

Nicola Cioffi · Mahendra Rai *Editors*

Nano-Antimicrobials

Progress and Prospects

 Springer

Nano-Antimicrobials

Nicola Cioffi • Mahendra Rai
Editors

Nano-Antimicrobials

Progress and Prospects

 Springer

Editors

Dr. Nicola Cioffi
Università degli Studi di Bari
Dipartimento di Chimica
via Orabona 4
70126 Bari
Italy
cioffi@chimica.uniba.it

Prof. Mahendra Rai
SGB Amravati University
Dept. Biotechnology
Amravati
India
mkrai@rediffmail.com

ISBN 978-3-642-24427-8 e-ISBN 978-3-642-24428-5
DOI 10.1007/978-3-642-24428-5
Springer Heidelberg Dordrecht London New York

Library of Congress Control Number: 2012932406

© Springer-Verlag Berlin Heidelberg 2012

This work is subject to copyright. All rights are reserved, whether the whole or part of the material is concerned, specifically the rights of translation, reprinting, reuse of illustrations, recitation, broadcasting, reproduction on microfilm or in any other way, and storage in data banks. Duplication of this publication or parts thereof is permitted only under the provisions of the German Copyright Law of September 9, 1965, in its current version, and permission for use must always be obtained from Springer. Violations are liable to prosecution under the German Copyright Law.

The use of general descriptive names, registered names, trademarks, etc. in this publication does not imply, even in the absence of a specific statement, that such names are exempt from the relevant protective laws and regulations and therefore free for general use.

Printed on acid-free paper

Springer is part of Springer Science+Business Media (www.springer.com)

Preface

There are alarming reports of new and emerging diseases caused by pathogenic microbes from all over the world. The dreaded diseases like AIDS and cancer needs new antimicrobial agents. The secondary infections caused by microbes in cancer patients are fatal and sometimes difficult to cure. Chemotherapy is one of the most effective strategies to treat malignant tumors. However, the resistance of cancer cells to the drugs remains a significant impediment to successful chemotherapy. Multidrug-resistant microbes are increasing with fast pace. The disease burden from multidrug-resistant strains of tuberculosis, malaria, hepatitis, and HIV is growing in both developed and developing countries. Therefore, there is a pressing need to search for a new generation of antimicrobial agents, which are effective, safe and can be used for the cure of multidrug-resistant microbial infections. Nano-antimicrobials offer effective solutions for the cure of such new and multidrug-resistant microbes.

The development of innovative nanosized materials capable of preventing the growth of undesired or pathogenic biological species is an emerging nanotechnological field. Nanophases composed of coinage metals and their compounds (e.g., Cu, Ag, Zn, etc.) are being frequently employed as a new bioactive element that is well tolerated by human beings. Organic and hybrid nano-antimicrobials are also being deeply studied. Several applications are envisaged for this class of materials, including food packaging and improvement of feedstock shelf-life, anti-fouling coatings and paints, antimicrobial textiles, biomedical devices and disposables, prevention of bio-contamination and diffusion of pandemic diseases in high-risk places (hospitals, airports, stations), etc. An exponentially growing number of patents and papers is being issued on these multidisciplinary aspects.

The present book is aimed at discussing the new technology of nano-antimicrobials. The book covers the synthesis of nanomaterials including Chemical, Physical, Mechanical, Photo- and Electro-Chemical methods. Particular emphasis is given to the microbial synthesis of bioactive nanomaterials, because the process is eco-friendly and economically viable. The antimicrobial potential of different nanoparticles is also covered, bioactivity mechanisms are elucidated,

and several applications are reviewed in detail. Finally, the toxicology of nano-antimicrobials is briefly assessed.

The book has been divided into four sections. Section I covers the synthesis and characterization of novel nano-antimicrobials, and the opening chapters have been prepared by two of the leading research groups working on silver nano-antimicrobials. The contributions by the groups of Professors Sen and Wang provide complementary points of view on either nanoparticle- or nanocomposite-based silver antimicrobials. Then, the chapters by Dr. Longano, Prof. Fernandez-Garcia, and Dr. Manna offer a comprehensive description of nano-antimicrobials, respectively based on copper, photo-catalytic titanium oxide, and zinc oxide. Finally, in the last chapter of the section, a short overview of the main methods for the characterization of nano-antimicrobials is provided by Prof. Regan.

Section II deals with the bioactivity and mechanisms of action of nano-antimicrobials. In this section, a contribution by the editors deals with the benefits and bottlenecks of the use of silver nano-antimicrobials. Then, a contribution by Prof. Mukherji assesses strain resistance or sensitivity towards nano-antimicrobials. The chapter by Dr. Ivask gives an insight into the different impact of soluble species and nanoparticles, in the bioactivity mechanisms of metal-containing antimicrobials. Finally, Dr. Debiemme-Chouvy's chapter describes an electrochemical approach to nanostructuring surfaces which shows interesting bioactivity properties.

Section III comprises six chapters providing some of the most exciting applications of nano-antimicrobials. The first chapter, by the group of Prof. Sannino, deals with the application of photo-reduction processes to the development of nano-silver coatings for textile and bio-medical applications. Then, a contribution by Prof. Duran deals with the industrial applications of bio-synthesized metal nano-antimicrobials, providing details about their effects, mechanisms of action, and toxicity. Prof. de Azeredo's chapter gives an expert opinion on bioactivity and applications of nano-antimicrobials used in the food-packaging industry. A chapter by Prof. Allaker elucidates, with plenty of detail, the application of nano-antimicrobials to the control of oral infections. Finally, antibacterial paper is the subject of Prof. Fan's chapter, while a contribution from the group of Prof. Cui reviews the use of nano-antimicrobials for water disinfection.

Last, but not least, Section IV offers two chapters on the toxicology of nano-antimicrobials. Prof. Dwahan's chapter deals with the use of micro-organisms as models for the assessment of toxicity, while a chapter by the group of Prof. Rai specifically assesses the toxicity of one of the most diffused classes of nano-antimicrobials, e.g. silver nanoparticles.

The book is of an interdisciplinary nature and will be very useful for students, teachers and scientists working in nanotechnology, materials science, biology, chemistry, physics, botany, zoology, chemical technology, medicine, pharmacology, mycology, microbiology, pathology, and biotechnology.

The contributions of eminent researchers in the field of nano-antimicrobials have been included in the present book. The editors greatly appreciate the contributions by leading scholars, and their patience during the publication of the book.

The authors wish to express sincere thanks to Dr. Pauly, Steffen, Springer, Germany for his continued interest, critical suggestions, and prompt response during the editing process. M.K.R. and N.C. gratefully acknowledge the help and support rendered by their students.

Bari, Italy
Amravati, India

Nicola Cioffi
Mahendra Rai

Contents

Section I Synthesis and Characterization of Novel Nano-Antimicrobials

- 1 Silver Nanoparticle Antimicrobials and Related Materials** 3
Hua Zhang, Meng Wu, and Ayusman Sen
- 2 Synthesis, Characterization and Application of Silver-Based Antimicrobial Nanocomposites** 47
Desong Wang, Jing An, Qingzhi Luo, Xueyan Li, and Luna Yan
- 3 Synthesis and Antimicrobial Activity of Copper Nanomaterials** 85
Daniela Longano, Nicoletta Ditaranto, Luigia Sabbatini, Luisa Torsi, and Nicola Cioffi
- 4 Titanium Dioxide–Polymer Nanocomposites with Advanced Properties** 119
Anna Kubacka, Marcos Fernández-García, María L. Cerrada, and Marta Fernández-García
- 5 Synthesis, Characterization, and Antimicrobial Activity of Zinc Oxide Nanoparticles** 151
Adhar C. Manna
- 6 Characterisation of Nano-antimicrobial Materials** 181
Timothy Sullivan, James Chapman, and Fiona Regan

Section II Bioactivity and Mechanisms of Action of Nano-Antimicrobials

- 7 Silver Nanoparticles as Nano-Antimicrobials: Bioactivity, Benefits and Bottlenecks** 211
Mahendra Rai, Alka Yadav, and Nicola Cioffi
- 8 Antimicrobial Activity of Silver and Copper Nanoparticles: Variation in Sensitivity Across Various Strains of Bacteria and Fungi** 225
Suparna Mukherji, Jayesh Ruparelia, and Shekhar Agnihotri
- 9 Metal-Containing Nano-Antimicrobials: Differentiating the Impact of Solubilized Metals and Particles** 253
Angela Ivask, Saji George, Olesja Bondarenko, and Anne Kahru
- 10 Electrosynthesis and Characterisation of Antimicrobial Modified Protein Nanoaggregates** 291
Catherine Debieuvre-Chouvy

Section III Applications of Nano-Antimicrobials

- 11 Engineering Nanostructured Silver Coatings for Antimicrobial Applications** 313
M. Pollini, F. Paladini, A. Licciulli, A. Maffezzoli, and A. Sannino
- 12 Biotechnological Routes to Metallic Nanoparticles Production: Mechanistic Aspects, Antimicrobial Activity, Toxicity and Industrial Applications** 337
Nelson Durán and Priscyla D. Marcato
- 13 Antimicrobial Activity of Nanomaterials for Food Packaging Applications** 375
Henriette Monteiro Cordeiro de Azeredo
- 14 The Use of Antimicrobial Nanoparticles to Control Oral Infections** 395
R.P. Allaker
- 15 Nanomaterial-Based Antibacterial Paper** 427
Wenbing Hu, Qing Huang, and Chunhai Fan
- 16 Antimicrobial Nanomaterials for Water Disinfection** 465
Chong Liu, Xing Xie, and Yi Cui

Section IV Toxicology of Nano-Antimicrobials

17 Microorganisms: A Versatile Model for Toxicity Assessment of Engineered Nanoparticles 497
 Ashutosh Kumar, Alok K. Pandey, Rishi Shanker, and Alok Dhawan

18 Nano-Silver Toxicity: Emerging Concerns and Consequences in Human Health 525
 Indarchand Gupta, Nelson Duran, and Mahendra Rai

Index 549

About the Editors 555

List of Contributors

Shekhar Agnihotri Centre for Research in Nanotechnology & Science (CRNTS), IIT Bombay, Powai, Mumbai, India

Rob P. Allaker Queen Mary University of London , Barts & The London School of Medicine and Dentistry, Institute of Dentistry, London, UK

Jing An School of Sciences, Hebei University of Science and Technology, Shijiazhuang, Hebei, PR China

Henriette M.C. deAzeredo Embrapa Tropical Agroindustry – CNPAT, Fortaleza, CE, Brazil

Olesja Bondarenko National Institute of Chemical Physics and Biophysics, Laboratory of Molecular Genetics, Tallinn, Estonia

María L. Cerrada Instituto de Ciencia y Tecnología de Polímeros (CSIC), Madrid, Spain

James Chapman Marine and Environmental Sensing Technology Hub (MESTECH), National Centre for Sensor Research, School of Chemical Sciences, Dublin City University, Dublin, Ireland

Nicola Cioffi Dipartimento di Chimica, Università degli Studi di Bari “Aldo Moro”, Bari, Italy

Yi Cui Material Science and Engineering, Stanford University, Stanford, CA, USA

Catherine Debiemme-Chouvy Laboratoire Interfaces et Systèmes Electrochimiques UPR 15 du CNRS, Paris, France

Alok Dhawan Nanomaterial Toxicology Group, CSIR-Indian Institute of Toxicology Research, Lucknow, Uttar Pradesh, India

Nicoletta Ditaranto Dipartimento di Chimica, Università degli Studi di Bari “Aldo Moro”, Bari, Italy

Nelson Duran Chemistry Institute, Biological Chemistry Laboratory, Universidade Estadual de Campinas (UNICAMP), Campinas, SP, Brazil; Center of Natural and Human Sciences (CCNH), Universidade Federal do ABC (UFABC), Santo André, SP, Brazil

Chunhai Fan Laboratory of Physical Biology, Shanghai Institute of Applied Physics, Chinese Academy of Sciences, Shanghai, China

Marcos Fernández-García Instituto de Catálisis y Petroleoquímica, Consejo Superior de Investigaciones Científicas, Madrid, Spain

Marcos Fernandez-Garcia Instituto de Catlisis y Petroleoquímica, Consejo Superior de Investigaciones Científicas, Madrid, Spain

Saji George University of California Center for Environmental Implications of Nanotechnology, Los Angeles, CA, USA

Indarchand Gupta Department of Biotechnology, SGB Amravati University, Amravati, Maharashtra, India

Wenbing Hu Laboratory of Physical Biology, Shanghai Institute of Applied Physics, Chinese Academy of Sciences, Shanghai, China

Qing Huang Laboratory of Physical Biology, Shanghai Institute of Applied Physics, Chinese Academy of Sciences, Shanghai, China

Angela Ivask National Institute of Chemical Physics and Biophysics, Laboratory of Molecular Genetics, Tallinn, Estonia; University of California Center for Environmental Implications of Nanotechnology, Los Angeles, CA, USA

Anne Kahru National Institute of Chemical Physics and Biophysics, Laboratory of Molecular Genetics, Tallinn, Estonia

Anna Kubacka Instituto de Catlisis y Petroleoquímica, Consejo Superior de Investigaciones Científicas, Madrid, Spain

Ashutosh Kumar Nanomaterial Toxicology Group, CSIR-Indian Institute of Toxicology Research, Lucknow, UP, India

Xueyan Li School of Sciences, Hebei University of Science and Technology, Shijiazhuang, Hebei, PR China

Antonio Licciulli Department of Engineering for Innovation, University of Salento, Lecce, Italy; Department of Engineering for Innovation, Silvertech Ltd, Lecce, Italy

Chong Liu Material Science and Engineering, Stanford University, Stanford, CA, USA

Daniela Longano Dipartimento di Chimica, Università degli Studi di Bari “Aldo Moro”, Bari, Italy

Qingzhi Luo School of Sciences, Hebei University of Science and Technology, Shijiazhuang, Hebei, PR China

Alfonso Maffezzoli Department of Engineering for Innovation, University of Salento, Lecce, Italy

Adhar C. Manna Basic Biomedical Sciences, Sanford School of Medicine, University of South Dakota, Vermillion, SD, USA

Priscyla D. Marcato Chemistry Institute, Biological Chemistry Laboratory, Universidade Estadual de Campinas (UNICAMP), CP 6154, CEP 130970, Campinas, SP, Brazil

Suparna Mukherji Centre for Environmental Science and Engineering (CESE), IIT Bombay, Powai, Mumbai, India

Federica Paladini Department of Engineering for Innovation, University of Salento, Lecce, Italy

Alok K. Pandey Nanomaterial Toxicology Group, CSIR-Indian Institute of Toxicology Research, Lucknow, UP, India

Mauro Pollini Department of Engineering for Innovation, University of Salento, Lecce, Italy

Mahendra Rai Department of Biotechnology, SantGadge Baba Amravati University, Amravati, Maharashtra, India

Fiona Regan Marine and Environmental Sensing Technology Hub (MESTECH), National Centre for Sensor Research, School of Chemical Sciences, Dublin City University, Glasnevin, Dublin

Jayesh Ruparelia Department of Chemical Engineering, Institute of Technology, Nirma University, Ahmedabad, India

Luigia Sabbatini Dipartimento di Chimica, Università degli Studi di Bari “Aldo Moro”, Bari, Italy

Alessandro Sannino Department of Engineering for Innovation, University of Salento, Lecce, Italy; Department of Engineering for Innovation, Silvertech Ltd, Lecce, Italy

Ayusman Sen Department of Chemistry, The Pennsylvania State University, University Park, PA, USA

Rishi Shanker Nanomaterial Toxicology Group, CSIR-Indian Institute of Toxicology Research, Lucknow, UP, India

Timothy Sullivan Marine and Environmental Sensing Technology Hub (MESTECH), National Centre for Sensor Research, School of Chemical Sciences, Dublin City University, Dublin, Ireland

Luisa Torsi Dipartimento di Chimica, Università degli Studi di Bari “Aldo Moro”, Bari, Italy

Desong Wang School of Sciences, Hebei University of Science and Technology, Shijiazhuang, Hebei, PR China

Meng Wu Department of Chemistry, The Pennsylvania State University, University Park, PA, USA

Xing Xie Civil and Environmental Engineering, Stanford University, Stanford, CA, USA

Alka Yadav Department of Biotechnology, SantGadge Baba Amravati University, Amravati, Maharashtra, India

Luna Yan College of Bioscience and Bioengineering, Hebei University of Science and Technology, Shijiazhuang, Hebei, PR China

Hua Zhang Department of Chemistry, The Pennsylvania State University, University Park, PA, USA

Section I
Synthesis and Characterization of Novel
Nano-Antimicrobials

Chapter 1

Silver Nanoparticle Antimicrobials and Related Materials

Hua Zhang, Meng Wu, and Ayusman Sen

1.1 Antimicrobial Mechanism of Silver and Silver Ion

Silver has a long history of usage in medicine in many cultures. The ancient Greeks, Romans, Egyptians, and many others used silver vessels for water and other liquids storage. It is recorded that Aristotle suggested that Alexander the Great (335 BC) should transport water in silver containers on many campaigns [1]. Pioneers who explored across the Wild West also used silver and copper coins to preserve drinking water from spoilage by bacteria and algae. They also put silver dollars into their milk to retain its freshness [2].

The first documented usage of silver in medical applications can be dated back to around AD 750. However, it was not until late 1800s that scientists proved that silver is an effective germicide. In 1869, Ravelin reported that silver, even in ultra-low concentration, shows antimicrobial activity [3]. Shortly after Ravelin's discovery, von Naegeli found silver ions (9.2×10^{-9} M) from metallic silver are able to kill *Spirogyra* commonly found in water [4]. In 1881, Carl Crede pioneered the treatment of eye infection of neonates by using 2% silver nitrate solution, a technique which has been widely used ever since [2]. In the early 1900s, silver foil was used as a dressing material for burn wound treatment. Silver in different forms, mostly colloidal silver, was extensively used by physicians, and this type of treatment was considered as "high-tech" at that time.

After World War II, novel and powerful antibiotics quickly replaced silver in bacterial infection treatment and the interest in silver as an antimicrobial agent declined sharply. Unfortunately, after decades of use, many bacteria have developed resistance towards one or more antibiotics. This has led to a resurgence in the use of silver in antibacterial applications. For example, in the 1970s, Margraf used a 0.5% silver solution to kill invasive bacteria in burn wounds. Silver sulphadiazine cream

H. Zhang • M. Wu • A. Sen (✉)

Department of Chemistry, The Pennsylvania State University, University Park, PA, USA

e-mail: huz111@psu.edu; asen@psu.edu

was also developed to replace diluted silver salt solutions, and is now used extensively in burn wards in America. This technique is considered as a gold standard of topical burn treatment [5]. Other commercial silver antibacterial products can also be found in the food industry, water supply systems, medical care products, clothing, electronic appliances, etc. For example, Agion[®] is a surface modification technique that turns regular surfaces into antibacterial surfaces by releasing silver ions. Similar techniques have been adopted in various products made by Honeywell[®], Dell[®], Motorola[®], Logitech[®], PPG[®], the North Face[®], Adidas[®], etc. Microban[®] 3G silver is another popular antibacterial solution for polymeric materials that combines antibacterial property of silver with other antibacterial agents.

Although silver has been used as a biocide for hundreds of years, the antimicrobial mechanism of silver has not been fully elucidated. A variety of mechanisms may be involved in the antimicrobial activity of silver against a broad spectrum of organisms. Some of the commonly accepted mechanisms include silver–amino acid interaction, silver–DNA interaction, generation of reactive oxidative species, and direct cell membrane damage.

1.1.1 Interaction with Thiol Groups on Amino Acids

The cytotoxicity of heavy metal ions like Ag^+ , Hg^{2+} , Cu^{2+} and Pb^{2+} , in many cases, is due to the interaction between metal ions and thiol groups in proteins or enzymes in microorganisms which leads to the inhibition of their crucial biological functions [6–11]. The thiol group in *L*-cysteine residues can undergo either reversible or irreversible oxidation by chemical agents, including heavy metal ions, causing death of microorganisms (Fig. 1.1) [1].

1.1.1.1 Inhibition of Respiratory Process of Bacteria Cells

Cellular respiration is the process by which cells convert biochemical energy from nutrient into adenosine triphosphate (ATP) and release waste products.

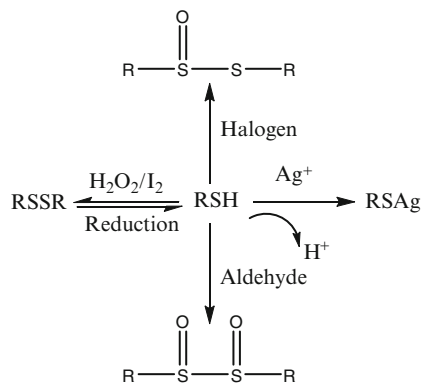


Fig. 1.1 Biocides interaction with thiol group (Reprinted from [1]. With permission from Elsevier)

In eukaryotes, oxidative phosphorylation occurs in the mitochondrial cristae. It involves the respiratory chain which establishes a proton gradient (chemiosmotic potential) across the inner membrane by oxidizing the nicotinamide adenine dinucleotide (NADH) produced from the Krebs cycle. ATP is synthesized by the ATP synthase enzyme, and the chemiosmotic gradient is used to drive the phosphorylation of ADP to form ATP. To complete the respiration process, the electrons are finally transferred to exogenous oxygen and, with the addition of two protons, water is formed. Bard [12] used microelectrode and other techniques to explore the inhibition of respiration of *Escherichia coli* treated by silver ions. The mechanism has been proposed that silver is able to cause cell membranes to be permeable to protons and therefore the proton gradient is lost. To compensate for the loss of the proton gradient, the acceleration of the respiratory process is triggered, attempting to expel more protons to restore the proton gradient. This uncontrolled process generates superoxide or hydroxyl radicals which are extremely harmful to the cells.

1.1.1.2 Enhanced Phosphate Efflux

Rosenberg [13, 14] studied the ability of silver ions to inhibit the intake of phosphate ions and enhanced efflux of phosphate of *Escherichia coli*. In the experiment, *Escherichia coli* was first incubated with either 5 mM succinate or 1 mM glucose to deplete the phosphate ions in cells. Then, the phosphate-depleted cells were washed to remove any extra sugar energy sources. Silver was added 2 min prior to radioactive ^{32}P addition. The ^{32}P uptakes by *Escherichia coli* cells (with silver and without silver) were compared with control (no cells) by radioactivity monitoring. The inhibition of uptake of phosphate by silver ions was observed. Alleviation of such inhibition could be done by adding KBr to decrease effective silver ion concentrations. In another experiment, where AgNO_3 was also added to suspension of cells which have already taken up ^{32}P , the enhanced efflux of ^{32}P was observed. Again, addition of KBr can either slow down the efflux of phosphate for the *Escherichia coli* AN710 strain or resume phosphate uptake for the *Escherichia coli* AN1080 strain. Besides the enhanced efflux of phosphate ions, the efflux of accumulated proline, glutamine, mannitol, and succinate was also discovered when *Escherichia coli* suspension was treated with silver ions. The efflux can be stopped and the uptake can be resumed by adding thiol compounds such as dithiothreitol or mercaptoethanol, presumably due to the detoxification reactions between silver ions and thiol compounds.

1.1.2 Interaction with DNA Molecules

DNA is responsible for the reproduction process. Any damage done to it will cause either mutation or death of the organism. The preferential interaction of silver ions with the bases found in DNA rather than the phosphate group is well documented [15–19].

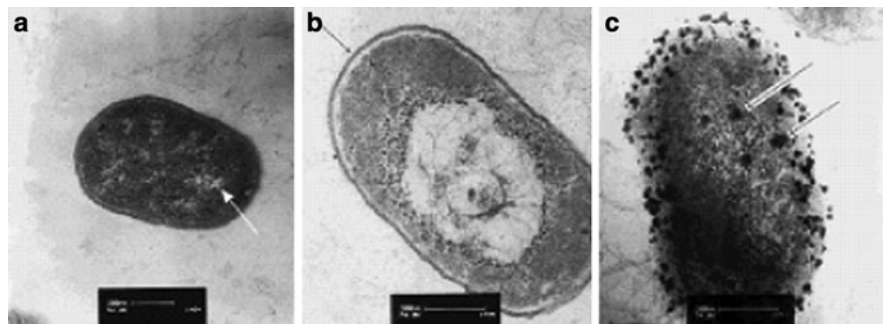


Fig. 1.2 Morphology comparison of untreated and treated *Escherichia coli*: (a) Untreated. (b) self-defense mechanism tries to protect DNA. (c) final stage of a dying *Escherichia coli* cell (Reprinted from [20]. With permission from Wiley)

Feng [20] probed the antibacterial mechanism of Ag^+ by treating *Escherichia coli* and *B. aureus* bacteria with AgNO_3 solution. After silver treatment, bacteria samples are subjected to TEM observation. It was found that silver-treated *Escherichia coli* cells showed a large electron-light region (DNA molecules) in the center whereas electron-light areas were evenly distributed in untreated cells (Fig. 1.2a, b). Another phenomenon was also noticed: a large amount of electron-dense granules appeared around the electron-light region but not in untreated bacteria. The researcher proposed that these electron-dense granules were generated by a cell self-defense mechanism as they tried to protect the DNA (electron-light region). When this self-defense mechanism failed to function due to the large amount of silver ions present, the cell was full of electron-dense granules with no electron-light regions at all and the cell wall also completely disappeared, both of which were captured by TEM images (Fig. 1.2c).

The assumption that silver ions may cause increased mutation frequency of microorganism has also been supported in a recent publication [21]. Three different silver materials were used in this research: silver nanopowder, silver-copper nanopowder, and colloidal silver. Both polymerase chain reaction (PCR) and *in vivo Escherichia coli* experiments were carried out and compared. A particular *rpsL* mutation assay was used in *in vitro* PCR. The *rpsL* gene encodes a small ribosomal protein S12, which caused resistance to the antibiotic streptomycin after mutation. When the PCR process was finished, the silver-treated genes were used to transform into host bacterial cells MF101. If mutation of *rpsL* gene occurs, the transformed bacteria will be streptomycin resistant. Therefore, the mutation frequency is calculated from the number of colonies surviving on both ampicillin and streptomycin agar plates divided by the total colonies surviving on ampicillin agar. A substantial increase of mutation frequency was observed: 1.63%, 1.54%, 2.15%, and 0.68% for silver nanopowder, silver-copper nanopowder, colloidal silver, and untreated samples, respectively. These results suggested that silver material treatment can cause significant gene mutation and that this mutation may lead to death of the bacterial cells. A similar observation was made with *in vivo Escherichia coli*

although the mutation frequency was lowered by four orders of magnitude than those in vitro perhaps due to the lower uptake of silver.

1.1.3 Catalytic Generation of Reactive Oxygen Species (ROS)

ROS are normal byproducts of the respiration process. ROS at low level can be controlled by the so-called antioxidant defense such as equilibrium between glutathione and glutathione disulfide. However, excess ROS production may generate free radicals which are extremely deleterious to cells because of the damage to lipids or DNA [22]. It is believed that metals can catalytically promote the generation of ROS with dissolved oxygen in solution [23]. If true, the silver nanomaterials can kill bacteria directly by the catalytic generation of ROS without the presence of silver ions. Hwang [24] found that the antimicrobial activity of carbon-supported silver was observable only in the presence of oxygen. In this case, it was apparent that generation of ROS by silver nanoparticles instead of biocidal silver ions was the predominate mechanism. Kim [25] verified free radicals generated from silver nanoparticles by spin resonance methods. In the same experiments, the biocidal action of both silver nanoparticles and silver ions was stopped with the presence of reductants, which led to the conclusion that the biocidal mechanism against *Staphylococcus aureus* and *Escherichia coli* is the generation of free radicals.

Besides silver nanomaterials, silver ions can also generate excess ROS. Park [26] used superoxide-responsive protein containing bacteria to detect the ability of silver ions to generate ROS. Usually, bacteria have their own ROS sensor systems. For example, *Escherichia coli* has two proteins as ROS sensing systems: SoxR and OxyR. When exposed to superoxide or nitric oxide radicals, the SoxR protein induces a single gene *soxS*. By monitoring *soxS* induction in the reporter strains, the ROS level in the solution can be determined. The increased *soxS* response found after ionic silver treatment suggested that ROS was generated. Another experiment conducted to validate this mechanism was comparing the antibacterial activity of silver ions under both aerobic and anaerobic conditions, since the generation of ROS requires the presence of dissolved oxygen. It was found that silver ions exhibited higher biocidal activity under aerobic conditions (3.3 log bacterial reductions under aerobic condition versus 1.9 log bacterial reductions under anaerobic condition). This result shows that generation of ROS is a plausible biocidal pathway and also suggests that the antibacterial mechanisms of silver ions may be a combination of ROS generation and silver–thiol interactions.

1.1.4 Direct Damage to Cell Membrane

Direct damage to cell membrane caused by silver nanomaterials has been reported recently. Morones and colleagues [27] explored the biocidal mechanism of silver nanoparticles against four kinds of bacteria: *Vibrio cholerae*, *Pseudomonas*

aeruginosa, *Scrub typhus*, and *Escherichia coli*. The accumulation of silver particles on the bacterial membrane surface was observed by using the High Angle Annular Dark Field (HAADF) microscopy technique. The researchers were also able to get electronic microscopy images of the bacterial cross-section. EDS mapping of the silver element showed that silver nanoparticles are able to penetrate the membranes and get enriched inside the cells. The ability of silver particles to get inside the cells is explained by the observation of membrane defects caused by silver nanoparticles. The researchers also compared silver nitrate-treated bacteria with silver nanoparticles-treated bacteria. Silver nitrate-treated bacteria showed both DNA agglomerated regions (electron-light regions) and electron-dense regions, which match with a previous publication [20]. However, this was not seen for silver nanoparticles-treated bacteria, which suggests that silver in different forms may operate differently.

The detailed mechanism of cell membrane penetration and accumulation of silver nanoparticles is not fully understood. One hypothesis is that the accumulation is caused by electrostatic attraction between negatively charged bacterial surfaces and positively charged silver nanoparticles [28]. However, this does not explain why negatively charged silver nanoparticles are able to adhere to and enter the bacteria cells. Another possibility is that the process is initiated by silver–thiol group interaction on the cell surface, and is supported by a recent publication [29].

Another explanation for cell membrane damage is proposed for Gram-negative bacteria such as *Escherichia coli*. Gram-negative bacteria possess an external membrane outside the peptidoglycan layer, which is lacking in Gram-positive bacteria. It was previously found that chelating agent EDTA can cause the depletion of Ca^{2+} and Mg^{2+} ions, resulting in pits and holes in the outer membranes due to the release of LPS (lipopolysaccharide) molecules [30]. Sondi [31] also observed a similar phenomenon by treating *Escherichia coli* bacteria with silver nanoparticles. The SEM images clearly showed that there were many holes in the cell membranes of silver-treated *Escherichia coli* bacteria (Fig. 1.3). The researchers postulated that silver may also generate pits and holes in the cell membrane by causing the release of LPS from cell membranes.

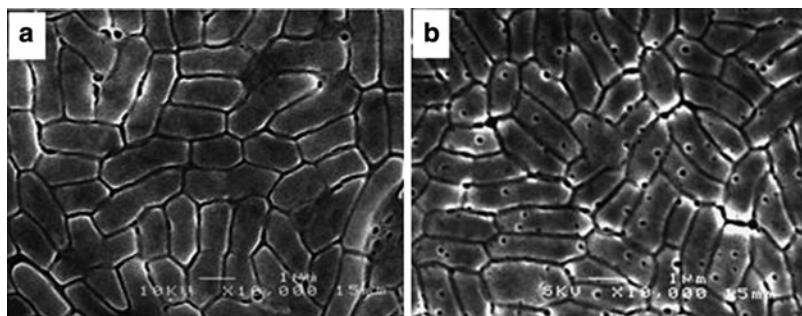


Fig. 1.3 SEM images of (a) native *Escherichia coli* bacteria and (b) *Escherichia coli* treated with 50 µm/mL silver nanoparticles (Reprinted from [31]. With permission from Elsevier)

1.2 Evaluation Methods and Criteria for Silver Antibacterial Materials

Standard evaluation methods and criteria for silver antimicrobial materials are important because quantitative data are necessary for materials screening in terms of antibacterial activities and inter-laboratory comparisons. Most evaluation methods used in publications are adopted from long-standing *in vitro* microbiology protocols for antibiotics.

1.2.1 Minimum Inhibitory Concentration (MIC)

The minimum inhibitory concentration (MIC) test is an *in vitro* test which determines the lowest concentration of antibiotics needed to inhibit the growth of (but not necessarily kill) bacteria. MIC test is extensively used to evaluate the antibiotic susceptibility of targeted bacteria in microbiology and clinic practice. In theory, it can also be used for antibacterial silver materials and it works practically very well on these samples. Usually, both MIC and minimum biocidal concentration (MBC) are reported for small molecule antibiotics and MBC is usually much higher in value than MIC. However, for silver antibacterial materials, only MIC data are typically reported.

1.2.1.1 Test Protocols

Typically, there are two standard techniques to determine MIC values: agar dilution and broth dilution. In agar dilution test, the antibiotic is mixed with agar powder and made into nutrient agar plates with different concentration of the antibiotic. Then, liquid broth with a predetermined concentration of bacteria is inoculated onto the agar plates. After incubation, bacterial colonies are visually counted. An absence of bacteria colonies means all bacteria are inhibited or killed at that concentration of antibiotics.

The broth dilution protocol uses liquid media with known amounts of bacteria, and different amounts of antibiotic are added to it. After incubation, the turbidity of the media is observed as an indication of bacterial growth. Based on the final media volume (bacterial solution + antibiotic solution), broth dilution can be categorized as microdilution (total volume $\leq 500 \mu\text{L}$) and macrodilution (total volume $\geq 2 \text{ mL}$) [32]. The final results given by the MIC test can be in mg/mL, mg/L, or $\mu\text{g/mL}$ depending on the antibacterial efficiency and bacteria tested. For silver antimicrobial materials, it is difficult to obtain uniformly blended agar plates. Therefore, broth dilution is the commonly used evaluation protocol.

1.2.1.2 Critical Parameters

In order to get reproducible and reliable MIC values for both intra-laboratory and inter-laboratory comparisons, additional parameters must be noted during the test: (a) *Bacteria*: Bacteria tested in the experiments must be isolated in their pure form. Their genus and species level must be identified. Most organisms can be obtained from hospital laboratories, the American Type Culture Collection (ATCC) or other national collections [32, 33]. (b) *Inoculum*: The typical bacterial concentration for MIC is 5×10^5 cfu/mL for final solution (broth dilution) or 1×10^4 cfu per agar plate (agar dilution). It has been documented [34] that more concentrated solutions of drug-resistant strains give increased MIC values due to the generation of enzymes capable of decomposing antibiotics. However, it is still not clear whether increased inoculum will affect the MIC value of silver antibacterial materials. (c) *Determination of bacteria concentration*: The concentration of bacterial media is usually expressed in cfu/mL (colony forming unit/mL). The turbidity of the bacterial solution is proportional to its optical absorption at 600 nm. A calibration curve is usually set up for a specific bioassay reader (or microplate reader) by plotting cfu numbers versus absorption values. The detailed procedure can be found in previous literature [32]. Once the calibration curve is set, the bacterial concentration can be readily calculated from its absorption. If the absorption value is greater than 1, it causes loss of linearity. Therefore, necessary dilution may be needed before obtaining the absorption value.

1.2.1.3 Limitations

The MIC test does not indicate whether tested materials are biocidal or biostatic. Even if the broth or agar plate shows no bacterial growth, there may be viable bacteria present because the tested materials may only inhibit the growth of bacteria (biostatic effect). Bacteria may continue to proliferate when the antibacterial material is removed. To differentiate whether the sample is biostatic or biocidal, aliquots of broth can be withdrawn and spread on a new agar plate with no antibacterial material present. If colonies are observed after incubation, the material is only biostatic at this concentration. Otherwise, the material is biocidal.

1.2.2 Zone of Inhibition (ZOI)

The ZOI test is another *in vitro* test, also widely known as the Kirby-Bauer disk diffusion test [35]. When bacteria are inoculated onto nutritious agar plates, they tend to form continuous spots called colonies. If there is an antibiotic present at a specific area in the agar, colony formation will be inhibited around that area due to

the leaching of the antibiotic, and the zone of inhibition can be visually observed and measured.

1.2.2.1 Test Protocol

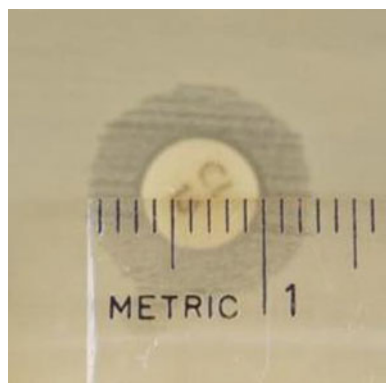
The general procedure is as follows: bacteria are first incubated in a liquid broth for a certain period of time (depending on the bacteria); several drops of bacterial broth are streaked onto an agar plate. Then, sample disks are placed over the agar plate and the whole agar plate is incubated. Finally, the net inhibition diameter can be calculated by subtracting the diameter of the sample disk from the diameter of the total zone of inhibition. Kirby and Bauer did a series of experiments comparing their method with the previously mentioned MIC test, and they found that these two tests are highly correlated [35]. Therefore, the net diameter of inhibition zone can be a benchmark for the activity of the specific antibiotic as long as the same type of agar is used during all the experiments (Fig. 1.4).

1.2.2.2 Modification

The ZOI test, though originally developed for water-soluble antibiotics, provides us with a semi-quantitative option to evaluate water-insoluble antibacterial materials when the MIC test cannot be carried out. The ZOI test is especially applicable to antibacterial coatings and films because these types of materials usually perform poorly in the MIC test due to limited availability of biocidal agents.

Due to the simplicity of this method, the FDA has recommended using this technique to evaluate new antibiotics. One disadvantage of the Kirby-Bauer method is the long incubation period, typically 12–16 h. In 1973, Ross [36] shortened this period to 6.5 h without sacrificing the accuracy by spraying cell stains on the agar plates. The live bacteria show a certain color depending on the dye, and the zone of inhibition remains unstained.

Fig. 1.4 Antibacterial material is placed on a bacteria-inoculated agar plate. A circle of poor bacterial growth surround the material shows the ZOI (Picture credited to Center of Disease Control and Prevention)



1.2.2.3 Limitation

ZOI tests do not necessarily indicate that the bacteria are killed by the antibacterial material. The antibacterial material may just prevent the bacteria growth. Sometimes, clear boundaries are not observed which makes measuring the ZOI diameter difficult. This method is also less quantitative than the MIC protocol.

1.3 Inorganic Silver Composites and Silver Nanomaterials

The increasing demands of better living conditions have prompted scientists to develop and commercialize effective yet affordable antimicrobial materials. Silver is introduced into inorganic substrates in the form of either pure silver nanoparticles or as sparingly soluble silver salts. Silver may either be present on the surface of the material or dispersed in the matrix. The preparations of inorganic silver composites are usually straightforward with little wet chemistry involved. Commonly used inorganic substrates or matrices are titania or silica particles, glasses, ceramics, inorganic fibers, and medical alloys.

1.3.1 Glass

Glass is widely used in windows, sliding doors, and containers which are prone to bacterial adhesion. Thus, antimicrobial modification on glasses is highly desirable. Traditional glasses are made by using melt–quench process, which makes it impossible to fabricate silicate glass/silver composites with a high silver loading. Instead, a sol–gel method is used [37–39]. The first step of this method is polycondensation. Silver salts are mixed with TEOS (tetraethyloxysilane) and triethyoxysilane, such as $\text{NH}_2(\text{CH}_2)_3\text{Si}(\text{OEt})_3$, in absolute ethanol. After mixing, aqueous ammonia is added under vigorous stirring to cause hydrolysis. The homogenous mixture is then heated and the solvent is removed under reduced pressure to obtain xerogels. The next step involves oxidation of the xerogels in heated quartz tubes under air flow to adjust elemental composition. In the final step, the composites are reduced by reheating under hydrogen flow to further decrease carbon and oxygen content. Glasses made by this method usually show a brown color due to the presence of silver colloids. An improved method has been developed for colorless antimicrobial glasses [40]. First, AgNO_3 , $\text{Al}(\text{NO}_3)_3$, water, and ethanol are mixed to obtain a solution A. Second, TEOS and equal amount of ethanol are mixed to form a solution B. Solution A is slowly added to solution B under vigorous stirring. The mixture is then poured into a polystyrene mold to dry and gelate for 7 days. Finally, the gel is milled into a fine powder, put into a mold and baked at 900–1,000°C. Instead of having silver particles, this product is infused with silver ions which are colorless.

As a test, this composite was soaked in *Streptococcus mutans* broth and incubated for 12 h. No surviving bacteria were found in the broth, indicating that the silver ions released from the glass had killed 100% of the bacteria.

1.3.2 Coatings and Films

Surface antimicrobial modification of medical alloy implants is especially important since the adherence and fouling by bacteria on implant surfaces may cause serious complications and sometimes even the death of the patient [41]. Surface modification of surgical materials with silver can greatly reduce this risk. The surface deposition of silver can be achieved by anodic oxidation, electroless plating, CVD (Chemical Vapor Deposition), and other physical or chemical coating techniques. Recently, Duszczuk [42] utilized the PEO (Plasma Electrolytic Oxidation) technique to plate Ag/TiO₂ film onto a commonly used surgical Ti-6Al-7Nb alloy. PEO is an anodic oxidation electrochemical process which uses a voltage higher than the dielectric breakdown point of the metal oxide layer. This technique significantly increases the surface roughness and interconnects the pores in the metal oxide layer. Thus, the metal oxide layers more readily absorb other species. The oxidation process is carried out in a calcium acetate and calcium glycerophosphate solution to create a bioactive porous oxide coating containing calcium and phosphate ions on titanium metal. During the oxidation process, silver nanoparticles present in the electrolyte solution are uniformly incorporated into the oxide coating (Fig. 1.5). Such Ti/Ag disks were incubated with broth medium inoculated with methicillin-resistant *Staphylococcus aureus* at 2×10^5 cfu. After 24 h of incubation, 100% of the bacteria were killed.

Alt [43] developed a double layer coating by using both PVD (Physical Vapor Deposition) and CVD (Chemical Vapor Deposition) techniques. Elemental silver was firstly coated by PVD on a stainless steel implant. This silver coating was covered by a layer of silicon carbide by CVD for better biocompatibility and mechanical durability. The coated implant was able to retain antibacterial activity for at least 28 days in animal experiments, and TEM images showed little silver particle loss after implanted in animal for 28 days (Fig. 1.6).

Besides the aforementioned surface modification of metal, ceramics and glasses are also popular substrates for antibacterial coatings and films. Wang [44] developed a convenient method to co-precipitate Ag/TiO₂ film on the surface of ceramic tiles. A dipping solution was firstly made by mixing an aqueous solution of ammonium hexafluorotitanate with silver nitrate and boric acid. Then, ceramic tiles were soaked in the dipping solution for several hours to form a surface coating. Use of a scanning electron microscope (SEM) and energy dispersion spectrum (EDS) confirmed the formation of the Ag/TiO₂ coating covering the ceramic tile surface. This film is able to leach out silver ions and kill over 99% of *Staphylococcus aureus* and *Escherichia coli* after incubation for 24 h. A variation on this technique has also been employed [45]. Titanium alkoxide was first stabilized by

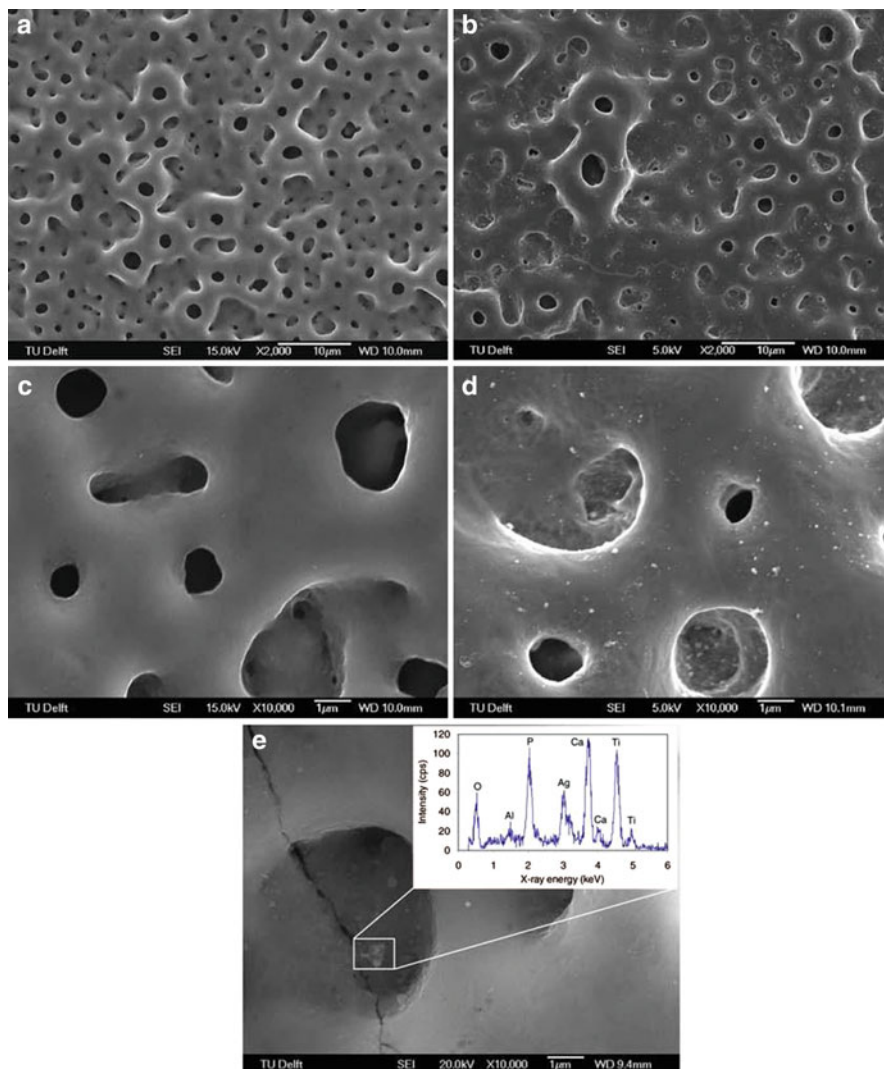


Fig. 1.5 SEM images of titanium oxide (a, c) and titanium oxide composite coating (b, d, e) produced at 20 A/dm^2 and 5 min oxidation time. EDS analysis indicated presence of Ag particles (Reprinted from [42]. With permission from Elsevier)

pentane-2,4-dione chelation and was then mixed with an AgNO_3 aqueous solution to obtain a dipping solution. Different substrates such as glass, aluminum, brass, and stainless steel were soaked in this solution. The coated substrates were finally annealed at 500°C for 1 h before use. Besides ceramics, silver can be coated on float glasses (a type of glass made by floating molten glass on a bed of molten metal) by a more sophisticated technique [46]. Initially, float glasses are pre-coated with silica to prevent diffusion of impurity into the float glasses, followed by a secondary

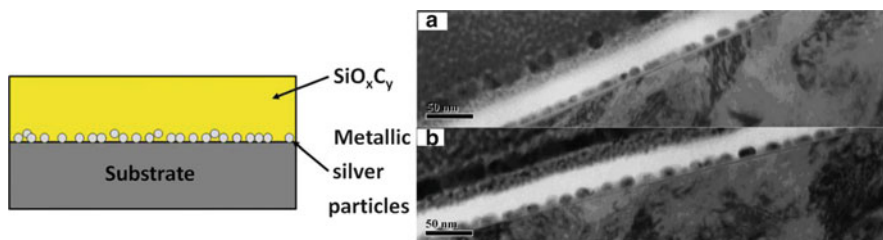


Fig. 1.6 Scheme for double layer coating (*left*) and TEM images of intersection: before implant (**a**) and after 28 days implant (**b**). TEM images show little silver particles loss before and after implant (Reprinted from [43]. With permission from Wiley)

coating of TiO_2 by CVD. Silver film was finally grown in a combustion CVD machine by nebulizing the AgNO_3 solution onto the substrate. This method gives the film a photolytic property from TiO_2 to decompose organic contaminants and antibacterial performance from silver. This material is able to kill over 99% of *Staphylococcus aureus*, 69% of *Escherichia coli* and over 99% of *Bacillus subtilis*.

Coating modification of textiles and fibers is another attractive research topic. Fisher [47] developed a silicon-based sol-gel coating solution with both antibacterial and waterproof properties. Triethoxytridecafluorooctyl silane and AgNO_3 were mixed to form a sol-gel solution followed by dipping textiles in this solution. Hydrolysis of silane was then initiated. Finally, the textile was dried and tested. It was found that water uptake of the treated textile was considerably reduced due to the highly hydrophobic nature of fluorinated silane. Nearly 100% bacterial inhibition of *Escherichia coli*, *Candida cariosilignicola*, and *Candida glabrata* were observed even after ten washes.

1.3.3 Pigment Materials

Titania and silica are the two most frequently used pigment materials. Antimicrobial modification of these materials is highly desirable as it may provide a more hygienic environment, especially in hospitals. Another application of such a pigment is in the fabric industry. Conventionally, silver nanoparticles are grafted onto fiber surfaces. However, it is almost impossible to maintain their antibacterial activity after extensive wash cycles. One possible solution is to use a metal oxide, titanium oxide for instance, as a carrier of silver particles so that the silver is less likely to be washed away by detergent. Yuan [48] designed $\text{Ag}/\text{TiO}_2\text{-C}$ composites with a TiO_2 core that gives regular pigment an antimicrobial property. To prepare the $\text{Ag}/\text{TiO}_2\text{-C}$ composite, activated carbon was formed on the surface of TiO_2 by dehydration of sucrose in an autoclave and by soaking $\text{TiO}_2\text{-C}$ powder in an AgNO_3 solution whereupon Ag is precipitated onto the $\text{TiO}_2\text{-C}$ surface. This composite was tested against *Escherichia coli* and *Staphylococcus aureus* at

10^5 cfu/mL for 24 h. Pure TiO_2 shows moderate antimicrobial activity whereas the Ag/ TiO_2 -C composite killed 100% of the microorganisms.

Porous silica particles can also be made into antibacterial pigments in a similar fashion. Kwon [49] developed a white pigment based on silica nanoparticles. The porous silica particles were initially synthesized from the hydrolysis reaction of TEOS in the presence of the triblock copolymer Pluronic[®] as the structure directing agent. The silica particles obtained were a few 100 nm in diameter and morphologically porous to AgNO_3 solutions. Then, the silica particles were treated with HCl vapor to generate AgCl. This antibacterial pigment is stable enough to undergo a melt-extruding process in a polypropylene (PP) matrix. In the antibacterial test, the doped PP composite was able to kill 99% *Escherichia coli* after 24 h incubation.

1.3.4 Absorbents/Filter Agents

Zeolites are aluminosilicate minerals with porous surfaces, commonly used as commercial absorbents, water cleaning agents, and filter agents. Adding antibacterial property to zeolites is quite natural and the process is very simple. Sasatsu [50] used commercially available sodium-type zeolites as the host compound. Silver ions were loaded by an ion exchange method that involved soaking Na-zeolite powder in AgNO_3 solution for 24 h, then washing with distilled water and drying in air. This zeolite/Ag composite was able to kill *Escherichia coli* in just 5 min. The fast biocidal action is due to the generation of ROS (reactive oxygen species) described earlier.

Another type of porous material is activated carbon. Hu [51] used charcoal obtained from pyrolysis of bamboo as a substrate for silver deposition. To prepare this material, bamboo charcoal was immersed in an $[\text{Ag}(\text{NH}_3)_2]\text{NO}_3$ solution for 1 h and then the silver ion was reduced by slowly adding diluted hydrazine solution under an inert atmosphere. Finally, a filter paper was impregnated with the obtained powder. The powder itself showed low MIC (0.3 $\mu\text{g}/\text{mL}$) towards tested bacteria such as *Staphylococcus aureus*, *Escherichia coli*, *Pseudomonas aeruginosa*, and *Bacillus subtilis*. The filter papers showed clear ZOI for bacteria-inoculated agar plates (Fig. 1.7).

Activated carbon in the form of fiber is also widely used as air filter to remove air pollutants, odor, and airborne microorganisms. An activated carbon fiber filter is also susceptible to bacteria adherence. Bacteria can grow on carbon fibers and thereby become the source of bioaerosols. Incorporation of silver in activated carbon fiber was reported by Hwang [24, 52]. Initially, Pd was introduced as a catalyst onto the activated carbon fiber. Then, an electroless plating technique was employed by immersing the Pd-loaded carbon fiber into a silver salt solution to deposit silver on the carbon fiber (Fig. 1.8). The silver-containing carbon fibers have ZOI of around 11 mm (*Escherichia coli*) and 12–15 mm (*Bacillus subtilis*) compared with none for the control fiber.

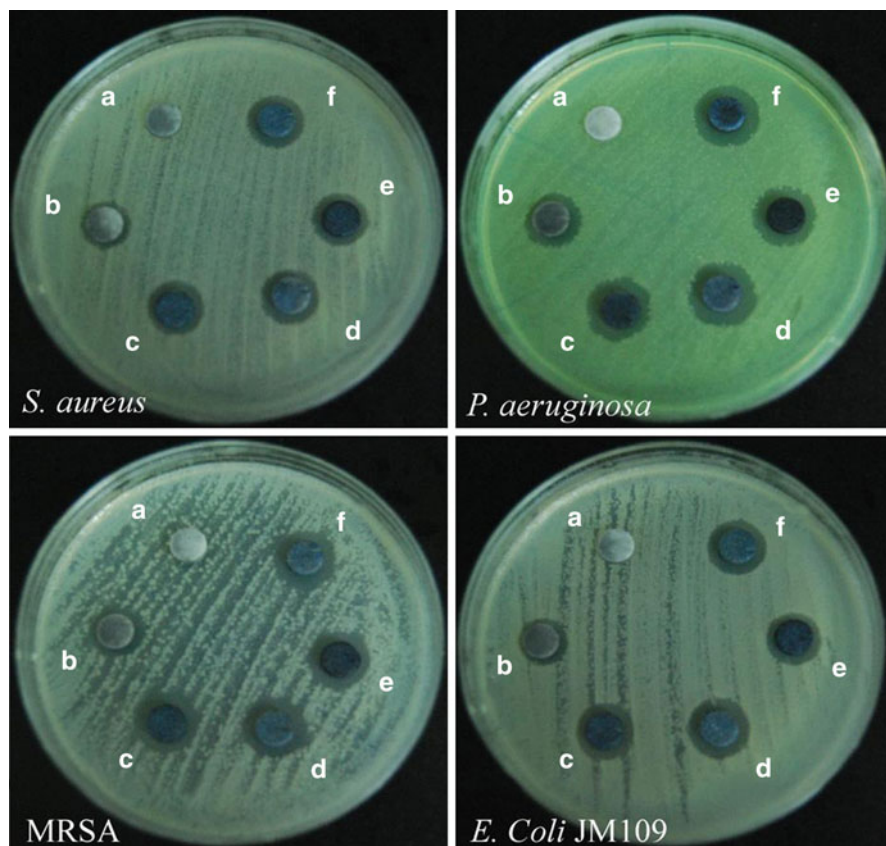


Fig. 1.7 Pictures of filter paper test samples on bacteria inoculated agar plates. Pure bamboo charcoal (a) shows no ZOI whereas all bamboo charcoal/Ag samples (b–f) show obvious ZOI (Reprinted from [51]. With permission from Elsevier)

1.3.5 Silver Nanomaterials

Contrary to bulk metallic forms or ionic forms, the antimicrobial action of silver in the nano-scale is due to the catalytic generation of reactive oxidative species (ROS) from dissolved oxygen in solution, which can directly attack cell membranes or DNA. The most common synthetic methods for silver nanomaterials are reduction of silver ions by either electrochemical processes or chemical reductants such as hydrazine [53, 54], NaBH_4 [55], hyperbranched poly (amidoamine) [56], and formamide [53]. The size of the silver nanomaterial depends on the reductant employed. Strong reductants like NaBH_4 usually lead to small silver nanoparticles whereas weak reductants like citrate yield larger nanoparticles with high size dispersion. Factors such as pH and the complexing agent (e.g., ammonia) also contribute to the different morphologies of the obtained silver nanoparticles.

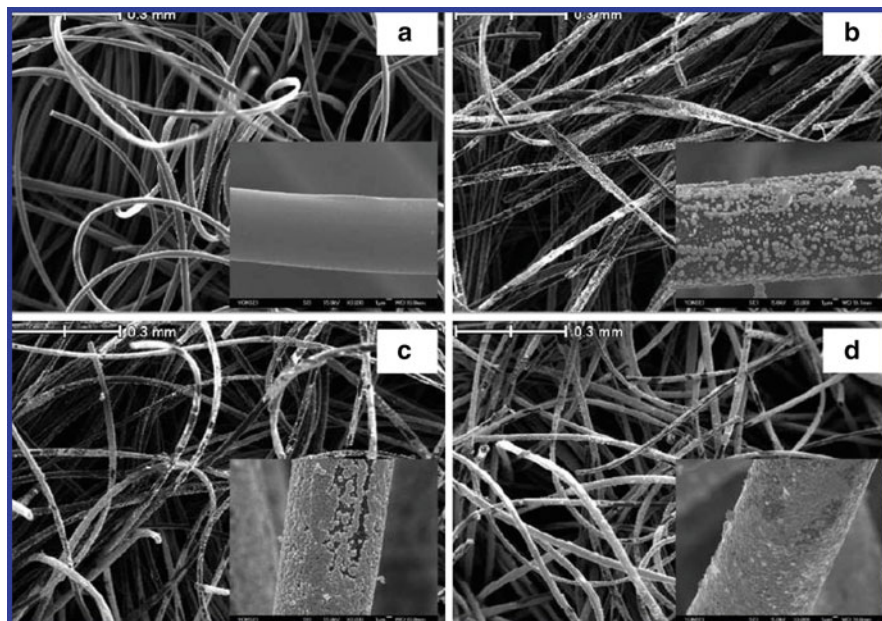


Fig. 1.8 SEM images of (a) pure carbon fiber, (b) carbon fiber with silver treatment for 10 mins, (c) carbon fiber with silver treatment for 20 mins and (d) carbon fiber with silver treatment for 30 mins (Reprinted from [52]. With permission from American Chemistry Society)

To avoid using toxic reductants, Zbořil [57] used saccharides as reductants. $\text{Ag}(\text{NH}_3)_2^+$ complex with glucose, galactose, maltose, or lactose were mixed in solution, and NaOH solution added to initiate the reduction. TEM images of silver colloid nanoparticles synthesized via this method are shown in Fig. 1.9. Besides silver nanoparticles, other silver nanostructures such as silver nanoflakes [58], silver nanofibers [59, 60], silver-coated fibers [61], titania/silver nanocomposites [62], and cross-linked micelles with silver nanoparticle cores [63] have been reported to have antibacterial properties.

Silver nanoparticles synthesized by biological approaches are becoming more and more popular. For more information, please refer to Sect. 2.1.1.3 in Chap. 2.

1.4 Polymeric Silver Composites

Besides inorganic materials, polymers are also encountered daily. Most polymeric materials, such as polyethylene, polypropylene, polystyrene, are not inherently antibacterial. Therefore, the antibacterial modifications of polymeric materials are also important and necessary.

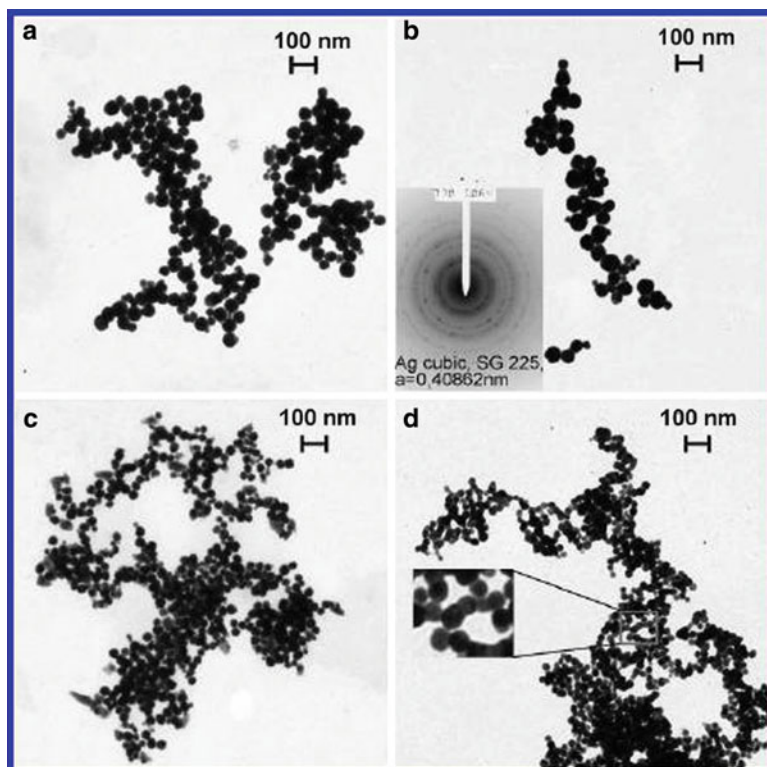


Fig. 1.9 TEM images of silver colloid nanoparticles synthesized via reduction of $\text{Ag}(\text{NH}_3)_2^+$ by glucose (a), galactose (b), lactose (c), and maltose (d) (Reprinted from [57]. With permission from American Chemistry Society)

1.4.1 Coatings and Films

Antibacterial polymeric coatings and films are very useful as surface modifiers that impart antibacterial properties to inherently non-antimicrobial surfaces such as glasses, metals, polymers, wood, and paper. The binding force can be either physical attachment or chemical bonding. Blending antibacterial agents into a polymer coating is one straightforward method. In a recent publication, Khor [64] used Ag/hydroxyapatite (HA) powder and polyetheretherketone (PEEK) to give glass surfaces antimicrobial properties. Ag/HA powder was synthesized by adding H_3PO_4 and AgNO_3 solution into a $\text{Ca}(\text{OH})_2$ solution, then ammonia solution was used to adjust the pH to 8. Stirred overnight, the Ag/HA powder was separated, washed, dried and mixed with PEEK powder. Later, the powder mixture was sprayed by compressed air at 150°C onto a glass substrate, which exhibited clear ZOI on *Escherichia coli*-inoculated agar plates after coating.

Layer-by-Layer (LbL) self-assembly is another versatile method to prepare functional coatings and films [65, 66]. Basically, electrostatic forces are involved

in the fabrication of LbL films. The glass substrate (negatively charged) is first dipped into a cationic polyelectrolyte solution and dried to form the first layer, then dipped into an anionic polyelectrolyte solution and dried to form the second layer. The two steps are repeated alternately to obtain a multi-layer structure to achieve the desired thickness. Usually, these LbL films are used as drug delivery systems, as water-soluble drugs can be loaded in their positive/negative bilayers and be released when an external stimulus is applied. The commercialization and large-scale preparation are easy due to the simplicity of this technique. For specific antibacterial applications, LbL films can be fabricated into films with multiple antimicrobial actions. First, silver ions or antibiotics (cetrimonium bromide, for example) can be loaded into the LbL films. Second, the positive charged layer can be an antibacterial cationic polymer (see Sect. 1.5.3.2) to offer extra antimicrobial activity. Grunlan [67] made LbL films of polyethylenimine (PEI) and polyacrylic acid (PAA), and loaded silver ions in the PEI polymer layer on polyethylene terephthalate (PET) substrate (Fig. 1.10). After coating, the sample remained transparent. The antibacterial activity of the PET-coated disks was evaluated by the ZOI test for *Staphylococcus aureus* or *Escherichia coli* (Fig. 1.11). The LbL-treated PET disks with different numbers of layers showed different ZOI radii compared to no ZOI for untreated PET.

Theoretically, the LbL technique can be used on any surface. However, in practice, problems often arise when the target substrate is a highly hydrophobic polymer such as polytetrafluoroethylene (PTFE), polyethylene (PE), and polypropylene (PP). Traditionally, a harsh and complicated “priming” such as plasma or oxidation is required prior to applying LbL. The priming process introduces reactive, hydrophilic hydroxyl groups on these polymeric surfaces. A recent paper proposed a novel strategy to address this issue. Messersmith [68] used PEI and hyaluronic acid (HA) (Fig. 1.12) molecules modified with dopamine moieties to mimic the protein structure of natural mussel adhesive. After the modification, the researcher was able to coat LbL film onto a PTFE substrate, which is considered to be the most challenging surface due to its extremely anti-adhesive nature. After three cycles of coating, fluorine composition on the PTFE surface sharply decreased from 69% to 1.6% and the contact angle of water dropped remarkably from 106° to 19.7°, both of which proved that LbL assembly was successful on the PTFE substrate. To grant this LbL coating of PTFE with antibacterial properties, silver nanoparticles were formed in situ inside the LbL coating from reduction of AgNO₃. Although only moderate biocidal efficiency was observed (approx. 18% of the total bacteria was killed after 4 h of incubation) from an antibacterial test on *Escherichia coli*, this work proposed a useful solution for antibacterial coating on surfaces like PTFE.

By combining the bacterial killing power of silver nanoparticles and the quaternary ammonium functionality, a dual-functional antibacterial coating was reported by Rubner [69]. The polystyrene substrate was first coated with ten bilayers of poly (allylamine hydrochloride) (PAH) and PAA. An additional ten bilayers of PAH and SiO₂ nanoparticles (~20 nm in diameter) were then deposited onto it. Later, ammonium groups were covalently bonded to the silica nanoparticles by reaction

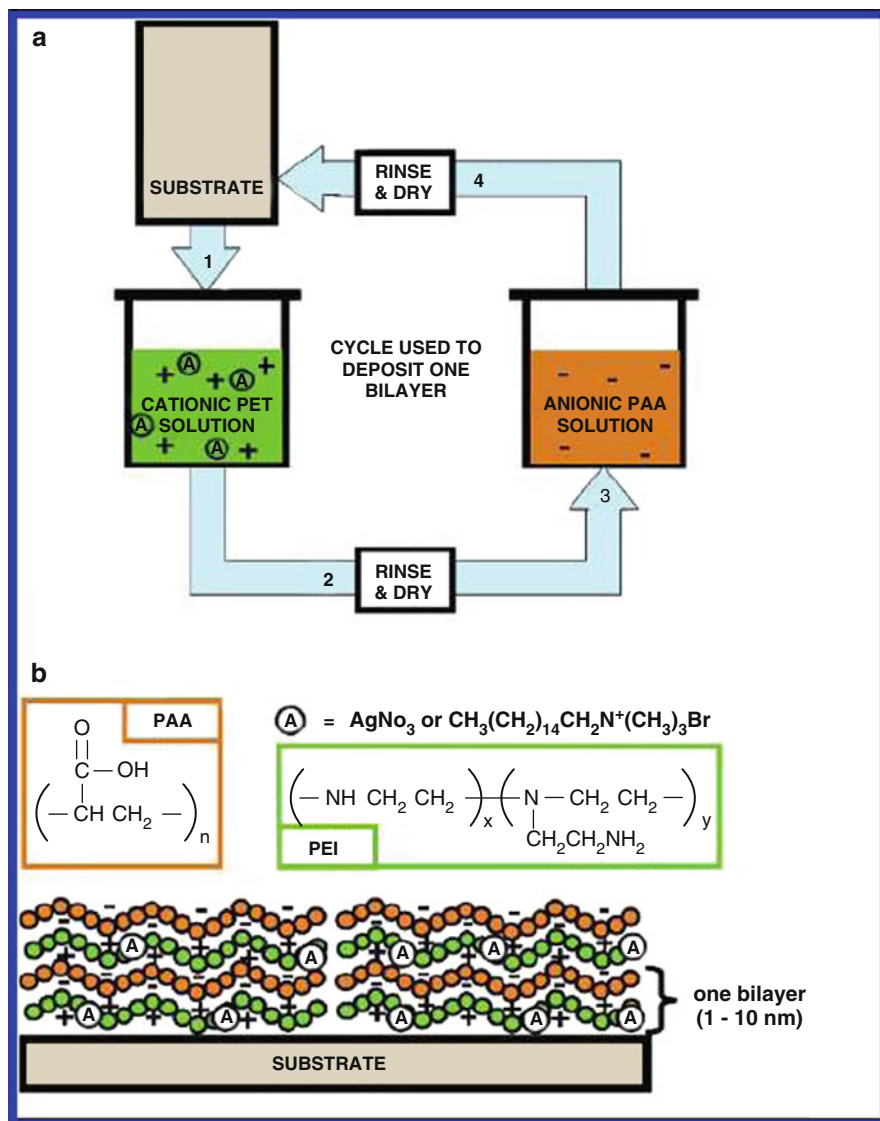


Fig. 1.10 Scheme of LbL self-assembly coating (Reprinted from [67]. With permission from American Chemistry Society)

with Si-OH groups. Finally, the coated substrate was dipped in silver acetate solution and the silver ions were subsequently reduced. The coating now had quaternary ammonium groups on the top surface to kill any bacteria on contact and silver nanoparticles beneath the protective silica particles layer to leach out biocidal silver ions (Fig. 1.13).

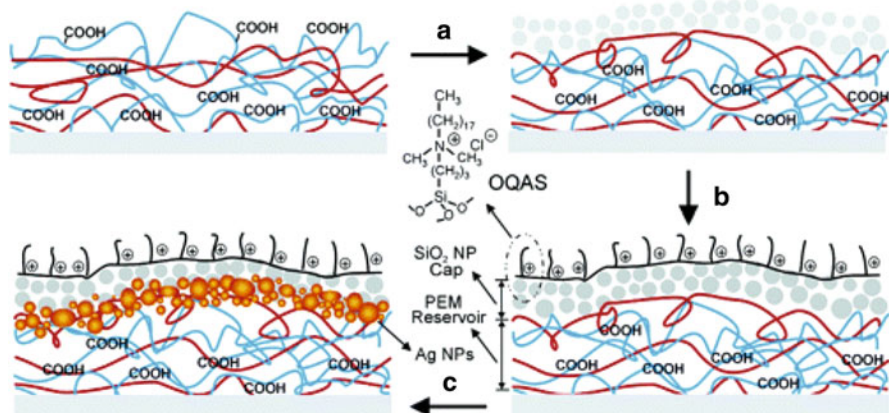


Fig. 1.13 Scheme showing the design of a two-level dual-functional antibacterial coating with both quaternary ammonium salts and silver. The coating process begins with LbL deposition of a reservoir made of bilayers of PAH and PAA. (a) A cap region made of bilayers of PAH and SiO₂ nanoparticles added to the top. (b) The SiO₂ nanoparticle cap modified with a quaternary ammonium silane, OQAS. (c) Ag⁺ loaded inside the coating using the available unreacted carboxylic acid groups in the LbL multilayers (Reprinted from [69]. With permission from American Chemistry Society)

PAMPS [poly(2-acrylamido-2-methyl-1-propanesulfonic acid)] and PHMA [poly(2-hydroxy-4-N-methacrylamidobenzoic acid)]-doped polypyrrole film. The films themselves are not antibacterial but silver ions can be anchored onto either PAMPS or PHMA by chelating to the polymer chains, giving these films antibacterial activity. Both *Escherichia coli* and *Staphylococcus aureus* were used to evaluate antibacterial activity of coated stainless steel and carbon fibers. Viable bacteria were significantly reduced when incubated with these samples. The advantages of this technique are: (1) simplicity in controlling the film thickness by altering the current, voltage and time, and (2) generation of robust film with high resistance to peeling force [71].

One interesting type of a polymer coating bearing silver nanoparticles was reported by John [72]. The monomer described in this publication was derived from unsaturated natural fatty acids. The unsaturated fatty acids readily undergo self-cross-linking reaction of the double bonds caused by external oxidants like oxygen (drying oil effect). The author utilized silver ions to oxidize the double bonds to form a cross-linked polymer film. This type of polymer film can kill bacteria on contact.

The design of an antibacterial coating with a stronger binding force is always desirable and can be achieved by chemical bonding between the coating material and the substrate. The Sen group has done extensive research on antibacterial materials. One of their papers proposed an antibacterial modification of various substrates by well-established silane chemistry [73]. This technique involved the irreversible reaction methoxysilane groups with free hydroxyl groups or alkoxy silane groups

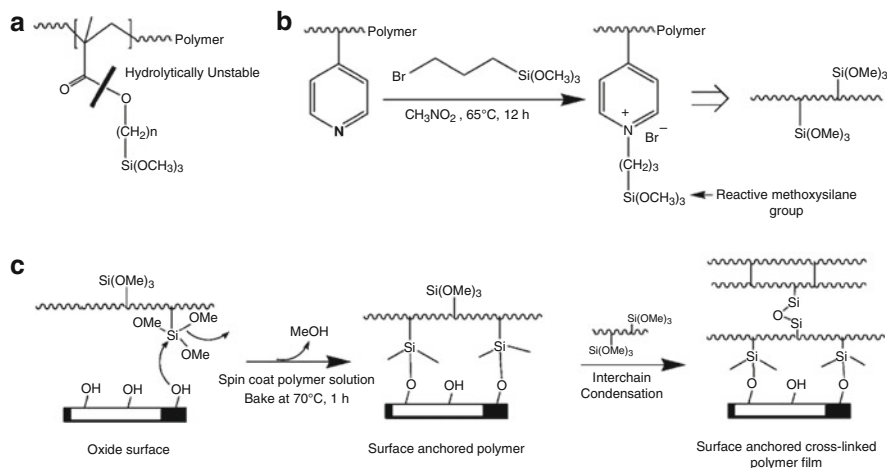


Fig. 1.14 Synthetic route to polymer coating and chemical reaction of polymer coating with OH groups on the substrates (Reprinted from [73]. With permission from American Chemistry Society)

to form strong Si-O-Si bonds. The polymer used in this method was poly (4-vinylpyridine). Most of the nitrogen atoms were quaternized by alkyl bromide to render the polymer antimicrobial, while some of the tertiary nitrogen atoms were quaternized by 1-bromopropylytrimethoxy silane to provide reactive anchor groups (Fig. 1.14). The polymer was then spin-coated onto solid surfaces or dip-coated onto fabrics. The antibacterial activity was further enhanced by adding $AgNO_3$ in polymer solution to form precipitated $AgBr$ nanoparticles that were incorporated into polymer films. This method provides a practical and facile surface modification option for virtually all substrates due to the universal presence of OH groups on glass, metals, ceramics, etc.

1.4.2 Hydrogels

Polymeric hydrogels are cross-linked three-dimensional polymer networks synthesized from hydrophilic monomers [74]. Generally, monomers used in hydrogel synthesis are: acrylic acid, acrylamide, N-isopropyl acrylamide, 2-hydroxyethyl methacrylate (HEMA), methacrylic acid, dimethylethylamino acrylate, etc. Hydrogels are ideal wound-dressing materials for multiple reasons. First, the water in the hydrogel keeps the wound hydrated and prevents the formation of a scar that is undesirable for cosmetic reasons. Second, the low abrasion property of hydrogels keeps the patient comfortable. Finally, the nutrients in the hydrogel can promote the healing process. Commercial products such as HDR[®] and AQUA-GEL[®] have been available on the market for years. Due to the high susceptibility of

wounds to infection, antibacterial modification of hydrogels is not only academically important but also practically urgent. The general strategies involved are releasing antimicrobial agents such as antibiotics or silver ions, using an inherently antibacterial polymer network, or a combination of the two.

Raju [75] used a semi-IPN hydrogel to obtain an antibacterial material. Acrylamide monomer, a cross-linker, ammonia persulfate (free radical polymerization initiator) and polyvinyl acetate (PVA) were mixed in water and the polymerization was carried out at 35°C for 8 h. Ionic silver solution was absorbed by dry gels, and silver ions were further reduced by NaBH₄ yielding hydrogel–silver nanoparticle composites. The resulting solution of the composite was dropped onto bacteria-inoculated agar plates. Pure hydrogel showed no antibacterial activity whereas hydrogel–silver composites showed significant ZOI. Interestingly, the hydrogel–silver nanoparticle composite has a higher antibacterial activity against *Escherichia coli* than the hydrogel–silver ion composite which is obtained without reduction.

Another hydrogel–silver composite for wound-dressing application was reported by Aggor [76]. The acrylamide-based hydrogel used N,N'-methylenebisacrylamide as cross-linker. Silver ions were directly incorporated into the hydrogel by mixing with AgNO₃ reaction mixture and then reduced to silver particles after the hydrogel was formed. Although no antibacterial test was done in this paper, antibacterial properties can be expected from this material.

1.4.3 Fabrics and Textiles

The development of antibacterial fabrics and textiles is receiving more and more attention for obvious reasons. First, antibacterial clothing minimizes cross-contaminations and risks for doctors, nurses, and patients. Second, antibacterial combat garments can increase soldiers' survivability in biological warfare. Other types of clothing, such as athletic garments, can be made to possess antibacterial activity. The most straightforward way to impart antibacterial activity to fabrics is by physical deposition of biocidal silver [77–80]. Baglioni [81] reported a simple way to modify some common fabrics like cotton, wool, and polyester. Silver nanosol was synthesized by reduction of Ag⁺/PAA solution by either NaBH₄ or UV irradiation. Wool, cotton, and polyester textiles were soaked in the solution, then squeezed, rinsed, and dried at elevated temperatures. ZOI test was used to evaluate the antibacterial activity (Fig. 1.15). Obvious ZOI were found for treated cotton sheets on different bacteria-inoculated agar plates.

Previously, the LbL method was used to obtain antibacterial coatings (see Sect. 1.4.1). It turns out to be useful in fabric and textile modifications as well [82]. To start with, silver nanoparticles are reduced by UV treatment with polymethacrylic acid (PMA) as a capping agent. Then, poly(diallyldimethylammonium chloride) (PDADMAC) and Ag/PMA are used as positively and negatively charged polymers for LbL self-assembly. By alternately dipping nylon or silk fibers into the two polymer solutions, antibacterial fibers with 10 or 20 layers

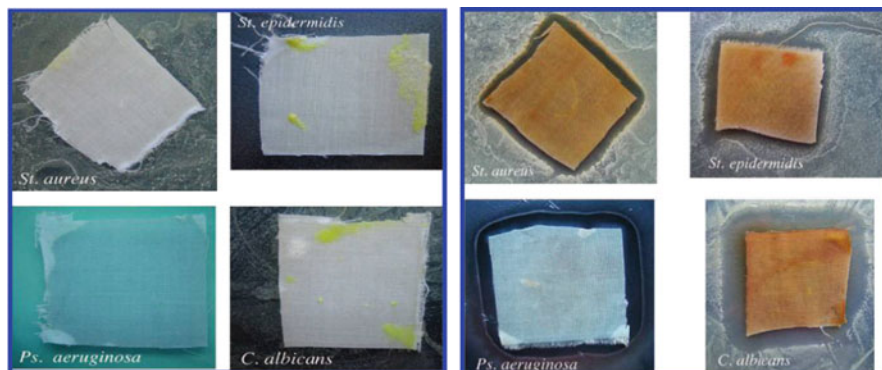


Fig. 1.15 Untreated cotton samples show intense bacterial growth (*left*) and treated cotton samples show ZOI against multiple bacteria (*right*) (Reprinted from [81]. With permission from American Chemistry Society)

of polymer were obtained. Antibacterial efficiencies of both fibers were compared by using *Staphylococcus aureus*. Generally, with the same number of polymer layers, silk showed a better antibacterial activity than nylon, attributed to a higher surface charge of the silk fibers, which facilitates the LbL process.

One challenge in antibacterial fabric and textile fabrication is to maintain antibacterial activity after multiple washing cycles. Silver ions are water soluble and may get depleted after laundry; mechanical abrasion and the usage of detergents during cleaning are also detrimental to the integrity of these materials. Previous reports utilized capillary forces to incorporate silver ions, which are weak in nature and may suffer significant loss of silver species after washing. To cope with this issue, stronger binding of silver onto fabrics was proposed and tested [83]. TiO_2 , silver nanoparticles and water-based polyurethane were mixed together and then allowed to soak into polyester fibers. When 90% uptake was achieved, the treated fiber was dried, baked and cleaned with soap. During a water-borne bacteria test, an interesting synergetic effect of TiO_2 and silver nanoparticles was discovered. Samples pretreated with UV irradiation before antibacterial test showed enhanced antibacterial activity because of the activation of TiO_2 particles by UV light. Samples without UV pretreatment showed only 70% biocidal efficiency comparing with the 84–100% for UV-pretreated samples. The researchers ran antibacterial tests after multiple wash cycles. The results looked promising as polyester samples were able to maintain up to approx. 86% biocidal efficiency against *Escherichia coli* and *Staphylococcus aureus* after 3,000 wash cycles.

A similar strategy was also proposed in another publication [84]. First, SiO_2/Ag nanoparticles were made by absorbing silver ions from solution onto SiO_2 nanoparticles. The SiO_2/Ag particles, PET, and coupling agents were mixed, heated, and extruded to get PET bulk material. Finally, bulk PET was subject to melt-spinning to form its corresponding fiber. The resultant PET fiber showed high antibacterial activity against *Escherichia coli* and *Staphylococcus aureus*. Also, the

PET sample with 5% antibacterial agent load can retain 80% efficiency after 30 wash cycles.

1.4.4 Bulk Materials

Bulk polymeric materials blended with silver can be considered as the counterpart of inorganic silver composite in glasses. For example, Nia [85] blended Ag/TiO₂ composite powder with polypropylene (PP) powder and melt-molded it into an antibacterial plastic. Plastic sheets were tested against *Staphylococcus* and over 99% kill was observed compared with pure PP sheets. Another recent example is using the sol-gel technique to synthesize PBAT polymer with SiO₂/Ag [86]. In addition, silver-doped polyurethane catheters are used as improved medical devices to inhibit bacterial infection [87].

One important application of bulk polymeric silver composites is in dental care materials. It was found that more bacteria or plaques tend to accumulate on conventional restorative resin [88]. Efforts have been made to address this problem by loading chlorhexidine into resin material [89]. However, the antibacterial activity is lost once the drug is depleted and loading of the drug compromises material integrity. Silver-containing dental materials with non-leaching properties were developed to overcome this problem. Preparation of antibacterial resin with silver nanoparticles was described in a recent paper [90]. Silver nanoparticles were synthesized as described in Sect. 1.3.5. Then, these nanoparticles were doped into liquid acrylate monomer and the mixture was cured into the desired shape resin. The material killed 100% *Escherichia coli* bacteria in solution. Similar work was reported by Asuta [91] using commercial silver-incorporated Novaron[®] and Amenitop[®]. Acrylate derivatives were used in this system and SiO₂ was added to form a paste, which was later cured under UV light to give a resin disk. In the MIC test, the silver-loaded resin showed no biocidal effect. However, in the ZOI test, the same sample killed *Streptococcus mutans* on contact. The reason for these conflicting results is that there are no silver ions leached into the liquid media, but the resin can kill bacteria on contact by catalytic generation of ROS with silver. The author also tested the silver ion concentration in water after 6 months exposure to water and no silver ions were detected.

1.5 Challenges and Future Prospects

1.5.1 Bacterial Resistance to Silver

Since silver-based antimicrobial materials are now widely used, it is almost inevitable that bacteria will develop a certain resistance to silver. The first report addressing this issue dates back to 1975 [92]. Research showed that the resistance

can be intrinsic. Intrinsic silver resistance of bacteria is defined as the phenotype demonstrated by micro-organisms before the use of an antimicrobial agent. Intrinsic silver-resistant bacteria are usually found in the areas where there is frequent silver exposure such as burn care wards in hospitals, hospital water distribution systems, and soils near silver mines. This resistance can also be acquired by genetic mutation or caused by the acquisition of silver-resistant plasmid or transposon [93].

1.5.1.1 Mechanism of Silver Resistance

Bacterial resistance to silver and other heavy metal ions is generally from genes encoded in either plasmids [94, 95] or chromosomes [96, 97]. Thus far, the silver resistance determinant studied in most detail is plasmid pMG101, which confers bacteria resistances to Ag^+ and Hg^{2+} , as well as to several antibiotics [92]. When this plasmid was transferred by conjugation with *Escherichia coli*, the mutant *Escherichia coli* was able to survive in 0.6 mM silver ions in broth media, a 600% greater tolerance compared to silver-susceptible *Escherichia coli*. Sequencing pMG101 revealed that it contains nine genes, and the functions of eight named genes and their protein products are considered responsible for silver resistance due to the fact that they are the homologues of proteins known for other metal resistance. The first protein product of pMG101 gene is SilCBA, one member of the potential-driven cation/proton efflux pump. It contains three polypeptides. SilA, SilB, and SilC [98]. SilA is a large inner membrane cation pump, SilC is the outer membrane protein, and SilB is the protein which connects SilA and SilC (Fig. 1.16). SilA and SilB together work as an antiporter that carries silver ions out of the cell

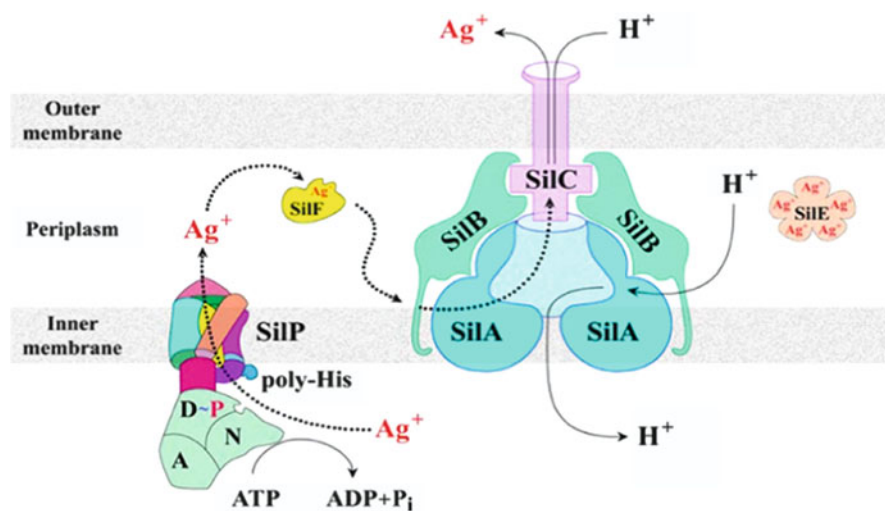


Fig. 1.16 Plasmid silver resistance mechanism (Reprinted from [100]. With permission from Springer)

while SilC is an ATPase that transports silver ions from the cytoplasm to the periplasm. Besides the SilCBA cation/proton pump, another set of pumps also exists: SilP and SilF, both of which are also the protein products of pMG101 gene. SilP is a P-type ATPase, which is a member of large family of cation pumps [96, 97]. SilF is a chaperone protein which picks up silver ions released from SilP and drops off to SilCBA. SilP, SilF, and SilCBA, when working together, complete a full cycle of silver ion efflux and protect bacteria from the deleterious effect of silver. In addition, SilE, another protein product, can also help to increase silver resistance by binding to five silver ions and preventing the silver ions entrance to cytoplasm (Fig. 1.16) [99, 100].

1.5.2 Material Fouling and Biofilm Formation

Fouling is defined as accumulation of undesired materials on a solid surface, mostly in aquatic environments. The most common fouling situation is the adhesion of marine species to ship hulls, which enhances drag, and lowers fuel economy. Similar to fouling on ship hulls, biomaterial surface is subject to protein absorption, which is considered to be the initial step of biofouling. In addition, many proteins such as fibronectin [101–105], fibrinogen [101, 106–108], vitronectin [109, 110], thrombospondin [111], and Von Willebrand factor [112] can enable the specific binding of *Staphylococcus aureus* to biomaterial surfaces. It has been reported that this type of fouling can result in many serious consequences such as heart valve failure [113].

To avoid biofilm formation is another challenge for antimicrobial materials. Defined as microorganism built-up adhering to either biological or non-biological surfaces [114], biofilm is an intrinsic defense mechanism of bacteria against antibiotics and human immune systems. NIH estimates that 75% of bacterial infection is biofilm based [115]. Bacteria within biofilms are 1,000 times or more resistant to antibiotics and inherently inert to host immune response [115]. In addition, exchanges of genes responsible for drug resistance across biofilms have resulted in many bacteria possessing multidrug resistance [116, 117].

1.5.3 Possible Solutions

To cope with ever increasing bacteria resistance to antibiotics, new antimicrobial strategies and new types of antibiotics that do not induce bacterial resistance must be developed. New synthetic materials that can avoid fouling or prevent biofilm formation will also significantly increase the antimicrobial effectiveness of silver and other antibiotics.

1.5.3.1 Cationic Antibacterial Peptides

Naturally occurring antimicrobial peptides focus on the fundamental structural difference between microorganisms and normal cells: the cell membrane. Bacterial membranes are usually constructed in such a way that the outermost layer is extensively occupied by negatively charged lipid head groups. In contrast, the outer layers of cell membranes of plants or animals are usually neutral with most negatively charged lipids pointed into the cytoplasm [118]. Despite the diversity of antimicrobial peptides present in nature, most function in a similar fashion. Peptides can adopt configurations in which the hydrophobic chains and cationic amino acids spatially organize into separate domains [119]. The Shai–Matsuzaki–Huang (SMH) model explains how antimicrobial peptides interact with microorganisms using their hydrophobic chains and cationic amino acids [118, 120, 121]. This model (Fig. 1.17) suggests that these peptides kill the microorganisms through the following steps. First, peptides are absorbed onto bacteria surfaces due to electrostatic forces. Second, lipid membranes are disrupted and membrane structures are altered. Sometimes, this process involves the entrance of peptides into the bacterial interior. Finally, bacteria are killed due to the leakage of internal contents. This model is indirectly supported by the following experimental observations: (1) cholesterol can lower peptide antibacterial activity by

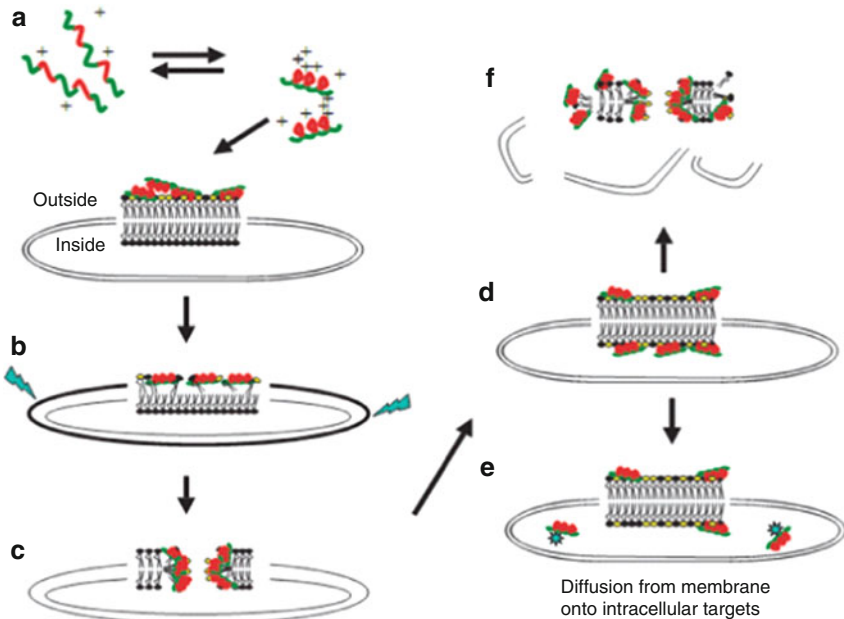


Fig. 1.17 The SMH model. (a) Peptides absorption on cell membranes. (b) “Thinning” process of cell membranes. (c) Disassociation of cell membrane creating “worm-hole.” (d) Transportation to inner lipid layer. (e) Diffusion into cytoplasm. (f) Fragmentation of cell membranes (Reprinted from [119]. With permission from Nature)

providing extra stabilization of membranes, and (2) increased ionic strength in solution weakens the antibacterial activity of peptides by shielding the electrostatic forces between cationic peptides and negatively charged membranes.

The detailed mechanism on how peptides kill these microorganisms is not clear. Suggested mechanisms include: disintegration of cell membranes which causes leakage of internal contents [120], disturbance of cell membranes by altering the distribution of lipids between leaflets of bilayers [118], damage to vital intracellular targets after insertion of peptides [122], and degradation of the cell wall by introduction of hydrolases [123].

The major motivation for the study of antimicrobial peptides is that their biocidal activity can even be extended to fungi and viruses. In addition, although these peptides are not as efficient as traditional antibiotics toward susceptible microbes, the peptides are able to kill drug-resistant pathogens at similar concentrations with much faster rates. Unlike antibiotics, acquisition of resistance by bacterial strains is also less likely to happen due to their unique antibacterial mechanism. Since the target site of antibacterial peptides is the cell membrane, to develop resistance towards peptides requires changes of membrane structure and alteration of composition and/or reorganization of lipids, which is very difficult for most microorganisms [119].

1.5.3.2 Synthetic Polymer Mimics of Natural Antimicrobial Peptides

Despite the attractive antibacterial properties of naturally occurring peptides, their extensive use is precluded by the high cost (\$50–400/g) compared to conventional antibiotics (approx. \$1/g) [124]. In addition, their susceptibility towards enzymatic degradation is a concern. Therefore, the design of synthetic polymer mimics is of great interest.

Polymers with quaternary ammonium and phosphonium groups are structurally designed to mimic the antibacterial peptides with positively charged blocks and hydrophobic alkyl chains, and have the advantage of low cost, ease of synthesis, and resistance to enzymatic degradation (Fig. 1.18). Generally, cationic quaternary polymers share the same antimicrobial mechanism with their peptide counterparts. First, electrostatic attraction between the cationic groups and negatively charged bacterial membrane brings them together. Second, the long hydrophobic alkyl chains are able to penetrate into the bacterial membrane through hydrophobic interactions. Finally, the polymer induces membrane disruption and leakage of cell contents.

In a recent publication [125], biodegradable quaternary ammonium polymers were synthesized as possible next generation drug to replace conventional antibiotics. An *in vitro* test showed that these polymers are able to kill

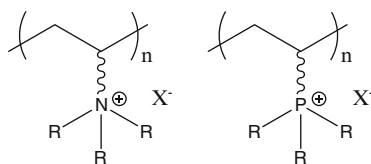


Fig. 1.18 General chemical structures of quaternary ammonium and phosphonium polymers

methicillin-resistant *Staphylococcus aureus*. Short-term in vivo toxicity studies on animal kidney and liver showed no functional abnormality of these vital organs.

Another desirable aspect of quaternary ammonium or phosphonium polymers is that silver halide particles can be introduced inside the polymer matrix if halide counter ions are used during the polymer synthesis. By combining the antimicrobial properties of both the quaternary-functionalized polymers and silver halides, the synthesized “dual action” antibacterial materials further increase the antibacterial performance. In a recent publication [126], Sen partially quaternized poly(4-vinylpyridine) with n-hexyl bromide. Then, soluble silver salts were added into the polymer solution to prepare a polymer–silver bromide composite. Finally, this polymer–silver bromide composite was coated onto glass slides by film casting. This film was subjected to multiple antimicrobial tests. ZOI tests showed bacteria-free areas around the coated slide. The size of ZOI was found to be dependent on the size of silver bromide particles: samples with small silver halide particles yielding larger ZOI and vice versa. MIC tests on both the polymer and polymer–silver bromide composite were also carried out, in which the composites showed much lower MIC values compared to pure polymer coating simply because of the additional antibacterial silver ions in the composite. Finally, the anti-biofilm property was tested using *Pseudomonas aeruginosa*. The pure polymer surface was susceptible to biofilm formation and prone to lose its antibacterial ability, whereas the polymer–silver bromide composite maintained the antimicrobial activity for a prolonged time period.

1.5.3.3 Anti-fouling or Anti-biofilm Modifications

Understanding how biofouling happens is especially important. It is now generally believed that hydration force is the key to surface fouling. In the past, the modeling for interaction of surfaces and foulants only considered electrostatic and electrodynamic (van der Waals) forces. Unfortunately, this model is not applicable for strong interactions within the 3-nm range [127, 128]. Within this range, the hydration force predominates [129] because the interactions between water-soluble moieties are best seen in terms of their interaction with water itself. When largely surrounded by water molecules, they repel each other, and the strength of this force was found to be independent of the charge. Thus, it is essential to create a hydration force barrier at short distances to prevent fouling. Two types of polymeric materials have been developed to address the fouling of biomaterials. The materials exhibit ultra-low fouling properties.

PEG and OEG

The ability of polyethylene glycol (PEG) and oligo ethylene glycol (OEG) to prevent protein absorption has been reported [130]. The hydration force barrier of

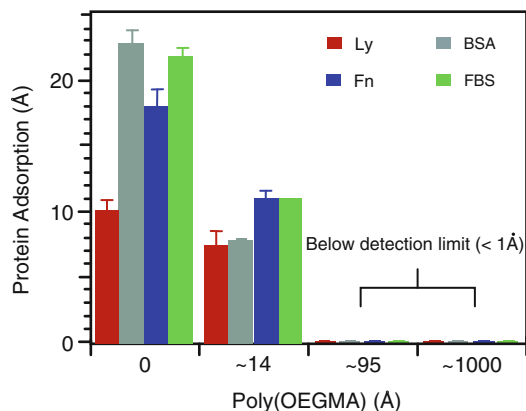


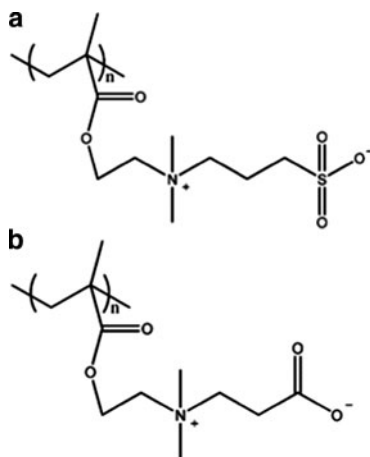
Fig. 1.19 Protein adsorption comparison of the poly(OEGMA) coating on SiO_2 and SiO_2 with only ATRP initiator but no polymer coating (control) measured by ellipsometry. The x-axis is the thickness of poly (OEGMA) coating (14, 95 or 1,000 Å; Control is labeled as a film with 0 Å thickness), and the y-axis is the thickness of the adsorbed protein. *Ly* lysozyme, *Fn* fibronectin, *BSA* bovine serum albumin, *FBS* fetal bovine serum (Reprinted from [135]. With permission from American Chemistry Society)

highly water-soluble PEG chains is believed to be responsible for the resistance to protein fouling because a large entropy penalty must be paid to force the PEG chains to collapse for proteins to adhere to the coated surface [131, 132]. Both self-assembly membranes and surface-initiated ATRP coating techniques have been employed to treat glass for anti-fouling applications [133, 134]. Protein absorption is substantially reduced by a PEG coating comparing to untreated glass [135] (Fig. 1.19).

Zwitterionic Polymers

One obvious disadvantage of PEG-type anti-fouling materials is that PEG chains are subject to oxidation by oxygen or transition metal ions, which are commonly present in the physiological environment. This prevents long-term application of PEG-type materials [136–138]. While PEG uses hydration force to avoid protein fouling, zwitterionic polymers such as phosphobetaine, sulfobetaine, and carboxybetaine can interact with water molecules even more strongly through electrostatically induced hydration [139, 140]. The first generation of anti-fouling zwitterionic polymers are phosphobetaine-based polymers. They are considered as biomimetic fouling-resistant materials, since they contain phosphorylcholine head-groups, which are abundantly present in the outside layer of cell membranes [141, 142]. However, the complicated synthesis process limits its application. Hence, polymers with similar structures, such as

Fig. 1.20 Zwitterionic polymer structure:
(a) polysulfobetaine,
(b) polycarboxybetaine



polysulfobetaine (PSB) and polycarboxybetaine (PCB) (Fig. 1.20), are used instead and have been experimentally proved to avoid non-specific protein absorption [143].

Jiang [144] compared the anti-fouling properties of PEG, PSB, and PCB polymers formed by both self-assembly and surface-initiated ATRP techniques to coat Au-coated glass slides. Ultra-low protein absorption on PSB and PCB polymer coatings was observed (Fig. 1.21) by SPR (Surface Plasmon Resonance). Jiang [145] also explored the optimum film thickness to achieve almost “zero-adhesion” (Fig. 1.22).

Anti-biofilm Materials

The concepts “anti-fouling” and “anti-biofilm” have different definitions and sometimes cause confusion. The term “anti-fouling” usually means resistance to adhesion of proteins and normal cells. However, “anti-biofilm” means the inhibition of adhesion of bacteria and the formation of biofilms. It is generally assumed that a surface that avoids protein adhesion can prevent biofilm formation. However, this correlation is not always true [137].

The PEG, PSB, and PCB polymers are able to avoid biofilm formation in addition to their ability to prevent protein fouling. Coatings created by both ATRP and SAM of PEG and PSB polymers on Au surface were subject to anti-biofilm tests [142]. Short-term adhesion (3 h) of Gram-positive *Staphylococcus epidermidis* and Gram-negative *Pseudomonas aeruginosa* were reduced compared with untreated glass surfaces. When long-term anti-biofilm experiments (18–24 h) were carried out, SAM coatings were less effective in inhibiting biofilm formation,

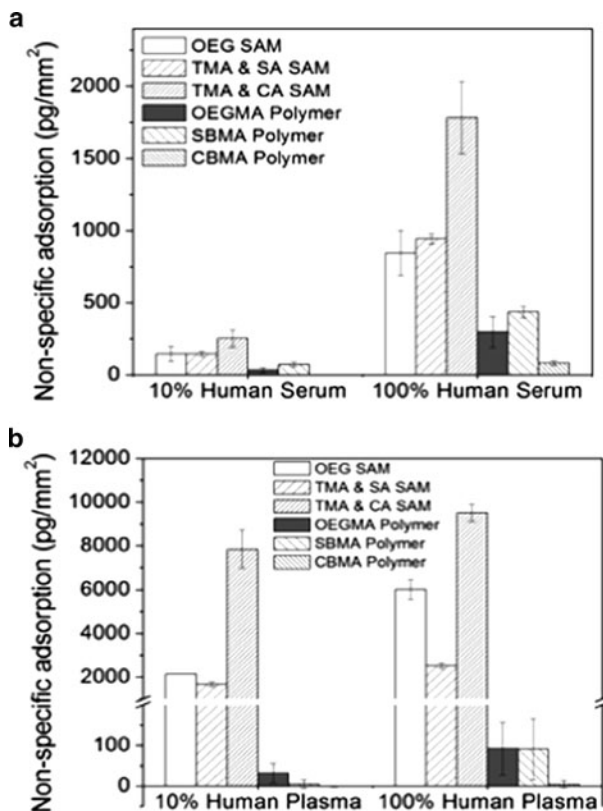


Fig. 1.21 Non-specific adsorption comparison for (a) 10% human serum in PBS and 100% human serum and (b) 10% human plasma in PBS and 100% human plasma. A full monolayer of protein on the surface is equivalent to 2,700 pg/mm² standard error of the mean. Surfaces used in these experiments are self-assembled monolayers of oligo(ethylene glycol) (OEG SAM), mixed trimethylamine and sulfonic acid (TMA&SA SAM), mixed trimethylamine and carboxylic acid (TMA&CA SMA), and ATRP-created poly(OEGMA) (OEGMA polymer), sulfobetaine methacrylate (SBMA polymer), and carboxybetaine methacrylate (CBMA polymer) (Reprinted from [144]. With permission from American Chemistry Society)

probably because of their long-term instability. The anti-biofilm capability of PCB polymer in prolonged period was studied [146], and the biofilm formation by *Pseudomonas aeruginosa* was considerably hindered by a PCB polymer coating with a thickness of 30 nm. At 25°C, an untreated glass surface was completely covered by biofilm within 48 h whereas a PCB surface exhibited less than 5% accumulation in 10 days. At 37°C, the optimum growth temperature of *Pseudomonas aeruginosa*, the glass surface showed 100% biofilm coverage in 15 h. In comparison, less than 7% biofilm buildup was observed for the PCB-treated glass surface (Fig. 1.23).

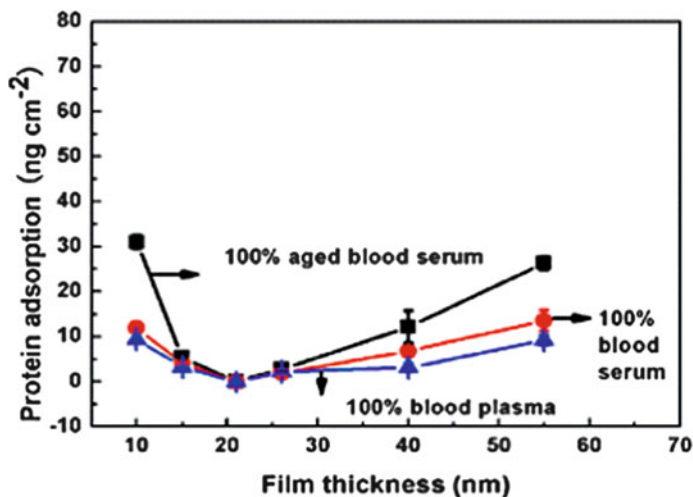


Fig. 1.22 Adsorption of undiluted blood serum, undiluted aging blood serum, and undiluted blood plasma versus film thickness of PCBAA grafted surfaces at 37°C as measured by SPR (Reprinted from [145]. With permission from American Chemistry Society)

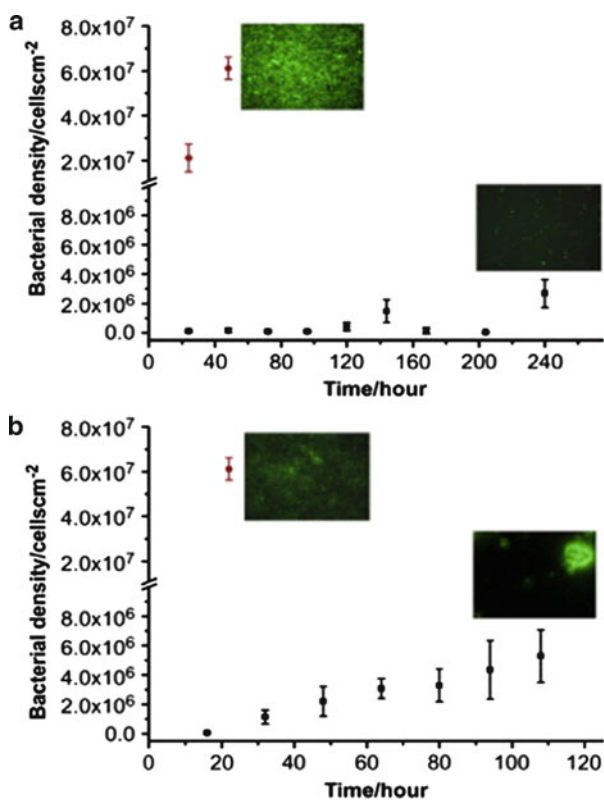


Fig. 1.23 *Pseudomonas aeruginosa* accumulation on PCB surface (■) and glass (●) surfaces as a function of time (a) tested with Method I at 25°C, (b) tested with Method II at 25°C, (c) tested with Method I at 37°C, and (d) tested with Method II at 37°C reported as the mean \pm SD ($n = 20$) (Reprinted from [146]. With permission from Elsevier)

1.5.4 Perspectives on Silver Antibacterial Materials

Currently, highly effective silver-containing antimicrobial materials are used in various ways, many of which are already commercialized. However, the warfare between humans and pathogenic microorganisms does not end. New threats to our health emerge, such as drug-resistant or silver-resistant pathogens and fouling of biomedical devices. To address these challenges, new approaches and novel materials are needed. The strategies may include (1) the search for novel anti-fouling or anti-biofilm modifications, (2) combining different antimicrobial agents, (3) better recognition and utilization of the antibacterial mechanisms of silver, and (4) the employment of new modification techniques to hitherto non-antibacterial materials. By combining modern material sciences and technologies, silver, this ancient antimicrobial agent, will broaden its current applications.

References

1. Russell AD, Hugo WB (1994) Antimicrobial Activity and Action of Silver. *Prog Med Chem* 31: 351-370. doi:[10.1016/S0079-6468\(08\)70024-9](https://doi.org/10.1016/S0079-6468(08)70024-9)
2. Hill JW (2009) Colloidal silver medical uses, toxicology & manufacture, 3rd ed. Clear Springs Press, Rainier, WA (USA) ISBN: 1884979084
3. Ravelin J (1869) Chemistry of vegetation. *Sic Nat* 11:93-102.
4. Von Naegelli V (1893) *Deut schr Schweiz Naturforsch Ges* 33:174-182.
5. Atiyeh BS, Costagliola M, Hayek SN, Dibo SA (2007) Effect of silver on burn wound infection control and healing: Review of the literature. *Burn* 33:139-148. doi: [10.1016/j.burns.2006.06.010](https://doi.org/10.1016/j.burns.2006.06.010)
6. Chappel JB, Greville GD (1954) Effect of silver ions on mitochondrial adenosine triphosphatase. *Nature* 174:930-931. doi: [10.1038/174930b0](https://doi.org/10.1038/174930b0)
7. Cecil R, McPhee JR (1959) The sulfur chemistry of proteins. *Adv Protein Chem* 14:255-389. doi: [10.1016/S0065-3233\(08\)60613-0](https://doi.org/10.1016/S0065-3233(08)60613-0)
8. Rogers KS (1972) Variable sulfhydryl activity toward silver nitrate by reduced glutathione and alcohol, glutamate and lactate dehydrogenases. *Biochim Biophys Acta* 263:309-314. doi: [10.1016/0005-2795\(72\)90084-0](https://doi.org/10.1016/0005-2795(72)90084-0)
9. Foster TJ (1983) Plasmid-determined resistance to antimicrobial drugs and toxic metal ions in bacteria. *Microbiol Mol Biol Rev* 47:361-409.
10. Rayman ML, Lo TCY, Sanwal BD (1972) Transport of succinate in *Escherichia coli*: II. Characteristics of uptake and energy coupling with transport in membrane preparations. *J Biol Chem* 247:6332-6339.
11. Shaw WHR (1954) The inhibition of urease by various metal ions. *J Am Chem Soc* 76:2160-2163. doi: [10.1021/ja01637a034](https://doi.org/10.1021/ja01637a034)
12. Holt KB, Bard AJ (2005) Interaction of silver(I) ions with the respiratory chain of *Escherichia coli*: An electrochemical and scanning electrochemical microscopy study of the antimicrobial mechanism of micromolar Ag⁺. *Biochemistry* 44:13214-13223. doi: [10.1021/bi0508542](https://doi.org/10.1021/bi0508542)
13. Rosenberg H, Cox GB, Butlin JD, Gutowski SJ (1975) Metabolite transport in mutants of *Escherichia coli* K12 Defective in electron transport and coupled phosphorylation. *Biochem J* 146:417-423.

14. Schreurs WJ, Rosenberg H (1982) Effect of silver ions on transport and retention of phosphate by *Escherichia coli*. *J Bacteriol* 152:7–13.
15. Duane M, Dekker CA, Schachmen HK (1966) Complexes of silver ion with natural and synthetic polynucleotides. *Biopolymers* 4:51–76. doi: [10.1002/bip.1966.360040107](https://doi.org/10.1002/bip.1966.360040107)
16. Jensen RH, Davidson N (1966) Spectrophotometric, potentiometric, and density gradient ultracentrifugation studies of the binding of silver ion by DNA. *Biopolymers* 4:17–32. doi: [10.1002/bip.1966.360040104](https://doi.org/10.1002/bip.1966.360040104)
17. Yakabe Y, Sano T, Ushio H, Yasunaga T (1980) Kinetic studies of the interaction between silver ion and deoxyribonucleic acid. *Chem Lett* 4:373–376. doi: [10.1246/cl.1980.373](https://doi.org/10.1246/cl.1980.373)
18. Richard H, Sreiber JP, Duane M (1973) Interactions of metallic ions with DNA V DNA renaturation mechanism in the presence of Cu²⁺. *Biopolymers* 12:1–10. doi: [10.1002/bip.1973.360120102](https://doi.org/10.1002/bip.1973.360120102)
19. Izatt RM, Christensen JJ, Rytting JH (1971) Sites and thermodynamic quantities associated with proton and metal ion interaction with ribonucleic acid, deoxyribonucleic acid, and their constituent bases, nucleosides, and nucleotides. *Chem Rev* 71:439–481. doi: [10.1021/cr60273a002](https://doi.org/10.1021/cr60273a002)
20. Feng QL, Wu J, Chen GQ, Cui FZ, Kim TN, Kim JO (2000) A mechanistic study of the antibacterial effect of silver ions on *Escherichia coli* and *Staphylococcus aureus*. *J Biomed Mater Res* 52:662–668. doi: [10.1002/1097-4636\(20001215\)52:4<662::AID-JBM10>3.0.CO;2-3](https://doi.org/10.1002/1097-4636(20001215)52:4<662::AID-JBM10>3.0.CO;2-3)
21. Yang W, Shen C, Ji Q, An H, Wang J, Liu Q, Zhang Z (2009) Food storage material silver nanoparticles interfere with DNA replication fidelity and bind with DNA. *Nanotechnology* 20:085102. doi: [10.1088/0957-4484/20/8/085102](https://doi.org/10.1088/0957-4484/20/8/085102)
22. Mendis E, Rajapakse N, Byun H-G, Kim S-K (2005) Investigation of jumbo squid (*Dosidicus gigas*) skin gelatin peptides for their in vitro antioxidant effects. *Life Sci* 77:2166–2178. doi: [10.1016/j.lfs.2005.03.016](https://doi.org/10.1016/j.lfs.2005.03.016)
23. Stohs SJ, Bagchi D (1995) Oxidative mechanisms in the toxicity of metal ions. *Free Radic Biol Med* 18:321–366. doi: [10.1016/0891-5849\(94\)00159-H](https://doi.org/10.1016/0891-5849(94)00159-H)
24. Yoon K-Y, Byeon JH, Park J-H, Ji JH, Bae GN, Hwang J (2008) Antimicrobial characteristics of silver aerosol nanoparticles against *Bacillus subtilis* bioaerosols. *Environ Eng Sci* 25:289–294. doi: [10.1089/ees.2007.0003](https://doi.org/10.1089/ees.2007.0003)
25. Kim JS, Kuk E, Yu KN, Kim J-H, Park SJ, Lee HJ, Kim SH, Park YK, Park YH, Hwang C-Y, Kim Y-K, Lee Y-S, Jeong DH, Cho M-H (2007) Antimicrobial effects of silver nanoparticles. *Nanomed Nanotechnol Biol Med* 3:95–101. doi: [10.1016/j.nano.2006.12.001](https://doi.org/10.1016/j.nano.2006.12.001)
26. Park H-J, Kim JY, Kim J, Lee J-H, Hahn J-S, Gu MB, Yoon J (2009) Silver-ion-mediated reactive oxygen species generation affecting bactericidal activity. *Water Res* 43:1027–1032. doi: [10.1016/j.watres.2008.12.002](https://doi.org/10.1016/j.watres.2008.12.002)
27. Morones JR, Elechiguerra JL, Camacho A, Holt K, Kouri JB, Ramírez JT, Yacaman MJ (2005) The bactericidal effect of silver nanoparticles. *Nanotechnology* 16:2346–2353. doi: [10.1088/0957-4484/16/10/059](https://doi.org/10.1088/0957-4484/16/10/059)
28. Raffi M, Hussain F, Bhatti T, Akhter J, Hameed A, Hasan MM (2008) Antibacterial characterization of silver nanoparticles against *Escherichia coli*. *J Mater Sci Technol* 24:192–196.
29. Hwang ET, Lee JH, Chae YJ, Kim YS, Kim BC, Sang B-I, Gu MB (2008) Analysis of the toxic mode of action of silver nanoparticles using stress-specific bioluminescent bacteria. *Small* 4:746–750. doi: [10.1002/smll.200700954](https://doi.org/10.1002/smll.200700954)
30. Amro NA, Kotra LP, Wadu-Mesthrige K, Bulychev A, Mobashery S, Liu G-Y (2000) High-resolution atomic force microscopy studies of the *Escherichia coli* outer membrane: structural basis for permeability. *Langmuir* 16:2789–2796. doi: [10.1021/la991013x](https://doi.org/10.1021/la991013x)
31. Sondi I, Salopek-Sondi B (2004) Silver nanoparticles as antimicrobial agent: a case study on *Escherichia coli* as a model for Gram-negative bacteria. *J Colloid Interface Sci* 275:177–182. doi: [10.1016/j.jcis.2004.02.012](https://doi.org/10.1016/j.jcis.2004.02.012)

32. Wiegand I, Hilpert K, Hancock REW (2008) Agar and broth dilution methods to determine the minimal inhibitory concentration (MIC) of antimicrobial substances. *Nat Protocols* 3:163–175. doi: [10.1038/nprot.2007.521](https://doi.org/10.1038/nprot.2007.521)
33. Clinical and Laboratory Standards Institute (2006) Performance standards for antimicrobial susceptibility testing; sixteenth informational supplement. CLSI document M100-S16CLSI, Wayne.
34. Thomson KS, Moland ES (2001) Cefepime, Piperacillin-Tazobactam, and the inoculum effect in tests with extended-spectrum beta-lactamase-producing Enterobacteriaceae. *Antimicrob Agents Chemother* 45:3548–3554. doi: [10.1128/aac.45.12.3548-3554.2001](https://doi.org/10.1128/aac.45.12.3548-3554.2001)
35. Bauer AW, Perry DM, Kirby WMM (1959) Single-disk antibiotic-sensitivity testing of *Staphylococci*: An analysis of technique and results. *Arch Int Med* 104:208–216.
36. Boyle VJ, Fancher ME, Ross RW, Jr. (1973) Rapid, modified Kirby-Bauer susceptibility test with single, high-concentration antimicrobial disks. *Antimicrob Agents Chemother* 3:418–424. doi: [10.1128/aac](https://doi.org/10.1128/aac).
37. Innocenzi P, Kozuka H (1994) Methyltriethoxysilane-derived sol-gel coatings doped with silver metal particles. *J Sol-Gel Sci Technol* 3:229–233. doi: [10.1007/bf00486561](https://doi.org/10.1007/bf00486561)
38. Breitscheidel B, Zieder J, Schubert U (1991) Metal complexes in inorganic matrixes. 7. Nanometer-sized, uniform metal particles in a silica matrix by sol-gel processing of metal complexes. *Chem Mater* 3:559–566. doi: [10.1021/cm00015a037](https://doi.org/10.1021/cm00015a037)
39. Brusilovsky D, Eyal M, Reisfeld R (1988) Absorption spectra, energy dispersive analysis of X-rays and transmission electron microscopy of silver particles in sol-gel glass films. *Chem Phys Lett* 153:203–209. doi: [10.1016/0009-2614\(88\)85213-8](https://doi.org/10.1016/0009-2614(88)85213-8)
40. Kawashita M, Tsuneyama S, Miyaji F, Kokubo T, Kozuka H, Yamamoto K (2000) Antibacterial silver-containing silica glass prepared by sol-gel method. *Biomaterials* 21:393–398. doi: [10.1016/s0142-9612\(99\)00201-x](https://doi.org/10.1016/s0142-9612(99)00201-x)
41. Zhang F, Wolf GK, Wang X, Liu X (2001) Surface properties of silver doped titanium oxide films. *Surf Coat Technol* 148:65–70. doi: [10.1016/s0257-8972\(01\)01305-6](https://doi.org/10.1016/s0257-8972(01)01305-6)
42. Necula BS, Fratila-Apachitei LE, Zaat SAJ, Apachitei I, Duszczek J (2009) In vitro antibacterial activity of porous TiO₂-Ag composite layers against methicillin-resistant *Staphylococcus aureus*. *Acta Biomater* 5:3573–3580. doi: [10.1016/j.actbio.2009.05.010](https://doi.org/10.1016/j.actbio.2009.05.010)
43. Khalilpour P, Lampe K, Wagener M, Stigler B, Heiss C, Ullrich MS, Domann E, Schnettler R, Alt V (2010) Ag/SiO_xCyplasma polymer coating for antimicrobial protection of fracture fixation devices. *J Biomed Mater Res B: Appl Biomater* 94B:196–202. doi: [10.1002/jbm.b.31641](https://doi.org/10.1002/jbm.b.31641)
44. Sun S-Q, Sun B, Zhang W, Wang D (2008) Preparation and antibacterial activity of Ag-TiO₂ composite film by liquid phase deposition (LPD) method. *Bull Mater Sci* 31:61–66.
45. Page K, Palgrave RG, Parkin IP, Wilson M, Savin SLP, Chadwick AV (2007) Titania and silver-titania composite films on glass-potent antimicrobial coatings. *J Mater Chem* 17:95–104. doi: [10.1039/b611740f](https://doi.org/10.1039/b611740f)
46. Brook LA, Evans P, Foster HA, Pemble ME, Steele A, Sheel DW, Yates HM (2007) Highly bioactive silver and silver/titania composite films grown by chemical vapour deposition. *J Photochem Photobiol A: Chem* 187:53–63. doi: [10.1016/j.jphotochem.2006.09.014](https://doi.org/10.1016/j.jphotochem.2006.09.014)
47. Mahltig B, Fischer A (2010) Inorganic/organic polymer coatings for textiles to realize water repellent and antimicrobial properties-A study with respect to textile comfort. *J Polym Sci, Part B: Polym Phys* 48:1562–1568. doi: [10.1002/polb.22051](https://doi.org/10.1002/polb.22051)
48. Tan S-X, Tan S-Z, Chen J-X, Liu Y-L, Yuan D-S (2009) Preparation and properties of antibacterial TiO₂@C/Ag core-shell composite. *Science and Technology of Advanced Materials* 10:045002. doi: [10.1088/1468-6996/10/4/045002](https://doi.org/10.1088/1468-6996/10/4/045002)
49. Min S-H, Yang J-H, Kim JY, Kwon Y-U (2010) Development of white antibacterial pigment based on silver chloride nanoparticles and mesoporous silica and its polymer composite. *Microporous Mesoporous Mater* 128:19–25. doi: [10.1016/j.micromeso.2009.07.020](https://doi.org/10.1016/j.micromeso.2009.07.020)
50. Inoue Y, Hoshino M, Takahashi H, Noguchi T, Murata T, Kanzaki Y, Hamashima H, Sasatsu M (2002) Bactericidal activity of Ag-zeolite mediated by reactive oxygen species under aerated conditions. *J Inorg Biochem* 92:37–42. doi: [10.1016/s0162-0134\(02\)00489-0](https://doi.org/10.1016/s0162-0134(02)00489-0)

51. Yang F, Wu K, Liu M, Lin W, Hu M (2009) Evaluation of the antibacterial efficacy of bamboo charcoal/silver biological protective material. *Mater Chem Phys* 113:474–479. doi: [10.1016/j.matchemphys.2008.07.126](https://doi.org/10.1016/j.matchemphys.2008.07.126)
52. Yoon KY, Byeon JH, Park CW, Hwang J (2008) Antimicrobial Effect of Silver Particles on Bacterial Contamination of Activated Carbon Fibers. *Environ Sci Technol* 42 (4):1251–1255. doi: [10.1021/es0720199](https://doi.org/10.1021/es0720199)
53. Rao CRK, Trivedi DC (2005) Synthesis and characterization of fatty acids passivated silver nanoparticles – their interaction with PPy. *Synth Met* 155:324–327. doi: [10.1016/j.synthmet.2005.01.038](https://doi.org/10.1016/j.synthmet.2005.01.038)
54. Zhang W, Qiao X, Chen J, Wang H (2006) Preparation of silver nanoparticles in water-in-oil AOT reverse micelles. *J Colloid Interface Sci* 302:370–373. doi: [10.1016/j.jcis.2006.06.035](https://doi.org/10.1016/j.jcis.2006.06.035)
55. Huang H, Yuan Q, Yang X (2004) Preparation and characterization of metal-chitosan nanocomposites. *Colloids Surf B Biointerfaces* 39:31–37. doi: [10.1016/j.colsurfb.2004.08.014](https://doi.org/10.1016/j.colsurfb.2004.08.014)
56. Zhang Y, Peng H, Huang W, Zhou Y, Zhang X, Yan D (2008) Hyperbranched poly (amidoamine) as the stabilizer and reductant to prepare colloid silver nanoparticles in situ and their antibacterial activity. *J Phys Chem C* 112:2330–2336. doi: [10.1021/jp075436g](https://doi.org/10.1021/jp075436g)
57. Panáček A, Kvítek L, Prucek R, Kolář M, Večeřová R, Pízürová N, Sharma VK, Nevěčná Tj, Zbořil R (2006) Silver colloid nanoparticles: synthesis, characterization, and their antibacterial activity. *J Phys Chem B* 110:16248–16253. doi: [10.1021/jp063826h](https://doi.org/10.1021/jp063826h)
58. Liu J, Sonshine DA, Shervani S, Hurt RH (2010) Controlled release of biologically active silver from nanosilver surfaces. *ACS Nano* 4:6903–6913. doi: [10.1021/nn102272n](https://doi.org/10.1021/nn102272n)
59. Holtz RD, Filho AGS, Brocchi M, Martins D, Durán N, Alves OL (2010) Development of nanostructured silver vanadates decorated with silver nanoparticles as a novel antibacterial agent. *Nanotechnology* 21:185102. doi: [10.1088/0957-4484/21/18/185102](https://doi.org/10.1088/0957-4484/21/18/185102)
60. Kong H, Jang J (2008) Synthesis and antimicrobial properties of novel silver/polyrhodanine nanofibers. *Biomacromolecules* 9:2677–2681. doi: [10.1021/bm800574x](https://doi.org/10.1021/bm800574x)
61. Lee HY, Park HK, Lee YM, Kim K, Park SB (2007) A practical procedure for producing silver nanocoated fabric and its antibacterial evaluation for biomedical applications. *Chem Commun* 28:2959–2961. doi: [10.1039/B703034G](https://doi.org/10.1039/B703034G)
62. Zhang H, Chen G (2009) Potent antibacterial activities of Ag/TiO₂ nanocomposite powders synthesized by a one-pot sol–gel method. *Environ Sci Technol* 43:2905–2910. doi: [10.1021/es803450f](https://doi.org/10.1021/es803450f)
63. Li Y, Hindi K, Watts KM, Taylor JB, Zhang K, Li Z, Hunstad DA, Cannon CL, Youngs WJ, Wooley KL (2010) Shell crosslinked nanoparticles carrying silver antimicrobials as therapeutics. *Chem Commun* 46:121–123. doi: [10.1039/B916559B](https://doi.org/10.1039/B916559B)
64. Sanpo N, Tan ML, Cheang P, Khor KA (2008) Antibacterial Property of Cold-Sprayed HA-Ag/PEEK Coating. *J Therm Spray Technol* 18:10–15. doi: [10.1007/s11666-008-9283-0](https://doi.org/10.1007/s11666-008-9283-0)
65. Bertrand P, Jonas A, Laschewsky A, Legras R (2000) Ultrathin polymer coatings by complexation of polyelectrolytes at interfaces: suitable materials, structure and properties. *Macromol Rapid Commun* 21:319–348. doi: [10.1002/\(sici\)1521-3927\(20000401\)21:7<319::aid-marc319>3.0.co;2-7](https://doi.org/10.1002/(sici)1521-3927(20000401)21:7<319::aid-marc319>3.0.co;2-7)
66. Decher G, Schlenoff JB (2003) Multilayer thin films-sequential assembly of nanocomposite materials. Wiley-VCH, Weinheim
67. Grunlan JC, Choi JK, Lin A (2005) Antimicrobial behavior of polyelectrolyte multilayer films containing cetrimide and silver. *Biomacromolecules* 6:1149–1153. doi: [10.1021/bm049528c](https://doi.org/10.1021/bm049528c)
68. Lee H, Lee Y, Statz AR, Rho J, Park TG, Messersmith PB (2008) Substrate-independent layer-by-layer assembly by using mussel-adhesive-inspired polymers. *Adv Mater* 20 (9):1619–1623. doi: [10.1002/adma.200702378](https://doi.org/10.1002/adma.200702378)
69. Li Z, Lee D, Sheng X, Cohen RE, Rubner MF (2006) Two-level antibacterial coating with both release-killing and contact-killing capabilities. *Langmuir* 22:9820–9823. doi: [10.1021/la0622166](https://doi.org/10.1021/la0622166)

70. Collier JH, Camp JP, Hudson TW, Schmidt CE (2000) Synthesis and characterization of polypyrrole–hyaluronic acid composite biomaterials for tissue engineering applications. *J Biomed Mater Res* 50:574–584. doi: [10.1002/\(sici\)1097-4636\(20000615\)50:4<574::aid-jbm13>3.0.co;2-i](https://doi.org/10.1002/(sici)1097-4636(20000615)50:4<574::aid-jbm13>3.0.co;2-i)
71. Ignatova M, Labaye D, Lenoir S, Strivay D, Jerome R, Jerome C (2003) Immobilization of silver in polypyrrole/polyanion composite coatings: preparation, characterization, and antibacterial activity. *Langmuir* 19:8971–8979. doi: [10.1021/la034968v](https://doi.org/10.1021/la034968v)
72. Kumar A, Vemula PK, Ajayan PM, John G (2008) Silver-nanoparticle-embedded antimicrobial paints based on vegetable oil. *Nat Mater* 7:236–241. doi: [10.1038/nmat2099](https://doi.org/10.1038/nmat2099)
73. Sambhy V, Peterson BR, Sen A (2008) Multifunctional silane polymers for persistent surface derivatization and their antimicrobial properties. *Langmuir* 24:7549–7558. doi: [10.1021/la800858z](https://doi.org/10.1021/la800858z)
74. Kickhoefer B, Wokalek H, Scheel D, Ruh H (1986) Chemical and physical properties of a hydrogel wound dressing. *Biomaterials* 7:67–72. doi: [10.1016/0142-9612\(86\)90092-x](https://doi.org/10.1016/0142-9612(86)90092-x)
75. Varaprasad K, Mohan YM, Ravindra S, Reddy NN, Vimala K, Monika K, Sreedhar B, Raju KM (2010) Hydrogel-silver nanoparticle composites: A new generation of antimicrobials. *J Appl Polym Sci* 115:1199–1207. doi: [10.1002/app.31249](https://doi.org/10.1002/app.31249)
76. Ahmed EM, Aggor FS (2010) Swelling kinetic study and characterization of crosslinked hydrogels containing silver nanoparticles. *J Appl Polym Sci* 117:2168–2174. doi: [10.1002/app.31934](https://doi.org/10.1002/app.31934)
77. Ilić V, Saponjić Z, Vodnik V, Lazović Sa, Dimitrijević S, Jovanić P, Nedeljković JM, Radetić M (2010) Bactericidal efficiency of silver nanoparticles deposited onto radio frequency plasma pretreated polyester fabrics. *Ind Eng Chem Res* 49:7287–7293. doi: [10.1021/ie1001313](https://doi.org/10.1021/ie1001313)
78. Pollini M, Russo M, Licciulli A, Sannino A, Maffezzoli A (2009) Characterization of antibacterial silver coated yarns. *J Mater Sci Mater Med* 20:2361–2366. doi: [10.1007/s10856-009-3796-z](https://doi.org/10.1007/s10856-009-3796-z)
79. Parikh DV, Fink T, DeLucca AJ, Parikh AD (2011) Absorption and swelling characteristics of silver (I) antimicrobial wound dressings. *Textile Research Journal* 81 (5):494–503. doi: [10.1177/0040517510380778](https://doi.org/10.1177/0040517510380778)
80. Mariscal A, Lopez-Gigosos R, Carnero-Varo M, Fernandez-Crehuet J (2011) Antimicrobial effect of medical textiles containing bioactive fibres. *Eur J Clin Microbiol Amp; Infect Dis* 30 (2):227–232. doi: [10.1007/s10096-010-1073-1](https://doi.org/10.1007/s10096-010-1073-1)
81. Falletta E, Bonini M, Fratini E, Lo NA, Pesavento G, Becheri A, Lo NP, Canton P, Baglioni P (2008) Clusters of poly (acrylates) and silver nanoparticles: structure and applications for antimicrobial fabrics. *J Phys Chem C* 112:11758–11766. doi: [10.1021/jp8035814](https://doi.org/10.1021/jp8035814)
82. Dubas S, Kumlangdudsana P, Potiyaraj P (2006) Layer-by-layer deposition of antimicrobial silver nanoparticles on textile fibers. *Colloids Surf Physicochem Eng Aspects* 289:105–109. doi: [10.1016/j.colsurfa.2006.04.012](https://doi.org/10.1016/j.colsurfa.2006.04.012)
83. Chen CC, Wang CC, Yeh JT (2009) Improvement of odor elimination and anti-bacterial Activity of polyester fabrics finished with composite emulsions of nanometer titanium dioxide-silver particles-water-borne polyurethane. *Tex Res J* 80:291–300. doi: [10.1177/0040517508100626](https://doi.org/10.1177/0040517508100626)
84. Shuhua W, Wensheng H, Liqiao W, Jinming D, Husheng J, Xuguang L, Bingshe X (2009) Structure and properties of composite antibacterial PET fibers. *J Appl Polym Sci* 112:1927–1932. doi: [10.1002/app.29672](https://doi.org/10.1002/app.29672)
85. Ahmadi Z, Ashjari M, Hosseini R, Nia JR (2009) Synthesis and morphological study of nanoparticles Ag/TiO₂ ceramic and bactericidal investigation of polypropylene-Ag/TiO₂ composite. *J Inorg Organomat P* 19:322–327. doi: [10.1007/s10904-009-9268-6](https://doi.org/10.1007/s10904-009-9268-6)
86. Wu C-S, Liao H-T (2011) Antibacterial activity and antistatic composites of polyester/Ag-SiO₂ prepared by a sol–gel method. *J Appl Polym Sci* 121:2193–2201. doi: [10.1002/app.33823](https://doi.org/10.1002/app.33823)

87. Guggenbichler J, Bösward M, Lugauer S, Krall T (1999) A new technology of microdispersed silver in polyurethane induces antimicrobial activity in central venous catheters. *Infection* 27 S16–S23. doi: [10.1007/bf02561612](https://doi.org/10.1007/bf02561612)
88. Weitman R, Eames W (1975) Plaque accumulation on composite surfaces after various finishing procedures. *J Am Dent Assoc* 91:101–106.
89. Jedrychowski JR, Caputo AA, Kerper S (1983) Antibacterial and mechanical properties of restorative materials combined with chlorhexidines. *J Oral Rehabil* 10:373–381. doi: [10.1111/j.1365-2842.1983.tb00133.x](https://doi.org/10.1111/j.1365-2842.1983.tb00133.x)
90. Kassae MZ, Akhavan A, Sheikh N, Sodagar A (2008) Antibacterial effects of a new dental acrylic resin containing silver nanoparticles. *J Appl Polym Sci* 110:1699–1703. doi: [10.1002/app.28762](https://doi.org/10.1002/app.28762)
91. Yoshida K, Tanagawa M, Atsuta M (1999) Characterization and inhibitory effect of antibacterial dental resin composites incorporating silver-supported materials. *J Biomed Mater Res* 47:516–522. doi: [10.1002/\(sici\)1097-4636\(19991215\)47:4<516::aid-jbm7>3.0.co;2-e](https://doi.org/10.1002/(sici)1097-4636(19991215)47:4<516::aid-jbm7>3.0.co;2-e)
92. Gail Larkin M, Robert CM, Cyrus CH, Morton NS (1975) *Salmonella typhimurium* resistant to silver nitrate, chloramphenicol, and ampicillin: A new treat in burn units? *The Lancet* 305:235–240. doi: [10.1016/S0140-6736\(75\)91138-1](https://doi.org/10.1016/S0140-6736(75)91138-1)
93. Russel AD, Chopra I (1990) Understanding antibacterial action and resistance. Ellis Horwood, Chichester
94. Gupta A, Phung LT, Taylor DE, Silver S (2001) Diversity of silver resistance genes in IncH incompatibility group plasmids. *Microbiology* 147:3393–3402
95. Davis IJ, Richards H, Mullany P (2005) Isolation of silver- and antibiotic-resistant *Enterobacter cloacae* from teeth. *Oral Microbiol Immunol* 20:191–194. doi: [10.1111/j.1399-302X.2005.00218.x](https://doi.org/10.1111/j.1399-302X.2005.00218.x)
96. Silver S, Phung L (2005) A bacterial view of the periodic table: genes and proteins for toxic inorganic ions. *J Ind Microbiol Biotechnol* 32:587–605. doi: [10.1007/s10295-005-0019-6](https://doi.org/10.1007/s10295-005-0019-6)
97. Silver S, Phung LT (1996) Bacterial heavy metal resistance: new surprises. *Annu Rev Microbiol* 50:753–789. doi: [10.1146/annurev.micro.50.1.753](https://doi.org/10.1146/annurev.micro.50.1.753)
98. Silver S (2003) Bacterial silver resistance: molecular biology and uses and misuses of silver compounds. *FEMS Microbiol Rev* 27:341–353. doi: [10.1016/s0168-6445\(03\)00047-0](https://doi.org/10.1016/s0168-6445(03)00047-0)
99. Gupta A, Matsui K, Lo J-F, Silver S (1999) Molecular basis for resistance to silver cations in *Salmonella*. *Nat Med* 5:183–188. doi: [10.1038/5545](https://doi.org/10.1038/5545)
100. Silver S, Phung L, Silver G (2006) Silver as biocides in burn and wound dressings and bacterial resistance to silver compounds. *J Ind Microbiol Biotechnol* 33:627–634. doi: [10.1007/s10295-006-0139-7](https://doi.org/10.1007/s10295-006-0139-7)
101. Herrmann M, Vaudaux PE, Pittet D, Auckenthaler R, Lew PD, Perdreaux FS, Peters G, Waldvogel FA (1988) Fibronectin, fibrinogen, and laminin act as mediators of adherence of clinical staphylococcal isolates to foreign material. *J Infect Dis* 158:693–701. doi: [10.1093/infdis/158.4.693](https://doi.org/10.1093/infdis/158.4.693)
102. Vaudaux P, Pittet D, Haeberli A, Huggler E, Nydegger UE, Lew DP, Waldvogel FA (1989) Host factors selectively increase staphylococcal adherence on inserted catheters: A role for fibronectin and fibrinogen or fibrin. *J Infect Dis* 160:865–875. doi: [10.1093/infdis/160.5.865](https://doi.org/10.1093/infdis/160.5.865)
103. Toy PT, Lai LW, Drake TA, Sande MA (1985) Effect of fibronectin on adherence of *Staphylococcus aureus* to fibrin thrombi in vitro. *Infect Immun* 48:83–86.
104. Vaudaux P, Suzuki R, Waldvogel FA, Morgenthaler JJ, Nydegger UE (1984) Foreign body infection: Role of fibronectin as a ligand for the adherence of *Staphylococcus aureus*. *J Infect Dis* 150:546–553. doi: [10.1093/infdis/150.4.546](https://doi.org/10.1093/infdis/150.4.546)
105. Vaudaux PE, Waldvogel FA, Morgenthaler JJ, Nydegger UE (1984) Adsorption of fibronectin onto polymethylmethacrylate and promotion of *Staphylococcus aureus* adherence. *Infect Immun* 45:768–774.
106. Francois P, Schrenzel J, Stoerman-Chopard C, Favre H, Herrmann M, Foster TJ, Lew DP, Vaudaux P (2000) Identification of plasma proteins adsorbed on hemodialysis tubing that

- promote *Staphylococcus aureus* adhesion. *J Lab Clin Med* 135:32–42. doi: [10.1016/s0022-2143\(00\)70018-7](https://doi.org/10.1016/s0022-2143(00)70018-7)
107. Cheung AL, Fischetti VA (1990) The role of fibrinogen in Staphylococcal adherence to catheters in vitro. *J Infect Dis* 161:1177–1186. doi: [10.1093/infdis/161.6.1177](https://doi.org/10.1093/infdis/161.6.1177)
108. McDevitt D, Francois P, Vaudaux P, Foster TJ (1994) Molecular characterization of the clumping factor (fibrinogen receptor) of *Staphylococcus aureus*. *Mol Microbiol* 11:237–248. doi: [10.1111/j.1365-2958.1994.tb00304.x](https://doi.org/10.1111/j.1365-2958.1994.tb00304.x)
109. Chhatwal GS, Preissner KT, Muller-Berghaus G, Blobel H (1987) Specific binding of the human S protein (vitronectin) to *streptococci*, *Staphylococcus aureus*, and *Escherichia coli*. *Infect Immun* 55:1878–1883
110. Liang OD, Maccarana M, Flock J-I, Paulsson M, Preissner KT, Wadström T (1993) Multiple interactions between human vitronectin and *Staphylococcus aureus*. *Biochim Biophys Acta (BBA) – Mol Basis Dis* 1225:57–63. doi: [10.1016/0925-4439\(93\)90122-h](https://doi.org/10.1016/0925-4439(93)90122-h)
111. Herrmann M, Suchard SJ, Boxer LA, Waldvogel FA, Lew PD (1991) Thrombospondin binds to *Staphylococcus aureus* and promotes staphylococcal adherence to surfaces. *Infect Immun* 59:279–288
112. Herrmann M, Hartleib J, Kehrel B, Montgomery RR, Sixma JJ, Peters G (1997) Interaction of von Willebrand Factor with *Staphylococcus aureus*. *J Infect Dis* 176:984–991. doi: [10.1086/516502](https://doi.org/10.1086/516502)
113. Que Y-A, Haefliger J-A, Piroth L, François P, Widmer E, Entenza JM, Sinha B, Herrmann M, Francioli P, Vaudaux P, Moreillon P (2005) Fibrinogen and fibronectin binding cooperate for valve infection and invasion in. *J Exp Med* 201:1627–1635. doi: [10.1084/jem.20050125](https://doi.org/10.1084/jem.20050125)
114. Hall-Stoodley L, Costerton JW, Stoodley P (2004) Bacterial biofilms: from the natural environment to infectious diseases. *Nat Rev Micro* 2:95–108. doi: [10.1038/nrmicro821](https://doi.org/10.1038/nrmicro821)
115. Musk DJ, Hergenrother PJ (2006) Chemical countermeasures for the control of bacterial biofilms: effective compounds and promising targets. *Curr Med Chem* 13:2163–2177
116. Klein E, Smith DL, Laxminarayan R (2007) Hospitalizations and deaths caused by Methicillin-resistant *Staphylococcus aureus*, United States, 1999–2005. *Emerg Infect Dis* 13:1840–1846
117. Kuehn BM (2007) MRSA Infections Rise. *J Am Med Assoc* 298:1389. doi: [10.1001/jama.298.12.1389-a](https://doi.org/10.1001/jama.298.12.1389-a)
118. Matsuzaki K (1999) Why and how are peptide-lipid interactions utilized for self-defense? Magainins and tachyplesins as archetypes. *Biochim Biophys Acta (BBA) – Biomembranes* 1462:1–10. doi: [10.1016/s0005-2736\(99\)00197-2](https://doi.org/10.1016/s0005-2736(99)00197-2)
119. Zasloff M (2002) Antimicrobial peptides of multicellular organisms. *Nature* 415:389–395. doi: [10.1038/415389a](https://doi.org/10.1038/415389a)
120. Yang L, Weiss TM, Lehrer RI, Huang HW (2000) Crystallization of antimicrobial pores in membranes: Magainin and Protegrin. *Biophys J* 79:2002–2009. doi: [10.1016/S0006-3495\(00\)76448-4](https://doi.org/10.1016/S0006-3495(00)76448-4)
121. Shai Y (1999) Mechanism of the binding, insertion and destabilization of phospholipid bilayer membranes by [alpha]-helical antimicrobial and cell non-selective membrane-lytic peptides. *Biochim Biophys Acta (BBA) – Biomembranes* 1462:55–70. doi: [10.1016/s0005-2736\(99\)00200-x](https://doi.org/10.1016/s0005-2736(99)00200-x)
122. Kragol G, Lovas S, Varadi G, Condie BA, Hoffmann R, Otvas L (2001) The antibacterial peptide Pyrrhocoricin inhibits the ATPase actions of DnaK and prevents chaperone-assisted protein folding. *Biochemistry* 40:3016–3026. doi: [10.1021/bi002656a](https://doi.org/10.1021/bi002656a)
123. Bierbaum G, Sahl H-G (1985) Induction of autolysis of staphylococci by the basic peptide antibiotics Pep 5 and nisin and their influence on the activity of autolytic enzymes. *Arch Microbiol* 141:249–254. doi: [10.1007/bf00408067](https://doi.org/10.1007/bf00408067)
124. Marr AK, Gooderham WJ, Hancock REW (2006) Antibacterial peptides for therapeutic use: obstacles and realistic outlook. *Curr Opin Pharmacol* 6:468–472. doi: [10.1016/j.coph.2006.04.006](https://doi.org/10.1016/j.coph.2006.04.006)

125. Nederberg F, Zhang Y, Tan JPK, Xu K, Wang H, Yang C, Gao S, Guo XD, Fukushima K, Li L, Hedrick JL, Yang Y-Y (2011) Biodegradable nanostructures with selective lysis of microbial membranes. *Nat Chem* 3:409–414. doi: [10.1038/nchem.1012](https://doi.org/10.1038/nchem.1012)
126. Sambhy V, MacBride MM, Peterson BR, Sen A (2006) Silver bromide nanoparticle/polymer composites: Dual action tunable antimicrobial materials. *J Am Chem Soc* 128:9798–9808. doi: [10.1021/ja061442z](https://doi.org/10.1021/ja061442z)
127. Langmuir I (1938) The role of attractive and repulsive forces in the formation of tactoids, thixotropic gels, protein crystals and coacervates. *J Chem Phys* 6:873–896. doi: [10.1063/1.1750183](https://doi.org/10.1063/1.1750183)
128. Derjaguin BV, Churaev NV (1974) Structural component of disjoining pressure. *J Colloid Interface Sci* 49:249–255. doi: [10.1016/0021-9797\(74\)90358-0](https://doi.org/10.1016/0021-9797(74)90358-0)
129. LeNeveu D, Rand R, Gingell D, Parsegian V (1976) Apparent modification of forces between lecithin bilayers. *Science* 191:399–400. doi: [10.1126/science.1246623](https://doi.org/10.1126/science.1246623)
130. Harris JM (1992) Poly (ethylene glycol) chemistry: biotechnical and biomedical applications. Plenum Press, New York
131. Harder P, Grunze M, Dahint R, Whitesides GM, Laibinis PE (1998) Molecular conformation in oligo (ethylene glycol)-terminated self-assembled monolayers on gold and silver surfaces determines their ability to resist protein adsorption. *J Phys Chem B* 102:426–436. doi: [10.1021/jp972635z](https://doi.org/10.1021/jp972635z)
132. Li L, Chen S, Zheng J, Ratner BD, Jiang S (2005) Protein adsorption on oligo(ethylene glycol)-terminated alkanethiolate self-assembled monolayers: The molecular basis for nonfouling behavior. *J Phys Chem B* 109:2934–2941. doi: [10.1021/jp0473321](https://doi.org/10.1021/jp0473321)
133. Ma H, Wells M, Beebe TP, Chilkoti A (2006) Surface-initiated atom transfer radical polymerization of oligo(ethylene glycol) methyl methacrylate from a mixed self-assembled monolayer on gold. *Adv Funct Mater* 16:640–648. doi: [10.1002/adfm.200500426](https://doi.org/10.1002/adfm.200500426)
134. Prime KL, Whitesides GM (1993) Adsorption of proteins onto surfaces containing end-attached oligo(ethylene oxide): a model system using self-assembled monolayers. *J Am Chem Soc* 115:10714–10721. doi: [10.1021/ja00076a032](https://doi.org/10.1021/ja00076a032)
135. Ma H, Li D, Sheng X, Zhao B, Chilkoti A (2006) Protein-resistant polymer coatings on silicon oxide by surface-initiated atom transfer radical polymerization. *Langmuir* 22:3751–3756. doi: [10.1021/la052796r](https://doi.org/10.1021/la052796r)
136. Luk Y-Y, Kato M, Mrksich M (2000) Self-assembled monolayers of alkanethiolates presenting mannitol groups are inert to protein adsorption and cell attachment. *Langmuir* 16:9604–9608. doi: [10.1021/la0004653](https://doi.org/10.1021/la0004653)
137. Ostuni E, Chapman RG, Liang MN, Meluleni G, Pier G, Ingber DE, Whitesides GM (2001) Self-assembled monolayers that resist the adsorption of proteins and the adhesion of bacterial and mammalian cells. *Langmuir* 17:6336–6343. doi: [10.1021/la010552a](https://doi.org/10.1021/la010552a)
138. Shen MC, Martinson L, Wagner MS, Castner DG, Ratner BD, Horbett TA (2002) PEO-like plasma polymerized tetraglyme surface interactions with leukocytes and proteins: In vitro and in vivo studies. *J Biomater Sci Polym Ed* 13:367–390. doi: [10.1163/156856202320253910](https://doi.org/10.1163/156856202320253910)
139. Chen S, Zheng J, Li L, Jiang S (2005) Strong resistance of phosphorylcholine self-assembled monolayers to protein adsorption: Insights into nonfouling properties of zwitterionic materials. *J Am Chem Soc* 127:14473–14478. doi: [10.1021/ja054169u](https://doi.org/10.1021/ja054169u)
140. He Y, Hower J, Chen S, Bernards MT, Chang Y, Jiang S (2008) Molecular simulation studies of protein interactions with zwitterionic phosphorylcholine self-assembled monolayers in the presence of water. *Langmuir* 24:10358–10364. doi: [10.1021/la8013046](https://doi.org/10.1021/la8013046)
141. Chang Chung Y, Hong Chiu Y, Wei Wu Y, Tai Tao Y (2005) Self-assembled biomimetic monolayers using phospholipid-containing disulfides. *Biomaterials* 26:2313–2324. doi: [10.1016/j.biomaterials.2004.06.043](https://doi.org/10.1016/j.biomaterials.2004.06.043)
142. Cheng G, Zhang Z, Chen S, Bryers JD, Jiang S (2007) Inhibition of bacterial adhesion and biofilm formation on zwitterionic surfaces. *Biomaterials* 28:4192–4199. doi: [10.1016/j.biomaterials.2007.05.041](https://doi.org/10.1016/j.biomaterials.2007.05.041)

143. Lowe AB, McCormick CL (2002) Synthesis and solution properties of zwitterionic polymers. *Chem Rev* 102:4177–4190. doi: [10.1021/cr020371t](https://doi.org/10.1021/cr020371t)
144. Ladd J, Zhang Z, Chen S, Hower JC, Jiang S (2008) Zwitterionic polymers exhibiting high resistance to nonspecific protein adsorption from human serum and plasma. *Biomacromolecules* 9:1357–1361. doi: [10.1021/bm701301s](https://doi.org/10.1021/bm701301s)
145. Yang W, Xue H, Li W, Zhang J, Jiang S (2009) Pursuing “zero” protein adsorption of poly (carboxybetaine) from undiluted blood serum and plasma. *Langmuir* 25:11911–11916. doi: [10.1021/la9015788](https://doi.org/10.1021/la9015788)
146. Cheng G, Li G, Xue H, Chen S, Bryers JD, Jiang S (2009) Zwitterionic carboxybetaine polymer surfaces and their resistance to long-term biofilm formation. *Biomaterials* 30:5234–5240. doi: [10.1016/j.biomaterials.2009.05.058](https://doi.org/10.1016/j.biomaterials.2009.05.058)

Chapter 2

Synthesis, Characterization and Application of Silver-Based Antimicrobial Nanocomposites

Desong Wang, Jing An, Qingzhi Luo, Xueyan Li, and Luna Yan

The different types of nanomaterials like copper, zinc, titanium, magnesium, gold, alginate, and silver possess the antimicrobial activity [1–3]. Among the various antimicrobials, silver is most promising because of its inherent properties of high thermal stability, little toxicity to mammalian cells and tissues [4, 5], versatile activity (such as good antimicrobial efficacy against bacteria, viruses, and other eukaryotic microorganisms), and long-term activity [6]. Therefore, the silver-containing materials having excellent antimicrobial activity against a broad spectrum of microbes have attracted much interest of the scientists [7].

The present chapter aims at reviewing the synthesis, characterization, and application of silver-based antimicrobial nanocomposites. Firstly, the common synthetic methods of silver nanomaterials, e.g., physical method, chemical reduction and all kinds of biological approach, are described. Secondly, the bioactivity of silver(I) complexes, silver nanoparticles, silver/inorganic nanocomposites, and silver–polymer nanocomposites are discussed, and especially the different antimicrobial mechanisms of diverse silver-based nanocomposites are emphatically summarized. Thirdly, the applications of the antimicrobial nanocomposites in the medical, pharmaceutical, and food packaging industry, in addition to water disinfection and microbial control, are introduced. Additionally, the toxicology of the antimicrobial nanocomposites is also mentioned. Finally, the current and possible developing trends of the antimicrobial silver-based nanocomposites are prospected.

D. Wang (✉) • J. An • Q. Luo • X. Li

School of Sciences, Hebei University of Science and Technology, Shijiazhuang, Hebei, PR China
e-mail: dswang06@126.com

L. Yan

College of Bioscience and Bioengineering, Hebei University of Science and Technology,
Shijiazhuang, Hebei, PR China

2.1 Synthesis of Silver-Based Antimicrobial Nanocomposites

2.1.1 Synthesis of Silver Nanoparticles

The application of nanoparticles varies widely on the basis of their physical properties, like apparent density, surface area, and morphology, which are strongly related to the preparation methods and preparing materials. For example, the antimicrobial activity of silver nanoparticles is closely related to their size and shape [8]. Thus, the control over the size, size distribution, and shape of nanoparticles is an important task in the synthesis of silver-based antimicrobial nanocomposites. Generally, silver nanoparticles can be prepared and stabilized by physical approaches (such as the evaporation–condensation method and laser ablation method), chemical approaches (such as the reduction method), and biological and biotechnological approaches, etc. [9–11].

2.1.1.1 Physical Approach

In the past, mechanical approaches such as homogenization and grinding/ball milling were used to prepare silver nanoparticles for antimicrobial application. But the obtained silver nanoparticles aggregated greatly and showed poor inhibitory and bactericidal effect. In recent physical processes, silver nanoparticles are generally synthesized by evaporation–condensation which could be carried out in a tube furnace. Simchi et al. [12] presented a design of silver nanoparticle synthesis by an inert-gas condensation process. Silver was heated in a small temperature-regulated crucible to produce vapors, then the vapors were rapidly quenched on the surface of a liquid nitrogen tank in a reduced atmosphere of argon gas. They found that source temperature, evaporation rate, and argon pressure greatly affected the average particle size and particle shape.

Laser ablation in liquids has received much attention as a novel nanoparticle-production technique [13]. In general, silver nanoparticles are obtained by irradiating intense laser light onto the metallic bulk material settled in solvents. One advantage of laser ablation compared to other conventional methods for preparing metal colloids is the absence of chemical reagents in the solutions. Therefore, pure colloids, which will be useful for further applications, can be produced by this method. Tsuji et al. [14, 15] carried out laser ablation of silver plates in polyvinylpyrrolidone (PVP) aqueous solutions and found the obtained colloidal silver nanoparticles were more stable than those obtained in neat water. Nanoparticles can also be modified in size and shape by the surfactant coating due to their further interaction with the laser light passing through. The nanoparticles formed by laser ablation in a solution of high surfactant concentration are smaller than those formed in a solution of low surfactant concentration.

Other physical methods, such as ultrasonic-assisted reduction [16], photoinduced synthesis [17], microwave-assisted synthesis [18], irradiation reduction [19], and so

on, have been employed to synthesize silver nanoparticles and silver-based nanocomposites. In these methods, silver nanoparticles with various morphologies and excellent antimicrobial activities can be obtained.

2.1.1.2 Chemical Approach

The chemical approach includes chemical reduction (chemical reduction of silver ions in aqueous solutions [20, 21] or non-aqueous solutions [22]), the template method [23, 24], electrochemical reduction [25], the microemulsion method [26], biochemical reduction [27], and so on.

Chemical reduction is the most frequently applied method for the preparation of silver nanoparticles as stable, colloidal dispersions in water or organic solvents. The reduction of silver ions (Ag^+) in aqueous solution generally yields colloidal silver with particle diameters of several nanometers. Initially, the reduction of various complexes with Ag^+ leads to the formation of silver atoms (Ag^0), which is followed by agglomeration into oligomeric clusters. These clusters eventually lead to the formation of colloidal silver particles. Commonly used reductants are borohydride, citrate, ascorbate, and elemental hydrogen [28–30]. The use of a strong reductant such as borohydride results in small particles that are somewhat monodispersed, while the use of citrate, a weaker reductant, results in a slower reduction rate and narrower size distribution. Moreover, nanoparticles with different shapes can be easily prepared by controlling the reaction conditions. However, the coalescence of the nanoparticles may lose their characteristic properties. Thus, the most important key in this method is to avoid the agglomeration of silver nanoparticles during the synthesis and preservation procedures. Usually, special organic compounds, such as surfactants, polymers, and stabilizing ligands, are used to passivate the particles and prevent them from aggregating.

To overcome the limitation of chemical reduction and prevent particle aggregation, the reverse microemulsion (reverse micelle) method is introduced to obtain the uniform and size-controlled nanoparticles. This method has the obvious advantage of synthesizing nanoparticles with specific diameter and morphology. The nucleation and growth are restricted within the water cores of inverse micelles. The droplet dimension can be modulated by various parameters, in particular the molar ratio of water and surfactant. Preparation of silver nanoparticles by the microemulsion method has many influencing factors, and the synthesis system also has some characteristics different from other systems.

Currently, in the microemulsion method, some natural compounds such as sodium citrate and reducing sugars are usually used as reducing agents, although the reduction activity is generally low and the reducing reaction takes place under a higher temperature and needs a long time. These reducing agents are mild, inexpensive, and nontoxic. Some of them simultaneously play dual roles as a protective agent and a reducing agent. For instance, silver particles prepared by citrate reduction are nearly spherical, and the crystallites have relatively large diameters (50–100 nm) and a wide range of distributions in size and shape. Citrate serves not only the dual roles of a reductant and stabilizer but also in the role of a template [31].

2.1.1.3 Biological and Biotechnological Approaches

The chemical method allows the preparation of uniform and size-controllable nanoparticles; however, highly deleterious organic solvents with potential risks for environment and biological hazards are employed. It has, therefore, been an increasing awareness towards green chemistry and biological processes leading to the development of an environment-friendly approach for the synthesis of nanoparticles. Unlike other processes in physical and chemical methods, which involve hazardous chemicals, microbial biosynthesis of nanoparticles is an eco-friendly approach. Research in biological and biotechnological approaches provides reliable, cost-effective processes for the synthesis of nanoscale materials.

It has been known for a long time that a variety of nanoparticles are synthesized by biological processes. The biological synthesis of nanoparticles germinated from the experiments on biosorption of metals with Gram-negative and Gram-positive bacteria. A few microorganisms, such as *Pseudomonas stutzeri*, *Klebsiella pneumonia*, *Escherichia coli*, and *Enterobacter cloacae*, have been explored as potential biofactories for synthesis of silver nanoparticles [32, 33]. Moreover, biological reduction is developed as a promising method because of its special advantages such as sufficient material sources, mild reaction conditions, and good dispersion of nanoparticles as well as few chemical additives and poisonous byproducts.

In recent years, fungi such as *Fusarium oxysporum*, *Colletotrichum* sp., *Trichothecium* sp., *Trichoderma asperellum*, *Trichoderma viride*, *Phanerochaete chrysosporium*, *Fusarium solanii*, *Aspergillus fumigatus*, *Coriolus versicolor*, *Aspergillus niger*, *Phoma glomerata*, *Penicillium brevicompactum*, *Cladosporium cladosporioides*, *Penicillium fellutanum*, and *Volvariella volvaceae* have been explored for silver nanoparticles synthesis. Fungi are more advantageous compared to other microorganisms in many methods [34]. For example, in *Fusarium oxysporum* fungus, the reduction of Ag^+ was attributed to an enzymatic process involving NADH (reduced nicotinamide adenine dinucleotide)-dependent reductase. Hen egg white lysozyme can act as the sole reducing agent and catalyzes the formation of silver nanoparticles in the presence of light. Stable silver colloids formed after mixing lysozyme and silver acetate in methanol, and the resulting nanoparticles are concentrated and transferred to aqueous solution without any significant changes in physical properties [35]. Figure 2.1 is the proposed formation mechanism of silver-lysozyme nanoparticles. In another example, the white rot fungus, *Phanerochaete chrysosporium*, reduced silver ions to form silver nanoparticles, in which a protein was suggested to cause the reduction of silver ions. Environmental SEM analysis revealed that silver nanoparticles were in the size range of 50–200 nm on the surface of the mycelium. This demonstrated the presence of reductase enzymes on the surface of the mycelium, which reduced silver ions to silver nanoparticles. Spent mushroom substrate (SMS) can also be used as a reducer and stabilizer to synthesize stable and monodisperse silver-protein (core-shell) nanoparticles [36].

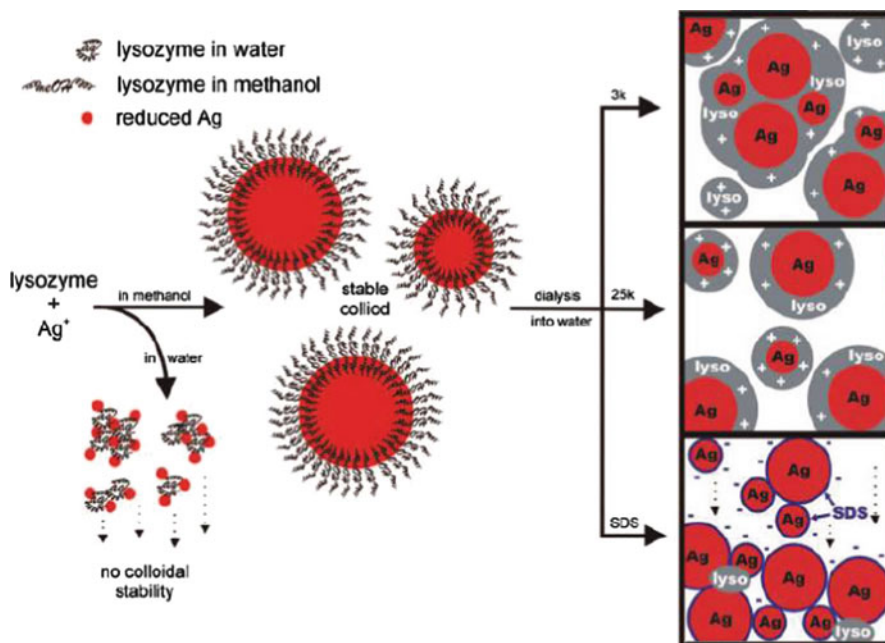


Fig. 2.1 Proposed mechanism of silver-lysozyme nanoparticle formation [35]

Extracts from microorganisms may act as both reducing and capping agents in silver nanoparticles synthesis. The reduction of silver ions by combinations of biomolecules found in these extracts such as enzymes/proteins, amino acids, polysaccharides, and vitamins is environmentally benign. For example, the extract of unicellular green algae *Chlorella vulgaris* was used to synthesize single-crystalline silver nanoplates at room temperature. Proteins in the extract provide the dual function of silver ions reduction and shape control in the nanoparticle synthesis. The carboxyl groups in aspartic and/or glutamine residues and the hydroxyl groups in tyrosine residues of the proteins were suggested to be responsible for the silver ion reduction [37].

Among biological molecules, deoxyribonucleic acid (DNA) is one of the most interesting template systems because of its large aspect ratio (length/diameter) and well-defined sequences of DNA base and a variety of superhelix structures. Sun et al. reported that a silver nanoparticles ring could be successfully fabricated by electrostatic assembling 4-aminothiophenol (4-ATP)-capped silver nanoparticles on a predefined extended circular plasmid pBR322 DNA [38].

Although biological methods are regarded as safe, cost-effective, sustainable, and environmentally friendly processes, they also have some drawbacks in the culturing of microbes, which is time-consuming and difficult to provide better control over size distribution, shape, and crystallinity. In order to improve the rate of synthesis and monodispersity of nanoparticles, factors such as microbial

cultivation methods and downstream processing techniques have to be improved and the combinatorial approach such as photobiological methods may be used.

2.1.2 Synthesis of Typical Silver-Based Antimicrobial Nanocomposites

Silver-based antimicrobial nanocomposites deserve special attention due to their unique properties, which differentiate them from other antimicrobial additives. According to the composition of nanocomposites, the silver-based antimicrobials can be placed in four categories: silver–polymer nanocomposites, silver–biopolymer nanocomposites, silver–inorganic compounds, and silver(I) complexes.

2.1.2.1 Silver–Polymer Nanocomposites

Polymer molecules are found to be very effective support for the stabilization of silver nanoparticles [39, 40]. In silver–polymer nanocomposites, the commonly used polymers are polyacrylate [41], poly(amidoamine) [42], polyaniline [43], poly(methyl methacrylate) [44], poly(ethylene oxide) [45], polyrhodanine [46], etc. So far, there are many chemical and physical methods to prepare silver–polymer nanocomposites [47].

One of the in situ syntheses of silver nanoparticles in the polymer matrix involves the dissolution and reduction of silver salts or complexes into the matrix [48]. Generally, the silver cations are first complexed with a certain polymer, and then reduced in situ by using various reducing agents to form the stable colloidal silver–polymer nanocomposites. Here, the polymers acted as templates, stabilizers or protecting agents. For instance, a nanoscale silver cluster protected by sodium polyacrylate (PAA) was prepared through the reduction of aqueous silver nitrate solution containing PAA. The silver nanoparticles in clusters of nanoscale dimension (nanoclusters) could be dispersed into the artificial heterogeneous matrix of polyacrylate and protein (bovine serum albumin, BSA) by adjusting the pH in the acidic region [41]. A series of colloid silver nanoparticles were successfully prepared by in situ reduction and stabilization of hyperbranched poly(amidoamine) with terminal dimethylamine groups [HPAMAM-N(CH₃)₂] in water [42]. The schematic procedure for the preparation of Ag-HPAMAMN(CH₃)₂ nanocomposite is shown in Fig. 2.2.

Another approach is a system in which simultaneous polymerization and metal reduction occur. For example, core–shell silver–polyaniline nanocomposites have been synthesized by the in situ gamma radiation-induced chemical polymerization method. An aqueous solution of aniline, a free-radical oxidant, and/or silver metal salt were irradiated by γ -rays. Reduction of the silver salt in aqueous aniline leads to the formation of silver nanoparticles which in turn catalyze oxidation of aniline to

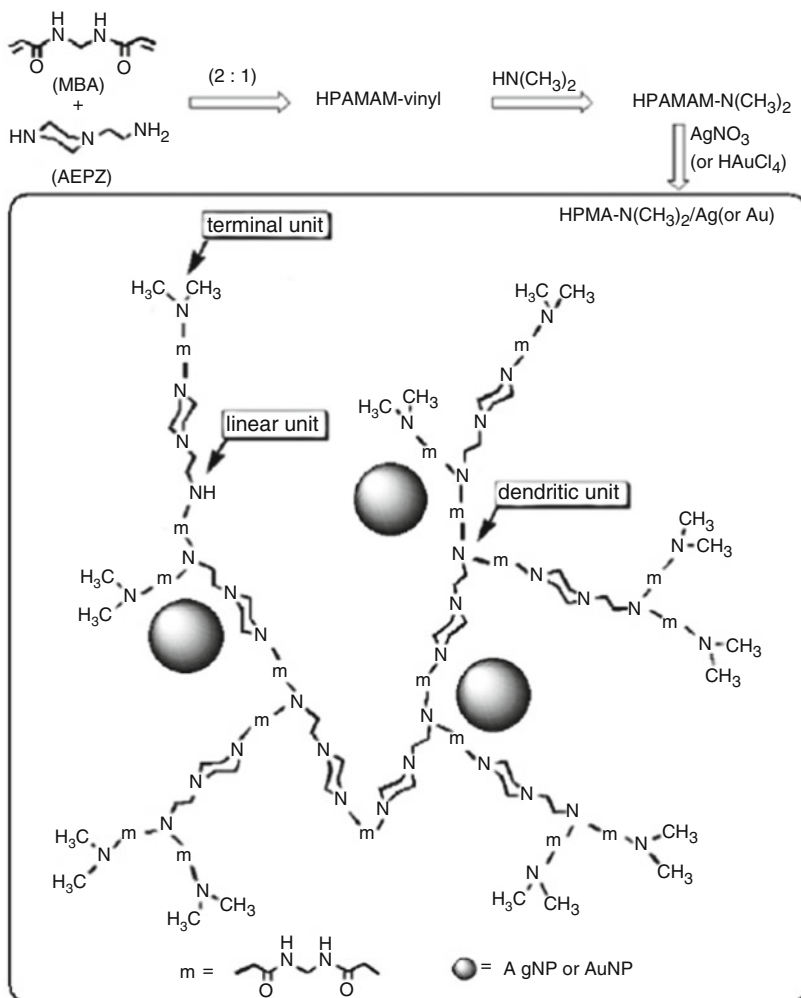


Fig. 2.2 Schematic procedure for the preparation of the Ag-HPAMAM- $\text{N}(\text{CH}_3)_2$ nanocomposite [42]

polyaniline [43]. Interestingly, in some reactions, silver ions can be used as an oxidant in the chemical oxidation polymerization. For example, during the synthetic process of silver- poly(amidoamine) (Ag-HPAMA) nanomaterials. Silver nanoparticles can be fabricated with HPAMA as the stabilizer and reductant while silver ions act as the oxidant [49]. The schematic plot of preparing Ag-HPAMAM- NH_2 nanocomposites is shown in Fig. 2.3.

Moreover, supercritical carbon dioxide (sc-CO_2) has been attracting interest as a polymerization and processing medium, primarily driven by the need to replace conventional solvents with more environmentally benign and economically viable systems [50, 51]. It possesses many advantages like non-flammability, high diffusivity, low cost, low viscosity, compressibility, etc. [52]. And the product can easily

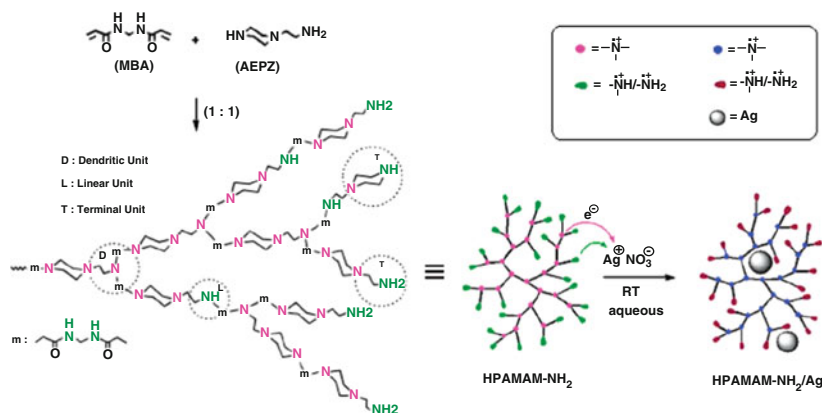


Fig. 2.3 Schematic plot of preparing Ag-HPAMAM-NH₂ nanocomposites [49]

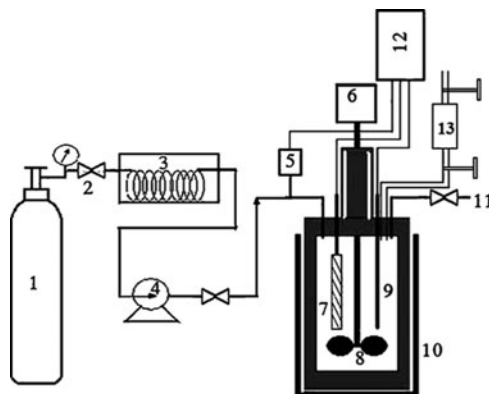
be separated by depressurizing CO₂. Many chemicals are not soluble in CO₂, but they can easily be emulsified in sc-CO₂ by selecting proper fluorinated or siloxane-based surfactants/stabilizers. Shiho and De Simone pioneered the dispersion polymerization of methyl methacrylate in sc-CO₂. They used the CO₂-soluble fluorinated homo-polymer, poly(dihydroperfluorooctyl acrylate) (PFOA) as a stabilizer for the polymerization reaction [53]. Kamrupi et al. [54] have elaborately explained one simple, effective and green route to synthesize silver-polystyrene nanocomposite particles in water-in-sc-CO₂ medium. Silver nanoparticles are synthesized by chemical reduction of silver nitrate using sodium borohydrate as a reducing agent and polydimethylsiloxane (PDMS) as a stabilizer in the water-in-sc-CO₂ medium. This work represents a simple, reproducible and universal way to prepare a variety of metal-polymer nanocomposite particles. The schematic diagram of the apparatus for preparing the silver nanocomposite by the above-mentioned method is displayed in Fig. 2.4.

2.1.1.2 Silver-Biopolymer Nanocomposites

To date, polysaccharide biopolymers, which are generally non-toxic and available from renewable agricultural sources, can integrate with inorganic nanoparticles, and the research on the hybrid systems of silver-biopolymers is a dramatic activity in current bio-nanoscience. Characteristic macromolecular and supramolecular properties of these biopolymers make them become the good controlled environments for growth of metallic and semiconductor nanocrystals [55]. For example, silver-cellulose colloids are obtained by immersing bacterial cellulose into the silver nitrate solution through chemical reduction [56].

The glycogen biopolymer from bovine liver has been used as stabilization agent for the growth of silver nanoparticles [57]. The nanoparticles encapsulated in

Fig. 2.4 Schematic diagram of the apparatus 1 Carbon dioxide cylinder, 2 back pressure valve, 3 refrigeration unit, 4 high-pressure liquid pump, 5 back pressure gauge, 6 motor for mechanical stirrer, 7 cooling unit, 8 mechanical stirrer, 9 heating probe, 10 SFE Vessel, 11 vent, 12 digital display unit, 13 specially designed dropper [54]



glycogen with various contents of silver are prepared by two different procedures that include fast (using microwave radiation) and slow (conventional) heating of the reaction mixtures.

Starch is the most extensively used biopolymer for the stabilization of the growth of metallic and semiconductor nanoparticles. Stable silver nanoparticles have been synthesized by using soluble starch as both the reducing and stabilizing agents [58]. The silver nanoparticles embedded in soluble starch have been proved to be an environmentally benign and renewable material. The use of a silver–starch nanocomposite like soluble starch offers numerous benefits of eco-friendliness and compatibility for pharmaceutical and biomedical applications.

Chitosan possesses many unique properties, including antimicrobial characteristics; hence, it has been used in various applications, such as medical, pharmaceutical, textile, water treatment, food, cosmetics, packaging, etc [59–61]. Silver nanoparticles can be formed by reduction of corresponding metal salts with a reductant such as NaBH_4 in the presence of chitosan, and then chitosan molecules are adsorbed onto the surface of as-prepared silver nanoparticles in the cross-linking process to form the corresponding silver–chitosan nanocomposites [62].

Silver-impregnated polymer nanofibers have been developed as a new class of biomedical materials by releasing biocidal silver with a protective polymer barrier against infection [63–65]. Kong et al. [66] reported the fabrication of novel silver–polyrhodanine nanofibers and their antimicrobial efficacy. Silver ions are reduced to silver nanoparticles by oxidizing rhodanine monomer and simultaneously complexed with the rhodanine due to coordinative interactions, resulting in the formation of silver nanoparticle-embedded polyrhodanine nanofibers. The synthesized nanofiber is found to have excellent antimicrobial activities.

The other polysaccharide biopolymers such as poly(L-lactide) [67] and gum arabic [68] are also proving to be good stabilization agents for silver nanoparticles. To sum up, silver nanoparticles synthesized within the biopolymer are biocompatible and hydrophilic, which could be important for their application in biology and medicine.

2.1.2.3 Silver–Inorganic Compounds

In recent years, the use of inorganic–inorganic hybrid antimicrobial agents has attracted interest because of their industrial and medical applications. The key advantages of inorganic antimicrobial agents are improved safety and stability [69]. As can be observed, the integration of silver into nanocomposites and bimetallic nanoparticles is limitless. With each combination, silver is being used to generate nanoparticles with new characteristics.

Hydroxyapatite (HA) has been widely used for bone repair and substitute because of its good biocompatibility and the high silver ions exchange rate. The hydroxyapatite nanoribbon spherites have large surface, good bio-consistency and high physical/chemical activities [70]. The silver nanoparticles were controlled to be synthesized under the cooperation of the ethylenediamine and the cetyltrimethyl ammonium bromide. Then, under the electrostatic effect of the silver nanoparticles and with the strong adsorbability of the hydroxyapatite nanoribbon spherites, the two substances were combined to form special nanocomposite spheres [71].

The photocatalytic activity of anatase titanium dioxide (TiO_2) was discovered by Fujishima and Honda. This photodecomposition of organic compounds is also useful for killing bacteria. The antimicrobial activity of silver nanoparticles was enhanced when it was incorporated into an Ag/TiO_2 nanocomposite, and would result in higher toxicity levels in the ecosystem in the event of release to the environment [72]. Silver-hydroxyapatite/titania nanocomposite thin films were coated on commercially pure titanium by a modified dipping method, and the antimicrobial effect of this thin film on Gram-positive material proved to be excellent [73].

A combination antimicrobial property is achieved when silver nanoparticles are combined with other metal nanoparticles or oxides acting as a shell or a core to form bimetallic nanoparticles. For example, silver colloids are synthesized using polymer polyvinylpyrrolidone (PVP) as protecting agent, and the silica shell is then coated by means of the Stober process to fabricate Ag@SiO_2 core shell particles. The shell thickness can be easily controlled by the amount of tetraethyl orthosilicate (TEOS) [74]. The preparation process is described in Fig. 2.5.

Carbon nanofibers (CNFs) have some inherent advantages, such as excellent chemical stability and mechanical stability. As a substrate for an antimicrobial system, its nanofibrous structure can offer higher cell adherence compared with other structures. In addition, considering their other functional properties, they have been used for the fillers in polymer composites or used as the biosensors [75]. It is anticipated that the composite of carbon materials and silver nanoparticles can contribute to antimicrobial efficiency. One-dimensional (1D) carbon nanomaterials wrapped by silver nanoparticles were fabricated via a facile and environmentally benign route with the assistance of supercritical carbon dioxide [76].

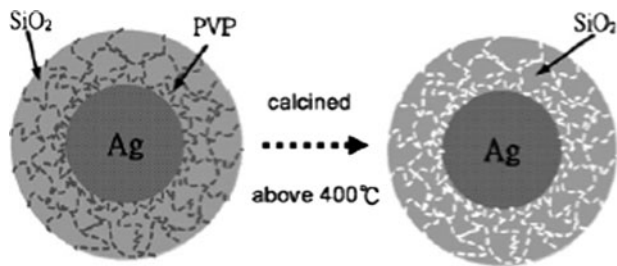


Fig. 2.5 Schematic illustration of the porous characteristics of an Ag@SiO₂ core shell particle [74]

2.1.2.4 Silver(I) Complexes

Silver(I) complexes have long been known to show powerful antimicrobial activity. A great number of silver(I) complexes have been prepared by impregnating silver salts into the corresponding chemical compound. Rowan et al. [77] provided the synthesis and structures of the related silver(I) complexes containing non-functionalized imidazole ligands. The imidazole complex salt [Ag(imH)₂]NO₃ has been prepared by reacting AgNO₃ with imH (ca. 1:4 molar ratio) and in the [Ag(imH)₂]⁺ cation, the metal is bonded to the imine N atoms of two neutral imidazole ligands in a similar fashion to that found in the core structure of [Ag₂(imH)₄](salH)₂. Chen et al. [78] synthesized thiourea chitosan (TU-CTS) by the reaction of chitosan with ammonium thiocyanate, which was easy to dissolve in 1% acetic acid solution. Ag⁺(TU-CTS-Ag⁺) complex was obtained by mixing TU-CTS and AgNO₃, which greatly enhanced the antimicrobial activity of chitosan as well as the stability of Ag⁺.

2.2 Bioactivity of Silver-Based Antimicrobial Nanocomposites

Silver compounds have also been exploited for their medicinal properties for centuries. They were popular remedies for tetanus and rheumatism in the nineteenth century and for colds and gonorrhea before the advent of antibiotics in the early part of the twentieth century [79]. Silver-based medical products, ranging from typical ointments and bandages for wound healing to coated stents, have been proven to be effective in retarding and preventing bacterial infections. Among the properties of silver compounds and silver-based nanocomposites, the bioactivity is most important for biomaterials (such as antimicrobial materials). Therefore, the knowledge about the bioactivity of silver-based antimicrobial nanocomposites will be summarized here.

2.2.1 Silver Salts and Silver(I) Complexes

The silver ion exhibits broad-spectrum biocidal activity toward many different bacteria, fungi, and viruses, and is believed to be the active component in silver-based antimicrobials. Simple silver salts have been known for centuries to exert anti-infective properties, and proven to have significantly low cytotoxicity. However, overdoses of all the forms of silver can lead to complications generally known as argyria. The delivery system becomes more stable when a positively charged silver ion is complexed to negatively charged ions (AgCl , AgNO_3 , Ag_2SO_4). The standard is 0.5% silver nitrate and the most popular silver salt solution used for typical burn wound therapy. Concentrations exceeding 1% silver nitrate are toxic to the tissues. Ionic silver solutions are highly bactericidal and have a beneficial effect in decreasing wound surface inflammation. However, the solutions are unstable and can produce typical black stains when exposed to light, and are therefore extremely impractical. On the other hand, nitrate is toxic to wounds and cells, and appears to decrease healing thus offsetting to some degree the antimicrobial effect of silver. Moreover, the reduction of nitrate to nitrite can cause cell damage, which is most likely the reason for the impaired re-epithelialization when used in partial thickness burns or donor sites.

Silver(I) complexes have been reported to show a different antimicrobial spectrum against microorganisms compared to the spectra of the ligand itself and the hydrated silver(I) ion [80]. Amongst the few silver(I) complexes, silver sulfadiazine complex (AgSD) is commonly prescribed today for the treatment of burns and wounds [81]. AgSD , introduced by Fox [82] in the 1970s, is usually used as a 1% water-soluble cream [83] and the additive in polymer or biopolymer composites [84, 85].

It has recently been reported that silver(I) complexes with hard donor atoms [i.e., complexes with silver(I)-N and silver(I)-O bonds] exhibit an excellent and wide spectrum of antimicrobial activities [86]. Yesilel et al. [87] have synthesized five new silver(I)-saccharinate complexes. In the complex with the molecular structure of $[\text{Ag}_2(\text{sac})_2(\text{tmen})_2]$ (sac = saccharinate, tmen = N,N,N',N'-tetramethylethylenediamine), the sac ligand acted as a bridge to connect the silver centres through N or O atom in the imino or carbonyl groups, leading to the formation of an eight-membered bimetallic ring with a chair conformation (Fig. 2.6). The complexes showed a better antimicrobial activity against the studied wild-type and clinical bacterial isolates than the corresponding silver salts.

2.2.2 Silver Nanoparticles

Silver nanoparticles have been proved to be most effective nanomaterials due to the good antimicrobial efficacy against bacteria, viruses and other eukaryotic microorganisms. The nanoparticles synthesized by inert gas condensation and

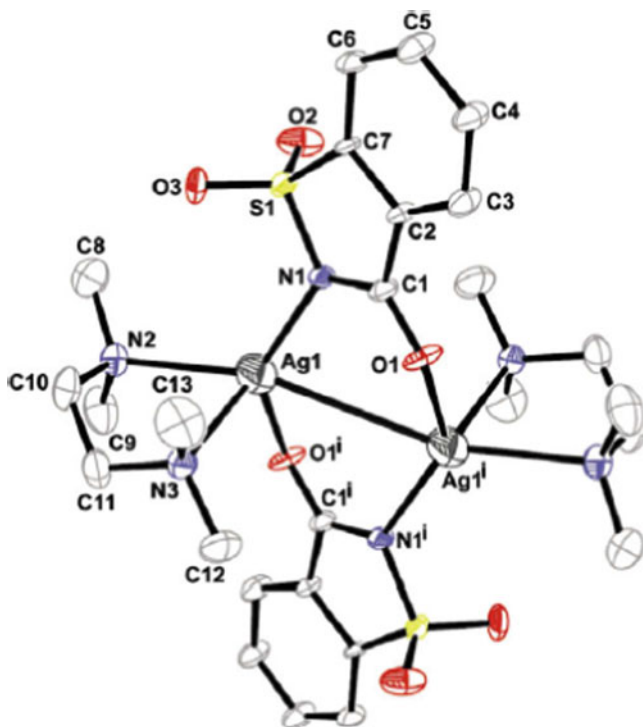


Fig. 2.6 Dimeric unit in $[Ag_2(sac)_2(tmen)_2]$ with the atom-labeling scheme and 50% thermal ellipsoids. H atoms have been omitted for clarity [Symmetry code: (i) 1-x, 1-y, 1-z] [87]

co-condensation techniques were observed to exhibit high antimicrobial activity at low concentrations. It is thought that the antimicrobial activity is related to their specific surface area, and the larger specific surface area generally leads to higher antimicrobial activity [88].

Morones et al. [89] studied the effect of silver nanoparticles on Gram-negative bacteria using high-angled annular dark field microscopy (HAADF) and TEM. The effect of different concentrations of silver nanoparticles with the size of about 16 nm on the growth of bacteria demonstrated that there was no significant bacterial growth observed at a concentration above 75 $\mu\text{g/mL}$. The HAADF images show that the smaller sized nanoparticles (~5 nm) depicted more efficiently antimicrobial activity. Panacek et al. [90] found the silver nanoparticles synthesized by a one-step protocol have high antimicrobial and bactericidal activity on Gram-positive and Gram-negative bacteria including multiresistant strains such as methicillin-resistant *Staphylococcus aureus*. They found that antimicrobial activity of silver nanoparticles was size dependent, and that nanoparticles 25 nm in size possessed the highest antimicrobial activity.

Pal et al. [91] investigated the antimicrobial properties of silver nanoparticles of different shapes, and found that silver concentration for the inhibition of bacterial

growth by spherical nanoparticles was 12.5 $\mu\text{g/mL}$, while it was 1 $\mu\text{g/mL}$ by the truncated triangular nanoparticles. Therefore, they concluded that the antimicrobial efficacy of silver nanoparticles is shape dependent.

Shahverdi et al. [92] investigated the combination effects of silver nanoparticles with antibiotics. It was observed that the antimicrobial activity of antibiotics like penicillin G, amoxicillin, erythromycin, clindamycin, and vancomycin increased in the presence of silver nanoparticles against *E. coli* and *S. aureus*. Ingle et al. [93] investigated the use of *Fusarium accuminatum*, isolated from infected ginger, for the synthesis of silver nanoparticles and analyzed its antimicrobial activity against human pathogenic bacteria. Results revealed that the antimicrobial activity of silver nanoparticles is 2.4–2.9 times that of silver ions.

2.2.3 Silver/Inorganic Nanocomposites

The incorporation of silver nanoparticles into solid inorganic materials in a controlled way can facilitate the application of the nanoparticles or combine the properties of the nanoparticles and the inorganic matrixes to produce some novel properties that are beyond those of the individual component alone.

Recently, it was reported that doping TiO_2 with silver greatly improved the photocatalytic inactivation of bacteria and viruses. Reddy et al. [94] demonstrated that 1 wt% silver in TiO_2 reduced the reaction time required for complete removal of 10^7 cfu/mL *E. coli* from 65 to 16 min under UV light irradiation. Silver nanoparticles in TiO_2 are believed to enhance photoactivity by facilitating electron–hole separation and/or providing a larger specific surface area for the adsorption of bacteria. Additionally, Ag/ TiO_2 nanocomposites can be excited by the visible light due to the plasmon effect of silver nanoparticles, then produce the electron–hole pairs which are capable of destroying the bacteria [95]. Therefore, Ag/ TiO_2 nanocomposites show promising antimicrobial activity under visible light irradiation.

Kim et al. [96] synthesized hybrid structures of Ag/ SiO_2 nanocomposites by the one-pot sol–gel method to prevent aggregation of Ag nanoparticles and increase their antimicrobial abilities. The antimicrobial properties of Ag/ SiO_2 nanocomposites annealed below Tammann temperature were excellent because silver nanoparticles were formed on the surface of SiO_2 nanoparticles without aggregation, while they were drastically decreased above Tammann temperature due to the growth of silver crystals. The above-mentioned nanocomposites annealed at the different temperatures of 25°C and 800°C could more effectively kill the Gram-negative bacteria than Gram-positive bacteria, because of the positive charged silver nanoparticles reacting easily with the former bacteria rather than the latter.

Ag/carbon nanocomposites were prepared by impregnating carbon materials (such as carbon fibers) into silver ions solution and then reducing the silver ions to metallic form [97, 98]. For example, silver ions were absorbed into a carbon matrix and then exposed to the fungus *Aspergillus ochraceus* to form intracellular silver

nanoparticles, and finally the prepared nanocomposites were heat treated in a nitrogen environment. The experimental results revealed that Ag/carbon nanocomposites possess excellent antimicrobial properties against both bacteria and viruses and have sustained activity due to silver nanoparticles firmly embedded into the carbonaceous matrix. It is anticipated that the composites of 1D carbon nanomaterials (carbon nanofibers or carbon nanotubes) and silver nanoparticles can contribute to antimicrobial efficiency [99]. Carbon nanofibers or nanotubes wrapped by silver nanoparticles (Ag/CNF or Ag/CNT) were fabricated via a facile and environmentally benign route with the assistance of supercritical carbon dioxide. The minimum inhibitory concentration (MIC) for Ag/CNF or Ag/CNT nanocomposite against *E. coli* is 0.5%, indicating that both the nanocomposites possessed the good antimicrobial activity [76]. Figure 2.7 shows the antimicrobial activities of Ag/CNT nanocomposite.

Ag/graphene oxide (Ag/GrO) nanocomposites were prepared by the chemical reduction of AgNO_3 in graphene oxide (GrO) suspension [100]. The size and shape of silver nanoparticles on the surface of GrO sheets was controlled by changing the concentration of AgNO_3 solution. The as-prepared Ag/GrO nanocomposites can efficiently inactivate Gram-negative bacteria such as *E. coli* and *P. aeruginosa*.

2.2.4 Silver–Polymer Nanocomposites

Silver–polymer nanocomposites, providing the antimicrobial efficacy with a sustained release of silver, have been synthesized with a great deal of effort to

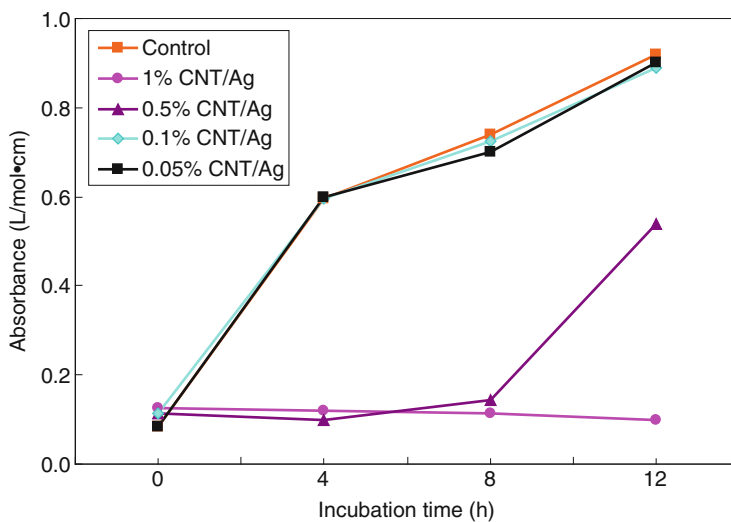


Fig. 2.7 Growth inhibition by Ag/CNT nanocomposites of various concentrations against *E. coli* [76]

prevent diseases in public health hygiene [101, 102]. Due to the stabilization of macromolecules, silver nanoparticles in a polymer matrix are more difficult to aggregate while the antimicrobial activity of silver–polymer nanocomposites is usually higher than that of silver nanoparticles and silver complexes at the same silver concentration [103, 104]. Kong et al. [105] prepared poly(methyl methacrylate) (PMMA) nanofiber containing silver nanoparticles by radical-mediated dispersion polymerization and investigated its antimicrobial activity against both Gram-negative and Gram-positive bacteria. The results showed that the silver–polymer nanofiber had an enhanced killing rate and effective antimicrobial activity than that of AgNO_3 . Figure 2.8 shows the plot of % reduction versus contact time (min) of different silver compounds on *E. coli*.

Silver-loaded acetate hollow fibers also show good antimicrobial activity. Composite membranes containing a 50-nm-thick chitosan layer on a poly(acrylic acid)/poly(ethylene glycol) diacrylate layer were found to exhibit potent antimicrobial activity towards Gram bacteria, and the antimicrobial activity of the membrane improved with increasing chitosan content [106]. In a similar way, nanocomposite membranes incorporating other functional (e.g., catalytic, photocatalytic, and antimicrobial) nanoparticles into water treatment membranes can be developed.

A recent study has reported on in vitro antimicrobial activity and in vitro cell compatibility of poly-(3-hydroxybutyrate-co-3-hydroxyvalerate) (PHBV) nanofibers loaded with metallic silver particles of a size of 5–13 nm [107]. Of the results, only silver-containing PHBV nanofibrous scaffolds showed a high antimicrobial activity and an inhibitory effect on the growth of both *S. aureus* and *Klebsiella pneumoniae* bacteria (Fig. 2.9). Moreover, the nanofibrous scaffolds having silver nanoparticles

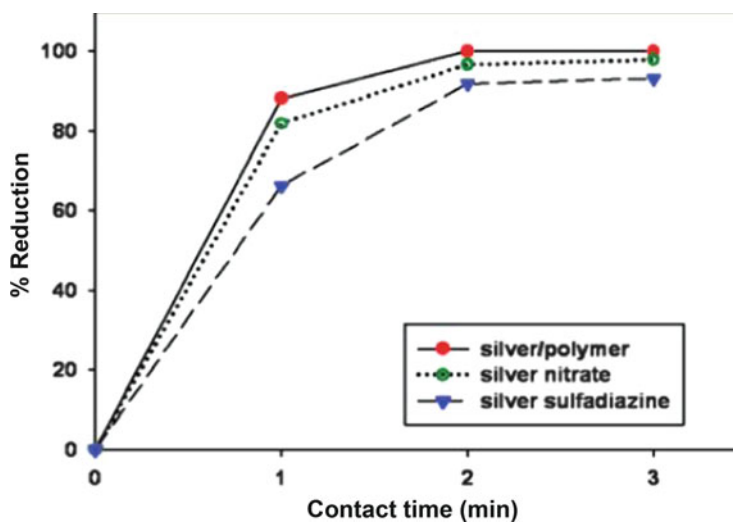


Fig. 2.8 The plot of % reduction versus contact time (min) of different silver compounds on *Escherichia coli* [105]

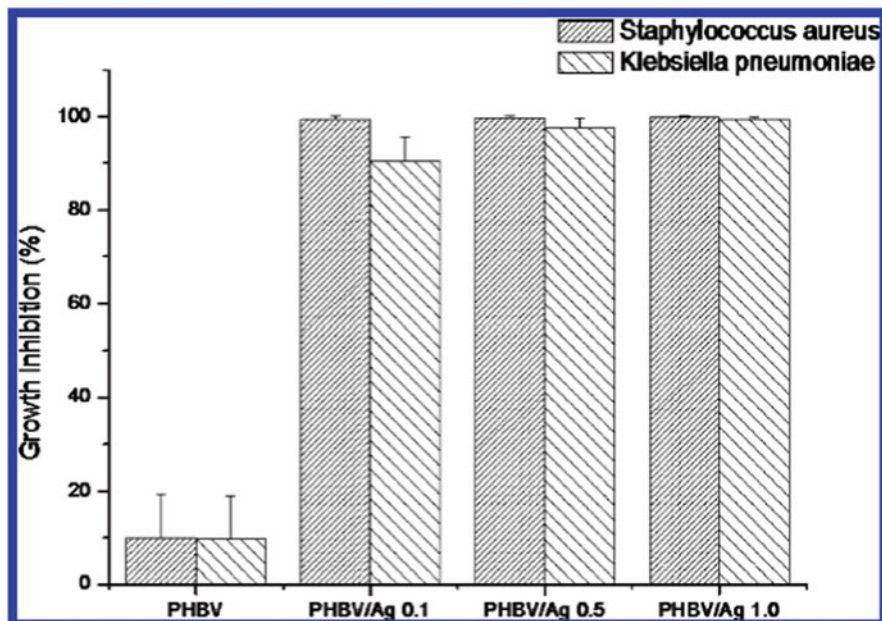


Fig. 2.9 Growth inhibition of PHBV nanofibrous scaffolds with different amounts of silver against *Staphylococcus aureus* and *Klebsiella pneumoniae* [107]

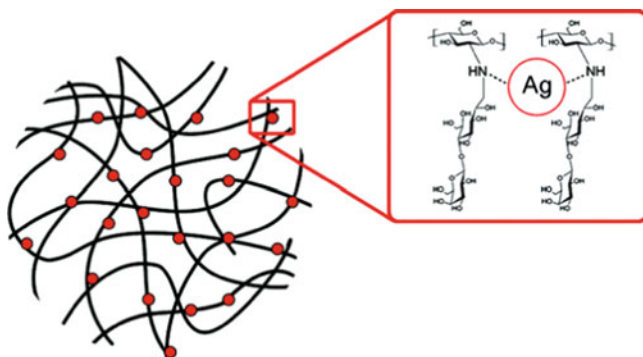


Fig. 2.10 Schematic representation of the polymeric chains of Chitlac providing the nitrogen atoms for the coordination and stabilization of silver nanoparticles [108]

<1.0% were free of in vitro cytotoxicity. Thus, the prepared nanofibrous scaffolds were considered to have a potential to be used in joint arthroplasty.

Travan et al. [108] prepared antimicrobial non-cytotoxic silver–polysaccharide nanocomposites with the polymeric chains of Chitlac providing the stabilization of silver nanoparticles (the schematic representation of the nanocomposites is shown in Fig. 2.10). The results show that these nanocomposite systems display a very

effective bactericidal activity toward both Gram-positive and Gram-negative bacteria. However, the hydrogel does not show any cytotoxic effect toward three different eukaryotic cell lines. This novel finding could advantageously contribute to responding to the growing concerns on the toxicity of nanoparticles and facilitate the use of silver–biopolymer composites in the preparation of biomaterials.

2.3 Antimicrobial Mechanisms of Silver-Based Nanocomposites

The study of antimicrobial mechanisms of silver-based nanocomposites offers a valuable contribution to nanobiotechnology. The antimicrobial nanocomposites with their unique chemical and physical properties could be synthesized on the basis of the antimicrobial mechanisms. Therefore, the diverse silver-based nanocomposites could be used to fight infections and prevent spoilage in a broader biological field.

The possible antimicrobial mechanism of silver ions, silver nanoparticles, and silver-based nanocomposites on the microbes has been suggested according to the morphological and structural changes found in the bacterial cells. In general, the antimicrobial mechanism of silver materials is linked with the interaction between silver atoms (ions) and thiol groups in the respiratory enzymes of bacterial cells [109].

One antimicrobial mechanism of silver ions has been reported with silver ions reacting with proteins by attaching the thiol group and then inactivating the proteins [110, 111]. The detailed explanation for the mechanism can be seen in Sects. 1.1–1.3 of Chap. 1

Another mechanism is believed to be that silver ions interact with three main components of the bacterial cell to produce the bactericidal effect: (1) the peptidoglycan cell wall and the plasma membrane, causing cell lysis; (2) the bacterial (cytoplasmic) DNA, preventing DNA replication; and (3) the bacterial proteins, disrupting protein synthesis (Fig. 2.11) [112].

It has been reported that the mode of antimicrobial action of silver nanoparticles is similar to that of silver ions. However, silver nanoparticles show more efficient antimicrobial properties because of their much larger specific surface area than that of ordinary solid silver salts. The nanoparticles firstly get attached to the cell membrane and also penetrate the bacteria, then interact with the sulfur-containing proteins in the bacterial membrane as well as with the phosphorus-containing compounds like DNA, and finally destroy the respiratory chain and lead the bacterial cells to death. In addition, the silver nanoparticles release silver ions in the bacterial cells, which can further enhance their bactericidal activity [89, 113]. Sondi et al. [114] reported on antimicrobial activity of silver nanoparticles against *E. coli* as a model for Gram-negative bacteria. From the SEM micrographs, the formation of aggregates composed of silver nanoparticles and dead bacterial cells were observed. It was also observed that the silver nanoparticles interacted with the building elements of the bacterial membrane and caused damage to the cell. The TEM

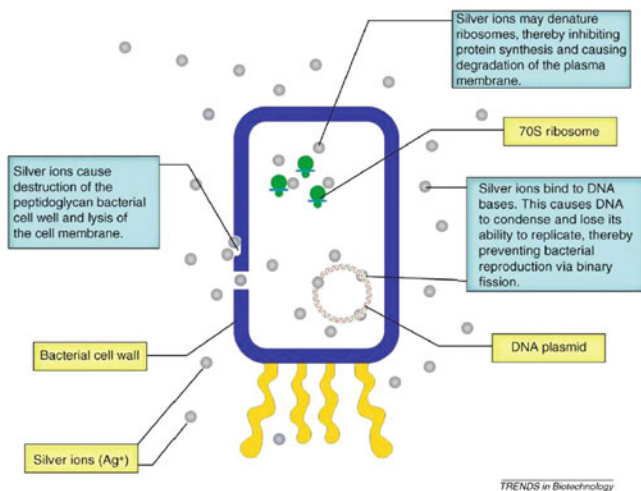


Fig. 2.11 Mechanisms of the antimicrobial activity of silver ions [112]

analysis and EDAX study confirmed the incorporation of silver nanoparticles into the membrane, which was recognized by the formation of pits on the cell surface.

However, because those studies include both positively charged silver ions and negatively charged silver nanoparticles, it is insufficient to explain the antimicrobial mechanism of positively charged silver nanoparticles. Therefore, we expect that there is another possible mechanism. Amro et al. [115] suggested that metal depletion may cause the formation of irregularly shaped pits in the outer membrane and change the membrane permeability, which is caused by progressive release of lipopolysaccharide molecules and membrane proteins. Although their inference involved some sort of binding mechanism, the mechanism of the interaction between silver nanoparticles and components of the outer membrane is still unclear.

Another mechanism of the growth-inhibitory effects of silver nanoparticles on microorganisms has been speculated by the Electron Spin Resonance (ESR) spectroscopy study of silver nanoparticles [116]. It has been revealed that the growth inhibition of bacteria may be related to the formation of free radicals from the surface of silver. Uncontrolled generation of free radicals can attack membrane lipids and then lead to a breakdown of membrane function [117]. Kim et al. [118] suggested that the antimicrobial mechanism of silver nanoparticles is related to the formation of free radicals and subsequent free radical-induced membrane damage. They confirmed that the antimicrobial activity of silver nanoparticles and silver nitrate was influenced by NAC (N-acetylcysteine), and also suggested that free radicals, probably derived from the surface of silver nanoparticles, were responsible for the anti-microbial activity through ESR.

The silver nanoparticles with smaller size possess a larger surface area to contact with the bacterial cells, and hence will have a higher antimicrobial activity than those bigger nanoparticles [119]. Panacek et al. [90] prepared a series of silver nanoparticles by the reduction of the $\text{Ag}(\text{NH}_3)_2^+$ complex cation by saccharides, and

found that Ag nanoparticles synthesized using disaccharides (such as maltose and lactose) have a much higher antimicrobial activity than those synthesized using monosaccharides (such as glucose and galactose). They investigated the sizes of the silver nanoparticles by TEM and concluded that silver nanoparticles prepared from disaccharide have a smaller size than those from monosaccharide. Therefore, they thought that the observed antimicrobial activity of silver nanoparticles is related to their size.

The antimicrobial efficacy of silver nanoparticles also depends on the shapes of the nanoparticles, which can be confirmed by studying the inhibition of bacterial growth by silver nanoparticles with different shapes [91]. Silver nanoparticles with different shapes (triangular, spherical, and rod) were tested against typical bacteria such as *E. coli*. The {111} facets of silver crystals have high-atom-density, which is favorable to the reactivity of silver. A triangular nanoplate has a high percentage of {111} facets whereas spherical and rod-shaped silver nanoparticles predominantly have {100} facets. According to Pal et al. [91], truncated triangular nanoparticles show bacterial inhibition with silver content of 1, 12.5 $\mu\text{g/L}$ for the spherical nanoparticles, and 50–100 $\mu\text{g/L}$ for the rod-shaped nanoparticles.

Enhanced antimicrobial activities have been reported in silver nanoparticles modified by surfactants, such as SDS and Tween 80, and in polymers, such as PVP 360 [120]. The results are presented in Fig. 2.12. The antimicrobial activity was significantly enhanced for most of the species when silver nanoparticles were modified by SDS while not significant when nanoparticles were modified by Tween 80. This result can be explained as follows [121]: (1) SDS provides more stability for silver nanoparticles than Tween 80, resulting in the decrement of nanoparticle aggregation; and (2) SDS is an ionic surfactant and may have the ability to penetrate or disrupt the cell wall, particularly of Gram-positive strains. The antimicrobial activities of PVP-modified silver nanoparticles were significant because the polymer is most effective in stabilizing particles against aggregation.

2.4 Applications of Silver-Based Antimicrobial Nanocomposites

It has been mentioned that microorganisms with resistance to the antimicrobial activity of silver are exceedingly rare [122, 123]. For decades, silver-based nanocomposites have been used extensively as antimicrobial agents in a number of areas, including medical and pharmaceutical, textile and fiber, coating and paint, food storage, and environmental applications.

2.4.1 Applications in the Medical and Pharmaceutical Industry

Silver has been used for the treatment of medical ailments for over 100 years due to its natural antimicrobial and antifungal properties [124]. Silver ions, silver

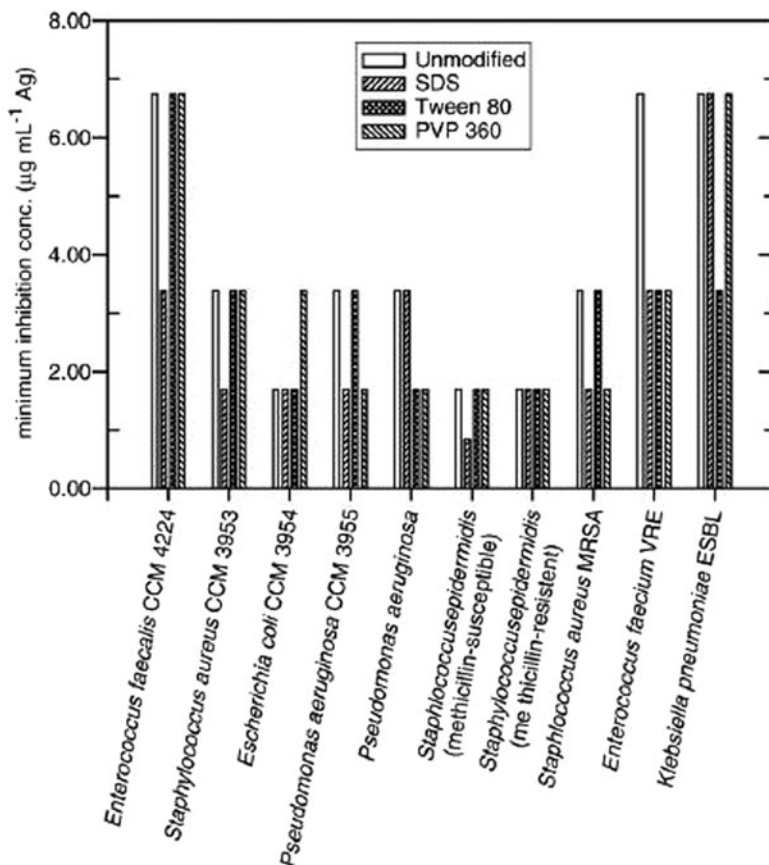


Fig. 2.12 A plot of minimum inhibition concentration (MIC) of the Ag nanoparticles prepared by the modified Tollens process with D-maltose and consequently modified by addition of SDS, Tween 80, and PVP 360 in a concentration of 1% (w/w) [120] (Data used with permission from the American Chemical Society)

compounds and polymer-supported silver nanoparticles have been widely used in various biomedical fields, such as wound dressing materials, body wall repairs, disinfecting medical devices, tissue scaffolds, antimicrobial filters [63], and so on.

2.4.1.1 Wound Dressing Materials

Silver has been used extensively for the treatment of burns, with silver ions or silver nanoparticles incorporated into bandages for use in large open wounds [125]. Many silver-coated and silver-containing dressings are now available for the treatment of wounds [126].

Silver sulfadiazine has been widely accepted as the standard treatment for burn injuries in both animals and humans [127]. It produces better healing of burn wounds due to its slow and steady reaction with serum and other body fluids [128].

The use of silver in the past has been restrained by the need to produce silver as a compound, thereby increasing the potential side effects. Nanotechnology has provided a way of reducing pure silver nanoparticles. This system also markedly increases the release rate of silver. The silver nanoparticles are reported to show better wound healing capacity, better cosmetic appearance, and scarless healing when tested using an animal model [129].

Nanocrystalline silver dressings, creams, and gel effectively reduce bacterial infections in chronic wounds [130, 131]. For example, the electrospun silver/poly(vinyl alcohol) fiber web show efficient antimicrobial property as a wound dressing [132, 133]. The silver/poly(N-vinyl-2-pyrrolidone) composite functioned as a bactericide applied in complicated cases of infected burns and purulent wounds. Pape et al. [134] developed an activated carbon fiber after-treated with silver nanoparticles. Yeo et al. [135] applied silver nanoparticles to produce antimicrobial as-spun mono-filament yarns. Fernández et al. [136] have developed silver nanoparticles on cellulose fibers to be used as the absorbent pad. They immersed fluff pulp and nano-structured lyocell fibers in silver nitrate and the subsequent transformation to silver nanoparticles were done by physical (thermal or UV) or chemical (sodium borohydride) methods. Fu et al. [137] have produced multi-layer composite films from heparin/chitosan/silver for biomedical applications. Khundkar et al. [138] presented an evaluation of the evidence available regarding the use of Acticoat™ (registration certificate number: SFDA 20043640127, made by Smith & Nephew, UK) in burn wounds. The studies show that the non-charged form of silver (Ag^0) in Acticoat™ reacts much more slowly with chloride and thus is deactivated less rapidly in wounds and does not need a carrier. In vitro studies confirm that Acticoat™ provides a sustained release of silver, lasting for a few days. In contrast, the silver ions released from silver nitrate are deactivated within a few hours.

2.4.1.2 Tissue Scaffolds

Bone cement is used for the secure attachment of joint prostheses in, for example, hip and knee replacement surgery. Silver nanoparticles has been used as an antimicrobial additive to poly(methyl methacrylate) (PMMA) bone cement. Ag-PMMA bone cement has been suggested as a means to decrease the incidence of resistance through its multifaceted mechanism of action, and has further shown impressive in vitro antimicrobial activity and low cytotoxicity [139].

Considering the large surface and strong adsorption properties of hydroxyapatite nano-ribbon to adsorb bacteria and high bioactivity of silver nanoparticles, the hydroxyl apatites nano-ribbon spherites containing silver nanoparticles have been successfully prepared by Liu et al. [140]. Hydroxy apatite/silver composite coating has been designed particularly for reducing bacterial infections after implant

placement [141]. Bioactivity, dissolution range, and resorption properties, which are close to those of natural bones, have presented in hydroxyapatite, so this material and its composites are the excellent candidates for wide applications in coating artificial joints and tooth roots. Vojislav et al. [142] synthesized the monophasic silver-doped hydroxyapatite nanopowders with high crystallinity and examined their antimicrobial and hemolytic activities. The atomic force microscopic studies illustrate that silver-doped hydroxyapatite samples cause considerable morphological changes of microorganism cells which might be the cause of cell death. Hemolysis ratios of the silver-doped hydroxyapatite samples were below 3%, indicating the good blood compatibility and promising biomaterials for tissue scaffolds. Kumar et al. [143] developed novel β -chitin/nanosilver composite scaffolds for wound healing applications using β -chitin hydrogel with silver nanoparticles. The prepared β -chitin/nanosilver composite scaffolds were bactericidal against *E. coli* and *S. aureus* and also showed good blood-clotting ability. Cell attachment studies using vero (epithelial) cells showed that the cells were well attached on the scaffolds.

2.4.1.3 Implantable Devices

Silver-impregnated medical devices like surgical masks and implantable devices show significant antimicrobial efficacy [144]. For example, poly(ethylene terephthalate) (PET) has been widely used in cardiovascular implants because of its excellent mechanical properties and moderate biocompatibility. However, the infection and thrombogenicity commonly exist in this kind of cardiovascular implants, which can lead to significant morbidity and mortality [145]. Fu et al. [137] has successfully prepared natural polyelectrolyte multilayer films containing nanosilver on aminolyzed PET film via a layer-by-layer fashion. The multilayer films containing well-dispersed nanosilver were effective in killing *E. coli*, and had good anticoagulation activity and low cell toxicity. The above investigated films with biocompatibility may have good potentials for surface modification of medical devices, especially for cardiovascular implants.

2.4.1.4 Disinfecting Medical Devices

The high incidence of infections caused by the use of implanted biomedical devices has a severe impact on human health and health care costs. Many studies suggest a strong antimicrobial activity of silver-coated medical devices [146]. These devices, such as dressings, heart valves, central venous catheters and urinary catheters, have been proved to effectively reduce the infections [147].

The silver-coated silicone catheters are effective at reducing the incidence of catheter-associated urinary tract infections and resistant organisms in an acute care hospital. In a randomized clinical study, a silver alloy-coated central venous catheter reduced the infection rate by 50% although there was no reduction of

catheter colonization or of catheter-associated sepsis. Akiyama and Okamoto [148] first described the use of a silver-coated urinary catheter in an uncontrolled study of 102 patients in which no episodes of bacteriuria occurred. Other research has also shown that there was a statistically significant difference in the occurrence of bacterial infection (defined as $>10^5$ organisms/mL) in patients treated with a silver alloy-coated catheter as compared to those treated with a standard device.

2.4.1.5 Biomedicine

Silver nanoparticles have been used to exhibit antimicrobial efficacy against viral particles. The recent emergence of nanotechnology has provided a new therapeutic modality in silver nanoparticles for use in medicine.

Monkeypox virus (MPV), an orthopoxvirus similar to variola virus, is the causative agent of monkeypox in many species of non-human primates [149]. Silver nanoparticles have been shown to exhibit promising cytoprotective activities towards HIV-infected T cells; however, the effects of these nanoparticles towards other kinds of viruses remain largely unexplored. Recently, a study revealed the potential cytoprotective activity of silver nanoparticles toward HIV-1 infected cells [150]. Thus, the use of silver nanoparticles as an anti-viral therapeutic may be a new area of developing nanotechnology-based anti-viral therapeutics.

In addition, many attempts have been made to use silver nanoparticles as an anti-cancer agent. The discovery of an anti-cancer mechanism would be a milestone for cancer treatment. The key to the mechanism is the specific binding of silver nanoparticles towards cancer cells but not the other body cells. One possible reason for this result could be because of the morphological differences between cancer cells and the other body cells, e.g., the morphology of cancer cells is more favorable to the anti-cancer activity of silver nanoparticles [151].

2.4.2 Antimicrobial Food Packaging

Antimicrobial packaging is a promising form of active food packaging material to prevent bacterial infection in foodstuffs. If silver-based antimicrobial nanocomposites are incorporated into packaging materials, the microbial contamination can be controlled by reducing the growth rate of microorganisms. Since the antimicrobial silver can be released from the package during an extended period, the activity can also be extended into the transport and storage phase of food distribution [152].

Many efforts have been made to load and/or to incorporate silver nanoparticles into acceptable packaging materials such as filter paper, low density polyethylene (LDPE), and poly(methyl methacrylate) (PMMA). Also, numerous biodegradable materials, e.g. polysaccharides (such as starch, chitosan, alginate, and konjak glucomannan) have been used to fabricate silver nanoparticle-based composite films. For example, silver zeolite has been developed as the most common

antimicrobial agent incorporated into plastics and used in food preservation, disinfection and decontamination of products [153]. The zeolite, in which some of surface atoms are replaced by silver atoms which are laminated as a thin layer (3–6 nm) in the surface of the food-contact packaging polymers, continuously releasing silver ions when silver nanoparticles are exposed to the aqueous solution from the food [154].

Recently, some studies focus on making the filter paper with degradable nature as an attractive alternative for eco-friendly packaging materials. Tankhiwale et al. [155] developed ordinary filter papers as antimicrobial packaging material by grafting vinyl monomers like acrylamide on paper macromolecules followed by loading of silver nanoparticles. This newly developed material shows a strong antimicrobial property against *E. coli*.

2.4.3 Water Disinfection and Microbial Control

The presence of bacteria is the main indication of water contamination. A World Health Organization (WHO) investigation showed that 80% of disease is due to contaminated drinking water [156]. To overcome this problem, chemical agents and physical treatments including silver-based nanocomposites are commonly used.

Silver nanoparticles are of great value to waste water treatment and to biological systems. The inhibitory effects of silver nanoparticles on microbial growth were evaluated at a treatment facility using an extant respirometry technique. The nitrifying bacteria were susceptible to inhibition by silver nanoparticles, which have detrimental effects on the microorganisms in waste water treatment [157]. For example, Fe₃O₄ containing silver nanoparticles can be used for water treatment [158].

Basri et al. [159] prepared silver-filled asymmetric polyethersulfone (PES) membranes by a simple phase inversion technique. The silver nanoparticles were formed in PES membranes when polyvinylpyrrolidone (PVP) was added during dope preparation. The improved silver dispersion on membrane surfaces was able to enhance the antimicrobial activity against *E. coli* and *S. aureus*, and the investigated results confirmed that the Ag-PES membrane can inhibit almost 100% bacterial growth in rich medium, indicating the potential of Ag-PES to be used in antimicrobial applications especially in water treatment.

The water-related diseases like diarrhea and dehydration can be reduced by improving the quality of the drinking water. Lv et al. [160] prepared silver nanoparticle-decorated porous ceramic composites by fixing silver nanoparticles to the interior walls of porous ceramic channels with the aminosilane coupling agent, 3-aminopropyltriethoxy silane (APTES), as a connecting bridge. On-line tests show that, at a flow rate of 0.01 L/min, the output count of *E. coli* was zero when the input water had a bacterial load of $\sim 10^5$ colony-forming units (CFU) per millilitre.

Combined with low cost and effectiveness in prohibiting the growth of *E. coli*, such materials should have wide applications in drinking water treatment.

To sum up, as antimicrobial agents, silver-based materials were applied in a wide range of applications from medical devices to water treatment. Therefore, the silver nanoparticles with their unique chemical and physical properties are proving an alternative for the development of new antimicrobial agents.

2.5 Toxicology of Silver-Based Antimicrobial Nanocomposites

With increasing public knowledge about health care in the world, people are more and more concerned about the rise of possible subsequent diseases caused by new technologies, including nanotechnology and the application of nano-materials especially through inhalation during manufacturing or usage.

Silver-based nanocomposites have been introduced as materials with good potentiality to be extensively used in biological and medical applications. The therapeutic property of silver has shown that it is a safer antimicrobial agent in comparison with some organic antimicrobial agents [161, 162], principally due to its antimicrobial activities having low toxicity to human cells [163].

Some evidence has proved the safety of the application of silver-based materials. There are very few reports in the literature of silver toxicity despite large exposures to silver in the treatment of burn wounds [164]. Skin-innoxiousness of silver nano-colloidal solution especially in the case of smaller nanoparticles has been demonstrated via the skin irritation test performed on rabbits [165]. Hendi et al. [166] reported that silver nanoparticles can promote wound healing and reduce scar appearance in a dose-dependent manner. Furthermore, the experimental results show that silver nanoparticles act by decreasing inflammation, and there were no side effects on the liver and kidney functions through a rat model. The potential benefits of silver nanoparticles in all wounds can therefore be enormous. Nontoxicity of the interaction of silver nanoparticles and the membrane surface has been proved by growing human fibroblasts on various concentrations of silver nanoparticles [167]. Jeong et al. applied a silver–sulfur (Ag/S) composition and observed that addition of sulfur enhances the antimicrobial properties and the stability of silver ions. They emphasized that the Ag/S composite is nontoxic even though sulfur is a toxic agent [168]. Ag/S nano-colloidal solution (SNSE) has also been used by Ki et al. for functionalization of wool [169].

Silver nanoparticles in most studies are suggested to be nontoxic. But some reports state that the biological activity of silver nanoparticles can be detrimental. Many nanoparticles are small enough to have access to skin, lungs, and brain [170]. Exposure of metal-containing nanoparticles to human lung epithelial cells generated reactive oxygen species, which can lead to oxidative stress and cellular damage. Nanoparticles and reactive oxygen production have an established link in vivo. Therefore, it is important to study the potential for the application of silver nanoparticles in the treatment of diseases that require maintenance of circulating

drug concentrations or targeting of specific cells or organs [171, 172]. Burd et al. [173] studied the cytotoxicity of five silver nanoparticle-impregnated commercially available dressings, and found that three of the silver dressings showed cytotoxicity effects in keratinocytes and fibroblast cultures. Braydich-Stolle et al. reported the toxicity of silver nanoparticles on C18-4 cells, a cell line with spermatogonial stem cell characteristics [74]. Both studies showed that the cytotoxicity of silver nanoparticles to mitochondrial activity increased with the increase in their concentration.

The comprehensive biologic and toxicologic information of silver nanoparticles is explored by Ahamed et al. [174], while the sources of their exposure and associated risk to human and environmental health are described schematically in Fig. 2.13.

The potent anti-inflammatory properties of silver ions and nanoparticles on a wound have been demonstrated histologically. Most of the reports are purely descriptive in nature identifying the decrease in erythema and increased healing. However, it must be realized that not all silver is anti-inflammatory, and that the anti-inflammatory properties depend on the delivery vehicle, the available concentration and species of silver, and the duration of release [175, 176]. Investigation of bio-innocuousness of silver revealed that smaller-sized silver particles are less toxic to skin than larger ones at the same concentration. Although a small irritation has been reported by applying the colloidal silver with 30-nm particle size, colloidal silver with a particle size of 2–3 nm has been known to be innocuous [177].

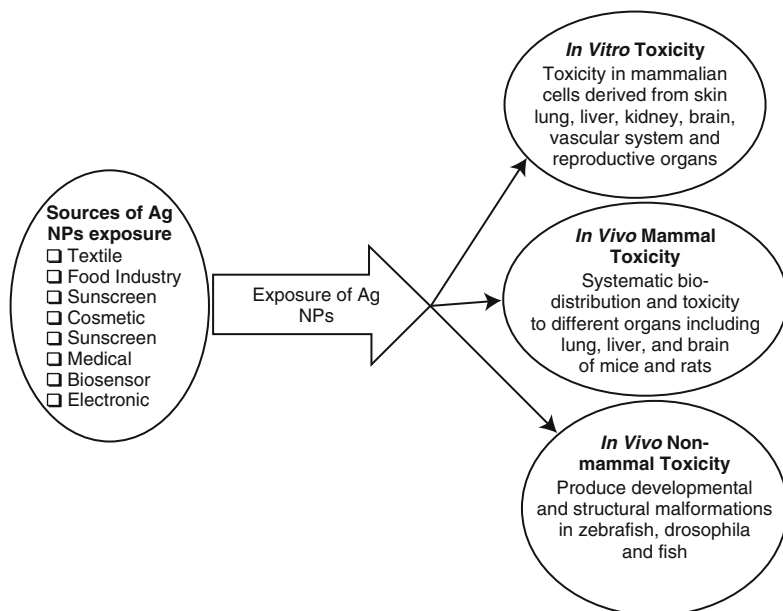


Fig. 2.13 Sources of silver nanoparticles exposure and its known adverse effects [174]

Argyria, a permanent disorder caused by silver deposition in the skin's microvessels in patients who are exposed to chronic silver toxicity [178], is only seen following large oral or inhaled intakes of silver dust or colloidal silver over an extended period of time, and has never been reported as a result of topical application. In addition, prolonged topical application of silver sulfadiazine cream can induce argyria even though it has never been reported as a result of topical application except locally [179]. *In vitro* studies showed that silver sulfadiazine is cytotoxic but that the cytotoxicity can be reduced by controlling the delivery of the active agent [180].

Additionally, silver nanoparticles are suggested to be hazardous to the environment due to their small size and variable properties [181]. The environmental risk of silver nanoparticles was recently investigated by determining released silver from commercial clothing (socks). The sock material and wash water contained silver nanoparticles of 10–500 nm diameter. The fate of silver in waste water treatment plants (WWTPs), which could treat a high concentration of influent silver, was also examined. The model suggested that WWTPs are capable of removing silver at concentrations much more than expected from the silver nanoparticles-containing consumer products. However, silver concentrations in the biosolids may exceed the concentration (5 mg/L), established by the USEPA. This may restrict the fertilizer application of biosolids to the agricultural lands.

Reactive oxygen species (ROS) generation and oxidative stress appear to be two possible mechanisms of silver nanoparticles toxicity [182]. Depletion of glutathione and protein bound sulfhydryl groups and changes in the activity of various antioxidant enzymes indicative of lipid peroxidation have been implicated in oxidative damage [183]. Oxidative stress occurs when generation of ROS exceed the capacity of the anti-oxidant defense mechanism. ROS and oxidative stress elicit a wide variety of physiologic and cellular events including stress, inflammation, DNA damage and apoptosis [184]. A number of investigators reported that cytotoxicity, DNA damage and apoptosis induced by silver nanoparticles were mediated through membrane lipid peroxidation, ROS and oxidative stress [185]. Mitochondria appear to be sensitive targets for silver nanoparticles toxicity. Asharani et al. suggested that the disruption of the mitochondrial respiratory chain by silver nanoparticles increased ROS production and interruption of ATP synthesis, thus leading to DNA damage. Interaction of silver nanoparticles with DNA led to cell cycle arrest at the G2/M phase [186]. Possible mechanisms of silver nanoparticle-induced toxicity are described in Fig. 2.14.

From the above studies, it can be concluded that longer-term studies and monitoring of humans exposed to silver nanoparticles are imperative to evaluate any potential toxicity. Care must also be taken in the use of silver-based antimicrobials in everyday applications so that the burden of silver ion and nanoparticles exposure does not exceed subtoxic levels. Furthermore, the environmental impact of silver ions and nanoparticles, which leach into the water system, must be considered to prevent ecological disaster.

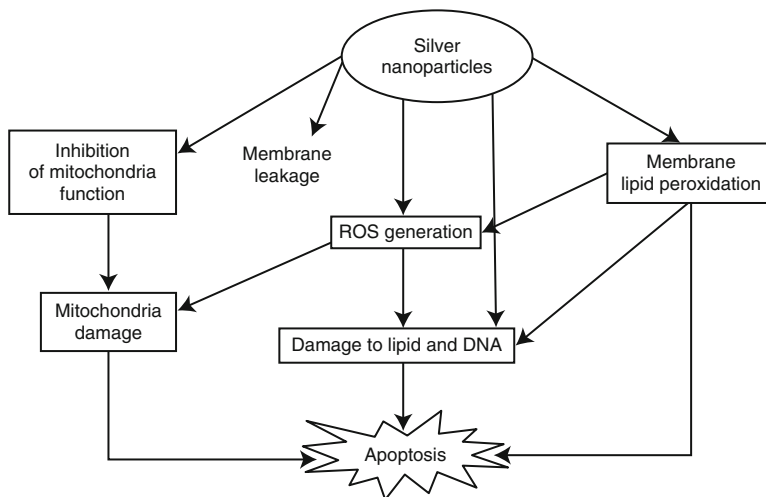


Fig. 2.14 Possible mechanism for silver nanoparticle-induced toxicity [186]

2.6 Future Perspectives

Silver-based nanomaterials exhibit remarkable biological and antimicrobial properties in many fields, and silver nanoparticle dressings are now the new gold standard for medical application. Implantable medical devices, such as neurosurgical and venous catheters, have greatly benefited from the broad antimicrobial activity of silver nanoparticles by reducing both patient infection and dependence on antibiotic use and the associated costs.

The application of silver-based nano-antimicrobials in biomedical and therapeutic applications has developed a wide area of nanotechnology, but the possible side effects of silver ion and nanoparticles have not been completely studied, and hence, detailed studies are needed before the introduction to the market of products related to nano-antimicrobial materials.

References

1. Retchkiman-Schabes PS, Canizal G, Becerra-Herrera R, Zorrilla C, Liu HB and Ascencio JA. Biosynthesis and characterization of Ti/Ni bimetallic nanoparticles. *Optical Materials*, 2006, 29: 95–99.
2. Gu H, Ho PL, Tong E, Wang L and Xu B. Presenting vancomycin on nanoparticles to enhance antimicrobial activities. *Nano Letters*, 2003, 3(9): 1261–1263.
3. Ahmad Z, Pandey R, Sharma S and Khuller GK. Alginate nanoparticles as antituberculosis drug carriers: formulation development, pharmacokinetics and therapeutic potential. *The Indian Journal of Chest Diseases & Allied Sciences*, 2005, 48: 171–176.
4. Chen X and Schluesener HJ. Nanosilver: a nanoparticle in medical application. *Toxicology Letters*, 2008, 176: 1–12.

5. Poon Vincent KM and Burd A. In vitro cytotoxicity of silver: implication for clinical wound care. *Burns*, 2004, 30: 140–147.
6. Mahendra R, Alka Y and Aniket G. Silver nanoparticles as a new generation of antimicrobials. *Biotechnology Advances*, 2009, 27: 76–83.
7. Gong P, Li H, He X, Wang K, Hu J and Tan W. Preparation and antibacterial activity of $\text{Fe}_3\text{O}_4@Ag$ nanoparticles. *Nanotechnology*, 2007, 18, 604–611.
8. Zahir MH, Suzuki T, Fujishiro Y and Awano M. Perovskites with cotton-like morphology consisting of nanoparticles and nanorods: their synthesis by the combustion method and their NO_x adsorption. *Applied Catalysis A*, 2009, 361: 86–92.
9. Li QL, Mahendra S, Delina YL, Lena B, Michael VL, Li D and Pedro JJ. Antimicrobial nanomaterials for water disinfection and microbial control: potential applications and implications. *Water Research*, 2008, 42: 4591–4602.
10. Andersson M, Pedersen JS and Palmqvist Anders EC. Silver nanoparticle formation in microemulsions acting both as template and reducing agent. *Langmuir*, 2005, 21(24): 11387–11396.
11. Das MR, Sarma RK, Saikia R, Kale VS, Shelke Manjusha V and Sengupta P. Synthesis of silver nanoparticles in an aqueous suspension of graphene oxide sheets and its antimicrobial activity. *Colloids and Surfaces B: Biointerfaces*, 2011, 83(1): 16–22.
12. Simchi A, Ahmadi R, Seyed Reihani SM and Mahdavi A. Kinetics and mechanisms of nanoparticle formation and growth in vapor phase condensation process. *Materials and Design*, 2007, 28: 850–856.
13. Phuoc TX, Soong Y and Chyu MK. Synthesis of Ag-deionized water nanofluids using multi-beam laser ablation in liquids. *Optics and Lasers in Engineering*, 2007, 45(12): 1099–1106.
14. Tsuji T, Mizuki T and Ozono S. Laser-induced silver nanocrystal formation in polyvinylpyrrolidone solutions. *Journal of Photochemistry and Photobiology A: Chemistry*, 2009, 206 (2–3): 134–139.
15. Tsuji T, Thang DH, Okazaki Y, Nakanishi M, Tsuboi Y and Tsuji M. Preparation of silver nanoparticles by laser ablation in polyvinylpyrrolidone solutions. *Applied Surface Science*, 2008, 254: 5224–5230.
16. Zheng M, Wang ZS and Zhu YW. Preparation of silver nanoparticle via active template under ultrasonic. *Transactions of Nonferrous Metals Society of China*, 2006, 16(6): 1348–1352.
17. Balan L, Malval JP, Schneider R, Nouen DL and Loungnot DJ. *In-situ* fabrication of polyacrylate-silver nanocomposite through photoinduced tandem reactions involving eosin dye. *Polymer*, 2010, 51(6): 1363–1369.
18. Gao F, Lu QY and Komarneni S. Interface reaction for the self-assembly of silver nanocrystals under microwave-assisted solvothermal conditions. *Chemistry of Materials*, 2005, 17(4): 856–860.
19. Jia HY, Xu WQ, An J, Li DM and Zhao B. A simple method to synthesize triangular silver nanoparticles by light irradiation. *Spectrochimica Acta Part A: Molecular and Biomolecular Spectroscopy*, 2006, 64(4): 956–960.
20. Wang W and Gu BH. Preparation and Characterization of Silver Nanoparticles at High Concentrations. *ACS Symposium Series*, Vol. 878, Chapter 1, pp. 1–14.
21. Li D, Hong BY, Fang WJ, Guo YS and Lin R. Preparation of well-dispersed silver nanoparticles for oil-based nanofluids. *Industrial and Engineering Chemistry Research*, 2010, 49(4): 1697–1702.
22. Gibbons Vernett L and Getman FH. The potential of silver in non aqueous solutions of silver nitrate. *Journal of American Chemical Society*, 1914, 36(10): 2091–2095.
23. Kora AJ, Sashidhar RB and Arunachalam J. Gum kondagogu (*Cochlospermum gossypium*): a template for the green synthesis and stabilization of silver nanoparticles with antibacterial application. *Carbohydrate Polymers*, 2010, 82(3): 670–679.
24. Yuan WY, Fu JH, Su K and Ji J. Self-assembled chitosan/heparin multilayer film as a novel template for in situ synthesis of silver nanoparticles. *Colloids and Surfaces B: Biointerfaces*, 2010, 76(2): 549–555.

25. Cheng WL, Dong SJ and Wang EK. Studies of electrochemical quantized capacitance charging of surface ensembles of silver nanoparticles. *Electrochemistry Communications*, 2002, 4(5): 412–416.
26. Zhang WZ, Qiao XL and Chen JG. Synthesis of silver nanoparticles-Effects of concerned parameters in water/oil microemulsion. *Materials Science and Engineering B*, 2007, 142: 1–15.
27. Narayanan KB and Sakhivel N. Biological synthesis of metal nanoparticles by microbes. *Advances in Colloid and Interface Science*, 2010, 156(1–2): 1–13.
28. Wagner J, Tshikhudo TR and Kohler JM. Microfluidic generation of metal nanoparticles by borohydride reduction. *Chemical Engineering Journal*, 2008, 135(15): S104–S109.
29. Yang ZQ, Qian HJ, Chen HY and Anker JN. One-pot hydrothermal synthesis of silver nanowires via citrate reduction. *Journal of Colloid and Interface Science*, 2010, 352(2): 285–291.
30. Miyoshi H, Ohno H, Sakai K, Okamura N and Kourai H. Characterization and photochemical and antibacterial properties of highly stable silver nanoparticles prepared on montmorillonite clay in n-hexanol. *Journal of Colloid and Interface Science*, 2010, 345(2): 433–441.
31. Tolaymat TM, Badawy Amro ME, Genaidy A, Kirk GS and Todd P. An evidence-based environmental perspective of manufactured silver nanoparticle in syntheses and applications: a systematic review and critical appraisal of peer-reviewed scientific papers. *Science of the Total Environment*, 2010, 408: 999–1006.
32. Sastry M, Ahmad A, Khan MI and Kumar R. Biosynthesis of metal nanoparticles using fungi and actinomycetes. *Current Science*, 2003, 85: 162–170.
33. Merin DD, Prakash S and Valentine Bhimba B. Antibacterial screening of silver nanoparticles synthesized by marine micro algae. *Asian Pacific Journal of Tropical Medicine*, 2010, 3: 797–799.
34. Narayanan KB and Sakhivel N. Biological synthesis of metal nanoparticles by microbes. *Advances in Colloid and Interface Science*, 2010, 156: 1–13.
35. Matthew ED, Schaeublin NM, Farrington KE, Hussain SM and Johnson GR. Lysozyme Catalyzes the formation of antimicrobial silver nanoparticles. *ACS Nano*, 2009, 3(4): 984–994.
36. Vigneshwaran N, Kathe AA, Varadarajan PV, Nachane RP and Balasubramanya RH. Silver-protein (core-shell) nanoparticle production using spent mushroom substrate. *Langmuir* 2007, 23: 7113–7117.
37. Xie JP, Lee JY and Wang DC. Silver nanoplates: from biological to biomimetic synthesis. *ACS Nano*, 2007, 1(5): 429–439.
38. Sun LL, Wei G, Song YH, Liu ZG, Wang L and Li Z. Fabrication of silver nanoparticles ring templated by plasmid DNA. *Applied Surface Science*, 2006, 252: 4969–4974.
39. Thirumurugan G, Shaheedha SM and Dhanaraju MD. In-vitro evaluation of antimicrobial activity of silver nanoparticles synthesized by using phytophthora infestans. *International Journal of ChemTech Research*, 2009, 3: 714–716.
40. Zezin AB, Rogacheva VB, Feldman VI, Afanasiev P and Zezin AA. From triple interpolyelectrolyte-metal complexes to polymer-metal nanocomposites. *Advances in Colloid and Interface Science*, 2010, 158: 84–93.
41. Mitra A and Bhaumik A. Nanoscale silver cluster embedded in artificial heterogeneous matrix consisting of protein and sodium polyacrylate. *Materials Letters*, 2007, 61: 659–662.
42. Zhang YW, Peng HS, Huang W, Zhou YF and Yan DY. Facile preparation and characterization of highly antimicrobial colloid Ag or Au nanoparticles. *Journal of Colloid and Interface Science*, 2008, 325: 371–376.
43. Karim MR, Lim KT, Lee CJ, Bhuiyan MT, Kim HJ, Park LS and Lee MS. Synthesis of core-shell silver-polyaniline nanocomposites by gamma radiolysis method. *Journal of Polymer Science Part A: Polymer Chemistry*, 2007, 45(24): 5741–5747.
44. Kong HY and Jang J. Antibacterial properties of novel poly(methyl methacrylate) nanofiber containing silver nanoparticles. *Langmuir* 2008, 24: 2051–2056.

45. Chen Q, Yue L, Xie FY, Zhou ML, Fu YB, Zhang YF and Weng J. Preferential facet of nanocrystalline silver embedded in polyethylene oxide nanocomposite and its antibiotic behaviors. *Journal of Physical Chemistry C*, 2008, 112: 10004–10007.
46. Kong HY and Jang J. Synthesis and antimicrobial properties of novel silver/polyrhodanine nanofibers. *Biomacromolecules* 2008, 9: 2677–2681.
47. Kvíték L, Panák A, Soukupová J, Kolář M, Veeřová R, Pucek R, Holecová M and Zbořil R. Effect of surfactants and polymers on stability and antibacterial activity of silver nanoparticles (NPs). *Journal of Physical Chemistry C*, 2008, 112(15): 5825–5834.
48. Nair AS, Binoy NP, Ramakrishna S, Kurup TRR, Chan LW, Goh CH, Islam MR, Utschig T and Pradeep T. Organic-soluble antimicrobial silver nanoparticle-polymer composites in gram scale by one-pot synthesis. *ACS Applied Materials Interfaces*, 2009, 1(11): 2413–2419.
49. Zhang YW, Peng HS, Huang W, Zhou YF and Yan DY. Hyperbranched poly(amidoamine) as the stabilizer and reductant to prepare colloid silver nanoparticles *in situ* and their antibacterial activity. *Journal of Physical Chemistry C*, 2008, 112: 2330–2336.
50. Zhang J and Han B. Supercritical CO₂-continuous microemulsions and compressed CO₂-expanded reverse microemulsions. *Journal of Supercritical Fluids*, 2009, 47: 531–536.
51. Shimizu R, Nibe A, Sawada K, Enokida Y and Yamamoto I. Preparation of hydrophobic platinum catalysts using a water-in-CO₂ microemulsion. *Journal of Supercritical Fluids*, 2008, 44: 109–114.
52. Lee H, Terry E, Zong M, Arrowsmith N, Perrier S, Thurecht KJ and Howdle SM. Successful dispersion polymerization in supercritical CO₂ using polyvinylalkylate hydrocarbon surfactants synthesized and anchored via RAFT. *Journal of American Chemical Society*, 2008, 130: 12242–12243.
53. Shiho H and DeSimone JM. Dispersion polymerization of glycidyl methacrylate in supercritical carbon dioxide. *Macromolecules*, 2001, 34(5): 1198–1203.
54. Kamrupi IR, Phukon P, Konwer BK and Dolui SK. Synthesis of silver-polystyrene nanocomposite particles using water in supercritical carbon dioxide medium and its antimicrobial activity. *The Journal of Supercritical Fluids*, 2011, 55: 1089–1094.
55. Travan A, Pelillo C, Donati I, Marsich E, Benincasa M, Scarpa T, Semeraro S, Turco G, Gennaro R and Paoletti S. Non-cytotoxic silver nanoparticle-polysaccharide nanocomposites with antimicrobial activity. *Biomacromolecules*, 2009, 10(6): 1429–1435.
56. Santa Maria LC, Santos ALC and Oliveira PC. Synthesis and characterization of silver nanoparticles impregnated into bacterial cellulose. *Materials Letters*, 2009, 63: 797–799.
57. Božanić DK, Dimitrijević-Branković S, Bibić N, Luyt AS and Djoković V. Silver nanoparticles encapsulated in glycogen biopolymer: Morphology, optical and antimicrobial properties. *Carbohydrate Polymers*, 2011, 83: 883–890.
58. Vigneshwaran N, Nachane RP, Balasubramanya RH and Varadarajan PV. A novel one-pot 'green' synthesis of stable silver nanoparticles using soluble starch. *Carbohydrate Research*, 2006, 341: 2012–2018.
59. Zheng LY and Zhu JF. Study on antimicrobial activity of chitosan with different molecular weights. *Carbohydrate Polymers*, 2003, 54: 527–530.
60. Rabea EI, Badawy MET and Stevens CV. Chitosan as antimicrobial agent: applications and mode of action. *Biomacromolecules*, 2003, 4: 1457–1465.
61. Sarasam AR, Brown P and Khajotia SS. Antibacterial activity of chitosan-based matrices on oral pathogens. *Journal of Materials Science: Materials in Medicine*, 2008, 19: 1083–1090.
62. Huang HZ, Yuan Q and Yang XR. Preparation and characterization of metal-chitosan nanocomposites. *Colloids and Surfaces B: Biointerfaces*, 2004, 39: 31–37.
63. Son WK, Youk JH and Lee TS. Preparation of antimicrobial ultrafine cellulose acetate fibers with silver nanoparticles. *Macromolecular Rapid Communications*, 2004, 25: 1632–1637.
64. Hong KH, Park JL and Sul IH. Preparation of antimicrobial poly(vinyl alcohol) nanofibers containing silver nanoparticles. *Journal of Polymer Science: Part B: Polymer Physics*, 2006, 44(17): 2468–2474.
65. Kong H and Jang J. Antibacterial properties of novel poly(methyl methacrylate) nanofiber containing silver nanoparticles. *Langmuir* 2008, 24: 2051–2056.

66. Kong H and Jang J. Synthesis and antimicrobial properties of novel silver/polyrhodanine nanofibers. *Biomacromolecules* 2008, 9: 2677–2681.
67. Xu XY, Yang QB, Wang YZ, Yu HJ, Chen XS and Jing XB. Biodegradable electrospun poly (l-lactide) fibers containing antibacterial silver nanoparticles. *European Polymer Journal*, 2006, 42(9): 2081–2087.
68. Gils PS, Ray D and Sahoo PK. Designing of silver nanoparticles in gum arabic based semi-IPN hydrogel. *International Journal of Biological Macromolecules*, 2010, 46(2): 237–244.
69. Lee SM, Lee BS, Byun TG and Song KC. Preparation and antibacterial activity of silver-doped organic-inorganic hybrid coatings on glass substrates. *Colloids and Surfaces A: Physicochemical and Engineering Aspects*, 2010, 355(1–3): 167–171.
70. Chen W, Liu Y, Courtney HS, Bettenga M, Agrawal CM, Bumgardner JD and Ong JL. In vitro anti-bacterial and biological properties of magnetron co-sputtered silver-containing hydroxyapatite coating. *Biomaterials*, 2006, 27(32): 5512–5517.
71. Liu JK, Yang XH and Tian XG. Preparation of silver/hydroxyapatite nanocomposite spheres. *Powder Technology*, 2008, 184: 21–24.
72. Nino-Martinez N, Martinez-Castanon GA, Aragon-Pina A, Martinez-Gutierrez F, Martinez-Mendoza JR and Ruiz F. Characterization of silver nanoparticles synthesized on titanium dioxide fine particles. *Nanotechnology*, 2008, 19: 1–8.
73. Moa A, Liao J, Xu W, Xian SQ, Li YB and Bai S. Preparation and antibacterial effect of silver-hydroxyapatite/titania nanocomposite thin film on titanium. *Applied Surface Science*, 2008, 255: 435–438.
74. Chou KS and Chen CC. Fabrication and characterization of silver core and porous silica shell nanocomposite particles. *Microporous and Mesoporous Materials*, 2007, 98(1–3): 208–213.
75. Zhang J, Lei JP, Liu YY, Zhao JW and Ju HX. Highly sensitive amperometric biosensors for phenols based on polyaniline-ionic liquid-carbon nanofiber composite. *Biosensors and Bioelectronics*, 2009, 24: 1858–1863.
76. Niu AP, Han YJ, Wu J, Yu N and Xu Q. Synthesis of one-dimensional carbon nanomaterials wrapped by silver nanoparticles and their antibacterial behavior. *Journal of Physical Chemistry C*, 2010, 114: 12728–12735.
77. Rowan R, Tallon T, Sheahan AM, Curran R, McCann M, Kavanagh K, Devereux M and McKee V. “Silver bullets” in antimicrobial chemotherapy: synthesis, characterisation and biological screening of some new Ag(I)-containing imidazole complexes. *Polyhedron*, 2006, 25: 1771–1778.
78. Chen SP, Wu GZ and Zeng HY. Preparation of high antimicrobial activity thiourea chitosan-Ag⁺ complex. *Carbohydrate Polymers*, 2005, 60: 33–38.
79. Warriner R and Burrell R. Infection and the chronic wound: a focus on silver. *Advances in Skin Wound Care*, 2005, 18(8): 2–12.
80. Kasuga NC, Sato M, Amano A, Hara A, Tsuruta S, Sugie A and Nomiya K. Light-stable and antimicrobial active silver(I) complexes composed of triphenylphosphine and amino acid ligands: synthesis, crystal structure, and antimicrobial activity of silver(I) complexes constructed with hard and soft donor atoms. *Inorganica Chimica Acta*, 2008, 361: 1267–1273.
81. Muller MJ, Hollyoak MA, Moaveni Z, Brown TL, Herndon DN and Hegggers JP. Retardation of wound healing by silver sulfadiazine is reversed by aloe vera and nystatin. *Burns*, 2003, 29(8): 834–836.
82. Fox CL. Silver sulphadiazine, addendum to local therapy modern treatment, Hoeber Medical Division. New York: Harper and Row, 1967, p. 1259–1267.
83. Stanford W, Rappole BW and Fox CL Jr. Clinical experience with silver sulphadiazine, a new topical agent for control of pseudomonas infections in burns. *Journal of Trauma*, 1969, 9: 377–388.
84. Sambhy V, MacBride MM, Peterson BR and Sen A. Silver Bromide Nanoparticle/Polymer Composites: dual Action Tunable Antimicrobial Materials. *Journal of American Chemical Society*, 2006, 128(30): 9798–9808.

85. Atiyeh BS, Costagliola M, Hayek SN and Dibo SA. Effect of silver on burn wound infection control and healing: review of the literature. *Burns*, 2007, 33: 139–148.
86. Kasuga NC, Yamamoto R, Hara A, Amano A and Nomiya K. Molecular design, crystal structure, antimicrobial activity and reactivity of light-stable and water-soluble Ag-O bonding silver(I) complexes, dinuclear silver(I) N-acetyltylglycinate. *Inorganica Chimica Acta*, 2006, 359(13): 4412–4416.
87. Yesilel OZ, Tas GK, Darcan C, Ilker I, Pasaog˘lu H and Bykngr O. Syntheses, thermal analyses, crystal structures and antimicrobial properties of silver(I)-saccharinate complexes with diverse diamine ligands. *Inorganica Chimica Acta*, 2010, 363: 1849–1858.
88. Baker C, Pradhan A and Pakstis L. Synthesis and antibacterial properties of silver nanoparticles. *Journal of Nanoscience and Nanotechnology*, 2005, 2: 244–249.
89. Morones JR, Elechiguerra JL, Camacho A and Ramirez JT. The bactericidal effect of silver nanoparticles. *Nanotechnology*, 2005, 16: 2346–2353.
90. Panacek A, Kvittek L, Pucek R, Kolar M, Vecerova R and Pizurova N. Silver colloid nanoparticles: synthesis, characterization, and their antibacterial activity. *Journal of Physical Chemistry B*, 2006, 110(33): 16248–16253.
91. Pal S, Tak YK and Song JM. Does the antibacterial activity of silver nanoparticles depend on the shape of the nanoparticle? A study of the gram-negative bacterium *Escherichia coli*. *Applied and Environmental Microbiology*, 2007, 27(6): 1712–1720.
92. Shahverdi AR, Fakhimi A, Shahverdi HR and Minaian S. Synthesis and effect of silver nanoparticles on the antibacterial activity of different antibiotics against *Staphylococcus aureus* and *Escherichia coli*. *Nanomedicine-Nanotechnology Biology and Medicine*, 2007, 3(2): 168–171.
93. Ingle A, Gade A, Pierrat S, Sonnichsen C and Rai M. Mycosynthesis of silver nanoparticles using the fungus *Fusarium acuminatum* and its activity against some human pathogenic bacteria. *Current Nanoscience*, 2008, 4: 141–144.
94. Reddy KM. Selective toxicity of zinc oxide nanoparticles to prokaryotic and eukaryotic systems. *Applied Physics Letter*, 2007, 90: 2139021–2139023.
95. Seery MK, George R, Floris P and Pillai SC. Silver doped titanium dioxide nanomaterials for enhanced visible light photocatalysis. *Journal of Photochemistry and Photobiology A-Chemistry*, 2007, 189(2–3): 258–263.
96. Kim YH, Kim CW, Cha HG, Lee DK, Jo BK, Ahn GW, Hong ES, Kim JC and Kang YS. Bulk like thermal behavior of antibacterial Ag-SiO₂ nanocomposites. *Journal of Physics Chemistry C*, 2009, 113: 5105–5110.
97. Wei QF, Ye H, Hou DY, Wang HB and Gao WD. Surface functionalization of polymer nanofibers by silver sputter coating. *Journal of Applied Polymer Science*, 2006, 99: 2384–2388.
98. Park SJ and Jang YS. Preparation and Characterization of Activated Carbon Fibers Supported with Silver Metal for Antibacterial Behavior. *Journal of Colloid Interface Science*, 2003, 261: 238–242.
99. Vijayakumar PS and Prasad BLV. Intracellular biogenic silver nanoparticles for the generation of carbon supported antiviral and sustained bactericidal agents. *Langmuir*, 2009, 25(19): 11741–11747.
100. Manash RD, Sarma RK, Saikia R, Kale Vinayak S, Shelke MV and Sengupta P. Synthesis of silver nanoparticles in an aqueous suspension of graphene oxide sheets and its antimicrobial activity. *Colloids and Surfaces B: Biointerfaces*, 2011, 83(1): 16–22.
101. Lu L, Rininsland FH, Wittenburg SK, Achyuthan KE, McBranch DW and Whitten DG. Biocidal activity of a light-absorbing fluorescent conjugated polyelectrolyte. *Langmuir*, 2005, 21: 10154–10159.
102. Rosemary MJ, MacLaren I and Pradeep T. Investigations of the antibacterial properties of ciprofloxacin@SiO₂. *Langmuir*, 2006, 22: 10125–10129.
103. Shi ZL, Neoh KG and Kang ET. Surface-Grafted Viologen for Precipitation of Silver Nanoparticles and Their Combined Bactericidal Activities. *Langmuir*, 2004, 20: 6847–6852.
104. Nirmala R, Nam KT, Park DK, Wooil Baek, Navamathavan R and Kim H Y. Structural, thermal, mechanical and bioactivity evaluation of silver-loaded bovine bone hydroxyapatite

- grafted poly(ϵ -caprolactone) nanofibers via electrospinning. *Surface & Coatings Technology*, 2010, 205: 174–181.
105. Kong H and Jang J. Antibacterial Properties of Novel Poly(methyl methacrylate) Nanofiber Containing Silver Nanoparticles. *Langmuir*, 2008, 24: 2051–2056.
 106. Don TM, Chen CC, Lee CK, Cheng WY and Cheng LP. Preparation and antibacterial test of chitosan/PAA/PEGDA bilayer composite membranes. *Journal of Biomaterials Science - Polymer Edition*, 2005, 16(12): 1503–1519.
 107. Xing ZC, Chae WP, Baek JY, Choi MJ, Jung Y and Kang IK. In vitro assessment of antibacterial activity and cytocompatibility of silver-containing PHBV nanofibrous scaffolds for tissue engineering. *Biomacromolecules*, 2010, 11(5): 1248–1253.
 108. Travan A, Pelillo C, Donati I, Marsich E, Benincasa M, Scarpa T, Semeraro S, Turco G, Gennaro R and Paoletti S. Non-cytotoxic silver nanoparticle-polysaccharide nanocomposites with antimicrobial activity. *biomacromolecules*, 2009, 10: 1429–1435.
 109. Yamanaka M, Hara K and Kudo J. Bactericidal actions of a silver ion solution on *Escherichia coli*, studied by energy-filtering transmission electron microscopy and proteomic analysis. *Applied and Environmental Microbiology*, 2005, 71(11): 7589–7593.
 110. Feng QL, Wu J, Chen GQ, Cui FZ, Kim TN and Kim JO. A mechanistic study of the antibacterial effect of silver ions on *Escherichia coli* and *Staphylococcus aureus*. *Journal of Biomedical Materials*, 2000, 52(4): 662–668.
 111. Kim JS, Kuk E, Yu KN, Kim JH, Park SJ, Lee HJ, Kim SH, Park YK, Park YH and Hwang CY. Antimicrobial effects of silver nanoparticles. *Nanomedicine: Nanotechnology, Biology, and Medicine*, 2007, 3: 95–101
 112. Chaloupka K, Malam LY and Seifalian AM. Nanosilver as a new generation of nanoparticle in biomedical applications. *Trends in Biotechnology*, 2010, 28(11): 580–588.
 113. Song HY, Ko KK, Oh LH and Lee BT. Fabrication of silver nanoparticles and their antimicrobial mechanisms. *European Cells and Materials*, 2006, 11: 58–63.
 114. Sondi I and Salopek-Sondi B. Silver nanoparticles as antimicrobial agent: a case study on *E. coli* as a model for gram-negative bacteria. *Journal of Colloid and Interface Science*, 2004, 275: 177–182.
 115. Amro NA, Kotra LP, Wadu-Mesthrige K, Bulychev A, Mobashery S and Liu G. High-resolution atomic force microscopy studies of the *Escherichia coli* outer membrane: structural basis for permeability. *Langmuir*, 2000, 16: 2789–2796.
 116. Danilczuk M, Lund A, Saldo J, Yamada H and Michalik J. Conduction electron spin resonance of small silver particles. *Spectrochimica Acta: Part A*, 2006, 63: 189–191.
 117. Mendis E, Rajapakse N, Byun HG and Kim SK. Investigation of jumbo squid (*Dosidicus gigas*) skin gelatin peptides for their in vitro antioxidant effects. *Life Science*, 2005, 77: 2166–2178.
 118. Kim JS, Kuk E, Yu KN, Kim JH, Park SJ, Lee HJ, Kim SH, Park YK, Park YH, Hwang CY, Kim YK, Lee YS, Jeong DH and Cho MH. Antimicrobial effects of silver nanoparticles. *Nanomedicine: Nanotechnology, Biology, and Medicine*, 2007, 3: 95–101.
 119. Raimondi F, Scherer G G, Kotz R and Wokaun A. Nanoparticles in energy technology: examples from electrochemistry and catalysis. *Angewante Chemie, International Edition*, 2005, 44: 2190–2209.
 120. Kvitek L, Panacek A, Soukupova J, Kolar M, Vecerova R and Prucek R. Effect of Surfactants and Polymers on Stability and Antibacterial Activity of Silver Nanoparticles (NPs). *Journal of Physical Chemistry C*, 2008, 112(15): 5825–5834.
 121. Carpenter PL. *Microbiology*. Philadelphia: W. B. Saunders, 1972. p. 245.
 122. Sadeghi B, Jamali M and Kia SA. Synthesis and characterization of silver nanoparticles for antibacterial activity. *International Journal of Nanotechnology*, 2010, 1(2): 119–124.
 123. Yoksan R and Chirachanchai S. Silver nanoparticle-loaded chitosan-starch based films: fabrication and evaluation of tensile, barrier and antimicrobial properties. *Materials Science and Engineering C*, 2010, 30(6): 891–897.

124. Wang YZ, Yang QB, Shan GY, Wang C, Du JS, Wang SG, Li YX, Chen XS, Jing XB and Wei Y. Preparation of silver nanoparticles dispersed in polyacrylonitrile nanofiber film spun by electrospinning. *Materials Letter*, 2005, 59(24–25): 3046–3049.
125. George N, Faoagali J and Muller M. Silver nanoparticles (silver sulfadiazine and chlorhexidine) activity against 200 clinical isolates. *Burns*, 1997, 23: 493–495.
126. Illingworth B, Bianco RW and Weisberg S. In vivo efficacy of silver coated fabric against *Staph. Epidermidis*. *Journal of Heart Valve Disease*, 2000, 9: 135–141.
127. Tsiouras N, Rix CJ and Brady PH. Passage of silver ions through membrane-mimetic materials, and its relevance to treatment of burn wounds with silver sulfadiazine cream. *Clinical Chemistry*, 1997, 43(2): 290–301.
128. Fox CL and Modak SM. Mechanism of silver sulfadiazine action on burn wound infections. *Antimicrobial Agents and Chemotherapy*, 1974, 5(6): 582–528.
129. Tian J, Wong KKY, Ho CM, Lok CN, Yu WY, Che CM, Chiu JF and Tam PKH. Topical delivery of silver nanoparticles promotes wound healing. *ChemMedChem*, 2006, 1: 171–180.
130. Richard JW, Spencer BA, McCoy LF, Carina E, Washington J and Edgar P. Acticoat versus silverlon: the truth. *Journal of Burns and Surgical Wound Care*, 2002, 1: 11–20.
131. Ip M, Lui SL, Poon VKM, Lung I and Burd A. Antimicrobial activities of silver dressings an in vitro comparison. *Journal of Medical Microbiology*, 2006, 55: 59–63.
132. Jia J, Duan YY, Wang SH, Zhang SF and Wang ZY. Preparation and characterization of antibacterial silver-containing nanofibers for wound dressing applications. *Journal of US-China Medical Science*, 2007, 4(2): 52–54.
133. Hong KH. Preparation and properties of electrospun poly(vinyl alcohol)/silver fiber web as wound dressings. *Polymer Engineering & Science*, 2007, 47(1): 43–49.
134. Pape HL, Serena FS, Contini P, Devillers C, Maftah A and Leprat P. Evaluation of the antimicrobial properties of an activated carbon fibre supporting silver using a dynamic method. *Carbon*, 2002, 40: 2947–2954.
135. Yeo SY, Lee HJ and Jeong SH. Preparation of nanocomposite fibers for permanent antibacterial effect. *Journal of Materials Science*, 2003, 38: 2143–2147.
136. Fernández A, Soriano E, López-Carballo G, Picouet P, Lloret E, Gavara R and Hernández-Muñoz P. Preservation of aseptic conditions in absorbent pads by using silver nanotechnology. *Food Research International*, 2009, 42: 1105–1112.
137. Fu J, Ji J, Fan D and Shen J. Construction of antibacterial multilayer films containing nanosilver via layer-by-layer assembly of heparin and chitosan-silver ions complex. *Journal of Biomedical Materials Research: Part A*, 2006, 79A(3): 665–674.
138. Khundkar R, Malic C and Burge T. Use of Acticoat™ dressings in burns: What is the evidence? *Burns*, 2010, 36: 751–758.
139. Alt V. An in vitro assessment of the antibacterial properties and cytotoxicity of nanoparticulate silver bone cement. *Biomaterials*, 2004, 25: 4383–4391.
140. Liu JK, Yang XH and Tian XG. Preparation of silver/hydroxyapatite nanocomposite spheres. *Powder Technology*, 2008, 184: 21–24.
141. Chen W, Liu Y, Courtney HS, Bettenga M, Agrawal CM, Bumgardner JD and Ong JL. In vitro anti-bacterial and biological properties of magnetron cosputtered silver-containing hydroxyapatite coating. *Biomaterials*, 2006, 27: 5512–5517.
142. Vojislav S, Djordje J, Suzana D, Sladjana BT, Miodrag M, Mirjana SP, Aleksandra K, Dragoljub J and Slavica R. Synthesis of antimicrobial monophase silver-doped hydroxyapatite nanopowders for bone tissue engineering. *Applied Surface Science*, 2011, 257: 4510–4518.
143. Kumar PT, Abhilash S, Manzoor K, Nair SV, Tamura H and Jayakumar R. Preparation and characterization of novel b-chitin/nanosilver composite scaffolds for wound dressing applications. *Carbohydrate Polymers*, 2010, 80: 761–767.
144. Furno F, Morley KS, Wong B, Sharp BL, Arnold PL and Howdle SM. Silver nanoparticles and polymeric medical devices: a new approach to prevention of infection? *Journal of Antimicrobial Chemotherapy*, 2004, 54: 1019–1024.

145. Wang J, Huang N, Yang P, Leng YX, Sun H, Liu ZY and Chu PK. The effects of amorphous carbon films deposited on polyethylene terephthalate on bacterial adhesion. *Biomaterials*, 2004, 25: 3063–3070.
146. Ciresi DL, Albrecht RM, Volkers PA and Scholten DJ. Failure of antiseptic bonding to prevent central venous catheter related infection and sepsis. *American Surgeon*, 1996; 62: 641–645.
147. Shao W and Zhao Q. Influence of reducers on nanostructure and surface energy of silver coatings and bacterial adhesion. *Surface & Coatings Technology*, 2010, 204: 1288–1294.
148. Akyiama H and Okamoto S. Prophylaxis of indwelling urethral catheter infection: clinical experience with a modified Foley catheter and drainage system. *Journal of Urology*, 1979, 121: 40–48.
149. James EM and Browning ND. Practical aspects of atomic resolution imaging and analysis in STEM. *Ultramicroscopy*, 1999, 78: 125–139.
150. Elechiguerra JL, Burt JL, Morones JR, Bragado AC, Gao X and Lara HH. Interaction of silver nanoparticles with HIV-1. *Journal of Nanobiotechnology*, 2005, 3: 1–10.
151. Vaidyanathan R, Kalishwaralal K, Gopalram S and Gurunathan S. Nanosilver-The burgeoning therapeutic molecule and its green synthesis. *Biotechnology Advances*, 2009, 27: 924–937.
152. Quintavalla S and Vicini L. Antimicrobial food packaging in meat industry. *Meat Science*, 2002, 62: 373–380.
153. Matsuura T, Abe Y, Sato K, Okamoto K, Ueshige M and Akagawa Y. Prolonged antimicrobial effect of tissue conditioners containing silver zeolite. *Journal of Dent*, 1997, 25: 373–377.
154. Ishitani T. Active packaging for food quality preservation in Japan. In P. Ackermann, M. Jagerstad, & T. Ohlson (Eds.), *Food and food packaging materials-chemical interactions*. Cambridge, England: Royal Society of Chemistry, 1995, 81: 177–188.
155. Tankhiwale R and Bajpai SK. Graft copolymerization onto cellulose-based filter paper and its further development as silver nanoparticles loaded antibacterial food-packaging material. *Colloids and Surfaces B: Biointerfaces*, 2009, 69: 164–168.
156. Prashant J and Pradeep T. Potential of silver nanoparticle-coated polyurethane form as an antibacterial water filter. *Biotechnology and Bioengineering*, 2005, 90: 59–66.
157. Jain P and Pradeep T. Potential of silver nanoparticle-coated polyurethane foam as an antibacterial water filter. *Biotechnology and Bioengineering*, 2005, 90(1): 59–63.
158. Gong P, Li H, He X, Wang K, Hu J and Tan W. Preparation and antibacterial activity of Fe₃O₄@Ag nanoparticles. *Nanotechnology*, 2007, 18: 604–611.
159. Basri H, Ismail AF, Aziz M, Nagai K, Matsuura T, Abdullah MS and Ng BC. Silver-filled polyethersulfone membranes for antibacterial applications-Effect of PVP and TAP addition on silver dispersion. *Desalination*, 2010, 261: 264–271.
160. Lva YH, Liu H, Wang Z, Liu SJ, Hao LJ, Sang YH, Liu D, Wang JY and Boughtone RI. Silver nanoparticle-decorated porous ceramic composite for water treatment. *Journal of Membrane Science*, 2009, 331: 50–56.
161. Dastjerdi R, Mojtahedi MRM, Shoshtari AM and Khosroshahi A. Investigating the production and properties of Ag/TiO₂/PP antibacterial nanocomposite filament yarns. *Journal of the Textile Institute*, 2010, 101: 204–213.
162. Mucha H, Hofer D, Bflag SA and Swere M. Antimicrobial finishes and modification. *Melliand Textile Berichte*, 2002, 83(4): 53–56.
163. Dastjerdi R, Mojtahedi MRM and Shoshtari AM. Comparing the effect of three processing methods for modification of filament yarns with inorganic nanocomposite filler and their bioactivity against *Staphylococcus aureus*. *Macromolecular Research*, 2009, 17(6): 378–387.
164. Dunn K and Edwards-Jones V. The role of Acticoat TM with nanocrystalline silver in the management of burns. *Burns*, 2004, 30(Suppl 1): S1–9.
165. Lee HJ and Jeong SH. Bacteriostasis and skin innocuousness of nanosize silver colloids on textile fabrics. *Textile Research Journal*, 2005, 75(7): 551–556.

166. Hendi A. Silver nanoparticles mediate differential responses in some of liver and kidney functions during skin wound healing. *Journal of King Saud University (Science)*, 2011, 23: 47–52.
167. Wen HC, Lin YN, Jian SR, Tseng SC, Weng MX, Liu YP, Lee PT, Chen PY, Hsu RQ, Wu WF and Chou CP. Observation of growth of human fibroblastson silver nanoparticles. *Journal of Physics: Conference Series*, 2007, 61: 445–449.
168. Jeong SH, Hwang YH and Yi SC. Antibacterial properties of padded PP/PE nonwovens incorporating nano-sized silver colloids. *Journal of Materials Science*, 2005, 40: 5413–5418.
169. Ki HY, Kim JH, Kwon SC and Jeong SH. A study on multifunctional wool textiles treated with nano-sized silver. *Journal of Material Science*, 2007, 42: 8020–8024.
170. AshaRani PV, Kah Mun GL, Hande MP and Valiyaveettil S. Cytotoxicity and Genotoxicity of Silver Nanoparticles in Human Cells. *ACS Nano*, 2009, 3(2): 279–290.
171. Moghimi SM, Hunter AC and Murray JC. Long-circulating and target-specific nanoparticles: theory to practice. *Pharmacological Reviews*, 2001, 53: 283–318.
172. Panyam J and Labhasetwar V. Biodegradable nanoparticles for drug and gene delivery to cells and tissue. *Advanced Drug Delivery Reviews*, 2003, 55: 329–347.
173. Burd A, Kwok CH, Hung SC, Chan HS, Gu H and Lam WK. A comparative study of the cytotoxicity of silver-based dressings in monolayer cell, tissue explant, and animal models. *Wound Repair and Regeneration*, 2007, 15: 94–104.
174. Ahamed M, AlSalhi MS and Siddiqui MKJ. Silver nanoparticle applications and human health. *Clinica Chimica Acta*, 2010, 411: 1841–1848.
175. Warriner R and Burrell R. Infection and the chronic wound: a focus on silver. *Advances in Skin and Wound Care*, 2005, 18(8): 2–12.
176. Wright JB, Lam K, Buret AG, Olson ME and Burrell RE. Early healing events in a porcine model of contaminated wounds: effects of nanocrystalline silver on matrix metalloproteinases, cell apoptosis, and healing. *Wound Repair and Regeneration*, 2002, 10: 141–147.
177. Lee HJ and Jeong SH. Bacteriostasis and skin innocuousness of nanosize silver colloids on textile fabrics. *Textile Research Journal*, 2005, 75(7): 551–556.
178. Wan AT, Conyers RA, Coombs CL and Masterton JP. Determination of silver in blood, urine, and tissues of volunteers and burn patients. *Clinical Chemistry*, 1991, 37: 1683–1687.
179. Chaby G, Viseux V, Poulain JF, De CB, Denoeux JP and Lok C. Topical silver sulfadiazine-induced acute renal failure. *Annales Dermatologie Et De Venereologie*, 2005, 132(11 Pt 1): 891–893.
180. Kuroyanagi Y, Kim E and Shioya N. Evaluation of a synthetic wound dressing capable of releasing silver sulfadiazine. *Journal of Burn Care and Research*, 1991, 12: 106–115.
181. Braydich-Stolle L, Hussain S, Schlager J and Hofmann MC. In vitro cytotoxicity of nanoparticles in mammalian germ line stem cells. *Toxicological Science*, 2005, 88: 412–419.
182. Nel A, Xia T, Madler L and Li N. Toxic potential of materials at the nanolevel. *Nature*, 2006, 311: 622–627.
183. Ahamed M and Siddiqui MKJ. Low level lead exposure and oxidative stress: current opinions. *Clinica Chimica Acta*, 2007, 383: 57–64.
184. Ahamed M, Siddiqui MA, Akhtar MJ and Siddiqui MKJ. Genotoxic potential of copper oxide nanoparticles in human lung epithelial cells. *Biochemical and Biophysical Research Communication*, 2010, 396: 578–583.
185. Park EJ, Yi J, Kim Y, Choi K and Park K. Silver nanoparticles induce cytotoxicity by a Trojan-horse type mechanism. *Toxicology In Vitro*, 2010, 24: 872–878.
186. Asharani PV, Mun GK, Hande MP and Valiyaveettil S. Cytotoxicity and genotoxicity of silver nanoparticles in human cells. *ACS Nano*, 2009, 3: 279–290.

Chapter 3

Synthesis and Antimicrobial Activity of Copper Nanomaterials

Daniela Longano, Nicoletta Ditaranto, Luigia Sabbatini, Luisa Torsi, and Nicola Cioffi

3.1 Introduction

There is a great concern about the resistance of microorganisms towards multiple antibiotics or disinfecting agents, therefore great efforts are being devoted to the development of novel and effective agents against pathogenic microorganisms [1]. Several real-life applications could be involved including food processing and packaging, health care and biomedical devices, surgery and implants, disinfection of hospitals, textiles, household furnishing and paints, airports, and production facilities; these needs might have implications even in more extreme scenarios, such as germ warfare, space exploration, and in the prevention of pandemic diseases like SARS (Severe Acute Respiratory Syndrome), influenza viruses, etc.

In this regard, the development of non-conventional antibacterial and antifungal agents is becoming a key research field. Recently, inorganic bactericides have attracted special interest due to their activity, chemical stability, and heat resistance [2, 3]. Furthermore, the development of nanoscience and nanotechnology presents novel opportunities for exploring the bactericidal effect of innovative nanomaterials containing metals with a marked bioactivity such as silver, copper, and zinc [3–7], to cite just a few.

In most studies on metal-based nano-antimicrobials, the biological effectiveness of the material is demonstrated to be significantly higher or longer than the (well-known) bioactivity of the bulk metal itself. This has been suggested to be due to several aspects, including the nano-metal size-dependent properties, as well as the high surface-to-volume ratio of ultrafine particles, and, finally, non-conventional features related to the presence of surface stabilizers. In fact, capping agents have

D. Longano (✉) • N. Ditaranto • L. Sabbatini • L. Torsi • N. Cioffi
Dipartimento di Chimica, Università degli Studi di Bari “Aldo Moro”, Bari, Italy
e-mail: longano@chimica.uniba.it

been frequently demonstrated to tune the nanoparticle ionic release and, consequently, its anti-biofilm properties.

The need for hygienic living conditions prompts new challenges for the development of affordable and efficacious antimicrobial materials that should be environmentally friendly and absolutely non-toxic towards human beings.

Finely dispersed bioactive nanomaterials are expected to exert an improved disinfecting effect due to their size, providing higher environmental mobility and allowing them to interact closely with bacterial membranes. On the other hand, the same properties may give rise to severe risks for human health, thus greatly limiting the development of nanoparticle real-life applications.

The growing international concern in nanoparticle toxicology towards humans is presently supporting the development of “smart” nano-antimicrobials. Such non-toxic nanomaterials can still reduce the risks of transmitting diseases by preventing microorganism survival and proliferation in several application contexts, but are also expected to ensure environmental compatibility and absence of human toxicity, since they are impregnated or covalently linked or co-polymerized or somehow confined in a dispersing/supporting matrix. The latter component acts as an immobilizing component in a nanocomposite formulation or a hybrid nanomaterial, and it might also bring additional properties to the final product coating.

The usefulness of copper as an antibacterial agent has been known for a long time. Different forms of copper compounds were used by ancient civilizations for several afflictions and to maintain hygiene [8]. The ancient Egyptians sterilized drinking water and wounds using metals such as silver and copper. The Romans catalogued numerous medicinal uses of copper for various diseases. The Aztecs treated sore throats with copper, while in Persia and India, copper was applied to treat boils, eye infections, and venereal ulcers [9].

Soluble copper compounds have been shown to provide excellent antimicrobial activity against a number of microorganisms including bacteria, fungi, algae, and viruses, while these species are relatively safe for humans [10]. Copper appears to exert its killing effect by generating reactive hydroxyl radicals that can cause irreparable damage such as the oxidation of proteins, cleavage of DNA and RNA molecules, and membrane damage due to lipid peroxidation [11, 12].

Bioactivity of copper, both as free ion and complex species, is well-known and has been documented for many years; nevertheless, only few papers and patents have been issued so far about the antibacterial properties of copper-containing nano-sized materials [13–15].

This chapter focuses on the synthesis and bioactivity of antimicrobial copper nanomaterials and on their applications to real life.

The number of publications dealing with possible approaches to the synthesis of copper nanomaterials is very large, and the authors have recently published a specific review dealing with copper nano-phases [16]. In the present chapter, we have focused our attention only on those papers where the antimicrobial properties of copper nanomaterials were explicitly assessed.

These studies are here reviewed and classified firstly as a function of the synthesis approach and secondly as a function of the target microorganism used for testing the antimicrobial activity.

3.2 Synthesis of Cu Nano-Antimicrobials

Several approaches to the preparation of copper nanomaterials are nowadays available. Plenty of details are available in a recent review specifically dealing with the synthesis and characterization of copper nanomaterials [16]. In the present chapter, the different studies dealing with antimicrobial copper nanomaterials have been classified on the basis of the preparation method. Three different classes of syntheses are outlined in the following: chemical, electrochemical, and physical/mechanical approaches.

3.2.1 Chemical Approaches

The redox syntheses of metal nanomaterials, including copper, are certainly the most frequently used, and they are usually indicated as *wet-chemical* processes. Key aspects of the overall synthetic method include the choice of the reaction medium and the stabilizer agent, the experimental conditions (pressure, temperature, microwave assistance, etc.), and the use of additional dispersing/supporting materials. Some of these issues will be explicitly assessed in the following subparagraphs.

3.2.1.1 Unsupported Copper Nanoparticles

Among the simplest processes, the direct reduction of a salt (such as copper nitrate) into copper nanoparticles (CuNPs) has to be mentioned. As an example, Ruparelia et al. have reported on the synthesis of CuNPs involving the well-known wet-chemical reaction between sodium borohydride and copper nitrate, used as precursor. The resulting nanoparticles were dried in a reducing environment and stored in air-tight containers until biological testing. The presence of nanoparticles in suspension would ensure a continuous release of ions into the nutrient media [17]. Many redox processes can be used similarly. Among these, we outline the possible use of vitamin C [18], citrate [19], glucose [20] or similar nutrients/food additives to reductively produce CuNP colloids. At present, these nanomaterials have not been tested specifically as nano-antimicrobials, although such an application could have unprecedented advantages from the use of non-toxic reductants in the colloidal formulation.

Recently, low-polydispersion copper nanoparticles (NPs) (Fig. 3.1) and nanorods (CuNRs) (Fig. 3.2) were synthesized by thermal decomposition of copper (II) acetylacetonate [Cu(acac)₂] precursors in the presence of surfactants [21]. CuNPs were synthesized in phenyl ether using Cu(acac)₂ as a salt precursor, oleyamine as a surfactant, and 1,2-tetradecanediol as a reducing agent. The solution was degassed and stirred while its temperature was raised at a rate of $\sim 2^\circ\text{C}/\text{min}$ to 155°C and was

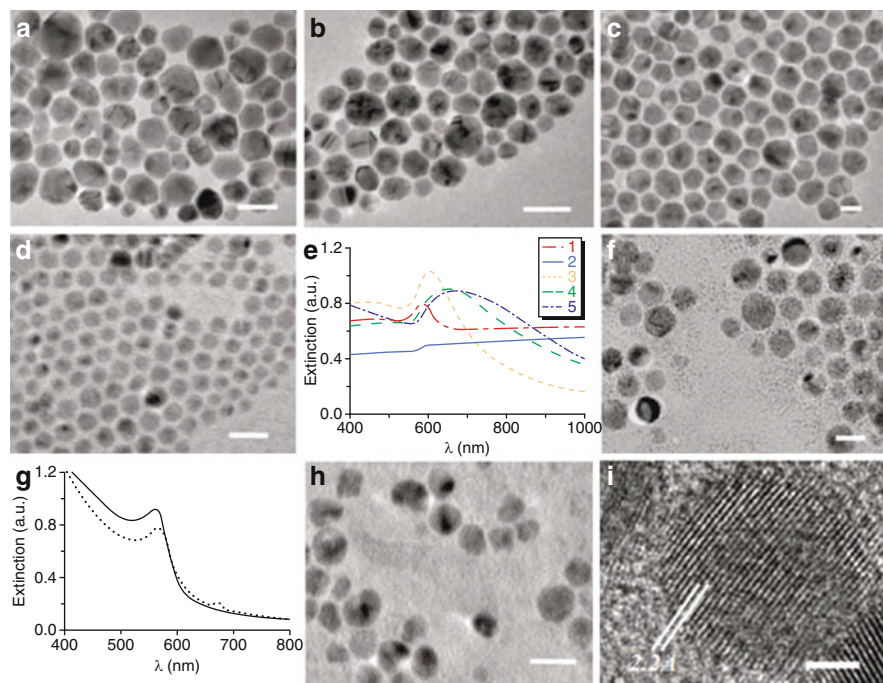


Fig. 3.1 TEM images of Cu nanoparticles prepared with different ratio of OAM to $\text{Cu}(\text{acac})_2$ (a–d). (e) UV–vis spectra of CuNPs in toluene: 1 freshly prepared CuNPs coated with OAM, 2 Cu/OAM NPs stored under argon for 10 days, 3 freshly prepared CuNPs protected with 1-undecanethiol 4 and 5 CuNPs coated with 1-undecanethiol and stored under argon for 10 and 20 days, respectively. (f) A representative TEM image of CuNPs coated with 1-undecanethiol. (g) UV–vis spectra of freshly prepared CuNPs in H_2O (solid curve) and the same NPs stored in water for 2 months (dotted curve). (h) A representative image of Cu/TMA NPs. (i) The HRTEM image of alkylthiol-coated CuNPs (synthesized at $\chi = 100$) (Reprinted with permission from [21]. Copyright 2010 American Chemical Society)

held there for an additional 1 h. During heating, the color of the reaction mixture changed from blue to dark red, signifying the formation of CuNPs. Cu nanorods were obtained by the same route as CuNPs, except that 0.1 equivalent of dodecylammonium bromide was added as structure-directing surfactant. The Cu nanostructures prepared by this route could be further functionalized by exchanging weakly bound surfactants to tighter binding alkane-thiols. This functionalization allowed for the control of surface chemistry and solubility of CuNPs and CuNRs in different solvents, and yielded nanostructures that were stable in solution for prolonged periods of time. Noticeably, copper nanoparticles functionalized with positively charged thiols were stable in water for several months. Cu-containing particles could be precipitated from phenyl ether with ethanol and re-dispersed in toluene or hexane for further use [21].

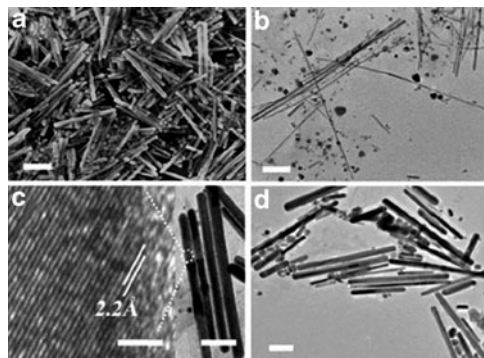


Fig. 3.2 (a) SEM image of Cu nanorods, $\chi = 100$, average aspect ratio, $R \approx 13$ (average length/width 841.6 nm/63.5 nm). (b) TEM image of Cu nanorods, $\chi = 60$, $R \approx 64$ (average length/width 1,338 nm/21 nm). (c) HRTEM image of Cu nanorods, $\chi = 100$; distance between two adjacent lattice planes is 2.2 Å. (d) TEM image of Cu nanorods coated with 1-undecanethiol after storing under atmosphere for several months. Scale bars (a) 400 nm, (b, d) 200 nm, and (c) 2 nm for the left and 200 nm for the right image (Reprinted with permission from [21]. Copyright 2010 American Chemical Society)

3.2.1.2 Copper Nanomaterials Supported on Organic Substrates

Metal nanoparticles (MeNPs) can be immobilized and coated onto surfaces for their better utilization. Since it is known that CuNPs may aggregate quickly in colloidal media, the extent of agglomeration can be effectively reduced by lowering the surface energy by adsorption of stabilizers such as polymers or surfactants present in the medium. The incorporation of smaller inorganic particles into larger polymers is also desirable in order to combine the key properties of both the materials. A few years ago, the group of C. Neckers reported on the synthesis of functionalized CuNPs/polymer composites. The preparation protocol was based on two steps: at first, functionalized CuNPs were obtained by a modification of the Brust's procedure, introducing a polymerizable acrylic functionality into the NPs shell. Then, CuNPs were integrated into the polymer backbone by means of a specific cross-linking process, providing a way to control on the ionic release from the particles [22].

Colloidal CuNPs have been recently synthesized in a solution of hyperbranched polyamine (HBPA) by a reduction in the presence of NaBH_4 . Hence, hyperbranched polymer was simultaneously supporting the stabilization of metal colloidal solution, and preventing agglomeration and precipitation of the particles [23].

Weickmann et al. developed polymethyl-methacrylate (PMMA)/bentonite/Cu nanocomposites by an electroless copper-plating process involving aqueous Pd/bentonite dispersions that were first blended with a PMMA dispersion and then treated with an electroless plating bath. As a result, 14-nm copper nanospheres were selectively immobilized at the bentonite nano-platelet surface. Key feature of this technology is the in situ formation of bentonite-supported metal nanoparticles which are assembled at the surface of the cationic polymer latex. As a consequence,

a fragile inorganic shell is obtained, which is ruptured during melt processing, producing very uniform fine dispersions of bentonite/metal hybrid nanoparticles. This approach was demonstrated for PMMA but offers several new preparation routes for other acrylic and styrene monomers [24].

Nanoparticulate hybrid systems derived from inorganic solids and carbon nanotubes (CNTs) were developed by Mohan and co-workers [25]. Chemically active surface and high-temperature stability are the basic attributes to use CNTs as the template for the growth of nanoparticles. Cu-grafted carbon nanotubes (Cu-MWCNTs) were prepared by a simple chemical reduction method divided into three steps. In the first step, acid groups were introduced on the carbon nanotube surface through sulphuric acid treatment, followed by the introduction of Cu ions in the second step. Finally, ions introduced on the surface were subjected to chemical reductions leading to the formation of Cu-MWCNTs [25].

Among the wide variety of polymer matrices, biopolymers are optimal candidates as CuNP-dispersing matrix, since they are readily available, inexpensive, environmentally friendly and fully compatible with scaling up industrial needs. Moreover, the biopolymer oxygen-rich functionalities and their affinity towards metals make them ideal candidates for the stabilization of nanoparticles [26, 27]. For example, agarose has been utilized to prepare bioactive composite films containing metal/semiconductor nanoparticles by introducing a metal/semiconductor precursor solution followed by a reducing agent, such as hydrazine hydrate, during the agarose gelation process. In a typical synthesis, agarose powder was dissolved in Luria-Bertani (LB) broth kept at 80°C with constant stirring. CuSO₄ was added to this system at two different concentrations (about 3 and 6 µg of Cu per millilitre of LB broth), followed by the addition of N₂H₄ hydrate solution. The immediate appearance of wine red color was observed, indicating the formation of CuNPs which became faint upon solidification, and then was masked by the components of LB broth. The nanoparticles were trapped in the LB agarose matrix, which was then employed to check the NPs antibacterial activity, without further modification [26].

Cárdenas et al. have described the preparation and characterization of colloidal Cu nanoparticles/chitosan composite films (Fig. 3.3) by a solution-casting technique, assisted by microwave heating [28–30]. This method gives an appropriate nanoparticle size for its inclusion in chitosan matrix. The film-forming solution exhibited good dispersion and film-forming property due to the high density of amino and hydroxyl groups of chitosan, avoiding the aggregation of metallic particles. Cu nanoparticles incorporated in chitosan matrix improved the film barrier properties, decreasing the permeability to oxygen and water vapor. Furthermore, they increased the material protection against UV light [28, 29].

Recently, Mary et al. proposed a novel cellulose-based fiber, obtained by periodate-induced oxidation of cotton cellulose fibres to give di-aldehyde cellulose, followed by covalent attachment of –NH₂ group of chitosan through a coupling reaction [31]. This novel chitosan-bound cellulose fiber has been used for the immobilization of Cu²⁺ ions, producing a material the authors named “copper-bound chitosan-attached cellulose”, while, copper nanoparticles-loaded fibers (NCLCAC) were produced by

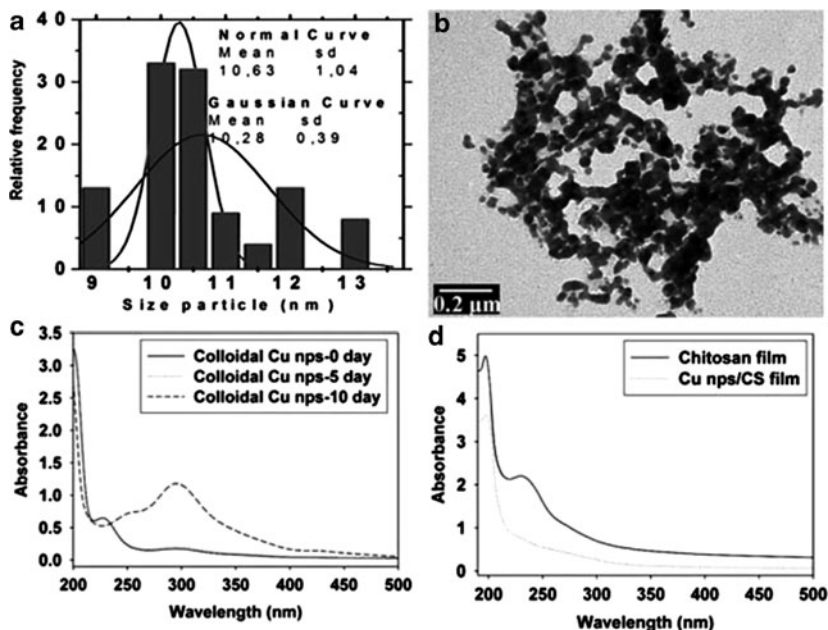


Fig. 3.3 (a) Particle size distribution of colloidal Cu NPs, (b) TEM micrograph of colloidal Cu NPs, (c) UV-vis spectra of colloidal Cu NPs, (d) UV-vis spectra of films (Reprinted from [28], Fig. 3.1. With kind permission from Springer Science+Business Media)

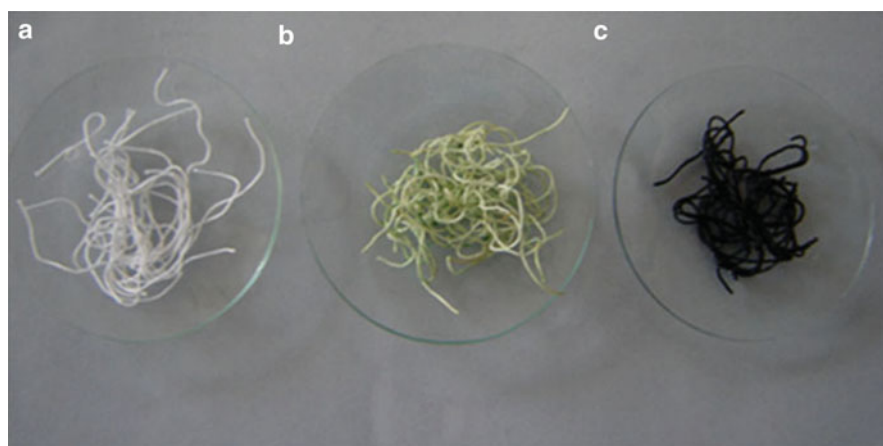


Fig. 3.4 Photograph showing (a) plain cotton cellulose fibers, (b) copper-bound chitosan-attached cellulose fibers, and (c) nanocopper-loaded chitosan-attached cotton fibers. Copyright permission requested (Reprinted with permission from [31]. Copyright 2009 John Wiley and Sons)

borohydride-induced reduction of Cu^{2+} (Fig. 3.4) [31]. The same authors have also developed copper nanoparticles-loaded alginate–cotton fibers, which were prepared by immersing cotton fibers in aqueous solution of sodium alginate, followed by cross-

linking of alginate chains in presence of Cu^{2+} ions; finally, the fibers were reduced with sodium borohydride [9].

Very recently, a new method for preparing antibacterial cotton bandages has been developed by treating fabric surfaces with CuO NPs obtained via ultrasound irradiation [32]. The sonication process involved an in situ generation of CuO NPs and their subsequent deposition on fabrics in a one-step reaction. CuO-coated bandages were prepared as follows: a cotton bandage was added to an $\text{Cu}(\text{Ac})_2$ H_2O solution of ethanol and then irradiated for 1 h with a high intensity ultrasonic Ti-horn. After adding the ammonium solution to the reaction cell, the color of the reaction mixture changed from light blue to deep blue and then became dark brown. The product was washed thoroughly, and then dried under vacuum. The as-prepared CuO NPs were thrown at the surface of the bandages by sonochemical microjets resulting from the collapse of the sonochemical bubble [32].

Copper-loaded carboxymethyl-chitosan (CMCS-Cu) nanoparticles have been successfully prepared by chelation under aqueous conditions [33]. CuSO_4 was added to a CMCS solution under magnetic stirring, and the pH value of the solution was kept acidic. The resulting particles were purified by centrifugation and then extensively rinsed, re-dispersed in water and, lastly spray-dried before further use or analysis [33].

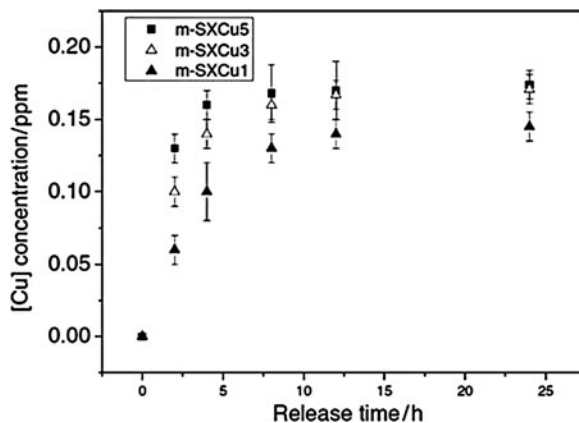
3.2.1.3 Fully Inorganic Copper Nanomaterials

Compared to organic hybrid antibacterial materials, fully inorganic antibacterial materials may offer several advantages, such as long-lasting action, stability (chemical, thermal, mechanical), simplified manufacturing and storage characteristics. The preparation of inorganic antibacterial materials has attracted interest in recent years, although it should be noted that – in the case of weak interactions of these agents with their supporting/dispersing media – this approach might suffer from NP leaching/releasing in aqueous media, which might give rise to nanotoxicology drawbacks.

A significant approach is that of synthesizing CuNPs in the presence of a supporting oxide, such as alumina, titania, and mesoporous silica. Based on the NP chemical stability, and on the interactions between CuNPs and the supporting oxide, the copper release properties can be delayed for such a long time that Cu-supported materials become attractive for antibacterial applications. Kim et al. reported on the synthesis and characterization of a well-dispersed Cu-SiO₂ nanocomposite that was obtained by depositing copper nanophases onto preformed SiO₂ NPs [34]. In this process, CuCl_2 was added to a SiO₂ NPs slurry under several mixing ratios and with or without making use of catalysts, at room temperature and under vigorous stirring. Finally, Cu-SiO₂-1, Cu-SiO₂-2, Cu-SiO₂-3, and Cu-SiO₂-4 nanocomposites were obtained [34].

Very recently, Wu et al. developed a novel biocompatible material composed of mesoporous copper-doped silica xerogels (m-SXCu) by a sol-gel process using tetraethoxy-orthosilicate and $\text{CuSO}_4 \cdot 5\text{H}_2\text{O}$ as precursors. Copper ions were demonstrated

Fig. 3.5 Change of Cu concentration in the SBF soaking m-SXCu over time (Reprinted with permission from [35]. Copyright 2009 IOP Publishing Ltd)



to be released from m-SXCu into the simulated body fluid at release rates depending on the nanocomposite composition (Fig. 3.5) [35].

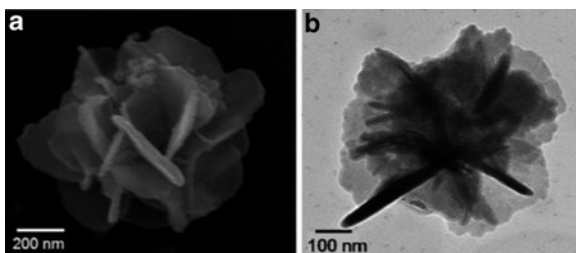
A few years later, this simple, low cost method was used to prepare SiO₂-Cu core-shell composites using SiO₂ spheres as the supporting core and CuNPs as the shell [36]. Uniform spherical particles of SiO₂ were fabricated according to an improved Stöber method. To deposit CuNPs on the surface of SiO₂ spheres, the specified amounts of CuSO₄·5H₂O and Fe powder were added to SiO₂ slurry. When the reaction was over, a fluid contained a brown-red precipitation was obtained. SiO₂-Cu-1, SiO₂-Cu-2, SiO₂-Cu-3, and SiO₂-Cu-4 were synthesized by adding different amounts of Fe powder [36].

Copper-based zeolites were synthesized by Petranovskii and co-workers [37]. The zeolitic raw mineral was ground and purified in order to remove the non-zeolitic mineral phases. Then, an ion exchange, a multistep process involving washing, drying and reduction in hydrogen was carried out, in order to obtain dispersed metal species. The advantage of copper zeolites is their low cost and high permitted maximum concentration of copper accordingly to the World Health Organization (WHO) requirements. In fact, WHO have classified zeolite minerals as a function of their toxicity versus human health [37].

In a recent work of Stanić, the synthesis of copper-doped hydroxyapatite (HAP) nanopowders was done by an acid-base neutralization method [38]. This method was chosen because of its simplicity, the relatively inexpensive chemicals, the possibility of preparing pure products, and its suitability for industrial production. A required amount of CuO was dissolved in a solution of H₃PO₄, and the slow addition to suspension of Ca(OH)₂ was applied to obtain a monophasic product. The slow reactant addition was found to yield pure, well-crystallized HAP, due to low supersaturation and avoidance of local inhomogeneity [38].

A new form of Au₃Cu₁ hollow nanostructure was prepared by the reaction of Cu nanoparticles with HAuCl₄. Following a course of aging, the biomineral botallackite Cu₂(OH)₃Cl nanoflowers (Fig. 3.6) were developed with the aid of Au₃Cu₁ hollow nanostructures at room temperature. In a typical preparation of hollow nanospheres

Fig. 3.6 (a) SEM image of a single nanoflower. (b) TEM image of a single nanoflower (Reprinted with permission from [39]. Copyright 2006 American Chemical Society)



and nanoflowers, a laser-prepared Cu colloidal solution was added to HAuCl_4 thus forming a greyish-blue dispersion of hollow nanospheres [39].

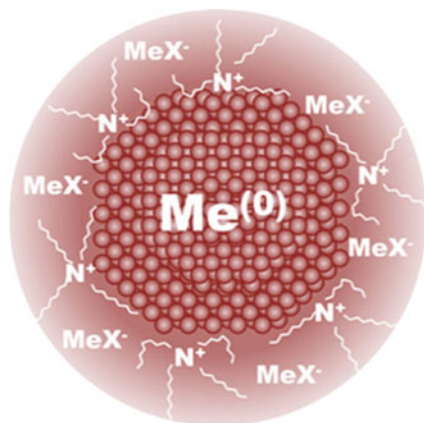
Finally, in a very recent work by Esteban-Tejeda et al., a low melting point soda-lime glass powder containing CuNPs was obtained following a simple and reliable bottom-up route starting from n-Cu sepiolite as source of the copper nanoparticles [40]. The glass was milled down and homogeneously mixed in isopropyl alcohol with the corresponding fraction of n-Cu sepiolite to obtain a copper-doped glass that was further treated, thus obtaining glass bars or pellets, that were finally milled down to $<30 \mu\text{m}$ [40].

3.2.2 Electrochemical Syntheses

Electrochemical routes to metal nanoparticles (MeNPs) are of great interest since they allow for high purity products and for a strict control over the cluster morphology, without the need for chemical reductants.

In 2004, the so-called “sacrificial anode” method (proposed by Reetz in 1994 [41]) was applied in the authors’ laboratory to the electrochemical preparation of core-shell copper nanoparticles [42]. CuNPs were prepared using a small-scale electrolytic process, performed by using a three-electrode cell, equipped with a copper sheet as sacrificial electrode, a platinum sheet as cathode electrode, and Ag/AgNO_3 0.1 M in acetonitrile as reference electrode. During such a process, when the applied potential is sufficiently high, the anode dissolves under the form of metal ions that are subsequently reduced at the cathode surface in the presence of proper surfactants, such as tetra-n-alkyl-ammonium salts, which stabilize the nanoparticle under the form of a core-shell structure in which the copper core is surrounded by quaternary ammonium ions (Fig. 3.7) [42–46]. Core-shell CuNPs were directly obtained as nanocolloidal dispersion in a solution of disinfecting quaternary ammonium species, and then they could be easily mixed to water-insoluble polymers which were ultrasonically dissolved in the electrolysis solution. Several dispersing polymers were tested, including polyvinyl-methyl-ketone (PVMK), polyvinyl-chloride (PVC), polyvinylidene-fluoride (PVDF), estel 1100, etc., as a function of the final application envisaged. The resulting CuNPs/polymer hybrid solutions – with different CuNPs loadings – were directly spin-coated onto proper substrates for further characterization or applications.

Fig. 3.7 Nanoparticle with a core-shell structure in which the copper core is surrounded by quaternary ammonium ions



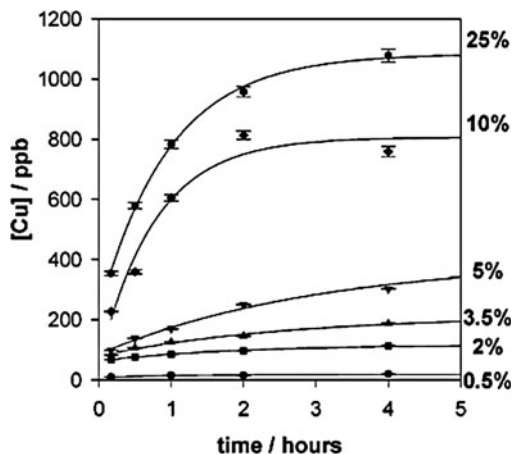
Moreover, despite unsupported copper colloids being extremely active against a wide range of bacterial pathogens [26], bioactivity experiments carried out on nanoparticles embedded in a polymer matrix showed that supported CuNPs may provide very high ion-release and eventually a significant efficiency in preventing microbial growth. Using supported materials in place of unsupported ones, affords a higher environmental compatibility for a wider range of applications, either as free-standing nanocomposites or as deposited thin nanostructured films. Lipophilic nanoparticles embedded into water-insoluble polymers cannot be released into the environmental media or when allowed in contact with aqueous solutions. Using different amounts of core-shell particles or properly choosing the stabilizing shell was shown to provide a way to finely select the concentration levels of released Cu ions. In fact, the stabilized structure of the CuNPs allowed a gradual and controlled copper ions release, when the nanocoatings were exposed to aqueous solutions (Fig. 3.8). The release extent of bioactive ions was demonstrated to be easily tuneable by a proper selection of preparation parameters, such as, for instance, the metal loading in the film. Noteworthy, the latter is a key aspect in order to kill or inhibit the growth of harmful species, without affecting the health of human beings [42, 47].

3.2.3 Physical/Mechanical Approaches

Physical approaches are frequently preferred to other routes when the simultaneous deposition of both nano-Cu and a proper dispersing medium (either organic or inorganic) is desired. The main difference between this approach and those described in the previous paragraphs is that the former does not necessarily provide NPs stabilization with a chemisorbed layer of surfactants or capping agents.

For example, the ion beam co-sputtering (IBS) technique can be employed to deposit different polymers and inorganic materials in an extremely controlled

Fig. 3.8 Copper release from CuNP-containing nanocomposites as function of time. Different CuNPs loadings in PVMK dispersing polymers were employed, relative weight percentages are reported on the right. Release curves are modelled as a first-order process (Reprinted with permission from [45]. Copyright 2005 American Chemical Society)



fashion, just by selecting the composition of appropriate targets and adjusting the IBS experimental conditions [48].

To the best of the authors' knowledge, the first work aiming to deposit copper-based nano-antimicrobials by IBS was published by Ivanov-Omskii et al. in 2000 [49]. The authors reported on the modification of hydrogenated amorphous carbon (a-C:H) films with nanosized copper clusters by IB co-sputtering of copper and graphite targets in argon–hydrogen (80% Ar and 20% H₂) DC magnetron plasma. The copper concentration in the growing film was varied within the range from 0 to 12 at.%, and it was controlled by changing the relative areas of graphite and copper targets. So, copper trapped into the a-C:H matrix was shown to deeply modify the structure and chemical characteristics of the layer [50].

In 2005, bioactive copper–fluoropolymer (Cu–CF_x) nanocomposites were successfully deposited on different substrates by co-sputtering a Teflon target and a copper target with Ar⁺ ion beams at room temperature. The ion-beam properties (energy, current) and the growth rate ratio were chosen in order to obtain copper–fluorocarbon composites with a copper volume fraction comprised in the interval $0 \leq \varphi \leq 0.25$ [48]. The analytical characterization of these layers revealed that inorganic nanoparticles composed of Cu²⁺ species could be evenly dispersed in a branched fluoropolymer matrix at different copper/fluoropolymer concentration ratios. So, the IBS technique enabled the controlled and reproducible inclusion of inorganic NPs in a polymer-dispersing matrix, thus obtaining active coatings with tuneable properties [48].

Recently, Kelly et al. have co-deposited TiN/Cu nanocomposites with varying copper contents (0 to ~26 at.%) in a dual-pulsed magnetron sputtering system [49, 51]. The rig was equipped with two vertically opposed closed field unbalanced magnetrons. The power applied to the Ti target was kept constant for the deposition of TiN-based coatings, while the power applied to the Cu target was varied in order to obtain different coating compositions [49].

In 2010, Chang and co-workers proposed nanostructured Cr₂N/Cu multilayer thin films that were deposited by the bipolar asymmetry reactive pulsed DC magnetron sputtering system [52]. Several multilayered thin films were deposited by alternately rotating the substrates from the plasma of Cr target to the plasma of Cu target. The target power values of Cr and Cu were adjusted to achieve a Cr₂N/Cu thickness ratio of around 9:1. Different bi-layer periods (Λ) were achieved by controlling the substrate holding time in the plasma of Cr or Cu. In order to investigate the effects of Cu layer thickness on the antibacterial activity of the coatings with the same Λ , four thickness ratios of Cr₂N/Cu layers were prepared [52].

In a study by Zhang et al. in 2006, copper was incorporated into the surface of polyethylene (PE) specimens by means of a plasma immersion ion implanter (PIII) [53]. One of the advantages of this approach is that low-energy Cu PIII can introduce a large amount of Cu into the polymer without causing too much damage to the polymer surface [53–55]. In a later study by the same authors, medical-grade PE specimens were implanted with Cu in a plasma immersion ion implanter equipped with a copper cathodic arc plasma source and nitrogen PIII was performed to change the structure of the implanted region of the substrate [56]. Compared to single plasma implantation processes, this dual PIII process (Cu/N₂ PIII) provided a better control over the copper release rate and improved the long-term antibacterial properties of the Cu–PE nanomaterials, producing new polar unsaturated functional groups such as C = N and C \equiv N in the near surface of the polymer [56].

Ren and co-workers prepared copper oxide (CuO) nanoparticles using thermal plasma (TesimaTM) technology in 2009. The procedure allowed the preparation of CuO, Cu, and Cu₂O nanoparticles with extremely high surface areas and unusual crystal morphologies [57]. On the other hand, drawbacks are represented by the cost of the processing apparatus and, most of all, by the potential risks related to handling copper-based nanoparticulate matter that could be unintentionally inhaled.

Finally, a low cost approach to nanoparticles and nanoparticulate coatings has been proposed by Yates et al., who used a flame-assisted chemical vapor deposition technique (FACVD) employing aqueous solutions of cupric nitrate as precursor, leading to nanostructured metal oxide thin films [58]. FACVD is a relatively simple atmospheric pressure chemical vapor deposition (CVD) technique that is compatible with both small volume batch and high volume continuous coating processes. Use of this method with low hazard aqueous solutions of simple metal salts can yield metal oxide thin films, which represents a major advantage in terms of precursor cost and environmental impact compared to alternative CVD methods [58].

3.3 Antimicrobial Activity

Copper shows an excellent antimicrobial activity against a wide range of microorganisms [1, 10], and such a property is greatly improved when Cu is properly nano-dispersed [59].

All papers reviewed in the previous section deal with the growth inhibition or killing effects of novel copper nanostructures towards several microorganisms. In this section, these studies have been classified according to the bioactivity towards three target classes: bacteria, fungi, and algae.

Most of the bacteria in the body are rendered harmless by the protective effects of the immune system, and a few are beneficial; however, some species of bacteria are pathogenic and may cause infectious diseases. Fungi have an essential role in the decomposition of organic matter and have fundamental roles in nutrient cycling and exchange, but many species produce bioactive compounds, including mycotoxins, that are toxic to animals including humans. Finally, the various sorts of algae play significant roles in aquatic ecology, even if some of them are common constituents of the biofilm formed during marine biofouling.

Genetic and biochemical studies have been conducted with microbial model systems including bacteria and yeast, establishing that cells have developed a sophisticated homeostatic mechanism to uptake copper [11, 12].

Microbial sensitivity to nanostructures has been found to be extremely different, depending on the microbial species and on the experimental set-up. Different methods that have been used to test the antimicrobial activity of copper nanomaterials are itemized as follows: disc diffusion test also defined zone of inhibition (ZOI), minimum inhibitory concentration (MIC), minimum bactericidal concentration (MBC) and counting the number of colony-forming units.

MIC is defined as the lowest concentration of a material that inhibits the growth of an organism; while MBC is defined as the lowest concentration of a material that inhibits the growth of an organism in batch cultures, this can be determined from broth dilution MIC tests by subculturing to agar media without antibiotics.

Hence, a quantitative comparison of the bioactivity effects of Cu-nano-antimicrobials is not possible in all cases, since the antimicrobial effectiveness was studied using different experimental parameters, such as methods, time of contact, and microorganism strain, as well as its initial concentration.

3.3.1 Antimicrobial Tests Against Bacteria

Bacteria are a large group of single-celled prokaryote microorganisms. There are two different types of cell wall in bacteria, called Gram-positive and Gram-negative. The names originate from the reaction of cells to the Gram stain, a test long-employed for the classification of bacterial species.

Gram-positive bacteria possess a thick cell wall containing many layers of peptidoglycan and teichoic acids, while Gram-negative bacteria have a relatively thin cell wall consisting of a few layers of peptidoglycan surrounded by a second lipid membrane containing lipopolysaccharides and lipoproteins.

3.3.1.1 *Escherichia coli*

Escherichia coli represents the most important model microorganism in studies on the antibacterial activity towards Gram-negative bacteria. Many papers mentioned in paragraph two deal with the assessment of the nano-antimicrobial activity against *E. coli*, tested using different protocols [9, 17, 25, 26, 31, 32, 34–36, 38, 40, 44, 45, 48, 52, 53, 57, 58].

Three different methods have been used to study the effects of CuNPs synthesized by Ruparelia and co-workers towards *E. coli* (four strains): disc diffusion test, MIC and MBC. The MIC and MBC values observed in this study are, respectively, in the range of 140–280 and 160–300 $\mu\text{g/mL}$. A good negative correlation was observed between the inhibition zone observed in disc diffusion test and MIC/MBC determined based on liquid cultures with the various strains ($r^2 = -0.75$) [17].

Copper oxide nanoparticles in suspension were used to determine the lowest bactericidal concentration required to prevent the growth of *E. coli* (NCTC 9001). As a result, a MBC value of 250 $\mu\text{g/mL}$ was found [57], which is very similar to that observed by Ruparelia et al.

The disc diffusion test was also used to evaluate the antimicrobial properties of nanocopper-loaded fibers [31], nanocopper alginate–cotton cellulose fibers [9], Cu-SiO₂ nanocomposite [34], SiO₂-Cu composites [36], and copper-doped hydroxyapatite nanopowders [38].

The results of antibacterial action of nanocopper-loaded fibers, namely NCLCAC (2) and NCLCAC (4), clearly indicate that Petri dishes with plain fibers show dense populations of bacterial colonies. In contrast, Petri dishes supplemented with nanocopper-loaded fibers, NCLCAC (2) and NCLCAC (4), show less growth of colonies, as indicated by a clear zone of inhibition around the bunch of the amount of CuNPs present in the fibers which, in turn, depends upon the concentration of Cu²⁺ solution used for copper loading [31]. In another paper, the same authors showed that nanocopper alginate–cotton cellulose fibres efficiently inhibit bacterial growth (Fig. 3.9) [9].

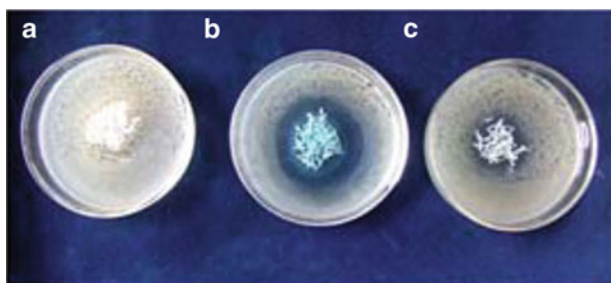


Fig. 3.9 Antibacterial activity of copper nanoparticles loaded alginate cotton cellulose fibres (Reprinted with permission from [31]. Copyright 2009 John Wiley and Sons)

The disk diffusion assay of Cu-SiO₂ nanocomposites was determined by placing an 8-mm disk saturated with 50 μL of Cu-SiO₂-1, Cu-SiO₂-3, and Cu-SiO₂-4 nanocomposite aqueous slurry onto an agar plate seeded with *E. coli* (ATCC 25922). After 24 h of incubation, the diameters of the inhibition zones were measured. The antibacterial activity of Cu-SiO₂-1 was not detected, while the inhibition zones of SiO₂-4 and Cu-SiO₂-3 were determined as 11 and 15 mm. The antibacterial activities of the Cu-SiO₂-3 nanocomposite were higher than those of Cu-SiO₂-4 because Cu nanoparticles of the Cu-SiO₂-3 nanocomposite were well formed and not aggregated on the surface of the SiO₂ nanoparticle [34].

The antimicrobial activity of SiO₂@Cu composites was examined against *E. coli* by two methods: paper disk agar diffusion assay and MIC. The inhibition zones of SiO₂@Cu-2, SiO₂-Cu-3, SiO₂-Cu-4 were determined, respectively, as 16.8, 10.1 and 12.1 mm. SiO₂-Cu-2 showed the best antibacterial properties and perfect core-shell structure. In order to calculate antimicrobial activity quantitatively, the MIC method was performed [36].

The antimicrobial activity of copper-doped hydroxyapatite nanopowders was tested against *E. coli* (ATCC 25922) by the so-called “agar diffusion” and “liquid challenge” methods. The diffusion technique was carried out by pouring agar into Petri dishes to form 4-mm-thick layers and adding a dense inoculum of the tested microorganisms in order to obtain semiconfluent growth. The results of antimicrobial disk diffusion tests showed that only CuHAP2 affects *E. coli* and that the average inhibition zone was 2 mm. The quantitative test was performed according to Radetić et al. [60] with some modifications. The results of the quantitative antimicrobial tests in liquid medium demonstrated that all metal-doped HAP samples show viable cells reduction [38].

Cioffi et al. carried out biological tests against *E. coli* on electrosynthesized copper nanoparticles dispersed in several polymers, and on IBS-deposited composites and copper fluoropolymer nanocomposites films. The screening of the antimicrobial activity was performed using a two-steps protocol. In the first step, properly diluted cultures containing the living cells were allowed to be in contact, under sterile conditions, with the nanostructured layers for a controlled interaction time. In the second step, a plate counter agar solid culture medium was poured onto the glass plates, which were subsequently incubated so that the vital cells, eventually present, could grow into colonies.

The microorganism colony presence was then evaluated, by counting the colony-forming units per Petri plate (CFU/mL). In the case of the CuNPs stabilized by tetra-butyl-ammonium-perchlorate (TBAP) and embedded in polymer matrixes like PVMK, PVC, and PVDF, it was observed that the samples always exerted clear biostatic activity on *E. coli*. Moreover, it was systematically observed that the CuNPs-PVMK films exhibited the strongest biostatic effect, while the least effective were the CuNPs-PVDF films.

The CFUs counted in the plates with the bare polymers and the polymers added with TBAP were comparable, within the experimental error, to the control experiment, indicating that neither the bare polymers nor the alkyl-ammonium salt exert any short-term biostatic activity on the growth of the microorganisms [45].

In contrast, in the case of the CuNPs stabilized by tetraoctylammonium chloride (TOAC) and embedded in polymer matrixes like PVMK, the ammonium salt gave rise to a strong growth inhibition effect, causing a significant decrease in the cellular growth. Interestingly, these nanocomposites were characterized by increased biological activity due to the simultaneous action of the TOAC and the embedded metal species [44].

Moreover, Cu-CFx coatings showed an even more striking disinfectant action towards *E. coli* thanks to the extremely high concentration of released copper species [48].

The viable *E. coli* cells were monitored by counting the number of colony-forming units, and the effect was quantitatively determined by the killing percentage for Cu-MWCNTs [25], CuO–cotton nanocomposites [32], Agarose–CuNPs composites [26], m-SXCu [35], Cr₂N/Cu layer [52], Cu PIII PE samples [53], Cu PIII PE and Cu/N₂ PIII PE samples [56].

Cu-MWCNTs were also investigated against bacteria, following the requirement of ISO 14729:2001(E) regulations. An amount of 20 μL of the bacterial suspension in USP phosphate buffer pH 7.2 was transferred to 1 mL of the prepared sample (21 μg of MWCNT-COOH/mL and 21 μg of Cu-MWCNT/mL) in a test tube. A series of tenfold dilutions in neutralizing broth were prepared and plated out in Trypticase Soy Agar. The plates were incubated at 37°C for 72 h and counted for colony-forming units. The results were expressed as:

$$\%Kill = [(N_{\text{control}} - N_{\text{sample}})/N_{\text{control}}] \times 100$$

where N_{sample} represented the counts of survived bacterial inoculums in the neutralization broth containing 21 μL of Cu-MWCNTs or pristine MWCNTs. Pure MWCNTs exhibited a relatively low effect against *E. coli* bacteria ($20 \pm 2.5\%$) at the concentration level of the 21 μg/mL. Cu-MWCNTs exhibited a fairly good antimicrobial efficiency (~75%) as compared to pure CuNPs showing a killing percentage of about 52% [25].

CuO–cotton nanocomposites tested against *E. coli* led to the complete inhibition of cell growth [32].

Agarose–CuNPs composites at two different concentrations (3 and 6 μg of Cu per millilitre of LB broth) were employed to check the antibacterial activity of *E. coli*. Complete inhibition was observed even at the lower concentration (at about 3 μg of Cu per gram of composite gel) [26].

The antibacterial performances of m-SXCu against *E. coli* (ATCC 8723) were quantitatively determined using the same relationship used in the case of Cu-MWCNTs. m-SXCu showed good antibacterial activity against *E. coli*; for instance, the antibacterial rate reached 99% for the sample coded as “m-SXCu5” at 1 h, while it reached 99% for all m-SXCu samples at 24 h (Fig. 3.10). The antibacterial rate was improved with the increase of the amount of Cu, indicating that addition of Cu ions to m-SX enhanced its antibacterial activity [35].

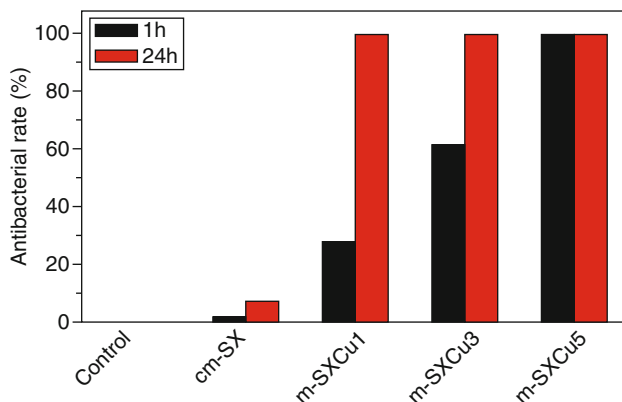


Fig. 3.10 Antibacterial rate of m-SX and m-SXCu against *E. coli* (Reprinted with permission from [35]. Copyright 2009 IOP Publishing Ltd)

The antibacterial tests of coatings with various bilayer periods (Λ) and different $\text{Cr}_2\text{N}/\text{Cu}$ thickness ratios were performed to evaluate the bactericidal ability towards *E. coli* (ATCC25922). A film attachment method (modifying the method JIS Z 2801:2000) was adopted for evaluating the antibacterial activity in this work. The effect was quantitatively determined using the same relationship used in the case of Cu-MWCNTs. Apparently, the coating antibacterial rate against each bacterium increased with increasing bilayer period and reached a maximum value of 100% at $\Lambda = 20$ nm, followed by a drastic decrease when the bilayer period increased to 40 nm. In order to investigate the effects of Cu layer thickness, the antibacterial rates of the coatings with fixed $\Lambda = 12$ nm and different $\text{Cr}_2\text{N}/\text{Cu}$ layer thickness ratios were also studied. As expected, the antimicrobial rate increased with increasing Cu layer thickness and reached a maximum value for the *E. coli* test of 100% at a $\text{Cr}_2\text{N}/\text{Cu}$ layer thickness ratio of 7:3[52].

Cu PIII PE samples were tested against *E. coli* (ATCC10536) suspensions with a concentration of 10^6 CFU/mL. The antibacterial performance was determined by the plate-counting method and the antibacterial effect was quantitatively determined using the same relationship used for Cu-MWCNTs. The effectiveness of the antimicrobial properties was as high as 96% [53].

In a more recent work, the antimicrobial properties of the Cu PIII PE and Cu/N_2 PIII PE samples were studied at immersion times of 0, 14, 28 days. The tested microorganisms were *E. coli* suspensions with a concentration of 10^6 CFU/mL. The antibacterial performance was determined by the plate-counting method and the antibacterial effect was quantitatively evaluated using the same relationship of the previous paper [25]. Both Cu PIII PE and Cu/N_2 PIII PE showed excellent antibacterial effects against *E. coli*. This was hypothesized to mainly stem from the surface-deposited Cu that can deliver immediate antimicrobial effects. After 14 days, the Cu PIII PE and Cu/N_2 PIII PE samples still possessed good antibacterial performances against such a concentrated cell suspension, the antimicrobial effects against *E. coli* being higher than 70% and 80%, respectively [56].

Finally, the viable *E. coli* cells were monitored by counting the number of colony-forming units, and the effect was quantitatively determined by the logarithm of reduction for n-Cu sepiolite and the n-Cu-doped glass powder [40] on copper oxide thin films [58].

Biocide tests were performed to investigate the effect of the n-Cu sepiolite and the n-Cu-doped glass powder towards *Escherichia coli JM 110*; the nanomaterials were added over the cultures to obtain a final concentration of copper in each culture of 0.036 and 0.054 wt%. The survivals from each culture were counted every 24 h, after plating serial dilution. The effectiveness of the biocide agent was expressed as the logarithm of reduction, and it is defined as follows:

$$\log \eta = \log A - \log B$$

where A is the average number of viable cells from inoculums control after 24 or 48 h and B is the average number of viable cells from the substance after 24 or 48 h. The activity against *E. coli* of n-Cu glass powder was very high ($\log \eta$ of 8.2 for the n-Cu glass powder versus 0.76 for the n-Cu sepiolite) after 48 h. Consequently, the MIC for the n-Cu glass powder as an antibacterial agent is <0.036 wt% [40].

Biocidal activity of copper oxide thin films on glass was determined by monitoring the survival rate of *E. coli* (ATCC 10536). The used test was a modification of the standard test described by BS EN 13, 697:2001 [61]. The films deposited at 400°C and with 30 passes were found to be highly bioactive and achieved high kill rates of >5 log reduction over 12 min. A much thinner sample of CuO, deposited at 400°C and with two passes, was also tested; in this case, the killing rate was much slower, taking 80 min for a 3 log reduction. The much slower growth rate was hypothesized to be correlated to a lower amount of CuO [58].

3.3.1.2 *Staphylococcus aureus*

Staphylococcus aureus represents the most frequently used target microorganism in studies on the antibacterial activity towards Gram-positive bacteria.

The antimicrobial properties of copper nanoparticles were investigated using *S. aureus* (three strains) by the disc diffusion test, MIC and MBC. The MIC and MBC values observed in this study are, respectively, 140 and 160 $\mu\text{g/mL}$ [17].

Copper oxide nanoparticles in suspension were used to determine the MBC value for *S. aureus* EMRSA-16, *S. aureus* EMRSA-1, *S. aureus* 252, *S. aureus* (Golden) and *S. aureus* (Oxford) that were respectively equal to 1,000, 250, 1,000, 2,500 and 100 $\mu\text{g/mL}$ [57].

Micro-MIC assays were performed for both Au_3Cu_1 hollow nanostructure and the derived $\text{Cu}_2(\text{OH})_3\text{Cl}$ nanoflowers. Both MIC50 and MIC90 were defined as the minimal concentrations of the nanoparticles to achieve 50% and 90% growth inhibition of the bacteria, respectively, as referenced to the non-treated control. As shown in Fig. 3.11, antimicrobial activities of both nanomaterials were observed.

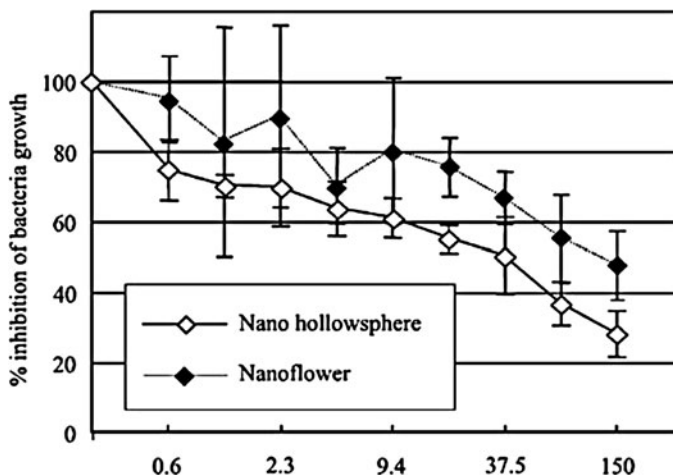


Fig. 3.11 Bacteria growth inhibition for *S. aureus* as referenced to the untreated control revealed dose-dependent antimicrobial activity of both hollow nanospheres (Au_3Cu_1) and nanoflowers ($\text{Cu}_2(\text{OH})_3\text{Cl}$) (Reprinted with permission from [39]. Copyright 2006 American Chemical Society)

However, the hollow nanospheres showed stronger antibacterial effects than the nanoflowers with MIC₅₀ values of 39.6 and 127.2 $\mu\text{g}/\text{mL}$, respectively [39].

Bentonite-immobilized copper/PMMA hybrid nanocomposites exhibited only bacteriostatic behavior against *S. aureus* [24].

The antimicrobial activity of $\text{SiO}_2\text{-Cu}$ composites was examined not only against *E. coli* but also against *S. aureus*. The inhibition zones of $\text{SiO}_2\text{-Cu}_2$, $\text{SiO}_2\text{-Cu}_3$, and $\text{SiO}_2\text{-Cu}_4$ were determined, respectively, as 16.0, 9.5 and 11.2 mm; thus, $\text{SiO}_2\text{-Cu}_2$ showed the best antibacterial properties. The $\text{SiO}_2\text{-Cu}_2$ composites exhibited high efficiency for destruction of *S. aureus* with a MIC value of 0.8 mg/mL [36].

The antimicrobial activity of Cu-doped hydroxyapatite nanopowders was tested against *S. aureus* (ATCC 25923) by the agar diffusion method and the liquid challenge method in buffer solution with the same protocol used for *E. coli*. The results of antimicrobial disk diffusion tests showed no inhibition zone. The results of the quantitative antimicrobial tests in liquid medium demonstrated viable cell reduction by all the metal-doped HAP samples [38].

ZoI and a nitro-blue tetrazolium (NBT) redox dye were used against *S. aureus* to determine the antimicrobial effectiveness of TiN/Cu nanocoatings following incubation. For the NBT assays, colony-forming units were counted following submersion in the NBT dye for 5 h. For the ZoI assays, the zones of inhibition from the surface were measured using an electronic micrometer. For the NBT assays, significant reduction in the number of viable cells was observed with increasing Cu content, compared to the 'pure' nitride surfaces, while no zones of inhibition were observed. This could be explained by considering that the latter assay is sensitive to ion leaching from the surface into the agar [49].

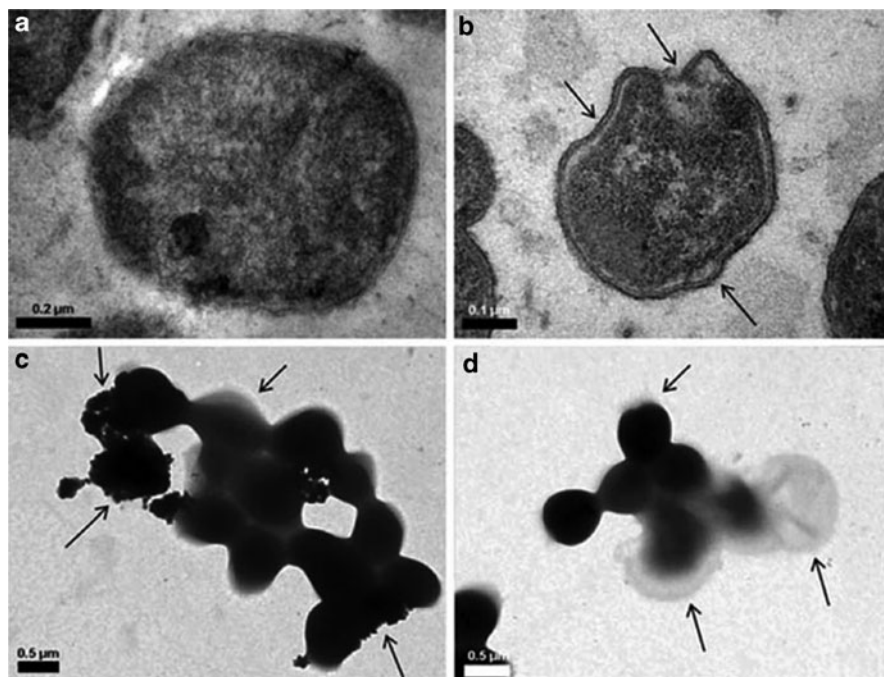


Fig. 3.12 (a) TEM micrograph of thin section of untreated *S. aureus*. (b) TEM micrograph of thin section of *S. aureus* treated with composite film. (c, d) TEM micrograph of deposition onto copper grid of *S. aureus* treated with composite film (Reprinted from [28], Fig. 3.6. With kind permission from Springer Science+Business Media)

In a recent work, Cu nanoparticles/chitosan composite films were tested against *S. aureus* (ATCC 25923). A standard plate count method on Mueller–Hinton Agar was used to determine the concentration of bacteria capable of reproducing. The composite film was effective in reducing microbial concentration in the bulk fluid for the microorganism tested. Cell wall deformation is related to the cytoplasmic volume decrease (Fig. 3.12) and the detrimental structural change was the result of the cell shrinkage [28].

CuO–cotton nanocomposites were also tested against *S. aureus*. Treatment for 1 h with the coated cotton led to the complete inhibition of cell growth [32].

The antibacterial performance of m-SXCu against *S. aureus* (AATCC 6538) was determined by the method of plate counting. Similar results to *E. coli* were obtained, since the antibacterial rate of m-SXCu increased with the increase of Cu amounts at 1 h as shown in Fig. 3.13 [35].

In the authors' laboratories, TBAP-capped CuNPs were dispersed in several polymers and employed in biological experiments against *S. aureus* and *Listeria monocytogenes* following the experimental protocol previously described. A similar approach was also used for Cu-CF_x ultra-thin coatings. In all cases, a clear correlation was found between ion release properties and bioactivity of these nanomaterials [45, 48].

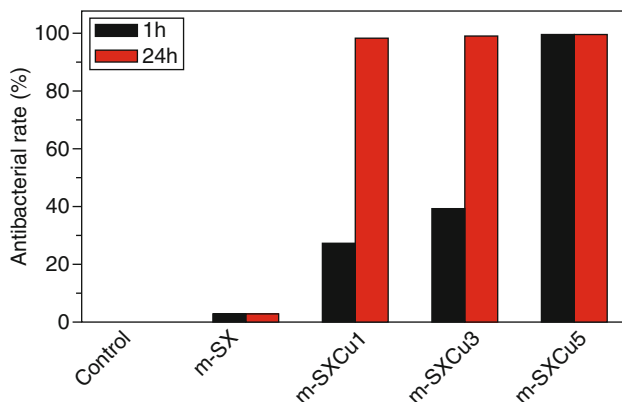


Fig. 3.13 Antibacterial rate of m-SX and m-SXCu against *S. aureus* (Reprinted with permission from [35]. Copyright 2009 IOP Publishing Ltd)

The antibacterial activity of 1,000-nm carboxymethyl-chitosan (CMCS) particles and of ~100-nm copper-loaded CMCS particles were evaluated against *S. aureus* by the vibration method. Results showed that the antibacterial efficiency of nanoparticles reached 99%, which is much more efficient than the 68.9% of the normal 1 of 1,000 nm and the 6.1% of CMCS [33].

Antibacterial tests of coatings with various bilayer periods and different Cr₂N/Cu thickness ratios were performed against *S. aureus* and showed that the antibacterial rate reaches 100% at Cr₂N/Cu layer thickness ratios of 5:5 [52].

Cu PIII PE samples were also tested against *S. aureus* (ATCC 6538) and their antibacterial effect was as high as 86% [53].

Finally, the antimicrobial activity of Cu-SiO₂ nanocomposite was measured by the paper disk diffusion method against *S. aureus* (ATCC 25923). Only the antibacterial activity of Cu-SiO₂-3 and Cu-SiO₂-4 was detected [34].

3.3.1.3 Gram+ and Gram– Bacteria

In view of real-life applications, copper nanomaterial antimicrobial properties were tested towards several bacteria.

Bacillus subtilis (three strains), although it is not a human pathogen, may contaminate food and causes food poisoning and, as such, it has been chosen as a target species [17]. Tests on this microorganism were carried out by MIC and MBC approaches. The MIC and MBC values observed in this study are, respectively, 20 and 40 µg/mL. As a result, copper nanoparticles have been hypothesized to show a great affinity to surface-active groups of *B. subtilis*.

Glass-supported copper oxide thin films were also tested against *Staphylococcus epidermidis* (NCTC 11047). This bacterium was chosen since it can grow on plastic devices, such as intravenous catheters, and on medical prostheses placed within the body. Interestingly, the rate of kill exerted by the afore-mentioned

Cu-nano-antimicrobials was similar for both *E. coli* and *S. epidermidis*. Generally, Gram-positive bacteria such as *S. epidermidis* are considered to be more resistant than Gram-negative bacteria such as *E. coli*, but in this case there was little difference [58]. Not only copper oxide thin films on glass but also copper oxide nanoparticles in suspension were used to determine the lowest bactericidal concentration required to prevent the growth of two strains of *S. Epidermidis*. The MBC value for *S. Epidermidis* SE-51 and SE-4 was 2,500 µg/mL. Moreover, the MBC value was 5,000 µg/mL for *Proteus* spp. [57].

Cu nanoparticles/chitosan composite films were also tested against *Salmonella enterica* serovar *Typhimurium* with the same protocol used for *S. aureus*. The cell wall of *S. Typhimurium* is very rough due to the cell wall components, which are also possibly cross-linked, resulting in heterogeneous surfaces. Treated cells with composite film appeared smooth, collapsed and cracked, and markedly shrank [28].

Very recently, copper-containing nanomaterials such as TiN/Cu nanocoatings, Cr₂N/Cu multi-layered thin films and copper oxide nanoparticles were tested against *Pseudomonas aeruginosa*. Usually, this microorganism infects the pulmonary and urinary tracts, as well as burns, wounds, and also causes other blood infections. As a consequence, *P. aeruginosa* is a target species of considerable applicative interest. In the case of TiN/Cu films, similar considerations to *S. aureus* could be done about the biological results as reported in Sect. 3.1.2 [49]. In the case of Cr₂N/Cu multi-layered thin films, the antibacterial rate reached 100% at a Cr₂N/Cu layer thickness ratio of 3:7 [52]. Finally, copper oxide nanoparticles in suspension were used to determine the lowest bactericidal concentration required to prevent the growth of *P. aeruginosa*; the resulting MBC value was 5,000 µg/mL [57].

The activity of the Cu-SiO₂ nanocomposite against *Enterobacter cloacae* (ATCC 29249), which is associated with infections of the urinary and respiratory tracts, was measured by the paper disk diffusion method [34].

The antimicrobial effect of the n-Cu sepiolite and the n-Cu-doped glass powder was also performed against *Micrococcus luteus*, which colonizes the human mouth, mucosae, oropharynx and upper respiratory tract. For a copper content in the cultures of 0.036 wt%, n-Cu sepiolite and n-Cu glass powder showed similar bioactivity (log η of 3.36 versus 3 after 48 h of biocide test). However, at an increasing content of copper in the cultures, the biocide activity of n-Cu glass powder was significantly higher [40].

In the authors' laboratories, tests on the bioactivity of CuNPs-Estel nanomaterials were recently performed against *Arthrobacter histidinolovorans* (ATCC 11442), yielding a complete inhibition of the microorganism growth [46]. The importance of this evidence relies in the perspective application of Cu/Estel nano-antimicrobials to the field of the cultural heritage. The proposed material behaved as a multifunctional coating, capable of combining the antimicrobial properties of nanostructured copper with those of the formulations applied to the restoration of stone artworks.

Copper NPs/polymer composites synthesized by Neckers and co-workers were tested against cyanobacterial strains of *Synechocystis* sp. PCC 6803 (freshwater) and *Synechococcus* sp. PCC 7002 (marine). The Cu NP/polymer composite pellets were immersed in flasks containing the growing cells at the start of the culture period. Cell

growth of the cyanobacteria was correlated with absorbance measured at 24-h intervals at 680 nm. All tested Cu NP species exhibited good antibacterial activity, especially when NPs were chemically attached to the polymer backbone [22].

3.3.2 Antimicrobial Tests Against Fungi

The fungus kingdom encompasses an enormous diversity of taxa with varied ecologies, life cycle strategies, and morphologies ranging from single-celled aquatic chytrids to large mushrooms.

So far, more than ten papers have dealt with the bioactivity of the novel copper nanostructures towards fungi. The different studies on each nanomaterial are itemized and classified in the following in terms of the function of the target microorganism.

Among the different species of fungi, *Saccharomyces cerevisiae* is a model organism for studying the antifungal activity of nanomaterials. In 2004 and following years, we choose this microorganism to test copper nanoparticles/polymer composites and copper fluoropolymer nanocomposites films. The screening of the antifungal activity was performed using a two-step protocol, as previously described. The microorganism colony presence was then evaluated, by counting the colony-forming units per Petri plate (CFU/mL).

In the case of the CuNPs stabilized by TBAP and embedded in polymer matrixes like PVMK, PVC, and PVDF, it was observed that the samples always exerted clear biostatic activity on the yeast cell growth. Moreover, it was systematically observed that composites exerting the highest release of Cu ions exhibited the strongest biostatic effect [45]. The results clearly showed that the higher the nanoparticle loading, the lower the number of residual CFU; i.e., the stronger the antifungal effect (Fig. 3.14) [42].

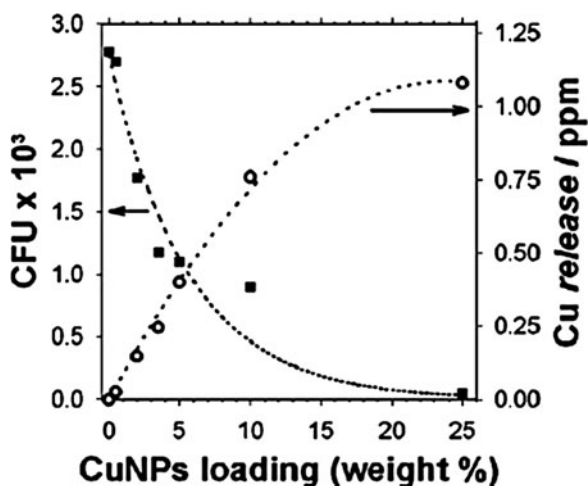


Fig. 3.14 The left Y axis reports the amount of the CFU/mL for seven different PVMK nanocomposites loaded with different bulk concentrations of CuNPs. The right Y axis reports the copper concentration released by the nanocomposites in the culture broth after 4 h exposure (Reprinted with permission from [42]. Copyright 2004, American Institute of Physics)

Similar results were obtained for Cu-CF_x coatings. Higher loadings of unstabilized metal nanoparticles resulted in higher copper surface availability and in a much higher release of copper ions; eventually, this gave rise to a significantly increased bioactivity [48].

Finally, in the case of CuNPs stabilized by TOAC and embedded in polymer matrixes like PVMK, it was observed that the ammonium salt itself was strongly inhibiting the fungi growth. As a consequence, Cu/TOAC/polymer hybrid materials showed an increased biological activity, thanks to synergistic action of the quaternary ammonium species and of copper ions [43, 44].

Effective antifungal activity of hyperbranched polyamine CuNPs, Cu-SiO₂ nanocomposites, SiO₂-Cu and copper-doped hydroxyapatite nanopowders were observed against *Candida albicans* fungus, which can be a pathogenic agent, causing candidiasis in the oral cavity, the esophagus, the gastrointestinal tract, the urinary bladder and the genital tract. The results of antifungal studies clearly demonstrated that the colloidal hyperbranched polyamine/CuNPs inhibited the growth of *C. albicans* even at very low total concentrations of copper (1.4 g/100 L) [23].

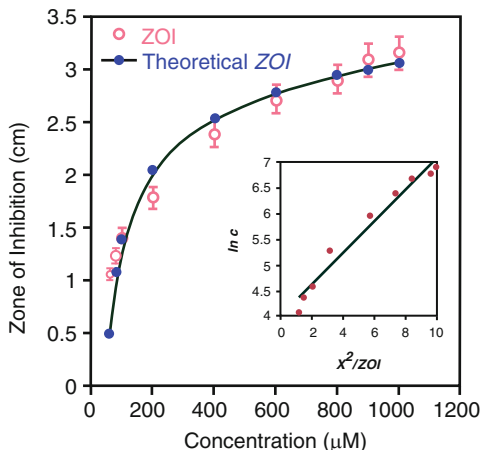
The antimicrobial activity of the Cu-SiO₂ nanocomposite was measured by the paper disk diffusion method. The disk diffusion assay was determined by placing an 8-mm disk saturated with 50 μL of several Cu-SiO₂ nanocomposite aqueous slurries onto an agar plate seeded with *C. albicans* and *Penicillium citrinum*. The latter produced ochratoxin and citrinin which may cause growth retardation, hepatic necrosis and nephropathy. After 24 h of incubation, the diameters of the inhibition zones were measured and selected samples were shown to be active against *C. albicans* [34].

In a recent paper, the antimicrobial activity of SiO₂-Cu composites was examined by two methods, namely paper disk agar diffusion assay and MIC. The ZoI comprised between 9 and 10.6 mm, as a function of the amount of copper on the SiO₂ surface. In order to calculate antimicrobial activity quantitatively, the MIC method was performed. The SiO₂-Cu core-shell composite was dissolved in ultra-pure deionized water to form colloidal solutions with different SiO₂-Cu concentrations. High efficiency for the destruction of *C. albicans* was obtained at nano-antimicrobial concentrations of 0.9 mg/mL [36].

The antimicrobial activity of copper-doped hydroxyapatite nanopowders was tested against yeast *C. albicans* (ATCC 24433) by the agar diffusion method and the liquid challenge method in buffer solution. The diffusion technique was carried out by pouring agar into Petri dishes to form 4-mm-thick layers and adding a dense inoculum of the tested microorganisms in order to obtain semiconfluent growth. The results of antimicrobial disk diffusion tests showed that only some samples affected *C. albicans* and the average inhibition zone was 3 mm. The results of the quantitative antimicrobial tests in liquid medium demonstrated that all metal-doped HAP samples show viable cell reduction [38].

Low-polydispersion copper nanoparticles and nanorods exhibited antifungal properties against *Stachybotrys chartarum*, which is a common indoor house mold that has been linked to various health effects and the “sick building

Fig. 3.15 Antifungal and catalytic properties of CuNPs. Radii of the inhibition zones plotted as a function of CuNP concentration. Critical inhibitory concentration $55.46 \mu\text{M}$ is estimated from the y-intercept (Reprinted with permission from [21]. Copyright 2010 American Chemical Society)



syndrome". The disk diffusion assay and MIC tests were used. In the first assay, the radii, r , of the inhibition zone surrounding CuNP reservoirs depended on the concentration of the nanoparticles (Fig. 3.15). Following the standard procedure, these radii were fitted to the solution of the one-dimensional, radial diffusion equation:

$$(r - r_0)^2 = 4Dt \ln(c/c_0)$$

where $r_0 = 5 \text{ mm}$ is the radius of the NP reservoir, D is the diffusion constant of CuNPs/ Cu^{2+} , t is the time, and c_0 is the critical NP concentration required to inhibit any growth of the fungus. Rearranging this equation and plotting

$$\ln c = (r - r_0)^2 / 4Dt + \ln c_0$$

gave the critical concentration (from the y-intercept) of $55.46 \mu\text{M}$ in terms of Cu atoms, which is close to the minimum inhibitory concentration of $40 \mu\text{M}$ determined by the MIC assay. This MIC value is lower than the *Stachybotrys chartarum* MIC values reported for carneic acid ($75 \mu\text{M}$, $25 \mu\text{g/mL}$), penicillin G ($299 \mu\text{M}$, $100 \mu\text{g/mL}$), or itraconazole ($142 \mu\text{M}$ – 142 mM ; 0.1 – 100 mg/mL) but higher than the $2.5 \mu\text{M}$ ($3.12 \mu\text{g/mL}$) [43] for actinomycin D (which, however, is highly toxic) [21].

To investigate the effect of the n-Cu sepiolite and the n-Cu-doped glass powder on *Issatchenkia orientalis*, the nanomaterials were added over the culture to obtain a final concentration of copper in each culture of 0.036 and 0.054 wt%, respectively. The survivals from each culture were counted every 24 h after plating serial dilution. No activity was detected for the n-Cu sepiolite, while n-Cu glass powder was active at a Cu concentration of 0.054 wt%. This activity could be explained by considering the synergistic effect of n-Cu with Ca^{2+} lixiviated from the glass [40].

In 2000, the fungistatic action of a-C:H:Cu films was tested towards five species of fungi: *Aspergillus niger* (giving rise to aspergillosis upon spore inhalation); *Chaetomium globosum* (which is a cause of infections in humans); *Cladosporium cladosporioides* and *Epicoccum nigrum* (which are fungal plant pathogens); and *Pestalotia heteromorpha*. In these tests, samples were inoculated with fungi spores in distilled water (pH = 6.8), and stored in closed chambers for 21 days at $T = 27^{\circ}\text{C}$ and 100% humidity. Quantitative estimation of fungal growth, based on the so-called coefficients of biodeterioration (K), was expressed as the ratio between the area covered by fungi and the whole area of the analyzed field. No pathological fungal growth was detected on a-C:H:Cu films containing 9 at.% of copper [50].

Three species of black fungi (*Cladosporium cladosporioides*, *Phaeococcomyces chersonesos*, *Ulocladium chartarum*), isolated from marble were used to demonstrate fungicide action of Cu-based zeolites. Zeolite powder concentrations were in a range from 0.005 to 0.5 g/cm² for each series of samples. Marble samples were exposed in closed chambers for 21 days at $T = 27^{\circ}\text{C}$ and 100% humidity. Morphological characteristics, mycelia patterns formation on solid media, growth rate, and fungal biomass amount in stationary growth phase were used for the characterization of fungicide activity of zeolite samples. Minimal inhibiting concentration of zeolite powder, sufficient for preventing fungal growth, lay in the range 0.05–0.1 g/cm² and depended on the fungal strain [37].

3.3.3 Antimicrobial Tests Against Algae

Algae are a large and diverse group of simple, typically autotrophic organisms, ranging from unicellular to multicellular forms. Among the referenced studies on Cu-nano-antimicrobials, only the group of Neckers has chosen strains of green algae and diatoms to detect the biological activity of different functionalized copper NPs/polymer composites. A freshwater green alga, *Chlamydomonas* sp. strain CD1 Red, and the marine diatom, *Phaeodactylum tricorutum* CCMP 1327, were used as test organisms. Cu NP/polymer composite pellets were immersed into the flasks containing the growing cells at the start of the culture period. Two controls were established: the culture without any polymers or biocides, and the polymer lacking any copper particles. The latter was important to probe the effects of the polymer matrix or the irradiated photo-initiator on cell growth. Cell growth of the green algae was correlated with absorbance measured at 24-h intervals at 680 nm. The cell growth of the diatoms was monitored daily by measuring in vivo chlorophyll fluorescence ($\lambda_{\text{ex}} = 436$ nm; $\lambda_{\text{em}} = 680$ nm). The antimicrobial activity of the acrylated copper nanoparticles developed by Neckers' group matched well with conventionally used biocides [22].

3.4 Applications of Antimicrobial Copper Nanomaterials

Despite the difficulty of a quantitative comparison regarding the biological activity of the copper-based nanomaterials, the results mentioned in the previous paragraphs demonstrate the great potentialities of these novel nanostructures as efficient biocide agents with a widespread action.

Moreover, the large number of possible approaches to the synthesis of these nanostructures are reasonable to envisage a great development of this research field thanks to the perspective growth of their real-life applications.

The use of stabilized and/or polymer-dispersed CuNPs provides better control over ion release properties, especially when NPs are chemically interacting with the polymer backbone [22], or when they are further stabilized, due to a tuneable core-shell structure [47]. Biological activity is not compromised by the use of controlled releasing of Cu-nanomaterials; on the contrary, we have recently demonstrated that these materials may have a great value for the development of antibacterial paints and coatings for household materials, textiles, biomedical devices, hospital and food storage equipment, etc. [47]. Thus, metal-polymer nanocomposites can be a valid option for such purposes because of the highly dispersed nature of the metal releasing-clusters and a large nanoparticles-polymer interface area that ensures high reactivity. Advanced antifungal coating materials, such as hyperbranched polyamine/Cu nanoparticles, low-polydispersion copper NPs and NRs, functionalized CuNPs and Cu-grafted carbon nanotubes, are very important innovations for a number of biotechnological applications [21, 22, 25].

Microscopic fungi play an important role in the deterioration of the cultural heritage; stone monuments represent an important part of this heritage. Due to their prevalently outdoor location, they are generally subject to a complex series of weathering and decay processes causing aesthetic, biogeophysical and biogeochemical damages. The most recent approaches to the development of novel antimicrobial agents are based on the application of Cu-zeolites, amorphous hydrogenated carbon films doped with copper, and CuNPs mixed with Estel 1100, commonly used as a water repellent/consolidant [37, 46, 50].

The porous nature of agarose polymer films coupled with CuNPs can find application in antimicrobial membrane filters and coatings. This kind of nanomaterial can be utilized in food packaging, sanitation and fabrics, because of the ability of agarose to form transparent gels and films [26].

Similarly, biopolymer films, such as chitosan, modified with CuNPs were demonstrated to be effective in reducing the fluid concentration of two microorganisms affecting food quality and could therefore be used to improve food quality and extend its shelf life [28].

Metal nanoparticle-loaded fibres (particularly cotton cellulose fibers) could be used in a number of biomedical and textile applications such as medical devices, burn/wound dressings, healthcare (including disposables), personal care products, veterinary, military and bio-defence, protective suits, clothing, etc. [31, 32].

Among the fibrous products, alginate-based products are currently the most popular ones used in developing antimicrobial agent-releasing systems or textile materials. In particular, copper nanoparticle-loaded composite fibers show fair mechanical strength, excellent Cu^{2+} -releasing capacity due to their ion-exchange property and a high degree of antibacterial activity against the model bacterium *E. coli* [9].

An inorganic antimicrobial agent incorporated into an organic biomedical polymer can significantly increase its usefulness in medicine [53, 56], and even inorganic nanocomposites such as mesoporous copper-doped silica xerogels have been proposed as biomedical materials (for instance, in the treatment of traumatic wounds), because of their excellent *in vitro* and *in vivo* biocompatibility [35]. Moreover, the application of $\text{Cr}_2\text{N}/\text{Cu}$ multilayered coating on the surfaces of implanted medical devices seems particularly promising [52].

Metal-doped hydroxyapatite nanopowders can be applied as antimicrobial materials of various purpose, such as for bone defects and implant coating in orthopaedic surgery, for the treatment of skin infections, for the treatment of microbiologically polluted water, and as polymer additives [38].

CuO nanoparticles were demonstrated to be effective in killing a range of bacterial pathogens involved in hospital infections. Notably, hospitals and transport are two key fields that offer great opportunities for the use of copper nano-antimicrobials to prevent infections and pandemic diseases. Wall coatings, equipment, clothing, seats and bedding are all potential risk areas for the spread of infections, and this could be particularly important in the case of microorganisms that have developed a resistance towards conventional disinfecting agents and antibiotics [57].

The number of potential applications is evidently enormous, and it is expected to grow further, considering that other metals – such as silver and zinc – can be used for similar purposes, and multi-metal nanomaterials could also be developed.

3.5 Conclusions

A selection of recent studies dealing with the development of novel antimicrobial copper nanomaterials and their applications has been reviewed in the present chapter.

The referenced routes to copper nano-antimicrobials offer different advantages. Wet chemical syntheses are very simple and they are presently the most diffused methods. Electrochemical processes do not require chemical reductants and hence they allow for a high purity of products and for a tight control over the cluster morphology. Physical/mechanical approaches do not involve surfactants or capping agents, but they might result in poly-disperse NPs. Therefore, the choice of the appropriate route is a function of the final application of the antimicrobial nanomaterials.

Bulk copper materials provide themselves an excellent antimicrobial activity against a wide range of microorganisms (such as bacteria, fungi, algae, and viruses), and such a property is greatly improved when copper is properly nano-dispersed.

In CuNP bioactivity experiments, the Gram-negative *E. coli*, the Gram-positive *S. aureus*, and the yeast *S. cerevisiae* are the most common microorganisms employed to test the biological activity of antimicrobial agents. It should be noted, however, that, aiming at real-life applications, Cu-nanoantimicrobial properties have often been tested towards several other species. No matter the microorganism type, Cu-nano-antimicrobials proved to effectively kill it or to significantly inhibit its growth.

It may be useful to create a sort of index of the antimicrobial effectiveness of the nanomaterials classified in this chapter. However, a quantitative comparison of the bioactivity effects of Cu-nano-antimicrobials demonstrated in the existing literature is actually impossible. The referenced studies have been carried out by using different experimental parameters, and frequently the studied microorganisms belonged to different classes.

Thanks to the large number of possible approaches to these nanostructures and to the prospective growth of their real-life applications, it is reasonable to envisage a great development of this research field. The main limitations seem to reside in the need for carefully assessing any possible nano-toxicology effect related to the exposure of humans to brand new nanomaterials with unknown properties. Until now, confinement of the Cu-containing nanophases into insoluble dispersing polymer networks inhibiting NP leaching phenomena appears to be one of the most promising ways to solve these issues.

References

1. SCI Finder ScholarTM, American Chemical Society
2. Fang M, Chen JH, Xu XL, Yang PH, Hildebrant HF (2006) Antibacterial activities of inorganic agents on six bacteria associated with oral infections by two susceptibility tests. *Int J Antimicrob Ag* 27:513–517
3. Trapalis CC, KokkOris M, Perdikakis G, Kordas G (2003) Study of antibacterial composite Cu/SiO₂ thin coatings. *J Sol-Gel Sci Techn* 26:1213–1218
4. Pal S, Tak YK, Song JM (2007) Does the antibacterial activity of silver nanoparticles depend on the shape of the nanoparticle? A study of the Gram-negative bacterium *Escherichia coli*. *Appl Environ Microb* 73:1712–1720
5. Sambhy V, MacBride MM, Peterson B, Sen A (2006) Silver bromide nanoparticle/polymer composites: Dual action tunable antimicrobial materials. *J Am Chem Soc* 128:9798–808
6. Holt KB, Bard AJ (2005) Interaction of silver(I) ions with the respiratory chain of *Escherichia coli*: An electrochemical and scanning electrochemical microscopy study of the antimicrobial mechanism of micromolar Ag⁺. *Biochemistry* 44:13214–13223
7. Kawashita M, Tsuneyama S, Miyaji F, Kokubo T, Kozuka H, Yamamoto K (2000) Antibacterial silver-containing silica glass prepared by sol-gel method. *Biomaterials* 21:393–398

8. Faundez G, Troncoso M, Navarrete P, Figueroa G (2004) Antimicrobial activity of copper surfaces against suspensions of salmonella enterica and campylobacter. *BMC Microbial* 4:19–25
9. Mary G, Bajpai SK, Chand N (2009) Copper Alginate-Cotton Cellulose (CACC) fibers with excellent antibacterial properties. *J Eng Fiber Fabr* 4:24–35
10. Grass G, Rensing C, Solioz M (2011) Metallic copper as an antimicrobial surface. *App Environ Microb* 77:1541–1547
11. Peña MMO, Koch KA, Thiele DJ (1998) Dynamic regulation of copper uptake and detoxification genes in *Saccharomyces cerevisiae*. *Mol Cell Biol* 18:2514–2523
12. Halliwell B, Gutteridge JMC (1984) Oxygen toxicity, oxygen radicals, transition metals and disease. *Biochem J* 219:1–14
13. Nyden M, Fant C (2006) PCT Int. Appl. 27 pp. Application: WO 2006-SE318 20060313
14. Stupp SI, Hartgerink JD, Beniash E (2003) PCT Int. Appl. 54 pp. Application: WO 2003-US4779 20030218
15. Lin J, Yang CY, Chou CC, Su HL, Hung TJ (2009) U.S. Pat. Appl. Publ. 27 pp. Application: US 2008–253037 20081016
16. Cioffi N, Ditaranto N, Torsi L, Sabbatini L (2009) Approaches to synthesis and characterization of spherical and anisotropic copper nanomaterials. In: Challa Kumar (ed) *Metallic Nanomaterials*, Wiley-VCH, Weinheim (Germany)
17. Ruparelia JP, Chatterjee AK, Duttagupta SP, Mukherji S (2008) Strain specificity in antimicrobial activity of silver and copper nanoparticles. *Acta Biomat* 4:707–716
18. Xiong J, Wang Y, Xue QJ, Wu XD (2011) Synthesis of highly stable dispersions of nanosized copper particles using L-ascorbic acid. *Green Chem* 13:900–904
19. Ding LP, Fang Y (2007) The study of resonance Raman scattering spectrum on the surface of Cu nanoparticles with ultraviolet excitation and density functional theory. *Spectrochim Acta A* 67:767–771
20. Panigrahi S, Kundu S, Ghosh SK, Nath S, Praharaj S, Basu S, Pal T (2006) Selective one-pot synthesis of copper nanorods under surfactantless condition. *Polyhedron* 25:1263–1269
21. Wei Y, Chen S, Kowalczyk B, Huda S, Gray TP, Grzybowski BA (2010) Synthesis of stable, low-dispersity copper nanoparticles and nanorods and their antifungal and catalytic properties. *J Phys Chem C* 114:15612–15616
22. Anyaogu KC, Fedorov AV, Neckers DC (2008) Synthesis, characterization, and antifouling potential of functionalized copper nanoparticles. *Langmuir* 24:4340–4346
23. Mahapatra SS, Karak N (2009) Hyperbranched polyamine/Cu nanoparticles for epoxy thermoset. *J Macromol Sci* 46:296–303
24. Weickmann H, Tiller JC, Thomann R, Mülhaupt R (2005) Metallized organoclays as new intermediates for aqueous nanohybrid dispersions, nanohybrid catalysts and antimicrobial polymer hybrid nanocomposites. *Macromol Mater Eng* 290:875–883
25. Mohan R, Shanmugaraj AM, Hun RS (2011) An efficient growth of silver and copper nanoparticles on multiwalled carbon nanotube with enhanced antimicrobial activity. *J Biomed Mater Res B* 96:119–126
26. Datta KKR, Srinivasan B, Balaram H, Eswaramoorthy M (2008) Synthesis of agarose–metal/semiconductor nanoparticles having superior bacteriocidal activity and their simple conversion to metal–carbon composites. *J Chem Sci* 120:579–586
27. Liu JC, He F, Durham E, Zhao D, Roberts CB (2008) Polysugar-stabilized Pd nanoparticles exhibiting high catalytic activities for hydrodechlorination of environmentally deleterious trichloroethylene. *Langmuir* 24:328–336
28. Cárdenas G, Díaz JV, Meléndrez MF, Cruzat CC, Cancino AG (2009) Colloidal Cu nanoparticles/chitosan composite film obtained by microwave heating for food package applications. *Polym Bull* 62:511–524
29. Cárdenas G, Díaz JV, Meléndrez MF, Cruzat CC (2008) Physicochemical properties of edible films from chitosan composites obtained by microwave heating. *Polym Bull* 61:737–748

30. Lima CAS, Oliva R, Cárdenas G, Silva EN, Miranda LCM (2001) Influence of the thermal annealing on the electrical resistivity and thermal diffusivity of Pd:Ag nanocomposites. *Mater Lett* 51:357–362
31. Mary G, Bajpai SK, Chand N (2009) Copper (II) Ions and copper nanoparticles-loaded chemically modified cotton cellulose fibers with fair antibacterial properties. *J Appl Polym Sci* 113:757–766
32. Perelshtein I, Applerot G, Perkas N, Wehrschuetz E, Hasmann A, Guebitz G, Gedanken A (2009) CuO–cotton nanocomposite: Formation, morphology, and antibacterial activity. *Surf Coat Tech* 204:54–57
33. Chunju Gu, Bin Sun, Wenhua Wu, Fengchuan Wang, Meifang Zhu (2007) Synthesis, characterization of copper-loaded carboxymethyl-chitosan nanoparticles with effective antibacterial activity. *Macromol Symp* 254:160–166
34. Kim YH, Lee DK, Cha HG, Kim CW, Kang YC, Kang YS (2006) Preparation and characterization of the antibacterial Cu nanoparticle formed on the surface of SiO₂ nanoparticles. *J Phys Chem B* 110:24923–24928
35. Wu X, Ye L, Liu K, Wang W, Wei J, Chen F, Liu C (2009) Antibacterial properties of mesoporous copper-doped silica xerogels. *Biomed Mater* 4:1–6
36. Zhang N, Gao Y, Zhang H, Feng X, Cai H, Liu Y (2010) Preparation and characterization of core–shell structure of SiO₂@Cu antibacterial agent. *Colloid Surf B–Biointerfaces* 81:537–543
37. Petranovskii V, Panina L, Bogomolova E, Belostotskaya G (2003) Microbiologically active nanocomposite media. *Proceedings of SPIE* 5218:244–255
38. Stanić V, Dimitrijević S, Antić-Stanković J, Mitrić M, Jokić B, Plečaš IB, Raičević S (2010) Synthesis, characterization and antimicrobial activity of copper and zinc doped hydroxyapatite nanopowders. *Appl Surf Sci* 256:6083–6089
39. Hsiao MT, Chen SF, Shieh DB, Yeh CS (2006) One-pot synthesis of hollow Au₃Cu₁ spherical-like and biomineral botallackite Cu₂(OH)₃Cl flowerlike architectures exhibiting antimicrobial activity. *J Phys Chem B* 110:205–210
40. Esteban-Tejeda L, Malpartida F, Esteban-Cubillo A, Pecharrómán C, Moya JS (2009) Antibacterial and antifungal activity of a soda-lime glass containing copper nanoparticles. *Nanotechnology* 20:505701–505707
41. Reetz MT, Helbig W (1994) Size-selective synthesis of nanostructured transition-metal clusters. *J Am Chem Soc* 116:7401–7402
42. Cioffi N, Torsi L, Ditaranto N, Sabbatini L, Zambonin PG (2004) Antifungal activity of polymer-based copper nanocomposite coatings. *Appl Phys Lett* 85:2417–2419
43. Cioffi N, Torsi L, Ditaranto N, Picca RA, Tantillo G, Sabbatini L, Zambonin PG (2004) Synthesis analytical characterization and bio-activity of Ag- and Cu-containing nanostructured membranes. *J Appl Biomater Biomec* 2:200
44. Cioffi N, Ditaranto N, Torsi L, Picca RA, De Giglio E, Sabbatini L, Novello L, Tantillo G (2005) Synthesis, analytical characterization and bioactivity of Ag and Cu nanoparticles embedded in poly-vinyl-methyl-ketone films. *Anal Bioanal Chem* 382:1912–1918
45. Cioffi N, Torsi L, Ditaranto N, Tantillo G, Ghibelli L, Sabbatini L, Bleve-Zacheo T, D’Alessio M, Zambonin PG, Traversa E (2005) Copper nanoparticle/polymer composites with antifungal and bacteriostatic properties. *Chem Mater* 17:5255–5262
46. Ditaranto N, Loperfido S, van der Werf I, Mangone A, Cioffi N, Sabbatini L (2011) Synthesis and analytical characterisation of copper-based nanocoatings for bioactive stone artworks treatment. *Anal Bioanal Chem* 399:473–481
47. Cioffi N, Ditaranto N, Sabbatini L, Torsi L, Zambonin PG (2008) European Patent Application 9 pp Application: EP 2008-EP2123797A1
48. Cioffi N, Ditaranto N, Torsi L, Picca RA, Sabbatini L, Valentini A, Novello L, Tantillo G, Bleve-Zacheo T, Zambonin PG (2005) Analytical characterization of bioactive fluoropolymer ultra-thin coatings modified by copper nanoparticles. *Anal Bioanal Chem* 381:607–616

49. Kelly PJ, Li H., Benson PS, Whitehead KA, Verran J, Arnell RD, Iordanova I (2010) Comparison of the tribological and antimicrobial properties of CrN/Ag, ZrN/Ag, TiN/Ag, and TiN/Cu nanocomposite coatings. *Surf Coat Tech* 205:1606–1610
50. Ivanov-Omskii VI, Panina LK, Yastrebov SG (2000) Amorphous hydrogenated carbon doped with copper as antifungal protective coating. *Carbon* 38:495–499
51. Kelly PJ, Li H, Whitehead KA, Verran J, Arnell RD, Iordanova I (2009) A study of the antimicrobial and tribological properties of tin/Ag nanocomposite coatings. *Surf Coat Tech* 204:1137–1140
52. Chang YJ, Li CL, Lee JW, Wu FB, Chang LC (2010) Evaluation of antimicrobial abilities of Cr₂N/Cu multilayered thin films. *Thin Solid Films* 518:7551–7556
53. Zhang W, Zhang YH, Ji JH, Zhao J, Yan Q, Chu PK (2006) Antimicrobial properties of copper plasma-modified polyethylene. *Polymer* 47:7441–7445
54. Chu PK (2004) Recent developments and applications of plasma immersion ion implantation. *J Vac Sci Technol B* 22:289–296
55. Chu PK, Tang BY, Wang LP, Wang XF, Wang SY, Huang N (2001) Third-generation plasma immersion ion implanter for biomedical materials and research. *Rev Sci Instrum* 72:1660–1665
56. Zhang W, Zhang Y, Ji J, Yan Q, Huang A, Chu PK (2007) Antimicrobial polyethylene with controlled copper release. *J Biomed Mater A* 83:838–844
57. Ren G, Hu D, Cheng EWC, Vargas-Reus MA, Reip P, Allaker RP (2009) Characterisation of copper oxide nanoparticles for antimicrobial applications. *Int J Antimicrob Ag* 33:587–590
58. Yates HM, Brook LA, Sheel DW, Ditta IB, Steele A, Foster HA (2008) The growth of copper oxides on glass by flame assisted chemical vapour deposition. *Thin Solid Films* 517:517–521
59. Medina C., Santos-Martinez MJ, Radomski A, Corrigan OI, Radomski MW (2007) Nanoparticles: Pharmacological and toxicological significance. *Brit J Pharmacol* 150:552–558
60. Radetić M, Illić V, Vodnik V, Dimitrijević S, Jovančić P, Šaponjić Z, Nedeljković JM (2008) Antibacterial effect of silver nanoparticles deposited on corona-treated polyester and polyamide fabrics. *Polym Adv Technol* 19:1816–1821
61. Anon BS N 697:2001 Chemical Disinfectants and Antiseptics - Quantitative Non-porous Surface Test for the Evaluation of Bactericidal and/or Fungicidal Activity of Chemical Disinfectants Used in Food, Industrial, Domestic and Institutional Areas - Test Method and Requirements Without Mechanical Action (phase 2/step 2), British Standards Institution, London (2001)

Chapter 4

Titanium Dioxide–Polymer Nanocomposites with Advanced Properties

Anna Kubacka, Marcos Fernández-García, María L. Cerrada,
and Marta Fernández-García

4.1 Introduction

Nanotechnology refers to that technology able to manipulate and organize a substance at the nanometer level. The control at this stage makes it possible to create new materials and devices with fascinating functions allowing the best use of the special properties of nanosized substances. Accordingly, the term of nanocomposite has emerged strongly in scientific literature and technological applications during the last decade. In general, nanocomposites essentially consist of a multiphase material in which one of the phases has one, two or three dimensions of less than 100 nanometers (nm).

In particular, organic/inorganic nanocomposite materials, where the organic major component is based on polymers, are a fast-growing area of research in order to meet new requirements and challenges in performance properties of the resulting materials that allow for further development and progress of the present and future society. The excellent characteristics of titanium dioxide, TiO_2 (known also as titania), make it an ideal candidate as an inorganic component in these promising titania-based polymeric nanocomposites. Therefore, the primary aim of the present chapter consists of describing the model examples of these materials from the standpoint of either their advanced properties or their preparation protocol. Especial emphasis is placed on those exhibiting biocidal characteristics. As a prior stage, the striking photocatalytic properties found in the titania material and involving or related to its disinfection capability are discussed.

A. Kubacka • M. Fernández-García (✉)
Instituto de Catálisis y Petroleoquímica (ICP-CSIC), Madrid, Spain
e-mail: mfg@icp.csic.es

M.L. Cerrada • M. Fernández-García (✉)
Instituto de Ciencia y Tecnología de Polímeros (ICTP-CSIC), Madrid, Spain
e-mail: martafg@ictp.csic.es

4.2 Nanostructured Titanium Dioxide: Photocatalysis

Photo-induced processes are studied in several industrial-oriented applications, which have been developed since their first descriptions in the scientific literature. Despite the differences in character and utilization, all photo-induced processes have the same origin. A semiconductor can be excited by light energy higher than the band gap inducing the formation of energy-rich electron–hole pairs. It is commonly understood that the term photo-catalysis refers to any chemical process catalyzed by a solid where the external energy source is an electromagnetic field with wave numbers in the UV-visible–infrared range [1–6]. Normally, photocatalysts are solid semiconductors that are able to absorb visible and/or UV light, chemically and biologically inert and photostable, inexpensive and non-toxic. TiO_2 , ZnO , SrTiO_3 , CeO_2 , WO_3 , Fe_2O_3 , Bi_2O_3 , GaN , CdS , ZnS , CdS , ZnSe or more complex oxides, nitrides or chalcogenides can act as photoactive materials for redox processes due to their electronic structure, which is characterized by a filled valence band and an empty conduction band. Among these possible semiconductors, titanium dioxide, TiO_2 , is the most widely used photocatalytic material as it fulfils all of these requirements and exhibits adequate conversion values [7].

TiO_2 appears in nature in three different crystallographic phases: rutile, anatase, and brookite, anatase being the most commonly employed in photocatalytic applications due to its inherent exceptional photocatalytic properties [6–8]. Anatase is the least thermodynamically stable polymorph of TiO_2 as a bulk phase, although it appears from energy calculations as the more likely phase when the grain size is below 15–20 nm [9]. High surface TiO_2 materials would therefore present the anatase polymorph as a general rule. The crystalline structure of the TiO_2 oxides can be described in terms of TiO_6 octahedral chains differing by the distortion of each octahedron and the assembly pattern of such octahedra chains. The Ti–Ti distances in the anatase structure are greater than in the rutile, whereas Ti–O distances are shorter [10]. These structural variations cause different mass densities and lead to distinct electronic structures of the bands. The anatase phase is 9% less dense than the rutile, presenting a more pronounced localization of the Ti 3*d* states and, consequently, a narrower 3*d* band. Also, the O 2*p*–Ti 3*d* hybridization is different in the two structures (more covalent mixing than in rutile), with anatase exhibiting a valence and conduction band with more pronounced O 2*p*–Ti 3*d* characters, respectively, and less non-bonding self-interaction between similar ions (e.g., anion–anion and cation–cation interactions) [11]. The importance of the covalent versus ionic contributions to the Metal–Oxygen bond is discussed in a more general context for several photocatalytic oxides by Wiswanathan [12]. In any case, these differential structural features, which distinguish anatase and rutile, are presumably responsible for the difference in the mobility of charge carriers during light excitation.

Nanostructured anatase- TiO_2 has been synthesized by an enormous number of techniques including liquid-phase sol–gel, microemulsion, hydro- and solvothermal, aerogel, sonochemical or surfactant-templated methods. Also, solid-state chemistry

methods related to the oxidation or chemical vapor deposition of (solid) precursors have been used. Review articles itemize specific details of such methods and the physico-chemical properties of the resulting titania solids [13, 14]. In brief, TiO_2 nanoparticles would appear basically amorphous below 3–4 nm and will display the anatase structure in the stability region mentioned above, e.g. below ca. 15–20 nm. Truncated bi-pyramidal shapes mainly exposing {101}, {001}, and {100} surfaces are essentially expected for anatase nanoparticles, although very recent studies show unforeseen shapes for “molecular” (e.g., below 1.5 nm) TiO_2 entities, which may be potentially present near the low 3–4 nm limit [15]. Figure 4.1 shows that anatase nanoparticles can exhibit two main or “extreme” morphologies: elongated (along the c crystallographic axis) shapes dominated by {100} and {101} faces, and more isotropically ones with certain additional main contribution from {001} faces. Typical anatase nanoparticle morphologies can be thus represented by an aspect parameter ($B-A$ in Fig. 4.1) that usually get values of 0.3–0.4 and may display a maximum value of 0.57 [16]. Modulation/control of the c -axis elongation of the particle by the presence of unusual surface species, such as fluorine ions during preparation conditions [17], as well as morphology control with formation of nanostructures (other than nanoparticles as, for example, nanosheets), having dominant presence of {001} facets [18–21] have also been recently reported. Recent work indicates that nanoparticle morphology (primary particle size/shape) (1) is governed by thermodynamic (specifically the initial local order, around 3–6 Angstroms, in the solid precursor state of the oxide at nucleation states) and not only kinetic parameters of the anatase genesis process [22]; and (2) surface OH density and net charge (e.g., hydration of surface layers) [16, 23] together with the number of kinks/edges [24] are key factors to control surface energy and thus morphology and can be envisaged to be key parameters in controlling the elongation along the c axis (e.g., particle shape) in the case of OH species.

Several paths have been explored in order to optimize the photo-activity of anatase- TiO_2 systems. Almost from the conception of the use of photocatalysis, the photo-activity of anatase- TiO_2 systems was typically improved with the addition of

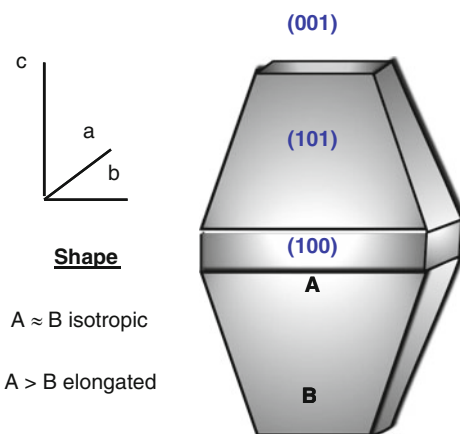


Fig. 4.1 Typical morphological characteristics of anatase nanocrystals

surface noble metals such as Pt, Pd, and Ag, which act as electron trapping centers, and/or oxide–oxide contact using SnO, ZrO₂ and others with an appropriate electronic structure to positively influence the electron–hole charge separation process [1, 5, 6, 25]. Another methodology, central in the current research, takes into account the extension of the solid light-absorption spectrum to the visible region. This would facilitate the use of sunlight, an inexpensive, renewable energy source, as the excitation energy of the photocatalytic processes. Several alternatives, mainly based on the use of inorganic solids as metals, chalcogenides, nitrides, and other non-Ti-based oxides with adequate optical properties, other (polymeric or molecular species) sensitizers, or hypothetical cubic-type TiO₂ polymorphs, have been tested in reaching this goal [1, 26]. Additional studies involving TiO₂ and aimed at enhancing its optical absorption and photocatalytic performance are focused on anatase modification by cation and/or anion doping [1, 4–6, 27].

4.3 TiO₂ and Its Disinfection Capability

Photocatalytic disinfection or photo-killing has undergone a boost in the last decades and promising results have been obtained with a significant number of microorganisms including Gram-negative bacteria (*Escherichia coli*, *Enterobacter cloacae*, *Erwinia caratovora*, *Klebsiella pneumoniae*, *Legionella pneumophila*, *Listeria monocytogenes*, *Microbacterium* sp., *Salmonella typhimurim*, *choleraesuis*, *enterica*, and *faecalis*, *Shigella flexnerii*, and *Pseudomonas aeruginosa*, and *fluorescens*), Gram-positive bacteria (*Bacillus anthracis*, *stearothermophilus*, *pumilus*, *cereus*, *subtilis* and spp., *Lactobacillus helveticus*, *acidophilus*, and *plantarum*, *Staphylococcus aureus*, and *Streptococcus faecalis*, *mutans*, *sobrinus* AHT, *Enterococcus faecalis*), yeasts (*Pichia jadini* and *Zygosaccharomices rouxii*), fungus (*Aspergillus niger*, *Candida albicans*, *Cereviside*, *Fusarium solani*, *anthopiluml equiseti* and *verticilliosides*, and *Penicillium chysogenum* and *expansum*), protozoa (*Acanthamoeba polyphaga*, *Giardia lambia*), and viruses (*Bacteriophage MS2*, *polvirus*, *Herpes simplex*, *Hepatitis B 1*, *Influenza*, *Avian A/H5N2*, *Lactobacillus case phage PL-1*) [5, 6, 28–37]. Titania is used as a powder but also supported on plastics, metals, ceramics, and other materials, which facilitate its use and recovery [5, 6, 28, 29, 31, 32, 34, 36, 37]. These studies showed that photokilling performance is sensitive to several experimental factors, which include among others:

- Excitation energies, fluences (power × time) and irradiation conditions (pulsed, continuous) used in experiments with titania as they all significantly influence the photokilling performance, possibly in a more pronounced way than in the traditional use of anatase in the photodegradation of organic waste. For example, while *E. coli* and *B. fragilis* require prolonged illumination for effective killing, *B. pumilis* inactivation is better obtained by using intermittent illumination [38–40].

The photon energy is also important as TiO₂ materials are mostly effective under ultraviolet light excitation, but their interaction with certain polymeric matrices [33, 35] and/or their modification by adding additional components (such as Ag, PdO, etc.) or doping allows the use of visible and sunlight as excitation sources [41, 42].

- A second factor concerns the state and nature of the biocidal oxide. TiO₂ works by surface/near-surface contact and displays significant variability in efficiency while used as powders or being immobilized on a support. As is well known, as a powder it may present typically a onefold order of magnitude greater activity (for example, in the case of *E. coli*) due to the fact that nanoparticles in suspension/powders can be ingested by microorganisms by phagocytosis, causing rapid cellular damage in addition to that triggered by photo-activity [40].
- Another variable is related to the effect of temperature as typically the inactivation rate increases/decreases with temperature for Gram-positive/Gram-negative bacteria. However, coliform bacteria are the exception to this rule. All microorganisms display, in any case, very narrow temperature ranges where photocatalytic disinfection activity reaches maximum values [5, 6, 40].
- Titania photokilling operation seems to decrease in the order virus > Gram-negative > Gram-positive > bacterial spores ≈ yeasts > fungus [5, 6, 43]. This appears to be connected with the increasing cell wall complexity, which goes from the thin peptidoglycan layer of Gram-negative bacteria, to the thicker and more compact walls of Gram-positive bacteria and cocci, and ending with the thick eukaryotic cell membrane containing sugar polymers for yeasts and/or complex peptidoglycan chains for fungus.
- The last point is specific for the measurements of cell inactivation reaction rates as they show a linear relationship with the initial bacteria concentration, a fact that should be considered when comparing results.

In spite of these variables, good efficiencies, close to those considered functional for bacteria disinfection (4–5 log reduction in the temporal range of minutes) are customarily reported in studies reviewed here. Note, however, that waste water or other real targets for disinfection having significant turbidity (water, for example, contains significant amounts of solids in suspension) as well as dissolved organic matter may complicate the functionality of titania photocatalysts. Tests of titania performance with real municipal waste water have nevertheless been proven successful [6]. In addition, the presence of microorganism aggregations forming biofilms is another aspect of relevance due to the limited use of current technologies. Related to that, only a few titania-based photocatalysts show an adequate performance for effectively reducing microorganism populations [33].

The mechanism leading to cell death appears as key information in order to optimize the photokilling process but is not yet fully understood. Adherence of the microorganism seems the first important step in the process while using TiO₂ powders [44], but it may not be as dramatic in the case of polymer-based composites as the surface contact area is then orders of magnitude superior than that corresponding to the powders. The photocatalytic attack appears to be carried

out by hole-related species under UV light [45–47], while oxide (e.g., superoxide and singlet oxygen) species appear as the key intermediate under visible light [47]. The photokilling sensitivity to the microorganism structural surface properties, particularly to the chemical complexity and thickness of the cell wall, suggests that it is initiated by a cell wall and/or cytoplasmic membrane attack. Kinetic studies with *E. coli* spheroplasts (*E. coli* bacteria from which the cell wall is almost completely removed, as by the action of penicillin) strongly support such a mechanism [48]. Recent microscopy studies indicate that cell walls suffer a continuous collapse by which the photo-process leads initially to round-shaped and lysed cells with a restricted number of breaks in their walls. This decreases the cell volume by a factor of $2/3$, but the microorganism may subsequently re-grow under dark conditions. In a subsequent step, viability of cells is, however, fully lost by further attack of TiO_2 -derived radicals [33]. The viability loss would be a function of the cell wall chemical complexity and thickness and of the efficiency of the microorganism repair/protection mechanisms, using the superoxide dismutase (an enzyme that dismutates superoxide radicals to H_2O_2 and O_2) and catalase (an enzyme that reduces intracellular concentration of H_2O_2 and converts it to H_2O and O_2) enzymes.

Early proposals, however, suggested that photokilling mechanisms not only imply external or cell wall effects but also processes occurring at the core of the cell and thus called internal effects. So, the use of hole-related species in the oxidation of the intracellular coenzyme A, (CoA), was presumed to inhibit cell respiration [38]. Subsequent direct TiO_2 –microorganism contact would result in cell death. Damage of nucleic acid entities was also claimed in a more recent contribution [49]. Although it is obvious that internal and external cell damage processes coexist, it is not clear at the moment which of them are key in the photokilling of microorganisms, nor the exact time evolution and potential interrelationship(s) among such processes [37, 50].

4.4 Titanium Dioxide–Polymeric Nanocomposites

In recent years, organic–inorganic hybrid or nanocomposite materials that combine attractive qualities of dissimilar components have received great attention for a wide range of mechanical, electronic, magnetic, biological, and optical properties. These novel materials are not merely physical mixtures but can be broadly defined as complex materials having both organic and inorganic components intimately connected at nanometric length scale. The methodologies used for their preparation are mainly: sol–gel, in situ polymerization, solution and melt processes. They can be classified as defined by Novak [51] and others [52] established: type I for soluble, preformed organic polymers embedded in an inorganic network; type II for embedded, preformed organic polymer owing covalent bonds to the inorganic network; type III for mutually interpenetrating organic–inorganic networks; type IV for mutually interpenetrating networks with covalent bonds between the organic

and inorganic phases; and type V for “non-shrinking” sol–gel composite materials. Obviously, there are materials falling between these categories which make their classification difficult.

Here, we present a short summary of the titania-containing polymeric nanocomposites with a general description of their utility. Description of antimicrobial materials is postponed to a separate, last section of the chapter due to the significant photokilling characteristics presented by TiO_2 .

4.4.1 Polymeric Nanocomposites with In Situ Preparation of Titania

Lantelme et al. [53] obtained a hybrid organic–inorganic material by in situ polymerization of titanium isopropoxide in polyvinylacetate, PVAc. The use of a titanium alkoxide as the inorganic precursor enables a chemical cross-linking of PVAc resulting from transesterification reactions. The results showed a higher cross-linking density of the Ti clusters or stronger interactions between clusters and polymer matrix. These strong chemical interactions prevent a macroscopic phase separation and allow manufacturing composites at nanometer scale (size < 10 nm) where the clusters are randomly dispersed in the PVAc matrix and are bound to the matrix through an interphase made of a titanium dioxide network interpenetrated by polymer chains. Nevertheless, the major inconvenience of these nanocomposites is that Ti-based clusters contain some residual isopropoxy groups and the TiO_2 phase could display limited crystallinity.

Nandi et al. [54] prepared poly(amic acid) solution from condensation of 3,3',4,4'-bezophenone tetracarboxylic dianhydride, BTDA, and 4,4'-oxydianiline, ODA. Then tetraethyl titanate precursor was added, followed by thermal imidization to form polyimide/titania, PI/ TiO_2 , hybrid nanocomposites. The results reported showed that TiO_2 nanosized and dispersed in PI films had an average diameter of 1.5 nm at TiO_2 content of 12 wt%. Hu and Marand [55] prepared poly (amide–imide)/ TiO_2 , PAI/ TiO_2 , composite films by sol–gel process using tetraethyl titanate as precursor. In this case, the hydrogen bonding interactions between the amide group in the PAI polymer and the hydroxyl groups on the inorganic oxide allow the obtaining of a high mixing degree of the organic–inorganic system and the formation of the nanosized TiO_2 domains. The size of these domains increases from 5 to 50 nm when the TiO_2 content rises from 3.7% to 17.9% by weight. These composite films exhibit higher optical transparency, higher glass transition temperature, an increase and flattening of the rubbery plateau modulus and a decrease in polymer crystallinity over the pure PAI.

Transparent poly(trimethylhexamethyleneterephthalamide)-based titania nanocomposites have been prepared by the in situ generation of inorganic network structure via the sol–gel process [56]. In this article, different concentrations of tetrapropylorthotitanate, TPOT, as precursor are added to a dimethylformamide,

DMF, solution of polyamide, resulting hybrid films with particle sizes ranging from 3 to 14 nm. The mechanical properties increases with the inorganic content, but at higher concentrations the nanocomposites deteriorate due to agglomeration. The glass transition temperature, T_g , and the storage modulus indicate the better cohesion between inorganic and organic components. Finally, the analysis of the nanocomposites thermal degradation reveals that the incorporation of the titania contents increases their stability.

Liaw and Chen [57] prepared a series of poly(imide siloxane)/TiO₂, PIS/TiO₂, nanocomposites from condensation of BTDA, 2,2'-bis[4-(3-aminophenoxy)phenyl] sulfone, polysiloxane, trimethoxyvinyl silane as coupling agent, and titanium alkoxides as several TiO₂ contents to study the effect of the composition on the morphology, thermal and mechanical properties of the material. The in situ incorporation of titania together with the adoption of a coupling agent, which minimize the degree of aggregation and enhance organic–inorganic interfacial cohesiveness, and significantly improves the material's Young's modulus, which increases as does the TiO₂ content. However, these materials are brittle and, consequently, with lower tensile strength and elongation at break values. In addition, their thermal stability is slightly lower than the one observed in the pure PIS.

Whang and Chiang [58] prepared hybrid nanocomposite films of titania in a polyimide matrix. The synthesis was performed by imidization of the homogeneous mixture of tetraethyl titanate precursor and poly(amic acid) functional polymer. The titania particle size on these nanocomposites increases from 10 to 40 nm as does the TiO₂ content from 5 to 30 wt%. All the films exhibit good optical transparency within this range. Other dianhydrides and/or diamines, which produce poly(amic acid), are utilized for the synthesis of PI/TiO₂ nanocomposites [59, 60]. Polyurethane/titania hybrid materials [61] with high refractive indexes are also attained by modification of polyurethane with (3-isocyanatopropyl) triethoxysilane, which allows the formation of covalent bonds between titania moiety and polymer segments, restricting the polymer chain motion and preventing the phase separation.

In most of these hybrid systems, the TiO₂ exists in an amorphous state and still contains unreacted alkoxide and hydroxyl groups. This is a constant while using preparation methods which do not allow calcination of titania over 673 K in order to obtain reasonable crystalline oxide phases, and will not be mentioned again for subsequent works. Works mentioned after this point use TiO₂ materials previously synthesized to the nanocomposite system although the inorganic oxide is not always calcined at high temperature.

4.4.2 Polymeric Nanocomposites with Titania Prior Synthesized

Yuwono et al. [62] also successfully prepared transparent nanohybrid thin films (250–350 nm in thickness) consisting of nanocrystalline TiO₂ particles in poly(methyl methacrylate), PMMA. The methyl methacrylate, MMA, and 3-(trimethoxysilyl) propyl methacrylate, MSMA, monomers were partially copolymerized by free radical

polymerization using benzoyl peroxide, BPO, as initiator in tetrahydrofuran, (THF). The sol solution was prepared using titanium isopropoxide, deionized water, ethanol, and hydrochloric acid. Then, both solutions were mixed, spin-coated on quartz substrates and finally heated to finish the polymerization reaction. All nanohybrid thin film samples exhibit a nonlinear optical behavior with a very fast characteristic relaxation time of ~ 1.5 ps, which has been measured by a pump probe technique. Similar nanomaterials based on MMA and styrene using the same silane coupling agent have been developed by pseudo-dispersion polymerization in supercritical carbon dioxide [63] (see Fig. 4.2 for illustration). In this case, the presence of 3-(trimethoxysilyl) propylmethacrylate modified TiO_2 nanoparticles serves not only as an inorganic filler but also as an effective stabilizer for the MMA polymerization in the supercritical fluid. The authors reported that the morphologies of these two composites are quite different from each other, which was attributed to the difference in the interaction mechanisms between the carbonyl group of the monomers and the hydroxyl group on the TiO_2 surface.

Nanocomposites of polymer electrolytes have been prepared with TiO_2 with a particle size of 10 [64], 13 [65, 66], 20 [67], and 21 nm [68–70]. Decreasing the particle size of inorganic TiO_2 fillers leads to the enhancement of the interaction between the polymer matrix and inorganic fillers that might change the ionic conductivity of polymeric electrolyte nanocomposites. Ahmad et al. [71] demonstrated the effect of nanosized TiO_2 addition in different concentrations to PMMA based gel polymeric electrolytes on their conductivity as well as their thermal and rheological properties. The addition of nanoparticles enhances the ionic conductivity with negligible effect on other electrochemical properties. In addition, no changes appear in X-ray diffraction pattern but an increase in T_g of the resulting electrolytes is noticeable. These nanocomposite polymeric electrolytes are prepared by PMMA addition into a propylene carbonate homogenous dispersion of commercial anatase TiO_2 nanoparticles ($d = 15$ nm), in different weight percentages with respect to liquid electrolyte weight. Free radical suspension polymerization in water medium with in situ sol–gel transformation is also used by these authors to prepare PMMA/ TiO_2 polymeric nanocomposites [72]. Electrolytes based on these polymeric materials show superior properties compared to those found in conventional polymer electrolytes.

Nanocrystalline Ag/ TiO_2 composite thin films were synthesized using a two-step synthesis methodology: the in situ precipitation of Ag nanoparticles followed by an

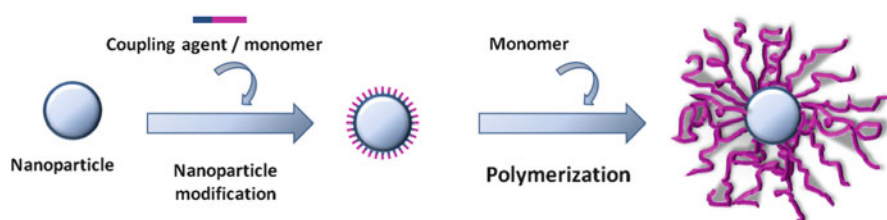


Fig. 4.2 Molecular imprinting polymer-coated titania

in situ sol–gel reaction of titanium isopropoxide in a weak polyion multilayer template formed by the layer-by-layer (LbL) self-assembly of negatively charged poly(acrylic acid), PAA, and positively charged poly(allylamine chloride), PAH [73]. In this procedure, the thickness of the nanocomposite films is controlled by the number of layers in the polyion template on the nanometer scale. The results demonstrated that the addition of Ag enhances the titania UV and visible photoactivity, followed by the decomposition of methylene blue, whereas a simultaneous increase in the content and size of the Ag nanoparticles reduces its photocatalysis.

Acrylamide has been polymerized in aqueous solution in the presence of titania nanoparticles (average diameter 30 nm and a specific surface area 50 m²/g) and N, N'-methylene bisacrylamide as cross-linker agent, and potassium peroxydisulfate as initiator to obtain photocatalytic degradable nanocomposites [74]. The results illustrate that these nanocomposites present higher photocatalytic efficiency under UV irradiation for discoloration of the methyl orange solution used as target substance.

Surface-modified TiO₂ nanoparticles, obtained with 6-palmitate ascorbic acid, are encapsulated in PMMA by in situ radical polymerization thermally initiated by 2,2'-azobisisobutyronitrile, AIBN, in toluene solutions [75]. These nanoparticles are previously synthesized from controlled hydrolysis of titanium tetrachloride, having an average diameter of 4.5 nm. The resulting nanocomposites have similar T_g which could be unexpected, since the presence of inorganic nanoparticles is reported in the literature to lead to an increase of T_g [55]. This fact is explained as a result of two opposing effects. Specifically, the existing palmitoyl chains in the modified nanoparticles could act as a plasticizer, reducing the T_g of PMMA, while the presence of TiO₂ particles might trigger an increase of T_g. On the other hand, the thermal stability analyzed either in inert or air atmospheres exhibits a significant increase. The nanocomposite degradation curves under nitrogen atmosphere do not show any peak at 180°C indicating the lack of head-to-head bonds (polymer chain double bond at the end) in PMMA chains, responsible for the first degradation stage. The improvement of the degradation under a thermo-oxidative atmosphere is attributed to the presence of ascorbic acid chains.

Acrylic acid and allyl acetylacetone have also been chosen as coupling agents to modify the titania surface and, then, methyl methacrylate is conventional free radical polymerized using BPO as initiator [76]. When acrylic acid is used as compatibilizer, the starting metal alkoxide is titanium butoxide, while titanium isopropoxide is used when allyl acetylacetone is selected, because it is difficult to obtain transparent hybrid materials using titanium butoxide. The hybrid materials achieved with the latest one show a reversible thermochromic effect. They are red and transparent at room temperature and change to yellow and opaque when they are cooled. Methacrylic acid, MA, has also been used as a functionalization agent since it can chemically link TiO₂ nanomaterials and polymer matrix. Then, the double bond in MA was copolymerized with methyl methacrylate to form TiO₂-PMMA nanocomposites (see Fig. 4.3) [77]. The analysis of these materials revealed that the glass transition temperature, thermal degradation temperature, and dynamic

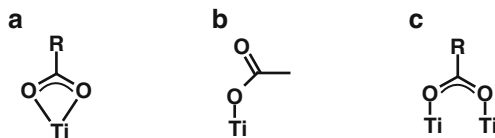


Fig. 4.3 Three possible structures of carboxylate coordinated to a titania surface. In the first structure, carboxylate is bound to one Ti^{4+} center in a chelating bidentate mode (a). The carboxylate could also be bound to one Ti^{4+} in a monodentate mode (b), and finally, the carboxyl group could bind with each of its oxygen atoms to two Ti^{4+} atoms yielding the bridging bidentate mode (c)

elastic moduli of the nanocomposites increase with the weight percentage of nanofibers in the composite.

Similar approach is utilized to manufacture hybrid materials with different morphologies (hexagonal and cubic mesostructures) by self-assembly of trifluoroacetic acid-modified titania with poly(ethylene oxide)-*b*-poly(propylene oxide)-*b*-poly(ethylene oxide), PEO-PPO-PEO, amphiphilic triblock copolymers [78]. Information about molecular proximities and interfaces, which is unavailable from TEM and SAXS experiments, has been attained by solid-state NMR techniques, such as cross-polarization and two-dimensional (2D) experiments.

Bead milling with centrifugal bead separation is used to prepare PMMA/TiO₂ nanocomposite materials from stable nanoparticle–monomer dispersions with the addition of (3-acryloxypropyl)trimethoxysilane as coupling agent, followed by monomer polymerization [79]. These well-dispersed titania nanoparticles have little effect on the transmittance of visible light through MMA but enhance the UV absorbing properties of MMA. Their refractive index at 633 nm increases from 1.4853 to 1.5070 for pure PMMA and 0.10 TiO₂ mass fraction in PMMA film. Improvements on achieving monodisperse nanocomposite particles are made by the coupling of an electrospray method after the bead milling protocol [80]. In this work, authors find that an increase on concentration of titania nanoparticles (~15 nm, rutile phase) leads to a decrease on secondary particle size (aggregation size), making their distribution uniform.

Commercial titania nanoparticles (diameter approx. 30 nm) have also been encapsulated by using styrene microemulsion polymerization [81]. This synthesis method requires two steps to attain stable microemulsions: (1) the TiO₂ nanoparticles must be successfully dispersed in the monomer phase and (2) this phase must be dispersed in an aqueous surfactant solution to form stable submicron droplets. In this work, the effect of nanoparticle concentration on the mini-emulsification step is proved by increasing the droplet size as amount of titania is added to mini-emulsion.

The effect of titania nanoparticle surface modification on the physical properties of the polypropylene-based, PP/TiO₂, nanocomposites after processing by injection molding has been studied by Zhang et al. [82]. They describe how the incorporation of small amount of TiO₂ nanoparticles, lower than 1% in weight, does not promote any toughening effect in the injection-molded nanomaterials although their ductility is enhanced.

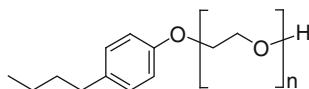
On the other hand, PMMA/TiO₂ nanocomposites have been prepared by the polymerization with photo-excited TiO₂ nanoparticles as initiator [83]. The titania, as mentioned before, is a semiconductor that under UV-irradiation produces valence hole and conduction electron in pairs, and then catalyzes reactions on the surface [84]. Polymerization initiated by the excited nanoparticles is called photocatalytic polymerization. XPS results show that the Ti 2p doublet of the TiO₂ in the composites shifts to lower binding energy by 1.0 eV. This downshift could reveal that the Ti⁴⁺ cation interacts with PMMA.

Finally, the photopolymerization kinetics of MMA initiated by TiO₂ nanoparticles in aqueous suspensions have been studied [85], demonstrating the pH dependence of polymerization rate while the tacticity of polymer remains unchanged.

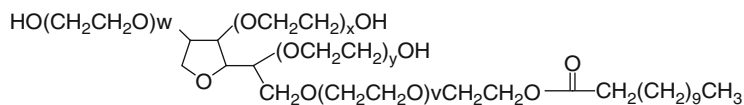
Polyaniline nanocomposites, PANI/TiO₂, [86] have been prepared by the chemical oxidative polymerization in a reverse micelle of aniline/TiO₂/hydrochloride acid precursor solution with ammonium peroxydisulfate used as oxidant. The nano-dimensional TiO₂ colloidal dispersion is previously prepared by the hydrolysis of titanium chloride. After 60 days, the nanocomposites create spherical nanoparticles self-organized in different morphologies depending on the surfactant system used. Then, a sea urchin-like morphology is developed when this non-ionic system is polyethylene glycol p-(1,1,3,3-tetramethylbutyl)-phenyl ether (Triton-x100); a triangle shape is promoted in sodium bis(2-ethylhexyl) sulfosuccinate, AOT/ anionic system; and nanoclusters are observed in cetyltrimethyl ammonium bromide, CTAB, cationic system (see Fig. 4.4 for surfactant information). These nanoclusters are built up by needle-like nanowires with the same aspect ratio as the nanowires in the Triton-x100 surfactant system, and these needle-like nanowires are comprised of spherical particles of PANI/TiO₂.

Li et al. [87] have also prepared PANI/TiO₂ nanocomposites using in situ chemical oxidative polymerization of aniline in the TiO₂ suspension. The nanoparticles, prepared by sol-gel using tetrabutyl titanate, are mostly anatase with an average particle size of approx. 15 nm and BET specific surface area of ca. 70 m²/g. PANI exhibits high absorption in the UV range and in the visible light region. As a consequence, the absorption of PANI/TiO₂ nanocomposite increases over the entire range of visible light compared with the one presented by pure TiO₂, whereas it decreases in the UV range. Therefore, this method can be effective to extend the absorption of TiO₂ to visible light range. In addition, these nanocomposites show good stability under irradiation conditions and they keep their perfect photocatalytic activity after several cycles with only a small decrease after each cycle due to slight aggregation of nanoparticles during the catalytic process.

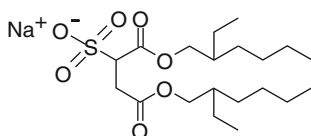
Tang's group [88] also utilizes oxidative reaction to chemically graft PANI on the surface of the self-assembled monolayer-coated TiO₂ nanoparticles (commercial anatase with an average particle size of 15 nm). The γ -aminopropyltriethoxysilane is used as a coupling agent to make a dense aminopropylsilane monolayer with active sites for grafting polymerization of aniline. This approach to produce PANI/TiO₂ nanocomposites improves its thermal stability at high temperatures (>400 °C), due to the covalent bonds formed between PANI chains and titania nanoparticles. As happened in the previous system, photocatalytic activity is observed under visible

a

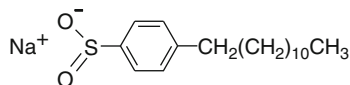
Triton-x100

Sum of $w+x+y+z=20$ $v=x-1$

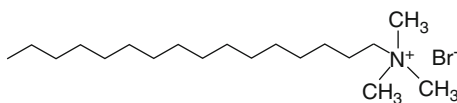
Tween 20

b

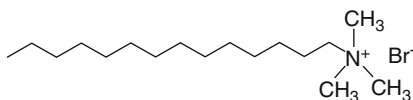
AOT



NaDBS

c

CTAB



TTAB

Fig. 4.4 Structure of surfactants: (a) non ionic Triton-x100 and Tween 20. (b) anionic sodium bis (2-ethylhexyl) sulfosuccinate (AOT) and sodium dodecylbenzenesulfonate (NaDBS). (c) cationic cetyltrimethyl ammonium (CTAB) and tetradecyltrimethyl ammonium bromide (TTAB)

light excitation; therefore, this will be another approach to extend the titania photoactivity.

This group [89] also reports in situ photocatalytic polymerization to achieve molecular imprinting polymer-coated photocatalysts. In this work, *o*-phenylenediamine,

OPDA, is selected as the functional monomer, since it has two NH_2 groups in its molecule capable of forming a hydrogen bond with the target molecules or templates, 4-chlorophenol, 4CP, or 2-chlorophenol, 2CP. The photodegradation of the mixture of 2 mg/L 4CP and 500 mg/L phenol is confirmed in the nanocomposites, where a rapid degradation with a half-time of approximately 8 min occurs for 4CP, while the relative concentration of phenol apparently remains almost unchanged. Therefore, these formed nanocomposites can promote the selectivity of TiO_2 photocatalysis.

Nanocomposite particles can be also prepared through in situ emulsion polymerization in the presence of nano- TiO_2 colloid obtained by the hydrolysis of titanium tetrachloride [90]. Authors used three different initiators: 2,2'-azobis (2-amidinopropane) dihydrochloride, AIBA, as cationic, and AIBN as non-ionic and ammonium persulfate, APS, as anionic initiators (see Fig. 4.5), where the latter is the most appropriate initiator in the polymerization since a cooperative effect can be formed by the negatively charged titania particles and the SO_4^{2-} terminal anionic group of APS. The formed particles are based on PMMA or poly(*n*-butyl acrylate) as core and TiO_2 as shell. The diameter of nanocomposite particles is about 150 nm, and the thickness of the TiO_2 -shell approx. 4–10 nm. In this case, the pH value has to be strictly controlled to obtain a tight TiO_2 coating without nanoparticle aggregation, adjusting the pH at about 3 during polymerization, and after that the pH ranges from 8.0 to 10.5. These materials could be used in the field

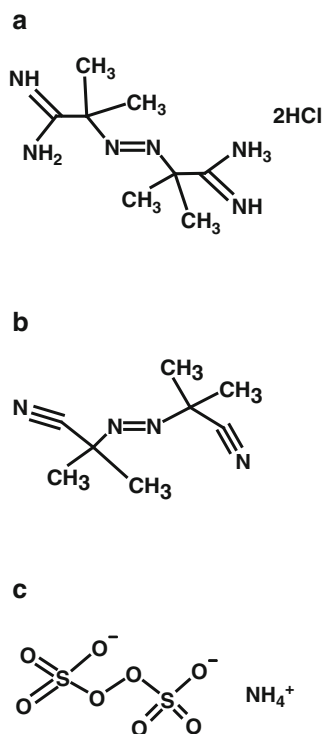


Fig. 4.5 Structure of different initiators used in radical polymerization. (a) 2,2'-azobis (2-methylpropionamide) dihydrochloride (AIBA). (b) 2,2'-azobisisobutyronitrile (AIBN). (c) ammonium persulfate

of photocatalytic coating, keeping in mind the coexistence of rutile and anatase structures in the nanocomposite.

In a recent article [91], TiO_2 nanoparticles are modified by adding a small amount of polythiophene to improve the dispersion of TiO_2 nanoparticles and to enhance the photocatalytic activity of the resulting nanocomposites. These nanomaterials have been synthesized by via oxidative polymerization of thiophene using FeCl_3 in the presence of three different surfactants: sodium dodecylbenzene-sulfonate, NaDBS, as anionic, tetradecyltrimethyl ammonium bromide, TTAB, as cationic, and poly(ethylene oxide) (20) sorbitan monolaurate, Tween 20, as non-ionic (see Fig. 4.4). In this case, the titania nanocrystal is the core and the polymer the shell. The best semiconductor property is observed when an anionic surfactant is used, which is attributed to differences in the stability of the nanocomposites. Consequently, the decomposition temperature when the anionic system is used is higher than that obtained in the hybrid materials prepared using the non-ionic, cationic or doped ones.

Surface modification by brushes allows dispersion and stability of the nanoparticles in various solvents or polymeric matrices while they maintain their physical characteristics. The modification of TiO_2 nanoparticles (primary particle diameter between 70 and 100 nm) by grafting polystyrene, PS, on its surface, and further polymerization of styrene allow preparing photodegradable PS/ TiO_2 nanocomposite films [92]. The presence of TiO_2 nanoparticles in polymer films promotes the photocatalytic oxidation of PS films under the UV-irradiation or the sunlight illumination, through its oxidative reaction with the active oxygen radicals [93]. Accordingly, the mass loss rate of the nanocomposite films is much higher than that for the neat PS film.

PS/ TiO_2 nanocomposites are also built up through a direct polymer grafting reaction from the surfaces of titanium oxide nanoparticles ($d \approx 15$ nm) [94]. In this case, a controlled radical polymerization method, nitroxide-mediated radical polymerization, NMP, is used to obtain the polystyrene and poly(3-vinylpyridine), P3VP, brushes. The initiator for NMP with a phosphoric acid group is chemisorbed onto the nanoparticles, and then monomer is polymerized giving controlled polymer graft layers on the surface (which means controlled molecular weights and low polydispersity indexes) (Fig. 4.6 illustrates the general procedure). The PS- and

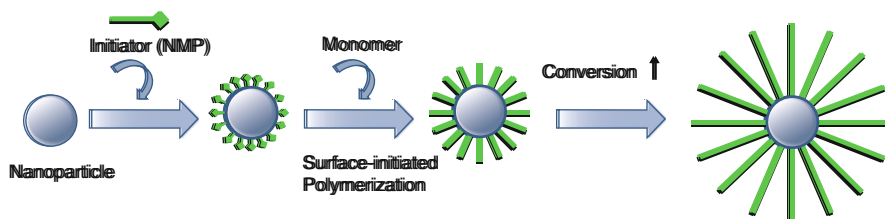


Fig. 4.6 Genesis sequence of nanocomposite synthesis: the initiator is chemisorbed onto the nanoparticles and, subsequently, the monomer is polymerized giving controlled polymer graft layers on the surface (the increment of conversion implies a linear augment on molecular weight)

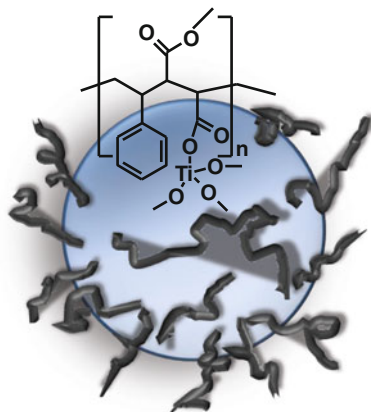
P3VP-modified nanoparticles are stably dispersed in organic solvents, such as tetrahydrofuran, toluene, and ethyl acetate. The dispersion of grafted and non-grafted nanoparticles in the PS matrix is later studied. The nanoparticles dispersed in chloroform are mixed to a PS matrix chloroform solution. It is found that the nanocomposite film becomes clouded and the transparency is drastically decreased, along with an increase in the weight ratio of nanoparticles, when non-grafted TiO₂ particles are added to the PS matrix. On the contrary, the PS-grafted TiO₂ nanoparticles are finely dispersed in PS matrix.

Transparent PMMA/TiO₂ nanocomposite particles have been prepared by graft polymerization of MMA from the surface of the modified TiO₂ particles with [γ -(methacryloxy)-propyl]trimethoxysilane by in situ emulsion polymerization [95]. These nanocomposite particles present either higher glass transition temperature or thermal stability than the pure PMMA. This coupling agent is also used to obtain PS/TiO₂ nanocomposite by in situ polymerization in toluene solution [96, 97].

Anatase TiO₂ nanoparticles have also been modified with 3-(trimethoxysilyl)propyl methacrylate to obtain PMMA/TiO₂ nanocomposites with high transparency and UV-absorption characteristics [98]. The anatase TiO₂ nanocrystals are prepared by a non-aqueous sol-gel approach involving the mixing of titanium isopropoxide and benzyl alcohol. The nanoparticles obtained exhibit a diameter ranging from 10 to 20 nm. As happened in the previous materials, the surfaces are modified to make the nanoparticles easily dispersible in non-polar media like xylene and dichloromethane as well as compatible with the PMMA matrix. The synthesis of PMMA/TiO₂ functional nanocomposite particles have been performed by atom transfer radical polymerization, ATRP, using commercial titanium dioxide nanoparticles (80% anatase and 20% rutile, an average particle size 34 nm and BET specific surface area 45 m²/g) where catechol-terminated initiator is anchored by chemisorption [99]. This specific biomimetic initiator is synthesized because of mussels secreting adhesive proteins that are mainly formed by catecholic amino acid, L-3,4-dihydroxyphenylalanine, which is believed to interact strongly with a variety of metal, metal oxide, and polymers. Therefore, it has a robust anchoring to titania surface. However, the controlled polymerization is not achieved when higher initiator concentrations are used. This group also studies the effect on the final properties of these nanocomposite particles when are incorporated into a PMMA matrix [100]. Their glass transition temperature and elastic modulus increase with respect to those presented in the pure PMMA. In contrast, nanocomposites obtained using unmodified nanoparticles lead to a decrease in these ultimate properties. This behavior demonstrates the influence that interfacial modification of nanoparticles produces on the nanocomposite homogeneity.

Another way to produce hybrid materials is using functional polymers that can interact with the inorganic component. This is the case of poly(styrene-*alt*-maleic anhydride), PSMA, alternating copolymer [101] with highly regular anhydride groups on the backbone chains that may provide regular sites for combination. This copolymer is dissolved along with tetrabutyl titanate precursor and both hydrolyzed at the same time. Acrylate groups are created from the reaction between uncondensed Ti-OH and maleic acid during the sol-gel process. Consequently,

Fig. 4.7 Structure of PSMA/TiO₂ nanocomposites



TiO₂ is covalent bonded with PSMA (see Fig. 4.7). Similar processes are described for nanocomposites based on poly(methyl methacrylate-*co*-butyl methacrylate-*co*-methacrylic acid) statistical copolymer [102] and other polymers [103] using the same titania precursor. In addition, functional poly(butyl acrylate-*co*-methyl methacrylate-*co*-(3-methacryloxypropyl)trimethoxysilane) terpolymer [104] and titanium *n*-butoxide are used for the synthesis of hybrid materials with higher hardness, elastic modulus, thermal stability and refractive index than those presented by the neat acrylic resin.

Sangermano et al. [105] prepared titania-containing coatings by cationic photopolymerization of an epoxy resin either by dispersion of commercial TiO₂ nanoparticles or by their in situ generation through a sol–gel dual-cure process. The rate of polymerization and, therefore, the epoxy group conversion decreases as increasing the TiO₂ concentration. All the cured films showed an increase of hydrophilicity on the surface of the coatings with increasing TiO₂ content. The results showed that completely transparent polymeric films are always obtained in the sol–gel-generated dual-cure systems, while systems containing dispersed TiO₂ with content higher than 3 wt% are non-transparent coatings. This indicates a more efficient and uniform distribution within the matrix for the in situ-generated titania particles in the nanometric size level. A solution process has been used to synthesize hybrid films of PMMA containing titanium dioxide nanoparticles of around 20 nm in diameter [106]. These nanoparticles are produced by sol–gel from titanium tetraisopropoxide, within the hydrophilic core of micelles, formed using poly(acrylic acid-*block*-methyl methacrylate) in toluene solution. The thermal stabilities of the obtained nanocomposites increase in comparison to the one shown by the pure PMMA. In addition, they exhibit high transparency in the visible light region even at 30 wt% titania, over 87% at 500 nm. The refractive index of the hybrid films at 633 nm linearly increases with TiO₂ content to attain a value of 1.579, which is 0.1 higher than that observed in PMMA [107]. Other nanocomposites based on poly(vinyl alcohol), polyvinylpyrrolidone, and poly(4-vinylpyridine) and titania also exhibit an enhancement of their refractive indexes by addition of

nanoparticles [108]. Very recently, Liou et al. [60] developed polyimide–nanocrystalline–titania hybrid optical films with a relatively high titania content (up to 50 wt %) and thickness (20–30 μm) from soluble polyimides containing hydroxyl groups. They synthesized two series of soluble polyimides. The hydroxyl groups on the backbone of the polyimides provide the organic–inorganic bonding, arising homogeneous hybrid solutions by controlling the mole ratio of titanium butoxide/hydroxyl group. The flexible hybrid films could be successfully obtained and revealed relatively good surface planarity, thermal dimensional stability, tunable refractive index, and high optical transparency.

Membranes of polyethersulfone/ TiO_2 with application for direct methanol fuel cells [109] were obtained by solving sulfonated polyethersulfone with a sulfonation degree of 70% and titania obtained from hydrolysis of titanium isopropoxide. It is well known that barrier properties in membranes, in terms of mass transport, increase by incorporation of inorganic fillers due to their higher tortuosity. However, the addition of nanoparticles produces in this case the contrary effect, i.e., a diminishment of proton conductivity [109, 110].

PS/ TiO_2 nanocomposite membranes for ultrafiltration can be prepared by blending titania sol in a polymer solution and posterior cast-evaporation [111]. The resulting membranes develop a network of pores that avoids the formation of macrovoids. They show higher hydrophilicity, porosity and permeability in comparison with the unfilled polymeric membranes. Polysulfone has also been utilized for ultrafiltration technology [112]. At 2 wt% TiO_2 content, the membranes present excellent water permeability, hydrophilicity, mechanical strength and good anti-fouling ability with almost unchanged retentions. However, higher titania content than 2 wt% cause particle aggregation; therefore, their performances decay.

Xiao-e et al. [113] prepared titania nanocomposites to study the oxygen dependence on the system photocatalytic activity. To do this, they used UV excitation of 10–15 nm diameter anatase nanocrystalline TiO_2 deposited on acetate substrate in the presence of excess organic electron donor components ('sacrificial' electron donor or SED). The organic SED added (50% mass relative to TiO_2) was methanol. Poly(vinyl chloride), PVC, and polyethylene glycol with different molecular weights were used. The results demonstrate that UV light in the presence of excess organic hole scavengers can lead to the deoxygenation of a closed environment. Optimum deoxygenation is observed using methanol as a hole scavenger, although efficient deoxygenation is also observed for a range of different polymer/ TiO_2 nanocomposite films deposited on glass and plastic substrates. Transient absorption spectroscopy is used to probe the kinetics of the deoxygenation reaction, focusing on the oxygen reduction step by photogenerated TiO_2 electrons.

PVC nanocomposite films with pure and modified TiO_2 have been casted from tetrahydrofuran solutions [114, 115]. Hyperbranched poly(3-caprolactone) with carboxylic acid groups are utilized to increase the compatibility of titania with the PVC matrix. The resulting well-dispersed nanocomposites show photocatalytic degradation where chloride acid is not formed. Therefore, they present a potential application as an eco-friendly alternative for the disposal of PVC wastes to the current waste landfill and dioxin-generating incineration.

Photo-active nanomaterials are also obtained by spin-coating of homogeneous solutions of low molecular weight poly[2-methoxy-5-(2'-ethyl-hexyloxy)phenylene-vinylene], MEH-PPV, and oleic acid surface-coating TiO₂ anatasa (rod and dot) nanocrystals onto low resistivity indium tin oxide, ITO, substrates [116]. The authors report photo-induced electron and hole transfer at the interface between anatase TiO₂ nanorods or nanoparticles and MEH-PPV conjugated polymer within these solution blends, being higher for spherical TiO₂ nanoparticles. In a very recent article [117], proton exchange membranes consisting of Nafion[®] and crystallized titania nanoparticles have been developed to improve water-retention and proton conductivity at elevated temperature and low relative humidity. The anatase-type titania nanoparticles ($d = 3\text{--}6$ nm) were synthesized in situ in Nafion (sulfonated tetrafluoroethylene) solution through the sol–gel process. The formed nanoparticles are well dispersed in Nafion solution at the titania concentration of 5 wt%. The glass transition temperature of the formed nanocomposite membrane is about 20°C higher than that of neat Nafion membrane. At elevated temperature (above 100°C), this nanocomposite membrane shows higher water uptake ability and improved proton conductivity compared to pure Nafion membrane.

There is in the literature many fewer articles dealing with the preparation of TiO₂ nanocomposites by melting process, although it is the most attractive methodology from an industrial standpoint. The effect of the content and nature of TiO₂ nanoparticles on the crystalline structure of high density polyethylene and isotactic polypropylene have been studied [33, 35, 42, 46, 118, 119]. The degree of crystallinity, the unit cell dimensions, the average lamellar thickness, or the average spherulite size are not usually altered in the polymer by the presence of nanoparticles. Moreover, location of the glass transition as well as melting temperatures in these nanocomposites is rather independent of the nanoparticles content. However, their photodegradation is enhanced by the nanoparticles presence.

The effect on the rheological behavior of the nanoparticle coating as well as of the nanoparticle amount has been studied in high impact polystyrene nanocomposites performed by this melting method [120]. These coated nanoparticles are obtained by in situ emulsion polymerization of styrene. The nanocomposite melts with coated nanoparticles presenting higher shear viscosity due to their strong interfacial interaction than the uncoated ones.

Very recently, polypropylene-titania nanocomposites, PP/TiO₂, have been prepared [121] by this process using titanium *n*-butoxide premixed with PP in the molten state. Under these conditions, the nanocomposites present TiO₂ nanoparticles with primary particle sizes with a mean diameter as low as 5 nm. The authors found that a fractal structure of these particles is observed at the highest concentrations, with a characteristic aggregates size of $d_{\text{aggr}} \approx 130$ nm. In addition, the rheological properties demonstrate that, in this case, the inorganic filler concentration at the percolation threshold is lower than 6 wt % (volume fraction ≈ 0.014). The appearance of a second plateau modulus at low frequency is mainly correlated to the formation of an aggregate–particle network.

4.5 TiO₂-Nanocomposites with Biocidal Properties

There is significant interest in the development of antimicrobial materials for application in the health and biomedical devices, food packaging, and personal hygiene industries [122–136]. Among several possibilities currently being explored, titania can be seen as a potential candidate for polymer modification with a significant number of advantages, the most obvious resulting from the absence of the releasing of dangerous materials into the media. This is a direct, positive input when compared with other current nanomaterials, like silver, with antimicrobial purposes. As deduced from recent contributions, there are additional benefits derived from the specific nanocomposite organization although, unfortunately, there are only a few articles exploring the use of TiO₂ nanocomposites for biocidal purposes. Below, the main results reported in these contributions are itemized.

Probably the earliest work of photo-active TiO₂-containing polymer-based nanocomposites was carried out by Kim et al. which aimed to reduce biofouling effects on polymer-based (polyamide) membrane systems [137, 138]. The nanocomposite material showed efficient control of *E. coli* in a period of hours, thus establishing the potential of the system in microorganism control and killing. The presence of TiO₂ on polymer-based membranes was recently reviewed although it appears that, apart from the already mentioned contributions, there is an essential lack of information concerning disinfection applications of these materials [139]. As detailed in the review article, some disinfection studies considered a technology derived from the combination of TiO₂ slurries and polymer-based membranes, but the use of nanocomposites was/is certainly scarce.

Only recently, several groups have tried to build up some general work aiming to test the potential antimicrobial properties of polymer-based composite systems containing TiO₂ as a biocidal agent. In this line, Kubacka et al. [33] describe the preparation by a melting process of ethylene-vinyl alcohol copolymer, EVOH/TiO₂ nanocomposite films with different amounts of the inorganic TiO₂ component with anatase structure, primary particle size of ~9 nm and a BET surface area of 104 m²/g. These nanoparticles are synthesized by a microemulsion method, and EVOH copolymers are selected because of their extensive commercial applications in food packaging, health, and biomedical industrial areas. The use of compatibilizer or coupling agent(s) is not needed in these nanocomposites due to the amphiphilic nature of EVOH copolymer, which is able to include titania nanoparticles in the final material with a good adhesion at interfaces between the two components. These nanocomposites present extraordinary antimicrobial properties against a number of Gram-positive and Gram-negative bacteria (*E. coli*, *carotovora*, and *faecalis*, and *P. aeruginosa* and *fluorescens*), Gram-positive cocci (*S. aureus*), and yeasts (*Z. rouxii* and *P. jadinii*). Figure 4.8 exemplifies this feature for a series of samples having different weight loadings of the inorganic component. The study showed that a key advantage of polymer-based materials biocidal properties (with respect to oxide-alone ones or even of polymer-based systems incorporating biocidal agents like Ag) relies on the fact that the whole nanocomposite surface becomes biocidal

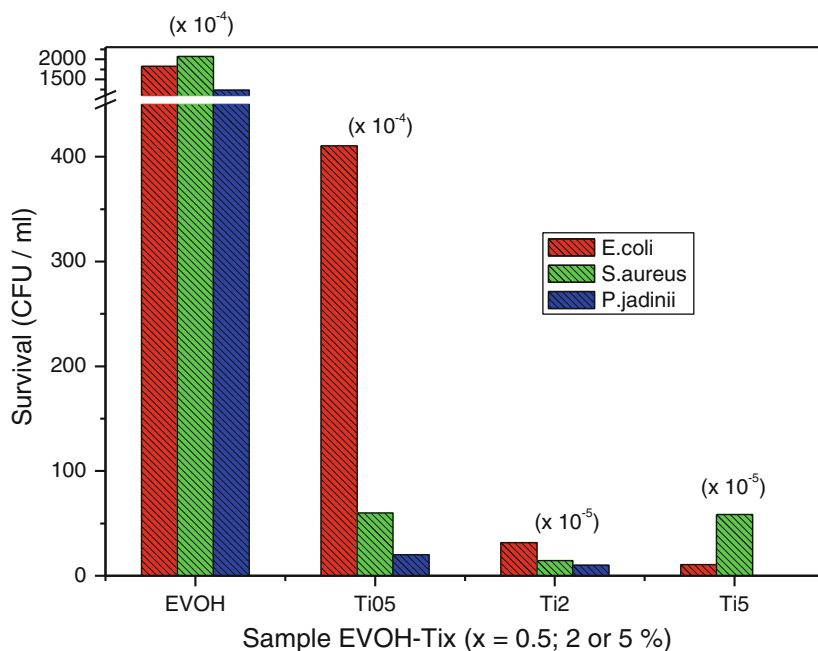


Fig. 4.8 Photokilling performances of EVOH-TiO₂ composites with variable inorganic content

and thus relaxes the requirement for direct biocidal agent to microorganism contact. These nanocomposites exhibit an astonishing biocidal behavior in comparison with that presented by well-known biocide agents such as Ag-based systems, AgBr particles coating with poly(vinylpyridine) or simple chemicals (glutaraldehyde, formaldehyde, H₂O₂, phenol, cupric ascorbate, or sodium hypochlorite) [31, 130, 133, 140, 141]. The outstanding biocidal capability comes from a close contact at nanometric scale between polymer and oxide nanoparticles, this contact being proved by the presence of new electronic states, not present in the individual components, in the nanocomposite systems. The optimum handling of charge carriers through the organic–inorganic interface occurs for oxide loading between 2 and 5 wt% as a compromise is found between the maximization of the components inter-area and the aggregation of the inorganic component [33, 35, 142].

Figure 4.9 displays the results of a SEM study illustrating how the incorporation of TiO₂ nanoparticles influences the biokilling potential of the nanocomposites, not only affecting the cell viability but also bacteria aggregation and biofilm formation. Biofilm formation control is a major issue in microbial control and killing, and the high effectiveness shown by these systems appears as a distinctive advantage of polymer-TiO₂ nanocomposites with respect to the bare oxide and/or traditional chemical agents. Note that the advantage against the bare oxide comes directly from the fact that, as explained above, the composite system is a type of non-contact agent, relaxing some of the inherent limitations of the inorganic biocide.

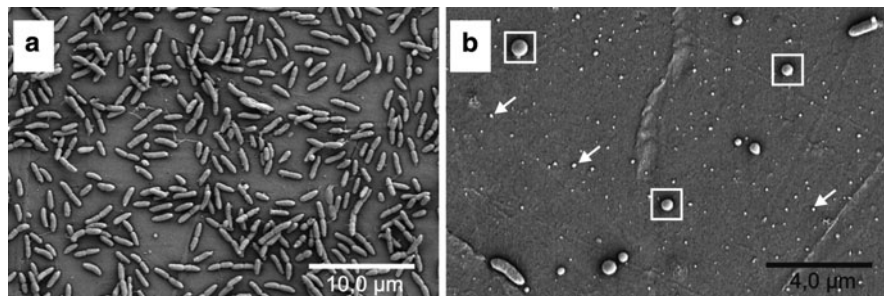


Fig. 4.9 SEM images of the *P. aeruginosa* cells sited at the surface of the TiO₂-EVOH nanocomposite with a 2 wt% of nanoparticle content in the absence (a) and presence of UV light (b)

In addition, these nanocomposites are easily photodegraded by exposure to sunlight. Therefore, they could be considered as environmentally friendly polymeric nanomaterials with potential applicability in the productive sector [33].

The physico-chemical characterization of these nanocomposites has additionally shown that the EVOH crystallinity does not practically vary by incorporation of titania nanoparticles, although the crystal size slightly increases with nanoparticle content at low compositions. The values of glass transition and melting temperatures do not differ significantly with the increase of titania composition, indicating a slight effect of TiO₂ nanoparticles on the transitions related to the amorphous and crystalline phases within the polymeric component. However, a considerable microhardness improvement is observed as the TiO₂ amount rises in the nanocomposites [35]. Such features would indicate that the conventional applicability of the EVOH copolymer is not affected or even reasonably improved by the presence of the biocidal oxide.

In additional works, these authors have evaluated isotactic polypropylene, iPP, as a matrix and, once more, anatasa titania nanoparticles to verify their straightforward and cost-effective approach as well as the biocidal possibilities of these other nanocomposites [46, 143], also with applications in the packaging sector. In this case, an interfacial agent (a low molecular weight polypropylene with maleic anhydride grafted, PP-*g*-MAH) is required to be added to improve the interfacial contact between the organic matrix and the nanoparticles due to the hydrophobic nature of iPP [144]. The antimicrobial activity is substantially enhanced in the resulting nanocomposites by efficiently managing charge carrier handling through the organic-inorganic interface, making the whole system biocidal. As occurred in EVOH/TiO₂ nanocomposites, crystallinity degree of the iPP matrix remains practically unchanged by the presence of nanoparticles in the polymer.

The antimicrobial performance exhibited by these TiO₂-polymer nanocomposites surface can even be improved by extending the oxide absorption power into the visible region through an oxide-surface doping process. Consequently, TiO₂-doped nanoparticles have been prepared by photodeposition of metallic entities (e.g., silver) in a content of 1 wt% [42] or by addition of a similar amount of certain oxides like Cu₂O/CuO or ZnO using impregnation procedures [145]. Afterwards, different

amounts of these doped nanoparticles have been incorporated into an EVOH copolymer through, once more, a melting process without using any compatibilizer. These nanocomposites demonstrate very effective germicide activity toward Gram-negative and Gram-positive bacteria/cocci (*E. coli*, *P. putida*, *S. aureus*), and yeasts (*P. jadinii*) using both UV and visible light sources, the latter up to 500 nm wavelengths. Figure 4.10 compares the film performance of TiO₂-EVOH and doped-TiO₂-EVOH nanocomposites with a 2 wt% of inorganic content for both the UV and visible light excitation cases. The plots display nanocomposites killing performances after 30 min contact with Gram-positive (*E. coli*) and -negative (*S. aureus*) bacteria. As expected, the surface doping of the oxide is effective with respect to TiO₂ as inorganic phase of the nanocomposite under all illumination conditions, but particularly while exposed to visible light irradiation. Photoluminescence studies indicate that such a positive effect is based on the influence of the additives in charge recombination, allowing hole-related charge species to interact more efficiently with microorganism targets. In addition, the materials show exceptional resistance to biofilm formation, which is responsible of microorganism antibiotic resistance. In summary, the presence of minuscule amounts of metallic Ag or Cu₂O/CuO or ZnO oxides greatly boosts the antimicrobial power (in comparison to TiO₂-EVOH systems) through several optical effects under UV light and introduces the successful use of visible-light sources. Such optical effects concern visible-light plasmonic resonances for the Ag metal and the optimization of the optical absorption capability

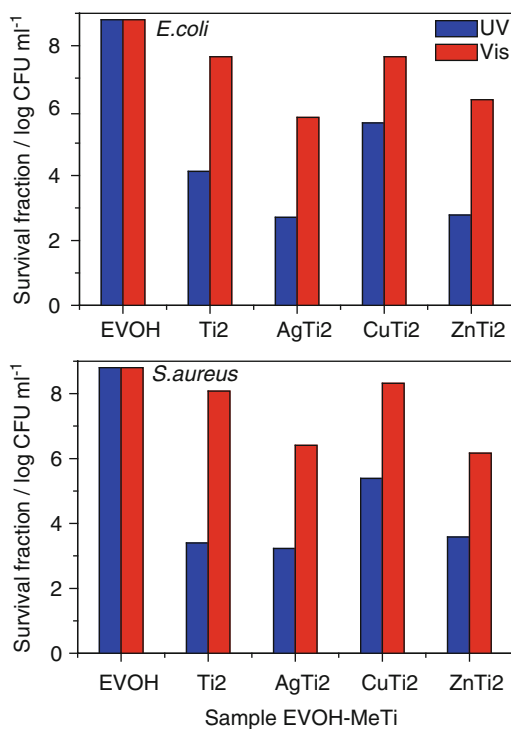


Fig. 4.10 Photokilling performances of EVOH-TiO₂ composites with a modified TiO₂ component at 2 wt% by surface addition of several inorganic phases (Ag, Cu or Zn). See text for details

in the UV/visible range for, respectively, ZnO and Cu₂O/CuO oxides, but, common to all of doping agents, is the already mentioned adequate handling of charge carriers generated upon light excitation through the corresponding inorganic–inorganic and inorganic–organic interfaces.

Other valuable works concern the use of an industrial TiO₂ material, called P25 from Degusa, to produce a polyester-based composite film which was coated on the walls of a photo-catalytic reactor to disinfect the air of a typical room (ca. 60 m³) using a recirculation system which can be installed, for example, in air conditioning apparatus. Using UV light, the system efficiently eliminated bacteria although showed a limited performance with fungi [146]. Also, Zhang et al. [147] reported the incorporation of titania to a polyurethane matrix using a surfactant (SDS) as interfacial agent. The presence of the latter component also increases the hydrophilicity of the final nanocomposite material. The system was tested against bacteria (*E. coli*, *C. albicans*) and a virus (*A. niger*) under both UV and visible (typical indoor conditions from fluorescence illumination) excitations. *E. coli* seems to be efficiently eliminated while some deficiencies were surprisingly observed in the photokilling of *C. albicans* and *A. niger*. Very recently, in 2010, two contributions described additional uses of these TiO₂-polymer composite materials. Tyllianakis et al. [148] described the use of complex biocidal agents containing silver, titania and quaternary ammonium salts in order to obtain highly efficient nanocomposite films showing outstanding activity against *E. coli*, *S. epidermis*, *S. aureus*, and *C. paraprilosis* and potential use in biomedical applications as scaffolds. Excellent performance is observed both in the presence or absence of light excitation and attributed to the combined effect of silver and quaternary salts while in dark conditions and titania upon illumination. Similarly, Kong et al. [149] reported the preparation of titania nanocomposites exhibiting antimicrobial performances even under dark conditions, since the secondary amine-containing antifouling copolymer shell provides additional antimicrobial activity to the one provided by TiO₂ nanoparticles. These materials are obtained by photo-induced copolymerization of 2-(*tert*-butylamino)ethyl methacrylate and ethylene glycol dimethacrylate to form core–shell poly(tBAM-*co*-EGDMA)/commercial anatase needle-like TiO₂ nanoparticles. They show enhanced photocatalytic antibacterial properties than neat TiO₂ nanoparticles against both *E. coli* and *S. aureus* due to the synergic antibacterial performances of the biocidal polymer shell and light-activated biocidal TiO₂ core.

Finally, we can mention that a system currently explored concerns the use of a natural polymer as chitosan incorporating the titania oxide as biocidal component. Presence of the inorganic component helps in mitigating chitosan biocidal deficiencies, typical of aqueous media at acidic pH and due to solubility deficiencies and limited availability of amino groups. Multilayer systems containing these two components [150] showed outstanding activity as well as that observed in more complex formulations using an additional layer containing Ag–AgBr [151] under, respectively, UV and visible light excitation conditions for the inactivation of *E. coli*. Also, TiO₂-chitosan composites immobilized in cotton fibers were shown to obtain 2/3 log reductions for *E. coli* and *S. aureus* upon 12 h visible light interaction. A lower activity of 97% was observed in the case of the virus *A. niger*

[152]. Some of the previous results on chitosan-based nanocomposite films containing additional (typically silver) antimicrobial agents were reviewed by Li et al. [124].

Acknowledgments A. Kubacka acknowledges MICINN for financial support (Ramón y Cajal postdoctoral grant). Funding of MICINN is fully acknowledged by the authors (CTQ2010-14872/BQU, MAT2010-17016, MAT2010-19883, PLE2009-0037).

References

1. Hoffmann MR, Martin BT, Choi W, Bahnemann DW (1995) Environmental applications of semiconductor photocatalysis. *Chem Rev* 95:69
2. Linsebigler AL, Lu G, Yates JT (1995) Photocatalysis on TiO₂ surfaces – principles mechanisms and selected results. *Chem Rev* 95:735
3. Bahnemann DW (2004) Photocatalytic water treatment: solar energy applications. *Solar Energy* 77:445
4. Serpone N (2006) Is the band gap of pristine TiO₂ narrowed by anion- and cation-doping of titanium dioxide in second-generation photocatalysts? *J Phys Chem B* 110:24287
5. Colón G, Belver C, Fernández-García M (2007) Nanostructured oxides in Photocatalysis. In: Rodríguez JA, Fernández-García (eds) *Synthesis Properties and Applications of Solid Oxides*. M Wiley, New York
6. Carp O, Huisman CL, Reller A (2004) Photoinduced reactivity of titanium dioxide. *Prog Solid State Chem* 32:33
7. Fox MA, Dulay MT (1993) Heterogeneous photocatalysis. *Chem Rev* 93:341
8. Fujishima A, Rao TN, Tryk DA (2000) Titanium dioxide photocatalysis. *J Photochem Photobiol C* 1:1
9. Barnard AS, Xu H (2008) An environmentally sensitive phase map of titania nanocrystals. *ACS Nano* 2:2237
10. Burdett JK, Hughbands T, Gordon JM, Richardson JW, Smith J (1987) Structural electronic relationships in inorganic solids – powder neutron-diffraction studies of the rutile and anatase polymorphs of titanium-dioxide at 15 and 295-K. *J Am Chem Soc* 109:3639
11. Asahi R, Taga Y, Mannstadt W, Freeman AJ (2000) Electronic and optical properties of anatase TiO₂. *Phys Rev B* 61:7459
12. Wiswanathan B (2003) Photocatalytic processes – selection criteria for the choice of materials. *Bull Catal Soc India* 2:71
13. Chen X, Mao SS (2007) Titanium dioxide nanomaterials: synthesis properties modifications and applications. *Chem Rev* 107:2891
14. Luan J, Ma K, Zhang L, Li M, Li Y, Pan B (2010) Research on different preparation methods of new photocatalysts. *Current Org Chem* 14:683
15. Catlow CRA, Bromley ST, Hamad S, Mora-Fonz M, Sokol AA, Woodley SM (2010) Modelling nano-clusters and nucleation. *Phys Chem Chem Phys* 12:786
16. Barnard AS, Curtiss LA (2005) Prediction of TiO₂ nanoparticle phase and shape transitions controlled by surface chemistry. *Nano Lett* 5:1261
17. Yang HG, Sun CH, Qiao SZ, Zou J, Liu G, Smith SC, Cheng MH, Lu GQ (2008) Anatase TiO₂ single crystals with a large percentage of reactive facets. *Nature* 453:638
18. Sakai N, Ebina K, Takada K, Sasaki T (2004) Electronic band structure of titania semiconductor nanosheets revealed by electrochemical and photoelectrochemical studies. *J Am Chem Soc* 126:5851
19. Marshall MSJ, Castell MR (2009) Shape transitions of epitaxial islands during strained layer growth: Anatase TiO₂(001) on SrTiO₃(001). *Phys Rev Lett* 102:146102
20. Dai YQ, Copley CM, Zeng J, Sun YM, Xia YN (2009) Synthesis of anatase TiO₂ nanocrystals with exposed {001} facets. *Nano Lett* 9:2455

21. Zhang DQ, Li GS, Wang HB, Chang KM, Yu JC (2010) Biocompatible anatase single-crystal photocatalysts with tunable percentage of reactive facets. *Cryst Growth Design* 10:1130
22. Fernández-García M, Belver C, Hanson JC, Wang X, Rodríguez JA (2007) Anatase-TiO₂ nanomaterials: Analysis of key parameters controlling crystallization. *J Am Chem Soc* 129:13604
23. Li G, Li L, Boerio-Goates J, Woodfield BF (2005) High purity anatase TiO₂ nanocrystals: Near room-temperature synthesis grain growth kinetics and surface hydration chemistry. *J Am Chem Soc* 127:8659
24. Hummer DR, Kubicki JD, Kent PRC, Post JE, Heaney PJ (2009) Origin of nanoscale phase stability reversals in titanium oxide polymorphs. *J Chem Phys C* 113:4240
25. Lee S-K, Mills A (2003) Platinum and palladium in semiconductor photocatalytic system. *Plat Metals Rev* 47:61
26. Mattesini M, de Almeida JS, Dubrovinsky L, Dubrovinskaia N, Johansson B, Ahuja R (2004) Cubic TiO₂ as a potential light absorber in solar-energy conversion. *Phys Rev B* 70:115101
27. Kubacka A, Fernández-García M, Colón G (2008) Nanostructured Ti-M mixed-metal oxides: Toward a visible light-driven photocatalyst. *J Catal* 254:272
28. Robertson JMC, Robertson PKJ, Lawton LA (2005) A comparison of the effectiveness of TiO₂ photocatalysis and UVA photolysis for the destruction of three pathogenic microorganisms. *J Photochem Photobiol A* 175:51
29. Lonnen J, Kilvington S, Kehoe SC, Al-Touati F, McGuigan KG (2005) Solar and photocatalytic disinfection of protozoan fungal and bacterial microbes in drinking water. *Water Res* 39:877
30. Vohra A, Goswami DY, Desphande DA, Block SS (2006) Enhanced photocatalytic disinfection of indoor air. *Appl Catal B* 65:57
31. Pal A, Pehkonen SO, Yu LE, Ray MB (2007) Photocatalytic inactivation of Gram-positive and Gram-negative bacteria using fluorescent light. *J Photochem Photobiol A* 186:335
32. Mitoraj D, Janczyk A, Strus M, Kisch H, Stochel G, Heczko PB (2007) Visible light inactivation of bacteria and fungi by modified titanium dioxide. *Photochem Photobiol Sci* 6:642
33. Kubacka A, Serrano C, Ferrer M, Lundsford H, Bielecki P, Cerrada ML, Fernández-García M, Fernández-García M (2007) High-performance dual-action polymer-TiO₂ nanocomposite films via melting processing. *Nano Lett* 7:2529
34. Guillard C, Bui TH, Felix C, Moules V, Lina B, Lejeune P (2008) Microbiological disinfection of water and air by photocatalysis. *Comptes Rendus Chim* 11:107
35. Cerrada ML, Serrano C, Fernández-García M, Fernández-Martín F, Jiménez-Rioboo RJ, de Andrés A, Kubacka A, Ferrer M, Fernández-García M (2008) Self-sterilized EVOH-TiO₂ nanocomposites: Interface effects on biocidal properties. *Adv Funct Mater* 18:1949
36. Li QL, Mahendra S, Lyon DY, Brunet L, Liga MV, Li D, Alvarez PJJ (2008) Antimicrobial nanomaterials for water disinfection and microbial control: Potential applications and implications. *Water Res* 42:4591
37. Dalrymplei OK, Slefankos E, Trutz MA, Goswami DY (2010) A review of the mechanism and modeling of photocatalytic disinfection. *Appl Catal B* 98:27
38. Matsunaga T, Tomoda R, Nakajima T, Wake H (1985) Photoelectrochemical sterilization of microbial cells by semiconductor powders. *FEMS Microbiol Lett* 29:211
39. Phan HN, McDowell T, Wilkins E (1995) Photocatalytically-mediated disinfection of water using TiO₂ as a catalyst and spore-forming *bacillus-pumilus* as a model. *J Environ Sci Health A* 30:627
40. Rincón AG, Pulgarin C (2003) Photocatalytical inactivation of *E coli*: Effect of (continuous-intermittent) light intensity and of (suspended-fixed) TiO₂ concentration. *Appl Catal B* 44:263
41. Wu PG, Xie RC, Shang JK (2008) Enhanced visible-light photocatalytic disinfection of bacterial spores by palladium-modified nitrogen-doped titanium oxide. *J Am Ceram Soc* 91:2957
42. Kubacka A, Cerrada ML, Serrano C, Fernández-García M, Ferrer M, Fernández-García M (2009) Plasmonic nanoparticle/polymer nanocomposites with enhanced photocatalytic antimicrobial properties. *J Phys Chem C* 113:9182

43. Zhang D, Li G, Yu JC (2010) Inorganic materials for photocatalytic water disinfection. *J Mater Chem* 20:4529
44. Elahifard MR, Rahimnejad S, Haghghi S, Gholami MR (2007) Apatite-coated Ag/AgBr/TiO₂ visible-light photocatalyst for destruction of bacteria. *J Am Chem Soc* 129:9552
45. Yan G, Chen J, Hua Z (2009) Roles of H₂O₂ and OH radical in bactericidal action of immobilized TiO₂ thin-film reactor: An ESR study. *J Photochem Photobiol A* 207:153
46. Kubacka A, Ferrer M, Cerrada ML, Serrano C, Sánchez-Chaves M, Fernández-García M, de Andrés A, Jiménez-Riobóo RJ, Fernández-Martín F, Fernández-García M (2009) Boosting TiO₂-anatase antimicrobial activity: Polymer-oxide thin Films. *Appl Catal B: Environ* 89:441
47. Rengifo-Herrera JA, Pierzchala K, Sienkiewicz A, Forró L, Kiwi J, Pulgarin C (2009) Abatement of organics and *Escherichia coli* by N S co-doped TiO₂ under UV and visible light Implications of the formation of singlet oxygen (O-1(2)) under visible light. *Appl Catal B* 88:398
48. Sunada K, Watanabe T, Hasimoto K (2003) Studies on photokilling of bacteria on TiO₂ thin film. *J Photochem Photobiol A* 156:227
49. Gogniat G, Dunkan S (2007) TiO₂ photocatalysis causes DNA damage via Fenton reaction generated hydroxyl radicals during the recovery period. *Appl Environ Microbiol* 73:7740
50. Wu D, You H, Jin D, Li X (2011) Enhanced inactivation of *E coli* with Ag-coated TiO₂ thin film under UV-C irradiation *J Photochem Photobiol A* 217:177
51. Novak BM (1993) Hybrid nanocomposite materials – between inorganic glasses and organic polymers. *Adv Mater* 5:422
52. Sanchez C, Julian B, Belleville Ph, Popall M (2005) Application of hybrid organic-inorganic composites. *J Mater Chem* 15:3559
53. Lantelme B, Dumon M, Mai C, Pascault JP (1996) In situ polymerization of titanium alkoxides in polyvinylacetate. *J Non-Crystal Solids* 194:63
54. Nandi M, Conklin JA, Salvati Jr L, Sen A (1991) Molecular level ceramic/polymer composites. 2. Synthesis of polymer-trapped silica and titania nanoclusters. *Chem Mater* 3:201
55. Hu Q, Marand E (1999) In situ formation of nanosized TiO₂ domains within poly(amide-imide) by a sol-gel process. *Polymer* 40:4833
56. Sarwar M, Zulfiqar S, Ahmad Z (2007) Preparation and properties of polyamide–titania nanocomposites. *J Sol-Gel Sci Technol* 44:41
57. Liaw W-Ch, Chen K-P (2007) Preparation and characterization of poly(imide siloxane) (PIS)/titania(TiO₂) hybrid nanocomposites by sol–gel processes. *Eur Polym J* 43:2265
58. Chiang P-C, Whang W-T (2003) The synthesis and morphology characteristic study of BAO-ODPA polyimide/TiO₂ nano hybrid films. *Polymer* 44:2249
59. Chiang PC, Whang WT, Tsai MH, Wu SC (2004) Physical and mechanical properties of polyimide/titania hybrid films. *Thin Solid Film* 447–448:359
60. Liou G-S, Lin P-H, Yen H-J, Yu Y-Y, Chen W-C (2010) Flexible nanocrystalline-titania/polyimide hybrids with high refractive index and excellent thermal dimensional stability. *J Polym Sci Part A: Polym Chem* 48:1433
61. Lü C, Cui Z, Guan C, Guan J, Yang B, Shen J (2003) Research on preparation structure and properties of TiO₂/polythiourethane hybrid optical films with high refractive index. *Macromol Mater Eng* 288:717
62. Yuwono AH, Xue J, Wang J, Elim HI, Ji W, Li Y, White TJ (2003) Transparent nanohybrids of nanocrystalline TiO₂ in PMMA with unique nonlinear optical behaviour. *J Mater Chem* 13:1475
63. Matsuyama K, Mishima K (2009) Preparation of poly(methyl methacrylate)–TiO₂ nanoparticle composites by pseudo-dispersion polymerization of methyl methacrylate in supercritical CO₂. *J Supercritical Fluids* 49:256
64. Lin CW, Hung CL, Venkateswarlu M, Hwang BJ (2005) Influence of TiO₂ nano-particles on the transport properties of composite polymer electrolyte for lithium-ion batteries. *J Power Sources* 146:397

65. Croce F, Appetecchi GB, Persi L, Scrosati B (1998) Nanocomposite polymer electrolytes for lithium batteries. *Nature* 394:456
66. Croce F, Curini R, Martinelli A, Persi L, Ronci F, Scrosati B, Caminiti R (1999) Physical and chemical properties of nanocomposite polymer electrolytes. *J Phys Chem B* 103:10632
67. Bloise AC, Donoso JP, Magon CJ, Rosario AV, Pereira EC (2003) NMR and conductivity study of PEO-based composite polymer electrolytes. *Electrochim Acta* 48:2239
68. Forsyth M, MacFarlane DR, Best A, Adebahr J, Jacobsson P, Hill AJ (2002) TiO₂ nanoparticles in polymer electrolytes: Surface interactions. *Solid State Ionics* 147:203
69. Best AS, Adebahr J, Jacobsson P, MacFarlane DR, Forsyth M (2001) Microscopic interactions in nanocomposite electrolytes. *Macromolecules* 34:4549
70. Byrne N, Efthimiadis J, MacFarlane DR, Forsyth M (2004) The enhancement of lithium ion dissociation in polyelectrolyte gels on the addition of ceramic nano-fillers. *J Mater Chem* 14:127
71. Ahmad S, Ahmad S, Agnihotry SA (2006) The effect of nanosized TiO₂ addition on poly (methylmethacrylate) based polymer electrolytes. *J Power Sources* 159:205
72. Ahmad S, Agnihotry SA, Ahmad S (2008) Nanocomposite polymer electrolytes by in situ polymerization of methyl methacrylate: For electrochemical applications. *J Appl Polym Sci* 107:3042
73. Logar M, Jančar B, Sturm S, Suvorov D (2010) Weak polyion multilayer-assisted in situ synthesis as a route toward a plasmonic Ag/TiO₂ photocatalyst. *Langmuir* 26:12215
74. Tang Q, Lin J, Wu Z, Wu J, Huang M, Yang Y (2007) Preparation and photocatalytic degradability of TiO₂/polyacrylamide composite. *Eur Polym J* 43:2214
75. Džunuzović E, Jeremić K, Nedeljković JM (2007) In situ radical polymerization of methyl methacrylate in a solution of surface modified TiO₂ and nanoparticles. *Eur Polym J* 43:3719
76. Zhang J, Luo S, Gui L (1997) Poly(methyl methacrylate)-titania hybrid materials by sol-gel processing. *J Mater Sci* 32:1469
77. Khaled SM, Sui R, Charpentier PA, Rizkalla AS (2007) Synthesis of TiO₂ - PMMA nanocomposite: Using methacrylic acid as a coupling agent. *Langmuir* 23:3988
78. Boettcher SW, Bartl MH, Hu JG, Stucky GD (2005) Structural analysis of hybrid titania-based mesostructured composites. *J Am Chem Soc* 127:9721
79. Inkyo M, Tokunaga Y, Tahara T, Iwaki T, Iskandar F, Hogan CJ Jr, Okuyama K (2008) Beads mill-assisted synthesis of poly methyl methacrylate (PMMA)-TiO₂ nanoparticle composites. *Ind Eng Chem Res* 47:2597
80. Yu KM, Suryamas AB, Hirakawa C, Iskandar F, Okuyama K (2009) A new physical route to produce monodispersed microsphere nanoparticle-polymer composites. *Langmuir* 25:11038
81. Erdem B, Sudol ED, Dimonie VL, El-Aasser MS (2000) Encapsulation of inorganic particles via miniemulsion polymerization II Preparation and characterization of styrene miniemulsion droplets containing TiO₂ particles. *J Polym Sci A: Polym Chem* 38:4431
82. Zhang H, Zhang Z, Park H-W, Zhu X (2008) Influence of surface-modified TiO₂ nanoparticles on fracture behavior of injection molded polypropylene. *Front Mater Sci China* 2:9
83. Wang J, Ni X (2008) Interfacial structure of poly(methyl methacrylate)/TiO₂ nanocomposites prepared through photocatalytic polymerization. *J Appl Polym Sci* 108:3552
84. Hoffman AJ, Yee H, Mills G, Hoffman MR (1992) Photoinitiated polymerization of methylmethacrylate using q-sized ZnO colloids. *J Phys Chem* 96:5540
85. Ni X, Ye J, Dong C (2006) Kinetics studies of methyl methacrylate photopolymerization initiated by titanium dioxide semiconductor nanoparticles. *J Photochem Photobiol A: Chem* 18:119
86. Sui X, Chu Y, Xing S, Yu M, Liu C (2004) Self-organization of spherical PANI/TiO₂ nanocomposites in reverse micelles. *Colloids and Surfaces A: Physicochem Eng Aspects* 251:103
87. Li X, Wang D, Cheng G, Luo Q, An J, Wang Y (2008) Preparation of polyaniline-modified TiO₂ nanoparticles and their photocatalytic activity under visible light illumination. *Appl Catal B: Environ* 81:267

88. Li J, Zhu L, Wu Y, Harima Y, Zhang A, Tang H (2006) Hybrid composites of conductive polyaniline and nanocrystalline titanium oxide prepared via self-assembling and graft polymerization. *Polymer* 47:7361
89. Shen X, Zhu L, Li J, Tang H (2007) Synthesis of molecular imprinted polymer coated photocatalysts with high selectivity. *Chem Commun* 11:1163
90. Ai Z, Sun G, Zhou Q, Xie C (2006) Polyacrylate-core/TiO₂-shell nanocomposite particles prepared by in situ emulsion polymerization. *J Appl Polym Sci* 102:1466
91. Uygun A, Turkoglu O, Sen S, Ersoy E, Yavuz AG, Batir GG (2009) The electrical conductivity properties of polythiophene/TiO₂ nanocomposites prepared in the presence of surfactants. *Curr Appl Phys* 9:866
92. Zan L, Tian L, Liu Z, Peng Z (2004) A new polystyrene–TiO₂ nanocomposite film and its photocatalytic degradation. *Appl Catal A: General* 264:237
93. Zan L, Wang S, Fa W, Hu Y, Tian L, Deng K (2006) Solid-phase photocatalytic degradation of polystyrene with modified nano-TiO₂ catalyst. *Polymer* 47:8155
94. Kobayashi M, Matsuno R, Otsuka H, Takahara A (2006) Precise surface structure control of inorganic solid and metal oxide nanoparticles through surface-initiated radical polymerization. *Sci Technol Adv Mater* 7:617
95. Yang M, Dan Y (2005) Preparation and characterization of poly(methyl methacrylate)/titanium oxide composite particles. *Colloid Polym Sci* 284:243
96. Zan L, Liu Z, Zhong J, Peng Z (2004) Organic modification on TiO₂ nanoparticles by grafting polymer. *J Mater Sci* 39:3261
97. Rong Y, Chen H-Z, Wu G, Wang M (2005) Preparation and characterization of titanium dioxide nanoparticle/polystyrene composites via radical polymerization. *Mater Chem Phys* 91:370
98. Koziej D, Fischer F, Kränzlin N, Caseri WR, Niederberger M (2009) Nonaqueous TiO₂ nanoparticle synthesis: a versatile basis for the fabrication of self-supporting transparent and UV-absorbing composite films. *Appl Mat Interf* 1:1097
99. Fan X, Lin L, Messersmith PB (2006) Surface-initiated polymerization from TiO₂ nanoparticle surfaces through a biomimetic initiator: A new route toward polymer–matrix nanocomposites. *Compos Sci Technol* 66:1198
100. Hamming LM, Qiao R, Messersmith PB, Brinson LC (2009) Effects of dispersion and interfacial modification on the macroscale properties of TiO₂ polymer–matrix nanocomposites. *Compos Sci Technol* 69:1880
101. Wang S, Wang M, Lei Y, Zhang L (1999) “Anchor effect” in poly(styrene maleic anhydride)/TiO₂ nanocomposites. *J Mater Sci Lett* 18:2009
102. Perrin FX, Nguyen V, Vernet JL (2002) Mechanical properties of polyacrylic–titania hybrids – microhardness. *Studies Polym* 43:6159
103. Su B, Liu X, Peng X, Xiao T, Su Z (2003) Preparation and characterization of the TiO₂/polymer complex nanomaterial. *Mater Sci Eng A* 349:59
104. Xiong M, Zhou S, Wu L, Wang B, Yang L (2004) Sol–gel derived organic–inorganic hybrid from trialkoxysilane-capped acrylic resin and titania: effects of preparation conditions on the structure and properties. *Polymer* 45:8127
105. Sangermano M, Malucelli G, Amerio E, Bongiovanni R, Priola A, Di Gianni A, Voit B, Rizza G, (2006) Preparation and characterization of nanostructured TiO₂/epoxy polymeric films. *Macromol Mater Eng* 291:517
106. Yamada S, Wang Z, Yoshinaga K (2009) Incorporation of TiO₂ nanoparticles formed via sol-gel process in micelle of block copolymer into poly(methyl methacrylate) to fabricate high refractive and transparent hybrid materials. *Chem Lett* 38:828
107. Aspnes DE (1982) Local-field effects and effective-medium theory – a microscopic perspective. *Am J Phys* 50:704
108. Nussbaumer RJ, Caseri WR, Smith P, Tervoort T (2003) Polymer-TiO₂ nanocomposites: A route towards visually transparent broadband UV filters and high refractive index materials. *Macromol Mater Eng* 288:44

109. Prashantha K, Park SG (2005) Nanosized TiO₂-filled sulfonated polyethersulfone proton conducting membranes for direct methanol fuel cells. *J Appl Polym Sci* 98:1875
110. Wu G, Gan S, Cui L, Xu Y (2008) Preparation and characterization of PES/TiO₂ composite membranes. *Appl Surf Sci* 254:7080
111. Yang Y, Wang P (2006) Preparation and characterizations of a new PS/TiO₂ hybrid membranes by sol-gel process. *Polymer* 47:2683
112. Yang Y, Zhang H, Wang P, Zheng Q, Li J (2007) The influence of nano-sized TiO₂ fillers on the morphologies and properties of PSF UF membrane. *J Membr Sci* 288:231
113. Xiao-e L, Green ANM, Haque SA, Mills A, Durrant JR (2004) Light-driven oxygen scavenging by titania/polymer nanocomposite films. *J Photochem Photobiol A: Chem* 162:253
114. Cho S, Choi W (2001) Solid-phase photocatalytic degradation of PVC-TiO₂ polymer composites. *J Photochem Photobiol A: Chem* 143:221-228
115. Kim SH, Kwak S-Y, Suzuki T (2006) Photocatalytic degradation of flexible PVC/TiO₂ nanohybrid as an eco-friendly alternative to the current waste landfill and dioxin-emitting incineration of post-use PVC. *Polymer* 47:3005
116. Petrella A, Tamborra M, Cozzoli PD, Curri ML, Striccoli M, Cosma P, Farinola GM, Babudri F, Naso F, Agostiano A (2004) TiO₂ nanocrystals-MEH-PPV composite thin films as photoactive material. *Thin Solid Films* 451-452:64
117. Ye G, Li K, Xiao Ch, Chen W, Zhang H, Pan M (2011) Nafion® - titania nanocomposite proton exchange membranes. *J Appl Polym Sci* 120:1186
118. Ma D, Akpalu YA, Li Y, Siegel RW, Schadler LS (2005) Effect of titania nanoparticles on the morphology of low density polyethylene. *J Polym Sci Part B: Polym Phys* 43:488
119. Zan L, Fa W, Wan S (2006) Novel photodegradable low-density polyethylene-TiO₂ nanocomposite film. *Environ Sci Technol* 40:1681
120. Tang CY, Yue TM, Chen DZ, Tsui CP (2007) Effect of surface coating on the rheological properties of a highly opaque nano-TiO₂/HIPS composite. *Mater Lett* 61:4618
121. Bahloul W, Bounor-Legaré V, David L, Cassagnau P (2010) Morphology and viscoelasticity of PP/TiO₂ nanocomposites prepared by in situ sol-gel method. *J Polym Sci Part B: Polym Phys* 48:1213
122. Appendini P, Hotchkiss JH (2002) Review of antimicrobial food packaging. *Innovative Food Sci Emerg Technol* 3:113
123. Devlieghere F, Vermeiren L, Debevere J (2004) New preservation technologies: Possibilities and limitations. *Int Dairy J* 14:273
124. Li Q, Mahendra S, Lyon DY, Brunet L, Liga MV, Li D, Álvarez PJJ (2008) Antimicrobial nanomaterials for water disinfection and microbial control. *Water Res* 42:4591
125. Noimark S, Dunnill CW, Wilons M, Parkin IP (2009) The role of surfaces in catheter-associated infections. *Chem Soc Rev* 38:3435
126. Brody AL (2003) "Nano nano" food packaging technology. *Food Technol* 57:52
127. Tang HZ, Doerksen RJ, Tew GN (2005) Synthesis of urea oligomers and their antibacterial activity. *Chem Commun* 12:1537
128. Ignatova M, Voccia S, Gilbert B, Markova N, Cossement D, Gouttebaron R, Jerome R, Jerome C (2006) Combination of electrografting and atom-transfer radical polymerization for making the stainless steel surface antibacterial and protein antiadhesive. *Langmuir* 22:255
129. Brayner R, Ferrari-Iliou R, Brivois N, Djediat S, Benedetti MF, Fievet F (2006) Toxicological impact studies based on *Escherichia coli* bacteria in ultrafine ZnO nanoparticles colloidal medium. *Nano Lett* 6:866
130. Sambhy V, MacBride M, Peterson BR, Sen A (2006) Silver bromide nanoparticle/polymer composites: Dual action tunable antimicrobial materials. *J Am Chem Soc* 128:9798
131. Dizman B, Elasi MO, Mathias LJ (2005) Synthesis characterization and antibacterial activities of novel methacrylate polymers containing norfloxacin. *Biomacromolecules* 6:514
132. Iconomopoulou SM, Voyiatzis GA (2005) The effect of the molecular orientation on the release of antimicrobial substances from uniaxially drawn polymer matrixes. *J Controlled Release* 103:451

133. Sagripanti JC, Bonifacio A (2000) Resistance of *Pseudomonas aeruginosa* to liquid disinfectants on contaminated surfaces before formation of biofilms. *J AOAC Int* 83:1415
134. Chen Y, Worley SD, Kim J, Wei TY, Santiago JI, Williams JF, Sun G (2003) Biocidal poly (styrenehydantoin) beads for disinfection of water. *Ind Eng Chem Res* 42:280
135. Robbins ME, Hopper ED, Schoenfish MH (2004) Synthesis and characterization of nitric oxide-releasing sol-gel microarrays. *Langmuir* 20:10296
136. Klibanov AM (2007) Permanently microbicidal materials coatings. *J Mater Chem* 17:2479
137. Kwak SY, Kim SH (2001) Hybrid organic/inorganic reverse osmosis membranes for bactericidal antifouling. *Environ Sci Technol* 35:2388
138. Kim SH, Kwak SY, Sohn BH, Park TH (2003) A TiO₂-based membrane with antifouling properties. *J Membr Sci* 211:157
139. Kim J, der Bruggen B (2010) The use of nanoparticles in polymeric and ceramic membrane structures. *Environ Pollut* 158:2335
140. Cowan MM, Abshire KZ, Houk SL, Evans SM (2003) Antimicrobial efficacy of a silver-zeolite matrix coating on stainless steel. *J Ind Microbiol Biotechnol* 30:102
141. Mazzola PG, Martins AMS, Penna TCV (2006) Chemical resistance of the gram-negative bacteria to different sanitizers in a water purification system. *BMC Infect Dis* 6:131
142. Jiménez Riobóo RJ, De Andrés A, Kubacka A, Fernández-García M, Cerrada ML, Serrano C, Fernández-García M (2010) Influence of nanoparticles on elastic and optical properties of a polymeric matrix: Hypersonic studies on ethylene–vinyl alcohol copolymer–titania nanocomposites. *Eur Polym J* 46:397
143. Kubacka A, Cerrada ML, Serrano C, Fernández-García M, Ferrer M, Fernández-García M (2008) Light-driven novel properties of TiO₂-modified polypropylene-based nanocomposite films. *J Nanosci Nanotechnol* 8:3241
144. Cerrada ML, Fernández-García M, Serrano C, Sánchez-Chaves M, Fernández-García M, De Andrés A, Jiménez Riobóo RJ, Fernández-Martín F, Kubacka A, Ferrer M, Fernández-García M (2009) Biocidal capability optimization in organic-inorganic nanocomposites based on titania. *Environ Sci Technol* 43:1630
145. Kubacka A, Ferrer M, Fernández-García M, Serrano C, Cerrada ML, Fernández-García M (2011) Tailoring polymer-TiO₂ properties by presence of metal (Ag, Cu, Zn) species: Optimization of antimicrobial properties. *Appl Catal B* 104:346–352
146. Paschoalino MP, Jardim WF (2008) An efficient polymer-based disinfection material. *Indoor Air* 18:473
147. Zhang X, Su H, Zhao Y, Tan T (2008) TiO₂-Polyurethane composites for indoor application. *J Photochem Photobiol A* 199:123
148. Tyllianakis M, Sevastos D (2010) Ag-TiO₂ nanocomposites for biomedical applications. *J Mater Chem* 21:2201
149. Kong H, Song J, Jang J (2010) Photocatalytic antibacterial capabilities of TiO₂ – biocidal polymer nanocomposites synthesized by a surface-initiated photopolymerization. *Environ Sci Technol* 44:5672
150. Yuan WY, Ji J, Fu JH, Shen JC (2008) Multilayer TiO₂-chitosan materials with antimicrobial properties. *J Biomed Mater Res B* 85:556
151. Yuan WY, Ji J, An Q, Liu YF, Chen JC (2009) Multilayer chitosanbased films with outstanding antimicrobial properties. *Nanotechnol* 20:245101
152. Quian T, Su H, Tan T (2011) The bactericidal and middle-proof activity of a TiO₂-chitosan composite. *J Photochem Photobiol A* 218:130

Chapter 5

Synthesis, Characterization, and Antimicrobial Activity of Zinc Oxide Nanoparticles

Adhar C. Manna

5.1 Introduction

In recent years, research and the use of nanomaterials has attracted much interest due to their small size (1–100 nm) and novel structures that exhibit significantly improved physical, chemical, and biological properties compared to their bulk or molecular precursors. In this context, a new branch of multidisciplinary science integrating engineering with biology, chemistry, and physics has emerged as nanosciences or nanotechnology, due to their existence and potential applications in a wide variety of fields such as electronics, ceramics, catalysis, magnetic data storage, structural components, food, cosmetics, biological, and medical [1–3]. Metal oxides, in particular the transition metal oxides, have profound applications in various fields due to their excellent optical, magnetic, electrical, and chemical properties. As the size decreases from the micrometer to the nanometer range, the materials exhibit enhanced diffusivity, increased mechanical strength and chemical reactivity, higher specific heat and electrical resistivity, and enhanced biological properties. This is in part because as particles become smaller, the proportion of atom found at the surface increases relative to the proportion inside its volume, which means that composite materials containing nanoparticles can be more reactive and have enhanced chemical properties. Nanostructure metal oxides are more interesting in that they can be synthesized with a very high surface-to-volume ratio and with unusual morphologies that contain numerous edge/corner and other reactive surface sites, which can be easily functionalized with different groups for the desired applications. An increasing use of nanomaterials has been reported in biological- and medical-related applications such as imaging, sensing, target drug delivery, fighting human pathogens, healthcare products, cosmetics, and food

A.C. Manna

Basic Biomedical Sciences, Sanford School of Medicine, University of South Dakota, Vermillion, SD, USA

e-mail: 1-605-677-63361-605-677-6381 amanna@usd.edu

preservative agents due to better safety and stability compared to bulk precursors or their organic counterparts.

The development of agents with antimicrobial activity and surface coatings has been attracting increased interest among various researchers in recent years due to the continuous emergence and spread of multiple or pan-antibiotic-resistant strains of various infectious organisms worldwide. In addition, microbial contamination is a serious health issue in both hospital- and community-associated settings and in the food industries. The antimicrobial activity of nanoparticles has been studied for several metal and metal oxide nanoparticles and bulk powders with different pathogenic and nonpathogenic bacteria [3–19]. Inorganic materials with antibacterial activity can be used in different forms such as powders, coated on the surface of hospital or medical devices, and/or as a part of organic/inorganic nanocomposite coatings in numerous industrial sectors including environmental, food, textiles, packaging, husbandry, healthcare, and medical care, as well as construction and decoration [1–3]. The main advantages of using inorganic oxides when compared with organic antimicrobial agents are their stability at higher temperatures and/or pressures, their ability to withstand harsh processes, and their robustness and long shelf life [3, 4]. Some of the inorganic or bulk oxide powders that have been tested for their antimicrobial activity are TiO_2 , ZnO , MgO , CaO , CuO , Al_2O_3 , AgO , and CeO_2 under different conditions [4, 6–8, 10–19]. Interestingly, several metal oxides (e.g., CaO , MgO , and ZnO) showed antimicrobial activity without photo-activation in contrast to others like TiO_2 that required photo-activation [4, 8, 9, 20, 21]. This has attracted much more attention toward developing an alternative compound to substitute for the conventional organic compounds like quaternary ammonium salt and chlorine disinfectant. Among the inorganic materials, metal oxides such as TiO_2 , ZnO , MgO , and CaO are not only stable under harsh conditions but also regarded as safe materials for human beings and animals, and are part of essential minerals for human health [1, 4, 20]. Furthermore, TiO_2 and ZnO have been used extensively in the formulation of various personal care products [22].

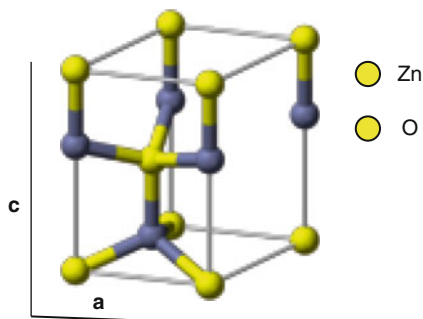
ZnO is a wurtzite-type semiconductor and piezo-electrical material exhibiting excellent electrical, optical and chemical properties with band-gap energy of 3.1–3.4 eV. It has a very large excitation binding energy of 60 meV at room temperature, which is very close to that of TiO_2 [14]. It is considered to be more suitable for photocatalysis applications due to its high photosensitivity, and chemical stability. Recently, special interest has been shown in its morphology, as ZnO can form various nanostructures suitable for a wide variety of applications in UV-shielding materials, gas sensors, biosensors, semiconductors, piezoelectric devices, field emission displays, photocatalytic degradation of pollutants, and antimicrobial treatments [1–3]. Several physical parameters such as surface area, particle size, surface charge, and zeta potential of a material are very important for its applications and function. These physical factors of nanoparticles very often govern the stability, uptake, persistence, and chemical or biological activities inside the living cells. ZnO nanoparticles are considered to be non-toxic, biosafe, and biocompatible and have been found in many biological applications in daily life such

as drug carriers, and in cosmetics, and as fillings in medical materials or devices [3, 4, 20]. Discovery of antimicrobial properties of metal oxides either powders or nanoscale materials has gained increased interest over the past decade largely due to the increasing emergence and spread of multiple antibiotic-resistant strains against organic antimicrobial agents. The majority of research and interest in the antimicrobial properties of metal oxides regards their use as antimicrobial coatings of the surfaces of various devices to eliminate survival of microorganisms on surfaces in the environment, community and health care settings that will eventually stop the spread of the diseases. In addition, coatings are expected to have better stability and safety, although nanoscale materials may pose a health-related hazard upon inhalation [10, 22]. It has been recognized that nanoscale materials pose more cytotoxicity than larger particles of the same material [20]. In this context, ZnO has advantages over other metal oxides such as TiO_2 for developing metal oxide-based antimicrobial agents at ambient conditions as its activity does not require photo-activation [10]. Antimicrobial activity and stability of ZnO nanoparticles can be enhanced by incorporating agents during synthesis. Because of the multifunctional nature of ZnO nanoparticles, it would be difficult to cover all aspects of interest. In this chapter, we will focus on the following aspects: synthesis, characterization, mechanism of antimicrobial activity, and biological applications.

5.2 Zinc Oxide Crystal Structure and Band Structure

Zinc oxide normally crystallizes in a hexagonal wurtzite structure, which is its most thermodynamically stable phase. This phase is where each anion is surrounded by four cations at the corners of a tetrahedron with a typical sp^3 covalent bonding [3, 23, 24]. It exhibits partial polar characteristics with lattice parameters $a_o = 0.32495$ nm, $c_o = 0.52069$ nm and $a_o/c_o = 1.602$ – 1.633 . As shown in Fig. 5.1, the ZnO structure can be described as number of alternative unit cells composed of tetrahedrally coordinated O^{2-} and Zn^{2+} stacked alternatively along the c -axis, resulting in the absence of inversion symmetry structure. For nanoparticle ZnO, the concentration of zinc and oxygen atoms located on the surface is greatly increased due to the

Fig. 5.1 The hexagonal wurtzite structure model of ZnO. The lattice constants are $a = 0.325$ nm and $c = 0.5207$ nm. All atoms are tetrahedrally coordinated. The fundamental band gap is direct with a value of 3.3 eV at room temperature (Adapted from http://en.wikipedia.org/wiki/Wurtzite_crystal_structure)



very large surface area, which affects its density and renders it with novel physical, chemical, and optoelectronic properties or responses. The most interesting characteristic of ZnO is that its polar surface is induced by its strong sensitivity to normal light at room temperature. Specifically, once a ZnO crystal is exposed to normal light, it readily deforms by the basal plane or growth direction $\{0001\}$ and forms polar surfaces. One end of the basal polar plane terminates with partially positive Zn lattice sites and the other end terminates with partially negative oxygen sites, resulting in a normal dipole moment and spontaneous polarization along the c -axis as well as variation in surface energy. To maintain a stable structure, the polar surfaces generally have facets or exhibit surface deformations, but nano-ZnO surfaces are exceptions as they are atomically flat, stable and exhibit no deformations. However, for nano-ZnO, there have been many conflicting views regarding the superior stability, electron transport, band structure and other characteristics compared to the bulk ZnO, although discussions are ongoing among the theoretical physicists and chemists [1, 3, 4]. In addition to growth surface or facet $\{0001\}$, two more commonly observed facets for ZnO are the top surface $\{2110\}$ and side surface $\{0110\}$, which are non-polar and have lower energy. ZnO exhibits various novel structures which can be grown by turning the growth rates along different directions of the facets.

The crystal structure, size, and shape of the synthesized ZnO nanoparticles can be investigated using several methods such as nitrogen physisorption (N_2), powder X-ray diffraction (XRD), and scanning and transmission electron microscopies (SEM and TEM) [3, 4, 23–31]. The crystallographic orientation of ZnO nanoparticles synthesized using hydrothermal methods is determined by XRD. A typical XRD pattern of a 12-nm-diameter particle synthesized ZnO nanoparticles by a hydrothermal method is shown in Fig. 5.2a. Nine peaks appeared at the positions

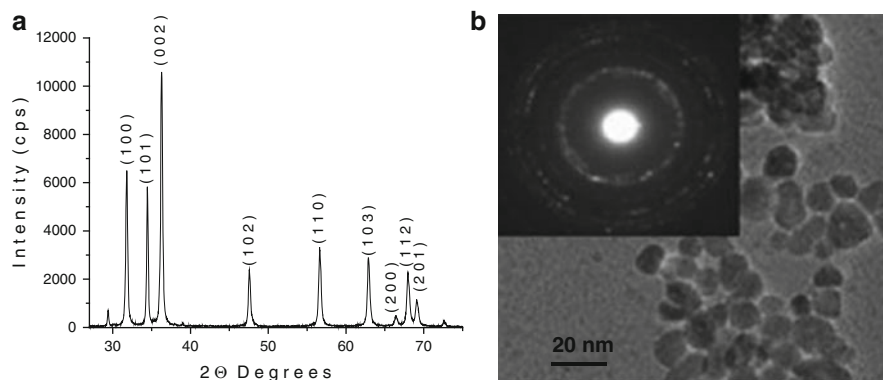


Fig. 5.2 (a) Typical X-ray diffraction (XRD) pattern for a 25-nm-diameter ZnO nanoparticle prepared using hydrothermal method. (b) TEM image of a 13-nm-diameter ZnO nanoparticle synthesized by force hydrolysis of zinc acetate at 160°C . The inset shows a selected area electron diffraction pattern confirming the crystalline ZnO phase (TEM image reproduced from [47]). With permission of the American Institute of Physics)

of $2\theta = 31.63^\circ, 34.50^\circ, 36.25^\circ, 47.50^\circ, 56.50^\circ, 62.80^\circ, 66.35^\circ, 67.92^\circ,$ and 68.91° , which correspond to $\{100\}, \{002\}, \{101\}, \{102\}, \{110\}, \{103\}, \{200\},$ and $\{201\}$, respectively, which are in good agreement with the assigned standard wurtzite-type ZnO structure (JCPDS 36–1,451) [31]. The specific surface areas, pore volumes, and diameters of ZnO nanoparticles can be determined using nitrogen physisorption studies in a Quantachrome Nova 2200e series surface area analyzer or similar instruments. For example, the surface areas of ZnO nanoparticles can be calculated using the Brunauer–Emmett–Teller equation in the relative pressure range (P/P_0) of 0.05–0.30. The average particle diameter (D) of the zinc oxide particles can also be estimated under the assumption that all particles are spherical in shape, and using the equation ($D = 6/S \rho$), where S is specific surface area per unit gram of the sample and ρ is the density of zinc oxide. The morphology and the size of the synthesized nanoparticles can be determined using various high resolution microscopes such as SEM or TEM [3, 19, 31]. A typical TEM pattern for ZnO nanoparticles synthesized through a hydrothermal method is shown in Fig. 5.2b. Lattice spacing of 0.28 and 0.16 nm indicate the presence of the $\{100\}$ and $\{110\}$ planes. In addition, electron diffraction studies can be performed to determine the crystal structure and the growth orientation of the ZnO nanoparticles.

5.3 Synthesis of ZnO Nanoparticles

Significant progress has been made in understanding fundamental aspects of the synthesis of nanoparticles in different forms. Various routes have been developed for the small- and large-scale production of nanoparticles. Several methods have been employed for the preparation of different forms of ZnO nanoparticles to investigate various functions and further improvements; however, a more fundamental approach of the exact growth mechanism of nanoparticles synthesis remains largely unknown. The different synthesis methods with different parameters and stringent growth conditions like temperature, pressure, hydrolysis ratio, and precursors has been adopted to achieve different forms of ZnO nanoparticles such as nanospheres, nanotubes, nanorods, nanobelts, nanowires, nanocombs, nanorings, nanoloops, nanobows, and nanoribbons [24–29]. These methods include metal–organic chemical vapor deposition, hydrothermal synthesis, thermal evaporation via a vapor liquid solid process assisted by a catalyst, and oxidation of metallic zinc powder without metal [24–26]. In addition, synthesis of ZnO nanoparticles largely depends on whether they will be used in biological and/or non-biological related systems. The relatively simple room temperature synthesis is more important than other methods for either coatings or biological applications. In low temperatures, synthesis is primarily focused on redox–reaction processes for metal chalcogenides or limited precipitation and/or crystallization for some metal salts and hydroxides. Overall, these methods are broadly classified into two main routes of nanoparticles synthesis: vapor phase and solution phase synthesis.

5.3.1 Vapor or Gas Phase Synthesis of ZnO

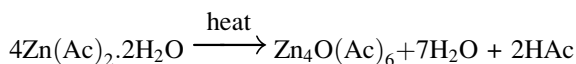
Various approaches have been developed for the synthesis of metal and ceramic nanoparticles with well-defined and narrow size distribution in the gas or vapor phase synthesis route using an inert gaseous environment in closed chambers. Normally, the synthesis of ZnO nanoparticles is carried out at higher temperatures from 500°C to 1,500°C, which is below the melting point of 1,975°C. Some of the commonly used gas phase methods are vapor phase transport that includes vapor solid and vapor liquid solid growth, physical vapor deposition, chemical vapor deposition, metal organic chemical vapor deposition, thermal oxidation of pure Zn and condensation, and microwave-assisted thermal decomposition [24]. Different sources such as evaporation, sputtering and laser are used to evaporate materials from the surface of solids into clusters, which are then condensed, transported, and collected on a cold finger to form the nanoparticles. Various types of ZnO nanoparticles such as nanowires, sheets, and tetrapods can be synthesized by physical vaporization of zinc powder with or without the presence of catalysts and exposure to air or N₂/O₂ mixture at relatively high temperature ranging from 800°C to 850°C [27]. One-dimensional high purity ZnO nanobelts have been synthesized using thermal evaporation of zinc sulfide (ZnS) powders in a hydrogen–oxygen mixture gas at 1,050°C [28] for potential application in optoelectronic devices. Generally, to synthesize ZnO nanoparticles, the metal bulk of zinc is placed inside the vacuum chamber and then, by setting the heating current, vacuum pressure and vaporized temperature, it melts and vaporizes into gas. Inside the chamber, the material vapor collides with inert gas to cool off, which then flows into a low temperature collector and forms nanoparticles. This simple principle has been used to synthesize different structures of ZnO or metallic Zn nanoparticles for fabrication on the surface of potential applications. Several methods which have been described for growing the different ZnO nanostructures or nanoparticles in the solution phase are also part of the gas phase synthesis.

5.3.2 Solution Phase Synthesis

Solution phase synthesis is often known as the hydrothermal growth process because the synthesis is carried out in aqueous solutions at a relatively low temperature. Some of the solution phase synthesis methods are the zinc acetate hydrate-derived nanocolloidal sol–gel route, zinc acetate hydrate in alcoholic solution with hydroxide (s), temperature-assisted synthesis, spray pyrolysis for growth of thin film, and electrophoresis [24, 25]. Numerous methods have been reported which are beyond the scope of description in this chapter; instead, we will present several of the most frequent methods used.

5.3.2.1 Sol–Gel Synthesis of ZnO Nanoparticles

The sol–gel processing method has been used for producing metal oxide and ceramic powders with high purity and high homogeneity [24, 29]. The sol–gel offers a degree of control of composition, shape, and morphologies of nanoparticles at the molecular level. The process involves the preparation of a colloidal suspension (“sol”), which is subsequently converted to viscous gels and solid materials using the principles of hydrolyzation, condensation, and polymerization reactions. Templates or precursors such as zinc acetate hydrates in an alcohol or ethanolic suspension are refluxed and distilled to form a transparent sol to remove the solvents and followed by drying. Small ZnO nanoparticles (>5 nm) can be formed under high concentration conditions by addition of hydroxides (e.g., LiOH, NaOH, etc.) and subsequent condensation and polymerization reactions. There are several factors, such as the nature of the alkyl group and the solvent, the concentration of each species in the solvent, the temperature, the water to alkoxide molar ratio, and the presence of acid or base catalysts, known to affect the different steps for the growth of ZnO nanoparticles. When zinc acetate, $\text{Zn}(\text{Ac})_2$, is heated in alcohol, the following reaction initially occurs:



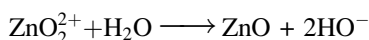
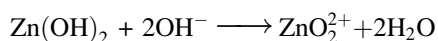
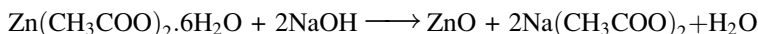
The tetrahedral oxy-acetate, $\text{Zn}_4\text{O}(\text{Ac})_6$, is also known as basic zinc acetate and is a well-designed molecular model of ZnO. Zinc acetate can form larger homologues like ethoxy acetate, $[\text{Zn}_{10}\text{O}_4(\text{Ac})_{12}]$ and hydroxy-double salt, $[(\text{Zn-HDS})\text{Zn}_5(\text{OH})_8(\text{Ac})_2(\text{H}_2\text{O})_2]$ from $\text{Zn}_4\text{O}(\text{Ac})_6$. The by-products such as H_2O , acetic acid, etc. are removed by distillation. ZnO nanoparticles are formed by continuous refluxing from these sol substrates. It has been observed that $\text{Zn}_4\text{O}(\text{Ac})_6$ is more stable than zinc acetate hydrate, while the stability of ethoxy acetate is enhanced in the presence of H_2O and ethanol. There is spontaneous formation of zinc hydroxyl double salts due to the presence of water and the higher stability of Zn-HDS monomer with respect to the oxy-acetate clusters. The zinc ethoxy-acetate is most the stable precursor because free Zn^{2+} ions do not exist in alcoholic zinc acetate hydrate solutions due to a strong chemical bond exists between Zn^{2+} ions and Ac ligands. The sol–gel process has been useful for synthesizing metal oxides as a result of the presence of metal–oxygen bonds. The process has distinct advantages over other methods for preparing metal oxide nanoparticles that include faster nucleation and growth, the formation of high purity powders as a result of homogenous mixing of the raw materials and the large-scale industrial production of nanopowders. The disadvantage of the process is the high cost for the precursors of the metal materials.

5.3.2.2 Hydrothermal Synthesis of ZnO Nanoparticles

Hydrothermal or wet chemical synthesis processes are solution-based processing routes used for the synthesis of nanoparticles. These include precipitation of solids from a supersaturated solutions, homogeneous liquid phase chemical reduction, and ultrasonic decompositions of chemical precursors [24, 29, 30]. These methods are more attractive due to their simplicity, versatility, and availability of low cost precursors.

Room Temperature Synthesis

The simplest route used to synthesize ZnO nanoparticles is room temperature synthesis using an acid-base precipitation method [22, 25, 29, 31]. In a typical synthesis, the precursor solution of zinc such as zinc nitrate, zinc acetate, or zinc sulfate, and an aqueous solution of base like NaOH, KOH, trimethyl (or ethyl) ammonium hydroxide, or NH_4OH are prepared in nanopure water. The acid solution is mixed with the base by varying the molar hydrolysis ratio of $\text{Zn}^{2+}/\text{OH}^-$ from 1 to 10, and the precipitate is harvested, washed, and dried in a static air oven at 80–90°C for several hours. The following reactions occur during the formation of ZnO nanoparticles:



Liu and Zeng [17] used similar room temperature solution synthesis to synthesize ZnO nanorods using the precursor solution of zinc nitrate [$\text{Zn}(\text{NO}_3)_2 \cdot 6\text{H}_2\text{O}$] and a NaOH solution in deionized water with different molar ratios of Zn^{2+} to OH^- varying from 1:3 to 1:40 at room temperature ($25 \pm 2^\circ\text{C}$) under constant stirring for 1–12 days. In addition, several reports of hydrothermal synthesis in aqueous solution have been reported with modification of the reaction conditions and the precursor materials used to achieve desired sizes and morphologies of the synthesized ZnO nanostructures/nanoparticles [24, 31]. For example, zinc acetate hexahydrate was mixed with sodium hydroxide in water with varying molar ratios of Zn^{2+} and OH^- at room temperature for 2 h, followed by sonication for 30 min to impart uniformity. Synthesis of ZnO nanoparticles can be carried out in an autoclave at different temperatures from 80°C to 180°C with varying reaction times from 12 to 48 h. For more simplicity of hydrothermal synthesis, the mixture of zinc salts (e.g., zinc acetate) and base (e.g., NaOH or NH_4OH) with adjustment in pH (>7.0) and/or heat (100–200°C) for 2 h is also very effective in forming a crystalline ZnO nanopowder.

Conveniently, the particle size and morphology can be manipulated during the growth of ZnO nanoparticles by using different precursors such as zinc nitrate, zinc sulfate, zinc chloride; bases like potassium hydroxide, ammonium hydroxide, tetramethylammonium hydroxide (TMAH), tetraethylammonium hydroxide (TEAH), diethanolamine; growth temperature; pressure; pH; and addition of macromolecules such as different surfactants such as polyvinyl alcohol (PVA), polyethylene glycol (PEG), sodium dodecyl sulphate (SDS), and cetyltrimethyl ammonium bromide (CTAB) [24]. Similar modification followed a significant change in morphology from rod-like to polyhedral, which was observed using ZnCl_2 and NaOH in hydrothermal synthesis with different organic compounds. In this example, crystalline nanoparticles of 10–20 nm were synthesized at room temperature by adding TMAH to an ethanolic solution of zinc acetate dehydrate, whereas addition of water to the ethanolic solution prior to adding TMAH produced ZnO nanoflakes [24]. Spherical ZnO nanoparticles of diameters ranging from 39 to 320 nm were synthesized by oxidation of zinc acetate in supercritical water [32]. Thus, particle size and morphology can be modulated by varying conditions like temperature, pressure and/or the reaction atmosphere.

Synthesis of Different Structures ZnO Nanostructures

The synthesis of nanoparticles can be divided into four steps: precursor formation, nucleation, growth, and aging. The kinetics of these processes determines the properties of the final product. The chemistry of precursor formation depends on the solvent and reactants present in the solution. The presence of water helps speed up the nucleation process during synthesis. Condensation reactions lead to nucleation that determines the detailed structure of the solid material. Faster nucleation processes combined with relatively slow growth and aging kinetics, is desirable for monodispersed colloids. The growth process does not significantly alter the particle size and size distribution; rather, aging can influence the types of aggregation or coarseness of the final product. Most of the nanostructures of ZnO such as nanowires, nanorods, nanobelts, etc., are important for various applications during fabrication and can be easily synthesized using different controlling agents such as surfactants, doping agents, or changing solvents. ZnO nanowires can be formed on glass surfaces by thermal decomposition of highly water soluble methenamine and zinc nitrate. These probably act as shape-inducing polymer surfactants, thereby blocking the growth of ZnO to other faces (e.g., {2110} and {0110}) and leaving only the polar {0001} face. There are numerous investigations regarding variation in the morphology of ZnO nanostructures using different surfactants, growth on substrates, and the control of reaction conditions. Tang et al. [33] synthesized ZnO nanorods using single precursor, zinc acetylacetonate hydratein, and the presence of four different surfactants (PVA, PEG, SDS, and CTAB). Similarly, carbamide was used as a surfactant for the synthesis of ZnO nanobelts in a hydrothermal growth process with ZnSO_4 and NaOH. Zhang et al. [34] has been able to synthesize bundles of ZnO nanostructures through a macromolecular surfactant (L64 and

F68) using a hydrothermal growth route. Nanoflowers of ZnO structure with hexagonal nanorod petals as long as 2–4 μm were synthesized at a temperature of 90°C in 30 min using zinc acetate dehydrate and sodium hydroxide through the hydrothermal method [24]. The growth of flower-like and cabbage-like nanostructures was also achieved using the hydrothermal growth method and the surfactant CTAB at temperatures of 120°C, 150°C, and 180°C. The flower-like micro- and nanostructures of ZnO nanorods are preferentially formed at a temperature of 120°C, whereas cabbage-like nanostructures are formed at higher temperatures of 150°C and 180°C due to repeated growth of two-dimensional ZnO sheets of 50 m or 100 nm. Overall, the nanoparticle size and morphologies can be modulated during the hydrothermal growth process of ZnO by changing different precursors, solvents, molar ratio, temperature, pressure, atmosphere of reaction, and the presence of catalysts or surfactants.

Other Hydrothermal Processes for the Synthesis of ZnO Nanoparticles or Nanostructures

At present, numerous processes have either been developed or are under development for producing nanoparticles in a manner that reduces both synthesis time and cost. Metal nanoparticles can be generated using either ultrasonic waves or microwave irradiation of metal salts or chemical precursors. Power ultrasonic waves can stimulate certain novel chemical processes such as nucleation, growth, and collapse of cavitation bubbles formed in liquid through localized hot spots in the liquid of extremely high temperature ($\sim 2,700^\circ\text{C}$) and pressure ($\sim 1,000$ atm). Increased use of microwaves mediated the synthesis of nanostructures or nanoparticles have been reported in comparing to this conventional oven. Microwave-assisted decomposition of zinc acetate precursor in the presence of an ionic liquid, 1-butyl-3-methylimidazolium bis(trifluoromethylsulfonyl) imide, [bmim][NTf₂], was used to synthesized ZnO nanoparticles [35]. Ma et al. [36] also synthesized ZnO micro- and nanoparticles using zinc acetate hexahydrate and pyridine in a hydrothermal process through microwave irritation at 90°C for 10 min. Adjusting the concentration of pyridine in the reaction, synthesis of various ZnO structures such as hexagonal columns, needles, nanorings, and hollow structures was reported. ZnO nanocrystallites synthesized using microwave irradiation were found to have more defects and were capable of exhibiting visible light photocatalysis without any doping with transition metals [24].

Several reports detailing the synthesis of ZnO nanostructures using simple routes have been published [24, 37]. Large arrays of ZnO nanorods on zinc foil have been synthesized in the absence of zinc salts, oxidant or coating of metal oxide layers by simply dipping the zinc foil into a 25% aqueous ammonium solution and heating at 80°C [24]. Vijayan et al. [37] successfully synthesized thin films of ZnO using a double dip method where sodium zincate served as the first dipping solution prior to dipping in hot water. The parameters of ZnO microstructures or nanoparticles can

vary based on the temperature of the hot water, the pH, and the amount of zinc sulfate used for preparation of the sodium zincate solution.

5.4 Antimicrobial Activity of ZnO Nanoparticles

Zinc oxide nanoparticles have attracted much attention due to their versatile and promising applications in biological sciences (antibacterial, antifungal, antifouling, and biosensors), ultraviolet applications (catalysis, sunscreen, paint, polymer nanocomposite, and rubber), and opto-electronics (light-emitting diodes, field effect transistors, field emitters, solar cells, toners, and sensors) [3, 38]. In addition, there are other applications such as in ferrite, varistor, pigment, ceramic flux, animal food, pollutant filter, dental fillings, hydrogen fuel, and nanotextiles. The main advantages of using ZnO nanoparticles compared with organic or bulk oxide is their chemical stability, thermal resistance, robustness, and long shelf life [3, 4, 39]. This is important for harsh conditions such as high temperatures and pressures that occur during product manufacturing, storage, and transportation. Considering the continuous emergence of multiple drugs and antibiotic-resistant microorganisms, in particular, seen amongst pathogenic bacteria, it has become an emerging public health issue. The morbidity and mortality associated with bacterial diseases as well as the cost associated with treatment remains high, due to continuous emergence of multiple antibiotic-resistant pathogenic strains that either acquire resistance readily or are naturally resistant [40–42]. Some of these emerging bacterial diseases that occur frequently include large outbreaks of food- and water-borne infections, hospital-acquired (nosocomial) infections, bioterrorism-associated infections, microbiota shift diseases and antibiotic resistance. In addition, several pathogens are capable of forming biofilms, typically on either host organs or medical and non-medical devices, which makes treatment difficult due to reduced drug penetration [42, 43]. The capacity of various bacterial pathogens to cause a multitude of animal diseases is due to the organisms' ability to produce multiple factors associated with survival and virulence when they are in their environmental settings [40–43]. Many of these factors are associated with colonization, neutralization of host immune systems, host tissue damage, and spreading of pathogens in their environmental settings. Therefore, alternative therapeutics that control the spread of pathogens and eliminate resistant pathogenic bacteria from different environmental settings such as community, hospital, and various food industries are being sought.

A literature survey revealed that over the last 20 years, efforts have been carried out to develop nanomaterial agents with novel properties that have specific antibacterial activities to combat the growing threat of infectious diseases [1–3]. Some of the inorganic nanoparticles or the bulk oxide powders that have been tested for their antibacterial activity are TiO₂, ZnO, MgO, CaO, CuO, Al₂O₃, AgO, and CeO₂ [4–19]. Among these metallic oxide nanoparticles, photocatalytic inactivation of bacteria by TiO₂ has been studied over the last 20 years [6, 7]. TiO₂ can kill both

Gram-negative (*Escherichia coli*), and Gram-positive (*Bacillus subtilis*, *Staphylococcus aureus*) organisms as well as viruses including poliovirus 1, *hepatitis B virus*, *Herpes simplex virus* and MS2 bacteriophage with different sensitivity [44]. Similar to TiO_2 , various structures of ZnO have attracted much interest due to extensive applications in sunscreens, coating, and paints [10], and also due to their piezoelectricity and band gap in the near ultraviolet range and large excitation binding energy at room temperature. ZnO has been shown to have different modes of action towards microorganisms from other metal oxides [5, 8, 9, 11, 19, 46, 47]. Specifically, studies have demonstrated the antimicrobial activity of bulk or larger particle-sized ZnO in the range of 0.1–1.0 μm under visible light [21], whereas similar studies on ZnO nanoparticles showed higher antibacterial activities against *E. coli*, *S. aureus*, and *B. subtilis* [8, 9, 11, 21, 30, 39, 45–49]. Studies by several groups have shown that functional activities and consequent toxicity of ZnO nanoparticles may be influenced by particle size and concentration which is inversely proportional to the size and concentration of ZnO nanoparticles used against *S. aureus* and *E. coli* [9, 21, 31, 46]. Specifically, studies on *E. coli* with particle sizes ranging from microns (2 μm) to nanometers (45 and 12 nm) showed more effective antibacterial effect with smaller nanoparticles compared with larger sized particles [46]. Size-dependent growth inhibition and viability of *S. aureus* were demonstrated in the presence of 6 mM concentration of hydrothermally synthesized ZnO particle sizes ranging from 302 to 12 nm as shown in Fig. 5.3 [31]. This is due to the fact that smaller particles will have both a higher number and a higher surface area to volume

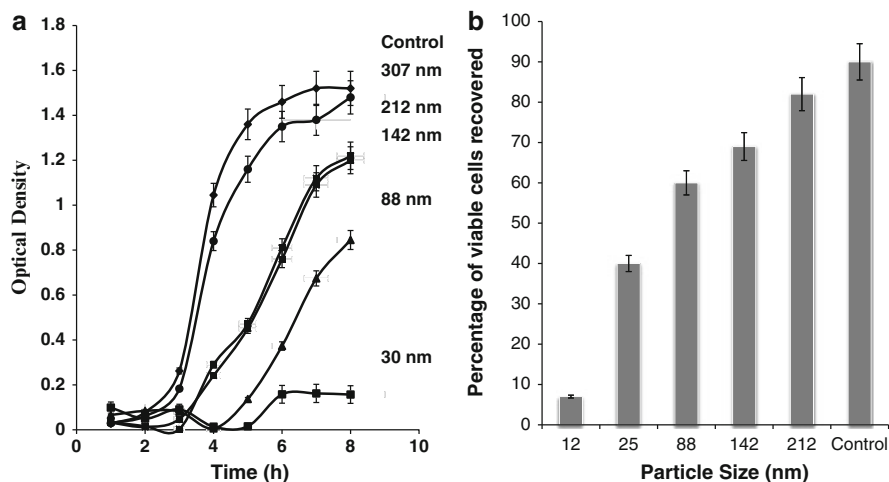


Fig. 5.3 Effect of different sizes ZnO nanoparticles on the growth of *S. aureus*. **(a)** Growth analysis curves measured by monitoring the culture turbidity as a qualitative measure of cell growth using the optical density (OD) at 600 nm. **(b)** The percentage of growth inhibition as counted the viable *S. aureus* colonies recovered from TSA (tryptic soy broth agar) plates and plotted against ZnO particle sizes. The results demonstrate that size-dependent bacterial growth inhibition of *S. aureus* exists in the presence of 6 mM of different sizes of ZnO nanoparticles (Adapted from [31]; American Chemical Society)

ratio to cover target microorganisms and attribute higher surface reactivity compared to larger particles. Contradictory results have been reported where size-dependent effects were not found to influence the antimicrobial activity of ZnO [50]. In addition to the particle size-dependent antibacterial effect of ZnO nanoparticles, most of the studies in the literature strongly indicate that dose-dependent antibacterial activity exists for various forms of ZnO nanoparticles against both Gram-positive and Gram-negative bacteria. Interestingly, the antibacterial effect of the nanoparticles was significantly more pronounced on the Gram-positive bacteria than on the Gram-negative bacteria probably due to the complexity of the cell membrane structure that exhibits significant changes in membrane permeability and other surface properties in the presence of metal oxide nanoparticles. It has been reported that more than 95% inhibition of *S. aureus* growth could be seen at ZnO nanoparticle (diameter ~13 or 8 nm) concentration of ≥ 1 or 1 mM, whereas complete inhibition of *E. coli* growth was observed with ≥ 3 mM of ZnO nanoparticles of about 11 nm diameter [9, 19, 47, 51].

Although most of the studies on the antibacterial activity of either ZnO bulk or nanoparticles has been performed using Gram-negative *E. coli* and Gram-positive *S. aureus*, very few studies have been performed using other bacterial species. Some of the bacterial species that have been tested for various sizes ZnO nanoparticles or bulk are *Streptococcus* (*mutans*, *pyogenes*, and *agalactiae*), *Enterococcus* (*faecalis*), *Staphylococcus epidermidis*, *Bacillus* (*subtilis* and *atrophaeus*), *Lactobacillus* (*casei* and *helveticus*), *Vibrio fischer*, *Salmonella typhimurium*, *Shigella* (*dysenteriae* and *flexinari*), *Pseudomonas* (*aeruginosa*, *chlororaphis*, and *alcaligenes*), *Campylobacter jejuni*, and *Proteus vulgaris* [8, 9, 13, 31, 48, 51–54]. Figure 5.4 represents a typical growth inhibition assay for several bacterial pathogens with various concentrations of ZnO nanoparticles (particle size ~ 12 nm) under normal ambient lighting conditions [31]. These results demonstrate that most of the bacterial growth (>95%) could be inhibited for most of the bacteria, except for a select few such as *S. typhimurium*. In addition to the growth inhibition assays, viable cell counts of the ZnO nanoparticle-treated cultures demonstrated that the number of recovered bacteria was significantly fewer compared to the untreated control, which correlates with growth inhibition patterns. The antibacterial activity of ZnO nanoparticles varies from species to species due to the characteristic difference of the organisms tested. For example, among the Gram-negative bacteria, the minimal inhibitory concentration (MIC) of ZnO nanoparticles (~30 nm) for *C. jejuni* (0.05–0.25 mg/mL) is 8- to 16-fold lower than *Salmonella enterica* and *E. coli* O157:H7 (0.4 mg/mL) strains [54]. It has also been reported that strains within a species vary significantly in terms of infectivity and tolerance to various agents including antibiotics. Analysis of the antibacterial activity of various clinical isolates of *S. aureus* suggest that there is a variation in antibacterial activity of ZnO nanoparticles to some of the isolates, although majority of the isolates showed similar patterns of inhibition [9, 31]. In addition to these microorganisms, efficient growth inhibition or killing activity of both bulk and nanoscale ZnO has been demonstrated for fungi (*Candida albicans*, *Saccharomyces cerevisiae*, *Neurospora crassa*, and *Aspergillus oryzae*) and algae (*Nitzschia pallida* and *Crustaceans*

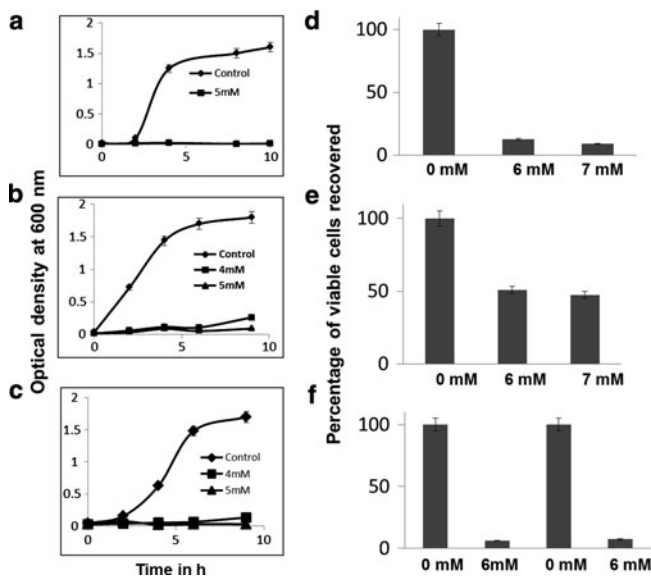


Fig. 5.4 Growth inhibition assays of various microorganisms in the presence of different concentrations of ZnO nanoparticles (~12 nm particle diameter). The different strains of microorganisms are: (a) *S. aureus* strain MW2 (community-associated MRSA). (b) *S. aureus* strain Newman (MSSA). (c) *S. aureus* strain Cowan (hospital-associated MRSA). (d) *Proteus vulgaris*. (e) *Salmonella typhimurium*. (f) *Shigella flexinari* (left) and *Bacillus cereus* (right). The results demonstrate that the concentration range of 4–7 mM colloidal suspension of ZnO nanoparticles could inhibit more than 95% of growth for most of the microorganisms, except *S. typhimurium* (Adapted from [31]; American Chemical Society)

daphnia magna) and nematodes (*C. elegans*) [50, 52, 55, 56]. Overall, published reports clearly suggest that ZnO nanoparticles have significantly higher antibacterial or antifungal activity compared to the bulk ZnO, target a wide range of microorganisms, and that their activity does not require any photo-activation.

The properties of regular spherical or different shapes nanoparticles depend strongly on their dimensions and morphologies [57–60]. The relationship between the different forms of ZnO with the antibacterial activity is not clear, in spite of the fact that different structures and morphologies of ZnO can be efficiently synthesized using various synthesis methods. Studies have demonstrated that antibacterial activity increases with the increase of the lattice constant value of c_0 in the hexagonal structure of ZnO powder and is also due to enhanced generation of hydrogen peroxide [60]. The relationship between antibacterial activity and various orientations of ZnO nanowire arrays indicate differential antibacterial activity among ZnO nanoarrays, in spite of having similar average diameter. Randomly oriented ZnO nanoarrays exhibited superior antibacterial activity compared with less or well-defined oriented ZnO nanoarrays in *E.coli* [57]. Although the exact mechanism of the antibacterial actions of different orientations of ZnO nanoarrays is not known, the probable mechanism is considered to be due to the generation of

hydrogen peroxide as well as surface abrasiveness [46]. The aggregation of ZnO nanoparticles does not greatly affect the antibacterial activity, rather the size of the nanoparticles greatly influences the antibacterial activity against various microorganisms. The dimension and morphology of ZnO nanoparticles play important roles in determining the antibacterial activity, although it has not been well investigated compared to other non-biological applications.

In summary, both bulk and nanoparticle preparation of ZnO can effectively inhibit both Gram-positive and Gram-negative bacteria as well as algae and fungi under normal ambient lighting conditions. The antibacterial activity of ZnO can be observed against various states of bacteria such as vegetative and spores that naturally resist both high temperature and high pressure treatments. Antibacterial activity of ZnO nanoparticles is size dependent, as smaller particle sizes have more efficient antibacterial activity than the larger size nanoparticles or bulk particles. The antibacterial activity of ZnO depends on the surface area and concentration of the particles, while the crystalline structure and particle shape have little effect. Thus, increasing the concentration and surface area improves the effectiveness of ZnO particles against most of the tested microorganisms. High temperature treatment of ZnO nanoparticles (calcination) does not have a significant effect on antibacterial activity [31], whereas high temperature treatment of ZnO bulk decreases its antibacterial properties [60].

5.5 Mechanism of Antibacterial Activity of ZnO Nanoparticles

To date, a number of mechanisms have been proposed to interpret the antibacterial or cytotoxic activity of ZnO powders or nanoparticles. These include toxicity based on chemical composition (e.g., release of toxic ions); production of reactive oxygen species (ROS) due to the presence of nanoparticles; stress of stimuli caused by the surface, size, and shape of particles; damage to membrane cell wall through adhesion on the cell membrane; penetration through the membrane cell wall; and cellular internalization of nanoparticles [4, 5, 19, 46, 55, 61, 62]. Although there are numerous studies regarding the antibacterial effect of ZnO mostly using *E. coli* and *S. aureus*, little is known regarding ZnO interactions with other bacteria and the mechanism underlying the antimicrobial effects. It is clear from numerous studies that interactions of ZnO nanoparticles or powders in water produce various reactive oxygen species, predominantly hydroxyl radicals (OH^\cdot), singlet oxygen or superoxide anion (O_2^\cdot), and hydrogen peroxide (H_2O_2), which play a crucial role in nanoparticle-induced antimicrobial activity. As direct proof, the formation of hydroxyl radicals and singlet oxygen species of a suspension of ZnO was determined by electron spin resonance (ESR) [46, 63], while hydrogen peroxide formation was evident by direct quantification [5, 11, 12]. It has been shown that, under ordinary room light with a light intensity of $10 \mu\text{W}/\text{cm}^2$ (or the intensity of UV light $\sim 1 \mu\text{W}/\text{cm}^2$), is sufficient to induce ROS production in suspension of ZnO in water [63]. However, the level of ROS production increases significantly when the

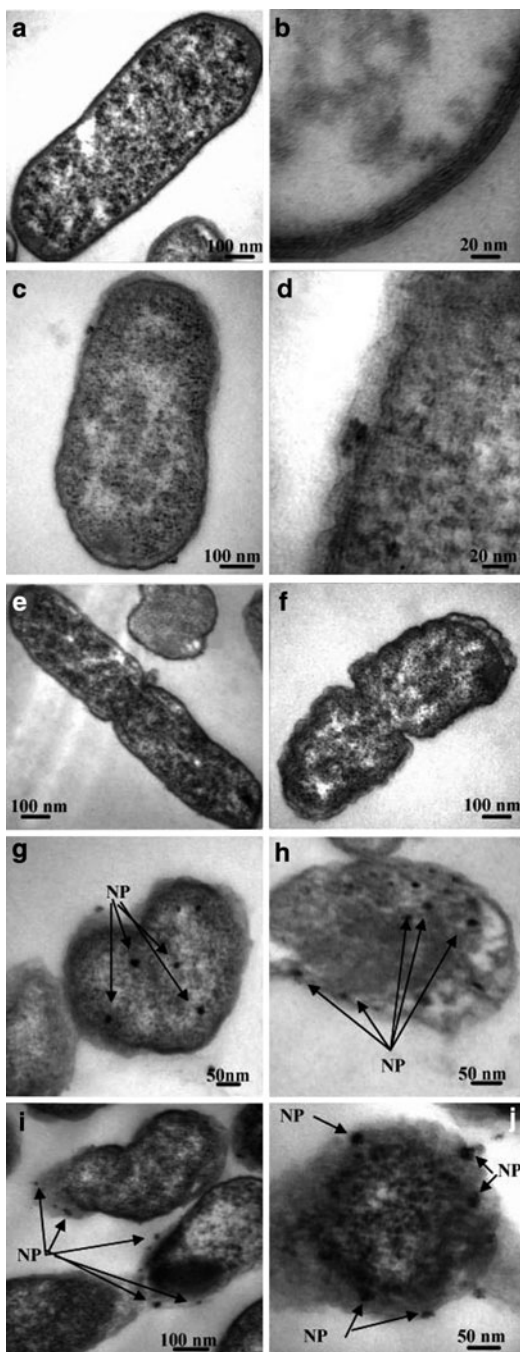
suspension was subjected to irradiation with visible light at the range of 400–500 nm or UV light, which subsequently increased either the antimicrobial activity or ecotoxicity toward various microorganisms or environmental species [55, 63]. As a basic principle, ZnO with defects can be activated by both UV and visible light, and electron hole pairs (e^-h^+) can be created. The holes split H_2O molecules into OH^- and H^+ . Consequently, oxygen molecules are transformed to superoxide radical anions (O_2^-), which in turn react with H^+ to generate ($HO_2\cdot$) radicals that subsequently collide with free electrons to produce hydrogen peroxide anions (HO_2^-). Transient hydrogen peroxide anions react with hydrogen ions to produce molecules of hydrogen peroxide (H_2O_2). The hydroxyl radicals and superoxides are negatively charged particles, which are unable to penetrate into the cell membrane and remain in direct contact with the outer surface of the microorganisms, whereas hydrogen peroxide can easily penetrate into the cell [46]. The generation of active oxygen species and the disruption of cell membranes caused by ZnO nanoparticles may actually be bacteriocidal. The generation of hydrogen peroxide depends on the surface area of ZnO as the smaller size of the nanoparticles means higher the surface area yielding increases in the production of ROS and higher antimicrobial activity [9, 46].

A comparative study of the effect of particle size on ROS production in TiO_2 suggested that a sharp increase in ROS generation per unit surface area of dry samples occurs only for particles with a size range of 10–30 nm, and a relatively constant ROS generation per unit surface area were observed for particles below 10 nm and above 30 nm [64]. In addition to particle size, aggregation of nanoparticles in solution or medium may strongly impact their interaction with biological systems, activity, and toxicity [64]. For example, nanoparticles and bulk ZnO formed similar-sized aggregates in solution, yet the primary size appears to be more important than aggregate size in determining the toxicity of ZnO particles, probably due to the increased surface area and ROS generation [45]. Contradicting this is the finding that aggregate size determines both the uptake and response of immortalized brain microglia to nano- TiO_2 and the bioavailability of nanoparticles to plant roots, algae, and fungi [65]. It is interesting that ZnO nanoparticles decreased the ability of growth of bacteria such as *E. coli* [66] and *S. aureus* [9] even in the dark compared to ambient light, which is probably due to the generation of super oxide anion (O_2^-) or alternative modes of ZnO nanoparticles activity. Photo-activation and antibacterial properties of ZnO nanoparticles are similar to TiO_2 and are receiving increasing application in numerous areas. However, information describing phototoxicity of ZnO nanoparticles has been very limited. Increases in the antibacterial activity of ZnO nanoparticles were demonstrated when *S. aureus* and ZnO nanoparticles were exposed to UV light [31]. Similarly, phototoxicity of nano-ZnO and bulk-ZnO was dramatically enhanced under natural sunlight illumination as compared to artificial laboratory light illumination, which is due to increased generation of ROS in *C. elegans* [67]. Generation of ROS by nanoparticles such as TiO_2 and ZnO interacting with environmental agents (e.g., UV) can be enhanced significantly to cause oxidative stress and can eventually elicit toxicity to bacteria [68]. Overall, the literature suggests that ZnO powder or

nanoparticles produce greater amounts of hydrogen peroxide which mediate its antibacterial effect, whereas hydrogen peroxide production was not detected using similar CaO and MgO powders [5].

Although the detailed mechanism for the antimicrobial activity of ZnO is still under debate, several studies have shown that the production of ROS is not the only contributing factor [19, 46]. One of the several alternative mechanisms suggested is that ZnO nanoparticles have abrasive surface defects as confirmed by the photoluminescence spectrum of ZnO [4, 46]. The abrasiveness of nanoparticles compared with the bulk is caused by uneven surface texture due to rough edges and corners, which contributes to mechanical damage of the cell membrane by electrostatic interaction [4]. It has been shown that increased antibacterial effect of ZnO nanoparticles against *E. coli* can be observed as the particle diameter is reduced from 2 μm to 45 nm to 12 nm, and that this is attributed to the enhanced effect of the greater surface area to volume ratio and mechanical damage to cells due to increase abrasiveness of the smaller nanoparticles [46]. Upon interaction with bacterial cells, ZnO nanoparticles can either be transported into the cytoplasm, be deposited on the surface, penetrate into the cell wall or membranes, and/or a combination of all of these scenarios can occur. In fact, it has been reported that all these scenarios can occur in both Gram-negative (e.g., *E. coli*) and Gram-positive (e.g., *S. aureus*) bacteria [19, 31, 68]. It has been reported that ZnO nanoparticles cause damage to the membrane of *E. coli*, which yielded as accumulation of ZnO and cellular internalization [19]. Figure 5.5 represents the cell membrane disorganization and cellular internalization of ZnO nanoparticles in *E. coli* as a probable mechanism of ZnO nanoparticles-mediated antibacterial activity [19]. These scenarios, along with ROS generation, lead to extensive disorganization of the cell membranes or wall and cell death. It has also been suggested that the orientation of ZnO can affect bioactivity, as randomly oriented ZnO nanowires demonstrated higher antimicrobial activity than regularly oriented ZnO nanowires [57]. Thus, the mechanism of antibacterial activity of ZnO nanoparticles is complex and not fully understood. Furthermore, the role of Zn^{2+} ions released from dissolution of ZnO is not very clear [11, 20, 31, 68]. Zinc ions are known to inhibit multiple activities in bacteria, such as glycolysis, transmembrane proton translocation and acid tolerance. Thus, the presence of zinc ions is likely to inhibit proliferation by binding to the membrane of bacteria, which can prolong the lag phase of growth, and contribute to the antimicrobial activity of ZnO [68]. It is estimated that the minimal inhibitory concentration (MIC) of zinc ions is 1,917 (*P. aeruginosa*), 9 (*S. aureus*), and 39 (*Candida albicans*) $\mu\text{g/mL}$, varying for different organisms [68], yet the antibacterial effects of ZnO are similar to these organisms, although zinc ions are reported to be bacteriostatic rather than bacteriocidal [69]. However, the release of Zn^{2+} ions from ZnO nanoparticles suspension compared to the precursor is not significantly high enough, about 354-fold less [31] or five to ten times less [47, 63], to impart its cytotoxicity. Zinc is a ubiquitous essential metal ion and plays a role in catalysis, protein structure and perhaps as signaling molecules in living systems [70]; therefore, low concentration of zinc ions will be metabolized and may not have any antimicrobial or ecotoxicity effect. In addition, the pH of the ZnO

Fig. 5.5 Transmission electron microscopic micrographs of *E. coli* thin section under various conditions: (a, b) *E. coli* grown in Luria Broth (LB) medium without any ZnO nanoparticles treatment. (c, d) *E. coli* grown with diethylene glycol (DEG) in LB medium (used for ZnO nanoparticles synthesis). (e, f) *E. coli* cellular division when cells are grown in LB and DEG media, respectively. (g–j) *E. coli* grown in the presence of 1 mM concentration of ZnO nanoparticles (~14 nm average diameter). The results showed that the *E. coli* grown with DEG in LB medium indicates changes in the morphology of the cells (c, d). Damage and disorganization in the cell wall as well as cell morphology were prominent in case of *E. coli* grown the presence of DEG (f) compared with in the absence in (c). Micrographs in (g, h) of *E. coli* grown in the presence of ZnO nanoparticles demonstrated that more cellular internalization of ZnO nanoparticles and cell wall disorganization. The results also showed more extensive damage of the cell membrane and the leakage of intracellular contents. NP ZnO nanoparticles (TEM images reprinted from [19]. With permission of the American Chemical Society)



nanoparticle suspension in water, saline or medium does not change in a neutral region (pH 7), and thus its suitability for bacterial survival and antibacterial activity [59]. It should be noted that the solubility of ZnO increases sharply when pH is below 6 or above 11 and it becomes completely dissolved around pH 6 and 12 [38], thus using ZnO for the antibacterial agent or the biological applications will be more suitable.

Several factors, in particular host-specific factors, play crucial roles in the antibacterial effect as well as differential activity of ZnO nanoparticles. Similarly, differential antibacterial effect among the Gram-negative (*E. coli*) and Gram-positive (*S. aureus*) microorganisms against ZnO nanoparticles has been observed [9, 54], probably due to, firstly, the nature and difference of the cell wall or outer layer structures of Gram-negative and Gram-positive bacteria. Specifically, in Gram-positive bacteria (*S. aureus*) the cell wall is thick and lacks any periplasmic region, consisting of a large amount of peptidoglycans as well as other components such as lipoteichoic acids (LTA). On the other hand, Gram-negative bacteria (*E. coli*) have relatively thin cell walls, but with inner and outer membranes in-between the periplasmic region. Secondly, there is differential resistance to oxidant and UV due to production of carotenoid pigments as *S. aureus* produces more pigments than *E. coli*. And, thirdly, *S. aureus* has developed efficient pathways to defend against oxidative stresses by increasing the expression of oxidative stress-responsive gene products such as superoxide dismutase (the *sodA* and *sodM* gene products converts O_2^- to H_2O_2), catalase (the *katA* gene product converts H_2O_2 to H_2O and O_2), thioredoxin reductase (*trxB*; maintains thioredoxin in reduced form to protect cells against toxic oxygen species), thioredoxin (encoded by *trxA*), alkyl hydroperoxide reductase sub C and F (*ahpCF*, having activity against organic peroxides, peroxyxynitrate, and H_2O_2) and endopeptidase (*clpC*) in combating oxidative stress [71, 72]. In contrast, *E. coli* has less efficient pathways to eliminate oxidative stresses. Quantitative PCR analysis (RT-qPCR) for various genes suggests a significant increase in the expression levels of two oxidative genes, *katA* (52-fold) and *ahpC* (7-fold), and a general stress response gene, *dnaK* (17-fold), under ZnO nanoparticle treatment conditions, which demonstrate that the antibacterial activity of ZnO nanoparticles is most likely due to disruption of the cell membrane and oxidative stress in *Camplobacter jejuni* [54]. A similar transcriptional analysis for various oxidative stress-responsive genes of *S. aureus* strains treated with bulk, 8- or 12-nm-diameter ZnO nanoparticles suggest that there was no significant variation in the expression levels of the *katA*, *sodA*, *sodM*, *trxA*, *trxB*, and *perR* (hydrogen peroxide regulator) genes, except for the *ahpCF* genes [31]. The results suggest that the production of ROS by ZnO nanoparticles or powder may not be high enough to induce the expression of most of the ROS-specific genes in *S. aureus*, although the antibacterial activity of these ZnO agents has been investigated.

In addition, other factors, such as differences in the mode of association of the particles to the cell surface, capacity of solubilizing and metabolizing ZnO, cell permeability, and the various pump and transporter systems for transporting and exporting ZnO nanoparticles, may also play important roles for the effectiveness of

ZnO against a particular bacterium. It is also important that, within the same species such as *Staphylococcus*, different clinical strains may have different effectiveness towards the same ZnO nanoparticles, as has been demonstrated in the antibiotic resistance or sensitivity profiles of different isolates [42, 43]. Therefore, the evidence suggests that different forms of ZnO yield different degrees of antimicrobial activity towards the same or different bacteria, and presumably microorganisms are unlikely to develop resistance against zinc or ZnO nanoparticles, as they do against conventional and narrow-target antibiotics, because the metal oxide or metal attack a broad range of targets within the bacteria. This means that bacteria would have to develop a large number of mutations simultaneously to protect themselves; therefore, ZnO nanoparticles may demonstrate improved effectiveness with an ability to target more microorganisms than conventional organic antibiotics.

5.6 Enhancement of ZnO Antibacterial Activity by Surface Modification

Surface coating or modification of nanomaterials has been recognized as one of the most advanced and intriguing approaches to increasing their affinity or activity and improving their applicability. Since surface area and surface defects play an important role in the photocatalytic activities of metal oxides, therefore the doping of metal oxides and/or transient metals increases the surface defects leading to higher biological activity and also affects the optical and electronic properties, probably shifting the optical absorption towards the visible region. Doping is a widely used method for modification of nanoparticles, in particular for ZnO, to enhance their electrical, optical and biological properties. Although different approaches have been adopted to synthesize ZnO nanoparticles, doping and fabrication of ZnO nanoparticles is done using the wet chemical synthesis method which offers many advantages such as ease to synthesis, reduced reaction temperature, increased yield, and formation of well-defined nanostructures or nanoparticles. Work performed in the area of transient metal doping of ZnO single crystals and thin films indicates that ZnO nanorods doped with manganese (Mn), chromium (Cr), and cobalt (Co) can be formed using hydrothermal synthesis, and the morphology of the doped ZnO nanorods was different from that of the undoped ZnO [73]. Doping of Mn into the ZnO offers an interesting method to alter various properties such as the band gap of ZnO (3.37–3.70 eV), which can alter the emission properties by providing an efficient channel for the recombination of electron and hole. ZnO doped with Mn has also been synthesized using the co-precipitation method. It has been demonstrated that Mn-doped ZnO nanoparticles have increased antibacterial activity against both Gram-negative and Gram-positive bacteria than undoped ZnO nanoparticles [40]. Enhanced antibacterial activity against *E. coli* was reported with hydrothermally synthesized ZnO doped with transient metals such as Fe and Co [74]. It has also been reported

that tyrosine-assisted addition of silver (Ag) metal to ZnO nanoparticles enhanced photo-degradation of organic dye pollutants and destruction of bacteria [75]. Similarly, ZnO-Al₂O₃ or MgO-ZnO composites have been prepared using zinc–aluminum layered double hydroxides [76] or mixing MgO/ZnO solid solution powders and heating at 1,400°C for 3 h in air [77]. In this instance, higher antibacterial properties were observed with decreasing amount of doped ZnO nanoparticles. A different type of doping of ZnO nanoparticles with non-metal nitrogen has been reported using the mechano-chemical method, which exhibits high photocatalytic activity under visible light irradiation [78].

Antimicrobial activity can be enhanced by antibiotic–nanoparticle interaction or by the combination of antibiotics and ZnO nanoparticles against different antibiotic-resistant bacteria. Although there are no reports on antibiotics coupled with ZnO nanoparticles, several studies have been described on antibiotics–nanoparticles interaction and their antibacterial activity. It has been demonstrated that when amoxicillin and silver nanoparticles are combined, its efficiency was enhanced against *E. coli* compared to amoxicillin and silver nanoparticles alone. Similarly, when vancomycin was covalently attached to TiO₂ nanoparticles, its antibacterial activity against *S. aureus* increased and was sustained for a longer period of time [79]. Combination of ZnO nanoparticles ranging from 20 to 45 nm with ciprofloxacin-enhanced antibacterial activity against *E. coli* and *S. aureus* [49]. A probable cause of the synergistic effect may be due the action of nanoparticles on the surface of the bacteria complementing the action of the antibiotic. The advantage of using double agents to kill or inhibit bacterial growth will be more beneficial as the mode of inhibition or killing for each individual agent are different. For example, resistant strains can be targeted using antibiotics–nanoparticles, as a particular antibiotic may be ineffective to kill bacteria, but nanoparticles will restrict growth or eliminate the bacteria. Several potential applications with respect to the biological activity of ZnO nanoparticles has been demonstrated using thin layer coating on different surfaces such as cotton, fabric, glass or paper, which showed significant bacterial growth inhibition or protection from UV light [79–81]. ZnO or other nanoparticles have been successfully used for water disinfection and purification [73]. Functionalized ZnO with sepiolite (ZnO-Sepiolite) has been used in weaning piglet diets to fulfill the Zn requirement as well as the health requirement to protect from bacterial infection [82]. Therefore, observations in the published literature indicate that ZnO nanoparticles or functionalized ZnO nanoparticles have extensive biological applications and benefits and can be further developed to suit desired applications.

5.7 Potential Toxicity of ZnO Nanoparticles

During the last few years, research on toxicologically relevant properties of nanoparticles, in particular engineered nanoparticles, has increased substantially. Most of the experimental toxicological work on nanoparticles has been based on

a small set of nanoparticles such as carbon black, TiO₂, iron oxides and amorphous silica, while little is known related to ZnO nanoparticles [83, 84]. Because a wide range of applications can lead to large-scale production and finally release to the environment, it is still uncertain whether engineered nanoparticles are inherently toxic or safe to health and environment. It should be stressed that natural nanoparticles including metal oxides existing in all ecosystems play an important role in biogeochemical processes and thus living systems have adapted to their presence in the environment. The greatest current risk is to the occupational health of workers involved in research and manufacture of nanoparticles and nanofabrics. In addition, various nanostructures of ZnO, including particles, rods, wires, belts, tubes, and rings, have attracted a great deal of attention because of their useful electronic and opto-electronic properties and novel applications. Therefore, significant increases in production and demand in the products could lead to unintended exposure via possible various routes such as inhalation, dermal absorption, and oral absorption of various nanoparticles including ZnO by the living systems. Due to their unique properties, including small size and corresponding large surface area, it is believed different degrees of biological effects are imposed related to their bulk [62, 83, 84].

Several studies have been directed toward the potential toxicity of ZnO nanoparticles or powders in various animal systems such as in rats [85, 86], mice [87–89], guinea pigs [90], human skin [91], and zebra fish [92], as well as *C. elegans* [55] and *Daphnia* [93]. In addition, the cytotoxicity of both bulk and nanoparticles of ZnO has also been performed in several cell culture-based studies including mouse embryo fibroblast cells [94], human bronchoalveolar carcinoma-derived cells [76], mouse neural stem cells [95], phagocytic cells and bronchial epithelial cells [61], and NIH 3T3 fibroblast, epithelial, and endothelial cells [96]. Nanoparticles can deposit in the respiratory tract after inhalation of 0.5, 2.5 and 12.5 mg/m³, which can induce inflammatory reactions or oxidative-stress responses in the respiratory tracts and lungs [86]. Oral exposure of experimental mice with two different sizes (20 and 120 nm) of ZnO nanoparticles and with the doses of – 5 g/kg body weight demonstrated that the liver, spleen, heart, pancreas, and bone are the target organs for oral exposure [89]. Exposure to human skin with 20–30 nm ZnO nanoparticles suggested that ZnO nanoparticles stayed in the stratum corneum and accumulated into skin folds and/or hair follicle roots, which indicate that the form of ZnO nanoparticles studied is unlikely to result in safety concerns [91]. There is no doubt that ZnO nanoparticles impart cytotoxicity against different culture cells, mostly due to the induction of oxidative and inflammatory responses, and that the mechanism is often misleading owing to the small number of reported studies. Cell viability assays with 10-, 30-, 60-, and 200-nm particles indicated that ZnO nanoparticles manifested dose-dependent, rather than size-dependent, toxic effects on mouse neural stem cells, where Zn ions from ZnO nanoparticles in the culture or inside cells caused cell damage at 12 ppm or higher for 24-h treatment [95]. Similar studies in human bronchoalveolar carcinoma-derived cells with 70- and 120-nm ZnO particles suggest that size- and dose-dependent cytotoxicity as reflected in oxidative stress, lipid peroxidation, cell membrane damage, and

oxidative DNA damage, which is mediated by neither Zn ions nor metal impurity in the ZnO particle samples, and rather the cytotoxicity is caused by localization of ZnO in vesicles [76]. A comparative study on the effect of three nanoparticles, ZnO, TiO₂, and CeO₂, in macrophage and epithelial cells suggested that non-activated TiO₂ did not cause any toxicological injury to these cells, whereas CeO₂ exerted a cytoprotective effect due to its antioxidant properties. Interestingly, ZnO nanoparticles exhibited major toxicity toward these cells due to particle dissolution and the release of Zn²⁺ that engaged in oxidant-mediated injury of cells [63]. The cytotoxicity of ZnO nanoparticles depends on the availability or the concentration as zinc is an essential element. Thus, low concentrations are not cytotoxic, rather living systems utilize it for growth. Several studies have demonstrated efficient growth inhibition or killing activity of both bulk and nanostructures ZnO or TiO₂ for algae (*Nitzschiapallea*, and *Crustaceans daphnia magna*) and nematodes (*C. elegans*) in environmental systems [50, 52, 55]. The genotoxicity of ZnO nanoparticles to human sperm and lymphocytes can be enhanced by UV irradiation [97]. The control of pathogenic bacteria by antimicrobial nanoparticles is a promising approach to limit the spread of multiple drug-resistant pathogens such as *S. aureus*; however, it is expected that the same agent will affect the population of the microbes that play beneficial roles in the environment. Toxicity studies on manufactured metal oxide nanoparticles such as TiO₂ and ZnO are expanding rapidly, but the effectiveness is not sufficient to draw a conclusion due to the lack of environmentally relevant conditions used in the experiments [50]. It should also be noted that, for the environmental conditions, it is known that the type and amount of natural organic matter in the ecosystem or environment affects nanoparticle stability and bioavailability, because the interaction of nanoparticles with environmental organic and inorganic colloids may strongly influence their behavior and potential cytotoxicity. Thus, there is currently little evidence from skin penetration studies that dermal applications of metal oxide nanoparticles, in particular TiO₂ and ZnO₂ used in sunscreens, lead to systemic exposure, nor for inhalation of nanoparticles over longer periods or uptake of nanoparticles in the gastrointestinal tract after oral intake of various designs of food and pharmacological components. Therefore, it is safe to conclude that ZnO powders or nanoparticles are biosafe and environmentally safe up to a certain amount, but may become hazardous at higher concentrations as it has been reported that ZnO nanoparticles have reduced the viability of human T cells at an elevated concentration (≥ 5 mM) [47]. Zinc oxide is listed as “generally recognized as safe” by the U.S. Food and Drug Administration (21CFR1828991). As a food additive, it is the most commonly used zinc source in the fortification of cereal-based foods. Due to its antimicrobial properties, ultrafine ZnO has been incorporated into the lining of food cans in packages for meat, fish, corn, and peas to preserve colors and to prevent spoilage. Although, presently, there are no set threshold limit values for various forms of ZnO to the community members due to lack sufficient experimental studies and data, the recommended threshold limit values of ZnO for welders and others in the workplace have been set at 5 mg/m³ [98].

5.8 Conclusion and Future Perspective

Metal oxide, in particular ZnO, is an environmentally friendly wide band gap semiconductor (3.37 eV) with a large excitation binding energy, and high mechanical and thermal stability. This makes it suitable for applications in opto-electronic and piezo-electrical fields. Moreover, ZnO can be manipulated easily to change its size and morphology, so that the physical and chemical properties can be modulated to suit its applications. Extensive research in terms of synthesis and modification such as coatings, and doping has been performed for several decades to improve and enhance its novel properties, which opens up opportunities for new technological applications mostly in solar cells, sensors, detectors, and energy generators. ZnO nanoparticles are being increasingly used as a photocatalyst for degrading harmful contaminants like pesticides from ground water. A wide variety of synthetic approaches have been employed to prepare various forms of ZnO colloids and films, which are generally classified as gas and liquid phase synthesis. Some of them are sol-gel synthesis, hydrothermal synthesis, spray pyrolysis, metal-organic chemical vapor deposition, sonochemical processing, and pulsed laser deposition. The choice of synthesis methods is purely dependent upon the application, cost effectiveness, purity, and downstream fabrication. Simple methods, such as wet chemical synthesis, and in particular hydrothermal methods, have gained more popularity for their simplicity and their further applications such as thin layer coatings and surface modification due to synthesis temperature and other synthesis conditions.

The antimicrobial activity of ZnO has been known for a long time and it has been used as an active ingredient in antibacterial creams, lotions, and ointments. The last decade has seen a logarithmic growth in the field of antimicrobial properties of ZnO nanoparticles and potential applications in various forms that leads to substantial progress in the development, process, functionalization and applications of nanoparticles. Studies of antimicrobial activity of ZnO nanoparticles suggested several important points such as antimicrobial activity can be achieved under normal ambient light condition and can be enhanced with UV irradiation; activity is size-dependent, the smaller-sized ZnO nanoparticles exhibit higher activity; and there is activity against wide variety of both Gram-positive and Gram-negative bacteria as well as fungi, algae, and nematodes. The mechanism of antimicrobial activity of ZnO is not well defined; numerous studies demonstrate that the production of reactive oxygen species (ROS), in particular H_2O_2 , from ZnO is proportional to ZnO concentration and surface area that may contribute to cell death or inhibition of bacterial growth. However, ROS-mediated killing is not the main mechanism of antibacterial activity of ZnO, several other probable interactions between bacteria-ZnO nanoparticles also play important roles. Interactions between bacteria-ZnO nanoparticles or the antibacterial activity of ZnO nanoparticles can be enhanced by engineering ZnO with a transient metal such as Mn, Ag, and Mg. Since ZnO dissolves easily and both ZnO and Zn^{2+} have antibacterial activity, aquatic organisms can be highly sensitive to zinc; therefore, its application in drinking

water treatment is limited. One possible application could be in combination with existing disinfection technologies such as UV disinfection systems, although ZnO nanoparticles in water treatment is not very reasonable because loss of zinc to water may have potential impacts on human health and ecosystems.

Application of ZnO nanoparticles in controlling the spread and colonization of potential pathogens is very a promising finding that has motivated many investigations into the application and fundamental knowledge of nanoparticles and improvement in the techniques for synthesis and fabrication of new nanomaterials with controlled properties and dimensions. The use of ZnO nanoparticles or other nanomaterial coatings is still limited because the application requires control of the synthesis of nanoparticles. Several methods have been developed to fabricate nanoparticles that can be routinely prepared using conventional fabrication processes, but their application is limited to the small scale. It would be interesting to determine if any derivate of ZnO nanoparticles with chemical groups or bioagents are more effective at eliminating various microorganisms. Several reports have suggested that modification of nanoparticle surfaces can efficiently target and kill both Gram-positive and Gram-negative bacteria. Therefore, in the future, ZnO nanoparticle-containing formulations may be utilized as antibacterial agents in ointments, lotions, mouthwashes, and surface coatings on various substrates to prevent microorganisms from attaching, colonizing, spreading, and forming biofilms on surfaces in the community, health care and environmental settings. In summary, more research is needed to achieve better technologies to formulate and retain nanomaterials in order to reduce costs associated with premature material loss and to prevent potential human health and environmental impacts.

Acknowledgements The author thank Dr. Vector Huber for the critical reading the manuscript. The author would like to thank Dr. R.T. Koodali and Krishna R. Raghupathi for their help in preparation of this article.

References

1. Rosi NL, Mirkin CA (2005) Nanostructures in biodiagnostics. *Chem Rev* 105:1547–1562.
2. Rotello V (2003) *Nanoparticles: Building Blocks for Nanotechnology*, Kluwer Academia, Boston.
3. Wang ZL (2004) Zinc oxide nanostructures: growth, properties and applications. *J Phys: Condens Matter* 16:R829.
4. Stoimenov PK, Klinger RL, Marchin GL, Klabunde KJ (2002) Metal Oxide nanoparticles as bactericidal agents. *Langmuir* 18:6679–6686.
5. Sawai J, Shoji S, Igarashi H, Hashimoto A, Kokugan T, Shimizu M, Kojima H (1998) Hydrogen peroxide as an antibacterial factor in zinc oxide powder slurry. *J Ferment Bioeng* 86:521–522.
6. Matsunaga T, Tomoda R, Nakajima T, Wake H (1985) Photoelectrochemical sterilization of microbial cells by semiconductor powders. *FEMS Microbiol Lett* 29:211–214.

7. Wei C, Lin WY, Zainal Z, William NE, Zhu K, Kruzic AP, Smith RL, Rajeshwar K (1994) Bactericidal activity of TiO₂ photocatalyst in aqueous media: toward a solar-assisted water disinfection system. *Environ Sci Tech* 28:934–938.
8. Fang M, Chen J-H, Xu X-L, Yang P-H, Hildebrand HF (2006) Antibacterial activities of inorganic agents on six bacteria associated with oral infections by two susceptibility tests. *Int J Antimicrobiol Agents* 27:513–517.
9. Jones N, Ray B, Koodali RT, Manna AC (2008) Antibacterial activity of ZnO nanoparticles suspensions on a broad spectrum of microorganisms. *FEMS Microbiol Lett* 279:71–76.
10. Fu G, Vary PS, Lin CT (2005) Anatase TiO₂ nanocomposites for antimicrobial coating. *J Phys Chem B* 109:8889–8898.
11. Sawai J (2003) Quantitative evaluation of antibacterial activities of metallic oxide powders (ZnO, MgO and CaO) by conductimetric assay. *J Microbiol Method* 54:177–182.
12. Sawai J, Yoshikawa T (2004) Quantitative evaluation of antifungal activity of metallic oxide powders (MgO, CaO and ZnO) by an indirect conductimetric assay. *J Appl Microbiol* 96:803–809.
13. Liu H-L, Yang TC-K (2003) Photocatalytic inactivation of *Escherichia coli* and *Lactobacillus helveticus* by ZnO and TiO₂ activated with ultraviolet light. *Proc Biochem* 39:475–481.
14. Sondi I, Salopak-Sondi B (2004) Silver nanoparticles as antimicrobial agent: a case study on *E. coli* as a model for Gram-negative bacteria. *J Colloid Interface Sci* 275:177–182.
15. Cioffi N, Torsi L, Ditaranto N, Tantillo G, Ghibelli L, Sabbatini L, Blevè-Zacheo T, D'Alessio M, Zambonin, PG, Traversa E (2005) Copper nanoparticle/polymer composites with antifungal and bacteriostatic properties. *Chem Mater* 17:5255–5262.
16. Thill A, Zeyons O, Spalla O, Chauvat F, Rose J, Auffan M, Flank AM (2006) Cytotoxicity of CeO₂ nanoparticles for *Escherichia coli*, physicochemical insight of the cytotoxicity mechanism. *Environ Sci Technol* 40:6151–6156.
17. Sunada K, Kikuchi Y, Hashimoto K, Fujishima K (1998) Bactericidal and detoxification effects of TiO₂ thin film photocatalysts. *Environ Sci Technol* 32:726–728.
18. Bellantone M, Williams HD, Hench LL (2002) Broad-spectrum bactericidal activity of Ag₂O-doped bioactive glass. *Antimicrob Agents Chemother* 46:1940–1945.
19. Brayner R, Ferrari-Iliou R, Brivois N, Djediat S, Benedetti MF, Fievet F (2006) Toxicological impact studies based on *Escherichia coli* bacteria in ultrafine ZnO nanoparticles colloidal medium. *Nano Lett* 6:866–870.
20. Roselli M, Finamore A, Garaguso I, Britti MS, Mengheri E (2003) Zinc oxide protects cultured enterocytes from the damage induced by *Escherichia coli*. *J Nutr* 133:4077–4082.
21. Yamamoto O (2001) Influence of particle size on the antibacterial activity of zinc oxide. *Int J Inorgan Mater* 3:643–646.
22. Li Y, Leung P, Yao L, Song QW, Newton E (2006) Antimicrobial effect of surgical masks coated with nanoparticles. *J Hosp Infect* 62:58–63.
23. Campo EJA, Peiteado M, Caballero AC, Villegas M, Modriguez-Paez JE (2009) Room temperature synthesis of high purity 2D ZnO nanoneedles. *J Ceramic Proc Res* 10:477–481.
24. Baruah S, Dutta J (2009) Hydrothermal growth of ZnO nanostructures. *Sci Technol Adv Mater* 10:013001 (18pp).
25. Liu B, Zeng HC (2004) Room temperature solution synthesis of monodispersed single-crystalline ZnO nanorods and derived hierarchical nanostructures. *Langmuir* 20:4196–4204.
26. Xu F, Zhang P, Navrotsky A, Yuan ZT, Ren TZ, Halasa M, Su B-L (2007) Hierarchically assembled porous ZnO nanoparticles: synthesis, surface energy, and photocatalytic activity. *Chem Mater* 19:5680–5686.
27. Kim H, Sigmund W (2004) ZnO nanocrystals synthesized by physical deposition. *J Nanosci Nanotechnol* 4:275–278.
28. Chen ZG, Li F, Liu G, Tang Y, Cong H, Lu GQ, Cheng HM (2006) Preparation of high purity ZnO nanobelts by thermal evaporation of ZnS. *J Nanosci Nanotechnol* 6:704–707.
29. Meulenkamp EA (1998) Synthesis and growth of ZnO nanoparticles. *J Phys Chem B* 102:5566–5572.

30. Tam KH, Djurisic AB, Chan CMN, Xi YY, Tse CW, Leung YH, Chan WK, Leung FCC, Au DWT (2008) Antibacterial activity of ZnO nanorods prepared by a hydrothermal method. *Thin Solid Films* 516:6167–6174.
31. Raghupati RK, Koodali RT, Manna AC (2011) Size-dependent bacterial growth inhibition and mechanism of antibacterial activity of zinc oxide nanoparticles. *Langmuir* 27:4020–4028.
32. Vishwanathan R, Gupta RB (2003) Formation of zinc oxide nanoparticles in supercritical water. *J Supercritical Fluids* 27:187–193.
33. Tang L, Bao X-B, Zhou H, Yuan A-H (2008) Synthesis and characterization of ZnO nanorods by a simple single-source hydrothermal method. *Physica E* 40:924–928.
34. Zhang Z, Mu J (2007) Hydrothermal synthesis of ZnO nanobundles controlled by PEO–PPO–PEO block copolymers. *J Colloid Interface Sci* 307:79–82.
35. Jalal R, Goharshadi EK, Abareshi M, Moosavi M, Yousefi A, Nancarrow P (2010) ZnO nanofluids: green synthesis, characterization, and antibacterial activity. *Matters Chem Phys* 121:198–201.
36. Ma M-G, Zhu YJ, Cheng GF, Huang YH (2007) Microwave synthesis and characterization of ZnO with various morphologies. *Mater Lett* 62:507–510.
37. Vijayan TA, Chandramohan R, Valanarasu S, Thirumalai J, Venkateswaran S, Mahalingam T, Srkumar SR (2008) Optimization of growth conditions of ZnO nano thin films by chemical double dip technique. *Sci Technol Adv Mater* 9:035007.
38. Dange C, Phan T, Andre V, Rieger J, Persello J, Foissy A (2007) Adsorption mechanism and dispersion efficiency of three anionic additives [poly(acrylic acid), poly(styrene sulfonate) and HEDP] on zinc oxide. *J Colloid Interface Sci* 315:107–115.
39. Zhang L, Jiang Y, Ding Y, Povey M, York D (2007) Investigation into the antibacterial behaviour of suspension of ZnO nanoparticles (ZnO nanofluids). *J Nanoparticles Res* 9:479–489.
40. Desselberger U (2000) Emerging and re-emerging infectious diseases. *J Infect* 40:3–15.
41. Costello EK, Lauber CL, Hamady M, Fierer N, Gordon JI, Knight R (2009) Bacterial community variation in human body habitats across space and time. *Science* 326:1694–1697.
42. Donlan RM, Costerton JW (2002) Biofilms: Survival mechanisms of clinically relevant microorganisms. *Clin Microbiol Rev* 15:167–193.
43. Gilbert P, Collier PJ, Brown MR (1990) Influence of growth rate on susceptibility to antimicrobial agents: biofilms, cell cycle, dormancy, and stringent response. *Antimicrob Agents Chemother* 34:1865–1868.
44. Hajokova P, Spatenka P, Horsky J, Horska I, Kolouch A (2007) Photocatalytic effect of TiO₂ films on various virus and bacteria. *Plasma Process Polym* 4:S397–S401.
45. Adama LK, Lyon DY, Alvarez PJJ (2006) Comparative eco-toxicity of nanoscale TiO₂, SiO₂, and ZnO water suspensions. *Water Res* 40:3527–3532.
46. Padmavathy N, Vijayaraghavan R (2008) Enhanced bioactivity of ZnO nanoparticles – an antibacterial study. *Sci Technol. Adv Mater* 9:035004 (7pp).
47. Reddy KM, Feris K, Bell J, Hanley C, Punnoose A (2007) Selective toxicity of zinc oxide nanoparticles to prokaryotic and eukaryotic systems. *Appl Phys Lett* 90:213902 (3 pp).
48. Rekha K, Nirmala M, Nair MG, Anukaliani A (2010) Structure, optical, photocatalytic and antibacterial activity of zinc oxide and manganese doped zinc oxide nanoparticles. *Physica B* 405:3180–3185.
49. Banooe M, Seif S, Nazari ZE, Jafari-Fesharaki P, Shahverdi HR, Moballegh A, Moghaddam KM, Shahverdi AR (2005) ZnO nanoparticles enhanced antibacterial activity of ciprofloxacin against *Staphylococcus aureus* and *Escherichia coli*. *J Biomed Mater Res B: Appl Biomater* 93B:557–561.
50. Franklin NM, Rogers NJ, Apte SC, Batley GE, Gadd GE, Casey PS (2007) Comparative toxicity of nanoparticulate ZnO, bulk ZnO, and ZnCl₂ to a freshwater microalga (*Pseudokirchneriella subcapitata*): the importance of particle solubility. *Environ Sci Technol* 41:8484–8490.

51. Liu Y, He L, Mustapha A, Li H, Hu ZQ, Lin M (2009) Antibacterial activities of zinc oxide nanoparticles against *Escherichia coli* O157:H7. *J Appl Microbiol* 107:1193–1201.
52. Heinlaan M, Ivask A, Blinova I, Dubourguir HC, Kahru A (2008) Toxicity of nanosized and bulk ZnO, CuO and TiO₂ to bacteria *Vibrio fischeri* and crustaceans *Daphnia magna* and *Thamnocephalus platyurus*. *Chemosphere* 71:1308–1316.
53. Huang Z, Zheng X, Yan D, Yin G, Liao X, Kang Y, Yao Y, Huang D, Hao B (2008) Toxicological effect of ZnO nanoparticles based on bacteria. *Langmuir* 24:4140–4144.
54. Xie Y, He Y, Irwin PL, Jin T, Shi X (2011) Antibacterial activity and mechanism of zinc oxide nanoparticles on *Campylobacter jejuni*. *Appl Environ Microbiol* 77:2325–2331.
55. Ma H, Bertsch PM, Glenn TC, Kabengi NJ, Williams PL (2009) Toxicity of manufactured zinc oxide nanoparticles in the nematode *Caenorhabditis elegans*. *Environ Toxicol Chem* 28:1324–1330.
56. Wang H, Wick RL, Xing B (2009) Toxicity of nanoparticulate and bulk ZnO, Al₂O₃ and TiO₂ to the nematode *Caenorhabditis elegans*. *Environ Pollut* 157:1171–1177.
57. Wang X, Yang F, Yang W, Yang X (2007) A study on the antibacterial activity of one-dimensional ZnO nanowire arrays: Effects of the orientation and plane surface. *Chem Commun* 4419–4421.
58. Zhou D, Keller AA (2010) Role of morphology in the aggregation kinetics of ZnO nanoparticles. *Water Res* 44:2948–2956.
59. Ohira T, Yamamoto O, Iida Y, Nakagawa Z (2008) Antibacterial activity of ZnO powder with crystallographic orientation. *J Mater Sci Mater Med* 19:1407–1412.
60. Yamamoto O, Komatsu M, Sawai J, Nakagawa Z (2004) Effect of lattice constant of zinc oxide on antibacterial characteristics. *J Mater Sci Med* 15:847–851.
61. Xia T, Kovochich M, Liang M, Adler LM, Gilbert B, Shi H, Yeh JI, Zink JI, Nel AE (2008) Comparison of the mechanism of toxicity of zinc oxide and cerium oxide nanoparticles based on dissolution and oxidative stress properties. *ACS Nano* 2:2121–2134.
62. Nel A, Xia T, Madler L, Li N (2006) Toxic potential of materials at the nanolayers. *Science* 311:622–627.
63. Lipovsky A, Tzitrinovich Z, Friedmann H, Applerot G, Gedanken A, Lubart R (2009) EPR study of visible light-induced ROS generation by nanoparticles of ZnO. *J Phys Chem C* 113:15997–16001.
64. Jiang J, Oberdrster G, Elder A, Gelein R, Mercer P, Biswas P (2008) Does nanoparticle activity depend upon size and crystal phase? *Nanotoxicology* 2:33–42.
65. Navarro E, Baun A, Behra R, Hartmann NB, Filser J, Miao AJ, Quigg A, Santschi PH, Sigg L (2008) Environmental behavior and ecotoxicity of engineered nanoparticles to algae, plants, and fungi. *Ecotoxicology* 17:372–386.
66. Hirota K, Sugimoto M, Kato M, Tsukagoshi K, Tanigawa T, Sugimoto H (2010) Preparation of zinc oxide ceramics with a sustainable antibacterial activity under dark conditions. *Ceramics Int* 36:497–506.
67. Ma H, Kabengi NJ, Bertsch PM, Unrine JM, Glenn TC, Williams PL (2011) Comparative phototoxicity of nanoparticle and bulk ZnO to a free-living nematode *Caenorhabditis elegans*: the importance of illumination mode and primary particles size. *Environ Pollut* 159:1473–1480.
68. Applerot G, Perkas N, Amirian G, Girshevit O, Gedanken A (2009) Coating of glass with ZnO via ultrasonic irradiation and a study of its antibacterial properties. *Appl Surf Sci* 256:53–58.
69. McCarthy TJ, Zeelie JJ, Krause DJ (1992) The antibacterial action of zinc ion/antioxidant combination. *J Clin Pharm Ther* 17:51–54.
70. Blencowe DK, Morby AP (2003) Zn (II) metabolism in prokaryotes. *FEMS Microbiol Rev* 27:291–311.
71. Foster TJ (2005) Immune invasion by staphylococci. *Nat Rev Microbiol* 3:948–958.
72. Storz G, Imlay JA (1999) Oxidative stress. *Curr Opin Microbiol* 2:188–194.

73. Li Q, Mahendra S, Lyon DY, Brunet L, Liga MV, Li D, Alvarez PJJ (2008) Antimicrobial nanomaterials for water disinfection and microbial control: Potential applications and implications. *Water Res* 42:4591–4602.
74. Dutta RK, Sharma PK, Bhargava R, Kumar N, Pandey AC (2010) Differential susceptibility of *Escherichia coli* cells towards transition metal-doped and matrix-embedded ZnO nanoparticles. *J Phy Chem B* 114:5594–5599.
75. Lu W, Liu G, Gao S, Xing S, Wang J (2008) Tyrosine-assisted preparation of Ag/ZnO nanocomposites with enhanced photocatalytic performance and synergistic antibacterial activities. *Nanotechnology* 19:445711 (10pp).
76. Lin Y-J, Xu X-Y, Huang L, Evans DG, Li D-Q (2009) Bactericidal properties of ZnO-Al₂O₃ composites formed from layered double hydroxide precursors. *J Mater Sci Mater Med* 20:591–595.
77. Yamamoto O, Sawai J, Sasamoto T (2000) Change in antibacterial characteristic with doping of ZnO in MgO-ZnO solid solution. *Int J Inorganic Mater* 2:451–454.
78. Moribe S, Ikoma T, Akiyama K, Zhang Q, Saito F, Tero-Kubota S (2007) EPR study on paramagnetic species in nitrogen-doped ZnO powders prepared by a mechanochemical method. *Chem Phys Lett* 436:373–377.
79. Jose B, Antoci V, Zeiger AR, Wickstrom E, Hickok NJ (2005) Vancomycin covalently bonded to titanium beads kills *Staphylococcus aureus*. *Chem Biol* 12:1041–1048.
80. Perelshtein I, Applerot G, Perkas N, Wehrschetz E, Hasmann A, Guebitz GM, Gedanken A (2009) Antibacterial properties of an in situ generated and simultaneously deposited nanocrystalline ZnO on Fabrics. *Appl Mater Interfaces* 1:361–366.
81. Koga H, Kitaoka T, Wariishi H (2009) In situ synthesis of silver nanoparticles on zinc oxide whiskers incorporated in a paper matrix for antibacterial applications. *J Mater Chem* 19:2135–2140.
82. Vila B, Escribano F, Esteban A, Fontgibell A, Esteve-Garcia E, Brufau J (2010) Application of ZnO-functionalised-sepiolite in weaning piglet diets. *Livestock Sci* 134:232–235.
83. Oberdorster G, Oberdorster E, Oberdorster J (2005) Nanotoxicology: an emerging discipline evolving from studies of ultrafine particles. *Environ Health Perspect* 113:823–839.
84. Adisehah P, Hall JB, McNeil SE (2009) Nanomaterial standards for efficacy and toxicity assessment. *WIREs Nanomed Nanobiotechnol* 2:99–112.
85. Hirano S, Higo S, Tsukamoto N, Kobayashi E, Suzuki KT (1989) Pulmonary clearance and toxicity of zinc oxide instilled into the rat lung. *Arch Toxicol* 63:336–342.
86. Ma-Hock L, Burkhardt S (2008) Inhalation toxicity of nano-scale zinc oxide in comparison with pigmentary zinc oxide using short-term inhalation test protocol. *Naunyn-Schmiedeberg Arch Pharmacol* 377:354.
87. Wesselkamper SC, Chen LC, Gordon T (2001) Development of pulmonary tolerance in mice exposed to zinc oxide fumes. *Toxicol Sci* 60:144–151.
88. Wesselkamper SC, Chen LC, Gordon T (2005) Quantitative trait analysis of the development of pulmonary tolerance to inhaled zinc oxide in mice. *Respir Res* 6:73.
89. Wang B, Feng WY et al (2008) Acute toxicological impact of nano- and submicro-scaled zinc oxide powder on healthy adult mice. *J Nanopart Res* 10:263–276.
90. Lam HF, Chen LC, Ainsworth D, Peoples S, Amdur MO (1988) Pulmonary function of guinea pigs exposed to freshly generated ultrafine zinc oxide with and without spike concentrations. *Am Ind Hyg Assoc J* 49:333–341.
91. Zvyagin AV, Zhao X, Gierden A, Sanchez W, Ross JA, Roberts MS (2008) Imaging of zinc oxide nanoparticle penetration in human skin *in vitro* and *in vivo*. *J Biomed Opt* 13:064031 doi:[10.1117/1.3041492](https://doi.org/10.1117/1.3041492).
92. Zhu X, Zhu L, Duan Z, Qi R, Li Y, Lang Y (2008) Comparative toxicity of several metal oxide nanoparticle aqueous suspensions to Zebrafish (*Danio rerio*) early developmental stage. *J Environ Sci Health Part A-Toxic/Hazard Subs Environ Engineer* 43:278–284.
93. Zhu X, Zhu S et al (2009) Acute toxicities of six manufactured nanomaterial suspension to *Daphnia magna*. *J Nanoparticle Res* 11:67–75.

94. Yang H, Liu C, Yang D, Zhang H, Xi Z (2009) Comparative study of cytotoxicity, oxidative stress and genotoxicity induced by four typical nanomaterials: The role of particle size, shape and composition. *J Toxicol Sci* 34:119–122.
95. Deng XY, Luan QX, Chen WT, Wang YL, Jiao Z (2009) Nanosized zinc oxide particles induce neural stem cell apoptosis. *Nanotechnology* 20:11510.
96. Lee J, Kang BS, Hicks B, Chancellor TF, Chu BH, Wang H-T, Keselowsky BG, Ren F, Lele TP (2008) The control of cell adhesion and viability by zinc oxide nanorods. *Biomaterials* 29:3743–3749.
97. Gopalan RC, Osman IF, Amani A, De Matas M, Anderson D (2009) The effect of zinc oxide and titanium dioxide nanoparticles in the comet assay with UVA photoactivation of human sperm and lymphocytes. *Nanotoxicology* 3:33–39.
98. Beckett WS, Chalupa DF, Paul-Brown A, Speers DM, Stewart JC, Frampton MW, Well MJ, Haug LS, Cox C, Zareba W, Oberdorster G (2005) Comparing inhaled ultrafine versus fine zinc oxide particles in healthy adults: a human inhalation study. *Am J Respir Crit Care Med* 171:1129–1135.

Chapter 6

Characterisation of Nano-antimicrobial Materials

Timothy Sullivan, James Chapman, and Fiona Regan

6.1 Introduction to Characterisation of Nano-antimicrobial Materials

Nanomaterials, synthesised through a variety of different methods [1–3], have increasingly been of theoretical and commercial interest, owing to their potential antimicrobial properties [4–7]. Nanomaterials are increasingly incorporated into bulk materials for this purpose and some of the more recent biotechnological advances in this area have included the application of nanoparticles in materials such as textiles, wound repair and as preservatives in cosmetics [1].

Recent work has indicated that the mechanism of preparation and synthesis of nanoparticles or materials may influence subsequent antimicrobial effects. Material substrates range from polymer membranes like poly (methyl methacrylate), hydrogels [8], ultrafiltration membranes [9] or on matrices like rice paper [10] or as a self-assembled thin film composite [11].

Currently, materials incorporating silver (Ag) nanoparticles in antimicrobial applications are the most widely used nano-antimicrobial material. This is not surprising given that the history of Ag as an antimicrobial material dates back as far as the twelfth century, when Ag containers were used to store water, and the eighteenth century North Americans put Ag coins into potable water containers. Ag has been shown to be an effective biocide against bacteria, yeasts, fungi and moulds. Ghosh and co-workers have demonstrated the antimicrobial activity of Ag nanoparticles embedded in a thin film and have shown that the nature of attack on

T. Sullivan • J. Chapman

Marine and Environmental Sensing Technology Hub (MESTECH), National Centre for Sensor Research, Dublin City University, Dublin, Ireland

F. Regan (✉)

Marine and Environmental Sensing Technology Hub (MESTECH), National Centre for Sensor Research, School of Chemical Sciences, Dublin City University, Dublin, Ireland
e-mail: fiona.regan@dcu.ie

the studied organisms is linked to cell wall destruction [2]. Ag metal nanoparticle-doped hydroxyapatite powder has been shown to have antimicrobial properties with potential for use in medical applications using bone tissue [12]. The antibacterial effect of Ag nanoparticle-coated foam was investigated by Jain and Pardeep [13]. It was found that following exposure to the cultures no viable bacterial cells were detected and the untreated foam generated 'substantial growth'. Polymer nanofibres containing Ag nanoparticles [14] were characterised using UV-Visible (UV-Vis) spectral analysis and Transmission Electron Microscopy (TEM), and demonstrated effective antimicrobial activity. Studies involving nano-antimicrobial materials focused at the water quality sensor market are also evident. Exploitation of these metals at the nanoscale [15] have the potential to lead to new effective treatments and biotechnological applications. Nanotechnology recently introduced in the food packaging industry can potentially provide solutions to challenges encountered in this industry, such as short shelf life [16]. Antimicrobial packaging is a new generation of nano-food packaging based on metal nanocomposites which can be produced by incorporating metal nanoparticles into polymer films. Packaging that incorporates nanomaterials can be smart/intelligent which means that it can respond to environmental conditions or repair itself or alert a consumer to contamination and/or the presence of pathogens [16]. Self-healing packaging materials use nano/micro-encapsulated repairing agents. Small amounts of an encapsulated reagent will be released by crack propagation or other triggering mechanisms, which have been incorporated into polymeric coatings.

Figure 6.1 shows the range of characterisation and analysis options for the study of nano-antimicrobial materials. The focus of this chapter is on the surface and interface techniques as these provide information on material activity and efficacy. Antimicrobial properties of a nanomaterial must be characterised in terms of two interrelated aspects. The nature of the nanomaterial in question must be fully characterised in terms of chemical and physical properties, i.e. particle morphology, and the elemental composition of the particle. Once this has been done, it is necessary to characterise the material in terms of antimicrobial ability. Of course this process can be empirically done in reverse, i.e. production of the material, subsequent testing for antimicrobial properties, and, upon discovery of any antimicrobial efficacy, full characterisation of the nanomaterials. The first approach is preferred in terms of the development of materials and understanding of the nature of matrix/nanomaterial interaction. However, the second approach may generate unexpected results arising from interactions between the nanomaterial and the matrix within which it is presented to the microbial community.

Characterisation of materials relying on nanotechnology is important, given the range of nanomaterials that can be produced and the effect of material morphology and composition on antimicrobial properties. A large suite of characterisation techniques are available for the study of nano-antimicrobial materials. Most of these techniques are common to characterisation of nanotechnology while a few are specific to antimicrobial aspects of nanotechnology. The choice of technique depends on the material properties in question and the information required.

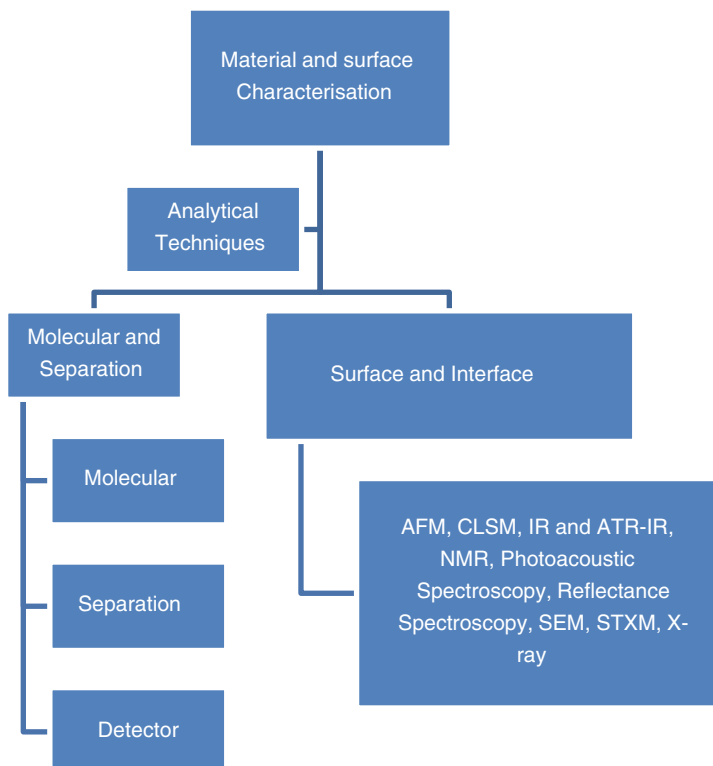


Fig. 6.1 Material and surface characterisation methods of interest with greatest attention from surface and interface techniques in relation to nanoantimicrobial materials

This chapter provides a general guide and overview of characterisation techniques available to researchers studying nano-antimicrobial materials. The following sections deal with the techniques typically used for the characterisation of nanomaterials, materials containing nanoparticles and characterisation of the antimicrobial activity where relevant.

6.2 Microscopic Characterisation of Nano-antimicrobials

Direct visual evaluation of materials is often one of the key requirements when assessing the functional characteristics of any material. This is particularly true of nanomaterials including nano-antimicrobial materials, where the nature and distribution of the particle incorporated within a bulk matrix often dictate the subsequent functional behaviour of the material. Frequently, data are required on nanoparticle concentrations, size distribution, shape and degree of particle aggregation, making

some form of direct visual characterisation crucial to material analysis. Additionally, antimicrobial materials based on the incorporation of nanomaterials require visualisation of microbe–material interactions. The understanding of such interactions is required to determine the mechanisms and efficacy of the antimicrobial properties of the generated material. Thus, the microscopy technique(s) chosen for characterisation of nano-antimicrobials will depend very much on the nature of the material under investigation and the resolution required. Figure 6.2 illustrates the range of common microscopy techniques that are currently used for characterisation of most nano-antimicrobial materials.

Additional factors that will influence the microscopy technique chosen will depend on the bulk matrix which for nano-antimicrobials may include sol–gels [17], fibreglass [18], gels [19] and textiles [20]. Direct microscopic visualisation of the nanoscale materials in situ within the matrix or bulk material is one of the most useful methods of characterisation, although also perhaps one of the most difficult to achieve without the introduction of significant spurious imaging artefacts. Most sample types, including fully hydrated samples, can now be visualised by a range of microscopic methods. However, no single technique will be able to provide all the required information, as pointed out by Samberg et al. [21] in their study of the antibacterial effects of Ag nanoparticles. A comparison of methods is needed in order to realise complete characterisation of any antimicrobial effects.

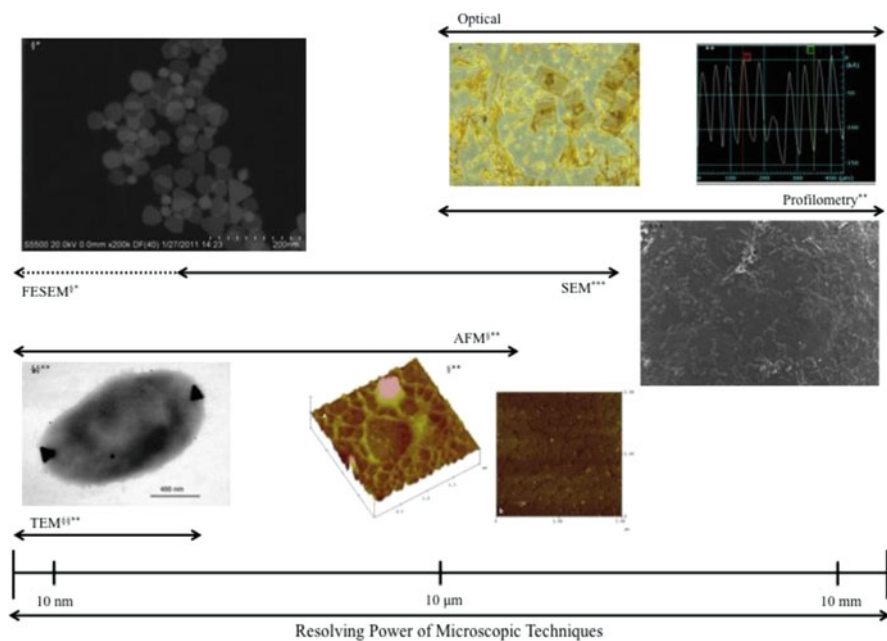


Fig. 6.2 Schematic illustrating the range of characterisation techniques and measurement ranges

6.2.1 Atomic Force Microscopy (AFM)

The field of scanning probe microscopy (SPM) now covers a wide variety of imaging techniques, having been founded with the invention of the scanning tunnelling microscope in 1981. Since then, a number of high-resolution imaging techniques have been developed based on the basic principle of SPM, which consists of scanning a probe across the surface of a sample and recording the interaction force between the tip and the sample [22]. This is facilitated by the use of piezoelectric actuators to record the changes in the electrical potential of a sample.

AFM has become one of the most widely used, and one of the most important, tools associated with SPM techniques. Invented in the 1980s and with the first commercial instruments available in 1989, AFM has been widely used for the characterisation of nanostructures since its inception. It is now considered the best choice for all-round visual characterisation of nanoscale materials, and is particularly effective when corroborated with transmission electron microscopy (TEM). Information provided by AFM includes direct 3-D visualisation that can be used for both qualitative and quantitative data on size, morphology, surface texture and roughness [23]. A number of studies on the antimicrobial effects of nanoparticles have utilised AFM as the primary method of visualisation [15].

AFM operates by the use of an oscillating cantilever which is scanned over the material under study in order to measure the electrostatic interactions occurring between the tip and the surface. Electrostatic forces as low as 10^{-12} N can be measured and a height resolution of circa 0.5 nm can be achieved. Typically, AFM can provide characteristic measurements of nanoscale materials with a vertical resolution of less than 0.1 nm with XY resolution of approximately 1 nm and is capable of material sensing [24].

AFM also provides information on the surface roughness profile or surface texture of a substrate, an important requirement when analysing microbial retention or removal from a substrate [12, 25]. Hansma et al. reviewed AFM of biopolymers with some specific examples including: EPS, condensed deoxyribonucleic acid (DNA), DNA constructs and even DNA–protein interaction [22]. Van der Aa and Dufrene (2002) investigated bacterial adhesion to polystyrene under aqueous conditions using AFM, and cell morphologies and cell interactions across the surfaces were realised [26]. AFM not only provides data on the nanoparticles used as antimicrobial agents in materials but also provides information on the bactericidal properties of the material such as the mechanism of action of the materials on microorganisms (Fig. 6.3). For instance, cell death and changes in the morphology of the cell membrane nanoparticles have been directly visualised using AFM [27]. The potential of AFM in demonstrating the more subtle effects of microbial membrane integrity upon interaction with nanoparticles is illustrated by the ability to detect changes in membrane elasticity under fully hydrated conditions [14].

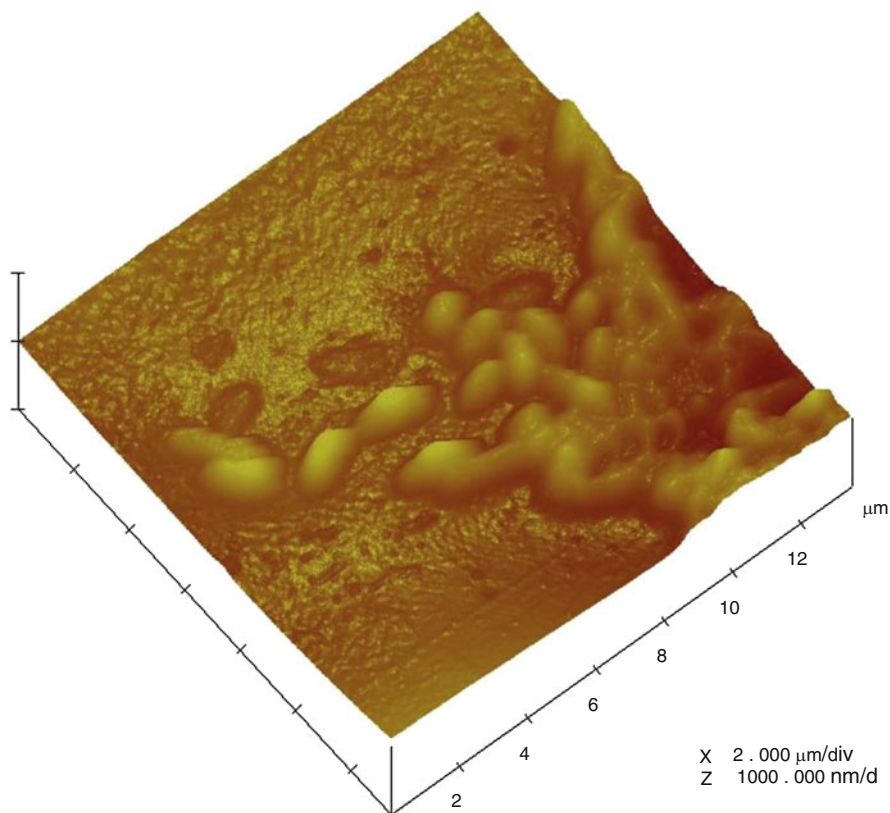


Fig. 6.3 Atomic force micrograph illustrating microorganisms adhered to a polymer thin film

AFM is a technique that has many advantages over the other methods of visual characterisation such as electron microscopy when considering nano-antimicrobial materials. AFM does not require extensive sample preparation (i.e. sputter coating or chemical fixation) for visualisation, and is a relatively non-destructive technique. As the sample does not need to be in a vacuum for analysis, live microorganisms can be viewed in situ. Unlike electron microscopy techniques, the sample can be either a conductor or insulator and no staining is required in order to achieve contrast. Chemical fixation and dehydration, a frequent cause of artefacts in EM techniques, is unnecessary if the sample is rapidly imaged. AFM, in conjunction with an EM method, often offers the best solution for visual characterisation of most nanoscale materials.

Of course, this must be balanced against the speed of EM techniques where (low resolution) information can be obtained in near real-time. The scan speed of AFM is slow and can lead to problems with thermal drift, although some promising techniques have been recently developed in order to achieve faster scan speeds [28, 29].

6.2.2 *Electron Microscopy (EM)*

Electron microscopy covers a broad range of microscope techniques that operate by visualising the interaction between a finally focused electron beam and the sample of interest. The type of signals generated when the electron beam interacts with the sample includes secondary electrons (SE), backscattered electrons (BSE), Auger electrons (AE), characteristic X-rays, and photons of various energies. All these signals can be used in some capacity to generate information about both the nature of the nanomaterial and microbial interaction with these materials, making EM one of the most popular and versatile techniques for nano-antimicrobial material characterisation. Semi-quantitative analysis of materials such as nanoparticles including states of aggregation, dispersion, sorption, size, structure and shape can be resolved for most particles, and EM can readily be coupled to other analytical instrumentation for further analysis. Depending on the technique used, sample and method of sample preparation, sub-nanometre resolution (>0.1 nm) can be attained using transmission electron microscopy (TEM) or scanning TEM (STEM). Undoubtedly, EM offers many advantages in terms of visualisation of nanoparticle-based materials; however, difficulties are encountered when trying to attain quantitative information. This is due to the fact the EM can only give information in 2-D and lacks detailed information on 3-D morphology of samples without specialised software and imaging techniques.

Obvious disadvantages of using EM for nanoparticle visualisation are related to the destructive nature of the sample preparation techniques required for EM when subjecting samples to the high vacuum conditions required for most high-resolution EM. Artefacts are easily introduced during the sample preparation process during dehydration, fixation or embedding.

6.2.2.1 *Scanning Electron Microscopy (SEM)*

Conventional SEM has been the workhorse of visual characterisation of nanometre scale materials for decades. Commercial instruments often have a sub-nanometre theoretical resolution; however, the ultra-high resolution required for modern nanoscale material analysis has meant that problems are frequently encountered in resolving such structures due to lens aberration at ultra-high magnification. Conventional SEM has a number of advantages when used for characterisation of nano-antimicrobial materials. These include the capability to image large samples (up to several square centimetres in area or larger) and a large magnification range. SEM can provide information on the material surface and morphology of attached microorganisms such as bacteria, and, in some cases, SEM provides valuable insights into the relationship between microbe and substrate [28, 29].

Unfortunately, SEM suffers from a number of disadvantages when used as a means of characterisation of microbe–substrate interactions. Chemical fixation such as protein cross-linking using reagents such as glutaraldehyde, formaldehyde,

ethanol or methanol is necessary to retain some semblance of structural integrity of soft biological specimens. Samples must be dehydrated prior to introduction into the vacuum chamber, usually by dehydration using an alcohol or acetone series, further increasing the probability of sample artefacts.

It is also difficult to image non-conducting specimens using conventional SEM due to the build-up of surface-charging artefacts disrupting electron collection. To counteract this, it is often necessary to coat the surface of the specimen with a conductive coating; usually gold (Au), chromium (Cr) or carbon (C). Sputter-coatings facilities are readily available for this, meaning that most samples can be imaged. The ability to carbon sputter-coat a sample is especially desirable if further elemental analysis such as energy dispersive spectroscopy (EDS) is to be performed on the sample. Of course, if ultra-high-resolution imaging is required, the deposition of a conductive coating may obscure features of interest and sputter-coating of samples is one further area where spurious sample artefacts may be introduced. Experimentation with various methods of sample preparation for SEM is desirable and usually necessary for characterisation of novel nano-antimicrobial materials.

6.2.2.2 Field Emission SEM (FeSEM)

Field emission scanning electron microscopy (FeSEM) offers one of the highest resolution techniques for nanoscale material visualisation. By definition, FeSEM involves the use of a field emission source also called a cold cathode field emitter, usually composed of tungsten (W) wire sharpened to a fine point (<100 nm). The advantages of this over conventional SEM emission sources are clear when it is understood that the filament requires no heating in order to emit electrons. Instead, the field emission source is placed in a large electrical potential gradient, such that the electrical field is highly concentrated on the fine source, resulting in a reduction in the work function of the material and thus the emission of electrons. This results in a greater spatial resolution than conventional SEM which relies on thermionic emission, and an increase in resolution of four to six times that of conventional SEM is achievable with less electrostatic distortion. Figure 6.4 illustrates a field emission scanning electron micrograph of gallium nanoparticles doped on a nylon membrane.

Current FeSEM instruments have a number of useful imaging modes that can be employed to gather supplementary data about nanoparticles and nanomaterials. These include low-angle BSE (combining SE and BSE), high-angle BSE, and scanning transmission microscopy (STEM). STEM is a particularly useful imaging mode and has been used to confirm the presence of metal nanoparticles within the bacterial cell membrane [4].

STEM is an excellent probe of the electronic properties of nanoparticles and utilises a number of signals from elastically scattered electrons including direct and diffracted beams giving dark field (DF) and bright field (BF) images incoherent scattering (for Z contrast).

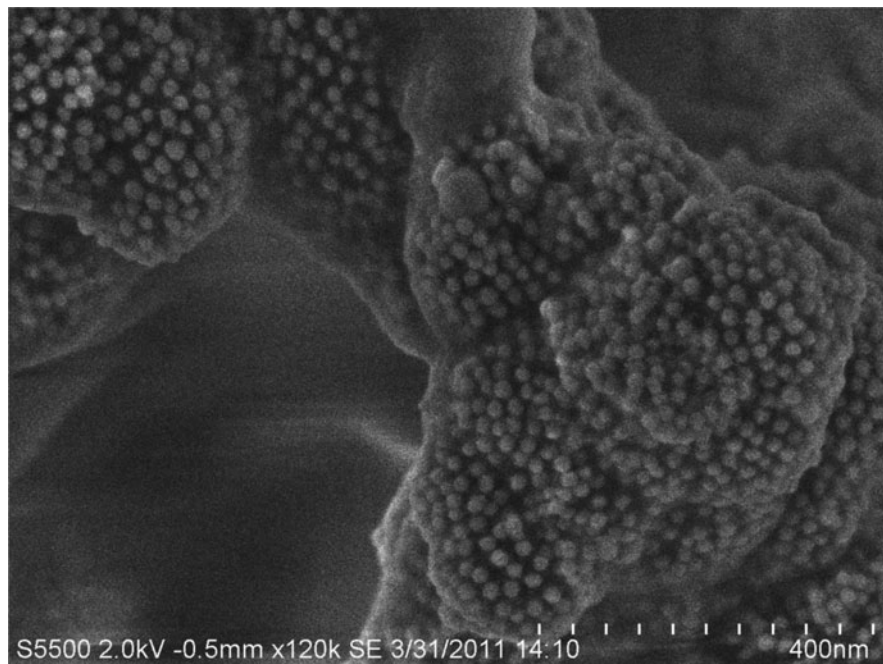


Fig. 6.4 Field emission scanning electron micrograph of gallium nanoparticles doped on a nylon membrane for antimicrobial and antifouling purposes

TEM using high-angle annular dark field (HAADF) detection in scanning transmission microscopy (STEM) mode can be used to visualise biological systems and has been done successfully by Shrivasta et al. [30]. Most TEM methods are 2-D; however, STEM coupled to high annular angled dark field microscopy (HAADF) allows 3-D analysis by HAADF STEM tomography. STEM is limited if nanoparticles do not adhere to the surface of the substrate for measurement resulting in poor images. The geometry of the tip may lead to inaccurate measurements, and standard operational protocols for specific imaging techniques are still not developed thereby leading to some error.

By using a number or all of these imaging modes, it is possible to completely characterise the morphology of most currently prepared nanoscale materials. The additional information gained on nanoparticle morphology by the use of STEM can readily be seen when compared to just SE imaging. Such information will prove vital in understanding the results of subsequent microbial–nanoparticle interactions. In addition to this, many FeSEM instruments are now equipped with cryo-stage capabilities, thus further extending the versatility and sample range possibilities, especially with regard to biological specimens (see notes on sample preparation for EM techniques).

For the advantages cited above, FeSEM has become the visualisation method of choice for analysing metal nanoparticles, given the excellent resolution that can be

achieved and the minimal sample preparation required. The applications of FeSEM to analyse nanoparticles prior to material doping or incorporation into anti-microbial materials is almost unlimited, especially with regard to morphology. In addition, FeSEM is usually coupled with EDS capability as standard, similar to conventional SEM, and thus information on nanoparticle elemental composition and distribution are readily gathered. FeSEM has been actively utilised to visualise a number of exotic nanoparticle types including chitosan NPs [7] and magnetic NPs [31]. FeSEM has also been utilised to demonstrate the distribution and shape of particles in preparation methods such as spin coating of Co and Ag particles [6] or binding to fibre materials, an important consideration for incorporation of nanoparticles into antimicrobial materials. Biological material is less suited to FeSEM, given it is classified as a high vacuum method requiring 1×10^{-7} Pa from two ion pumps.

In terms of sample preparation, FeSEM offers an advantage over conventional SEM, as it eliminates the requirement of using a conductive coating on poorly insulating materials for visualisation and spatial resolution is improved [17]. FeSEM imaging was used in the studies by Daoud et al. [32] for the determination of the level of TiO₂ nanoparticles adhering to the surface of the cellulose fibres.

6.2.2.3 Energy-Dispersive X-Ray Spectroscopy (EDS)

EDS is an analytical technique that is used in elemental analysis or chemical characterisation of a sample. Figure 6.5 is a typical spectrum that is produced when the surface of an antimicrobial material has been characterised. The observed energy peaks correspond to the elements present in the sample. Energy-dispersive

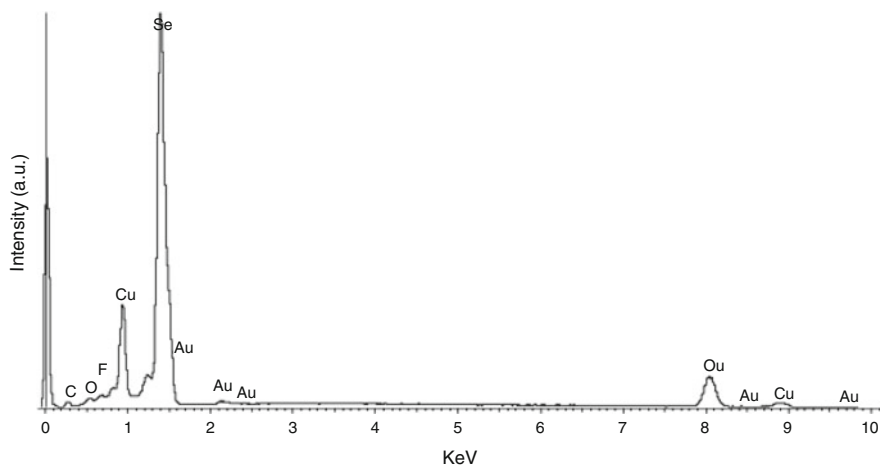


Fig. 6.5 Energy dispersive X-ray analysis of Se-nanotree confirming elemental composition. Working distance of 10 mm with 20.0 kV accelerating voltage and probe currents of 35–50 eV

X-ray (EDS) analysis is a feature of electron microscopy and has been used extensively in research to establish the chemical composition of nanocomposite membranes [11, 17]. By focusing the electron beam on a single Ag nanoparticle, Zeng et al. [10] were able to confirm the formation of particles on the substrate. Figure 6.5 illustrates a typical EDS obtained from selenium nanoparticles using FeSEM-EDS.

6.2.2.4 Transmission Electron Microscopy (TEM)

When coupled with AFM, TEM provides one of the most useful and complete microscopic methods of nanomaterial characterisation. TEM is a valuable tool in the determination of size, shape, dispersion, structure, morphology and orientation of biological and physical samples. Magnifications are typically in the region of $\geq 40,000$ to 0.2 nm. Despite the extensive sample preparation required, TEM and variations of TEM are one of the most common techniques utilised for the visualisation of nanoparticles both in situ and of separated particles.

Samples should be very thin to allow transmission of electrons [33] through the sample, which poses a number of problems during sample preparation of bulk materials; however, this is balanced by the quantity and quality of information that TEM analysis can provide. TEM scopes fitted with field-emission guns (to provide coherent electron waves) can be adapted to record the magnetic fields within and surrounding nanoparticles or metal clusters [34]. A number of recent studies on the antimicrobial effects of Ag nanoparticle materials have used TEM as a means of studying the interaction between cell and nanoparticle, including uptake and transport of nanoparticles across the cell membrane [35]. As with all EM techniques, caution should be exercised when interpreting information acquired using TEM as the images may not be representative; to counter this, many images must be captured to give a true representation of the surface [36].

Aside from solely examining the nanomaterial properties of a potential nano-antimicrobial material, TEM can assist in discerning the mode of action of the material through analysis of cell–nanoparticle interactions. Carefully prepared thin-sections through microorganisms such as bacteria can show the uptake and distribution of nanoparticles within the cell when imaged using TEM. Shrivastava et al. [30] used TEM to investigate the interaction between microbial cells and metal nanoparticles. From their investigation, they found that Gram-positive bacteria had reduced interaction with Ag nanoparticles compared to Gram-negative bacteria.

6.2.2.5 Scanning Transmission X-Ray Microscopy (STXM)

STXM is a powerful tool that can be applied successfully to fully hydrated biological systems. It uses a near-edge X-ray absorption spectroscopy (NEXAFS) as the contrast mechanism. The soft X-rays penetrate through water molecules coupled with the presence of reduced radiation damage (compared with the electron

beam of a transmission electron microscope (TEM)). Macromolecule components have previously been mapped using STXM and TEM showing biofilm composition (protein, polysaccharides, lipids and nucleic acids) [37].

Lawrence et al. [38] demonstrated a combination of multi-microscopic techniques and created a detailed map of biofilm structure and composition. It should also be noted that they were able to detect metals using the STXM. STXM is capable of providing chemical maps at environmentally relevant concentrations (i.e. mg kg^{-1}) with spatial resolutions up to 50 nm [37].

6.2.3 Optical Microscopy Techniques

Optical microscopy plays a key role in understanding many biological systems. It was one of the first tools ever developed for assessing microbial organisms, and the ability to now couple automation and digital imagery with extension to in situ analysis means that optical microscopic techniques are vital to characterisation of nano-antimicrobial materials. High-resolution optical imaging of thick specimens (optical sectioning) is possible and naturally fluorescent samples or samples treated with fluorescent dyes are detectable.

Optical methods for nanomaterial characterisation are generally limited by the diffraction limit of light, although modern near-field scanning optical microscopy (NSOM) can obtain a resolution of 50–100 nm. Thus, optical microscopy is primarily used for rapid in situ examination of material–microbial interactions when characterising nano-antimicrobial materials. A range of well-established techniques such as epifluorescence microscopy, phase contrast, differential interference contrast (DIC), super-resolution microscopy, and stereomicroscopy are routine when examining antimicrobial materials. Techniques such as fluorescence microscopy or confocal microscopy often necessitate the use of specialised fluorophores for the target of interest of which a broad range are now available. Live cell imaging or time-lapse microscopies are additional useful tools to understand microbial organism–nanomaterial interactions.

6.2.3.1 Laser Scanning Confocal Microscopy (LSCM)

No discussion of the characterisation of antimicrobial materials would be complete without a description of confocal microscopy, an imaging technique that has revolutionised the imaging of biological specimens since the first commercial instruments became available in 1987. This complex technique, capable of imaging a single molecule, relies on the excitation of a fluorophore using scanning laser source of precise wavelength and excitation intensity [10]. Confocal microscopy in contrast to conventional wide field microscopy has only recently been applied in colloid characterisation and has been combined with fluorescence correlation spectroscopy (FCS) to characterise fluorescent species in complex systems.

In preparation for LSCM, microbial cells are stained or probed with green fluorescent protein (GFP), for example to allow visualisation and quantification of the organisms. LSCM offers great potential for the investigation of antimicrobial properties of nanocomposite materials as the structure of an attached biofilm can be investigated by 3-D imaging [39]. Microbial structures can be monitored in situ enabling the observation of a developing microbial community in an undisturbed and non-destructive manner [40, 41]. Stewart et al. have shown structural heterogeneity of microbial consortia attached to substrata through SEM and LSCM. They used a cryo-embedding technique followed by the tandem microscopy techniques. The authors compare three different microscopy methods illustrating differences in the additional information that can be gained through use of complementary techniques.

LSCM of live, fully hydrated systems is possible [42]. LSCM also provides 3-D structural information of various components within a cellular matrix either by autofluorescence (algae) or labelling with specific dyes for DNA [43].

6.2.3.2 Epifluorescence and Nano-antimicrobial Materials

Epifluorescence microscopy is one of the most wide-ranging techniques for characterisation of biological composition on materials. Fluorescence has a number of advantages over transmitted light, including improved contrast, the detection of sub-resolution structures, detection of low abundance molecules and high specificity. In addition, epifluorescence can be used to detect several biomarkers simultaneously with high specificity.

The principle is simple in that the target material is stained with one of more fluorophores that have a characteristic excitation and emission spectrum separated by a Stokes shift. If the correct filter set is used to absorb or deflect non-transmitted wavelengths, the emission spectrum from the region of interest can be detected. Further advantages include the fact that many research laboratories have access to epifluorescence as this technique does not have the costs associated with instrument upkeep as do many of the higher end electron microscopy techniques or LSCM.

Staining for epifluorescence or immunofluorescence of microbial cells allows for cell enumeration, determination of metabolic activity and, importantly, in situ assessment of adhered bacteria [44]. Many microbial stains are used, e.g. crystal violet, acridine orange and 4',6'-diamidino-2-phenylindole (DAPI), in conjunction with high throughput instrumentation and can provide a rapid form of biological assessment, depending on the parameter under investigation. Simple commercial staining kits such as Live/Dead[®] BacLight[™] are now available to quantify information such as viability of bacterial cells after exposure to the nanomaterial. The capability for automated cell enumeration is desirable as this can be labour intensive. Staining methods can be easily applied for the study of nano-antimicrobial materials in environmental or medical settings to establish the degree and nature of bacterial adhesion.

A generic protocol followed for antimicrobial assessment of nanomaterials usually includes a number of steps that may involve fixation, permeabilisation of the cell membrane. Non-adhered microorganisms are usually removed through rinsing of the surface.

Acridine orange and DAPI (4',6'-diamidino-2-phenylindole) staining are fluorochromic staining methods used for direct cell counts. Acridine orange stain attaches to DNA and RNA of cells present in solution or on a surface and can be used as a rapid and simple stain for cell counting. Adherent cells are viewed by fluorescence microscopy and can be counted manually using the epifluorescence microscope or imported into image analysis software for automated enumeration. A number of useful free software programmes, e.g. ImageJ, with extensive ability to handle large and varied file formats have been developed for such applications [45].

The fluorescence generated can be detected with an epifluorescence microscope and indicates the presence of DNA from the bacteria (Fig. 6.6). Azevedo et al. [46] and Kerr et al. [47] used DAPI to determine the total cell counts following bacterial exposure of surfaces. This stain was applied directly to the surface under investigation and viewed by epifluorescence microscopy. DAPI staining was used as the method for screening antifouling materials by Leroy et al. where these were incubated with cultures using 96-well plates. This enabled the study of multiple samples simultaneously [48] using DAPI to quantify bacterial adhesion. Figure 6.6 shows an epifluorescence image of microorganisms attached to a polymer surface when samples are stained with 0.1% w/v acridine orange.

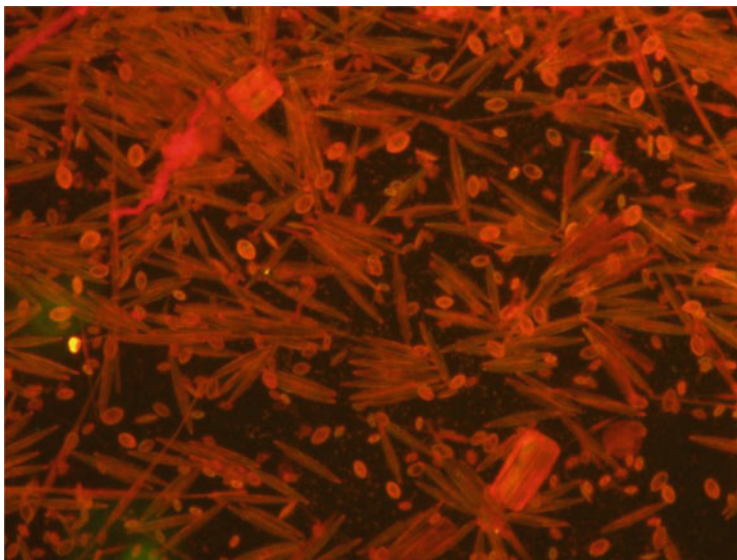


Fig. 6.6 Epifluorescence image of microorganisms attached to a polymer surface showing the diversity of attached organisms including diatoms (*Bacillariophyceae*) settled on underlying bacterial cells (samples stained with 0.1% w/v acridine orange, Leica 200 × magnification)

6.3 Spectroscopic Methods of Characterisation

In order to quantify the antimicrobial properties of a nanomaterial, it is frequently necessary to expose the material to a number of representative organisms, depending on the envisioned end use of the material. Figure 6.7 shows a light microscopy image of a polymer surface exposed to a natural marine microbial community; the complexity and diversity of a natural microbial community can be seen, including adhesion of unicellular algal cells such as diatoms. In order to quantify the degree of colonisation by natural microbial communities it is frequently necessary to resort to biochemical or spectroscopic methods of quantification.

6.3.1 Photoacoustic Spectroscopy (PAS)

PAS is based on the absorption of electromagnetic radiation that is contained within a sample. The combination of optical spectroscopy and ultrasonic tomography allows depth-resolved analysis of both optical and acoustic media. Schmid et al. presented a PAS sensor system for the analysis of biofilms [49]. Outer and inner

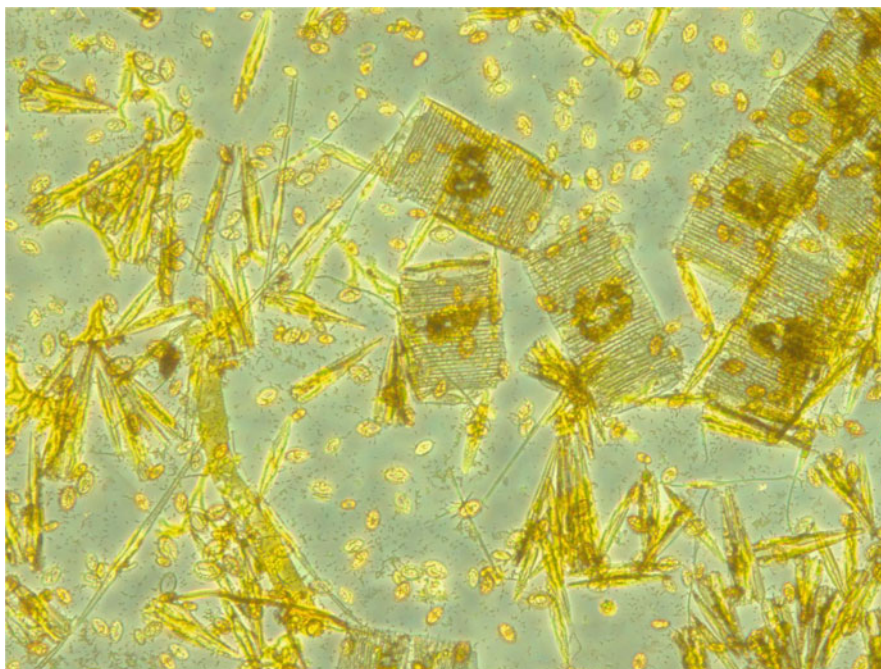


Fig. 6.7 Light microscopy image of a number of diatom species attached to a material surface

surfaces of the biofilms were analysed for Fe (III) oxide particles that had been adsorbed; this was performed in situ.

A multiple suite of PAS sensor heads can also be used to investigate the efficacy of biocides used to deter biofilm formation. Monitoring the photoacoustic signal amplitude in the visible spectral range allows observation of the biofilm detachment induced from the use of a biocide [50]. Immobilisation of furanones (a group of natural product antimicrobial compounds) was investigated using XPS [51] and tapping mode AFM; each technique was applied following each immobilisation step.

6.3.2 Nuclear Magnetic Resonance (NMR)

For the purpose of characterising metal nanoparticles, NMR has two uses: it can be used to probe the ligand that surrounds the metal core *and* probe the more difficult task of investigating the intra-core metallic atoms. The use of NMR in characterising nano-antimicrobial materials is not widely reported.

NMR has provided detailed information for live prokaryotic cell suspensions and extracts as eukaryotic cell and tissue samples [52]. In particular, ^1H and ^1H -detected ^{13}C NMR provide for the direct time-resolved monitoring of metabolite concentrations, metabolic pathways and even flux rates for in situ studies [53]. Recent investigations by Vrouwenvelder et al. studied biofouling of reverse osmosis membranes using 2-D NMR velocity imaging, where substrates were analysed over 4 days. The substrates are specifically created using a non-magnetic spacer membrane and then fitted into a radio frequency coil which directly mounts into the instrument [54].

Exopolymeric substances (EPS), which are generally produced by microorganisms when adhered to a substrate, are comprised of carbohydrates, proteins, water and organic particulates. Therefore, the determination of such molecules allows the assessment of the degree of activity upon a substrate. This approach is preferred to the use of measurements of biomass, among other techniques, to assess microbial growth as it relates directly to EPS.

6.3.3 UV-Visible Spectrophotometry (UV-Vis)

UV-vis spectroscopy is used abundantly in nanomaterial based research and represents a versatile technique that can be applied to characterise a range of systems ranging from [55]:

- Nanoparticle solutions;
- Nanomaterials (where transmission is possible);
- Photoactivity of a nano-antimicrobial material;
- Optical Density (OD) for the determination of cell numbers and or activity in a given system.

In each case, UV-Vis spectroscopy displays wide ranging capabilities and, furthermore, has the ability to characterise both the component of a material, e.g. a nanoparticle, the material itself, e.g. a nanoparticle-doped transparent polymer, and a given system; this material is in situ, e.g. a pure culture bacterial matrix.

6.3.3.1 Nanoparticle Characterisation

UV-Vis spectroscopy is commonly used to confirm the presence of nanoparticles in a liquid [17] and is particularly effective in characterising metal nanoparticles. It is useful for characterisation of metal nanoparticles where the surface plasmon absorbance is in the visible region of the spectrum, e.g. Ag, Au, Cu, etc.

A sharp peak on the UV-Vis spectrum can indicate a narrow size distribution of nanoparticles. Figure 6.8 shows typical spectra achieved for UV-Vis spectroscopy whereby an example of shape tuning observed a range of colours being produced, highlighting the optical properties of such nanoparticles. The shape of the nanoparticles can also be indicated by UV-Vis spectroscopy, but confirmation is usually performed using imaging methods, such as TEM or FeSEM [17]. There are many advantages to this method. The instrumentation is relatively inexpensive compared with other instruments used for characterisation. UV-Vis spectroscopy is also a very simple and quick method for characterisation as there is no or little sample preparation. However, UV-Vis spectroscopy does not offer detail of the size distribution of the particles and visualisation is recommended to determine the shape of the nanoparticle. Although only small areas can be observed at one time, requiring multiple measurements in order to obtain representative data, UV-Vis observations are widely used among all researchers for initial confirmation of nanoparticle occurrence [51, 56]. In a study by Slistan-Grijalva [57] and co-workers, the surface plasmon absorption band was characterised to illustrate spherical Ag nanoparticles in water and ethylene glycol. The study demonstrated that the maximum absorbance of Ag nanoparticles is higher in ethylene glycol than in water, whereas the surface plasmon peak occurs at longer wavelengths under the same conditions. This result relates to the different refractive index in different solvents.

6.3.3.2 Bacterial Characterisation on Nano-antimicrobial Substrates

For a bacterial system, OD measurement is based on an assessment of turbidity of the bacteria present in a clear liquid medium. This method provides a quick estimation of bacteria present in solution. The OD values obtained via a spectrophotometric reading are directly related to the concentration of cells in the media under the Beer–Lambert Law. A disadvantage is that this method does not distinguish between dead and viable cells. However, it is a rapid technique for the determination of approximate cell numbers in a non-destructive manner.

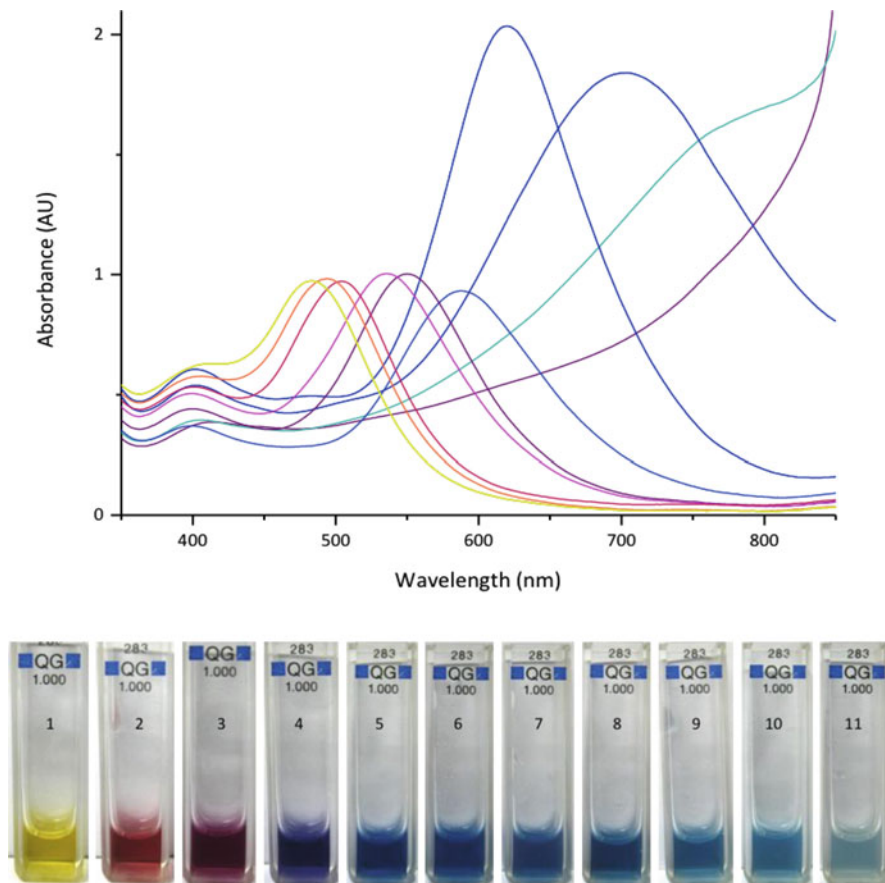


Fig. 6.8 UV-Visible spectra of silver nanoparticles with tuned {111} facet. From *left to right* yellow small {111} edge through to purple with a larger {111} edge. *Bottom* photograph showing relevant nanoparticle solutions used to generate the spectra

By reading the optical density of cultures exposed to a potential nano-antimicrobial, an indication of bacterial kinetics can be determined.

Bacterial kinetics, following exposure to nanoparticles and nanoparticle-doped materials, has been studied by using both plate counting and by monitoring optical density. Lee and Tsao [58] placed 1 g of a hydrogel containing Ag nanoparticles in a flask with sterile water and *Escherichia coli* cells. Bacterial growth was monitored over time by withdrawing samples of liquid periodically, performing a serial dilution and preparing pour plates. Colonies were counted following incubation to determine viability. Cioffi et al. [36] monitored Ag and Cu nanoparticles at various concentrations over a fixed duration of time.

Diffusion methods are also sound techniques in assessing the efficacy of a nano-antimicrobial material. The inoculation and subsequent diffusion of the

antimicrobial agent through agar in a pure culture system enables effective concentrations to be monitored. If there is an anti-bacterial effect, a zone of inhibition will be present. The test works on the basis that the greater the zone of inhibition the greater the anti-bacterial properties of the test material. The Kirby Bauer test is one such test and was used by Fekete et al. [59] and Sambhy et al. [60] for the determination of the antibacterial properties of the test agent. This type of analysis is easy to perform, and nanoparticle-containing composites have been tested using this method by Sambhy et al. [6] and Kim et al. [61] among others. This is a very cost effective and quick method to confirm the antibacterial ability of a material. A disk diffusion method using Muller-Hinton agar was used by Shahverdi et al. [62] for the assessment of Ag nanoparticles and their effect on different antibiotics against common bacterial species.

The minimum inhibitory concentration (MIC) shows the lowest concentration at which an antimicrobial agent will inhibit the growth of a microorganism. The method is well established for the interrogation of future antimicrobial agents such as metal nanoparticles [63]. Typically, the antimicrobial agent is diluted in a liquid solution where a series of concentrations are made. The series of concentrations are then inoculated with a standard number of known organisms. The lowest concentration that inhibits growth represents the MIC. Numerous authors have used this method in screening novel antimicrobial agents including Zeng et al. [10] and Pal et al. [64].

One method that is closely linked to MIC is the minimum bactericidal concentration (MBC). This method indicates the lowest concentration by which 99.9% of microorganisms are killed by the investigated compound. The MBC is the lowest concentration of the antimicrobial agent that restricts the growth of the organism when subcultured into antibiotic-free media. Advantages of the MIC method are ease of preparation and efficacy of the analysis. No special apparatus or instrumentation is required, but researchers using this method with the inclusion of agar will find it is more time consuming.

6.3.4 *Infra-Red (IR) Spectroscopy*

IR spectroscopy is a useful non-destructive technique that provides a fingerprint of the fundamental functional groups of some biomolecules. This method relies on IR energy being absorbed by quantum energy levels associated with atomic vibrations or rotations. Fourier transform (FT) refers to a pair of mechanical expressions which essentially relates to a continuous function and its decomposition into weighted frequency components.

Suci et al. [65] report that water absorbs very strongly in the mid-infra-red range, which is where most biological molecules have strong resonance vibrations. This is because the absorption in the region centres at 1,640 and 3,300 cm^{-1} will mask whatever compounds are also in this region. They also reported that bacteria have distinct bands and have shown RNA (DNA) can be detected at 1,000 cm^{-1} . Osiro

et al. reported biofilms being analysed on FT-IR using a KBr disc method [66], where the sample was ground up before being analysed. They reported weak signalling bands of $1,740\text{ cm}^{-1}$ of the C=O bond found in fatty acids, phospholipids, lipopolysaccharides and in the acetate group of xathan [67, 68]. They also reported that signals at $1,650\text{ cm}^{-1}$ show typical amide bands from within proteins, carboxylate anions, and OH absorption of polysaccharides. The most important bands relating to polysaccharide stretching C–O bonds are in the region of 950 and $1,150\text{ cm}^{-1}$.

ATR-IR spectroscopy is also another feature of IR data analysis that can be used to readily acquire in situ information from a sample or substratum [69]. It has the added advantage that whole cells can be readily analysed and studied. As mentioned above, Suci et al. have also combined interference contrast microscopy and ATR-FT-IR spectroscopy in order to characterise the architecture and chemistry of the attached biofilms in situ [65]. Similarly, Chongdar et al. used microscopy coupled with ATR-FT-IR to interrogate the mechanism of microbes in influencing corrosion upon a substrate. Steel electrodes were incubated in phosphate-buffered solution with two different microbes, and the biofilm was then subsequently scraped and analysed using FT-IR spectroscopy [70, 71]. Pink et al. [72] gave an interpretation of the ATR-FT-IR data in the $1,500$ – $1,180\text{ cm}^{-1}$ region. Their results provide the first detection of excess proteins on the surface of a substrate from pure culture studies using *Pseudomonas aeruginosa* [72].

6.4 Further Characterisation Techniques

Direct characterisation possibilities of nano-antimicrobials offered by microscopy are invaluable when assessing both the nature of the nanomaterial and the antimicrobial properties of the material. However, further characterisation by non-visual methods are often warranted to understand the physiochemical characteristics that may influence the efficacy of the material in terms of antimicrobial ability.

A range of further techniques are relevant and have been used in assessment of nano-antimicrobials to date, including methods of characterising the chemical nature of the surfaces and spectroscopic methods to assess the biological activity on the surface.

6.4.1 Contact Angle and Surface Free Energy

Contact angle (CA) measurements provide an indication of the surface free energy (SFE) of a surface by measuring the hydrophobicity or hydrophilicity. This is important as it has been demonstrated that surface free energy (SFE) alters the antimicrobial characteristics of a surface by altering the ability a microorganism to adhere to or approach a surface [73]. The SFE can be approximated using contact

angle measurements as a function of the surface “wettability”, whereby the contact angle is the angle at which the drop of liquid touches the substratum described by Young’s equation:

$$\gamma_{lv} \cos \theta = \gamma_{sv} - \gamma_{sl} \quad (6.1)$$

where γ_{sl} , γ_{sv} and γ_{lv} correspond to the surface tension of solid, liquid and solid–liquid interfaces. Both wetting and adhesion properties can be estimated through calculation of the surface tension induced by the solid–liquid interface.

Polymers do not tend to adhere to this equation as they are regarded as non-ideal surfaces due to liquid penetration into the matrix causing swelling phenomena.

A typical sessile drop technique for CA measurement is shown in Fig. 6.9. Here, the photograph shows the water droplet that has been dispersed on a nanoparticle doped poly(vinylchloride) (PVC) thin film. Images are taken on a side profile and the data for advancing and receding (hysteresis) measurements are collected. An advantage of this method, aside from its relatively straightforward nature, is the fact that, with substrates with large enough surface areas, multiple droplets can be deposited in various locations upon the sample thus determining heterogeneity. Some disadvantages include the converse to the aforementioned, and therefore with fewer samples heterogeneity cannot be determined and is sometimes therefore

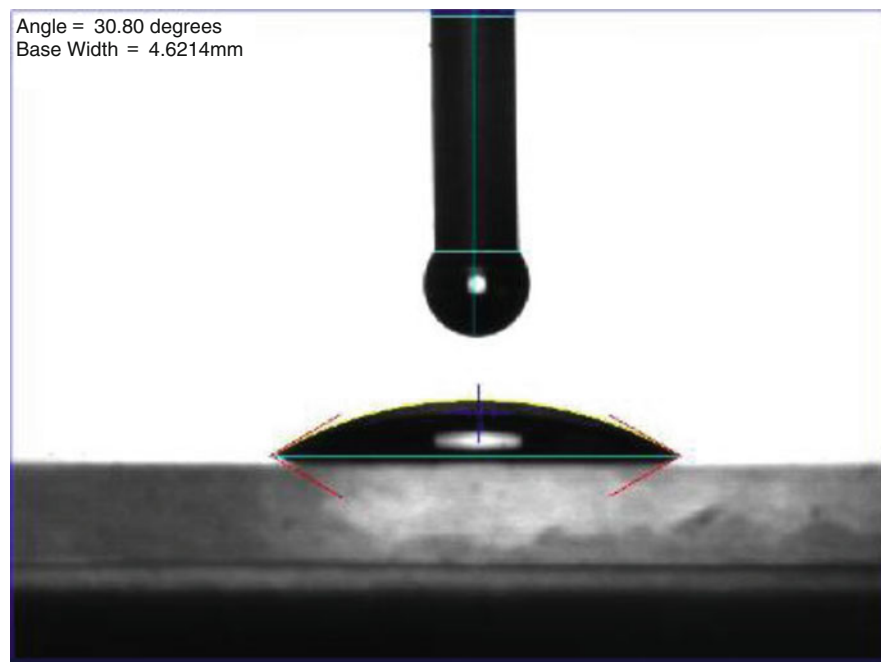


Fig. 6.9 Contact angle of nanoparticle doped sol-gel showing hydrophilic properties. Static drop method at room temperature and pressure

assumed. Furthermore, the sample spotting of water droplets does not reflect the 'true' environment the substrate/material is being subjected to, as more often than not samples are completely submerged.

One drawback of contact angle measurements is that external factors will influence the result. To reduce error, it is important to keep the environment controlled and to limit exposure to potential contaminants, as contamination of the surface under investigation will affect the results. Sometimes, researchers define the contact angle in terms of surface energy, given the sessile drop technique, but this is not always well defined. The values obtained using the sessile drop depend not only on the solid substrate but equally on the liquid (probe) being used.

6.4.2 Powder X-Ray Diffraction (XRD)

XRD has been shown to be a powerful characterisation tool in the study of Ag nanoparticles in natural rubber [74]. XRD analysis is based on the principle that each crystalline solid possesses its own characteristic X-ray powder pattern [20, 75]. The X-rays are scattered by diffraction owing to the unique crystalline structure of each of the materials analysed. From this analysis, the particular crystalline structure and hence the chemical composition of the material under investigation can be obtained. XRD is regularly used for the characterization of nanoparticles. Kwak et al. [11] analysed commercially obtained TiO₂ nanoparticles by XRD for comparative purposes. It has been noted that sometimes an identifying peak might not be present, owing to the nanoparticle being embedded in the gel composite [11]. However, this method of characterisation is particularly good as it is a non-destructive technique, which can be used to calculate the phase content and investigate changes in phase structure of the samples before and after a treatment. XRD was used effectively to characterise Ag-glycogen nanocomposite films developed by Božanić and coworkers [33].

6.4.3 Dynamic Light Scattering (DLS)

DLS is a technique that can be used to measure the profile size and or distribution of particles held in a solution or suspension. The laser energy produced from the instrument hits the particles and scatters (Rayleigh scattering); these motion data are then processed to derive a size distribution of the given sample, where the size is given by the Stokes radius of the particle. This is of particular relevance to nanoparticles which can be characterised in this manner. The key strengths of this method include:

- (a) Analysis of samples containing broad distributions of species of different molecular masses can be measured;

- (b) Small amounts of higher mass species can be detected; and
- (c) Batch mode processing can be carried out, without dilution in most cases [76].

Nanoparticles have been characterised in this manner in a wide range of publications, [77–86] illustrating the versatility of the technique. In particular, Chinnapongse et al. characterised singly dispersed nanoparticles that were a product of free suspensions in natural freshwaters [82], highlighting a potential fate and product for the use of silver nanoparticles when incorporated into a material.

6.4.4 Electrophoretic Mobility Shift Assay (EMSA)

An evaluation of DNA binding capabilities can be realised through the use of EMSA. The technique can determine the effectiveness of binding to a given DNA or ribonucleic acid (RNA) sequence and has the capability of indicating if more than protein is involved in a binding complex sequence. A mobility shift is a type of electrophoretic separation at which different molecules move through a gel at the rate of their size and charge [87–90]. This is of particular relevance to an antimicrobial material, as the effectiveness can be assessed against selected microorganisms. Assays conducted in this manner have been reported in Liu et al. [91] and Wan et al. [92]. In a paper by Wang et al. chiral polymer composites were synthesised using an electrophoretic deposition method [93]. The composites have the potential to be used as cell adhesion antagonists and therefore could present a viable option as a novel antimicrobial material or as applications in the cell-based biosensor fields [94].

6.5 Conclusions

This chapter provides a general guide and overview of characterisation techniques available to researchers studying nano-antimicrobial materials. The techniques typically used for the characterisation of nanomaterials, materials containing nanoparticles and characterisation of the antimicrobial activity where relevant are described.

The techniques described are common to the characterisation of nanotechnology and some are more specific to antimicrobial aspects of nanotechnology. The choice of technique depends on the material properties in question and the information required.

Many studies have focused on the potential antimicrobial activity that nanomaterials possess. Recent work has indicated that the mechanism of preparation and synthesis of the nanomaterials may have additional antimicrobial effects. In order to determine the antimicrobial nature of nanomaterials, the assessment of the attachment of microorganisms on that material is desirable.

This chapter deals with the assessment of materials involving two approaches:

1. The characterisation of the nano-antimicrobial material itself in terms of occurrence and distribution of nanoparticles, fibres, etc., physical characteristics and surface characteristics like roughness or surface energy;
2. The characterisation of the microbial attachment on the surface of the nano-antimicrobial material in terms of adhesion of bacteria or other organisms, scale of development and integrity of a microbial community and identification of the microorganisms.

A range of physical methods are described with key techniques used in the majority of assessments including SEM, LSCM as well as TEM where available. In addition to the physical methods of material assessment, visualisation techniques are also used to assess the nature of the microorganism attachment on the materials under study. These techniques can provide information on the type of organisms interacting with a surface as well as indicating the mechanisms of efficacy of the antimicrobial material, e.g. bacterial cell wall damage, etc.

In addition to the physical characterisation methods, many researchers use biological methods, staining, bacterial enumeration, protein and carbohydrate analysis, etc. to ascertain the viability of a biofilm and the degree of adhesion to the surfaces. It is desirable to utilise physical methods such as visualisation in conjunction with biological assays to confirm the mechanisms of antimicrobial activity and to determine the efficacy of the nano-antimicrobial materials. While there are other physical techniques that are used for the study of materials, those described here relate to the most widely available and widely used methods to provide the required information.

References

1. S. Panigrahi, et al. (2004) General method of synthesis for metal nanoparticles. *J. Nanopart. Res.* 6(4), pp. 411–414.
2. S. D. Solomon, et al. (2007) Synthesis and study of silver nanoparticles. *J. Chem. Educ.* 84(2), pp. 322.
3. W. Li, Q. Jia and H. L. Wang. (2006) Facile synthesis of metal nanoparticles using conducting polymer colloids. *Polymer* 47(1), pp. 23–26.
4. J. R. Morones, et al. (2005) The bactericidal effect of silver nanoparticles. *Nanotechnology* 16(10), pp. 2346–2353.
5. J. Jain, et al. (2009) Silver nanoparticles in therapeutics: Development of an antimicrobial gel formulation for topical use. *Mol. Pharm.* 6(5), pp. 1388–1401.
6. V. Sambhy, et al. (2006) Silver bromide nanoparticle/polymer composites: Dual action tunable antimicrobial materials. *J. Am. Chem. Soc.* 128(30), pp. 9798–9808.
7. B. L. Cushing, V. L. Kolesnichenko and C. J. O'Connor. (2004) Recent advances in the liquid-phase syntheses of inorganic nanoparticles. *Chem. Rev.*, vol. 104, pp. 3893–3946, Sep. 2004.
8. T. Endo, et al. (2008) Stimuli-responsive hydrogel-silver nanoparticles composite for development of localized surface plasmon resonance-based optical biosensor. *Anal. Chim. Acta* 611(2), pp. 205–211.

9. C. Yang, et al. (2003) Highly dispersed metal nanoparticles in functionalized SBA-15. *Chem. Mater* 15(1), pp. 275–280.
10. F. Zeng, et al. (2007) Silver nanoparticles directly formed on natural macroporous matrix and their anti-microbial activities. *Nanotechnology* 18(055605), pp. 055605.
11. S. Y. Kwak, S. H. Kim and S. S. Kim. (2001) Hybrid organic/inorganic reverse osmosis (RO) membrane for bactericidal anti-fouling. 1. preparation and characterization of TiO₂ nanoparticle self-assembled aromatic polyamide thin-film-composite (TFC) membrane. *Environ. Sci. Technol.* 35(11), pp. 2388–2394.
12. V. Stanić, et al. (2010) Synthesis, characterization and antimicrobial activity of copper and zinc-doped hydroxyapatite nanopowders. *Appl. Surf. Sci.* 256(20), pp. 6083–6089.
13. P. Jain and T. Pradeep. (2005) Potential of silver nanoparticle-coated polyurethane foam as an antibacterial water filter. *Biotechnol. Bioeng.* 90(1), pp. 59–63.
14. W. K. Son, J. H. Youk and W. H. Park (2006). Antimicrobial cellulose acetate nanofibers containing silver nanoparticles. *Carbohydr. Polym.* 65(4), pp. 430–434.
15. S. Ghosh, et al. (2010) Antimicrobial activity of highly stable silver nanoparticles embedded in agar–agar matrix as a thin film. *Carbohydr. Res.* 345(15), pp. 2220–2227.
16. J.E. Morris (2008) Nanopackaging: nanotechnologies and electronics packaging, Springer book series.
17. J. Chapman, E. Weir and F. Regan. (2010) Period four metal nanoparticles on the inhibition of biofouling. *Colloids and Surfaces B: Biointerfaces* 78(2), pp. 208–216.
18. G. Nangmenyi, X. Li, S. Mehrabil, E. Mintz, J. Economy, (2011) Silver-modified iron oxide nanoparticle impregnated fiberglass for disinfection of bacteria and viruses in water, *Materials letters*, 65(8) pp 1191–1193
19. Y. Xiang and D. Chen. (2007 10). Preparation of a novel pH-responsive silver nanoparticle/poly(HEMA–PEGMA–MAA) composite hydrogel. *European Polymer Journal*, 43(10), pp. 4178–4187.
20. R. Dastjerdi and M. Montazer. (2010 8/1). A review on the application of inorganic nanostructured materials in the modification of textiles: Focus on anti-microbial properties. *Colloid. Surface. B* 79(1), pp. 5–18.
21. M. E. Samberg, P. E. Orndorff and N. Monteiro-Riviere. (2010 11/01; 2011/02). Antibacterial efficacy of silver nanoparticles of different sizes, surface conditions and synthesis methods. *Nanotoxicology* pp. 1–10. Available: <http://dx.doi.org/10.3109/17435390.2010.525669>
22. H. G. Hansma and L. Pietrasanta. (1998) Atomic force microscopy and other scanning probe microscopies. *Curr. Opin. Chem. Biol.* 2(5), pp. 579–584.
23. J. Roqué, et al. (2005) Evidence of nucleation and growth of metal Cu and Ag nanoparticles in lustre: AFM surface characterization. *J. Non Cryst. Solids* 351(6–7), pp. 568–575.
24. G. Binnig, C. F. Quate and C. Gerber. (1986) Atomic force microscope. *Phys. Rev. Lett.* 56(9), pp. 930–933.
25. J. Verran, et al. (2010) Use of the atomic force microscope to determine the strength of bacterial attachment to grooved surface features. *J. Adhes. Sci. Technol.* 24 13(14), pp. 2271–2285.
26. B. C. van der Aa and Y. F. Dufrière. (2002 2) In situ characterization of bacterial extracellular polymeric substances by AFM. *Colloid. Surface. B* 23(2–3), pp. 173–182.
27. V. Stanić, et al. (2011 2/15) Synthesis of antimicrobial monophase silver-doped hydroxyapatite nanopowders for bone tissue engineering. *Appl. Surf. Sci.* 257(9), pp. 4510–4518.
28. I. B. Beech. (1996) The potential use of atomic force microscopy for studying corrosion of metals in the presence of bacterial biofilms — an overview. *Int. Biodeterior. Biodegrad.* 37 (3–4), pp. 141–149.
29. I. B. Beech, et al. (2002 2) The use of atomic force microscopy for studying interactions of bacterial biofilms with surfaces. *Colloid. Surface. B* 23(2–3), pp. 231–247.
30. S. Shrivastava, et al. (2007) Characterization of enhanced antibacterial effects of novel silver nanoparticles. *Nanotechnology* 18, pp. 225103.
31. J. Park, et al. (2005) One-nanometer-scale size-controlled synthesis of monodisperse magnetic iron oxide nanoparticles. *Angew. Chem. Int. Ed.* 44(19), pp. 2872–2877.

32. W. A. Daoud, J. H. Xin and Y. H. Zhang. (2005) Surface functionalization of cellulose fibers with titanium dioxide nanoparticles and their combined bactericidal activities. *Surf. Sci.* 599 (1–3), pp. 69–75.
33. D. K. Božanić, et al. (2011 1/10). Silver nanoparticles encapsulated in glycogen biopolymer: Morphology, optical and antimicrobial properties. *Carbohydr. Polym.* 83(2), pp. 883–890.
34. J. M. Thomas, et al. (2008 05/01). Electron holography for the study of magnetic nanomaterials. *Acc. Chem. Res.* 41(5), pp. 665–674. Available: <http://dx.doi.org/10.1021/ar700225v>
35. O. Choi, et al. (2010 12). Interactions of nanosilver with escherichia coli cells in planktonic and biofilm cultures. *Water Res.* 44(20), pp. 6095–6103. Available: <http://www.sciencedirect.com/science/article/B6V73-50GJ2H2-2/2/9c64599a3eae0f260bf0c0957a8e9d8c>
36. N. Cioffi, et al. (2005) Synthesis, analytical characterization and bioactivity of ag and cu nanoparticles embedded in poly-vinyl-methyl-ketone films. *Anal. Bioanal. Chem.* 382(8), pp. 1912–1918.
37. T. R. Neu and J. R. Lawrence. (2010). Extracellular polymeric substances in microbial biofilms, in *Microbial Glycobiology* Otto Holst, Patrick J. Brennan and Mark von Itzstein, Eds.
38. M. Obst, et al. (2009 7/15). Precipitation of amorphous CaCO₃ (aragonite-like) by cyanobacteria: A STXM study of the influence of EPS on the nucleation process. *Geochim. Cosmochim. Acta* 73(14), pp. 4180–4198.
39. V. Lazarova and J. Manem. (1995 10) Biofilm characterization and activity analysis in water and wastewater treatment. *Water Res.* 29(10), pp. 2227–2245.
40. P. S. Stewart, et al. (1995 8) Biofilm structural heterogeneity visualized by three microscopic methods. *Water Res.* 29(8), pp. 2006–2009.
41. P. S. Stewart and J. William Costerton. (2001 7/14) Antibiotic resistance of bacteria in biofilms. *The Lancet* 358(9276), pp. 135–138.
42. G. Wolf, J. G. Crespo and M. A. M. Reis. (2002) Optical and spectroscopic methods for biofilm examination and monitoring. *Rev. Environ. Sci. Biotechnol.* 1(3), pp. 227–251.
43. Y. Zhang, et al. (2008 9/15) Facile preparation and characterization of highly antimicrobial colloid ag or au nanoparticles. *J. Colloid Interface Sci.* 325(2), pp. 371–376.
44. M. G. Weinbauer, C. Beckmann and M. G. Hofle. (1998) Utility of green fluorescent nucleic acid dyes and aluminum oxide membrane filters for rapid epifluorescence enumeration of soil and sediment bacteria. *Appl. Environ. Microbiol.* 64(12), pp. 5000.
45. W. S. Rasband and U. ImageJ. (1997) National institutes of health. *Bethesda, Maryland, USA 2007*
46. L. C. Simões, et al. (2006) Drinking water biofilm assessment of total and culturable bacteria under different operating conditions. *Biofouling* 22(2), pp. 91–99.
47. A. Kerr, et al. (1998 4) The early stages of marine biofouling and its effect on two types of optical sensors. *Environ. Int.* 24(3), pp. 331–343.
48. C. Leroy, et al. (2007) A marine bacterial adhesion microplate test using the DAPI fluorescent dye: A new method to screen antifouling agents. *Lett. Appl. Microbiol.* 44(4), pp. 372–378.
49. T. Schmid, et al. (2004 3) Investigation of biocide efficacy by photoacoustic biofilm monitoring. *Water Res.* 38(5), pp. 1189–1196.
50. T. P. Trainor, A. S. Templeton and P. J. Eng. (2006 2) Structure and reactivity of environmental interfaces: Application of grazing angle X-ray spectroscopy and long-period X-ray standing waves. *J. Electron Spectrosc.* 150(2–3), pp. 66–85.
51. X. Liu, et al. (2007) Fabrication and characterization of Ag/polymer nanocomposite films through layer-by-layer self-assembly technique. *Thin Solid Films* 515(20–21), pp. 7870–7875.
52. J. Grivet and A. Delort. (2009 1) NMR for microbiology: In vivo and in situ applications. *Prog. Nucl. Magn. Reson. Spectrosc.* 54(1), pp. 1–53.
53. L. Brecker and D. W. Ribbons. (2000 5/1) Biotransformations monitored in situ by proton nuclear magnetic resonance spectroscopy. *Trends Biotechnol.* 18(5), pp. 197–202.
54. H. S. Vrouwenvelder, et al. (1998 9/20) Biofouling of membranes for drinking water production. *Desalination* 118(1–3), pp. 157–166.

55. L. Baia and S. Simon. (2007) UV-VIS and TEM assessment of morphological features of silver nanoparticles from phosphate glass matrices.
56. V. K. Sharma, R. A. Yngard and Y. Lin. (2009 1/30) Silver nanoparticles: Green synthesis and their antimicrobial activities. *Adv. Colloid Interface Sci.* 145(1–2), pp. 83–96.
57. A. Slistan-Grijalva, et al. (2005) Classical theoretical characterization of the surface plasmon absorption band for silver spherical nanoparticles suspended in water and ethylene glycol. *Phys. E: Low-Dimens. Sys. Nanostructures* 27(1–2), pp. 104–112.
58. C. Lee, et al. (2011 4/6) Transmembrane pores formed by human antimicrobial peptide LL-37. *Biophys. J.* 100(7), pp. 1688–1696.
59. T. Fekete, et al. (1994 4) A comparison of serial plate agar dilution, bauer-kirby disk diffusion, and the vitek automicrobic system for the determination of susceptibilities of klebsiella spp., enterobacter spp., and pseudomonas aeruginosa to ten antimicrobial agents. *Diagn. Microbiol. Infect. Dis.* 18(4), pp. 251–258.
60. V. Sambhy, et al. (2005) Silver bromide nanoparticle/polymer composites: Dual action tunable antimicrobial materials. *Molecules* 6, pp. 514–520.
61. D. Kim, et al. (2007 6/25) Formation and immobilization of silver nanoparticles onto chromia surface by novel preparation route involving polyol process. *Surf. Coat. Technol.* 201(18), pp. 7663–7667.
62. A. R. Shahverdi, et al. (2007) Synthesis and effect of silver nanoparticles on the antibacterial activity of different antibiotics against staphylococcus aureus and escherichia coli. *Nanomedicine: Nanotechnology, Biol. Med.* 3(2), pp. 168–171.
63. I. Sondi and B. Salopek-Sondi. (2004) Silver nanoparticles as antimicrobial agent: A case study on E. coli as a model for gram-negative bacteria. *J. Colloid Interface Sci.* 275(1), pp. 177–182.
64. S. Pal, Y. K. Tak and J. M. Song. (2007 3) Does the antibacterial activity of silver nanoparticles depend on the shape of the nanoparticle? A study of the Gram-negative bacterium Escherichia coli. *Appl. Environ. Microbiol.* 73, pp. 1712–1720.
65. P. A. Suci, J. D. Vraný and M. W. Mittelman. (1998) Investigation of interactions between antimicrobial agents and bacterial biofilms using attenuated total reflection fourier transform infrared spectroscopy. *Biomaterials* 19(4–5), pp. 327–339.
66. D. Osiro, et al. (2004) A kinetic model for xylella fastidiosa adhesion, biofilm formation, and virulence. *FEMS Microbiol. Lett.* 236(2), pp. 313–318.
67. M. Kansız, et al. (1999) Fourier transform infrared microspectroscopy and chemometrics as a tool for the discrimination of cyanobacterial strains. *Phytochemistry* 52(3), pp. 407–417.
68. D. Naumann. (2000) Infrared spectroscopy in microbiology.
69. N. Branan and T. A. Wells. (2007) Microorganism characterization using ATR-FTIR on an ultrathin polystyrene layer. *Vib. Spectrosc.* 44(1), pp. 192–196.
70. G. Gunasekaran, et al. (2004 8). Influence of bacteria on film formation inhibiting corrosion. *Corros. Sci.* 46(8), pp. 1953–1967.
71. S. Chongdar, G. Gunasekaran and P. Kumar. (2005 8/30) Corrosion inhibition of mild steel by aerobic biofilm. *Electrochim. Acta* 50(24), pp. 4655–4665.
72. C. Sandt, et al. (2008 9) Quantification of local water and biomass in wild type PA01 biofilms by confocal raman microspectroscopy. *J. Microbiol. Methods* 75(1), pp. 148–152.
73. M. Strathmann, J. Wingender and H. Flemming. (2002 8). Application of fluorescently labelled lectins for the visualization and biochemical characterization of polysaccharides in biofilms of pseudomonas aeruginosa. *J. Microbiol. Methods* 50(3), pp. 237–248.
74. N. Abu Bakar, J. Ismail and M. Abu Bakar. (2007) Synthesis and characterization of silver nanoparticles in natural rubber. *Mater. Chem. Phys.* 104(2–3), pp. 276–283.
75. M. Montazer, et al. Photo induced silver on nano titanium dioxide as an enhanced antimicrobial agent for wool. *J. Photoch. Photobiolo. B* (In Press, Corrected Proof)
76. S. K. Brar and M. Verma. (2011 1) Measurement of nanoparticles by light-scattering techniques. *TRAC-Trend. Anal. Chem.* 30(1), pp. 4–17.
77. T. Zhang, T. F. Sturgis and B. C. Youan. pH-responsive nanoparticles releasing tenofovir for the prevention of HIV transmission. *Eur. J. Pharm. Biopharm.* (In Press, Accepted Manuscript)

78. S. Jaiswal, et al. (2010 9) Enhancement of the antibacterial properties of silver nanoparticles using β -cyclodextrin as a capping agent. *Int. J. Antimicrob. Agents* 36(3), pp. 280–283.
79. A. Bankar, et al. (2010 10/1) Banana peel extract mediated synthesis of gold nanoparticles. *Colloid. Surface. B* 80(1), pp. 45–50.
80. H. Zhou, et al. (2011 2) Nucleic acids determination using the complex of eriochrome black T and silver nanoparticles in a resonance light scattering technique. *Spectrochim. Acta A* 78(2), pp. 681–686.
81. F. Rispoli, et al. (2010 8/15) Understanding the toxicity of aggregated zero valent copper nanoparticles against *Escherichia coli*. *J. Hazard. Mater.* 180(1–3), pp. 212–216.
82. S. L. Chinnapongse, R. I. MacCuspie and V. A. Hackley. (2011 5/15) Persistence of singly dispersed silver nanoparticles in natural freshwaters, synthetic seawater, and simulated estuarine waters. *Sci. Total Environ.* 409(12), pp. 2443–2450.
83. Y. H. Ngo, et al. (2011 3/15) Paper surfaces functionalized by nanoparticles. *Adv. Colloid Interface Sci.* 163(1), pp. 23–38.
84. J. C. Garay-Jimenez and E. Turos. A convenient method to prepare emulsified polyacrylate nanoparticles from for drug delivery applications. *Bioorg. Med. Chem. Lett.* (In Press, Corrected Proof)
85. I. Rezić. Determination of engineered nanoparticles on textiles and in textile wastewaters. *TRAC-Trend. Anal. Chem.* (In Press, Corrected Proof)
86. J. Zhang, et al. (2007 12) Self-assembled nanoparticles based on hydrophobically modified chitosan as carriers for doxorubicin. *Nanomedicine: Nanotechnology, Biol. Med.* 3(4), pp. 258–265.
87. Y. Lee, et al. (2006 11/10) Preparation of au colloids by polyol process using NaHCO_3 as a buffering agent. *Mater. Chem. Phys.* 100(1), pp. 85–91.
88. L. Huo, et al. Antimicrobial and DNA-binding activities of the peptide fragments of human lactoferrin and histatin 5 against *Streptococcus mutans*. *Arch. Oral Biol.* (In Press, Corrected Proof)
89. R. Potter, L. Truelstrup Hansen and T. A. Gill. (2005 8/15) Inhibition of foodborne bacteria by native and modified protamine: Importance of electrostatic interactions. *Int. J. Food Microbiol.* 103(1), pp. 23–34.
90. D. Guzey and D. J. McClements. (2006 1) Characterization of β -lactoglobulin–chitosan interactions in aqueous solutions: A calorimetry, light scattering, electrophoretic mobility and solubility study. *Food Hydrocoll.* 20(1), pp. 124–131.
91. S. -. Liu, et al. (2000) Lipophilization of lysozyme by short and middle chain fatty acids. *J. Agric. Food Chem.* 48(2), pp. 265–269.
92. J. Wan, A. Wilcock and M. J. Coventry. (1998) The effect of essential oils of basil on the growth of *Aeromonas hydrophila* and *Pseudomonas fluorescens*. *J. Appl. Microbiol.* 84(2), pp. 152–158.
93. Y. Wang, X. Pang and I. Zhitomirsky. Electrophoretic deposition of chiral polymers and composites. *Colloid. Surface. B* (In Press, Corrected Proof)
94. I. Hirata, et al. (2000) Surface modification of Si₃N₄-coated silicon plate for investigation of living cells. *Jpn. J. Appl. Phys., Part 1* 39(11), pp. 6441–6442.

Section II
Bioactivity and Mechanisms of Action of
Nano-Antimicrobials

Chapter 7

Silver Nanoparticles as Nano-Antimicrobials: Bioactivity, Benefits and Bottlenecks

Mahendra Rai, Alka Yadav, and Nicola Cioffi

7.1 Introduction

Nanotechnology is defined as miniaturization of structures with a dimension less than 100 nm. It is a field of applied science and technology whose unifying theme relates to control of matter at the molecular level in scales smaller than 1 μm for fabrication of materials (Rai et al. 2009a; Sau and Rogach 2010). The term “nanotechnology” was introduced by physicist Professor Richard Feynman in his historical talk “There’s plenty of room at the bottom”. Feynman envisioned the manipulation of atoms by developing small-scale machine tools that would evolve into future generations of smaller and smaller tools (Feynman 1959), while Professor Norio Taniguchi coined the term nanotechnology to describe precision manufacturing of materials at the nanoscale level (Taniguchi 1974).

Nanoparticles can be explained as microscopic particles with size 1–100 nm (Sharma et al. 2009). Nanoparticles exhibit a number of special properties relative to bulk material as they possess a very high surface area to volume ratio (Rai et al. 2008). Nanoparticles can be synthesized using different methods, including chemical, physical, and biological (Rai et al. 2009b; Sau and Rogach 2010; Thakkar et al. 2010). Nanoparticles are classified on the basis of material into metallic, bimetallic or core–shell and semiconductor nanoparticles (Liu 2006; Song and Kim 2009). Metal nanoparticles like silver, gold, platinum, zinc, silica, and titanium have many applications and are used in a number of fields including medicine, pharmacology, environmental monitoring, and electronics (Liu 2006; Huang et al. 2007; Rai et al. 2008; Kumar and Yadav 2009; Thakkar et al. 2010).

M. Rai (✉) • A. Yadav
Department of Biotechnology, Sant Gadge Baba Amravati University, Amravati,
Maharashtra, India
e-mail: mkrai123@rediffmail.com; pmkrai@hotmail.com

N. Cioffi
Dipartimento di Chimica, Università degli Studi di Bari “Aldo Moro”, Bari, Italy

Silver has been used widely for thousands of years in different applications like jewellery, utensils, water purification, dental alloys, photography, etc. (Chen and Schluenser 2008). The much exploited properties of silver are in areas of hygiene and medicine (Castellano et al. 2007; Sharma et al. 2009). Silver vessels have been used since ancient times to preserve water and wine (Chen and Schluesener 2008; Thakkar et al. 2010). The German scientist C.S.F. Crede in 1884 used 1% silver nitrate in the form of eye drops for the treatment of ophthalmia neonatorum (Landsdown 2002), while Moyer in 1960 used 0.5% silver nitrate for the treatment of burns (Moyer et al. 1965). In 1968, silver nitrate was combined with sulfonamide to form silver sulfadiazine cream which proved to be a broad-spectrum antimicrobial agent and was used in treatment of burns (Fox and Modak 1974). The introduction of different broad spectrum antibiotics reduced the use of silver, but with the advancement of modern science and engineering technologies, metallic silver has made a comeback in the form of silver nanoparticles (Duran et al. 2007; Sharma et al. 2009). Due to their extremely small size, SNPs show significant physicochemical properties and biological activities (Rai et al. 2009a, b).

Silver nanoparticles (SNPs) are nanosized particles of silver with size 1–100 nm (Sharma et al. 2009). SNPs can be synthesized using physical, chemical, and biological methods (Rai et al. 2008; Mohanpuria et al. 2008; Gade et al. 2010). SNPs in their present form show improved physical, chemical, and optical properties compared to bulk metal and thus are efficient in killing microbes (Kim et al. 2007; Kumar and Yadav 2009; Pattabi et al. 2010). Thus, SNPs in the present scenario are harnessed as efficient antimicrobial agents (Sanghi and Verma 2009; Saxena et al. 2010). The present review focuses on SNPs as antimicrobial agents, their activity against different microorganisms, different applications offered by SNPs, and also implications of SNPs.

7.2 Bioactivity of Silver Nanoparticles Against Pathogenic Micro-organisms

The antimicrobial activity of silver ions has been documented by clinicians over several years (Matsumura et al. 2003; Leaper 2006; Chen and Schluesener 2008; Rai et al. 2009a). SNPs possess unique physical and chemical properties due to their large surface area compared to volume, which provides better contact with microorganisms (Gong et al. 2007; Rai et al. 2009a; Lara et al. 2010). Due to these improved properties, SNPs get attached to the cell membrane and penetrate inside the microbial cell (Egger et al. 2009; Jo et al. 2009; Gajbhiye et al. 2009). The microbial cell contains electron donor groups like sulfur, oxygen, and nitrogen. Electrostatic interaction takes place between negatively charged electron donor groups and positively charged SNPs, which brings structural and functional changes in the microbial cell membrane (Lala et al. 2007; Rai et al. 2009a; Sharma et al. 2009). The nanoparticles also attack on the respiratory chain and cell division

finally leading to cell death (Feng et al. 2000; Sondi and Salopek 2004; Morones et al. 2005; Lala et al. 2007; Rai et al. 2009a; Pattabi et al. 2010).

The size, shape, and dispersity of SNPs have also been shown to have immense impact on the antimicrobial efficacy of SNPs (Sondi and Salopek 2004; Pal et al. 2007; Rai et al. 2009a). The nano size of the particles possesses a large surface area for contact with the microbial cell and hence exhibits better interaction than bigger particles (Morones et al. 2005; Rai et al. 2009a; Egger et al. 2009). Regarding the shape of nanoparticles, truncated and triangular nanoparticles show better inhibition (Pal et al. 2007). Thus, among the different antimicrobial agents involved, silver as an antimicrobial agent possesses great potential and can be used efficiently in diverse applications (Gade et al. 2008; Sharma et al. 2009; Lara et al. 2010). Gade et al. (2008) observed the potential bioactivity of silver nanoparticles produced by *Aspergillus niger*. They obtained spherical particles of around 20 nm that showed maximum activity against *S. aureus* and minimum activity against *E. coli* (Fig. 7.1).

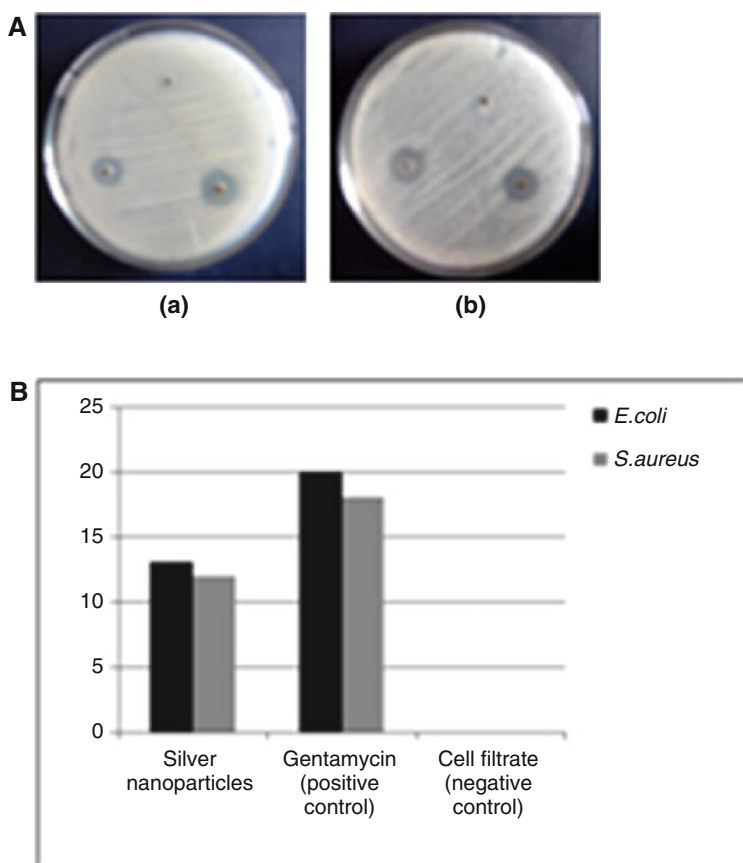


Fig. 7.1 (a) Antibacterial activity of silver nanoparticles against (1) *Escherichia coli* and (2) *Staphylococcus aureus*, in each image: (a) cell filtrate, (b) Gentamycin and (c) silver nanoparticles. (b) Graphical representation of the size of zone of inhibition for the four tested bacteria cultures (Image adopted from Gade et al. 2008)

Silver has long been known to possess strong bactericidal activity, and with the advent of SNPs it has become an eminent antibacterial, antifungal, and antiviral agent (Rai et al. 2009a; Lara et al. 2010).

7.2.1 Antibacterial Activity of Silver Nanoparticles

Gong et al. (2007) synthesized $\text{Fe}_3\text{O}_4@\text{Ag}$ nanoparticles possessing super paramagnetic properties, which showed excellent antibacterial activity against *Escherichia coli*, *Staphylococcus epidermis*, and *Bacillus subtilis*. The authors observed that the antibacterial potential of SNPs was better against Gram-negative bacteria compared to Gram-positive bacteria. Ingle et al. (2008) also observed efficient antibacterial activity of SNPs biosynthesized using *Fusarium acuminatum* against *E. coli* and *S. aureus* (Fig. 7.2).

Jung et al. (2008) studied the antibacterial activity of SNPs against *E. coli* and *S. aureus* in experiments using a silver laundry machine with contaminated fabric. The authors found that the efficacy of SNPs was better against *E. coli* than against *S. aureus* possibly due to the thickness of the peptidoglycan layer. Nithya and Raghunathan (2009) also reported that SNPs show more activity against Gram-negative bacteria compared to Gram-positive bacteria due to the presence of a peptidoglycan layer in case of Gram positive bacteria. Similar findings were also reported by Esteban-Tejeda et al. (2009) while evaluating antibacterial activity of SNPs against Gram-negative and Gram-positive bacteria. Birla et al. (2009) studied the antibacterial activity of SNPs along with commercially available antibiotics against *E. coli* and *S. aureus*. The authors reported comprehensive activity of SNPs against Gram-positive and Gram-negative bacteria. Gade et al. (2010) also reported

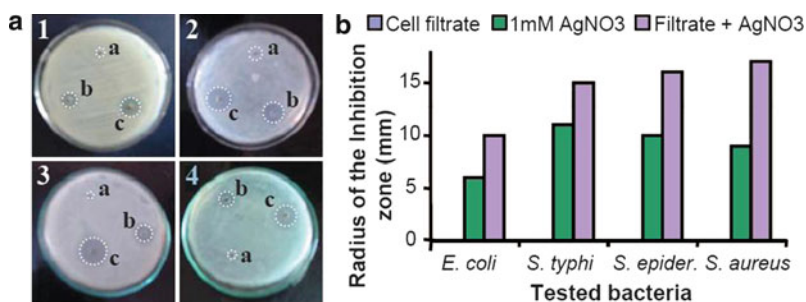


Fig. 7.2 (a) Antibacterial activity of silver nanoparticles against (1) *Escherichia coli*, (2) *Salmonella typhi*, (3) *Staphylococcus epidermis* and (4) *S. aureus*. In each image: (a) Cell filtrate, (b) AgNO_3 (1 mM) and (c) silver nanoparticles. (b) Graphical representation of the size of the zone of inhibition for the four tested bacterial cultures (Image reprinted with permission from Ingle et al. 2008)

remarkable antibacterial activity of SNPs in combination with antibiotics. Patabi et al. (2010) evaluated the antibacterial activity of SNPs against selected Gram-positive and Gram-negative bacteria and found that SNPs showed the maximum activity against Gram-negative bacteria while the minimum activity was observed against Gram-positive bacteria. Saxena et al. (2010) also depicted effective antibacterial activity of SNPs against *E. coli* and *Salmonella typhimurium*. Kathiresan et al. (2010) synthesized silver nanoparticles using *E. coli* and *Aspergillus niger* isolated from coastal mangroves of southeast India. These biosynthesized silver nanoparticles from bacteria and fungi were further tested for their antimicrobial activity, and it was found that the silver nanoparticles possess more pronounced antibacterial activity while the antifungal activity was comparatively less distinct. Also, the antimicrobial activity of silver nanoparticles synthesized from *E. coli* was better compared to silver nanoparticles synthesized from *A. niger*. Similar results were also obtained by Mubarakali et al. (2011) using *Mentha piperita* extract for synthesis of silver and gold nanoparticles. The silver nanoparticles were active against clinically isolated pathogens, *E. coli* and *S. aureus*. Li et al. (2011) studied the antibacterial activity and also the mechanism of action of silver nanoparticles against *S. aureus*. For the study, bacterial cells were treated with increasing concentrations of SNPs for a time period of 6–12 h. After treating the bacterial cells with 50 µg/mL SNPs for 6 h, the DNA of the bacterial cell was condensed to a tension state and also stopped replicating, while after an exposure of 12 h with 50 µg/mL SNPs, the bacterial cell completely broke down with release of its cellular components into the surrounding environment. Sintubin et al. (2011) also investigated the antibacterial activity of SNPs and its mode of action. The authors found that antibacterial activity of SNPs is mainly related to the release of silver ions and, due to the release of higher concentration of free silver ions, the activity of biogenic SNPs is better compared to ionic silver.

7.2.2 Antifungal Activity of Silver Nanoparticles

SNPs are also known to possess broad spectrum antifungal activity (Sharma et al. 2009; Gajbhiye et al. 2009). Esteban-Tejeda et al. (2009) reported efficient antifungal activity of soda lime containing SNPs against *L. oreintalis*. The authors correlated the higher antifungal activity to inhibitory effects of Ca^{2+} percolated from soda lime containing SNPs on the fungal cells. Jo et al. (2009) reported that SNPs also show remarkable activity against phytopathogenic fungi. Gajbhiye et al. (2009) studied antifungal activity of SNPs in combination with fluconazole against *Phoma glomerata*, *Phoma herbarum*, *Fusarium semitectum* and *Trichoderma* sp. The antifungal activity of SNPs was found to be increased in combination with fluconazole. The maximum inhibition was reported against *P. glomerata* and *Trichoderma* sp. while, for *P. herbarum* and *F. semitectum*, no significant activity was observed.

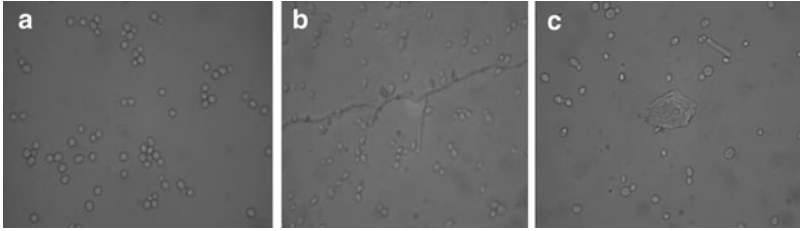


Fig. 7.3 The effect of nano-Ag on the dimorphic transition in *C. albicans*. Yeast control without 20% FBS and nano-Ag (a), without treated nano-Ag (b), or with 2 $\mu\text{g/mL}$ of nano-Ag (c) (Image adopted from Keuk-Jun et al. 2008)

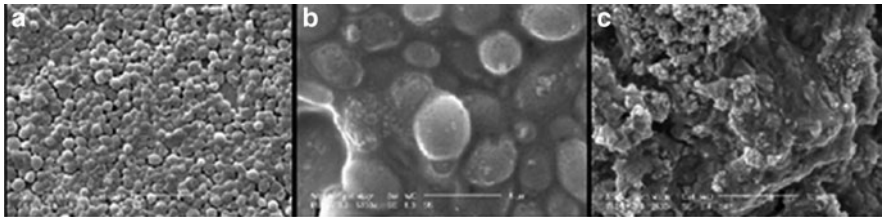


Fig. 7.4 Scanning electron microscopy images of *Candida albicans*. Normal cells (A) and cells influence by 0.5mg/ml (MIC 50) concentration of Ag-NPs (B) and cells influence by 2 mg/ml (MIC 90) concentration of Ag-NPs (C) (10ppm) (Reprinted with permission from Nashrollahi et al. 2011).

Anticandidal activity of SNPs was evaluated by Keuk-Jun et al. (2008) against *Candida* sp. (*C. albicans*, *C. glabrata*, *C. parapsilosis*). The authors reported that SNPs show prominent activity against *C. albicans* and *C. glabrata* at low concentrations but it showed the minimum activity against *C. parapsilosis* (Fig. 7.3).

Kim et al. (2008) also reported that SNPs showed considerable antifungal activity against *Candida* sp. Egger et al. (2009) studied antimicrobial activity of silver nanocomposites, silver nitrate and silver zeolite. The results of the MIC (Minimum Inhibitory Concentration) and MBC (Minimum Bactericidal Concentration) showed that maximum activity of SNPs was found against *C. albicans* compared to silver nitrate and silver zeolite. Panacek et al. (2009) reported effective antifungal activity of SNPs against *Candida* sp. The authors also studied the MIC, MFC and time dependency and found that SNPs at 0.2 mg/L concentration inhibited candidal growth. Gajbhiye et al. (2009) also studied anticandidal activity of SNPs. The authors reported the maximum activity of SNPs against *C. albicans*. Nasrollahi et al. (2011) reported the antifungal activity of silver nanoparticles against *C. albicans* and *Saccharomyces cerevisiae* using the MIC technique and compared with antifungal drugs like Amphotericin B and Fluconazole. The authors found that SNPs possess considerable activity compared to the commercially available antifungal agents (Fig. 7.4). Lkhagvajav et al. (2011) also

reported antifungal activity of SNPs against *C. albicans* and found that only a small quantity of nanosilver (2–4 µg/mL) is required to completely inhibit the growth of fungus.

7.2.3 Antiviral Activity of Silver Nanoparticles

SNPs are also observed to show efficient antiviral activity. It has been reported that SNPs undergo size-dependent interaction with HIV-1 virus (Elechiguerra et al. 2005). HIV-1 virus consists of a lipid membrane intervened with a glycoprotein knob which comprises two sub-units, gp120 surface glycoprotein subunit and gp41 trans-membrane subunit. The main function of the gp120 subunit is to bind with CD4 receptor sites on host cells (Foster et al. 2000). The gp subunit consists of nine disulfide bonds out of which three are located in the vicinity of the CD4 binding domain and these exposed disulfide bonds form the preferential sites for the SNPs to bind with HIV-1 virus. Also, the spatial arrangement and the center to center spacing arrangement of the glycoprotein knob (~22 nm) are similar to those of SNPs (~28 nm). Hence, it could be presumed that the spatial arrangement, the center to center distance between nanoparticles and the preferential binding to disulfide bonds and glycoprotein knobs suggest the strong interaction of SNPs to the HIV-I virus. Also, the smaller size of nanoparticles (<14 nm) serve for a more stable surface interaction (Elechiguerra et al. 2005; Kumar and Yadav 2009). Lara et al. (2010) also explained the antiviral action of SNPs against HIV-1 depicting that SNPs act as a virucidal agent by binding to gp120 and preventing CD4-dependent virion binding, fusion, and infectivity. The authors depicted that SNPs show antiviral activity at an early stage of replication. Also, the resistance developed by antiretroviral HIV strains does not affect the efficiency of SNPs. Virus adsorption assay was conducted to study binding of virus or fusion at initial stages of the HIV-1 cycle; gp120 capture ELISA and cell-based fusion assay were also conducted. It was observed from the above tests that the antiviral activity of SNPs increase with incubation time. Thus, the authors hypothesized that SNPs initially bind with gp120 and inhibit viral activity by irreversibly modifying viral structures. Also, silver ions possess the capability to complex with electron donor groups like sulfur, oxygen or nitrogen, and, hence, inhibit the post-entry stages of viral infection by blocking HIV-1 proteins and other gp120 or reducing reverse transcription or proviral transcription by directly binding to DNA or RNA (Lara et al. 2010).

7.3 Different Benefits of Bioactivity: Multiple Applications

Due to efficient antimicrobial potential, SNPs show varied applications in different areas of science and technology (Richardson et al. 2006; Mohanpuria et al. 2008; Rai et al. 2009a; Thakkar et al. 2010)

- Dressings play a major role in the treatment of wounds whether it is an open or chronic wound by prevention of infection (Rai et al. 2009b). Dressings impregnated with silver are called silver dressings. Since historic times, silver has been known as an antibacterial agent and used for the treatment of burns. Hence, SNPs- coated dressings are used in the present scenario as they provide the highest and sustained release of silver to a wound without any toxicity (Leaper 2006). SNPs containing creams and gel are also observed to effectively reduce bacterial infections in chronic wounds (Richard et al. 2002; Leaper 2006; Ip et al. 2006; Sharma et al. 2009). Jain et al. (2009) reported excellent antifungal and anticandidal activity of antimicrobial gel formulated using silver nanoparticles.
- Wound healing is a complex process with the ultimate aim of speedy and scarless recovery of wounds (Jain et al. 2009). SNPs have become a new therapeutic approach in treatment of burn wounds (Jain et al. 2009; Rai et al. 2009a). SNPs are reported to show better wound healing capacity and better cosmetic appearance with fewer scars when tested on burn wounds of an animal model (Tian et al. 2006). In the present study, SNPs depicted positive effects through their antimicrobial properties, reduction in wound inflammation, and modulation of fibrogenic cytokines.
- Surface coating of medical devices with silver nanoparticles is a proficient technique to reduce medical device-related infections (Rai et al. 2009b). In this application, SNPs are directly deposited on medical device surfaces or applied in a polymeric surface coating (Knetsch and Koole 2011). Medical devices like surgical masks, implantable impregnated with SNPs, show significant antimicrobial efficacy (Furno et al. 2004; Rai et al. 2009b; Kumar and Yadav 2009). Catheters coated with SNPs are found to be active against most of the noscomial infections related to catheters which predominantly accumulate at the site of insertion. SNPs serve as a protective means against these infections with no risk of systemic toxicity (Roe et al. 2008).
- Household oil paints are generally prepared from vegetable-derived drying oils which contain a variety of polyunsaturated fatty acids. Development of bactericidal coatings using green chemical protocols could be an environmental-friendly application of common household paints (Kumar et al. 2008). Eco-friendly nanopaints embedded with SNPs are found to possess excellent antimicrobial activity against Gram-positive and Gram-negative bacteria and can be directly used on different surfaces like wood, glass, steel, etc. (Kumar et al. 2008; Rai et al. 2009b).
- In recent years, ready to eat food products have gained considerable demand due to their fresh-like and healthy features (Fernandez et al. 2010). Food packaging systems with proper antimicrobial efficacy could actively prevent post-processing contamination and increase shelf life of food products (Fernandez et al. 2009). Silver in trace quantities functions as a broad-spectrum antimicrobial agent and prevents biofilm preparation in food-contact surfaces (Rai et al. 2009b; Fernandez et al. 2010). Silver zeolite is used in food preservation, disinfection and decontamination of products (Matsumura et al. 1997; Nikawa

et al. 1997; Nair and Laurencin 2007). Nanocoating of fruits and vegetables with the help of SNPs has emerged as a recent interest in the field of food nanotechnology, protecting the fruits and vegetables by applying a waxy coat does not safeguard them from water loss and high respiration rate and thus results in loss of water and protein during storage. This technique also increases the shelf life of food products (Fayaz et al. 2009).

- Increasing pollution and ground water contamination from a wide variety of industrial, municipal and agricultural sources has seriously tainted water quality in these sources, effectively reducing the supply of freshwater for human use (Jain and Pradeep 2005). Nanoparticles and nanostructured membranes contribute towards the development of efficient and cost-effective water filtration technology (Theron et al. 2008). SNPs-coated polyurethane foams can be used for drinking water filtration where there is a high risk of bacterial contamination (Jain and Pradeep 2005; Parikh et al. 2008). Silver nanoparticle and chitosan composites form a cost-effective means of removing pesticides from drinking water (Saiffudin et al. 2011).
- SNPs are used as selective coatings for absorption of solar energy and intercalation material for electrical batteries, as catalyst in chemical reactions, as fluorescents and as optical receptors (Safaepour et al. 2009; Sau and Rogach 2010). Recently, smart gating nanochannels are being devised which can be used for photoelectric conversion system in specially designed photoelectrochemical cells (PEC). Bioinspired smart switching surfaces have been devised using semiconductor nanoparticles which can respond to external stimuli like temperature, pH, light, electricity, etc. (Wen et al. 2010).
- Nonlinear optical (NLO) materials are essential for high speed optical network systems dealing with a large amount of data. In particular, organic third-order NLO materials are powerful candidates for developing photonic devices, due to their fast response and easy chemical modification in comparison to the inorganic systems (Satyavathi et al. 2010). The other applications of nanoparticles include enhanced Raman scattering, bioreactors, and biosensors (Zhu and Zhou 2011). SNPs have recently been used for the synthesis of eco-friendly nonlinear optical materials (Satyavathi et al. 2010).

7.4 Complications in Use of Silver Nanoparticles

The proficient antimicrobial activity of SNPs makes it a frequently used product in a number of commercial and medical applications (Nair and Laurencin 2007; Sharma et al. 2009; Thakkar et al. 2010). But, due to this wide range of exploitation of SNPs, a number of complications are also involved in this field (Chen and Schluesener 2008; Fadeel and Bennett-Garcia 2010). In most of the studies, it is observed that SNPs are non-toxic in low concentrations (Rai et al. 2009a). But repeated exposure to silver through silver-impregnated dressings results in the forming of agryria (Leaper 2006). SNPs due to their extremely small size and

variable properties are also supposed to be hazardous to the environment (Braydich-Stolle et al. 2005). The toxicity of variable sizes of SNPs was studied by Hussain et al. (2005) using rat liver cell line (BRL 3A) (ATCC, CRL-1442 immortalized rat liver cells). The authors reported that after an exposure of 24 h, the mitochondrial cells displayed abnormal size, cellular shrinkage, and irregular shape. Burd et al. (2007) also studied the cytotoxic effect of five SNPs-impregnated commercially available dressings. In the study, three silver dressings depicted cytotoxicity effects in keratinocytes and fibroblast cultures. Chen and Schluesener (2008) reported that SNPs generally react with proteins and enzymes with thiol groups in the mammalian cells. These proteins and enzymes are responsible for the cells' antioxidant defense mechanism, and SNPs may deplete this antioxidant defense mechanism, which results in the accumulation of reactive oxygen species due to which inflammatory response is initiated and destruction of mitochondria takes place. The interaction of SNPs with thiol group proteins also results in damage of cell membranes as the latter are abundant in thiol group proteins (Chen and Schluesener 2008).

Thus, it can be concluded that the use of nanoparticles in biomedical and therapeutic applications has opened up a new area of nanotechnology, but the possible complications related to the use of SNPs needs to be briefly studied.

7.5 Conclusion and Future Prospects

Among the different antimicrobial agents available, silver has been most extensively studied and used since ancient times to fight infections and prevent spoilage. The antibacterial, antifungal, and antiviral properties of SNPs prove them to be efficient antimicrobial agents in all respects. Hence, SNPs have also found varied applications in textile fabrics, wound dressings, coatings for medical devices and catheters, etc. The major advantage of using SNPs for impregnation in medical devices is that there is continuous release of silver ions, which enhances the better healing of wounds with less chance of infections. But there are certain points which need to be considered before the large-scale exploitation of silver nanoparticles in different commercial applications. The exact mechanism of interaction of SNPs with microbial cells and mammalian cells needs to be briefly studied with the help of animal models and clinical studies. A better understanding of the interaction of SNPs- impregnated dressings and medical devices with open wounds should also be evaluated. Eco-toxicity of nanoparticles is also a matter of great concern as accumulation of large amounts of SNPs in plants may be hazardous to the environment.

Hence, it can be concluded that SNPs are efficient antimicrobial agents with a broad spectrum activity, but certain studies related to the mechanism and toxicity of SNPs need to be appraised.

References

- Braydich-Stolle L, Hussain S, Schlager J, Hofmann M C (2005) *In vitro* cytotoxicity of nanoparticles in mammalian germ line stem cells. *Toxicol Sci* 88:412–419 792
- Birla S S, Tiwari V V, Gade A K, Ingle A P, Yadav A P, Rai M K (2009) Fabrication of silver nanoparticles by *Phoma glomerata* and its combined effect against *Escherichia coli Pseudomonas aeruginosa* and *Staphylococcus aureus*. *Lett Appld Microbiol*, 48: 173–179
- Burd A, Kwok C H, Hung S C, Chan H S, Gu H, Lam W K (2007) A comparative study of the cytotoxicity of silver-based dressings in monolayer cell, tissue explant, and animal Models. *Wound Repair Regener* 15: 94–104
- Castellano J J, Shafiq S M, Ko F, Donate G, Wright T E, Mannari R J, Payne W G, Smith D J, Robson MC (2007) Comparative evaluation of silver-containing antimicrobial dressings and drugs. *Int Wound J* 4(2): 114–122
- Chen X, Schluesener H J (2008) Nanosilver: A nanoparticle in medical application. *Toxicol Lett* 176: 1–12
- Duran N, Marcato P D, De Souza G I H, Alves O L, Esposito E (2007) Antibacterial effect of silver nanoparticles produced by fungal process on textile fabrics and their effluent treatment. *J Biomed Nanotechnol* 3: 203–208
- Egger S, Lehmann R P, Height MJ, Loessner MJ, Schuppler, M (2009) Antimicrobial properties of a novel silver-silica nanocomposite material. *Appl Environ Microbiol* 75(9): 2973–2976
- Elechiguerra J L, Burt J L, Morones J R, Camacho-Bragado A, Gao X, Lara H H, Yacaman M J (2005) Interaction of silver nanoparticles with HIV-1. *J Nanobiotechnol* 3: 1–6
- Esteben-Tejeda L, Malpartida F, Esteban-Cubillo A, Peccharoman C, Moya J S (2009) The antibacterial and antifungal activity of a soda-lime glass containing silver nanoparticles. *Nanotechnology* 20(8): 085103
- Fadeel B, Bennett-Garcia A E (2010) Better safe than sorry: Understanding the toxicological properties of inorganic nanoparticles manufacture for biomedical applications. *Adv Drug Deliver Rev* 62: 362–374
- Fayaz A M, Balaji K, Girilal M, Kalaichelvan P T, Venkatesan R (2009) Mycobased synthesis of silver nanoparticles and their incorporation into sodium alginate films for vegetable and fruit preservation. *J Agric Food Chem* 57: 6246–6252
- Feng Q L, Wu J, Chen G Q, Cui F Z, Kim T N, Kim J O (2000) A mechanistic study of the antibacterial effect of silver ions on *Escherichia coli* and *Staphylococcus aureus*. *J Biomed Mater* 52(4): 662–668
- Feynman R, Lecture at the California Institute of Technology, December 29, 1959
- Fernandez A, Soriano E, Lopez-Carballo G, Picouet P, Lloret E, Gavara R, Hernandez-Munoz P (2009) Preservation of aseptic conditions in absorbent pads by using silver nanotechnology. *Food Res Internat* 42: 1105–1112
- Fernandez A, Picouet P, Lloret E (2010) Cellulose-silver nanoparticle hybrid materials to control spoilage-related microflora in absorbent pads located in trays of fresh cut melons. *Internat J Food Microbiol* 142: 222–228
- Fox C L, Modak S M (1974) Mechanism of silver sulfadiazine action on burn wound infections. *Antimicro Agents Chemother* 5(6): 582–588
- Foster M J, Mulloy B, Mermut M V (2000) Molecular modeling study of HIV p17gag (MA) protein shell utilizing data from electron microscopy and X-ray crystallography. *J Mol Biol* 298: 841–857
- Furno F, Morley K S, Wong B, Sharp B L, Arnold P L, Howdle S M, Bayston R, Brown P D, Winship P D, Reid H J (2004) Silver nanoparticles and polymeric medical devices: a new approach to prevention of infection? *J Antimicro Chemother* 54: 1019–1024
- Gade A, Gaikwad S, Tiwari V, Yadav A, Ingle A, Rai M (2010) Biofabrication of silver nanoparticles by *Opuntia ficus-indica*: *In vitro* antibacterial activity and study of the mechanism involved in the synthesis. *Curr Nanosci* 6: 370–375
- Gade A K, Bonde P, Ingle A P, Marcato P D, Duran N, Rai M K (2008) Exploitation of *Aspergillus niger* for synthesis of silver nanoparticles. *J Biobased Mater Bioenergy* 2: 243–247.

- Gajbhiye M, Kesharwani J, Ingle A, Gade A, Rai M (2009) Fungus-mediated synthesis of silver nanoparticles and their activity against pathogenic fungi in combination with fluconazole. *Nanomed: Nanotechnol Biol Med* 5: 382-386
- Gong P, Li H, He X, Wang K, Hu J, Tan W, Zhang S, Yang X (2007) Preparation and antibacterial activity of Fe₃O₄@Ag nanoparticles. *Nanotechnology* 18: 604-611
- Huang J, Chen C, He N, Hong J, Lu Y, Qingbiao L, Shao W, Sun D, Wang X H, Wang Y, Yang X (2007) Biosynthesis of silver and gold nanoparticles by novel sundried *Cinnamomum camphora* leaf. *Nanotechnology* 18: 105-106
- Hussain S, Hess K, Gearhart J, Geiss K, Schlager J (2005) *In vitro* toxicity of nanoparticles in BRL3A rat liver cells. *Toxicol In vitro* 19: 975-83
- Ingle A, Gade A, Pierrat S, Sonnichsen C, Rai M K (2008) Mycosynthesis of silver nanoparticles using the fungus *Fusarium acuminatum* and its activity against some human pathogenic bacteria. *Curr Nanosci* 4: 141-144
- Ip M, Lui S L, Poon V K M, Lung I, Burd A (2006) Antimicrobial activities of silver dressings: An *in vitro* comparison. *J Med Microbiol* 55: 59-63
- Jain P, Pradeep T (2005) Potential of silver nanoparticle-coated polyurethane foam as an antibacterial water filter. *Biotechnol Bioeng* 90(1): 59-63
- Jain J, Arora S, Rajwade J M, Omray P, Khandelwal S, Paknikar K M (2009) Silver nanoparticles in therapeutics: Development of an antimicrobial gel formulation for topical use. *Mol Pharmaceutics* 6(5): 1388-1401
- Jo K Y, Kim B H, Jung G (2009) Antifungal activity of silver ions and nanoparticles on phytopathogenic fungi. *Plant Disease* 93(10): 1037-1043
- Jung W K, Koo H C, Kim K W, Shin S, Kim S H, Park Y H (2008) Antibacterial activity and mechanism of action of silver ion in *Staphylococcus aureus* and *Escherichia coli*. *Appl Environ Microbiol* 74(7): 2171-2178
- Kathiresan K, Alikunhi N M, Patnamaban S, Nabikhan A, Kandasamy S (2010) Analysis of antimicrobial silver nanoparticles synthesized by coastal strains of *Escherichia coli* and *Aspergillus niger*. *Can J Microbiol* 56(2): 1050-1059
- Keuk-Jun K, Sang W S, Moon S K, Choi J S, Kim J G, Lee D G (2008) Antifungal effect of silver nanoparticles on dermatophytes. *J Microbiol Biotechnol* 18(8): 1482-1484
- Kim J S, Kuk E, Yu K N, Kim J H, Park S J, Lee H J, Kim S H, Park Y K, Park Y H, Hwang C Y, Kim Y K, Lee Y S, Jeong D H, Cho M H (2007) Antimicrobial effects of silver nanoparticles. *Nanomed: Nanotechnol Biol Med* 3: 95-101
- Kim J K, Sung W S, Suh B K, Moon S K, Choi J S, Kim J G, Lee D G (2008) Antifungal activity and mode of action of silver nanoparticles on *Candida albicans*. *Biometals* 22(2): 235-242
- Knetsch M L W, Koole L H (2011) New strategies in the development of antimicrobial coatings: The example of increasing usage of silver and silver nanoparticles. *Polymers* 3(1): 340-366
- Kumar A, Vemula P K, Ajayan P M, John G (2008) Silver-nanoparticle-embedded antimicrobial paints based on vegetable oil. *Nat Mater* 7(3): 236-241
- Kumar V, Yadav S K (2009) Plant-mediated synthesis of silver and gold nanoparticles and their applications. *J Chem Technol Biotechnol* 84: 151-157
- Lala N L, Ramakrishnan R, Li B, Sundarrajan S, Barhate R S, Ying-Jun L, Ramakrishna S (2007) Fabrication of nanofibres with antimicrobial functionality used as filters: Protection against bacterial contaminants. *Biotechnol Bioeng* 97(6): 1357-1365
- Landsdown A B G (2002) Silver I: Its antibacterial properties and mechanism of action. *J Wound Care* 11: 125-138
- Lara H H, Ayala-nunez N V, Ixtapan-Turrent L, Rodriguez-Padilla C (2010) Mode of antiviral action of silver nanoparticles against HIV-1. *J Nanobiotechnol* 8: 1-10
- Leaper D L (2006) Silver dressings: Their role in wound management. *Int Wound J* 3(4): 282-294
- Li W R, Xie X B, Shi Q S, Duan S S, Ouyang Y S, Chen Y B (2011) Antibacterial effect of silver nanoparticles on *Staphylococcus aureus*. *Biometals* 24(1): 135-141
- Liu W T (2006) Nanoparticles and their biological and environmental applications. *J Biosci Bioeng* 102(1): 1-7

- Lkhagvajav N, Yasa I, Celik E, Koizhaiganova M, Sari O (2011) Antimicrobial activity of colloidal silver nanoparticles prepared by sol gel method. *Digest J Nanomater Biomater* 6(1): 149–154
- Matsumura Y, Yoshikata K, Kunisaki S I, Tsuchido T (2003) Mode of bactericidal action of silver zeolite and its comparison with that of silver nitrate. *Appl Environ Microbiol* 69(7): 4278–4281
- Mohanpuria P, Rana N K, Yadav S K (2008) Biosynthesis of nanoparticles: Technological concepts and future applications. *J Nanopar Res* 7: 9275–9280
- Morones J R, Elechiguerra J L, Camacho J B, Ramirez J T (2005) The bactericidal effect of silver nanoparticles. *Nanotechnology* 16: 2346–2353
- Moyer C A, Brentano L, Gravens D L, Margraf H W, Monafu W W (1965) Treatment of large human burns with 05% silver nitrate solution. *Arch Surgery* 90: 812–867
- Mubarakali D, Thajuddin N, Jeganathan K, Gunashekar M (2011) Plant extract mediated synthesis of silver and gold nanoparticles and its antibacterial activity against clinically isolated pathogens. *Colloids Surf B Biointerfaces* 85(2):360–365
- Nair L S, Laurencin C T (2007) Silver nanoparticles: Synthesis and therapeutic applications. *J Biomed Nanotechnol* 3: 301–316
- Nasrollahi A, Pourshamsian K H, Mansourkiaee P (2011) Antifungal activity of silver nanoparticles on some of fungi. *Int J Nano Dim* 1(3): 233–239
- Nikawa H, Yamamoto H T, Rahardjo M B, Murata N S (1997) Antifungal effect of zeolite-incorporated tissue conditioner against *Candida albicans* growth and/or acid production. *J Oral Rehab* 25: 30–357
- Nithya R, Ragunathan R (2009) Synthesis of silver nanoparticles using *Pleurotus sajor caju* and its antimicrobial study. *Digest J Nanomater Biostruct* 4(4): 623–629
- Pal S, Tak Y K, Song J M (2007) Does the antibacterial activity of silver nanoparticles depend on the shape of the nanoparticle? A study of the gram-negative bacterium *Escherichia coli*. *Appl Environ Microbiol* 27(6): 1712–1720
- Panacek A, Kolar M, Vecerova R, Pucek R, Soukupova J, Krystof V, Hamal P, Zboril R, Kvitek L (2009) Antifungal activity of silver nanoparticles against *Candida* spp. *Biomaterials* 30(31): 6333–63340
- Parikh R Y, Singh S, Prasad B L V, Patole M S, Sastry M, Shouche Y S (2008) Extracellular synthesis of crystalline silver nanoparticles and molecular evidence of silver resistance from *Morganella* sp: Towards understanding biochemical synthesis mechanism. *ChemBioChem* 9: 1415–1422
- Pattabi R M, Sridhar K R, Gopakumar S, Vinayachandra B, Pattabi M (2010) Antibacterial potential of silver nanoparticles synthesized by electron beam irradiation. *Int J Nanopar* 3(1): 53–64
- Rai M, Yadav A, Gade A (2008) Current trends in phytosynthesis of metal nanoparticles. *Crit Rev Biotechnol* 28(4): 277–284
- Rai M, Yadav A, Gade A (2009a) Silver nanoparticles: As a new generation of antimicrobials. *Biotechnol Adv* 27: 76–83
- Rai M, Yadav A, Bridge P, Gade A (2009b) Myconanotechnology: A new and emerging science. *In: Applied Mycology*, eds Rai MK and Bridge P D 14, 258–267, CAB International, New York
- Richard J W, Spencer B A, McCoy L F, Carina E, Washington J, Edgar P (2002) Acticoat versus silverlon: the truth. *J Burns Surg Wound Care* 1: 11–20
- Richardson A, Chan B C, Crouch R D, Janiec A, Chan B C, Crouch R D (2006) Synthesis of silver nanoparticles: An undergraduate laboratory using green approach. *Chem Edu* 11: 331–333
- Roe D, Karandikar B, Bonn-Savage N, Gibbns B, Jean-Baptiste R (2008) Antimicrobial surface functionalisation of plastic catheters by silver nanoparticles. *J Antimicrob Chemoth* 61(4): 869–876
- Safaepour M, Shahverdi A R, Shahverdi H R, Khorramzadeh M R, Gohari A R (2009) Green synthesis of small silver nanoparticles using geraniol and its cytotoxicity against fibrosarcoma-wehi 164. *Avicenna J Med Biotechnol* 1: 111–115

- Saiffudin N, Nian C Y, Zhan L W, Ning K X (2011) Chitosan-silver nanoparticle composite as point-of-use drinking water filtration system for household to remove pesticides in water. *Asian J Biochem* 6(2): 142–159
- Sanghi R, Verma P (2009) Biomimetic synthesis and characterization of protein capped silver nanoparticles. *Biores Technol* 100: 502–504
- Satyavathi R, Krishna M B, Rao S V, Saritha R, Rao D N (2010) Biosynthesis of silver nanoparticles using *Coriandrum sativum* leaf extract and their application in non-linear optics. *Adv Sci Lett* 3: 1–6
- Sau T K, Rogach A L (2010) Nonspherical noble metal nanoparticles: Colloid-chemical synthesis and morphology control. *Adv Mater* 22(16): 1781–1804
- Saxena A, Tripathi R M, Singh R P (2010) Biological synthesis of silver nanoparticles by using Onion (*Alium cepa*) extract and their antibacterial activity. *Digest J Nanomater Biostruc* 5(2): 427–432
- Sharma V K, Yngard R A, Lin Y (2009) Silver nanoparticles: Green synthesis and their antimicrobial activities. *Adv Colloid Interface Sci* 145: 83–96
- Sintubin L, De Guesseme B, Van der Meeren P, Pycke B F, Verstraete W, Boon N (2011) The antibacterial activity of biogenic silver and its mode of action. *Appl Microbiol Biotechnol* 9(1): 153–162
- Sondi I, Salopek-Sondi B (2004) Silver nanoparticles as antimicrobial agent: A case study on *E coli* as a model for gram-negative bacteria. *J Colloids Interface* 275: 177–182
- Song J Y, Kim B S (2009) Biological synthesis of bimetallic Au/Ag nanoparticles using Persimmon (*Diopyros kaki*) leaf extract. *Korean J Chem Eng* 25(4): 808–811
- Taniguchi N (1974) On the Basic Concept of Nano-Technology. Proceedings of the International Conference on Production Engineering Tokyo, Part II Japan Society of Precision Engineering
- Thakkar K N, Mhatre S S, Parikh R Y (2010) Biological synthesis of metallic Nanoparticles. *Nanomedicine* 6(2): 257–262
- Theron J, Walker J A, Cloete T E (2008) Nanotechnology and water treatment: applications and emerging opportunities. *Crit Rev Microbiol* 34: 43–69
- Tian J, Wong K K Y, Ho C M, Lok C N, Yu W Y, Che C M, Chiu J F, Tam P K H (2006) Topical Delivery of silver nanoparticles promotes wound healing. *ChemMedChem* 2(1): 171–180
- Wen R L, Xie X B, Shi Q S, Zeng H Y, Yang Y S, Chen Y B (2010) Antibacterial activity and mechanism of silver nanoparticles on *Escherichia coli*. *Appl Microbiol Biotechnol* 85(4): 1115–1122
- Zhu S, Zhou W (2011) Optical properties and immunoassay applications of noble metal nanoparticles. *J Nanomater*. doi:10.1155/2010/562035

Chapter 8

Antimicrobial Activity of Silver and Copper Nanoparticles: Variation in Sensitivity Across Various Strains of Bacteria and Fungi

Suparna Mukherji, Jayesh Ruparelia, and Shekhar Agnihotri

8.1 Introduction

Prevention of infectious diseases through control of pathogenic microorganisms has been a major challenge across the globe. Infectious diseases may spread through consumption of contaminated food and water, hospital-acquired diseases, and pandemics. Numerous antibiotics and antifungal formulations are available for control of disease-causing microorganisms; however, their efficacy is known to vary. Moreover, with the widespread use of antibiotics, antibiotic-resistant strains are developing to cause an even greater threat to public health. Thus, there is a need for exploring alternative strategies for controlling the spread of infectious diseases.

Chemical disinfectants, such as chlorine, are commonly used for inactivating harmful microorganisms in water so as to render it fit for drinking purposes. However, in the presence of trace organics in water, chlorine-based disinfectants are known to form disinfection byproducts (DBPs), such as trihalomethanes (THMs) and haloacetic acids (HAAs), that pose a threat to human health. THMs and HAAs are disinfection byproducts that have been implicated both in genotoxic risk and carcinogenic risk. Since halomethanes were discovered in chlorinated water in 1974, alleviation of DBPs has become a prime concern in water treatment.

S. Mukherji (✉)

Centre for Environmental Science and Engineering (CESE), IIT Bombay, Powai, Mumbai, India
e-mail: mitras@iitb.ac.in

J. Ruparelia

Department of Chemical Engineering, Institute of Technology, Nirma University, Ahmedabad, India
e-mail: jruparelia@gmail.com

S. Agnihotri

Centre for Research in Nanotechnology & Science (CRNTS), IIT Bombay, Powai, Mumbai, India
e-mail: agnish@iitb.ac.in

Thus, more research is targeted towards enhancing the efficiency of the disinfection process without formation of DBPs (Sadiq and Rodriguez 2004).

With the emergence of nanoscience and technology, research has been initiated to exploit the unusual and unique properties of nanomaterials. Nanotechnology and nanoscience research involves a wide spectrum of focus areas from fundamental sciences (i.e., biology, chemistry, and physics) to applied sciences (i.e., electronics and materials). Currently, there is a lot of interest in the environmental application of nanoparticles. Studies with various types of nanoparticles suggest that they may possess antibacterial and antifungal properties. Silver nanoparticles (SNP) have been studied extensively in this regard. The literature suggests that, while the antimicrobial activity of silver nanoparticles may be due to the release of silver ions, it is also possible that they exhibit additional effects that cannot be explained solely by the release of silver ions in solution.

Research on development of nanoparticles with antimicrobial properties and verification of antimicrobial activity of nanoparticles have primarily focused on nanoparticles of silver since the antimicrobial effect of silver ions is well established (Morones et al. 2005). Since antimicrobial activity associated with copper ions is also well established, some research has also been conducted with copper nanoparticles (CNP). Silver and copper nanoparticles have been reported to exhibit antimicrobial effects even at concentration as low as 1.69 and 10 $\mu\text{g/mL}$, respectively (Panacek et al. 2006; Yoon et al. 2007). No notable antimicrobial activity has been reported for gold and platinum nanoparticles at 100 $\mu\text{g/mL}$ (Williams et al. 2006; Cho et al. 2005); however, some growth inhibition was reported for 240 $\mu\text{g/mL}$ of gold nanoparticles (Burygin et al. 2009). Silica (33,000 $\mu\text{g/mL}$) and silica/iron oxide (2,200 $\mu\text{g/mL}$) nanoparticles also failed to depict any antimicrobial activity (Williams et al. 2006). Makhluif et al. (2005) reported some growth inhibition for MgO nanoparticles at a concentration of 1,000 $\mu\text{g/mL}$; however, Jones et al. (2008) reported negligible antimicrobial activity for MgO and also for TiO₂, CuO, and CeO₂. Mild antimicrobial activity of ZnO and Al₂O₃ nanoparticles have also been reported at high nanoparticle concentration (Jones et al. 2008; Jin et al. 2009; Sadiq et al. 2009).

The quantification of antimicrobial effects of silver and copper nanoparticles has been performed primarily with a few strains of Gram-positive and Gram-negative bacteria. Variation in response across a wide range of strains has not been studied. This chapter reviews methodologies adopted for experimental studies and depicts the results obtained by various researchers and variability in response observed for various reference strains. The mechanism of antimicrobial activity of nanoparticles is also discussed. The response of various groups of microorganisms, and also the species and strain level response, to silver and copper nanoparticles needs to be studied further using standard protocols before recommending use of such nanoparticles in commercial applications.

Although the toxicity/adverse effects of silver and copper nanoparticles to higher organisms is outside the scope of this chapter, it needs to be emphasized that the toxicity of nanoparticles may differ significantly from that of soluble forms

of silver and copper. The toxicity of silver and copper to human and other higher organisms is typically considered to be low compared to their toxic effect on microorganisms (Bosetti et al. 2002). As per World Health Organization (WHO) guidelines for drinking water quality, there are no adverse effects for exposure to silver at a concentration less than 0.1 mg/L. Only about 10% of the silver entering the body is absorbed and about 4–6% is retained by the tissues (Drake and Hazelwood 2005). The predominant adverse effect of exposure to silver is argyria, a bluish-gray discoloration of the skin, hair and eyes reported for silver levels in the blood exceeding 200 $\mu\text{g/L}$ (Hardes et al. 2007). Other chronic effects manifested for silver concentration in blood exceeding 300 $\mu\text{g/L}$ include: leucopenia, liver damage, kidney damage, and irritation of eyes, skin, respiratory and intestinal tract. Although metallic silver is reported to pose a lower risk compared to soluble silver, silver nanoparticles may pose a significantly higher risk due to specific effects on mitochondria and generation of reactive oxygen species (ROS) (Klaine et al. 2008; Costa et al. 2010). Silver nanoparticles have been reported to cause deformities, abnormalities and higher mortality in zebra fish embryos (Asharani et al. 2008) at concentrations exceeding 50 mg/L. Researchers have reported various cytotoxic and genotoxic effects of silver nanoparticles in higher organisms (Ahamed et al. 2008; Asharani et al. 2009). The maximum contaminant level goal (MCLG) for soluble copper in drinking water specified by US Environment Protection Agency (USEPA) is 1.3 mg/L. Potential adverse effects for chronic exposure at concentrations exceeding this value include liver and kidney damage. However, greater toxic effects are implicated for copper nanoparticles compared to soluble copper ions. Copper nanoparticles (80 nm) resulted in adverse morphological effects on gills and also affected gene expression patterns in zebra fish exposed to concentrations exceeding 0.1 mg/L (Klaine et al. 2008). The chronic toxicity associated with silver and copper nanoparticles needs to be explored through extensive research before recommending use of these nanoparticles for antimicrobial applications.

8.2 Antimicrobial Activity and Strain Specificity

A considerable amount of literature is available on the antibacterial effects of silver and copper nanoparticles against various bacteria. Bacteria tested with silver/copper nanoparticles include, *Escherichia coli*, *Staphylococcus aureus*, *Bacillus subtilis*, *Bacillus megaterium*, *Proteus vulgaris*, *Pseudomonas aeruginosa*, *Staphylococcus epidermidis*, *Enterococcus faecium*, *Klebsiella pneumoniae*, *Pseudomonas fluorescens*, *Salmonella Enteritidis*, *Salmonella Typhimurium*, *Bacillus cereus*, *Listeria monocytogenes*, *Micrococcus luteus*, and *Streptococcus mutans* among others (Sondi and Salopek-Sondi 2004; Kim et al. 2007; Panacek et al. 2006; Gogoi et al. 2006; Lok et al. 2006; Falletta et al. 2008; Hernandez-Sierra et al. 2008; Chudasama et al. 2009, 2010; Dallas et al. 2010; Egger et al. 2009; Fayaz et al. 2010; Fernandez et al. 2008). The antifungal properties of nanoparticles have

been tested and reported for fungal species *Candida albicans*, *Candida tropicalis*, *Candida parapsilosis*, *Issatchenkia orientalis*, *Saccharomyces cerevisiae*, *Trichosporon beigelii*, and *Aspergillus niger* (Dallas et al. 2010; Dorjnamjin et al. 2008; Esteban-Tejeda et al. 2009a, b; Gittard et al. 2009; Ilic et al. 2009; Kim et al. 2009a, b; Panacek et al. 2009; Egger et al. 2009; Jain et al. 2009). These studies provide support for the utilization of silver and copper nanoparticles as a unique class of biocidal agents.

The antimicrobial effects are commonly quantified using either the disc diffusion method or by dilution of the antimicrobial agent in broth cultures. In the disc diffusion method, the diameter of the inhibition zone (DIZ) surrounding a disc indicate the sensitivity of microorganisms to the nanoparticles on the disc as illustrated in Fig. 8.1. The assay based on liquid culture is used to quantify the minimum inhibitory concentration (MIC) and minimum bactericidal/fungicidal concentration (MBC/MFC) of nanoparticles as illustrated in Fig. 8.2. The minimum inhibitory concentration (MIC) is defined as the lowest concentration of antimicrobial agent that inhibits growth while the minimum bactericidal/fungicidal concentration (MBC/MFC) represents the lowest concentration of antimicrobial agent that kills 99.9% of the bacteria/fungi (Qi et al. 2004; Williams et al. 2006; Ruparelia et al. 2008a).

Several studies that utilized either the disk diffusion method or the broth dilution test, have simply reported growth inhibition in the presence of silver and copper nanoparticles and have not reported the DIZ, MIC, or MBC/MFC values (An et al. 2009; Mahltig et al. 2009; Mary et al. 2009; Asavavisithchai et al. 2010; Musarrat et al. 2010). The studies reporting the DIZ, MIC and MBC/MFC values provide a quantitative measure of antibacterial activity; however, there is still significant non-uniformity in the experimental methods reported. Variations in growth medium employed, differences in the initial concentration of microorganisms, and the size, shape and composition of nanoparticles used may cause variations in DIZ, MIC, and MBC for the same microbial strain exposed to silver/copper nanoparticles. Thus, comparison with respect to sensitivity of different strains to copper or silver nanoparticles is often not feasible although a large amount of literature is available.

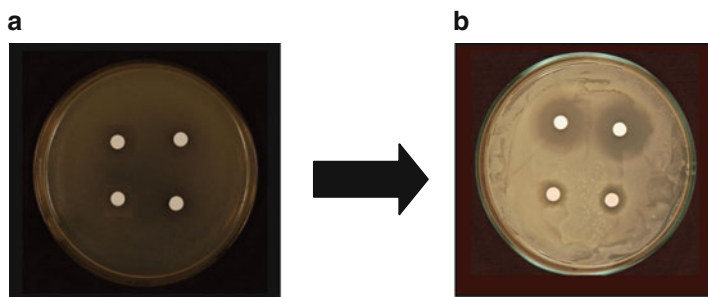


Fig. 8.1 Illustration of the disc diffusion test: *B. subtilis* exposed to copper (two upper discs) and silver nanoparticles (two lower discs) before (a) and after (b) incubation

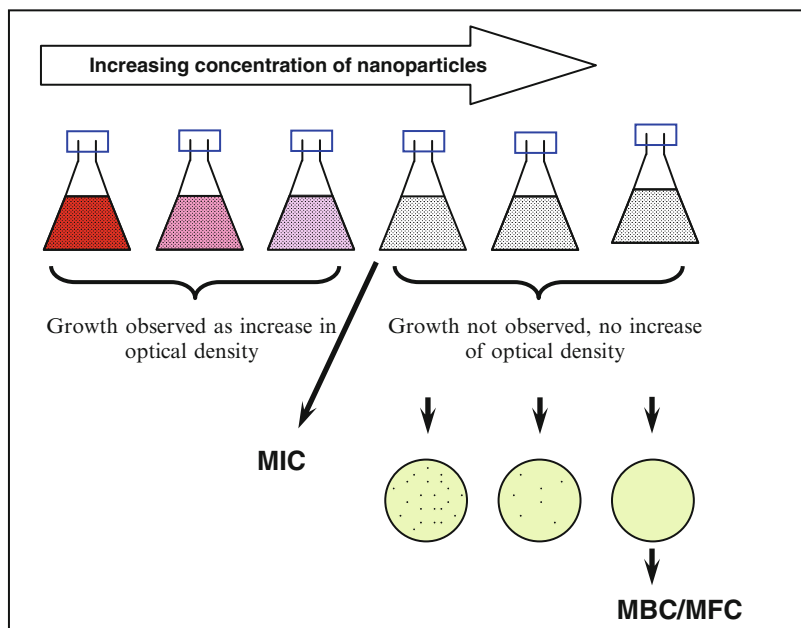


Fig. 8.2 Schematic illustration of broth dilution protocol for determination of MIC and MBC/MFC

The strain specificity in antibacterial and antifungal activities of silver and copper nanoparticles is discussed below.

8.2.1 Antibacterial Activity

The DIZ reflects magnitude of susceptibility of the microorganism to the antimicrobial agent. The susceptible strains are characterized by larger DIZ compared to the resistant strains. The antibacterial activity of metal nanoparticles has been compared for various microorganisms using the diameter of inhibition zone in disc diffusion susceptibility tests (Gittard et al. 2009; Jain et al. 2009; Kong and Jang 2008; Ruparelia et al. 2008a; Saravanan and Nanda 2010; Wu et al. 2009). Ruparelia et al. (2008a) reported that discs with silver nanoparticles were surrounded by a larger DIZ compared to copper nanoparticles for all *Escherichia coli* and *Staphylococcus aureus* strains selected for their study. Further, in the disc diffusion studies, strain specificity was not observed across the various strains of *E. coli* MTCC 443 (ATCC 25922), MTCC 739 (ATCC 10536), MTCC 1302 and MTCC 1687 (ATCC 8739) (obtained from IMTECH, Chandigarh, India) and *S. aureus* NCIM 2079 (ATCC 6538P), NCIM 5021 (ATCC 25923), and NCIM 5022 (ATCC 29213) strains (obtained from NCL, Pune, India). The lower DIZ for the

copper nanoparticle-impregnated discs compared to the silver nanoparticle-impregnated discs may have been due to the size difference in the copper (9.3 nm) and silver (3.3 nm) nanoparticles. Energy dispersive X-ray spectroscopy suggested the presence of an oxide layer on the copper nanoparticles, but not on the silver nanoparticles. However, *Bacillus subtilis* (MTCC 441/ATCC 6633) depicted a high sensitivity to the copper nanoparticles and the DIZ with copper nanoparticles was almost 90% greater compared to that observed with silver nanoparticles. Higher sensitivity of *B. subtilis* to copper nanoparticles was also reported by Yoon et al. (2007).

Jain et al. (2009) reported DIZ values for silver nanoparticles (size range 7–20 nm) in a proprietary gel formulation using various reference cultures and also multidrug-resistant clinical isolates. The clinical isolates included *Pseudomonas* sp. (eight strains), *Staphylococcus* sp. (five strains), *E. coli* (six strains) and *Klebsiella* sp. (three strains). The reference strains used were *E. coli* ATCC 117, *P. aeruginosa* ATCC 9027, *Salmonella abony* NCTC 6017, *Salmonella typhimurium* ATCC 23654, *Klebsiella aerogenes* ATCC 1950, *Proteus vulgaris* NCIB 4157, *Staphylococcus aureus* ATCC 6538, *Bacillus subtilis* ATCC 6633 and *Staphylococcus epidermis* ATCC 1228. Strain-specific variation in the diameter of inhibition zone was observed. The corrected inhibition zone (CIZ) was defined as the difference in diameter of inhibition zone and diameter of the well/disc. The *E. coli* and *S. aureus* reference strains depicted comparable inhibition zones as also shown by Ruparelia et al. (2008a) (Fig. 8.3). Ruparelia et al. (2008a) used filters loaded with 100 µg silver nanoparticles while Jain et al. used gel containing silver nanoparticles at 0.1 mg/g. *E. coli* and *S. aureus* strains have commonly been used for representing sensitivity to Gram-negative and Gram-positive organisms. *Pseudomonas* sp. depicted the largest inhibition zone which was more than double that

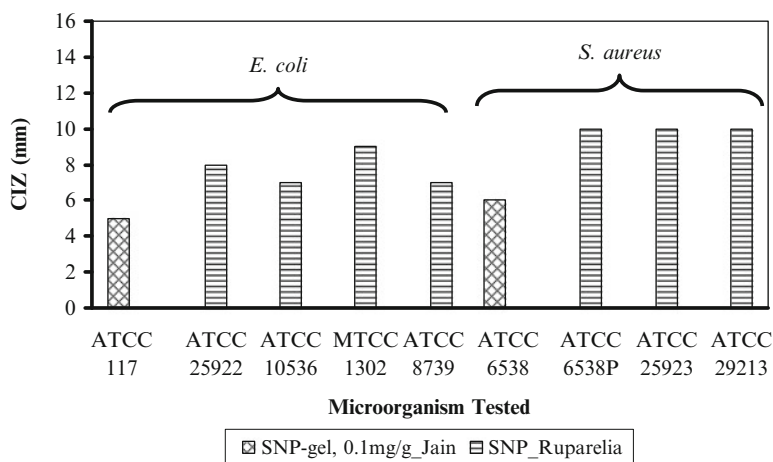


Fig. 8.3 Corrected inhibition zone (CIZ, mm) for *E. coli* and *S. aureus* strains reported by Ruparelia et al. (2008a) and Jain et al. (2009) in disc diffusion tests with silver nanoparticles (SNP)

observed for *E. coli* (CIZ 13 mm for 0.1 mg/g silver nanoparticles in the gel). *K. aerogenes*, *S. typhimurium*, *P. vulgaris*, and *B. subtilis* also depicted higher sensitivity compared to *E. coli* and *S. aureus* (CIZ 8–9 versus CIZ 5–6 nm, respectively).

The MIC and MBC of a particular antimicrobial agent is an important parameter with respect to a particular microbe because it is quantitatively measured in vitro through the micro-/macro-dilution test. For antibacterial studies in suspension, a greater lag phase and lower maximum absorbance has been reported as the concentration of nanoparticles increase until complete growth inhibition is observed at the MIC (Sondi and Salopek-Sondi 2004; Ruparelia et al. 2008a). The MIC and MBC values have been reported by various researchers for silver and copper nanoparticles and silver-containing nanocomposites in suspension (Egger et al. 2009; Fernandez et al. 2008; Ruparelia et al. 2008a; Hernandez-Sierra et al. 2008; Jain et al. 2009; Sharma et al. 2009). However, large variations are observed due to variations in initial bacterial concentration, size of nanoparticles and growth media used. The factors affecting the antimicrobial effect of silver nanoparticles include the particle size, shape, crystallinity, surface chemistry, and capping agents, as well as environmental factors such as pH, ionic strength and presence of ligands, divalent cations, and macromolecules (Marambio-Jones et al. 2010; Pal et al. 2007). In the majority of the literature, all such parameters vary, therefore a comparison among strains reported by various researchers is not feasible. The range of MIC and MBC values reported for *E. coli* and *S. aureus* often chosen as representative of Gram-negative and Gram-positive bacteria is reported in Tables 8.1 and 8.2, respectively. Several researchers have reported the impact of bacterial cell wall structure on MIC and MBC values based on difference in response observed for *E. coli* and *S. aureus*. For both *E. coli* (ATCC 10536) and *S. aureus* (ML 422), silver nanoparticles demonstrated greater bactericidal efficiency compared to penicillin (Sarkar et al. 2007). Synergistic effect between silver nanoparticles and antibiotics, such as, amoxicillin has also been reported (Li et al. 2005).

Some researchers have reported the MIC of *E. coli* in the presence of silver nanoparticles to be in the range of 3–25 $\mu\text{g/mL}$ for an initial bacterial concentration of 10^5 – 10^8 CFU/mL (Cho et al. 2005; Panacek et al. 2006; Gogoi et al. 2006). In contrast, other studies have reported negligible growth inhibition of silver nanoparticles on *E. coli* up to 100 $\mu\text{g/mL}$ (Sondi and Salopek-sondi 2004; Panacek et al. 2006). The latter studies employed silver nanoparticles of size 12–40 nm and a higher initial concentration of bacteria in the batch cultures of 10^5 – 10^8 CFU/mL. *E. coli* ATCC 25922 and strain F220 were found to have identical MIC values although the experimental conditions differed (Ruparelia et al. 2008a; Li et al. 2005). The range of MIC and MBC values observed for various *E. coli* strains is typically found to range from 12.5 to 180 $\mu\text{g/mL}$ and 12.5 to 220 $\mu\text{g/mL}$, respectively. Even for the same strain *E. coli* ATCC 25922, Fernandez et al. (2008) and Ruparelia et al. (2008a) have reported values that differ significantly due to differences in the experimental conditions. Some difference in methodology was observed for these studies reporting different MIC and MBC for the same strains. Fernandez et al. (2008) used Mueller–Hinton broth with initial bacterial

Table 8.1 Strain specificity of *E. coli* and range of MIC and MBC values reported for silver and copper nanoparticles and nanocomposites in broth studies

Strain of <i>E. coli</i>	Type & size (nm)	MIC (µg/mL)	MBC (µg/mL)	Initial count (CFU/mL)	Media used	Synthesis method	Reference
F220	SNP 20 nm	40	NR	5×10^6	Luria-Bertani broth	$\text{AgNO}_3 + \text{NH}_3 \rightarrow [\text{Ag}(\text{NH}_2)_2]^+$ Rxn with 5% SDS and ascorbic acid at 70°C, 1 h	Li et al. (2005)
ATCC 25922	SNP 10 nm	12.5	12.5	5×10^5	Mueller-Hinton broth	$\text{NBu}_4\text{Ag}(\text{C}_6\text{F}_5) + \text{AgClO}_4 \rightarrow \text{Ag}(\text{C}_6\text{F}_5)$; Rxn with hexadecylamine; reflux in toluene for 5 h	Fernandez et al. (2008)
ATCC 25922	SNP 3 nm	40	60	10^3 – 10^4	Nutrient broth	$\text{AgNO}_3 + \text{NaBH}_4 + \text{surfactant} \rightarrow \text{SNP}$; drying in H_2 atmosphere	Ruparelia et al. (2008a)
ATCC 10536	SNP 3 nm	180	220	10^3 – 10^4	Nutrient broth	$\text{AgNO}_3 + \text{NaBH}_4 + \text{surfactant} \rightarrow \text{SNP}$; drying in H_2 atmosphere	Ruparelia et al. (2008a)
MTCC 1302	SNP 3 nm	120	160	10^3 – 10^4	Nutrient broth	$\text{AgNO}_3 + \text{NaBH}_4 + \text{surfactant} \rightarrow \text{AgNP}$; drying in H_2 atmosphere	Ruparelia et al. (2008a)
ATCC 8739	SNP 3 nm	140	180	10^3 – 10^4	Nutrient broth	$\text{AgNO}_3 + \text{NaBH}_4 + \text{surfactant} \rightarrow \text{SNP}$; drying in H_2 atmosphere	Ruparelia et al. (2008a)
NR	SNP 8 nm	100	NR	10^5	Nutrient broth	$\text{AgNO}_3 + \text{Oleyamine}$ heated to 180°C; Rxn with Pluronic F-127	Chudasama et al. (2010)
NR	SNP 5 – 40 nm	35	NR		Mueller-Hinton broth	Biogenic synthesis: $\text{AgNO}_3 + \text{culture filtrate of } Trichoderma \text{ viride}$	Fayaz et al. (2010)
CCM 3954	SNC_Fe 10 nm	78	NR	10^6	Mueller-Hinton broth	AgNO_3 reduction by surface active amines of a phosphotriazine based polymer also containing oleic acid stabilized Fe_2O_3 nanoparticles	Dallas et al. (2010)
ATCC 27325	SNC_Si 10 nm	62.5	125	10^7	Luria Bertani broth	SNP embedded in a matrix of amorphous SiO_2 using flame spray pyrolysis	Egger et al. (2009)
ATCC 25922	CNP 9 nm	140	160	10^3 – 10^4	Nutrient broth	$\text{CuNO}_3 + \text{NaBH}_4 + \text{surfactant} \rightarrow \text{CNP}$; drying in H_2 atmosphere	Ruparelia et al. (2008a)

ATCC 10536	CNP 9 nm	220	260	10^3 – 10^4	Nutrient broth	CuNO ₃ + NaBH ₄ + surfactant → CNP; drying in H ₂ atmosphere	Ruparella et al. (2008a)
MTCC 1302	CNP 9 nm	200	220	10^3 – 10^4	Nutrient broth	CuNO ₃ + NaBH ₄ + surfactant → CNP; drying in H ₂ atmosphere	Ruparella et al. (2008a)
ATCC 8739	CNP 9 nm	280	300	10^3 – 10^4	Nutrient broth	CuNO ₃ + NaBH ₄ + surfactant → CNP; drying in H ₂ atmosphere	Ruparella et al. (2008a)
ATCC 15224	CNP 12–15 nm	100	–	10^4	Nutrient broth	Inert gas condensation of Cu wire under vacuum	Raffi et al. (2010)

NR not reported, *SNP* silver nanoparticles, *SNC_Fe* silver-containing nanocomposite with iron, *SNC_Si* silver-containing nanocomposite with silica, *SDS* sodium dodecyl sulphate

Table 8.2 Strain specificity of *S. aureus* and range of MIC and MBC values reported for silver and copper nanoparticles and nanocomposites in broth studies

Strain of <i>S. aureus</i>	Type & size nm	MIC $\mu\text{g/mL}$	MBC $\mu\text{g/mL}$	Initial count CFU/mL	Media used	Synthesis method	Reference
ATCC 25923	SNP10 nm	12.5	25	5×10^5	Mueller Hinton broth	$\text{NBu}_4\text{Ag}(\text{C}_6\text{F}_5) + \text{AgClO}_4 \rightarrow \text{Ag}(\text{C}_6\text{F}_5)$; Rxn with hexadecylamine; reflux in toluene for 5 h	Fernandez et al. (2008)
ATCC 6538P	SNP 3 nm	120	160	10^3 – 10^4	Nutrient broth	$\text{AgNO}_3 + \text{NaBH}_4 + \text{surfactant} \rightarrow \text{SNP}$; drying in H_2 atmosphere	Ruparella et al. (2008a)
ATCC 25923	SNP 3 nm	120	160	10^3 – 10^4	Nutrient broth	$\text{AgNO}_3 + \text{NaBH}_4 + \text{surfactant} \rightarrow \text{SNP}$; drying in H_2 atmosphere	Ruparella et al. (2008a)
ATCC 29213	SNP 3 nm	120	160	10^3 – 10^4	Nutrient broth	$\text{AgNO}_3 + \text{NaBH}_4 + \text{surfactant} \rightarrow \text{SNP}$; drying in H_2 atmosphere	Ruparella et al. (2008a)
NR	SNP 8 nm	350	NR	10^5	Nutrient broth	$\text{AgNO}_3 + \text{Oleylamine}$ heated to 180°C ; Rxn of SNP with Pluronic F-127	Chudasama et al. (2010)
CCM 3953	SNP 10 nm	78	NR	10^6	Mueller-Hinton broth	AgNO_3 reduction by surface active amines of a phosphotriazine based polymer also containing oleic acid stabilized Fe_2O_3 nanoparticles	Dallas et al. (2010)
MRSA	SNP 10 nm	78	NR	10^6	Mueller-Hinton broth	AgNO_3 reduction by surface active amines of a phosphotriazine based polymer also containing oleic acid stabilized Fe_2O_3 nanoparticles	Dallas et al. (2010)
NR	SNP 5–40 nm	80	NR	NR	Mueller-Hinton broth	Biogenic synthesis; $\text{AgNO}_3 + \text{culture filtrate of } Trichoderma \text{ viride}$	Fayaz et al. (2010)
29213	SNC_S1 10 nm	250	1000	10^7	Brain-heart infusion broth	SNP embedded in a matrix of amorphous SiO_2 using flame spray pyrolysis	Egger et al. (2009)
BEC9393 (MRSA)	SNC_V, 20 nm	6.75–12.5	NR	NR	Mueller-Hinton broth	$\text{NH}_4\text{VO}_3 + \text{AgNO}_3 \rightarrow \text{hydrothermal treatment} \rightarrow \text{SNP on Sg-vanadate nanowires}$	Holtz et al. (2010)

Rib1 (MRSA)	SNC_V, 20 nm	6.75–12.5	NR	Mueller–Hinton broth	$\text{NH}_4\text{VO}_3 + \text{AgNO}_3 \rightarrow$ hydrothermal treatment \rightarrow SNP on Sg-vanadate nanowires	Holtz et al. (2010)
ATCC 29213	SNC_V, 20 nm	3.4–6.75	NR	Mueller–Hinton broth	$\text{NH}_4\text{VO}_3 + \text{AgNO}_3 \rightarrow$ hydrothermal treatment \rightarrow SNP on Sg-vanadate nanowires	Holtz et al. (2010)
6538P	CNP 9 nm	140	10^3 – 10^4	Nutrient broth	$\text{CuNO}_3 + \text{NaBH}_4 +$ surfactant \rightarrow CNP; drying in H_2 atmosphere	Ruparelia et al. (2008a)
25923	CNP 9 nm	140	10^3 – 10^4	Nutrient broth	$\text{CuNO}_3 + \text{NaBH}_4 +$ surfactant \rightarrow CNP; drying in H_2 atmosphere	Ruparelia et al. (2008a)
29213	CNP 9 nm	140	10^3 – 10^4	Nutrient broth	$\text{CuNO}_3 + \text{NaBH}_4 +$ surfactant \rightarrow CNP; drying in H_2 atmosphere	Ruparelia et al. (2008a)

NR not reported, SNP silver nanoparticles, SNC_Fe silver-containing nanocomposite with iron, SNC_Si silver-containing nanocomposite with silica, SNC_V SNP nanocomposite with silver vanadate nanowires

concentration of 10^5 CFU/mL whereas Ruparelia et al. (2008a) used nutrient broth and initial bacterial concentration of 10^3 – 10^4 CFU/mL. A higher initial concentration is expected to raise the MIC; however, the reverse results were observed. Release of ions in these two studies may have differed due to difference in the growth medium used and also due to differences in the size of nanoparticles and their surface characteristics. The relatively low MIC reported by Fernandez et al. (2008) was possibly affected by the production approach which resulted in a homogeneous population of spherical nanoparticles with a narrow size distribution.

In broth culture studies, Ruparelia et al. (2008a) reported that *E. coli* strains showed large variation in the sensitivity to silver nanoparticles. *E. coli* ATCC 25922 was found to be the most sensitive *E. coli* strain with MIC and MBC of 40 and 60 $\mu\text{g/mL}$, respectively, while the corresponding values for the other strains were in the range of 120–180 $\mu\text{g/mL}$ and 180–220 $\mu\text{g/mL}$, respectively. The *E. coli* strain ATCC 25922 also showed higher sensitivity to copper nanoparticles compared to the other *E. coli* strains. The MIC and MBC values for copper nanoparticles ranged from 140 to 280 $\mu\text{g/mL}$ and 160 to 300 $\mu\text{g/mL}$, respectively. The antibiotic gentamycin is reported to exhibit MBC value of 240 $\mu\text{g/mL}$ for *E. coli* ATCC 700926 (Burygin et al. 2009). Thus, *E. coli* is more sensitive to silver nanoparticles compared to gentamycin but less sensitive to copper nanoparticles compared to gentamycin. Sensitivity of the various *S. aureus* strains to silver or copper nanoparticles observed in the broth cultures were comparable across the various strains. From these results, it appears that, for comparing sensitivity across various strains, it is better to perform both disc diffusion and the broth culture tests. For assays conducted in a batch bioreactor with AgCl-coated silver wires that released silver ions in solution, complete disinfection was achieved in a shorter time for *E. coli* ATCC 25922 compared to *E. coli* ATCC 10536, irrespective of the initial cell concentration (Sharma 2010). Thus, *E. coli* ATCC 25922 depicts high sensitivity to both silver ions and silver nanoparticles. Using commercially available silver nanoparticles, Lee et al. (2009) reported the order of susceptibilities across various strains as *E. coli* > *B. subtilis*. However, Ruparelia et al. (2008a) reported comparable sensitivity for *E. coli* and *B. subtilis* for some strains and greater susceptibility for *B. subtilis* compared to *E. coli* for other strains.

Jain et al. (2009) reported comparable MIC and MBC for the various reference cultures other than *S. aureus* when cultures exposed to silver nanoparticles in a proprietary gel formulation was introduced into 96-well microtiter plates and observed after 24 h. Almost 66% of all strains tested showed MIC less than 3.12 $\mu\text{g/mL}$ and most had MBC of 12.5 $\mu\text{g/mL}$. In contrast, *S. aureus* was reported to have MBC higher than 50 $\mu\text{g/mL}$. The kill rate of the various cultures at the MIC and MBC concentration studied over an 8-h period showed significant variability. The time required to achieve 1 log unit reduction in all the tested strains were between 3.5 and 10 h, other than for *S. aureus*. Based on the broth culture studies, they found that *E. coli* and *P. aeruginosa* were more vulnerable to the silver nanoparticles compared to the other cultures while *S. aureus* was most resistant. The trend based on DIZ did not match the trend based on MIC/MBC across the various cultures. Interestingly an order of magnitude lower MIC and MBC values

are reported by Jain et al. (2009) compared to those reported by Ruparelia et al. (2008a). Starting with an initial concentration of 10^5 CFU/mL, Jain et al. (2009) reported a continuous decreasing trend in cell count for silver nanoparticles present at MIC and MBC concentrations. In contrast, Ruparelia et al. (2008a) demonstrated culture growth at nanoparticle concentration below the MIC for initial concentration of 10^3 – 10^4 CFU/mL, respectively, and identified MIC based on no increase in absorbance. It thus appears that it is difficult to compare across various studies.

The range of MIC values observed for various *S. aureus* strains in the presence of silver nanoparticles was found to range from 12.5 to 350 $\mu\text{g/mL}$ and values differing significantly has been reported even for the same strain (ATCC 25923) as shown in Table 8.2. Panacek et al. (2006) and Ruparelia et al. (2008a) did not observe strain specificity in the response for *S. aureus* to silver nanoparticles for the reference strains used in their study. However, strain specificity is apparent from the results reported by Holtz et al. (2010) for silver nanoparticles loaded on silver vanadate nanowires. Holtz et al. (2010) performed a comparative study with the antibiotic oxacillin and silver vanadate nanowires decorated with silver nanoparticles against three strains of *S. aureus* and reported very promising results. The MIC value against a multidrug-resistant *S. aureus* (MRSA) strain BEC 9393 was found to be tenfold lower for the nanocomposite than for the antibiotic oxacillin. For the strain Rib1, MIC values were almost comparable with oxacillin, and for strain ATCC 29213, the MIC values with the nanocomposite were higher than oxacillin. Dallas et al. (2010) also reported an MIC value against MRSA as 78 $\mu\text{g/L}$ and this value was lower than that observed for oxacillin. Thus, the trend in bactericidal efficiency of antimicrobial agents for *S. aureus* is silver nanoparticles > oxacillin > copper nanoparticles. Chudasama et al. (2010) reported higher MIC for *S. aureus* (350 $\mu\text{g/mL}$) compared to *E. coli* (100 $\mu\text{g/mL}$) for silver nanoparticles synthesized using oleylamine as reducing and capping agent and pluronic acid used for facile phase transformation. Various other bacteria, i.e., *Bacillus megaterum*, *Proteus vulgaris* and *Shigella sonnei*, had MIC in the intermediate range between 200 and 300 $\mu\text{g/mL}$. Although several studies suggest that Gram-positive *S. aureus* is more resistant to silver nanoparticles compared to Gram-negative *E. coli* (Chudasama et al. 2010; Kim et al. 2007; Jain et al. 2009), this result is not always true (Ruparelia et al. 2008a).

8.2.2 Antifungal Activity

Since most studies on antimicrobial effects of silver nanoparticles are focused on bacteria, not much is known regarding the effects on fungi. Only limited studies are available on effects of silver nanoparticles on some yeast strains, such as *Saccharomyces cerevisiae* (Lee et al. 2009; Nasrollahi et al. 2011) and *Candida* sp. (Dallas et al. 2010; Nasrollahi et al. 2011) and some plant fungi belonging to the ascomycetes and basidiomycetes groups (Min et al. 2009; Kim et al. 2009b). The limited studies that are available have demonstrated antifungal activity of

silver nanoparticles, and both inhibition in growth and development and cell wall damage have been reported.

The antifungal efficacy of silver nanoparticles on fungal pathogens responsible for skin diseases was investigated by Kim et al. (2008). This study demonstrated silver nanoparticles as a potent antifungal agent by comparing the antifungal activity to that of known antifungal drugs, i.e., amphotericin B and fluconazole. Silver nanoparticles (3 nm) showed antifungal effects against *Candida albicans* (ATCC 90028), *Candida glabrata* (ATCC 90030), *Candida tropicalis*, and *Trichophyton mentagrophytes* as shown by IC₈₀ values of 1–7 µg/mL (80% inhibitory concentration, IC₈₀, is the lowest concentration that causes 80% inhibition in microbial growth). The IC₈₀ values of silver nanoparticles were comparable to the IC₈₀ of amphotericin B (1–5 µg/mL), and were significantly lower than those of fluconazole (10–30 µg/mL). The silver nanoparticles were thus more potent than fluconazole. However, these nanoparticles expressed less potent antifungal activity than amphotericin B for the strains *Candida parapsilosis* and *Candida krusei*. Nasrollahi et al. (2011) demonstrated lower IC₉₀ for silver nanoparticles compared to amphotericin B and fluconazole for *Candida albicans*; however, the IC₉₀ for silver nanoparticles and amphotericin B were comparable for *Saccharomyces cerevisiae*. Thus, it is hypothesized that variation in the sensitivity of a particular microbe against nanoparticles may depend upon the nature of the strain, type of isolate and physiological variation in the microbial species. Subsequently, Kim et al. (2009a, b) explored the antifungal activity of silver nanoparticles against fungal strains *Saccharomyces cerevisiae* (KCTC 7296), *Trichosporon beigelii* (KCTC 7707), *Candida albicans* (ATCC 90028), and *Raffaelea* sp. The MIC value of silver nanoparticles was 2 µg/mL for *C. albicans*, *T. beigelii*, and *S. cerevisiae*, which was similar to that of amphotericin B, an antifungal compound with MIC range 2.5–5 µg/mL (Kim et al. 2009a).

Panacek et al. (2009) reported the minimum fungicidal concentration (MFC) of silver nanoparticles against *Candida* spp. to be in the range of 0.21–1.69 µg/mL. This is comparable or even better than the fungicidal activity of antifungals, such as, amphotericin B (MFC around 2–16 µg/mL), posaconazole (MFC around 8 µg/mL), itraconazole and voriconazole (MFC more than 10 µg/mL) or caspofungin (MFC around 1 µg/mL). Gajbhiye et al. (2009) demonstrated that silver nanoparticles with fluconazole can be used as an effective antifungal agent against *Candida* sp. In this study, *Candida albicans* was depicted as the most sensitive fungal strain followed by *Trichoderma* sp. and *Phoma glomerata*. No significant antifungal activity was found for *Fusarium semitectum* and *Phoma herbarum*, and hence they were reported as the most resistant among all the fungal strains tested.

Kim et al. (2009b) reported antifungal activity of silver nanoparticles (of 4–8 nm size range) on a phytopathogenic *Raffaelea* sp. at concentrations of 10 µg/mL and above. Min et al. (2009) also reported antifungal activity on phytopathogenic sclerotium forming species *Rhizoctonia solani*, *Sclerotinia sclerotiorum*, and *S. minor*. Sclerotia are primary asexual survival structures that facilitate disease dissemination and initiation. Inhibition of hyphal growth was observed at silver nanoparticles concentration greater than 5 µg/mL and *R. solani* showed the highest

sensitivity among the three strains. Maximum adverse effect of silver nanoparticles on sclerotium germination was observed for *S. sclerotiorum*.

Some studies have compared the effect of silver nanoparticles on bacteria and fungi. Most of these studies indicate a comparatively higher MIC for fungi compared to bacterial strains such as *E. coli* (Lee et al. 2009) when studied over the same time period. Dallas et al. (2010) reported antibacterial and antifungal effect of strains by testing growth inhibition after 24 h for bacteria but after 36 h for fungi. The bacterial strains *E. coli* (CCM 3954), *S. aureus* (CCM 3953 and MSRA), *S. epidermis*, *Enterococcus faecalis* (CCM 4224 and VRE), and *K. pneumoniae* depicted MIC in the range of 78–150 µg/mL. The fungal strains *Candida albicans* (I and II) and *Candida parasilosis* also depicted MIC in the same range. Egger et al. (2009) also used lower initial cell concentration (10^6 instead of 10^7) and longer time period (72 instead of 24 h) for determining the MIC and MBC/MFC of bacterial/fungal strains in presence of silver nanoparticles loaded on silica. They reported comparable MIC for *E. coli* (ATCC 27325), *K. pneumoniae* (ATCC 4352) *P. fluorescens* (LME 233), *Salmonella enteritidis* (D1), *Salmonella typhimurium* (DB 7155), and *Enterobacter faecalis* (ATCC 19433) as 62.5 µg/mL and MBC in the range of 125–250 µg/mL. However, the MIC and MBC/MFC were significantly higher for *Listeria monocytogenes*, *S. aureus* and *C. albicans* (MIC 125–250 µg/mL; MBC/MFC 500–2,000 µg/mL). Kokura et al. (2010) investigated the antimicrobial efficacy of silver nanoparticles against a mixed bacterial suspension containing *Escherichia coli* ATCC 8739, *Pseudomonas aeruginosa* ATCC 9027, *Staphylococcus aureus* ATCC 6538, mixed fungal suspension *Candida albicans* ATCC 10231, *Aspergillus niger* ATCC 16404, *Penicillium citrium* ATCC 9849, and *Aureobasidium pullulans* IFO 6353 and a waste suspension (filtered kitchen drainage). At a concentration of 1 ppm of silver nanoparticles, microbial growth was reduced to less than or equal to 10 CFU/g within 7 days in all the microbial suspensions with initial cell concentrations in the range of 10^5 – 10^6 CFU/g.

Gutierrez et al. (2010) evaluated the antibacterial and antifungal activity of silver nanoparticles (20–25 nm) and found them to be comparable to that of commercial antibiotics for bacteria and fungi. For example, MICs of 0.53, 0.37, and 0.74 µg/mL were obtained for bacterial strains *Escherichia coli* (ATCC 25922), *Pseudomonas aeruginosa* (ATCC 27853), and *Staphylococcus aureus* (ATCC 25923), respectively, using silver nanoparticles. The corresponding MICs were 0.83, 1.33, and 0.42 µg/mL for gentamicin. The fungal strain, *Candida albicans* (ATCC 14053) displayed MIC of 6 µg/mL for silver nanoparticles when the corresponding MIC with amphotericin B and fluconazole was 0.25 and 64 µg/mL, respectively. *Mycobacterium smegmatis* (ATCC 700084), which showed a MIC of 0.46 µg/mL with silver nanoparticles, had a MIC of 0.85 µg/mL with rifampicin. Interestingly, the average MIC values for bacterial and fungal strains were found to be 0.4–1.7 µg/mL and 3–25 µg/mL, respectively, which were significantly better than previous studies with nanoparticles of similar size (Panacek et al. 2006).

Very few studies have reported the antifungal activity of copper nanoparticles. For the first time, Cioffi et al. (2004) reported the usage of a copper/polymer nanocomposite as an efficient antifungal coating. Here, copper nanoparticles

(3.2 nm) were embedded inside the polymeric matrices of polyvinylmethyl ketone (PVMK), poly(vinyl chloride) (PVC), and polyvinylidene fluoride (PVDF) by the spin-coating method and their bioactivity was evaluated in vitro against bacterial species, yeast, and molds (Cioffi et al. 2004, 2005). Among the three nanocomposites, Cu-PVMK was the most bioactive composite. It caused 100%, 99.99%, 99.97%, 100%, and 94.3% reduction in counts for *S. cerevisiae*, *E. coli*, *S. aureus*, *L. monocytogenes*, and molds, respectively, after an incubation period of 4 h. The results also demonstrated that antifungal activity of the resulting nanocomposites increased with higher loading of copper.

8.3 Mechanism of Antimicrobial Activity of Copper and Silver Nanoparticles

Various researchers have attempted to elucidate the mechanism of action of silver ions and silver nanoparticles as summarized by Rai et al. (2009). Ionic silver (Ag^+) is highly toxic to microorganisms. It acts through multiple mechanisms and is found to cause structural and morphological changes as observed in studies with silver nitrate at concentrations of 10 mg/L and above. In transmission electron microscopy (TEM), an electron light region containing a highly condensed substance has been observed in the center of the *E. coli* and *S. aureus* exposed to silver ions. A big gap between the cytoplasmic membrane and the cell wall has also been reported. These observations indicate that silver ions penetrate the cell wall and condense the DNA. Ag^+ ions can form complexes with the bases in DNA such that DNA loses its replication ability. Interaction between the silver ions and ribosomes suppress the expression of enzymes and proteins necessary for ATP production. Reaction of Ag^+ with the thiol, carboxylate, phosphate, hydroxyl, amine, imidazole, and indole groups on enzymes can lead to enzyme inactivation and cell death (Lin et al. 1998). Ag^+ ions are reported to inhibit phosphate uptake and exchange in *E. coli*. They promote efflux of accumulated phosphate as well as mannitol, succinate, glutamine, and proline. Silver ions can collapse the proton motive force in bacteria and can thus cause cell death (Lok et al. 2006). Silver ions can also react with electron donors containing sulfur, oxygen and nitrogen. Siva Kumar et al. (2004) proposed that oxygen associates with silver and reacts with the sulfhydryl ($-\text{S}-\text{H}$) groups on the cell wall to form $\text{R}-\text{S}-\text{S}-\text{R}$ bonds, thus blocking respiration and causing cell death. Silver ions are also reported to generate reactive oxygen species that inhibit respiration.

The specific bactericidal effect of silver nanoparticles is due to their small size and high surface to volume ratio, which allows them to interact closely with microbial membranes (Morones et al. 2005). Sondi and Salopek-Sondi (2004) reported the incorporation of silver nanoparticles into the bacterial membrane which appeared as pits on the cell surface. Cho et al. (2005) reported that the surface of the cell walls of *E. coli* treated with silver nanoparticles were severely

damaged compared to untreated *E. coli*. It is hypothesized that nanoparticles can cause interruption in transmembrane electron transfer and can disrupt the cell envelope (Lok et al. 2006). This allows them to penetrate into the cell and oxidize the cell components by production of reactive oxygen species (ROS) and dissolved metal ions (Li et al. 2010). Some researchers have reported that nanoparticles can directly react with cellular proteins and DNA. They attack the respiratory chain and eventually affect cell division. However, with a detailed study of DNA/protein migration profiles, Gogoi et al. (2006) demonstrated that silver nanoparticles have no direct effects on either cellular DNA or protein, although the silver nanoparticles were more efficient bactericidal agents compared to the silver ions.

Silver nanoparticles in aqueous solution promote a sustained release of silver ions as they are depleted from the solution. Thus, it is often difficult to distinguish its mechanism of action from that of silver ions, and similar effects as observed for silver ions have also been reported for silver nanoparticles (Lok et al. 2006). Media components such as chlorides and deposition of surface layer on the nanoparticles (i.e., oxide or chloride layer) may increase the rate and extent of release of ions from the nanoparticles (Ruparelia et al. 2008a).

Li et al. (2010, 2011) demonstrated that the effect of silver nanoparticles on *E. coli* and *S. aureus* varied with changes in the concentration of the silver nanoparticles and exposure time. The DNA was condensed upon exposure of *S. aureus* (10^7 CFU/mL) to SNP at a concentration of 50 $\mu\text{g/L}$ for 6 h. Upon 12 h exposure, the cellular contents were released due to breakdown of the cell wall. Reduced enzymatic activity of respiratory chain dehydrogenase indicated inhibition in respiration for both *E. coli* and *S. aureus*. The expression of various proteins was altered fivefold to sevenfold in *S. aureus* cells treated with SNPs. The increased expression of formate acetyl transferase indicated that the cells were unable to utilize oxygen as the terminal electron acceptor. A significant decrease was observed for aerobic glycerol-3-phosphate dehydrogenase, ABC transporter ATP binding protein and recombinase A protein indicating adverse effects on transfer of substrate and nutrients across the cell membrane and a faulty DNA repair mechanism.

Copper ions can react with negatively charged cell wall components such as peptidoglycan through electrostatic attraction. Recycling redox reactions between Cu^{2+} and Cu^+ can occur at the bacterial cell surface. These reactions generate H_2O_2 that damages the cytoplasmic membrane. The presence of copper ions inside bacterial cells can disrupt biochemical processes (Kim et al. 2000; Stohs and Bagchi 1995). However, the exact mechanism behind the bactericidal effect of copper nanoparticles is not known. It is generally believed that toxicity is exerted through several parallel mechanisms both by the direct action of the nanoparticles and by the release of Cu^{2+} ions from the nanoparticles. Formation of pits and cavities has been observed in the presence of *E. coli* exposed to copper nanoparticles (Raffi et al. 2010). For oxidized copper nanoparticles embedded in an inert, Teflon-like matrix, Cioffi et al. (2005) demonstrated significant antimicrobial activity due to release of ions. One hypothesis is that Cu^{2+} ions can damage proteins present on the cell envelope and may also damage the proteins within the cell. Copper is reported to

displace essential metals from their native binding sites in the proteins. Copper ions may bind with DNA molecules and lead to disorder of the helical structure by cross-linking within and between the nucleic acid strands. Direct interaction of copper nanoparticles with the proteins is also hypothesized. These interactions may cause conformational changes in protein structure or in the active site of the protein. This causes inhibition or neutralization of the biological activities of the protein (Borkow and Gabbay 2009). Some bacterial cultures exhibit high sensitivity to copper nanoparticles possibly due to the greater abundance of functional groups, such as amines and carboxyl groups on *B. subtilis*, that have a great affinity to react with the copper ions and nanoparticles (Ruparelia et al. 2008a; Beveridge and Murray 1980).

The mechanism of antifungal effect of silver nanoparticles has been elucidated only recently (Kim et al. 2009a) using the yeast, *Candida albicans*. TEM images revealed pits in the fungal cell wall and pores in the plasma membrane upon exposure to 3-nm spherical silver nanoparticles. The nanoparticles attached to the membrane and disrupted the membrane potential as revealed through flow cytometry. The fluorescence anisotropy upon exposure to a plasma membrane probe (1,6 diphenyl 1,3,5 hexatriene) measured in a fluorescence spectrofluorometer at 350 and 425 nm was increased with increasing concentration of silver nanoparticles indicating disruption of the plasma membrane. They also demonstrated that creation of transmembrane pores caused leakage of intracellular components such that the level of extracellular glucose and trehalose was increased upon exposure. Silver nanoparticles also interfered with the budding process in yeast. Kim et al. (2009b) demonstrated antifungal activity of silver nanoparticles on an ascomycetous phytopathogen, *Raffaelea* sp. Growth inhibition in *Raffaelea* sp. was found to be due to detrimental effects on hyphae. Healthy hyphae sprayed with 10 ppm silver nanoparticles were observed by scanning electron microscopy. Breakage of the hyphal tips, detachment of conidia, surface damage of hyphae and shrinkage due to release of cellular material was observed. Min et al. (2009) also reported similar adverse effects of silver nanoparticles on hyphae and adverse effect on sclerotial germination for various phytopathogenic fungi.

8.4 Immobilization of Nanoparticles and Their Antibacterial Effects

Application of nanoparticles for drinking water disinfection would require recovery of the nanoparticles using membrane filters or immobilization of the nanoparticles onto support surfaces in a reactor (Li et al. 2008). Conceptually, the various immobilization approaches used can be divided into two main groups, i.e., the entrapment of segregated nanoparticles within porous matrix and the use of solid support as a substrate for immobilization of the stabilized nanoparticles. The solid support can be fabricated into various structures such as nanofibers, thin films, and porous gel that act as a template for immobilizing silver nanoparticles. However,

most of the polymeric supports are chemically inert. For the application to be successful, the support must be surface functionalized. Common surface modification techniques include treatment by blending, coating, radiation with electromagnetic waves, electron beam, ion beam (Brown 1993) or atomic beam, corona or plasma treatment (Chu et al. 2002), chemical vapor deposition (CVD), gas oxidation, chemical modifications using wet-treatment, and surface grafting polymerization (Uyama et al. 1998; Kato et al. 2003). Immobilization is achieved through surface modification that allows favorable interaction between the nanoparticles and the support matrix. Organic functional groups, such as hydroxyl, amino, mercapto, carboxyl, imidazole, indole, and pyridyl, can be employed to immobilize metal nanoparticles onto these exposed surfaces. Although the discussion in this section focuses on immobilization and entrapment of silver nanoparticles, similar methods can also be used for immobilization and entrapment of copper nanoparticles (Cioffi et al. 2004, 2005; Sheikh et al. 2011). Sheikh et al. (2011) fabricated polyurethane nanofibers containing copper nanoparticles by electrospinning and demonstrated good bactericidal effect of this material on *E. coli* and *B. subtilis*.

The release of silver ions from silver-containing bactericidal agents is a key parameter in evaluating their applicability. It will determine the stability and durability of the agent to a large extent. Silver-impregnated polymeric nanofibers was reported to provide antimicrobial efficacy with a sustained release of silver (Silver 2003). The antimicrobial ability of silver-impregnated composites is related to their silver content, the size of the silver nanoparticles and their distribution (Chou et al. 2005; Su et al. 2011). The common techniques used for fabricating nanofibers are self-assembly, phase separation, and electrospinning. A nanofibrous mesh prepared by any of the above methods has a high surface area-to-volume ratio with high porosity. This allows higher loading of silver nanoparticles with sustained release of silver (Silver 2003) and ultimately such nanofibers are expected to exhibit stronger antibacterial activity. Klueh et al. (2000) demonstrated the antibacterial efficacy of silver-coated polyethylene-terephthalate (PET) fabric, which effectively prevented the attachment of microorganisms on the silver active surface. Jin et al. (2005) prepared electrospun poly-N-vinylpyrrolidone (PVP) nanofibers containing silver nanoparticles for utilizing their expected strong antimicrobial activity. They also concluded that PVP containing Ag nanoparticles could be used to introduce Ag nanoparticles into other polymer nanofibers that are miscible with PVP such as chitosan, collagen, poly(4-vinylphenol), bisphenol, poly(epichlorohydrin), and poly(chloromethyl methacrylate). Chou et al. (2005) reported the fabrication of a cellulose acetate hollow fiber membrane loaded with silver nanoparticles, fabricated via wet-jet spinning technique for antibacterial applications. Activated carbon fiber with dispersed silver particles spun using conventional spinning techniques has been shown to have a good potential for water purification (Oya et al. 1993; Pape et al. 2002). Su et al. (2011) fabricated silver nanoparticle-impregnated (3–20 nm) cotton textiles using polyethylene glycol 600 as stabilizer. This fabric showed excellent antimicrobial activity against *S. aureus* ATCC6538 and *E. coli* ATCC11229 with good antibacterial durability retained in multiple washings.

Various researchers have attempted to incorporate silver nanoparticles in carbon nanotubes. Since carbon nanotubes (CNTs) are reported to promote sorption of pollutants (Ruparelia et al. 2008b), CNTs loaded with nanoparticles may serve a dual role in water treatment, i.e., removal of trace contaminants from water along with disinfection. Lukhele et al. (2010) fabricated a cyclodextrin polyurethane polymer containing about 1% multi-walled CNTs loaded with silver nanoparticles and applied it for disinfection of natural water samples. They reported that 300 mg of this polymeric material with 0.019% silver could cause 3-log unit reduction in *E. coli* (initial count 10^2 – 10^4 CFU/100 mL) and almost complete removal of *Vibrio cholera* (initial count 10^1 – 5×10^2 CFU/100 mL) within 90 min when 250 mL of natural water samples were passed through this material. The treated water was found to contain less than 0.1 ppm of silver, which was well within the WHO guidelines for drinking water (WHO 2006). Mohan et al. (2011) successfully grafted silver and copper nanoparticles on to multi-walled carbon nanotubes and demonstrated good antimicrobial efficiency using *E. coli* as the test organism. Results showed that silver and copper containing carbon nanotubes at 21 $\mu\text{g/mL}$ concentration in the culture broth demonstrated 97% and 75% kill, respectively, while the plain carbon nanotubes demonstrated only 20% kill. The free silver and copper nanoparticles demonstrated lower antimicrobial efficacy of 85% and 52%, respectively. The higher antimicrobial efficacy of silver and copper nanoparticles grafted on to carbon nanotubes was attributed to their higher surface area.

Over the past few decades, advances in hydrogel technologies have opened new dimensions for the development of surfaces for antimicrobial applications. Hydrogels usually have well-defined structures that can be modified to yield tailorable functionality and release profile. This attracted many researchers to explore their usage for the antibacterial applications either by directly taking the polymer(s) having antibacterial property or by incorporating the antibacterial agent on the polymeric hydrogel network. Several studies have utilized chitin and its derivative form, chitosan, for making antibacterial hydrogels owing to their innate antibacterial property. Zhao et al. (2003) created hydrogels of carboxymethylated chitin derivatives by high electron beam irradiation which exhibited excellent mechanical properties, with good swelling behavior and satisfying antibacterial activity against *E. coli*. Silver-hyalurone-based hydrogel complexes have shown that the presence of silver ions drastically reduced the adhesion and proliferation of *Staphylococcus epidermidis* (Barbucci et al. 2002). Recently, a hydrogel based on polyvinyl alcohol/polyvinyl pyrrolidone (PVA/PVP) has been prepared by using the γ -irradiation technique which exhibited antibacterial properties. The results showed that, while *Pseudomonas aeruginosa* and *Candida albicans* were resistant against PVA/PVP based hydrogel, *Bacillus subtilis* was very sensitive (Abd El-Mohdy et al. 2009). Since most of the studies regarding incorporation of silver nanoparticles in a hydrogel network were focused on the opto-electronics, biosensors and catalysis applications (Mohan et al. 2006; Pich et al. 2006; Wang et al. 2004), more focused studies are needed to explore their applicability for environmental and biomedical applications.

To date, nanoparticles of copper, silver, gold, silica, titania, and zinc oxide have been incorporated into multilayered assemblies for various applications. However, multilayered films with incorporated silver nanoparticles represent another class of nanocomposites that may contribute to long-term antibacterial effects due to nanoparticle immobilization. Dai and Bruening (2002) synthesized multilayered films by alternate adsorption of polyacrylic acid (PAA) and polyethyleneimine (PEI)-stabilized silver colloids. Post-deposition reduction of the silver ions by heating or exposure to NaBH_4 yielded composite films containing silver nanoparticles which could be used in catalysis and/or antimicrobial coatings. Grunlan et al. (2005) incorporated silver ions and/or cetrимide into the multilayers. They showed that these multilayered assemblies are biocompatible in nature and can provide a sustained release of silver ions. The multilayers exhibited strong antibacterial property and the substitution of cetrимide with silver dramatically enhanced the antimicrobial efficacy of these films. Yuan et al. (2007) prepared a multifunctional antibacterial coating by incorporating silver nanoparticles into the hybrid chitosan/heparin multilayer films which showed long-term antibacterial activity when exposed to low intensity UV light. In another study, polyelectrolyte multilayers (PEMs) including chitosan and dextran sulfate-stabilized silver nanoparticles were deposited on the aminolyzed poly(L-Lactic acid) membrane in a layer-by-layer (LBL) self-assembly process (Yu et al. 2007). These PEMs possessed antibacterial activity against methicilin-resistant *Staphylococcus aureus*.

8.5 Conclusions

The current review was aimed to compare sensitivity across microbial strains against metal/metal oxide nanoparticles. In the literature, antimicrobial activity of silver nanoparticles has been widely reported; however, there are very few studies on interactions of microbes with copper nanoparticles. Due to variations in the methodology adopted for determining the antimicrobial activity of nanoparticles, comparison of results across studies is not feasible. The bactericidal effect of nanoparticles is dependent on the size, shape, surface characteristics and concentration of nanoparticles, the media used and the initial concentration of microorganisms.

In summary, we can conclude that silver nanoparticles exhibit broad spectrum biocidal activity toward bacteria and fungi. This motivates its use in biomedical and environmental applications. Although some studies suggest Gram-positive bacteria have greater resistance to silver nanoparticles, such a conclusion is not supported by this review, since large strain-specific variations is observed even for the same species. Some strains of *B. subtilis* exhibits resistance to silver nanoparticles; however, this is not true for all strains. More studies are needed with copper nanoparticles across various strains before its use can be recommended. Although there are significant prospects for the use of silver and copper nanoparticles, further studies are needed to promote understanding of the antimicrobial mechanisms and

difference in sensitivity towards various bacterial and fungal strains through standardized experimental studies.

With the use of silver nanoparticles in various applications, it is important to re-evaluate the threat posed by these nanoparticles to higher organisms including human beings. There is an urgent need for more toxicological studies. However, the parameters such as surface chemistry, reactivity, and state of dispersion achieved in the laboratory for toxicology studies may not be relevant for assessing behavior in real systems due to the wide variation of pH, ionic strength, ionic composition, and natural organic matter encountered in natural systems. Such factors may change the aggregation state of metal nanoparticles. Thus, antimicrobial activities and toxicities may vary widely in real systems, and microorganisms in these conditions may exhibit different altered susceptibility to metallic nanoparticles than predicted in the laboratory.

Sufficient studies are not available on long-term antimicrobial efficacy of silver nanoparticles or of silver nanoparticles immobilized on surfaces. Disinfection applications need to focus on the recovery of the silver nanoparticles to ensure cost effectiveness. As discussed earlier, the leaching of silver nanoparticles to the environment may be detrimental to the aquatic ecosystem. Immobilization of silver and copper nanoparticles on to surfaces may prove to be more effective for prolonged release of silver ions and for reducing potential environmental risks. However, the potential for direct release of nanoparticles from the surfaces and their toxic effects on human and other organisms needs to be explored further.

References

- Abd El-Mohdy HL, Ghanem S (2009) Biodegradability, antimicrobial activity and properties of PVA/PVP hydrogels prepared by γ -irradiation. *J Polym Res Taiwan* 16:1–10. doi:[10.1007/s10965-008-9196-0](https://doi.org/10.1007/s10965-008-9196-0)
- Ahamed M, Karns M, Goodson M, Rowe J, Hussain SM, Schlager JJ, Hong Y (2008) DNA damage response to different surface chemistry of silver nanoparticles in mammalian cells. *Toxicol Appl Pharm* 233:404–410. doi:[10.1016/j.taap.2008.09.015](https://doi.org/10.1016/j.taap.2008.09.015)
- An J, Wang D, Luo Q, Yuan X (2009) Antimicrobial active silver nanoparticles and silver/polystyrene core-shell nanoparticles prepared in room-temperature ionic liquid. *Mater Sci Eng C* 29:1984–1989. doi:[10.1016/j.msec.2009.03.015](https://doi.org/10.1016/j.msec.2009.03.015)
- Asavavisithchai S, Oonpradern A, Rungsardthong Ruktanonchai U (2010) The antimicrobial effect of open-cell silver foams. *J Mater Sci: Mater Med* 21:1329–1334. doi:[10.1007/s10856-009-3969-9](https://doi.org/10.1007/s10856-009-3969-9)
- Asharani PV, Wu YL, Gong Z, Valiyaveetil S (2008) Toxicity of silver nanoparticles in zebrafish models. *Nanotechnology* 19:1–8. doi:[10.1088/0957-4484/19/25/255102](https://doi.org/10.1088/0957-4484/19/25/255102)
- Asharani PV, Kah Mun GL, Hande MP, Valiyaveetil S (2009) Cytotoxicity and genotoxicity of silver nanoparticles in human cells. *ACS Nano* 3:279–290. doi: [10.1021/nn800596w](https://doi.org/10.1021/nn800596w)
- Barbucci R, Leone G, Magnani A, Montanaro L, Arciola CR, Peluso G, Petillo O (2002) Cu^{2+} and Ag^{1+} complexes with a hyaluron-based hydrogel. *J Mater Chem* 12:3084–3092. doi:[10.1039/b205320a](https://doi.org/10.1039/b205320a)
- Beveridge TJ, Murray RG (1980) Sites of metal deposition in the cell wall of *Bacillus subtilis*. *J Bacteriol* 141:876–887.

- Borkow G, Gabbay J (2009) Copper, An ancient remedy returning to fight microbial, fungal and viral infections. *Curr Chem Biol* 3:272–278.
- Bosetti M, Masse A, Tobin E, Cannas M (2002) Silver coated materials for external fixation devices: *in vitro* biocompatibility and genotoxicity. *Biomaterials*, 23:887–892. doi:[10.1016/S0142-9612\(01\)00198-3](https://doi.org/10.1016/S0142-9612(01)00198-3)
- Brown IG (1993) Metal–ion implantation for large scale surface modification. *J Vac Sci Technol A* 11:1480–1485.
- Burygin GL, Khlebtsov BN, Shantrokha AN, Dykman LA, Bogatyrev VA, Khlebtsov NG (2009) On the enhanced antibacterial activity of antibiotics mixed with gold nanoparticles. *Nanoscale Res Lett* 4:794–801. doi:[10.1007/s11671-009-9316-8](https://doi.org/10.1007/s11671-009-9316-8)
- Cho KH, Park JE, Osaka T, Park SG (2005) The study of antimicrobial activity and preservative effects of nanosilver ingredient. *Electrochim Acta* 51:956–960. doi:[10.1016/j.electacta.2005.04.071](https://doi.org/10.1016/j.electacta.2005.04.071)
- Chou WL, Yu DG, Yang MC (2005) The preparation and characterization of silver-loading cellulose acetate hollow fiber membrane for water treatment. *Polym Advan Technol* 16:600–607. doi:[10.1002/pat.630](https://doi.org/10.1002/pat.630)
- Chu PK, Chen JY, Wang LP, Huang N (2002) Plasma surface modification of biomaterials. *Mater Sci Eng Res* 36:143–206. doi:[10.1016/S0927-796X\(02\)00004-9](https://doi.org/10.1016/S0927-796X(02)00004-9)
- Chudasama B, Vala, AK, Andhariya N, Upadhyay RV, Mehta RV (2009) Enhanced antibacterial activity of bifunctional Fe₃O₄-Ag core-shell nanostructures. *Nano Res* 2: 955–965. doi:[10.1007/s12274-009-9098-4](https://doi.org/10.1007/s12274-009-9098-4)
- Chudasama B, Vala, AK, Andhariya N, Mehta RV, Upadhyay RV (2010) Highly bacterial resistant silver nanoparticles: synthesis and antibacterial activities. *J Nanopart Res* 12:1677–1685. doi:[10.1007/s11051-009-9845-1](https://doi.org/10.1007/s11051-009-9845-1)
- Cioffi N, Torsi L, Ditaranto N, Sabbatini L, Giorgio P (2004) Antifungal activity of polymer-based copper nanocomposite coatings. *Appl Phys Lett* 85:2417–2419. doi:[10.1063/1.1794381](https://doi.org/10.1063/1.1794381)
- Cioffi N, Torsi L, Ditaranto N, Tantillo G, Ghibelli L, Sabbatini L, Blevè-Zacheo T, D’Alessio M, Giorgio Zambonin P, Traversa E (2005) Copper nanoparticle/polymer composites with antifungal and bacteriostatic properties, *Chem Mater* 17:5255–5262. doi:[10.1021/cm0505244](https://doi.org/10.1021/cm0505244)
- Costa CS, Ronconi JVV, Daufenbach JF, Gonçalves CL, Rezin GT, Streck EL, Marques da Silva PM (2010) *In vitro* effects of silver nanoparticles on the mitochondrial respiratory chain. *Mol Cell Biochem* 342:51–56. doi: [10.1007/s11010-010-0467-9](https://doi.org/10.1007/s11010-010-0467-9)
- Dai J, Bruening ML (2002) Catalytic nanoparticles formed by reduction of metal ions in multilayered polyelectrolyte films. *Nano Lett* 2:497–501. doi:[10.1021/nl0255471](https://doi.org/10.1021/nl0255471)
- Dallas P, Tucek J, Jancik D, Kolar M, Panacek A, Zboril R (2010) Magnetically controllable silver nanocomposite with multifunctional phosphotriazine matrix and high antimicrobial activity. *Adv Funct Mater* 20:2347–2354. doi:[10.1002/adfm.200902370](https://doi.org/10.1002/adfm.200902370)
- Drake PL, Hazelwood KJ (2005) Exposure-related health effects of silver and silver compounds: a review. *Ann Occup Hyg* 49:575–585. doi:[10.1093/annhyg/mei019](https://doi.org/10.1093/annhyg/mei019)
- Dorjnamjin D, Ariunaa M, Shim YK (2008) Synthesis of silver nanoparticles using hydroxyl functionalized ionic liquids and their antimicrobial activity. *Int J Mol Sci* 9: 807–820. doi:[10.3390/ijms9050807](https://doi.org/10.3390/ijms9050807)
- Egger S, Lehmann RP, Height MJ, Loessner MJ, Schuppler M (2009) Antimicrobial properties of a novel silver-silica nanocomposite material. *Appl Environ Microbiol* 75:2973–2976. doi:[10.1128/aem.01658-08](https://doi.org/10.1128/aem.01658-08)
- Esteban-Tejeda L, Malpartida F, Esteban-Cubillo A, Pecharroman C, Moya JS (2009a) The antibacterial and antifungal activity of a soda-lime glass containing silver nanoparticles. *Nanotechnology* 20:085103. doi:[10.1088/0957-4484/20/8/085103](https://doi.org/10.1088/0957-4484/20/8/085103)
- Esteban-Tejeda L, Malpartida F, Esteban-Cubillo A, Pecharroman C, Moya JS (2009b) Antibacterial and antifungal activity of a soda-lime glass containing copper nanoparticles. *Nanotechnology* 20:505701. doi:[10.1088/0957-4484/20/50/505701](https://doi.org/10.1088/0957-4484/20/50/505701)
- Fayaz AM, Balaji K, Girilal M, Yadav R, Kalaichelvan PT, Venketesan R (2010) Biogenic synthesis of silver nanoparticles and their synergistic effect with antibiotics: a study against

- gram-positive and gram-negative bacteria. *Nanomedicine-NBM* 6:103–109. doi:[10.1016/j.nano.2009.04.006](https://doi.org/10.1016/j.nano.2009.04.006)
- Falletta E, Bonini M, Fratini E, Nostro AL, Pesavento G, Becheri A, Nostro PL, Canton P, Baglioni P (2008) Clusters of poly(acrylates) and silver nanoparticles: structure and applications for antimicrobial fabrics. *J Phys Chem C* 112:11758–11766. doi:[10.1021/jp8035814](https://doi.org/10.1021/jp8035814)
- Fernandez EJ, Garcia-Barrasa J, Laguna A, Lopez-de-Luzuriaga JM, Monge M, Torres C (2008) The preparation of highly active antimicrobial silver nanoparticles by an organometallic approach. *Nanotechnology* 19:185602. doi:[10.1088/0957-4484/19/18/185602](https://doi.org/10.1088/0957-4484/19/18/185602)
- Gajbhiye M, Kesharwani J, Ingle A, Gade A, Rai M (2009) Fungus-mediated synthesis of silver nanoparticles and their activity against pathogenic fungi in combination with fluconazole. *Nanomedicine-NBM* 5:382–386. doi:[10.1016/j.nano.2009.06.005](https://doi.org/10.1016/j.nano.2009.06.005)
- Gittard SD, Hojo D, Hyde GK, Scarel G, Narayan RJ, Parsons GN (2009) Antifungal textiles formed using silver deposition in supercritical carbon dioxide. *J Mater Eng Perform* 19:368–373. doi:[10.1007/s11665-009-9514-7](https://doi.org/10.1007/s11665-009-9514-7)
- Gogoi SK, Gopinath P, Paul A, Ramesh A, Ghosh SS., Chattopadhyay A (2006) Green fluorescent protein-expressing *Escherichia coli* as a model system for investigating the antimicrobial activities of silver nanoparticles. *Langmuir* 22:9322–9328. doi: [10.1021/la060661v](https://doi.org/10.1021/la060661v)
- Grunlan JC, Choi JK, Lin A (2005) Antimicrobial behavior of polyelectrolyte multilayer films containing cetrimide and silver. *Biomacromolecules* 6:1149–1153. Doi: [10.1021/bm049528c](https://doi.org/10.1021/bm049528c)
- Gutierrez FM, Olive PL, Banuelos A, Orrantia E, Nino N, Sanchez EM, Ruiz F, Bach H, Av-Gay Y (2010) Synthesis, characterization, and evaluation of antimicrobial and cytotoxic effect of silver and titanium nanoparticles. *Nanomedicine-NBM* 6:681–688. doi:[10.1016/j.nano.2010.02.001](https://doi.org/10.1016/j.nano.2010.02.001)
- Hardes J, Ahrens H, Gebert C, Streitbuerger A, Buerger H, Erren M, Gonsel A, Wedemeyer C, Saxler G, Winkelmann W, Goshager G (2007) Lack of toxicological side-effects in silver-coated megaprotheses in humans. *Biomaterials* 28:2869–2875. doi:[10.1016/j.biomaterials.2007.02.033](https://doi.org/10.1016/j.biomaterials.2007.02.033)
- Hernández-Sierra JF, Ruiz F, Pena DCC, Martínez-Gutiérrez F, Martínez AE, Guillén AJP, Tapia-Pérez H, Martínez Castañón G (2008) The antimicrobial sensitivity of *Streptococcus mutans* to nanoparticles of silver, zinc oxide, and gold. *Nanomedicine-NBM* 4:237–240. doi:[10.1016/j.nano.2008.04.005](https://doi.org/10.1016/j.nano.2008.04.005)
- Holtz RD, Filho AGS, Brocchi M, Martins D, Duran, N, Alves OL (2010) Development of nanostructured silver vanadates decorated with silver nanoparticles as a novel antibacterial agent. *Nanotechnology* 21:185102. doi: [10.1088/0957-4484/21/18/185102](https://doi.org/10.1088/0957-4484/21/18/185102)
- Ilic V, Saponjic Z, Vodnik V, Molina R, Dimitrijevic S, Jovancic P, Nedeljko J, Radetic M (2009) Antifungal efficiency of corona pretreated polyester and polyamide fabrics loaded with Ag nanoparticles. *J Mater Sci* 44:3983–3990. doi:[10.1007/s10853-009-3547-z](https://doi.org/10.1007/s10853-009-3547-z)
- Jain J, Arora S, Rajwade JM, Omray P, Khandelwal S, Paknikar KM (2009) Silver nanoparticles in therapeutics: Development of an antimicrobial gel formulation for topical use. *Mol Pharmaceutics* 6:1388–1401. doi:[10.1021/mp900056g](https://doi.org/10.1021/mp900056g)
- Jin WJ, Lee HK, Jeong EH, Park WH, Youk JH (2005) Preparation of polymer nanofibers containing silver nanoparticles by using poly(N-vinylpyrrolidone). *Macromol Rapid Commun* 26:1903–1907. doi:[10.1002/marc.200500569](https://doi.org/10.1002/marc.200500569)
- Jin T, Sun D, Su JY, Zhang H, Sue HJ (2009) Antimicrobial efficacy of zinc oxide quantum dots against *Listeria monocytogenes*, *Salmonella enteritidis*, and *Escherichia coli* O157:H7. *J Food Sci* 74:M46–M52. doi:[10.1111/j.1750-3841.2008.01013.x](https://doi.org/10.1111/j.1750-3841.2008.01013.x)
- Jones N, Ray B, Ranjit KT, Manna AC (2008) Antibacterial activity of ZnO nanoparticle suspensions on a broad spectrum of microorganisms. *FEMS Microbiol Lett* 279:71–76. doi:[10.1111/j.1574-6968.2007.01012.x](https://doi.org/10.1111/j.1574-6968.2007.01012.x)
- Kato K, Uchida E, Kang ET, Uyama Y, Ikada Y (2003) Polymer surface with graft chains. *Prog Polym Sci* 28:59–89. doi:[10.1016/S0079-6700\(02\)00032-1](https://doi.org/10.1016/S0079-6700(02)00032-1)
- Kim JH, Cho H, Ryu SE, Choi MU (2000) Effects of metal ions on the activity of protein tyrosine phosphatase VHR: Highly potent and reversible oxidative inactivation by Cu²⁺ ion. *Arch Biochem Biophys* 382:72–80. doi:[10.1006/abbi.2000.1996](https://doi.org/10.1006/abbi.2000.1996)

- Kim JS, Kuk E, Yu KN, Kim J, Park SJ, Lee HJ, Kim SH, Park YK, Park YH, Hwang C, Kim Y, Lee Y, Jeong DH, Cho M (2007) Antimicrobial effects of silver nanoparticles. *Nanomedicine: NBM* 3:95–101. doi:[10.1016/j.nano.2006.12.001](https://doi.org/10.1016/j.nano.2006.12.001)
- Kim KJ, Sung WS, Moon SK, Choi JS, Kim JG, Lee DG (2008) Antifungal effect of silver nanoparticles on dermatophytes. *J Microbiol Biotechnol* 18:1482–1484.
- Kim KJ, Sung WS, Suh BK, Moon SK, Choi JS, Kim JG, Lee DG (2009a) Antifungal activity and mode of action of silver nanoparticles on *Candida albicans*. *Biometals* 22: 235–242. doi:[10.1007/s10534-008-9159-2](https://doi.org/10.1007/s10534-008-9159-2)
- Kim SW, Kim KS, Lamsal K, Kim YJ, Kim SB, Jung M, Sim SJ, Kim HS, Chang SJ, Kim JK, Lee YS (2009b) An *in vitro* study of the antifungal effect of silver nanoparticles on oak wilt pathogen *Raffaella sp.* *J Microbiol Biotechnol* 19:760–764.
- Clueh U, Wagner V, Kelly S, Johnson A, Bryers JD (2000) Efficacy of silver-coated fabric to prevent bacterial colonization and subsequent device-based biofilm formation. *J Biomed Mater Res* 53:621–631 doi:[10.1002/1097-4636\(2000\)53:6<621::aid-jbm2>3.0.co;2-q](https://doi.org/10.1002/1097-4636(2000)53:6<621::aid-jbm2>3.0.co;2-q)
- Claine SJ, Alvarez PJJ, Batley GE, Fernandes TF, Handy RD, Lyon DY, Mahendra S, McLaughlin MJ, Lead JR (2008) Nanoparticles in the environment: behaviour, fate, bioavailability and effects. *Environ Toxicol Chem* 27:1825–1851. doi:[10.1897/08-090.1](https://doi.org/10.1897/08-090.1)
- Kokura S, Handa O, Takagi T, Ishikawa T, Naito Y, Yoshikawa T (2010) Silver nanoparticles as a safe preservative for use in cosmetics. *Nanomedicine: NBM* 6:570–574. doi:[10.1016/j.nano.2009.12.002](https://doi.org/10.1016/j.nano.2009.12.002)
- Kong H, Jang J (2008) Synthesis and antimicrobial properties of novel silver/polyrhodanine nanofibers. *Biomacromolecules* 9:2677–2681. doi: [10.1021/bm800574x](https://doi.org/10.1021/bm800574x)
- Lee S, Lee J, Kim K, Sim SJ, Gu MB, Yi J, Lee J (2009) Eco-toxicity of commercial silver nanopowders to bacterial and yeast strains. *Biotechnol Bioproc Eng* 4:490–495. doi: [10.1007/s12257-008-0254-6](https://doi.org/10.1007/s12257-008-0254-6)
- Li P, Li J, Wu C, Wu Q, Li J (2005) Synergistic antibacterial effects of β -lactam antibiotic combined with silver nanoparticles. *Nanotechnology* 16:1912–1917. doi: [10.1088/0957-4484/16/9/082](https://doi.org/10.1088/0957-4484/16/9/082)
- Li Q, Mahendra S, Lyon DY, Brunet L, Liga MV, Li D, Alvarez PJ (2008) Antimicrobial nanomaterials for water disinfection and microbial control: potential applications and implications. *Water Res* 42:4591–4602. doi:[10.1016/j.watres.2008.08.015](https://doi.org/10.1016/j.watres.2008.08.015)
- Li WR, Xie XB, Shi QS, Zeng HY, Ou-Yang YS, Chen YB (2010) Antibacterial activity and mechanism of silver nanoparticles on *Escherichia coli*. *Appl Microbiol Biotechnol* 85:1115–1122. doi: [10.1007/s00253-009-2159-5](https://doi.org/10.1007/s00253-009-2159-5)
- Li WR, Xie XB, Shi QS, Duan SS, Ouyang YS, Chen YB (2011) Antibacterial effect of silver nanoparticles on *Staphylococcus aureus*. *Biometals* 24:135–141. doi: [10.1007/s10534-010-9381-6](https://doi.org/10.1007/s10534-010-9381-6)
- Lin YE, Vidic RD, Stout JE, McCartney CA, Yu VL (1998) Inactivation of *Mycobacterium avium* by copper and silver ions. *Water Res* 32:1997–2000. doi:[10.1016/S0043-1354\(97\)00460-0](https://doi.org/10.1016/S0043-1354(97)00460-0)
- Lok C, Ho C, Chen R, He Q, Yu W, Sun H, Tam PK, Chiu J, Che C (2006) Proteomic analysis of the mode of antibacterial action of silver nanoparticles. *J Proteome Res* 5:916–924. doi: [10.1021/pr0504079](https://doi.org/10.1021/pr0504079)
- Lukhele LP, Mamba BB, Momba MNB, Krause RWM (2010) Water disinfection using novel cyclodextrin polyurethane containing silver nanoparticles supported on carbon nanotubes. *J Appl Polym Sci* 10:65–70. doi:[10.3923/jas.2010.65.70](https://doi.org/10.3923/jas.2010.65.70)
- Mahltig B, Gutmann E, Reibold M, Meyer DC, Böttcher H (2009) Synthesis of Ag and Ag/SiO₂ sols by solvothermal method and their bactericidal activity. *J Sol-Gel Sci Technol* 51:204–214.
- Makhluif S, Dror R, Nitzan Y, Abramovich Y, Jelinek R, Gedanken A (2005) Microwave assisted synthesis of nanocrystalline MgO and its use as a bactericide. *Adv Funct Mater* 15:1708–1715. doi:[10.1002/adfm.200500029](https://doi.org/10.1002/adfm.200500029)
- Marambio-Jones C, Hoek EMV (2010) A review of the antibacterial effects of silver nanomaterials and potential implications for human health and the environment. *J Nanopart Res* 12:1531–1551. doi:[10.1007/s11051-010-9900-y](https://doi.org/10.1007/s11051-010-9900-y)

- Mary G, Bajpai SK, Chand N (2009) Copper (II) ions and copper nanoparticles-loaded chemically modified cotton cellulose fibers with fair antibacterial properties. *J Appl Poly Sci* 113:757–766. doi:[10.1002/app.29890](https://doi.org/10.1002/app.29890)
- Min JS, Kim KS, Kim SW, Jung JH, Lamsal K, Kim SB, Jung M, Lee YS (2009) Effects of colloidal silver nanoparticles on sclerotium forming phytopathogenic fungi. *Plant Pathol J* 25:376–380.
- Mohan YM, Premkumar T, Lee K, Geckeler KE (2006) Fabrication of silver nanoparticles in hydrogel networks. *Macromol Rapid Commun* 27:1346–1354. doi:[10.1002/marc.200600297](https://doi.org/10.1002/marc.200600297)
- Mohan R, Shanmugharaj AM, Hun RS (2011) An efficient growth of silver and copper nanoparticles on multiwalled carbon nanotube with enhanced antimicrobial activity. *J Biomed Mater Res B* 96:119–126. doi:[10.1002/jbm.b.31747](https://doi.org/10.1002/jbm.b.31747)
- Morones JR, Elechiguerra JL, Camacho A, Holt K, Kouri JB, Ramirez JT, Yacaman MJ (2005) The bactericidal effect of silver nanoparticles. *Nanotechnology* 16:2346–2353. doi:[10.1088/0957-4484/16/10/059](https://doi.org/10.1088/0957-4484/16/10/059)
- Musarrat J, Dwivedi S, Singh BR, Al-Khedhairi AA, Azam A, Naqvi A (2010) Production of antimicrobial silver nanoparticles in water extracts of the fungus *Amylomyces rouxii* strain KSU-09. *Bioresource Technol* 101:8772–8776. doi:[10.1016/j.biortech.2010.06.065](https://doi.org/10.1016/j.biortech.2010.06.065)
- Nasrollahi A, Pourshamsian K, Mansourkiaee P (2011) Antifungal activity of silver nanoparticles on some of fungi. *Int J Nano Dimens* 1:233–239.
- Oya A, Yoishida S, Abe Y, Iizuka T, Makiyama N (1993) Antibacterial activated carbon fiber derived from phenolic resin containing silver nitrate. *Carbon* 31:71–73. doi:[10.1016/0008-6223\(93\)90157-6](https://doi.org/10.1016/0008-6223(93)90157-6)
- Pal S, Tak YK, Song JM (2007) Does the antimicrobial activity of silver nanoparticles depend on the shape of the nanoparticle? A study of the gram-negative bacterium *Escherichia coli*. *Appl Environ Microbiol* 73:172–1720. doi:[10.1128/aem.02218-06](https://doi.org/10.1128/aem.02218-06)
- Panacek A, Kvitek L, Prucek R, Kolar M, Vecerova R, Pizurova N, Shurma VK, Nevecna T, Zboril R (2006) Silver colloid nanoparticles: synthesis, characterization, and their antibacterial activity. *J Phys Chem B* 110:16248–16253. doi:[10.1021/jp063826h](https://doi.org/10.1021/jp063826h)
- Panacek A, Kolar M, Vecerova R, Prucek R, Soukupova J, Krystof V, Hamal P, Zboril R, Kvitek L (2009) Antifungal activity of silver nanoparticles against *Candida* spp. *Biomaterials* 31:6333–6340. doi:[10.1016/j.biomaterials.2009.07.065](https://doi.org/10.1016/j.biomaterials.2009.07.065)
- Pape HL, Sarena SF, Contini P, Devillers C, Maftah A, Laprat P (2002) Evaluation of the antimicrobial properties of an activated carbon fibre supporting silver using a dynamic method. *Carbon* 40:2947–2954. doi:[10.1016/S0008-6223\(02\)00246-4](https://doi.org/10.1016/S0008-6223(02)00246-4)
- Pich A, Karak A, Lu Y, Ghosh AK, Adler H (2006) Preparation of hybrid microgels functionalized by silver nanoparticles. *Macromol Rapid Commun* 27:344–350. doi: [10.1002/marc.200500761](https://doi.org/10.1002/marc.200500761)
- Qi L, Xu Z, Jiang X, Hu C, Zou X (2004) Preparation and antibacterial activity of chitosan nanoparticles. *Carbohydrate Res* 339:2693–2700. doi:[10.1016/j.carres.2004.09.007](https://doi.org/10.1016/j.carres.2004.09.007)
- Rai M, Yadav A, Gade A (2009) Silver nanoparticles as a new generation of antimicrobials. *Biotechnol Adv* 27:76–83. doi:[10.1016/j.biotechadv.2008.09.002](https://doi.org/10.1016/j.biotechadv.2008.09.002)
- Raffi M, Mehrwan S, Bhatti TM, Akhter JI, Hameed A, Yawar W, Hasan MM (2010) Investigations into the antibacterial behavior of copper nanoparticles against *Escherichia coli*. *Annal Microbiol* 60:75–80. doi:[10.1007/s13213-010-0015-6](https://doi.org/10.1007/s13213-010-0015-6)
- Ruparelia JP, Duttgupta SP, Chatterjee AK, Mukherji S (2008a) Strain specificity in antimicrobial activity of silver and copper nanoparticles. *Acta Biomater* 4:707–716. doi:[10.1016/j.actbio.2007.11.006](https://doi.org/10.1016/j.actbio.2007.11.006)
- Ruparelia JP, Duttgupta SP, Chatterjee AK, Mukherji S (2008b) Potential of carbon nanomaterials for removal of heavy metals from water. *Desalination* 232:145–156. doi:[10.1016/j.desal.2007.08.023](https://doi.org/10.1016/j.desal.2007.08.023)
- Sadiq R, Rodriguez MJ (2004) Disinfection by-products (DBPs) in drinking water and predictive models for their occurrence: a review. *Sci Total Environ* 321:21–46. doi:[10.1016/j.scitotenv.2003.05.001](https://doi.org/10.1016/j.scitotenv.2003.05.001)

- Sadiq IM, Chowdhury B, Chandrasekaran N, Mukherjee A (2009) Antimicrobial sensitivity of *Escherichia coli* to alumina nanoparticles. *Nanomedicine NBM* 5:282–286. doi:[10.1016/j.nano.2009.01.002](https://doi.org/10.1016/j.nano.2009.01.002)
- Saravanan M, Nanda A (2010) Extracellular synthesis of silver bionanoparticles from *Aspergillus clavatus* and its antimicrobial activity against MRSA and MRSE. *Colloid Surf B* 77:214–218. doi:[10.1016/j.colsurfb.2010.01.026](https://doi.org/10.1016/j.colsurfb.2010.01.026)
- Sarkar S, Jana AD, Samanta SK, Mostafa G (2007) Facile synthesis of silver nano particles with highly efficient anti-microbial property. *Polyhedron* 26:4419–4426. doi:[10.1016/j.poly.2007.05.056](https://doi.org/10.1016/j.poly.2007.05.056)
- Sharma VK, Yngard RA, Lin Y (2009) Silver nanoparticles: green synthesis and their antimicrobial activities. *Adv Colloid Interface Sci* 145:83–96.
- Sharma V (2010) Bactericidal action of chemically treated silver surfaces for water disinfection. M Tech. Thesis, IIT Bombay, Mumbai, India.
- Sheikh FA, Kanjwal MA, Saran S, Chung WJ, Kim H (2011) Polyurethane nanofibers containing copper nanoparticles as future materials. *Appl Surf Sci* 257:3020–3026. doi:[10.1016/j.apsusc.2010.10.110](https://doi.org/10.1016/j.apsusc.2010.10.110)
- Siva Kumar V, Nagaraja BM, Shashikala V, Padmasri AH, Madhavendra SS, Raju BD, Rama Rao KS (2004) Highly efficient Ag/C catalyst prepared by electro-chemical deposition method in controlling microorganisms in water. *J Mol Cat-A Chem* 223:313–319. doi:[10.1016/j.molcata.2003.09.047](https://doi.org/10.1016/j.molcata.2003.09.047)
- Silver S (2003) Bacterial silver resistance: molecular biology and uses and misuses of silver compounds. *FEMS Microbiol Rev* 27:41–353. doi:[10.1016/S0168-6445\(03\)00047-0](https://doi.org/10.1016/S0168-6445(03)00047-0)
- Sondi I, Salopek-Sondi B (2004) Silver nanoparticles as antimicrobial agent: a case study on *E. coli* as a model for gram-negative bacteria. *J Colloid Interf Sci* 275:177–182. doi:[10.1016/j.jcis.2004.02.012](https://doi.org/10.1016/j.jcis.2004.02.012)
- Stohs SJ, Bagchi D (1995) Oxidative mechanisms in the toxicity of metal ions. *Free Radic Bio Med* 18:321–336. doi:[10.1016/0891-5849\(94\)00159-h](https://doi.org/10.1016/0891-5849(94)00159-h)
- Su W, Wei SS, Hu SQ, Tang JX (2011) Antimicrobial finishing of cotton textile with nanosized silver colloids synthesized using polyethylene glycol. *J Text Inst* 102:150–156. doi:[0.1080/00405001003603098](https://doi.org/10.1080/00405001003603098)
- Uyama Y, Kato K, Ikada Y (1998) Surface modification of polymers by grafting. *Adv Poly Sci* 137:1–39. doi:[10.1007/3-540-69685-7_1](https://doi.org/10.1007/3-540-69685-7_1)
- Wang C, Flynn NT, Langer R (2004) Controlled structure and properties of thermo responsive nanoparticle-hydrogel composites. *Adv Mater* 16:1074–1079. doi: [10.1002/adma.200306516](https://doi.org/10.1002/adma.200306516)
- Williams DN, Ehrman SH, Holoman TRP (2006) Evaluation of the microbial growth response to inorganic nanoparticles. *J Nanobiotechnol* 4:3. doi:[10.1186/1477-3155-4-3](https://doi.org/10.1186/1477-3155-4-3)
- WHO (2006) Guidelines for drinking water quality, 3rd edn. World Health Organization, Geneva.
- Wu Y, Jia W, An Q, Liu Y, Chen J, Li G (2009) Multi-action antibacterial nanofibrous membranes fabricated by electrospinning: an excellent system for antibacterial applications. *Nanotechnology* 20:245101. doi:[10.1088/0957-4484/20/24/245101](https://doi.org/10.1088/0957-4484/20/24/245101)
- Yoon KY, Byeon JH, Park CW, Hwang J (2007) Antimicrobial effect of silver particles on bacterial contamination of activated carbon fibers, *Environ Sci Technol* 42: 1251–1255. doi:[10.1021/es0720199](https://doi.org/10.1021/es0720199)
- Yu DG, Lin WC, Yang MC (2007) Surface modification of poly(L-lactic acid) membrane via layer-by-layer assembly of silver nanoparticle-embedded polyelectrolyte multilayers. *Bioconjugate Chem* 18:1521–1529. doi:[10.1021/bc060098s](https://doi.org/10.1021/bc060098s)
- Yuan W, Ji J, Fu J, Shen J (2007) A facile method to construct hybrid multilayered films as a strong and multifunctional antibacterial coating. *J Biomed Mater Res B: Appl Biomater* 16:556–563. doi:[10.1002/jbm.b.30979](https://doi.org/10.1002/jbm.b.30979)
- Zhao L, Mitomo H, Zhai M, Yoshii F, Nagasawa N, Kume T (2003) Synthesis of antibacterial PVA/CM-chitosan blend hydrogels with electron beam irradiation. *Carbohydr Polym* 53:439–446. doi:[10.1016/S0144-8617\(03\)00103-6](https://doi.org/10.1016/S0144-8617(03)00103-6)

Chapter 9

Metal-Containing Nano-Antimicrobials: Differentiating the Impact of Solubilized Metals and Particles

Angela Ivask, Saji George, Olesja Bondarenko, and Anne Kahru

9.1 Metal-Containing Antimicrobials: Past, Current and Future

Antiseptics and disinfectants are used extensively in hospitals and other health care settings for a variety of topical and hard-surface applications. In particular, they are an essential part of infection control practices and aid in the prevention of nosocomial infections. Increasing concerns over the potential for microbial contamination and infection risks have led to increased use of antiseptics and disinfectants in health care premises, food processing facilities, public amenities and in many general consumer applications. A wide variety of active chemical agents (or “biocides”) are used in the above-mentioned areas, many of which have been used for hundreds of years for antiseptics, disinfection, and preservation (for a review, see McDonnell and Russell 1999).

A. Ivask (✉)

National Institute of Chemical Physics and Biophysics, Laboratory of Molecular Genetics,
Tallinn, Estonia

University of California Center for Environmental Implications of Nanotechnology, Los Angeles,
CA, USA

e-mail: angela.ivask@kbfi.ee

S. George

University of California Center for Environmental Implications of Nanotechnology, Los Angeles,
CA, USA

School of Chemical and Life Sciences, Nanyang Polytechnic, Singapore

e-mail: saji_GEORGE@nyp.gov.sg

O. Bondarenko • A. Kahru

National Institute of Chemical Physics and Biophysics, Laboratory of Molecular Genetics,
Tallinn, Estonia

e-mail: olesja.bondarenko@kbfi.ee; anne.kahru@kbfi.ee

Based on the type of biocidal active ingredients, antimicrobial agents can be broadly divided into two types: organic and inorganic. One of the earliest used organic antiseptics was phenol (carbolic acid) that Joseph Lister started to use in operating theatres for sterilization of surgical instruments in 1865, which significantly reduced mortality rates associated with surgical procedures. Most of the currently used antibiotics are also of organic nature as they have originally been synthesized by various microorganisms (mostly fungi) to fight their competitors. The inorganic metal-based disinfectants/drugs, however, have an even longer history: silver has been used to fight infections as far back as the days of ancient Greece and Egyptian civilizations. In World War I, before the advent of antibiotics, silver compounds were used to prevent and treat infections. The journal *Lancet* (May 31, 1919) published information on the drugs used in Paris hospitals at that time “. . . Certain popular drugs have only recently been inscribed on the official list, e.g., novocain in 1908, *colloidal silver* in 1909, arsenobenzol in 1911, novarsenobenzol in 1912, and galyl in 1915. Other new remedies still on trial in Paris hospitals include certain *colloidal metals* and organo-therapeutic extracts prepared for intravenous medication. . .”. Moreover, copper materials have been used since 2200 BC to produce drink and food storage vessels which due to their antimicrobial properties prevented spoilage (Dollwet and Sorenson 1985). The onset of zinc as antimicrobial is, however, more recent: since 1977, ZnO has been authorized by US FDA (<http://www.fda.gov/>) in externally applied drugs as well as in cosmetics. Currently, ZnO is used, e.g., as an antiseptic in surgical tapes, deodorants, and soaps, to provide topical relief in skin irritation, diaper rash, minor burns, and cuts. The increasing interest in the use of metals and metal oxides as antimicrobials is attributed to their ability to withstand harsh process conditions, durability and the sustained antimicrobial action which are often the shortcomings of organic antimicrobial compounds.

Along with the rapid development of nanotechnology witnessed during the past 10 years and due to a vast number of studies showing higher effectiveness of nano-sized materials than their micro- or macro-sized counterparts, the metal-containing nano-antimicrobials may present revolutionizing applications in consumer and patient care products. The higher activity of nano-sized materials compared to their ‘larger’ analogues has been mainly attributed to their relatively higher specific surface area and, thus, high amount of active molecules/atoms present on the surface. As an example, a 1-nm nanoparticle would have ~76% of its atoms present on the surface. Thus, the *physical dimensions* as well as the *chemical composition and stability* determine the reactivity of each nanomaterial and govern their specific type of nano–bio interaction. In the following paragraphs, we discuss the current knowledge about the contribution of physical dimensions and chemical characteristics (including dissolution) of the most widely applied and/or most promising metal-containing nano-antimicrobials, Ag, ZnO, TiO₂, and CuO, in their antimicrobial activity. We also present and discuss the (bio)analytical methods that have been developed and/or applied to discriminate between the antimicrobial effects mediated by metal dissolution and particles *per se*.

9.2 Antimicrobial Action of Metal-Containing Nano-Antimicrobials with Special Emphasis on Their Dissolution

As previously mentioned, metal-containing antimicrobials have been considered to bring a revolutionary breakthrough in hygiene as well as in medical applications. However, while we start to enjoy the primary benefit of nanotechnology-based improvements in antimicrobial applications, one of the main questions that need to be answered is: how likely are these nanomaterials to exert their toxic effects on non-target biological systems? This question can only be answered based on extensive knowledge about the detailed mechanisms of action of these metallic nano-antimicrobials. Therefore, it is of utmost importance to understand the key mechanisms of action of already applied or potential antimicrobial compounds *prior* to their large-scale application. Yet, the early studies on metal-containing nanomaterials toxicity did not address the issue but rather reported empirical observations on cellular viability. Only since 2007 have major efforts been made to link the toxicological and antimicrobial potency of nanomaterials to their physico-chemical properties. The observations have indicated that the potency of metal-containing nanomaterials is controlled by their physical dimensions and, most importantly, their chemical stability. Examples of the properties related to nanomaterials' (NMs') physical properties that have been demonstrated to modulate their toxicity are: *size* (Panáček et al. 2006) (Choi and Hu 2008) and *shape* (Pal et al. 2007). Examples of toxicologically important properties related to NMs' chemical composition and stability are: *surface coating* (El Badawy et al. 2010), *doping* (George et al. 2010) and *dissolution* (Cioffi et al. 2005; Morones et al. 2005; Franklin et al. 2007; Smetana et al. 2008; Heinlaan et al. 2008; Kahru et al. 2008; Rai et al. 2009; Jiang et al. 2009; Allaker 2010). Although all these NMs properties may be observed separately, the final toxicological outcome of a nanomaterial is usually due to the joint action (that may lead to synergy) between the key physico-chemical properties. *Metal ion dissolution* from metal-containing nanomaterials may be considered as one of the most important key factors in their toxicity. Due to the fact that bacteria have rigid cell envelopes and do not have internalization mechanisms for supramolecular and colloidal particles, the effect of nano-sized materials on bacterial cells is mostly restricted to the effects at or near the cell wall. Differently from bacteria that are unicellular prokaryotic organisms, most eukaryotic systems have highly developed molecular machineries for internalization of nano- and microscale particles. Therefore, in eukaryotic systems, the physical properties of the NMs may have a markedly greater role than in prokaryotes. Specific examples emphasizing the role of dissolution will follow below for each of the nano-antimicrobials separately, but at this stage, we wanted to emphasize that the dissolution rate of metal oxide NMs has been used in one of the very few nano-QSAR (quantitative structure–activity relationship) models currently available, as a single predictor for their toxicity to *E. coli* in *in vitro* tests (Puzyn et al. 2011).

According to that model, the metal oxides (M) that had lower enthalpy (ΔH_{M^+}) to form a gaseous cation (M^{n+}) in the reaction:



are more likely to be transformed to cations and thus exert toxic effects to *E. coli*.

In the following sections, we give an overview about recent findings on mechanisms of toxic action of the most widely used and most promising metal and metal oxide nano-antimicrobials: TiO₂, Ag, ZnO and CuO.

9.2.1 Nano-TiO₂

9.2.1.1 Importance of Nano-TiO₂ as an Antimicrobial

Nano-TiO₂ is a semiconductor that shows antimicrobial properties during photoactivation and is probably the highest production volume nanomaterial (Mueller and Nowack 2008). The exact current production volumes for TiO₂ are relatively difficult to estimate, however, the current production volume of TiO₂ in USA is estimated to be between 7,800 and 38,000 t/year (Hendren et al. 2011). Robichaud et al. (2009) have estimated that the annual production of this nano metal oxide will reach 2.5 million tonnes by 2025.

The use of TiO₂ in different consumer products including food has a long history and as stated by Dr. Wetter in her presentation on behalf of ETC Group at US FDA Nanotechnology Public Meeting on October 10, 2006 (<http://www.fda.gov/ScienceResearch/SpecialTopics/Nanotechnology/NanotechnologyTaskForce/ucm111425.htm>): "...FDA approved TiO₂ as a food color additive as early as in 1966 with the stipulation that the additive was not to exceed 1% by weight and TiO₂ is also approved as a food packaging additive. Currently TiO₂ is being formulated at the nano-scale and the transparent particles are being used in clear plastic food wraps for UV protection. Apparently, this percent-by-weight limit set back in the 1960s for micro-scale TiO₂ particles is not relevant to today's nano-scale formulations since tiny amounts can produce large effects. And nano-scale TiO₂ in food is just one example...". In addition to the use of TiO₂ in coatings for its white color and UV protection of food, textiles or human skin, the TiO₂-coated surface also has a strong antimicrobial activity when exposed to sunlight. For the first set of applications, TiO₂ natural form, rutile, is used, whereas for antimicrobial applications, a rarer TiO₂ polymorph, anatase, is used (Mueller and Nowack 2008). A large number of studies on the photocatalytic disinfection efficiency of TiO₂ for water purification (Wei et al. 1994), as well as for self-cleaning surfaces (Gelover et al. 2006), has been published. For example, Chen et al. (2008) showed that when TiO₂ particles were attached onto bacterial surfaces, fast antimicrobial effects were observed after UV illumination. Such laboratory research findings are being translated into commercial products: TiO₂ is already used in home air purifiers, e.g. 3Q Multistage Air Purifier and

NanoBreeze Room Air Purifier, to remove volatile organic compounds and kill bacteria. TiO₂ as an antimicrobial is suitable for large-scale antimicrobial applications because it is stable, relatively non-toxic by incidental ingestion, and is low-cost.

9.2.1.2 Evidence for Nano-TiO₂ Antimicrobial Properties

As reported by Kahru and Dubourguier (2010), toxicity of TiO₂ was considerably lower in comparison to other current and potential nano-antimicrobials: ZnO, Ag and CuO. However, it must be noted that, due to the requirement for photoactivation, the available toxicity data for nano-TiO₂ are relatively inconsistent. The reason for this may be varying light exposure conditions and illumination duration, and the test media, as well as TiO₂ concentrations used. Interestingly, our recent data (A. Ivask, unpublished data) showed that the antibacterial effect of TiO₂ is not linearly related to the applied dose and that addition of highly concentrated (>100 µg/mL) nano-TiO₂ aqueous suspension to a photoactivation experiment decreased its antibacterial effects. This may be the reason why TiO₂ exerts its optimal photocatalytic antimicrobial activity when immobilized on to a surface (Ireland et al. 1993). Currently, the inhibitory potential of TiO₂ against *Escherichia coli*, *Bacillus subtilis* (Ireland et al. 1993; Adams et al. 2006), *Staphylococcus aureus* (Tsuang et al. 2008), MRSA (methicillin-resistant *Staphylococcus aureus*) (Sunada et al. 1998; Wei et al. 1994), *Enterococcus hirae*, *Pseudomonas aeruginosa*, *Bacterioides fragilis* (Tsuang et al. 2008) and natural bacterial community (Gelover et al. 2006) has been reported. The reported concentrations of TiO₂ required to affect bacterial viability usually vary between 100 and 1,000 µg/mL, depending on the size of the particles and the intensity and wavelength of the light applied for photoactivation (Wei et al. 1994). Gelover et al. (2006) showed that 15-min exposure to 87 µg/mL of TiO₂ was enough to completely inactivate fecal coliforms. On the other hand, 10,000 µg/mL of TiO₂ was reported as an effective concentration to inactivate *S. aureus*, *E. hirae* and *P. aeruginosa*, *B. fragilis* and *E. coli* after 50-min exposure to UV light (Tsuang et al. 2008). As mentioned above, these differences in effective concentrations may be due to the differences in exposure conditions and properties of the nanomaterials.

9.2.1.3 Modes of Antimicrobial Action of Nano-TiO₂

Toxicity and antimicrobial properties of TiO₂ have almost exclusively been linked to its photoexcitation under UV light. Upon UV light exposure, electrons in the valence band get excited to a conduction band leaving behind a hole. The conduction band electron and valence band hole can react with molecular oxygen and water molecules, respectively, to generate superoxide and hydroxyl radical. Thus, the most commonly formed ROS include hydroxyl radicals, superoxide and peroxide production under UV irradiation (Kikuchi et al. 1997). For a more detailed

discussion on the mechanisms of antibacterial action of TiO₂ nanoparticles, the reader is directed to the excellent review by Foster et al. (2011). In addition to bacteria, TiO₂ nanoparticles in combination with UV light have been shown to inactivate microorganisms such as blue-green algae *Anabaena*, *Microcystis*, and *Melosira* (Kim and Lee 2005) and *Chroococcus* sp. (Hong et al. 2005) by potentially destroying the algal cell surface. In addition, a specific aggregation of algal cells with TiO₂ particles leading to poorer growth or decreased photosynthetic ability of the algae have been reported by several groups (Aruoja et al. 2009; Sadiq et al. 2011). Toxicity data of TiO₂ are also available for a number of other (eco)toxicological model organisms. However, these data are often variable, which may be the result of different exposure conditions used as well as of different physico-chemical properties of TiO₂ used in the experiments (Menard et al. 2011).

9.2.1.4 The Role of Dissolution in Antimicrobial Action of TiO₂

Currently, no reports showing the release of metal ions from TiO₂ nanomaterials and their significant effects in toxicity have been published and, thus, the antimicrobial effect of this material may be attributed solely to its photocatalytic and surface redox properties. However, as TiO₂ nanoparticles have also shown toxicity to *Bacillus subtilis* and *E. coli* in dark conditions (Adams et al. 2006), the mechanisms of action of bactericidal properties of nano-TiO₂ warrants further investigations.

9.2.2 Nano-ZnO

9.2.2.1 Importance of Nano-ZnO as an Antimicrobial

ZnO is probably the second highest volume of metal-containing nanomaterials produced after TiO₂. As mentioned above, ZnO is typically used to provide relief in skin irritation, diaper rash, minor burns and cuts but also in cosmetics such as deodorants and soaps. Since nano-sized ZnO is believed to exert a higher efficacy than the micro- or macro-sized ZnO, the applications of nano-ZnO include packaging materials in the food industry (Tayel et al. 2011), dental applications to prevent biofilm formation (Allaker 2010), antimicrobial wallpaper (Ghule et al. 2006) or in textiles (Rajendran et al. 2010). ZnO-impregnated textiles have been shown to retain their antimicrobial properties even after 50 washing cycles (Rajendran et al. 2010).

9.2.2.2 Evidence for Nano-ZnO Antimicrobial Properties

The antibacterial activity of nano-ZnO has been demonstrated towards both Gram-negative and Gram-positive bacteria although at relatively high concentrations. The reported effective concentrations of nano-ZnO fall usually between 80 and

10,000 µg/mL depending on the observed endpoint and test conditions. EC₅₀ values for nano-ZnO have been reported between 1.8 and 1,000 µg/mL (Adams et al. 2006; Brayner et al. 2006; Heinlaan et al. 2008; Gajjar et al. 2009; Baek and An 2011) whereas complete growth inhibition has been observed at higher concentrations even reaching 10,000 µg/mL (Ren et al. 2009; Applerot et al. 2009; Liu et al. 2009). The efficacy of nano-ZnO has also been shown towards yeast *Saccharomyces cerevisiae* at 120–130 µg/mL (Kasemets et al. 2009).

9.2.2.3 Modes of Antimicrobial Action of Nano-ZnO

Based on the current literature, three mechanisms leading to nano ZnO toxicity and antimicrobial effects may be pointed out: (1) *dissolution*, (2) *size*, and (3) *induction of reactive oxygen species* (ROS) (Table 9.1). As mentioned above, these mechanisms can be related to each other and also combined.

Dissolution of ZnO to Zn ions has been considered as the mechanism for (nano-) ZnO toxicity in a vast number of papers and these are discussed below (Sect. 9.2.2.4). Here, we discuss the evidence for size-related and ROS-dependent toxicity mechanisms of nano-ZnO.

Nanosize has been considered as an important property leading to nano-ZnO toxicity by Jones et al. (2008) and Applerot et al. (2009). In the first study, it was demonstrated that 5-nm initial-sized particles were five-fold more toxic than 50–70-nm particles (Jones et al. 2008), and the second study showed that 6.8-nm ZnO particles exerted much higher antibacterial activity than 260 or 800-nm particles (Applerot et al. 2009). In addition to the increased surface area of the smaller particles, smaller sized nano-ZnO has even been suggested and/or proven to enter the cells of *E. coli* and *S. aureus* (Brayner et al. 2006; Liu et al. 2009; Applerot et al. 2009) (Fig. 9.1b,c). The internalization of ZnO nanoparticles by bacterial cells is surprising since the sizes of nanoparticles are approximately 50 times larger than the pore sizes of the membrane pumps and, according to the available information, bacteria have no internalization mechanisms for supramolecular and colloidal particles. The authors suggested that possibly, the *de novo* formation of respective membrane channels for small nanoparticles takes place in real time (Applerot et al. 2009). Indeed, bacteria have shown to internalize <5-nm CdSe and CdSe/ZnS quantum dots, probably by oxidative damage of the cell membrane potentialized by light (Kloepfer et al. 2005).

The evidence for induction of ROS as one of the toxicity mechanisms of nano-ZnO has been presented by Sawai (2003), Ghule et al. (2006), Zhang et al. (2007), Applerot et al. (2009), and Ivask et al. (2010). Sawai (2003) even suggested the photocatalytic generation of hydrogen peroxide to be one of the primary mechanisms of ZnO toxicity. Indeed, ZnO is a semiconductor that upon absorption of photons transports its electrons between the valence and conduction band. The photogenerated electrons and electron holes undergo reactions with dissolved molecular oxygen, surface hydroxyl groups or adsorbed water molecules to form

Table 9.1 Selected studies reporting on the contribution of dissolved metal ions in antimicrobial effects of metal containing nanomaterials

Nanomaterial Type	Description	Test organism	Toxicity endpoint	Quantity dissolved (method used for metal ion separation)	Contribution of dissolved ions in toxicity	Additional reported toxicity mechanisms	Reference
Ag	Commercial, nano-Ag, <100 nm	<i>E. coli</i> bioluminescent cells	Inhibition of bioluminescence	3.3% of Ag solubilized (bioavailable Ag ions analyzed by cellular Ag biosensors)	100% of toxicity caused by solubilized Ag ions.	ROS due to solubilized ions	Ivask et al. (2010)
Commercial, nano-Ag, <100 nm	ROS inducible <i>E. coli</i>	Induction of bioluminescence by ROS	3.3% of Ag solubilized (bioavailable Ag ions analyzed by cellular Ag biosensors)	Nano-Ag induced more ROS than could be expected from Ag ions	ROS due to nanoparticles per se at subtoxic concentrations	Ivask et al. (2010)	
Citrate-stabilized nano-Ag, 10 nm	<i>E. coli</i>	Bacterial growth (number of cells)	0.1% of the total silver in nano Ag (filtration, 3,000 kDa cutoff)	Nano-Ag was 10 ³ –10 ⁴ times more toxic than Ag dissolution predicted	ROS due to nanoparticles, enhanced intracellularization of nano Ag compared to Ag ⁺ , intracellular release of ions	Lok et al. (2007)	
16 nm nano-Ag particles in carbon matrix	<i>E. coli</i> , <i>P. aeruginosa</i>	Bacterial growth (number of cells)	<5 μM (stripping voltammetry)	Nano-Ag was more toxic than respective concentration of soluble Ag salt	Accumulation of nano Ag in cell membrane and intracellularly	Morones et al. (2005)	
In-house SMAD synthesized nano-Ag, 3–100 nm	<i>E. coli</i>	10-minute decrease in viable colonies	Qualitative estimation (addition of NaCl and observation of white precipitate formation and reduction in toxicity)	Formation of Ag ⁺ was the only cause for nano-Ag toxicity	None	Smetana et al. (2008)	
Nano-Ag-coated plastic catheters	<i>E. coli</i> , <i>E. faecalis</i> , <i>S. aureus</i> , <i>P. aeruginosa</i> , <i>C. albicans</i>	Biofilm formation	15% of Ag release in 10 days (radioactive ^{110m} Ag released)	Catheter surface decreased bacterial biofilm formation; however no quantitative correlations with Ag release was performed	None	Roe et al. (2008)	

Polymer-immobilized nano-AgBr	<i>E. coli</i> , <i>B. cereus</i>	MIC, biofilm formation	2.8–3.65 ppm/g AgBr dissolved (filtration, 200 nm filter)	Toxicity of AgBr composites was due to the release of Ag ions to test media for prolonged periods	None	Sambly et al. (2006)
In-house synthesized nano-Ag, 3 nm	<i>E. coli</i> , <i>S. aureus</i> , <i>B. subtilis</i>	Growth inhibition	0.3% in DI water, and 4% in nutrient media (filtration, 200 nm filter)	Toxicity of nano-Ag was higher than respective amount of soluble Ag salt	Mechanical membrane damage	Ruparella et al. (2008)
In-house synthesized nano-Ag	yeast, <i>E. coli</i> , <i>S. aureus</i>	Growth inhibition	No Ag ions quantified	Nano-Ag and Ag ions exhibited similar effect towards <i>E. coli</i> at similar concentration	ROS generation	Kim (2007)
ZnO 30 nm	<i>V. fischeri</i>	Inhibition of bioluminescence	100% between 0.1 and 1 mg/L of ZnO (bioavailable Zn ions analyzed by cellular Zn biosensors)	100% of toxicity was due to solubilized Zn ions	None	Heinlaan et al. (2008)
Commercial ZnO, 30 nm	<i>E. coli</i> bioluminescent cells	Inhibition of bioluminescence	100% between 0.1 and 1 mg/L of ZnO (bioavailable Zn ions analyzed by cellular Zn biosensors)	100% of toxicity was due to solubilized Zn ions	H ₂ O ₂ in addition to solubilized Zn ions	Ivask et al. (2010)
Commercial ZnO, 30 nm	ROS inducible <i>E. coli</i>	Induction of bioluminescence by ROS	100% between 0.1 and 1 mg/L of ZnO (bioavailable Zn ions analyzed by cellular Zn biosensors)	100% of toxicity was due to solubilized Zn ions	H ₂ O ₂ in addition to solubilized Zn ions	Ivask et al. (2010)
Commercial ZnO, 30 nm	<i>S. cerevisiae</i>	Growth inhibition	100% between 0.1 and 1 mg/L of ZnO (bioavailable Zn ions analyzed by	100% of toxicity was due to solubilized Zn ions	None	Kasemets et al. (2009)

(continued)

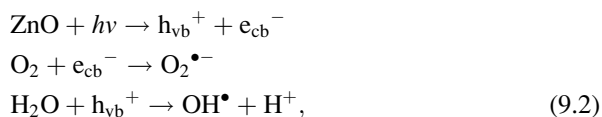
Table 9.1 (continued)

Nanomaterial Type	Description	Test organism	Toxicity endpoint	Quantity dissolved (method used for metal ion separation)	Contribution of dissolved ions in toxicity	Additional reported toxicity mechanisms	Reference
Commercial ZnO		<i>P. chlororaphis</i>	Growth inhibition	cellular Zn biosensors 15–30% (at pH 7.12 and 6–5, respectively) (centrifugation at 15,000 g)	Some toxicity was due to solubilized ions	None	Dimkpa et al. (2011)
Commercial ZnO	<100 nm	<i>E. coli</i>	Viability, growth	1.90%, depending on dissolution media (centrifugation at 10,000 g 30 min, filtration through 200 nm)	All toxicity of ZnO was due to solubilized Zn ions	None	Li et al. (2011)
Commercial and in-house synthesized, 20–30 nm		<i>E. coli</i> , <i>P. putida</i> , <i>B. subtilis</i>	Viability	30% of total Zn in nanomaterial (filtration, 100-nm filter)	All toxicity due to Zn ions, no nano-specific effect detected	None	Li et al. (2010)
In-house synthesized ZnO		<i>E. coli</i> , <i>S. aureus</i>	Viability	Not quantified; 1.6–5 mg/L of Zn was considered as maximum solubilization from ZnO	No toxicity due to Zn ions, mainly due to membrane damage, OH [•] production	Formation of OH [•] on the nanomaterials surface	Applerot et al. (2009)
CuO	Polymer nanocomposite loaded with nano-CuO	<i>S. cerevisiae</i> , mold, <i>E. coli S. aureus</i> , <i>L. monocytogenes</i>	Growth inhibition	Qualitative (electro-thermal atomic absorption spectroscopy ETAAS)	Toxicity increased with increasing CuO (and, thus, Cu ion) concentration in the polymer-matrix	None	Cioffi et al. (2005)
In-house synthesized, CuO, 7–17 nm		<i>E. coli</i> , <i>B. subtilis</i> , <i>S. aureus</i>	Growth inhibition	17% in rich media, 0.5% in water (not specified)	n.d	None	Ruparella et al. (2008)

In-house synthesized Cu-doped TiO ₂ , 20 nm	<i>M. smegmatis</i> ; <i>S. onidenstis</i>	Growth inhibition	Qualitative (ultracentrifugation, filtration, EDTA chelation)	100% of Cu doped to TiO ₂ was in soluble form toxicity increased with increasing Cu doping in TiO ₂	None	Wu et al. (2009)
Commercial CuO, 30 nm	<i>V. fischeri</i>	Inhibition of bioluminescence	33% (between 1 and 20 mg/L) (bioavailable Cu ions analyzed by cellular Cu biosensors)	Contribution from solubilized ions relatively high (almost 100%)	None	Heinlaan et al. (2008)
Commercial CuO, 30 nm	<i>E. coli</i>	Inhibition of bioluminescence	33% (between 1 and 20 mg/L) (bioavailable Cu ions analyzed by cellular Cu biosensors)	100% of toxicity was due to solubilized Cu ions	None	Ivask et al. (2010)
Commercial CuO, 30 nm	O ₂ ⁻ inducible <i>E. coli</i>	Induction of bioluminescence by O ₂ ⁻	33% (bioavailable Cu ions analyzed by cellular Cu biosensors)	100% of ROS generation was due to solubilized Cu ions	O ₂ ⁻ radicals were only due to solubilized Cu ions	Ivask et al. (2010)
Commercial CuO, 30 nm	H ₂ O ₂ and DNA damage inducible <i>E. coli</i>	Induction of bioluminescence by H ₂ O ₂ and ssDNA	20% (bioavailable Cu ions analyzed by cellular Cu biosensors)	100% of ROS generation was due to solubilized Cu ions	H ₂ O ₂ and DNA damage were only due to solubilized Cu ions	O. Bondarenko et al. (unpublished data, 2011)
Commercial CuO, 30 nm	<i>S. cerevisiae</i>	Growth inhibition	33% (bioavailable Cu ions analyzed by cellular Cu biosensors)	50% of toxicity was due to solubilized Cu ions	ROS	Kasemets et al. (2009)
Commercial CuO, 33 nm	<i>P. chlororaphis</i>	Growth inhibition	0.25–2% at pH 6 and 7 (centrifugation)	Partial toxicity due to Cu ions	None	Dimkpa et al. (2011)

ROS reactive oxygen species

hydroxyl (OH^\bullet) and superoxide ($\text{O}_2^{\bullet-}$) radicals, as suggested by (Niazi and Gu 2009):



where e_{cb}^- is a conducting band electron and h_{vb}^+ is the valence-band hole. Neal (2008) has suggested that ZnO-induced ROS may lead to disruption of bacterial membranes and thereby induce their porosity, which could further result in uptake of ZnO nanoparticles *via* the damaged cell wall. Membrane deformations and impaired morphology of bacterial cells after exposure to nano-ZnO have been demonstrated by Zhang et al. (2007) and Li et al. (2011) (see also Fig. 9.1). Also, electrochemical

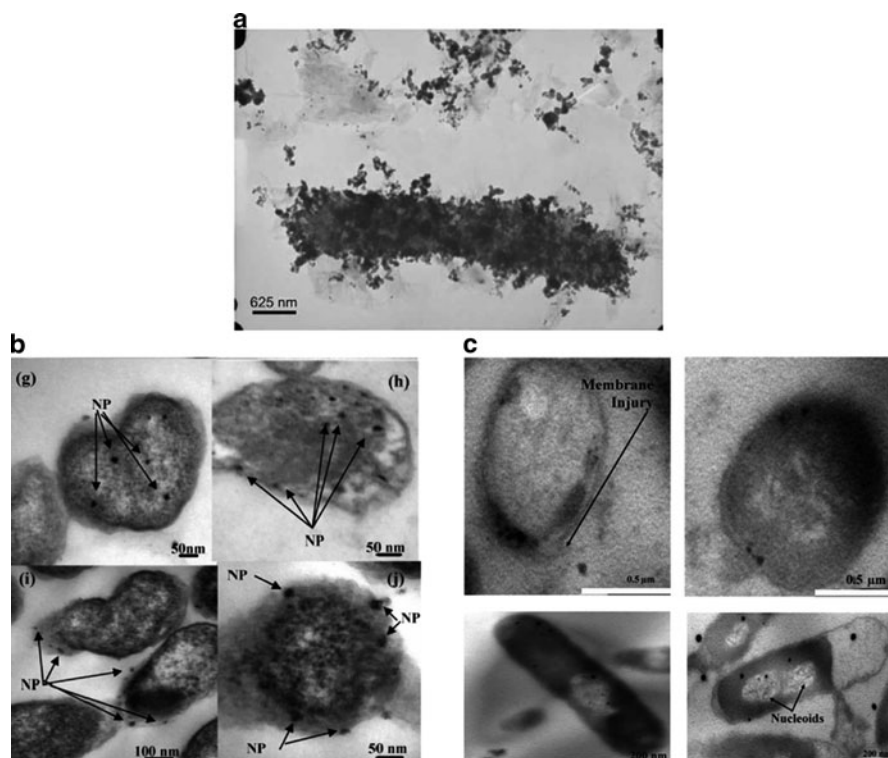
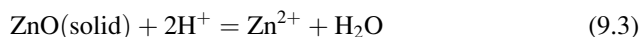


Fig. 9.1 Evidence for surface attachment and internalization of nano-ZnO by bacterial cells. (a) Attachment of ZnO nanoparticles to *E. coli* surface (cells were exposed to 100 $\mu\text{g}/\text{mL}$ of ZnO) (Reprinted from Jiang et al. 2009. With permission from Elsevier). (b) Intracellular nano-ZnO in *E. coli* cells (ZnO particles are shown with *black arrows*) (Reprinted from Brayner et al. 2006. Copyright American Chemical Society). (c) Internalization of nano-ZnO (primary size 6.8 nm) in *S. aureus* (*upper row*) and *E. coli* (*lower row*) cells (Reprinted from Applerot et al. 2009. Copyright Wiley; reproduced with permission)

measurements using a model 1,2-dioleoyl-sn-glycero-3-phosphocholine (DOPC) lipid monolayer suggest a tight interaction between ZnO nanoparticles and the bacterial membranes and resulting membrane damage (Zhang et al. 2007).

9.2.2.4 The Role of Dissolution in Antimicrobial Action of Nano-ZnO

ZnO could certainly be suggested as a metal-containing nanomaterial the effect of which has most often been directly connected with its dissolution and shedding of the toxic heavy metal ion, Zn^{2+} (Table 9.1). Hereby, it is interesting to note that the Material Safety Data Sheets for ZnO and nano ZnO (CAS 1314-13-2) state that this material is *poorly soluble* or even *insoluble* or the solubility data are missing, leading, thus, to erroneous conclusions and precautions by end-users. Dissolution of ZnO has been believed to occur during surface hydrolysis of this metal oxide:



The first paper discussing the dissolution of ZnO as a reason for toxicity was by Franklin et al. (2007) using freshwater algae. These authors demonstrated that, even at pH 7.6, a very rapid dissolution of ZnO bulk and nano forms took place, and at 100 μg of ZnO/mL, at least 15 $\mu\text{g}/\text{mL}$ was present as Zn ions. They showed that, if dissolved Zn from ZnO was used as the concentration unit, the obtained EC_{50} values for nano-ZnO and a soluble Zn salt coincided. Li et al. (2011) showed almost complete dissolution of ZnO nanomaterials in most commonly used bacteriological media, LB (rich organic media) and Minimal Davis (mineral media with citrate) media – at 100 μg of nano-ZnO/mL, 90% and 40% of it was detected as soluble Zn, respectively. Interestingly, solubility of nano ZnO in other environments – saline, water and PBS (phosphate-buffered saline) – was markedly lower but still 12%, 7% and about 1% of nano ZnO was present as dissolved ions, respectively. Li et al. (2010) showed marked dissolution of Zn ions from nano-ZnO – at 1 $\mu\text{g}/\text{mL}$, the dissolution rate was 0.3 $\mu\text{g}/\text{mL}$ being completely responsible for their observed antibacterial effects as proven by parallel testing with a soluble Zn salt. Thus, the authors concluded that no measurable ‘nano effect’ was associated with ZnO bacterial toxicity. Liberation of Zn ions from ZnO nanoparticles has been shown as the sole mechanism for their antibacterial (Adams et al. 2006; Heinlaan et al. 2008; Ivask et al. 2010; Wu et al. 2010), algacidal (Aruoja et al. 2009) and antifungal activity (Kasemets et al. 2009). Similarly to antibacterial effects of ZnO, systematic investigations into the mammalian toxicity of ZnO nanoparticles also pointed towards the dissolution and release of Zn^{2+} ion as the principal mechanism of toxicity (Xia et al. 2008; George et al. 2010). Limiting the dissolution of ZnO in aqueous media by iron doping reduced the toxicity of ZnO in mammalian cells and higher organisms (Xia et al. 2008; George et al. 2011). In addition to ZnO dissolution due to physico-chemical processes in the surrounding environment, cellular activities (excretion of acids as metabolic by-products, for example) may also lead

to its dissolution. For example, Fasim et al. (2002) showed that the bacteria *P. aeruginosa* can solubilize nano-ZnO and other solid Zn salts, and total dissolution of 14 mM (1,140 µg/mL) ZnO in 3 days was achieved. It is interesting to note that along with ZnO dissolution, pH of bacterial culture decreased to 3.5 which by itself could be one additional reason for the observed ZnO dissolution. Finally, we want to emphasize that the solubility of nano-ZnO may not necessarily be solely due to its nano-property. This is supported by the fact that at least up to a certain concentration of ZnO, several studies have shown similar dissolution and also toxicological effects of bulk and nano-ZnO materials (Heinlaan et al. 2008; Kasemets et al. 2009; Aruoja et al. 2009; Ivask et al. 2010; Li et al. 2011). Keeping this finding in mind, the past consideration of “insolubility” of ZnO is even more surprising.

9.2.3 Nano-Ag

9.2.3.1 Importance of Nano-Ag as an Antimicrobial

Silver has probably the longest application history among all the metal-containing antimicrobials. Even today, its antimicrobial application is increasing due to its efficacy, high durability and resistance to high temperature processing. One can safely say that, among all antimicrobial nanomaterials, *nano-Ag* is used in the highest number and variety of consumer products from cosmetic applications, clothing, shoes, and detergents to dietary supplements, surface coatings, respirators, water filters, cell phones, laptop keyboards and children’s toys (Maynard 2007). About 300 of over 1,000 nanomaterial-containing consumer products currently on the market contain nano-Ag (www.nanotechproject.org). Although the history of intended use of Ag in consumer products dates back to 2000, nano-Ag-containing products have been on the market for hundreds of years. Nanoscale silver colloids, known under different trade names such as Collargol, Argyrol, and Protargol entered the market in the early part of the twentieth century and over a 50-year period their use became widespread. These nanosilver products were sold as over-the-counter medications and also used by medical doctors to treat various diseases such as syphilis and other bacterial infections. Moreover, after the establishment of the EPA in 1970, all silver registrations in the next 23 years until 1993 were for nano-silver (colloidal silver) or for silver nanocomposites (for a review, see Nowack et al. 2011). Warningly, the increasing use of colloidal silver in over-the-counter drugs and also in these available the Internet have increased reports in cases of argyria in people, i.e. skin coloration due to hematogenous spread after topical application (Sebastian Tomi et al. 2004) or ingestion of *argentum proteinatatum* (colloidal silver) preparations (White et al. 2003). Nowadays, nano-sized silver preparations may be used in a number of forms – as metallic silver nanoparticles, silver-impregnated zeolite powders and activated carbon materials, dendrimer–silver

complexes, silver–titanium dioxide composite nanopowders, and silver nanoparticles coated onto polymers like polyurethane (Marambio-Jones and Hoek 2010).

9.2.3.2 Evidence for Nano-Ag Antimicrobial Properties

There are numerous publications showing the toxicity of nano-Ag to microorganisms (Kahru and Savolainen 2010). The list of microbes that have been reported as sensitive to nano-Ag consist of but is not limited to bacteria *E. coli*, *Staphylococcus aureus*, *S. epidermis*, *Leuconostoc mesenteroides*, *Bacillus subtilis*, *Klebsiella mobilis*, and *K. pneumoniae*, *Enterococcus faecalis*, and *Pseudomonas aeruginosa* (Balogh et al. 2001; Sondi and Salopek-Sondi 2004; Kim 2007; Kim et al. 2007; Benn and Westerhoff 2008; Chen and Chiang 2008; Falletta et al. 2008; Jung et al. 2008; Roe et al. 2008; Ruparelia et al. 2008; Smetana et al. 2008; Vertelov et al. 2008; Yoon et al. 2008; Zhang et al. 2008; Kim et al. 2009a; El-Rafie et al. 2010), yeasts *Candida albicans* and *Saccharomyces cerevisiae*, fungi *Aspergillus niger* and *Penicillium citrinum* (Kim et al. 2007; Roe et al. 2008; Vertelov et al. 2008; Zhang et al. 2008; Kim et al. 2009b). Given that nano-Ag is effective towards such a wide range of microbes, it is highly likely that nano-Ag would also adversely affect useful microflora, e.g., present in soil, human skin and gut. Although the variety of nano-Ag materials that have been tested for antimicrobial effects is high; ranging from uncoated to coating-stabilized and polymer-embedded nanoparticles, generally the toxicity of nano-Ag as measured by bacterial growth inhibition falls between 0.2 and 300 µg/mL. Gajjar et al. (2009) showed a decrease in CFU (colony-forming units) of *Pseudomonas putida* at 0.2 µg of nano-Ag/mL, while Vertelov et al. (2008) showed growth inhibition of *E. coli* and *S. aureus* cells by 5 µg of differentially coated Ag nanomaterials/mL. Kvitek et al. (2008) showed that the MIC (minimal inhibitory concentration) for non-coated nano-Ag aqueous suspension for *S. aureus*, *E. faecalis*, *E. coli*, and *P. aeruginosa* ranged from 1.6 to 13.5 µg/mL. Smetana et al. (2008) showed a decreasing effect of 30 µg/mL aqueous dispersion of Ag nanomaterials to *E. coli*, CFU after 10 min of exposure. Raffi et al. (2008) showed that *E. coli* cells were completely inhibited by 60 µg of nano-Ag/mL, Sambhy et al. (2006) demonstrated growth inhibition of *E. coli* and *Bacillus cereus* by 50 µg of AgBr-cationic polymer-embedded particles/mL and Ren et al. (2009) reported that 100 µg of nano-Ag/mL was MIC for *S. aureus*, *E. coli* and *P. aeruginosa*. The only study reporting very different antimicrobial activity of nano-Ag is by Kim et al. (2007) who showed that 13.4-nm silver nanoparticles prepared by reduction with borohydride had MIC of 0.00043 µg/mL for *E. coli*, 0.00356 µg/mL for *S. aureus* and 0.001 µg/mL for yeast isolated from bovine mastitis.

9.2.3.3 Modes of Antimicrobial Action of Nano-Ag

Despite the vast number of papers discussing the antimicrobial effects of nano-Ag, there is still no common agreement concerning the mechanisms of the observed

effects. Generally, there are three mechanisms that are brought up to explain the antibacterial mechanism of Ag nanomaterials: (1) *release of silver ions* by dissolution (Hwang et al. 2008; Smetana et al. 2008; Rai et al. 2009); (2) *generation of reactive oxygen species* (ROS) by reactions taking place on nano-Ag surface with molecular oxygen (Kim et al. 2007; Hwang et al. 2008) and (3) *surface reactivity* due to different crystal defects on nanomaterials surface (Morones et al. 2005; Pal et al. 2007) (Table 9.1). Whether all these mechanisms function independently or synergistically, is still unclear. Although there is evidence for the generation of ROS, and papers are emerging showing the importance of surface reactivity in nano-Ag toxicity, the final toxic outcome is most likely a joint/additive (or, potentially, even synergistic) effect of all these factors combined with the ‘nano’ effect of these particles and dissolution. For example, even when Navarro et al. (2008) observed that the toxicity of Ag nanoparticles for *Chlamydomonas reinhardtii* was higher than what could be predicted based on their dissolution rate, they finally suggested that the enhanced toxicity of nano-Ag was due to increased dissolution of Ag⁺ ions when Ag nanoparticles interacted with H₂O₂ generated by the algae. Another study by Lok et al. (2007) showed that Ag nanoparticles exerted 1,000-fold higher antimicrobial activity than could be predicted from their dissolution rate (0.1% of nanoparticles were in dissolved form). Again, the authors suggested that the final cause of the observed toxicity were still dissolved Ag ions released upon internalization of 10 nm nano-Ag. Additional evidence for nano-Ag ‘nano effect’ combined with dissolution was presented by Choi and Hu (2008). These authors observed an increased bactericidal activity of 5-nm-sized Ag nanoparticles compared to what could be expected based on their dissolution and suggested that, upon direct contact with membranes, local dissolution of nano-Ag occurred and the released Ag ions acted on membrane-bound enzymes of nitrifying bacteria. Indeed, as also discussed by Morones et al. (2005) and Sondi and Salopek-Sondi (2004), direct association of nano-Ag with bacterial membranes and subsequent local release of Ag ions may be involved in nano-Ag toxicity (Fig. 9.2). Also, Kim et al. (2007) and El Badawy et al. (2010) have shown that efficient binding of Ag nanomaterials onto bacterial surfaces is a prerequisite for their toxicity. El Badawy et al. (2010) even presented a clear decrease in nano-Ag toxicity to *E. coli* when the surface charge was converted to negative by certain surface coatings and, thus, the binding efficacy of nanoparticles onto membranes was decreased. Ruparelia et al. (2008) suggested that the bound Ag nanomaterials may exert toxic effects due to membrane damage. Liao et al. (1997) evidenced that this large-scale membrane damage by degrading the cell surfaces and forming pits as shown by Sondi and Salopek-Sondi (2004) (Fig. 9.2c) could be due to ROS production by Ag nanomaterials. Production of ROS by Ag nanomaterials either related to the dissolution or surface reaction with molecular oxygen has been evidenced in a number of papers (Kim 2007; Lok et al. 2007; Ivask et al. 2010). ROS induction by nano-Ag is indeed a property that has also been observed using other types of organisms, e.g., in fish cell lines (Carlson et al. 2008; Farkas et al. 2010).

The importance of surface reactivity in nano-Ag toxicity is a relatively less studied phenomenon. Morones et al. (2005) noticed that, among Ag nanoparticles with different crystal lattices, the crystal facet with a {111} lattice indices was

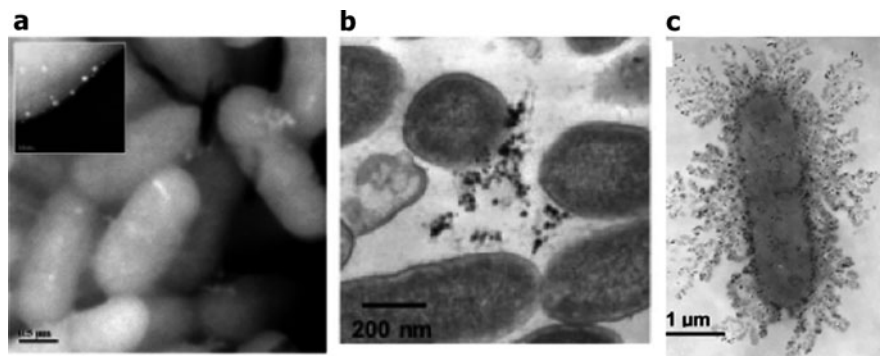
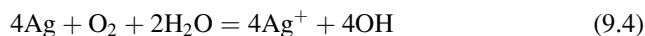


Fig. 9.2 Association of nano Ag with bacterial cells. (a, b) Transmission electron micrographs (TEM) of *Pseudomonas aeruginosa* cells after treatment with 100 µg/mL of nano Ag. Attachment of nano-Ag on bacterial surface (a, b) and the resulting membrane disruption (b) may be seen (Reprinted from Morones et al. 2005. Copyright IOP Science). (c) TEM images of *Escherichia coli* cells treated with 50 µg/mL of nano Ag. Degraded outer membrane structures (lipopolysaccharides) may be observed (Reprinted from Sondi and Salopek-Sondi 2004. With permission from Elsevier)

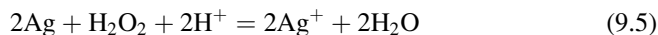
preferred for interactions with the bacterial cell membrane and, in particular, sulfur-containing membrane proteins. They inferred that the {111} crystal facet, which has high-atom-density compared to other lattice structures, leads to direct interaction with the bacterial membrane. Later, studies by Pal et al. (2007) demonstrated that crystal structure indeed has an influence to the toxicity of Ag nanoparticles to bacterial cells wherein the rod-shaped and triangular particles were markedly more toxic for bacteria than the spherical structures. According to their explanation, the planar nano-Ag structures were more reactive due to the high proportion of crystallographic faces available for nanoparticle–bacteria contact. Indeed, among different shapes, particles with a higher proportion of exposed crystallographic faces showed higher electrocatalytic reactivity (Bansal et al. 2010), which could be due to increased frequency of crystal defects in these structures. Although these surface reactivities are not yet discussed in relevance to the toxicity of Ag nanoparticles with different crystal structures, data emerging from our laboratory suggest the role of crystal defects in enhancing the toxicity of plate-shaped Ag nanoparticles.

9.2.3.4 The Role of Dissolution in Antimicrobial Action of Nano-Ag

Regardless of the myriad of different opinions, there is no doubt that the release of Ag ions either alone or in combination with other, previously discussed mechanisms is one of the most important factors determining the toxicity of nano-Ag. Differently from nano-ZnO, the chemical reactions behind the dissolution of Ag involve redox reactions either in the presence of oxygen (Fan and Bard 2001; Le Pape et al. 2004; Smetana et al. 2008; Choi et al. 2008):



or as suggested by AshaRani et al. (2008) in the presence of hydrogen peroxide originating from mitochondria of eukaryotic cells:



Marambio-Jones and Hoek (2010) hypothesized that a similar process involving hydrogen peroxide could also occur in bacterial membranes. As the dissolution of Ag either following reaction in Eqs. 9.4 or 9.5 involves transfer of electrons, formation of ROS, such as superoxide anions ($\text{O}_2^{\bullet-}$) and hydroxyl radicals (OH^{\bullet}), in this process is very likely. On the other hand, Park et al. (2009) also showed that dissolved Ag^+ ions could induce $\text{O}_2^{\bullet-}$ in bacterial cells. Therefore, the induction of intracellular ROS by nano-Ag observed in studies by Kim et al. (2007), Lok et al. (2007) and Ivask et al. (2010) may be due to the combination of these factors.

The summary of selected studies on nano-Ag dissolution and its impacts on its toxicity is given in Table 9.1. For example, in the case of nano-Ag incorporating surface coatings, release of ions has been directly related to their antimicrobial activity, and in order to prolong and control that release of antimicrobial Ag ions, embedding of Ag nanomaterials, e.g., to cationic polymer poly(4-vinyl-*N*-hexylpyridinium bromide), has been used (Sambhy et al. 2006). Shedding of Ag from Ag nanoparticles is also evidenced by the fact that some ligand-capped silver nanoparticles – although highly stable and monodisperse in suspension – were less bioactive, and authors concluded that the capping agent hindered the release of silver ions (Smetana et al. 2008). By using bacterial Ag sensor cells, Ivask et al. (2010) showed that all the observed antimicrobial effects of nano-Ag were due to solubilized ions. Lok et al. (2006) showed that the proteomic response of *E. coli* to nano-Ag and AgNO_3 was similar. Both compounds showed altered expression profile of envelope and stress response proteins. This kind of change in protein expression level could be expected as Ag ions are known to interact with membrane-bound thiol-rich respiratory chain enzymes (Dibrov et al. 2002) leading to collapse in the transmembrane pH gradient and membrane electric potential (Holt and Bard 2005). Finally, we want to emphasize that the dissolution of Ag ions from nano-Ag may take place either in the surrounding environment following the chemical equilibria or at the particle–cell membrane interface. The latter is especially likely because of the oxidizing environment on bacterial surface as discussed with Eq. 9.5. As these processes – abiotic dissolution of nano Ag and its dissolution after binding to bacterial surfaces or even internalization – may occur simultaneously, the separation of Ag dissolution from other factors important in nano Ag toxicity is a complicated task.

9.2.4 Nano-CuO

9.2.4.1 Importance of Nano-CuO as an Antimicrobial

Although not yet widely applied in commercial products, Cu nanomaterials are discussed in this chapter due to their high antimicrobial potential. Cu has long been known for its antimicrobial effects and was applied, e.g., in antifungal treatments and antifouling agents. Cu nanomaterials have been proposed as antimicrobials in polymer nanocomposites (Cioffi et al. 2005) that could serve as antimicrobial surfaces for packaging and in medicine. Borkow et al. (2010) used *nano-CuO* in wound dressings and showed its antimicrobial and antifungal properties by removing 99.9% of microbial cells even at high microbial loads within minutes. Akhavan and Ghaderi (2010) immobilized Cu and CuO nanoparticles in silica thin films to produce antimicrobial surfaces.

9.2.4.2 Evidence for Nano-CuO Antimicrobial Properties

Compared with the previously discussed nano-antimicrobials, CuO has the least number of toxicity data available (Kahru and Savolainen 2010). However, its effectiveness towards *Staphylococcus aureus*, *Escherichia coli*, *Pseudomonas aeruginosa*, *P. putida*, *Bacillus subtilis*, and *Vibrio fischeri* has been demonstrated (Heinlaan et al. 2008; Gajjar et al. 2009; Ren et al. 2009; Baek and An 2011). The effective concentrations for this nanomaterial towards microbes reported in different publications vary from 10 to 5,000 $\mu\text{g/mL}$, whereas in most of the studies, toxicity has been observed between 10 and 100 $\mu\text{g/mL}$. Gajjar et al. (2009) showed that 10 μg of CuO/mL decreased both the CFU (colony forming unit) and bioluminescence of a recombinant *P. putida* strain. A similar concentration has been shown to inhibit bioluminescence in recombinant *E. coli* strain by Ivask et al. (2010), and Heinlaan et al. (2008) showing that 80 $\mu\text{g/mL}$ decreased the natural bioluminescence of *V. fischeri* by 50% and at 200 $\mu\text{g/mL}$, 100% inhibition was observed. Kasemets et al. (2009) showed that 30 $\mu\text{g/mL}$ of nano-CuO inhibited the growth of yeast *Saccharomyces cerevisiae*. And 28–65 $\mu\text{g/mL}$ has been shown as EC_{50} of nano-CuO for *E. coli*, *B. subtilis*, and *S. aureus* (Baek and An 2011). Relatively lower toxicity of nano-CuO for *S. aureus*, *E. coli*, and *P. aeruginosa* ranging from 100 to 5,000 $\mu\text{g/mL}$ was reported by Ren et al. (2009), which, however, may be due to their experimental setup that involved the observation of inhibition by nanomaterials only after the transfer of bacteria to fresh growth media.

9.2.4.3 Modes of Antimicrobial Action of Nano-CuO

Based on the currently published articles, it is still disputable whether the observed antimicrobial effects of CuO nanomaterials are due to specific ‘nano effects’ or due to the release of Cu ions and their mediated toxicity (Table 9.1). Very few reports

are available on the mechanism of bactericidal action of copper nanoparticles. However, based on the current literature, three mechanisms for antimicrobial action of nano CuO can be proposed: (1) *metal dissolution*, (2) specific *nano-effects* and (3) induction of *reactive oxygen species* (ROS) (Table 9.1). The effect of dissolution in toxicity of nano-CuO is discussed in the next section (Sect. 9.2.4.4.). The ‘nano effect’ as a reason for nano-CuO toxicity was exclusively highlighted by Baek and An who reported that the dissolution rate of nano-CuO did not explain its toxicity (Baek and An 2011). However, the mechanisms behind this observed ‘nano effect’ were not proposed. A ‘nano-effect’ combined with solubility as a toxicity mechanism has been presented by Heinlaan et al. (2008) and Ivask et al. (2010). Using *E. coli* and *V. fischeri*, these authors demonstrated that the nano-size of CuO resulted in higher solubility and thus, toxicity (see Sect. 9.2.4.4.). Induction of intracellular ROS by CuO particles in *E. coli* bacteria has been observed by Ivask et al. (2010) and by O. Bondarenko (unpublished data, 2011; see Table 9.1). However, these authors also proved that the ability of CuO nanoparticles to induce ROS is again clearly dependent on the dissolution rate of nano CuO; similar results but for abiotic systems have been shown by Rice et al. (2009).

9.2.4.4 The Role of Dissolution in Antimicrobial Action of Nano-CuO

As already mentioned, the importance of dissolution of Cu nanomaterials in determining their antibacterial properties has been highlighted in many papers (Trapalis et al. 2003; Ruparelia et al. 2008; Ren et al. 2009; Akhavan and Ghaderi 2010) (see summary in Table 9.1) and indirect evidence on this process has been reported. Cioffi et al. (2005) showed that increasing the load of nano-Cu in polymer nanocomposites increased the bactericidal activity of the material towards *Saccharomyces cerevisiae*, *Escherichia coli*, *Staphylococcus aureus*, *Listeria monocytogenes* and molds. With increasing nano-Cu load in polyvinylmethyl ketone, there was a concomitant increase in the solubilized Cu, which apparently is thought to be the reason for toxicity of these materials. Similarly, decreased release of Cu ions from polyvinylidene fluoride–nano-Cu composite showed reduced antimicrobial activity. Thus, the authors concluded that, by using differently controlled Cu release in different nano-CuO–polymer composites, it is possible to control their antimicrobial properties. The studies on Cu-doped Ti and Se nanoparticles showed that the antibacterial action of the particles correlated well with the content of Cu ions in the coating (Trapalis et al. 2003). The addition of 20 mg/L ethylenediaminetetraacetic acid (EDTA) abolished the toxicity of Cu-TiO₂, showing that their toxicity to bacteria *Mycobacterium smegmatis* and *Shewanella oneidensis* was fully caused by Cu ions (Wu et al. 2009). Indirect evidence on participation of dissolved Cu ions in CuO toxicity has also been shown with eukaryotic cells. Studer et al. (2010) showed that if the carbon layer preventing the dissolution of Cu ions was used to coat nano-CuO, it was significantly less toxic.

Only a few studies have been aimed to differentiate the effects of dissolved Cu ions and the CuO particles *per se* in detail. Heinlaan et al. (2008) quantified the

dissolution of Cu ions from nano-CuO and reported that the toxicity of nano-CuO to *V. fischeri* was entirely explained by the dissolved Cu ions. In a similar experimental setup, Ivask et al. (2010) showed that the toxicity of nano-CuO to *E. coli* cells was due to solubilized ions. As discussed in Sect. 9.2.3.4, induction of ROS has been shown as one of the mechanisms of toxicity of nano-CuO. Mostly, this property of nano-CuO may be attributed to dissolved Cu ions that are well known for their redox reactive properties (Kimura and Nishioka 1997). The fact that intracellular ROS induced by nano-CuO were solely the result of solubilized Cu ions was shown by Ivask et al. (2010) and O. Bondarenko et al. (unpublished data, 2011; see Table 9.1) by the parallel use of biosensor systems that allowed the detection of dissolved ions and ROS in parallel. The formation of both, superoxide anions and hydrogen peroxide by nano-CuO was detected. These studies were supported by Rice et al. (2009) who showed by using cell-free media that the generation of OH[•] radicals was solely due to Cu ions solubilized from nano-CuO.

9.3 Environmental Parameters Affecting the Dissolution of Metal-Containing Nano-Antimicrobials

Although in previous chapters we discussed mainly the inherent properties of nanoparticles that determine their dissolution, the final dissolution of each of the nanomaterials depends on the conditions used in the test. Perhaps one of the best examples on how the test conditions may affect the dissolution of metal-containing nanoparticles has been given by Li et al. (2011) who studied the dissolution of ZnO nanomaterials in different test media and observed almost complete dissolution (90% at 100 µg of nano-ZnO/mL) in LB medium (bacterial medium containing organics) and very high dissolution rate (40% at 100 µg of nano-ZnO/mL) in Minimal Davis media (bacterial mineral medium containing citrate). For comparison, dissolution of nano-ZnO in saline, water or PBS (phosphate-buffered saline) was 12%, 7% and about 1%, respectively. The authors suggested that the affinity of Zn to the ligands present in these media was responsible for nanomaterial dissolution. The authors suggested that organic ligands in LB media and citrate in Minimal Davis media were the reasons for high solubility of nano ZnO and the low solubility of ZnO in PBS was due to the formation and immediate precipitation of Zn-phosphate complexes. As these complexes were removed when nanoparticles and dissolved ions were separated (using centrifugation combined with filtration, see Sect. 9.4), the final dissolved amount of Zn in PBS was very low. Proteins and organic substances have also been shown to increase the dissolution of nanoparticles of ZnO, CdSe, iron oxides, aluminium oxides and oxyhydroxides as well as CuO nanoparticles in earlier studies (Xia et al. 2008; Käkinen et al. 2011), and also explained by the organic ligand-enhanced dissolution.

Ag ion dissolution is determined by several factors such as nanomaterial surface functional groups (Liu et al. 2010), level of dissolved oxygen, temperature and

presence of organics (Liu and Hurt 2010). Differently from Zn^{2+} ion, which is relatively soluble, Ag^+ easily forms complexes with most of the inorganic anions. The pK values of Ag complexes with different inorganic ligands are 9.75 for chloride, 4.9 for sulfate, 4.9 for sulfide, and 7.8 for hydroxide (Choi et al. 2008; Gao et al. 2009). Thus, as suggested by Jin et al. (2010), even if Ag ions are solubilized from nano-Ag material, there is a high possibility that these ions re-precipitate forming insoluble complexes with inorganic ligands. Therefore, nanomaterials in aqueous suspensions must be considered as a dynamic system where the apparent speciation is controlled by the aquatic media pH, redox potential, and ionic composition as well as exposure to light.

As a final note, we would like to emphasize that in case of nanomaterials the dissolution is also dependent on the agglomeration/aggregation state of the material. Thus, in addition to controlling the dissolution as such, an environmental factor also determines the dispersion state of the nanomaterial. For example, high salt concentration that is known to decrease the electrical double layer (Nel et al. 2009) and thus, cause nanomaterial aggregation, is perhaps acting also as a limitation for dissolution process due to loss of surface area. pH of the medium close to the nanomaterials isoelectric point also promotes nanoparticle aggregation but its effect on dissolution depends on the speciation properties of the respective metal.

9.4 Currently Used Methods to Separate Dissolved Metal Ions from Metal Containing Nano-Antimicrobials

As discussed above, there is much evidence available that suggests the importance of dissolved metal ions in the toxicity of metal-containing nano-antimicrobials. However, often the presented evidence does not allow the clear differentiation between the roles of dissolved ions and 'nano-specific' effects in the observed toxic properties. Thus, the experimental design is of utmost importance in mechanistic studies of nano-antimicrobials and nanomaterials in general. The suggested design would include the combination of measurement of dissolved metals by analytical methods, including parallel experiments with a soluble metal salt, and experiments with re-engineered materials to deliberately decrease or increase the solubility of the nanomaterial. Measurement of dissolved metal ions is, however, a key step in this experimental setup that requires a *prior* separation of nano-sized non-dissolved materials and solubilized metal ions. It should be emphasized that this task is not the most straightforward as the extremely small size of nanomaterials may cause difficulty in separating particles from solubilized metal ions and their potential complexes with organics present in the test media. Luckily, in most aqueous test environments that contain salts (e.g., microbial media), nanomaterials agglomerate heavily enabling their easier separation. However, the presence of individual nano-sized particles in these agglomerated samples cannot be ruled out and care should be taken when using any separation techniques.

Selection of a method to be used for nanomaterial–dissolved ion separation depends on the nature of the material. Usually, in cases of polymer/surface immobilized nanomaterials, no special separation techniques have been used and the presence of metals in overlaying water or media as analyzed by analytical techniques has been used to judge the level of metal dissolution. In a study by Roe et al. (2008), radioactive isotope ^{110m}Ag was used instead of common analytical detection techniques to measure the fraction of solubilized metals from a nano-Ag-containing polymer. Metal solubilization has also been analyzed based on their characteristics to form certain complexes. For example, due to its nature to form (visually opaque) chloride complexes, NaCl at 0.5 g/mL has been used to detect solubilized Ag ions from Ag nanomaterials (Smetana et al. 2008). A similar principle was applied by Rice et al. (2009) who used spectrophotometric measurement of Cu chelated by oxalic acid bis(cyclohexylidene hydrazide) to quantify solubilized Cu ions.

In this section, we introduce in detail some of the most commonly applied and perhaps most appropriate techniques for separation of dissolved metal ions from metal nanoparticles: *centrifugation* and *filtration*. We also discuss *metal ion chelation* as a method to determine whether the observed toxicity of nanomaterials was due to metal dissolution. In addition, we discuss some methods that may be used for speciation analysis of the dissolved metals: *assessment of labile and bioavailable metal ions* and *models that may be used for metal speciation analysis*.

9.4.1 Separation of Dissolved Metal Ions by Centrifugation

Centrifugal force leads to the sedimentation of particles while leaving the dissolved ions in the solution which can then be detected using analytical techniques. When selecting an appropriate condition for centrifugation, both the size and density of the nanomaterials has to be taken into account. Kaegi et al. (2008) showed that centrifugation at 330 g for 6 minutes is enough to sediment particles with size up to 1.8 μm if their density is 1.1 g/cm^3 , particles with size up to 410 nm if their density is 2.7 g/cm^3 and particles with size up to 300 nm if their density is 4.2 g/cm^3 . Two hours of centrifugation at 2,700 g was enough to sediment particles of less than 130 nm with a density of 1.1 g/cm^3 , particles of less than 30 nm with a density of 2.7 g/cm^3 and particles of less than 20 nm with a density of 4.2 g/cm^3 (Kaegi et al. 2008). Thus, by simple centrifugation at low to moderate speeds, it is possible to separate particles as small as 20 nm from the nanomaterial suspension. A relatively low centrifugal speed was also used by Fasim et al. (2002) who isolated Zn dissolved from ZnO nanomaterials by 20-min centrifugation at 2,000 g. However, many studies have applied relatively high centrifugal speeds to ensure the sedimentation and separation of nanomaterials. Dimkpa et al. (2011) used a higher speed and longer duration of centrifugation (15,500 g for 30 min) for ion separation from commercial CuO and ZnO nanomaterial suspensions. However, they calculated that the actual time needed to sediment the nanoparticles at that speed was 5 min.

Midander et al. (2009) and Wu et al. (2010) used centrifugation at 19,000 g in combination with filtration (200 nm) to ensure the separation of Cu ions from CuO nano-suspensions. Indeed, as centrifugation could be considered as procedurally difficult and a technique with relatively low resolution power for size separation, the combination of this technique with other separation methods could be suggested.

9.4.2 Separation of Dissolved Metal Ions by Filtration

Filtration of nanomaterial suspension through membranes with controlled pore size is another method to separate metal-containing nanomaterials and solubilized ions. By selecting a filter with an appropriate pore size, it is possible to control the size of particles that pass the membrane or will be retained. There is a selection of filters available ranging from micro-sized pores from 0.1 to 1 μm to ultrafiltration (pore size around 0.01 μm) and nanofiltration (pore size around 0.001 μm). In addition to pore size, the material used to fabricate the filter is of importance as contamination or sorptive loss of the metals can become important at low (nanomolar) concentrations (Handy et al. 2008).

Filtration procedures have been discussed in detail by Behnke (1983) and Buffle et al. (1992). In most of the published reports on nanomaterial separation, filtration through 0.2- μm (i.e. 200-nm) filters has been used. There are reports showing the use of a 200-nm filter to separate nano CuO and Cu ions (Ruparelia et al. 2008; Wu et al. 2009). Baek and An (2011) used 200-nm nylon material filter to separate solubilized ions from ZnO, CuO, NiO and Sb₂O₃ nanomaterials in LB media without *prior* centrifugation. Li et al. (2011) used combined centrifugation (30 min at 10,000 g) and filtration through a 200-nm filter to separate solubilized Zn ions from ZnO nanomaterials. Heinlaan et al. (2011) used filtration of CuO suspensions through 100-nm polyethersulfone (PES) filters to separate solubilized Cu ions from nanomaterials. Interestingly, these authors showed that when filtration is applied as a single method to separate dissolved metal ions and nanomaterials, a 100-nm pore size may not be small enough cutoff to eliminate the presence of all nanomaterials. Indeed, they showed that, in the filtrates, a fraction of nanoparticles below 100 nm was present. A 100-nm pore-size filter was also used to separate dissolved Zn from ZnO nanomaterials by Li et al. (2010). These authors showed that application of a 100-nm pore size produced a similar yield to centrifugation at 15,000 g or dialysis through a 3,000-Da membrane. A similar comparison was done by Franklin et al. (2007) who showed that dialysis through a 1,000-Da cutoff filter that should restrict the passage of nanomaterials well below nanometer size yielded similar results to filtration of a nano-ZnO suspension through a 100-nm pore size filter. Differential results showing either complete or incomplete separation of nanomaterials from dissolved ions by using micro-sized filtration may be due to the differential dispersion state of nanomaterials. If the particles aggregate to >100 nm before filtration, the filter will certainly set a suitable limit to entrap the

particles; however, in the case of smaller particles, the cutoff may not be small enough.

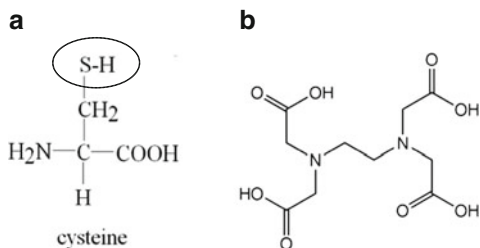
Compared to macro-sized filtration, dialysis may provide a more complete separation method for small nanoparticles. For example, the molecular weight cutoff of 7,500 Da in dialysis membranes corresponds to 1-nm particles, 75,000 Da to 10-nm particles and 750,000 Da to 100-nm particles. Although dialysis offers an accurate degree of separation for particles and solutes, this procedure often involves scaling up of the test procedure and the dilution of the sample. This may change the dissolution kinetics of the nanomaterial, and therefore the results may deviate from the actual situation in the toxicity test. Thus, perhaps a more accurate method for metal ion separation is centrifugal ultrafiltration where the sample is centrifuged through a dialysis membrane. For example, Navarro et al. (2008) used centrifugation of silver nanomaterials suspensions at 3,000 g for 30 min through a 3,000-Da membrane and considered the filtered concentration of Ag as the soluble fraction. Also, 3,000-Da centricon membranes were used to separate dissolved Ag ions by Lok et al. (2007).

9.4.3 Qualitative Determination of the Presence of Dissolved Metal Ions by Chelation

Chelation, i.e. complexation of free metal ions in suspensions of metal-containing nanomaterials has also been used as a method to separate the effects of nanomaterials and their dissolved metal ions. However, this method only offers a qualitative proof for the presence of dissolved ions, as the addition of a chelating agent either removes or does not remove the observed toxic effect of the nanomaterial. Usually, a chelating compound is added to the nanomaterial suspension and its biological effects are evaluated in comparison with nanosuspensions with no chelator added. If addition of a chelating compound removes or decreases the observed adverse effects, the toxicity of the metal-containing nanomaterial may at least be partially attributed to its solubility.

The most popular chelating compounds for metallic compounds are sulfur-containing molecules that have been shown to efficiently bind metal ions. For example, SH-groups in cysteine (Fig. 9.3) have been used to chelate Ag ions from Ag nanomaterials. Indeed, the addition of cysteine abolished the toxic effects

Fig. 9.3 Structure of cysteine (a) and EDTA (b) molecules. Sulfide group of cysteine reacting with metal ions is indicated, in the case of EDTA metal ions form coordinative bonds with nitrogen and oxygen cluster



of Ag nanomaterials to a green algae (Navarro et al. 2008). In another study, the effect of inorganic ligands on Ag ion complexation was studied, and it was shown that of the tested ligands, SO_4^{2-} , S^{2-} , Cl^- , PO_4^{3-} and EDTA (ethylenediaminetetraacetic acid), only S^{2-} showed efficacy in decreasing nanosilver toxicity. By adding a small aliquot of sulfide that was stoichiometrically complexed with nano-Ag, the nanosilver toxicity to nitrifying organisms was reduced by up to 80% (Choi et al. 2009).

While in the case of Ag ions, sulfide anions were the most effective complexing agents and EDTA did not prove particularly efficient, Cu ions, including those liberated from CuO nanomaterials, were effectively chelated by EDTA (Wu et al. 2009). Actually, every metal may have its specific chelator ('specific antidote'): for Cu, a specific chelator is bathocuproine (1,10-dimethyl-4,7-diphenyl 1,10-phenanthroline disulfonate) which has been used to specifically complex Cu ions from nano-CuO (Dimkpa et al. 2011).

9.4.4 Speciation of Dissolved Metals by Detection of Free and Labile Metal Ions

In addition to the determination of total dissolved fraction of metals from metal-containing nanomaterials, the speciation of dissolved metal ions may be of interest. This is important because not all (even soluble) metal complexes formed in aqueous systems are equally toxic. The most reactive and toxic form of the metal is its free ion. However, when some organic components or even inorganic phosphates are present in the media, the amount of free ions usually markedly decreases and most of the dissolved metal in the sample may exist in the form of different organic or phosphate complexes. Knowledge about free and complexed metal species has been considered very valuable in environmental risk assessment (International Council on Mining and Metals 2007). However, as the nano-research is just in its infancy, and there are serious issues connected with attempts to separate the total solubilized fraction of metals, the sophisticated models and measurements necessary for gaining information about metal speciation have not yet been fully applied in the nano-field.

The techniques to separate free and labile metal ions were established for metal speciation in environmental samples such as soils and sediments decades ago (Pesavento et al. 2009). Due to the fact that environmental samples usually contain a range of colloidal or nanosized particles, these samples may be relatively similar to nanomaterial suspensions (Ivask et al. 2010) and thus, the techniques for free and labile metal ion detection may also be applicable in case of metal-containing nanomaterials.

Broadly, the techniques used to separate the free and labile metal ions may be categorized into electrochemical methods such as voltammetric techniques detecting the current from free/labile metals on the surface of an electrode, and non-electrochemical methods based on ion exchange, complexing resins or micro-

extraction. The working principles of some of these methods, stripping voltammetry, diffusive gradients in thin films (DGT) and ion selective electrode (ISE), are shown in Fig. 9.4. As stated earlier, the application of these techniques has not yet been established for nanomaterial suspensions, which may be due to the relatively sophisticated experimental design or low sensitivity of some of the methods. For example,

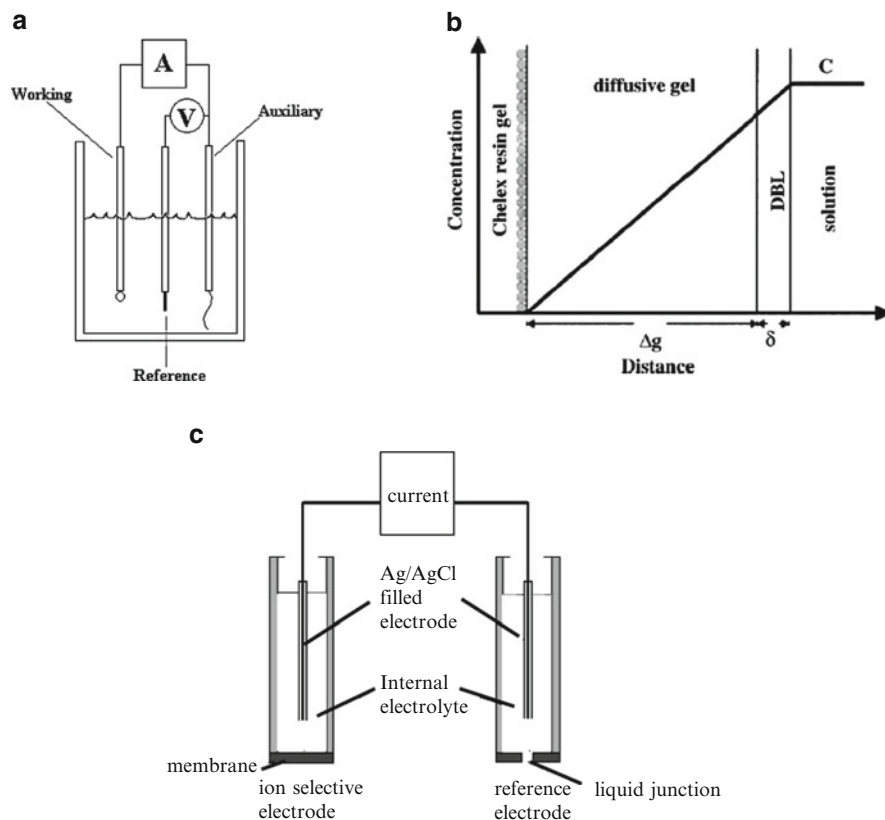


Fig. 9.4 Metal speciation techniques commonly used for metal speciation in environmental studies. (a) Stripping voltammetry is based on binding of the free/labile metals on the working electrode (usually a mercury film/drop) during a deposition step and a following oxidation of the deposited metals during a stripping step. The potential at which the stripping occurs indicates the nature and concentration of the analyte. (b) DGT technique based on passive sampling of free/labile metal species by a device incorporating hydrogel and a metal-binding resin, e.g., Chelex. As the resin is selective for free or weakly complexed metal species, analysis of passed metal concentrations provides a proxy for the labile fraction of metals in solution (Reprinted from Pesavento et al. 2009. With permission from Elsevier). (c) Ion-selective electrode is based on the measurement of the potential generated across a metal-specific membrane. The difference in potential of ion selective electrode and reference electrode upon immersing into a sample indicates the passage of charged metal ions through the membrane. Differently from stripping voltammetry and DGT that detect free and labile metal forms, ISEs are capable of detecting only free metal ions

the detection limits for ISEs fall usually between 10^{-6} – 10^{-8} M that may not be enough for low-concentration samples (Pesavento et al. 2009).

There are a few papers reporting on the application of voltammetric methods or micro-extraction methods such as stripping voltammetry, DGT and ISE in the separation of solubilized metal ions from metal-containing nanomaterials. Navarro et al. (2008) used both, ISE and DGT to separate Ag ions from Ag nanoparticles. These authors showed that the results from these two different techniques were comparable and agreed with the results obtained by membrane dialysis of the samples, all indicating that 1% of Ag dissolved from 0.006 $\mu\text{g/mL}$ Ag nanomaterial was in soluble form. Choi et al. (2008) used Ag ISE to separate dissolved and immobilized nano Ag when they synthesized Ag nanomaterials and colloids by AgNO_3 reduction. Stripping voltammetry was used for the specific quantification of Ag ions released from Ag nanomaterials by Morones et al. (2005). These authors found a relatively low concentration of silver solubilized from nano-Ag suspension with the maximum being less than 0.5 $\mu\text{g/mL}$. K  inen et al. (2011) used Cu-ISE and bacterial Cu-biosensor in parallel, to study the speciation of Cu in suspensions of CuO nanoparticles. They showed that the speciation of nano-CuO in toxicological test systems was not only determined by the complexation of Cu ions but also by differential dissolution of nano-CuO in different test conditions leading to a new speciation equilibrium.

In addition to separation of free and labile metal ions by electrochemical techniques and semipermeable membranes or hydrogels, there are specific chemicals available that bind certain free ions. For example, quantification of Cu ions released from CuO was quantified by Cu ion binding to bathocuproine disulfate (Dimkpa et al. 2011). This chemical, a derivative of 1,10-phenantroline, may be successfully used to bind and colorimetrically detect Cu(I) between 0.1 and 10 $\mu\text{g/mL}$ as it forms a red complex at physiological pH.

9.4.5 Models Used for Speciation of Dissolved Metals

As mentioned above, speciation of metals is an important factor in their apparent toxicity, but the respective models/calculations are not often used in nano-safety research. In previous paragraphs, we discussed some of the practical approaches that could be used to study the speciation of dissolved metal-containing nanomaterials. Here, we discuss some of the most promising speciation models. As in the case of speciation techniques, the speciation models have been primarily developed for environmental risk assessment (International Council on Mining and Metals 2007). These models are based on the equilibrium between the stability of free metal ions and of complexes that may be formed between the metal ion and the potential ligands in the study environment. The most widely used speciation models in environmental studies are WHAM (Windermere Humic Aqueous Model) (http://windermere.ceh.ac.uk/Aquatic_Processes/wham/) that allow the modeling of the aqueous interactions between metal ions and humic substances, and Visual Minteq (<http://www2.lwr.kth.se/English/OurSoftware/vminteq/>) that allows the modeling

of the aqueous interactions between metal ions and selected inorganic and organic ligands. No widely used speciation model is currently available for soils; for sediments, the SEM-AVS (Simultaneously Extracted Metal–Acid Volatile Sulfides) concept (Allen et al. 1991) has been used. Perhaps the most straightforward of these models is Visual Minteq. Indeed, a recent paper by Li et al. (2011) has applied this model to calculate the speciation of Zn that was dissolved from ZnO nanoparticles. In this case, the authors determined the total dissolved amount of Zn and then determined the speciation of this dissolved fraction in their test media. The amount of main anions and cations as well as organic ligands (such as citrate) were fed into the Visual Minteq model. Unfortunately, the results were not compared with toxicological tests or alternative speciation tests.

9.4.6 Speciation of Dissolved Metals by Detection of Bioavailable Metals Using Cellular Biosensors

As discussed above, formation of different metal complexes between the dissolved metal ions released from metal-containing nanomaterials and test media components may result in a decrease in toxicity due to the formation of non-bioavailable complexes. To predict the bioavailable fraction of metals, models like FIAM (Free Ion Activity Model) (Campbell 1995) and BLM (Biotic Ligand Model) (Paquin et al. 2002) have been applied in environmental risk assessment studies. These models take into account the chemical speciation as well as the affinity of certain biological ligands (e.g., on the biological surface, such as fish gills) that may facilitate the entrance of metal ions into the cells, to calculate the bioavailable, i.e., potentially toxic, fraction of metals. These models are, however, relatively sophisticated and have not so far been applied for nanomaterials.

There are very few tools available that allow the direct measurement of bioavailable metals. Here, we describe a novel approach involving recombinant metal-specific microbial sensors that has been used by Heinlaan et al. (2008), Kasemets et al. (2009), Aruoja et al. (2009) and Ivask et al. (2010) to quantify the bioavailable fraction of metals from metal-containing nanomaterials (including Ag, ZnO and CuO discussed in this chapter). This approach can be used as an analytical tool, and pre-separation of the particles from the solubilized fraction is not obligatory. As this methodology is relatively new, the methodological nuances of the approach will be discussed here. The analytical basis of this method is cellular biosensors that are recombinant microbes responding specifically towards certain heavy metals by increased bioluminescence. The bioluminescent response is induced, however, only if the particular heavy metal crosses the cell biological envelopes and enters the cytoplasmic space, that is if the metal is accessible or bioavailable to the sensing system. Mostly, the sensors are based on bacteria (Ivask et al. 2009) but also on yeast cells (Leskinen et al. 2003). These recombinant constructs contain genetic elements in which a metal-binding transcriptional regulator and its regulated promoter originating from microbial precisely regulated resistance

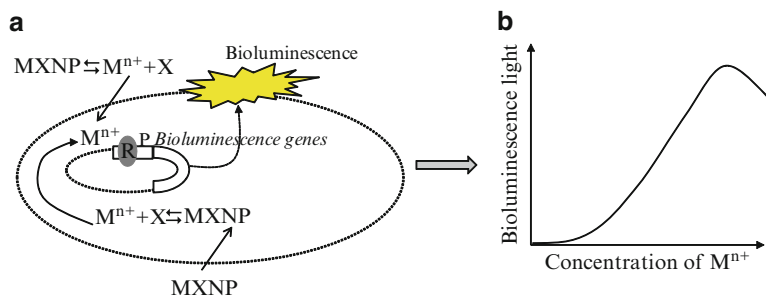


Fig. 9.5 Working mechanism of a cellular metal ion biosensor. (a) Metal ions (M^{n+}), released from metal-containing nanomaterials extracellularly or by intracellular dissolution bind a protein functioning as a transcriptional regulator (R). Regulator R binds a promoter (P), which is fused with bioluminescence encoding genes allowing the expression of the latter. The transcriptional regulator binds only certain metal ions and, thus, results in metal-specific expression of bioluminescence-encoding genes and resulting bioluminescence production. (b) With increasing metal ion concentration, the bioluminescence increases until the metal-binding transcriptional regulator is saturated (stable high bioluminescence is achieved) and/or a toxic concentration for the cell (bioluminescence decreasing) is reached. As only intracellular metal ions result in increased bioluminescence, this system may be detecting only bioavailable metals

systems towards heavy metals, are fused to bioluminescence-encoding (*lucFF* or *luxCDABE*) genes (Fig. 9.5).

Recombinant microbial heavy metal sensors have been developed for Cd, Pb, Hg, Cr, Ni, Co, Zn, Cu and As (for review, see Daunert et al. 2000) and have been widely used for heavy metal speciation studies in environmental analysis (Ivask et al. 2004, 2007, 2010; Kahru et al. 2005) offering a unique possibility for the quantification of bioavailable concentrations of target metals in complex environmental samples. The analysis scheme that can be used to evaluate the impact of solubilization of metals from metal-containing nanoparticles by recombinant metal-specific microbial sensors was first shown by Heinlaan et al. (2008). Since then, the methodology has been successfully used to demonstrate the toxic effect of solubilized Zn (using Zn-sensing bacteria) and Cu (using Cu-sensing bacteria and yeast) from nanoparticles of ZnO and CuO, respectively, towards algae (Aruoja et al. 2009), crustaceans and bacteria (Heinlaan et al. 2008; Ivask et al. 2010), protozoa (Mortimer et al. 2010) and yeast (Kasemets et al. 2009). Heinlaan et al. (2011) and O. Bondarenko et al. (unpublished data, 2011) have shown that solubilized Cu determined from nano-CuO suspensions by these cellular Cu biosensors and filtration combined with analytical detection methods (AAS) were in good agreement ($R^2 = 0.88$). However, as a rule, the AAS values on dissolution of nano-CuO exceeded the values obtained by Cu-sensor bacteria. The difference could be explained by the fact that, after filtering the nanosuspensions through 100-nm pore-size filters the filtrate contained (<100 nm) CuO nanoparticles that did not induce the bioluminescence of Cu-sensor bacteria but were quantified during AAS analysis. Thus, these results indicate that, due to the complexity of separation of nanoparticles from the dissolved copper, the biosensors

seem to be even more relevant tools for the analysis of Cu ions than chemical methods to distinguish dissolved metal ions and insoluble (nano)materials.

9.5 Final Comments

In this chapter, we have discussed the potential mechanisms of toxicity of metal-containing nanomaterials keeping the main emphasis on their dissolution. Although dissolution of metal ions may be among the most important factors determining the toxicity of discussed nano-antimicrobials Ag, ZnO and Cu/CuO, their actual toxic outcome is certainly influenced by other physical/chemical properties of the nanomaterial: size, shape, surface characteristics and reactivity, photochemistry, etc. Figure 9.6 represents the summary of all potential factors leading to the toxic and antimicrobial effects of metallic nanomaterials that could be derived from the current literature. Due to the complexity of the process and inter-dependence of different physical and chemical properties in orchestrating the resultant reactivity and potency of nanomaterials, it is a daunting task to identify the contribution from

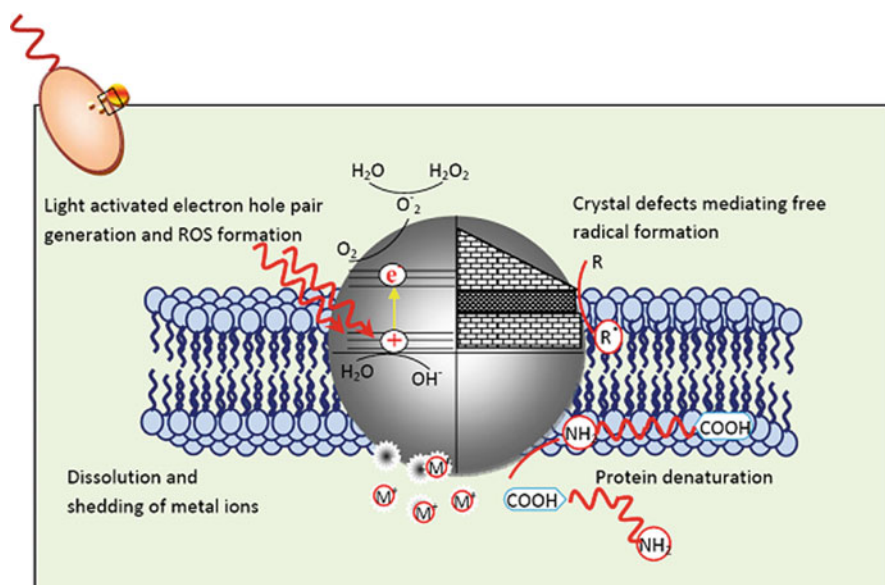


Fig. 9.6 Properties of metal/metal oxide nanomaterials responsible for their toxic and antibacterial activities. Lower left corner: dissolution of metal ions (M^+) from metal-containing nanomaterials. This process can take place either extra- or intracellularly. Upper right corner: 'nano-specific' properties such as crystal defects, surface reactivity that lead to reactive free radical formation resulting in lipid peroxidation and protein deformation. Upper left corner: activation of nanomaterials by external agents such as UV illumination resulting in reactive oxygen species formation and their following reactions with biological molecules

each individual factor separately. Unveiling the functional relationship between physical/chemical properties of nanomaterials and toxicity may require the use of specifically designed nanomaterial libraries. Often this level of sophistication demands inter-disciplinary expertise wherein the key steps for establishing functional relationship between material property and toxicity are (1) synthesis and characterization of a library of nanomaterials with systematic variation in a critical nanoscale parameter, (2) identification of an appropriate toxicity endpoint in the target biological system, and (3) correlation of the toxicity data to the systematically varied physical/chemical parameter. We believe that only intelligent experimental planning including parallel testing of soluble metal forms and nanomaterials, measurement of dissolved metals by analytical methods, decreasing of dissolution rates e.g., by doping, would lead to meaningful information about dissolution as a separate factor in metallic nanomaterials toxicity. Unfortunately, even if all these possible controls are taken into account, some effects may remain unexplained. This may be due to e.g., locally increased dissolution and aggregation/disaggregation of nanomaterials, taking place in cellular-processes that are difficult if not impossible to measure by conventional experimental methods. Bearing this in mind, all the studies discussed in this chapter have a certain degree of simplification, but each of them provides a piece of information useful in assembling an integral picture about the behavior of metal-containing nanomaterials in biological systems.

Acknowledgements European Social Fund and Estonian Science Foundation programs Mobilitas, Do-Ra3, EU FP7 Project NanoValid (grant agreement No 263147) and projects ETF6975 and ETF8561 as well as Estonian Ministry of Science and Education project SF0690063s08 are acknowledged for the support.

References

- Adams LK, Lyon DY, Alvarez PJJ (2006) Comparative eco-toxicity of nanoscale TiO₂, SiO₂, and ZnO water suspensions. *Water Res* 40(19): 3527–3532.
- Akhavan O, Ghaderi E (2010) Cu and CuO nanoparticles immobilized by silica thin films as antibacterial materials and photocatalysts. *Surf Coat Technol* 205(1): 219–223.
- Allaker RP (2010) The use of nanoparticles to control oral biofilm formation. *J Dent Res* 89(11): 1175–1186.
- Allen HE, Fu G, Boothman W, DiToro D, Mahony JD (1991) Draft Analytical Method for Determination of Acid Volatile Sulfide in Sediment. U.S. Environmental Protection Agency, Washington, DC.
- Applerot G, Lipovsky A, Dror R, Perkas N, Nitzan Y, Lubart R, Gedanken A (2009) Enhanced antibacterial activity of nanocrystalline ZnO due to increased ROS-mediated cell injury. *Adv Funct Mater* 19(6): 842–852.
- Aruoja V, Dubourguier HC, Kasemets K, Kahru A (2009) Toxicity of nanoparticles of CuO, ZnO and TiO₂ to microalgae *Pseudokirchneriella subcapitata*. *Sci Total Environ* 407(4): 1461–1468.
- AshaRani PV, Low Kah Mun G, Hande MP, Valiyaveetil S (2008) Cytotoxicity and genotoxicity of silver nanoparticles in human cells. *ACS Nano* 3(2): 279–290.

- Baek YW, An YJ (2011) Microbial toxicity of metal oxide nanoparticles (CuO, NiO, ZnO, and Sb₂O₃) to *Escherichia coli*, *Bacillus subtilis* and *Streptococcus aureus*. *Sci Total Environ* 409(8): 1603–1608.
- Balogh L, Swanson DR, Tomalia DA, Hagnauer GL, McManus AT (2001) Dendrimer – silver complexes and nanocomposites as antimicrobial agents. *Nano Lett* 1(1): 18–21.
- Bansal V, Li V, O'Mullane AP, Bhargava SK (2010) Shape dependent electrocatalytic behaviour of silver nanoparticles. *Cryst Eng Comm* 12(12): 4280–4286.
- Behnke U (1983) T. D. Brock: Membrane Filtration. A User's Guide and Reference Manual. 381 Seiten, 115 Abb., 27 Tab. Springer-Verlag, Berlin/Heidelberg/New York/Tokyo 1983, Preis: 87,- DM. *Food/Nahrung* 27(10): 1025.
- Benn TM, Westerhoff P (2008) Nanoparticle silver released into water from commercially available sock fabrics. *Environ Sci Technol* 42(11): 4133–4139.
- Borkow G, Okon-Levy N, Gabbay J (2010) Copper oxide impregnated wound dressing: biocidal and safety studies. *Wounds* 22(12): 301–310.
- Brayner R, Ferrari-Iliou R, Brivois N, Djediat S, Benedetti MF, Fiévet F (2006) Toxicological impact studies based on *Escherichia coli* bacteria in ultrafine ZnO nanoparticles colloidal medium. *Nano Lett* 6(4): 866–870.
- Buffle A, Perret D, Newman M (1992) The use of filtration and ultrafiltration for size fractionation of aquatic particles, colloids and macromolecules. In: Buffle A, Leeuwen HP (eds) *Environmental Particles*, vol. 1. Lewis Publishers, Boca Raton.
- Campbell PGC (1995) Interactions between trace metals and aquatic organisms: a critique of the free-ion activity model. In: Tessier A, Turner DR (eds) *Metal Speciation and Bioavailability in Aquatic Systems*. Wiley, Chichester.
- Carlson C, Hussain SM, Schrand AM, Braydich-Stolle K, Hess L, Jones KL and Schlager JJ (2008) Unique cellular interaction of silver nanoparticles: size-dependent generation of reactive oxygen species. *J Phys Chem B* 112(43): 13608–13619.
- Chen CY, Chiang CL (2008) Preparation of cotton fibers with antibacterial silver nanoparticles. *Mater Lett* 62(21–22): 3607–3609.
- Chen WJ, Pei-Jane T, Chen YC (2008) Functional Fe₃O₄/TiO₂ core/shell magnetic nanoparticles as photokilling agents for pathogenic bacteria. *Small* 4: 485–491.
- Choi O, Hu Z (2008) Size dependent and reactive oxygen species related nanosilver toxicity to nitrifying bacteria. *Environ Sci Technol* 42(12): 4583–4588.
- Choi O, Deng KK, Kim NJ, Ross JL, Surampalli RY, Hu Z (2008) The inhibitory effects of silver nanoparticles, silver ions, and silver chloride colloids on microbial growth. *Water Res* 42(12): 3066–3074.
- Choi O, Clevenger TE, Deng B, Surampalli RY, Ross JL, Hu Z (2009) Role of sulfide and ligand strength in controlling nanosilver toxicity. *Water Res* 43(7): 1879–1886.
- Cioffi N, Torsi L, Ditaranto N, Tantillo G, Ghibelli L, Sabbatini L, Blevè-Zacheo T, D'Alessio M, Zamboni PG, Traversa E (2005) Copper nanoparticle/polymer composites with antifungal and bacteriostatic properties. *Chem Mater* 17: 5255–5262.
- Daunert S, Barrett G, Feliciano J, Shetty R, Shrestha S, Smith-Spencer W (2000) Genetically engineered whole-cell sensing systems: coupling biological recognition with reporter genes. *Chem Rev* 100(7): 2705–2738.
- Dibrov P, Dzioba J, Gosnik KK, Häse CC (2002) Chemiosmotic mechanism of antimicrobial activity of Ag⁺ in *Vibrio cholerae*. *Antimicrob Agents Chemother* 46(8): 2668–2670.
- Dimkpa CO, Calder A, Britt DW, McLean JE, Anderson AJ (2011) Responses of a soil bacterium, *Pseudomonas chlororaphis* O6 to commercial metal oxide nanoparticles compared with their metal ions. *Environ Pollut* 159(7): 1749–1756.
- Dollwet HHA, Sorenson JRJ (1985) Historic uses of copper compounds in medicine. *J Trace Elem Med Biol* 2(2): 80–87.
- El Badawy AM, Silva RG, Morris B, Scheckel KG, Suidan MT, Tolaymat TM (2010) Surface charge-dependent toxicity of silver nanoparticles. *Environ Sci Technol* 45(1): 283–287.
- El-Rafie MH, Mohamed AA, Shaheen TI, Hebeish A (2010) Antimicrobial effect of silver nanoparticles produced by fungal process on cotton fabrics. *Carbohydr Polym* 80(3): 779–782.

- Falletta E, Bonini M, Fratini E, Lo Nostro A, Pesavento G, Becheri A, Lo Nostro P, Canton P, Baglioni P (2008) Clusters of poly(acrylates) and silver nanoparticles: structure and applications for antimicrobial fabrics. *J Phys Chem C* 112(31): 11758–11766.
- Fan FRF, Bard AJ (2001) Chemical, electrochemical, gravimetric and microscopic studies on antimicrobial silverfilms. *J Phys Chem B* 106(2): 279–287.
- Farkas J, Christian P, Gallego-Urrea JA, Roos N, Hasselov M, Tollefsen KE, Thomas KV (2010) Uptake and effects of manufactured silver nanoparticles in rainbow trout (*Oncorhynchus mykiss*) gill cells. *Aquat Toxicol* 101(1): 117–125.
- Fasim F, Ahmed N, Parsons R, Gadd GM (2002) Solubilization of zinc salts by a bacterium isolated from the air environment of a tannery. *FEMS Microbiol Lett* 213(1): 1–6.
- Foster H, Ditta I, Varghese S, Steele A (2011) Photocatalytic disinfection using titanium dioxide: spectrum and mechanism of antimicrobial activity. *Appl Microbiol Biotechnol* 90(6): 1847–1868.
- Franklin NM, Rogers NJ, Apte SC, Batley GE, Gadd GE, Casey PS (2007) Comparative toxicity of nanoparticulate ZnO, bulk ZnO and ZnCl₂ to a freshwater microalga (*Pseudokirchneriella subcapitata*): the importance of particle solubility. *Environ Sci Technol* 41(24): 8484–8490.
- Gajjar P, Pettee B, Britt DB, Huang W, Johnson WP, Anderson AJ (2009) Antimicrobial activities of commercial nanoparticles against an environmental soil microbe, *Pseudomonas putida* KT2440. *J Biol Eng* 3(9): 1–13.
- Gao J, Youn S, Hovsepyan A, Llaneza VL, Wang Y, Bitton G, Bonzongo JCJ (2009) Dispersion and toxicity of selected manufactured nanomaterials in natural river water samples: effects of water chemical composition. *Environ Sci Technol* 43(9): 3322–3328.
- Gelover S, Gómez LA, Reyes K, Teresa Leal M (2006) A practical demonstration of water disinfection using TiO₂ films and sunlight. *Water Res* 40(17): 3274–3280.
- George S, Pokhrel S, Xia T, Gilbert B, Ji Z, Schowalter M, Rosenauer A, Damoiseaux R, Bradley KA, Mädler L, Nel AE (2010) Use of a rapid cytotoxicity screening approach to engineer a safer zinc oxide nanoparticle through iron doping. *ACS Nano* 4(1): 15–29.
- George S, Xia T, Rallo R, Zhao Y, Ji Z, Lin S, Wang X, Zhang H, France B, Schoenfeld D, Damoiseaux R, Liu R, Lin S, Bradley KA, Cohen Y, Nel AE (2011) Use of a high-throughput screening approach coupled with in vivo zebrafish embryo screening to develop hazard ranking for engineered nanomaterials. *ACS Nano* 5(3): 1805–1817.
- Ghule K, Ghule AV, Chen BJ, Ling YC (2006) Preparation and characterization of ZnO nanoparticles coated paper and its antibacterial activity study. *Green Chemistry* 8(12): 1034–1041.
- Handy R, von der Kammer F, Lead J, Hassellöv M, Owen R, Crane M (2008) The ecotoxicological and chemistry of manufactured nanoparticles. *Ecotoxicol* 17(4): 287–314.
- Heinlaan M, Ivask A, Blinova, Dubourguier HC, Kahru A (2008) Toxicity of nanosized and bulk ZnO, CuO and TiO₂ to bacteria *Vibrio fischeri* and crustaceans *Daphnia magna* and *Thamnocephalus platyurus*. *Chemosphere* 71(7): 1308–1316.
- Heinlaan M, Kahru A, Kasemets K, Arbeille B, Prensier G, Dubourguier HC (2011) Changes in the *Daphnia magna* midgut upon ingestion of copper oxide nanoparticles: a transmission electron microscopy study. *Water Res* 45(179–190).
- Hendren CO, Mesnard X, Dröge J, Wiesner MR (2011) Estimating production data for five engineered nanomaterials as a basis for exposure assessment. *Environ Sci Technol* 45(7): 2562–2569.
- Holt K, Bard AJ (2005) Interaction of silver(I) ions with the respiratory chain of *Escherichia coli*: An electrochemical and scanning electrochemical microscopy study of the antimicrobial mechanism of micromolar Ag⁺. *Biochem* 44(39): 13214–13223.
- Hong J, Ma H, Otaki M (2005) Controlling algal growth in photo-dependent decolorant sludge by photocatalysis. *J Biosci Bioeng* 99(6): 592–597.
- Hwang ET, Lee JH, Chae YJ, Kim YS, Kim BC, Sang BI, Gu MB (2008) Analysis of the toxic mode of action of silver nanoparticles using stress-specific bioluminescent bacteria. *Small* 4(6): 746–750.

- Ireland JC, Klostermann P, Rice EW, Clark RM (1993) Inactivation of *Escherichia coli* by titanium dioxide photocatalytic oxidation. *Appl Environ Microbiol* 59(5): 1668–1670.
- Ivask A, Francois M, Kahru A, Dubourguier H-C, Virta M, Douay F (2004) Recombinant luminescent bacterial sensors for the measurement of bioavailability of cadmium and lead in soils polluted by metal smelters. *Chemosphere* 22: 147–156.
- Ivask A, Green T, Polyak B, Mor A, Kahru A, Virta M, Marks R. (2007). Fibre-optic bacterial biosensors and their application for the analysis of bioavailable Hg and As in soils and sediments from Aznalcollar mining area in Spain. *Biosens Bioelectron* 22: 1396–1402.
- Ivask A, Rolova T, Kahru A (2009) A suite of recombinant luminescent bacterial strains for the quantification of bioavailable heavy metals and toxicity testing. *BMC Biotechnol* 9(1): 41.
- Ivask A, Bondarenko O, Jepihina N, Kahru A (2010) Profiling of the reactive oxygen species-related ecotoxicity of CuO, ZnO, TiO₂, silver and fullerene nanoparticles using a set of recombinant luminescent *Escherichia coli* strains: differentiating the impact of particles and solubilised metals. *Anal Bioanal Chem* 398(2): 701–716.
- Ivask A, Dubourguier H-C, Pöllumaa L, Kahru A (2011) Bioavailability of Cd in 110 polluted topsoils to recombinant bioluminescent sensor bacteria: effect of soil particulate matter. *J Soil Sediment* 11(2): 231–237.
- Jiang W, Mashayekhi H, Xing B (2009) Bacterial toxicity comparison between nano- and micro-scaled oxide particles. *Environ Pollut* 157(5): 1619–1625.
- Jin X, Li M, Wang J, Marambio-Jones C, Peng F, Huang X, Damoiseaux R, Hoek EMV (2010) High-throughput screening of silver nanoparticle stability and bacterial inactivation in aquatic media: influence of specific ions. *Environ Sci Technol* 44(19): 7321–7328.
- Jones N, Ray B, Ranjit KT, Manna AC (2008) Antibacterial activity of ZnO nanoparticle suspensions on a broad spectrum of microorganisms. *FEMS Microbiol Lett* 279(1): 71–76.
- Jung WK, Koo HC, Kim KW, Shin S, Kim SH, Park YH (2008) Antibacterial activity and mechanism of action of the silver ion on *Staphylococcus aureus* and *Escherichia coli*. *Appl Environ Microbiol* 74(7): 2171–2178.
- Kaegi R, Ulrich A, Sinnet B, Vonbank R, Wichser A, Zuleeg S, Simmler H, Brunner S, Vonmont H, Burkhardt M, Boller M (2008) Synthetic TiO₂ nanoparticle emission from exterior facades into the aquatic environment. *Environ Pollut* 156(2): 233–239.
- Kahru A, Dubourguier H-C (2010) From ecotoxicology to nanoecotoxicology. *Toxicology* 269: 105–119.
- Kahru A, Savolainen K (2010) Potential hazard of nanoparticles: from properties to biological and environmental effects. *Toxicol* 269(2–3): 89–91.
- Kahru A, Ivask A, Kasemets K, Pöllumaa L, Kurvet I, François M, Dubourguier H-C (2005) Biotests and biosensors in ecotoxicological risk assessment of field soils polluted with zinc, lead and cadmium. *Environ Toxicol Chem* 24(11): 2973–2982.
- Kahru A, Dubourguier HC, Blinova I, Ivask A, Kasemets K (2008) Biotests and biosensors for ecotoxicol of metal oxide nanoparticles: A minireview. *Sensors* 8(8): 5153–5170.
- Käkinen A, Bondarenko O, Ivask A, Kahru A (2011) The effect of composition of different ecotoxicological test media on free and bioavailable copper from CuSO₄ and CuO nanoparticles: comparative evidence from a Cu-selective electrode and a Cu-biosensor. *Sensors* 11(11):10502–10521.
- Kasemets K, Ivask A, Dubourguier HC, Kahru A (2009) Toxicity of nanoparticles of ZnO, CuO and TiO₂ to yeast *Saccharomyces cerevisiae*. *Toxicol in Vitro* 23(6): 1116–1122.
- Kikuchi Y, Sunada K, Iyoda T, Hashimoto K, Fujishima A (1997) Photocatalytic bactericidal effect of TiO₂ thin films: dynamic view of the active oxygen species responsible for the effect. *J Photochem Photobiol A: Chemistry* 106(1–3): 51–56.
- Kim JS (2007) Antibacterial activity of Ag + ion-containing silver nanoparticles prepared using the alcohol reduction method. *J Ind Eng Chem* 13(5): 718–722.
- Kim SC, Lee DK (2005) Preparation of TiO₂-coated hollow glass beads and their application to the control of algal growth in eutrophic water. *Microchem J* 80(2): 227–232.
- Kim JS, Kuk E, Yu KN, Kim J-H, Park SJ, Lee HJ, Kim SH, Park YK, Park YH, Hwang C-Y, Kim Y-K, Lee Y-S, Jeong DH, Cho M-H (2007) Antimicrobial effects of silver nanoparticles. *Nanomed Nanotech Biol Med* 3(1): 95–101.

- Kim J, Jungeun L, Soonchul K, Sunghoon J (2009a) Preparation of biodegradable polymer/silver nanoparticles composite and its antibacterial efficacy. *J Nanosci Nanotechnol* 9: 1098–1102.
- Kim KJ, Sung W, Suh B, Moon SK, Choi JS, Kim J, Lee D (2009b) Antifungal activity and mode of action of silver nano-particles on *Candida albicans*. *BioMetals* 22(2): 235–242.
- Kimura T, Nishioka H (1997) Intracellular generation of superoxide by copper sulphate in *Escherichia coli*. *Mutat Res-Gen Tox En* 389(2–3): 237–242.
- Kloepfer JA, Mielke RE, Nadeau JL (2005) Uptake of CdSe and CdSe/ZnS quantum dots into bacteria *via* purine-dependent mechanisms. *Appl Environ Microbiol* 71(5): 2548–2557.
- Kvitek L, Panaček A, Soukupova J, Kolar M, Večerova R, Pucek R, Holecova M, Zboril R (2008) Effect of surfactants and polymers on stability and antibacterial activity of silver nanoparticles (NPs). *J Phys Chem C* 112(15): 5825–5834.
- Le Pape H, Solano-Serena F, Contini P, Devillers C, Maftah A, Leprat P (2004) Involvement of reactive oxygen species in the bactericidal activity of activated carbon fibre supporting silver: bactericidal activity of ACF(Ag) mediated by ROS. *J Inorg Biochem* 98(6): 1054–1060.
- Leskinen P, Virta M, Karp M (2003) One-step measurement of firefly luciferase activity in yeast. *Yeast* 20(13): 1109–1113.
- Li M, Pokhrel S, Jin X, Mädler L, Damoiseaux R, Hoek EMV (2010) Stability, bioavailability, and bacterial toxicity of ZnO and iron-doped ZnO nanoparticles in aquatic media. *Environ Sci Technol* 45(2): 755–761.
- Li M, Zhu L, Lin D (2011) Toxicity of ZnO nanoparticles to *Escherichia coli*: mechanism and the influence of medium components. *Environ Sci Technol* 45(5): 1977–1983.
- Liau, SY, Read DC, Pugh WJ, Furr JR, Russell AD (1997) Interaction of silver nitrate with readily identifiable groups: relationship to the antibacterial action of silver ions. *Lett Appl Microbiol* 25: 279–283.
- Liu J, Hurt, RH (2010) Ion release kinetics and particle persistence in aqueous nano-silver colloids. *Environ Sci Technol* 44(6): 2169–2175.
- Liu Y, He L, Mustapha A, Li H, Hu ZQ, Lin M (2009) Antibacterial activities of zinc oxide nanoparticles against *Escherichia coli* O157:H7. *J Appl Microbiol* 107(4): 1193–1201.
- Liu J, Sonshine DA, Shervani S, Hurt RH (2010) Controlled release of biologically active silver from nanosilver surfaces. *ACS Nano* 4(11): 6903–6913.
- Lok CN, Ho CM, Chen R, He QY, Yu WY, Sun H, Tam P, Chiu JF, Che CM (2006) Proteomic analysis of the mode of antibacterial action of silver nanoparticles. *J Proteome Res* 5(4): 916–924.
- Lok CN, Ho CM, Chen R, He QY, Yu WY, Sun H, Tam P, Chiu JF, Che CM (2007) Silver nanoparticles: partial oxidation and antibacterial activities. *JBIC* 12(4): 527–534.
- Marambio-Jones C, Hoek EMV (2010) A review of the antibacterial effects of silver nanomaterials and potential implications for human health and the environment. *JNR* 12: 1531–1551.
- Maynard AD (2007) Nanotechnology – toxicological issues and environmental safety and environmental safety. In: Project on Emerging Nanotechnologies, vols–14. Woodrow Wilson International Center for Scholars, Washington, DC.
- McDonnell G, Russell AD (1999) Antiseptics and disinfectants: activity, action and resistance. *Clin Microbiol Rev* 12(1): 147–179.
- Menard A, Drobne D, Jemec A (2011) Ecotoxicity of nanosized TiO₂. Review of in vivo data. *Environ Pollut* 159(3): 677–684.
- International Council on Mining and Metals (2007) MERAG: Metals Environmental Risk Assessment Guidance. London, UK.
- Midander K, Cronholm P, Karlsson HL, Elihn K, Möller L, Leygraf C, Wallinder IO (2009) Surface characteristics, copper release, and toxicity of nano- and micrometer-sized copper and copper(II) oxide particles: a cross-disciplinary study. *Small* 5(3): 389–399.
- Morones JR, Elechiguerra JL, Camacho A, Holt KB, Kouri JB, Ramirez JT, Yacaman MJ (2005) The bactericidal effect of silver nanoparticles. *Nanotechnol* 16: 2346–2353.

- Mortimer M, Kasemets K, Kahru A (2010) Toxicity of ZnO and CuO nanoparticles to ciliated protozoa *Tetrahymena thermophila*. *Toxicol* 269(2–3): 182–189.
- Mueller NC, Nowack B (2008) Exposure modeling of engineered nanoparticles in the environment. *Environ Sci Technol* 42(12): 4447–4453.
- Navarro E, Piccapietra F, Wagner B, Marconi F, Kaegi R, Odzak N, Sigg L, Behra R (2008) Toxicity of silver nanoparticles to *Chlamydomonas reinhardtii*. *Environ Sci Technol* 42(23): 8959–8964.
- Neal A (2008) What can be inferred from bacterium–nanoparticle interactions about the potential consequences of environmental exposure to nanoparticles? *Ecotoxicol* 17(5): 362–371.
- Nel A, Madler L, Velegol D, Xia T, Hoek EMV, Somasundaran P, Klaessig F, Castranova V, Thompson M (2009) Understanding biophysicochemical interactions at the nano-bio interface. *Nat Mater* 8(7): 543–557.
- Niazi JH, Gu MB (2009) Toxicity of metallic nanoparticles in microorganisms - a review. In: Kim YK, Platt U, Gu MB, Iwahashi H (eds) *Atmospheric and Biological Environmental Monitoring*. Springer, Dordrecht/Heidelberg/London/New York.
- Nowack B, Krug HF, Height M (2011) 120 years of nanosilver history: implications for policy makers. *Environ Sci Technol* 45(4): 1177–1183.
- Pal S, Tak YK, Song JM (2007) Does the antibacterial activity of silver nanoparticles depend on the shape of the nanoparticle? A study of the gram-negative bacterium *Escherichia coli*. *Appl Environ Microbiol* 73(6): 1712–1720.
- Panaček A, Kvítek L, Pucek R, Kolář M, Večeřová R, Pizúrová N, Sharma VK, Nevěčná TJ, Zbořil R (2006) Silver colloid nanoparticles: synthesis, characterization and their antibacterial activity. *J Phys Chem B* 110(33): 16248–16253.
- Paquin PR, Gorsuch JW, Apte S, Batley GE, Bowles KC, Campbell PGC, Delos CG, Di Toro DM, Dwyer RL, Galvez F, Gensemer RW, Goss GG, Hogstrand C, Janssen CR, McGeer JC, Naddy RB, Playle RC, Santore RC, Schneider U, Stubblefield WA, Wood CM, Wu KB (2002) The biotic ligand model: a historical overview. *Comp Biochem Physiol C* 133: 3–35.
- Park HJ, Kim JY, Kim J, Lee JH, Hahn JS, Gu MB, Yoon J (2009) Silver-ion-mediated reactive oxygen species generation affecting bactericidal activity. *Water Res* 43(4): 1027–1032.
- Pesavento M, Alberti G, Biesuz R (2009) Analytical methods for determination of free metal ion concentration, labile species fraction and metal complexation capacity of environmental waters: a review. *Anal Chim Acta* 631(2): 129–141.
- Puzyn T, Rasulev B, Gajewicz A, Hu X, Dasari TP, Michalkova A, Hwang HM, Toropov A, Leszczynska D, Leszczynski J (2011) Using nano-QSAR to predict the cytotoxicity of metal oxide nanoparticles. *Nat Nano* 6(3): 175–178.
- Raffi M, Hussain F, Bhatti T, Akhter J, Hameed A, Hasan M (2008) Antibacterial characterization of silver nanoparticles against *E. coli* ATCC-15224. *J Mater Sci Tech Ser* 24: 192–196.
- Rai M, Yadav A, Gade A. (2009). Silver nanoparticles as a new generation of antimicrobials. *Biotechnology Advances* 27(1): 76–83.
- Rajendran R, Balakumar C, Mohammed Ahammed HA, Jayakumar S, Vaideki K, Rajesh EM (2010) Use of zinc oxide nano particles for production of antimicrobial textiles. *Int J Eng Sci* 2(1): 202–208.
- Ren G, Hu D, Cheng EWC, Vargas-Reus MA, Reip P, Allaker RP (2009) Characterisation of copper oxide nanoparticles for antimicrobial applications. *Int J of Antimicrob Ag* 33(6): 587–590.
- Rice RH, Vidrio EA, Kumfer BM, Qin Q, Willits NH, Kennedy IM, Anastasio C (2009) Generation of oxidant response to copper and iron nanoparticles and salts: stimulation by ascorbate. *Chem-Biol Interact* 181(3): 359–365.
- Robichaud CO, Uyar AE, Darby MR, Zucker LG, Wiesner MR (2009) Estimates of upper bounds and trends in nano-TiO₂ production as a basis for exposure assessment. *Environ Sci Technol* 43(12): 4227–4233.
- Roe D, Karandikar B, Bonn-Savage N, Gibbins B, Rouillet JB (2008) Antimicrobial surface functionalization of plastic catheters by silver nanoparticles. *J Antimicrob Chemother* 61(4): 869–876.

- Ruparelia JP, Chatterjee AK, Duttgupta SP, Mukherji S (2008) Strain specificity in antimicrobial activity of silver and copper nanoparticles. *Acta Biomater* 4(3): 707–716.
- Sadiq IM, Dalai S, Chandrasekaran N, Mukherjee A (2011) Ecotoxicity study of titania (TiO₂) NPs on two microalgae species: *Scenedesmus sp.* and *Chlorella sp.* *Ecotoxicol Environ Saf* 74(5): 1180–1187.
- Sambhy V, MacBride MM, Peterson BR, Sen A (2006) Silver bromide nanoparticle/polymer composites: dual action tunable antimicrobial materials. *J Am Chem Soc* 128(30): 9798–9808.
- Sawai J (2003) Quantitative evaluation of antibacterial activities of metallic oxide powders (ZnO, MgO and CaO) by conductimetric assay. *J Microbiol Meth* 54(2): 177–182.
- Sebastian Tomi N, Kränke B, Aberer W (2004) A silver man. *Lancet* 363(9408): 532.
- Smetana AB, Klabunde KJ, Marchin GR, Sorensen CM (2008). Biocidal activity of nanocrystalline silver powders and particles. *Langmuir* 24(14): 7457–7464.
- Sondi I, Salopek-Sondi B (2004) Silver nanoparticles as antimicrobial agent: a case study on *E. coli* as a model for gram-negative bacteria. *J Colloid Interface Sci* 275(1): 177–182.
- Studer AM, Limbach LK, Van Duc L, Krumeich F, Athanassiou EK, Gerber LC, Moch H, Stark, WJ (2010) Nanoparticle cytotoxicity depends on intracellular solubility: comparison of stabilized copper metal and degradable copper oxide nanoparticles. *Toxicol Lett* 197(3): 169–174.
- Sunada K, Kikuchi Y, Hashimoto K, Fujishima A. (1998). Bactericidal and Detoxification Effects of TiO₂ Thin Film Photocatalysts. *Environmental Science & Technology* 32(5):726–728.
- Tayel AA, El-Tras WF, Moussa S, El-Baz AF, Mahrous H, Salem MF, Brimer L (2011) Antibacterial activity and mechanism of action of zinc oxide nanoparticles against foodborne pathogens. *J Food Safety*: 31(2): 211–218.
- Trapalis CC, Keivanidis P, Kordas G, Zaharescu M, Crisan M, Szatvanyi A, Gartner M (2003) TiO₂(Fe₃⁺) nanostructured thin films with antibacterial properties. *Thin Solid Films* 433(1–2): 186–190.
- Tsuang YH, Sun JS, Huang YC, Lu CH, Chang WHS, Wang CC (2008) Studies of photokilling of bacteria using titanium dioxide nanoparticles. *Artif Organs* 32(2): 167–174.
- Vertelov GK, Krutyakov TA, Eremenkova OV, Olenin AY, Lisichkin, GV (2008) A versatile synthesis of highly bactericidal Myramistin® stabilized silver nanoparticles *Nanotechnol* 19(35): 355707. doi:10.1088/0957-4484/19/35/355707.
- Wei C, Lin WY, Zainal Z, Williams NE, Zhu K, Kruzic AP, Smith RL, Rajeshwar K (1994) Bactericidal activity of TiO₂ photocatalyst in aqueous media: toward a solar-assisted water disinfection system. *Environ Sci Technol* 28(5): 934–938.
- White JML, Powell AM, Brady K, Russell-Jones R (2003) Severe generalized argyria secondary to ingestion of colloidal silver protein. *Clin Exp Dermatol* 28(3): 254–256.
- Wu B, Huang R, Sahu M, Feng X, Biswas P, Tang YJ (2009) Bacterial responses to Cu-doped TiO₂ nanoparticles. *Sci Total Environ* 408(7): 1755–1758.
- Wu B, Wang Y, Lee YH, Horst A, Wang Z, Chen DR, Sureshkumar R, Tang YJ (2010) Comparative eco-toxicities of nano-ZnO particles under aquatic and aerosol exposure modes. *Environ Sci Technol* 44(4): 1484–1489.
- Xia T, Kovochich M, Liang M, Mädler L, Gilbert B, Shi H, Yeh JI, Zink JI, Nel AE (2008) Comparison of the mechanism of toxicity of zinc oxide and cerium oxide nanoparticles based on dissolution and oxidative stress properties. *ACS Nano* 2(10): 2121–2134.
- Yoon KY, Byeon JH, Park CW, Hwang J (2008) Antimicrobial effect of silver particles on bacterial contamination of activated carbon fibers. *Environ Sci Technol* 42(4): 1251–1255.
- Zhang L, Jiang Y, Ding Y, Povey M, York D (2007) Investigation into the antibacterial behaviour of suspensions of ZnO nanoparticles (ZnO nanofluids). *JNR* 9(3): 479–489.
- Zhang Y, Peng H, Huang W, Zhou Y, Yan D (2008) Facile preparation and characterization of highly antimicrobial colloid Ag or Au nanoparticles. *J Colloid Interface Sci* 325(2): 371–376.

Chapter 10

Electrosynthesis and Characterisation of Antimicrobial Modified Protein Nanoaggregates

Catherine Debiemme-Chouvy

10.1 Introduction

To fight against biofouling, the best way is to avoid the first step of its formation which consists of macromolecule adsorption or microfouling. Adsorption can be avoided or at least limited by modifying surface properties. Microfouling can be hampered through the action of a biocide. To achieve this goal, different strategies have been considered [1]. One is based on the release of a biocide from a coating. The oldest example is that of tri-butyl tin (TBT) mixed with marine paints. However, it is presently prohibited because of its high toxicity leading to environmental damage. Today, TBT is mainly replaced by some metal cations such as Cu^{2+} and Ag^+ . These cations are produced by simple release of nanoparticles (see Chap. 9, for example) or by anodic dissolution of the corresponding metal.

In addition, for water disinfection, biocides such as chlorine or bromine are used in inorganic form: hypochlorous acid (HOCl), monochloramine (NH_2Cl), hypobromous acid (HOBr) [2]. For these species, halide atoms are in the oxidation state +I, i.e. in an oxidizing form. In organic compounds, chloramine or bromamine groups ($>\text{N-X}$; X being Cl or Br) also retains the oxidizing properties of halide atoms, and therefore these compounds have biocidal properties. Thus, in the 1980s, the study of low molecular weight organic molecules containing chloramine or bromamine functions (N-halamine) for water disinfection was developed [3, 4]. Some examples of such molecules are depicted in Fig. 10.1. Notice that an N-halamine compound can be defined as a species containing one or more nitrogen–halogen covalent bonds that is normally formed by the halogenation of imide, amide, or amine groups. Actually, nitrogen–halogen covalent bonds in organic compounds are in general named

C. Debiemme-Chouvy (✉)
Laboratoire Interfaces et Systèmes Electrochimiques, UPR 15 du CNRS; Université
P. et M. Curie, Paris, France
e-mail: catherine.debiemme-chouvy@upmc.fr

haloamine (chloramine, bromamine) by biologists and N-halamine by physico-chemists.

The small halogenated organic molecules (Fig. 10.1) which are soluble in water suffer from some disadvantages such as toxicity to the environment and short-term antimicrobial ability [5]. To overcome these problems, antimicrobial functional groups should be immobilized into insoluble molecules. This has been behind the origin of the development of organic polymers containing N-halamine moieties [6, 7]. Some examples of N-halamine polystyrene polymers are depicted in Fig. 10.2. In fact, several methods of achieving antimicrobial N-halamine organic polymers have been developed. One is the grafting of the biocidal function to the monomer. Another way is to add the antimicrobial function to the polymer after its synthesis. The modification of a natural polymer such as chitin (second-most abundant biopolymer in nature) modified by deacetylation leading to chitosan has also been developed. Indeed, if the organic polymer contains amine, amide or imine groups, it can be rendered biocidal by exposure to dilute bleach [8]. For example, upon chlorine bleach treatment

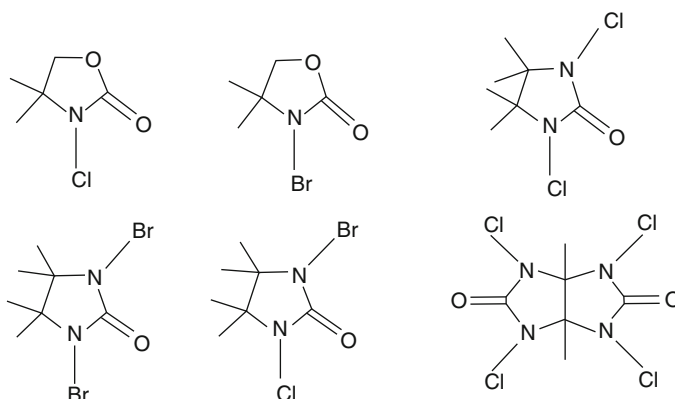


Fig. 10.1 Structures of some organic N-halamines tested as compounds for water disinfectant (Adapted from [4])

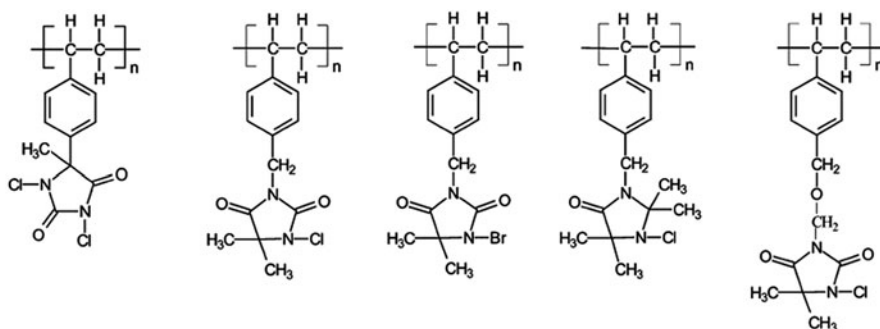


Fig. 10.2 Structures of some biocidal N-halamine polystyrene polymers (Adapted from [6])

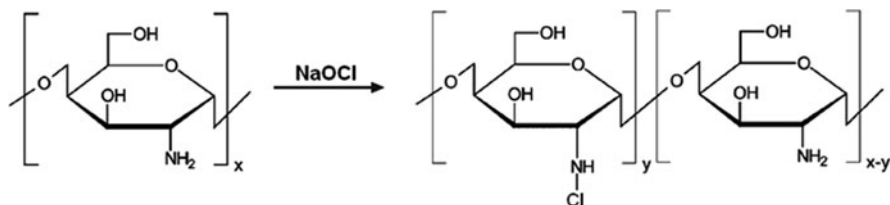


Fig. 10.3 Synthesis of N-halamine-based chitosan

some amino groups in chitosan can be transformed into N-halamine structures [9]; the reaction scheme is shown in Fig. 10.3.

Notice that the polymer could be cyclic, as shown in Fig. 10.2, or acyclic N-halamine compounds [10–14]. It has been shown that N-halamine polymers have excellent biocidal functions against a wide range of microorganisms including bacteria, viruses, fungi, and spores. Therefore, these antimicrobial polymers are attractive candidates for many applications such as water treatment, biocidal functional modifications of textiles or paints, and polymeric materials [15–23].

Another original way to obtain organic coatings having antibacterial properties is to modify protein with chlorine and/or bromine and to use the protein as a monomer. It is the aim of this chapter to present this new route to designing surfaces having biocidal properties.

The process is based on local electro-generation of hypochlorous acid and/or hypobromous acid by oxidation of chloride and/or bromide ions which react with natural organic compounds: proteins (bovine serum albumin, BSA) present in the medium. The first condition to implement this process is the adsorption of the proteins used on the material. The second one is the anodic oxidation of chloride and/or bromide ions at the material surface (conductive material). Both conditions are notably satisfied for Sb-doped SnO_2 films [24]. Indeed, this transparent and conductive film (generally deposited on glass) allows chloride and bromide oxidation leading to hypochlorous and hypobromous acid [25, 26]:



in water, Cl_2 and Br_2 disproportionate into HOCl (at $\text{pH} > 2.5$) and HOBr (at $\text{pH} > 5.7$):



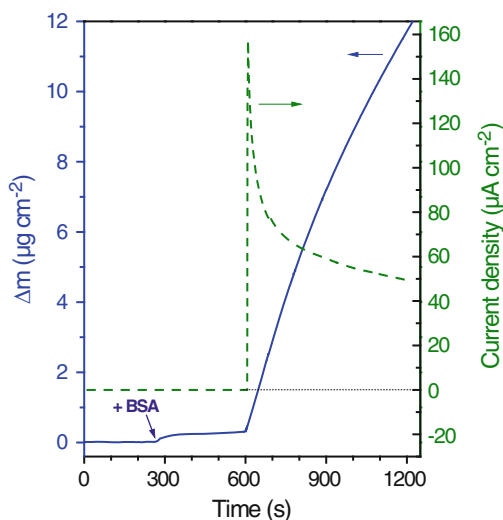
Therefore, in the first part of this chapter, the way to obtain nanoclusters of modified proteins by electrogenerated hypochlorous and/or hypobromous acid in the presence of bovine serum albumin (BSA) is described. Then, the chemical characterization of these aggregates is presented and the reaction mechanism which leads to their formation is discussed. Finally, the capability of these nano-aggregates to prevent surface colonization by bacteria (*Escherichia coli*) is shown.

10.2 Electrogeneration of N-Halamine-Based Protein Nanoclusters

First of all, the protein used to form the aggregates has to adsorb on the surface to be protected against biofilm. To verify this point, the quartz crystal microbalance (QCM) is a powerful means since it allows one to follow the mass of the material deposited on the quartz. On SnO_2 film deposited on quartz, it has been shown that after addition of BSA in the medium the mass of the SnO_2 film slightly increases; this increase was attributed to protein adsorption (Fig. 10.4) [27]. If the BSA tertiary structure (three-dimensional structure) is preserved, the mass of the equivalent of one BSA monolayer is between 0.2 and $0.7 \mu\text{g cm}^{-2}$ depending on the orientation of the macromolecules on the surface [28]. Since in the presence of BSA, at open circuit potential (no applied potential), the SnO_2 mass increase is of $0.4 \pm 0.1 \mu\text{g cm}^{-2}$, it has been concluded that the equivalent of one monolayer of BSA adsorbs on it. Actually, it has been shown that, on hydrophilic surfaces, BSA adsorbs in a two-step process [29] and that the deposited layer prevents further protein adsorption. This is in good agreement with the fact that the as-prepared SnO_2 surface is hydrophilic [30].

In addition, if BSA and chloride and/or bromide ions are present in the medium, under anodic polarization, i.e. when halide anions are oxidized (reactions (10.1) and (10.2)), the mass of the SnO_2 film progressively increases (Fig. 10.4; $t > 600$ s). This increase which depends on the polarization time, could be very high indicating that an important and continuous deposit is formed onto the SnO_2 film [27]. This finding has been verified by SEM observations. The SEM images reported in Fig. 10.5 show that, after an anodic polarization at 1.5V/SCE for 2 h in the presence of chlorides and BSA, nanoclusters are present on the SnO_2 surface (Fig. 10.5c, d) [31]. The same results,

Fig. 10.4 Mass variation (blue line) and current density (dashed green line) versus time of a SnO_2 film in contact with a 0.5-M NaCl solution first at open circuit potential before and after addition of BSA into the solution (arrow) then, after 600 s, under polarization at 1.5V/SCE (oxidation of chloride ions). BSA concentration: 0.5 mg/mL (Adapted from [27])



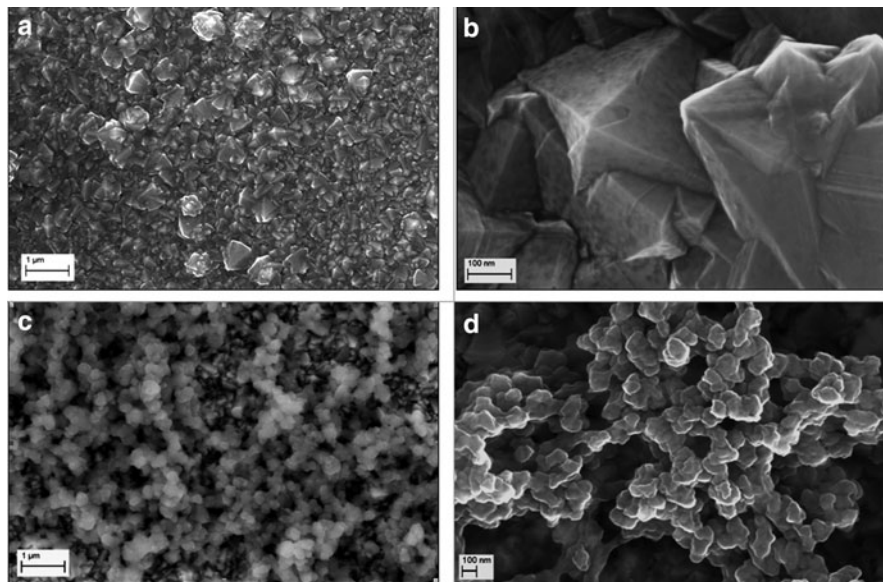


Fig. 10.5 SEM images obtained from SnO₂ samples (a, b) as-deposited (c, d) after polarization at 1.5V/SCE for 2 h in 0.5-M NaCl solution containing 1 mg mL⁻¹ BSA (From [31]. With permission of Elsevier)

i.e. formation of nano-aggregates, have been obtained using BSA-containing NaBr solution or seawater [32]. In seawater, the concentrations of chloride and bromide ions are 0.55 and 8×10^{-4} M, respectively. These anions are both oxidized at a SnO₂ electrode polarized at 1.5V/SCE; therefore, at this potential, HOCl and HOBr species are produced.

Moreover, it has been observed that if BSA molecules are present in the electrolyte but not halide ions, the anodic current at 1.5V/SCE is lower (due to water oxidation) and the mass of the SnO₂ electrode does not increase. Finally, if halide ions are present in the solution but there is no BSA, no deposit is formed on the electrode when it is anodically polarized, i.e. when the halide ions are oxidized.

Therefore, the mass increase of the SnO₂ electrode is due to the presence of BSA and to the electrogeneration of hypohalous acid (HOCl and/or HOBr).

10.3 Chemical Characterization of the Deposit (EDX, XPS, TNB Reagent): N-Halamine Evidence

After an anodic polarization in the presence of halide ions and BSA, an important deposit is present on the SnO₂ film. The chemical nature of this deposit was determined by energy dispersive X-ray spectroscopy (EDX). Figure 10.6 shows the spectra recorded for various SnO₂ samples. One without treatment (a, as-deposited

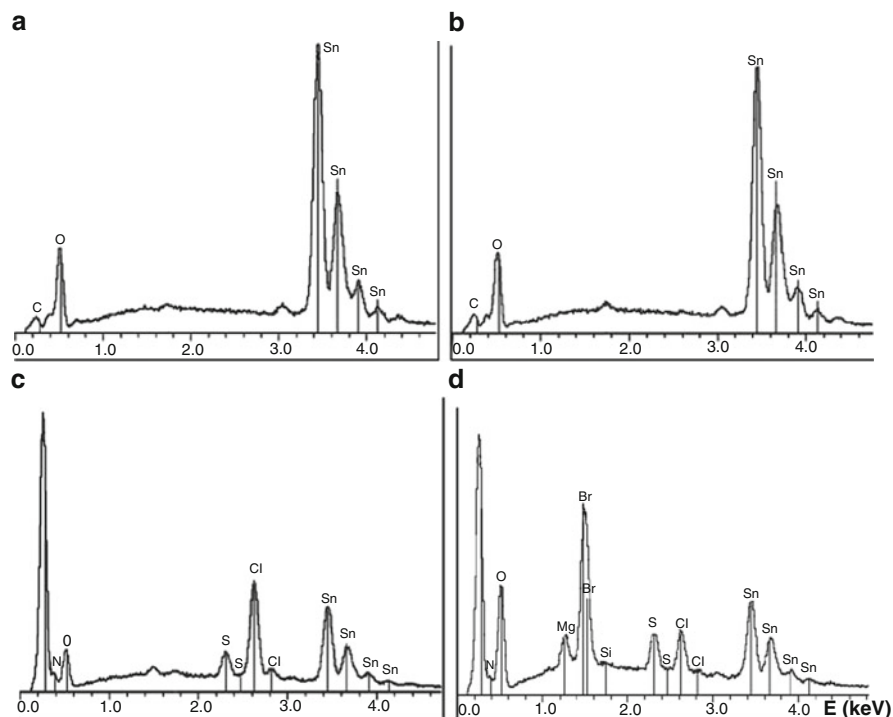


Fig. 10.6 EDX spectra obtained from SnO_2 sample (a) as-deposited, (b) after 54 h at open circuit potential, (c) and (d) after polarization at 1.5V/SCE for 2 h, in (b, c) 0.5-M NaCl solution containing 1 mg mL^{-1} BSA, (d) seawater containing 1 mg mL^{-1} BSA (Adapted from [27] and [32])

SnO_2 film), one after contact with a BSA solution at open circuit potential, i.e. without applied potential (b) and two after polarization in BSA-containing NaCl solution (c) or seawater (d). Taking into account spectra (c) and (d), the main features are the large intensity of the carbon peak (at 0.25 keV), the presence of sulfur (at 2.3 keV), obviously these elements are due to proteins, and finally the presence of chlorine (at 2.6 keV); in the case of seawater, the contribution of bromine (at 1.5 keV) was also detected (spectrum d). Moreover, the decrease of the intensity of the tin signals (in comparison with spectra a and b) confirms that the SnO_2 film is covered with a thick organic deposit: BSA molecules modified with Cl and/or Br.

The environment and the oxidation state of the elements present in the nanoclusters formed during oxidation of halide ions (chloride and/or bromide) in the presence of BSA have been determined using X-ray photoelectron spectroscopy (XPS) which is a surface analysis technique (thickness analyzed: less than 10 nm). For the SnO_2 films anodized in BSA-containing NaCl solution or seawater, the photopeaks of C, N, O, and S were detected on the survey spectrum [27, 31]. Obviously these elements are characteristic of the BSA molecules. The photopeaks due to Cl (Br) atoms were also present on the survey spectrum. For most of the

elements detected by XPS (all expected H and He), the high-resolution spectrum allows one to determine their oxidation state; it is notably the case for C, S, Cl and Br elements.

For the C1s signal, it has been shown that the shapes of the photopeak obtained on one hand for the BSA powder and on the other hand for the deposit formed during electro-oxidation of halide ions in the presence of BSA are the same [27]. This finding is important because it implies that the primary structure of the protein (amino acid sequence) is preserved in the aggregates.

For the SnO₂ film at which halide ions (Cl⁻ and/or Br⁻) were oxidized in the presence of BSA, the organic deposit contains sulfur. The S2p peak was well fitted with two pairs of doublet (Fig. 10.7, spectrum C). The contribution at the lower binding energy (163.7 eV) which is also observed for BSA powder (spectrum A) and for SnO₂ film after contact with a BSA-containing solution (substrate coated with a BSA monolayer, spectrum B) is due to S(-II) (amino acid: cysteine and methionine, structures are depicted in Fig. 10.8) or S(-I) (cystine). The same values were reported for unbound alkanethiols and dialkyl disulfides i.e. 163 and 164 eV [36, 37]. Taking into account the S2p peak, the main finding is that for the

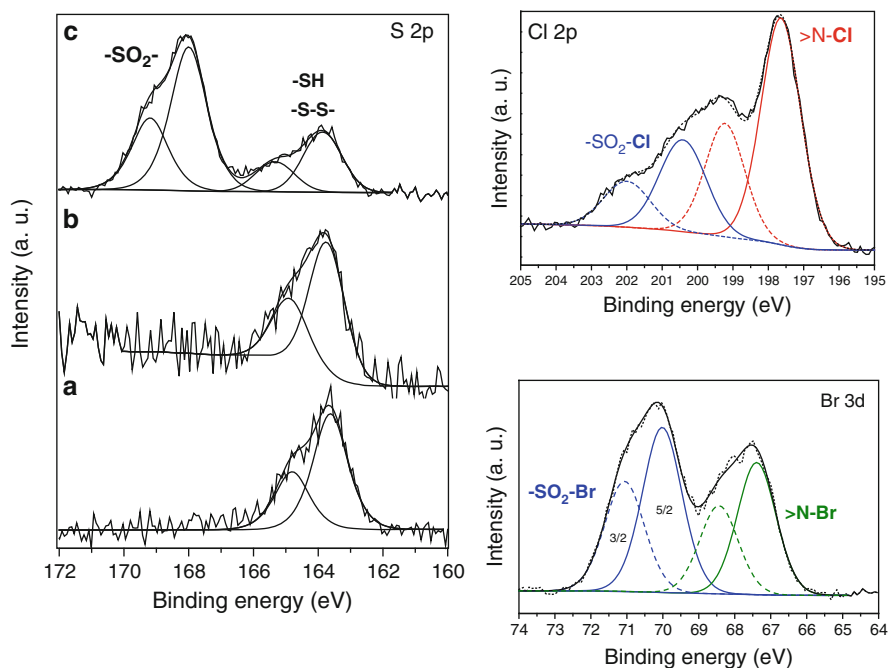


Fig. 10.7 Left S2p XPS spectra from (a) BSA powder, (b, c) SnO₂ films after contact with 1 mg/mL BSA + 0.5 M NaCl solution (b) at open circuit potential for 2 h, (c) under polarization at 1.5V/SCE for 2 h. Right Cl2p XPS spectrum (top) of a SnO₂ film after polarization at 1.5V/SCE for 2 h in 1 mg/mL BSA + 0.5 M NaCl solution. Br3d XPS spectrum (bottom) of a SnO₂ film after polarization at 1.5V/SCE for 2 h in seawater containing 1 mg/mL BSA (Adapted from [31] and [32])

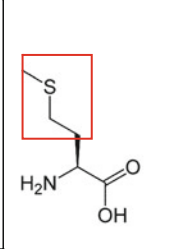
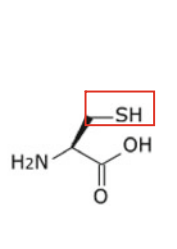
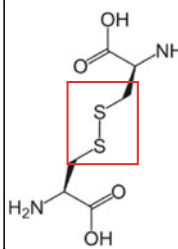
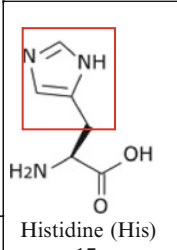
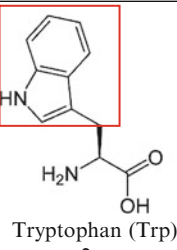
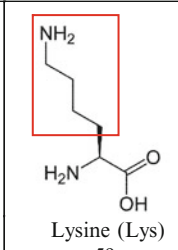
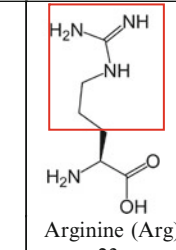
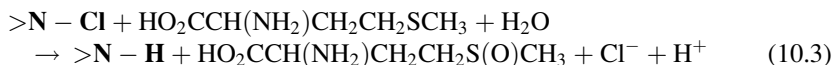
				
	Methionine (Met)	Cysteine (Cys)	cystine	
n	4	1	17	
k_2 (HOCl)	$4 \cdot 10^7 \text{ M}^{-1} \text{ s}^{-1}$	$3.2 \cdot 10^7 \text{ M}^{-1} \text{ s}^{-1}$	$1.6 \cdot 10^5 \text{ M}^{-1} \text{ s}^{-1}$	
k_2 (HOBr)	$3.6 \cdot 10^6 \text{ M}^{-1} \text{ s}^{-1}$	$1.2 \cdot 10^7 \text{ M}^{-1} \text{ s}^{-1}$	$7.2 \cdot 10^5 \text{ M}^{-1} \text{ s}^{-1}$	
				
	Histidine (His)	Tryptophan (Trp)	Lysine (Lys)	Arginine (Arg)
n	17	2	59	23
k_2 (HOCl)	$10^5 \text{ M}^{-1} \text{ s}^{-1}$	$10^4 \text{ M}^{-1} \text{ s}^{-1}$	$8 \cdot 10^3 \text{ M}^{-1} \text{ s}^{-1}$	$26 \text{ M}^{-1} \text{ s}^{-1}$
k_2 (HOBr)	$3 \cdot 10^6 \text{ M}^{-1} \text{ s}^{-1}$	$3.7 \cdot 10^6 \text{ M}^{-1} \text{ s}^{-1}$	$2.9 \cdot 10^5 \text{ M}^{-1} \text{ s}^{-1}$	$1.8 \cdot 10^3 \text{ M}^{-1} \text{ s}^{-1}$

Fig. 10.8 Structure of some amino acids, number of residues (n) in BSA [33] and second-order rate constant (k_2) for the reaction of HOCl and HOBr with amino acid side chain (framed in red) obtained from [34] and [35], respectively

electrochemically treated SnO_2 film a second contribution around 168 eV was observed. It was ascribed to sulfur oxidized at oxidation state +6, i.e. $-\text{SO}_2^-$ groups present in the organic matter. This means that a part of the sulfur-containing amino acids of the BSA molecules have been oxidized during the anodic polarization of SnO_2 . The $\text{S}2\text{p}_{3/2}$ contribution of $\text{SO}_2\text{-N}$ group has also been reported to be located at 168.6 eV [38].

For the SnO_2 films at which the oxidation of chloride ions has been performed in the presence of BSA, a $\text{Cl}2\text{p}$ photopeak is detected. The deconvolution of this peak yields components for the $\text{Cl}2\text{p}_{3/2}$ level at 200.6 and 197.8 eV (see Fig. 10.7). These contributions have been ascribed to sulfonyl chloride groups ($-\text{SO}_2\text{-Cl}$) and to chloramine groups ($>\text{N-Cl}$), respectively [31]. This assignment has been verified: a SnO_2 film anodically polarized in BSA-containing NaCl solution was soaked in a 0.1 M methionine solution for 4 h since it is well known that methionine reacts with the chloramines according to [34], and [39]

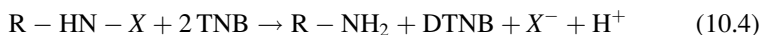


Effectively, after this treatment, the intensity of the photopeak located at 197.8 eV is nearly null [31]. Therefore, the chlorine atoms for which the binding energy of the 2p_{3/2} electrons is 197.8 eV are really implied in the chloramine group.

For the SnO₂ films anodically polarized in BSA-containing 0.5 M NaBr solution or seawater, photopeaks due to bromine (Br3d and Br3p levels) were also detected on the survey spectrum [30]. As for the Cl2p peak, the peaks due to Br were fitted with two contributions, the one at the lower binding energy being ascribed to bromamine and the other one to sulfonyl bromide groups (Fig. 10.7).

The presence of the chloramine and/or bromamine groups in the organic aggregates formed during oxidation of chloride and/or bromide ions in the presence of BSA was also confirmed using a chemical reagent. It was shown by reaction with 5-thio-2-nitrobenzoic acid (TNB), by measuring the bleaching of a TNB solution, at 412 nm ($\epsilon_{412} = 14,100 \text{ M}^{-1} \text{ cm}^{-1}$) [40].

The yellow-colored TNB reacts with chloramines and bromamines (>N-X, X being Cl or Br) to regenerate colorless 5,5'-dithiobis(2-nitrobenzoic acid) (DTNB), according to the reaction:



For this aim, the SnO₂ film electrochemically treated in BSA-containing 0.5 M NaCl/NaBr solution or seawater was soaked in a TNB solution. After polarization, the SnO₂ electrode was rinsed with water and then dipped into the yellow TNB solution. It was observed that immediately the solution began to bleach. The same sample was soaked successively for 30 s, 2 and 5 min in a TNB solution. After 5 min of immersion, the TNB solution has become totally bleached. The same observations were done for SnO₂ films anodically polarized in BSA-containing 0.5 M NaBr solution, when the TNB solution bleached [32]. To confirm the specificity of the electrochemically treated SnO₂ surface, the same experiments were conducted on the one hand with an as-deposited SnO₂ film and on the other hand by adding BSA powder in the TNB solution. In both cases the TNB solution did not bleach and the solution absorbance remained unchanged [27].

Finally, both methods were coupled (treatment with methionine and TNB reagent) to confirm that the TNB solution bleaching is really due to the presence of chloramine (bromamine) groups in the organic nanoclusters. Before immersion in the TBN solution, a SnO₂ film coated with the organic deposit formed during halide ion oxidation in the presence of BSA was dipped into a 0.1 M methionine solution. After the methionine treatment, the sample was soaked in the TNB solution, its absorbance only slightly decreased (Fig. 10.9, sample C, red spectra). Whereas for other coated film the TNB solution absorbance at 412 nm has decreased (Fig. 10.9, sample B, blue lines). Therefore, chloramine (bromamine)

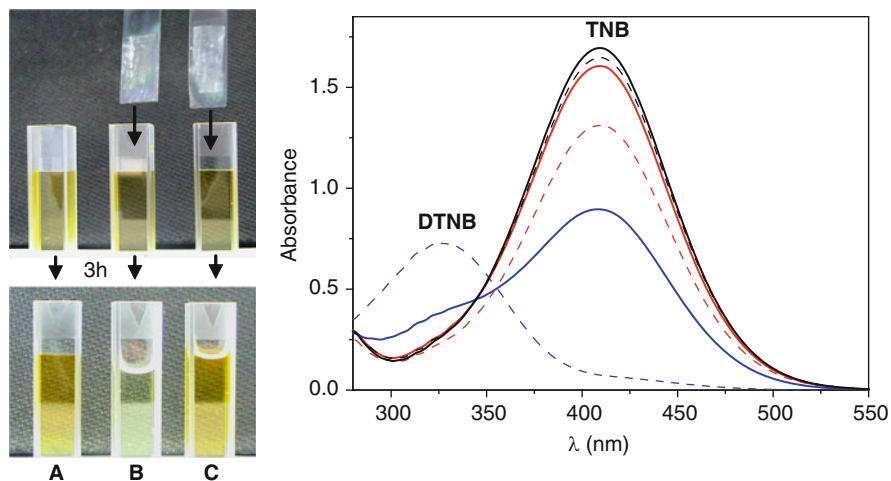
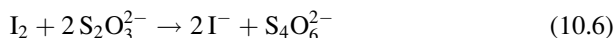
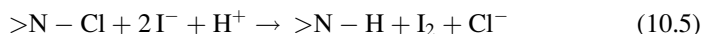


Fig. 10.9 Chemical characterization of chloramines. *Left* SnO₂ films and optical images of cuvettes (1 cm) containing the TNB solution. *Top* before immersion of the SnO₂ films coated with a very large organic deposit. *Bottom* sample (b) after a 3-h immersion of the SnO₂ films polarized at 1.5V/SCE in 0.5 M NaCl solution containing 1 mg/mL BSA; sample (c) as sample (b) but before immersion the SnO₂ film was dipped for 4 h in 0.1 M methionine solution. *Right* optical absorbance spectra of TNB solutions (cuvette length: 0.2 cm). *Black lines* reference (a); *blue and red lines* correspond to samples (b) and (c), respectively. *Full and dotted lines* spectra recorded after 30 min and 3 h, respectively, of immersion of the SnO₂ films (From [27]. With permission of ACS)

groups are really present in the organic deposit formed during oxidation of chloride (bromide) ions in the presence of BSA. Thus, it is an effective method to immobilize on a surface such oxidizing functions (N-halamine).

Notice that in general for the N-halamine polymers, the active chlorine (Cl(+I)) content of polymer is determined by iodometric titration [41]. First, iodide ions reduce the chlorine atoms leading to the release of iodine which is then titrated with thiosulfate:



10.4 Mechanism of N-Halamine and Nanocluster Formation

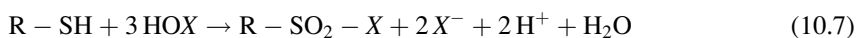
Obviously, during the oxidation of halide ions in the presence of BSA, two processes take place: (1) formation of N-halamine groups and (2) protein aggregation.

Since by XPS analysis, the C1s peak obtained from the nanostructured deposit is identical to the one obtain from the BSA powder, it has been concluded that the protein primary structure is conserved into the cross-linking [31]. Thus, chlorination and/or bromination of the BSA occurs on the amino acid side chains.

In addition, to discuss the mechanism, it should be underlined that many studies of the reactions occurring between proteins and HOCl or HOBr have been conducted by biologists, since these hypohalous acids which are generated by the human immune system are implicated in the development of some human inflammatory diseases [42–44]. It has been shown that these acids notably react with proteins [44, 45]. Second-order rate constants for the reaction of HOCl or HOBr with protein side chains have been estimated [35, 37], some values are reported in Fig. 10.8. From these values and from Fig. 10.10 which shows the proportion of HOCl reacting with each amino acid residue (Fig. 10.10a) and the percentage of each residue remaining in function of the ratio HOCl/HSA (Fig. 10.10b), it is obvious that the HOCl reactivity for protein residues is Met > Cys >> cystine > His > R-amino > Trp > Lys >> Tyr > Arg > backbone amides.

Therefore, the chemical modification of the SnO₂ surface during halide ion oxidation (reactions (10.1) and (10.2)) is due to the reaction of hypohalous acid with the protein side chains. Actually, during the process, two types of reaction occur: oxidation of sulfur atoms and substitution of H of some amine/imine/amide functions. The oxidation and the halogenation of the protein side-chain take place according to the following reactions [43, 46, 47]:

Cystein side chain oxidation :



Cystine oxidation :

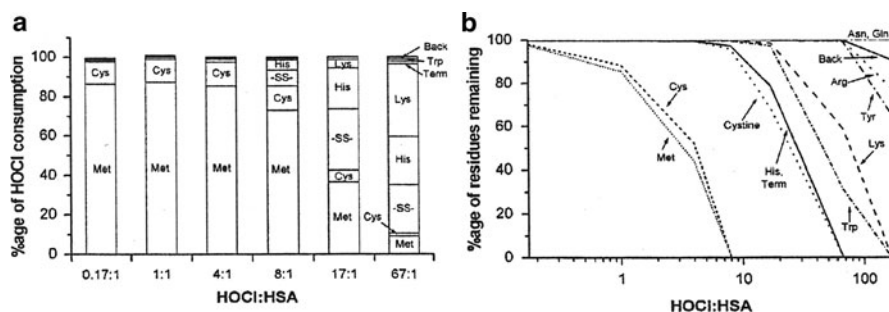
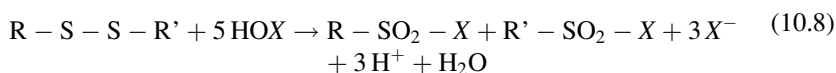
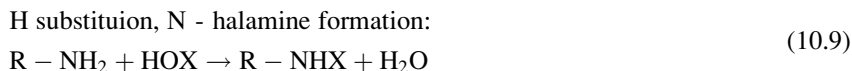
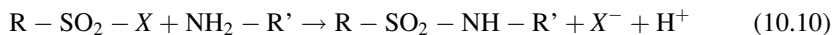


Fig. 10.10 Predicted reactivity of various molar excesses of HOCl with human serum albumin (HSA) using constants reported in Fig. 10.8 showing (a) the proportion of HOCl reactivity at each amino acid residue and (b) the percentage of each residue remaining. –SS– cystine, *Term* terminal amino group, *Back* backbone amides (From [34]. With permission of ACS)



Reactions (10.7) and (10.8) yield sulfonyl chloride/bromide groups. These groups are at the origin of the protein aggregation (polymerisation). Indeed, protein aggregation has been explained by intermolecular sulphonamide formation from oxidized thiol (sulfonyl halide) and amine group of proteins [48–50]:



Reaction pathways including this reaction have been proposed by Fu et al. [50]. They are shown in Fig. 10.11.

10.5 Antibacterial Properties

The antibacterial properties of the chlorinated/brominated protein aggregates has been confirmed by testing the adhesion and growth of bacteria on these surfaces. Figure 10.12 shows SEM images obtained after incubation of various samples in the

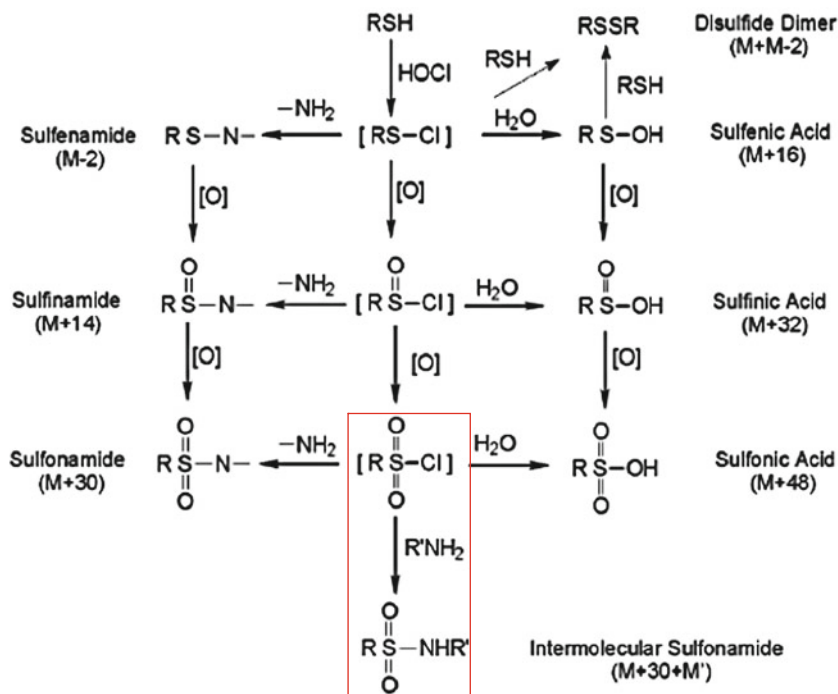


Fig. 10.11 Proposed reaction pathways for thiol oxidation by HOCl and S-N cross-linking (From [50]. With permission of ACS)

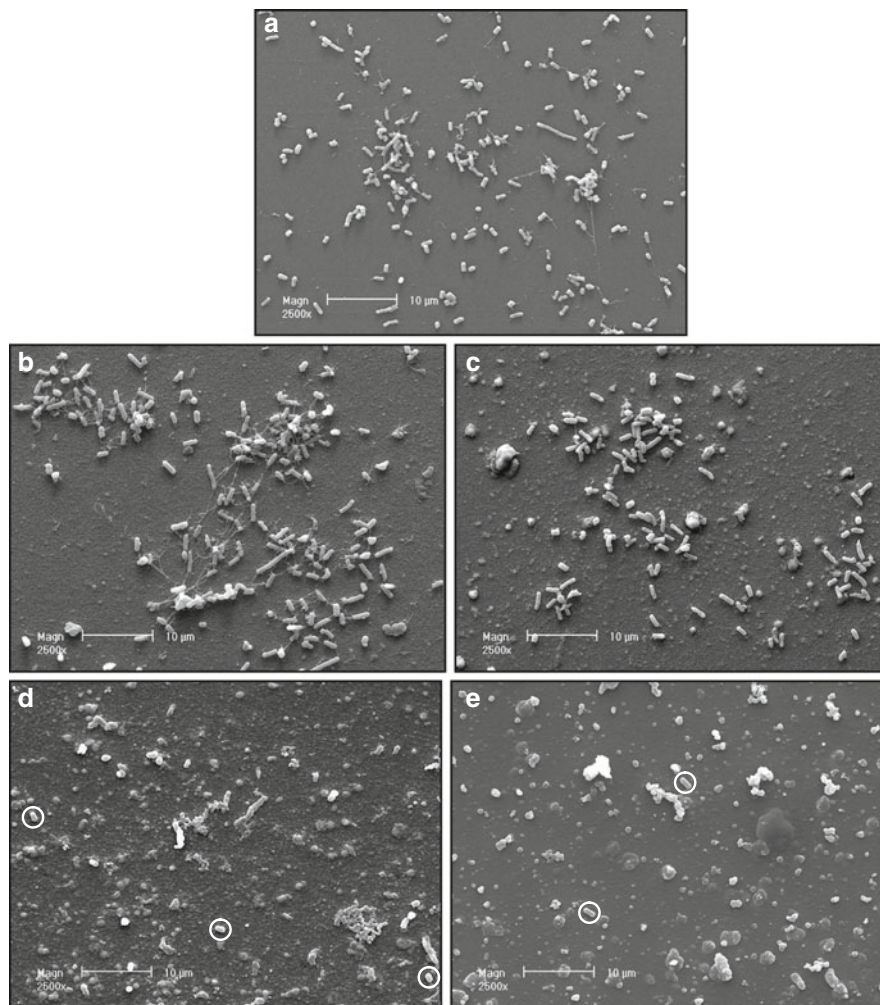


Fig. 10.12 SEM images after 17 h at 37°C in contact with 5×10^7 *Escherichia coli*/mL of (a) Thermanox (reference substrate), (b–e) treated SnO₂. (b, c) At open circuit potential for 54 h. (d, e) Polarized for 2 h in 0.5 M NaCl + BSA solution. BSA concentration: (b, d) 0.5 mg/mL, (c, e) 1 mg/mL. (d, e) White circles are aids for visualization of bacteria (From [51]. With permission of Elsevier)

presence of bacteria (*Escherichia coli*). For the reference substrate (Thermanox) and SnO₂ samples held at open circuit potential in the presence of BSA (surface coated with a monolayer of BSA, see Part 1), many bacteria are present on the sample surface (images a–c), whereas on the SnO₂ surfaces anodically polarized in the presence of BSA and chlorides, only a few bacteria were detected [31, 51]. All the images shown in Fig. 10.12 are corroborated with the average data reported in

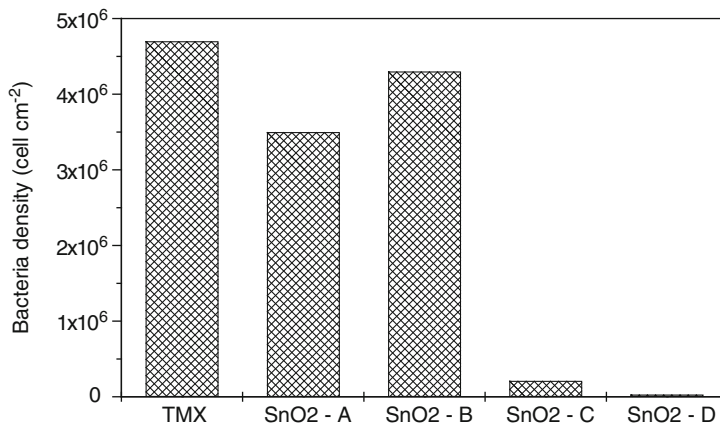


Fig. 10.13 Average number of adhered *Escherichia coli* per square centimeter on thermanox (TMX) and SnO₂ after incubation for 17 h in the presence of 5×10^7 bacteria/mL, at 37°C. SnO₂ pre-treatment in BSA + 0.5 M NaCl solution: (a, b) at open circuit potential for 54 h; (c, d) at 1.5 V/SCE for 2 h. BSA concentration: (a, c) 1 mg/mL; (b, d) 0.5 mg/mL (Adapted from [51])

Fig. 10.13. Clearly, after electrochemical pre-treatment in the presence of BSA and chlorides, the bacterial density on the SnO₂ surface is very low. The number of bacteria on reference surfaces (Thermanox and SnO₂ held at open circuit potential) is much higher than on the electrochemically pre-treated ones.

These findings were confirmed by fluorescence microscopy performed after incubation of the substrates in the presence of bacteria. In Fig. 10.14, the fluorescence is very low for two specimens (images b and f). Both have been anodically polarized in the presence of halide ions and BSA before contact with the bacteria suspension.

Similar antibacterial activity has been demonstrated for many chlorinated organic polymers or compounds immobilized onto fibrous materials: for example, for chloromelamine-based cellulosic fibrous material (cotton) [53] or for some other textiles such as nylon or polyester fibers [11, 54]. Antimicrobial properties have also been indicated for paints resulting from addition of polymeric N-halamine latex emulsions into commercial water-based latex paints [22]. Obviously, in all cases, the antibacterial efficacy is due to the oxidizing properties of chlorine atoms which are at the oxidation state +I. Finally, it is interesting to note that the mode of action of the N-halamine polymers is described by some researchers as direct transfer of oxidative halogen (Cl(+I) or Br(+I)) from the haloamine groups to the cell wall of the microorganism by direct contact followed by oxidation, rather than dissociation of Cl(+I) or Br(+I) into water followed by diffusion over to a microorganism [21, 55–57], whereas for other researchers both processes take place [22, 53, 58]. In all cases, it is obvious that the process consumes chlorines or bromines. However, the consumed chlorines/bromines can be readily recharged by a halogenation treatment performed by exposure of the polymer to an aqueous solution containing hypochlorite or hypobromite ions.

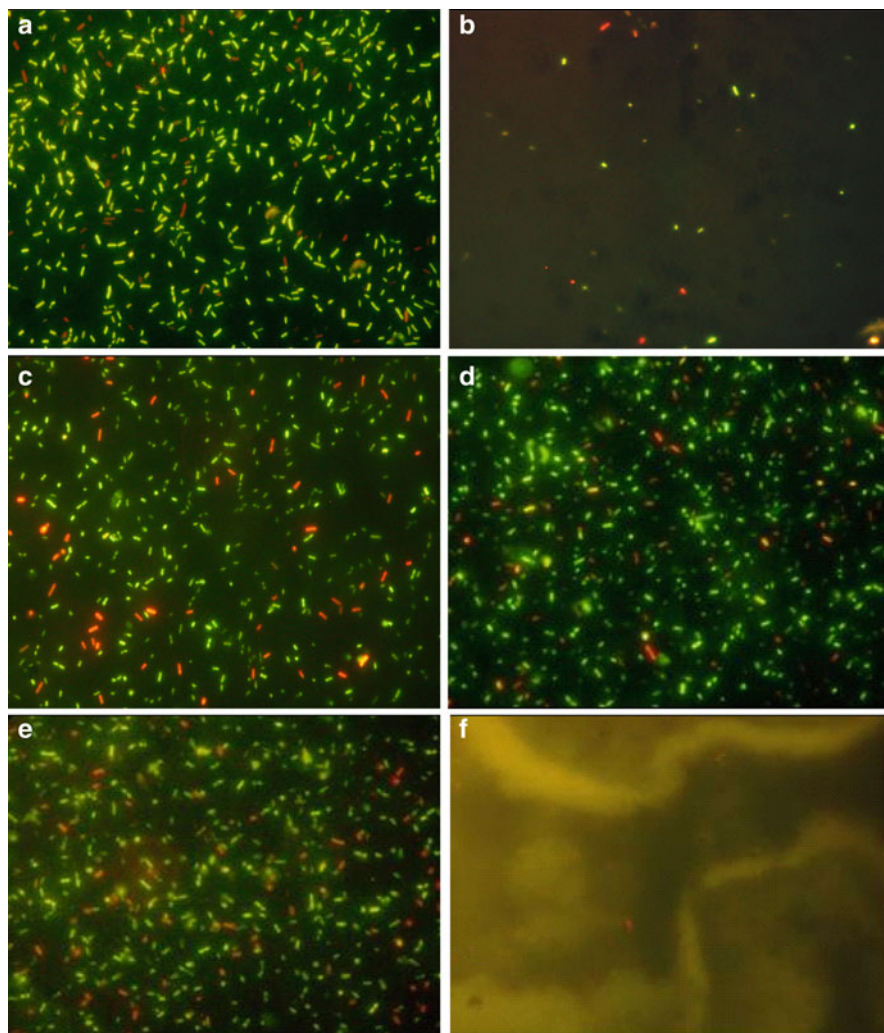


Fig. 10.14 Fluorescence microscopy images of SnO₂ films after incubation for 17 h at 37°C in the presence of *Escherichia coli*. (a) As-deposited. (b–f) Pre-treated films. Pre-treatments: (b) polarisation at 1.5V/SCE for 2 h in 0.5 M NaCl + 1 mg/mL BSA, (c) as (b) followed by immersion in a methionine solution for 5 h, (d) holding for 2 h at open circuit potential (no polarization) in seawater +1 mg/mL BSA, (e, f) polarisation at 1.5V/SCE for 2 h in seawater (e) in the absence of BSA, (f) in the presence of 1 mg/mL BSA (From [51] and [52])

10.6 Conclusion

In this chapter, the electrode material to be protected against bacteria settlement is a conductive transparent film of Sb-doped SnO₂. However, it is important to notice that other conductive materials such as a-CN_x, boron-doped diamond or stainless

steel also yield the formation of antimicrobial nano-aggregates of protein when halide ions are electro-oxidized at their surface [59].

As indicated by Worley et al. in their review concerning antimicrobial polymers [7] “The ideal antimicrobial polymer should possess the following characteristics: (1) easily and inexpensively synthesized, (2) stable in long-term usage and storage at the temperature of its intended application, (3) not soluble in water for a water disinfection application, (4) does not decompose to and/or emit toxic products, (5) should not be toxic or irritating to those who are handling it, (6) can be regenerated upon loss of activity, and (7) biocidal to a broad spectrum of pathogenic microorganisms in brief times of contact.”. It seems reasonable to think that the process described in this chapter allows one to obtain a polymer which meets all these criteria.

Finally, it should be underlined that this new process corresponds to a ‘green chemistry’ process since no organic solvent or toxic products are used for the synthesis of the polymer. Moreover, the protein polymerization and the halogenation of some amino acid residues lead to a non-toxic and biodegradable compound. Obviously, this process could only be used to coat conductive substrates at which halide ion electro-oxidation could be performed. However, a chemical way involving hypohalous acid and peptides or proteins is currently being developed in order to treat non-conductive substrates or to obtain an antibacterial powder.

References

1. Delauney L, Compère C, Lehaitre M (2010) Biofouling protection for marine environmental sensors. *Ocean Sci.* 6: 503–511.
2. White’s handbook of chlorination and alternative disinfectants – 5th edition/Black & Veatch, John Wiley, Hoboken (USA), 2010.
3. Worley SD, Williams DE (1988) Halamine water disinfectants. *CRC Crit. Rev. Environ. Control* 18: 133–175.
4. Worley SD, Williams DE, Barnela SB (1987) The stabilities of new N-halamine water disinfectants. *Wat. Res.* 21: 983–988.
5. Worley SD, Burkett HD, Price JF (1984) The tendency of a new water disinfectant to produce toxic trihalomethanes. *Wat. Resour. Bull.* 20: 369–371.
6. Chen Y, Worley SD, Huang TS, Weese J, Kim J, Wei CI, Williams JF (2004) Biocidal polystyrene beads. III. Comparison of N-halamine and quat functional groups. *J. Appl. Polym. Sci.* 92: 363–367.
7. Kenawy ER, Worley SD, Broughton R (2007) The chemistry and applications of antimicrobial polymers: A state-of-the-art review. *Biomacromol.* 8: 1359–1384.
8. Kou L, Liang J, Ren XH, Kocer HB, Worley SD, Broughton RM, Huang TS (2009) Novel N-halamine silanes. *Colloids Surf. A-Physicochem. Eng. Aspects* 345: 88–94.
9. Cao ZB, Sun YY (2008) N-Halamine-based chitosan: Preparation, characterization, and antimicrobial function. *J. Biomed. Mat. Res. Part A* 85A: 99–107.
10. Sun J, Sun YY (2006) Acyclic N-halamine-based fibrous materials: Preparation, characterization, and biocidal functions. *J. Polym. Sci. Part A-Polym. Chem.* 44: 3588–3600.
11. Ren XH, Zhu CY, Kou L, Worley SD, Kocer HB, Broughton RM, Huang TS (2010) Acyclic N-Halamine Polymeric Biocidal Films. *J. Bioact. Comp. Polym.* 25: 392–405.

12. Luo J, Sun YY (2008) Acyclic N-halamine-based biocidal tubing: Preparation, characterization, and rechargeable biofilm-controlling functions. *J. Biomed. Mat. Res. Part A* 84A: 631–642.
13. Liu S, Sun G (2009) New Refreshable N-Halamine Polymeric Biocides: N-Chlorination of Acyclic Amide Grafted Cellulose. *Ind. Eng. Chem. Res.* 48: 613–618.
14. Badrossamay MR, Sun G (2008) Acyclic halamine polypropylene polymer: Effect of monomer structure on grafting efficiency, stability and biocidal activities. *React. Funct. Polym.* 68: 1636–1645.
15. Sun Y, Chen TY, Worley SD, Sun G (2001) Novel refreshable N-halamine polymeric biocides containing imidazolidin-4-one derivatives. *J. Polym. Sci., Part A: Polym. Chem.* 39: 3073–3084.
16. Chen ZB, Sun YY (2005) N-chloro-hindered amines as multifunctional polymer additives. *Macromol.* 38: 8116–8119.
17. Sun G, Xu XJ, Bickett JR, Williams JF (2001) Durable and regenerable antibacterial finishing of fabrics with a new hydantoin derivative. *Ind. Eng. Chem. Res.* 40: 1016–1021.
18. Lin J, Winkelman C, Worley SD, Broughton RM, Williams JF (2001) Antimicrobial treatment of nylon. *J. Appl. Polym. Sci.* 81: 943–947.
19. Sun Y, Sun G (2002) Durable and regenerable antimicrobial textile materials prepared by a continuous grafting process. *J. Appl. Polym. Sci.* 84: 1592–1599.
20. Braun M, Sun YY (2004) Antimicrobial polymers containing melamine derivatives. I. Preparation and characterization of chloromelamine-based cellulose. *J. Polym. Sci. Part A-Polym. Chem.* 42: 3818–3827.
21. Lin J, Cammarata V, Worley SD (2001) Infrared characterization of biocidal nylon. *Polymer* 42: 7903–7906.
22. Cao ZB, Sun YY (2009) Polymeric N-Halamine latex emulsions for use in antimicrobial paints. *ACS Appl. Mat. Interface* 1: 494–504.
23. Ahmed AEI, Hay JN, Bushell ME, Wardell JN, Cavalli G (2008) Biocidal polymers (I): Preparation and biological activity of some novel biocidal polymers based on uramil and its azo-dyes. *React. Funct. Pol.* 68: 248–260.
24. Bruneaux J, Cachet H, Froment M, Messad A (1994) Structural, electrical and interfacial properties of sprayed SnO₂ Films. *Electrochim. Acta* 39: 1251–1257.
25. Connick RE, Chia YT (1959) The hydrolysis of chlorine and its variation with temperature. *J. Am. Chem. Soc.* 81: 1280–1284.
26. Ed, Bard, AJ, Parsons, R, Jordan, J, Dekker, A Standard potentials in aqueous solution. Marcel Dekker, New York, 1985, pp. 76–77.
27. Debiemme-Chouvy C, Haskouri S, Folcher G, Cachet H (2007) An original route to immobilize an organic biocide onto a transparent tin dioxide electrode. *Langmuir* 23: 3873–3879.
28. Bendedouch D, Chen SH (1983) Structure and Interparticle Interactions of Bovine Serum-Albumin in Solution Studied by Small-Angle Neutron-Scattering. *J. Phys. Chem.* 87: 1473–1477.
29. Sweryda-Krawiec B, Devaraj H, Jacob G, Hickman JJ (2004) A new interpretation of serum albumin surface passivation. *Langmuir* 20: 2054–2056.
30. Cachet H, Folcher G, Haskouri S, Tribollet B, Festy D (2004) Protection antisalissure, active et passive, d'un film transparent de dioxyde d'étain par voie électrochimique. *Mat. & Tech.* 7–8: 1–4.
31. Debiemme-Chouvy C, Haskouri S, Cachet H (2007) Study by XPS of the chlorination of proteins aggregated onto tin dioxide during electrochemical production of hypochlorous acid. *Appl. Surf. Sci.* 253: 5506–5510.
32. Debiemme-Chouvy C, Hua Y, Hui F, Duval JL, Cachet H (2011) Electrochemical treatments using tin oxide anode to prevent biofouling. *Electrochim. Acta* 56: 10364–10370.
33. Hirayama K, Akashi S, Furuya M, Fukuhara K (1990) Rapid confirmation and revision of the primary structure of bovine serum-albumin by Esims and Frit-Fab Lc Ms. *Biochem. Biophys. Res. Comm.* 173: 639–646.
34. Pattison DI, Davies MJ (2001) Absolute rate constants for the reaction of hypochlorous acid with protein side chains and peptide bonds. *Chem. Res. Toxicol.* 14: 1453–1464.

35. Pattison DI, Davies MJ (2004) Kinetic analysis of the reactions of hypobromous acid with protein components: Implications for cellular damage and use of 3-bromotyrosine as a marker of oxidative stress. *Biochem.* 43: 4799–4809.
36. Lindberg BJ, Hamrin K, Johansson G, Gelius U, Fahlman A, Nordling C, Siegbahn K (1970) Molecular spectroscopy by means of ESCA [electron spectroscopy for chemical analysis]. II. Sulfur compounds. Correlation of electron binding energy with structure. *Phys. Scr.* 1: 286–298.
37. Castner DG, Hinds K, Grainger DW (1996) X-ray photoelectron spectroscopy sulfur 2p study of organic thiol and disulfide binding interactions with gold surfaces. *Langmuir* 12: 5083–5086.
38. Schick GA, Sun ZQ (1994) Spectroscopic characterization of sulfonyl chloride immobilization on silica. *Langmuir* 10: 3105–3110.
39. Peskin AV, Winterbourn CC (2001) Kinetics of the reactions of hypochlorous acid and amino acid chloramines with thiols, methionine, and ascorbate. *Free Radic. Biol Med.* 30: 572–579.
40. Kettle AJ, Winterbourn CC (1994) Assays for the Chlorination Activity of Myeloperoxidase. *Methods Enzymol.* 502–512.
41. Sun XB, Cao ZB, Porteous N, Sun YY (2010) Amine, melamine, and amide n-halamines as antimicrobial additives for polymers. *Ind. Eng. Chem. Res.* 49: 11206–11213.
42. Hawkins CL, Pattison DI, Davies MJ (2003) *Amino Acids* 25: 259–263.
43. Senthilmohan R, Kettle AJ (2006) Bromination and chlorination reactions of myeloperoxidase at physiological concentrations of bromide and chloride. *Arch. Biochem. Biophys.* 445: 235–244.
44. Pattison DI, Davies MJ (2006) Reactions of myeloperoxidase-derived oxidants with biological substrates: Gaining chemical insight into human inflammatory diseases. *Curr. Med. Chem.* 13: 3271–3290.
45. Prutz WA (1998) Interactions of hypochlorous acid with pyrimidine nucleotides, and secondary reactions of chlorinated pyrimidines with GSH, NADH, and other substrates. *Arch. Biochem. Biophys.* 349: 183–191.
46. Pattison DI, Davies MJ (2005) Kinetic analysis of the role of histidine chloramines in hypochlorous acid mediated protein oxidation. *Biochem.* 44: 7378–7387.
47. Hawkins CL, Davies MJ (2005) The role of aromatic amino acid oxidation, protein unfolding, and aggregation in the hypobromous acid-induced inactivation of trypsin inhibitor and lysozyme. *Chem. Res. Toxicol.* 18: 1669–1677.
48. Winterbourn CC, Brennan SO (1997) Characterization of the oxidation products of the reaction between reduced glutathione and hypochlorous acid. *Biochem. J.* 326: 87–92.
49. Pullar JM, Vissers MCM, Winterbourn CC (2001) Glutathione oxidation by hypochlorous acid in endothelial cells produces glutathione sulfonamide as a major product but not glutathione disulfide. *J. Biological Chem.* 276: 22120–22125.
50. Fu XY, Mueller DM, Heinecke JW (2002) Generation of intramolecular and intermolecular sulfenamides, sulfnamides, and Sulfonamides by hypochlorous acid: A potential pathway for oxidative cross-linking of low-density lipoprotein by myeloperoxidase. *Biochem.* 41: 1293–1301.
51. Haskouri S, Cachet H, Duval JL, Debiemme-Chouvy C (2006) First evidence of the antibacterial property of SnO₂ surface electrochemically modified in the presence of bovine serum albumin and chloride ions. *Electrochem. Comm.* 8: 1115–1118.
52. Haskouri S. University Paris 7. (2006) Thesis.
53. Chen ZB, Luo J, Sun YY (2007) Biocidal efficacy, biofilm-controlling function, and controlled release effect of chloromelamine-based bioresponsive fibrous materials. *Biomaterials* 28: 1597–1609.
54. Gao Y, Cranston R (2008) Recent advances in antimicrobial treatments of textiles. *Textile Res. J.* 78: 60–72.
55. Liang J, Wu R, Huang TS, Worley SD (2005) Polymerization of a hydantoinylsiloxane on particles of silicon dioxide to produce a biocidal sand. *J. Appl. Polym. Sci.* 97: 1161–1166.

56. Liang J, Chen Y, Barnes K, Wu R, Worley SD, Huang TS (2006) N-halamine/quat siloxane copolymers for use in biocidal coatings. *Biomaterials* 27: 2495–2501.
57. Kocer HB, Akdag A, Ren XH, Broughton RM, Worley SD, Huang TS (2008) Effect of alkyl derivatization on several properties of N-Halamine antimicrobial siloxane coatings. *Ind. Eng. Chem. Res.* 47: 7558–7563.
58. Ahmed AESI, Hay JN, Bushell ME, Wardell JN, Cavalli G (2009) Optimizing halogenation conditions of N-Halamine polymers and investigating mode of bactericidal action. *J. Appl. Polym. Sci.* 113: 2404–2412.
59. Debiemme-Chouvy C, Unpublished results. Study of antibacterial properties of tin dioxide electrochemically modified in the presence of chlorides and proteins.

Section III
Applications of Nano-Antimicrobials

Chapter 11

Engineering Nanostructured Silver Coatings for Antimicrobial Applications

M. Pollini, F. Paladini, A. Licciulli, A. Maffezzoli, and A. Sannino

11.1 Introduction

The interest in nanotechnologies is growing worldwide thanks to the enormous number of publications devoted to the fundamental aspects of nanosciences. Physiology, industrial bioprocessing, biology and medicine represent just some examples of the areas for nanotechnology application [1, 2]. Compared with silver metal, silver nanoparticles are known for their higher antimicrobial activity, due to their high specific surface area [3] and the large surface to volume ratio [4], against a broad spectrum of bacteria and also against drug-resistant bacteria [5], fungi [6], and viruses [7–9]. The use of silver nanoparticles incorporated into various categories of consumer products, such as cosmetics, clothes, electronics, aerospace, textiles, and medicines, is growing thanks to the interesting and unique properties they confer to the product due to their nanometric size [10, 11]. This is a very important matter related to the emergence of an increased number of microbial organisms resistant to multiple antibiotics and the continuing emphasis on health care costs [12].

In hospital practice, the risk of infection associated with the use of indwelling medical devices is very high [13], and many cases of morbidity and mortality have been reported [14]. Microorganisms commonly attach to the surface of indwelling medical devices forming a biofilm [15, 16] that is, by definition, an accumulation of microorganisms and of their extracellular products forming a structured community highly resistant to antimicrobial treatment and tenaciously bound to the surface [17]. Many strategies have been employed to reduce this problem, among them one

M. Pollini (✉) • A. Licciulli • A. Sannino
Department of Engineering for Innovation, University of Salento, Lecce, Italy

Department of Engineering for Innovation, Silverttech Ltd, Lecce, Italy
e-mail: mauro.pollini@unisalento.it; alessandro.sannino@unisalento.it

F. Paladini • A. Maffezzoli
Department of Engineering for Innovation, University of Salento, Lecce, Italy

approach for prevention is the use of antimicrobials which can be incorporated into, or used to coat, medical polymeric devices like catheters [18]. Heparin coatings on catheters and stents [19, 20], the use of chlorhexidine and silver sulfadiazine coatings [21] and also the use of silver nanoparticles have been demonstrated to be efficacious against bacterial proliferation [22, 23]. As shown in Fig. 11.1, many uses of silver and silver nanoparticles can be applied in medicine. Silver can be used to stop epistaxis and post-traumatic granulomas, to improve skin regeneration and for its antibacterial and anti-inflammatory effects. The use of silver nanoparticles in medicine is related to their prophylactic environmental and antibacterial effect in bone cement and implants, for venous catheters and neurosurgical shunts [24].

In hospitals, in addition to the treatment of medical devices, silver represents a promising instrument for advanced textile for wound dressing [24–26], antiseptic bandages [27], for hospital gowns, flax and for surgical masks, in particular when the replacement cannot always be done immediately [28], in order to prevent infections and generation of bad odors. Textiles, in fact, can easily become carriers of fungi and bacteria [29], so the use of silver can also be helpful in treatment of skin diseases [30] and to ensure a major degree of hygiene and daily welfare. Silver treatment can be applied according to two different methods: the first is the insertion of silver nanoparticles as host inside the textile matrix [31], while in the second silver is applied as a coating on the material [32].

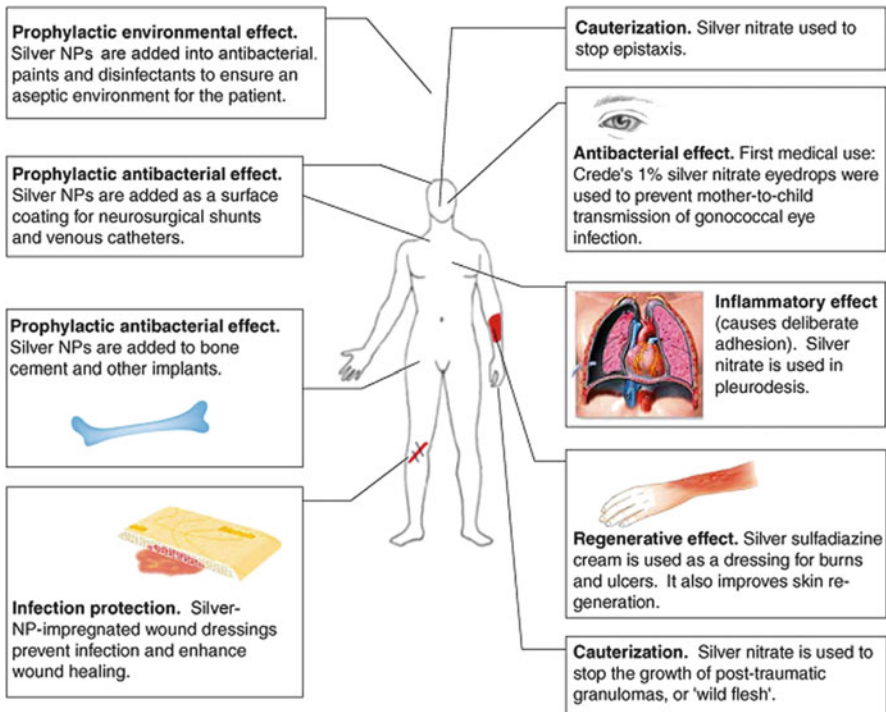


Fig. 11.1 Uses of silver (*right*) and silver nanoparticles (*left*) in medicine (Adapted from [24])

The innovative technology presented in this paper is a surface engineering process, an interesting alternative to more expensive ways of silver deposition and a very effective technique to treat many different types of substrates. Three case studies will be explored, that is textile, temporary medical devices and artificial leather. For each type of substrate, the method of silver deposition chosen for the specific application will be explored and the characterization of samples will be discussed.

11.2 Past and Present Uses of Antimicrobial Silver

The antimicrobial spectrum of silver is exceptionally broad against fungi [6], viruses [7–9] and bacteria [5]. Panacek et al. demonstrated the antifungal activity of silver nanoparticles against pathogenic *Candida* [6]; Lu et al. hypothesized that the direct interaction between silver nanoparticles and Hepatitis B virus double-stranded DNA or viral particles is responsible for their antiviral mechanism [8]; a study carried out by Feng et al. on *Escherichia coli* and *Staphylococcus aureus* suggested that morphological and structural changes in bacterial cells, the formation of small electron-dense granules around the cell wall and the inactivation of bacterial proteins occur after addition of Ag^+ . DNA loses its replication ability once the bacteria have been treated with silver ions [24, 33]. Figure 11.2 summarizes

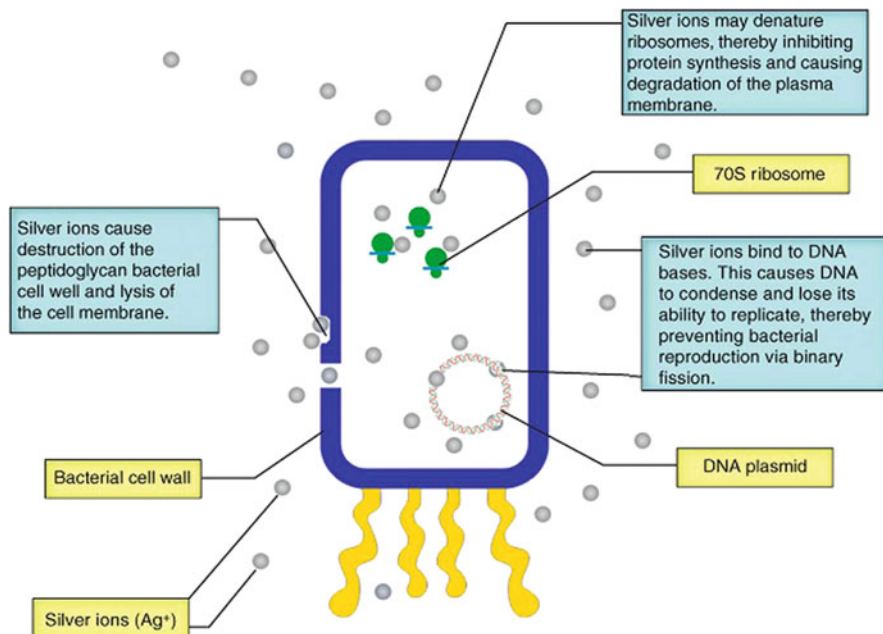


Fig. 11.2 Mechanisms of the antibacterial activity of silver ions (Adapted from [24])

some possible mechanisms of action of silver ions in a schematic bacterial cell, like the interactions of silver ions with peptidoglycan cell wall, plasma membrane, bacterial (cytoplasmic) DNA, and bacterial proteins [24].

Silver and its antimicrobial properties are known since antiquity. Herodotus, the Greek philosopher and historian, described the use of silver for water purification; Pliny the Elder, the famous Roman physician, reported the properties of silver in 79 AD in his encyclopedia *Natural History* in which he wrote that silver was extremely effective in causing wounds to close [34]; Hippocrates, the father of modern medicine, believed silver powders to have a beneficial healing effect for ulcers [35].

Since the nineteenth century, many studies have been carried out and many applications of silver have been employed in different fields of medical research [36]. In 1884, in Germany, Carl Siegmund Franz Credé introduced an eye prophylaxis to prevent ocular infection by using silver nitrate solution on neonates [25]. In the 1920s, colloidal silver was accepted by the US Food and Drug Administration (FDA) as being effective for wound management [37] and through the first half of the twentieth century it was used in controlling infection in burn wounds [25]. In the 1940s, penicillin was introduced as a healing method and antibiotics became the standard treatment for bacterial infections, so the use of silver diminished [37, 38]. The resistance of pathogenic bacteria to many antibiotics and the growing interest in nanotechnologies and nano-sized materials have led to many technological advances of nano-sized silver and to the development of many applications, such as coatings for medical devices, silver dressings, silver coatings on textile fabrics [36, 39], water sanitization [40] and so on. Today, also NASA uses silver to purify drink water in space flights [25].

11.3 Review of Nanosilver Coating Deposition Methods and Properties

Many procedures have been developed for the synthesis of Ag nanoparticles (NPs) [41] and several methods have been described in order to obtain thin silver coatings. The biological activity and the interaction of silver nanoparticles with bacteria depend on their size [22] and shape [42]. Morones et al. studied the interaction of silver nanoparticles with different types of Gram-negative bacteria. Their results demonstrated the dependence of the antibacterial capability both on concentration of particles and on their size [22]. Pal et al. investigated the antibacterial capability of silver nanoparticles synthesized in different shapes (truncated triangular, spherical, rods) against *Escherichia coli*. They demonstrated that the reactivity of silver particles changes as a function of their shapes, probably due to the really effective surface area in terms of active facets [42]. The results of their research are shown in Figs. 11.3 and 11.4. Images obtained by energy-filtering transmission electron microscopy (EFTEM) of silver NPs with different shapes are shown in Fig. 11.3.

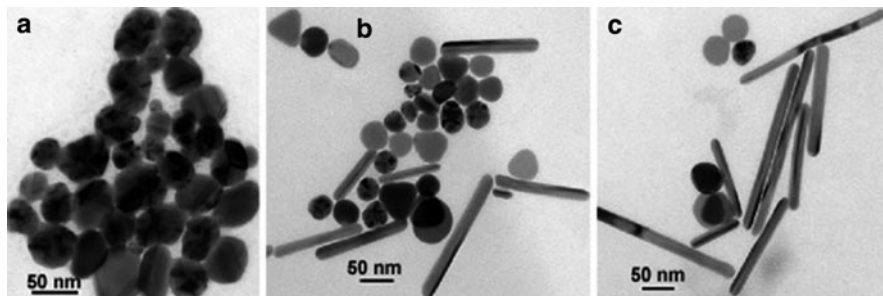


Fig. 11.3 EFTEM images of silver nanoparticles. (a) Spherical nanoparticles synthesized by citrate reduction. (b) Silver nanoparticles of different shapes. (c) Purified rod-shaped nanoparticles (From [42])

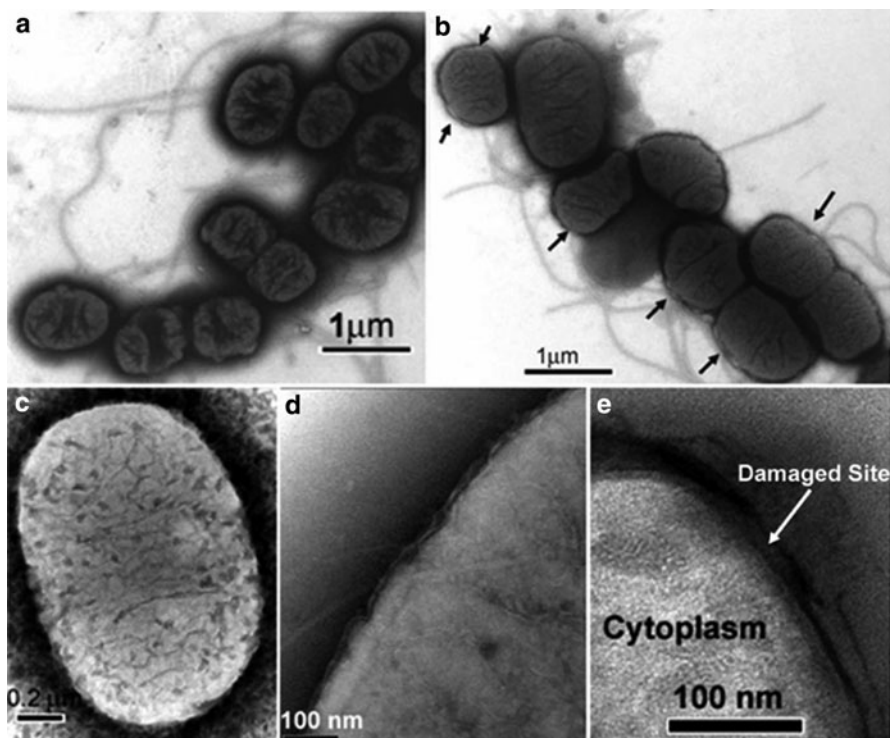


Fig. 11.4 EFTEM images of *E. coli* cells. (a) Untreated *E. coli*. (b) *E. coli* grown on agar plates supplemented with AgNO_3 . (c) *E. coli* treated with triangular silver nanoplates. (d) *E. coli* treated with spherical silver nanoparticles. (e) Enlarged image of part of the bacterial cell membrane treated with triangular silver nanoparticles (Adapted from [42])

The effect obtained against a bacterial cell of *Escherichia coli* after treatments with AgNO_3 , triangular and spherical silver nanoparticles are shown in Fig. 11.4, where both the partial (Fig. 11.4b) and multiple (Fig. 11.4e) damages on bacterial membrane

and also the presence of dark irregular pits on the cell surface are visible, compared with untreated *E. coli*.

Nanostructured materials incorporated into larger mesoscopic and macroscopic systems and the enhancing of coating functionality and coating process represent a crucial key in the success of nanotechnology in many different applications [43]. Surface modification is very effective in the interactions with biological systems. A relevant strategy widely used in biomedical research consists in modifying the material surface by plasma treatment, such as plasma etching, plasma deposition, plasma polymerization and so on, in order to modify material surfaces without altering bulk properties of the material [44]. Plasma processes can also be combined with colloidal lithography, a patterning technique used to texture surfaces with nanofeatures and some recent research on plasma-aided micro- and nanostructuring processes for biomedical applications have been reported by Sardella et al. [45]. Gomathi et al. provided an overview of recent advances in biomedical applications of plasma surface-modified polymers [46]. Korner et al. described the combination of deposition of plasma polymer coatings with embedded Ag nanoparticles and the sputtering of Ag atoms from an Ag target, with incorporation of Ag nanoparticles in the growing polymer matrix [47]. The deposition of plasma coatings using combined deposition/etching/sputtering processes enabled the formation of multifunctional surfaces [48].

Among techniques for the deposition of silver coatings, the use of magnetron sputtering combined with atom beam source has been demonstrated to be effective for coatings on thermally sensitive polymeric substrates [49]. Magnetron sputtering, already tried on substrates like SiO₂, polypropylene and nonwoven fabrics to fix Ag nanoparticles has also been used by Mejía et al. to produce cotton–Ag composites [50]. Nanostructured silver films were deposited at room temperature on polypropylene non-woven by radio frequency magnetron sputter coating to obtain the antibacterial properties. The relationship between sputter parameters and antibacterial properties were investigated by Wang [51, 52]. He found that both the antibacterial capability and the grain size depend on the deposition time, while no effect of sputtering power and argon pressure have been discovered during his experiments.

Another method for textile modification is the sol–gel technique for preparing bioactive materials for biomedical applications [53]. Antimicrobial coatings for textile based on silver-containing silica have been developed by Mahltig et al. The release of biocides from these coatings and the biocidal effect can be controlled by modifying the content of the biocide in the silica sol [54]. An alternative method to constrain silver in nanodimensions reported in the literature is the loading of zeolite with silver ions [55].

In addition to the most commonly applied dip-coating methods, sonochemical coating using ultrasound irradiation as well as the sputter deposition of Ag NPs onto textile surfaces were performed [44]. The sonochemical irradiation of wool fibers in an aqueous solution of silver nitrate containing ethylene glycol under a reducing atmosphere of an argon/hydrogen gas mixture resulted in the coating of the neat wool fibers with silver nanoparticles [56]. Perelshtein et al. have described

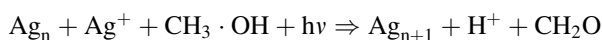
a process carried out by ultrasound radiation in a one-step reaction procedure to obtain nylon, polyester and cotton with antibacterial properties [57]. The chemical reduction method involves the reduction of AgNO_3 by a reducing agent in the presence of a suitable stabilizer, which is necessary in protecting the growth of silver particles through aggregation. In the formation of silver nanoparticles by the chemical reduction method, the size and aggregation of silver nanoparticles are affected by various parameters, such as initial AgNO_3 concentrations, reducing agent/ AgNO_3 molar ratios, and stabilizer concentrations [58]. Nair and Laurencin provided an overview about the synthesis of silver nanoparticles by the reduction of a silver salt and their stabilization, both in solution and on surfaces, with particular attention to biomedical applications [59].

Microwave irradiation [60], electrochemical synthesis [61] and photo-reduction [62] have also been proposed to obtain silver nanoparticles.

11.4 In Situ Photoreduction and Deposition of Silver Metal Clusters

The researchers of University of Salento (Lecce, Italy) have developed, and patented in 2004, a new technique based on the photo-reduction of silver ions in the form of nanoparticles directly on the substrate [63]. A spin-off company, Silvertch Ltd, has been started in 2008 to promote the technology transfer. The technique is suitable for many different substrates, natural or synthetic, from textile to medical devices, making them antibacterial with a very cheap process. The antibacterial treatment of the substrate is obtained by impregnating natural or synthetic substrates with an alcoholic solution, a photo-reducing agent and a silver salt, and afterwards by exposing them to UV rays until the silver ions are reduced to metal silver. Methanol is not only the solvent but also the reducing agent that activates the photo-reduction process on the surface. The amount of methanol used for this purpose is strictly related to the amount of silver used for the treatment. The solution can be prepared also using different solvents such as water or ethanol. The only requirement is that the molar ratio methanol/silver nitrate is more than one. The effect of the in situ reduction of silver ions consists of a strong antibacterial coating made of neat silver clusters. Silver nanoparticles do not form inside the solution after the mixing of precursor and solvent; they form as a consequence of UV exposure directly on the substrate to which they bond strongly, independently of the nature of the substrates and of the way of deposition.

The photochemical reaction on which the process is based is the following:



In order to obtain information about the size of silver nanoparticles and about the lattice parameters of silver, transmission electron microscopy, TEM, has been

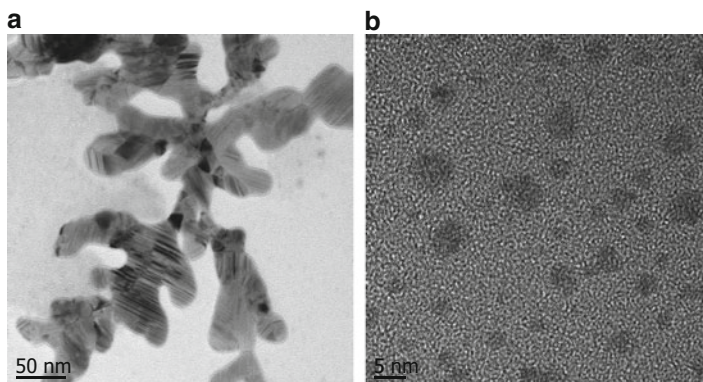


Fig. 11.5 TEM images obtained from silver solution deposited on carbon-covered copper grid, showing an extensive crystal structure (a) and a good distribution of small nanoparticles (b)

performed. Images obtained by TEM analysis of coatings made of a solution of silver salt and alcohol deposited onto a carbon-covered copper grid are reported in Fig. 11.5. They show the presence of both extensive crystal structures and very small silver particles with a size of about 2–3 nm; the identified lattice parameters (lattice fringes of 2.36 Å) correspond to metallic silver and in particular to atomic planes {111}.

According to the specific application to which the substrate is destined, it is possible to modify the composition of the silver solution and the mechanism of deposition, according to costs and to the degree of antibacterial effect to be achieved. For example, silver-coated textiles for daily use realized to improve the degree of hygiene and for personal care do not require a very high degree of antimicrobial activity; silver-coated medical devices instead need a very high antibacterial capacity to reduce the risk of infections.

In this chapter, some examples of applications joined by the common needs of hygiene and control of the bacterial proliferation and the results obtained by the characterization of the treated substrates will be shown and discussed. The application fields of Silvertex technology chosen to be exposed as case studies are textiles, temporary medical devices and artificial leather.

11.4.1 Silver Deposition on Fibers and Textile

The deposition of silver on textile fibers and fabrics represents a very interesting way to confer antibacterial properties to textile materials that can be used in fields of application that require a high degree of hygiene and the control of bacterial proliferation. For example, the introduction of silver in hospital textiles, such as cotton or flax used for sheets of patients or gowns for nurses and doctors, can represent an effective instrument to contain the diffusion of diseases. In addition,

there are many other applications of silver-treated textiles in the sector of daily comfort. Textile with antimicrobial properties used for the production of common knitwear or underwear can guarantee to customers a major welfare benefit by reducing unpleasant odors caused by bacterial proliferation in corporeal areas most exposed to perspiration. Cotton textile was selected for silver deposition because it is a substrate suitable both for medical field and common clothing. Cotton is made up of many short fibers (1–3 cm) with flattened and irregular sections. Their extension and contraction occurring by the absorption of humidity can irritate the skin [64] and an excellent environment for microorganisms to grow can develop owing to their ability to retain moisture [65]. Colonization of several types of bacteria, especially *Staphylococcus aureus*, represents the most common complication in patients affected by atopic dermatitis (AD) [66], a chronic disease of pruritus and eczematous lesions [67]. In the treatment of AD, various solutions have been tried, among them antibacterial drugs or topical steroids, or the use of special textiles with the antimicrobial capability to contain bacterial colonization [68]. Daeschlein et al. investigated in patients affected by AD the bacterial contamination in textiles containing silver versus placebo and in particular the effect of silver textiles on *S. aureus* and total bacteria colonizing the skin of AD patients. The obtained data were in agreement with those of Gauger et al. [69], who found a significant decrease in *S. aureus* on the skin of AD patients when they wore a silver textile [70].

Various methods, depending on the particular active agent and fiber type, have been developed to confer antimicrobial activity to textiles. For synthetic fibers, the antimicrobial active agents can be incorporated into the polymer prior to extrusion or blended into the fibers during their formation [71] and during the melt spinning. There are numerous ways by which antimicrobial properties can be accomplished in textiles: incorporation of volatile and non-volatile antimicrobial agents directly into fibers, coating or adsorbing antimicrobials onto fiber surfaces, immobilization of antimicrobials to fibers by ion or covalent linkages, and the use of fibers that are inherently antimicrobial [72]. To produce commercial silver-coated nylon fabrics, 12% by weight of silver is added during manufacturing by an electroless plating process [73], while the antimicrobial capability of nylon substrates coated with metallic silver has been checked against *Pseudomonas aeruginosa*, *Staphylococcus aureus* and *Candida albicans* [74].

Silvertech technology, cheap and effective because it implies the treatment of only the surface of the material, has been adopted both for synthetic yarn and natural yarn [32]. Different deposition methods, like impregnation, dipping or spraying, related to the nature of the substrate and the amount of silver solution required have been developed. As provided by the technology, after the deposition of the solution on the substrate, the UV irradiation occurs with consequent synthesis of silver nanoparticles firmly bonded to the substrate, so the wet yarns are exposed to strong lamps in special containers for this treatment. Here, mild reducing conditions are applied for the treatment of cotton, all involving a silver salt and a reducing agent. In some cases, fiber pretreatment after improved silver adhesion is also proposed. The comparison between a silver-treated textile substrate and an

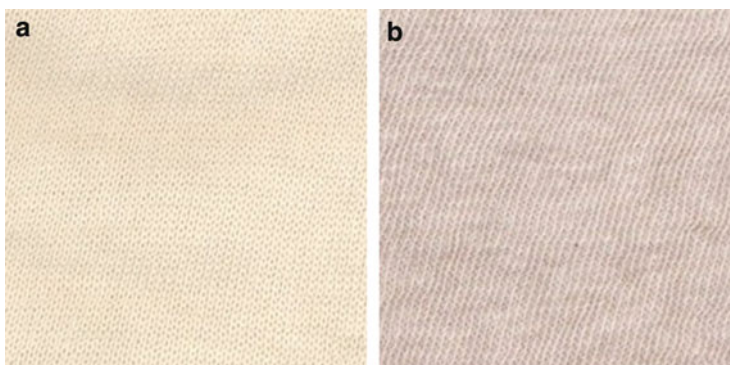


Fig. 11.6 Visual comparison of untreated cotton (a) and silver-treated cotton (b)

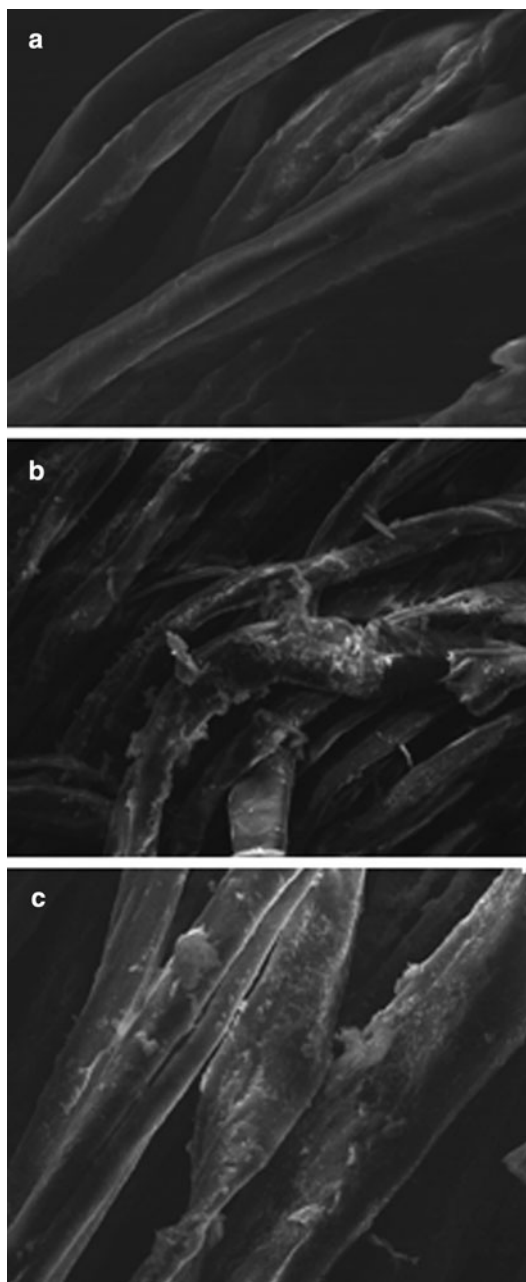
untreated one is shown in Fig. 11.6, in which the turning brown color of the treated sample due to the presence of silver nanoparticles is clearly visible.

The method of deposition chosen to deposit silver on textile was nebulization. As explained above, all samples have been washed before testing in order to remove unreacted silver salt. In textile, furthermore, this is not the only reason. In fact, it is necessary to ensure the presence of silver also after many washings, to check that silver nanoparticles exert their benefits for a very long time despite the user conditions. For this purpose, samples of cotton have been subjected to washing up to 20 times and they have been tested before and after washings with respect both to microscopy and the antibacterial activity. Images obtained by scanning electron microscopy (SEM) are shown in Fig. 11.7. The presence of nanometric particles on the surface of the treated sample that are not present on the untreated sample is clearly visible. The treated sample reveals a quite uniform distribution of silver on the surface and the very small size of the particles that sometimes aggregate in clusters of larger dimensions, even after 20 industrial washings.

The antibacterial activity of silver-treated cotton was checked before and after washings according to standard 'SNV 195920-1992', which is an agar diffusion test that relates the antibacterial capability to the dimension of the bacterial inhibition zone around the treated samples. The results of the Agar diffusion tests are shown in Fig. 11.8, in which the differences between the untreated sample and the silver-treated one are clearly visible. It is possible to assert that there are no great differences between the unwashed treated sample and the washed treated one because the bacterial inhibition growth area is very similar in the two cases. This confirms that washings do not reduce the benefits induced by treatment thanks to the very firmly bonded silver coating.

Another confirmation of this matter lies in the quantitative study of the amount of silver on the surface of the sample, carried out by thermogravimetric analysis (TGA) on unwashed and washed silver-treated samples. TGA is a testing that records the change in the weight of the sample as a function of the increasing

Fig. 11.7 SEM images obtained from untreated cotton fibers (a), silver-treated cotton fibers (b) and silver-treated cotton fibers after 20 industrial washings (c)



temperature. The comparison between the TGA data of an untreated sample and a silver-treated sample leads to the quantification of silver as the incombustible solid residue at 900°C, the temperature to which all the substrate has burnt. These

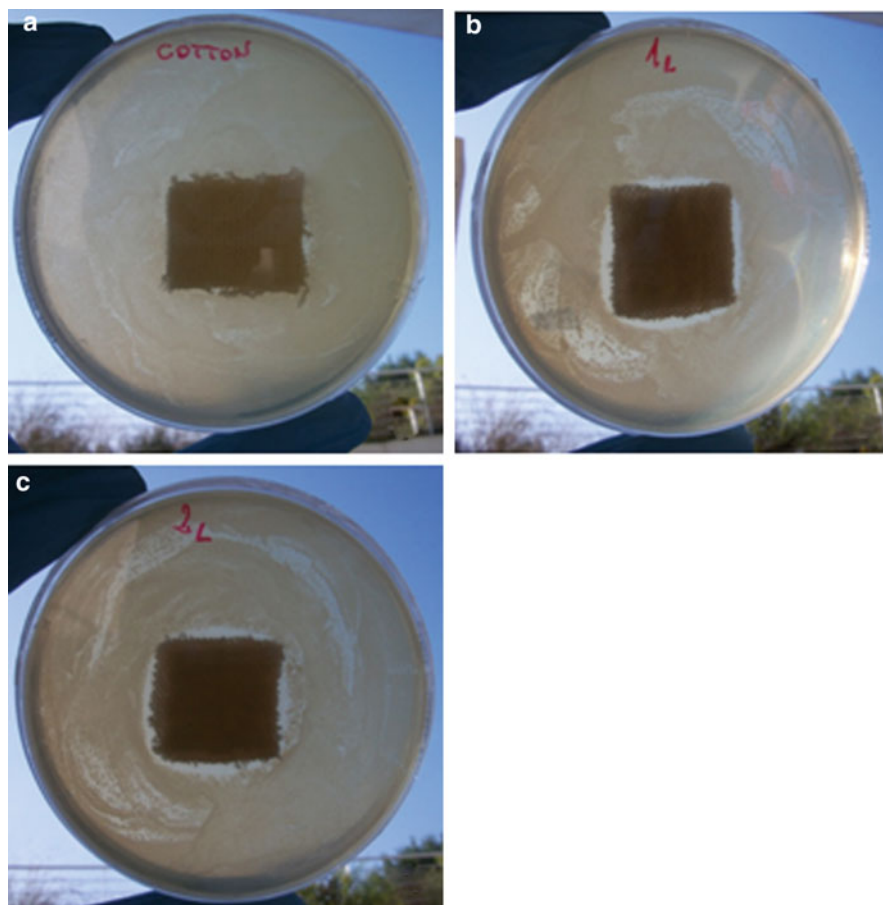


Fig. 11.8 Test of *Escherichia coli* growth on the sample of silver-treated cotton before washings (b) and after washings (c) in comparison with the untreated one (a)

results are shown in Table 11.1, in which the calculated amount of silver is reported for each substrate used in the case studies. The results have not revealed any significant differences between washed and unwashed cotton samples, being 2.72 wt% the amount of silver for the unwashed sample and 2.42 wt% for the sample washed 20 times. That means that washings do not remove silver nanoparticles from the substrate.

11.4.2 Silver Deposition on Catheters

The risk of infections associated with the use of indwelling medical devices is very high. In particular, bloodstream infections deriving from catheterization are

Table 11.1 Data collected by TGA analysis reporting the amount of silver for each type of silver-treated substrate

Substrate	Silver content (wt%)
Untreated cotton yarn	–
Silver-treated cotton yarn	2.72
Silver-treated cotton yarn after 20 washings	2.42
Untreated catheter	–
Silver-treated catheter	0.51
Untreated synthetic leather	–
Silver-treated synthetic leather	3.08

reported as one of the major cause of morbidity and mortality in hospitalized patients [75]. This happens because of the formation of bacterial biofilm growing on the surface of the device with consequent proliferation of infection [76]. So, it is very important to avoid the growth of bacteria on the surface of the device. For this purpose many strategies have been employed to reduce dialysis catheter-related infections, such as the impregnation in antibiotic and antiseptics, or the use of substances containing silver [77].

Biological responses to polymeric materials depend basically on surface chemistry and structure. So the surface modification of biomaterials is carried out to retain the key physical properties with modification of the outermost surface to influence bio-interaction. The surface modification techniques include physical/chemical methods, such as physical deposition of coatings, grafting or chemical modification, and biological methods, such as protein adsorption or immobilization of biomolecules [78]. A technology developed at the University of Erlangen provides for the impregnation of the entire catheter with a distribution of billions of silver nanoparticles (0.8–1.5 wt%) in the catheter matrix (polyurethane, silicone) on a carrier, preferably barium sulphate [40, 79].

The silver nanoparticles distributed on the carrier surfaces can be dispersed in a polymer matrix by thermoplastic processing [80]. Serghini-Monim et al. reported the results of adsorption of a silver complex on plasma-modified polyurethane surface performed to confer antibacterial properties to catheters. The purpose of the plasma modification treatment was to increase the concentration of adsorption sites for a chemical vapor deposition (CVD) reaction and to increase the surface biomedical compatibility through the incorporation of amine groups to mimic amino acids [81].

The method of silver deposition developed by Silvertex and the University of Salento for these medical devices consists of the treatment of the inner and outer surface of the catheter because it is subjected to the risk of contamination on both sides. Temporary double lumen polyurethane “Carbothane” catheters 30 cm long and with an outer diameter of 4 mm were coated. They penetrate into the jugular vein with a length of 10–15 cm and remain in contact with the blood stream inside and outside the lumina for about 30 days for acute dialysis and blood filtration. To ensure a good deposition of silver coating on the polymeric surface of catheters, the method of deposition chosen for this particular purpose is the dipping of the

device into the silver solution, made for this application only by silver salt and alcohol. The reason for these choices, about the deposition technique and the composition of the solution, derives from visual considerations about the color. That must be more uniform as possible in the final product. The treatment in this case consists of dipping the catheters in the silver solution followed by UV irradiation in a special box containing strong UV lamps. In order to ensure the treatment of the internal surface of the catheter, after dipping the catheters, the solution is forced by a syringe to flow inside the device and then it is expelled. The result after silver treatment is shown in Fig. 11.9 and, like the previous example of substrate, the polyurethane substrate also shows the typical browning due to the presence of silver on the surface.

After the silver deposition and an initial vigorous wash, scanning electron microscopy was carried on in order to verify the occurred photo-reduction of the salt and the uniformity of the coating on this type of substrate. SEM images are reported in Fig. 11.10 for the treated catheter, on the outer and inner surfaces, and for an untreated one. Due to the presence of small white inclusions in the untreated sample, an EDX analysis was combined with the SEM analysis in order to identify which particles were definitely silver. EDX has revealed the presence of elements belonging to the substrate and of barium, as expected, which is added in form of barium sulfate into the polymeric matrix to make it radio-opaque.

The amount of silver identified by EDS analysis on the treated catheter is slightly different between the internal and the external surface. The values obtained are 0.54 and 0.51 wt%, respectively for the external and the internal surface of the device. The reason for this result is the different superficial roughness of the polyurethane and the major difficulty of the UV irradiation to reach the internal surface of the catheter. This hypothesis is confirmed by SEM images in which a good coverage of the polyurethane surface and a quite good distribution of small particles are visible on the external surface, compared with the smaller coverage of the internal surface. As expected, no silver traces were revealed in the untreated sample by EDX.



Fig. 11.9 Visual comparison of untreated catheter (a) and silver-treated catheter (b)

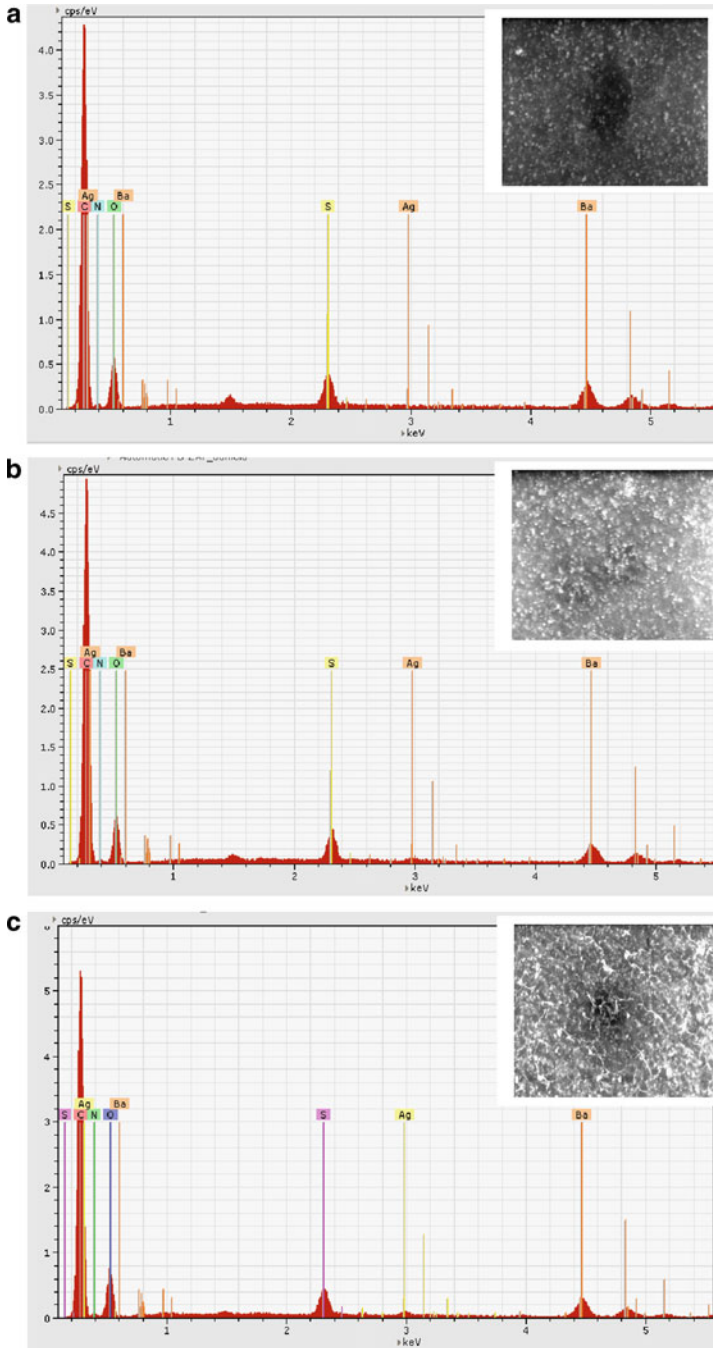


Fig. 11.10 SEM-EDX analysis on an untreated catheter (a) and a silver-treated catheter, on outer (b) and inner surfaces (c)

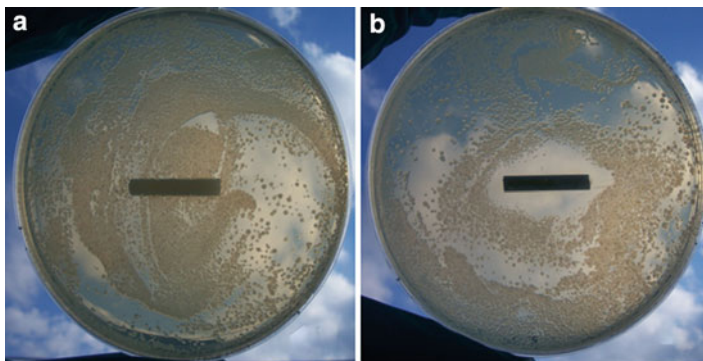


Fig. 11.11 Test of *Escherichia coli* growth on the silver-treated catheter (b) in comparison with the untreated one (a)

The antibacterial activity of silver-coated catheters was confirmed by an Agar diffusion test and a great inhibition zone to bacterial proliferation was observed, as shown in Fig. 11.11.

For this specific application, a strong antibacterial activity is required, so it is important to obtain a good compromise between the antibacterial capability and the amount of silver used for the treatment. The results of antibacterial test carried out on *E. coli* confirm that the small amount of silver used for the deposition is enough to ensure the inhibition of bacterial growth.

In order to evaluate the amount of silver, thermogravimetric analysis was also carried out and the data obtained are reported in Table 11.1. The value obtained is similar to the percentage of silver obtained by EDS and, in particular, it is 0.51 wt% for the treated catheter.

11.4.3 Silver Deposition on Leather Substrates

Public places and the public transport system represent an important field for the application of antibacterial technologies. The high number of users of trains, buses or taxis cannot guarantee a good degree of hygiene and welfare, causing allergies, dermatitis or skin irritation due to the proliferation of bacteria inside chairs or carpets. For this purpose, antibacterial coatings based on deposition of silver nanoparticles could represent an interesting solution to reduce such unpleasant consequences.

Substrates for public transport treated with Silvertch technology can be natural, such as the leather of chairs in trains and cars, and synthetic, such as polyurethane substrates for bus seats. For this work, synthetic substrates have been chosen and the adopted deposition process provides a roll coating in order to coat plain substrates of material more uniformly as possible. Moreover, this method makes

it possible to treat just one side of the sample, that is the one in direct contact with people, with consequent reduction in costs. Synthetic leather simulates the microstructure of natural leather because the superfine fiber is similar to the fineness and structure of the fibril. The natural leather has a stereoscopic structure with the continuously changing degree of fiber cross-linking. The synthetic leather has a three-dimensional structure of superfine fiber non-wovens and microporous polyurethane. The uniform braiding structure of the synthetic leather is its advantage, but it is restricted technically by the lack of a grain layer. The chemical composition of the silver solution used for this application is made of a small percentage of silver salt dissolved in a mixture of water and alcohol. It is enough to be effective against bacteria and cheap at the same time. The amount of alcohol in the solution has to be directly proportional to the amount of silver salt, because alcohol represents the reducing agent that activates the photo-reduction, so the presence of at least a minimum percentage of it is necessary to guarantee the synthesis of the silver nanoparticles on the treated surface. The capacity to absorb the solution depends on the porosity of the substrates and, hence, changes of the colors of substrates also depends on it, being related to the amount of solution used for the treatment. Figure 11.12 shows images of a silver-treated sample and an untreated one, in which the difference in colors between them is not so great, due to the small amount of silver used for the deposition and to the nature of the substrate.

As for catheters, SEM analysis of synthetic leather has also revealed the presence of many inclusions on the surface of the sample, so EDS analysis was carried out during the scanning electron microscopy session in order to identify silver particles. The SEM images in Fig. 11.13 of the treated sample, carried at the low magnification of $\times 500$, show a great porosity of the substrate and pores with different sizes and depths that influence the distribution of the coating. Some particles are visible on the side walls of pores and some larger aggregates are visible on the surface of the sample. The greater aggregates are not identified as silver, but they are more likely due to inclusions of other elements inside the synthetic leather, probably derived from the processing of the material.

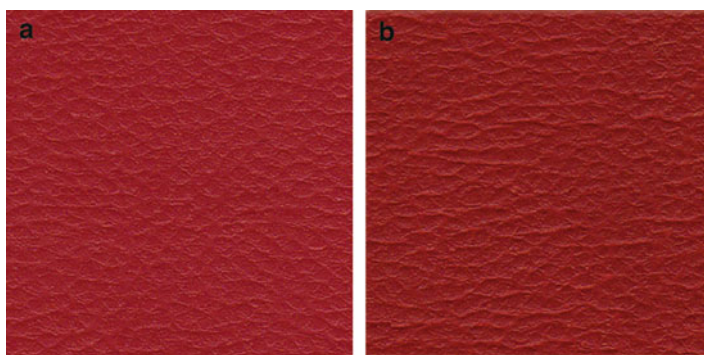


Fig. 11.12 Visual comparison of untreated synthetic leather (a) and a silver-treated one (b)

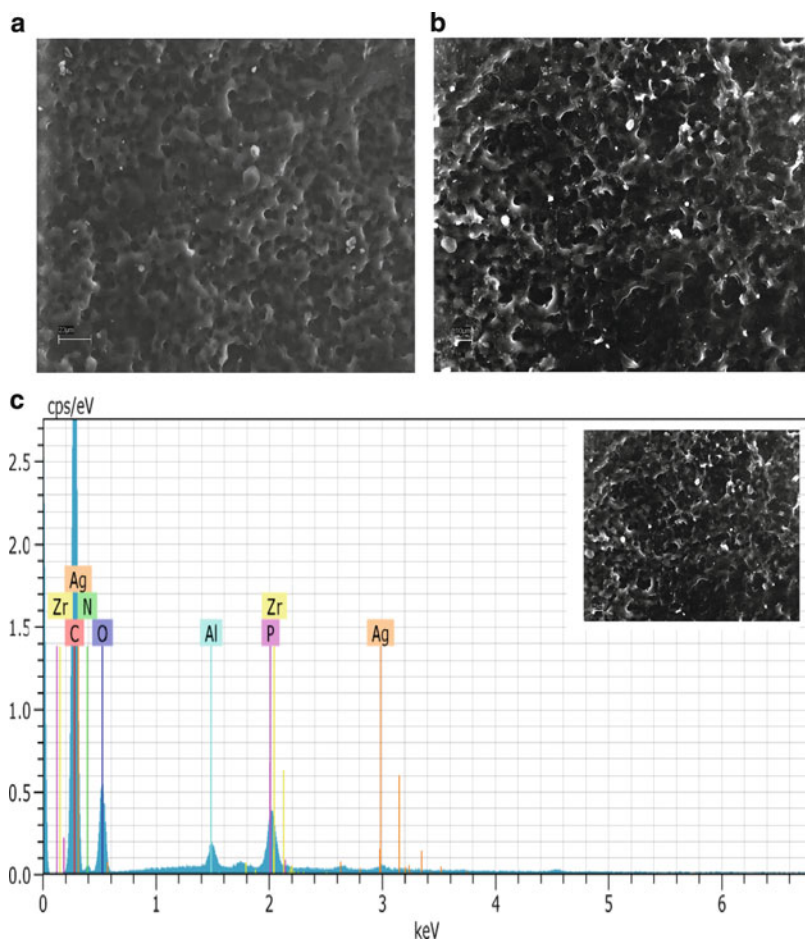


Fig. 11.13 SEM images on synthetic leather on an untreated sample (a) and on a silver-treated one (b) at low magnification and SEM-EDS analysis on a silver-treated sample (c)

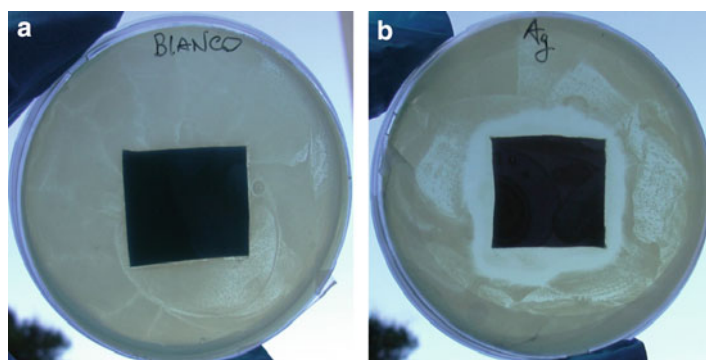


Fig. 11.14 Test of *Escherichia coli* growth on the sample of silver-treated synthetic leather (b) in comparison with the untreated one (a)

The antibacterial capability of silver-treated artificial leather was checked against *Escherichia coli* and the results are shown in Fig. 11.14. It was confirmed that silver particles on the surface reduce the bacterial growth on the sample, as visible from the comparison of the dimension of the bacterial growth inhibition area between the untreated sample and the silver-treated sample.

For this specific application of Silvertech technology, it is very important to satisfy both the antibacterial capability of the material and the necessity to limit costs. In fact, these substrates are intended to be used for a large number of external coverings for seats and chairs in public places, so the amount of silver has to be reduced in order to avoid increasing costs and ensuring at the same time a good reduction of bacterial proliferation. The amount of silver used in this example satisfies both the requirements. It has been calculated by thermogravimetric analysis, and the experimental data, reported in Table 11.1, show a percentage of silver corresponding to 3.08 wt%.

11.5 Conclusions and Future Trends

In this chapter, various properties and applications of antibacterial silver coatings have been reviewed.

In particular, an innovative and cheap technique to obtain antibacterial silver nanoparticles in situ developed in the University of Salento (Lecce, Southern Italy) has been described and discussed. The technology, suitable for many different types of substrates, consists of the photo-reduction of a silver salt in the presence of a reducing agent by UV illumination occurring directly on the substrate. According to the specific application of the substrate, the chemical composition of the silver solution (percentages of silver salt, alcohol, and water) and the method of depositing it on the material can be chosen in order to obtain the required antibacterial capability.

Three applications have been described in detail: antimicrobial textile, temporary implantable devices and artificial leather. For each of them, the silver deposition treatment and the experimental results obtained by the characterization of the treated substrates have been demonstrated. Despite the different natures of the treated substrates, it is possible to assert that the degree of coverage is good enough for each case and that there is a good distribution of silver nanoparticles on the materials. The small percentages of silver used for the treatment are enough to ensure a good antibacterial capability, as shown by the results of antibacterial tests carried out against *Escherichia coli*.

Experimental data revealed in this paper derive from many extensive studies carried out in applications in which this silver deposition technology can be considered ready for an industrial scale-up. One can expect that many other fields will be explored in order to extend the use of silver as an antimicrobial agent and to use it to improve health and welfare.

References

1. Silva GA (2004) Introduction to nanotechnology and its applications to medicine. *Surg Neurol* 61:216–220. doi:[10.1016/j.surneu.2003.09.036](https://doi.org/10.1016/j.surneu.2003.09.036)
2. Roco MC (2003) Nanotechnology: convergence with modern biology and medicine. *Curr Opin Biotechnol* 14:337–346. doi:[10.1016/S0958-1669\(03\)00068-5](https://doi.org/10.1016/S0958-1669(03)00068-5)
3. Shahverdi AR, Fakhimi A, Shahverdi HR, Minaian S (2007) Synthesis and effect of silver nanoparticles on the antibacterial activity of different antibiotics against *Staphylococcus aureus* and *Escherichia coli*. *Nanomed Nanotechnol Biol Med* 3:168–171. doi:[10.1016/j.nano.2007.02.001](https://doi.org/10.1016/j.nano.2007.02.001)
4. Guzmán MG, Dille J, Godet S (2008) Synthesis of silver nanoparticles by chemical reduction method and their antibacterial activity. *World Acad Sci Eng Technol* 43:357–364. <http://www.omnis-mg.hr/Radovi/4bak-4siz-peru.pdf>
5. Lara HH, Ayala-Nunez NV, Ixtapan Turrent LC, Rodríguez Padilla C (2010) Bactericidal effect of silver nanoparticles against multidrug-resistant bacteria. *World J Microbiol Biotechnol* 26:615–621. doi: [10.1007/s11274-009-0211-3](https://doi.org/10.1007/s11274-009-0211-3)
6. Panacek A, Kolar M, Vecerova R, Prucek R, Soukupova J, Krystof V, Hamal P, Zboril R, Kvizek L (2009) Antifungal activity of silver nanoparticles against *Candida* spp. *Biomaterials* 30:6333–6340. doi:[10.1016/j.biomaterials.2009.07.065](https://doi.org/10.1016/j.biomaterials.2009.07.065)
7. Elechiguerra JL, Burt JL, Morones JR, Camacho-Bragado A, Gao X, Lara HH, Yacaman MJ (2005) Interaction of silver nanoparticles with HIV-1. *J Nanobiotechnol*. doi: [10.1186/1477-3155-3-6](https://doi.org/10.1186/1477-3155-3-6)
8. Lu L, Sun RW, Chen R, Hui CK, Ho CM, Luk JM, Lau GK, Che CM (2008) Silver nanoparticles inhibit hepatitis B virus replication. *Antivir Ther* 13:253–262 <http://www.intmedpress.com/journals/avt/abstract.cfm?id=130&pid=88>
9. Lara HH, Ayala-Nunez NV, Ixtapan-Turrent L, Rodríguez-Padilla C (2010) Mode of antiviral action of silver nanoparticles against HIV-1. *J Nanobiotechnol*. doi:[10.1186/1477-3155-8-1](https://doi.org/10.1186/1477-3155-8-1)
10. Shrivastava S, Bera T, Roy A, Singh G, Ramachandrarao P, Dash D (2007) Characterization of enhanced antibacterial effects of novel silver nanoparticles. *Nanotechnol* 18: 225103. doi:[10.1088/0957-4484/18/22/225103](https://doi.org/10.1088/0957-4484/18/22/225103)
11. Sharma VK, Yngard RA, Lin Y (2009) Silver nanoparticles: Green synthesis and their antimicrobial activities. *Adv Colloid Interface Sci* 145:83–96. doi:[10.1016/j.cis.2008.09.002](https://doi.org/10.1016/j.cis.2008.09.002)
12. Kim JS, Kuk E, Yu KN, Kim JH, Park SJ, Lee HJ, Kim SH, Park YK, Park YH, Hwang CY, Kim YK, Lee YS, Jeong DH, Cho MH (2007) Antimicrobial effects of silver nanoparticles. *Nanomed Nanotechnol Biol Med* 3:95–101. doi:[10.1016/j.nano.2006.12.001](https://doi.org/10.1016/j.nano.2006.12.001)
13. Dickinson GM, Bisno AL (1989) Infections associated with indwelling devices: concepts of pathogenesis; Infections associated with intravascular devices. *Antimicrob Agents Chemother* 33:597–601. <http://www.ncbi.nlm.nih.gov/pmc/articles/PMC172497/>
14. Sitges-Serra A, Girvent M (1999) Catheter-related Bloodstream Infections. *World J Surg* 23:589–595. doi: [10.1007/PL00012352](https://doi.org/10.1007/PL00012352)
15. Donlan RM (2001) Biofilms and device-associated infections. *Emerg Infect Dis* 7:277–281. <http://www.cdc.gov/ncidod/eid/vol7no2/donlan.htm>. Accessed 5 March 2009
16. Francolini I, Donelli G, Stoodley P (2003) Polymer designs to control biofilm growth on medical devices. *Rev Environ Sci Biotechnol* 2:307–319. doi: [10.1023/B:RESB.0000040469.26208.83](https://doi.org/10.1023/B:RESB.0000040469.26208.83)
17. Tenke P, Riedl CR, Jones GL, Williams GJ, Stickler D, Nagy E (2004) Bacterial biofilm formation on urologic devices and heparin coating as preventive strategy. *Int J Antimicrob Agents* 23:67–74. doi:[10.1016/j.ijantimicag.2003.12.007](https://doi.org/10.1016/j.ijantimicag.2003.12.007)
18. Elliot TS (1999) Role of antimicrobial central catheters for prevention of associated infections. *J Antimicrob Chemother* 43:441–446. doi:[10.1093/jac/43.4.441](https://doi.org/10.1093/jac/43.4.441)
19. Mojibian H, Spector M, Ni N, Eliseo D, Pollak J, Tal M (2009) Initial clinical experience with a new heparin coated chronic hemodialysis catheter. *Hemodial Int* 13:329–334. doi:[10.1111/j.1542-4758.2009.00339.x](https://doi.org/10.1111/j.1542-4758.2009.00339.x)

20. Riedl CR, Witkowski M, Plas E, Pflueger H (2002) Heparin coating reduces encrustation of ureteral stents: a preliminary report. *Int J Antimicrob Agents* 19:507–510. doi:[10.1016/S0924-8579\(02\)00097-3](https://doi.org/10.1016/S0924-8579(02)00097-3)
21. Sherertz RJ, Carruth WA, Hampton AA, Byron MP, Solomon DD (1993) Efficacy of antibiotic-coated catheters in preventing subcutaneous *Staphylococcus aureus* Infection in Rabbits. *J Infect Dis* 167:98–106. doi:[10.1093/infdis/167.1.98](https://doi.org/10.1093/infdis/167.1.98)
22. Morones JR, Elechiguerra JL, Camacho A, Holt K, Kouri JB, Tapia Ramirez J, Yacaman MJ (2005) The bactericidal effect of silver nanoparticles. *Nanotechnol* 16:2346–2353. doi:[10.1088/0957-4484/16/10/059](https://doi.org/10.1088/0957-4484/16/10/059)
23. Raffi M, Hussain F, Bhatti TM, Akhter JI, Hameed A, Hasan MM (2008) Antibacterial characterization of silver nanoparticles against *E. coli* ATCC-15224. *J Mater Sci Technol* 24:192–196. <http://www.jmst.org/EN/abstract/abstract8045.shtml>. Accessed 10 October 2009
24. Chaloupka K, Malam Y, Seifalian AM (2010) Nanosilver as a new generation of nanoparticle in biomedical applications. *Trends Biotechnol* 28:580–588. doi:[10.1016/j.tibtech.2010.07.006](https://doi.org/10.1016/j.tibtech.2010.07.006)
25. Dunn K, Edwards-Jones V. (2004) The role of Acticoat™ with nanocrystalline silver in the management of burns. *Burns* 30:S1–S9 doi:[10.1016/S0305-4179\(04\)90000-9](https://doi.org/10.1016/S0305-4179(04)90000-9)
26. Maneerung T, Tokura S, Rujiravanit R (2008) Impregnation of silver nanoparticles into bacterial cellulose for antimicrobial wound dressing. *Carbohydr Polym* 72:43–51. doi:[10.1016/j.carbpol.2007.07.025](https://doi.org/10.1016/j.carbpol.2007.07.025)
27. Gupta P, Bajpai M, Bajpai SK (2008) Investigation of antibacterial properties of silver nanoparticle-loaded poly(acrylamide-co-itaconic acid)-grafted cotton fabric. *J Cotton Sci* 12:280–286. <http://www.cotton.org/journal/2008-12/3/>
28. Lia Y, Leung P, Yao L, Song QW, Newton E (2006) Antimicrobial effect of surgical masks coated with nanoparticles. *J Hosp Infect* 62:58–63. doi:[10.1016/j.jhin.2005.04.015](https://doi.org/10.1016/j.jhin.2005.04.015)
29. Wollina U, Heide M, Müller-Litzb W, Obenauf D, Ash J (2003) functional textiles in prevention of chronic wounds, wound healing and tissue engineering. *Text skin. Curr Probl Dermatol* 31:82–97. doi: [10.1159/000072239](https://doi.org/10.1159/000072239)
30. Kim KJ, Sung WS, Moon SK, Choi JS, Kim JG, Lee DG (2008) Antifungal effect of silver nanoparticles on dermatophytes. *J Microbiol Biotechnol* 18:1482–1484. <http://www.nanoarchive.org/13/>. Accessed 10 October 2008
31. Ravindra S, Murali Mohan Y, Narayana Reddy N, Mohana Raju K (2010) Fabrication of antibacterial cotton fibres loaded with silver nanoparticles via “Green Approach”. *Colloids Surf A: Physicochem. Eng Aspects* 367:31–40. doi:[10.1016/j.colsurfa.2010.06.013](https://doi.org/10.1016/j.colsurfa.2010.06.013)
32. Pollini M, Russo M, Licciulli A, Sannino A, Maffezzoli A (2009) Characterization of antibacterial silver coated yarns. *J Mater Sci Mater in Med* 20:2361–2366. doi:[10.1007/s10856-009-3796-z](https://doi.org/10.1007/s10856-009-3796-z)
33. Feng QL, Wu J, Chen GQ, Cui FZ, Kim TN, Kim JO (2000) A mechanistic study of the antibacterial effect of silver ions on *Escherichia coli* and *Staphylococcus aureus*. *J Biomed Mater Res* 52:662–668. doi: [10.1002/1097-4636\(20001215\)52:4<662::AID-JBM10>3.0.CO;2-3](https://doi.org/10.1002/1097-4636(20001215)52:4<662::AID-JBM10>3.0.CO;2-3)
34. Borsuk D, Gallant M, Richard D, Williams H (2007) Silver-coated nylon dressings for pediatric burn victims. *Can J Plast Surg* 15:29–31. <http://www.ncbi.nlm.nih.gov/pmc/articles/PMC2686041/>
35. Chen X, Schluessener HJ (2008) Nanosilver: A nanoparticle in medical application. *Toxicol Lett* 176:1–12. doi:[10.1016/j.toxlet.2007.10.004](https://doi.org/10.1016/j.toxlet.2007.10.004)
36. Jo YK, Kim BH, Jung G (2009) Antifungal activity of silver ions and nanoparticles on phytopathogenic fungi. *Plant Dis* 93:1037–1043. doi:[10.1094/PDIS-93-10-1037](https://doi.org/10.1094/PDIS-93-10-1037)
37. Chopra I (2007) The increasing use of silver-based products as antimicrobial agents: A useful development or a cause for concern? *J Antimicrob Chemother* 59:587–590. doi:[10.1093/jac/dkm006](https://doi.org/10.1093/jac/dkm006)
38. Kim J, Kwon S, Ostler E (2009) Antimicrobial effect of silver-impregnated cellulose: Potential for antimicrobial therapy. *J Biol Eng*. doi:[10.1186/1754-1611-3-20](https://doi.org/10.1186/1754-1611-3-20)

39. Rai M, Yadav A, Gade A (2009) Silver nanoparticles as a new generation of antimicrobials. *Biotechnol Adv* 27:76–83. doi:[10.1016/j.biotechadv.2008.09.002](https://doi.org/10.1016/j.biotechadv.2008.09.002)
40. Jain P, Pradeep T (2005) Potential of silver nanoparticle-coated polyurethane foam as an antibacterial water filter. *Biotechnol Bioeng* 90:59–63. doi:[10.1002/bit.20368](https://doi.org/10.1002/bit.20368)
41. Krutyakov YA, Kudrinskiy AA, Olenin AY, Lisichkin GV (2008) Synthesis and properties of silver nanoparticles: Advances and prospects. *Russ Chem Rev* 77:233–257. doi:[10.1070/RC2008v077n03ABEH003751](https://doi.org/10.1070/RC2008v077n03ABEH003751)
42. Pal S, Tak YK, Myong Song J (2007) Does the antibacterial activity of silver nanoparticles depend on the shape of the nanoparticle? A study of the Gram-negative bacterium *Escherichia coli*. *Appl Environ Microbiol* 73:1712–1720. doi:[10.1128/AEM.02218-06](https://doi.org/10.1128/AEM.02218-06)
43. Baer DR, Burrows PE, El-Azab AA (2003) Enhancing coating functionality using nanoscience and nanotechnology. *Prog Org Coat* 47:342–356. doi:[10.1016/S0300-9440\(03\)00127-9](https://doi.org/10.1016/S0300-9440(03)00127-9)
44. Chu PK, Chen JY, Wang LP, Huang N (2002) Plasma-surface modification of biomaterials. *Mater Sci Eng* 36:143–206. doi:[10.1016/S0927-796X\(02\)00004-9](https://doi.org/10.1016/S0927-796X(02)00004-9)
45. Sardella E, Favia P, Gristina R, Nardulli M, D'Agostino R (2006) Plasma-aided micro- and nanopatterning processes for biomedical applications. *Plasma Process Polym* 3:456–469. doi:[10.1002/ppap.200600041](https://doi.org/10.1002/ppap.200600041)
46. Gomathi N, Sureshkumar A, Neogi S (2008) RF plasma-treated polymers for biomedical applications. *Curr Sci* 94:1478–1486. <http://www.ias.ac.in/currsci/jun102008/contents.htm>. Accessed 10 June 2008
47. Korner E, Aguirre MH, Fortunato G, Ritter A, Ruhe J, Hegemann D (2010) Formation and distribution of silver nanoparticles in a functional plasma polymer matrix and related Ag⁺ release properties. *Plasma Process Polym* 7:619–625. doi:[10.1002/ppap.200900163](https://doi.org/10.1002/ppap.200900163)
48. Hegemann D, Hossain MM, Balazs DJ (2007) Nanostructured plasma coatings to obtain multi-functional textile surfaces. *Prog Org Coat* 58:237–240. doi:[10.1016/j.porgcoat.2006.08.027](https://doi.org/10.1016/j.porgcoat.2006.08.027)
49. Dowling DP, Donnelly K, McConnell ML, Eloy R, Arnaud MN (2001) Deposition of antibacterial silver coatings on polymeric substrates. *Thin Solid Films* 398:602–606. doi:[10.1016/S0040-6090\(01\)01326-8](https://doi.org/10.1016/S0040-6090(01)01326-8)
50. Mejía MI, Restrepo G, Marín JM, Sanjines R, Pulgarín C, Mielczarski E, Mielczarski J, Kiwi J. (2010) Magnetron-sputtered Ag surfaces. New evidence for the nature of the Ag ions intervening in bacterial inactivation. *ACS Appl Mater Interf* 2:230–235. doi:[10.1021/am900662q](https://doi.org/10.1021/am900662q)
51. Wang HB, Wei QF, Wang JY, Hong JH, Zhao XY (2008) Sputter deposition of nanostructured antibacterial silver on polypropylene non-wovens. *Surf Eng* 24:70–74. doi:[10.1179/174329408X277493](https://doi.org/10.1179/174329408X277493)
52. Wang HB, Wang JY, Wei QF, Hong JH, Zhao X (2007) Nanostructured antibacterial silver deposited on polypropylene nonwovens. *Surf Rev Lett* 14:553–557. doi:[10.1142/S0218625X07009839](https://doi.org/10.1142/S0218625X07009839)
53. Gupta R, Kumar A (2008) Bioactive materials for biomedical applications using sol–gel technology. *Biomed Mater* 3(2008):034005. doi:[10.1088/1748-6041/3/3/034005](https://doi.org/10.1088/1748-6041/3/3/034005)
54. Mahltig B, Textor T (2010) Silver containing sol–gel coatings on polyamide fabrics as antimicrobial finish-description of a technical application process for wash permanent antimicrobial effect. *Fibers Polym* 11:1152–1158. doi:[10.1007/s12221-010-1152-z](https://doi.org/10.1007/s12221-010-1152-z)
55. Shamel K, Ahmad M, Zargar M, Yunus W, Ibrahim N (2011) Fabrication of silver nanoparticles doped in the zeolite framework and antibacterial activity. *Int J Nanomed* 6:331–334. doi:[10.2147/IJN.S16964](https://doi.org/10.2147/IJN.S16964)
56. Hadad L, Perkas N, Gofer Y, Calderon-Moreno J, Ghule A, Gedanken A. (2007) Sonochemical deposition of silver nanoparticles on wool fibers. *J Appl Polym Sci* 104:1732–1737. doi:[10.1002/app.25813](https://doi.org/10.1002/app.25813)
57. Perelshtein I, Applerot G, Perkas N, Guibert G, Mikhailov S, Gedanken A (2008) Sonochemical coating of silver nanoparticles on textile fabrics (nylon, polyester and cotton) and their antibacterial activity. *Nanotechnology* 19:245705. doi:[10.1088/0957-4484/19/24/245705](https://doi.org/10.1088/0957-4484/19/24/245705)

58. Song KC, Lee SM, Park TS, Lee BS. (2009) Preparation of colloidal silver nanoparticles by chemical reduction method. *Korean J Chem Eng* 26:153–155. doi: [10.1007/s11814-009-0024-y](https://doi.org/10.1007/s11814-009-0024-y)
59. Nair LS, Laurencin CT (2007) Silver nanoparticles: synthesis and therapeutic applications. *J Biomed Nanotechnol* 3:301–316. doi: [10.1166/jbn.2007.041](https://doi.org/10.1166/jbn.2007.041)
60. Yin H, Yamamoto T, Wada Y, Yanagida S (2004) Large-scale and size-controlled synthesis of silver nanoparticles under microwave irradiation. *Mater Chem Phys* 83:66–70. doi: [10.1016/j.matchemphys.2003.09.006](https://doi.org/10.1016/j.matchemphys.2003.09.006)
61. Starowicz M, Stypuła B, Banas J (2006) Electrochemical synthesis of silver nanoparticles. *Electrochem Commun* 8:227–230. doi: [10.1016/j.elecom.2005.11.018](https://doi.org/10.1016/j.elecom.2005.11.018)
62. Coronato Courrol L, Rodrigues de Oliveira Silva F, Gomes L (2007) A simple method to synthesize silver nanoparticles by photo-reduction. *Colloids Surf A: Physicochem Eng Asp* 305:54–57. doi: [10.1016/j.colsurfa.2007.04.052](https://doi.org/10.1016/j.colsurfa.2007.04.052)
63. Pollini M, Sannino A, Maffezzoli A, Licciulli A (2008) Antibacterial surface treatments based on Silver clusters deposition. EP20050850988 (2008-11-05)
64. Haug S, Roll A, Schmid-Grendelmeier P, Johansena P, Wüthricha B, Kündiga TM, Senti G (2006) Coated textiles in the treatment of atopic dermatitis. *Curr Probl Dermatol* 33:144–151. doi: [10.1159/000093941](https://doi.org/10.1159/000093941)
65. Chen CY, Chiang CL (2008) Preparation of cotton fibers with antibacterial silver nanoparticles. *Mater Lett* 62:3607–3609. doi: [10.1016/j.matlet.2008.04.008](https://doi.org/10.1016/j.matlet.2008.04.008)
66. Biederman T (2006) Dissecting the role of infections in atopic dermatitis. *Acta Derm Venereol* 86:99–109. doi: [10.2340/00015555-0047](https://doi.org/10.2340/00015555-0047)
67. Huang JT, Abrams M, Tloutan B, Rademaker A, Paller AS, (2009) Treatment of *Staphylococcus aureus* colonization in atopic dermatitis decreases disease severity. *Pediatrics* 123:808–814. doi: [10.1542/peds.2008-2217](https://doi.org/10.1542/peds.2008-2217)
68. Ricci G, Patrizi A, Mandrioli P, Specchia F, Medri M, Menna G, Masi M (2006) Evaluation of the antibacterial activity of a special silk textile in the treatment of atopic dermatitis. *Dermatology* 213:224–227. doi: [10.1159/000095040](https://doi.org/10.1159/000095040)
69. Daeschlein G, Assadian O, Arnold, Haase H, Kramer A, Jünger M (2010) Bacterial burden of worn therapeutic silver textiles for neurodermitis patients and evaluation of efficacy of washing. *Skin Pharmacol Physiol* 23:86–90. doi: [10.1159/000265679](https://doi.org/10.1159/000265679)
70. Gauger A, Fischer S, Mempel M, Schaefer T, Foelster-Holst R, Abeck D, Ring J (2006) Efficacy and functionality of silver-coated textiles in patients with atopic eczema. *Eur Acad Dermatol Venereol* 20:534–41. doi: [10.1111/j.1468-3083.2006.01526.x](https://doi.org/10.1111/j.1468-3083.2006.01526.x)
71. Gao Y, Cranston R (2008) Recent advances in antimicrobial treatments of textiles. *Text Res J* 78:60–72. doi: [10.1177/0040517507082332](https://doi.org/10.1177/0040517507082332)
72. Kostic M, Radic N, Obradovic BM, Dimitrijevic S, Kuraica MM, Skundric P (2009) Silver-loaded cotton/polyester fabric modified by dielectric barrier discharge treatment. *Plasma Process Polym* 6:58–67. doi: [10.1002/ppap.200800087](https://doi.org/10.1002/ppap.200800087)
73. MacKeen PC, Person S, Warner SC, Snipes W, Stevens SE Jr (1987) Silver-coated nylon fiber as an antibacterial agent. *Antimicrob Agents Chemother* 31:93–99. <http://aac.asm.org/cgi/reprint/31/1/93.pdf>
74. Deitch EA, Marino AA, Gillespie TE, Albright JA (1983) Silver-nylon: a new antimicrobial agent. *Antimicrob Agents Chemother* 23:356–359. <http://aac.asm.org/cgi/reprint/23/3/356>
75. Canaud B (1999) Haemodialysis catheter-related infection: time for action. *Nephrol Dial Transplant* 14:2288–2290. doi: [10.1093/ndt/14.10.2288](https://doi.org/10.1093/ndt/14.10.2288)
76. Reid G. (1999) Biofilms in infectious disease and on medical devices. *Int J Antimicrob Agents* 11:223–226. doi: [10.1016/S0924-8579\(99\)00020-5](https://doi.org/10.1016/S0924-8579(99)00020-5)
77. Tobin EJ, Bambauer R (2003) Silver coating of dialysis catheters to reduce bacterial colonization and infection. *Ther Apher Dial* 7:504–509. doi: [10.1046/j.1526-0968.2003.00097.x](https://doi.org/10.1046/j.1526-0968.2003.00097.x)
78. Pavithra D, Doble M (2008) Biofilm formation, bacterial adhesion and host response on polymeric implants—issues and prevention. *Biomed Mater*. doi: [10.1088/1748-6041/3/3/034003](https://doi.org/10.1088/1748-6041/3/3/034003)

79. Guggenbichler JP, Boswald M, Lugauer S, Krall T (1999) A new technology of microdispersed silver in polyurethane induces antimicrobial activity in central venous catheters. *Infection* 27:16–23. doi:[10.1007/BF02561612](https://doi.org/10.1007/BF02561612)
80. Guggenbichler J-P (2003) Central venous catheter associated infections pathophysiology, incidence, clinical diagnosis, and prevention—A review. *Mat-wiss Werkstofftech* 34(12):1145. doi: [10.1002/mawe.200300712](https://doi.org/10.1002/mawe.200300712)
81. Serghini-Monim S, Norton PR, Puddephatt RJ (1997) Chemical vapor deposition of silver on plasma-modified polyurethane surfaces. *J Phys Chem B* 101:7808–7813. doi: [10.1021/jp9713827](https://doi.org/10.1021/jp9713827)

Chapter 12

Biotechnological Routes to Metallic Nanoparticles Production: Mechanistic Aspects, Antimicrobial Activity, Toxicity and Industrial Applications

Nelson Durán and Priscyla D. Marcato

12.1 Introduction

This chapter will describe the biogenic metallic nanoparticles synthesis and their mechanistic aspects in the syntheses and in their antimicrobial activities.

12.1.1 General Aspects of Biotechnological Processes Applied to Biogenic Synthesis of Nanoparticles

Nanobiotechnology has appeared as one of the most promising areas in nanotechnology, since nanoparticles, specifically in special nanometals, as carriers of drugs to treat and diagnose important diseases, form a major topic in nanomedicine. Among the metal nanoparticles, silver nanoparticles have been extensively studied. The most common synthetic methods of silver nanoparticle production are chemical reduction, photochemical methods, ultrasonic-assisted reduction, electrochemical methods, templates, and irradiating reduction (Zhang et al. 2007).

As indicated previously, there are many processes for metallic nanoparticle production, but the biological one is playing an important role in order to minimize the environmental pollution caused by physical and chemical procedures. In this

N. Durán (✉)

Chemistry Institute, Biological Chemistry Laboratory, Universidade Estadual de Campinas (UNICAMP), CP 6154, CEP 130970, Campinas, SP, Brazil

Center of Natural and Human Sciences (CCNH), Universidade Federal do ABC (UFABC), Santo André, SP, Brazil

e-mail: duvan@iqm.unicamp.br

P.D. Marcato

Chemistry Institute, Biological Chemistry Laboratory, Universidade Estadual de Campinas (UNICAMP), CP 6154, CEP 130970, Campinas, SP, Brazil

regard, fungi, bacteria, algae, yeasts, and plants have inherent capacities to reduce metal through their specific metabolic pathway. In fact, some biomimetic (peptides) procedures are also used in their study. Different types of metallic nanoparticles like copper, zinc, titanium, gold, and silver, among others, have been produced by biological methods. However, the interest in silver nanoparticles has been increasing due to their high antimicrobial activity against bacteria, viruses and eukaryotic microorganisms (Rai et al. 2009). The synthesis of metallic nanoparticles using a green procedure is of great interest in terms of introducing environmentally friendly synthesis procedures (Durán et al. 2010a; Marcato and Durán 2011). The importance of these nanoparticles is testified by the publication of many reviews on the biosynthesis and properties of metallic nanoparticles in the last 4 years (Rai et al. 2008; Mohanpuria et al. 2008; Bhattacharya and Mukherjee 2008; Chen and Schluesener 2008; Sharma et al. 2009; Singh et al. 2009; Sinha et al. 2009; Korbekandi et al. 2009; Hennebel et al. 2009; Krumov et al. 2009; Kumar and Yadav 2009; Das et al. 2009; Durán et al. 2010b, 2011; Narayanan and Sakthivel 2010; Popescu et al. 2010; Gade et al. 2010a; Thakkar et al. 2010; Marambio-Jones and Hoek. 2010; Arya 2010; Blanco-Andujar et al. 2010; Zhang et al. 2011). For example, Sinha et al. (2009) reviewed the knowledge and production by bioreductive approaches of Ag, Au, Cd, Pt, and Pd nanoparticles and oxides by bacteria, actinomycetes, yeasts, algae, fungi, higher angiospermic plants and their perspectives. Biosynthesis of Au, Ag, Au–Ag alloy, Se, Te, Pt, oxides and quantum dots by bacteria, actinomycetes, fungi, yeasts and viruses have been discussed as well as the current status of microbial synthesis and applications of metals (Narayanan and Sakthivel 2010).

The new uses of metallic nanoparticles require techniques to synthesize nanoparticles that are both cost-effective and environmentally benign. As discussed before, many processes for metallic nanoparticle synthesis have been reported; however, the synthesis of nanoparticles with precise control over size distribution, shape selectivity, and stability remains a challenge. Why is it important to synthesize these metallic nanoparticles? The small size and large surface area of metallic nanoparticles makes them useful for many different applications. The importance of these nanoparticles has been described as follows:

- Ag^0 . The small size and large surface area makes it useful for applications in non-linear optics, spectrally selective coatings for solar energy absorption, optical receptors, catalysts in chemical reactions, biolabeling, antistatic materials, cryogenic superconducting materials, and biosensor materials, and as antibacterials.
- Au^0 . Gold nanoparticles are used in opto-electronic devices, catalysis, biomedical including DNA labeling and drug delivery, cell imaging, immunostaining, and biosensors.
- Cd^0 . Cadmium is extremely toxic to the reproductive system of humans (accumulating in the body, particularly in the kidneys and the liver). Cadmium is widely used in alloys, pigments, solid-state batteries, metal coatings for protective coatings on steel, plastics and fertilizers.

- *Cu⁰*. Due to copper toxicity as ions, the biological system attempts to prevent copper toxicity by its reduction. Common plants can transform copper into metallic nanoparticles inside and near roots, with evidence of assistance by endomycorrhizal fungi when grown in contaminated soil in the natural environment.
- *Fe⁰*. Nano-scale zero-valent iron (nZVI) is of increasing interest for use in a variety of environmental remediations. In comparison to larger-sized ZVI particles, nZVI has a greater reactivity due to a greater surface area to volume ratio.
- *Pd⁰*. Palladium in terms of market prices is both economically and environmentally important due to their high global level. Palladium nanoparticles possess higher catalytic properties than their macro-scale counterparts.
- *Pt⁰*. Platinum exhibits excellent catalytic properties. The traditional methods are environmentally negative, and now the development of non-toxic, clean, eco-friendly and inexpensive synthetic protocols is needed ('green' processes).
- *Se⁰*. The reduction of the soluble oxyanions selenate [Se(VI)] or selenite [Se(IV)] to the elemental state [Se(0)] represents a method of removing elements from wastewaters.
- *Te⁰*. Nano-scale tellurium compounds, such as CdTe, have significant potential as solar-cell materials and are currently under intensive research scrutiny.
- *Ti⁰*. Titanium, by weight, is one of the strongest metals readily available with a wide range of practical applications. Titanium is suggested for use in desalination plants because of its strong resistance to corrosion from sea water. In medical applications, titanium pins are used because of their non-reactive nature when contacting bone and flesh.

12.2 Biogenic Synthesis of Metallic Nanoparticles

In this section of the chapter, selected cases of biogenic synthesis will be discussed in which some types of mechanism was proposed.

12.2.1 Silver Nanoparticles

12.2.1.1 Amino Acids and Peptides

In a biomimetic synthesis of silver nanoparticles through silver-binding peptides were incubated in an silver nitrate solution and, after a few hours, the solution turned reddish and a reddish-colored precipitate was obtained by centrifugation. No change in the color or precipitate was observed with non-specific peptides (Naik et al. 2002).

The silver-binding peptides (selected from the PhD-12C phage display peptide library) interact with preformed nanoclusters of silver metal present in the aqueous silver nitrate solution and this cluster gives the reducing moiety to obtain the silver nanoparticles. It has been demonstrated that the selected peptides containing specific amino acids permits the recognition and reduction of silver ions (Asn-Pro-Ser-Ser-Leu-Phe-Arg-Tyr-Leu-Pro-Ser-Asp), since the pure amino acids (e.g., proline, arginine or serine) or other non-silver binding peptides were unable to reduce the silver ion to silver nanoparticles. The amino acids, which are probably important in this process, are arginine, cysteine, lysine, and methionine, all known to interact with silver ions (Naik et al. 2002).

Aqueous silver sulfate solution and aqueous solution of tyrosine in basic medium at boiling temperature changed into a yellow solution, indicating the formation of silver nanoparticles. Under neutral and acidic pH conditions, this reaction did not occur. This result indicated the crucial role of tyrosine as a pH-dependent reducing agent (Selvakannan et al. 2004a). Silver-peptide nanoconjugate (peptide-SNPs) was formed from an aqueous solution of silver nitrate and a mixture of peptide NH₂-Leu- α -aminoisobutyric acid {Aib}-Trp-OMe). In this case, a color change from colorless to yellow was observed at pH 11. Similarly, peptide Tert-butyloxy-carbonyl {Boc}-Leu-Aib-Trp-OH) was used for synthesizing silver nanoparticles. The tryptophan residue was responsible for the reduction of metal ions to the respective metal atoms by donation of an electron to the metal ion and is itself converted to a transient tryptophyl radical, and then finally to finishing in a native tryptophan or in a ditryptophan/kynurenine form of the peptide (Si and Mandal 2007).

12.2.1.2 Fungi

Many of the *Fusarium oxysporum* strains studied were able to produce silver nanoparticles; however, this reduction was dependent on the nitrate reductase/2-acetyl-3,8-dihydroxy-6-methoxy anthraquinone or its isomers at 2-acetyl-2,8-dihydroxy-6-methoxy anthraquinone (Durán et al. 2005).

Silver nanoparticles were obtained from the fungal mycelia of *Trichoderma asperellum* that was resuspended in water in order to obtain a fungal filtrate in which aqueous solution of silver nitrate was added. The possible mechanism of the biosynthesis of silver nanoparticles was studied by FTIR. The β -carbon in cysteine loses one hydrogen radical and one electron in a concerted step, or two consecutive steps, and reduces Ag⁺ ion to Ag nanoparticles, probably through NADPH-dependent dehydrogenase. During the process, other changes show that this process follows the hypothetical mechanisms shown in Fig. 12.1.

FTIR analysis showed that there is a decrease of the amide linkage in the aqueous solution after the formation of silver nanoparticles, suggesting that the peptide linkage undergoes a hydrolysis to generate free carboxylic acid and amino groups which can act as capping agent to the silver nanoparticles and not the -SH group as in other fungi. The surface-enhanced resonance Raman spectroscopy

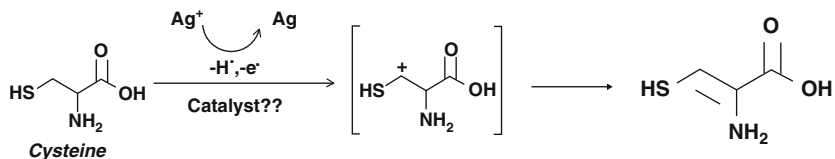
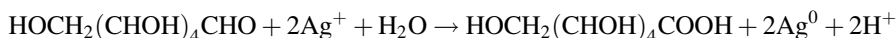


Fig. 12.1 Schematic representation of the mechanism for the formation of silver nanoparticles (Modified from Mukherjee et al. 2008)

showed this clearly since a very strong chemical bond between silver nanoparticles and nitrogen of the amino group in the amino acid appeared (Ag-N bond) (Mukherjee et al. 2008).

12.2.1.3 Bacteria

Lactic acid bacteria, such as *Lactobacillus* spp., *Pediococcus pentosaceus*, *Enterococcus faecium*, and *Lactococcus garvieae*, were able to reduce silver ions to silver nanoparticles (Sintubin et al. 2009). The mechanism of silver ions biosorption by resting cells of *Lactobacillus* sp. strain A09 and reduction to silver nanoparticles was studied at the molecular level using spectroscopic techniques. The silver ions in the presence of *Lactobacillus* sp biomass were rapidly absorbed and reduced by the free aldehyde group of the hemiacetalic hydroxyl group from glucose that was oxidized to the carboxyl group. Assays with free glucose demonstrated this process. The redox reaction of glucose on silver ions was proposed as follows (Lin et al. 2005):



In an other study, different lactic acid bacteria (*Lactobacillus* spp., *Pediococcus pentosaceus*, *Enterococcus faecium*, and *Lactococcus garvieae*) were studied to produce silver nanoparticles. Mainly the size distribution was species dependent and the final yields of nanoparticles were pH dependent (Sintubin et al. 2009). The authors suggest that exopolysaccharides from lactic acid bacteria (glucose, galactose and rhamnose) might serve in the reduction of silver ions to silver nanoparticles. Similar results were also reported by Lin et al. (2005). A reduction mechanism for these results is demonstrated in Fig. 12.2. The observation that the biosorption of silver nanoparticles decrease the pH is a good indication that silver ions compete with protons (Fig. 12.2a, $-\text{RH}$). At high pH, the aldehyde form (Fig. 12.2c) exerts its reducing power forming silver nanoparticles (Fig.12.2c).

It has been suggested that the enzyme involved in the intracellular synthesis of silver nanoparticles from *B. licheniformis* (Kalimuthu et al. 2008) could be NADH-nitrate reductase dependent and mediated by an electron shuttle, in a similar way as has been suggested in fungi (Durán et al. 2005). *B. licheniformis* is known to secrete

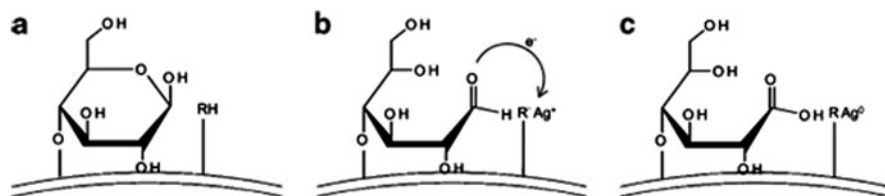


Fig. 12.2 Hypothetical mechanisms of bacterial reduction of silver ions to silver nanoparticles (From Sintubin et al. 2009. By permission of Springer)

the cofactor NADH and NADH-dependent enzymes, especially nitrate reductase, present in the membrane. The purified nitrate reductase was shown to have these properties confirming the possible mechanism (Kumar et al. 2007a).

A possible mechanism of silver nanoparticle production by *Morganella* sp., via extracellular synthesis, has been studied. In order to understand the silver resistance, it was studied at phenotypic and genotypic levels. In this case, three gene homologues, *silE*, *silP* and *silS*, were identified. The homologue of *silE* from *Morganella* sp. showed similarity with the gene which encodes a periplasmic silver-binding protein (Gupta et al. 1999). It was a good indication that silver-resistance machinery might have a similar role to play in *Morganella* sp. and could be associated with silver nanoparticle synthesis. A mechanistic speculation was proposed whereby an extracellular microenvironment created by the bacterium with several silver-specific proteins is secreted outside the cell during the growth. These proteins might specifically interact with silver ions and reduce it to silver nanoparticles stabilized by these proteins (Parikh et al. 2008).

12.2.1.4 Plants

Silver nanoparticles were efficiently synthesized by reacting silver ions with *Capsicum annuum* L. extract. In order to explain the mechanisms of the nanoparticles formation, Li et al. (2007) applied the model of recognition–reduction–limited nucleation and growth in the reaction solutions. In the first stage of the recognition process, the silver ions were trapped on the surface of proteins through electrostatic interactions. In the second stage, silver ions were reduced by proteins from the extract, and the secondary structures of the proteins changed with subsequent formation of silver nuclei. In the third stage, the silver nuclei grew by continuous reduction of silver ions and accumulation on these nuclei. The final stage is where the flexible linkage of the proteins and the large numbers of biomolecules coexist in the reaction solutions leading to an isotropic growth and the formation of the spherical silver nanoparticles. In the fifth stage, with an increase in aging time, large-sized silver nanoparticles formed and the crystalline phase changed from polycrystalline to single crystalline through Ostwald ripening (Li et al. 2007).

In another work, silver nanoparticles were prepared by reacting an aqueous solution containing silver ions, geraniol oil from Geranium leaves (*Pelargonium*

Fig. 12.3 Hypothetical mechanisms of silver nanoparticles prepared from geraniol (Modified from Safaepour et al. 2009)

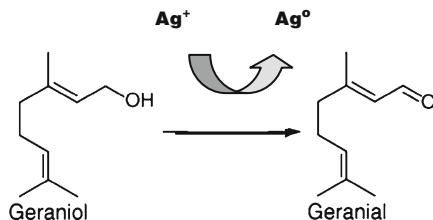
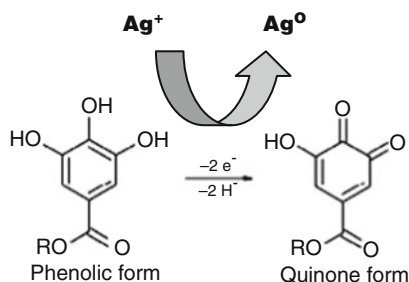


Fig. 12.4 Oxidation of phenolic group to quinones (Modified from Sivaraman et al. 2009)



graveolens) and an aqueous solution of polyethylene glycol 4,000 at pH >10 in a microwave for 40 s (Safaepour et al. 2009). The hypothetical mechanism of this reduction is illustrated in Fig. 12.3, with the genera *Pelargonium* exhibiting NADPH-dehydrogenases. The conversion of geraniol into geranial is catalyzed by NADP⁺-geraniol dehydrogenase in *Polygonum minus* (Maarof et al. 2010).

Tannic acid, a polyphenolic compound derived from tea or oak wood extracts, was used as the reducing agent for silver nanoparticles synthesis (Fig. 12.4). Silver nanoparticle sizes were controlled by molar ratio variation of tannic acid to silver nitrate. Tannic acid were used as a reducing and stabilizing agent to synthesize silver nanoparticles for an extremely short period of time (seconds). An increase in particle size with increasing molar ratio of tannic acid/silver nitrate indicates that tannic acid acts as an organizer for facilitating nucleation (Sivaraman et al. 2009).

Isolation of phyllanthin from leaf powder of the plant *Phyllanthus amarus* has been used in the synthesis of silver nanoparticles. After the addition of phyllanthin extract to the aqueous silver nitrate, the solution changed from colorless to pale orange which is indicative of the formation of silver nanoparticles. At different concentrations of phyllanthin, different silver nanoparticle morphologies were obtained. At low concentration, quasispherical forms were exhibited, and at high concentration, ellipsoidal nanoparticles were formed. On the basis of UV-vis spectroscopy, transmission electron microscopy, FT-IR spectrometry, cyclic voltametry and thermogravimetric analyses, a mechanism was proposed as shown in Fig. 12.5 (Kasthuri et al. 2009).

Green synthesis of silver nanoparticles using silver nitrate and different volume fractions of latex from *Jatropha curcas* has been studied (Bar et al. 2009a). The TEM analysis showed two broad size distributions of particle, one having diameter in the range 20–30 nm and others with some larger diameters and uneven shapes. It is known

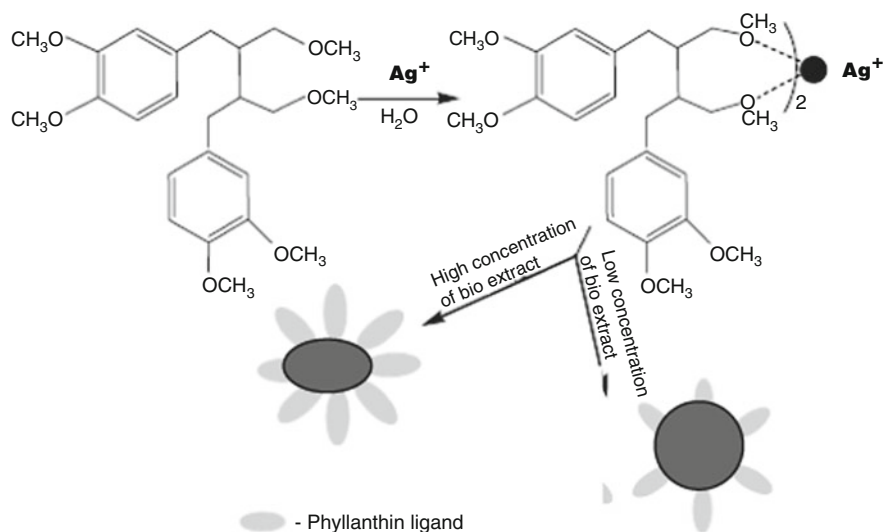


Fig. 12.5 Schematic diagram of the formation of phyllanthin-stabilized silver nanoparticles (Modified from Kasthuri et al. 2009)

that major components of *J. curcas* latex are curcacycline A (an octapeptide), curcacycline B (a nonapeptide) and curcain (an enzyme) (Bar et al. 2009a and references therein). Calculations on curcacycline A and curcacycline B using a semi-empirical AM1 method suggested that there are a number of different size pockets within the cavity in both structures having radii in the range ~20–35 nm. The authors suggested that silver ions were first entrapped into the core structure of the cyclic protein, and then reduced and stabilized in situ by the amide group of the host peptide under the present experimental conditions. This results in the formation of silver nanoparticles having a radius similar to that of the cavity of cyclic peptides, and probably, the enzyme, curcain, in the latex with its large folded structure helps to stabilize the silver nanoparticles with a larger size and having irregular shapes. Then, the most probable mechanisms in this case might be as shown in Fig. 12.6.

In a similar way, Bar et al. (2009b) synthesized silver nanoparticles using the aqueous seed extract of *J. curcas*. The particles were spherical and the size of the particles was controlled by varying the silver nitrate concentration. These nanoparticles were stable for several months due to protein capping.

Silver nanoparticles were synthesized in a short period of time (30 min) using leaf extract of *Acalypha indica*. Probably, quercetin and polysaccharides present in *A. indica* may be responsible for the nanoparticles synthesis. These molecules belong to a group of plant pigments called flavonoids, indicating that the plants with these compounds are able to reduce silver ions to silver nanoparticles (Krishnaraj et al. 2010).

Medicago sativa seeds were used to obtain silver nanoparticles from silver nitrate solution. The silver ion concentration, amount of exudate and pH determined the

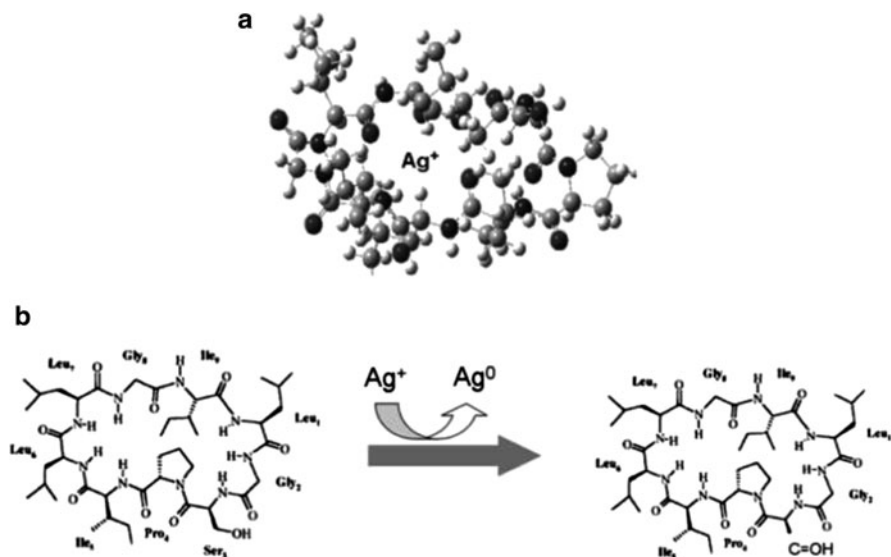


Fig. 12.6 Schematic representation of silver ion stabilization and reduction by curcacycline B. (a) Stabilization of silver ions in the curcacycline B pocket (Modified from Bar et al. 2009a) and (b) possible redox mechanism of the silver nanoparticles production, as suggested by Durán et al. 2011. By permission of Springer

particle size and morphology. At low silver ion concentration, largely spherical nanoparticles were produced, and at high concentration, flower-like clusters were observed. Pre-dilution of the exudate induced the formation of silver nanoplates, forming hexagonal particles and nanotriangles. These data are indicative that the formation of particles appears to follow a clear pathway, and the authors hypothesized that there were different primary growth mechanisms and combinations of these mechanisms, by which the particles (in particular, the nanotriangles) self-assembled in the silver exudate system. This exudate contained a large amount of quercetin, and the proposed oxidized structure for quercetin is that of a ketone, as quercetin possesses the readily oxidized hydroxyl group in the C ring next to the carbonyl group (Fig. 12.7). This further supports that this oxidized form of quercetin may dictate the growth of the Ag nanotriangles along the {111} direction and cap the Ag nanoparticles in the *M. sativa* seed exudate system.

This biogenic synthesis by *M. sativa* was mimicked by commercial quercetin and showed similar results to those observed in the biological systems (Fig. 12.8) (Lukman et al. 2011). These facts showed that the quercetin acts as an intermediate compound in the biosynthesis of metallic nanoparticles in plants (Egorova and Revina 2000; Materska 2008).

It is known that plants growing under different ecological conditions (e.g., xerophytes, mesophytes, and hydrophytes) are able to metabolize metallic nanoparticles (Jha et al. 2009). In the case of xerophytes (e.g., *Bryophyllum* sp.), during night-time CO_2 enters the leaf tissue and then the cells, CO_2 reacts with

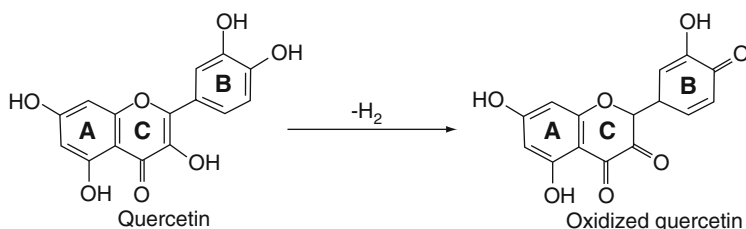


Fig. 12.7 Quercetin oxidation

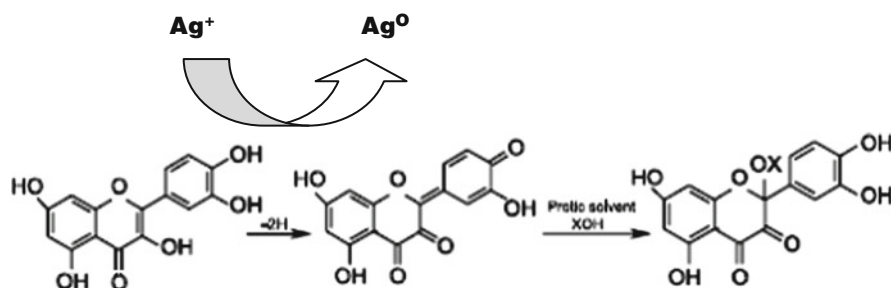


Fig. 12.8 Pathway of oxidative changes in quercetin reaction with silver nanoparticles in protic solvents (Modified from Materska 2008)

phosphoenol pyruvate (PEP) under PEP carboxylase to form oxalo-acetic acid which is reduced by Malate dehydrogenase/NADH to malic acid (by night). During the day, malic acid is oxidized to pyruvate, regenerating PEP by PEP carboxykinase at pH variations (pool of organic acids). These redox reactions indicate that the changes must be due to redial transformation of silver. The authors suggested that emodin (anthraquinones, similar to Durán et al. 2005) can undergo a redial tautomerization producing the silver nanoparticles (Fig. 12.9).

In mesophytes, it appeared that nano-transformation is produced by the tautomerization of quinones. The candidate mesophytic genera, *Cyperus* sp., contained three types of benzoquinones, e.g., cyperoquinone (type I), dietchequinone (type II) and remirin (type III) were able to produced silver nanoparticles via redial tautomerization (Fig. 12.10).

Hydrophytes (*Potamogeton* sp.) exhibit a translocation of ammonia and this is dissolved in water to give its hydroxide. This plant due to high salinity must be protected from the levels of reactive oxygen species (ROS), since an excessive level of ROS leads to oxidative damage to cellular molecules, aging and cell death. Due to this fact, the antioxidative species must be kept at appropriate levels (ascorbic acid). Dehydroascorbate (DHA) reductase (DHAR) catalyze the re-reduction of DHA to ascorbate. In addition, this presence of catechol and protocatechuic acid have also been reported along with other important phytochemicals in *Hydrilla*. In both the cases, reactive hydrogen gets liberated which participates in the synthesis of silver nanoparticles (Fig. 12.11).

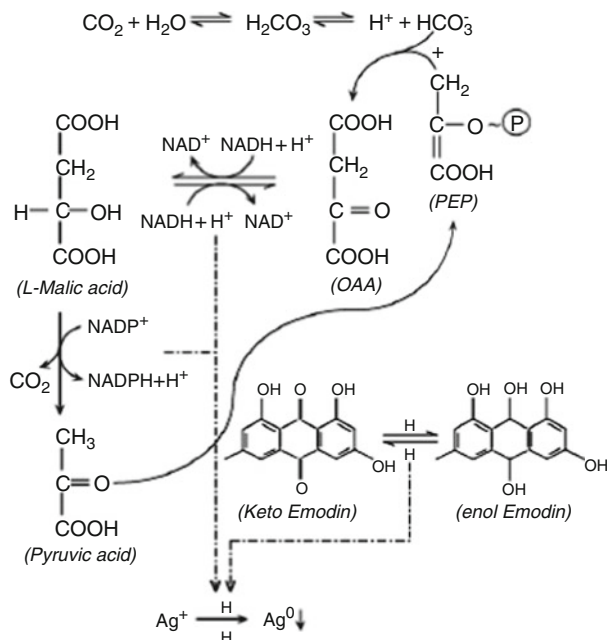


Fig. 12.9 Proposed mechanism of silver nanoparticles using xerophytes (From Jha et al. 2009. By permission of Elsevier)

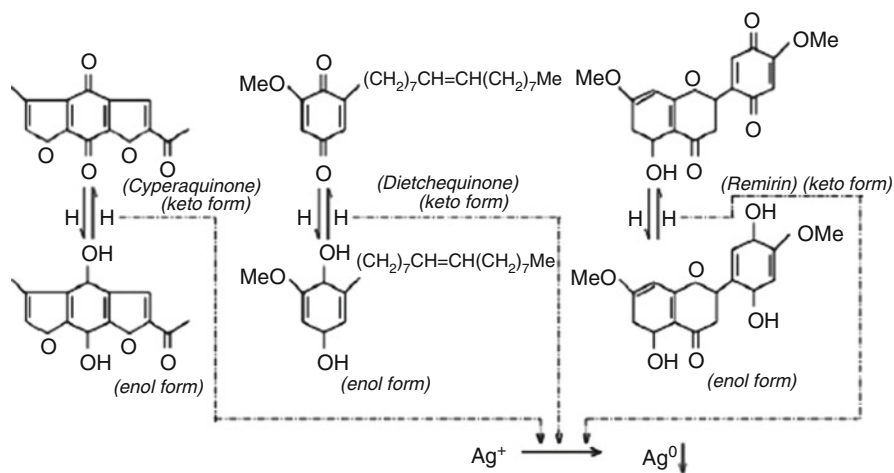


Fig. 12.10 Proposed mechanisms of silver nanoparticles using mesophytes (From Jha et al. 2009. By permission of Elsevier)

However, another intermediate for biosynthesis of silver nanoparticles has been proposed using xerophytic plant *O. ficus-indica*, commonly known as Opuntia. In this mechanism, quercetin was proposed as intermediate. This compound is the main bioactive products in this plant, thus probably this metabolite plays a major

Fig. 12.11 Proposed mechanism of silver nanoparticles using hydrophytes (From Jha et al. 2009. By permission of Elsevier)

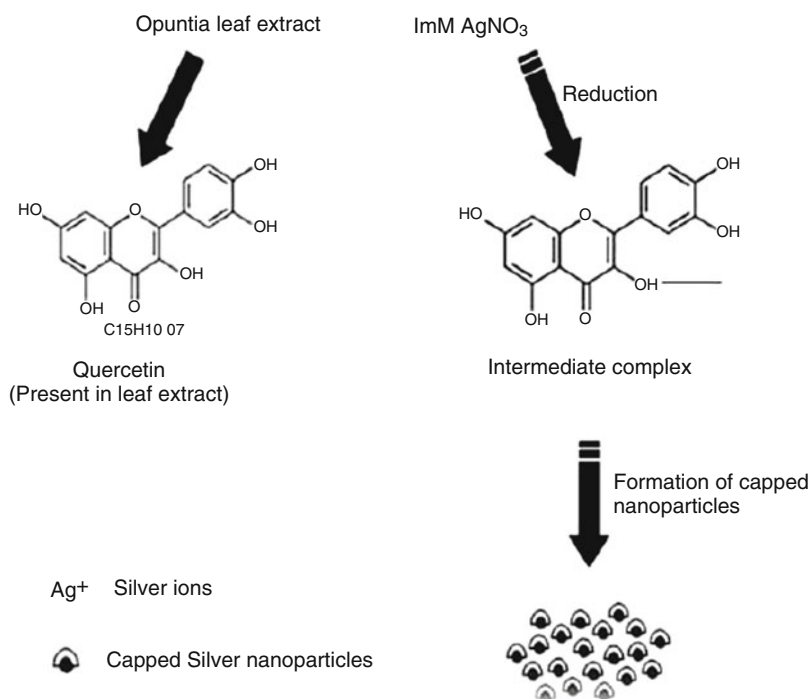
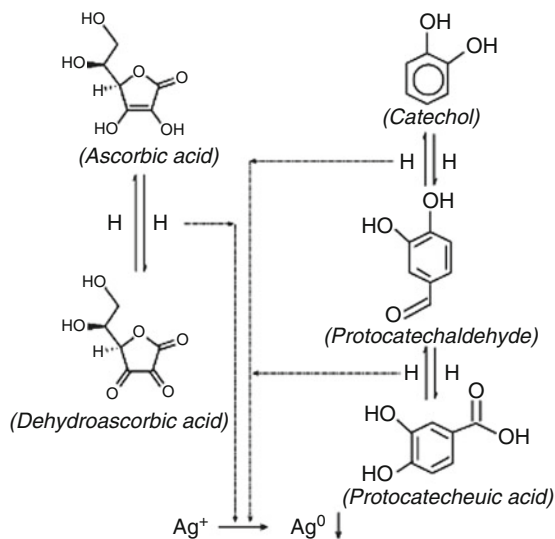


Fig. 12.12 A two-step hypothetical mechanism of biosynthesis of silver nanoparticles (From Gade et al. 2010b. By permission of Bentham Science)

role in the reduction of silver ions and formation of an intermediate complex which is further responsible for the formation of silver nanoparticles (Fig. 12.12) (Gade et al. 2010b).

Finally, the silver nanoparticle production by plants depends on their metabolism where different metabolites such as organic acids or quinones or flavonoids such as quercetin, or metabolic fluxes and other redox systems such as ascorbates or catechol/protocatechuic acid play important roles in the mechanism of silver nanoparticle formation (Jha et al. 2009).

12.2.2 Gold Nanoparticles

There are very few publications on the mechanistic aspect of gold biosynthesis.

12.2.2.1 Aminoacids and Peptides

Gold nanoparticles can be produced by using peptide and aminoacid. It has been reported that some short model peptides can be self-assembled into fibrous structures under appropriate conditions (this was not observed in peptide–silver ions interaction). Bhattacharjee et al. (2005) used the capacity of self-assembly of surface-adsorbed fibril-forming peptides. The authors mentioned that similar kinds of large aggregated structures have also been prepared by the self-assembly of gold nanoparticles using other biological interactions (e.g., Brown 2001). Previously, it was reported that tyrosine was redox active and the probable mechanism suggested was spin delocalization that was in agreement with a role for the peptide bond in tyrosyl radical-based electron-transfer reactions (Pujols-Ayala et al. 2003). Bhattacharjee et al. (2005) showed that the tripeptide (H₂N-Leu- α -aminoisobutyric acid {Aib}-Tyr-OMe-1) containing a C-terminally located tyrosine residue reduced gold salt to metallic gold nanoparticles in situ (Fig. 12.13). Stable nanoparticles were obtained due to the presence of tripeptide on the gold nanoparticles surface as self-assembled into three-dimensional structures.

In 2005, analyses were carried out of the reduction potential of cowpea chlorotic mottle viruses of unmodified SubE (plasmid expressed in yeast), (HRE)-SubE engineered with interior HRE peptide epitopes (Ala-His-His-Ala-His-His-Ala-Ala-Asp) and wild-type as viral templates for synthesis of gold nanoparticles (Slocik et al. 2005). SubE, (HRE)-SubE, and wild-type were added to water with

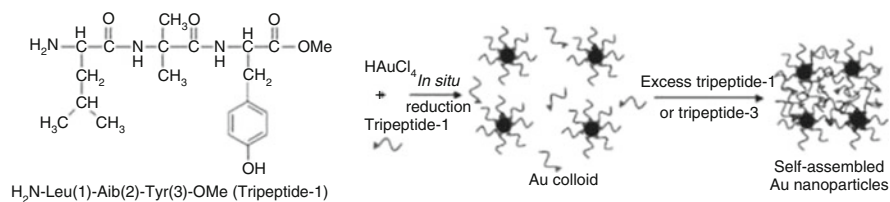


Fig. 12.13 Structure of tripeptide-1 and the self-assembled process for gold nanoparticles (Modified from Bhattacharjee et al. 2005 and from Durán et al. 2011. By permission from Springer)

AuCIP(CH₃)₃ leading to the rapid reduction to form gold nanoparticles (either aerobically or anaerobically). Tyrosine played an important role in the gold reduction and it was demonstrated by the decay of the tyrosine fluorescence and correlated with an increase of the plasmon absorbance of gold nanoparticles. In addition, a sequence analysis of cowpea chlorotic mottle virus demonstrated that there were four tyrosine residues in close proximity to the C-terminus of each subunit that presented multiple reduction sites. This research showed a unique surface chemistry of viruses with a large potential in many nanomaterials (Slocik et al. 2005).

In another work (Selvakannan et al. 2004b), it was demonstrated that tryptophan is a reductant agent of gold ions and that the temperature can impact on the synthesis process by increasing the reduction rate and favoring the formation of gold nanoparticles in anisotropic shapes (triangles and hexagons). Through surface-enhanced Raman scattering (SERS), it was demonstrated how tryptophan caps the gold nanoparticles after the reduction process, stabilizing the nanoparticles. Figure 12.14 shows the SERS spectra from the tryptophan-reduced gold nanoparticles synthesis (tryptophan alone did not exhibit Raman signal). Furthermore, the influence of temperature in the SERS spectra can be seen in this figure. Gold nanoparticles synthesized at 60°C and 80°C (spectra b and c) provide higher Raman enhancement compared to the particles synthesized at 20°C (spectrum a). The SERS is expected to be higher for anisotropic nanoparticles, because symmetry breaking allows for plasmon localization and more intense electromagnetic field generation at the edge and tips of nanoparticles. The SERS spectrum also demonstrated that the band at 1,123 cm⁻¹, which corresponded to NH₂ twisting vibration mode, is relating to the positive charge of the secondary amino group (glycine moiety of tryptophan), interacting with the negative charge of the gold nanoparticles surface by electrostatic interaction. Another observation by SERS

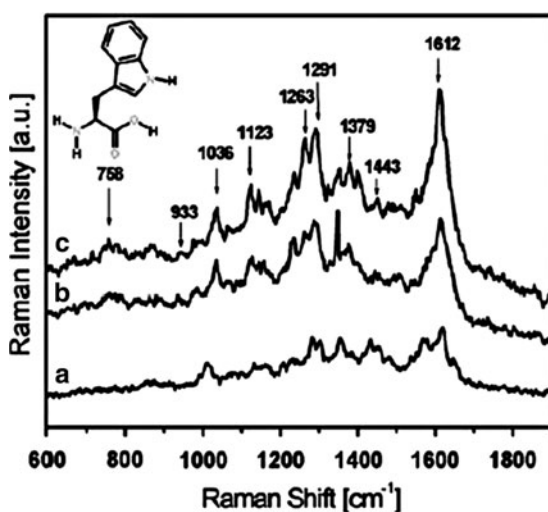


Fig. 12.14 SERS spectra of tryptophan-protected gold nanoparticles as synthesized at (a) 22°C, (b) 60°C, and (c) 80°C. The inset shows the molecular structure of tryptophan (From Iosin et al. 2010. By permission from Springer)

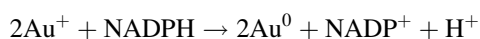
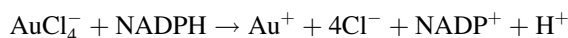
spectrum shows an enhancement of the band at $1,612\text{ cm}^{-1}$ (asymmetric stretching of the COO^- group). The authors concluded that the indole ring did not interact with the gold nanoparticles surface, while both amino and carboxy groups of tryptophan were the preferential terminal groups to attach onto the surface of the gold nanoparticles (Iosin et al. 2010).

12.2.2.2 Fungi

Biosynthesis of size-controlled gold nanoparticles using the fungus *Penicillium* sp. was carried out by bioreduction of AuCl_4^- ions, and led to the assembly and formation of intracellular gold nanoparticles with spherical morphology and monodispersity index. Temperature was an important physiological parameter for growth of *Penicillium* sp., and to control the size of the biosynthesized gold nanoparticles. FTIR spectra analysis of the fungus exposed to gold ions solution indicated that the intracellular reducing sugar played an important role in the occurrence of intracellular gold ions reduction and in the gold nanoparticle growth (Zhang et al. 2009).

12.2.2.3 Bacteria

An intracellular biosynthesis of gold nanoparticles by *Stenotrophomonas maltophilia* isolated from soil samples was reported by Nangia et al. (2009). This study suggested that biosynthesis and stabilization of gold nanoparticles via charge capping involved a NADPH-dependent reductase enzyme through electron shuttle process. The reduction of gold ions solution was probably processed in two steps. At the first step, AuCl_4^- ions were reduced to Au^+ species, and in a second step, the latter product was then reduced by NADPH to metallic gold and subsequently followed by the encapsulation of gold nanoparticles by charged NADP^+ species as shown in the equations below.



All the data in this study suggested a potential mechanism of gold nanoparticles synthesis by *Stenotrophomonas maltophilia* based on enzymatic reduction (Fig. 12.15).

12.2.2.4 Plants

A bioreductive approach of anisotropic gold using the phyllanthin extract with tunable optical properties has been studied (Kasthuri et al. 2009). The presence of

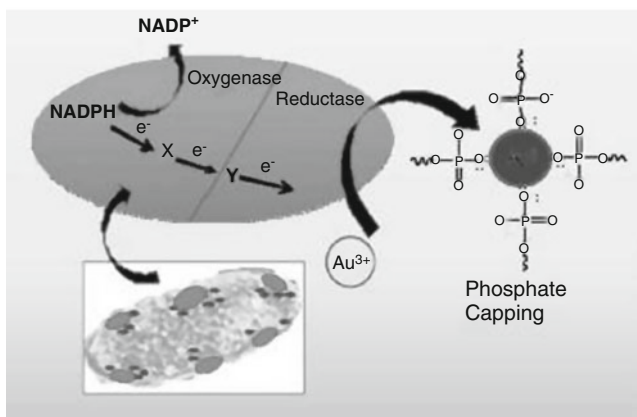


Fig. 12.15 Proposed synthesis mechanism of GNPs by *Stenotrophomonas maltophilia* through enzymatic reduction (From Nangia et al. 2009. By permission of American Institute of Physics)

a small amount of phyllanthin extract led to a slow reduction of AuCl_4^- ions favoring the formation of triangular- or hexagonal-shaped nanoparticles. However, a large amount of phyllanthin extract leads to a higher population of spherical nanoparticles. As in the case of silver nanoparticles (see Fig. 12.5), the electron-donating nature of the $-\text{OCH}_3$ group of the phyllanthin extract plays an important role in this process (Kasthuri et al. 2009).

12.2.2.5 Algae

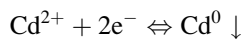
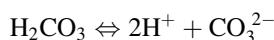
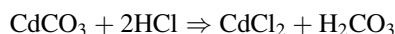
Shewanella algae cell extract produced spherical, triangular, truncated triangular, and hexagonal nanoplates with an edge length of 100–200 nm. Through the FTIR technique, it was shown that there was no difference in the FTIR spectra between the *S. algae* extract and the spherical gold particle suspension in a short period, indicating that the components of the *S. algae* extract did not participate in the formation of spherical gold nanoparticles. The FTIR spectra of the gold particle suspension after longer periods of interaction showed a different peak shape for the carbonyl group ($\text{C}=\text{O}$) centered at $1,645\text{ cm}^{-1}$ as the gold particle morphology changed from spherical nanoparticles to nanoplates. This result indicates that the carbonyl group in the *S. algae* extract contributes to the formation of gold nanoplates (Ogi et al. 2010).

12.2.3 Cadmium Nanoparticles

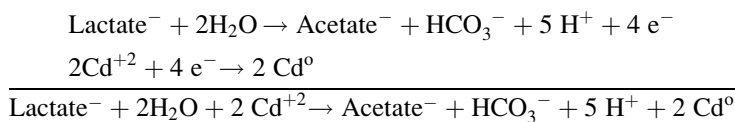
In this specific case of cadmium nanoparticles, no mechanistic aspects were found with fungi, yeast or plants.

12.2.3.1 Bacteria

NAD-independent lactate dehydrogenases (iLDHs) are commonly responsible for lactate utilization during the stationary phase of aerobic growth in *Lactobacillus plantarum*. In *L. plantarum*, two stereospecific nLDHs are present (LdhD, responsible for D-lactate; and LdhL, responsible for L-lactate). Under the experimental conditions used, the NAD-independent lactate dehydrogenase activities do not seem to be involved in this process (Goffin et al. 2004). Then, cadmium nanoparticles were prepared using *L. plantarum* from *Lactobacillus* strains found in buttermilk using the procedure adopted by Nair and Pradeep (2002) with slight modifications (Jha and Prassada 2010). The filtrate from buttermilk was diluted and a suitable sugar solution was added to the culture solution and this was allowed to incubate overnight. Then, to each culture, cadmium carbonate solution was added. After 3–4 days, the culture solution was observed to have distinctly marked deposits at the bottom of the conical flask. A remarkable change in pH was observed at this stage, which is currently under standardization. A possible synthetic mechanism was suggested as follows:



Although the authors do not say which part was the reductant, the reduction agents should be lactate (oxidation to acetate). The mechanistic aspect in lactate to acetate as suggested by Goffin et al. (2004) is the following. Lactate is oxidized to acetate by the bacteria by requiring transfer of four electrons to an exogenous electron acceptor (Marsili et al. 2008). Then, the final equation summing up both semi-reductions should be:



12.2.4 Copper Nanoparticles

No mechanistic aspects with fungi or other biological systems were found.

12.2.4.1 Bacteria

Synthesis for copper nanoparticles using *Pseudomonas stutzeri* biomass in an aqueous CuSO_4 solution has been studied (Varshney et al. 2010). High resolution

transmission electron microscopy analysis showed that the particles produced were almost spherical, a thin coating layer can be observed on all particles and the thickness is a few nanometers. This was an indication that the bacterial surface acts both as a reducing as well as capping agent and that these micrographs also demonstrate that Cu nanoparticles were well dispersed and stable for months.

12.2.4.2 Yeast

Biocatalytic reduction and removal of copper ions was observed in the aqueous–organic phase by induction of copper reductase in yeast grown in catabolic repression conditions by addition of inducer (copper ions) during the initial growth phase of *Saccharomyces cerevisiae*. Excess of glucose under catabolic repression conditions was used to induce the Cyt P450 in the yeast cells. The harvested biomass was lysed using cell disrupter and the microsomes were obtained. The most important parameters in the biocatalytic reduction were initial substrate concentration, time of reaction, initial pH of the reaction mixture (optimization of the enzyme) and concentration and time of addition of the inducer (yeast growth) (Chandran et al. 2001).

12.2.5 Iron Nanoparticles

The biosynthesis and mechanistic views were only found with plant extracts.

12.2.5.1 Plants

A green single-step synthesis of iron nanoparticles using tea (*Camellia sinensis*) polyphenols has been described (Hoag et al. 2009). The rapid reaction between polyphenols and ferric nitrate occurred at room temperature. As was previously discussed (Fig. 12.4), the plant polyphenols act as a reducing and a capping agent, resulting in green synthesized nano-scale-sized zero-valent iron particles.

12.2.6 Palladium Nanoparticles

In this biosynthesis, no mechanistic data with fungi or other organisms were found.

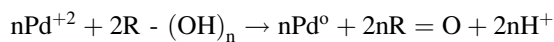
12.2.6.1 Bacteria

Desulfovibrio fructosivorans mutants were constructed using marker exchange mutagenesis, and the *D. fructosivorans* wild-type strain and mutant strains with deletions of NiFe hydrogenase, Fe hydrogenase, and Fe and NiFe hydrogenases

were grown anaerobically. Pd⁰ was visible within the periplasmic spaces of the parent strain and the Fe hydrogenase mutants; however, Pd clusters (in wild-type and Fe hydrogenase-negative cells) were distributed randomly throughout the whole width of the periplasmic space, but Pd nanoparticles were localized on the cytoplasmic membrane in NiFe hydrogenase-negative and double-mutant cells. In both treated cells – double-mutant and wild-type periplasmically – or intact ones, Pd clusters were associated only with the inner cytoplasmic membrane. This result and the hydrogenase localization suggested that the enzyme serves as a nucleation site and assists initial Pd nanoparticle growth by supplying the electrons for Pd⁺² reduction (Mikheenko et al. 2008). However, in another study using *Cupriavidus necator*, *Pseudomonas putida*, and *Paracoccus denitrificans* in palladium nanoparticle biosynthesis, no evidence was for the involvement of active hydrogenases or the participation of other active enzymes in nucleating Pd⁺² reduction (Bunge et al. 2010). Pd⁰ was located in the periplasmic space, and the size of the nanoparticles was defined by the distance of inner and outer membranes. From this, the authors postulated a hydrogenase-independent mechanism, contrary to findings with *Desulfovibrio* spp (Mikheenko et al. 2008). Although active enzymes appear not to be required, it is possible that the coordination of Pd⁺² to chemical groups on the cell surface contributes to nucleating the reduction process. This is an indication that the microbial surface operates as a scaffold for binding Pd⁺² before reduction to Pd⁰, with the cell surface acting as a type of biological stabilizer that prevents agglomeration (Bunge et al. 2010).

12.2.6.2 Plant

Palladium nanoparticles were obtained by a simple procedure using broth of *Cinnamomum camphora* leaf extract (Yang et al. 2010). According to the size distribution of the Pd nanoparticles, it was found that a higher concentration of Pd⁺² in the solution produces smaller Pd nanoparticles. Polyols such as flavones, terpenoids, and polysaccharides in the broth played a critical role in reduction of Pd⁺² ions. FTIR spectra of the reaction were indicative that polyols were oxidized to aldehydes or ketones confirming that the water-soluble fractions in the leaf broth played a leading role in bioreduction of the precursors. The proposed mechanism by Yang et al. (2010), in function of FTIR, was:



Where 2R-(OH)_n could be polyol and R=O could be an aldehyde or ketone.

12.2.7 Platinum Nanoparticles

In this case, only the mechanistic aspects with bacteria, fungi and plants are discussed.

12.2.7.1 Bacteria

Platinum nanoparticles were produced using a consortium of sulfate-reducing bacteria (SRB) cells that were suspended in a buffer (pH 7.6) under both anaerobic and aerobic environments with platinum salt [Pt(IV)-H₂PtCl₆] or [(Pt(II)-Na₂PtCl₄]. On the basis of the results obtained, a probable mechanism for the platinum nanoparticles was proposed (Fig. 12.16) (Riddin et al. 2009). The endogenous production of hydrogen/electrons via the oxidation of organic compounds, evolved by the cytoplasmic hydrogenase, would be rapid (Fig. 12.16, step 1). The periplasmic hydrogenase (Fig. 12.16, step 2) acting as an electron donor for the Pt (II) ion (Fig. 12.16, step 2). No inhibition of copper ions exerted on the bioreduction of the Pt(IV) ion was observed, while the rate limiting step was that of Pt(II) to Pt(0) further supporting the hypothesis that a periplasmic hydrogenase was involved using endogenously produced hydrogen during the reduction of Pt(II). Thus, a mixed consortium of SRB was capable of reducing Pt(IV) to Pt(0) via the intermediate cation Pt(II) in a two-step process: (1) A cytoplasmic hydrogenase, that was oxygen sensitive and not inhibited by Cu(II), required no exogenous electron donors and produced hydrogen (and excess electrons) from metabolite oxidation and/or Pt(IV) reduction, and (2) a periplasmic hydrogenase that was oxygen-tolerant/protected, was inhibited by Cu(II) and used the endogenously formed hydrogen donors [and Pt(II) ions] to form Pt(0) nanoparticles (Fig. 12.16).

Later on, in a study with cell-free and cell-soluble protein extract, it was demonstrated that in order to form stable platinum nanoparticles the ratio of the initial concentration of the platinum salt and total protein were also critical to control the shape and size (Riddin et al. 2010).

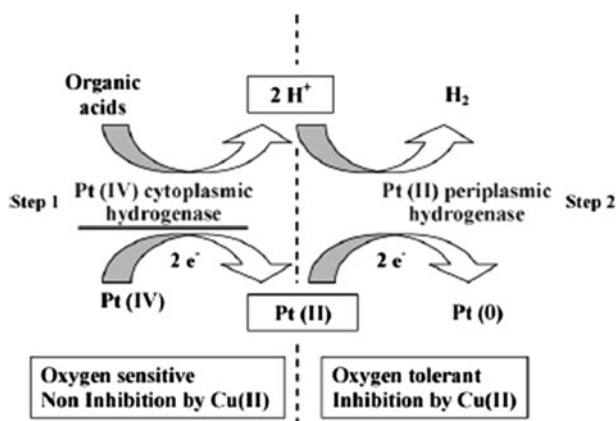
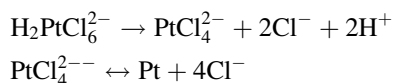


Fig. 12.16 Suggested mechanism for the double two-electron bioreduction of Pt(IV) into nanoparticles via an intermediary Pt(II) (From Riddin et al. 2009. By permission from Elsevier)

12.2.7.2 Fungi

The biosynthesis of platinum nanoparticles was obtained from cell-free extract of *Fusarium oxysporum* containing hydrogenase or purified enzyme and exposed to aqueous solutions of H_2PtCl_6 at the appropriate pH and temperature under an atmosphere of hydrogen (Govender et al. 2010). Experiments with cell-free extract from *F. oxysporum* with the platinum salts showed that there was a decrease in the concentration of the platinum salt after 1–3 h. Thereafter, there was a gradual increase in platinum salt concentration after 8 h incubation. This increase could have been as a result of, first, the bioreduction of H_2PtCl_6 to produce platinum with the release of HCl ions, followed by a reverse reaction and the in situ formation of PtCl_4^{2-} . By analogy, these authors with other results by Duff et al. (1995) proposed a two-stage reaction:



However, the study with purified hydrogenase enzyme under conditions at its optimum pH and temperature, showed no bioreduction. The cell-free extract contained other factors that were contributing to the bioreduction at the same conditions. The authors pointed out that a continuing study must be necessary to identify this intermediate and understand more about the mechanism of the platinum bioreduction (Govender et al. 2010).

12.2.7.3 Plants

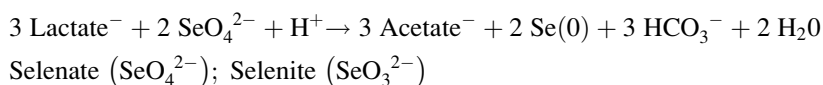
AQ leaf extract of *Diopyros kaki* was used as a reducing agent in the extracellular synthesis of platinum nanoparticles from an aqueous $\text{H}_2\text{PtCl}_6 \times 6\text{H}_2\text{O}$ solution. Results of this biosynthesis showed that platinum nanoparticles synthesized with *D. kaki* extract were surrounded by some metabolites like terpenoids, that have functional groups of amines, alcohols, ketones, aldehydes, and carboxylic acids, and not by proteins. The platinum nanoparticle synthesis using *D. kaki* is not an enzyme-mediated process because the rate of platinum nanoparticle synthesis was greatest at temperatures over 95°C and there were no peaks associated with proteins/enzymes on FTIR analysis. It appears more likely that the reduction of platinum ions and stabilization of synthesized platinum nanoparticles was the responsibility of many functional groups, which are present in various metabolites such as terpenoids and reducing sugars (Song et al. 2010).

12.2.8 Selenium Nanoparticles

The selenium nanoparticle biosynthesis and mechanistic views were only found with bacteria.

12.2.8.1 Bacteria

Bacillus arsenicoselenatis (strain E1H) and *Bacillus selenitireducens* (strain MLS10) isolated from a lake sediment were able to reduce oxyanions selenate-Se(VI) to selenite-Se(IV) and selenite-Se(IV) to selenium nanoparticles-Se(0), respectively, by a dissimilatory reduction with a concomitant of lactate to acetate and CO₂ (Blum et al. 1998). Growth of strain E1H in the oxidation of lactate to acetate consumed two electrons for reduction of Se(VI) to Se(IV); however, MLS10 consumed four electrons in the lactate oxidation for the Se(IV) reduction to Se(0). The co-culture of these two isolates was in agreement with the six-electron stoichiometry of complete selenate reduction to the elemental state as given by the equation (Oremland et al. 1994):



Species of selenate- and selenite-respiring bacteria, *Sulfurospirillum barnesii*, *Bacillus selenitireducens*, and *Selenihalanaerobacter shriftii*, growing with selenium oxyanions as the electron acceptor, formed extracellular granules of stable, uniform nanospheres of Se⁰. Intracellular packets of Se⁰ were also noted, but the extracellular Se⁰ accumulation was more common than the intracellular one. Because the Se⁰ nanospheres eventually migrate from the individual cells, the Se⁰ particles correspond to all the Se(VI) added at the initial incubation time. This also suggests that the external and internal Se⁰ nanospheres arise independently of each other and by different mechanisms. The external nanosphere accumulation is probably directly tied to the respiratory Se reductases (Oremland et al. 2004).

The reduction of Se (IV) by *Klebsiella pneumoniae* and the formation of intracellular selenium nanoparticles were investigated. The appearance of a red color in the culture flasks suggested the formation of elemental selenium. *K. pneumoniae* cells containing the red selenium particles which were disrupted using a wet heat sterilization process (Fesharaki et al. 2010). Probably, a similar mechanism as described for *Bacillus selenitireducens* (Oremland et al. 1994) is also applied.

Bacillus cereus generated selenium nanoparticles by transformation of toxic selenite (SeO₃²⁻) anions into red elemental selenium (Se⁰) under aerobic conditions. Microscopic analysis showed spherical Se⁰ nanospheres adhering to bacterial biomass (intracellular) as well as free particles (extracellular). Data suggested a hypothetical mechanism for the biogenesis of selenium nanoparticles involving membrane-associated reductase enzyme(s) that reduces selenite (SeO₃²⁻) to Se⁰ through an electron shuttle enzymatic metal reduction process as shown in Fig. 12.17 (Dhanjal and Cameotra 2010).

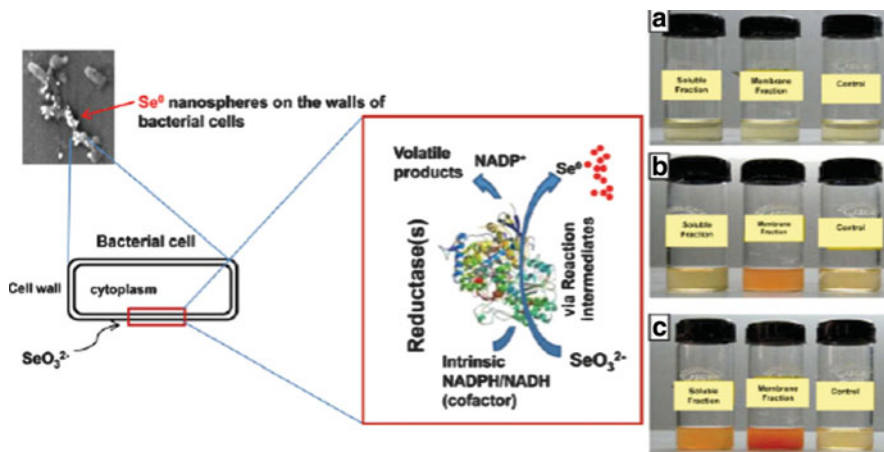


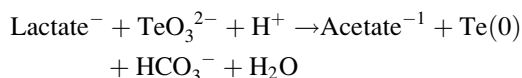
Fig. 12.17 Schematic representation of proposed mechanism of biogenesis of Selenium (Se⁰) nanospheres. (a) Selenite reduction at 0 h. (b) Formation of red elemental selenium in membrane fraction after 3–4 h of incubation. (c) Prolonged incubation of 12 h resulted also in formation of red elemental selenium in soluble fraction (From Dhanjal and Cameotra 2010. By permission from BioMed Central)

12.2.9 Tellurium Nanoparticles

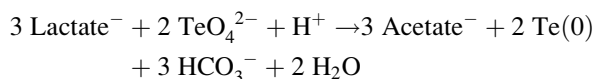
In the case of tellurium nanoparticles, biosynthesis was only found the mechanistic aspect involving bacteria.

12.2.9.1 Bacteria

Tellurium occurs in nature in four oxidation states: 6, 4, 0, and 2. The first two form the partially soluble oxyanions tellurate [TeO_4^{2-} , or Te(VI)] and tellurite [TeO_3^{2-} , or Te(IV)], and with respect to the latter two, the occurrence of native tellurium [Te(0)] is rare. Two anaerobes previously shown to be capable of respiring oxyanions of selenium also achieve growth by reduction of either tellurate [Te(VI)] or tellurite [Te(IV)] to elemental tellurium [Te(0)]. Those tellurium nanoparticles formed by *Bacillus selenitireducens* were initially nanorods, which cluster together forming larger rosettes composed of numerous individual shards. In contrast, *Sulfurospirillum barnesii* forms extremely small, irregularly shaped nanospheres that coalesce into larger composite aggregates (Baesman et al. 2007). The linkage of lactate oxidation to these reductions demonstrated that these Te derivatives served as terminal electron acceptors for anaerobic respiration. The biological oxidation of organic matter using Te(IV) as an electron acceptor support the growth of *B. selenitireducens*, and following the stoichiometry:



Growth of *S. barnesii* on lactate and Te(VI) also following the stoichiometry:



12.2.10 Titanium Nanoparticles

The biosynthesis and mechanistic aspect for titanium nanoparticles synthesis were only found with bacteria.

12.2.10.1 Bacteria

Titanium dioxide was added to curdled milk and whey from boiled milk that contained lactic acid bacteria, and with extra sugar after a few days the titanium nanoparticles were deposited in the flask. Nanoparticles containing the culture solution was filtered under the laminar flow through filter paper (Prasad et al. 2007). The nanotransformation from *Lactobacillus sporogens* was found superior to the *Lactobacilli* and was less expensive, more reproducible, emphatically least time-consuming and a truly green approach, and probably follows the same type of mechanisms as other metallic nanoparticles (Jha and Prasad 2010).

12.3 Antibacterial Potential of Metallic Nanoparticles

Silver nanoparticles exhibit special chemical and physical properties and have been appearing in the recent years as a possible new antibiotic or with other biological activities, since is possible to use them in wound dressing, medical tools, textiles, etc., and escape from antibiotic resistance (Durán et al. 2005, 2010a, b, c, 2011; Nair and Laurencin 2007; Singh et al. 2009; Rai et al. 2009; Dastjerdi and Montazer 2010; Vijayaraghavan and Nalini 2010; Marcato and Durán 2011). One important fact is that silver nanoparticles with different shapes and sizes exhibit variable antimicrobial activity. However, the mechanisms of antimicrobial activity of silver ions and silver nanoparticles, and their toxicity to human tissues, are not fully characterized. A recent review evaluated the potential use of silver nanoparticles to control pathogens with emphasis on their action against pathogenic bacteria, their toxicity and possible mechanisms of action (Durán et al. 2010b). In the last 3 years, many important results with silver nanoparticles on antibacterial activities have been published. Now we will discuss the most recent results on biogenic metallic nanoparticles and their antimicrobial activities.

Many aspects of the inhibitory effect of silver ions have been discussed previously, but silver nanoparticles also have inhibitory and lethal effects on bacterial species such as *E. coli*, *S. aureus* and even against yeast (Durán et al. 2010b and references therein).

Raffi et al. (2008) observed that silver nanoparticles were completely cytotoxic to *E. coli* at a low concentration. Gade et al. (2008) produced silver nanoparticles by extracellular biosynthesis using *Aspergillus niger* isolated from soil and these were cytotoxic to *E. coli*. A recent synthesis of silver nanoparticles using a reduction of aqueous silver ions with the culture supernatants of *Staphylococcus aureus* found them to be active against a methicillin-resistant *Staphylococcus aureus* (MRSA) followed by methicillin-resistant *Staphylococcus epidermidis* (MRSE) and *Streptococcus pyogenes*. However, when *Salmonella typhi* and *Klebsiella pneumoniae* were treated with silver nanoparticles, a moderate antimicrobial activity was observed (Nanda and Saravanan 2009). The synthesis of silver nanocrystals encapsulated in mesoporous silica nanoparticles showed a complete inhibition of bacterial growth (Liong et al. 2009).

The effect of shape on the antibacterial activity of silver nanoparticles was recently discussed studying the different synthesis of the silver nanoparticles (Sharma et al. 2009 and references therein). Silver nanoparticles with different shapes (triangular, spherical and rod) were tested against *E. coli*. The truncated triangular silver nanoplates displayed the strongest biocidal action when compared with spherical, rod-shaped nanoparticles and with silver ions. Furthermore, the antibacterial activity was also particle size-dependent (Sharma et al. 2009 and references therein). The influence of size was also related to the total surface area of the nanoparticles. Smaller particles with larger surface to volume ratios have greater antibacterial activity (Choi and Hu 2008).

The chemically synthesized silver nanoparticles exhibited high antibacterial activity against both Gram-negative *E. coli* and Gram-positive *S. aureus* bacteria. TEM images showed the interaction and bactericidal mechanism of silver nanoparticles. After interacting with bacteria, silver nanoparticles had adhered to the cell wall and penetrated the cell membrane, resulting in the inhibition of bacterial cell growth and multiplication due to their well-developed surface (Le et al. 2010). In this direction, on the basis of new research by Li et al. (2010), the action model of silver nanoparticles on *E. coli* was described as first making a break through the permeability of the outer membrane by lysis of cellular components. Then, second, the silver nanoparticles enter the inner membrane and inactivate respiratory chain dehydrogenases inhibiting respiration and growth of cells. Probably, silver nanoparticles could also affect some proteins and lipids and induce a collapse of the membrane, resulting in cell death (Le et al. 2010). This is very similar to that observed in biogenic silver nanoparticles acting as antimicrobial agents.

The availability of biosynthetically produced silver nanoparticles opened the possibility to investigate the association of these biological particles with antibiotics (Basavaraja et al. 2008; Parikh et al. 2008). A recent study was carried out with clindamycin associated to silver nanoparticles produced chemically or biosynthetically (Durán et al. 2008). Results with methicillin-resistant *S. aureus*

strains (MRSA) and *Staphylococcus epidemidis* showed a significant bactericidal activity of both formulations with slightly lower MIC values observed with the biosynthetic nanoparticles. In addition, a study on the effect of silver nanoparticles associated with clindamycin on leishmaniasis was published (Marcato et al. 2008). The effect of a combination of silver nanoparticles with different antibiotics was investigated against several bacterial strains. Silver nanoparticles were associated with penicillin G, amoxicillin, erythromycin, clindamycin, and vancomycin, etc. The association of antibiotics with silver nanoparticles increased the antibacterial activity against all bacteria strains studied (Durán et al. 2010b and references therein). Ampicillin, gentamycin, kanamycin, streptomycin and vancomycin were tested with silver nanoparticles produced from *Phoma glomerata*, and a synergistic activity was observed with *E. coli* and *Pseudomonas aeruginosa* (Birla et al. 2009).

In another study, silver nanoparticles as active carriers for chloramphenicol in polyvinylpyrrolidone showed substantially enhanced activity against clinically isolated *S. typhi* (Patil et al. 2009).

Silver ions exposed to a filtrate of *T. viride* produced silver nanoparticles and the antibacterial activities of a combination of these nanoparticles with ampicillin, kanamycin, erythromycin, and chloramphenicol showed an increase of the antibiotic effect. A mechanistic suggestion on the function of the synergistic effect between silver nanoparticles and ampicillin has been proposed (Fig. 12.18). First, the antimicrobial groups came into contact with silver nanoparticles forming a core with ampicillin molecules. The ampicillin molecules act on the cell wall producing a lysis increasing the penetration of the silver nanoparticles into the bacterium. Finally, the silver nanoparticles–ampicillin complex interacts with DNA which produced serious damage to the bacterial cells (Fayaz et al. 2010).

Revision of all the data published suggests possible mechanisms of the silver nanoparticles as antimicrobial activity, and a recent review discussed the three most common mechanisms of toxicity proposed to date which are: (1) the uptake of free silver ions followed by disruption of ATP production and DNA replication, (2) the silver nanoparticle and silver ion generation of reactive oxygen species (ROS), and (3) silver nanoparticle direct damage to cell membranes (Marambio-Jones and Hoek 2010 and references therein). Figure 12.19 summarizes all these hypotheses in one scheme.

Recently, a review focuses on the work done in the last few years developing gold nanoparticles as therapeutics and diagnostic agents (Arvizo et al. 2010). These particles also exhibit antibacterial activity. Das et al. (2009) studied the antimicrobial activity of gold nanoparticles, produced by a native *Rhizopus oryzae* strain, against *P. aeruginosa*, *E. coli*, *B. subtilis*, *S. aureus*, *Salmonella* sp., *S. cerevesiae*, and *C. albicans* by the cup-plate method. Exposure of microbial cells to gold nanoparticles resulted in a significant decrease in cell viability compared to the control cells. The SEM images of cells exposed to gold nanoparticles showed morphological changes compared to that of the control. After incubation with the nanoparticles, the integrity of most of the microbial cells was lost, indicating irreversible cell damage and ultimate cell death.

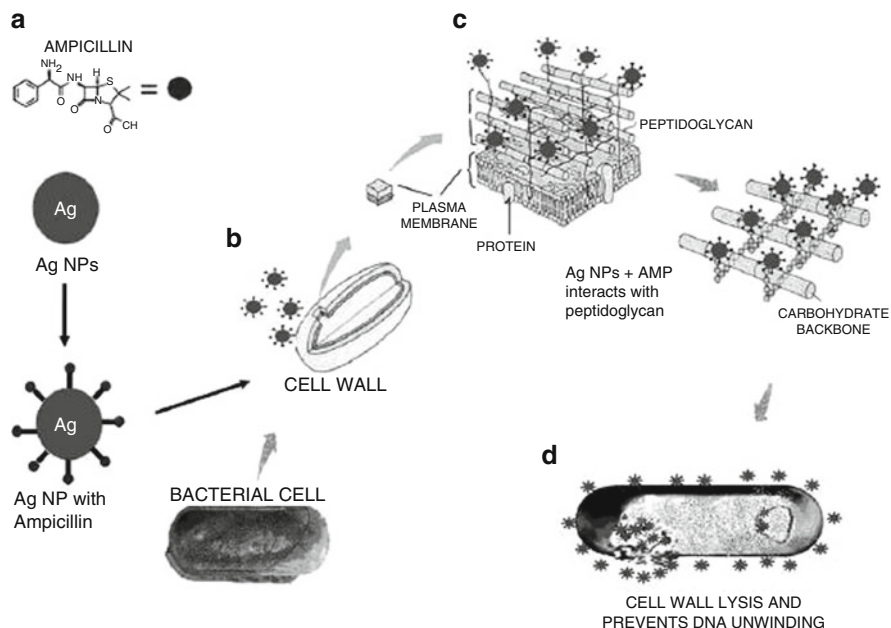


Fig. 12.18 Synergistic activity of silver nanoparticles with ampicillin (*Amp*) against bacteria. (a) Formation of core silver nanoparticles with ampicillin. (b) Interaction of silver nanoparticles complex over the cell wall of bacteria. (c) Silver nanoparticles–Amp complex inhibits the formation of cross-links in the peptidoglycan layer (which provides rigidity to the cell wall), leading to cell wall lysis. (d) Silver nanoparticles–Amp complex prevents the DNA unwinding (From Fayaz et al. 2010.. By permission from Elsevier)

The antimicrobial activity of silver nanoparticles and platinum nanoparticles, stabilized with sodium dodecyl sulfate and poly(*N*-vinyl-2-pyrrolidone), against *S. aureus* and *E. coli* was studied. The growth of Gram-positive (*S. aureus*) and Gram-negative (*E. coli*) bacteria was inhibited by silver nanoparticles, but the silver nanoparticles either stabilized with sodium dodecyl sulfate or the platinum nanoparticles with any stabilizer did not show antimicrobial activity (Cho et al. 2005).

The selenium nanoparticles prepared by *Klebsiella pneumoniae* exhibited a good antimicrobial effect on fungi such as *Aspergillus terreus*, *A. niger*, *A. flavus*, *A. fumigatus*, *Malassezia sympodialis* and *M. furfur*, with a MIC ranging from 10 to 260 $\mu\text{g mL}^{-1}$ for all isolate microorganisms (Shakibaie et al. 2010).

The antibacterial activity of silver and copper nanoparticles (both synthesized chemically) was compared for various strains of microorganisms (*Escherichia coli*, *Bacillus subtilis*, and *Staphylococcus aureus*). The effectiveness of silver nanoparticles was higher than those observed with copper nanoparticles for all *E. coli* and *S. aureus* strains selected for this study. However, copper nanoparticles showed a significantly higher activity than silver nanoparticles against *B. subtilis* (Ruparelia et al. 2008).

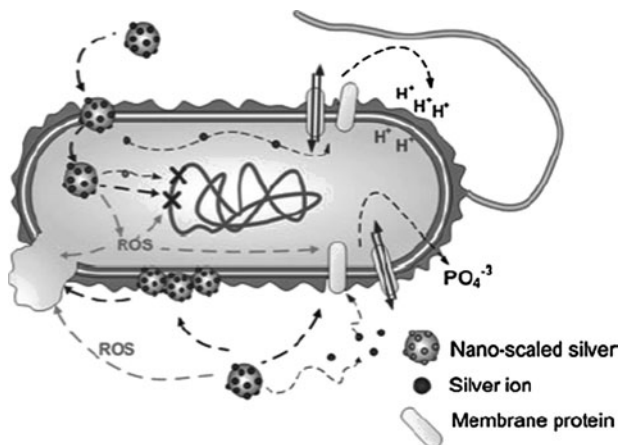


Fig.12.19 Diagram summarizing nano-scaled silver interaction with bacterial cells. Nano-scaled silver may (1) release silver ions and generate ROS; (2) interact with membrane proteins affecting their correct function; (3) accumulate in the cell membrane affecting membrane permeability; and (4) enter into the cell where it can generate ROS, release silver ions, and affect DNA. Generated ROS may also affect DNA, cell membrane, and membrane proteins, and silver ion release will likely affect DNA and membrane proteins (From Marambio-Jones and Hoek 2010. By permission from Springer)

The effective *E. coli* inactivation by Fe⁰ nanoparticles (chemically synthesized) was compared with several iron compounds. No significant inactivation of *E. coli* was achieved with iron oxide (magnetite) nanoparticles and microscale Fe⁰ powder. In contrast, Fe⁰ nanoparticles showed strong activity. These results suggest that the biocidal effect of Fe⁰ nanoparticles originates from both a size-related physical property of the nanoparticles and a chemical interaction of elemental iron with *E. coli*. Furthermore, Fe⁰ nanoparticles showed a higher bactericidal activity than silver nanoparticles (Lee et al. 2008).

12.4 Cytotoxicity and Toxicity of Metallic Nanoparticles

As described in the previous section, the beneficial effect on human health of metallic nanoparticles is clear but it does not mean that they are risk-free (El-Ansary and Al-Daihan 2009; Hussain and Schlager 2009). The small particle size possibly leads them to penetrate easily by inhalation, by oral ingestion and probably by contact with the skin, and disseminate throughout the body. In many cases, the cytotoxicity will depend on the support of the nanoparticles matrix or the concentration (Durán et al. 2010b).

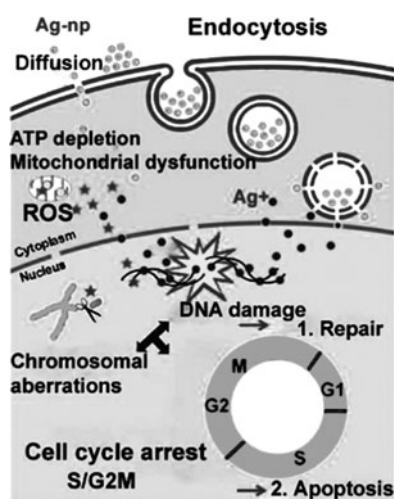
Recently, ActicoatTM (commercial silver support) was used in post-cardiac surgery for mediastinitis, and in all four patients, negative cultures were obtained within a maximum of 72 h (Totaro and Rambaldini 2009). Acute toxicity of

different metallic nanoparticles in vitro using a rat liver-derived cell line or neural cells treated with different silver nanoparticle sizes resulted in dose-dependent cytotoxicity. The toxicity on the C18-4 cells of a mouse cell line with spermatogonial stem cell characteristics showed that silver nanoparticles were the most toxic among other metallic (molybdenum, and aluminum) nanoparticles tested. Toxicity and biocompatibility of silver nanoparticles were evaluated in vivo using zebrafish embryos, and the results showed the same as before, that is dose-dependence of silver nanoparticles. Another important fact was observed in an alga where it was found that silver nanoparticle toxicity was mediated by silver ions (Durán et al. 2010b and references therein). Some reports have summarized the hazardous effects of silver nanoparticles to human health through biodistribution, organ accumulation, degradation and possible adverse effects and toxicity (Panyala et al. 2008; Chen and Schluesener 2008).

A possible mechanism of toxicity using human lung fibroblast and glioblastomacells of silver nanoparticles has been proposed. The mechanism involves disruption of the mitochondrial respiratory chain leading to production of reactive oxygen species (ROS) and interruption of ATP synthesis, which in turn cause DNA damage (Fig. 12.20) (AshaRani et al. 2009).

The immunological response of macrophages to gold and silver nanoparticles showed that both nanoparticles enter the cells but only gold nanoparticles up-regulate the expressions of pro-inflammatory genes interleukin-1 (IL-1), interleukin-6 (IL-6), and tumor necrosis factor (TNF- α). Probably, the gold nanoparticles might adsorb serum protein due to partial negative charge and enter cells via a complex endocytotic pathway, resulting in higher cytotoxicity and immunological activity for gold rather than silver nanoparticles (Yen et al. 2009). Using of gene expression data, it was suggested that silver nanoparticles may produce neurotoxicity by generating free radical-induced oxidative stress (Rahman et al. 2009).

Fig.12.20 A possible mechanism of toxicity which involves disruption of the mitochondrial respiratory chain by silver nanoparticles leading to production of ROS and interruption of ATP synthesis, which in turn cause DNA damage (From AshaRani et al. 2009. By permission from ACS Publications)



Histopathological examinations of inflammatory response and pulmonary function changes in rats treated by inhalation exposure to silver nanoparticles indicated dose-dependent increases in lesions related to silver nanoparticle exposure, such as infiltrated mixed cell and chronic alveolar inflammation, including thickened alveolar walls and small granulomatous lesions (Sung et al. 2008, 2009).

In vitro interactions of 7–20 nm spherical silver nanoparticles with primary fibroblasts and primary liver cells remained unaltered up to 25 and 100 $\mu\text{g mL}^{-1}$ silver nanoparticles, respectively. Many biological processes and morphological transformations have been suggested to the effect that, although silver nanoparticles seem to enter the eukaryotic cells, cellular antioxidant mechanisms protect the cells from possible oxidative damage (Carlson et al. 2008; Arora, et al. 2009).

Silver nanoparticles prepared by dispersing them in fetal bovine serum showed cytotoxicity to cultured RAW264.7 cells by cellular apoptosis, decreasing intracellular glutathione level, increasing NO secretion, increasing TNF- α in protein and gene levels, and increasing gene expression of matrix metalloproteinases. All the data suggested that silver nanoparticles were ionized in the cells to cause cytotoxicity by a Trojan-horse type mechanism (Park et al. 2010).

Investigations on the in vitro cytotoxicity of gold nanoparticles showed that they induced cytotoxicity in Cos-1 cells and in human dermal fibroblasts, but not in human leukemic cells or murine macrophages, where particles were taken up and stored in intracellular perinuclear vesicles. Gold nanoparticles induced a mild cytotoxicity in human alveolar type-II (ATII)-like cell lines A549 and NCIH441 (Uboldi et al. 2009, and references therein).

The cytotoxicity of the selenium nanoparticles prepared by *Bacillus* sp. MSh-1 was evaluated in vitro against the fibrosarcoma cell line (HT-1080), and the cytotoxicity analysis showed a direct dose–response effect; the higher the concentration, the higher the toxicity. The presence of a low dose level (10 $\mu\text{g mL}^{-1}$) showed a small cytotoxicity with a viability percentage of more than 80% (Shakibaie et al. 2010). Apoptosis had been shown previously with selenium nanoparticles (Chen et al. 2008).

Previous data of copper nanoparticles (chemically synthesized) showed, in vivo, a potent toxic effect (cytotoxic and genotoxic) (Chen et al. 2006). Earlier, the effect of copper nanoparticles inducing single-stranded breaks in cultured human lung cells was reported (Midander et al. 2009), and also, recently, in cultured cancer cell lines (Studer et al. 2010). The DNA degradation potential and anti-cancer activities of copper nanoparticles through singlet oxygen have been reported. The same authors observed that the copper nanoparticles exhibited a cytotoxic effect towards human histiocytic lymphoma cell (U937) and human cervical cancer (Hela cells) by inducing apoptosis (Jose et al. 2011).

As far as we know, no cytotoxic or toxic studies with nanoparticles of cadmium, copper, iron, palladium, platinum, tellurium or titanium have been found in the literature.

12.5 Industrial Applications

The strong antibacterial activity of silver nanoparticles discussed in this chapter can be as coatings and on certain implants and other applications such as treatment of wounds and burns, in contraception and also marketed as a water disinfectant and a room spray. Thus, the use of silver nanoparticles appears to be an important issue in medicine and related fields. Many aspects related to biodistribution, organ accumulation, degradation, possible adverse effects and toxicity have been reviewed focusing on major questions associated with the increased medical use of silver nanoparticles and related nanomaterials (Chen and Schluesener 2008).

Metal nanoparticles have many physicochemical and opto-electronic properties. Due to all these diverse properties, nanoparticles have multiple applications in various fields like electronics, agriculture, and medicine. Some of the nanoparticles that can be produced by fungi may be of particular relevance to new and emerging technologies. The use of silver coatings in solar absorption systems has already been mentioned (Durán et al. 2010c). Other applications in such areas include the use of gold nanoparticles as precursors to coatings for electronic applications (Mukherjee et al. 2001) and platinum nanoparticles in the production of fuel cells (Riddin et al. 2006). Applications in the field of medicine includes the formulations of many potential antimicrobial agents, which are effective against many human pathogens including multidrug-resistant bacteria (Ingle et al. 2008).

Most studies in the literature on the production of sterile materials (fabrics, textiles), using metal nanoparticles involve production by chemical methods (Gao and Cranston 2008; Gupta et al. 2010). One which was biogenic produced silver nanoparticles (from *F. oxysporum*) for sterilized fabrics (Durán et al. 2007) by the impregnation of biogenic silver nanoparticles in cotton and polyester fabrics. The padding method appeared to yield more homogeneous impregnations than the centrifugation process (Huber et al. 2009) with high resistance to washing with maintainance of the antibacterial activity, demonstrating the large adhesion of these particles in the fabric fibers probably due to the fungal protein capping the silver nanoparticles (Durán et al. 2005). Many fabric materials having silver nanoparticles are commercially available but they release the silver nanoparticles to the environment at the first washing.

Silver nanoparticle applications in fabrics, cosmetics and agriculture were recently discussed by Rai et al. (2011).

12.6 Conclusions

This chapter has described biogenic metallic nanoparticle synthesis and their mechanistic aspects in the syntheses and in their antimicrobial activities. Although many aspects have already been studied with silver and gold nanoparticles, many questions are still open to discussion related to the final consequence of the other

metallic nanoparticles such as cadmium, copper, iron, palladium, platinum, tellurium or titanium.

In the applications dealt with, the use of silver nanoparticles appears to be an important issue in medicine and related fields, such as coatings on certain implants, treatment of wounds and burns, in contraception and as a water disinfectant and a room spray. Many aspects related to biodistribution, organ accumulation, degradation and adverse effects were reviewed focusing on major questions associated with the medical use of silver nanoparticles and related nanomaterials. The physicochemical and opto-electronic properties of metal nanoparticles have multiple applications in various fields like electronics, agriculture and medicine. The uses of metallic nanoparticles in coating in solar absorption systems, or for electronic applications and production of fuel cells were also discussed. Their applications as antimicrobials against multidrug-resistant bacteria, and production of sterile materials are no less important than the previous issues mentioned.

Acknowledgements Support from FAPESP, CNPq and DST/CNPq Brazil-India Project is acknowledged.

References

- Arora, S., J. Jain, J.M. Rajwade and K.M. Paknikar. (2009). Interactions of silver nanoparticles with primary mouse fibroblasts and liver cells. *Toxicol. Appl. Pharmacol.* 236: 310–318.
- Arvizo, R., R. Bhattacharya and P. Mukherjee. (2010). Gold nanoparticles: opportunities and challenges in nanomedicine. *Expert Opin. Drug Deliv.* 7: 753–763.
- Arya, V. (2010). Living systems: eco-friendly nanofactories. *Digest J. Nanomater. Biostruct.* 5: 9–21.
- AshaRani, P.V., G.L.K. Mun, M.P. Hande and S. Valiyaveetti. (2009). Cytotoxicity and genotoxicity of silver nanoparticles in human cells. *ACS Nano.* 3: 279–290.
- Baesman, S.M., T.D. Bullen, J. Dewald, D. Zhang, S. Curran, F.S. Islam, T.J. Beveridge and R.S. Oremland. (2007). Formation of tellurium nanocrystals during anaerobic growth of bacteria that use the oxyanions as respiratory electron acceptors. *Appl. Environ. Microbiol.* 73: 2135–2143.
- Bar, H., D.K. Bhui, G.P. Sahoo, P. Sarkar, S.P. De and A. Misra. (2009a). Green synthesis of silver nanoparticles using latex of *Jatropha curcas*. *Colloids Surf. A Physicochem. Eng. Asp.* 339: 134–139.
- Bar, H., D.K. Bhui, G.P. Sahoo, P. Sarkar, S. Pyne and A. Misra. (2009b). Green synthesis of silver nanoparticles using seed extract of *Jatropha curcas*. *Colloids Surf. A Physicochem. Eng. Asp.* 348: 212–216.
- Basavaraja, S., S.D. Balaji, A. Lagashetty, A.H. Rajasab and A. Venkataraman. (2008). Extracellular biosynthesis of silver nanoparticles using the fungus *Fusarium semitectum*. *Mater. Res. Bull.* 43: 1164–1170.
- Bhattacharjee, R.R., A.K. Das, D. Haldar, S. Si, A. Banerjee and T.K. Mandal. (2005). Peptide-assisted synthesis of gold nanoparticles and their self-assembly. *J. Nanosci. Nanotechnol.* 5: 1141–1147.
- Bhattacharya, R. and P. Mukherjee. (2008). Biological properties of “naked” metal nanoparticles. *Adv. Drug Deliv. Rev.* 60: 1289–1306.

- Birla, S.S., V.V. Tiwari, A.K. Gade, A.P. Ingle, A.P. Yadav and M.K. Rai. (2009). Fabrication of silver nanoparticles by and its combined effect against *Escherichia coli*, *Pseudomonas aeruginosa*, *Phoma glomerata* and *Staphylococcus aureus*. *Lett. Appl. Microbiol.* 48: 173–179.
- Blanco-Andujar, C., D. Tung and N.T.K. Thanh. (2010). Synthesis of nanoparticles for biomedical applications. *Annu. Rep. Prog. Chem. Sect. A.* 106: 553–568.
- Blum, J.S., A.B. Bindi, J. Buzzelli, J.F. Stolz and R.S. Oremland. (1998). *Bacillus arsenico-selenatis*, sp. nov., and *Bacillus selenitireducens*, sp. nov.: two haloalkaliphiles from Mono Lake, California that respire oxyanions of selenium and arsenic. *Arch. Microbiol.* 171: 19–30.
- Brown, S. (2001). Protein-mediated particle assembly. *Nano Lett.* 1: 391–394.
- Bunge, M., L.S. Søjberg, A.S.E. Rotaru, D. Gauthier, A.T. Lindhardt, G. Hause, K. Finster, P. Kingshott, T. Skrydstrup and R.L. Meyer. (2010). Formation of palladium(0) nanoparticles at microbial surfaces. *Biotechnol. Bioeng.* 107: 206–215.
- Carlson, C., S.M. Hussain, A.M. Schrand, L.K. Braydich-Stolle, K.L. Hess, R.L. Jones and J.J. Schlager. (2008). Unique cellular interaction of silver nanoparticles: Size-dependent generation of reactive oxygen species. *J. Phys. Chem. B.* 112: 13608–13619.
- Chandran, C.B., T.V. Subramanian and P.A. Felse. (2001). Chemometric optimization of parameters for biocatalytic reduction of copper ion by a crude enzyme lysate of *Saccharomyces cerevisiae* grown under catabolic repression conditions. *Biochem. Eng. J.* 8: 31–37.
- Chen, X. and H.J. Schluesener. (2008). Nanosilver: a nanoparticle in medical application. *Toxicol. Lett.* 176: 1–12.
- Chen, Z., H. Meng, G. Xing, C. Chen, Y. Zhao, G. Jia, T. Wang, H. Yuan, C. Ye, F. Zhao, Z. Chai, C. Zhu, X. Fang, B. Ma and L. Wan. (2006). Acute toxicological effects of copper nanoparticles *in vivo*. *Toxicol. Lett.* 163: 109–120.
- Chen, T., Y.S. Wong, W. Zheng, Y. Bai and L. Huang. (2008). Selenium nanoparticles fabricated in *Undaria pinnatifida* polysaccharide solutions induce mitochondria-mediated apoptosis in A375 human melanoma cells. *Colloids Surf. B Biointerfaces.* 67: 26–31.
- Cho, K.H., J.E. Park, T. Osaka and S.G. Park. (2005). The study of antimicrobial activity and preservative effects of nanosilver ingredient. *Electrochim. Acta* 51: 956–960.
- Choi, O. and Z. Hu. (2008). Size dependent and reactive oxygen species related nanosilver toxicity to nitrifying bacteria. *Environ. Sci. Technol.* 42: 4583–4588.
- Das, S.K., A.R. Das and A.K. Guha. (2009). Gold nanoparticles: microbial synthesis and application in water hygiene management. *Langmuir* 25: 8192–8199.
- Dastjerdi, R. and M. Montazer. (2010). A review on the application of inorganic nano-structured materials in the modification of textiles: focus on anti-microbial properties. *Colloids Surf. B Biointerface* 79: 5–18.
- Dhanjal, S. and S.S. Cameotra. (2010). Aerobic biogenesis of selenium nanospheres by *Bacillus cereus* isolated from coalmine soil. *Microb. Cell Fact.* 9: 52. doi:10.1186/1475-2859-9-52.
- Duff, D.G., P.P. Edwards and B.F.G. Johnson. (1995). Formation of a polymer-protected platinum sol: a new understanding of the parameters controlling morphology. *J. Phys. Chem.* 99: 15934–15944.
- Durán, N., P.D. Marcato, O.L. Alves, G.I.H. De Souza and E. Esposito. (2005). Mechanistic aspects of biosynthesis of silver nanoparticles by several *Fusarium oxysporum* strains. *J. Nanobiotechnol.* 3: 8. doi:10.1186/1477-3155-3-8.
- Durán, N., P.D. Marcato, G.I.H. De Souza, O.L. Alves and E. Esposito. (2007). Antibacterial effect of silver nanoparticles produced by fungal process on textile fabrics and their effluent treatment. *J. Biomed. Nanotechnol.* 3: 203–208.
- Durán, N., P.D. Marcato, R. De Conti, O.L. Alves and M. Brocchi. (2008). Silver nanoparticles: control of pathogens, toxicity and cytotoxicity. *Nanotoxicology* 2: S32.
- Durán, N., P.D. Marcato, A. Ingle, A. Gade and M. Rai. (2010a). Fungi-mediated synthesis of silver nanoparticles: characterization processes and applications. In *Progress in Mycology* (Mahendra Rai and George Kövics, Eds), Scientific Publishers, Jodhpur, India, Ch 16, pp. 425–449.

- Durán, N., P.D. Marcato, R. De Conti, O.L. Alves, F.T.M. Costa, and M. Brocchi. (2010b). Potential use of silver nanoparticles on pathogenic bacteria, their toxicity and possible mechanisms of action. *J. Braz. Chem. Soc.* 21: 949–959.
- Durán, N., P.D. Marcato, A. Ingle, A. Gade and M. Rai. (2010c). Fungi-mediated synthesis of silver nanoparticles: characterization processes and applications. In *Progress in Mycology* (Mahendra Rai and George Kövics, Eds), Scientific Publishers, Jodhpur, India, Ch 16, pp. 425–449. ISBN: 978-81-7233-636-3.
- Durán, N., P.D. Marcato, M. Durán, A. Yadav, A. Gade and M. Rai. (2011). Mechanistic aspects in the biogenic synthesis of extracellular metal nanoparticles by peptides, bacteria, fungi and plants. *Appl. Microbiol. Biotechnol.* 90: 1609–1624.
- Egorova, E.M. and A.A. Revina. (2000). Synthesis of metallic nanoparticles in reverse micelles in the presence of quercetin. *Colloids Surf. A Physicochem. Eng. Asp.* 168: 87–96.
- El-Ansary, A. and S. Al-Daihan. (2009). On the toxicity of therapeutically used nanoparticles: an overview. *J. Toxicol.* 2009: 754–810.
- Fayaz, A.M, K. Balaji, M. Girilal, R. Yadav, P.T. Kalaichelvan and R. Venketesan. (2010). Biogenic synthesis of silver nanoparticles and their synergistic effect with antibiotics: a study against gram-positive and gram-negative bacteria. *Nanomedicine NBM.* 6: 103–109.
- Fesharaki, P.J., P.Nazari, M. Shakibaie, S. Rezaie, M. Banoe, M. Abdollahi and A.R. Shahverdi. (2010). Biosynthesis of selenium nanoparticles using *Klebsiella pneumoniae* and their recovery by a simple sterilization process. *Braz. J. Microbiol.* 41: 461–466.
- Gade, A.K., P. Bonde, A.P. Ingle, P.D. Marcato, N. Durán and M.K. Raí. (2008). Exploitation of *Aspergillus niger* for synthesis of silver nanoparticles. *J. Biobased Mater. Bioenergy* 2: 243–247.
- Gade, A., A. Ingle, C. Whiteley and M. Rai. (2010a). Mycogenic metal nanoparticles: progress and applications. *Biotechnol. Lett.* 32: 593–600.
- Gade, A., S. Gaikwad, V. Tiwari, A. Yadav, A. Ingle and M. Rai. (2010b). Biofabrication of silver nanoparticles by *Opuntia ficus-indica*: *in vitro* antibacterial activity and study of the mechanism involved in the synthesis. *Curr. Nanosci.* 6: 370–375.
- Gao, Y. and R. Cranston. (2008). Recent advances in antimicrobial treatments of textiles. *Textile Res. J.* 78: 60–72.
- Goffin, P., F. Lorquet, M. Kleerebezem and P. Hols. (2004). Major role of NAD-dependent lactate dehydrogenases in aerobic lactate utilization in *Lactobacillus plantarum* during early stationary phase. *J. Bacteriol.* 186: 6661–6666.
- Govender, Y., T.L. Riddin, M. Gericke and C.G. Whiteley. (2010). On the enzymatic formation of platinum nanoparticles. *J. Nanopart. Res.* 12: 261–271.
- Gupta, A., K. Matsui, L. Jeng-Fan and S. Silver. (1999). Molecular basis for resistance to silver cations in *Salmonella*. *Nat. Med.* 5: 183–188.
- Gupta, B., R.A. Agarwal and M.S. Alam. (2010). Textile-based smart would dressing. *Indian J. Fibre Textile Res.* 35: 174–187.
- Hennebel, T., B.De Gussem, N. Boon and W. Verstraete. (2009). Biogenic metals in advanced water treatment. *Trends Biotechnol.* 27: 90–98.
- Hoag, G.E., J.B. Collins, J.L. Holcomb, J.R. Hoag, M.N. Nadagouda and S. Rajender, Varma, R.S. (2009). Degradation of bromothymol blue by ‘greener’ nano-scale zero-valent iron synthesized using tea polyphenols. *J. Mater. Chem.* 19: 8671–8677.
- Huber, S.C., P.D. Marcato, G. Nakazato, D. Martins and N. Durán. (2009). Textile fabrics loading biosynthetic silver nanoparticles: bactericidal activity against gram-positive and gram-negative bacteria. *CIFARP-2009, 7th. Intern. Congress of Pharm. Sci.*, 6–9 September, Riberão Preto, SP, 2009, Abstr. FQ 012.
- Hussain, S.M. and J.J. Schlager. (2009). Safety evaluation of silver nanoparticles: inhalation model for chronic exposure. *Toxicol. Sci.* 108: 223–224.
- Ingle, A., A. Gade, S. Pierrat, C. Sönnichsen and M. Rai. (2008). Mycosynthesis of silver nanoparticles using the fungus *Fusarium acuminatum* and its activity against some human pathogenic bacteria. *Curr. Nanosci.* 4: 141–144.

- Iosin, M., P. Baldeck and S. Astilean. (2010). Study of tryptophan assisted synthesis of gold nanoparticles by combining UV-Vis, fluorescence, and SERS spectroscopy. *J. Nanopart. Res.* doi: 10.1007/s11051-010-9869-6
- Jha, A.K. and K. Prasad. (2010). Biosynthesis of metal and oxide nanoparticles using Lactobacilli from yoghurt and probiotic spore tablets. *Biotechnol. J.* 5: 285–291.
- Jha, A.K., K. Prasad, K. Prasad and A.R. Kulkarni. (2009). Plant system: nature's nanofactory. *Colloids Surf. B Biointerfaces* 73: 219–223.
- Jose, G.P., S. Santra, S.K. Mandal and T.K. Sengupta (2011). Singlet oxygen mediated DNA degradation by copper nanoparticles: potential towards cytotoxic effect on cancer cells. *J. Nanobiotechnol.* 9: 1–8.
- Kalimuthu, K., R.S. Babu, D. Venkataraman, M. Bilal and S. Gurunathan. (2008) Biosynthesis of silver nanocrystals by *Bacillus licheniformis*. *Colloids Surf. B Biointerfaces* 65: 150–153.
- Kasthuri, J., K. Kathiravan and N. Rajendiran. (2009). Phyllanthin-assisted synthesis of silver and gold nanoparticles: a novel biological approach. *J. Nanopart. Res.* 11: 1075–1085.
- Korbekandi, H., S. Irvani and S. Abbasi. (2009). Production of nanoparticles using organisms. *Crit. Rev. Biotechnol.* 29: 279–306.
- Krishnaraj, C., E.G. Jagan, S. Rajasekar, P. Selvakumar, P.T. Kalaichelvan and N. Mohan. (2010). Synthesis of silver nanoparticles using *Acalypha indica* leaf extracts and its antibacterial activity against water borne pathogens. *Colloids Surf. B Biointerfaces* 76: 50–56.
- Krumov, N., I. Perner-Nochta, S. Oder, V. Gotcheva, A. Angelov and C. Posten. (2009). Production of inorganic nanoparticles by microorganisms. *Chem. Eng. Technol.* 32: 1026–1035.
- Kumar, V. and S.K. Yadav. (2009). Plant-mediated synthesis of silver and gold nanoparticles and their applications. *J. Chem. Technol. Biotechnol.* 84: 151–157.
- Kumar, S.A., M.K. Abyaneh, S.W. Gosavi, S.K. Kulkarni, R. Pasricha, A. Ahmad and M.I. Khan. (2007a). Nitrate reductase-mediated synthesis of silver nanoparticles from AgNO₃. *Biotechnol. Lett.* 29: 439–443.
- Le, A.T., L.T. Tam, P.D. Tam, P.T. Huy, T.Q. Huy, N.V. Hieu, A.A. Kudrinskiy and Y.A. Krutyakov. (2010). Synthesis of oleic acid-stabilized silver nanoparticles and analysis of their antibacterial activity. *Mat. Sci. Eng. C.* 30: 910–916.
- Lee, C., J.Y. Kim, W.I. Lee, K.L. Nelson, J. Yoon and D.L. Sedlak. (2008). Bactericidal effect of zero-valent iron nanoparticles on *Escherichia coli*. *Environ. Sci. Technol.* 42: 4927–4933.
- Li, S., Y. Shen, A. Xie, X. Yu, L. Qiu, L. Zhang and Q. Zhang (2007). Green synthesis of silver nanoparticles using *Capsicum annum* L. extract. *Green Chem.* 9: 852–858.
- Li, W.R., X.B. Xie, Q.S. Shi, H.Y. Zeng, Y.S. OU-Yang and Y.B. Chen. (2010). Antibacterial activity and mechanism of silver nanoparticles on *Escherichia coli*. *Appl. Microbiol. Biotechnol.* 85: 1115–1122.
- Lin, Z.Y., C.H. Zhou, J.M. Wu, J.Z. Zhou and L. Wang. (2005). A further insight into the mechanism of Ag⁺ biosorption by *Lactobacillus sp.* strain A09. *Spectrochim. Acta A Mol. Biomol. Spectrosc.* 61: 1195–1200.
- Liong, M., B. France, K.A. Bradley and J.I. Zink. (2009). Antimicrobial activity of silver nanocrystals encapsulated in mesoporous silica nanoparticles. *Adv. Mater.* 21: 1684–1689.
- Lukman, A.I., B. Gong, C.E. Marjo, U. Roessner and A.T. Harris. (2011). Facile synthesis, stabilization, and anti-bacterial performance of discrete Ag nanoparticles using *Medicago sativa* seed exudates. *J. Colloid Interface Sci.* 353: 433–444.
- Maarof, N.D., Z.M. Ali, N.M. Nor and M. Hassan. (2010). Isolation of NADP⁺- geraniol dehydrogenase from *Polygonum minus*. *Nat. Biotechnol. Sem.* (Kerala, Kampur) A34: 1–4.
- Marambio-Jones, C. and E.M.V. Hoek. (2010). A review of the antibacterial effects of silver nanomaterials and potential implications for human health and the environment. *J. Nanopart. Res.* 12: 1531–1551.
- Marcato, P.D. and N. Durán. (2011). Biogenic silver nanoparticles: applications in medicines and textiles and their health implications, In: *Metal Nanoparticles in Microbiology* (Mahendra Rai, Nelson Duran and Gordon Southam, Eds), Springer, Germany, Ch 11, pp. 249–283, ISBN:978-3-642-18311-9.

- Marcato, P.D., R. De Conti, B.R. Bergmann and N. Durán. (2008). Silver nanoparticles/c lindamycin: antileishmanial activity. *Proceeding of the 7th Brazilian MRS Meeting (SBPMAT)*, Guarujá, Brazil, 2008.
- Marsili, E., D.B. Baron, I. D. Shikhare, D. Coursolle, J.A. Gralnick and D.R. Bond. (2008). *Shewanella* secretes flavins that mediate extracellular electron transfer. *Proc. Natl. Acad. Sci. USA* 105: 3968–3973.
- Materska, M. (2008). Quercetin and its derivatives: chemical structure and bioactivity – a review. *Pol. J. Food Nutr. Sci.* 58: 407–413.
- Midander, K., P. Cronholm, H.L. Karlsson, K. Elihn, L. Möller, C. Leygraf and I.O. Wallinder (2009). Surface characteristics, copper release, and toxicity of nano and micrometer-sized copper and copper(II) oxide particles: a cross disciplinary study. *Small* 5: 389–399.
- Mikheenko, I.P., M. Rousset, S. Dementin and L.E. Macaskie. (2008). Bioaccumulation of palladium by *Desulfovibrio fructosivorans* wild-type and hydrogenase-deficient strains. *Appl. Environ. Microbiol.* 74: 6144–6146.
- Mohanpuria, P., N.K. Rana and S.K. Yadav. (2008). Biosynthesis of nanoparticles: technological concepts and future applications. *J. Nanopart. Res.* 10: 507–517.
- Mukherjee, P., A. Ahmad, D. Mandal, S. Senapati, S.R. Sainkar and M. Khan. (2001). Bioreduction of acyl ions by the fungus, *Verticillium* species and surface trapping of the gold nanoparticles formed. *Angew Chem. Int. Ed.* 40: 3585–3583.
- Mukherjee P, M. Roy, B.P. Mandal, G.K. Dey, P.K. Mukherjee, J. Ghatak, A.K. Tyagi and S.P. Kale. (2008) Green synthesis of highly stabilized nanocrystalline silver particles by a non-pathogenic and agriculturally important fungus *T. asperellum*. *Nanotechnology* 19: 1–7.
- Naik, R.R., S.J. Stringer, G. Agarwal, S.E. Jones and M.O. Stone. (2002) Biomimetic synthesis and patterning of silver nanoparticles. *Nat. Mater.* 1: 169–172.
- Nair, L.S. and C.T. Laurencin. (2007). Silver nanoparticles: Synthesis and therapeutic applications. *J. Biomed. Nanotechnol.* 3: 301–316.
- Nair, B. and T. Pradeep. (2002). Coalescence of nanoclusters and formation of submicron crystallites assisted by *Lactobacillus* strains. *Cryst. Growth Des.* 4: 295–298.
- Nanda, A. and M. Saravanan. (2009). Biosynthesis of silver nanoparticles from *Staphylococcus aureus* and its antimicrobial activity against MRSA and MRSE *Nanomed. NBM* 5: 452–456.
- Nangia, Y., N. Wangoo, S. Sharma, J.S. Wu, V. Dravid, G.S. Shekhawat and C.R. Suri. (2009). Facile biosynthesis of phosphate capped gold nanoparticles by a bacterial isolate *Stenotrophomonas maltophilia*. *Appl. Phys.Lett.* 94: 233901.
- Narayanan, K.B. and N. Sakthivel. (2010). Biological synthesis of metal nanoparticles by microbes. *Adv. Colloid Interface Sci.* 156: 1–13.
- Ogi, T., N. Saitoh, T. Nomura and Y. Konishi. (2010). Room-temperature synthesis of gold nanoparticles and nanoplates using *Shewanella* algae cell extract. *J. Nanopart. Res.* 12: 2531–2539.
- Oremland, R.S., J.S. Blum, C.W. Culbertson, P.T. Visscher, L.G. Miller, P. Dowdle and F.E. Strohmaier. (1994) Isolation, growth, and metabolism of an obligatory anaerobic, selenate-respiring bacterium, strain SES-3. *Appl. Environ. Microbiol.* 60: 3011–3019.
- Oremland, R.S., M.J. Herbel, J.S. Blum, S. Langley, T.J. Beveridge, P.M. Ajayan, T. Sutto, A.V. Ellis and S. Curran. (2004). Structural and spectral features of selenium nanospheres produced by Se-respiring bacteria. *Appl. Environ. Microbiol.* 70: 52–60.
- Panyala, N.R., E.M. Peña-Méndez and J. Havel. (2008). Silver or silver nanoparticles: a hazardous threat to the environment and human health? *J. Appl. Biomed.* 6: 117–129.
- Parikh, R.Y., S. Singh, B.L.V. Prasad, M.S. Patole, M. Sastry and Y.S. Shouche. (2008). Extracellular synthesis of crystalline silver nanoparticles and molecular evidence of silver resistance from *Morganella sp.*: towards understanding biochemical synthesis mechanism. *ChemBioChem.* 9: 1415–1422.
- Park, E.J., J. Yi, Y. Kim, K. Choi and K. Park. (2010). Silver nanoparticles induce cytotoxicity by a Trojan-horse type mechanism. *Toxicol. In Vitro* 24: 872–878.

- Patil, S.S., R.S. Dhumal, M.V. Varghese, A.R. Paradkar and P.K. Khanna (2009). Synthesis and antibacterial studies of chloramphenicol loaded nano-silver against *Salmonella typhi*. *Synth. React. Inorg. Met. Org. Nano Met. Chem.* 39: 65–72.
- Popescu, M., A. Velea and A. Lőrinczi. (2010). Biogenic production of nanoparticles. *Digest J. Nanomater. Biostruct.* 5: 1035–1040.
- Prasad, K., A.K. Jha and A.R. Kulkarni. (2007). Lactobacillus assisted synthesis of titanium nanoparticles. *Nanoscale Res. Lett.* 2: 248–250.
- Pujols-Ayala, I., C.A. Sacksteder and B.A. Barry. (2003). Redox-active tyrosine residues: Role for the peptide bond in electron transfer. *J. Am. Chem. Soc.* 125: 7536–7538.
- Raffi, M., F. Hussain, T.M. Bhatti, J.I. Akhter, A. Hameed and M.M. Hasan. (2008). Antibacterial characterization of silver nanoparticles against *E. coli* ATCC-15224. *J. Mater. Sci. Technol.* 24: 192–196.
- Rahman, M.F., J. Wang, T.A. Patterson, U.T. Saini, B.L. Robinson, G.D. Newport, R.C. Murdock, J.J. Schlager, D.M. Hussain and S.F. Ali. (2009). Expression of genes related to oxidative stress in the mouse brain after exposure to silver-25 nanoparticles. *Toxicol. Lett.* 187: 15–21.
- Rai, M.K., A.P. Yadav and A.K. Gade. (2008). Current trends in phytosynthesis of metal nanoparticles. *Crit. Rev. Biotechnol.* 28: 277–284.
- Rai, M., A. Yadav and A. Gade (2009). Silver nanoparticles as a new generation of antimicrobials. *Biotechnol. Adv.* 27: 76–83.
- Rai, M., S. Birla, I. Gupta, A. Ingle, A. Gade, K. Abd-Elsalam, P.D. Marcato and N. Durán. (2011). In Diversity in synthesis and bioactivity of inorganic nanoparticles: progress and pitfalls (Vladimir Torchilin-Northeastern University, USA, Chief Editor) *Biomedical Nanotechnology Series*. Vol 5. Pan Stanford Publishing, USA.
- Riddin, T.L., M. Gericke and C.G. Whiteley. (2006). Analysis of the inter- and extracellular formation of platinum nanoparticles by *Fusarium oxysporum* f. sp. *lycopersici* using response surface methodology. *Nanotechnology* 17: 3482–3489.
- Riddin, T.L., Y. Govender, M. Gericke and C.G. Whiteley. (2009). Two different hydrogenase enzymes from sulfate-reducing bacteria are responsible for the bioreductive mechanism of platinum into nanoparticles. *Enzyme Microb. Technol.* 45: 267–273.
- Riddin, T.L., M. Gericke and C.G. Whiteley. (2010). Biological synthesis of platinum nanoparticles: effect of initial metal concentration. *Enzyme Microb. Technol.* 46: 501–505.
- Ruparelia, J.P., A.K. Chatterjee, S.P. Duttagupta and S. Mukherji. (2008). Strain specificity in antimicrobial activity of silver and copper nanoparticles. *Acta Biomater.* 4: 707–716.
- Safaepour, M., A.R. Shahverdi, H.R. Shahverdi, M.R. Khorramizadeh and A.R. Gohari. (2009). Green synthesis of small silver nanoparticles using geraniol and its cytotoxicity against fibrosarcoma-wehi 164. *Avicenna J. Med. Biotechnol.* 1: 111–115.
- Selvakannan, P.R., A. Swami, D. Srisathianarayanan, P.S. Shirude, R. Pasricha, A.B. Mandale and M. Sastry. (2004a). Synthesis of aqueous Au core-Ag shell nanoparticles using tyrosine as a pH-dependent reducing agent and assembling phase-transferred silver nanoparticles at the air-water interface. *Langmuir* 20: 7825–7836.
- Selvakannan, P., S. Mandal, S. Phadtare, A. Gole, R. Pasricha, S.D. Adyanthaya and M. Sastry. (2004b). Water-dispersible tryptophan-protected gold nanoparticles prepared by the spontaneous reduction of aqueous chloroaurate ions by the amino acid. *J. Colloid Interface Sci.* 269: 97–102.
- Shakibaie, M., M.R. Khorramizadeh, M.A. Faramarzi, O. Sabzevari and A.R. Shahverdi. (2010). Biosynthesis and recovery of selenium nanoparticles and the effects on matrix metalloproteinase-2 expression. *Biotechnol. Appl. Biochem.* 56: 7–15
- Sharma, V.K., R.A. Yngard and Y. Lin. (2009). Silver nanoparticles: green synthesis and their antimicrobial activities. *Advan. Colloid Interface Sci.* 145: 83–96.
- Si, S. and T.K. Mandal. (2007). Tryptophan-based peptides to synthesize gold and silver nanoparticles: a mechanistic and kinetic study. *Chem. Eur. J.* 13: 3160–3168.
- Singh, M., S. Singh, S. Prasad and I.S. Gambhir. (2009). Nanotechnology in medicine and antibacterial effect of silver nanoparticles. *Digest J. Nanomater. Biostruct.* 3: 115–122.

- Sinha, S., I. Pan, P. Chanda and S.K. Sen. (2009). Nanoparticles fabrication using ambient biological resources. *J. Appl. Biosci.* 19: 1113–1130.
- Sintubin, L., W.E. Windt, J. Dick, J. Mast, D.V. Ha, W. Verstarete and N. Boon. (2009). Lactic acid bacteria as reducing and capping agent for the fast and efficient production of silver nanoparticles. *Appl. Microbiol. Biotechnol.* 84: 741–761.
- Sivaraman, S.K., I. Elango, S. Kumar and V. Santhanam. (2009). A green protocol for room temperature synthesis of silver nanoparticles in seconds. *Curr. Sci.* 97: 1055–1059.
- Slocik, J.M., R.R. Naik, M.O. Stone and D.W. Wright. (2005). Viral templates for gold nanoparticle synthesis. *J. Mater. Chem.* 15: 749–753.
- Song, J.Y., E.Y. Kwon and B.S. Kim. (2010). Biological synthesis of platinum nanoparticles using *Diopyros kaki* leaf extract. *Bioproc. Biosyst. Eng.* 33: 159–164.
- Studer, A.M., L.K. Limbach, L. Van Duc, F. Krumeich, E.K. Athanassiou, L.C. Gerber, H. Moch and W.J. Stark. (2010). Nanoparticle cytotoxicity depends on intracellular solubility: comparison of stabilized copper metal and degradable copper oxide nanoparticles. *Toxico. Lett.* 197: 169–174.
- Sung, J.H., J.H. Ji, J.U. Yoon, D.S. Kim, M.Y. Song, J. Jeong, B.S. Han, J.H. Han, Y.H. Chung, J. Kim, T.S. Kim, H.K. Chang, E.J. Lee, J.H. Lee and I.J. Yu. (2008). Lung function changes in Sprague-Dawley rats after prolonged inhalation exposure to silver nanoparticles. *Inhalation Toxicol.* 20: 567–574.
- Sung, J.H., J.H. Ji, J.D. Park, J.U. Yoon, D.S. Kim, K.S. Jeon, M.Y. Song, J. Jeong, B.S. Han, J.H. Han, Y.H. Chung, H.K. Chang, J.H. Lee, M.H. Cho, B.J. Kelman and I.J. Yu. (2009). Sub-chronic inhalation toxicity of silver nanoparticles. *Toxicol. Sci.* 108: 452–461.
- Thakkar, K.N., S.S. Mhatre and R.Y. Parikh. (2010). Biological synthesis of metallic nanoparticles. *Nanomed. NBM.* 6: 257–262.
- Totaro, P. and M. Rambaldini. (2009). Efficacy of antimicrobial activity of slow release silver nanoparticles dressing in post-cardiac surgery mediastinitis. *Interact. Cardiovasc. Thorac. Sur.* 8:153–154.
- Uboldi, C., D. Bonacchi, G. Lorenzi, M.I. Hermanns, C. Pohl, G. Baldi, R.E. Unger and C.J. Kirkpatrick. (2009). Gold nanoparticles induce cytotoxicity in the alveolar type-II cell lines A549 and NCIH441. *Particle Fibre Toxicol.* 6: 1–12.
- Varshney, R., S. Bhadauria, M.S. Gaur and R. Pasricha. (2010). Characterization of copper nanoparticles synthesized by a novel microbiological method. *JOM. J. Miner. Met. Mater. Soc.* 62: 102–104.
- Vijayaraghavan, K. and S.P.K. Nalini. (2010). Biotemplates in the green synthesis of silver nanoparticles. *Biotechnol. J.* 5: 1098–110.
- Yang, X., Q. Li, H. Wang, J. Huang, L. Lin, W. Wang, D. Sun, Y. Su, J.B. Opiyo, L. Hong, Y. Wang, N. He and L. Jia. (2010). Green synthesis of palladium nanoparticles using broth of *Cinnamomum camphora* leaf. *J. Nanopart. Res.* 12: 1589–1598.
- Yen, H.J., S.H. Hsu and C.L. Tsai. (2009). Cytotoxicity and immunological response of gold and silver nanoparticles of different sizes. *Small.* 5: 1553–1561.
- Zhang, W., X. Qiao and J. Chen. (2007). Synthesis of silver nanoparticles. Effects of concerned parameters in water/oil microemulsion. *Mater. Sci. Eng. B* 142: 1–15.
- Zhang, X.R., X.X. He, K.M. Wang, Y.H. Wang, H.M. Li and W.H. Tan. (2009). Biosynthesis of size-controlled gold nanoparticles using fungus, *Penicillium sp.* *J. Nanosci. Nanotechnol.* 9: 5738–5744.
- Zhang, X., S. Yan, R.D. Tyagi and R.Y. Surampalli. (2011). Synthesis of nanoparticles by microorganisms and their application in enhancing microbiological reaction rates. *Chemosphere* 82: 489–494.

Chapter 13

Antimicrobial Activity of Nanomaterials for Food Packaging Applications

Henriette Monteiro Cordeiro de Azeredo

13.1 Introduction

The main function of food packaging systems is to protect food against environmental factors such as microorganisms, chemical contaminants, oxygen and water vapor, extending food shelf stability and improving food safety. Conventional food packaging systems are designed to protect the food in a passive way, that is to say, they are supposed not to interact with the food, but rather to act exclusively as a barrier between the food and the surrounding environment.

On the other hand, active food packaging systems are supposed to perform some role other than providing an inert barrier to external conditions (Rooney 1995). The most common active packaging systems are the antimicrobial ones, which release antimicrobial agents into the food surface, where microbial growth predominates, inhibiting or retarding microbial growth and spoilage.

Nanocomposite antimicrobial systems are particularly effective, because of the high surface-to-volume ratio and enhanced surface reactivity of the nano-sized antimicrobial agents, making them able to inactivate more microbial molecules and cells when compared to larger-scale counterparts (Luo and Stutzenberger 2008). Nanoscale materials have been investigated for antimicrobial activity as growth inhibitors (Cioffi et al. 2005), killing agents (Stoimenov et al. 2002; Qi et al. 2004; Huang et al. 2005; Kumar and Münstedt 2005; Lin et al. 2005), or as antimicrobial carriers (Gu et al. 2003; Bi et al. 2011).

Antimicrobial food packaging systems are extremely useful to minimize the growth of post-processing contaminant microorganisms, extending food shelf life and improving food safety.

In this review, the main types of antimicrobial nanomaterials as they are applied in food packaging are discussed. The discussion has been focused on antimicrobial

H.M.C. de Azeredo (✉)

Embrapa Tropical Agroindustry - CNPAT, Fortaleza, CE, Brazil
e-mail: ette@cpat.embrapa.br

mechanisms and effectivity, as well as applications in food packaging systems, including not only conventional food packaging but also edible coatings used as primary packages which can be consumed with the food product.

13.2 Nano-Antimicrobials Materials and Applications

13.2.1 Silver Nanoparticles

Silver has long been known to have a broad spectrum of antimicrobial activities (Liau et al. 1997), besides having some processing advantages such as high temperature stability and low volatility (Kumar and Münstedt 2005).

Most nanocomposites used as antimicrobial food packaging are based on silver nanoparticles (AgNP), which are effective antimicrobials (Aymonier et al. 2002; Sondi and Salopek-Sondi 2004; Son et al. 2006; Yu et al. 2007; Tankhiwale and Bajpai 2009), even more than larger silver particles, thanks to their larger surface area available for interaction with microbial cells (An et al. 2008; Kvítek et al. 2008). Damm et al. (2008) observed that polyamide 6 filled with 0.06 wt% AgNP was able to completely eliminate a bacterial population within 24 h, while a polyamide 6/silver-microcomposite incorporated with 1.9 wt% of silver killed only about 80% of the bacteria within the same time.

The antimicrobial activity of AgNPs seems to be dependent on release of Ag⁺ ions (Morones et al. 2005; Kumar and Münstedt 2005). According to findings by Kumar and Münstedt (2005), Ag⁺ binds to electron donor groups in biological molecules containing sulfur, oxygen or nitrogen. Feng et al. (2000) suggested that interactions of Ag⁺ ions with thiol groups in proteins may induce inactivation of bacterial enzymes; as a reaction to the protein denaturation effects of Ag⁺ ions, DNA molecules may become condensed and unable to replicate. An other mechanism proposed for the antimicrobial activity of AgNP was based on adhesion to the cell surface, degradation of lipopolysaccharides and formation of “pits” in the membranes, largely increasing permeability (Sondi and Salopek-Sondi 2004).

Tankhiwale and Bajpai (2009) demonstrated that grafting of acrylamide onto filter paper, followed by incorporation of AgNPs, results in a biomaterial effective against *Escherichia coli* (*E. coli*), which can be used as an antibacterial packaging material.

Yoksan and Chirachanchai (2010) produced AgNPs by γ -ray irradiation reduction of silver nitrate in a chitosan solution, and incorporated them into chitosan–starch-based films. The AgNP-loaded films were active against both Gram-positive and Gram-negative bacteria. Gottesman et al. (2011) developed a method to coat paper with nano-sized coatings (90–150 nm in thickness) of AgNPs by using ultrasonic radiation. AgNPs penetrated the paper to more than 1 μ m in depth, resulting in high stability of the coatings. The coated paper was

effective against *Escherichia coli* and *Staphylococcus aureus*, suggesting its potential application as an active food packaging material.

Tankhiwale and Bajpai (2010) loaded AgNPs into a lactic acid grafted chitosan film. The nanocomposite film showed strong antibacterial properties against *Escherichia coli* and thus has potential as an antibacterial food packaging material.

Fayaz et al. (2009) biosynthesized highly stable AgNPs using *Trichoderma viride* and incorporated them into sodium alginate for vegetable and fruit preservation. The nanobiocomposite film showed good antibacterial activity against test strains, and increased shelf life of carrot and pear when compared to uncoated controls.

An et al. (2008) coated green asparagus with a nanocomposite coating based on polyvinylpyrrolidone (PVP) incorporated with silver nanoparticles, and compared their microbial stability with that of uncoated asparagus. The coating significantly hindered the growth of total aerobic psychrotrophics, yeasts and molds, and reduced the visual changes in asparagus throughout a 25-day storage.

Emamifar et al. (2010) demonstrated the effectiveness of the application of a low-density polyethylene (LDPE) nanocomposite packaging film containing AgNP on reducing microbial growth in fresh orange juice at 4°C. The authors stated that the resulting concentration of Ag⁺ ions in orange juice (migrated from the film) was less than its allowable concentration (10 ppm).

In addition to their antimicrobial activity, AgNP have been reported to absorb and decompose ethylene, which may contribute to their effects on extending shelf life of fruits and vegetables (Hu and Fu 2003; Fernández et al. 2010). Moreover, AgNP have been reported to improve thermal properties and tensile properties of polymers used for food packaging. The incorporation of AgNPs into polyvinyl alcohol (PVOH) films resulted in improved thermal stability, higher glass transition temperature, and better tensile properties (Young's modulus and tensile strength) (Mbhele et al. 2003).

13.2.1.1 Nanostructured Calcium Silicate–Ag Complexes

Nanostructured calcium silicate (NCS) was used by Johnston et al. (2008) to adsorb Ag⁺ ions from a solution. The resulting NCS–Ag complex exhibited effective antimicrobial activity at desirably low levels of silver down to 10 mg kg⁻¹, and could be incorporated into food packaging as an antimicrobial agent.

13.2.1.2 AgNPs Synthesized in Polymer Matrices

Ex situ AgNP synthesis consists on synthesizing AgNPs beforehand (by chemical reduction) and then dispersing them into a polymerizable formulation. Besides the hazards related to handling dry nanoparticles, this method often involves contamination of AgNP surfaces with chemicals which raise their toxicity. Moreover, it is limited by the difficulty to control the monodispersity of the nanoparticles

(Balan and Burget 2006; Vimala et al. 2010). In the in situ approach, on the other hand, the nanoparticles are generated in a polymerizable medium from cationic precursors which exhibit better dispersion ability (Balan et al. 2010).

In situ synthesis methods involving a stabilization process by reducing Ag^+ ions in water soluble polymers have been suggested and proved efficient (Fernández et al. 2010; Valodkar et al. 2010; Vimala et al. 2010). The AgNPs become attached to the polymer, and the method provides a single-step synthesis and stabilization of AgNPs (Sanpui et al. 2008).

Cellulose is able to bind electropositive transition metal atoms such as silver by electrostatic interactions. Consequently, Ag^+ ions are adsorbed by cellulose during immersion in silver nitrate (Fernández et al. 2010). Afterwards, the nanoporous structure and the high oxygen density of cellulose fibers make them effective nanoreactors for in situ synthesis of AgNP (He et al. 2003). Fernández et al. (2010) stored fresh-cut melon pieces under modified atmosphere packaging containing cellulose absorbent pads loaded with AgNP. The lag phases of the microorganisms were incremented by the pads, and microbial loads remained about 3 log CFU/g below the control (melon cuts packed without the pads) during storage time.

Chitosan has strong affinity towards silver ions, thanks to the presence of amine and hydroxyl groups (Varma et al. 2004), and is able to reduce Ag^+ ions to AgNPs under alkaline conditions (Murugadoss and Chattopadhyay 2008). Sanpui et al. (2008) reported that the presence of a low concentration (2.15%, w/w) of AgNPs in a chitosan composite was enough to significantly enhance inactivation of *E. coli* as compared with unchanged chitosan.

13.2.2 Metal Oxides

Metal oxide materials such as TiO_2 , ZnO and MgO have been recognized as antibacterial agents. Generation of reactive oxygen species (ROS) seems to be one of the mechanisms of their antibacterial activity (Dong et al. 2010b). A great advantage of metal oxides over organic-based antimicrobial agents is their much higher stability (Zhang et al. 2010).

13.2.2.1 Titanium Dioxide (TiO_2)

TiO_2 has been widely applied as a photocatalytic disinfecting material for surface coatings (Fujishima et al. 2000). TiO_2 photocatalysis, which promotes peroxidation of the phospholipids present in microbial cell membranes (Maness et al. 1999), has been used to inactivate food-related pathogenic bacteria (Kim et al. 2005; Robertson et al. 2005). Chawengkijwanich and Hayata (2008) developed a TiO_2 powder-coated packaging film able to reduce *E. coli* contamination on food

surfaces. Gelover et al. (2006) demonstrated the efficacy of TiO₂-coated films exposed to sunlight to inactivate fecal coliforms in water.

Metal doping improves visible light absorbance of TiO₂ (Anpo et al. 2001), and increases its photocatalytic activity under UV irradiation (Choi et al. 1994). It has been demonstrated that doping TiO₂ with silver greatly improved photocatalytic bacterial inactivation (Page et al. 2007; Reddy et al. 2007). This combination was explored by Cheng et al. (2006), who have obtained effective antibacterial activity from a polyvinyl chloride (PVC) nanocomposite with TiO₂/Ag⁺ nanoparticles. Li et al. (2009) observed that the same combination was effective in reducing physicochemical and sensory changes in Chinese jujubes.

However, TiO₂ nanoparticles, combined or not to Ag⁺, are incompatible with organic matrices, and may agglomerate. Although such drawbacks decrease their antimicrobial properties, they can be suppressed by surface modification of the nanoparticles. Cheng et al. (2006) modified TiO₂/Ag⁺ nanoparticles by grafting γ -aminopropyltriethoxy-silane (APS), which resulted in improved dispersion of the nanoparticles in a PVC matrix.

13.2.2.2 Zinc Oxide (ZnO)

ZnO has been reported to present antibacterial activity against bacteria, including thermo-resistant spores (Sawai et al. 1996), which has been at least partly attributed to generation of hydrogen peroxide (H₂O₂) (Sawai et al. 1998). The antibacterial activity of ZnO powder has been reported to increase with decreasing particle size (Sawai et al. 1996; Yamamoto 2001).

ZnO nanoparticles deposited on a glass surface exhibited antibacterial activities against both *E. coli* (Gram-negative) and *S. aureus* (Gram-positive) cultures (Applerot et al. 2009b).

Emamifar et al. (2010) demonstrated that the application of LDPE packages containing nano-ZnO prolonged the microbial shelf life of fresh orange juice, without any negative effects on sensory attributes, although nano-ZnO had presented a lower antimicrobial activity on yeast and molds when compared to AgNPs. In another study, the same authors (Emamifar et al. 2011) observed that orange juice sterilized and inoculated with *Lactobacillus plantarum* presented reduced numbers of the inoculated bacteria when packed in LDPE films containing silver or ZnO nanoparticles.

Li et al. (2011a) reported that PVC films coated with ZnO nanoparticles presented excellent bacteriostatic and bactericidal effects against *E. coli*. In an in vitro test, the efficiency of ZnO-coated film was proved to be relatively constant within the pH range of 4.5–8.0. In an actual test, the number of *E. coli* cells from cut apple stored in a ZnO-coated bag was reduced in about 30% in 1 day. Moreover, fruit decay was reduced in nano-coated apples, the growth of aerobic psychrophilic microorganisms was inhibited, and the yeast and mold growth was lower than in uncoated fruit (Li et al. 2011b).

Li et al. (2010) produced chitosan/Ag/ZnO blend films via sol-cast transformation. Ag and ZnO nanoparticles were uniformly distributed within the chitosan polymer. Chitosan/Ag/ZnO blend films presented higher antimicrobial activities than nanocomposite films containing only Ag or ZnO nanoparticles. The blend films showed a wide spectrum of effective antimicrobial activities.

ZnO nanoparticles in aqueous media tend to agglomerate into large flocculates, due to their hydrophobicity, and thus do not interact effectively with microorganisms (Applerot et al. 2009a). Gordon et al. (2011) combined ZnO with FeO to produce magnetic composite nanoparticles with improved colloidal stability. The effectivity of the nanoparticles was reported to be increased by higher Zn/Fe weight ratios; moreover, the antibacterial activity was higher for Gram-positive than for Gram-negative bacteria.

13.2.3 Metal Hydroxides

Ca(OH)₂ has been reported as an effective antibacterial agent (Mendonça et al. 1994), its efficiency being highly dependent on the release of OH⁻ ions (Beltes et al. 1997).

Mg(OH)₂ is an approved drug and food additive (Dong et al. 2010b). Dong et al. (2010a, b) demonstrated the effectiveness of Mg(OH)₂ nanoparticles and nanoplatelets against *E. Coli*. Their antibacterial effect was attributed to two possible mechanisms (Dong et al. 2010a). The first is related to a direct penetration of Mg(OH)₂ nanoparticles into cell walls and damages to membrane proteins, leading to cell death. The second is adsorption of water on the nanoparticle surfaces, forming a thin layer of highly concentrated in OH⁻ ions, which, in contact with bacteria, could damage the membranes.

13.2.4 Chitosan Nanostructures

Chitosan is a linear polysaccharide consisting of (1,4)-linked 2-amino-deoxy-β-D-glucan units, prepared by alkali deacetylation of chitin. Since the deacetylation is usually incomplete, chitosan is a copolymer comprised of deacetylated and acetylated units (Dutta et al. 2009; Aranaz et al. 2010), as shown in Fig. 13.1. It is a polycation whose charge density depends on the degree of deacetylation and pH

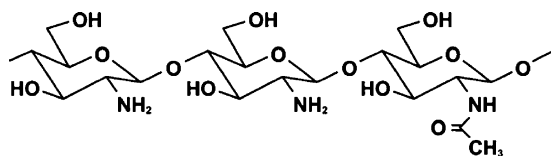


Fig. 13.1 Scheme of the chemical structure of chitosan

(Aranaz et al. 2010). Chitosan has long been reported as an antibacterial agent against a wide variety of microorganisms (Tsai and Su 1999; Entsar et al. 2003; Wu et al. 2005).

Nano-scale chitosan and its derivatives have antimicrobial effects towards bacteria (No et al. 2002; Qi et al. 2004), viruses (Chirkov 2002) and fungi (Badawy et al. 2005). The minimum inhibitory concentrations (MIC) depend on the organism, pH, molecular weight, degree of polymerization, and the presence of lipids and proteins (No et al. 2002). Antimicrobial activity of chitosan may be attributed to interactions between the positively charged chitosan and the negatively charged cell membranes, increasing membrane permeability and eventually causing rupture and leakage of the intracellular material. Indeed, it has been reported that both bulk chitosan and its nanoparticles are ineffective at pH lower than six, probably because of the absence of protonated amino groups (Qi et al. 2004). According to Shi et al. (2006), chitosan nanoparticles (CSN) exhibit higher antibacterial activity than bulk chitosan because of their higher surface area and charge density, favoring a higher interaction with the negatively charged surfaces of bacterial cells. Results by Xing et al. (2009) indicate that oleoyl–chitosan nanoparticles act by damaging cell membrane and putative binding to extracellular (such as phosphate groups) or intracellular (such as DNA and RNA) targets.

Keawchaon and Yoksan (2011) produced carvacrol-loaded CSN, which presented higher antibacterial activity when compared to unloaded chitosan nanoparticles. Carvacrol is a major component of essential oil fractions of oregano and thyme, which has been known for its bactericidal effects (Ultee et al. 1999).

Ali et al. (2011) synthesized CSN by ionic gelation with sodium tripolyphosphate (TPP) and loaded them with Ag⁺ ions to produce silver loaded chitosan nanoparticles (Ag-CSN). The minimum inhibitory concentrations of CSN and Ag-CSN against *S. aureus* were reported to be respectively 50 and 500 times lower than that of bulk chitosan.

Chitosan nanostructures have been demonstrated to disperse well in biopolymers such as starch (Chang et al. 2010) and hydroxypropyl methylcellulose (De Moura et al. 2009), having the potential to be used as antimicrobial agents in edible or biodegradable food packaging systems.

Watthanaphanit et al. (2010) observed that the incorporation of chitosan whiskers into alginate imparted antibacterial activity against both Gram-positive and Gram-negative bacteria to the nanocomposite material.

13.2.5 Carbon Nanotubes

Carbon nanotubes (CNTs) are arrangements of carbon hexagons into tube-like fullerenes, having diameters of a few nanometers with lengths up to centimeters. They may consist of a one-atom-thick single-wall nanotube (SWNT), or a number of concentric tubes called multi-walled nanotubes (MWNT) (Zhou et al. 2004). They have received much attention because of their very interesting mechanical,

electrical and thermal properties (Mi et al. 2007), and have been incorporated into polymer matrices such as PVOH (Chen et al. 2005), polypropylene (López Manchado et al. 2005; Prashantha et al. 2009), polyamide (Zeng et al. 2006), and PLA (Brody 2006).

CNTs have also been reported to have antibacterial properties. Direct contact with aggregates of CNTs have been demonstrated to kill *E. coli* (Kang et al. 2007). The antibacterial activity of CNTs has been related not only to their adsorption ability (Upadhyayula et al. 2009) but mainly to puncture of microbial cells by their needle-like structure, causing irreversible damage and leakage of intracellular material (Narayan et al. 2005; Kang et al. 2007). Indeed, Kang et al. (2008) have demonstrated that single-walled carbon nanotubes (SWNTs) are much more toxic to bacteria than multi-walled carbon nanotubes (MWNTs), thus providing evidence that the diameter of CNTs is a key factor governing their antibacterial effects.

13.2.6 Nanoclays

Layered silicates or nanoclays typically have a stacked arrangement of negatively charged silicate layers (nanoplatelets) which are 1 nm thick and several microns long depending on the particular silicate (Sorrentino et al. 2007). Layered silicates have been incorporated into polymer matrices in order to enhance polymer mechanical and barrier properties (Bharadwaj et al. 2002; Uyama et al. 2003).

13.2.6.1 Organically Modified Nanoclays as Antimicrobials

Hong and Rhim (2008) have reported antibacterial activity from two organically modified montmorillonites (OMMT), namely Cloisite 30B and Cloisite 20A, while an unmodified montmorillonite (Cloisite Na⁺) has not shown any antibacterial activity, even though the three nanoclays have the same basic montmorillonite (MMT) structure. The OMMT ruptured cell membranes and inactivated both Gram-positive and -negative bacteria. The contrast between the antimicrobial activity of the OMMT and the inefficacy of the unmodified MMT may be attributed to the presence of quaternary ammonium groups in the OMMT (Rhim et al. 2006; Hong and Rhim 2008). When comparing the effects of the two organoclays, the authors of the study (Hong and Rhim 2008) reported that Cloisite 30B showed significantly higher antimicrobial activity than Cloisite 20A, which were partly attributed to their degrees of hydrophobicity. Since Cloisite 20A is more hydrophobic, it may keep bacteria from being adsorbed into the clay surface, thus reducing clay antimicrobial activity.

Other studies (Rhim et al. 2009; Sothornvit et al. 2009) reported Cloisite 20A not to present any antibacterial activity, and Cloisite 30B to provide films only with some bacteriostatic activity. However, even those results were not very consistent with one another. While Sothornvit et al. (2009) observed that Cloisite 30B provided whey protein isolate (WPI) films with bacteriostatic effects against

Gram-negative bacteria, Rhim et al. (2009) observed that poly-(lactic acid) (PLA) films with Cloisite 30B presented bacteriostatic effect against *Listeria monocytogenes*, a Gram-positive bacteria, but not against the Gram-negative bacteria tested.

13.2.6.2 Nanoclays in Chitosan Films

Although unmodified nanoclays themselves do not have antimicrobial activity, they may adsorb bacteria from a solution enabling a better interaction with antimicrobial polymers such as chitosan (Wang et al. 2006). Indeed, some studies reported antimicrobial properties from the combination between chitosan and unmodified nanoclays.

Han et al. (2010) observed that chitosan–MMT nanocomposites exhibited significantly higher antimicrobial activity against *S. aureus* and *E. coli* than pure chitosan and Na–MMT. Since the antimicrobial activity of chitosan has been ascribed to its cationic character, the increased antimicrobial activity of the nanocomposites seems contradictory, because the positive charges of chitosan are neutralized via electrostatic interactions with anionic silicate layers. The authors concluded that the nanocomposites exhibited synergistic effects between the components, because the chitosan molecules were evenly distributed through the inorganic matrix.

Wang et al. (2006, 2007, 2009) have carried out a series of studies on chitosan/rectorite intercalated nanocomposites with antimicrobial properties. In their first study (Wang et al. 2006), using unmodified Ca^{2+} -rectorite and organic rectorite, they observed that, although pristine rectorite by itself had not inhibited bacterial growth, the chitosan/rectorite nanocomposites presented stronger antibacterial activity than pure chitosan, particularly against Gram-positive bacteria. In a further study (Wang et al. 2007), the authors suggested that the antibacterial mechanism of the nanocomposites were divided into two stages: the first being the adsorption of the bacteria from solution and immobilization on the clay surface, and the second being related to chitosan accumulation on the clay surface, inhibiting bacterial growth. Finally, in a more recent study, the authors (Wang et al. 2009) prepared nanocomposites of quaternized chitosan and OREC, which presented strong inhibition against bacteria (both Gram-positive and -negative) and fungi, but mainly against Gram-positive bacteria. The excellent antimicrobial activity of the nanocomposites was attributed to the high affinity and strong interaction between quaternized chitosan and OREC, combining the adsorption and immobilization capacity of OREC with the antimicrobial activity of quaternized chitosan. In the three studies of the group (Wang et al. 2006, 2007, 2009), the authors observed that the antimicrobial activity was directly proportional to the amount or the interlayer distance of the nanoclay, thanks to an increase in effective layers per unit weight, causing more bacteria to be adsorbed and immobilized on the clay surface.

13.2.6.3 Nanoclays with Ag⁺ Ions

Incoronato et al. (2010) obtained Ag-MMT antimicrobial nanoparticles by bringing Na-MMT in contact with AgNO₃ solutions at various concentrations in order to replace exchangeable Na⁺ ions of Na-MMT with Ag⁺ ions. The nanoparticles were incorporated into three different polymeric matrices (agar, zein, and polycaprolactone), but only the agar nanocomposites presented antimicrobial activity, which was ascribed to the highest water content (and thus the highest level of macromolecular mobility) of the agar hydrogel. The release kinetics of Ag⁺ ions was controlled because of the weak electrostatic interactions established with surface platelets of MMT. In a further study (Incoronato et al. 2011), the authors evaluated the effectiveness of an active packaging system of agar with Ag-MMT nanoparticles on the stability of Fior di Latte cheese. The nanocomposite packaging system markedly increased the shelf life of the cheese, without affecting the functional dairy microbiota and the sensory quality of the product.

Costa et al. (2011) obtained Ag-MMT nanoparticles by replacing the Na⁺ ions of natural MMT by Ag⁺ ions from nitrate solutions. The nanoparticles were used to extend stability of a fruit salad. Sensory and microbiological tests indicated that the Ag-MMT nanoparticles were effective in inhibiting microbial growth.

Busolo et al. (2010) studied the antimicrobial performance of polylactic acid (PLA) containing a silver-based nanoclay for use in food packaging applications. The nanobiocomposite showed strong activity against *Salmonella* spp. In addition to the strong biocidal properties, the films exhibited enhanced water vapour barrier. A silver migration study using a slightly acidified water medium as a food simulant suggested that migration levels were within levels specified by the European Food Safety Agency (EFSA).

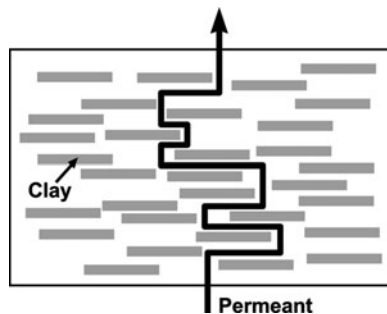
13.2.6.4 Effects of Nanoclays on Solubility, Release and Stability of Antimicrobials

Besides the direct or indirect antimicrobial effects of some nanoclays by themselves, Sánchez-García et al. (2008) reported that mica clay has been reported to enhance the solubility of the antimicrobial thymol in a polycaprolactone (PCL) matrix, by retention of the apolar thymol on the surface of the clay nanoplatelets. On the other hand, the thymol diffusion coefficient has decreased with the addition of mica clay to the biocomposite, probably because of the increased tortuosity effect (Fig. 13.2) imposed to thymol diffusion by the dispersed nanoclay. Thus, it was possible to control the release of thymol from the matrix.

Tunç and Duman (2011) observed that the release of the antimicrobial carvacrol from cellulose/carvacrol/MMT nanocomposite films was controlled by MMT concentration in the films.

An OMMT was reported by Konwar et al. (2010) to act as a supporting material for the stabilization of AgNPs in polyester/clay silver nanocomposites, preventing their aggregation.

Fig. 13.2 Tortuosity effect imposed by a nanoclay to diffusion of a permeant such as thymol through a polymer matrix (Adapted from Ray and Okamoto 2003)



13.2.7 *Tourmaline Nanocrystals*

Tourmaline is a naturally complex group of hydrous silicate minerals containing Li, Al, B, and Si and various quantities of alkalis (K and Na) and metals (Fe, Mg, and Mn) (Rhim and Ng 2007). Nanoparticles like tourmaline are classified as isodimensional nanoparticles, since their three dimensions are nanometric, while the layered silicate nanoplatelets have only one dimension in the nanometer range (Rhim and Ng 2007; Sorrentino et al. 2007).

Ruan et al. (2003) incorporated tourmaline nanocrystals into cellulose films and the resulting material presented antimicrobial action against *S. aureus*.

13.2.8 *Nano-Hybrid Systems with Antimicrobial Properties*

Hybrid organic–inorganic systems have aroused great attention, particularly those in which fillers are dispersed at a nanometric level in a polymeric matrix, forming nano-hybrid composite systems.

Marini et al. (2007) coated polyethylene (PE) films with antibacterial nano-hybrid coatings prepared by a sol–gel process from tetraethoxysilane (TEOS), triethoxysilane terminated poly(ethylene glycol)-block-poly(ethylene) (PE-PEG-Si), and triethoxysilane terminated quaternary ammonium salt (QAS-Si). The objective of bonding the quaternary ammonium salt (QAS) to the organic–inorganic network was to reduce QAS diffusivity and to enhance its stability. The coated PE films showed good activity against both Gram-negative and Gram-positive bacteria.

Layered double hydroxides (LDHs), also known as “anionic clays”, act as ion delivery vehicles, because of their anion exchange properties. They are cheap, eco-friendly, and can be organically modified with several organic anions, generally much more numerous than organic cations commonly involved in modification of cationic clays (Bugatti et al. 2010). Intercalation compounds of ZnAl-LDH with benzoate and derivatives (antimicrobial agents) were elaborated by Bugatti et al. (2010), and the resulting nano-hybrids were incorporated into polycaprolactone

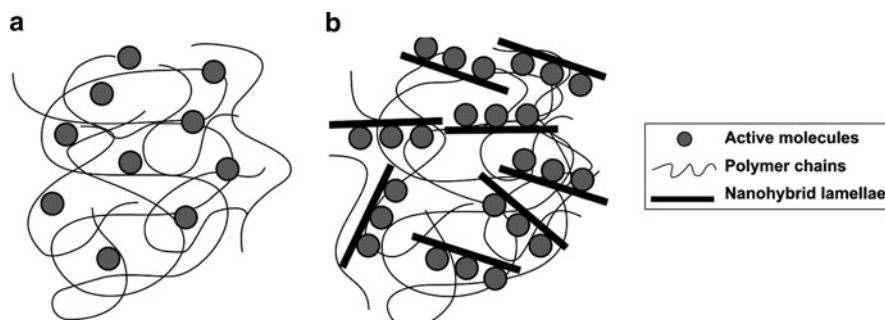


Fig. 13.3 Schematic picture of active molecules into a polymeric matrix: (a) free dispersed; (b) fixed on inorganic lamellae and dispersed as exfoliated filler (Source: Bugatti et al. 2011)

(PCL) films. The benzoate anions in the nano-hybrids exhibited much slower and controlled release when compared to those directly dispersed in PCL. According to Bugatti et al. (2011), the release of active molecules directly dispersed into a polymeric matrix (Fig. 13.3a) is only driven by diffusion, whereas when they are fixed on the inorganic lamellae of a clay by ionic bonds (Fig. 13.3b) the release depends on many factors, such as diffusion of water molecules carrying counter-anions inside the matrix.

13.3 Nanocarriers of Antimicrobials

Some nanoparticles, although not having antimicrobial properties themselves, may be used as carriers of antimicrobials, deserve mentioning in this review.

Bi et al. (2011) elaborated phytyglycogen-based nanoparticles to prolong the efficacy of an antimicrobial peptide (nisin) against *Listeria monocytogenes*, a food-related pathogen, in order to minimize nisin loss during storage and meanwhile provide an effective release in the presence of bacteria. Phytyglycogen was subjected to β -amylolysis as well as subsequent succinate or octenyl succinate substitutions. Nisin loading and retention were favored by nanoparticles, especially by those subjected to β -amylolysis, with a high degree of substitution with hydrophobic octenyl succinate moieties.

13.4 Toxicological Aspects and Final Considerations

The food packaging sector can benefit from antimicrobial nanocomposites, which can be used to reduce microbial growth on food surfaces. However, safety concerns have to be considered, since nano-sized materials frequently exhibit different properties than those of the corresponding starting materials. The much larger surface area of nanoparticles allows a greater contact with cell membranes,

as well as a greater capacity for absorption and migration (Li and Huang 2008). Hence, their toxicity profiles cannot be extrapolated from those of their non-nano-sized counterparts (Restuccia et al. 2010). Moreover, nanostructures can have more free movement through the body when compared to their larger-scale counterparts (Brayner 2008).

Exposure to nanoparticles present in food packaging can occur through dermal contact, inhalation, or ingestion of nanoparticles which have migrated to food (Carlson et al. 2008; Li and Huang 2008; Restuccia et al. 2010). Moreover, nanoparticles may eventually be released into the environment and enter the food chain indirectly (Hoet et al. 2004).

Several studies have already been conducted on toxicological aspects of the nano-antimicrobial materials indicated in this study. Carbon nanotubes may be cytotoxic to human cells, at least when in contact to skin (Shvedova et al. 2003; Monteiro-Riviere et al. 2005) or lungs (Warheit et al. 2004), which would affect people manipulating the nanotubes in processing stages rather than consumers. Although bulk ZnO is non-toxic (Li et al. 2011a), Sharma et al. (2009) demonstrated that ZnO nanoparticles have a genotoxic potential in human epidermal cells. Some nanoparticles cause more inflammation than larger respirable particles elaborated from the same material at the same mass dose (Brayner 2008).

Although there are limited scientific data available about the migration of nanostructures from packaging materials into food, it is prudent to consider that, once present in the food packaging material, nanoparticles might eventually migrate into food. Thus, it is mandatory to know about any eventual health effects from ingestion of nanoparticles. The toxicity issue is even more important when edible coatings are concerned, since edible coatings must be considered as part of the food itself, and not just as a food contact material. Hence, actual applications of nanocomposite packaging requires further studies focused on the potential toxicity of nanotechnology products.

Acknowledgements The authors gratefully acknowledge the financial support of CNPq. H.M.C. Azeredo thanks CNPq for the Research Productivity Fellowship.

References

- Ali, S.W., Rajendran, S., & Joshi, M. (2011). Synthesis and characterization of chitosan and silver loaded chitosan nanoparticles for bioactive polyester. *Carbohydrate Polymers*, 83(2), 438–446.
- An, J.; Zhang, M; Wang, S., & Tang, J. (2008). Physical, chemical and microbiological changes in stored green asparagus spears as affected by coating of silver nanoparticles-PVP. *LWT - Food Science and Technology*, 41(6), 1100–1107.
- Anpo, M., Kishiguchi, S., Ichihashi, Y., Takeuchi, M., Yamashita, H., Ikeue, K., Morin, B., Davidson, A., & Che, M. (2001). The design and development of second-generation titanium oxide photocatalysts able to operate under visible light irradiation by applying a metal ion-implantation method. *Research on Chemical Intermediates*, 27(4–5), 459–467.
- Applerot, G., Lipovsky, A., Dror, R., Perkash, N., Nitzan, Y., Lubart, R., & Gedanken, A. (2009a). Enhanced antibacterial activity of nanocrystalline ZnO due to increased ROS-mediated cell injury. *Advanced Functional Materials*, 19, 842–852.

- Applerot, G., Perkas, N., Amirian, G., Girshevitz, O., & Dedanken, A. (2009b). Coating of glass with ZnO via ultrasonic irradiation and a study of its antibacterial properties. *Applied Surface Science*, 256 S, S3–S8.
- Aranaz, I., Harris, R., & Heras, A. (2010). Chitosan amphiphilic derivatives. *Chemistry and applications*. *Current Organic Chemistry*, 14, 308–330.
- Aymonier, C., Schlotterbeck, U., Antonietti, L., Zacharias, P., Thomann, R., Tiller, J. C., & Mecking, S. (2002). Hybrids of silver nanoparticles with amphiphilic hyperbranched macromolecules exhibiting antimicrobial properties. *Chemical Communications*, 2002(24), 3018–3019.
- Badawy, M. E. I., Rabea, E. I., Rogge, T. M., Stevens, C. V., Steurbaut, W., Hofte, M., & Smaghe, G. (2005). Fungicidal and insecticidal activity of O-acyl chitosan derivatives. *Polymer Bulletin*, 54 (4–5), 279–289.
- Balan, L., & Burget, D. (2006). Synthesis of metal/polymer nanocomposite by UV-radiation curing. *European Polymer Journal*, 42, 3180–3189.
- Balan, L., Malval, J. P., & Lougnot, D. J. (2010). In situ photochemically assisted synthesis of silver nanoparticles in polymer matrixes, In: *Silver nanoparticles*, Perez, D. P. (Ed.), 79–91. InTech, Available from: <http://www.intechopen.com/articles/show/title/in-situ-photochemically-assisted-synthesis-of-silver-nanoparticles-in-polymer-matrixes>.
- Beltes, P. G., Pissiotis, E., Koulaouzidou, E., & Kortsaris, A. H. (1997). In vitro release of hydroxyl ions from six types of calcium hydroxide nonsetting pastes. *Journal of Endodontics*, 23(7), 413–415.
- Bharadwaj, R. K., Mehrabi, A. R., Hamilton, C., Trujillo, C., Murga, M., Fan, R., Chavira, A., & Thompson, A. K. (2002). Structure-property relationships in cross-linked polyester-clay nanocomposites. *Polymer*, 43(13), 3699–3705.
- Bi, L., Yang, L., Narsimhan, G., Bhunia, A. K., & Yao, Y. (2011). Designing carbohydrate nanoparticles for prolonged efficacy of antimicrobial peptide. *Journal of Controlled Release*, 150(2), 150–156.
- Brayner, R. (2008). The toxicological impact of nanoparticles. *Nano Today*, 3(1–2), 48–55.
- Brody, A. L. (2006). Nano and food packaging technologies converge. *Food Technology*, 60(3), 92–94.
- Bugatti, V., Constantino, U., Gorrasi, G., Nocchetti, M., Tammaro, L., & Vittoria, V. (2010). Nano-hybrids incorporation into poly(ϵ -caprolactone) for multifunctional applications: Mechanical and barrier properties. *European Polymer Journal*, 46, 418–427.
- Bugatti, V., Gorrasi, G., Montanari, F., Nocchetti, M., Tammaro, L., & Vittoria, V. (2011). Modified layered double hydroxides in polycaprolactone as a tunable delivery system: in vitro release of antimicrobial benzoate derivatives. *Applied Clay Science*, 52, 34–40.
- Busolo, M. A., Fernandez, P., Ocio, M. J., & Lagaron, J. M. (2010). Novel silver-based nanoclay as an antimicrobial in polylactic acid food packaging coatings. *Food Additives & Contaminants: Part A*, 27(11), 1617–1626.
- Carlson, C., Hussain, S. M., Schrand, A. M., Braydich-Stolle, K. L., Hess, K. L., Jones, R. L., & Schlager, J. J. (2008). Unique cellular interaction of silver nanoparticles: Size-dependent generation of reactive oxygen species. *Journal of Physical Chemistry B*, 112(43), 13608–13619.
- Chang, P. R., Jian, R., Yu, J., & Ma, X. (2010). Fabrication and characterisation of chitosan/plasticized starch composites. *Food Chemistry*, 120(3), 736–740.
- Chawengkijwanich, C., & Hayata, Y. (2008). Development of TiO₂ powder-coated food packaging film and its ability to inactivate *Escherichia coli* in vitro and in actual tests. *International Journal of Food Microbiology*, 123(3), 288–292.
- Chen, W., Tao, X., Xue, P., & Cheng, X. (2005). Enhanced mechanical properties and morphological characterizations of poly(vinyl alcohol)–carbon nanotube composite films. *Applied Surface Science*, 252, 1404–1409.
- Cheng, Q., Li, C., Pavlinek, V., Saha, P., & Wang, H. (2006). Surface-modified antibacterial TiO₂/Ag + nanoparticles: Preparation and properties. *Applied Surface Science*, 252, 4154–4160.

- Chirkov, S. N. (2002). The antiviral activity of chitosan (review). *Applied Biochemistry and Microbiology*, 38(1), 1–8.
- Choi, W., Termin, A., & Hoffmann, M. (1994). The role of metal ion dopants in quantum size TiO_2 : correlation between photoreactivity and charge carrier recombination dynamics. *The Journal of Physical Chemistry*, 98(51), 13669–13679.
- Cioffi, N., Torsi, L., Ditaranto, N., Tantillo, G., Ghibelli, L., Sabbatini, L., Bleve-zacheo, T., D'alesio, M., Zambonin, P. G., & Traversa, E. (2005). Copper nanoparticle/polymer composites with antifungal and bacteriostatic properties. *Chemistry of Materials*, 17, 5255–5262.
- Costa, C., Conte, A., Buonocore, G. G., & Del Nobile, M. A. (2011). Antimicrobial silver-montmorillonite nanoparticles to prolong shelf life of fresh fruit salad. *International Journal of Food Microbiology*, 148(3), 164–167.
- Damm, C., Münsted, H., & Rösch, A. (2008). The antimicrobial efficacy of polyamide 6/silver-nano- and microcomposites. *Materials Chemistry and Physics*, 108, 61–66.
- De Moura, M. R., Aouada, F. A., Avena-Bustillos, R. J., McHugh, T. H., Krochta, J. M., & Mattoso, L. H. C. (2009). Improved barrier and mechanical properties of novel hydroxypropyl methylcellulose edible films with chitosan/tripolyphosphate nanoparticles. *Journal of Food Engineering*, 92, 448–453.
- Dong, C., Cairney, Sun, Q., Maddan, O. L., He, G., & Deng, Y. (2010a). Investigation of $\text{Mg}(\text{OH})_2$ nanoparticles as an antibacterial agent. *Journal of Nanoparticles Research*, 12, 2101–2109.
- Dong, C., Song, D., Cairney, J., Maddan, O. L., He, G., & Deng, Y. (2010b). Antibacterial study of $\text{Mg}(\text{OH})_2$ nanoplatelets. *Materials Research Bulletin*, 46(4), 576–582.
- Dutta, P. K., Tripathi, S., Mehrotra, G. K., & Dutta, J. (2009). Perspectives for chitosan based antimicrobial films in food applications. *Food Chemistry*, 114(4), 1173–1182.
- Emamifar, A., Kadivar, M., Shahedi, M., & Soleimani-Zad, S. (2011). Effect of nanocomposite packaging containing Ag and ZnO on inactivation of *Lactobacillus plantarum* in orange juice. *Food Control*, 22, 408–413.
- Emamifar, A., Kadivar, M., Shahedi, M., & Soleimani-Zad, S. (2010). Evaluation of nanocomposite packaging containing Ag and ZnO on shelf life of fresh orange juice. *Innovative Food Science and Emerging Technologies*, 11, 742–748.
- Entsar, I. R., Badawy, M. E. T., Stevens, C. V., Smagghe, G., & Walter, S. (2003). Chitosan as antimicrobial agent: Application and mode of action. *Biomacromolecules*, 4, 1457–1465.
- Fayaz, A.M., Balaji, K., Girilal, M., Kalaichelvan, P.T., & Venkatesan, R. (2009). Mycobased synthesis of silver nanoparticles and their incorporation into sodium alginate films for vegetable and fruit preservation. *Journal of Agricultural and Food Chemistry*, 57(14), 6246–6252.
- Feng, Q. L., Wu, J., Chen, G. Q., Cui, F. Z., Kim, T. N., Kim, J. O. (2000). A mechanistic study of the antibacterial effect of silver ions on *Escherichia coli* and *Staphylococcus aureus*. *Journal of Biomedical Materials Research*, 52(4), 662–668.
- Fernández, A., Picouet, P., & Lloret, E. (2010). Cellulose-silver nanoparticle hybrid materials to control spoilage-related microflora in absorbent pads located in trays of fresh-cut melon. *International Journal of Food Microbiology*, 142, 222–228.
- Fujishima, A., Rao, T. N., & Tryk, D. A. (2000). Titanium dioxide photocatalysis. *Journal of Photochemistry and Photobiology C: Photochemistry Reviews*, 1(1), 1–21.
- Gelover, S., Gómez, L. A., Reyes, K., & Leal, M. T. (2006). A practical demonstration of water disinfection using TiO_2 films and sunlight. *Water Research*, 40, 3274–3280.
- Gordon, T., Perlstein, B., Houbara, O., Felner, I., Banin, E., & Margel, S. (2011). Synthesis and characterization of zinc/iron oxide composite nanoparticles and their antibacterial properties. *Colloids and Surfaces A: Physicochemical and Engineering Aspects*, 374, 1–8.
- Gottesman, R., Shukla, S., Perkast, N., Solovyov, L. A., Nitzan, Y., & Gedanken, A. (2011). Sonochemical coating of paper by microbicidal silver nanoparticles. *Langmuir*, 27(2), 720–726.
- Gu, H. W., Ho, P. L., Tong, E., Wang, L., & Xu, B. (2003). Presenting vancomycin on nanoparticles to enhance antimicrobial activities. *Nano Letters*, 3, 1261–1263.

- Han, Y. S., Lee, S. H., Choi, K. H., & Park, I. (2010). Preparation and characterization of chitosan-clay nanocomposites with antimicrobial activity. *Journal of Physics and Chemistry of Solids*, 71, 464–467.
- He, J., Kunitake, T., & Nakao, A. (2003). Facile in situ synthesis of noble metal nanoparticles in porous cellulose fibers. *Chemistry of Materials*, 15, 4401–4406.
- Hoet, P. H., Brüske-Hohlfeld, I., & Salata, O. V. (2004). Nanoparticles - known and unknown health risks. *Journal of Nanobiotechnology*, 2(1), 12.
- Hong, S. I., & Rhim, J. W. (2008). Antimicrobial activity of organically modified nano-clays. *Journal of Nanoscience and Nanotechnology*, 8(11), 5818–5824.
- Hu, A. W., & Fu, Z. H. (2003). Nanotechnology and its application in packaging and packaging machinery. *Packaging Engineering*, 24, 22–24.
- Huang, L., Li, D. Q., Lin, Y. J., Wei, M., Evans, D. G., & Duan, X. (2005). Controllable preparation of nano-MgO and investigation of its bactericidal properties. *Journal of Inorganic Biochemistry*, 99, 986–993.
- Incoronato, A. L., Buonocore, G. G., Conte, A., Lavorgna, M., & Del Nobile, M. A. (2010). Active systems based on silver-montmorillonite nanoparticles embedded into bio-based polymer matrices for packaging applications. *Journal of Food Protection*, 73(12), 2256–2262.
- Incoronato, A. L., Conte, A., Buonocore, G. G., & Del Nobile, M. A. (2011). Agar hydrogel with silver nanoparticles to prolong shelf life of Fior di Latte cheese. *Journal of Dairy Science*, 94(4), 1697–1704.
- Johnston, J. H., Borrmann, T., Rankin, D., Cairns, M., Grindrod, J. E., & McFarlane, A. (2008). Nano-structured composite calcium silicate and some novel applications. *Current Applied Physics*, 8(3–4), 504–507.
- Kang, S., Herzberg, M., Rodrigues, D. F., & Elimelech, M. (2008). Antibacterial effects of carbon nanotubes: Size does matter! *Langmuir*, 24(13), 6409–6413.
- Kang, S., Pinault, M., Pfefferle, L. D., & Elimelech, M. (2007). Single-walled carbon nanotubes exhibit strong antimicrobial activity. *Langmuir*, 23, 8670–8673.
- Keawchaon, L., & Yoksan, R. (2011). Preparation, characterization and in vitro release study of carvacrol-loaded chitosan nanoparticles. *Colloids and Surfaces B: Biointerfaces*, 84, 163–171.
- Kim, T. Y., Lee, Y. H., Park, K. H., Kim, S. J., & Cho, S. Y. (2005). A study of photocatalysis of TiO₂ coated onto chitosan beads and activated carbon. *Research on Chemical Intermediates*, 31(4–6), 343–358.
- Konwar, U., Karak, N., & Mandal, M. (2010). Vegetable oil based highly branched polyester/clay silver nanocomposites as antimicrobial surface coating materials. *Progress in Organic Coatings*, 68, 265–273.
- Kumar, R., & Münstedt, H. (2005). Silver ion release from antimicrobial polyamide/silver composites. *Biomaterials*, 26, 2081–2088.
- Kvítek, L., Panáček, A., Soukupová, J., Kolář, M., Večeřová, R., Pucek, R., Holecová, M., & Zbořil, R. (2008). Effect of surfactants and polymers on stability and antibacterial activity of silver nanoparticles (NPs). *The Journal of Physical Chemistry C*, 112(15), 5825–5834.
- Li, S. D., & Huang, L. (2008). Pharmacokinetics and biodistribution of nanoparticles. *Molecular Pharmaceutics*, 5(4), 496–504.
- Li, H., Li, F., Wang, L., Sheng, J., Xin, Z., Zhao, L., Xiao, H., Zheng, Y., & Hu, Q. (2009). Effect of nano-packing on preservation quality of Chinese jujube (*Ziziphus jujuba* Mill. var. *inermis* (Bunge) Rehd). *Food Chemistry*, 114(2), 547–552.
- Li, L. H., Deng, J. C., Deng, H. R., Liu, Z. L., & Li, X. L. (2010). Preparation, characterization and antimicrobial activities of chitosan/Ag/ZnO blend films. *Chemical Engineering Journal*, 160, 378–382.
- Li, W., Li, X., Zhang, P., & Xing, Y. (2011a). Development of nano-ZnO coated food packaging film and its inhibitory effect on *Escherichia coli* in vitro and in actual tests. *Advanced Materials Research*, 152–153, 489–492.

- Li, X., Li, W., Xing, Y., & Jiang, Y. (2011b). Effects of nano-ZnO powder-coated PVC film on the physiological properties and microbiological changes of fresh-cut 'Fuji' apple. *Advanced Materials Research*, 152–153, 450–453.
- Liau, S. Y., Read, D. C., Pugh, W. J., Furr, J. R., & Russell, A. D. (1997). Interaction of silver nitrate with readily identifiable groups: Relationship to the antibacterial action of silver ions. *Letters in Applied Microbiology*, 25, 279–283.
- Lin, Y. J., Li, D. Q., Wang, G., Huang, L., & Duan, X. (2005). Preparation and bactericidal property of MgO nanoparticles on γ -Al₂O₃. *Journal of Materials Science: Materials in Medicine*, 16, 53–56.
- López Manchado, M. A., Valentini, L., Biagotti, J., & Kenny, J. M. (2005). Thermal and mechanical properties of single-walled carbon nanotubes–polypropylene composites prepared by melt processing. *Carbon*, 43, 1499–1505.
- Luo, P.G., & Stutzenberger, F.J. (2008). Nanotechnology in the detection and control of microorganisms. *Advances in Applied Microbiology*, 63, 145–181.
- Maness, P. C., Smolinski, S., Blake, D. M., Huang, Z., Wolfrum, E. J., & Jacoby, W. A. (1999). Bactericidal activity of photocatalytic TiO₂ reaction: Toward an understanding of its killing mechanism. *Applied and Environmental Microbiology*, 65(9), 4094–4098.
- Mbhele, Z.H., Salemane, M.G., van Sittert, C.G.C.E., Nedeljković, V., & Luyt, A.S. (2003). Fabrication and characterization of silver-polyvinyl alcohol nanocomposites. *Chemistry of Materials*, 15(26), 5019–5024.
- Marini, M., Bondi, M., Iseppi, R., Toselli, M., & Pilati, F. (2007). Preparation and antibacterial activity of hybrid materials containing quaternary ammonium salts via sol-gel process. *European Polymer Journal*, 34, 3621–3628.
- Mendonça, A. F., Amoroso, T. L., & Knabel, S. J. (1994). Destruction of Gram-negative food-borne pathogens by high pH involves disruption of the cytoplasmic membrane. *Applied and Environmental Microbiology*, 60(11), 4009–4014.
- Mi, Y., Zhang, X., Zhou, S., Cheng, J., Liu, F., Zhu, H., Dong, X., & Jiao, Z. (2007). Morphological and mechanical properties of bile salt modified multi-walled carbon nanotube/poly(vinyl alcohol) nanocomposites. *Composites: Part A*, 38, 2041–2046.
- Monteiro-Riviere, N. A., Nemanich, R. J., Inman, A. O., Wang, Y. Y., & Riviere, J. E. (2005). Multi-walled carbon nanotube interactions with human epidermal keratinocytes. *Toxicology Letters*, 155(13), 377–384.
- Morones, J. R., Elechiguerra, J. L., Camacho, A., Holt, K., Kouri, J. B., Ramirez, J. T., & Yacaman, M. J. (2005). The bactericidal effect of silver nanoparticles. *Nanotechnology*, 16, 2346–2353.
- Murugadoss, A., Chattopadhyay, A. (2008). A 'green' chitosan–silver nanoparticle composite as a heterogeneous as well as micro-heterogeneous catalyst. *Nanotechnology*, 19(1), 015603.
- Narayan, R. J., Berry, C. J., & Brigmon, R. L. (2005). Structural and biological properties of carbon nanotube composite films. *Materials Science and Engineering B*, 123, 123–129.
- No, H. K., Park, N. Y., Lee, S. H., & Meyers, S. P. (2002). Antibacterial activity of chitosans and chitosan oligomers with different molecular weights. *Int. Journal of Food Microbiology*, 74 (1–2), 65–72.
- Page, K., Palgrave, R. G., Parkin, I. P., Wilson, M., Savin, S. L. P., & Chadwick, A. V. (2007). Titania and silver-titania composite films on glass-potent antimicrobial coatings. *Journal of Materials Chemistry*, 17(1), 95–104.
- Prashantha, K., Soulestin, J., Lacrampe, M. F., Krawczak, P., Dupin, G., & Claes, M. (2009). Masterbatch-based multi-walled carbon nanotube filled polypropylene nanocomposites: assessment of rheological and mechanical properties. *Composites Science and Technology*, 69(11–12), 1756–1763.
- Qi, L. F., Xu, Z. R., Jiang, X., Hu, C., & Zou, X. (2004). Preparation and antibacterial activity of chitosan nanoparticles. *Carbohydrate Research*, 339, 2693–2700.
- Ray, S.S., & Okamoto, M. (2003). Polymer/layered silicate nanocomposites: a review from preparation to processing. *Progress in Polymer Science*, 28, 1539–1641.

- Reddy, M. P., Venugopal, A., & Subrahmanyam, M. (2007). Hydroxyapatite-supported Ag-TiO₂ as *Escherichia coli* disinfection photocatalyst. *Water Research*, 41, 379–386.
- Restuccia, D., Spizzirri, U. G., Parisi, O. I., Cirillo, G., Curcio, M., Iemma, F., Puoci, F., Vinci, G., & Picci, N. (2010). New EU regulation aspects and global market of active and intelligent packaging for food industry applications. *Food Control*, 21, 1425–1435.
- Rhim, J. W., Hong, S. I., & Ha, C. S. (2009). Tensile, water vapor barrier and antimicrobial properties of PLA/nanoclay composite films. *LWT – Food Science and Technology*, 42, 612–617.
- Rhim, J. W., Hong, S. I., Park, H. M., & Ng, P. K. W. (2006). Preparation and characterization of chitosan-based nanocomposite films with antimicrobial activity. *Journal of Agricultural and Food Chemistry*, 54, 5814–5822.
- Rhim, J. W., & Ng, P. K. W. (2007). Natural biopolymer-based nanocomposite films for packaging applications. *Critical Reviews in Food Science and Nutrition*, 47(4), 411–433.
- Robertson, J. M. C., Robertson, P. K. J., & Lawton, L. A. (2005). A comparison of the effectiveness of TiO₂ photocatalysis and UVA photolysis for the destruction of three pathogenic microorganisms. *Journal of Photochemistry and Photobiology A: Chemistry*, 175(1), 51–56.
- Rooney, M. L. (1995). Overview of active food packaging. In: *Active food packaging*, Rooney, M.L. (Ed.), 1–37. London: Chapman & Hall.
- Ruan, D., Zhang, L., Zhang, Z., Xia, X. (2003). Structure and properties of regenerated cellulose/tourmaline nanocrystal composite films. *Journal of Polymer Science Part B: Polymer Physics*, 42(3), 367–373.
- Sanpui, P., Murugadoss, A., Prasad, P. V. D., Ghosh, S. S., & Chattopadhyay, A. (2008). The antibacterial properties of a novel chitosan-Ag-nanoparticle composite. *International Journal of Food Microbiology*, 124, 142–146.
- Sawai, J., Igarashi, H., Hashimoto, A., Kokugan, T., & Shimizu, M. (1996). Effect of particle size and heating temperature of ceramic powders on antibacterial activity of their slurries. *Journal of Chemical Engineering of Japan*, 29, 251–256.
- Sawai, J., Shoji, S., Igarashi, H., Hashimoto, A., Kokugan, T., Shimizu, M., Kojima, H. (1998). Hydrogen peroxide as an antibacterial factor in zinc oxide powder slurry. *Journal of Fermentation and Bioengineering*, 86(5), 521–522.
- Sánchez-García, M. D., Gimenez, E., Ocio, M. J., & Lagaron, J. M. (2008). Novel polycaprolactone nanocomposites containing thymol of interest in antimicrobial film and coating applications. *Journal of Plastic Film and Sheeting*, 24, 239–251.
- Sharma, V., Shukla, R. K., Saxena, N., Parmar, D., Das, M., & Dhawan, A. (2009). DNA damaging potential of zinc oxide nanoparticles in human epidermal cells. *Toxicology Letters*, 185(3), 211–218.
- Shi, Z., Neoh, K.G., Kang, E.T., & Wang, W. (2006). Antibacterial and mechanical properties of bone cement impregnated with chitosan nanoparticles. *Biomaterials*, 27(11), 2440–2449.
- Shvedova, A., Castranova, V., Kisin, E., Schwegler-berry, D., Murray, A., Gandelsman, V., Maynard, A., & Baron, P. (2003). Exposure to carbon nanotube material: assessment of nanotube cytotoxicity using human keratinocyte cells. *Journal of Toxicology and Environmental Health, Part A*, 66(20), 1909–1926.
- Son, W. K., Youk, J. H., & Park, W. H. (2006). Antimicrobial cellulose acetate nanofibers containing silver nanoparticles. *Carbohydrate Polymers*, 65, 430–434.
- Sondi, I., & Salopek-Sondi, B. (2004). Silver nanoparticles as antimicrobial agent: a case study on *E. coli* as a model for Gram-negative bacteria. *Journal of Colloid and Interface Science*, 275, 177–182.
- Sorrentino, A., Gorrasi, G., & Vittoria, V. (2007). Potential perspectives of bio-nanocomposites for food packaging applications. *Trends in Food Science & Technology*, 18(2), 84–95.
- Sothornvit, R., Rhim, J. W., & Hong, S. I. (2009). Effect of nano-clay type on the physical and antimicrobial properties of whey protein isolate/clay composite films. *Journal of Food Engineering*, 91, 468–473.

- Stoimenov, P., Klinger, R. L., Marchin, G. L., & Klabunde, K. J. (2002). Metal oxide nanoparticles as bactericidal agents. *Langmuir*, 18, 6679–6686.
- Tankhiwale, R., & Bajpai, S. K. (2009). Graft copolymerization onto cellulose-based filter paper and its further development as silver nanoparticles loaded antibacterial food packaging material. *Colloids and Surfaces*, 69, 164–168.
- Tankhiwale, R., & Bajpai, S. K. (2010). Silver-nanoparticle-loaded chitosan lactate films with fair antibacterial properties. *Journal of Applied Polymer Science*, 115(3), 1894–1900.
- Tsai, G. J., & Su, W. H. (1999). Antibacterial activity of shrimp chitosan against *Escherichia coli*. *Journal of Food Protection*, 62(3), 239–243.
- Tunç, S., & Duman, O. (2011). Preparation of active antimicrobial methyl cellulose/carvacrol/montmorillonite nanocomposite films and investigation of carvacrol release. *LWT – Food Science and Technology*, 44(2), 465–472.
- Ultee, A., Kets, E. P. W., & Smid, E. J. (1999). Mechanisms of action of carvacrol on the food-borne pathogen *Bacillus cereus*. *Applied Environmental Microbiology*, 65(10), 4606–4610.
- Upadhyayula, V. K. K., Deng, S., Mitchell, M. C., & Smith, G. B. (2009). Application of carbon nanotube technology for removal of contaminants in drinking water: A review. *Science of the Total Environment*, 408(1), 1–13.
- Uyama, H., Kuwabara, M., Tsujimoto, T., Nakano, M., Usuki, A., & Kobayashi, S. (2003). Green nanocomposite from renewable resources: plant oil-clay hybrid materials. *Chemistry of Materials*, 15, 2492–2494.
- Valodkar, M., Bhadoria, A., Pohnerkar, J., Mohan, M., & Thakore, S. (2010). Morphology and antibacterial activity of carbohydrate-stabilized silver nanoparticles. *Carbohydrate Research*, 345, 1767–1773.
- Varma, A. J., Deshpande, S. V., & Kennedy, J. F. (2004). Metal complexation by chitosan and its derivatives: a review. *Carbohydrate Polymers*, 55, 77–93.
- Vimala, K., Mohan, Y. M., Sivudu, K. S., Varaprasad, K., Ravindra, S., Reddy, N. N., Padma, Y., Sreedhar, B., & Raju, K. M. (2010). Fabrication of porous chitosan films impregnated with silver nanoparticles: A facile approach for superior antibacterial application. *Colloids and Surfaces B: Biointerfaces*, 76, 248–258.
- Wang, X., Du, Y., Luo, J., Lin, B., & Kennedy, J. F. (2007). Chitosan/organic rectorite nanocomposite films: Structure, characteristic and drug delivery behaviour. *Carbohydrate Polymers*, 69, 41–49.
- Wang, X., Du, Y., Luo, J., Yang, J., Wang, W., & Kennedy, J. F. (2009). A novel biopolymer/rectorite nanocomposite with antimicrobial activity. *Carbohydrate Polymers*, 77, 449–456.
- Wang, X., Du, Y., Yang, J., Wang, X., Shi, X., & Hu, Y. (2006). Preparation, characterization and antimicrobial activity of chitosan/layered silicate nanocomposites. *Polymer*, 47, 6738–6744.
- Warheit, D.B., Laurence, B.R., Reed, K.L., Roach, D.H., Reynolds, G.A.M., & Webb, T.R. (2004). Comparative pulmonary toxicity assessment of single-wall carbon nanotubes in rats. *Toxicological Sciences*, 77, 117–125.
- Watthanaphanit, A., Supaphol, P., Tamura, H., Tokura, S., & Rujiravanit, R. (2010). Wet-spun alginate/chitosan whiskers nanocomposite fibers: Preparation, characterization and release characteristic of the whiskers. *Carbohydrate Polymers*, 79, 738–746.
- Wu, T., Zivanovic, S., Draughon, F. A., Conway, W. S., & Sams, C. E. (2005). Physicochemical properties and bioactivity of fungal chitin and chitosan. *Journal of Agricultural and Food Chemistry*, 53(10), 3888–3894.
- Xing, K., Chen, X.G., Liu, C.S., Cha, D.S., & Park, H.J. (2009). Oleoyl-chitosan nanoparticles inhibits *Escherichia coli* and *Staphylococcus aureus* by damaging the cell membrane and putative binding to extracellular or intracellular targets. *International Journal of Food Microbiology*, 132(2–3), 127–133.
- Yamamoto, O. (2001). Influence of particle size on the antibacterial activity of zinc oxide. *International Journal of Inorganic Materials*, 3(7), 643–646.

- Yoksan, R., & Chirachanchai, S. (2010). Silver nanoparticle-loaded chitosan-starch based film: Fabrication and evaluation of tensile, barrier and antimicrobial properties. *Materials Science and Engineering C*, 30, 891–897.
- Yu, H., Xu, X., Chen, X., Lu, T., Zhang, P., & Jing, X. (2007). Preparation and antibacterial effects of PVA-PVP hydrogels containing silver nanoparticles. *Journal of Applied Polymer Science*, 103, 125–133.
- Zeng, H., Gao, C., Wang, Y., Watts, P. C. P., Kong, H., Cui, X., & Yan, D. (2006). In situ polymerization approach to multiwalled carbon nanotubes-reinforced nylon 1010 composites: mechanical properties and crystallization behavior. *Polymer*, 47, 113–122.
- Zhang, L., Jiang, Y., Ding, Y., Daskalakis, N., Jeuken, L., Povey, M., O'Neill, A. J., & York, D. W. (2010). Mechanistic investigation into antibacterial behaviour of suspensions of ZnO nanoparticles against *E. coli*. *Journal of Nanoparticle Research*, 12, 1625–1636.
- Zhou, X., Shin, E., Wang, K. W., & Bakis, C. E. (2004). Interfacial damping characteristics of carbon nanotube-based composites. *Composites Science and Technology*, 64(15), 2425–2437.

Chapter 14

The Use of Antimicrobial Nanoparticles to Control Oral Infections

R.P. Allaker

14.1 Introduction

Nanotechnology represents the ability to image, manipulate and model functionalities on the nanometer scale. Nanoparticles can be classified as particles of a size no greater than 100 nm, and their unique attributes to combat infection have received considerable attention. Nanomaterials are increasingly finding uses in products such as antimicrobial surface coatings and semiconductors. Such nanoparticulate materials include spherical, cubic and needle-like nanoscaled particles (approximately 5–100 nm) and near-nanoscaled devices (up to micrometers) (Cushing et al. 2004). The properties of nanoparticles, for example hardness, active surface area, chemical reactivity and biological activity, can be dramatically different from those of micrometer-sized particles (Allaker and Ren 2008), and indeed the biocidal effectiveness of metallic nanoparticles has been suggested to be due to both their size and their high surface-to-volume ratio. Such characteristics should allow them to closely interact with microbial membranes, the effect not being solely due to the release of metal ions (Morones et al. 2005). Metallic and other nanoparticles are now being combined with polymers or coated onto surfaces which may have a variety of potential antimicrobial applications within the oral cavity (Monteiro et al. 2009; Hannig et al. 2007).

The mouth supports the growth of a wide diversity of micro-organisms including bacteria, yeasts, viruses, and (on occasions) protozoa. Bacteria are the predominant components of this resident microflora, and the high species diversity found reflects the wide range of endogenously derived nutrients, the varied types of habitat for colonisation, and the opportunity to survive on surfaces provided by a biofilm. Within this context, a biofilm can be classed as an aggregate of microorganisms in which cells adhere to each other and to a surface (Marsh and Martin 2009).

R.P. Allaker (✉)

Queen Mary University of London, Barts & The London School of Medicine and Dentistry,
Institute of Dentistry, London, UK
e-mail: R.P.Allaker@qmul.ac.uk

However, perhaps more commonly than elsewhere in the body, the relationship between this flora and the host in the oral cavity can be disrupted in a number of ways, resulting in the development of disease of the oral structures.

Potential habitats suitable for attachment within the oral cavity include either non-shedding, hard tooth surfaces or soft, constantly replaced epithelial surfaces, and conditions vary with respect to oxygen levels and anaerobiosis, availability of nutrients, exposure to salivary secretions or gingival crevicular fluid, masticatory forces and other variables such as oral hygiene procedures. As a result, the composition of the microbial flora of the mouth varies considerably from site to site and at different times. The composition of the oral microflora, in addition to being variable, is highly complex. Up to 1,000 different species of bacteria at 10^8 – 10^9 bacteria per mL saliva or mg dental plaque are known to be associated with the oral cavity, and it has been suggested that only 50% of the bacteria found at this site can be cultured (Marsh and Martin 2009).

In the majority of cases, infections of the oral cavity are bacterial, fungal or viral. Most bacterial infections within the oral cavity are polymicrobial in nature, and it is quite unusual to find any that are clearly due to a single species. The relative contribution of different bacterial components in such infections is thus difficult to determine. Oral infections may arise either from an endogenous source, i.e. one yielding microorganisms normally found in the mouth, such as plaque-related dental caries ('tooth decay') and periodontal disease ('gum disease'), or an exogenous source yielding micro-organisms not normally found as part of the oral microflora. Dental caries and periodontal disease involve the adherence of bacteria and development of biofilms on both the natural and restored tooth surface. The use of nano-sized antimicrobials offers the possibility to control the formation of these and other oral biofilms through the use of nanoparticles with biocidal, anti-adhesive and delivery capabilities.

14.2 Biofilms and Oral Infections

Biofilms of oral bacteria and yeasts can cause a number of localised diseases in the oral cavity, including dental caries, periodontal disease, candidosis ('oral thrush'), endodontic ('tooth root and pulp disease'), orthodontic ('dental braces') and dental implant ('titanium root') infections (Marsh and Martin 2009).

14.2.1 *Formation and Properties*

The survival of microorganisms within the oral cavity is dependent on their ability to adhere to surfaces and subsequently develop into a biofilm, a process influenced by the physical and chemical properties of the underlying surface (Hannig and Hannig 2009). On the tooth surface, the initial colonisers adhere to the acquired

pellicle, a salivary-/dietary-derived proteinaceous layer, which can then influence the subsequent sequence of colonisation by microorganisms (Marsh and Bradshaw 1995). The acquired pellicle also contains several antibacterial components such as secretory immunoglobulin A (IgA) and lysozyme, and provides both barrier and buffering functions (Hannig and Joiner 2006). Both de- and remineralisation processes of the teeth are also mediated by the pellicle. In terms of bacterial colonisation, many of the proteins that make up the pellicle act as receptors for the specific interaction with adhesins on the surface of pioneer bacterial species (Hannig and Joiner 2006). This layer is therefore of particular relevance as regards the interactions of both bacteria and nanoparticles with the tooth surface.

The strength of the forces involved in the initial attachment of bacteria is critical to their survival and the subsequent growth of the biofilm. The major growth of dental plaque mass then occurs by bacterial cell division within the biofilm rather than by co-aggregation at the surface of the developing biofilm (Kolenbrander et al. 2006). The initial communities of bacteria found within the supragingival plaque (above the gum margin) biofilm are of a relatively low diversity in comparison to those present in the mature communities of both supragingival and subgingival (below the gum margin) plaque. Initial colonisers include *Streptococcus oralis*, *S. sanguinis* and *S. mitis*. The coaggregating partners with these bacteria would then include predominantly Gram-negative species, for example *Eikenella corrodens*, *Veillonella atypica* and *Prevotella loescheii*. Coaggregation bridges between these early colonisers and *Fusobacterium nucleatum*, are common and the latter then co-aggregates with numerous late colonisers. Late colonisers include *Aggregatibacter actinomycetemcomitans*, *Prevotella intermedia*, *Treponema denticola* and *Porphyromonas gingivalis* (Kolenbrander et al. 2006). The interactions between oral bacteria are integral to the development and maturation of the biofilm. Such interactions occur at a number of levels and include physical contact, metabolic exchange, molecular communication and genetic material exchange.

Oral biofilms will accumulate on both the hard and soft tissues, and this community of microbial species is embedded in a matrix of bacterial components, salivary proteins/peptides and food debris (Marsh and Bradshaw 1995). Extracellular polymeric substances, produced by bacteria in a mature biofilm, contain large amounts of polysaccharides, proteins, nucleic acids and lipids. These maintain the structural integrity of the biofilm and provide an ideal matrix for bacterial cell growth and survival (Sutherland 2001). The biofilm mode of growth is thus clearly distinguished from planktonic growth by a number of features, which includes the resistance to antimicrobial agents at concentrations that approach 1,000 times greater than that required to kill planktonic microorganisms (Jenkinson and Lamont 2005; Lewis 2001). This is of major significance in the development of nano-antimicrobials and the extrapolation of in vitro findings.

14.2.2 Oral Biofilms and Disease

14.2.2.1 Dental Caries and Periodontal Disease

Dental caries is a destructive condition of the dental hard tissues that can progress to inflammation and death of vital pulp tissue, and if untreated it may lead to the eventual spread of infection to the periapical area of the tooth and beyond. The disease process involves acidogenic plaque bacteria, including *Streptococcus mutans*, *S. sobrinus* and *Lactobacillus* spp. (Hardie 1992), whereas periodontal diseases can involve both the soft and hard tissues and are initiated by components of the plaque biofilm that develop on the hard root surface adjacent to the soft tissues of the supporting periodontium. Periodontal disease may be confined to the gingiva (gingivitis) or extend to the deeper supporting structures with destruction of the periodontal ligament and the alveolar bone that supports the teeth (periodontitis). This loss of attachment, with associated periodontal pocket formation, may ultimately lead to loosening and loss of the affected teeth. *Porphyromonas gingivalis*, *Tannerella forsythia* and *Treponema denticola* are now regarded as the major pathogens in advancing periodontitis (Ximenez-Fyvie et al. 2000).

The prevention of dental caries and periodontal diseases is traditionally targeted at mechanical or non-specific control of the plaque biofilm because this is the precipitating factor. The use of antimicrobial agents represents a valuable complement to mechanical plaque control (Baehni and Takeuchi 2003). Such strategies should ideally control plaque biofilm formation without significantly affecting the biological equilibrium within the oral cavity. However, actual periods of exposure to antimicrobial agents during tooth brushing and mouth rinsing can be very short, and may amount to about 30 s, rather than the recommended 2 min (van der Ouderaa 1991).

14.2.2.2 Peri-implantitis

Implant systems are increasingly being used to replace missing teeth, and most integrate with bone without complications. Small amounts of plaque consisting mainly of streptococci and *Actinomyces* spp. will accumulate on successful implants. However, in peri-implantitis, anaerobic Gram-negative organisms predominate (Allaker and Hardie 1998). This infection is a key cause of dental implant failure whereby the induced inflammatory changes in the soft tissues surrounding oral implants lead to a progressive destruction of the supporting bone (classified as peri-implantitis and seen in up to 43% of implant-treated subjects) or soft tissues (classified as peri-implantitis mucositis and seen in up to 50% of implant-treated subjects) (Zitzmann and Berglundh 2008). Current forms of treatment are often inadequate and may result in chronic infection requiring implant removal and costly resective and regenerative procedures in an attempt to restore and reshape the implant support (Zitzmann and Berglundh 2008). The incorporation of nanoparticles into

implant coatings may well offer useful osteoconductive and antimicrobial functionalities to prevent dental implant failure.

14.2.2.3 Candidosis

The development of candidosis, including denture stomatitis (chronic atrophic candidosis), which can affect up to 65% of edentulous individuals (Chandra et al. 2001), involves the formation of a biofilm. Despite the use of antifungal drugs to treat denture stomatitis, infection can often become re-established. Chandra et al. (2001), using a poly (methyl methacrylate) (PMMA) biofilm model, demonstrated, that *C. albicans* biofilms are potentially highly resistant to the currently used antifungal agents, with resistance developing with time and showing a correlation with biofilm maturation.

14.2.3 Control of Oral Biofilms

Issues surrounding the uptake and penetration of antimicrobial agents into biofilms are key considerations in the administration of therapeutics (Stewart 2003). This is of particular importance within the oral cavity when these agents have to reach fewer accessible stagnation sites or through plaque to the enamel. Thus, there remains an interest in the development of plaque control measures that require a minimum of public compliance and professional health care intervention (Wilson 1996). Within this context, antimicrobial nanoparticles may be of particular value if retained at approximal teeth surfaces and below the gum margin. The anti-caries potential of fluoride and other more conventional antimicrobial/antiplaque agents, which are mostly deployed in mouthwashes and toothpastes, have been well characterised (Baehni and Takeuchi 2003). However, the potential of nanoparticles as constituents of topical agents to control oral biofilms through either their biocidal or anti-adhesive capabilities is now emerging as an area worthy of serious consideration. The studies by Robinson and co-workers using the 'Leeds in situ model', a device that allows dental plaque to develop in situ on a removable human enamel surface, have helped in the assessment of novel antimicrobial agents and take into account the very complex microbial composition and architecture of plaque biofilms (Watson et al. 2005). The use of such intact biofilms on natural tooth surfaces would be of particular value to a study of the penetration of nanoparticles and released ions in situ. This model has indicated that plaque contains voids and channels, sometimes extending completely through the biomass to the underlying enamel (Wood et al. 2000). The presence of channels may have considerable influence on the transfer of nanoparticles through biofilms. The main considerations are the physico-chemical characteristics of the particular nanoparticles used, including the surface charge and degree of hydrophobicity, the surface area-to-mass ratio of the plaque biofilm and the ability of the particles to adsorb to/be taken up at the

biofilm surface. Within this context, nanoparticles are potentially useful because it is possible to alter their surface charge, hydrophobicity, and other physical and chemical characteristics (Nel et al. 2009).

14.3 Nanometals and the Control of Oral Infections

14.3.1 Nanometals as Antimicrobial Agents

Metals have been used for centuries as antimicrobial agents. Silver, copper, gold, titanium and zinc have attracted particular attention, each having different properties and spectra of activity. Many oral products, including toothpastes, now incorporate powdered (micron-sized) zinc citrate or acetate to control the formation of dental plaque (Giersten 2004). Powdered titanium dioxide is also commonly used as a whitener in toothpastes.

With respect to nanoparticles, the antimicrobial properties of silver (Sondi and Salopek-Sondi 2004) and copper (Cioffi et al. 2005a) have received the most attention. Both of these have been coated onto or incorporated into various materials (Li et al. 2006), including PMMA (Boldyryeva et al. 2005) and hydrogels (Lee and Tsao 2006). An inverse relationship between nanoparticle size and antimicrobial activity has been clearly demonstrated, where nanoparticles in the size range of 1–10 nm have been shown to have the greatest biocidal activity against bacteria (Morones et al. 2005; Verran et al. 2007). Indeed, it has been shown that smaller silver nanoparticles are more toxic than larger particles, more so when oxidised (Lok et al. 2007). At the nanoscale, Ag⁺ ions are known to be released (leached) from the surface (Benn and Westerhoff 2008). Sotiriou and Pratsinis (2010) propose that the antimicrobial activity of small (<10 nm) nanosilver particles is dominated by Ag⁺ ions, while for larger particles (>15 nm), the contributions of Ag⁺ ions and particles to the antibacterial activity are comparable, the Ag⁺ ion release being proportional to the exposed nanosilver surface area.

As a result of their small size, particular nanoparticles may be able to offer other advantages to the biomedical field through improved biocompatibility (Kim et al. 2007). Also, it appears that bacteria are far less likely to acquire resistance to metal nanoparticles than they are to other conventional and narrow-target antibiotics (Pal et al. 2007). This is thought to occur because metals may act on a broad range of microbial targets, and many mutations would have to occur in order for microorganisms to resist their antimicrobial activity. Shape may also affect the activity of nanoparticles. Indeed, it has been demonstrated that the shape of silver nanoparticles can influence antimicrobial activity, as has been shown in the case of *Escherichia coli* (Pal et al. 2007). Truncated triangular silver nanoplates with a {111} lattice plane as the basal plane showed the greatest biocidal activity compared with spherical and rod-shaped nanoparticles. The differences appear to be explained by the proportion of active facets present in nanoparticles of different shapes.

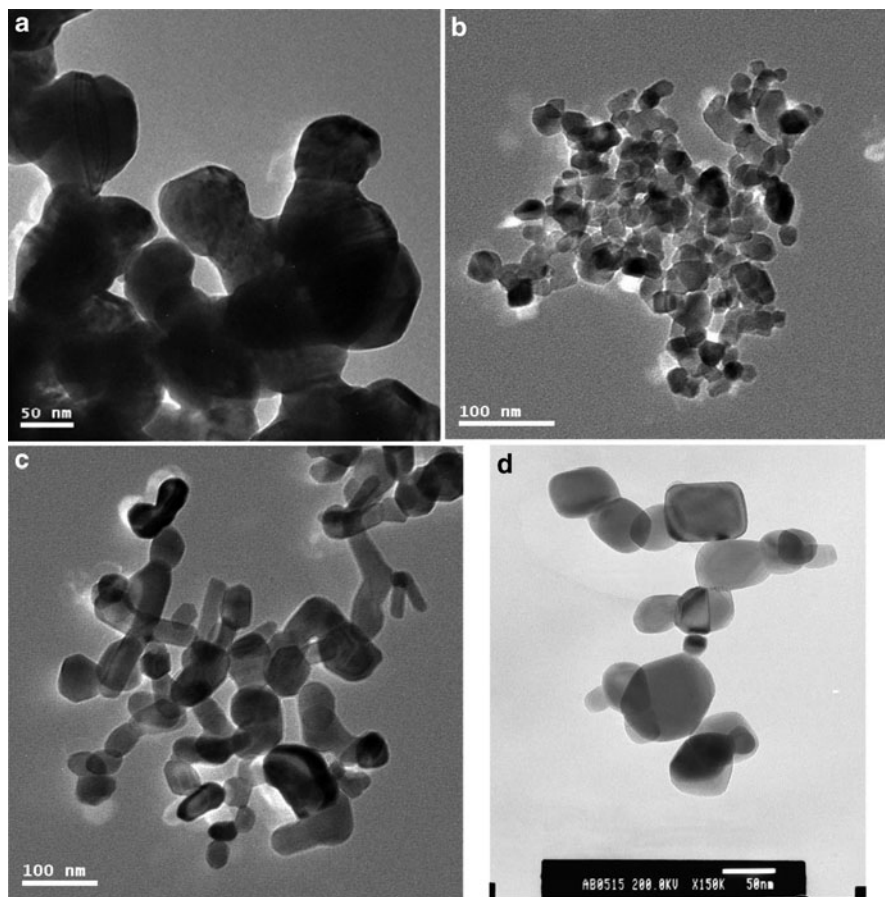


Fig. 14.1 Transmission electron microscopy images of agglomerated silver (a), titanium dioxide (b), zinc oxide (c) and copper oxide (d) nanoparticles

Exploitation of the toxic properties of nanoparticulate metals and metal oxides, in particular those that produce reactive oxygen species under UV light, such as titanium dioxide (TiO_2 ; Fig. 14.1b) and zinc oxide (ZnO ; Fig. 14.1c), are finding increasing use in antimicrobial formulations, with silver metal nanoparticles (5–40 nm) having been reported to inactivate most microorganisms, including HIV-1 (Elechiguerra et al. 2005). The high reactivity of nano-titanium dioxide and nano-silicon dioxide (SiO_2) is exploited extensively for their bacteriocidal properties in filters and coatings on substrates such as polymers, ceramics, glasses and alumina (Han et al. 2005). Significant activity using nanoparticles and their compound clusters (as produced by thermal plasma technology) against fungal and bacterial pathogens such as meticillin-resistant *Staphylococcus aureus* (MRSA) and *E. coli* has recently been demonstrated. These have also shown the capability to inactivate viruses, including SARS, H1N1 Influenza and H5N1 Bird Flu. For

example, new broad-spectrum materials (5–60 nm) can reduce virus levels by 80–100% through direct or indirect contact. Nanoparticle preparations, including those based on nickel (Ni, NiO), zirconium (ZrO₂), copper (Cu, CuO, and Cu₂O), titanium (TiO₂), zinc (ZnO), aluminum (Al₂O₃), silicon(IV) nitride (Si₃N₄), silver (Ag), and tungsten carbide (WC) have been compared as regards their antimicrobial potential. Significant activity with Ag, ZnO, TiO₂ (in the presence of UV light), SiO₂, Cu, Cu₂O, and CuO against bacterial pathogens, including MRSA and *Pseudomonas aeruginosa*, has been demonstrated. Minimum bacteriocidal concentrations (MBC) were found to be in the range of 0.1–5 mg mL⁻¹. In comparison, traditional antibiotics are effective at concentrations 1,000-fold lower. NiO, Ni, Al₂O₃, TiO₂ (in the absence of UV light), Si₃N₄, WC, and ZrO₂ were found to lack antimicrobial activity at the concentrations tested. The oral pathogens *Streptococcus intermedius*, *Porphyromonas gingivalis*, *Fusobacterium nucleatum*, *Prevotella intermedia* and *Aggregatibacter actinomycetemcomitans* were also found to be susceptible to Ag and CuO nanoparticles (Ren et al. 2009) with MBC values in the range 0.025–2.5 mg mL⁻¹ (R.P. Allaker and M.A. Vargas-Reus, 2011).

14.3.1.1 Silver (Ag)

The antibacterial and antiviral actions of elemental silver, Ag⁺ ions, and silver compounds have been extensively investigated (Monteiro et al. 2009). In comparison to other metals, silver is relatively less toxic to human cells, albeit at very low concentrations. Ag⁺ ions have been considered for a range of biomedical applications, including their use within the dental field as an antibacterial component in dental resin composites (Herrera et al. 2001). Silver also exhibits a strong affinity for zeolite, a porous crystalline material of hydrated aluminosilicate which can bind up to 40% Ag⁺ ions within its structure. Silver zeolite has been incorporated into tissue conditioners, acrylic resins, and mouth rinses within the dental field (Casemiro et al. 2008; Kawahara et al. 2000; Matsuura et al. 1997; Morishita et al. 1998). Silver nanoparticles (Fig. 14.1a), either alone or together with other antimicrobial agents, have shown particularly encouraging results (Sondi and Salopek-Sondi 2004; Li et al. 2005; Rai et al. 2009). The use of silver salt nanoparticles instead of elemental silver or complex silver compounds to prevent biofilm formation on surfaces for both biomedical and more general use has been investigated. Using silver bromide precipitation to synthesise polymer–nanocomposites, surfaces were shown to resist biofilm formation. It was also shown to be possible, through controlling the size of the embedded AgBr, to modify the release of biocidal Ag⁺ ions (Sambhy et al. 2006).

In comparison to conventional antimicrobials, surprisingly little is known about how nanoparticles behave in relation to microorganisms, particularly at the cellular level. The mechanism of the antimicrobial activity of silver is not completely understood, but is likely to involve multiple targets in comparison to the more defined targets of antibiotics. Studies have shown that the positive charge on the Ag⁺ ion is

critical for antimicrobial activity, allowing the electrostatic attraction between the negative charge of the bacterial cell membrane and positively charged nanoparticles (Kim et al. 2007). In terms of the molecular mechanisms of inhibitory action of Ag⁺ ions on microorganisms, it has been shown that DNA loses its ability to replicate (Feng et al. 2000), and the expression of ribosomal subunit proteins and other cellular proteins and enzymes necessary for ATP production becomes inactivated (Yamanaka et al. 2005). It has also been hypothesised that Ag⁺ ions affect membrane-bound respiratory enzymes (Bragg and Rainnie 1974). However, the precise mechanism(s) of biocidal activity of silver nanoparticles against bacteria remains to be fully elucidated. The work of Sondi and Salopek-Sondi (2004) demonstrated structural changes and damage to bacterial membranes resulting in cell death. These particular studies suggest that sulphur-containing proteins in the membrane or inside the cells and phosphorus-containing elements, such as DNA, are likely to be the preferential binding sites for silver nanoparticles. The contribution of Ag⁺ ion release from nanoparticles to the overall antimicrobial activity remains unclear. It is suggested that a bacterial cell in contact with silver nanoparticles will take up Ag⁺ ions, which possibly in turn will inhibit respiratory enzymes and so help to generate free radicals, and subsequent free radical-induced damage to the cell membrane. In order to determine the relationship between free radical formation and antimicrobial activity, the use of antioxidants does suggest that free radicals may be derived from the surface of silver nanoparticles (Kim et al. 2007).

14.3.1.2 Copper (Cu)

Alongside silver, copper is a traditionally well-known antimicrobial material. In comparison to silver, relatively few studies have reported the antimicrobial properties of copper. It is suggested that copper may well have a similar mode of action to that of silver. However, it remains unclear as to the precise mechanism by which copper nanoparticles exert their antimicrobial activity. As with silver, it is thought that copper partly elicits its antimicrobial activity by combining with the –SH groups of key enzymes. Yoon et al. (2007) demonstrated superior antimicrobial activity with copper nanoparticles against *E. coli* and *Bacillus subtilis* when compared to silver nanoparticles. However, in the author's laboratory, silver consistently demonstrated superior activity to copper with a wide range of different species and strains (Ren et al. 2009).

The antimicrobial properties of both silver and copper nanoparticles were also investigated by Ruparelia et al. (2008) using strains of *E. coli*, *B. subtilis*, and *S. aureus*. The bacteriocidal effect of the nanoparticles was compared using disc diffusion tests, and minimum inhibitory concentration (MIC) and minimum bacteriocidal concentration (MBC) determinations in batch cultures. Bacterial sensitivity was found to differ according to the species tested and the test system employed. For all strains of *S. aureus* and *E. coli*, the action of silver nanoparticles was found to be superior. Strain-specific variation for *S. aureus* was negligible, while some strain-specific variation was observed for *E. coli*. A higher sensitivity, as shown

with *B. subtilis*, may be attributed to more amine and carboxyl groups (in comparison to other species) on the cell surface, these groups having a greater affinity for copper (Beveridge and Murray 1980). Released copper ions within the cell may then disrupt nucleic acid and key enzymes (Stohs and Bagchi 1995). In theory, a combination of silver and copper nanoparticles may give rise to a more complete bacteriocidal effect, especially against a mixed population of bacteria. Indeed, the studies of Ren et al. (2009) demonstrated that populations of Gram-positive and Gram-negative bacteria could be reduced by 68% and 65%, respectively, in the presence of 1.0 mg mL⁻¹ nano-copper oxide within 2 h. This was significantly increased to 88% and 100%, respectively, with the addition of a relatively low concentration (0.05 mg mL⁻¹) of nano-silver.

14.3.1.3 Gold (Au)

In comparison to silver and copper, gold generally shows a weak antimicrobial effect. However, gold nanoparticles are employed in multiple applications involving biological systems. The binding properties of gold are exceptional, and this makes it particularly suitable for attaching ligands to enhance biomolecular interactions. Gold nanoparticles also exhibit an intense colour in the visible range and contrast strongly for imaging by electron microscopy (Lin et al. 2002). Despite all the current and potential applications for gold nanoparticles, there remains little information as to how these particles affect microorganisms. Growth inhibition studies, to measure the effect of gold nanoparticles (polyethylene glycol-coated to allow dispersion) on *E. coli* at various concentrations, demonstrated no significant activity (Williams et al. 2006). Studies in the author's laboratory with PEG-coated gold nanoparticles also showed no activity against *E. coli*. However, the growth of the Gram-negative species *Proteus* and *Pseudomonas aeruginosa* was inhibited at a concentration of 1.0 mg mL⁻¹.

14.3.2 Nanoparticulate Metal Oxides as Antimicrobial Agents

Nanoparticulate metal oxides have been of particular interest as antimicrobial agents as they can be prepared with extremely high surface areas and unusual crystal morphologies that have a high number of edges, corners and other potentially reactive sites (Stoimenov et al. 2002). However, certain metal oxides are now coming under close scrutiny because of their potential toxic effects (Karlsson et al. 2008). Oxides under consideration as antimicrobial agents include those of copper, zinc oxide, titanium dioxide (titania) and tungsten oxide (WO₃).

14.3.2.1 Copper Oxide (CuO)

Copper oxide (CuO) is a semi-conducting compound with a monoclinic structure. CuO has attracted particular attention because it is the simplest member of the

family of copper compounds and exhibits a range of potentially useful physical properties, such as high temperature superconductivity, electron correlation effects and spin dynamics (Cava, 1990; Tranquada et al. 1995). Limited information on the possible antimicrobial activity of nano CuO is available. Copper oxide is relatively cheap, easily mixed with polarised liquids (i.e. water) and polymers, and relatively stable in terms of both chemical and physical properties. Highly ionic nanoparticulate metal oxides, such as CuO, may be particularly valuable antimicrobial agents as they can be prepared with extremely high surface areas and unusual crystal morphologies (Stoimenov et al. 2002).

Copper oxide nanoparticles have been characterised, both physically and chemically, and investigated with respect to potential antimicrobial applications (Ren et al. 2009). It was found that nano-scaled CuO, as generated by thermal plasma technology, demonstrated particle sizes in the range 20–95 nm with a mean surface area of $15.7 \text{ m}^2 \text{ g}^{-1}$ (Fig. 14.1d). CuO nanoparticles in suspension showed activity against a range of bacterial pathogens, including MRSA and *E. coli*, with minimum bacteriocidal concentrations ranging from 0.1 to 5.0 mg mL^{-1} . As with silver, studies of CuO nanoparticles incorporated into polymers suggest that release of ions may be required for optimum killing (Ren et al. 2009). Incorporation of nano CuO into porous elastomeric polyurethane films has demonstrated potential for a number of applications. Studies have shown this approach to be effective against MRSA within 4 h of contact (Z. Ahmad and R.P. Allaker, unpublished observations).

14.3.2.2 Zinc Oxide (ZnO)

The antimicrobial mechanisms of zinc are not completely understood. In recent years, nano-zinc oxide has received increasing attention, partly because it is stable under harsh processing conditions but also because it is generally regarded as safe to man (Stoimenov et al. 2002). Studies have shown that some nanoparticulate metal oxides, such as ZnO, have a degree of selective toxicity to bacteria with a minimal effect on human cells (Brayner et al. 2006; Reddy et al. 2007; Zhang et al. 2007). The proposed mechanisms of antibacterial activity include induction of reactive oxygen species (Sawai, 2003; Jones et al. 2008) and damage to the cell membrane with subsequent interaction of the nanoparticle with the intracellular contents (Brayner et al. 2006).

In a study by Liu et al. (2009) the antimicrobial properties of ZnO nanoparticles were investigated against *E. coli* O157:H7. This strain was significantly inhibited as shown using SEM and TEM analyses to assess the morphological changes of bacterial cells. Leakage of intracellular contents and a degree of membrane disorganisation was observed. Using Raman spectroscopy, the intensities of lipid and protein bands were shown to increase after exposure to ZnO nanoparticles, whereas no significant change to nucleic acid was indicated. In comparison to silver nanoparticles (0.1 mg mL^{-1}), a higher concentration of zinc oxide (particle size: approx. 15–20 nm; surface area: $47 \text{ m}^2 \text{ g}^{-1}$) is required to have growth-inhibitory ($0.5\text{--}2.5 \text{ mg mL}^{-1}$) and killing effects ($>2.5 \text{ mg mL}^{-1}$) against a range of pathogens

including *E. coli* and MRSA. While with those organisms implicated in oral infections, including *A. actinomycetemcomitans*, *P. gingivalis*, *Prev. intermedia* and *F. nucleatum*, greater sensitivity was demonstrated, with growth inhibitory and killing concentrations of 0.25–2.5 and 0.25–2.5 mg mL⁻¹, respectively (R.P. Allaker, M.A. Vargas-Reus and K. Memarzadeh, 2011).

14.3.2.3 Titanium Dioxide (TiO₂)

Titanium dioxide (TiO₂) is the commonest titanium compound, and its ability to act as a photocatalytic antimicrobial compound is well established (Blake et al. 1999). TiO₂ is widely used in a number of applications, as a powder and increasingly in a nanoparticulate form, and is generally considered to be non-toxic at the concentrations normally employed. However, there are recent concerns that nano-titanium oxide may present a hazard to health through inflammation as generated by release of IL-1 α (Yazdi et al. 2010). The anatase form of nano TiO₂ and UV light excitation are required to ensure maximum antimicrobial activity. Such TiO₂ photocatalysis is able to promote the peroxidation of the polyunsaturated phospholipid component of the microbial lipid membrane, induce loss of respiratory activity, and elicit cell death (Maness et al. 1999). In comparison to silver and copper nanoparticles, there have been relatively few studies on nano-titanium/-titanium dioxide. The study of Tsuang et al. (2008) demonstrated TiO₂-mediated photocatalytic and bacteriocidal activities against obligate aerobes (*Pseudomonas aeruginosa*), facultative anaerobes (*S. aureus*, *E. coli* and *Enterococcus hirae*) and obligate anaerobes (*Bacteroides fragilis*). Concentrations of titanium oxide (predominantly anatase phase; in the absence of UV light; particle size: approx. 18 nm; surface area: 87 m² g⁻¹) required to have a growth inhibitory and killing effect against a range of pathogens including *E. coli* and MRSA. have been shown to be 1.0–2.5 and >2.5 mg mL⁻¹ respectively, while with those organisms implicated in oral infections, including *A. actinomycetemcomitans*, *P. gingivalis*, *Prev. intermedia* and *F. nucleatum*, growth inhibitory and killing concentrations are in the same order at 0.25–2.5 and >2.5 mg mL⁻¹, respectively (R.P. Allaker, M.A. Vargas-Reus and K. Memarzadeh, 2011).

14.3.3 Oral Applications of Nanoparticulate Metals and Metal Oxides

In order to reduce bacterial and fungal adhesion to oral materials and devices, silver nanoparticles are being investigated for a range of possible applications, for example, incorporation into denture materials (Fig. 14.2) (Monteiro et al. 2009) and orthodontic adhesives (Ahn et al. 2009). The optimum amount of silver nanoparticles used within such polymer materials will be of critical importance to avoid an adverse effect upon their physical properties. The study of Ahn et al. (2009) clearly

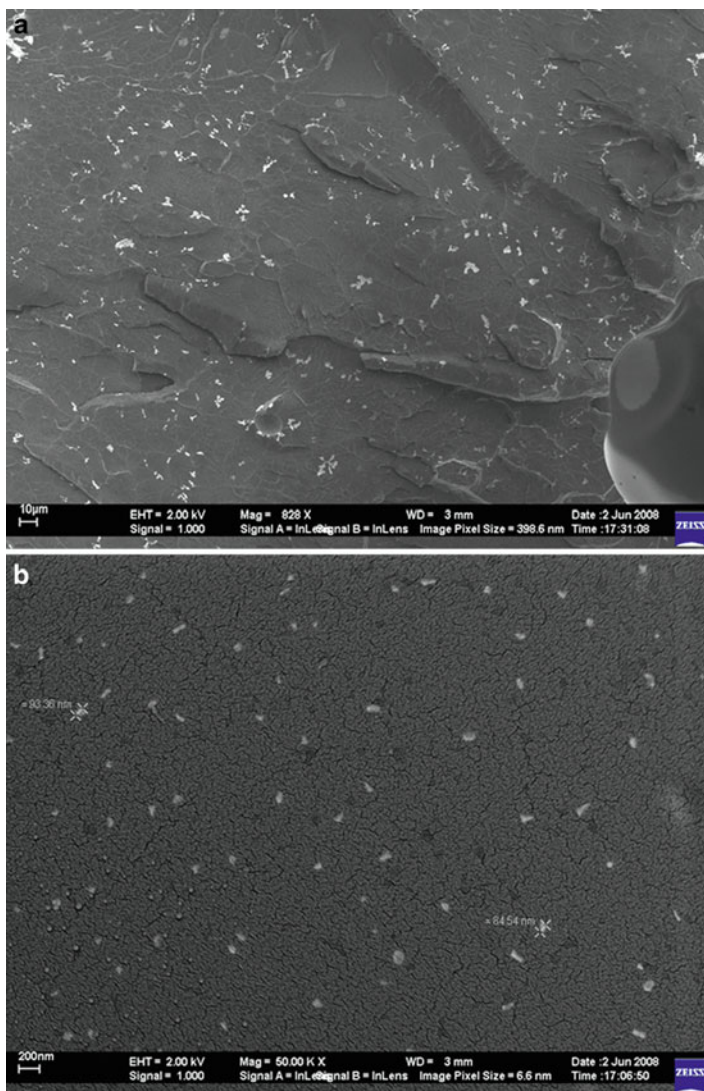


Fig. 14.2 Scanning electron micrograph of a fractured polymethyl methacrylate PMMA/Ag nanocomposite containing approximately 0.04% w/w silver. Distribution of silver particles in the PMMA acrylic resin shown. (a) White areas are agglomerated silver nanoparticles distributed in the PMMA ($\times 828$ magnification). (b) Silver nanoparticles (white dots) with approximate mean size 88 nm distributed in the PMMA matrix. ($\times 50,000$ magnification) (With permission; Monteiro et al. 2009)

demonstrated that experimental composite adhesives (ECAs) had rougher surfaces than conventional adhesives due to the addition of silver nanoparticles, although bacterial adhesion to ECAs was shown to be less than that to conventional adhesives

and was not influenced by saliva coating. However, no significant difference between ECAs and conventional adhesives was shown as regards bond shear strength.

Biofilm growth is known to contribute to secondary caries and the failure of resin-based dental composites. Within this context, zinc oxide nanoparticles have undergone in vitro testing using biofilm culture test systems (Aydin Sevnic and Hanley 2010). ZnO nanoparticles blended into a variety of composites were shown to significantly inhibit *S. sobrinus* biofilm growth at concentrations not less than 10% w/w over a 3-day test period. However, at this concentration, the impact on the structural characteristics of composites would need to be carefully assessed.

As regards dental implants, numerous companies currently market novel synthetic hydroxyapatite (HA) materials, as the optimal osteoconductive implant coating available, and some companies have developed nanoscaled varieties. Some have employed coatings and application methods different from the conventional coating techniques, including an HA material available in nanophase and a nanocrystalline silver-based antimicrobial coating that in theory should reduce the potential for bacterial colonisation. The antibacterial properties of an amorphous carbon film (Almaguer-Flores et al. 2010) incorporating silver nanoparticles in a 40- to 60-nm size range and deposited onto a standard titanium material have been evaluated. A significant reduction in mixed biofilm counts compared to the standard titanium material was observed after 7 days using the coating with silver nanoparticles.

14.3.4 Other Nano-Based Antimicrobials

14.3.4.1 Quaternary Ammonium Nanoparticles

Quaternary ammonium poly (ethylene imine) (QA-PEI) nanoparticles as an antimicrobial to incorporate into restorative composite resins have been developed by Yudovin-Faber et al. (2008). These may have distinct advantages over the currently used composite resins employed to restore hard tissues, which are known to have several disadvantages including development of biofilms on both teeth and the restorative material (Monteiro et al. 2009). The traditional methods for preparing antibacterial composite materials have been to impregnate them with low-molecular-weight agents, such as Ag⁺ ions or iodine, that are then released slowly. Apart from the possible adverse effects on the mechanical properties of the composite, difficulties in controlling the release of such agents may be a potential drawback.

The use of QA-PEI nanoparticles at a concentration of 1% w/w enabled complete in vitro growth inhibition of *Streptococcus mutans* to be achieved for a duration of at least 3 months (Yudovin-Farber et al. 2008). The proposed mechanism of action of QA-PEI is suggested to be as a result of transfusion across, and damage to, the bacterial cell wall. The hydrophobic nature and positive charge of these nanoparticles are also thought to further enhance the antimicrobial activity. Surface chemical analysis of the restorative composite embedded with QA-PEI

demonstrated a surface modification of higher hydrophobicity and the presence of quaternary amines when compared to the unmodified material. Further studies to optimise the release characteristics of QA-PEI and other potentially useful nanoparticles from dental materials will be required.

14.4 Anti-adhesive Nanoparticles and Oral Biofilm Control

14.4.1 Chitosan Nano- and Microparticles

Chitosan is a biopolymer derived by the deacetylation of chitin, a natural polymer occurring in the exoskeleton of crustaceans. Chitosan is positively charged and soluble in acidic to neutral solution, enabling it to bind to mucosal surfaces. Both chitosan nano- and microparticles have been investigated as a potential platform for local delivery of drugs (Wu et al. 2005). Although the currently used antimicrobial irrigants (without chitosan incorporation), employed to disinfect root canals in the treatment of endodontic infections, are capable of killing *Enterococcus faecalis*, the bacterium frequently associated with this condition, endodontic restorations often fail (Lin et al. 1992). The in vitro study of Kishen et al. (2008) demonstrated that root canal surfaces treated with cationic antibacterial nanoparticulates such as zinc oxide alone and a combination of zinc oxide and chitosan nanoparticulates are able to significantly reduce *E. faecalis* adherence to dentine. In theory such surface treatment could prevent bacterial recolonisation and biofilm formation in vivo.

14.4.2 Silica and Silicon Nanoparticles

Particles of a nano- and micro-size based upon the element silicon to rapidly deliver antimicrobial and anti-adhesive capabilities to the desired site within the oral cavity have received much attention (Stephen, 1993). Companies have used silica (silicon dioxide 'SiO₂' and often classed as 'microfine', but with a particle size within the definition of nanoparticles) in toothpastes for many years, and some are now actively seeking new directions in this area through the use of porous silicon and nanocrystalline silicon technology to carry and deliver antimicrobials, for example triclosan. These would offer advantages over some of the slower and more prolonged delivery systems under investigation.

The use of silica nanoparticles to polish the tooth surface may help protect against damage by cariogenic bacteria, presumably because the bacteria can more easily be removed. This has been investigated on human teeth ex vivo (Gaikwaad and Sokolov, 2008). Atomic force microscopy demonstrated lower nanometer-scale roughness obtained when silica nanoparticles were used to polish the surface of teeth as compared with conventional polishing pastes. It was also shown that

adherent *S. mutans* could be more easily removed. However, concerns remain as to the longevity of the effect, and whether the polished surface will inhibit mineralisation and plaque formation *in vivo*.

Spherical silica nanoparticles (up to 21 nm) deposited onto polystyrene surfaces by polycationic binding have been investigated with respect to the development of *C. albicans* biofilms and invasive filament formation (Cousins et al. 2007). Modified surfaces were shown to reduce attachment and growth of *C. albicans*, with the greatest effect observed with 7- and 14-nm particles. Such effects could possibly be attributed to the surface topography or slow dissolution of the bound silica. Such treatment has the advantages of being non-toxic, simple to apply and adaptable to 3-dimensional surfaces.

Other novel systems based upon silica have been investigated with respect to the control of oral biofilms. The use of nitric oxide (NO)-releasing silica nanoparticles to kill biofilm-based microbial cells has been described (Hetrick et al. 2009). The rapid diffusion of NO may well result in enhanced penetration into the biofilm matrix and therefore improved efficacy against biofilm-embedded bacteria. *In vitro*-grown biofilms of *Pseudomonas aeruginosa*, *E. coli*, *Staphylococcus aureus*, *Staphylococcus epidermidis* and *Candida albicans* were exposed to NO-releasing silica nanoparticles. Over 99% of cells from each type of biofilm were killed via NO release. In comparison to small-molecule NO donors, the physicochemical properties, for example hydrophobicity, charge and size, of nanoparticles can be altered to increase anti-biofilm efficacy (Nel et al. 2009).

Bioactive glasses of the $\text{SiO}_2\text{-Na}_2\text{O-CaO-P}_2\text{O}_5$ system have been shown to possess antimicrobial activity through the release of ionic alkaline species over time and are under consideration as dentine disinfectants to offer an alternative to calcium hydroxide (Waltimo et al. 2007). Those in the form of amorphous nanoparticles with a size of 20–60 nm may show an advantage over micron-sized material as the decrease in glass particle size should increase, by more than tenfold, the active exchange surface of glass and surrounding liquid. In turn, this would substantially increase ionic release into suspension and enhance antimicrobial efficacy. Waltimo et al. (2007) monitored ionic dissolution profiles in simulated body fluid. Antimicrobial activity was assessed against *Enterococcus faecalis* as a pathogen often isolated from root canal infections. They found that a shift from a micron- to a nano-size increased the release of silica by a factor of 10 and elicited a pH elevation of at least 3 units. The killing efficacy was also significantly higher.

14.4.3 Hydroxyapatite and Other Calcium Phosphate-Based Systems

The application of nano-scaled hydroxyapatite particles has been shown to impact on oral biofilm formation and provides a re-mineralisation capability (Roveri et al. 2008; Cross et al. 2007). Biomimetic approaches, based upon hydroxyapatite nanocrystals which resemble the structure at the nano-scale of abraded dental

enamel crystallites, should allow adsorbed particles to interact with bacterial adhesins and reduce bacterial adherence, and hence impact on biofilm formation (Venegas et al. 2006).

A number of oral health care products, including dentrifices and mouth rinses, have been developed containing nano-sized apatite particles with and without protein-based additives (Rahiotis et al. 2008; Reynolds et al. 2003). It is suggested that the efficacy of these compounds can be attributed to the size-specific effects of the apatite nanoparticulates. Casein phosphopeptide (CPP) – amorphous calcium phosphate (ACP) nanocomplex (Recaldent™) – is a particular technology based upon ACP and stabilised by casein phosphopeptide (CPP) (Reynolds 2008). Use of this technology has demonstrated anticariogenic activity under both in vitro and in vivo conditions. The levels of calcium and phosphate ions in supragingival plaque have been shown to increase upon delivery of CPP-ACP in a mouth rinse form and promote remineralisation of enamel subsurface lesions (Reynolds et al. 2003). Analysis of plaque samples demonstrated CPP-ACP nanocomplexes to be localised in plaque on the surface of bacterial cells and essentially confirm the studies by Rose (Rose 2000a; Rose 2000b) who demonstrated tight binding to *Streptococcus mutans* and the intercellular plaque matrix to provide a calcium ion reservoir. As a result of interaction with calcium binding sites and the masking of bacterial receptors on salivary molecules, CPP-ACP is thought to reduce bacterial colonisation as shown with CPP-ACP germanium-treated surfaces. (Rahiotis et al. 2008).

14.5 Incorporation of Nanoparticles into Polymeric Materials for Possible Oral Use

14.5.1 Properties of Polymer Matrix Nanocomposites

Nanocomposites are usually solid combinations of a bulk matrix and a nano-dimensional phase(s), which differ in structural and chemical properties. The physical properties of the nanocomposite will thus differ markedly from those of the component materials. In mechanical terms, this is attributed to the high surface-to-volume ratio of the nanoconstituents. With polymer-nanocomposites, properties related to local chemistry, thermoset cure, polymer chain mobility, conformation, and ordering can all vary markedly and continuously from the interface with the nanophase into the bulk of the matrix.

Polymer–matrix nanocomposites (nanofilled polymer composites) are, in their simplest case, made by appropriately adding nanoparticulates to a polymer matrix to enhance its functionality (Manias 2007). This can be particularly effective in producing high-performance composites when optimum dispersion of the nanofiller is achieved, and the properties of such a filler can markedly enhance those of the matrix, for example by reinforcement of a polymer matrix with more rigid nanoparticles of ceramics or carbon nanotubes. The high aspect ratio and/or

the high surface area-to-volume ratio of nanoparticulates provide such superior properties.

Silver nanoparticles have been investigated with a view to improving both the physical and the antimicrobial properties of dental polymeric materials, for example, in denture materials (Fig. 14.2) (Monteiro et al. 2009) and orthodontic adhesives (Ahn et al. 2009). K.P. Lackovic et al. (2008) investigated the use of silver nanoparticles in an attempt to improve the physical and antimicrobial properties of orthodontic bracket-bonding cement. Incorporation of silver nanoparticles at a concentration of less than 1% w/v was found not to decrease the modulus of the cement tested. However, no significant effect on either the attachment or growth of the cariogenic bacterium *Streptococcus mutans* was observed. Thus, an optimum amount of silver nanoparticles used within polymer materials may well be of critical importance to avoid an adverse effect upon the physical properties. The study of Ahn et al. (2009) clearly demonstrated that experimental composite adhesives (ECAs) had rougher surfaces than conventional adhesives owing to the addition of silver nanoparticles. Bacterial adhesion to ECAs was shown to be less than that of conventional adhesives and was not influenced by saliva coating. No significant difference between ECAs and conventional adhesives was shown as regards bond shear strength.

14.5.2 Methods of Combining Nanometals with Polymers

Combining nanoparticulate metals with a polymer matrix such that they remain adequately dispersed is a process that has presented some problems. Three general methods to formulate polymer–matrix nanocomposites have been utilised:

1. In situ synthesis of nanoparticles in the polymer matrix by reduction of a metal salt in the matrix or evaporation of the metal at the heated surface of the matrix.
2. Polymerisation of the matrix around the nanoparticles.
3. Incorporation of pre-synthesised nanoparticles into a pre-synthesised polymer matrix with the aid of a blending solvent (Corbierre et al. 2005).

However, the first and second methods have a tendency to produce undesirable nanospecies and polydisperse (range of particle sizes) polymer matrices. An approach involving the impregnation of silicone (as used in a wide variety of devices) with nanoparticulate silver, using supercritical carbon dioxide, has been investigated (Furno et al. 2004). This may be particularly applicable as regards implantable devices, as their use is a major risk factor for hospital-acquired infection. The initiation of infection involving biomaterials requires an initial adhesion event to the device or more often to the patient-derived glycoprotein coating (conditioning film) which is deposited from the time of implantation (Green et al. 1999). Following adhesion, microbial proliferation leads to the development of a biofilm which is more resistant to the effect of antimicrobials. Although approaches to prevent this type of infection, including the use of coatings

with nanoparticulate silver, have been proposed, unsatisfactory clinical results and on occasion further complications, have occurred (Riley et al. 2002). Possible reasons for the lack of activity include the inactivation of the antimicrobial coating by plasma components and a lack of inherent durability of the coatings used. Impregnation of polymers may well be more beneficial than the use of coatings or addition into the mix. A significant level of surface- or near-surface-deposited silver nanoparticles should provide an initial “burst” effect. However, Furno et al. (2004) showed that the majority of the antimicrobial activity, against both biofilms and planktonic cells, was simply removed by washing the polymer discs impregnated with silver nanoparticles. Further sustained release with significant antimicrobial activity would need to be carefully evaluated. The protection of both inner and outer surfaces against bacterial colonisation by impregnation of an antimicrobial agent is advantageous (Wilcox et al. 1988) and has been demonstrated in the clinical setting (Darouiche et al. 1999). The continued release of Ag⁺ ions at antimicrobial concentrations even in the presence of a plasma protein conditioning film, and the ability to offer protection to both the inner and outer surfaces of a catheter, are two distinct potential advantages of polymer impregnation (Furno et al. 2004).

14.5.3 *Polymeric Films Incorporating Nanometals*

It is possible to enhance the properties of certain materials by encapsulation in a polymeric film, for example by encapsulating and modifying the surface properties of denture acrylic polymers with an inorganic silicone polymeric film (Thorne and Vittori 1997) to prevent diffusion of food contaminants, bacteria and the ingrowth and adherence of *Candida* spp. hyphae that may lead to failure. The use of hydrophobic polymer-based materials as occlusive thin films for the prophylaxis of dental caries, dental erosion and dentine hypersensitivity has more recently been explored in vitro (Nielsen et al. 2011).

Nanotechnology is now beginning to be able to provide the tools required to synthesise films or layers with embedded metal nanoparticles. For copper nanoparticles embedded in an inert, Teflon (polytetrafluoroethylene)-like matrix, Cioffi et al. (2005b) demonstrated significant antimicrobial activity in vitro as a result of ion release. It is suggested that in such an experimental situation a bacterial growth medium facilitates the release of metallic ions, possibly as a consequence of a reaction with the nutrient media constituents. A greater release of copper ions into a liquid medium could well be due to the presence of an oxide layer on the copper nanoparticles and reaction with chloride ions in the medium. The copper–fluoropolymer (Cu-CFx) nano-composite films in this study were deposited by dual ion-beam sputtering, a technique to deposit different polymeric and inorganic materials in a very controlled manner. Analysis of the layers revealed that the inorganic Cu(II) nanoparticles were evenly dispersed in the branched fluoropolymer matrix. Through the use of electrochemical atomic absorption spectroscopy, copper release kinetics in solutions was measured. A correlation was

shown between the chemical composition (copper loading) of the material surface, the concentration of copper ions released into the microbial culture broths, and the bioactivity of the Cu-CFx coating. The Cu-CFx layers, used as coatings, were shown to inhibit the yeast *Saccharomyces cerevisiae* and the bacterial species *E. coli*, *S. aureus* and *Listeria* spp. Such use of Cu-CFx coatings, which allow variable metal loading, demonstrate good stability upon storage and microbial inhibitory activity, is being explored in a variety of applied fields, including food chemistry and biomedicine.

Sacrificial-anode electrochemical synthesis of metal nanoparticles in the presence of tetraoctylammonium (TAO) salts have allowed Cioffi et al. (2005c) to prepare copper- and silver-containing coatings by combining the metal colloid with a polymer-dispersing matrix. The surfactants used were capable of providing physical and chemical stabilisation of the metal nanoparticles through the formation of a protective organic shell. These materials were then able to show a significant inhibitory effect on the growth of *E. coli* and *Saccharomyces cerevisiae*. The marked effects of such nanocomposites can be attributed to the synergistic effect of the antimicrobial metal and the TAO salts. This study has provided further support for the use of metal nanoparticles in disinfecting/antifouling paint and other coating formulations.

To determine whether the localisation of controlled loadings of silver nanoparticles within nanometer-thick polymeric films could kill bacteria yet support the growth of mammalian cells, poly(allylamine hydrochloride) and poly(acrylic acid) were prepared using layer-by-layer deposition and were then loaded with silver nanoparticles in the range 0.4–23.6 $\mu\text{g cm}^{-2}$ (Agarwal et al. 2010). Suspensions of *Staphylococcus epidermidis* in contact with the film were reduced 6-log-fold with only 0.4 $\mu\text{g nanoparticles cm}^{-2}$. Polymeric films containing this concentration of silver nanoparticles were also shown to be non-toxic to mammalian fibroblast cells, allowing both growth and attachment.

14.6 Photodynamic Therapy and the Use of Nanoparticles to Control Oral Infections

Photodynamic therapy (PDT) is very well suited for the control of bacteria in oral plaque biofilms where there is relatively easy access for the application of the photosensitising agent and light sources to areas requiring treatment (Allaker and Douglas 2009). This approach is now being utilised within the clinical setting in some countries. The killing of microorganisms with light depends upon cytotoxic singlet oxygen and free radical generation by the excitation of a photo-activatable agent or sensitiser. The result of excitation is that the sensitiser moves from an electronic ground state to a triplet state that then interacts with microbial components to generate cytotoxic species (MacRobert et al. 1989). One of the advantages of light-activated killing is that resistance to the action of singlet oxygen is unlikely to become widespread in comparison to that experienced with more

traditional chemical antimicrobial agents. A sensitiser ideally should absorb light at red to near-infrared wavelengths because these wavelengths are able to penetrate more. The most commonly tested sensitisers on bacteria have been tricyclic dyes (for example methylene blue, erythrosine), tetrapyrroles (for example porphyrins) and furocoumarins (for example psoralen). The use of nanoparticles within this area is now under investigation. For example, a complex of biodegradable and biocompatible poly(lactic-co-glycolic acid) (PLGA) and colloidal gold nanoparticles, loaded with methylene blue and exposed to red light at 665 nm, have been tested against planktonic *E. faecalis* and in experimentally infected root canals (Pagonis et al. 2010). In theory, gold nanoparticle conjugates should have improved binding and cell wall penetration properties, and so should deliver a higher concentration of photoactive molecules. It remains to be fully established whether such conjugates will show an increased antibacterial activity when compared to more conventional treatments.

Most work on light-activated killing has been performed using suspensions of planktonic bacteria, with relatively few studies observing biofilm-grown microorganisms. In vitro biofilm-grown *Streptococcus mutans* cells demonstrated a 3-log reduction when treated with erythrosine and white light (500–650 nm) (Wood et al. 2006), while an approach using antibody- and erythrosine-labelled nanoparticles has shown the potential for targeting specific bacterial species in oral plaque biofilms (S.R. Wood, 2006). These in vitro studies, employing constant-depth film fermenters with gold nanoparticles conjugated to erythrosine and antibody to either *Streptococcus mutans* or *Lactobacillus casei*, have shown specific killing of target organisms in mixed-biofilm cultures.

Considerations in relation to the therapeutic use of light-activated killing of biofilms on host surfaces include: (1) direct toxicity of the sensitiser, (2) indirect toxicity of the sensitiser in terms of ‘by-stander’ damage to adjacent host cells, (3) penetration into the biofilm, (4) light exposure time required to kill bacteria within in vivo biofilms and (5) widespread relatively non-specific bacterial killing (Allaker and Douglas 2009). The photosensitiser erythrosine has an advantage over some other dyes because it is currently used in dentistry to visualise dental plaque in vivo, and so its lack of toxicity in the host is well established. For use in periodontitis, the dye needs to be applied subgingivally prior to fiber-optic laser light activation. However, when disease is present, the periodontal site has a marked flow of gingival crevicular fluid into the pocket, and most photosensitisers lose some activity in the presence of extraneous protein. Also, some have virtually no effect in the presence of saliva and other body fluids. This is because the agents complex with proteins and host cells in the gingival crevicular fluid and effectively compete for binding to bacteria. The use of nanoparticles as applied to PDT may help to overcome some of the issues associated with serum constituents.

14.7 Biocompatibility of Nano-Antimicrobials Within the Oral Cavity

Although the development and application of nanotechnology are of major importance in both industrial and consumer areas, knowledge regarding the possible toxicity of nanotechnology products to humans is limited. Whereas it is well known that copper in a non-nanoparticulate form is actively excreted from the normal body, non-nanoparticulate silver can accumulate within it. However the threat posed by these metals in a nanoparticulate form is far from clear (Seetharam and Sridhar 2006). In order to understand the mechanism of toxicity, a thorough knowledge of the toxico-kinetic properties of nanoparticles is required. This includes information on the absorption, distribution, metabolism and excretion (ADME) of nanoparticles (Hagens et al. 2007). In theory, certain nanoparticles may be retained within the body for longer than is desirable, and thus the safety profile becomes a matter of overriding significance. Nanomaterials are able to cross biological membranes and access cells, tissues and organs that larger-sized particles normally cannot. Nanomaterials can enter the blood stream following inhalation or ingestion, and some can even penetrate the skin. In vitro studies with lung epithelial cells, enterocytes and skin keratinocytes indicate marked differences in susceptibility to metallic nanoparticles according to cell type tested (R.P. Allaker and M.A. Vargas-Reus, 2010). However, a particle's surface chemistry, which in some cases can be modified, can govern whether it should be considered further for biomedical applications (Nel et al. 2009).

14.7.1 Toxicity to Cells in the Oral Cavity

Toxicology and biodynamic studies suggest that silica, silicon, and chitosan nanoparticles are relatively safe if introduced via the oral route (Seetharam and Sridhar 2006). Testing of NO-releasing silica nanoparticles (at the highest concentration tested of 8 mg mL^{-1}) with fibroblasts demonstrated that cell proliferation was inhibited to a lesser degree than with chlorhexidine (Hetrick et al. 2009). Likewise, quaternary ammonium poly(ethylene imine) (QA-PEI) nanoparticles incorporated into composite resins to restore teeth at 1% w/w demonstrate no additional toxic effects on cultured cells or experimental animal tissue in comparison to unmodified composites (Yudovin-Farber et al. 2008). In comparison to other metals, silver is less toxic to human cells, and is only ever used at very low concentrations in vivo (Sondi and Salopek-Sondi 2004). For example, silver nanoparticles have been shown to inhibit *Candida* spp. at a concentration of $0.2 \text{ } \mu\text{g mL}^{-1}$, which is markedly less than the concentration ($30 \text{ } \mu\text{g mL}^{-1}$) required to demonstrate a toxic effect against human fibroblasts (Panacek et al. 2009).

14.7.2 Alteration of Biocompatibility and Desired Function

The safe use of nanotechnology and the design of nanomaterials for biological applications, including the control of oral biofilms, involve a complete understanding of the interface between these materials and biological systems (Nel et al. 2009). The interface comprises three interacting components: (1) the surface of the nanoparticle, (2) the solid–liquid interface and the effects of the surrounding medium and (3) the contact zone with biological substrates (Fig. 14.3; Table 14.1). The nanoparticle characteristics of most importance as regards interaction with biological systems, whether mammalian or microbial, are chemical composition, surface function, shape and number of sides, porosity and surface crystallinity, heterogeneity, roughness, and hydrophobicity or hydrophilicity (Nel et al. 2006). For example, it has been shown that titanium dioxide nanoparticles (Luo et al. 2005) act to resist the formation of surface biofilms through increased hydrophilicity in comparison to an unmodified surface.

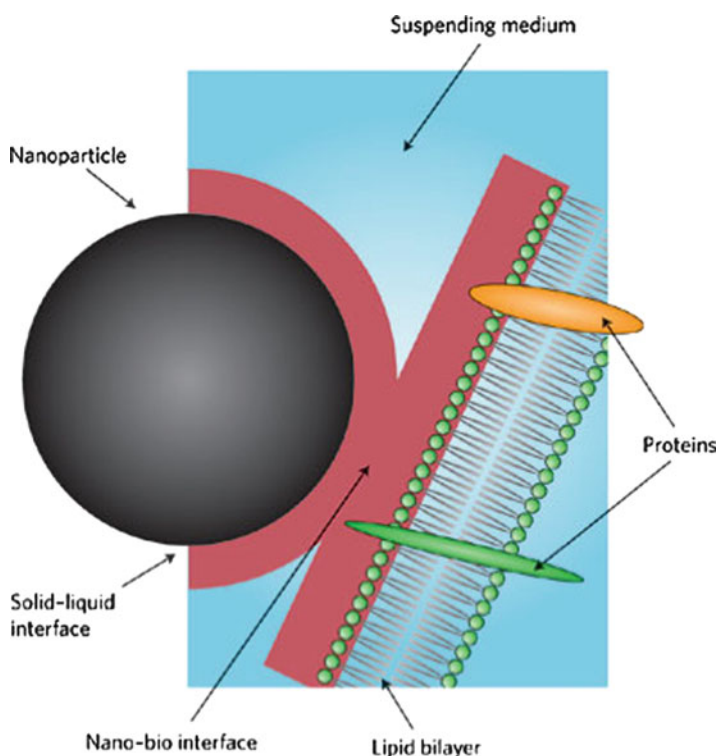


Fig. 14.3 Representation of the interface between nanoparticle and lipid bilayer. The properties of the material, modification of the surface properties of the material through interactions with the suspending medium, and the interactions of the solid–liquid interface with bio-molecules all impact on the interaction. See Table 14.1 for details (With permission; Nel et al. 2009)

Table 14.1 Biological, physical and chemical influences on the interface between nanomaterials and biological systems in man (Adapted with permission; Nel et al. 2009)

<i>Nanoparticle</i>
Size, shape and surface area
Surface charge, energy, roughness and porosity
Valence and conductance states
Functional groups
Ligands
Crystallinity and defects
Hydrophobicity and hydrophilicity
<i>Suspending media</i>
Water molecules
Acids and bases
Salt and multivalent ions
Natural organic matter (proteins, lipids)
Surfactants
Polymers
Polyelectrolytes
<i>Solid-liquid interface</i>
Surface hydration and dehydration
Surface reconstruction and release of free surface energy
Ion adsorption and charge neutralisation
Electrical double-layer formation, zeta potential, isoelectric point
Sorption of steric molecules and toxins
Electrostatic, steric and electrosteric interactions
Aggregation, dispersion and dissolution
Hydrophilic and hydrophobic interactions
<i>Nano-bio interface</i>
Membrane interactions: specific and non-specific forces
Receptor-ligand binding interactions
Membrane wrapping: resistive and promotive forces
Biomolecule interactions (lipids, proteins, DNA) leading to structural and functional effects
Free energy transfer to biomolecules
Conformational change in biomolecules
Oxidant injury to biomolecules
Mitochondrial and lysosomal damage, decrease in ATP

The characteristics of the surface layer, such as zeta potential (surface charge), nanoparticle aggregation, dispersion state, stability and hydration as influenced by the characteristics of the surrounding medium (including ionic strength, pH, temperature and presence of organic molecules or detergents) are of critical importance. The contribution of surface charge to both mammalian and microbial interactions has been clearly illustrated using surfactant-coated nanoparticles (McCarron et al. 2007). Both anti-adherent and antifungal effects were shown using buccal epithelial cells treated with non-drug-loaded poly (ethylcyanoacrylate) nanoparticles. Nanoparticles were prepared using emulsion polymerisation and stabilised with cationic, anionic or non-ionic surfactants. Cationic surfactants, for example cetrimide, which are known antimicrobial agents, were the most effective in reducing *Candida albicans*

blastospore adhesion, and showed a growth inhibitory and biocidal effect against the yeast. Production of nanoparticles with an anionic surfactant gave lower yields and wide particle size distributions. No evidence of killing against *C. albicans* was shown. Non-ionic surfactant-coated nanoparticles produced intermediate kill rates. These studies clearly demonstrate the importance of surface charge on the nanoparticle surface. It is envisaged that the buccal epithelium could possibly be treated using polymeric-type nanoparticles in a mouthwash-type formulation; effectively this would prime the potential target cells against adhesion and infection.

The *in vivo* screening of around 130 nanoparticles intended for therapeutic use has allowed detailed assessments as regards biocompatibility (Nel et al. 2009). It was shown that the main independent particle variables which determine compatibility are size, surface charge and dispersibility (particularly the effect of hydrophobicity). Cationic particles or particles with a high surface reactivity are more likely to be toxic (both to eukaryotes and prokaryotes). Larger, more hydrophobic or poorly dispersed particles, which are rapidly removed by the reticuloendothelial system, were shown to be less toxic. Karlsson et al. (2008) have recently shown that metal oxide nanoparticles are more toxic than at first envisaged at concentrations down to $40 \mu\text{g mL}^{-1}$ and show a high variation as regards different nanoparticle species to cause cytotoxicity, DNA damage and oxidative DNA lesions. Toxic effects on cultured cells were assessed using trypan blue staining together with the comet assay to measure DNA damage and an oxidation-sensitive fluoroprobe to quantify the production of reactive oxygen species (Karlsson et al. 2008). Copper oxide was found to be the most toxic and therefore may pose the greatest health risk. Nanoparticulate ZnO and TiO₂, both ingredients in sunscreens and cosmetics, showed cytotoxic and DNA-damaging effects. The potential mechanisms of toxicity for selected nanoparticles are listed in Table 14.2.

Table 14.2 Nanoparticle cytotoxicity to mammalian cells (Adapted with permission; Nel et al. 2009)

Nanoparticle	Cytotoxicity mechanism
TiO ₂	ROS (reactive oxygen species) production Glutathione depletion and toxic oxidative stress Cell membrane disruption
ZnO	ROS production Dissolution and release of toxic cations Lysosomal damage Inflammation
Ag	Dissolution and Ag ⁺ ion release inhibits respiratory enzymes and ATP production ROS production Disruption of membrane integrity and transport processes
Gold	Disruption of protein conformation
SiO ₂	ROS production Protein unfolding Membrane disruption
Cu/CuO	DNA damage and oxidative stress

In order to help prevent aggregation of nanoparticles, stabilising (capping) agents that bind to the entire nanoparticle surface can be used; these include water-soluble polymers, oligo- and poly-saccharides, sodium dodecyl sulfate, polyethylene glycol and glycolipids. The specific roles of surface capping, size scale and aspect ratio of ZnO particles towards antimicrobial activity and cytotoxicity have been investigated (Nair et al. 2009). Polyethylene glycol-capped ZnO nanoparticles demonstrated an increase in antimicrobial efficacy with a reduction in particle size. Again, gram negative bacteria were more affected than gram positive, which suggests that a membrane damage mechanism of action rather than one involving the production of reactive oxygen species (ROS) is of overriding significance. Polyethylene glycol-capped nanoparticles were highly toxic to human cells with a very low concentration (100 μ M) threshold for cytotoxic action, whereas the concentration for antibacterial activity was 50 times greater (5 mM). It is hypothesised that the toxicity to eukaryotic cells is related to nanoparticle-enhanced apoptosis by up regulation of the Fas ligand on the cell membrane.

An understanding of the interface between biological systems and nanomaterials should enable design features to be used to control the exposure, bioavailability and biocatalytic activities. A number of possible approaches are starting to be identified (Nel et al. 2009) including changing ability to aggregate, application of surface coatings, and altering charge density and oxidative state. However this may well compromise the intended selective toxicity of antimicrobial nanoparticles. It remains to be determined how potential mammalian toxicity issues will fully impact on the use of nanotechnology in the control of oral biofilms.

14.8 Concluding Remarks

The application of nano-antimicrobials to control oral infections, as a function of their biocidal, anti-adhesive and delivery capabilities, is of increasing interest. Their use as constituents of prosthetic device coatings, topically applied agents and within dental materials is currently being explored. Future developments are likely to concentrate on those nanoparticles with maximal antimicrobial activity and minimal host toxicity. Antimicrobial nanoparticulate metals have received particular attention as a result of their durability. Although certain nanoparticles may be toxic to oral and other tissues, the surface characteristics of a given particle will determine whether or not it will have potential for oral applications. Approaches to alter biocompatibility and desired function are now being identified and include changing the ability to aggregate, application of surface coatings, and altering oxidative state and charge density.

Acknowledgements The author is also grateful to International Journal of Antimicrobial Agents and Nature Materials for permission to use material from 34:103–110 (2009) and 8:543–557 (2009) respectively.

References

- Agarwal A, Weis TL, Schurr MJ, Faith NG, Czuprynski CJ, McAnulty JF, Murphy CJ, Abbott NL (2010) Surfaces modified with nanometer-thick silver-impregnated polymeric films that kill bacteria but support growth of mammalian cells. *Biomaterials* 31:680–690
- Ahn SJ, Lee SJ, Kook JK, Lim BS (2009) Experimental antimicrobial orthodontic adhesives using nanofillers and silver nanoparticles. *Dent Mater* 25:206–213
- Allaker RP, Douglas CWI (2009) Novel anti-microbial therapies for dental plaque-related diseases. *Int J Antimicrob Agents* 33:8–13
- Allaker RP, Hardie JM (1998) Oral Infections. *Topley and Wilson's Microbiology and Microbial infections*. 9th Edition. London: Arnold. 3:373–390.
- Allaker RP, Ren G (2008) Potential impact of nanotechnology on the control of infectious diseases. *Trans R Soc Trop Med Hyg* 102:1–2
- Almaguer-Flores A, Ximenez-Fyvie LA, Rodil SE (2010) Oral bacterial adhesion on amorphous carbon and titanium films: Effect of surface roughness and culture media. *J Biomed Mater Res B Appl Biomater* 92:196–204
- Aydin Sevcic B, Hanley L (2010) Antibacterial activity of dental composites containing zinc oxide nanoparticles. *J Biomed Mater Res B Appl Biomater* 94:22–31
- Baehni PC, Takeuchi Y (2003) Anti-plaque agents in the prevention of biofilm-associated oral diseases. *Oral Dis* 9 (Suppl 1):23–29
- Benn TM, Westerhoff P (2008) Nanoparticle silver released into water from commercially available sock fabrics. *Environ Sci Technol* 42:4133–4139
- Beveridge TJ, Murray RGE (1980) Sites of metal deposition in the cell wall of *Bacillus subtilis*. *J Bacteriol* 141:876–878
- Blake DM, Maness P-C, Huang Z, Wolfrum EJ, Jacoby WA, Huang J (1999) Application of the photocatalytic chemistry of titanium dioxide to disinfection and the killing of cancer cells. *Separation Purification Methods* 28:1–50
- Boldryryeva H, Umeda N, Plaskin OA, Takeda Y, Kishimoto N (2005) High-fluence implantation of negative metal ions into polymers for surface modification and nanoparticle formation. *Surf Coat Tech* 196:373–377
- Bragg PD, Rainnie DJ (1974) The effect of Ag⁺ ions on the respiratory chain of *E. coli*. *Can J Microbiol* 20:883–889
- Brayner R, Ferrari-Iliou R, Brivois N, Djediat S, Benedetti MF, Fievet F (2006) Toxicological impact studies based on *Escherichia coli* bacteria in ultrafine ZnO nanoparticles colloidal medium. *Nano Lett* 6:866–870
- Casemiro LA, Gomes-Martins CH, Pires-de-Souza FdeC, Panzeri H (2008) Antimicrobial and mechanical properties of acrylic resins with incorporated silver-zinc zeolite – part 1. *Gerodontology* 25:187–194
- Cava RJ (1990) Structural chemistry and the local charge picture of copper oxide superconductors. *Science* 247:656–662
- Chandra J, Kuhn DM, Mukherjee PK, Hoyer LL, McCormick T, Ghannoum MA (2001) Biofilm formation by the fungal pathogen *Candida albicans*: development, architecture, and drug resistance. *J Bacteriol* 183:5385–5394
- Cioffi N, Torsi L, Ditaranto N, Sabbatini L, Zambonin PG, Tantillo G, et al. (2005a) Copper nanoparticle/polymer composites with antifungal and bacteriostatic properties. *Chem Mater* 17:5255–5262
- Cioffi N, Ditaranto N, Torsi L, Picca RA, Sabbatini L, Valentini A, Novello L, Tantillo G, Bleve-Zacheo T, Zambonin PG (2005b) Analytical characterization of bioactive fluoropolymer ultrathin coatings modified by copper nanoparticles. *Anal Bioanal Chem* 381:607–616.
- Cioffi N, Ditaranto N, Torsi L, Picca RA, De Giglio E, Sabbatini L, Novello L, Tantillo G, Bleve-Zacheo T, Zambonin PG (2005c) Synthesis, analytical characterization and bioactivity of

- Ag and Cu nanoparticles embedded in poly-vinyl-methyl-ketone films. *Anal Bioanal Chem* 382: 1912–1918
- Cousins BG, Allison HE, Doherty PJ, Edwards C, Garvey MJ, Martin DS, Williams RL (2007) Effects of a nanoparticulate silica substrate on cell attachment of *Candida albicans*. *J Appl Microbiol* 102:757–765
- Corbierre MK, Cameron NS, Sutton M, Laaziri K, Lennox RB (2005) Gold nanoparticle/polymer nanocomposites: dispersion of nanoparticles as a function of capping agent molecular weight and grafting density. *Langmuir* 21:6063–6072
- Cross KJ, Huq NL, Reynolds EC (2007) Casein phosphopeptides in oral health chemistry and clinical applications. *Curr Pharm Des* 13:793–800
- Cushing BL, Kolesnichenko VL, O'Connor CJ (2004) Recent advances in the liquid-phase syntheses of inorganic nanoparticles. *Chem Rev* 104:3893–3946
- Darouiche RO, Raad II, Heard SO, Thornby JI, Wenker OC, Gabrielli A, Berg J, Khadori N, Hanna H, Hachem R, Harris RL, Mayhall G (1999) A comparison of two antimicrobial-impregnated central venous catheters. *Catheter Study Group. New Engl J Med* 340:1–8
- Elechiguerra JL, Burt JL, Morones JR, Camacho-Bragado A, Gao X, Lara HH, Yacaman MJ (2005) Interaction of silver nanoparticles with HIV-1. *J Nanobiotechnol* 3:6
- Feng QL, Wu J, Chen GQ, Cui FZ, Kim TM, Kim JO (2000) A mechanistic study of the antibacterial effect of Ag⁺ ions on *Escherichia coli* and *Staphylococcus aureus*. *J Biomed Mater Res* 52:662–668
- Furno F, Morley KS, Wong B, Sharp BL, Arnold PL, Howdle SM, Bayston R, Brown PD, Winship PD, Reid HJ (2004) Silver nanoparticles and polymeric medical devices: a new approach to prevention of infection? *J Antimicrob Chemother* 54:1019–1024
- Gaikwaad RM, Sokolov I (2008) Silica nanoparticles to polish tooth surfaces for caries prevention. *J Dent Res* 87:980–983
- Giersten E (2004) Effects of mouth rinses with triclosan, zinc ions, copolymer, and sodium lauryl sulphate combined with fluoride on acid formation by dental plaque in vivo. *Caries Res* 38:430–435
- Green RJ, Davies MC, Roberts CJ, Tendler SJ (1999) Competitive protein adsorption as observed by surface plasmon resonance. *Biomaterials* 20:385–391
- Hagens WI, Oomen AG, de Jong WH, Cassee FR, Sips AJ (2007) What do we (need to) know about the kinetic properties of nanoparticles in the body? *Reg Toxicol Pharmacol* 49:217–229
- Han J, Chen L, Duan S, Yang QX, Yang M, Gao C, Zhang BY, He H, Dong XP (2005) Efficient and quick inactivation of SARS coronavirus and other microbes exposed to the surfaces of some metal catalysts. *Biomed Environ Sci* 18:176–180
- Hannig M, Kriener L, Hoth-hannig W, Becker-Willinger C, Schmidt H (2007) Influence of nanocomposite surface coating on biofilm formation in situ. *J Nanosci Nanotechnol* 7:4642–4648
- Hannig C, Hannig M (2009) The oral cavity – a key system to understand substratum-dependent bioadhesion on solid surfaces in man. *Clin Oral Invest* 13:123–139
- Hannig M, Joiner A (2006) The structure, function and properties of the acquired pellicle. *Monogr Oral Sci* 19:29–64
- Hardie JM (1992) Oral microbiology: current concepts in the microbiology of dental caries and periodontal disease. *Brit Dent J* 172:271–278
- Herrera M, Carrion P, Baca P, Liebana J, Castillo A (2001) In vitro antibacterial activity of glass-ionomer cements. *Microbios* 104:141–148
- Hetrick EM, Shin JH, Paul HS, Schoenfish MH (2009) Anti-biofilm efficacy of nitric oxide-releasing silica nanoparticles. *Biomaterials* 30:2782–2789
- Jenkinson HF, Lamont RJ (2005) Oral microbial communities in sickness and in health. *Trends Microbiol* 13:589–595
- Jones N, Ray B, Ranjit KT, Manna AC (2008) Antibacterial activity of ZnO nanoparticle suspensions on a broad spectrum of microorganisms. *FEMS Microbiol Letters* 279:71–76

- Karlsson HL, Cronholm P, Gustafsson J, Moller L (2008) Copper oxide nanoparticles are highly toxic: a comparison between metal oxide nanoparticles and carbon nanotubes. *Chem Res Toxicol* 21:1726–1732
- Kawahara K, Tsuruda K, Morishita M, Uchida M (2000) Antibacterial effect of silver-zeolite on oral bacteria under anaerobic conditions. *Dent Mater* 16:452–455
- Kim JS, Kuk E, Yu KN, Kim JH, Park SJ, Lee HJ, Kim SH, Park YK, Park YH, Hwang CY, Kim YK, Lee YS, Jeong DH, Cho MH (2007) Antimicrobial effects of silver nanoparticles. *Nanomedicine* 3:95–101
- Kishen A, Shi Z, Shrestha A, Neoh KG (2008) An investigation on the antibacterial and antibiofilm efficacy of cationic nanoparticulates for root canal infection. *J Endod* 34:1515–1520
- Kolenbrander PE, Palmer RJ, Rickard AH, Jakubovics NS, Chalmers NI, Diaz PI (2006) Bacterial interactions and successions during plaque development. *Periodontol* 2000 42:47–79
- Lee WF, Tsao KT (2006) Preparation and properties of nanocomposite hydrogels containing silver nanoparticles by *ex situ* polymerization. *J Appl Poly Sci* 100:3653–3661
- Lewis K (2001) Riddle of biofilm resistance. *Antimicrob Agents Chemother* 45:999–1007
- Li P, Li J, Wu C, Wu Q, Li J (2005) Synergistic antibacterial effects of β -lactam antibiotic combined with silver nanoparticles. *Nanotechnology* 16:1912–1917
- Li Z, Lee D, Sheng X, Cohen RE, Rubner MF (2006) Two-level antibacterial coating with both release-killing and contact-killing capabilities. *Langmuir* 22:9820–9823
- Lin LM, Skribner JE, Gaengler P (1992) Factors associated with endodontic failures. *J Endod* 18:625–627
- Lin C, Yeh Y, Yang C, Chen C, Chen G, Chen CC, Wu YC (2002) Selective binding of mannose-encapsulated gold nanoparticles to type I pili in *Escherichia coli*. *J Am Chem Soc* 13:155–168
- Liu Y, He L, Mustapha A, Li H, Hu ZQ, Lin M (2009) Antibacterial activities of zinc oxide nanoparticles against *Escherichia coli* O157:H7. *J Appl Microbiol* 107:1193–1201
- Lok CN, Ho CM, Chen R, He QY, Yu WY, Sun H, Tam PKH, Chiu JF, Che CM (2007) Silver nanoparticles: partial oxidation and antibacterial activities. *J Biol Inorg Chem* 12:527–534
- Luo ML, Zhao JQ, Tang W, Pu S (2005) Hydrophilic modification of poly (ether sulfone) ultrafiltration membrane surface by self-assembly of TiO₂ nanoparticles. *Appl Surf Sci* 49:76–84
- MacRobert AJ, Bown SG, Phillips D (1989) What are the ideal photoproperties for a sensitizer? *Ciba Found Symp* 146:4–12
- Maness PC, Smolinski S, Blake DM, Huang Z, Wolfrum EJ, Jacoby WA (1999) Bacteriocidal activity of photocatalytic TiO₂ reaction: toward an understanding of its killing mechanism. *Appl Environ Microbiol* 65:4094–4098
- Manias, E. (2007) Nanocomposites: Stiffer by design. *Nature Mater* 6:9–11
- Marsh PD, Bradshaw DJ (1995) Dental plaque as a biofilm. *J Ind Microbiol* 15:169–175
- Marsh PD, Martin MV (2009) *Oral Microbiology*. 5th Edition. Edinburgh: Churchill Livingstone
- Matsuura T, Abe Y, Sato Y, Okamoto K, Ueshige M, Akagawa Y (1997) Prolonged antimicrobial effect of tissue conditioners containing silver-zeolite. *J Dent* 25:373–377
- McCarron PA, Donnelly RF, Marouf W, Calvert DE (2007) Anti-adherent and antifungal activities of surfactant-coated poly (ethylcyanoacrylate) nanoparticles. *Int J Pharmaceut* 340:182–190
- Monteiro DR, Gorup LF, Takamiya AS, Ruvollo-Filho AC, de Camargo ER, Barbosa DB (2009) The growing importance of materials that prevent microbial adhesion: antimicrobial effect of medical devices containing silver. *Int J Antimicrob Agents* 34:103–110
- Morishita M, Miyagi M, Yamasaki Y, Tsuruda K, Kawahara K, Iwamoto Y (1998) Pilot study on the effect of a mouthrinse containing silver zeolite on plaque formation. *J Clin Dent* 9:94–96
- Morones JR, Elechiguerra JL, Camacho A, Holt K, Kouri JB, Ramirez JT (2005) The bacteriocidal effect of silver nanoparticles. *Nanotechnology* 16:2346–2353
- Nair S, Sasidharan A, Rani VVD, Menon D, Nair S, Manzoor K, Raina S. (2009) Role of size scale of ZnO nanoparticles and microparticles on toxicity toward bacteria and osteoblast cancer cells. *J Mater Sci: Mater Med* 20:S235–S241

- Nel A, Xia T, Madler I, Li N (2006) Toxic potential of materials at the nanolevel. *Science* 311:622–627
- Nel AE, Madler L, Velegol D, Xia T, Hoek EMV, Somasundaran P, Klaessig F, Castranova V, Thompson M (2009) Understanding biophysicochemical interactions at the nano-bio interface. *Nature Mater* 8:543–557
- Nielsen BV, Nevell TG, Barbu E, Smith JR, Rees GD, Tisboulis J (2011) Multifunctional poly (alkyl methacrylate) films for dental care. *Biomed Mater* 6:1–9
- Pagonis TC, Chen J, Fontana CR, Devalapally H, Ruggiero K, Song X, Foschi F, Dunham J, Skobe Z, Yamazaki H, Kent R, Tanner AC, Amiji MM, Soukos NS (2010) Nanoparticle-based endodontic antimicrobial photodynamic therapy. *J Endod* 36:322–328
- Pal S, Tak YK, Song JM (2007) Does the antibacterial activity of silver nanoparticles depend on the shape of the nanoparticle? A study of the Gram-negative bacterium *Escherichia coli*. *Appl Environ Microbiol* 73:1712–1720
- Panacek A, Kolar M, Vecerova R, Prucek R, Soukupova J, Krystof V, Hamal P, Zboril R, Kvitek L (2009) Antifungal activity of silver nanoparticles against *Candida* spp. *Biomaterials* 30:6333–6340
- Rahiotis C, Vougiouklakis G, Eliades G. (2008) Characterization of oral films formed in the presence of a CPP-ACP agent: an in situ study. *J Dent* 36:272–280
- Rai M, Yadav A, Gade A (2009) Silver nanoparticles as a new generation of antimicrobials. *Biotechnol Adv* 27:76–83
- Reddy KM, Feris K, Bell J, Wingett DG, Hanley C, Punnoose A (2007) Selective toxicity of zinc oxide nanoparticles to prokaryotic and eukaryotic systems. *Appl Phys Lett* 90:213902
- Ren G, Hu D, Cheng EWC, Vargas-Reus MA, Reip P, Allaker RP (2009) Characterisation of copper oxide nanoparticles for antimicrobial applications. *Int J Antimicrob Agents* 33:587–590
- Reynolds EC (2008) Calcium phosphate-based remineralization systems: scientific evidence? *Aus Dent J* 53: 268–273
- Reynolds EC, Cai F, Shen P, Walker GD. (2003) Retention in plaque and remineralization of enamel lesions by various forms of calcium in a mouthrinse or sugar-free chewing gum. *J Dent Res* 82:206–211
- Riley DK, Classen DC, Stevens LE, Burke JP (2002) A large randomised clinical trial of a silver-impregnated urinary catheter: lack of efficacy and staphylococcal superinfection. *Am J Med* 98: 349–356
- Rose RK (2000a) Binding characteristics of *Streptococcus mutans* for calcium and casein phosphopeptide. *Caries Res* 34: 427–431
- Rose RK (2000b) Effects of an anticariogenic casein phosphopeptide on calcium diffusion in streptococcal model dental plaques. *Arch Oral Biol* 45: 569–575
- Roveri N, Battistello E, Foltran I, Foresti E, Iafisco M, Lelli M et al. (2008) Synthetic biomimetic carbonate-hydroxyapatite nanocrystals for enamel remineralization. *Adv Mater Res* 47–50: 821–824
- Ruparelia JP, Chatterje AK, Duttagupta SP, Mukherji S. (2008) Strain specificity in antimicrobial activity of silver and copper nanoparticles. *Acta Biomaterialia* 4:707–716
- Sambhy V, MacBride MM, Peterson BR, Sen A (2006) Silver bromide nanoparticle/polymer composites: dual action tunable antimicrobial materials. *J Am Chem Soc* 128:9798–9808
- Sawai J (2003) Quantitative evaluation of antibacterial activities of metallic oxide powders (ZnO, MgO and CaO) by conductimetric assay. *J Microbiol Methods* 54:177–182
- Seetharam RN, Sridhar KR (2006) Nanotoxicity: threat posed by nanoparticles. *Curr Sci* 93:769–770
- Sondi I, Salopek-Sondi B (2004) Silver nanoparticles as an antimicrobial agent: a case study on *E. coli* as a model for Gram-negative bacteria. *J Colloid Interface Sci* 275:177–182
- Sotiriou GA, Pratsinis SE (2010) Antibacterial activity of nanosilver ions and particles. *Environ Sci Technol* 44:5649–5654
- Stephen KW (1993) Dentrifices: recent clinical findings and implications for use. *Int Dent J* 43:549–553

- Stewart PS (2003) Diffusion in biofilms. *J Bacteriol* 185:1485–1491
- Stohs SJ, Bagchi D (1995) Oxidative mechanisms in the toxicity of metal ions. *Free Rad Biol Med* 18:321–336
- Stoimenov PK, Klinger RL, Marchin GL, Klabunde KJ (2002) Metal oxide nanoparticles as bactericidal agents. *Langmuir* 18:6679–6686
- Sutherland IW (2001) Biofilm exopolysaccharides: a strong and sticky framework. *Microbiology* 147:3–9
- Thorne K, Vittori G (1997) Proceedings of the 1997 Sixteenth Southern Biomedical Engineering Conference 202–205
- Tranquada JM, Sternlieb BJ, Axe JD, Nakamura Y, Uchida S (1995) Evidence for stripe correlations of spins and holes in copper oxide superconductors. *Nature* 375:561
- Tsuang YH, Sun JS, Huang YC, Lu CH, Chang WHS, Wang CC (2008) Studies of photokilling of bacteria using titanium dioxide nanoparticles. *Artif Organs* 32:167–174
- van der Ouderaa FJ (1991) Anti-plaque agents. Rationale and prospects for prevention of gingivitis and periodontal disease. *J Clin Periodontol* 18:447–454
- Venegas SC, Palacios JM, Apella MC, Morando PJ, Blesa MA (2006) Calcium modulates interactions between bacteria and hydroxyapatite. *J Dent Res* 85:1124–1128
- Verran J, Sandoval G, Allen NS, Edge M, Stratton J (2007) Variables affecting the antibacterial properties of nano and pigmentary titania particles in suspension. *Dyes Pigments* 73:298–304
- Waltimo T, Brunner TJ, Vollenweider M, Stark WJ, Zehnder M (2007) Antimicrobial effect of nanometric bioactive glass 45S5. *J Dent Res* 86:754–757
- Watson PS, Pontefract HA, Devine DA, Shore RC, Nattress BR, Kirkham J, Robinson C (2005) Penetration of fluoride into natural plaque biofilms. *J Dent Res* 84:451–455
- Wilcox M, Kite P, Dobbins B (1988) Antimicrobial intravascular catheters – which surface to coat? *J Hosp Infect* 40:322–323
- Williams DN, Ehrman SH, Pulliman Holoman TR (2006) Evaluation of the microbial growth response to inorganic nanoparticles. *J Nanobiotech* 4:3
- Wilson M (1996) Susceptibility of oral bacterial biofilms to antimicrobial agents. *J Med Microbiol* 44:79–87
- Wood SR, Kirham J, Marsh PD, Shore RC, Nattress B, Robinson C (2000) Architecture of intact natural human plaque biofilms studied by confocal laser scanning microscopy. *J Dent Res* 79:21–27
- Wood S, Metcalf D, Devine D, Robinson C (2006) Erythrosine is a potential photosensitizer for the photodynamic therapy of oral plaque biofilms. *J Antimicrob Chemother* 57:680–684
- Wu Y, Yang W, Wang C, Hu J, Fu S (2005) Chitosan nanoparticles as a novel delivery system for ammonium glycyrrhizinate. *Int J Pharmacol* 295:235–245
- Ximenez-Fyvie LA, Haffajee AD, Socransky SS (2000) Comparison of the microbiota of supra- and subgingival plaque in health and periodontitis. *J Clin Periodontol* 27:648–657
- Yamanaka M, Hara K, Kudo J (2005) Bactericidal actions of a silver ion solution on *Escherichia coli*, studied by energy-filtering transmission electron microscopy and proteomic analysis. *Appl Environ Microbiol* 71:7589–7593
- Yazdi AS, Guarda G., Riteau N, Drexler SK, Tardivel A, Couillin I, Tschopp J (2010) Nanoparticles activate the NLR pyrin domain containing 3 (Nlrp3) inflammasome and cause pulmonary inflammation through release of IL-1 α and IL-1 β . *PNAS* 107:19449–19454
- Yoon K.Y., Byeon J.H., Park J.H., Hwang J. (2007) Susceptibility constants of *Escherichia coli* and *Bacillus subtilis* to silver and copper nanoparticles. *Sci Tot Environ* 373:572–575
- Yudovin-Farber I, Beyth N, Nyska A, Weiss EI, Golenser J, Domb AJ (2008) Surface characterization and biocompatibility of restorative resin containing nanoparticles. *Biomacromolecules* 9:3044–3050
- Zhang LL, Jiang YH, Ding YL, Povey M, York D (2007) Investigation into the antibacterial behaviour of suspensions of ZnO nanoparticles (ZnO nanofluids). *J Nanopart Res* 9:479–489
- Zitzmann NU, Berglundh T (2008) Definition and prevalence of peri-implant diseases. *J Clin Periodontol* 35:286–291

Chapter 15

Nanomaterial-Based Antibacterial Paper

Wenbing Hu, Qing Huang, and Chunhai Fan

15.1 Synthesis and Characterization of Nanomaterial-Based Films

The nanomaterial-based film with antibacterial property can be fabricated by physical and chemical methods. Physical methods include spin-coating, dip-coating, vacuum filtration, electrospinning, and magnetron sputtering.

15.1.1 Spin-Coating

Spin-coating is applied to prepare uniform thin film by spreading the solution placed on the flat substrates at a constant rate. The thickness of the film is determined by centrifugal forces controlled by spin speed, solution viscosity, and spin time. TiO₂ film and silver nanoparticles (AgNPs)/TiO₂ composite film have been prepared by spin-coating technology.

TiO₂ nanoparticles have been synthesized using the sol-gel method [2]. In a typical experiment, TiO₂ sol was prepared from the hydrolysis of Ti(OC₄H₉)₄: 0.01 mol of Ti(OC₄H₉)₄ stirred in ice incubation was mixed with 0.15 mol of ethanol. The ethanol/H₂O/acetylacetone solution (0.1 mol ethanol, 0.02 mol deionized water, 0.01 mol acetylacetone) was added to the Ti(OC₄H₉)₄/ethanol solution under stirring in ice incubation, then the mixture was stirred for 2 h. The TiO₂ sol was matured for about 48 h before coating. TiO₂ thin films were coated on titanium plate by the sol-gel spin-coating method with a rotating speed of 2,000 rpm. The resulting films were subjected to heat treatment at 200°C for

W. Hu • Q. Huang (✉) • C. Fan (✉)

Laboratory of Physical Biology, Shanghai Institute of Applied Physics, Chinese Academy of Sciences, Shanghai, China

e-mail: huangqing@sinap.ac.cn; fchh@sinap.ac.cn

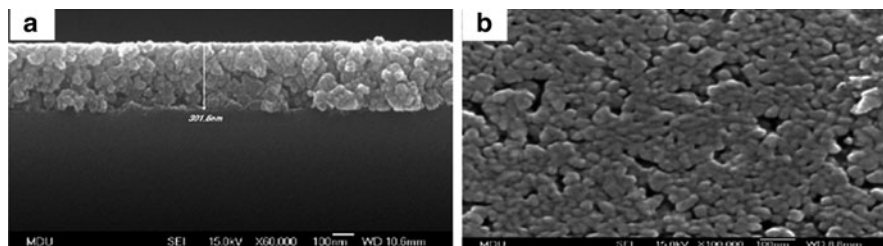


Fig. 15.1 The SEM images of TiO₂ film prepared by spin-coating technology cross-section (a) and surface structure (b) [3]. Immobilized TiO₂ nanoparticles were $\sim 15.2 \pm 0.6$ nm

15 min. By repeating this process, TiO₂ thin films with different thicknesses were obtained. Finally, the films were annealed at 500°C for 3 h in air for crystallization. The crystal structure and thickness of TiO₂ film were characterized by scanning electron microscopy (SEM) (Fig. 15.1) [3].

Zhang's [4] and Yang's [5] groups synthesized AgNPs/TiO₂ composite film according to the sol-gel spin-coating method. The SEM images and XRD suggested that the crystallinity and growth of AgNPs were improved by increasing the annealing temperature. Furthermore, the morphology of the AgNPs/TiO₂ composite film could be controlled by simply tuning the molar ratio of the silver nitrate, implying the morphology of composite film became rougher and rougher with the increase in the concentration of silver nitrate, while the diameter of AgNPs decreased. When the molar ratio of Ti⁴⁺ to Ag⁺ reached 5:1, the composite films were mesoporous. However, the AgNPs attached to the surface of TiO₂ nanoparticles by forming Ag-O-Ti bonds, rather than entering the lattice of the TiO₂ anatase phase [6].

15.1.2 Dip-Coating

The dip-coating method is a simple way to deposit thin film on the substrate. During the process, completely automated by computerized control system, the substrate is slowly dipped into and withdrawn from a tank containing the sol, with a uniform velocity, in order to obtain a uniform film. The film thickness is sensitive to flow conditions in the liquid bath and gas overhead, and is determined by the competition among viscous force, surface tension force and gravity. The faster the substrate was withdrawn, the thicker the film deposited. Many silver nanoparticles (AgNPs)-based films have been fabricated on glass and silica substrates with this procedure [7–10].

Zhang and co-workers [8] have reported a facile two-step method for the preparation of surface-silvered polymer films. The commercial polyimide (PI) film was functionalized by simply dipping the film into dopamine (DOPA) aqueous solution for a period of time. Poly (dopamine) was deposited on the surface of PI

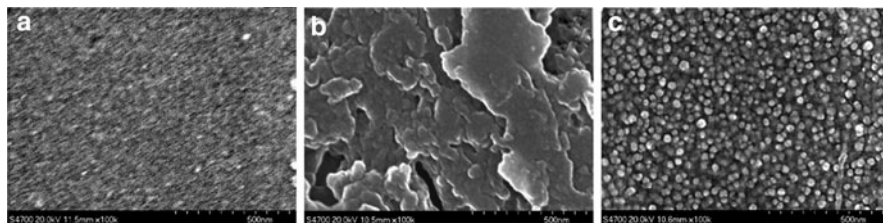


Fig. 15.2 SEM images of (a) the pristine PI film, (b) the PI-DOPA film, and (c) the AgNPs-immobilized PI film [8]

films and formed PI-DOPA films. Then, PI-DOPA films were immersed into an aqueous silver nitrate solution and subjected to UV irradiation in a self-made photochemical reactor for 15 min. The PI-DOPA films deposited with silver were washed thoroughly with doubly distilled water and then dried in a vacuum oven. The distribution and size of the silver nanoparticles could be controlled by changing the reaction time. In the SEM images of films, the surface of PI-DOPA film was much rougher than that of the pristine PI film (Fig. 15.2), resulting from the formation of the distinctive poly (dopamine) layer on the PI film, which facilitated the interlocking with the reduced silver nanoparticles. The silver nanoparticles with the diameter of ~ 20 nm were uniformly distributed on the surface of PI-DOPA film (Fig. 15.2).

15.1.3 Vacuum Filtration

Graphene oxide (GO) and reduced graphene oxide (rGO) papers were prepared by filtration of the suspension [11]. GO colloidal suspension was prepared from graphite by the modified Hummers method [12]. The GO was reduced to rGO with the aid of hydrazine hydrate [13]. The suspension was filtrated through a PVDF filter membrane (47 mm in diameter, 220 nm pore size) by vacuum at room temperature. The paper could be easily peeled off from the filter paper. The thickness of the paper was controlled by adjusting the volume of the colloidal suspension.

The thickness of GO sheets was ~ 1.1 nm as measured by atomic force microscope (AFM), suggesting the formation of a single-layer 2-D nanomaterial (Fig. 15.3a), while the thickness of rGO reduced to ~ 1.0 nm (Fig. 15.3b). The size of GO and rGO varied from nanometers to micrometers. The resulting GO paper was of ~ 1.5 μm thickness, and the rGO paper was ~ 4.6 μm as characterized by scanning electron microscope (SEM). Interestingly, the GO paper looked lack-luster while the rGO paper was lustrous (Fig. 15.3c, d).

The carbon nanotubes-deposited film or filter were fabricated by vacuum filtration, as described by the Elimelech group [14]. In a typical experiment, multi-walled carbon nanotubes (MWNTs) suspension with the concentration of 0.5 mg/mL in the

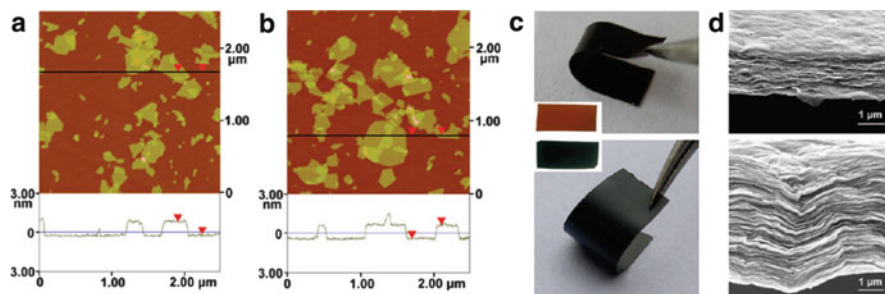


Fig. 15.3 Characterization of GO and rGO nanosheets and paper [11]. (a, b) AFM images of (a) GO and (b) rGO sheets. (c) Photographs of free-standing and flexible GO (upper) and rGO paper (lower) (inset of (c), the photos of GO (upper) and rGO (lower) paper penetrated by white light). (d) The thickness of GO (upper) and rGO (lower) paper as measured by SEM

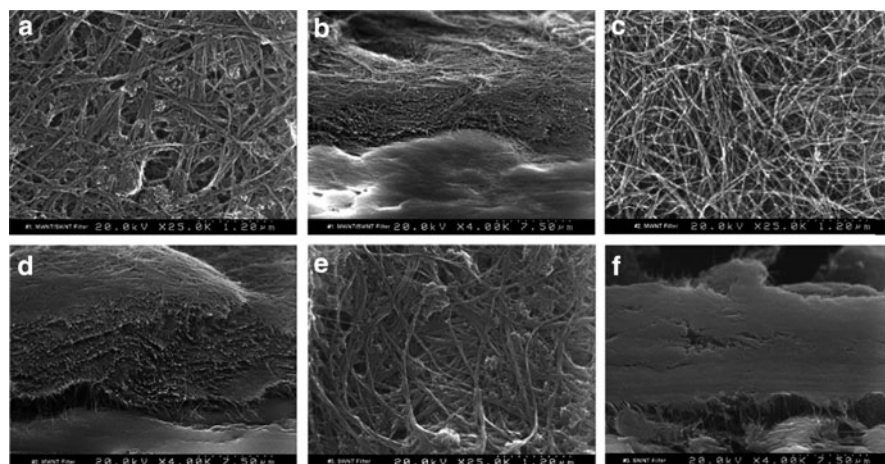


Fig. 15.4 FE-SEM images of the CNTs filters [14]. Aerial views of MWNT-SWNT filter (a), MWNT filter (c), and SWNT filter (e). The cross-section view of MWNT-SWNT filter (b), MWNT filter (d), and SWNT filter (f)

dimethyl sulfoxide (DMSO) was sonicated for 15 min at a power output of 50 W to achieve a more uniform dispersion. Bath sonication of the MWNTs suspension was also performed for 10 s immediately prior to filter deposition to disrupt any aggregates. Deposition of MWNTs from a 5-mL solution was achieved by vacuum filtration through the PTFE membrane (5 μm pore size; Omnipore filters) to attain a loading of 0.27 mg/cm^2 MWNTs on the base filter. The filter was rinsed with 50 mL of ethanol followed by 50 mL of deionized water to remove residual DMSO. And the single-walled carbon nanotubes (SWNTs) filter was made from the suspension with the concentration of 0.1 mg/mL . The MWNTs-SWNTs hybrid filter was made by deposition of SWNTs on the MWNTs filter. As shown in Fig. 15.4, the surface of the MWNTs-SWNTs filter appeared similar to that of the SWNTs filter,

and both filters showed increased bundling of the SWNTs in comparison with the MWNTs filter.

15.1.4 Electrospinning

Schiffman et al. [15] prepared the polysulphone (PSf)/single-walled carbon nanotubes (SWNTs) composite film on the commercial filter by electrospinning technology. In the experimental process, a solution of 4 g PSf and 20 mL DMF was mixed for 24 h. Various amounts of SWNTs (0, 0.4, 20, and 40 mg, corresponding to 0, 0.1, 0.5, and 1.0 wt%, respectively) were added, followed continuous strong ultrasonication for 1 h. The PSf/DMF solution containing SWNTs was loaded into a BD Luer-Lok tip syringe (Becton, Dickinson, Franklin Lakes, NJ, USA). A Precision Glide 21-gauge needle (Becton, Dickinson) was attached to the syringe prior to securing it to an advancement pump (Harvard Apparatus, Plymouth Meeting, PA, USA). Alligator clips were used to connect the positive anode of a high-voltage supply (Gamma High Voltage Research, Ormond Beach, FL, USA) to the needle and the negative anode to a copper plate wrapped in aluminum foil. The speed of the advancement pump, separation distance between the needle and collection plate, and applied voltage were held constant at 0.8 mL/h, 7 cm, and 20 kV, respectively.

The images displayed that PSf mats electrospun with 0, 0.1, 0.5, and 1.0 wt% SWNT loadings appear white, off-white, light ash gray, and deep gray, respectively (Fig. 15.5a), and the TEM images showed that the diameter of electrospun fiber increased with the enhancement of SWNTs contain (Fig. 15.5b–e), owing to incorporation of SWNTs into the electro-spinning solution increasing its conductivity.

15.1.5 Magnetron Sputtering (MS)

Weng's group [16] fabricated AgNPs/polyethylene oxide (PEO) composite film using magnetron sputtering. The fabrication process was accomplished in a bell jar vacuum chamber fed with Ar gas. Before the deposition on the p-silicon (100) wafers, the chamber was initially evacuated to a pressure below 1.3×10^{-3} Pa, refilled with Ar gas three times, and evacuated back to 1.3×10^{-3} Pa. In order to avoid poisoning, the sputtered target was mounted above the substrate, and the gas flowed directly to the pump after diffusing through the substrate. The silver target sputtering with 50 mm diameter, and monomer ethylene glycol dimethyl ether (EGDME) were the sources for AgNPs and PEO polymerization, respectively. DC electric power at 20 W and a suitable working pressure were employed in the MS. For the organic matrix polymerization, EGDME vapor was fed, which kept the constant flow rate by Ar (2 sccm) through the mass flow controller.

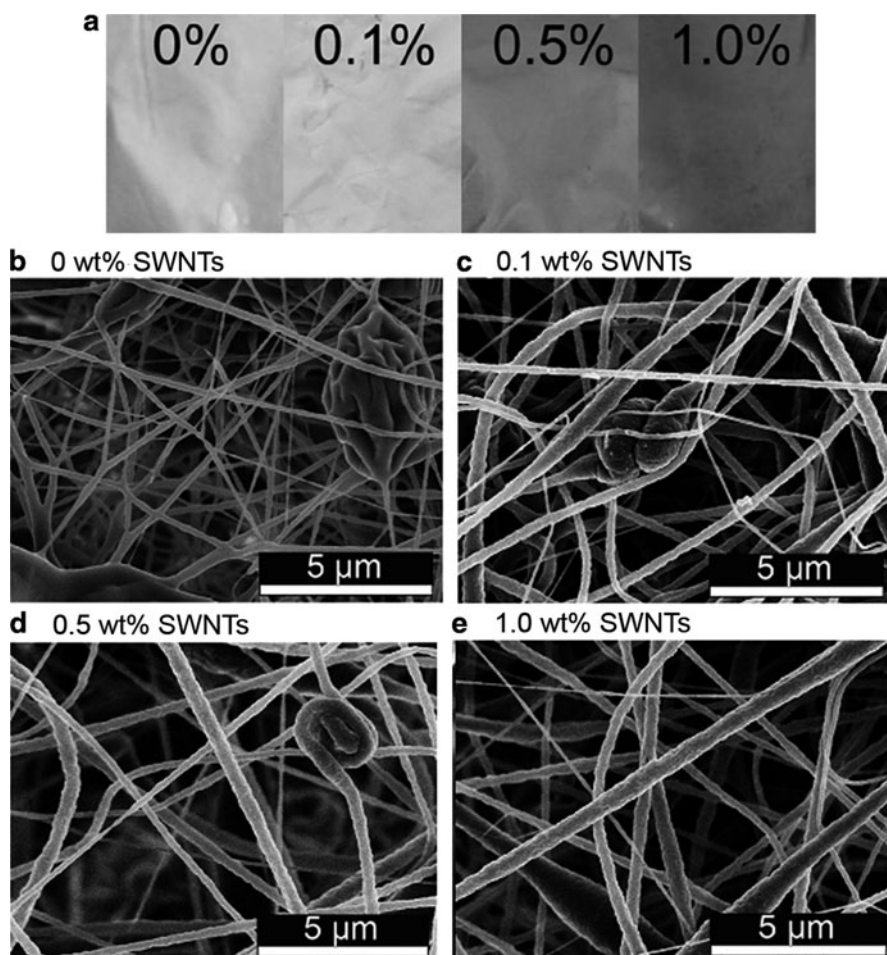


Fig. 15.5 Characterization of PSf/SWNTs films [15]. (a) Photographs of PSf films containing 0, 0.1, 0.5, 1.0 wt% loading of SWNTs. (b–e) The overall fiber SEM images of PSf films containing 0 (b), 0.1 (c), 0.5 (d), 1.0 wt% (e) loading of SWNTs

The TEM images and the selected area electron diffraction (SAED) presented the morphology of AgNPs embedded into PEO film. The pattern of discontinuous concentric rings showing in the SAED was characteristic of the silver, suggesting AgNPs in the matrix were of atomic status with preferential crystal orientation. When the working pressure was 0.2 Pa, the diameter of AgNPs with spherical shape was varied ranging from 5 to 10 nm (Fig. 15.6b), while the AgNPs were more than 20 nm when the working pressure was increased to 2.0 Pa (Fig. 15.6a), and the AgNPs shapes appeared spherical, triangular and elliptical, suggesting that the AgNPs diffused on the substrate had aggregated.

The peaks at $2\theta = 38.1^\circ$, 44.2° , 64.4° , and 77.3° that were assigned to {111}, {200}, {220}, and {311} crystalline planes of silver, respectively, also demonstrated

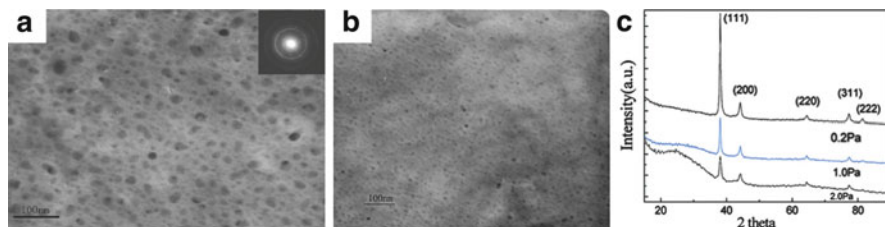


Fig. 15.6 Characterization of AgNPs/polyethylene oxide composite films [16]. (a, b) TEM images of AgNPs embedded into polyethylene oxide with the working pressure (a) 2.0 Pa and (b) 0.2 Pa. *Inset* at (a) displays the electron diffraction pattern of the AgNPs/polyethylene oxide composite films. (c) XRD patterns of AgNPs embedded in AgNPs/polyethylene oxide composite films with different working pressures

that AgNPs in the composite film were still crystal (Fig. 15.6c). Based on this pattern, the size of AgNPs could be calculated using the Scherer Formula $D = K\lambda/\beta\cos\theta$, where K depending on crystallite shape is constant (0.89), λ is the X-ray wavelength, β is the full width at half-max, and θ is the Bragg angle. The sizes of AgNPs were calculated as 7, 11 and 22 nm corresponding to 0.2, 1.0 and 2.0 Pa, respectively, which was in agreement with the TEM results that the AgNPs were grown with the increased working pressure.

15.1.6 Chemical Vapor Deposition

Chemical vapor deposition (CVD), as the most compatible approach to industrial scale production methods, could produce strongly adhesive, robust, durable, and highly active transparent thin films [17]. These film properties contrast with those produced by the coating approach that typically results in thicker films, which are less mechanically robust and often require post-coating annealing. A great many forms of CVD were developed and are frequently referenced in the literature with the different initiating means of chemical reactions and process conditions, such as atmospheric pressure CVD (APCVD), flame-assisted CVD (FACVD), thermal CVD, and so on.

Yates et al. [18] described the deposition of films of titania and copper oxide by atmospheric pressure CVD on pre-coated silica-coated barrier glass substrates. The precursor for TiO_2 film growth was titanium tetraisopropoxide (7.79×10^{-4} mol/min), transported to the reactor by N_2 via a bubbler. The substrate temperature for growth was set to 500°C . The CuO films were grown using an atmospheric pressure flame-assisted CVD coater with a propane/oxygen flame, previously described in detail [19]. The substrate temperature was set at 400°C . An aqueous solution of 0.5 M $\text{Cu}(\text{NO}_3)_2$ was nebulized into a carrier of N_2 , through the flame and onto the substrate. The resulting films were shown to be polycrystalline. The XRD and AFM studies demonstrated that both growth of TiO_2 above and below CuO film was in the form of anatase, and CuO

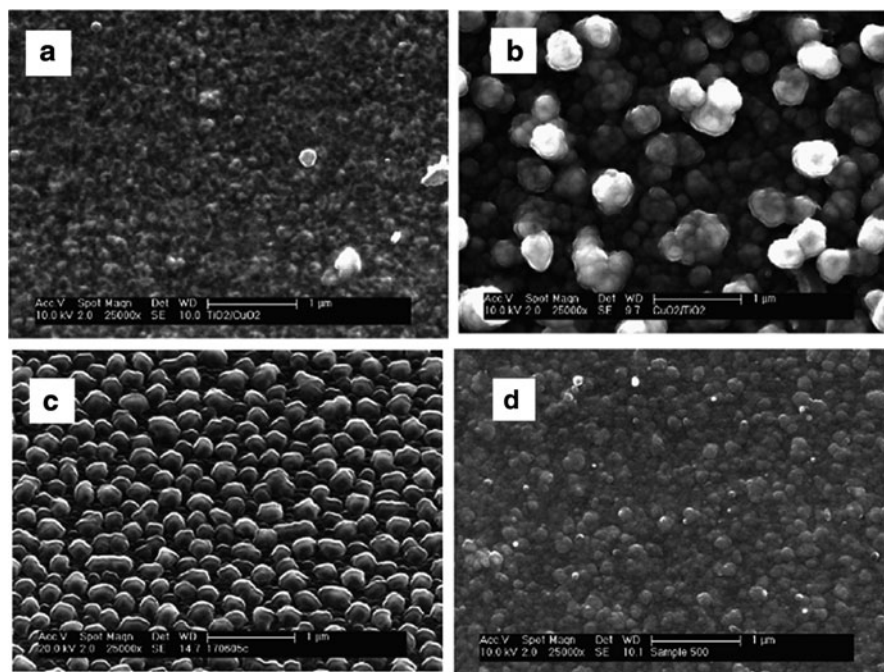


Fig. 15.7 SEM images of (a) CuO film over TiO₂, (b) TiO₂ film over CuO, (c) CuO film and (d) TiO₂ on the glass substrates [18]

film deposited above the TiO₂ film was in the form of copper II oxide, and Cu I oxide when CuO film was deposited on the TiO₂ film with over 61 nm thickness. Furthermore, CuO film deposited over TiO₂ film by FACVD consisted of an island growth-type structure of packed spherical nanoparticles, with size of ~100 nm (Fig. 15.7a), which was very similar in appearance to that of a single TiO₂ layer (Fig. 15.7d), rather than that of a single CuO film (Fig. 15.7c), suggesting the CuO film deposition was very much influenced by the underlying structure, in this case the change from amorphous smooth silica to crystalline titania. However, the TiO₂ film over thick CuO film had a much more pronounced particulate structure than the other surfaces, due to the existence of Cu₂O within this TiO₂ film (Fig. 15.7b).

15.2 Antibacterial Activity of Nanomaterial-Based Films

The antibacterial activity of nanomaterial-based films, including metal oxide nanoparticles (e.g., TiO₂ and ZnO), AgNPs, graphene, and carbon nanotubes, were determined against the model bacterium *E. coli*.

15.2.1 *TiO₂-Based Film*

TiO₂ nanoparticles were in the forms of anatase, brookite and rutile [20], where anatase TiO₂ was the most studied semiconductor after the discovery of its photocatalytic behavior [21]. So far, much attention has been focus on the photocatalysis and photo-induced hydrophilic effect mechanisms, improvement of photocatalytic activity by advancement of the microstructure, and applications including antimicrobial, and self-cleaning behaviors [22]. The biocidal activity of TiO₂ was first demonstrated by Matsunaga and co-workers [23]. Subsequently, a great deal of the considerable literature has shown that TiO₂ nanoparticles can kill cancer cells, bacteria, viruses, and algae under UV illumination [24–28], resulting in important applications in the disinfection of air, water, and surfaces. But most of these early work involved TiO₂ suspension and planktonic organisms. Recently, researchers had focused on the biocidal activity of the thin films of TiO₂ deposited on the substrate surfaces [29–32].

15.2.1.1 Comparison of the Test Methods

In order to compare the antibacterial activity of TiO₂ film prepared from different approaches, Yates' group [33] firstly compared the two-test methods, BS ISO 27447:2009 and in house standard (BS EN 13697). In a typical experiment, bacterial cells were collected by centrifugation at 12,000 rpm for 5 min, and washed three times with physiological saline solution. The cells were resuspended in a 1:500 dilution of Nutrient Broth and adjusted to OD 0.1 ~ 0.2 at 600 nm in a spectrophotometer to give approximately 2×10^8 colony-forming units (CFU) per milliliter. In the BS ISO 27447:2009 method, 50 μ L of cells suspension was inoculated onto each 20-mm² test sample and covered with a square of 1-mm² borosilicate glass to ensure close contact between the culture and the film. The samples were placed in 50-mm-diameter Petri dishes containing moistened filter paper to prevent drying out of the suspensions. The samples were irradiated with Blacklight Blue lamps with a maximum UV light intensity of 0.26 mW/cm². Plain borosilicate glass was used for a control experiment. Samples were removed after incubation time and immersed in 20 mL of sterile physiological saline solution, following vortexed for 60 s to resuspend the bacteria. The viability count was performed by serial dilution and plating on nutrient agar in triplicate and incubation at 37°C for 48 h. However, in the house standard method, the cells were resuspended in sterile water, and the samples were not covered with glass, but incubated in 55-mm-diameter Petri dishes kept humid by adding 2 mL sterile water under UVA lamp irradiation of 2.24 mW/cm². They found the control experiment remained viable after 24 h irradiation with only a 1-log reduction, while there was a 2-log reduction in the house standard method after 6 h irradiation. This difference could be attributed to the low concentration of Nutrient Broth in the resuspension medium in the BS ISO 27447:2009 method which meant that the bacterial cells

were less stressed and remained viable for longer. Also, the number of the viable cells in the BS ISO 27447:2009 method was much larger than that of the viable cells in the house standard method, owing to the reduced illumination levels by approximately tenfold, and the existence of oxidizable material in the resuspension medium (1/500 dilution of Nutrient Broth rather than distilled water) competing with the bacteria for reactive oxygen species (ROS).

15.2.1.2 Antibacterial Activity of TiO₂ Films

Kikuchi et al. [34] found that the survival ratio of *Escherichia coli* on the TiO₂ film under black light illumination (1.0 mW/cm²) decreased to a negligible level within 1 h (Fig. 15.8a), while the UV light only caused ~50% sterilization within 4 h. And the TiO₂ film in the dark did not affect the survival ratio, indicating that the film itself was not toxic for *E. coli*, which was also demonstrated by Sunada et al. [29]: when the initial cell concentration was 2×10^5 CFU/mL (Fig. 15.8b), bacterial cells on the TiO₂ film were killed within only ~90 min under the UV light illumination (1.0 mW/cm²). And they emphasized that the survival curve did not follow a simple single exponential decay process with the increasing of illumination time, but appeared to consist of two steps, a very low rate photokilling step, followed by a higher one, which was observed regardless of the initial cell concentration in the range of 2×10^5 – 2×10^8 . In the case of an initial cell concentration of 2×10^5 CFU/mL, the rate constants of the first and second steps were 0.015 and 0.085 min⁻¹, respectively, which was close to those obtained in the powder systems [35, 36]. Further studies

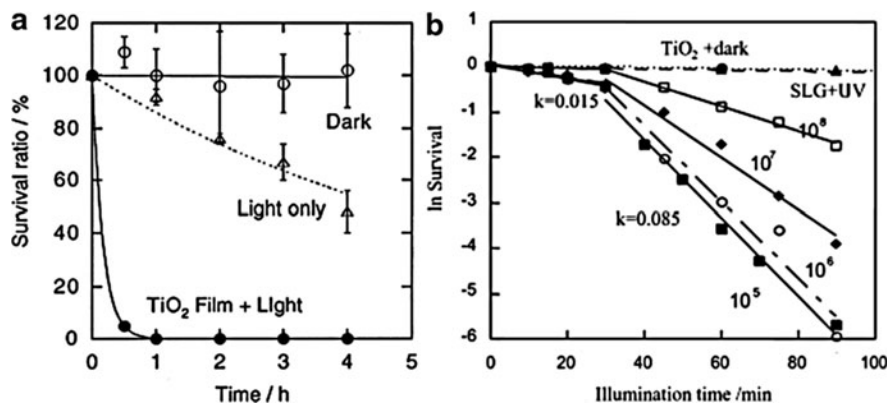


Fig. 15.8 (a) Survival ratio of *E. coli* with and without a TiO₂ thin film under black light illumination (1.0 mW/cm²) and with a TiO₂ thin film in the dark [29]. (b) The log plot of the survival of *E. coli* cells versus illumination time. The cell suspension was incubated on TiO₂ film under UV illumination (1.0 mW/cm²). The initial cell concentrations were 2×10^5 CFU/mL (■), 2×10^6 CFU/mL (○), 2×10^7 CFU/mL (◆), 2×10^8 CFU/mL (□), respectively. Survival was also determined for cells (2×10^5 CFU/ml) on the TiO₂ film in the dark (●), and on normal glass (soda-lime glass, SLG) without TiO₂ film under UV illumination (▲) (1.0 mW/cm²)

showed that various bacteria, *E. coli*, *Staphylococcus aureus*, and *Pseudomonas aeruginosa*, etc., were killed rapidly on TiO₂ film under UV illumination (320–380 nm, 1.0 mW/cm²) [37].

15.2.1.3 Antibacterial Activity of TiO₂-Based Composite Films

In order to overcome the disadvantages that the antibacterial activity of TiO₂ film was strongly weakened under the dark conditions and very low UV intensity, TiO₂ film deposited with the selected metal (and metal oxide) nanoparticles has been developed, such as silver and copper, which presented intrinsic antibacterial activity.

Zhang et al. [38] found AgNP-doped TiO₂ film exhibited much stronger antibacterial abilities toward both Gram-negative *E. coli* and Gram-positive *S. aureus* than that of pure anatase TiO₂ nanoparticles films. When the films were illuminated under 365 nm UV light (0.1 mW/cm²), almost all the bacteria were killed by AgNP-doped TiO₂ films (>99.9%), while the antimicrobial value only reached 77.0% and 72.9% for *E. coli* and *S. aureus* on pure anatase TiO₂ nanoparticle film, respectively. More importantly, the antimicrobial activities of the AgNP-doped TiO₂ film were still maintained even without exposure to UV light, such that the sterilizing rate reached 99.1% and 99.4% to *E. coli* and *S. aureus*, respectively. These results indicated that AgNPs promoted the antibacterial activity of TiO₂. Mai et al. [4] also synthesized AgNP-doped TiO₂ film on titanium plates by the sol–gel process. They found AgNPs deposited on TiO₂ film were of metallic nature and could grow to larger ones with an increase in the annealed temperature (Fig. 15.9a–c), and that the smaller the size of AgNPs, the better was the antibacterial ability whether in the dark or under visible light (Fig. 15.9d, e).

Sunada et al. [30] prepared the copper-deposited TiO₂ film, and demonstrated that the resulting film could inhibit the growth of copper-resistant *E. coli* not under dark conditions, but with a very weak UV intensity of 1 μW/cm², which corresponds to the typical UV intensity of indoor light (Fig. 15.10a). However, the copper-deposited TiO₂ film could represent photocatalytic antibacterial activity toward the normal *E. coli* (Fig. 15.10b). Foster et al. [33] also found CuO-doped TiO₂ film and CuO-TiO₂ co-deposited film gave a 2-log reduction after 4 h in the dark, and when the incubation time increased, the antibacterial activity of CuO-doped TiO₂ film was higher than that of CuO-TiO₂ co-deposited film, resulting from the reduced availability of CuO surface on the co-deposited film. However, under the UV illumination, the antibacterial activity of both CuO-doped TiO₂ and co-deposited film was greatly enhanced, giving a >6-log reduction after 2 h. Furthermore, Ondok et al. [39] and Sato et al. [40] reported that the antibacterial ability of CuO-doped TiO₂ film was enhanced when either the content of Cu or the UV intensity increased.

Recently, Dai et al. [31] reported photocatalytic hydrogen generation using a TiO₂ nanoparticle/MWNTs nanocomposite under visible light irradiation, which suggests that the photocatalytic activity of the MWNTs-doped TiO₂ nanoparticle

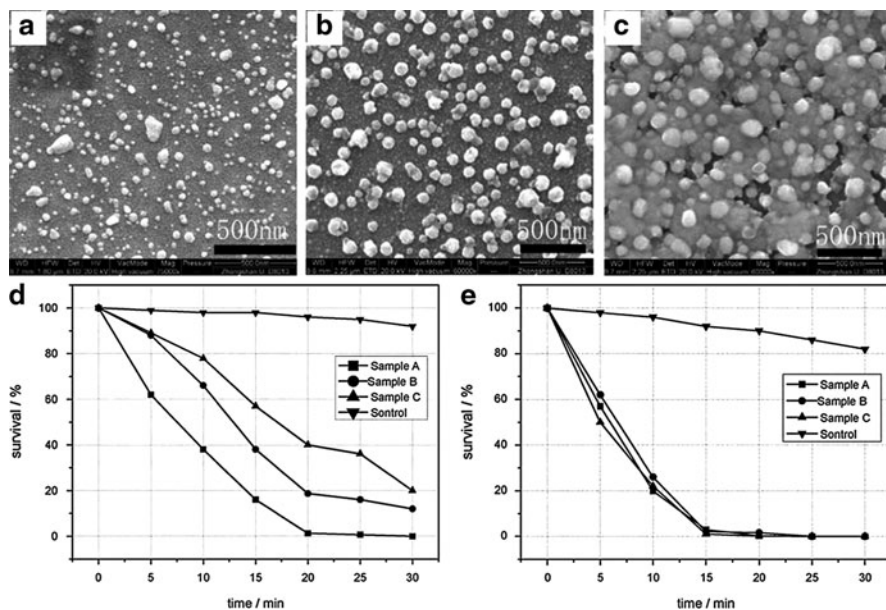


Fig. 15.9 (a–c) SEM images of the AgNPs-doped TiO₂ films annealed at different temperature. The sizes of AgNPs in the films were 20 ~ 30 nm (a), 60 ~ 80 nm (b) and >100 nm (c). (d, e) Survival curves of *E. coli* for the films (d) in the dark and (e) at visible light irradiation. The smaller size of AgNPs have the better antibacterial ability whether in the dark or under visible light [4]

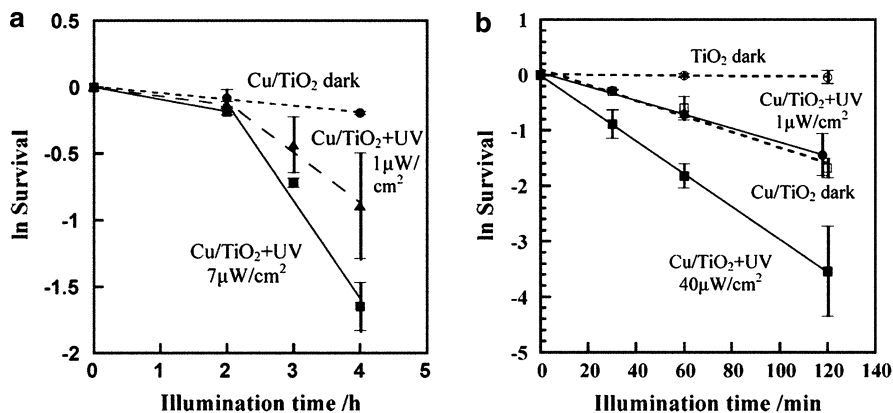


Fig. 15.10 (a) Changes in the survival of normal *E. coli* cells under the different illumination intensity. Cells (2×10^5 CFU/mL) were incubated on the TiO₂ film (O) and on the copper-deposited TiO₂ film (□) under dark conditions, respectively. The suspension was also incubated on the copper-deposited TiO₂ film under UV illumination at a UV light intensity of $40 \mu\text{W}/\text{cm}^2$ (■) and $1 \mu\text{W}/\text{cm}^2$ (●). (b) Changes in survival of copper-resistant *E. coli* cells on the copper-deposited TiO₂ film under dark condition (●) and under UV illumination at light intensity of $7 \mu\text{W}/\text{cm}^2$ (■) and $1 \mu\text{W}/\text{cm}^2$ (▲) [30]

was excited by visible light irradiation, rather than UV irradiation. Akhavan et al. [41] and Oh et al. [42] have shown that the MWNTs/TiO₂ nanocomposite could inactivate bacteria under the visible light irradiation and in the dark. Further, Akhavan et al. [32] tested the antibacterial property of MWNTs-doped TiO₂ film by varying the content of MWNTs and the post-annealing temperature. They found that the antibacterial activity of the MWNT-doped TiO₂ films in the dark gradually increased by increasing the MWNTs content of the films, independent from the post-annealing temperature (Fig. 15.18a). Especially, when the MWNTs content reached 20 wt%, the MWNTs-doped TiO₂ films annealed at 450°C showing an ability of complete inactivation of the bacteria under the visible light irradiation for 1 h, while the corresponding film annealed at 100°C could kill 93% of the bacteria under the same conditions.

15.2.1.4 Durability and Regenerate Ability of TiO₂ Films

Book and co-workers [43] demonstrated the durability and regenerate ability of TiO₂ film prepared by CVD. TiO₂ films were repeatedly cycled through the biocidal test procedure followed with a cleaning process (film was sonicated in methanol and then chloroform for 30 min), and then characterized the film photoactivity by the stearic acid test. They found no measurable reduction in maintained photoactivity, within the accuracy of the test, over three test cycles (Fig. 15.11b).

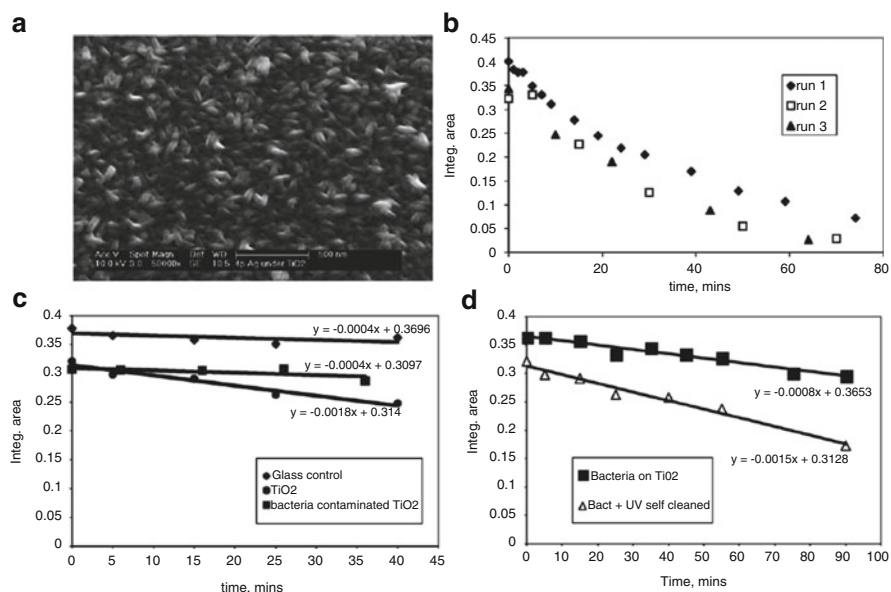


Fig. 15.11 (a) SEM image of TiO₂ over AgNPs films. (b) An example sample showing the retention of photoactivity after bioactivity testing. (c) Photoactivity after bio-contamination and (d) photoactivity after UV “self-regeneration” [43]

Additionally, it was known that TiO₂ film was mechanically durable, owing to the TiO₂ was hard and scratch resistant and had the longest term stability.

The TiO₂ surface can decompose organic contamination with the aid of UV light, suggesting the application of TiO₂ photocatalysis to novel “self-cleaning” techniques, which was first demonstrated by Watanabe et al. in 1992 [44]. And water could penetrate the molecular-level space between the stain and the superhydrophilic TiO₂ surface, so the surface was maintained clean with the supply of water current even though the photons excited by UV light may be insufficient to decompose the adsorbed stain [45]. After the biocidal test procedure, the TiO₂ film was visibly contaminated with dead bacteria residues, leading to significant reduction of photocatalytic activity (Fig. 15.11c). However, after the film contaminated with dead bacteria residues was treated with an additional UV irradiation, the film recovered a significant percentage of the original activity (Fig. 15.11d).

15.2.2 ZnO-Based Films

Owing to low cost, easy availability and unique chemical and physical properties, ZnO nanoparticles has sparked much interest. Jones et al. [46] reported that ZnO nanoparticles presented higher antibacterial activity on *S. aureus* than other metal oxide nanoparticles. Padmawathy et al. [46] demonstrated that nano-ZnO showed enhanced antibacterial activity as compared with bulk ZnO. And Zhang et al. [47] reported that the antibacterial activity of ZnO nanoparticles increased with decreasing particle size, and the dispersants (Polyethylene Glycol and Polyvinylpyrrolidone) did not much affect the antibacterial activity of ZnO nanoparticles but enhanced the stability of the suspensions. Thus, Bajpai et al. [48] prepared ZnO/chitosan film, and revealed that the film showed excellent antibacterial action against *E. coli*. And Chandramouleeswaran et al. [48] demonstrated that nano-ZnO/polypropylene film could kill almost all *Staphylococcus aureus* and *Klebsiella pneumoniae* with just nano-ZnO filler at a 3% level of loading. Shalumon et al. [49] demonstrated that sodium alginate/poly(vinyl alcohol)/nano-ZnO composite nanofiber mats could suppress the growth of *Staphylococcus aureus* and *Escherichia coli*.

15.2.3 AgNPs-Based Films

The antimicrobial properties of silver were well known to the ancient Egyptians and Greeks. Since then, silver has been used in different fields in medicine and surface coating for many years [50], due to a strong cytotoxic effect toward a broad range of microorganisms and remarkably low human toxicity compared to other heavy metal ions. Silver nanoparticles (AgNPs) also show efficient antimicrobial properties, because of their extremely large surface area which provides better contact with

microorganisms. Recently, not only silver ions or a silver nanoparticle colloid but also all kinds of silver-based films have attracted more and more attention.

Akhavan et al. [51] synthesized AgNPs film on the SiO₂ thin film, and found that the AgNPs film presented strong antibacterial activities against *E. coli* and *S. aureus* bacteria with relative rates of reduction of the viable bacteria of 1.05 and 0.73 h⁻¹ for initial concentration of ~10⁵ CFU/mL, respectively, and the difference was attributed to amount of peptidoglycan in the cell wall structure. The antibacterial activity of the AgNPs films was dependent on the AgNPs size corresponding to the surface-to-volume ratio. The smaller AgNPs with larger surface area could lead to a much greater bactericidal effect [52].

However, AgNPs were not stable and readily aggregated, and AgNP oxidation was accelerated by illumination with white lamps in air [53], resulting in the reduction of antibacterial activity. Therefore, the AgNP-based composite films, such as AgNP/TiO₂ film [54], AgNP/chitosan film [55–57], AgNP/polyethylene oxide film [16], AgNP/hyaluronan/poly (dimethyldiallylammonium chloride) film [58], AgNP/sodium alginate film [59], AgNP/polyvinyl alcohol [60], AgNP/polyester film [61], AgNP/poly (ethylenimine) film [7], AgNP/polyvinyl sulphonate film [62], AgNP/poly (vinyl alcohol)/poly (L-lactic acid) film [63], and AgNP/N-(2-aminoethyl)-3-aminopropyl-trimethoxysilane (DIAMO) film [64] were considered to overcome those challenges. Akhavan et al. [65] found the antibacterial activity of TiO₂-capped silver nanorods film in the dark was stronger than that of TiO₂-capped AgNPs film, with 2.34 h⁻¹ for the relative rate of reduction of the number of viable bacteria. Vimala et al. [66] successfully fabricated the AgNP/chitosan film by a three-step process: silver ion-poly (ethylene glycol) matrix preparation, addition of chitosan matrix, and removal of poly (ethylene glycol) from the film matrix. The AgNP/chitosan film can inhibit the growth of *E. coli*, *Bacillus*, and *K. pneumoniae*, and especially, after 350 min of incubation, AgNPschitosan film can killed ~75% of *E. coli*.

15.2.4 CNTs-Based Films

Carbon nanotubes are pseudo-one-dimensional carbon allotropes of high aspect ratio, high surface area, and excellent material properties, such as ultimate electrical and thermal conductivities and mechanical strength, which offer a wide range of opportunities and application potential in biology and also antibacterial nonmaterial [67]. Narayan et al. [68] showed that nanotube films formed via high temperature laser ablation of graphite on silicon completely inhibited bacterial colony formation. However, the nanotube structure was not well controlled and the process may not be amenable to many biomedical materials. Kang et al. [69], Rodrigues et al. [70] and Brady-Estévez et al. [71] tested the antibacterial activity of SWNTs filter against *E. coli*, showing inactivation of ~80% of *E. coli* after only 20 min incubation (Fig. 15.12) [71]. And then Kang et al. [69, 72] has revealed that the SWNTs filter presented higher antimicrobial activity than a MWNTs-coated filter, and the

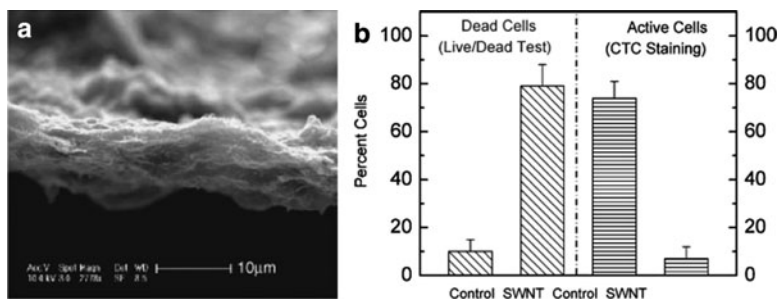


Fig. 15.12 (a) SEM image of the cross-section of a layer of SWNTs filtrated onto the PVDF membrane. The SWNTs film displayed highly porous structures. (b) Inactivation (*left row*) and metabolic activity (*right row*) of *E. coli* cells retained on the SWNTs film and on the control PVDF membrane. Inactivation test results based on the Live/Dead test showing the percent of *E. coli* cells that were not viable. Metabolic activity results based on CTC staining indicated the percent of metabolically active *E. coli* cells [71]

SWNT-coated filter could inactivate >60% of microorganisms in river water and wastewater treatment plant samples, while natural organic matter did not influence its antimicrobial activity [72]. Brady-Estévez et al. [14] prepared a novel SWNTs/MWNTs hybrid filter which was composed of a thin SWNTs layer on top of a thicker MWNTs layer supported by the PTFE membrane, and found that the hybrid filter not only exhibited high log removal of several model viruses (MS2, PRD1, T4) by depth filtration but also provided high levels of inactivation of model bacteria (*E. coli* K12 and *Staphylococcus epidermidis*), as well as microbes from river water and treated wastewater effluent.

They found the physicochemical properties (e.g., diameter, length, aspect ratio, sample purity, structural defects) determined the antimicrobial activity of MWNTs-coated filter, and functionalized [sonication in a mixture of H_2SO_4 and HNO_3 (3:1 v/v) for 1 h] and short MWNTs-coated filters represented excellent antibacterial activity, possibly due to increased density of the open tube ends [73]. However, Yang et al. [74] considered that longer SWNTs filters exhibited stronger antibacterial activity. Vecitis et al. [75] demonstrated for the first time that SWNTs electronic structure was a key factor regulating SWNTs antibacterial activity, and found that antibacterial activity of the high percent metallic (>95%) SWNTs filter was higher than that of the low percent metallic (<5%) SWNTs one, owing to the high percent metallic SWNTs-induced oxidative stress after SWNTs–bacteria contact and physical perturbation of the cell membrane.

In order to improve the antibacterial property of CNTs filter, large amounts of CNTs-based composite filters were introduced. Simmons et al. [76] prepared a flexible composite film by depositing SWNTs coated with polyvinylpyrrolidone-iodine (PVPI) in water, and found that the PVPI-coated SWNTs film could slowly release antiseptic iodine, resulting in the effective antibacterial property over 48 h incubation. Aslan et al. [77] found that *E. coli* and *S. epidermidis* viability and metabolic activity were significantly diminished on the SWNTs/polymer poly(lactic-co-glycolic acid)

(PLGA) film, and were correlated with SWNTs length and concentration (<2 wt%). Schiffman et al. [15] observed that the loss of viability of *E. coli* on the electrospun polysulphone/SWNTs mats was directly correlated to increased SWNTs incorporation within the mat, ranging from 18% for 0.1 wt% SWNTs to 76% for 1.0 wt% SWNTs, and the antimicrobial action of the polysulphone/SWNTs mats occurred after a short contact time of 15 min or less. Pangule et al. [78] incorporated conjugates of MWNTs with lysostaphin (Fig. 15.13a), a cell wall degrading enzyme, into films to impart bactericidal properties against methicillin-resistant *S. aureus* (MRSA) and *S. epidermidis*, and found that these enzyme–MWNTs films were highly efficient in killing MRSA (>99% within 2 h) without release of the enzyme into solution (Fig. 15.13b), and these films were reusable and stable under dry storage conditions for a month (Fig. 15.13c). Zhou and Qi [79] synthesized a novel epsilon–polylysine–MWNTs nanocomposite by covalent attachment of epsilon–polylysine on MWNTs with hexamethylene diisocyanate as the coupling agent,

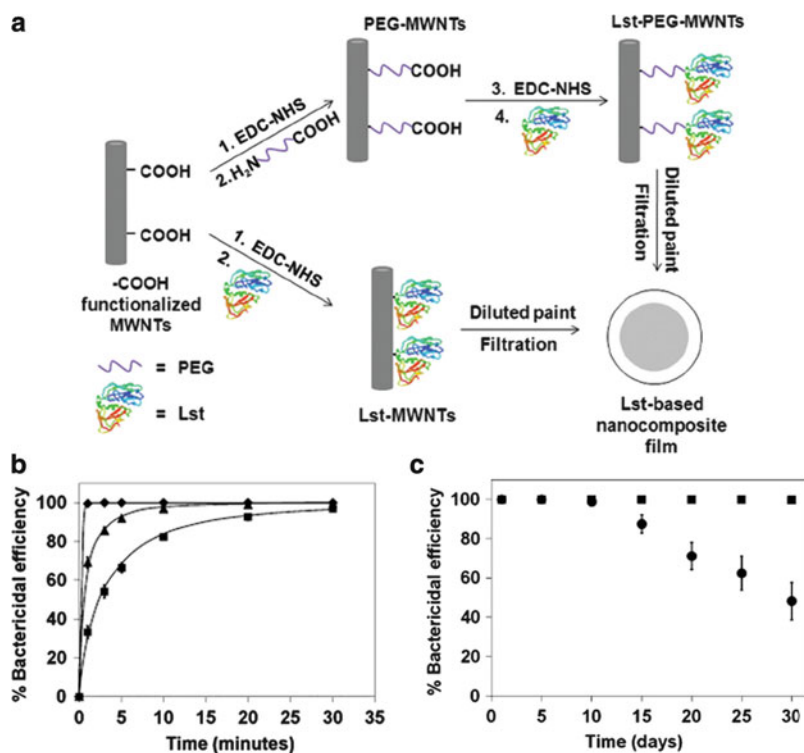


Fig. 15.13 (a) Scheme of antimicrobial nanocomposite films containing lysostaphin-MWNTs. (b) Comparison of bactericidal effect of Lst-MWNTs film (■) and Lst-PEG-MWNT film (▲) with the native enzyme (◆). These enzyme-MWNTs films were highly efficient in killing MRSA without release of the enzyme into solution. (c) Operational (●) and storage stability (■) of films containing 4% w/w Lst in the form of Lst-PEG-MWNT. The films were stored in dry conditions and at room temperature in between the two use cycles [78]

and found that the epsilon-polylysine-MWNTs film showed improved antibacterial activities and excellent anti-adhesive efficacy against *P. aeruginosa* and *S. aureus*.

Additionally, owing to outstanding electron transmitting property of CNTs, the antibacterial activity of CNTs films was enhanced by the aid of applied potential. Vecitis et al. [80] prepared an electrochemical MWNTs microfilter by depositing MWNTs on the PTFE membrane, and demonstrated that the MWNTs filter was effective for complete removal of bacteria by sieving and multilog removal of viruses by depth filtration in the absence of electrolysis, while concomitant electrolysis during filtration resulted in significantly increased inactivation of influent bacteria and viruses; especially, application of 2 and 3 V for 30-s post-filtration inactivated >75% of the sieved bacteria and >99.6% of the adsorbed viruses, leading to the number of bacteria and viruses in the effluent reaching below the limit of detection.

15.2.5 Graphene-Based Films

Graphene consisted of a monolayer of carbon atoms which were tightly packed into a two-dimensional crystal. Since the seminal work of Geim and coworkers on free-standing graphene in 2004 [81], many potential applications of graphene were actively pursued owing to its outstanding mechanical stiffness and electronic transport property [82, 83], such as nano-electronic devices [84], sensors [85], solar cells [86], and nanocomposite materials [82].

Hu et al. [11] demonstrated that the two water-dispersible graphene derivatives, graphene oxide (GO) and reduced graphene oxide (rGO) nanosheets, could effectively suppress the growth of *E. coli* cells, and the free-standing GO and rGO papers also presented antibacterial activity. And Akhavan et al. [87] further demonstrated that GO and rGO nanowalls could kill Gram-positive *S. aureus* bacteria. Park et al. [88] fabricated the Tween/rGO paper by simple filtration of a homogeneous aqueous colloidal suspension of a Tween/rGO hybrid, and found that the tween/rGO paper could inhibit nonspecific binding of Gram-positive bacteria *Bacillus cereus*, while rGO paper without tween showed nonspecific bacteria binding (Fig. 15.14).

15.3 Mechanism of Nanomaterial-Based Films Antibacterial Activity

15.3.1 TiO_2 -Based Films

As we know, the antibacterial activity of TiO_2 film was attributed to its photocatalysis property. In order to reveal the important molecules directly interacting with bacterial cells, Kikichi et al. [34] designed the membrane-separated

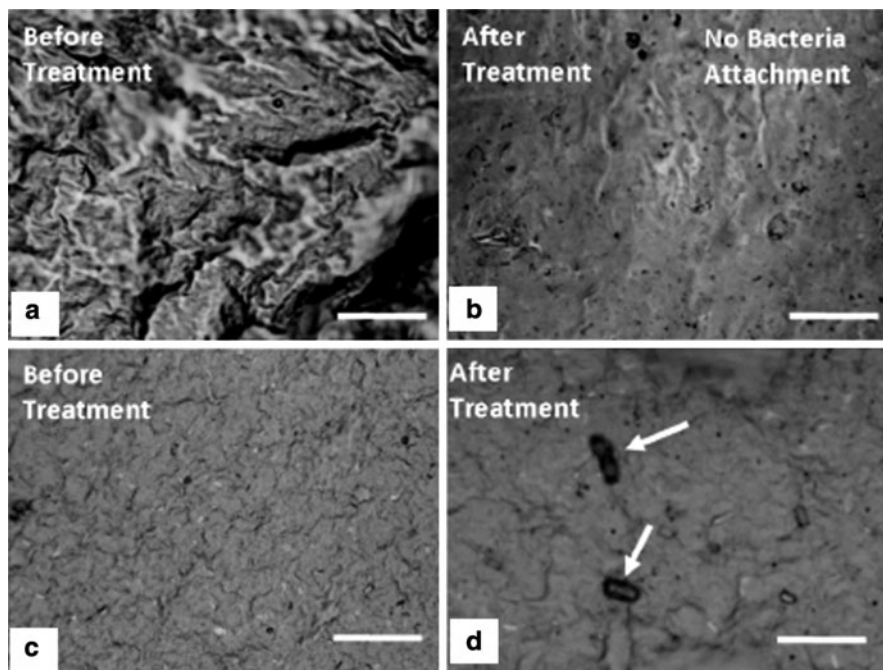


Fig. 15.14 (a, b) Optical microscopy image of the tween/rGO paper before and after the treatment with a DI-water suspension of the mature *Bacillus cereus* cells. The tween/rGO paper shows no bacterial attachment. (c, d) Optical microscopy image of the rGO paper before and after the bacterial treatment. The rGO paper shows bacterial attachment (marked by arrows) [88]. All scale bars 10 μm

system to fence out TiO_2 film and *E. coli* suspension by the PTFE membrane (50 μm thickness, 0.4 μm pore size). They found the survival ratio of bacteria on the film surface improved with the increase in both mannitol concentration and pH value which could suppress the activity of radical molecules ($\cdot\text{OH}$ and $\cdot\text{O}_2^-$), and that the existence of catalase in the suspension could enhance the bacterial survival ratio, suggesting the formation of radical molecules and H_2O_2 in the suspension under the UV illumination. So, it was clear that various reactive species (e.g., $\cdot\text{OH}$, $\text{HO}_2\cdot$, H_2O_2) were produced by UV illumination of TiO_2 in the presence of water and air by the following reactions [89, 90]



<Reduction reaction>



<Oxidation reaction>



These reactive oxygen species (ROS) can decompose organic compounds and extinguish cellular activity.

Sunada et al. [29] studied the photokilling process of *E. coli* on the TiO₂ film by means of AFM, which suggested that bacterial cells decomposed from the outside of the cell, resulting from the TiO₂ film photocatalysis (Fig. 15.15a–c). Additionally, Kühn et al. [91] observed that the killing rates of bacteria were dependent on the thickness and structure of cell walls. Based on these observations, they found that the photokilling of bacteria on the illuminated TiO₂ surface could be divided into three stages (Fig. 15.15d). First, disordering of the outer membrane of bacterial cells by reactive species ($\bullet\text{OH}$, O_2^- , H_2O_2). The outer membranes of *E. coli* cells were decomposed partially by the reactive species produced by the TiO₂ photocatalyst, while the bacteria cell viability was not lost very efficiently. Second, disordering of the inner membrane (the cytoplasmic membrane) and killing of the cell. Owing to the change of the permeability to reactive species when the partial outer membrane is decomposed, reactive species easily reached and attacked the inner membrane,

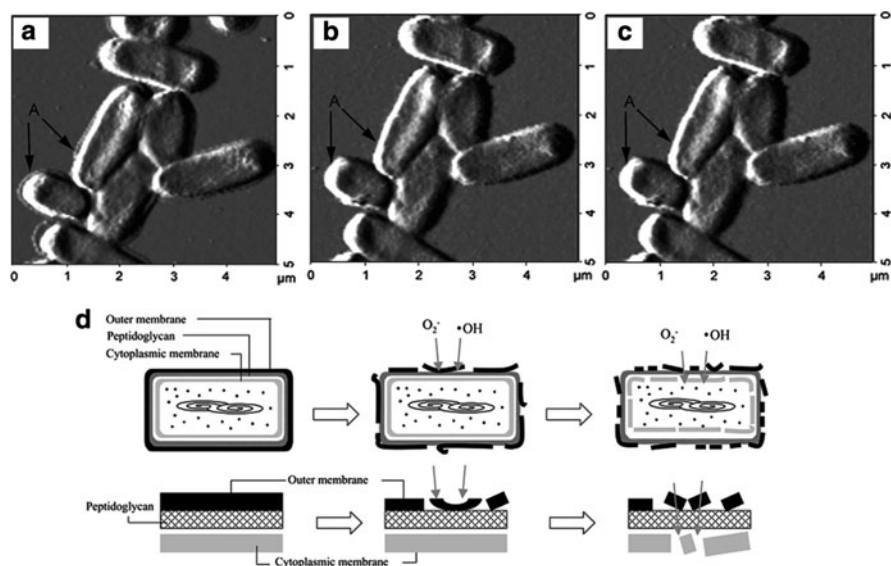


Fig. 15.15 (a–c) AFM images of *E. coli* cells on the TiO₂ film: (a) no illumination, (b) illumination for 1 day, (c) illumination for 6 days. Light intensity was 1.0 mW/cm². (d) Schematic illustration of the process of *E. coli* photokilling on TiO₂ film; in the lower row, the part of cell envelope was magnified [29]

leading to the peroxidation of the membrane lipid. The structural and functional disordering of the cytoplasmic membrane due to lipid peroxidation led to the loss of cell viability and cell death. And third, decomposition of the dead cell. If the illumination continued for a sufficiently long time, the dead cells were found to be decomposed completely.

As to the CuO-doped TiO₂ film, Sunada et al. [30] presumed that the valence state of the copper played the key role in the bactericidal process both in the dark and under the very weak UV illumination. It has been reported that the copper ions and metallic copper could be transformed into each other by the following redox reaction by the help of photo-generated electrons and holes [92–98].

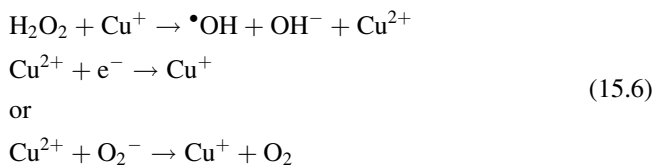
<Reduction reaction>



<Oxidation reaction>



Litter et al. [99] and Cieřla et al. [100] reported that the photocatalytic activity of TiO₂ was enhanced through converting photo-generated H₂O₂ into more reactive $\cdot\text{OH}$ by the following copper-mediated Fenton-type reactions.



Sato et al. [40] surmised a possible mechanism of the enhanced antibacterial activity of CuO-doped TiO₂ film, which was associated with photocatalysis under the weak UV illumination (Fig. 15.16). Through a series of photoreactions as expressed above, reactive oxygen species (ROS) such as $\cdot\text{OH}$, O_2^{-} and H₂O₂, were generated by TiO₂ photo-excitation on the CuO-doped TiO₂ film surface. Because H₂O₂ was more stable than $\cdot\text{OH}$ and O_2^{-} , it could diffuse from the CuO-doped TiO₂ film surface into the suspension. As shown in Fig. 15.16a, a small amount of copper ion could leach out of the CuO-doped TiO₂ solid phase into the suspension and was reduced into Cu⁺ by receiving electrons from photo-excited TiO₂ nanoparticles. Then, the free Cu⁺ reacted with H₂O₂ to produce $\cdot\text{OH}$ via Fenton-type reactions, contributing to the deactivation of microbial cells in the suspension. On the other hand, the following reactions are supposed to occur in solid phase (CuO-doped TiO₂ film) (Fig. 15.16b). Cu²⁺ could be reduced into Cu⁺ by electron from photo-excited TiO₂, and in turn Cu⁺ converted H₂O₂ into

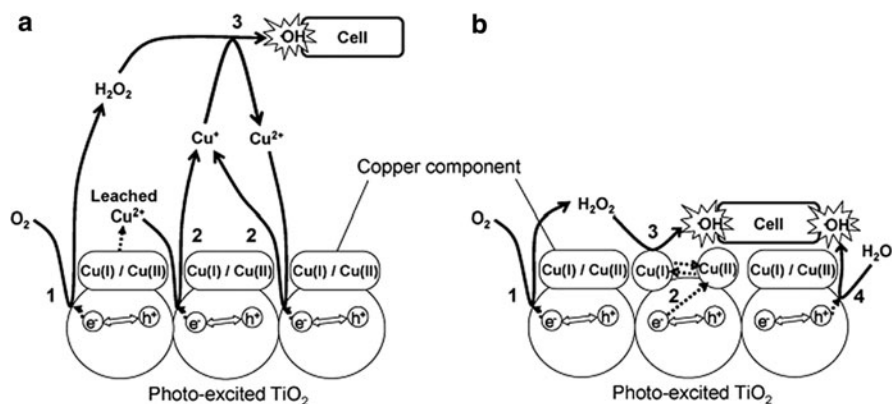


Fig. 15.16 Schematic illustration showing possible mechanism of deactivation on CuO-doped TiO₂ film in the liquid phase (a) and on the solid surface (b) [40]

·OH, while being oxidized into Cu²⁺ again, leading to much more deactivated bacterial cells. However, Sunada et al. [30] proposed that copper ions could penetrate the damaged membrane into cytoplasm, resulting in a direct disturbance in intracellular metabolic systems, and thus the bactericidal process for the bacterial cells on the CuO-doped TiO₂ film under weak UV illumination consisted of two steps (Fig. 15.17). First, the outer membrane was attacked by the reactive oxygen species produced by TiO₂ photocatalysis and the transformation between Cu²⁺ and Cu⁺ (Fig. 15.17b, c). And then copper ions (maybe and Cu⁺) were effectively taken into the cytoplasmic membrane (Fig. 15.17c, e). In this case, the photocatalytic reaction mainly played a critical role in assisting the intrusion of copper ions into the cells.

Therefore, the metal nanoparticles may play three roles in killing bacteria: (1) it could prevent photo-generated electrons and holes from surface recombination by trapping of photo-generated electrons with positive metal ions; (2) it increased the yield of hydroxyl radical through the Fenton-type process by reaction with photo-generated H₂O₂, and (3) it diffused into the cytoplasmic membrane of the bacteria and accelerated the lethal effect after the outer membrane of the bacteria was destroyed by oxidizing oxygen species. In addition, the metal ions can kill bacteria directly, which could explain the antibacterial activity of CuO-doped TiO₂ film in the dark.

On the other hand, Akhavan et al. [42] considered that the improved antibacterial property of the MWNTs-doped TiO₂ film could be assigned to the formation of Ti–C and Ti–O–C carbonaceous bonds at 450°C, which was confirmed by their XPS results. So a possible mechanism of the improvement in the photo-inactivation was proposed (Fig. 15.18b). First, the electrons generated by the photo-excited MWNTs were transmitted to the conduction band of the TiO₂ through the Ti–C bonds, leading to the formation of the positively charged MWNTs, which could capture electrons from the valence band of TiO₂ to generate the holes in the TiO₂ [101, 102]. And the electrons and holes induced the generation of ROS by a series

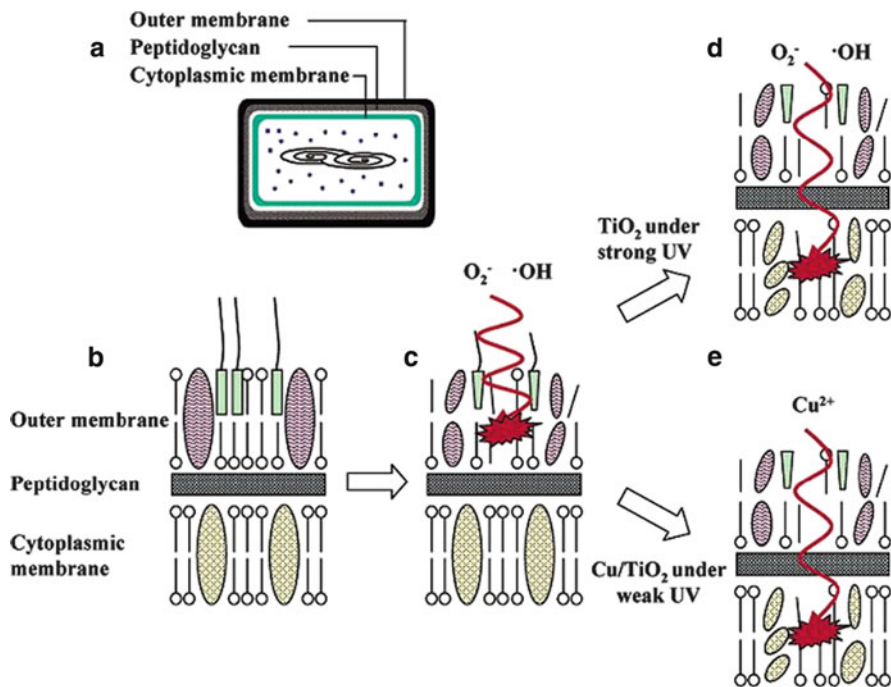


Fig. 15.17 Schematic illustration of the bactericidal process for the copper-resistant *E. coli* cell on the normal TiO₂ film and on the CuO-doped TiO₂ film: (a) illustration of *E. coli* cell, (b–e) enlarged illustration of cell envelope parts [30]

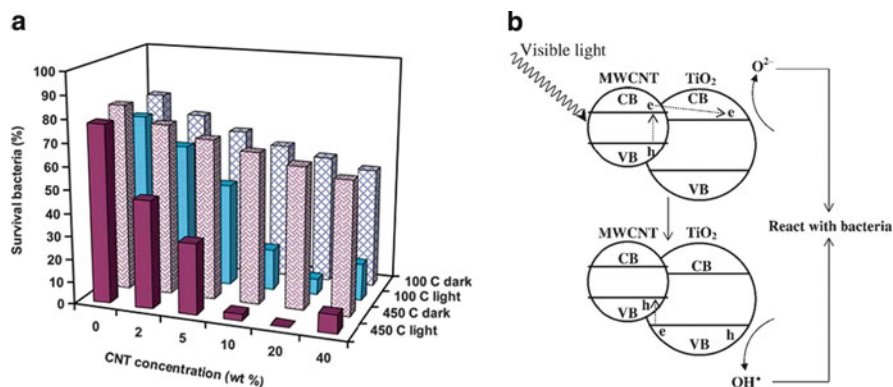


Fig. 15.18 (a) Percentage of survival ratio of *E. coli* bacteria on the surface of the MWNTs-doped TiO₂ film annealed at 100°C and 450°C with various MWNTs contents in the dark and under visible light irradiation for 1 h. (b) Schematic illustration of photocatalytic mechanism of the MWNTs-doped TiO₂ film under visible light irradiation [42]

of reactions as above described. And second, the formation of the heterojunction between TiO_2 and MWNTs resulted in giving rise to a charge space near the junction to equalize Fermi levels, ranging from several tens to hundreds of nanometres. Not only was the band gap energy within the MWNTs- TiO_2 heterojunction smaller than the band gap energy of the TiO_2 located out of the junction but also a driving force originated from interior electric field of the charge space could separate the photo-generated pairs which resulted in reduction of the recombination rate of the pairs. Additionally, the natural bactericidal activity of MWNTs also contributed to this property in the dark.

15.3.2 ZnO-Based Films

Premanathan et al. [103] suggested that ZnO nanoparticles killed HL 60 cells by generation of ROS and induction of apoptosis. The mechanism of antibacterial activity of ZnO nanoparticles was not well understood although the ZnO nanoparticles could effectively inhibit both Gram-positive and Gram-negative bacteria [104–107].

Antibacterial activity of ZnO nanoparticles may be attributed to several mechanisms. First, by induction of oxidative stress which led to interaction with proteins, DNA, and lipids causing death [108–110]. In 1996, Sawai et al. [107] discovered that H_2O_2 was produced in ZnO slurry and the concentration of H_2O_2 was linearly proportional to the ZnO particles, which confirmed by Yamamoto et al. [111]. It is known that ZnO possesses photocatalytic activity under the UV light [112]. However, most of the antibacterial tests were done under the dark conditions, so it was still not clear how the ROS species were produced and how to improve the active oxygen production in the dark. Second, by membrane destruction due to accumulation of ZnO nanoparticles in the bacterial membrane and also their cellular internalization [113]. Zhang et al. [47] showed that the ZnO nanoparticles damages the membrane of the bacterial cells by the aid of TEM studies, and the electrochemical measurements via a model DOPC monolayer further confirmed the direct interaction between ZnO nanoparticles and the bacterial membrane. And third, by the release of Zn ions that may be responsible for antimicrobial activity by contracting with the membrane of microorganisms [114]. However, the toxicity of ZnO nanoparticles was not directly related to their entering into the cell, rather their intimate contact onto the cell causes changes in the microenvironment in the vicinity of the organism–particle contact area to either increase metal solubilization or to generate ROS [115], which may ultimately damage the cell membrane [116].

15.3.3 AgNPs-Based Films

Although AgNP-based films represented excellent antibacterial activity, the antibacterial mechanism was not completely understood. Generally, it was clear

that the antimicrobial property of silver was related to the amount of silver and the rate of silver released. Silver in its metallic state was inert, but it reacted with moisture, and become ionized. The ionized silver was highly reactive. Silver ions interacted with thiol groups of membrane-bound enzymes and proteins, resulting in membrane structure and permeability changes [117–119]. After penetrating through the cell membrane, silver ions could uncouple the respiratory chain from oxidative phosphorylation [120], and bind to DNA and RNA by denaturing and inhibiting bacterial replication [121].

The antibacterial property of AgNPs-based films was attributed to silver ions generation and unique nanostructure of AgNPs. On the one hand, Akhavan et al. [51] demonstrated that silver ions were released over long periods from the film surface, even from TiO₂-capped AuNPs and silver nanorods films (Fig. 15.19) [65]. Agarwal et al. [122] also found that localization of AgNPs on the AgNPs/poly (allylamine hydrochloride)/poly (acrylic acid) film generated the concentrations of silver ions required for antibacterial activity at the surface, without requiring the high loading of silver AgNPs. On the other hand, free AgNPs released from films could directly interact with the microorganism by disrupting/penetrating the cell envelope, and generating reactive oxygen species (ROS) [108, 109] that caused deadly damage. Moreover, free AgNPs preferentially attacked the respiratory chain, cell division finally leading to cell death [123, 124]. So, compared to silver ions, the effective concentration of AgNPs was $\sim 10^3$ -fold lower, being at the nanomolar level [125]. In the AgNPs-based composite film, the improvement of antibacterial activity also partly arose from the action of the other components, such as AgNPs/TiO₂ films [126] and AgNPs/ZnO film [127].

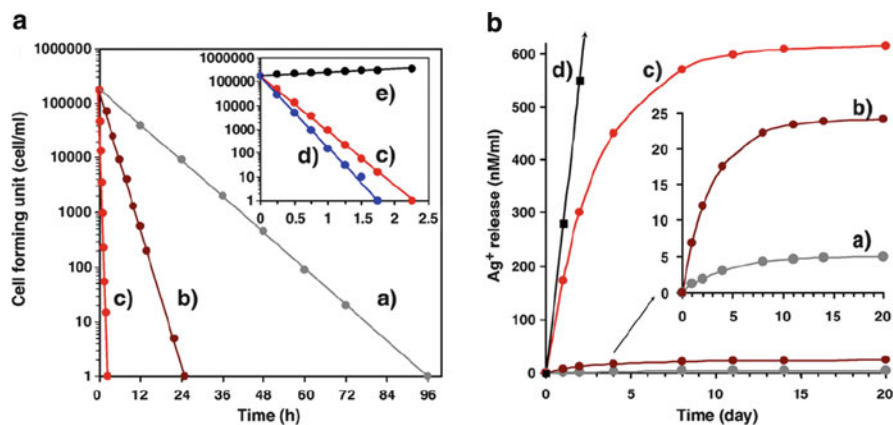


Fig. 15.19 (a) CFU of *E. coli* cultured for various periods in the medium containing different films. (b) The silver ion release curves of the TiO₂-capped AgNPs and silver nanorods films. (a) TiO₂-capped Ag film in the dark. (b) TiO₂-capped AgNPs film in the dark. (c) TiO₂-capped silver nanorods film in the dark. (d) Silver nanorods film in the dark. In the inset of (a): TiO₂-capped silver nanorods film in the dark (c) and under UV irradiation (d); (e) blank sample [65]

15.3.4 CNTs-Based Films

Despite agreement about the potential toxicity of CNTs on mammalian cells, the mechanism of CNTs toxicity is still elusive. Previous studies have proposed three hypothesized mechanisms: oxidative stress [128, 129], metal toxicity [130, 131], and physical piercing causing rupture [68, 132], where the generation of reactive oxygen species (ROS) and oxidative stress are the most developed paradigms for the mechanism of CNTs cytotoxicity. However, how do CNTs exert their antimicrobial activity? Two possible mechanisms have been proposed, i.e. mechanical disruption, where nanotubes act to physically pierce or otherwise perturb the bacterial membrane, and oxidative stress, where the high reductive potential of nanoscale carbon induced the generation of ROS to damage cell membranes and to disturb the metabolic pathway.

Kang et al. [69] and Brady-Estévez et al. [71] studied the scanning electron microscopic (SEM) images of CNTs-treated *E. coli*, and found that the treated *E. coli* cells became flattened, and lost their cellular integrity, suggesting irreversible cell membrane damage and cell death (Fig. 15.20), which confirmed that the antibacterial activity of CNTs was related to the surface characteristics of the bacteria [14]. The toxicity of CNTs against Gram-positive bacteria was smaller than that of CNTs against Gram-negative bacteria, owing to the thicker peptidoglycan in Gram-positive bacterial cell walls [133]. In 2008, Kang et al. [134] further found that the cytoplasmic nucleic acids were presented in the culture medium by DNA and RNA assays, and that genes related to the cell envelope integrity, including fatty acid biosynthesis, Tol/Pal system [135–137], and PhoPQ two-component system [138], were up-regulated in the SWNTs-treated *E. coli*, confirming the cell membrane damage. However, another kind of gene related to oxidative stress (e.g. *soxRS*, *oxyR*) was up-regulated in the DNA micro-array analysis, suggesting that oxidative stress was also responsible for the antibacterial property of CNTs.

Therefore, a three-step interaction process between CNTs and bacteria was proposed. First, by initial CNTs–bacteria contact. The bacteria were deposited

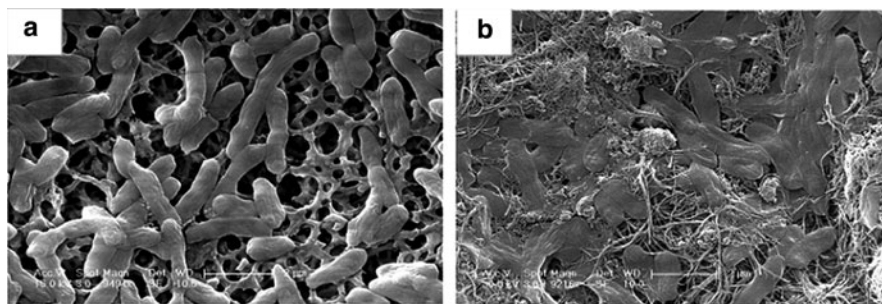


Fig. 15.20 SEM images of *E. coli* incubated for 60 min without (a) and with (b) SWNTs. The cell membrane of treated *E. coli* was damaged, leading to cell death [69]

onto CNTs resulting in direct bacteria–CNTs contact which could be mediated by the exposed CNTs surface area, bacteria concentration, and solution composition. Second, by perturbation of the cell membrane. The mechanism of this step could be clarified according to the toxicity of various classes of hydrocarbons against aquatic microorganisms [139]. The toxicity of hydrocarbons involved two parts: the non-specific and specific toxicity. The nonspecific toxicity was the disruption of the cell membrane, and dependent on the hydrophobicity of hydrocarbon. And the specific toxicity was described as how the hydrocarbons affected membrane proton transport, disrupted specific proteins, or chemically oxidized biomolecules (i.e. proteins, lipids, and DNA), which was attributed to the electrophilicity of hydrocarbon [140, 141]. Furthermore, Kang et al. [73] demonstrated that the perturbation of cell membrane was related to diameter and hydrophobicity of CNTs, the intensity of the open tube ends. And third, by bacterial oxidation. The cell death resulted from the ROS oxidation and regulation of cellular metabolic pathway (Fig. 15.21). The ROS were generated by the cell membrane damage and the interactions between CNTs and biomolecules (e.g., GSH [75]).

Vecitis et al. [80] proposed two primary mechanisms of electrochemical inactivation of *E. coli* and MS2: the direct oxidation of pathogen in contact with the MWNTs anode, and the indirect oxidation of pathogen via anodic production of an aqueous oxidant (e.g., Cl_2^- , HO^\cdot , or SO_4^{2-}). During the process, MWNTs provided positive holes (h^+). The oxidation reaction of pathogen with MWNTs and anodic one-electron oxidant resulted in the cell membrane damage and cell death, further confirmed by the SEM images of different potential-treated *E. coli*.

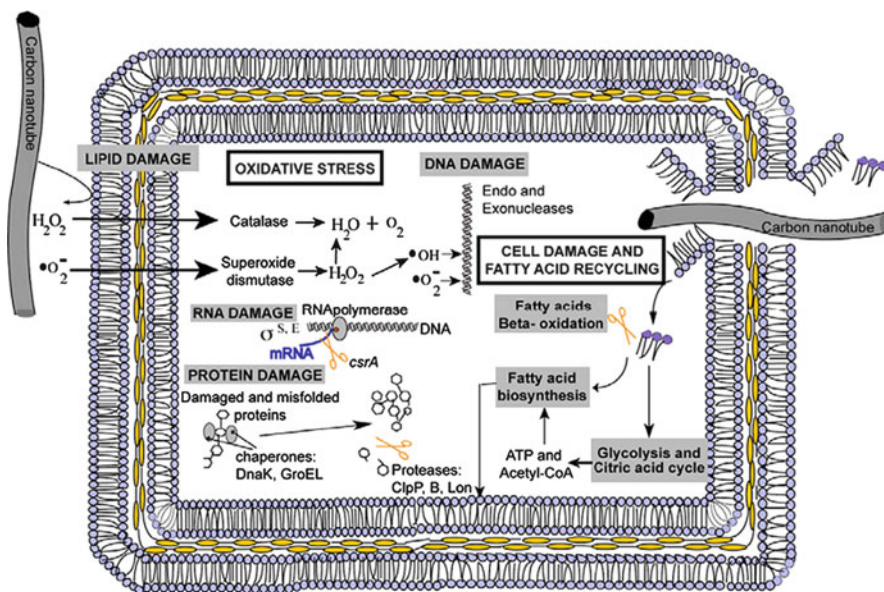


Fig. 15.21 Schematic summary of *E. coli* K12 gene expression stress responses under exposure to SWNTs and MWNTs, suggesting the mechanism of CNTs-induced antibacterial activity [73]

15.3.5 Graphene-Based Films

The antibacterial mechanism of graphene-based paper was attributed to graphene-induced cell membrane damage after interactions between graphene derivatives and bacterial cells. Akhavan et al. [87] reported that concentrations of RNA in the solutions of the bacteria exposed to the both GO nano-walls and rGO nano-walls were meaningfully higher than that of the control sample (Fig. 15.22a, b), suggesting the bacteria membrane damage. And the SEM images of *E. coli* attached on the surfaces of GO and rGO papers showed that treated *E. coli* cells on the paper lost the integrity of membranes (Fig. 15.22c, d) [11], further confirming this hypothesis. Additionally, in the tween/rGO composite paper, the tween-20 could prevent bacteria from adhering on the paper owing to its amphiphilic property [88].

15.4 Toxicity of Nanomaterial-Based Films

With the development of nanotechnology, artificial nanomaterials meeting different requirements were designed and applied. As a result, the biological effects of these artificial nanomaterials on humans and the environment became more and more

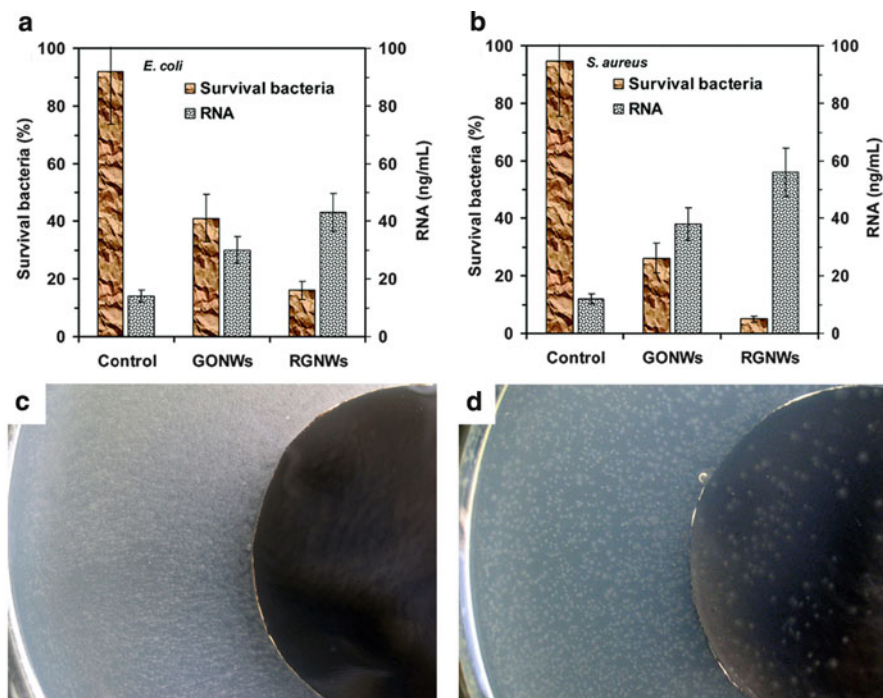


Fig. 15.22 (a, b) Cytotoxicity of GO nanowalls and rGO nanowalls to *E. coli* (a) and *S. aureus* (b), and concentrations of RNA in the PBS of the bacteria exposed to the nanowalls [87]. (c, d) Photographs of *E. coli* growth on GO (c) and rGO (d) paper (overnight incubation at 37°C) [11]

important. Owing to differences in test methods, the biological effect of the same nanomaterial was not always in agreement. However, it was known that high concentration of nanomaterials was toxic to mammalian cells.

Lagopati et al. [26] reported that TiO_2 nanoparticles could kill the mammalian cells via reactive oxygen species generated by photocatalysis, while Kommireddy et al. [142] revealed that TiO_2 thin film could speed the spread of mouse mesenchymal stem cells owing to the rough surface. The published literature shows that ZnO nanoparticles have been applied to drug delivery and cosmetics with non-toxicity [143], while Hanley et al. [144] demonstrated that ZnO nanoparticles could kill cancerous T cells owing to the generation of ROS. Huang et al. [145] also reported the cytotoxicity of ZnO nanoparticles with the size of 20 nm against human bronchial epithelial cells (BEAS-2B) was concentration- and time-dependent, resulting from elevating oxidative stress, disturbing calcium homeostasis and causing membrane damage. However, ZnO nanoparticles were considered and generally recognized as safe (GRAS) material by FDA [146].

Although silver could effectively suppress the growth of microorganisms, it also led to dose-related toxicity in tissue. It has been reported that silver ions accumulated in epithelial cells, macrophages, fibroblasts, and connective tissue [147, 148] and caused tissue toxicity and impaired wound healing [149, 150]. In vitro studies have also demonstrated that the concentrations of silver released from AgNPs-based film could be cytotoxic to mammalian cells involved in wound healing, including fibroblasts [151, 152], keratinocytes [151], and lymphocytes [153]. However, it was found that human osteoblast attached and grew well on the surface containing AgNPs [154, 155]. Agarwal et al. [122] employed molecularly thin polymeric films [poly (allylamine hydrochloride) and poly (acrylic acid)] prepared by layer-by-layer deposition to localize AgNPs on surfaces, and found that the resulting composite film could release silver ions, leading to antibacterial activity without cytotoxicity. Also, Zan et al. [63] considered that the high resistance of AgNPs/poly (vinyl alcohol)/poly (L-lactic acid) film to HeLa cells is not due to the embedded AgNPs, but to its high water content, hydrophilicity, and low interfacial tension between the hydrogel surface and the surrounding fluids.

Generally speaking, carbon-based nanomaterials were regarded as “safe” since the carbon element was inherently compatible with living systems. However, the high concentrations of CNTs and graphene derivatives were cytotoxic to the mammalian cells [132, 133], and the cytotoxicity could be mitigated by chemical modification [156–158]. Agarwal et al. [159] demonstrated that SWNTs thin film inhibits the proliferation, viability, and neurogenesis of PC 12 cells, and the proliferation of osteoblasts. The CNTs films can improve neural signal transfer [160]. The tendency of graphene oxide cytotoxicity was similar to that of CNTs cytotoxicity [161]. Agarwal et al. [159] and Chen et al. [162] showed that graphene-based paper displayed good biocompatibility against neuroendocrine PC 12 cells, osteoblast, and mouse fibroblast cell line L-929. Park et al. [88] also demonstrated that tween/rGO paper showed no cytotoxicity against African green monkey kidney cells, embryonic bovine cells, and Crandell Rees feline kidney cells.

15.5 Applications of Nanomaterial-Based Films

Despite the considerable concerns on public health and food safety, antibacterial materials have become more and more important in everyday use. However, traditional antibacterial materials have raised significant concerns on antibiotic resistance, environmental pollution, relatively complex processing and high cost [163, 164]. Owing to their excellent antibacterial property, nanomaterials-based films can inactivate bacteria attached on the surface, and thus nanomaterial-based films have been extensively applied to self-sterilizing surfaces of materials in public locations, food storage and clinical facilities, such as hospitals, elderly care facilities, wound care dressings, and orthopedic implants, where it was critical to control the surface and airborne bacteria.

Antimicrobial food packaging materials have been used to extend the lag phase and reduce the growth rate of microorganisms in order to extend shelf life and to maintain product quality and safety. Emamifar et al. [95] used AgNPs/LDPE and ZnO/LDPE films to store orange juice at 4 °C for 112 days, and found that the films could significantly suppress the growth of *Lactobacillus plantarum* in the orange juice, suggesting promising applications of nanomaterial-based film in food packaging.

Fujishima et al. [37] developed antibacterial tiles by covering ordinary tiles with TiO₂-Cu composite film, and tested such tiles on the floor and walls of the hospital operating room. The results showed that the bacterial counts decreased to negligible levels in a period of 1 h, and surprisingly, the bacterial counts in the surrounding air also significantly decreased, leading to commercial applications of such tiles in hospitals, hotels, and restaurants, among others [22]. Ohko et al. [121] fabricated TiO₂ film-coated silicone catheters, with repeated bending and resistibility to scratching. Further clinical studies showed TiO₂ film-coated silicone catheters presented better antibacterial activity compared to conventional catheters, suggesting the promising clinical application as an alternative to conventional catheters [165].

15.6 Conclusions

Recently, microorganism safety has attracted increasing attention. Particularly, the Severe Acute Respiratory Syndromes (SARS) virus, H1N1 flu virus and super-bacteria are seriously endangering people's health. The development of new nanomaterial-based antibacterial paper may provide a unique solution. In this chapter, we have summarized the preparation, antibacterial activity, and mechanisms, as well as potential applications, of nanomaterial-based paper. Although there still exist many challenges, such as the high cost, complex synthesis process, and environmental impact, we have witnessed significant advances toward the design and fabrication of novel antibacterial materials that may eventually find real-world applications.

References

1. Ip M, Lui SL, Poon VKM, Lung I, Burd A (2006) Antimicrobial activities of silver dressings: an *in vitro* comparison. *J Med Microbiol* 55:59–63
2. Mai L, Huang C, Wang D, Zhang Z, Wang Y (2009) Effect of C doping on the structural and optical properties of sol-gel TiO₂ thin films. *Appl Surf Sci* 255:9285–9289
3. Cheng TC, Chang CY, Chang CI, Hwang CJ, Hsu HC, Wang DY, Yao KS (2008) Photocatalytic bactericidal effect of TiO₂ film on fish pathogens. *Surf Coat Technol* 203:925–927
4. Mai L, Wang D, Zhang S, Xie Y, Huang C, Zhang Z (2010) Synthesis and bactericidal ability of Ag/TiO₂ composite films deposited on titanium plate. *Appl Surf Sci* 257:974–978
5. Yu BY, Leung KM, Guo QQ, Lau WM, Yang J (2011) Synthesis of Ag-TiO₂ composite nano thin film for antimicrobial application. *Nanotechnology* 22:115603
6. Kingery WD, Bowen HK, Uhlmann DR (1976) *Introduction to Ceramics*. Wiley, New York
7. Kim K, Lee HB, Lee JW, Shin KS (2010) Poly(ethylenimine)-stabilized silver nanoparticles assembled into 2-dimensional arrays at water-toluene interface. *J Colloid Interface Sci* 345:103–108
8. Liao YA, Wang YQ, Feng XX, Wang WC, Xu FJ, Zhang LQ (2010) Antibacterial surfaces through dopamine functionalization and silver nanoparticle immobilization. *Mater Chem Phys* 121:534–540
9. Lee SM, Lee BS, Byun TG, Song KC (2010) Preparation and antibacterial activity of silver-doped organic-inorganic hybrid coatings on glass substrates. *Colloid Surf A-Physicochem Eng Asp* 355:167–171
10. Fu JH, Ji J, Fan DZ, Shen JC (2006) Construction of antibacterial multilayer films containing nanosilver *via* layer-by-layer assembly of heparin and chitosan-silver ions complex. *J Biomed Mater Res Part A* 79A:665–674
11. Hu W, Peng C, Luo W, Lv M, Li X, Li D, Huang Q, Fan C (2010) Graphene-based antibacterial paper. *ACS Nano* 4:4317–4323
12. Hummers WS, Offeman RE (1958) Preparation of graphitic oxide. *J Am Chem Soc* 80:1339
13. Stankovich S, Dikin DA, Piner RD, Kohlhaas KA, Kleinhammes A, Jia Y, Wu Y, Nguyen ST, Ruoff RS (2007) Synthesis of graphene-based nanosheets via chemical reduction of exfoliated graphite oxide. *Carbon* 45:1558–1565
14. Brady-Estévez AS, Schnoor MH, Kang S, Elimelech M (2010) SWNT – MWNT hybrid filter attains high viral removal and bacterial inactivation. *Langmuir* 26:19153–19158
15. Schiffman JD, Elimelech M (2011) Antibacterial activity of electrospun polymer mats with incorporated narrow diameter single-walled carbon nanotubes. *ACS Appl Mater Interfaces* 3:462–468
16. Chen Q, Yue L, Xie FY, Zhou ML, Fu YB, Zhang YF, Weng J (2008) Preferential facet of nanocrystalline silver embedded in polyethylene oxide nanocomposite and its antibiotic behaviors. *J Phys Chem C* 112:10004–10007
17. Gordon R (1997) Chemical vapor deposition of coatings on glass. *J Noncryst Solids* 218:81–91
18. Yates HM, Brook LA, Ditta IB, Evans P, Foster HA, Sheel DW, Steele A (2008) Photo-induced self-cleaning and biocidal behaviour of titania and copper oxide multilayers. *J Photochem Photobiol Chem* 197:197–205
19. Davis MJ, Benito G, Sheel DW, Pemble ME (2004) Growth of thin films of molybdenum and tungsten oxides by combustion CVD using aqueous precursor solutions. *Chem Vapor Depos* 10:29–34
20. Reyes-Coronado D, Rodríguez-Gattorno G, Espinosa-Pesqueira M, Cab C, de Coss R, Oskam G (2008) Phase-pure TiO₂ nanoparticles: anatase, brookite and rutile. *Nanotechnology* 19:145605
21. Fujishima A (1972) Electrochemical photolysis of water at a semiconductor electrode. *Nature* 238:37–38

22. Fujishima A, Zhang X, Tryk DA (2008) TiO₂ photocatalysis and related surface phenomena. *Surf Sci Rep* 63:515–582
23. Matsunaga T, Tomoda R, Nakajima T, Wake H (1985) Photoelectrochemical sterilization of microbial cells by semiconductor powders. *FEMS Microbiol Lett* 29:211–214
24. Ogino C, Shibata N, Sasai R, Takaki K, Miyachi Y, Kuroda S, Ninomiya K, Shimizu N (2010) Construction of protein-modified TiO₂ nanoparticles for use with ultrasound irradiation in a novel cell injuring method. *Bioorg Med Chem Lett* 20:5320–5325
25. Fujishima A, Rao TN, Tryk DA (2000) Titanium dioxide photocatalysis. *J Photochem Photobiol C Photochem Rev* 1:1–21
26. Lagopati N, Kitsiou PV, Kontos AI, Venieratos P, Kotsopoulou E, Kontos AG, Dionysiou DD, Pispas S, Tsilibary EC, Falaras P (2010) Photo-induced treatment of breast epithelial cancer cells using nanostructured titanium dioxide solution. *J Photochem Photobiol Chem* 214:215–223
27. Matsui K, Segawa M, Tanaka T, Kondo A, Ogino C (2009) Antibody-immobilized TiO₂ nanoparticles for cancer therapy. *J Biosci Bioeng* 108:S36–S37
28. McCullagh C, Robertson JMC, Bahnemann DW, Robertson PKJ (2007) The application of TiO₂ photocatalysis for disinfection of water contaminated with pathogenic microorganisms: a review. *Res Chem Intermed* 33:359–375
29. Sunada K, Watanabe T, Hashimoto K (2003) Studies on photokilling of bacteria on TiO₂ thin film. *J Photochem Photobiol Chem* 156:227–233
30. Sunada K, Watanabe T, Hashimoto K (2003) Bactericidal activity of copper-deposited TiO₂ thin film under weak UV light illumination. *Environ Sci Technol* 37:4785–4789
31. Dai K, Peng T, Ke D, Wei B (2009) Photocatalytic hydrogen generation using a nanocomposite of multi-walled carbon nanotubes and TiO₂ nanoparticles under visible light irradiation. *Nanotechnology* 20:125603
32. Akhavan O, Azimirad R, Safa S, Larijani MM (2010) Visible light photo-induced antibacterial activity of CNT-doped TiO₂ thin films with various CNT contents. *J Mater Chem* 20:7386–7392
33. Foster HA, Sheel DW, Sheel P, Evans P, Varghese S, Rutschke N, Yates HM (2010) Antimicrobial activity of titania/silver and titania/copper films prepared by CVD. *J Photochem Photobiol Chem* 216:283–289
34. Kikuchi Y, Sunada K, Iyoda T, Hashimoto K, Fujishima A (1997) Photocatalytic bactericidal effect of TiO₂ thin films: dynamic view of the active oxygen species responsible for the effect. *J Photochem Photobiol Chem* 106:51–56
35. Wei C, Lin WY, Zainal Z, Williams NE, Zhu K, Kruzic AP, Smith RL, Rajeshwar K (1994) Bactericidal activity of TiO₂ photocatalyst in aqueous media: toward a solar-assisted water disinfection system. *Environ Sci Technol* 28:934–938
36. Watts RJ, Kong S, Orr MP, Miller GC, Henry BE (1995) Photocatalytic inactivation of coliform bacteria and viruses in secondary wastewater effluent. *Water Res* 29:95–100
37. Fujishima A, Hashimoto T, Watanabe T (1999) TiO₂ Photocatalysis: Fundamentals and Applications. BKC, Inc., Tokyo
38. Zhang QJ, Sun CH, Zhao Y, Zhou SY, Hu XJ, Chen P (2010) Low Ag-doped titanium dioxide nanosheet films with outstanding antimicrobial property. *Environ Sci Technol* 44:8270–8275
39. Ondok V, Musil J, Meissner M, Čerstvý R, Fajfrík K (2010) Two-functional DC sputtered Cu-containing TiO₂ thin films. *J Photochem Photobiol Chem* 209:158–162
40. Sato T, Taya M (2006) Copper-aided photosterilization of microbial cells on TiO₂ film under irradiation from a white light fluorescent lamp. *Biochem Eng J* 30:199–204
41. Akhavan O, Abdollahad M, Abdi Y, Mohajerzadeh S (2009) Synthesis of titania/carbon nanotube heterojunction arrays for photoinactivation of *E. coli* in visible light irradiation. *Carbon* 47:3280–3287
42. Oh WC, Jung AR, Ko WB (2009) Characterization and relative photonic efficiencies of a new nanocarbon/TiO₂ composite photocatalyst designed for organic dye decomposition and bactericidal activity. *Mater Sci Eng C* 29:1338–1347

43. Brook LA, Evans P, Foster HA, Pemble ME, Steele A, Sheel DW, Yates HM (2007) Highly bioactive silver and silver/titania composite films grown by chemical vapour deposition. *J Photochem Photobiol Chem* 187:53–63
44. Watanabe T, Hashimoto K, Fujishima A, Presented at the 1st International Conference on TiO₂ Photocatalytic Purification and Treatment of Water and Air, Toronto & Ontario, 1992.
45. Wang R, Hashimoto K, Fujishima A, Chikuni M, Kojima E, Kitamura A, Shimohigoshi M, Watanabe T (1998) Photogeneration of highly amphiphilic TiO₂ surfaces. *Adv Mater* 10:135–138
46. Padmavathy N, Vijayaraghavan R (2008) Enhanced bioactivity of ZnO nanoparticles-an antimicrobial study. *Sci Technol Adv Mater* 9:035004
47. Zhang L, Jiang Y, Ding Y, Povey M, York D (2007) Investigation into the antibacterial behaviour of suspensions of ZnO nanoparticles (ZnO nanofluids). *J Nanopart Res* 9:479–489
48. Chandramouleeswaran S, Mhaske ST, Kathe AA, Varadarajan PV, Prasad V, Vigneshwaran N (2007) Functional behaviour of polypropylene/ZnO-soluble starch nanocomposites. *Nanotechnology* 18:385702
49. Shalumon KT, Anulekha KH, Nair SV, Nair SV, Chennazhi KP, Jayakumar R (2011) Sodium alginate/poly(vinyl alcohol)/nano ZnO composite nanofibers for antibacterial wound dressings. *Int J Biol Macromol*. DOI: [10.1016/j.ijbiomac.2011.04.005](https://doi.org/10.1016/j.ijbiomac.2011.04.005)
50. Silver S (2003) Bacterial silver resistance: molecular biology and uses and misuses of silver compounds. *FEMS Microbiol Rev* 27:341–353
51. Akhavan O, Ghaderi E (2009) Bactericidal effects of Ag nanoparticles immobilized on surface of SiO₂ thin film with high concentration. *Curr Appl Phys* 9:1381–1385
52. Baker C, Pradhan A, Pakstis L, Pochan DJ, S.I. S (2005) Synthesis and antibacterial properties of silver nanoparticles. *J Nanosci Nanotechnol* 5:244–249
53. Ohko Y, Tatsuma T, Fujii T, Naoi K, Niwa C, Kubota Y, Fujishima A (2003) Multicolour photochromism of TiO₂ films loaded with silver nanoparticles. *Nat Mater* 2:29–31
54. Akhavan O (2009) Lasting antibacterial activities of Ag-TiO₂/Ag/a-TiO₂ nanocomposite thin film photocatalysts under solar light irradiation. *J Colloid Interface Sci* 336:117–124
55. Rhim JW, Hong SI, Park HM, Ng PKW (2006) Preparation and characterization of chitosan-based nanocomposite films with antimicrobial activity. *J Agric Food Chem* 54:5814–5822
56. Tankhiwale R, Bajpai SK (2010) Silver-nanoparticle-loaded chitosan lactate films with fair antibacterial properties. *J Appl Polym Sci* 115:1894–1900
57. Yoksan R, Chirachanchai S (2010) Silver nanoparticle-loaded chitosan-starch based films: fabrication and evaluation of tensile, barrier and antimicrobial properties. *Mater Sci Eng C* 30:891–897
58. Cui XQ, Li CM, Bao HF, Zheng XT, Lu ZS (2008) *In situ* fabrication of silver nanoarrays in hyaluronan/PDDA layer-by-layer assembled structure. *J Colloid Interface Sci* 327:459–465
59. Fayaz AM, Balaji K, Girilal M, Kalaichelvan PT, Venkatesan R (2009) Mycobased synthesis of silver nanoparticles and their incorporation into sodium alginate films for vegetable and fruit preservation. *J Agric Food Chem* 57:6246–6252
60. Dong G, Xiao X, Liu X, Qian B, Liao Y, Wang C, Chen D, Qiu J (2009) Functional Ag porous films prepared by electrospinning. *Appl Surf Sci* 255:7623–7626
61. Jiang SX, Qin WF, Guo RH, Zhang L (2010) Surface functionalization of nanostructured silver-coated polyester fabric by magnetron sputtering. *Surf Coat Technol* 204:3662–3667
62. Vasilev K, Sah VR, Goreham RV, Ndi C, Short RD, Griesser HJ (2010) Antibacterial surfaces by adsorptive binding of polyvinyl-sulphonate-stabilized silver nanoparticles. *Nanotechnology* 21:215102
63. Zan X, Kozlov M, McCarthy TJ, Su Z (2010) Covalently attached, silver-doped poly(vinyl alcohol) hydrogel films on poly(L-lactic acid). *Biomacromolecules* 11:1082–1088
64. Yliniemi K, Vahvaselka M, Van Ingelgem Y, Baert K, Wilson BP, Terryn H, Kontturi K (2008) The formation and characterisation of ultra-thin films containing Ag nanoparticles. *J Mater Chem* 18:199–206
65. Akhavan O, Ghaderi E (2009) Capping antibacterial Ag nanorods aligned on Ti interlayer by mesoporous TiO₂ layer. *Surf Coat Technol* 203:3123–3128

66. Vimala K, Mohan YM, Sivudu KS, Varaprasad K, Ravindra S, Reddy NN, Padma Y, Sreedhar B, MohanaRaju K (2010) Fabrication of porous chitosan films impregnated with silver nanoparticles: a facile approach for superior antibacterial application. *Colloid Surf B-Biointerfaces* 76:248–258
67. Lu F, Gu L, Mezziani MJ, Xin W, Luo PG, Veca LM, Cao L, Sun Y-P (2009) Advances in bioapplications of carbon nanotubes. *Adv Mater* 21:139–152
68. Narayan RJ, Berry CJ, Brigmon RL (2005) Structural and biological properties of carbon nanotube composite films. *Mater Sci Eng B* 123:123–129
69. Kang S, Pinault M, Pfefferle LD, Elimelech M (2007) Single-walled carbon nanotubes exhibit strong antimicrobial activity. *Langmuir* 23:8670–8673
70. Rodrigues DF, Elimelech M (2010) Toxic effects of single-walled carbon nanotubes in the development of *E. coli* biofilm. *Environ Sci Technol* 44:4583–4589
71. Brady-Estévez AS, Kang S, Elimelech M (2008) A single-walled-carbon-nanotube filter for removal of viral and bacterial pathogens. *Small* 4:481–484
72. Kang S, Mauter MS, Elimelech M (2009) Microbial cytotoxicity of carbon-based nanomaterials: implications for river water and wastewater effluent. *Environ Sci Technol* 43:2648–2653
73. Kang S, Mauter MS, Elimelech M (2008) Physicochemical determinants of multiwalled carbon nanotube bacterial cytotoxicity. *Environ Sci Technol* 42:7528–7534
74. Yang C, Mamouni J, Tang Y, Yang L (2010) Antimicrobial activity of single-walled carbon nanotubes: Length effect. *Langmuir* 26:16013–16019
75. Vecitis CD, Zodrow KR, Kang S, Elimelech M (2010) Electronic-structure-dependent bacterial cytotoxicity of single-walled carbon nanotubes. *ACS Nano* 4:5471–5479
76. Simmons TJ, Lee SH, Park TJ, Hashim DP, Ajayan PM, Linhardt RJ (2009) Antiseptic single wall carbon nanotube bandages. *Carbon* 47:1561–1564
77. Aslan S, Loebick CZ, Kang S, Elimelech M, Pfefferle LD, Van Tassel PR (2010) Antimicrobial biomaterials based on carbon nanotubes dispersed in poly(lactic-co-glycolic acid). *Nanoscale* 2:1789–1794
78. Pangule RC, Brooks SJ, Dinu CZ, Bale SS, Salmon SL, Zhu GY, Metzger DW, Kane RS, Dordick JS (2010) Antistaphylococcal nanocomposite films based on enzyme-nanotube conjugates. *ACS Nano* 4:3993–4000
79. Zhou J, Qi X (2011) Multi-walled carbon nanotubes/epsilon-polylysine nanocomposite with enhanced antibacterial activity. *Lett Appl Microbiol* 52:76–83
80. Vecitis CD, Schnoor MH, Rahaman MS, Schiffman JD, Elimelech M (2011) Electrochemical multiwalled carbon nanotube filter for viral and bacterial removal and inactivation. *Environ Sci Technol* 45:3672–3679
81. Novoselov KS, Geim AK, Morozov SV, Jiang D, Zhang Y, Dubonos SV, Grigorieva IV, Firsov AA (2004) Electric field effect in atomically thin carbon films. *Science* 306:666–669
82. Stankovich S, Dikin DA, Dommett GHB, Kohlhaas KM, Zimney EJ, Stach EA, Piner RD, Nguyen ST, Ruoff RS (2006) Graphene-based composite materials. *Nature* 442:282–286
83. Geim AK (2009) Graphene: status and prospects. *Science* 324:1530–1534
84. Lin YM, Dimitrakopoulos C, Jenkins KA, Farmer DB, Chiu HY, Grill A, Avouris P (2010) 100-GHz transistors from wafer-scale epitaxial graphene. *Science* 327:662
85. Schedin F, Geim AK, Morozov SV, Hill EW, Blake P, Katsnelson MI, Novoselov KS (2007) Detection of individual gas molecules adsorbed on graphene. *Nat Mater* 6:652–655
86. Wang X, Zhi L, Tsao N, Tomović Ž, Li J, Müllen K (2008) Transparent carbon films as electrodes in organic solar cells. *Angew Chem Int Ed* 47:2990–2992
87. Akhavan O, Ghaderi E (2010) Toxicity of graphene and graphene oxide nanowalls against bacteria. *ACS Nano* 4:5731–5736
88. Park S, Mohanty N, Suk JW, Nagaraja A, An J, Piner RD, Cai W, Dreyer DR, Berry V, Ruoff RS (2010) Biocompatible, robust free-standing paper composed of a tween/graphene composite. *Adv Mater* 22:1736–1740
89. Hoffmann MR, Martin ST, Choi W, Bahnemann DW (1995) Environmental applications of semiconductor photocatalysis. *Chem Rev* 95:69–96

90. Ishibashi K, Fujishima A, Watanabe T, Hashimoto K (2000) Generation and deactivation processes of superoxide formed on TiO₂ film illuminated by very weak UV light in air or water. *J Phys Chem B* 104:4934–4938
91. Kühn KP, Chaberny IF, Massholder K, Stickler M, Benz VW, Sonntag H-G, Erdinger L (2003) Disinfection of surfaces by photocatalytic oxidation with titanium dioxide and UVA light. *Chemosphere* 53:71–77
92. Fujihira M, Satoh Y, Osa T (1982) Heterogeneous photocatalytic reactions on semiconductor materials. III. effect of pH and Cu²⁺ ions on the photo-fenton type reaction. *Bull Chem Soc Jpn* 55:666–671
93. Ward MD, Bard AJ (1982) Photocurrent enhancement via trapping of photogenerated electrons of titanium dioxide particles. *J Phys Chem* 86:3599–3605
94. Okamoto K, Yamamoto Y, Tanaka H, Tanaka M, Itaya A (1985) Heterogeneous photocatalytic decomposition of phenol over TiO₂ powder. *Bull Chem Soc Jpn* 58:2015–2022
95. Wei TY, Wang YY, Wan CC (1990) Photocatalytic oxidation of phenol in the presence of hydrogen peroxide and titanium dioxide powders. *J Photochem Photobiol Chem* 55:115–126
96. Zang L, Liu CY, Ren XM (1995) Photochemistry of semiconductor particles. Part 4.-Effects of surface condition on the photodegradation of 2,4-dichlorophenol catalysed by TiO₂ suspensions. *J Chem Soc Faraday Trans* 91:917–923
97. Zhu H, Zhang M, Xia Z, Gary LKC (1995) Titanium dioxide mediated photocatalytic degradation of monocrotophos. *Water Res* 29:2681–2688
98. Brezová V, Blažková Ab, Borošová E, Čeppan M, Fiala R (1995) The influence of dissolved metal ions on the photocatalytic degradation of phenol in aqueous TiO₂ suspensions. *J Mol Catal Chem* 98:109–116
99. Litter MI (1999) Heterogeneous photocatalysis: Transition metal ions in photocatalytic systems. *Appl Catal B Environ* 23:89–114
100. Ciešla P, Kocot P, Mytych P, Stasicka Z (2004) Homogeneous photocatalysis by transition metal complexes in the environment. *J Mol Catal Chem* 224:17–33
101. An G, Ma W, Sun Z, Liu Z, Han B, Miao S, Miao Z, Ding K (2007) Preparation of titania/carbon nanotube composites using supercritical ethanol and their photocatalytic activity for phenol degradation under visible light irradiation. *Carbon* 45:1795–1801
102. Wang W, Serp P, Kalck P, Faria JL (2005) Visible light photodegradation of phenol on MWNT-TiO₂ composite catalysts prepared by a modified sol-gel method. *J Mol Catal Chem* 235:194–199
103. Premanathan M, Karthikeyan K, Jeyasubramanian K, Manivannan G (2011) Selective toxicity of ZnO nanoparticles toward Gram-positive bacteria and cancer cells by apoptosis through lipid peroxidation. *Nanomed Nanotechnol Biol Med* 7:184–192
104. Sawai J, Igarashi H, Hashimoto A, Kokugan T, Shimizu M (1995) Evaluation of growth inhibitory effect of ceramics powder slurry on bacteria by conductance method. *J Chem Eng Japan* 28:288–293
105. Sawai J, Saito I, Kanou F, Igarashi H, Hashimoto A, Kokugan T, Shimizu M (1995) Mutagenicity test of ceramic powder which have growth inhibitory effect on bacteria. *J Chem Eng Japan* 28:352–354
106. Sawai J, Igarashi H, Hashimoto A, Kokugan T, Shimizu M (1996) Effect of particle size and heating temperature of ceramic powders on antibacterial activity of their slurries. *J Chem Eng Japan* 29:251–256
107. Sawai J, Kawada E, Kanou F, Igarashi H, Hashimoto A, Kokugan T, Shimizu M (1996) Detection of active oxygen generated from ceramic powders having antibacterial activity. *J Chem Eng Japan* 29:627–633
108. Sawai J, Shoji S, Igarashi H, Hashimoto A, Kokugan T, Shimizu M, Kojima H (1998) Hydrogen peroxide as an antibacterial factor in zinc oxide powder slurry. *J Ferment Bioeng* 86:521–522
109. Sawai J (2003) Quantitative evaluation of antibacterial activities of metallic oxide powders (ZnO, MgO and CaO) by conductimetric assay. *J Microbiol Meth* 54:177–182

110. Adams LK, Lyon DY, Alvarez PJJ (2006) Comparative eco-toxicity of nanoscale TiO₂, SiO₂, and ZnO water suspensions. *Water Res* 40:3527–3532
111. Yamamoto O, Sawai J, Sasamoto T (2000) Effect of lattice constant of zinc oxide on antibacterial characteristics. *Int J Inorg Mater* 2:451–454
112. Karunakaran C, Rajeswari V, Gomathisankar P (2011) Optical, electrical, photocatalytic, and bactericidal properties of microwave synthesized nanocrystalline Ag-ZnO and ZnO. *Solid State Sci* 13:923–928
113. Brayner R, Ferrari-Iliou R, Brivois N, Djediat S, Benedetti MF, Fiévet F (2006) Toxicological impact studies based on *Escherichia coli* bacteria in ultrafine ZnO nanoparticles colloidal medium. *Nano Lett* 6:866–870
114. Gajjar P, Pettee B, Britt DW, Huang W, Johnson WP, Anderson AJ (2009) Antimicrobial activities of commercial nanoparticles against an environmental soil microbe *Pseudomonas putida* KT2440. *J Biol Eng* 3:1183–1189
115. Huang Z, Zheng X, Yan D, Yin G, Liao X, Kang Y, Yao Y, Huang D, Hao B (2008) Toxicological effect of ZnO nanoparticles based on bacteria. *Langmuir* 24:4140–4144
116. Heinlaan M, Ivask A, Blinova I, Dubourguier H-C, Kahru A (2008) Toxicity of nanosized and bulk ZnO, CuO and TiO₂ to bacteria *Vibrio fischeri* and crustaceans *Daphnia magna* and *Thamnocephalus platyurus*. *Chemosphere* 71:1308–1316
117. Liau SY, Read DC, Pugh WJ, Furr JR, Russell AD (1997) Interaction of silver nitrate with readily identifiable groups: relationship to the antibacterial action of silver ions. *Lett Appl Microbiol* 25:279–283
118. Zeiri L, Bronk BV, Shabtai Y, Eichler J, Efrima S (2004) Surface-Enhanced Raman Spectroscopy as a Tool for Probing Specific Biochemical Components in Bacteria. *Appl Spectrosc* 58:33–40
119. Ghandour W, Hubbard JA, Deistung J, Hughes MN, Poole RK (1988) The uptake of silver ions by *Escherichia coli* K12: toxic effects and interaction with copper ions. *Appl Microbiol Biotechnol* 28:559–565
120. Schreurs WJ, Rosenberg H (1982) Effect of silver ions on transport and retention of phosphate by *Escherichia coli*. *J Bacteriol* 152:7–13
121. Ohko Y, Utsumi Y, Niwa C, Tatsuma T, Kobayakawa K, Satoh Y, Kubota Y, Fujishima A (2001) Self-sterilizing and self-cleaning of silicone catheters coated with TiO₂ photocatalyst thin films: a preclinical work. *J Biomed Mater Res* 58:97–101
122. Agarwal A, Weis TL, Schurr MJ, Faith NG, Czuprynski CJ, McAnulty JF, Murphy CJ, Abbott NL (2010) Surfaces modified with nanometer-thick silver-impregnated polymeric films that kill bacteria but support growth of mammalian cells. *Biomaterials* 31:680–690
123. Feng QL, Wu J, Chen GQ, Cui FZ, Kim TN, Kim JO (2000) A mechanistic study of the antibacterial effect of silver ions on *Escherichia coli* and *Staphylococcus aureus*. *J Biomed Mater Res* 52:662–668
124. Sondi I, Salopek-Sondi B (2004) Silver nanoparticles as antimicrobial agent: a case study on *E. coli* as a model for Gram-negative bacteria. *J Colloid Interface Sci* 275:177–182
125. Dibrov P, Dzioba J, Gosink KK, Ha(·)se CC (2002) Chemiosmotic mechanism of antimicrobial activity of Ag⁺ in *Vibrio cholerae*. *Antimicrob Agents Chemother* 46:2668–2670
126. Kubacka A, Cerrada ML, Serrano C, Fernandez-Garcia M, Ferrer M (2009) Plasmonic nanoparticle/polymer nanocomposites with enhanced photocatalytic antimicrobial properties. *J Phys Chem C* 113:9182–9190
127. Emamifar A, Kadivar M, Shahedi M, Soleimani-Zad S (2011) Effect of nanocomposite packaging containing Ag and ZnO on inactivation of *Lactobacillus plantarum* in orange juice. *Food Control* 22:408–413
128. Manna SK, Sarkar S, Barr J, Wise K, Barrera EV, Jejelowo O, Rice-Ficht AC, Ramesh GT (2005) Single-walled carbon nanotube induces oxidative stress and activates nuclear transcription factor-κB in human keratinocytes. *Nano Lett* 5:1676–1684
129. Ding L, Stilwell J, Zhang T, Elboudwarej O, Jiang H, Selegue JP, Cooke PA, Gray JW, Chen FF (2005) Molecular characterization of the cytotoxic mechanism of multiwall carbon nanotubes and nano-onions on human skin fibroblast. *Nano Lett* 5:2448–2464

130. Shvedova AA, Kisin ER, Mercer R, Murray AR, Johnson VJ, Potapovich AI, Tyurina YY, Gorelik O, Arepalli S, Schwegler-Berry D, Hubbs AF, Antonini J, Evans DE, Ku B-K, Ramsey D, Maynard A, Kagan VE, Castranova V, Baron P (2005) Unusual inflammatory and fibrogenic pulmonary responses to single-walled carbon nanotubes in mice. *Am J Physiol Lung Cell Mol Physiol* 289:L698-708
131. Geslin C, Llanos J, Prieur D, Jeanthon C (2001) The manganese and iron superoxide dismutases protect *Escherichia coli* from heavy metal toxicity. *Res Microbiol* 152:901-905
132. Tang YJ, Ashcroft JM, Chen D, Min G, Kim C-H, Murkhejee B, Larabell C, Keasling JD, Chen FF (2007) Charge-associated effects of fullerene derivatives on microbial structural integrity and central metabolism. *Nano Lett* 7:754-760
133. Vollmer W, Blanot D, De Pedro MA (2008) Peptidoglycan structure and architecture. *FEMS Microbiol Rev* 32:149-167
134. Kang S, Herzberg M, Rodrigues DF, Elimelech M (2008) Antibacterial effects of carbon nanotubes: Size does matter! *Langmuir* 24:6409-6413
135. Davies JK, Reeves P (1975) Genetics of resistance to colicins in *Escherichia coli* K-12: cross-resistance among colicins of group A. *J Bacteriol* 123:102-117
136. Fognini-Lefebvre N, Lazzaroni JC, Portalier R (1987) *tolA*, *tolB*, and *excC*, three cistrons involved in the control of pleiotropic release of periplasmic proteins by *Escherichia coli* K12. *Mol Gen Genet MGG* 209:391-395
137. Bernadac A, Gavioli M, Lazzaroni J-C, Raina S, Lloubes R (1998) *Escherichia coli* tol-pal mutants form outer membrane vesicles. *J Bacteriol* 180:4872-4878
138. Murata T, Tseng W, Guina T, Miller SI, Nikaido H (2007) PhoPQ-mediated regulation produces a more robust permeability barrier in the outer membrane of *salmonella enterica* serovar typhimurium. *J Bacteriol* 189:7213-7222
139. Rand GM (1995) Fundamentals of Aquatic Toxicology. In: Rand GM (ed) Structure-Activity Relationships, Tayer and Francis Publisher, Washington
140. Verhaar HJM, van Leeuwen CJ, Hermens JLM (1992) Classifying environmental-pollutants 1. Structure-activity-relationships for prediction of aquatic toxicit. *Chemosphere* 25:471-491
141. Escher BI, Bramaz N, Eggen RIL, Richter M (2005) *In Vitro* assessment of modes of toxic action of pharmaceuticals in aquatic life. *Environ Sci Technol* 39:3090-3100
142. Kommireddy DS, Sriram SM, Lvov YM, Mills DK (2006) Stem cell attachment to layer-by-layer assembled TiO₂ nanoparticle thin films. *Biomaterials* 27:4296-4303
143. Guo D, Wu C, Jiang H, Li Q, Wang X, Chen B (2008) Synergistic cytotoxic effect of different sized ZnO nanoparticles and daunorubicin against leukemia cancer cells under UV irradiation. *J Photochem Photobiol B Biol* 93:119-126
144. Hanley C, Layne J, Punnoose A, Reddy K, Coombs I, Coombs A, Feris K, Wingett D (2008) Preferential killing of cancer cells and activated human T cells using ZnO nanoparticles. *Nanotechnology* 19:295103
145. Huang C, Aronstam RS, Chen D-R, Huang Y (2010) Oxidative stress, calcium homeostasis, and altered gene expression in human lung epithelial cells exposed to ZnO nanoparticles. *Toxicol Vitro* 24:45-55
146. Jin T, Sun D, Su JY, Zhang H, Sue HJ (2009) Antimicrobial efficacy of zinc oxide quantum dots against *Listeria monocytogenes*, *Salmonella Enteritidis*, and *Escherichia coli* O157:H7. *J Food Sci* 74:M46-M52
147. Klasen HJ (2000) Historical review of the use of silver in the treatment of burns. I. Early uses. *Burns* 26:117-130
148. Kristiansen S, Ifversen P, Danscher G (2008) Ultrastructural localization and chemical binding of silver ions in human organotypic skin cultures. *Histochem Cell Biol* 130:177-184
149. Atiyeh BS, Costagliola M, Hayek SN, Dibo SA (2007) Effect of silver on burn wound infection control and healing: review of the literature. *Burns* 33:139-148
150. Trop M, Novak M, Rodl S, Hellbom B, Kroell W, Goessler W (2006) Silver-coated dressing acticoat caused raised liver enzymes and argyria-like symptoms in burn patient. *J Trauma* 60:648-652

151. Poon VKM, Burd A (2004) *In vitro* cytotoxicity of silver: implication for clinical wound care. *Burns* 30:140–147
152. Lee ARC, Moon HK (2003) Effect of topically applied silver sulfadiazine on fibroblast cell proliferation and biomechanical properties of the wound. *Arch Pharm Res* 26:855–860
153. Hussain S, Anner RM, Anner BM (1992) Cysteine protects Na, K-ATPase and isolated human lymphocytes from silver toxicity. *Biochem Biophys Res Commun* 189:1444–1449
154. Alt V, Bechert T, Steinrücke P, Wagener M, Seidel P, Dingeldein E, Domann E, Schnettler R (2004) An *in vitro* assessment of the antibacterial properties and cytotoxicity of nanoparticulate silver bone cement. *Biomaterials* 25:4383–4391
155. Podsiadlo P, Paternel S, Rouillard JM, Zhang Z, Lee J, Lee J-W, Gulari E, Kotov NA (2005) Layer-by-layer assembly of nacre-like nanostructured composites with antimicrobial properties. *Langmuir* 21:11915–11921
156. Sayes CM, Liang F, Hudson JL, Mendez J, Guo W, Beach JM, Moore VC, Doyle CD, West JL, Billups WE, Ausman KD, Colvin VL (2006) Functionalization density dependence of single-walled carbon nanotubes cytotoxicity *in vitro*. *Toxicol Lett* 161:135–142
157. Dumortier H, Lacotte S, Pastorin G, Marega R, Wu W, Bonifazi D, Briand J-P, Prato M, Muller S, Bianco A (2006) Functionalized carbon nanotubes are non-cytotoxic and preserve the functionality of primary immune cells. *Nano Lett* 6:1522–1528
158. Zhu Y, Li W, Li Q, Li Y, Li Y, Zhang X, Huang Q (2009) Effects of serum proteins on intracellular uptake and cytotoxicity of carbon nanoparticles. *Carbon* 47:1351–1358
159. Agarwal S, Zhou X, Ye F, He Q, Chen GCK, Soo J, Boey F, Zhang H, Chen P (2010) Interfacing live cells with nanocarbon substrates. *Langmuir* 26:2244–2247
160. Lovat V, Pantarotto D, Lagostena L, Cacciari B, Grandolfo M, Righi M, Spalluto G, Prato M, Ballerini L (2005) Carbon nanotube substrates boost neuronal electrical signaling. *Nano Lett* 5:1107–1110
161. Chang Y, Yang ST, Liu JH, Dong E, Wang Y, Cao A, Liu Y, Wang H (2011) *In vitro* toxicity evaluation of graphene oxide on A549 cells. *Toxicol Lett* 200:201–210
162. Chen H, Müller MB, Gilmore KJ, Wallace GG, Li D (2008) Mechanically strong, electrically conductive, and biocompatible graphene paper. *Adv Mater* 20:3557–3561
163. Stewart PS, Costerton WJ (2001) Antibiotic resistance of bacteria in biofilms. *Lancet* 358:135–138
164. Adolfsson-Erici M, Pettersson M, Parkkonen J, Sturve J (2002) Triclosan, a commonly used bactericide found in human milk and in the aquatic environment in Sweden. *Chemosphere* 46:1485–1489
165. Sekiguchi Y, Yao Y, Ohko Y, Tanaka K, Ishido T, Fujishima A, Kubota Y (2007) Self-sterilizing catheters with titanium dioxide photocatalyst thin films for clean intermittent catheterization: basis and study of clinical use. *Int J Urol* 14:426–430

Chapter 16

Antimicrobial Nanomaterials for Water Disinfection

Chong Liu, Xing Xie, and Yi Cui

16.1 Introduction

To date, outbreaks of water-borne diseases, caused by pathogens, still occur at unexpectedly high levels, and they remain the leading cause of death in many developing countries. Worldwide, over one billion people lack reliable access to clean water, and water contamination causes two million deaths annually [1–3]. In addition, many people in the world live in water-stressed areas, and this number has kept on increasing over the last few years, which makes natural water disinfection and wastewater recycling and purification technologies urgently needed. Water disinfection and purification, the last procedure is to remove contaminated pathogens from drinking water, is critical for ensuring public health, and its importance can never be overemphasized.

Commonly, water treatment methods are based on two strategies, removing contaminated pathogens or inactivating them. Traditionally used water treatment methods include: size exclusion, chlorine disinfection, ozone disinfection, and UV disinfection. The use of size-exclusion membranes to remove bacteria is very effective and is not limited to certain kinds of pathogens. Even when the sizes of the microorganisms are very small, like some viruses, membrane filtration can also be quite effective by decreasing the pore sizes. However, the low treatment speed and high energy consumptions by using high pressures, limit its application. Chlorine disinfection is the most popular method for water treatment. However, research has revealed that, while increasing the efficiency of disinfection, the amount of harmful disinfection by-products (BDPs) is also increasing. Chemical

C. Liu • Y. Cui (✉)

Material Science and Engineering, Stanford University, Stanford, CA, USA

e-mail: yicui@stanford.edu

X. Xie

Civil and Environmental Engineering, Stanford University, Stanford, CA, USA

disinfectants such as free chlorine, chloramines and ozone can react with various content in natural water to form carcinogenic DBPs [4]. In addition, chlorine disinfection can cause unpleasant tastes and odors. UV disinfection has drawn more attention in recent decades because of its high efficiency and ease of use. However, the disinfection set-up is very expensive and the UV lamp needs to be changed frequently. Hence, there is an urgent need for innovative, low cost and high efficiency water treatment methods.

Recently, nanotechnology has opened an alternative way for water disinfection. Nanomaterials' high surface-to-volume ratios, crystallographic structure, and adaptability to various substrates increase their contact efficiency with contaminated pathogens and hence result in more effective inactivation [5]. Several natural and engineered nanomaterials have been demonstrated to have strong antimicrobial properties through diverse mechanisms. In this chapter, we will discuss some of the most popular nanomaterials used for disinfection. And based on recent work in this area, we will further discuss the disinfection mechanisms of these nanomaterials.

16.2 Antimicrobial Nanomaterials

Nanomaterials are usually defined as any materials smaller than one-tenth of a micrometer in at least one dimension. To date, several antimicrobial nanomaterials have been applied to water disinfection. They can be classified into three main categories: (1) oligodynamic metals, including silver (Ag), copper (Cu), zinc (Zn), titanium (Ti), and cobalt (Co) [6]; (2) photocatalytic semiconductors, including TiO_2 , ZnO, and WO_3 [7, 8]; and (3) carbon nanomaterials, including carbon nanotubes and fullerenes [9–11]. These nanomaterials can potentially be used as alternative disinfectants or coupled with current technologies to enhance the inactivation efficacy. In the following part of this section, we will briefly introduce the mechanisms of these nanomaterials used for water disinfection, and then mainly discuss how these nanomaterials are currently applied for water disinfection and what the advantages and disadvantages are of using these antimicrobial nanoparticles.

16.2.1 *nAg*

Silver is the most widely used oligodynamic metal for water disinfection, due to its wide range of antimicrobial effect, low toxicity to humans, and ease of operation [6]. The antimicrobial properties of silver have been known for centuries. Many examples of using silver to kill pathogens or prevent microbial growth can be found in history all over the world. To prevent water-borne diseases, people have used silver vessels to store water or have put silver coins in their barrels [12].

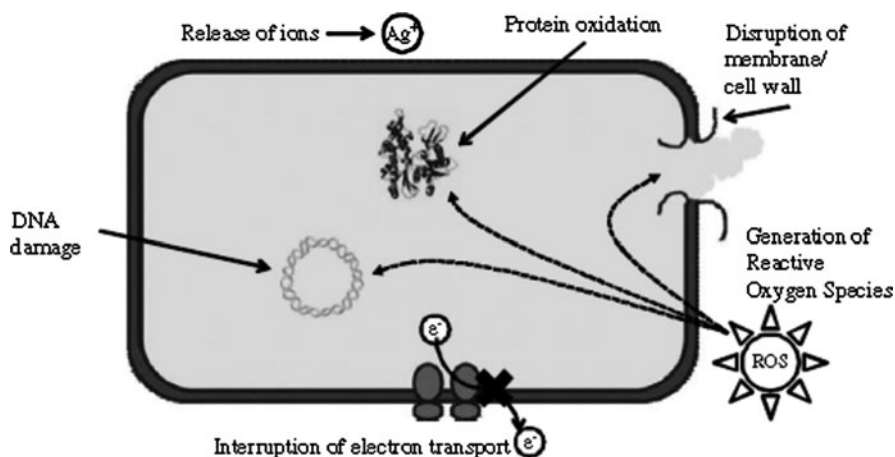


Fig. 16.1 A schematic of the possible mechanisms of antimicrobial activity of silver [4]

The antimicrobial effect of silver ions has been published many times in the literature and may include the following mechanisms: (1) interact with thiol groups and inactivate critical enzymes; (2) interact with DNA and prevent DNA replication; (3) catalyze the generation of reactive oxygen species (ROS); (4) change the permeability of the cell membrane; and (5) interrupt the electron transport [4, 6, 13–16]. Silver nanomaterials can disrupt the cell wall and penetrate through the cell membranes themselves, or they can kill the pathogens by releasing silver ions [4]. A schematic summarizing the possible mechanisms is shown in Fig. 16.1 [4]. Smaller silver particles, less than 10 nm, are more toxic, because smaller particles are able to more easily penetrate the cell membranes [16–18]. Furthermore, triangular silver nanoplates containing more {111} surface were found to be more toxic than nanorods, nanospheres, or silver ions [16, 17].

Silver disinfection is very promising for point-of-use (POU) application. One example, which has actually been commercialized and is widely used in many developing countries, is the silver nanoparticle-embedded ceramic filter, as shown in Fig. 16.2 [19–24]. Silver disinfectant products can also be found online when you are preparing an emergency package, such as the one called ASAP Silver Solution shown in Fig. 16.3. Large-scale applications are still under study. The most common idea is immobilizing silver nanomaterials on some porous substrate, such as various membranes and even paper [25–30]. Figure 16.4 shows a section of fiberglass impregnated with silver nanoparticles used for water filters [25].

Several issues need to be considered for water disinfection using silver nanomaterials. First, the antimicrobial effect of silver nanomaterials is caused by both direct contact and irreversibly releasing silver ions. Small particle size with big surface–volume ratio will enhance the inactivation efficacy, but it will also increase the rate of loss of silver. Therefore, it is very challenging to control the releasing rate of silver ions to have both a long life time and a sufficient killing effect. Secondly, a high concentration of silver in the treated water is also harmful to

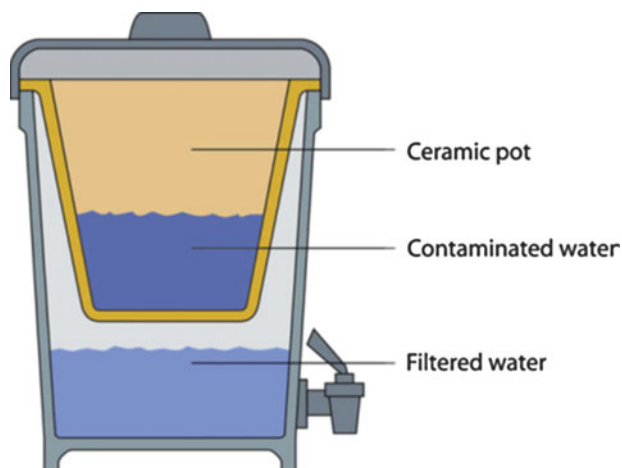
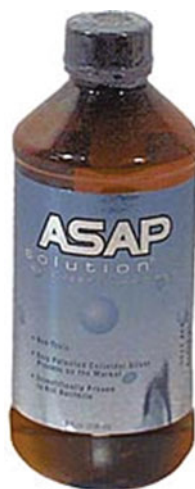


Fig. 16.2 A schematic of the silver nanoparticle-embedded ceramic pot [21]

Fig. 16.3 A bottle of ASAP silver solution (beprepared.com)



human health [31]. The U.S. Environmental Protection Agency (EPA) mean contamination level (MCL) for silver in drinking water is 0.1 mg/L [32]. Lastly, it has been reported that some microbes have been shown to be resistant to silver [33].

16.2.2 TiO_2

TiO_2 is the most commonly used photocatalyst. It is the most studied nanomaterial for water disinfection, although it has only been used for killing microbes for about 30 years [34]. The mechanisms of the antimicrobial effect of TiO_2 are mainly

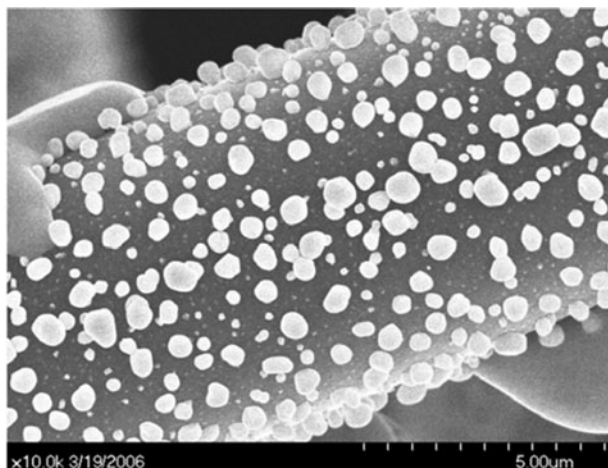


Fig. 16.4 SEM image of a silver nanoparticle impregnated fiberglass [25]

related to the generation of ROS, especially hydroxyl free radicals and peroxide, under UV-A irradiation ($300 \text{ nm} < \lambda < 390 \text{ nm}$) [7, 35]. Antimicrobial effect was also reported in the dark condition, indicating other non-photo-related mechanisms [36]. It has been reported that anatase phase TiO_2 showed higher photocatalytic activity than the rutile phase [37]. Doping with noble metals, especially silver, can increase the photocatalytic activity and extend the active absorption to visible light [38, 39]. Depending on the particle size and the intensity of the light, the normally used concentration of TiO_2 varies between 100 and 1,000 mg/L [40].

TiO_2 also has potential to be used in POU disinfection, because its photocatalytic activity can enhance solar disinfection [41, 42]. Figure 16.5 shows a photograph of a POU TiO_2 -assisted solar disinfection system called the SOLWATER and AQUACAT system [42]. Water from the feed tank is pumped through illuminated tubes connected in series in a compound parabolic concentrator solar collector. Electricity is provided by a solar panel on the right, as shown in the figure. However, solar disinfection usually requires long reaction times. In these applications, doping is critical to enhance the absorption of visible light to shorten the reaction time [4].

Many TiO_2 -based photocatalytic reactors have been studied, such as the annular slurry photoreactor (Fig. 16.6) [43], flow-through photoreactor (Fig. 16.7) [44], cascade photoreactor (Fig. 16.8) [45], etc. Although some of these reactors have been applied for treating organic contaminants, they can also be used for water disinfection. These reactors can be classified into two main configurations: (1) TiO_2 catalysts are suspended in the reactor; and (2) TiO_2 catalysts are immobilized onto an inert substrate [7].

To date, type 1 reactors are still preferred, due to the high total surface area of the TiO_2 per unit volume and the ease of the photocatalyst reactivation [7]. However, an additional downstream separation unit to recover the TiO_2 nanoparticles is required



Fig. 16.5 SOLWATER and AQUACAT solar disinfection system [42]

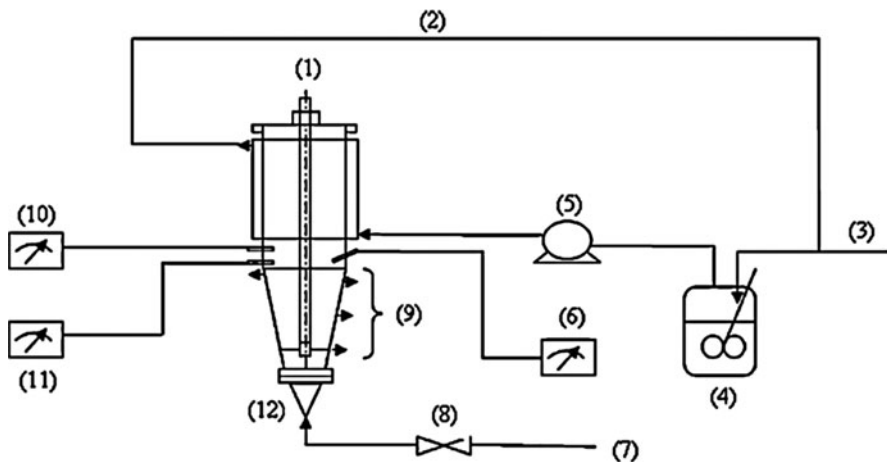
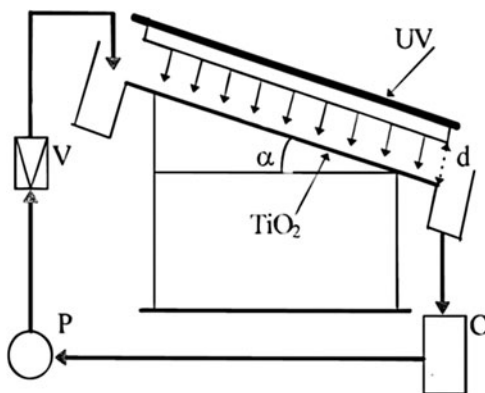


Fig. 16.6 The schematic of the annular photocatalytic reactor system: (1) UV light, (2) recirculation water line, (3) fresh cool water line, (4) cooling water vessel, (5) cooling water pump, (6) temperature meter, (7) compressed air supply line, (8) compressed air regulation valve, (9) sampling ports, (10) pH meter, (11) dissolved oxygen meter, and (12) photoreactor [43]

for continuous operation. This can be achieved by conventional sedimentation [46], cross-flow filtration [47], or membrane filtrations [48, 49]. But the optimal operating parameters are still under investigation [7]. For the type 2 reactors, various immobilizers have been tried as revealed in the literature, such as activated carbon [50, 51], mesoporous clays [52], fibers [53], or membranes [54]. Figure 16.9 shows that anatase TiO_2 nanoparticles with diameters around 10–20 nm are immobilized on titanate fibers with diameters around 100 nm [53].

Fig. 16.7 The schematic of the flow-through photoreactor system. *C* container, *P* pump, *V* venturi tube, *UV* UV lamps, *d* distance between the lamps and the plate, *TiO₂* glass plate with immobilized photocatalyst, α declination angle [44]



Advantages of using TiO_2 for water disinfection include that TiO_2 is very stable in water and ingestion of TiO_2 has low toxicity to human health [4]. One of the most important issues for TiO_2 disinfection is the impact from the water turbidity caused by the insoluble particles. On the one hand, these particles impede the penetration of UV light due to scattering and absorption [55]. On the other hand, they will also shield target pathogens from inactivation [7]. Normally, the turbidity of the water should be lower than five nephelometric turbidity units (NTU) to ensure the UV light utilization and photocatalytic reaction [56]. This limit could be achieved by prior treatment processes like screening, filtration, sedimentation, coagulation, and flocculation [7].

16.2.3 Carbon Nanotubes and Fullerenes

Carbon nanotubes (CNTs) and Fullerenes are two of the most typical carbon-based nanomaterials. They have been known to have cytotoxicity to mammalian cells with the toxicity decreasing from single-walled CNTs to multi-walled CNTs, and to Fullerenes [11, 57]. Recently, a few studies have also shown that these carbon nanomaterials also have antimicrobial capability [10]. Figure 16.10 shows the different cell morphologies of *E. coli* inoculated with or without single-walled carbon nanotubes (~1 nm diameter) [10]. The antimicrobial effect of CNTs are related to both physical interaction and changing the oxidative stress of the environment [10, 58, 59]. It is also reported that direct contact between CNTs and target microorganisms is required to have an inactivation effect [10]. The antimicrobial effect of Fullerenes may be attributed to ROS production [4, 60], but the understanding of the detailed mechanisms is still very limited.

It is very difficult to disperse CNTs in water without functionalizing or adding surfactants like sodium dodecyl benzenesulfate (SDBS), polyvinylpyrrolidone (PVP), or Triton-X [61]. Most of the current studies apply CNTs by coating them on a porous substrate, like a filter, textile or membrane [10, 62–64].

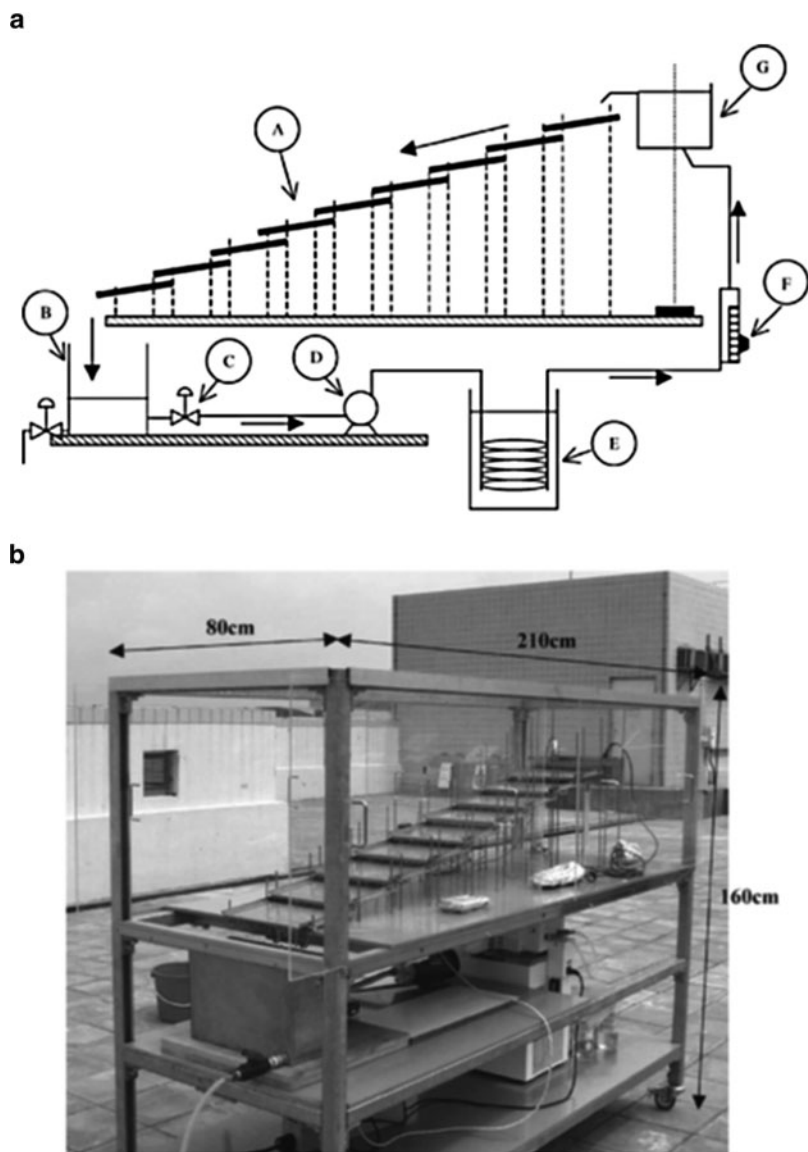


Fig. 16.8 (a) The schematic of the cascade photoreactor system. *A* TiO₂-coated plates; *B* tank with drain valve; *C* control; *D* centrifugal pump; *E* cooling coil in water bath; *F* flowmeter; *G* liquid reservoir. (b) Photograph of the pilot scale cascade photoreactor [45]

Fullerenes are also highly insoluble in water [65], but their derivatives can be soluble and still show antimicrobial effects [66]. Fullerenes can also form stable aqueous suspensions as nanoparticles with various particle sizes (Fig. 16.11) [67, 68].

Fig. 16.9 TEM image of TiO_2 nanoparticles decorated titanate fibers [53]

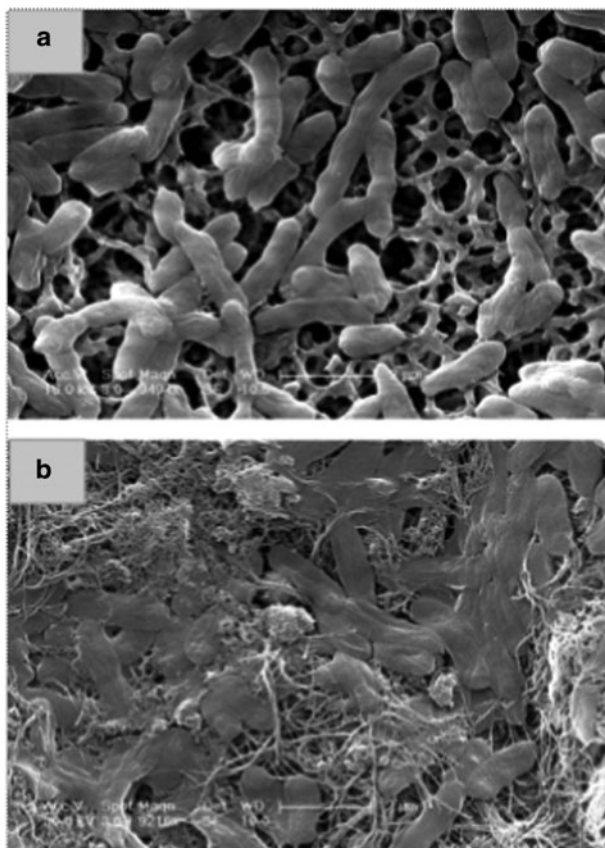
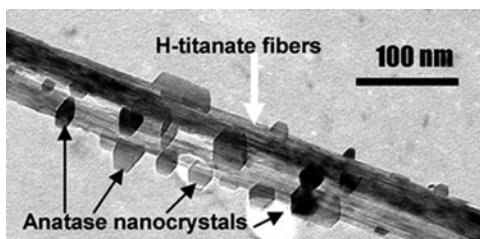


Fig. 16.10 SEM images of *E. coli*. (a) Cells incubated without SWNTs for 60 min. Cells were filtered and observed via SEM on the filter. (b) Cells incubated with SWNTs for 60 min [10]

16.3 Case Studies

Since nanotechnology has introduced new pathways for water disinfection, more and more researchers are investigating new methods for water disinfection using nanomaterials. As introduced in Sect. 16.2, oligodynamic metals, photocatalytic

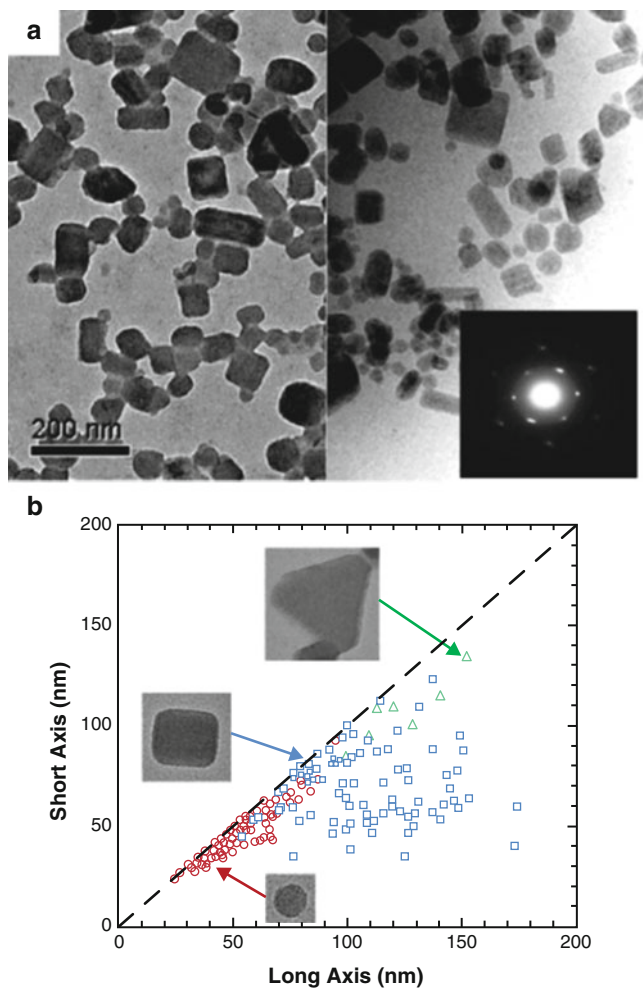


Fig. 16.11 (a) TEM image of dried (*left*) and flash-frozen (*right*) samples of nano-C60. (b) Particle size and shape distribution. Small aggregates are typically circular in cross-section, intermediate and large ones tending to be rectangular, together with a small fraction of triangular larger particles [68]

semiconductors and some carbon-based materials all have antimicrobial effect. However, their disinfection efficiency depends on a number of factors regarding nanomaterials' unique properties, such as nanomaterial synthesis methods, morphology difference, size difference and how they are used in real treatment devices. Therefore, in terms of large-scale application or commercialization, these nanomaterials need to be used more efficiently and effectively to save materials from synthesis, enhance disinfection efficiency and have lower cost and energy consumption.

In this chapter, we choose six studies carried out by different research groups using antimicrobial material for water disinfection. These studies include the three types of antimicrobial nanomaterials introduced in Chap. 2. Based on these cases, we want to introduce how these nanomaterials are designed and used for water treatment and how nanotechnology is involved in the water disinfection area.

16.3.1 Case-1: “TiO₂ Nanotube/CdS Hybrid Electrodes: Extraordinary Enhancement in the Inactivation of *Escherichia coli*”

Semiconducting materials are of great interest in wastewater treatment and among them TiO₂ is the most promising [69]. Under UV light, TiO₂ enhances the generation of hydroxyl free radicals, with hydrogen ion as a side product. This reaction is useful for bacteria inactivation in water treatment systems because hydroxyl radicals can inactivate bacteria as they will rapidly decimate the organic components of bacteria cells. However, the use of TiO₂ for photocatalytic inactivation of bacteria is limited by its relatively low efficiency of light utilization due to its wide band gap of 3.0–3.2 eV and its poor charge-transfer properties. Hence, the work done by the El-Sayed group introduced a complex system (CdS/TiO₂) to solve the above two limiting problems in order to increase bacteria inactivation efficiency [70]. And this system lowered the cost of a more complex Pt/CdS/TiO₂ system developed earlier by Kang Q. et al. by removing the high-cost Pt component [71].

They inherited the use of a TiO₂ nanotube (NT) structure developed by Baram et al. [72] for bacteria inactivation. TiO₂ NT arrays were synthesized using immobilized, anodic fabrication [73]. These TiO₂ NT arrays were aligned porous, crystallized, and oriented which made them attractive electron percolation pathways for vectorial charge transfer between interfaces. Moreover, to increase the utilization of visible light, small-band-gap nanocrystal CdS was anchored to this semiconducting metal oxide. CdS nanocrystals was deposited on the crystallized NT surfaces by the successive chemical bath deposition (CBD) method and resulted in enhancement of the charge carrier separation process [74]. SEM images of the materials were shown in Fig. 16.12.

By using this complex CdS/TiO₂ system, they have achieved a better bacteria inactivation in water solution. Two sets of experiments were performed to explore the inactivation efficiency of *E. coli*: one with light only—photochemical, and one with light and applied bias—photoelectrochemical. And to compare the performance of TiO₂/CdS electrodes, they also used TiO₂ thin films and TiO₂ NT arrays. The schematic diagram of the set-up used for the photochemical and photoelectrochemical is shown in Fig. 16.13. In the photochemical study, electrodes were immersed in separate solutions containing *E. coli* in sulfate buffer under stirring and illumination from a xenon lamp, with a water filter to cut off the IR effect, and samples were collected every 10 min. For the photoelectrochemical study, a two-electrode electrochemical cell was used with the semiconductor material as the

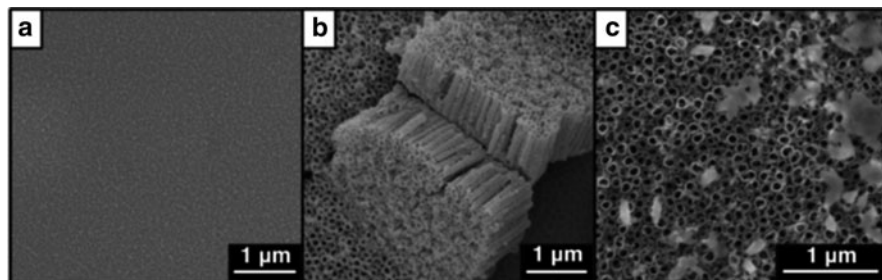
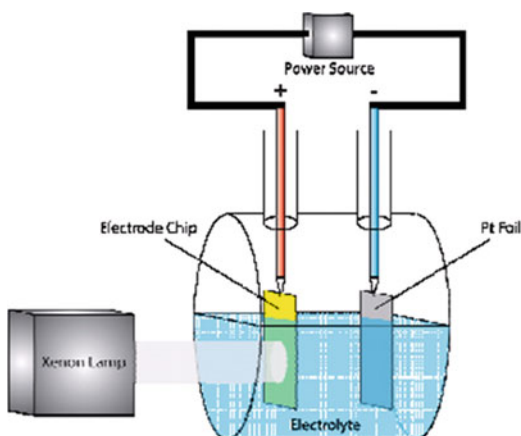


Fig. 16.12 FESEM images of (a) titania thin film, (b) titanium dioxide nanotubes, and (c) TiO₂/CdS hybrid electrode [70]

Fig. 16.13 Schematic diagram of the set-up used for the photochemical and photoelectrochemical disinfection of *E. coli* [70]



working electrode and a Pt foil as the counter electrode under a constant applied potential of 0.5 V. Illumination conditions were the same.

They also measured the diffuse reflectance spectroscopy (DRS)-UV-vis spectra of the three electrodes mentioned above (Fig. 16.14). The TiO₂/CdS electrode showed an absorption edge red-shifted to 570 nm while the other two electrodes' absorption edges were around 340–380 nm. This shifted absorption edge gave the TiO₂/CdS electrode a band-gap of 2.17 eV, which means that this hybrid array can harvest visible light.

The results of inactivation were shown as survivability with respect to time (Fig. 16.15). In the photochemical case, the hybrid electrode led to an almost complete inactivation of *E. coli* in only 10 min without any applied bias, which was much higher than both thin film and the pure NT arrays which led to the inactivation of only 40% and 45% of the bacteria, respectively. While with 0.5 V bias to help separate the charge carriers, the hybrid electrode showed an inactivation of *E. coli* in only 3 min.

This disinfection method is very attractive. The complex system of TiO₂ NT/CdS shows a lower band-gap, a higher absorption of visible light and a good charge

Fig. 16.14 DRS-UV-vis spectra of the three electrodes used to inactivate *E. coli*. CdS greatly increases the visible light absorption capability of the TiO₂ [70]

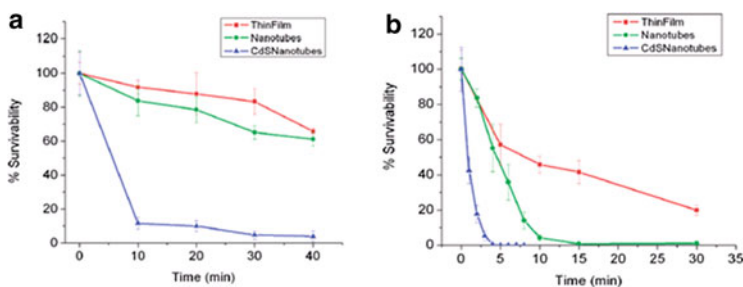
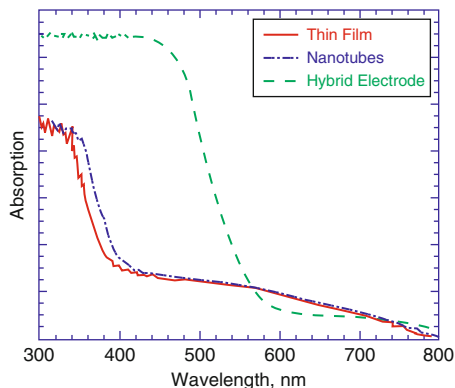


Fig. 16.15 Inactivation of *E. coli* in photochemical (a) and photoelectrochemical (b) experiments for TiO₂ thin film (red), TiO₂ nanotube array (green), and the hybrid CdS/TiO₂ nanotube array (blue) [70]

transport compared to other TiO₂-based water disinfection devices. Moreover, the main energy source to support this system is visible light which makes this method clean and of low cost. However, the fabrication process of the hybrid electrode is still relatively complicated compared to other innovative disinfection methods, and the toxicity of cadmium is a big concern. The mechanism of disinfection of this device is by generating hydroxyl free radicals which have high oxidation ability. This method would be more promising in terms of commercialization if the fabrication cost could be further lowered and the cadmium element could be replaced by another non-toxic element.

16.3.2 Case-2: “High Speed Water Sterilization Using One-Dimensional Nanostructures”

This work was done by the Cui group at Stanford University [62]. This water treatment device involves both silver nanowires (AgNWs) and carbon nanotubes

(CNTs); however, the disinfection mechanism is claimed not to be just silver disinfection or CNT disinfection. They have developed a high speed electrical assist disinfection device based on a conducting nanotextile. Though the conducting nanotextile is acting like a filter, the disinfection mechanism is not by size exclusion, because the nanotextile has pore sizes of several hundreds of microns which is much larger than the size of bacteria. This device is made through very simple processes and shows a high throughput and low energy consumption for bacteria inactivation in water.

The illustration of filtration set-up and filter fabrication is shown in Fig. 16.16. The filter was made of three components: cotton, CNT and AgNW. Cotton acted as the backbone of the filter since it is cheap, widely available, and chemically and mechanically robust. The conductivity was provided by CNT which was coated onto textile fibers by a simple dipping–drying process. AgNW, which is known to have antimicrobial property, was coated using the same method. AgNWs could form an efficient electrical transport network in filters and they have advantages over Ag nanoparticles (AgNP) in terms of disinfection since they significantly reduce the number of electron hopping times as compared to nanoparticles.

The disinfection idea was based on the fact that noble metal electrodes are known to exhibit antibacterial action under moderate currents, and the enhancement of a sheet of silver nanorods' antibacterial action when placed in an electric field has recently been observed [75, 76]. The experiment set-up was very simple. An external electric field was applied between a nanotextile filter and a counter electrode of copper mesh. Water flowed through the nanotextile filter by gravity force. Bacteria were inactivated while flowing through the nanotextile filter and with the presence of a moderate voltage. Disinfected water was collected from end of the funnel.

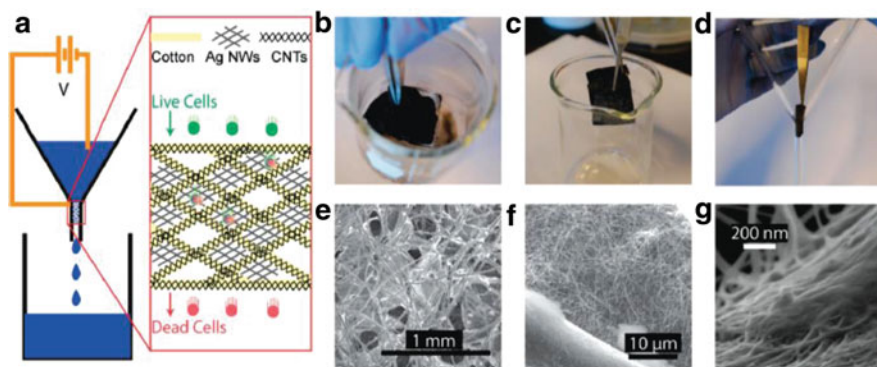
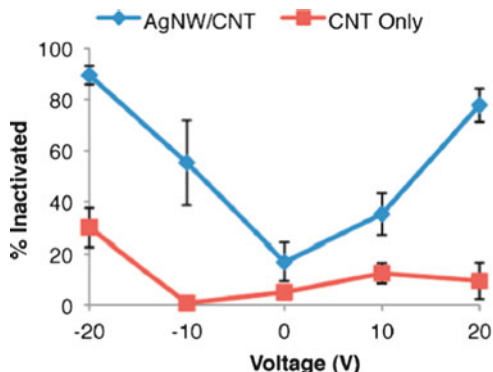


Fig. 16.16 Schematic, fabrication, and structure of cotton, AgNW/CNT device. (a) Schematic of active membrane device proposed. (b) Treatment of cotton with carbon nanotubes (CNTs). (c) Treatment of device with silver nanowires (AgNWs). (d) Integration of treated cotton into funnel. (e) SEM image showing large scale structure of cotton fibers. (f) SEM image showing AgNWs. (g) SEM image showing CNTs on cotton fibers [62]

Fig. 16.17 Inactivation efficiency at five biases for AgNW/CNT cotton as well as CNT-only cotton [62]

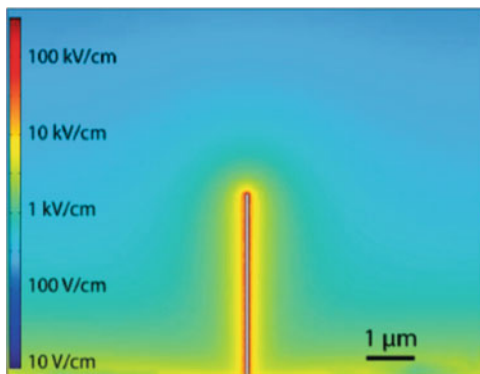


The efficiency of this water disinfection method was studied using *E. coli*. And the results were calculated by counting colonies of both the original bacteria solution and treated water solution cultured on agar plates. From the results, we can see that the AgNW coating can increase disinfection efficiency compared to the filter only with the CNT coating. And with an increased value of external voltage, a higher inactivation efficiency was achieved (Fig. 16.17). The flow rate of this device was 1 L/h and retention time was about 1 s. Moreover, this disinfection method was proved to be effective to different original bacteria concentration from 10^4 to 10^7 bacteria/mL. The best efficiency of this method reported by the paper was 98% by three times of filtration.

The authors put forward three possible hypotheses which could lead to bacteria inactivation, although the disinfection mechanism was not fully understood yet. The first factor is silver, in this device AgNW. Silver ion and AgNP are known to have antimicrobial properties and are used as coatings in other disinfection applications. In this case, the inactivation effect could be either from Ag^+ released from oxidized nanomaterial or nanomaterial itself without Ag^+ . However, the effect of silver cannot alone account for the dramatic improvement of killing efficiency observed when the AgNWs were placed at relatively moderate biases of 20 V. The second hypothesis is that the bacteria were inactivated by the strong external electric field which would cause irreversible electroporation to bacteria cells. By simulation, the electric field near AgNW surface could be as high as tens to hundreds of kilovolts per centimeter (Fig. 16.18). It is known that when electric fields exceeding 10^5 V/cm it will adversely affect cell viability by breaking down cell membranes in a process known as electroporation [77]. The third hypothesis is that changes to the solution chemistry during current flow are involved, including pH changes as well as in situ production of chemicals like chlorine, which have also been investigated as a route to sterilizing fluid [78]. Finally, it is also quite possible that two or more of these processes may work together and enhance the inactivation of bacteria.

This electrical assist water disinfection method is very attractive because of its short retention time, low cost of materials used and low energy consumption. And by introducing an external electric field, inactivation efficiency is significantly

Fig. 16.18 Simulation of e-field near NW surface in solution. Log plot of the electric field near a NW in solution at experimental anodic conditions [62]



improved which reveals that the electric field plays an important role in the bacteria inactivation mechanism. However, there is a health concern when using materials in the nano-sized range. In this chapter, it has been shown that the flow conditions studied did not result in mass material release over the time scales reported. Further work to accurately quantify the amount of material released should be carried out to make this disinfection more promising and capable of being commercialized.

16.3.3 Case-3: “Bactericidal Paper Impregnated with Silver Nanoparticles for Point-of-Use Water Treatment”

This work done by the Gray group at McGill University and was aimed to develop a cheap point-of-use water purification device [30]. This filter uses cheap and robust paper as substrate and embed silver nanoparticles in it. The inactivation mechanism of this filter is silver disinfection and the system for water filtration is really simple. Most of the bacteria were in effluent solution after percolation and they were inactivated by AgNPs during percolation as shown in Fig. 16.19.

The paper they used was absorbent blotting paper 0.5 mm thick and weighing 250 g/m² (Domtar). AgNPs were deposited by the in situ reduction of silver nitrate on the cellulose fibers of paper. The detailed synthesis process can be found publications by J. He et al. and T. Maneerung et al. [79, 80]. The characterization of the AgNPs on the paper was established by measuring the reflectance spectra of the AgNP with a diffuse reflectance attachment using a UV-vis reflectance spectrum. The shape and size distribution of AgNPs were characterized by electron microscopy (Fig. 16.20). The AgNPs’ size did not relate much to the precursor concentration and all samples of different mass loading of silver showed an average size of 7.1 ± 3.7 nm. With the increase of the precursor silver ion concentration, the silver content on the paper increased, which was also shown by the color change of the sheets. The paper turned darker with response to a higher silver concentration. And a comparison with paper made by soaking into AgNP suspension showed the lowest silver loading on the paper and displayed a gray color (Fig. 16.20).

Fig. 16.19 Schematic illustration of bacteria percolation through AgNP paper [30]

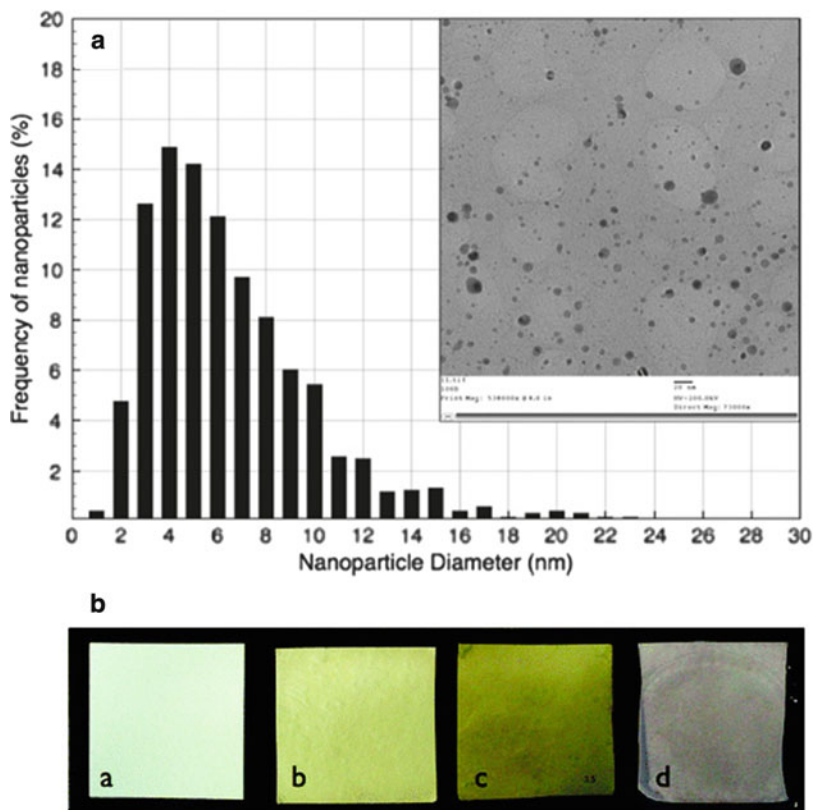
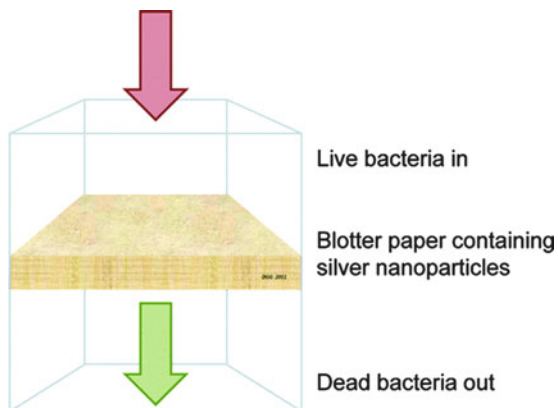


Fig. 16.20 (a) The distribution of silver nanoparticle diameters, as measured from a TEM image of AgNP on unstained paper fibers removed from sheet (*inset*, scale bar 20 nm). (b) Blotter papers (a) untreated and with silver nanoparticles, (b) 0.2 mg Ag/g paper, (c) 5.8 mg Ag/g paper, and (d) sheet soaked in preformed nanoparticle suspension, 0.06 mg Ag/g paper (each sheet is 6.5×6.5 cm) [30]

The bactericidal effectiveness of AgNP paper was evaluated by adding isolated effluent bacteria to agar plates and counting colonies. Two kinds of bacteria *E. coli* (Gram-negative) and *Enterococcus faecalis* (Gram-positive) were tested. The results are shown in Fig. 16.21. Paper prepared with AgNP suspensions showed a lower efficiency than in situ AgNP paper which achieved log-7.6 and log-3.4 removal efficiency of *E. coli* and *E. faecalis* bacteria. And for all the cases, Gram-positive bacteria *E. faecalis* constantly showed a lower efficiency of inactivation.

Considering potential health issue from AgNPs, the authors have analyzed the silver concentration in the effluent water. Graphite furnace atomic absorption was used to measure the total silver concentration including both silver ions and AgNP. The average content of silver was 0.048 (± 0.018) ppm in the effluent water which meets the US EPA guideline for drinking water of less than 0.1 ppm. However, AgNP suspension-soaked paper showed a higher concentration of silver content in the effluent water.

The mechanism of this method of water purification was silver inactivation of bacteria during percolation. Though the difference of inactivation effect by silver ions or by AgNP can hardly be analyzed, the TEM images of bacteria cells after inactivation showed some morphology changes which are similar to that of bacteria treated with AgNO₃ solution (Fig. 16.22).

This in situ synthesized AgNP paper shows great potential of easily transported and deployed use for emergency or outdoor activities. The bacteria removal efficiency is quite promising. However, the flow rate of 10 mL/min is not high enough compared to other treatment methods such as a ceramic/AgNP filter which has a flow rate of around 25 mL/min. And because of the natural properties of paper, the life time of this filter would not be very long which makes the in situ synthesis seem

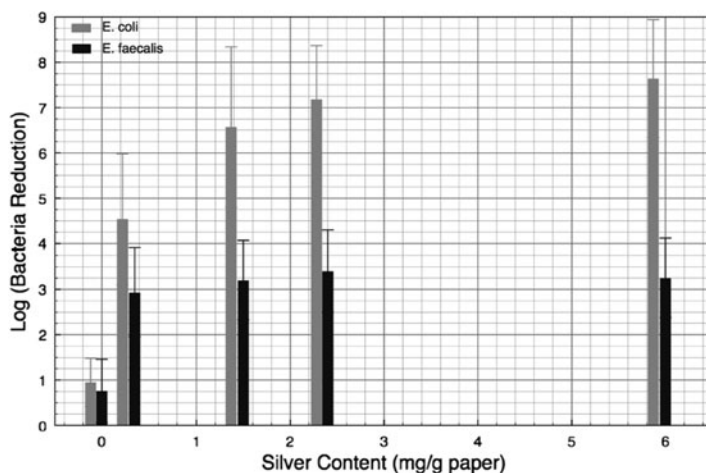


Fig. 16.21 Log reduction of *E. coli* and *E. faecalis* bacterial count after permeation through the silver nanoparticle paper, at different silver contents in paper. Initial bacterial concentration, 109 CFU/mL (log 9). Error bars standard deviation [30]

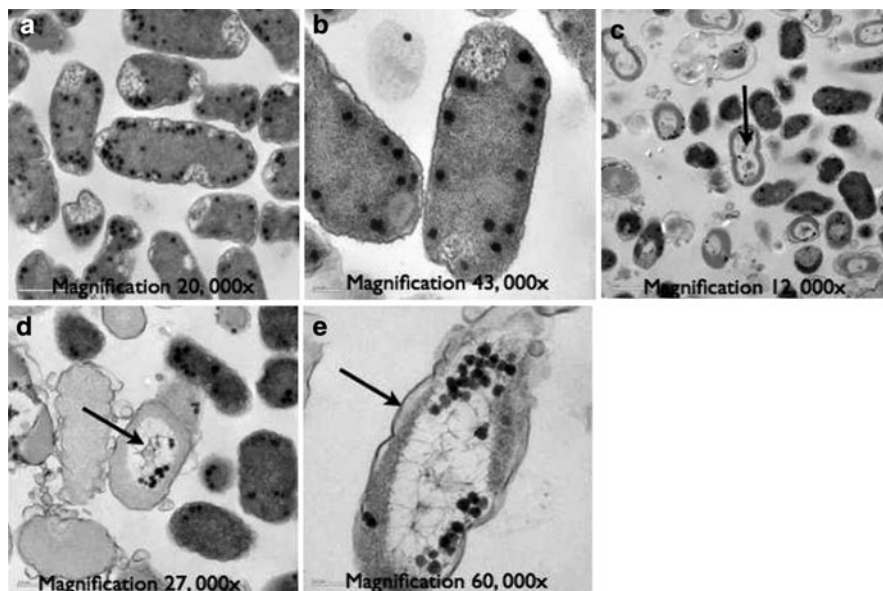


Fig. 16.22 Internal structure of *E. coli* bacteria imaging by TEM, following percolation experiments. (a, b) control paper (no silver). After exposure to Ag NP paper (c) low electron density region (*arrow*) in the centers of the cells. (d) Condensed form of DNA (*arrow*) in the center of the low electron density region. (e) A gap between the cytoplasm membrane and the cell wall (*arrow*); the cell wall shows serious damage. *Black dots* are not AgNP, but electron dense granules typical of *E. coli* [30]

a little bit complicated if this paper filter is designed for one-time use. But if the life time of this paper-based filter could be increased, this would be very attractive for commercialization.

16.3.4 Case-4: “Electrochemical Multiwalled Carbon Nanotube Filter for Viral and Bacterial Removal and Inactivation”

Carbon nanotubes have been reported to have an inherent antimicrobial activity [10]. Both single-walled carbon nanotube (SWNT)- and multiwalled carbon nanotube (MWNT)-based microfilters have been used for water disinfection to remove bacteria by a sieving mechanism. In addition, the conductive nature of carbon nanotubes allows the introduction of electrochemistry during filtration which could enhance the inactivation efficiency of pathogens in water. The work shown below was done by the Elimelech group at Yale University [63]. They took the advantages of porous and conductive properties of MWNT and made a filter functioning both by size screening and electrochemical disinfection with a small applied bias.

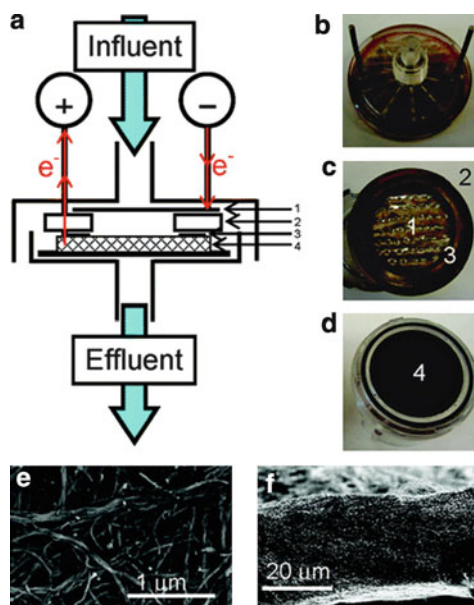


Fig. 16.23 Electrochemical MWNT filter design and characterization. (a) Depiction of modified electrolytic MWNT filtration setup, where 1 is the perforated stainless steel cathode, 2 is the insulating seal, 3 is the anodic titanium ring connector to the MWNT, and 4 is the anodic MWNT filter. (b) Top view of the modified upper piece of the Millipore filtration apparatus with anodic (*left*) and cathodic (*right*) connectors. (c) View of the upper piece of the filtration apparatus showing the perforated stainless steel cathode. (d) MWNT filter composed of 3 mg MWNTs (0.31 mg/cm^2 coverage) on a Teflon membrane ($5 \text{ }\mu\text{m}$ pore size) on the bottom piece of apparatus. (e) SEM aerial image of the MWNT filter. (f) SEM cross-section (*side*) image of the MWNT filter [63]

The filter design and operation is shown in Fig. 16.23. The MWNT filter was made by filtering MWNT solution onto a $5\text{-}\mu\text{m}$ PTFE membrane and the mass loading was 0.31 mg/cm^2 . The average pore diameter was $93 \pm 38 \text{ nm}$ and the thickness of the MWNT filter was $22 \pm 2 \text{ }\mu\text{m}$. The cathode was stainless steel which was on top of the anode CNT filter. An external voltage of 1–3 V was applied during filtration. Both inactivation of viruses (MS2) and of bacteria (*E. coli*) were studied.

The inactivation results showed that, after dispersing effluent water on to an agar plate, no bacteria colonies were formed. All bacteria were removed by the sieving mechanism using the $\sim 100\text{-nm}$ MWNT filter. And since MR2 virus sizes were much smaller, they measured the virus removal efficiency in effluent water according to bias change (Fig. 16.24). The bacteria and virus adsorbed onto the filter were also investigated. Viability was studied with different bias and exposure time. The experimental result is also shown in Fig. 16.24.

The mechanism of this disinfection method is that at low electric bias, 1–2 V, the dominant inactivation mechanism was direct oxidation by MWNT while at high bias, 3 V, bacteria and virus could be inactivated by indirect oxidation. Their

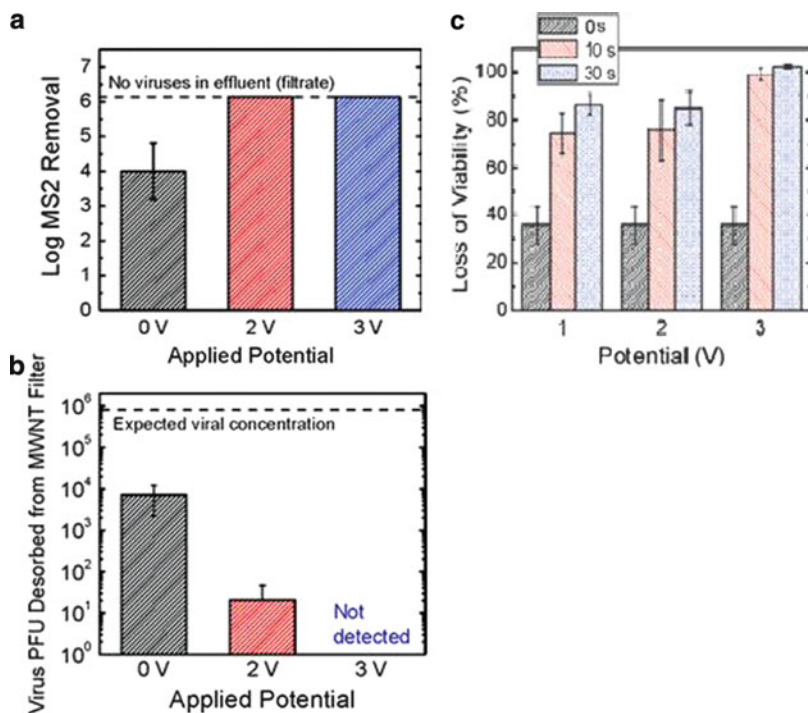


Fig. 16.24 Electrochemical MS2 removal and/or inactivation versus potential. (a) Log MS2 removal as a function of applied potential during filtration. In fluent was 10 mL of 10 mM NaCl (pH 5.7) and 106 viruses mL⁻¹ and was filtered at a rate of 4 mL min⁻¹ (filter approach velocity of 250 L m⁻² h⁻¹). Note that at 2 and 3 V, no viruses were detected in the filter effluent. (b) PFU of MS2 adsorbed on MWNT filter as a function of the post filtration applied potential. In fluent was 10 mL of 10 mM NaCl (pH 5.7) with 106 virus mL⁻¹ and was filtered at a rate of 4 mL min⁻¹ (filter approach velocity of 250 L m⁻² h⁻¹) in the absence of potential. Adsorbed viruses were then electrolyzed for 30 s at 2 or 3 V. (c) Electrochemical loss of *E. coli* viability versus potential and time. *E. coli* suspension [107 cells, (NaCl) = 10 mM, pH 5.7] first sieved onto the MWNT filter and then electrolyzed at an applied voltage of 1, 2, or 3 V for 10 or 30 s. Bacteria were stained immediately after electrolysis for viability assay. Each data point represents the mean of at least duplicate measurements at the same experimental conditions, with error bars representing standard deviations [63]

hypothesis was that at high bias, free radicals would form from electrolyte and oxidized pathogens. And in effluent water, bacteria were removed by the sieving mechanism and the virus was removed by both sieving and electrochemical inactivation.

This disinfection method shows a very effective inactivation of both bacteria and virus, and the filter fabrication is not complicated. However, limited by the small pore sizes of the MWNT filter, the flow rate can only achieve 4 mL/min. And by using the MWNT filter, there are still safety concerns of effluent water quality for point-of-use disinfection.

16.3.5 Case-5: “Converting Visible Light into UVC: Microbial Inactivation by Pr^{3+} -Activated Upconversion Materials”

This work done by the Kim group at Georgia institute of Technology who reported a light-activated antimicrobial surface composed of lanthanide-doped up-conversion luminescent nano- and microcrystalline Y_2SiO_5 [81]. This method, unlike that using TiO_2 which relies on photocatalytically-generated free radicals for disinfection, has a pure optical mechanism and this work is very innovative to use electromagnetic energy for disinfection purposes. This antimicrobial surface can absorb visible light and convert it into Germicidal UVC radiation (Fig. 16.25). Hence, the disinfection mechanism is similar to UV disinfection.

The surface antimicrobial effect was analyzed by studying the inactivation kinetics of *Bacillus subtilis*. Bacteria was deposited and dried on the coated surfaces. The reason this experiment can be carried out in dry condition is because the spores of this organism can remain viable in dry conditions [82]. The results are shown in Fig. 16.26. The sample with Pr^{3+} , Gd^{3+} and Li^+ showed the best performance and inactivation efficiency which could be enhanced by increasing light intensity and exposure time.

This method is innovative for a disinfection mechanism. The inactivation efficiency is relatively low compared to other methods since the group used the lowest excitation intensity to just evaluate the antimicrobial effect brought about by up-conversion materials. Although this technology has not been used in water solution systems, it demonstrates the potential of disinfection and further usage in the water disinfection area. So far, the kinetics is much slower than other methods; however, there is still room for this technology to improve.

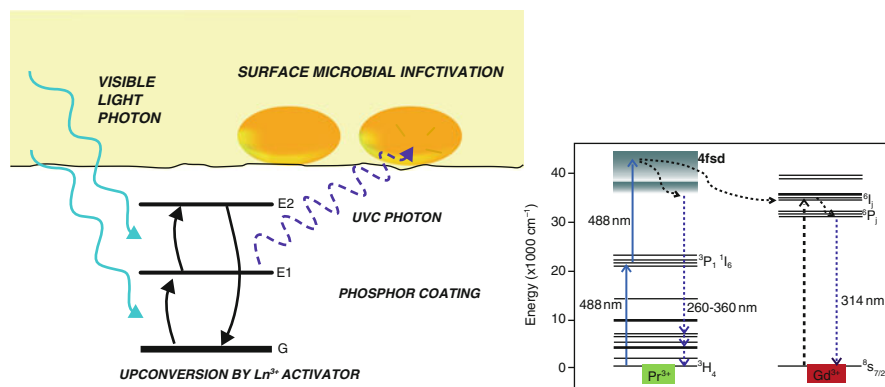


Fig. 16.25 Utilization of visible-to-ultraviolet upconversion phosphor coating for light-activated antimicrobial materials. The energy diagram depicts excited-state absorption of visible light from the ground-state configuration, G, to the excited states, E1 and E2, to emit a UVC photon upon relaxation (left). Up-conversion mechanisms of Pr^{3+} and Gd^{3+} UV emissions. Solid blue line shows visible light absorption; dotted black line shows nonradiative energy transfer; dotted purple line shows UV photon emission (right) [81]

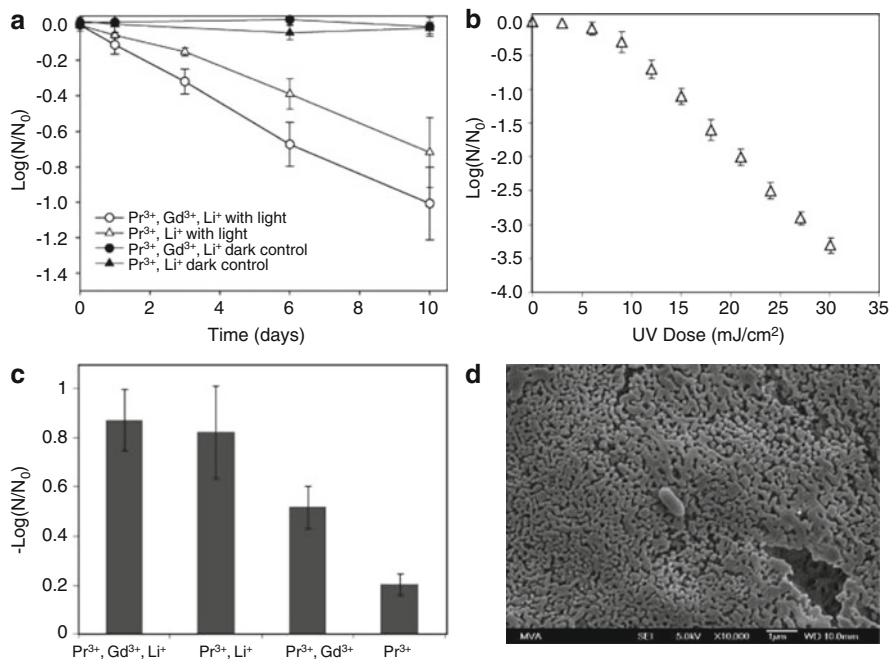


Fig. 16.26 Inactivation of *Bacillus subtilis* spores on dry phosphor-coated surfaces. (a) Inactivation kinetics of Y₂SiO₅ phosphors with different doping schemes exposed to “daylight” fluorescent lighting and dark controls. Unactivated surfaces showed no inactivation under visible light after 10 days (data not shown). (b) Inactivation dose–response of *B. subtilis* spores on dry surface exposed to known doses of UVC from low-pressure Hg bulbs, $\lambda = 254$ nm. The linear portion of this curve was used for biosimetric estimation of the upconversion efficiency of coated samples. (c) 10-day log inactivation of spores on Y₂SiO₅-coated surfaces with different doping schemes under visible light. (d) Scanning electron micrograph of a *B. subtilis* spore on a Y₂SiO₅: Pr³⁺, Li⁺ + nanocrystalline surface prepared through dip-coating in precursor sol solution. White scale bar 1 μm. All error bars standard deviations [81]

16.3.6 Case-6: “Sustainable Colloidal-Silver-Impregnated Ceramic Filter for Point-of-Use Water Treatment”

The Colloidal-Silver-Impregnated Ceramic Filter is one of the most representative examples of a commercialized water disinfection product using nanotechnology. In the late 1980s and early 1990s, ceramic filters were already appearing in third world markets; however, the price of those filters were too expensive for local people to afford in the long term. A U.S.-based nongovernmental organization (NGO) called Potters for Peace has developed a new method to fabricate these ceramic filters and has taught this method to local people. The filters look like ceramic pots and in operation they are put into a plastic container (Fig. 16.27). Ceramic filters can removal pathogens by size exclusion, and addition of colloidal silver particles to these filters will enhance the inactivation efficiency because of silver’s antimicrobial properties.



Fig. 16.27 A ceramic filter

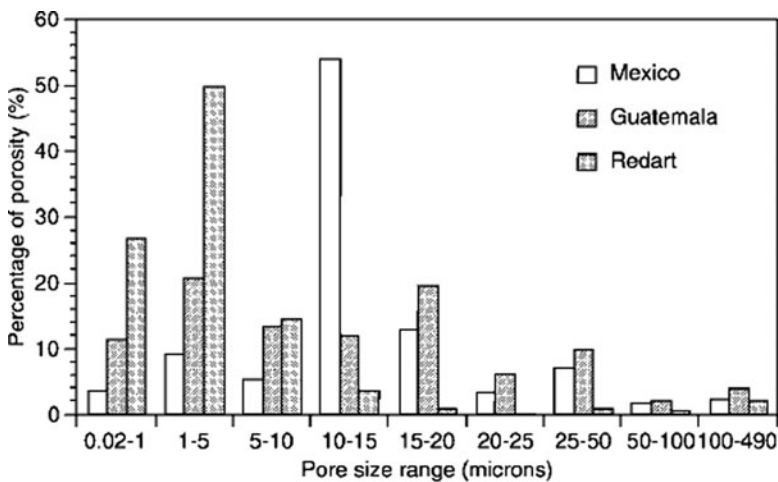


Fig. 16.28 Pore-size distribution for ceramic filters fabricated using Redart, Guatemalan, and Mexican soils [22]

V.A. Oyanedel-Craver and J.A. Simth at the University of Virginia fabricated this kind of ceramic filters using the same method as NGO and tested their performance in laboratory [22]. Filters made of three different soil samples were studied. The porosity study showed similar pore sizes for these three filters (Fig. 16.28). This means that ceramic filters could be fabricated by local labor and the transportation properties of the filters using different raw materials would not differ by very much.

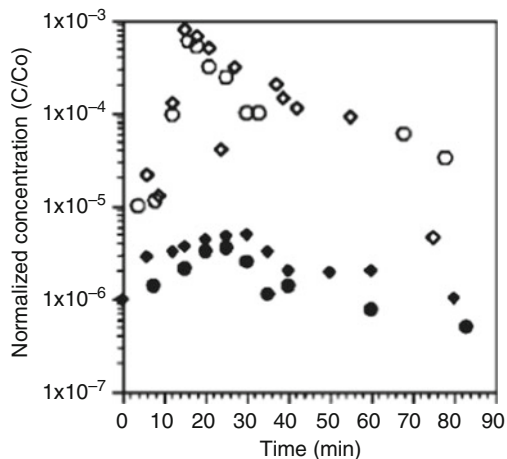


Fig. 16.29 Effluent *E. coli* concentrations normalized to the influent pulse concentration as a function of time for ceramic filters fabricated with Redart soils without colloidal silver (◇ and ○), and painted with (◆) and submerged in a 600-mg/L colloidal silver solution (●) [22]

To improve the efficiency of ceramic filters, colloidal silver nanoparticles were added. This was done by either painting them or submerging them using AgNPs suspensions. After saturation, bacteria removal experiments were done using ceramic filters both with and without silver colloidal particles. The results showed that silver nanoparticles can significantly improve bacteria removal efficiency (Fig. 16.29). And the methods used to adding AgNPs did not influence the efficiency very much, which proves the ease of commercialization of this Colloidal-Silver-Impregnated Ceramic Filter.

The Colloidal-Silver-Impregnated Ceramic Filter is very effective for point-of-use water treatment especially for the third world countries, because it is easy for it to be made by local labor and is of relatively low cost. This method provides a way to protect people in water-stressed areas from water borne diseases.

16.4 Challenges and Outlooks

Although antimicrobial nanomaterials have shown promising potential for water disinfection, several challenges still exist for large-scale practical applications.

1. Usually, the synthesis of nanomaterials includes several complex procedures and the scale-up is still challenging, meaning that the cost of the antimicrobial nanomaterials is still a concern based on current technology. Drinking water is essential for everyday life, but most of the antimicrobial nanomaterials are still not affordable for most people for daily use. The most commercialized ceramic filter as discussed previously costs about US\$ 25 each. However, this is still too

expensive for the people living in some developing countries who do not have safe drinking water access and who need POU disinfection techniques the most urgently.

2. We gain benefit from the antimicrobial effect of the nanomaterials by obtaining safe drinking water without pathogens. However, if these nanomaterials are discharged into the natural environment, they may also kill the microbes that are useful or even essential for the ecosystem. In addition, high concentrations of antimicrobial nanomaterials in the drinking water may also be harmful to human health [71]. Therefore, retaining the antimicrobial nanomaterials in the system is extremely important.
3. The antimicrobial effect of the nanomaterials is relevant to their high surface-to-volume ratio. Thus, smaller sizes will be preferable. However, smaller sizes will also cause more serious aggregation problems. It will also be more challenging to retain smaller nanomaterials in the system, no matter if it is a sedimentation process or a filtration process.
4. Since the antimicrobial nanomaterials are required to be retained in the treatment unit, no residual antimicrobial effects can be provided. It will be fine for POU applications, but will be a problem for remote applications with long-distance transport.
5. Most of the current studies on antimicrobial nanomaterials are conducted in a relatively clean solution [4]. The effects of the natural water qualities are still not well understood and many more studies on real application are required.

References

1. UNESCO, *Water a shared responsibility*, United Nations Educational, Scientific and Cultural Organization. Scientific and Cultural Organization. Paris, France: UNESCO; New York: Berghahn Books, 2006. p. 20–24.
2. Wolff, G., et al., *The biennial report on freshwater resources*, Washington, D.C., in *the world's water 2006–2007 the biennial report on freshwater resources*. Washington, DC: Island Press, 2006. p. 1–28.
3. WHO, *Water, sanitation and hygiene links to health*. 2004, World Health Organization. http://www.who.int/water_sanitation_health/publications/factsfigures04/en/
4. Li, Q., et al., *Antimicrobial nanomaterials for water disinfection and microbial control: Potential applications and implications*. Water Research, 2008. **42**(18): p. 4591–4602.
5. Diallo, M., et al., *Nanotechnology applications for clean water*. Norwich, NY: William Andrew, 2009. p. 3–15.
6. Nangmenyi, G. and J. Economy, *Nanometallic particles for oligodynamic microbial disinfection*, in *Nanotechnology Applications for Clean Water*, N. Savage, et al., Editors. 2009, William Andrew Inc.: Norwich. p. 3–15.
7. Chong, M.N., et al., *Recent developments in photocatalytic water treatment technology: A review*. Water Research, 2010. **44**(10): p. 2997–3027.
8. Gondal, M.A., M.A. Dastageer, and A. Khalil, *Synthesis of nano-WO₃ and its catalytic activity for enhanced antimicrobial process for water purification using laser induced photo-catalysis*. Catalysis Communications, 2009. **11**(3): p. 214–219.
9. Lee, J.S., et al., *Photochemical and antimicrobial properties of novel C60 derivatives in aqueous systems*. Environmental Science & Technology, 2009. **43**(17): p. 6604–6610.

10. Kang, S., et al., *Single-walled carbon nanotubes exhibit strong antimicrobial activity*. *Langmuir*, 2007. **23**(17): p. 8670–8673.
11. Magrez, A., et al., *Cellular toxicity of carbon-based nanomaterials*. *Nano Letters*, 2006. **6**(6): p. 1121–1125.
12. Russell, A.D. and W.B. Hugo, *Antimicrobial activity and action of silver*. *Progress in Medicinal Chemistry*, 1994. **31**: p. 351–370.
13. Jung, W.K., et al., *Antibacterial activity and mechanism of action of the silver ion in Staphylococcus aureus and Escherichia coli*. *Applied and Environmental Microbiology*, 2008. **74**(7): p. 2171–2178.
14. Inoue, Y., et al., *Bactericidal activity of Ag-zeolite mediated by reactive oxygen species under aerated conditions*. *Journal of Inorganic Biochemistry*, 2002. **92**(1): p. 37–42.
15. Li, W.R., et al., *Antibacterial effect of silver nanoparticles on Staphylococcus aureus*. *Biometals*, 2011. **24**(1): p. 135–141.
16. Morones, J.R., et al., *The bactericidal effect of silver nanoparticles*. *Nanotechnology*, 2005. **16**(10): p. 2346–2353.
17. Pal, S., Y.K. Tak, and J.M. Song, *Does the antibacterial activity of silver nanoparticles depend on the shape of the nanoparticle? A study of the gram-negative bacterium Escherichia coli*. *Applied and Environmental Microbiology*, 2007. **73**(6): p. 1712–1720.
18. Gogoi, S.K., et al., *Green fluorescent protein-expressing Escherichia coli as a model system for investigating the antimicrobial activities of silver nanoparticles*. *Langmuir*, 2006. **22**(22): p. 9322–9328.
19. Larimer, C., et al., *The segregation of silver nanoparticles in low-cost ceramic water filters*. *Materials Characterization*, 2010. **61**(4): p. 408–412.
20. Yaohui, L., et al., *Silver nanoparticle-decorated porous ceramic composite for water treatment*. *Journal of Membrane Science*, 2009. 331(1–2): p. 50–56.
21. van Halem, D., et al., *Assessing the sustainability of the silver-impregnated ceramic pot filter for low-cost household drinking water treatment*. *Physics and Chemistry of the Earth*, 2009. **34**(1–2): p. 36–42.
22. Oyanedel-Craver, V.A. and J.A. Smith, *Sustainable colloidal-silver-impregnated ceramic filter for point-of-use water treatment*. *Environmental Science & Technology*, 2008. **42**(3): p. 927–933.
23. Yang, L., et al., *Development and characterization of porous silver-incorporated hydroxyapatite ceramic for separation and elimination of microorganisms*. *Journal of Biomedical Materials Research Part B-Applied Biomaterials*, 2007. **81B**(1): p. 50–56.
24. Halem, D.v., et al., *Ceramic silver-impregnated pot filters for household drinking water treatment in developing countries: Material characterization and performance study*. *Water Science and Technology: Water Supply*, 2007. **7**(5–6): p. 9–17.
25. Nangmenyi, G., et al., *Synthesis and characterization of silver-nanoparticle-impregnated fibreglass and utility in water disinfection*. *Nanotechnology*, 2009. **20**(49): p. 1–10.
26. Nangmenyi, G., et al., *Bactericidal activity of Ag nanoparticle-impregnated fibreglass for water disinfection*. *Journal of Water and Health*, 2009. **7**(4): p. 657–663.
27. Zhang, X.L., et al., *Immobilizing silver nanoparticles onto the surface of magnetic silica composite to prepare magnetic disinfectant with enhanced stability and antibacterial activity*. *Colloids and Surfaces a-Physicochemical and Engineering Aspects*, 2011. **375**(1–3): p. 186–192.
28. Gangadharan, D., et al., *Polymeric microspheres containing silver nanoparticles as a bactericidal agent for water disinfection*. *Water Research*, 2010. **44**(18): p. 5481–5487.
29. De Gusseme, B., et al., *Virus disinfection in water by biogenic silver immobilized in polyvinylidene fluoride membranes*. *Water Research*, 2011. **45**(4): p. 1856–1864.
30. Dankovich, T.A. and D.G. Gray, *Bactericidal paper impregnated with silver nanoparticles for point-of-use water treatment*. *Environmental Science & Technology*, 2011. **45**(5): p. 1992–1998.

31. Panyala, N.R., E.M. Pena-Mendez, and J. Havel, *Silver or silver nanoparticles: A hazardous threat to the environment and human health?* Journal of Applied Biomedicine, 2008. **6**(3): p. 117–129.
32. USEPA, *National secondary drinking water regulations*. 2002. p. 6. <http://www.epa.gov/ogwdw/consumer/pdf/mcl.pdf>
33. Silver, S., *Bacterial silver resistance: Molecular biology and uses and misuses of silver compounds*. FEMS Microbiology Reviews, 2003. **27**(2–3): p. 341–353.
34. Matsunaga, T., et al., *Photoelectrochemical sterilization of microbial-cells by semiconductor powders*. FEMS Microbiology Letters, 1985. **29**(1–2): p. 211–214.
35. Kikuchi, Y., et al., *Photocatalytic bactericidal effect of TiO₂ thin films: Dynamic view of the active oxygen species responsible for the effect*. Journal of Photochemistry and Photobiology a-Chemistry, 1997. **106**(1–3): p. 51–56.
36. Adams, L.K., et al., *Comparative toxicity of nano-scale TiO₂, SiO₂ and ZnO water suspensions*. Water Science and Technology, 2006. **54**(11–12): p. 327–334.
37. Collins-Martinez, V., A.L. Ortiz, and A.A. Elguezabal, *Influence of the anatase/rutile ratio on the TiO₂ photocatalytic activity for the photodegradation of light hydrocarbons*. International Journal of Chemical Reactor Engineering, 2007. **5**: A29.
38. Page, K., et al., *Titania and silver-titania composite films on glass-potent antimicrobial coatings*. Journal of Materials Chemistry, 2007. **17**(1): p. 95–104.
39. Kim, J.P., et al., *Manufacturing of anti-viral inorganic materials from colloidal silver and titanium oxide*. Revue Roumaine De Chimie, 2006. **51**(11): p. 1121–1129.
40. Wei, C., et al., *Bactericidal activity of TiO₂ photocatalyst in aqueous-media - Toward a solar-assisted water disinfection system*. Environmental Science & Technology, 1994. **28**(5): p. 934–938.
41. Reed, R.H., *The inactivation of microbes by sunlight: Solar disinfection as a water treatment process*. Advances in Applied Microbiology, Vol 54, 2004. **54**: p. 333–365.
42. Blanco, J., et al., *Review of feasible solar energy applications to water processes*. Renewable & Sustainable Energy Reviews, 2009. **13**(6–7): p. 1437–1445.
43. Chong, M.N., et al., *Optimisation of an annular photoreactor process for degradation of Congo Red using a newly synthesized titania impregnated kaolinite nano-photocatalyst*. Separation and Purification Technology, 2009. **67**(3): p. 355–363.
44. Belhacova, L., et al., *Inactivation of microorganisms in a flow-through photoreactor with an immobilized TiO₂ layer*. Journal of Chemical Technology and Biotechnology, 1999. **74**(2): p. 149–154.
45. Chan, A.H.C., et al., *Solar photocatalytic thin film cascade reactor for treatment of benzoic acid containing wastewater*. Water Research, 2003. **37**(5): p. 1125–1135.
46. Fernandez-Ibanez, P., et al., *Application of the colloidal stability of TiO₂ particles for recovery and reuse in solar photocatalysis*. Water Research, 2003. **37**(13): p. 3180–3188.
47. Doll, T.E. and F.H. Frimmel, *Cross-flow microfiltration with periodical back-washing for photocatalytic degradation of pharmaceutical and diagnostic residues-evaluation of the long-term stability of the photocatalytic activity of TiO₂*. Water Research, 2005. **39**(5): p. 847–854.
48. Zhang, X.W., et al., *TiO₂ nanowire membrane for concurrent filtration and photocatalytic oxidation of humic acid in water*. Journal of Membrane Science, 2008. **313**(1–2): p. 44–51.
49. Zhao, Y.J., et al., *Fouling and regeneration of ceramic microfiltration membranes in processing acid wastewater containing fine TiO₂ particles*. Journal of Membrane Science, 2002. **208**(1–2): p. 331–341.
50. Lee, D.K., et al., *Photocatalytic oxidation of microcystin-LR in a fluidized bed reactor having TiO₂-coated activated carbon*. Separation and Purification Technology, 2004. **34**(1–3): p. 59–66.
51. Li, Y.J., M.Y. Ma, and X.H. Wang, *Inactivated properties of activated carbon-supported TiO₂ nanoparticles for bacteria and kinetic study*. Journal of Environmental Sciences-China, 2008. **20**(12): p. 1527–1533.
52. Chong, M.N., et al., *Synthesis and characterisation of novel titania impregnated kaolinite nano-photocatalyst*. Microporous and Mesoporous Materials, 2009. **117**(1–2): p. 233–242.

53. Zhu, H.Y., et al., *Hydrogen titanate nanofibers covered with anatase nanocrystals: A delicate structure achieved by the wet chemistry reaction of the titanate nanofibers*. Journal of the American Chemical Society, 2004. **126**(27): p. 8380–8381.
54. Kwak, S.Y., S.H. Kim, and S.S. Kim, *Hybrid organic/inorganic reverse osmosis (RO) membrane for bactericidal anti-fouling. 1. Preparation and characterization of TiO₂ nanoparticle self-assembled aromatic polyamide thin-film-composite (TFC) membrane*. Environmental Science & Technology, 2001. **35**(11): p. 2388–2394.
55. Tang, C. and V. Chen, *The photocatalytic degradation of reactive black 5 using TiO₂/UV in an annular photoreactor*. Water Research, 2004. **38**(11): p. 2775–2781.
56. Gelover, S., et al., *A practical demonstration of water disinfection using TiO₂ films and sunlight*. Water Research, 2006. **40**(17): p. 3274–3280.
57. Jia, G., et al., *Cytotoxicity of carbon nanomaterials: Single-wall nanotube, multi-wall nanotube, and fullerene*. Environmental Science & Technology, 2005. **39**(5): p. 1378–1383.
58. Kang, S., et al., *Antibacterial effects of carbon nanotubes: Size does matter*. Langmuir, 2008. **24**(13): p. 6409–6413.
59. Narayan, R.J., C.J. Berry, and R.L. Brigmon, *Structural and biological properties of carbon nanotube composite films*. Materials Science and Engineering B-Solid State Materials for Advanced Technology, 2005. **123**(2): p. 123–129.
60. Markovic, Z., et al., *The mechanism of cell-damaging reactive oxygen generation by colloidal fullerenes*. Biomaterials, 2007. **28**(36): p. 5437–5448.
61. Hu, L.B., D.S. Hecht, and G. Gruner, *Carbon nanotube thin films: Fabrication, properties, and applications*. Chemical Reviews, 2010. **110**(10): p. 5790–5844.
62. Schoen, D.T., et al., *High speed water sterilization using one-dimensional nanostructures*. Nano Letters, 2010. **10**(9): p. 3628–3632.
63. Vecitis, C.D., et al., *Electrochemical multiwalled carbon nanotube filter for viral and bacterial removal and inactivation*. Environmental Science & Technology, 2011. **45**(8): pp. 3672–3679.
64. Brady-Estevez, A.S., S. Kang, and M. Elimelech, *A single-walled-carbon-nanotube filter for removal of viral and bacterial pathogens*. Small, 2008. **4**(4): p. 481–484.
65. Heymann, D., *Solubility of fullerenes C-60 and C-70 in seven normal alcohols and their deduced solubility in water*. Fullerene Science and Technology, 1996. **4**(3): p. 509–515.
66. Spesia, M.B., A.E. Milanese, and E.N. Durantini, *Synthesis, properties and photodynamic inactivation of Escherichia coli by novel cationic fullerene C-60 derivatives*. European Journal of Medicinal Chemistry, 2008. **43**(4): p. 853–861.
67. Brant, J.A., et al., *Characterizing the impact of preparation method on fullerene cluster structure and chemistry*. Langmuir, 2006. **22**(8): p. 3878–3885.
68. Fortner, J.D., et al., *C-60 in water: Nanocrystal formation and microbial response*. Environmental Science & Technology, 2005. **39**(11): p. 4307–4316.
69. Zhang, D., G. Li, and J.C. Yu, *Inorganic materials for photocatalytic water disinfection*. Journal of Materials Chemistry, 2010. **20**(22): p. 4529.
70. Hayden, S.C., N.K. Allam, and M.A. El-Sayed, *TiO₂ nanotube/CdS hybrid electrodes: Extraordinary enhancement in the inactivation of Escherichia coli*. Journal of the American Chemical Society, 2010. **132**(41): p. 14406–14408.
71. Kang, Q., et al., *A ternary hybrid CdS/Pt-TiO₂ nanotube structure for photoelectrocatalytic bactericidal effects on Escherichia coli*. Biomaterials, 2010. **31**(12): p. 3317–3326.
72. Baram, N., et al., *Enhanced inactivation of E. coli bacteria using immobilized porous TiO₂ photoelectrocatalysis*. Electrochimica Acta, 2009. **54**(12): p. 3381–3386.
73. Allam, N.K. and C.A. Grimes, *Effect of cathode material on the morphology and photoelectrochemical properties of vertically oriented TiO₂ nanotube arrays*. Solar Energy Materials and Solar Cells, 2008. **92**(11): p. 1468–1475.
74. Allam, N.K., K. Shankar, and C.A. Grimes, *Photoelectrochemical and water photoelectrolysis properties of ordered TiO₂ nanotubes fabricated by Ti anodization in fluoride-free HCl electrolytes*. Journal of Materials Chemistry, 2008. **18**(20): p. 2341.

75. Spadaro, J.A., et al., *Antibacterial effects of silver electrodes with weak direct current*. *Antimicroblal Agents and Chemotherapy*, 1974. **6**(5): p. 637–642.
76. Akhavan, O. and E. Ghaderi, *Enhancement of antibacterial properties of Ag nanorods by electric field*. *Science and Technology of Advanced Materials*, 2009. **10**(1): p. 015003.
77. Tsong, T.Y., *Electroporation of cell-membranes*. *Biophysical Journal*, 1991. **60**: p. 297–306.
78. Li, X.Y., et al., *Electrochemical disinfection of saline wastewater effluent*. *Journal of Environmental Engineering*, 2002. **128**(8): p. 697–704.
79. He, J., T. Kunitake, and A. Nakao, *Facile in situ synthesis of noble metal nanoparticles in porous cellulose fibers*. *Chemistry of Materials*, 2003. **15**(23): p. 4401–4406.
80. Maneerung, T., S. Tokura, and R. Rujiravanit, *Impregnation of silver nanoparticles into bacterial cellulose for antimicrobial wound dressing*. *Carbohydrate Polymers*, 2008. **72**(1): p. 43–51.
81. Cates, E.L., M. Cho, and J.-H. Kim, *Converting visible light into UVC: Microbial inactivation by Pr³ + -activated upconversion materials*. *Environmental Science & Technology*, 2011, **45**(8): p. 3680–3686. doi: [10.1021/es200196c](https://doi.org/10.1021/es200196c)
82. Nicholson, W.L. and B. Galeano, *UV resistance of Bacillus anthracis spores revisited: Validation of Bacillus subtilis spores as UV surrogates for spores of B. anthracis Sterne*. *Applied and Environmental Microbiology*, 2003. **69**(2): p. 1327–1330.

Section IV
Toxicology of Nano-Antimicrobials

Chapter 17

Microorganisms: A Versatile Model for Toxicity Assessment of Engineered Nanoparticles

Ashutosh Kumar, Alok K. Pandey, Rishi Shanker, and Alok Dhawan

17.1 Introduction

Nanotechnology is the understanding and control of matter at the nanoscale, at dimensions between approximately 1 and 100 nm, where unique phenomena enable novel applications (www.nano.gov). The nano-structures exhibit significant novel and improved physical, chemical, biological properties and processes due to their size. Also, the unique optical, magnetic, electrical and physicochemical properties of engineered nanoparticles (ENPs) arise due to higher surface-to-volume ratios and an increased number of atoms on particle boundaries than their bulk counterparts. Due to their distinctive characteristics, ENPs are widely used in cosmetics, food packaging, drug delivery systems, therapeutics, biosensors, and others. Since the size of ENPs is approximately equivalent to the biological macromolecules and due to their antibacterial and antifungal properties, nanomaterials are extensively used for a number of commercial products such as wound dressings, detergents and antimicrobial coatings.

Microorganisms are the most important component of all known ecosystems and play an important primary role in biogeochemical cycles, degradation of pollutants, basis of food webs and soil health. They could serve as potential mediators of nanoparticle transformations that affect their mobility and toxicity. Wiesner et al. has stated that “Microbial ecotoxicology is a particularly important consideration in elucidating cytotoxicity mechanisms that could be extrapolated to eukaryotic cells” [1]. However, it is also clear that no single test system or living organism shows uniform sensitivity to all compounds, and therefore an array of different test systems with different sensitivity profiles are often recommended and used to get a broad idea of the risks posed by the nanoparticles.

A. Kumar • A.K. Pandey • R. Shanker • A. Dhawan (✉)
Nanomaterial Toxicology Group, CSIR-Indian Institute of Toxicology Research,
Lucknow-226001, UP, India
e-mail: dhawanalok@hotmail.com; alokdhawan@iitr.res.in

The use of nanotechnology in consumer products continues to grow on a rapid and consistent basis. The number of nano-products in March 2006 was 212, whereas more than 1,300 manufacturer-identified nanotechnology-enabled products are now available in the commercial market and this number is predicted to be ~3,400 by 2020 [2]. The existing inventory of the Project on Emerging Nanotechnologies (PEN) is dominated by health and fitness items (56%), with nano-silver products (24%) having the maximum share. According to the US National Nanotechnology Initiative, thousands of tons of silica, alumina, and ceria, in the form of ultrafine coarse particle mixtures including nanoparticles, are used each year in slurries for precision polishing of silicon wafers. The manufacture of fullerenes alone could soon match the production of engineered metal oxide nanoparticles with an annual production of 1,500 million tons. The zinc oxide industries with over 300 companies around the world are producing in excess of 1.2 million tons of ZnO nanoparticles per year. The production rate of metal oxide nanoparticles for cosmetics is estimated to be 1,000 tons per year [3]. Due to the large production and widespread use in consumer products, it is expected that ENPs will be released into aquatic, terrestrial, and atmospheric environments through washing and disposal, where their fate and behavior are still largely unknown (Fig. 17.1). Despite having several benefits in the application of ENPs, there are doubts about their environmental fate. Hence, the concern for the adverse effects of such ENPs, both to human and environmental health continues to grow with their diverse applications [4]. The unique properties of ENPs, such as high specific surface area, abundant reactive sites on the surface, and a large fraction of atoms located on the exterior face as well as mobility, could make them a special class of hazardous pollutant that may cause unexpected hazards to public and environmental health [1, 5].

The concern that the ENPs could be hazardous to ecosystems is partly fuelled by several examples in history that illustrate the unintentional environmental release of “beneficial” chemicals, such as DDT (Dichlorodiphenyltrichloroethane), which was used to control malaria but was later found to be carcinogenic to humans and toxic to several bird species. Endosulfan, an organochlorine insecticide, was used in

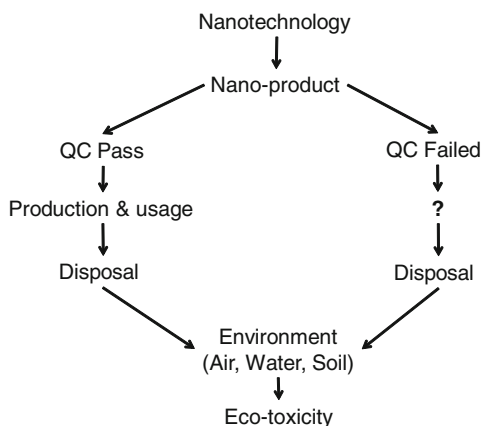


Fig. 17.1 Schematic showing the disposal of engineered nanoparticles in the ecosystems

agriculture around the world to control insects and pests. It was earlier considered safe but is now banned in 74 countries due to severe health implications including deformities in limbs, loss of motor nervous control, brain damage, delayed puberty and cancer. It persists in the environment for a long time, circulates globally and passes on from the mother to the child, causing intergenerational health effects.

Currently, ENPs are being incorporated into commercial products at a faster rate than the development of knowledge and regulations to mitigate potential environmental impacts associated with their manufacture, application and disposal. A variety of ENPs with different chemical compositions, synthesized through different methods, differing in size, shape, surface coatings, etc. have been shown to be genotoxic and cytotoxic using different models such as prokaryotes [6–8], plants [3, 9], human cell lines [10–13] and aquatic models [14, 15]. The bioavailability and toxicity of ENPs to microbes is a major area of concern because the microbes are primary degraders and perform a critical role in ecosystems. There is now considerable evidence that ENPs exhibit antibacterial activity in clinical bacterial isolates of *Escherichia coli*, *Pseudomonas aeruginosa* and *Staphylococcus aureus* (Table 17.1). Hence, there is a concern that, due to the ever-increasing use of nanoparticles in products, even the beneficial bacteria both in humans and the environment will get exposed (Fig. 17.2). This also raises the possibility that the release of ENPs may be detrimental to important bio-geochemical processes in the soil such as carbon or nitrogen cycling. Therefore, organisms, especially those that interact strongly with their immediate environment such as algae, plants, and fungi, are expected to be affected as a result of their exposure to ENPs. It is also likely that the ENPs can directly interact with the food web at different trophic levels and affect the ecological sustenance [50]. The bio-magnification of ENPs across the genera is of immediate concern. Any adverse effect caused by ENPs in living organisms will directly affect the carrying capacity of the ecosystems.

Other biological methods to test ENPs toxicity in organisms across all the major phyla currently depend on standard regulatory test species and whole organisms in ecotoxicity testing either in laboratory experiments [51] or field exposure scenarios [52]. A major constraint in risk assessment is to mimic the actual exposure to ENPs and biological variability with different test conditions. The models and methods currently used in toxicity assessment are costly, tedious, time consuming and require a culture facility with skilled personnel. A more viable option is microorganisms that can be cultured quickly and cost effectively, are easy to handle and could serve as an ideal alternative to different test models. Furthermore, the advancement in molecular biology and recombinant DNA technologies has created numerous possibilities for manipulating the microorganisms to study the ENPs-induced cellular and molecular responses. The microorganisms have a short doubling time which gives an additional benefit to express different proteins in a shorter time span. Several other 'omic' approaches can also be used to gather the information about the cellular responses to ENPs which could help in understanding the mechanism of toxicity in higher organisms (Fig. 17.3).

This chapter deals with the approaches, advantages and versatility of microbial systems for toxicity assessment of ENPs. In addition, an attempt has also been made

Table 17.1 Microorganisms used as models to assess toxicity responses of engineered nanoparticles (ENPs)

Organism	Particle type/size	Concentration	Assay	Results/outcome	Reference
<i>Bacteria</i>					
<i>Escherichia coli</i>	Zinc oxide nanoparticles/size not reported	15.63–1,000 µg/mL	Microtiter plate-based method using resazurin indicator dye solution for cytotoxicity assay, disk diffusion method	Antibacterial activity was observed at 500 µg/mL by resazurin dye method whereas for disk diffusion assay it was 400 µg/mL	[16]
	Zinc oxide nanoparticles/20–30 nm	5–45 µg/mL	Spectroscopic methods (OD ₆₀₀) for cytotoxicity assay	Antibacterial activity was observed at 15 µg/mL	[17]
	Zinc oxide nanoparticles/10–20 nm	1×10^{-3} – 10×10^{-3} M	Cell viability assay (standard plate count method)	Nanoparticles were internalized in the cells and induced toxicity at concentrations higher than 1.7×10^{-3} M	[18]
	Zinc oxide NPs/size not reported	2–40 mg/L	Spectroscopic methods (OD ₆₀₀) for cytotoxicity assay	No toxicity was observed	[19]
	Silver nanoparticle/10–15 nm	20–100 µg/mL	Bacterial growth kinetics by surface spread plate method and bacterial phosphotyrosine profile for signaling transduction	Exhibited antibacterial activity with a minimum inhibitory concentration (MIC) of 25 µg/mL	[20]
	Silver nanoparticles/<12 nm	10–60 µg/mL	Cell viability assay (standard plate count method)	Exhibited antibacterial activity with a MIC of 20 µg/mL	[21]
	Silver nanoparticle/truncated triangular plates, rods, and polyhedral plates/average size 39 nm	1–100 µg/mL	Cytotoxicity assay by surface spread plate method	Truncated triangular particles completely inhibited cell growth at 10 µg/mL whereas 100 µg/mL of rod shaped particles induced inhibition after prolonged exposure	[22]

Titanium dioxide (TiO ₂)/ 25 nm Degussa	0.01–1 mg/mL	Cell viability assay (standard plate count methods), lipid peroxidation assay, determination of cellular respiration using 2,3,5-triphenyltetrazolium formazan (TTF) dye	UV light activated particles exhibited higher toxicity than inactivated particles at concentration 0.1 mg/mL. Activated nanoparticles also induced significant membrane damage and lipid peroxidation at the same concentration	[23]
TiO ₂ /66 nm, 950 nm, and 44 µm), SiO ₂ /(14 nm, 930 nm, and 60 µm) ZnO/(67 nm and 820 nm)	10–5,000 ppm	Spectroscopic methods (OD ₆₀₀) and standard plate count methods for cell viability assay	The antibacterial activity of TiO ₂ was significantly higher in the presence of light	[24]
Al ₂ O ₃ /Degussa/spherical 11–13 nm, TiO ₂ /spherical/17 nm, MWCNT/elongated/L:1.5 µm and D:44.0 nm	10–500 mg/L	Live/Dead Viability Assay using flow cytometry and reactive oxygen species generation by DCFDA dye	Al ₂ O ₃ , TiO ₂ , MWCNT exhibited bactericidal effects at concentration 100 mg/L and also able to induce significant ROS at same concentration	[7]
Magnesium oxide/3.6 µm	100 mg/mL	Halo Test and conductance assay for cytotoxicity	MgO powder has antibacterial against <i>E. coli</i> and The zone of inhibition for <i>E. coli</i> was smaller than that of <i>S. aureus</i>	[25]
Multi-walled carbon nanotubes/D: 17–35 nm, L: 2.3–91 µm	4 mg/mL	Dead discrimination assay using PI dye by flow cytometry	Different shapes of MWCNT exhibit growth inhibition	[26]
Zinc oxide nanoparticles/20–30 nm	5–45 µg/mL	Spectroscopic methods (OD ₆₀₀) for cytotoxicity assay	Bacterial growth was inhibited at 15 µg/mL	[17]
Zinc oxide nanoparticles capped with tetramethylammonium hydroxide	39.1–5,000 µg/plate	Ames Test	Mutagenicity was negative in all strains at all concentrations	[27]

Salmonella typhimurium

(continued)

Table 17.1 (continued)

Organism	Particle type/size	Concentration	Assay	Results/outcome	Reference
<i>Staphylococcus aureus</i>	TiO ₂ / <25 nm and ZnO/30 nm	0.008–8 µg/plate	Ames Test	ZnO NPs induced frameshift mutation with metabolic activation system whereas TiO ₂ NPs induced frame shift mutation with and without metabolic activation system. Both NPs were also found to induce oxidative mutation in <i>E. coli</i> strain WP2uvrA	[28]
	Al ₂ O ₃ / <50 nm, Co ₃ O ₄ / <50 nm, CuO/ <50 nm, TiO ₂ / <100 nm ZnO/ <100 nm	100–1,600 µg/plate	Ames Test	TiO ₂ and ZnO NPs induced reverse mutants to <i>E. coli</i> strain WP2uvrA with metabolic activation	[29]
	MWCNT/0.2–1 µm	50–5,000 µg/plate	Ames test	Mutagenicity was negative in all strains at all concentrations	[30]
	MWCNT/D: 110–170 nm, L: 5–9 µm	0.01–9 µg/plate	Ames Test	Mutagenicity was negative in all strains at all concentrations	[31]
	FePt nanoparticles/3 nm	39.1–5,000 µg/plate	Ames Test	Mutagenicity was negative in all strains at all concentrations	[32]
<i>Staphylococcus aureus</i>	Zinc oxide nanoparticles/size not reported	15.63–1,000 µg/mL	Microtiter plate-based method using resazurin indicator dye solution for cytotoxicity assay, disk diffusion method	Antibacterial activity was observed at 500 µg/mL by resazurin dye method whereas for disk diffusion assay it was 400 µg/mL	[16]
	Zinc oxide nanoparticles/150 nm	0.0006–0.12 M	Cytotoxicity assay by surface spread plate method and disk diffusion assay	Exhibited antibacterial activity with a MIC of 0.12	[33]

Zinc oxide nanoparticles/ 20–30 nm	5–45 µg/mL	Spectroscopic methods (OD ₆₀₀) and standard plate count methods for cell viability assay	Microbial growth was inhibited at 15 µg/mL	[17]
MgO, TiO ₂ , Al ₂ O ₃ , CuO, CeO ₂ and ZnO nanoparticles/size not reported	1–10 mM	Spectroscopic methods (OD ₆₀₀) and standard plate count methods for cell viability assay	MgO, TiO ₂ , CuO and CeO ₂ , did not show any significant growth inhibition up to 10 mM suspension, whereas Al ₂ O ₃ and ZnO showed significant growth inhibition at 2 mM concentration	[34]
Zinc oxide nanoparticles/ 150 nm	0.0006–0.12 M	Cytotoxicity assay by surface spread plate method and disk diffusion assay	Exhibited an antibacterial activity with a MIC of 0.06 M	[33]
Zinc oxide nanoparticles/size not reported	15.63–1,000 µg/mL	Microtiter plate-based method using resazurin indicator dye solution for cytotoxicity assay, disk diffusion method	Antibacterial activity was observed at 500 µg/mL by resazurin dye method whereas for disk diffusion assay it was 400 µg/mL	[16]
Silver nanoparticle/ 65 ± 30 nm	20–2,000 ppb	Live/Dead Viability Assay using flow cytometry and spectroscopic methods (OD ₆₀₀) for cytotoxicity assay	Silver NPs are found to be internalized in cells and resulting into the thinning of biofilm (biomass)	[35]
Fullerene water suspensions/ 30–100 nm	0.2–1.2 mg/L	Spectroscopic methods (OD ₆₀₀) for cytotoxicity assay	Exhibited antibacterial activity with a MIC of 0.5 ± 0.13 mg/L	[36]
Silver nanoparticles/biogenic and chemically synthesized/2–11 nm	25 µg/mL	Live/Dead Viability Assay using flow cytometry and Cytotoxicity assay by spectrophotometer (OD ₆₀₀) and disk diffusion method	Diameter of the inhibition zone (DIZ) and the cytotoxicity of biogenic- Ag were greater than that observed with <i>E. coli</i>	[37]

(continued)

Table 17.1 (continued)

Organism	Particle type/size	Concentration	Assay	Results/outcome	Reference
	TiO ₂ /66 nm, 950 nm, and 44 µm), SiO ₂ /(14 nm, 930 nm, and 60 µm) ZnO/(67 nm and 820 nm)	10–5,000 ppm	Spectroscopic methods (OD ₆₀₀) and standard plate count methods for bacterial cytotoxicity	The antibacterial activity of TiO ₂ NPs was significantly greater in the presence of light than the dark and the toxicity was greater with <i>B. subtilis</i>	[24]
<i>Vibrio fischeri</i>	Zinc oxide nanoparticles/50–70 nm	0.1–1,000 mg/L	luminescence inhibition test	The luminescence of the treated cell reduced significantly and the observed EC50 was 4.8 mg/L	[38]
	Zinc oxide nanoparticles/50–70 nm, pH 6.5	0.1–1,000 mg/L	Toxicity of growth inhibition (<i>V. fischeri</i>), crustacean toxicity assays (SOP)	All Zn formulations were very toxic with an EC50 for bulk ZnO, nano ZnO and ZnSO ₄ ·7 H ₂ O of 1.8, 1.9, 1.1 mg/L, respectively	[39]
<i>Klebsiella pneumoniae</i>	Zinc oxide nanoparticles/20–30 nm	5–45 µg/mL	Spectroscopic methods (OD ₆₀₀) for cytotoxicity assay	Inhibition of the microbial growth was observed at 5 µg/mL	[17]
<i>Nitrifying bacterial culture</i>	Silver nanoparticles/9–21 nm	0.05–1 mg/L	Cytotoxicity assay by measuring dissolve oxygen level and ROS measurement by H ₂ DCFDA dye	Silver nanoparticles exhibited antibacterial activity with a MIC of 0.14 mg/L	[40]
<i>Mycobacterium smegmatis</i>	Zinc oxide NPs/size not reported	2–40 mg/L	Spectroscopic methods (OD ₆₀₀) for cytotoxicity assay	Inhibition of cell growth was observed at 40 mg/L ZnO NPs	[19]
<i>Cupriavidus metallidurans</i>	Al ₂ O ₃ /Degussa/spherical 11–13 nm, TiO ₂ /spherical/17 nm, MWCNT/elongated/L: 1.5 µm and D: 44.0 nm	10–500 mg/L	Live/Dead Viability Assay using flow cytometry and ROS measurement by DCFDA dye	Al ₂ O ₃ , TiO ₂ , MWCNT exhibited bactericidal effects at concentrations 100 mg/L	[7]

<i>Shewanella oneidensis</i>	Silver nanoparticles/biogenic and chemically synthesized/2–11 nm	25 µg/mL	Live/Dead Viability Assay using flow cytometry and Cytotoxicity assay by spectrophotometer(OD ₆₀₀) and disk diffusion method	DIZ and the cytotoxicity of biogenic-Ag were greater than the chemically synthesized	[37]
	Zinc oxide NPs/size not reported	2–40 mg/L	Spectroscopic methods (OD ₆₀₀) for cytotoxicity assay	ZnO NPs did not inhibit the cell growth	[19]
<i>Viruses</i>					
Bacteriophages MS2, ΦX174 and PRD-1	Al ₂ O ₃ , TiO ₂ , and CeO ₂ were treated with different halogens	20 mg/mL	Plaque formation assay	Showed promise disinfectants against bacteriophages MS2, ΦX174 and PRD-1	[41]
HIV-1 Virus	Silver nanoparticles/1–10 nm	>25 µg/mL	Interaction of NPs with HIV-1 using high angle annular dark field (HAADF) scanning transmission electron microscopy	AgNP binds with gp120 glycoprotein knobs of HIV-1 and inhibits the binding of the virus to host cells	[42]
<i>Yeast</i>					
<i>Saccharomyces cerevisiae</i>	Zinc oxide NPs/size not reported	2–40 mg/L	Spectroscopic methods (OD ₆₀₀) for cytotoxicity assay	<i>S. oneidensis</i> was not inhibited by ZnO NPs	[19]
	TiO ₂ NPs/25–70 nm, ZnO NPs/50–70 nm and CuO/30 nm	TiO ₂ : 1–20,000 mg/L ZnO: 10–1,000 mg/L CuO: 1–10,000 mg/L	Growth responses by viable cell count method	Growth was inhibited with an EC ₅₀ of 131–158 mg/L for ZnO, 873 mg/L for CuO and for TiO ₂ it was even more than 20,000 mg/L	[43]
<i>Algae</i>					
<i>Thalassiosira pseudonana</i> , <i>Chaetoceros gracilis</i> ,	Zinc oxide nanoparticles/D: 6.3–15.4 nm, L: 242–862 nm	10–80 mg/L	Cytotoxicity assay by algal cell count method	ZnO NPs stopped the growth of <i>T. pseudonana</i> and <i>C. gracilis</i> , whereas <i>P. tricornutum</i> was the least sensitive	[44]

(continued)

Table 17.1 (continued)

Organism	Particle type/size	Concentration	Assay	Results/outcome	Reference
<i>Phaeodactylum tricornutum</i>	Nickel oxide/20 nm	10–50 mg/L	Growth-inhibition test	Exhibited toxic responses with an EC ₅₀ of 32.28 mg/L for 72 h	[45]
<i>Chlorella vulgaris</i>	Zinc oxide NPs/size not reported	2–40 mg/L	Spectroscopic methods (OD ₆₀₀) for cytotoxicity assay	<i>Cyanothece</i> in aquatic media was inhibited at 40 mg/L	[19]
<i>Cyanothece</i>	TiO ₂ /34 nm and Al ₂ O ₃ /17 nm	5–100 mg/mL	Cytotoxicity assay by algal cell count method	TiO ₂ and Al ₂ O ₃ inhibited the growth of <i>C. dubia</i> and the EC ₅₀ values were 42 and 45 mg/L for TiO ₂ and Al ₂ O ₃ , respectively	[46]
<i>Pseudokirchneriella subcapitata</i> and <i>Ceriodaphnia dubia</i>	CuO/30 nm, ZnO/50–70 nm TiO ₂ /25–70 nm	ZnO: 0–0.5 mg/L TiO ₂ : 0–120 mg/L CuO: 0–7 mg/L	Cytotoxicity assay by fluorescence measurement assay and algal cell count method	Inhibit the algal growth with EC ₅₀ of 0.04 mg/L for ZnO, 5.83 mg/L for TiO ₂ and 0.71 mg/L for CuO	[47]
<i>Fungi</i> <i>Candida albicans</i> <i>Candida parapsilosis</i> , <i>Candida tropicalis</i>	Silver nanoparticles/25 nm	0.05–54 mg/L	Microdilution method	Exhibited fungicidal activity with a MIC of 0.1 mg/L for <i>Candida albicans</i> and 0.84 and 0.42 mg/L for <i>C. parapsilosis</i> and <i>C. tropicalis</i> respectively	[48]
<i>Botrytis cinerea</i> , <i>Penicillium expansum</i>	Zinc oxide/70 ± 15 nm	0–12 mM/L	Agar dilution method and morphological changes	Average growth of <i>B. cinerea</i> was inhibited by 63% to 80% whereas for <i>P. expansum</i> the reduction rate was varied from 61% to 91% in terms of colony growth with increasing concentration from 3 to 12 mmol/L	[49]

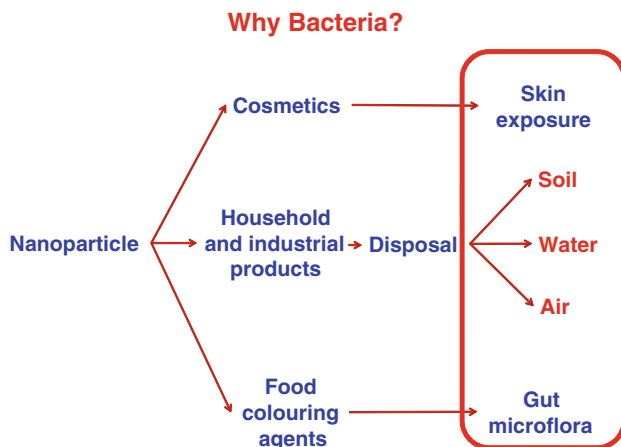


Fig. 17.2 The importance of bacteria in the ecosystem and possible routes of exposures to engineered nanoparticles

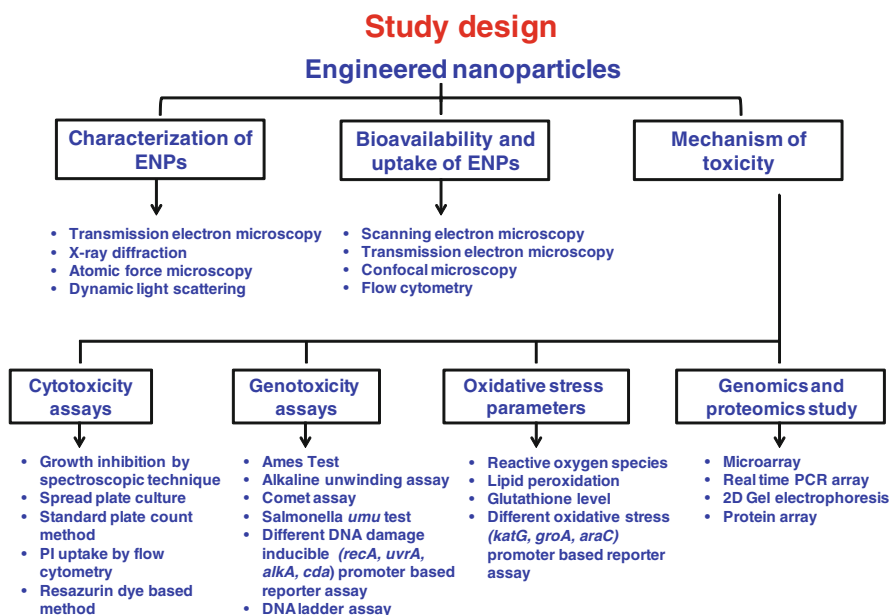


Fig. 17.3 Study design to evaluate the toxicity of engineered nanoparticles in bacteria

to address the knowledge gaps and problems in the experimentation and how these could be overcome. To assess the toxicity of ENPs, the primary criterion is to have full knowledge of the ENPs to be tested. Considering the novel characteristics of ENPs, unlike their chemical counterparts, it is imperative to undertake their comprehensive characterization prior to toxicity evaluation (Fig. 17.4).

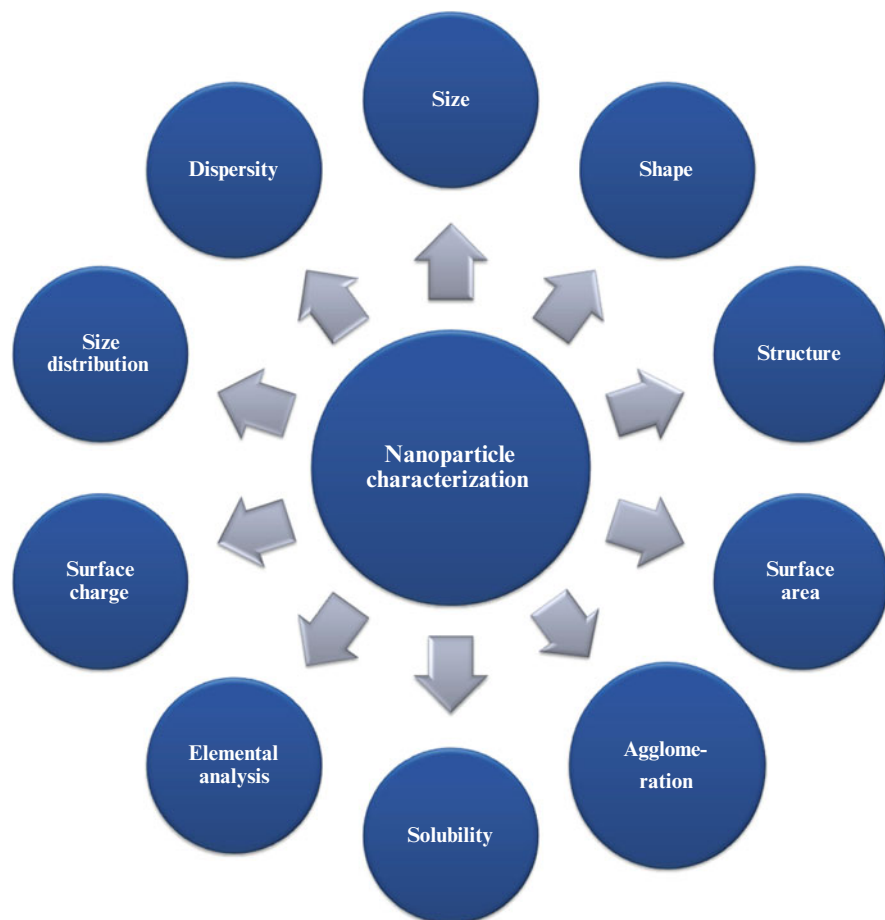


Fig. 17.4 Measurement of different physiochemical properties for engineered nanoparticles

17.2 Characterization

The behavior and activity of ENPs is largely dependent on a number of physical and chemical properties such as particle number, mass concentration, surface area, charge, chemistry and reactivity, size distribution, aggregation, elemental composition, as well as structure and shape. Therefore, a complete characterization is essential for interpreting the results. The characterization of ENPs should be carried out in order to learn about the specific physiochemical properties such as purity, crystallinity, solubility, chemical composition, surface chemistry, reactivity, size, shape, surface area, surface porosity, roughness, morphology, etc. Determination of the hydrodynamic size, size distribution, zeta potential, dispersity and the concentration and time at which agglomeration occurs should be done in the biological medium (Fig. 17.4; Table 17.2).

Table 17.2 Significance of measuring the physicochemical properties of engineered nanoparticles

Sl. No.	Nanoparticle property	Significance
1.	Size	Nanoparticles possess a unique physicochemical property due to their size; it also affects the mobility and transport behavior of the particles
2.	Shape	Particles with different shapes (e.g., spherical, tubular, and cubical) have different affinities and accessibilities towards the cell wall. Antibacterial activity of nanoparticles has also been reported due to their shape and size
3.	Structure	The structure of the nanoparticles can influence the stability and behavior of the particles (e.g. rutile and anatase are the possible crystal structures of TiO ₂ NPs)
4.	Surface area	As the size of nanoparticles reduces, the corresponding surface area increases leading to higher reactivity and sorption behaviour
5.	Agglomeration tendency	Agglomeration affects the surface properties of particles and their bio-availability to the cells
6.	Solubility	Some of the nanoparticles are reported to produce ions in soluble form which may be toxic to the cells e.g., ZnO, CuO
7.	Elemental composition	Elemental composition shows as to whether the nanoparticles have contamination that may lead to false positive results or nanoparticle behavior
8.	Size distribution	Size distribution of the particles gives an idea of the size range and helps in interpreting the results
9.	Surface charge and dispersity	Surface charge of the nanoparticles affects the particle solubility in suspension, whereas the dispersity of particles provides information about their tendency to agglomerate

Different microscopic and spectroscopic techniques have been used to characterize the ENPs. Microscopy-based methods include optical approaches, i.e. confocal microscopy, as well as electron and scanning probe microscopy. The dimensions of ENPs are below the diffraction limit of visible light; hence, they are beyond the range of optical microscopy. However, near-field scanning optical microscopy (NSOM) is the kind of scanning probe microscopy (SPM) technique that can achieve a spatial resolution of 50–100 nm through the use of a sub-wavelength diameter aperture. It is better than the conventional optical microscopes to visualize the agglomeration of ENPs. The diffraction of light is also the limiting factor for the conventional confocal microscopy. However, confocal laser scanning microscopy (CLSM) has a higher resolution (up to 200 nm), hence the fluorescent ENPs (natural and labeled) can be observed. Recently, for non-fluorescent particles, a reflection-based study using confocal microscopy has been reported [53, 54].

Electron microscopy (scanning electron microscopy, SEM; transmission electron microscopy, TEM; and atomic force microscopy, AFM) is the most popular and extensively used technique to characterize the ENPs. This technique not only gives visual images of the ENPs but also provides the information about the properties such as size, state of aggregation, dispersion, structure and shape [55]. In TEM, electrons are transmitted through a specimen; therefore, the specimen needs to be well distributed and spread on the grid (in the case of materials) to get

a good image, whereas in SEM, scattered electrons are detected at the sample interface for imaging. Analytical tools, mostly spectroscopic, are coupled with electron microscopes for additional elemental analysis. For example, energy dispersive X-ray spectroscopy (EDS) when combined with SEM and TEM provides percentage elemental composition of ENPs [28]. Other analytical tools, like electron energy loss spectroscopy (EELS) when coupled with TEM, detect the elements based on the loss of energy of the incident electron through the specimen [55]. Selected area electron diffraction (SAED) can also be combined with TEM to provide information on crystalline properties of particles [55].

Although electron microscopy is a very versatile tool for scientists in the area of nanotechnology, it has certain limitations. A critical limitation is that TEM and SEM are operated under vacuum, so it is difficult to analyze the liquid samples. The sample preparation steps of dehydration, cryo-fixation or embedding usually lead to sample alteration and dehydration artefacts [56]. Another disadvantage of the TEM is that the samples cannot be analyzed twice or used for validation of results. Further, the charging effects caused by the accumulation of static electric fields at the specimen due to the electron irradiation create confusion during imaging [57].

The atomic force microscopy (AFM) is also a kind of scanning probe microscope (SPM) which is a cost effective instrument and has several advantages in the characterization of ENPs. The main advantage of an AFM is that it images sub-nanometer structures under ambient air and liquid dispersion, and provides data about the size, shape, surface texture and roughness of the particles. In addition, multiple scanning of the sample can also be done to get robust statistics. There are some limitations of AFM for ENPs visualization; generally, the geometry of the probe is larger than the particles which lead to the overestimation of the lateral dimensions of the nanoparticles.

It can be summarized that a combination of microscopic techniques can be used to analyze the nanoparticles for size, shape, size distribution, etc. [58–60]. However, the analysis of the microscopic images is a crucial step because only small amounts of samples can be analyzed by microscopy which has an impact on the statistical significance of the results. The average particle size of ENPs is a value that depends on the number of particles counted and measured. As the ENPs in aqueous suspension have a tendency to agglomerate, it is important to count and measure sufficient numbers of particles to obtain robust statistics on each size fraction.

A wide range of spectroscopic techniques are available for the characterization of ENPs in suspension. Some of the important techniques used for the characterization of ENPs based on the light-scattering property are static (SLS) and dynamic light-scattering (DLS) and small-angle neutron-scattering (SANS).

Dynamic light-scattering (DLS) or photon correlation spectroscopy (PCS) measures time-dependent fluctuations in scattering intensity of light produced by particles in Brownian motion and yields the size of the particle by applying the Stokes–Einstein equation. DLS size of the nanoparticle is usually greater than that measured by other techniques, like TEM, Brunauer–Emmett–Teller (BET), etc. DLS is particularly very useful for sizing nanoparticles (based on intensity, volume and number) and determining particle stability/aggregation state in suspensions with respect to time and medium. It is a quantitative technique and gives the

statistically relevant data as compared to TEM [61]. Although DLS provides fast, in situ and real-time sizing, it also has certain limitations. For example, interference can be caused by a range of materials such as dust particles and nanoparticle impurities which influences the scattering intensity and skews the average hydrodynamic diameter towards the larger value. Also, the intensity of the scattered light is proportional to the sixth power of the particle diameter that makes it very sensitive to the presence of large particles, and the data obtained from samples containing particles with heterogeneous size distributions are difficult to interpret. DLS is considered an indispensable technique in toxicity studies, as it provides valuable information pertaining to the zeta potential, polydispersity and size range of the ENPs in the biological medium in which the organism is exposed.

Static light-scattering, also known as multi-angle (laser) light-scattering [MAL (L)S], provides information about the particle structure and, together with dynamic light-scattering, provides information about the shape of the particle [57]. In small-angle neutron-scattering (SANS), a beam of neutrons is focused on the sample, which can be solid (crystal, powder) or a suspension (aqueous, non-aqueous). These neutrons interact with the nuclei of the atoms and get scattered due to changes in the refractive index. The intensity of the scattered light gives information regarding the radius of gyration of a particle using Guinier's equation.

Therefore, it can be inferred that a combination of analytical methods is required to detect and characterize the nanoparticles in different matrices including air, soil, water and consumer products to which human beings and ecosystems are likely to be exposed. Additionally, this will also provide the broader idea related to the behavior of the particles which will be helpful for the toxicological and risk assessment of the nanoparticles.

17.3 Bioavailability and Uptake

Availability of the ENPs to the cell and their uptake is an important factor that can provide important information about their adverse and toxic effects on cellular systems. The exponential increase in usage of the ENPs-containing products in daily life has also enhanced the likelihood of their inadvertent release in the ecosystem through wastewater discharge or disposal/landfill. The environmental fate of the released ENPs largely depends on behavior, bioavailability and their interaction with aquatic colloids, such as natural organic matters (NOMs), humic substances, and salt ions. NOMs usually adsorb to the surface of the ENPs by different electrostatic, hydrogen bonding and hydrophobic interactions and affect the dispersity and bioavailability of the particles [62]. NOMs are classified into three major classes; (1) rigid biopolymers, such as polysaccharides and peptidoglycans produced by phytoplankton or bacteria, (2) fulvic compounds, mostly from terrestrial sources, originating from the decomposition products of plants, and (3) flexible biopolymers, composed of aquagenic refractory organic matter from a recombination of microbial degradation products [63]. ENPs in

aqueous suspension are dispersed due to the electrostatic and steric repulsion of the surface charge (positive/negative) present on the particle. As the surface charges of the particle skew towards the zero value, the repulsive forces between the particles reduce and ultimately settle down by gravitational forces. Due to agglomeration/aggregation, the physicochemical properties such as surface charge, size, size distribution, surface to volume ratio, surface reactivity of ENPs get altered which affects their bioavailability and toxicological responses. Fulvic compounds and flexible biopolymers have a tendency to modify the ENPs' surface charge which leads to the aggregation and non-bioavailability of the particle. An earlier report has demonstrated that humic acid coating of hematite reversed their charge from positive to negative leading to decreased attachment efficiencies from 1 to 0.01 mg/L to a sandy soil [64]. This resulted in the increased bioavailability and decreased agglomeration of the hematite. However, the rigid biopolymers, such as polysaccharides and peptidoglycans produced by phytoplankton and bacteria, coats the ENPs and increases their mobility and bioavailability to the cell [65]. Apart from the NOMs, several other factors can also influence the aggregation and bioavailability of the ENPs, examples being salt ion, presence of hydrophobic surfactant or polar groups on the surface of ENPs [66]. Trace metal ion speciation (especially oxides and oxide-coated ENPs) might alter the properties of ENPs, therefore altering their bioavailability and potential toxicity.

ENPs have also been demonstrated to absorb other pollutants on their surface due to their high surface area to volume ratio and complex-forming ability. Baun et al. showed that the toxicity of phenanthrene for *Daphnia magna* was increased by 60% in the presence of C₆₀ aggregates, and the availability of absorbed phenanthrene was also increased for the organisms [67]. The bioavailability of phenanthrene to plant roots also increased upon its adsorption to alumina ENPs [68]. In contrast, Knauer et al. has reported that presence of carbon black ENPs reduced the toxicity of diuron to green algae [69]. Fullerenes were found to decrease the toxicity of various chemicals to algae as a result of their decreased bioavailability [70].

Apparently, the formation of larger aggregates by high molecular weight NOMs compounds will favor the removal of ENPs from the sediments and is likely to decrease their bioavailability. However, solubilization by natural surfactants such as lower-molecular-weight NOM compounds will increase their mobility and further the bioavailability of ENPs. Furthermore, it is now clear that ENPs can serve as a transfer vectors for the pollutants in the environment. The ENPs can either enhance or diminish their bioavailability to the cells depending on the properties of the pollutant.

The detection of ENPs internalization in any model organism is a crucial step for understanding their behavior and toxicity. The commonly used methods for assessment of uptake of ENPs in the cells are transmission electron microscopy (TEM), scanning electron microscopy along with backscattered electron and energy-dispersive X-ray spectroscopy (SEM + BSE + EDS), confocal and fluorescence microscopy, reflection-based imaging and flow cytometry [10, 28, 71]. These techniques have several advantages for tracking the ENPs in the cells as well as in cellular organelles. The high resolution of TEM enables the imaging of membrane invagination, mode of ENPs uptake, and ultrastructural changes occurring in the cells subsequent to ENPs treatment.

SEM on the other hand is used to study the morphological changes and ENPs interaction with the cell. Whereas, EDS coupled with SEM provides an additional feature to analyze the elemental composition of the specimen based on the released energy by the corresponding element. Although these imaging techniques provide several advantages there are certain drawbacks, for example in TEM and SEM the samples have to be fixed, therefore live cell uptake cannot be monitored. It is also resource intensive, time consuming and confined to imaging of few cells. Furthermore, the staining process introduces electron dense artefacts that may be mistaken for nanoparticles [56]. Confocal and fluorescence microscopy, on the other hand, require that the particles be tagged with a probe or be doped with a fluorescence dye for their detection. Since the native nature of ENPs is lost, there is a likelihood that it may lead to their non-bioavailability leading to false/incorrect interpretation of observations.

Flow cytometry is another technique used to assess the uptake of ENPs in the cells. It is rapid, high throughput, cost effective, reliable, easy and sensitive technique that can analyse thousands of events rapidly in three dimensions, leading to the reduction of false negative or type II errors. In addition, flow cytometry provides a rapid, multi-parametric, single cell analysis with robust statistics, due to large number of events measured per treatment. In this method, a laser beam strikes on the stream of fluid containing a single cell suspension. The light diffracted, reflected and refracted by the cells is recorded by the photomultiplier tubes and the electronics convert these optical pulses to digital values. These values are then supplied to the computer with data representing the size and granularity of the cells as well as the intensity of the fluorochrome. It is well established that the light diffracted by the cells represent the forward light scatter and is used to measure the cellular size. However, the reflected and refracted light corresponds to the side scatter, which is a combined effect of the granularity and the cellular mass of the cell. ENPs in the host cell serve as granules and reflect/refract the light based on their intrinsic property. As the ENPs enter into the cell, the intensity of side scatter increases proportionately. However, a fluorescent particle can give an increased signal of side scatter as well as the fluorochrome intensity in a dose-dependent manner. Microbes have a very short dividing time, thus the internalization of the NPs in the cells and their retention for several generations can easily be monitored in a short time using flow cytometry. Several studies have demonstrated the internalization of the ENPs in cell lines using flow cytometry [10, 56, 72, 73].

Despite having several techniques to track the ENPs uptake in the bacterial cells, the precise mechanism of uptake is still unknown. The *silCBA* gene transportation operon is the most commonly accepted system for the transportation of silver NPs. The *silCBA* encodes a three-polypeptide efflux system including an inner membrane H^+ /cation antiporter. The protein SilA directly binds with the Ag^+ and transfers to the outer membrane protein SilC. The third protein SilB serves as an anchor, and transfers the silver to the inner membrane. Other gene clusters such as *silP*, *ORF105*, *silAB*, *ORF96*, *silC*, *silSR*, *silE* are the less-defined genes which also play an important role in ENPs transportation [74]. Nonspecific diffusion, nonspecific membrane damage and specific uptake (through porins) are the other possible mechanisms through which the ENPs could pass through the bacterial cell wall and membranes.

17.4 Microbe-Based Reporters

In this section of the chapter, the use of microbes as a bio-reporter to assess the toxic effects of ENPs and the possible mechanism is discussed.

17.4.1 Cytotoxicity

Cytotoxicity assessment is the first step towards understanding the alterations in normal cellular functions, when they interact with the ENPs. A wide range of methods are available to assess the cytotoxicity. Standard plate count, spread plate, spectroscopic (OD_{600}), flow cytometry using propidium iodide (PI) dye, and resazurin dye-based assay are some of the most commonly used methods. In the standard plate count method, the particle/treatment is mixed with the agar medium and bacterial cells are incubated on the plate. However, in the spread plate method, bacterial cells are treated with the ENPs in the broth for different time periods and spread on the agar plate. After the incubation period, these methods give information about the viable cells (culturable colonies). However, in flow cytometry, the damaged cells can be identified using PI dye. PI is a membrane-impermeable dye and enters into the cell and binds with the DNA, when the cellular wall is compromised due to the treatment. These methods allow us to calculate the minimum inhibitory concentration (MIC) of the antimicrobial agents and decide the dose for further studies such as genotoxicity, oxidative stress parameters, etc.

17.4.2 Genotoxicity

Genotoxic damage is the most extensively studied endpoint, because it has direct and long-lasting effects on the organism and the ecosystem. Additionally, assessment of DNA damage has been considered as an essential test for safe drug delivery to humans and animals. Hence, several rapid test systems have been developed to assess the mutagenic and carcinogenic potential of chemicals.

Ames test is one of the gold standard tests used for the evaluation of the mutagenic potential of the nanoparticles. The test system is based on the premise that a substance mutagenic to the bacterium is likely to be a carcinogen in laboratory animals, and hence, presents a risk to human and ecosystem health. Different histidine auxotrophic strains of *Salmonella typhimurium* (TA98, TA100, TA1535 and TA1537) and a tryptophan auxotrophic strain of *E. coli* are recommended by OECD Guideline [75] for testing of compounds to detect different mutation mechanisms. The test is carried out with and without the presence of the liver S9 fraction. Liver S9 fraction provides supplementary metabolic enzymes such as cytochrome P450s for the metabolic oxidation system. *S. typhimurium* strains

TA98 and TA1537 detects the frameshift mutation whereas TA100 and TA 1535 detects the base-pair substitution mutation. In TA 98, hisG gene: hisD3052 has one frameshift deletion, which is reverted to wild-type by various frame shift mutagens, whereas hisG46 marker in TA 100 results from the substitution of a leucine (GAG/CTC) by a proline (GGG/CCC). *E. coli* WP2uvrA used to detect oxidizing mutagens, such as free radical generators. This strain carries a tryptophan dependence due to a substitution in allele trpE65 by mechanisms of misreplication or misrepair at the AT sequence; mutagens which induce base-pair substitution can revert these mutations.

Several other genotoxicity assays based on the bacterial SOS repair system have also been used for fast screening of the mutagenic and carcinogenic potential. Among them, the *Salmonella umu* test is a quantitative reference test that is widely used for genotoxicity assay. This screening system is based on the induction of the *umuC-lacZ* genes by DNA damage to detect genotoxicity, thus the strain can sense the compounds that are capable of inducing SOS responses [76]. Later on, Justus and Thomas had improved the detection limit of the screening system by fusing the DNA-damage-inducible *umuC* gene to the *luxAB* gene (isolated from *Vibrio harveyi*) [77]. Furthermore, the structure activity relationship model also confirms the extensive predictive power and the overlapping response mechanisms of organic compounds between the SOS chromotest and the Ames fluctuation test [78]. Ptitsyn et al. constructed a plasmid by fusing the *lux* genes (from *Vibrio fischeri*) downstream to the *E. coli recA* promoter [79]. To validate his model, they investigated the genotoxic potential of several compounds with different methods and concluded that the sensitivity of SOS *lux* model was comparable with the other reported assays (Ames test, umu test, SOS chromotest). Furthermore, Vollmer et al. explored the differential sensitivity of three DNA-damage-inducible promoters (i.e. *recA*, *uvrA* and *alkA*) using *lux* gene as a reporter gene in *E. coli* [80]. They concluded *recA*, as the most sensitive promoter among three. Norman et al. described an *E. coli*-based bio-reporter that consists of a plasmid having a green fluorescent protein fused with a *cda* promoter [81]. The recombinant strain efficiency against genotoxic compound can be analyzed by flow cytometry. It has also demonstrated the higher sensitivity of *cda* promoter for a genotoxicity study than the traditional *recA*, *umuDC* and *sulA* promoters.

Apart from these promoter-based genotoxicity assessment methods, Comet assay and alkaline unwinding assay are the commonly used methods to evaluate the genotoxicity of ENPs. Comet assay is a versatile tool which can be used to assess the genotoxicity in various organisms ranging from bacteria to human [82]. In the Comet assay, single cell suspensions are embedded in agarose and layered on the slide. The embedded cells are then lysed using high salt concentration, subsequently electrophoresed and stained with fluorescent DNA binding dyes to quantify the DNA damage. However, alkaline unwinding assay is used to measure the DNA integrity based on the principle that the number of breaks in the phosphodiester backbone is directly proportional to the rate of transition of double-stranded DNA to single-stranded DNA under a pre-defined alkaline denaturing condition.

17.4.3 Oxidative Stress

Reactive oxygen species (ROS) generation has been previously proposed as a possible reason involved in the genotoxicity and cytotoxicity of ENPs. ENPs in aqueous suspension produce free radicals and their interaction with proteins results in the structural modification of cysteine, methionine, histidine, tryptophan, and other amino acids. ROS also attack DNA and produces chain break, modification of carbohydrate parts and nitro bases by oxidation, nitration, methylation or deamination reactions. Superoxide radical (O_2^-), hydrogen peroxide (H_2O_2) and nitric oxide (NO) are the main reactive species produced during the cellular metabolic pathway. A healthy cell regulates its balance between formation and breakdown. Whenever the cellular balance towards ROS gets altered, cells are under oxidative stress which could lead to the cellular damage at different target levels ranging from DNA damage to protein oxidation. Like all other cells, bacteria also have a strong defence system to encounter the oxidative stress. In *E. coli*, oxidative-stress-sensitive locus *oxyR* and *soxRS* acts as an inducer for a group of genes in protection against peroxide (H_2O_2) and superoxide stress (O_2^-), respectively. The *oxyR* regulon controls the expression of genes that are directly involved in antioxidant defensive activities such as hydroperoxidase I (*katG*), an alkyl hydroxy peroxidase (*ahpCF*), a small regulatory RNA (*oxyS*), glutathione reductase (*gorA*) and glutaredoxin I (*grxA*), while the *soxRS*-regulated genes include manganese binding superoxide dismutases (*Mn-SOD*), endonuclease IV (*nfo*), glucose-6-phosphate-dehydrogenase (*zwf*) and the outer membrane porin regulator *MicF* [83]. Manukhov et al. used a sensitive and specific *E. coli* (*pKatG-lux*) sensor for hydroperoxide compounds to assess the induction of oxidative stress by vegetable extracts [84]. Loui et al. generated deletion mutants of *arcA* (global regulator) and *arcB* (cognate sensor kinase of *arcA*) in *E. coli* and demonstrated that the *arcAB* global regulatory system plays an important role in the cell survival under hydrogen peroxide stress [85]. The *arcA* mutant *E. coli* was more susceptible toward H_2O_2 compared to the wild-type *E. coli*. Some oxidative stress-specific *E. coli* cell array chips consisting of 12 superoxide-sensitive strains with a diverse stress gene promoter fused with a *lux* reporter gene are also available to screen the oxidative stress inducers [86].

In addition to these molecular approaches, a battery of biochemical assays, such as measurement of ROS, lipid peroxidation (LPO), glutathione oxidase and reductase, catalase, and superoxide dismutase have been extensively used to demonstrate the oxidative stress induced by the ENPs. These oxidative stress parameters have been previously proposed as a possible reason involved in the genotoxicity and cytotoxicity of ENPs.

ROS in the cells can be measured by using dichlorofluorescein diacetate (DCFH-DA) dye. The deacetylation of the DCFH-DA in the cell by esters produces a non-fluorescent unstable DCFH, which becomes fluorescent DCF in the presence of oxygen free radicals. Whereas, LPO is a chain reaction process which propagates by an intermediate peroxy-radical and continues until the availability of unsaturated lipid molecules in the cell. Several types of damage including oxidation of sulfhydryl groups, reduction of disulfides, protein-protein cross-linking, peptide fragmentation

and modification of prosthetic group are documented due to LPO. It also generates reactive electrophiles, which degrade the poly-unsaturated fatty acid (PUFA) and resulted in the formation of malondialdehyde (MDA). MDA forms a stable pink colored adduct with thiobarbituric acid (TBA), and its quantification at 532 nm corresponds to the extent of LPO in the cell.

Glutathione (GSH) is a ubiquitous tripeptide which serves several vital functions including detoxifying electrophiles, scavenging free radicals and providing a reservoir for cysteine. The level of GSH in the cell can be quantified by measuring absorbance at 412 nm when dithionitrobenzoate (DTNB) binds with the reduced glutathione and forms a yellow colored product 5-thio-2-nitrobenzoic acid (TNB).

17.4.4 Genomics and Proteomics

Omic and bioinformatic tools provide a useful platform to study a new gene or protein as well as their differential expression for better understanding of toxicity mechanisms of ENPs. Microarray and real-time PCR are the commonly used genomic techniques that help to elucidate the pathway-specific responses induced by the ENPs and also serve as a basis to conduct further proteomic experimentation. The genomic data provide the preliminary idea about the ENPs response because, prior to becoming a functional protein, the mRNA have to be processed for the post-transcriptional modification, translational modification and post-translational modification. Hence, the degradation of mRNA or the formation of a non-functional protein may be the end product.

On the other hand, proteomics deals with the translational product of the exonic region of the gene which is a functional protein. 2D gel electrophoresis and protein array are the commonly used techniques that give the information about the whole protein expression profile of an organism. This provides more relevant data about the differential protein expression of the organism when exposed to ENPs.

17.5 Approaches and Knowledge Gaps in Toxicity of ENPs

The frequent release and interaction of ENPs with different component of the ecosystem necessitates the development of certain strategies to test the possible hazards of ENPs. We have critically discussed the fate, behavior and toxicity of different classes of ENPs in the ecosystem. It can be inferred from the above discussion that interactions of ENPs with microbes are dependent on their size, shape, chemical composition, surface charge, surface structure, area, solubility and aggregation state. Thus, it is essential to study these physiochemical properties of ENPs while assessing their biological hazards.

Among these physiochemical characteristics, surface properties of the ENPs are the most important factor that governs the stability and mobility of ENPs in the aqueous suspension. The agglomeration tendency of the ENPs is determined by the

ENPs' surface properties, which are mainly dependent on temperature, ionic strength, pH, particle concentration, size and the solvent property. But the study of these basic properties is very difficult because the relevant concentrations of ENPs in the ecosystem are in the nano- to picogram range which is lower than the detection limit of most of the test systems. On the other hand, the dosimetry of the ENPs is also a crucial step in designing the laboratory experiments, since the ENPs at higher concentrations have the tendency to agglomerate/aggregate which leads to their altered physicochemical properties and biological responses. Thus, the experimental design should also consider the concentration-induced aggregation effects of the ENPs concentration.

It may be speculated that at lower concentration range ENPs will tend to show less aggregation that leads to higher uptake and response than that expected from high concentrations. However, different surface modifications (particle coating, dispersant/surfactant, sonication) allow the particles to stabilize and avoid agglomerations; it also raises the concerns about what influences the effect of ENPs in biological systems. The durability of surface coatings in cellular/biological environments, the effects of cellular metabolites on the ENPs are the other key issues that need to be addressed in order to unravel the toxicological consequences of ENPs. Other possible effects of ENPs uptake could be the interaction with other (toxic) substances and their mobilization and bioavailability.

The environmental fate, behavior and bioavailability of ENPs are unknown; therefore, their persistence and the possible interaction/impact and biomagnification in food webs at different trophic levels are of immediate concern. Hence, to study the ENPs' effect in ecosystems, the study design should address the ENPs' interaction/impact directly with different trophic level organisms as well as the perturbations induced by the ENPs biomagnification (Fig. 17.5). ENPs' effect on other toxicant/pollutant also needs to be examined, because the transportation of the contaminant could be facilitated through their adsorption to ENPs which may have a negative impact on useful bacteria for natural remediation. The presence of impurities in the

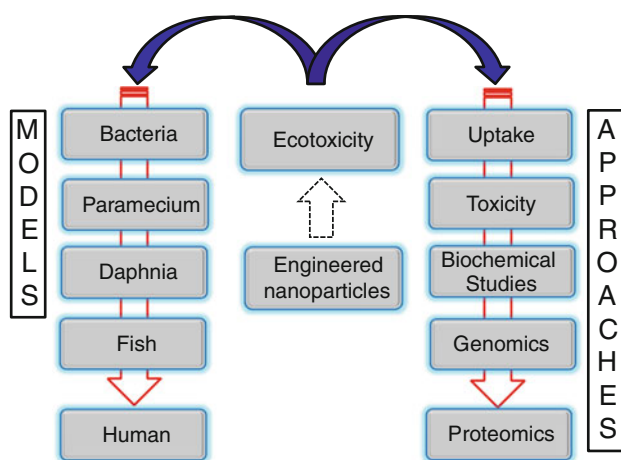


Fig. 17.5 Ecotoxicity of engineered nanoparticles: possible approaches and models

ENPs also influence the toxicity, thus the purity of the ENPs should also be considered in the study design. Elemental analysis using different analytical techniques could be helpful in analyzing the purity of ENPs.

Some of the metal oxide nanoparticles are known to release ions into the aqueous suspension which could alter the toxicity outcomes. Hence, the quantitation of soluble metal ions in the exposure medium is also a prerequisite in nanotoxicology studies. Lack of reference materials, appropriate methods to monitor ENPs behavior, dose problem and exposure methods, ENPs behavior in environmental matrices, regulatory toxicology test methods are certain other hurdles that need to be addressed by ecotoxicologists. Therefore, prior to use the ENPs-based consumer products in daily life activities, it is important for nanotoxicology research to understand their fate in the environment, so that their undesirable effects can be avoided.

17.6 Conclusion

The use of ENPs is continuously increasing in numerous applications which also increase their likelihood to interact with the various components of the ecosystem. Currently, the rate of ENPs incorporation in commercial products is much faster than the development of regulation and knowledge to mitigate their potential adverse effects. This can be attributed to the lack of guidelines, suitable models and the problems in experimental protocols and study design.

A systematic study design including characterization, nanoparticle uptake and toxicity studies using cytotoxicity assays, genotoxicity assays, oxidative stress parameters, and genomics and proteomics approaches can give the relevant information about the toxicity of ENPs in bacteria which could help to extrapolate the understanding of ENPs toxicity response in higher organisms.

Acknowledgements The authors gratefully acknowledge the funding from CSIR, New Delhi under its network project (NWP34, NWP35), OLP 006 and OLP 009. The funding from the Department of Science and Technology, Government of India under the nano mission project DST-NSTI grant (SR/S5/NM-01/2007) and UK India Education and Research Initiative (UKIERI) standard award to Indian Institute of Toxicology Research, Lucknow, India (DST/INT/UKIERI/SA/P-10/2008) and The Department of Biotechnology, under the New INDIGO programme (NanoLINEN project) is gratefully acknowledged. A.K. acknowledges the financial support through the Senior Research Fellowship of the Indian Council of Medical Research, New Delhi.

References

1. Wiesner MR, Lowry GV, Jones KL, Hochella Jr MF, Digiulio RT, Casman E, Bernhardt ES (2009) Decreasing uncertainties in assessing environmental exposure, risk, and ecological implications of nanomaterials. *Environmental Science and Technology* 43:6458–6462.
2. PEN. (2009) Project of the Emerging Nanotechnologies (PEN) Available at <http://www.nanotechproject.org>

3. Kumari M, Khan SS, Pakrashi S, Mukherjee A, Chandrasekaran N (2011) Cytogenetic and genotoxic effects of zinc oxide nanoparticles on root cells of *Allium cepa*. *Journal of Hazardous Materials* 190:613–621.
4. Handy RD, von der Kammer F, Lead JR, Hasselov M, Owen R, Crane M (2008) The ecotoxicology and chemistry of manufactured nanoparticles. *Ecotoxicology (London, England)* 17:287–314.
5. Maynard AD (2007) Nanotechnology: the next big thing, or much ado about nothing? *The Annals of Occupational Hygiene* 51:1–12.
6. Kumar A, Pandey AK, Singh SS, Shanker R, Dhawan A (2011) Cellular response to metal oxide nanoparticles in bacteria. *Journal of Biomedical Nanotechnology* 7:102–103.
7. Simon-Deckers A, Loo S, Mayne-L’Hermite M, Herlin-Boime N, Menguy N, Reynaud C, Gouget B, Carriere M (2009) Size-, composition- and shape-dependent toxicological impact of metal oxide nanoparticles and carbon nanotubes toward bacteria. *Environmental Science and Technology* 43:8423–8429.
8. Brayner R (2008) The toxicological impact of nanoparticles. *Nano Today* 3:48–55.
9. Vajpayee P, Khatoun I, Patel CB, Singh G, Gupta KC, Shanker R (2011) Adverse effects of chromium oxide nano-particles on seed germination and growth in *Triticum aestivum* L. *Journal of Biomedical Nanotechnology* 7:205–206.
10. Shukla RK, Kumar A, Pandey AK, Singh SS, Dhawan A (2011) Titanium dioxide nanoparticles induce oxidative stress-mediated apoptosis in human keratinocyte cells. *Journal of Biomedical Nanotechnology* 7:100–101.
11. Sharma V, Shukla RK, Saxena N, Parmar D, Das M, Dhawan A (2009) DNA damaging potential of zinc oxide nanoparticles in human epidermal cells. *Toxicology Letters* 185:211–218.
12. Dhawan A, Taurozzi JS, Pandey AK, Shan W, Miller SM, Hashsham SA, Tarabara VV (2006) Stable colloidal dispersions of C60 fullerenes in water: evidence for genotoxicity. *Environmental Science and Technology* 40:7394–7401.
13. Vallabani NV, Mittal S, Shukla RK, Pandey AK, Dhakate SR, Pasricha R, Dhawan A (2011) Toxicity of graphene in normal human lung cells (BEAS-2B). *Journal of Biomedical Nanotechnology* 7:106–107.
14. Fabrega J, Luoma SN, Tyler CR, Galloway TS, Lead JR (2011) Silver nanoparticles: behaviour and effects in the aquatic environment. *Environment International* 37:517–531.
15. Allen HJ, Impellitteri CA, Macke DA, Heckman JL, Poynton HC, Lazorchak JM, Govindaswamy S, Roose DL, Nadagouda MN (2011) Effects from filtration, capping agents, and presence/absence of food on the toxicity of silver nanoparticles to *Daphnia magna*. *Environmental Toxicology and Chemistry/SETAC* 29:2742–2750.
16. Premanathan M, Karthikeyan K, Jeyasubramanian K, Manivannan G (2011) Selective toxicity of ZnO nanoparticles toward gram-positive bacteria and cancer cells by apoptosis through lipid peroxidation. *Nanomedicine* 7:184–192.
17. Wahab R, Mishra A, Yun SI, Kim YS, Shin HS (2010) Antibacterial activity of ZnO nanoparticles prepared via non-hydrolytic solution route. *Applied Microbiology and Biotechnology* 87:1917–1925.
18. Brayner R, Ferrari-Iliou R, Brivois N, Djediat S, Benedetti MF, Fievet F (2006) Toxicological impact studies based on *Escherichia coli* bacteria in ultrafine ZnO nanoparticles colloidal medium. *Nano Letters* 6:866–870.
19. Wu B, Wang Y, Lee YH, Horst A, Wang Z, Chen DR, Sureshkumar R, Tang YJ (2010) Comparative eco-toxicities of nano-ZnO particles under aquatic and aerosol exposure modes. *Environmental Science and Technology* 44:1484–1489.
20. Shrivastava S, Bera T, Roy A, Singh G, Ramachandrarao P, Dash D (2007) Characterization of enhanced antibacterial effects of novel silver nanoparticles. *Nanotechnology* 18: 225103–225112.
21. Sondi I, Salopek-Sondi B (2004) Silver nanoparticles as antimicrobial agent: a case study on *E. coli* as a model for Gram-negative bacteria. *Journal of Colloid and Interface Science* 275:177–182.

22. Pal S, Tak YK, Song JM (2007) Does the antibacterial activity of silver nanoparticles depend on the shape of the nanoparticle? A study of the gram-negative bacterium *Escherichia coli*. *Applied and Environmental Microbiology* 73:1712–1720.
23. Maness PC, Smolinski S, Blake DM, Huang Z, Wolfrum EJ, Jacoby WA (1999) Bactericidal activity of photocatalytic TiO₂ reaction: toward an understanding of its killing mechanism. *Applied and Environmental Microbiology* 65:4094–4098.
24. Adams LK, Lyon DY, Alvarez PJJ (2006) Comparative eco-toxicity of nanoscale TiO₂, SiO₂, and ZnO water suspensions. *Water Research* 40:3527–3532.
25. Sawai J, Kojima H, Igarashi H, Hashimoto A, Shoji S, Sawaki T, Hakoda A, Kawada E, Kokugan T, Shimizu M (2000) Antibacterial characteristics of magnesium oxide powder. *World Journal of Microbiology and Biotechnology* 16:187–194.
26. Kang S, Mauter MS, Elimelech M (2008) Physicochemical determinants of multiwalled carbon nanotube bacterial cytotoxicity. *Environmental Science and Technology* 42:7528–7534.
27. Yoshida R, Kitamura D, Maenosono S (2009) Mutagenicity of water-soluble ZnO nanoparticles in Ames test. *Journal of Toxicological Sciences* 34:119–122.
28. Kumar A, Pandey AK, Singh SS, Shanker R, Dhawan A (2011) Cellular uptake and mutagenic potential of metal oxide nanoparticles in bacterial cells. *Chemosphere* 83:1124–1132.
29. Pan X, Redding JE, Wiley PA, Wen L, McConnell JS, Zhang B (2010) Mutagenicity evaluation of metal oxide nanoparticles by the bacterial reverse mutation assay. *Chemosphere* 79:113–116.
30. Wirtzner U, Herbold B, Voetz M, Ragot J (2009) Studies on the in vitro genotoxicity of baytubes, agglomerates of engineered multi-walled carbon-nanotubes (MWCNT). *Toxicology Letters* 186:160–165.
31. Di Sotto A, Chiaretti M, Carru GA, Bellucci S, Mazzanti G (2009) Multi-walled carbon nanotubes: lack of mutagenic activity in the bacterial reverse mutation assay. *Toxicology Letters* 184:192–197.
32. Maenosono S, Yoshida R, Saita S (2009) Evaluation of genotoxicity of amine-terminated water-dispersible FePt nanoparticles in the Ames test and in vitro chromosomal aberration test. *Journal of Toxicological Sciences* 34:349–354.
33. Huang Z, Zheng X, Yan D, Yin G, Liao X, Kang Y, Yao Y, Huang D, Hao B (2008) Toxicological effect of ZnO nanoparticles based on bacteria. *Langmuir* 24:4140–4144.
34. Jones N, Ray B, Ranjit KT, Manna AC (2008) Antibacterial activity of ZnO nanoparticle suspensions on a broad spectrum of microorganisms. *FEMS Microbiology Letters* 279:71–76.
35. Fabrega J, Fawcett SR, Renshaw JC, Lead JR (2009) Silver nanoparticle impact on bacterial growth: effect of pH, concentration, and organic matter. *Environmental Science and Technology* 43:7285–7290.
36. Lyon DY, Adams LK, Falkner JC, Alvarez PJ (2006) Antibacterial activity of fullerene water suspensions: effects of preparation method and particle size. *Environmental Science and Technology* 40:4360–4366.
37. Suresh AK, Pelletier DA, Wang W, Moon JW, Gu B, Mortensen NP, Allison DP, Joy DC, Phelps TJ, Doktycz MJ (2010) Silver nanocrystallites: biofabrication using *Shewanella oneidensis*, and an evaluation of their comparative toxicity on gram-negative and gram-positive bacteria. *Environmental Science and Technology* 44:5210–5215.
38. Mortimer M, Kasemets K, Heinlaan M, Kurvet I, Kahru A (2008) High throughput kinetic *Vibrio fischeri* bioluminescence inhibition assay for study of toxic effects of nanoparticles. *Toxicology in Vitro* 22:1412–1417.
39. Heinlaan M, Ivask A, Blinova I, Dubourguier HC, Kahru A (2008) Toxicity of nanosized and bulk ZnO, CuO and TiO₂ to bacteria *Vibrio fischeri* and crustaceans *Daphnia magna* and *Thamnocephalus platyurus*. *Chemosphere* 71:1308–1316.
40. Choi O, Hu Z (2008) Size dependent and reactive oxygen species related nanosilver toxicity to nitrifying bacteria. *Environmental Science and Technology* 42:4583–4588.
41. Haggstrom JA, Klabunde KJ, Marchin GL (2010) Biocidal properties of metal oxide nanoparticles and their halogen adducts. *Nanoscale* 2:399–405.

42. Elechiguerra JL, Burt JL, Morones JR, Camacho-Bragado A, Gao X, Lara HH, Yacaman MJ (2005) Interaction of silver nanoparticles with HIV-1. *Journal of Nanobiotechnology* 3:6.
43. Kasemets K, Ivask A, Dubourguier HC, Kahru A (2009) Toxicity of nanoparticles of ZnO, CuO and TiO₂ to yeast *Saccharomyces cerevisiae*. *Toxicology In Vitro* 23:1116–1122.
44. Peng X, Palma S, Fisher NS, Wong SS (2011) Effect of morphology of ZnO nanostructures on their toxicity to marine algae. *Aquatic Toxicology* 102:186–196.
45. Gong N, Shao K, Feng W, Lin Z, Liang C, Sun Y (2011) Biototoxicity of nickel oxide nanoparticles and bio-remediation by microalgae *Chlorella vulgaris*. *Chemosphere* 83:510–516.
46. Li M, Pokhrel S, Jin X, Madler L, Damoiseaux R, Hoek EM (2011) Stability, bioavailability, and bacterial toxicity of ZnO and iron-doped ZnO nanoparticles in aquatic media. *Environmental Science and Technology* 45:755–761.
47. Aruoja V, Dubourguier HC, Kasemets K, Kahru A (2009) Toxicity of nanoparticles of CuO, ZnO and TiO₂ to microalgae *Pseudokirchneriella subcapitata*. *Science of the Total Environment* 407:1461–1468.
48. Panacek A, Kolar M, Vecerova R, Prucek R, Soukupova J, Krystof V, Hamal P, Zboril R, Kvitel L (2009) Antifungal activity of silver nanoparticles against *Candida* spp. *Biomaterials* 30:6333–6340.
49. He L, Liu Y, Mustapha A, Lin M (2011) Antifungal activity of zinc oxide nanoparticles against *Botrytis cinerea* and *Penicillium expansum*. *Microbiological Research* 166:207–215.
50. Kumar A, Dhawan A, Shanker R (2011) The need for novel approaches in ecotoxicity of engineered nanomaterials. *Journal of Biomedical Nanotechnology* 7:79–80.
51. Oberdarster G, Oberdarster E, Oberdarster J (2005) Nanotoxicology: an emerging discipline evolving from studies of ultrafine particles. *Environmental Health Perspectives* 113:823–839.
52. Oberdarster G, Stone V, Donaldson K (2007) Toxicology of nanoparticles: a historical perspective. *Nanotoxicology* 1:2–25.
53. Lindfors K, Kalkbrenner T, Stoller P, Sandoghdar V (2004) Detection and spectroscopy of gold nanoparticles using supercontinuum white light confocal microscopy. *Physical Review Letters* 93:037401.
54. Van Dijk MA, Lippitz M, Orrit M (2005) Far-field optical microscopy of single metal nanoparticles. *Accounts of Chemical Research* 38:594–601.
55. Mavrocordatos D, Pronk W, Boiler M (2004) Analysis of environmental particles by atomic force microscopy, scanning and transmission electron microscopy. *Water Science and Technology* 50:9–18.
56. Dhawan A, Sharma V (2010) Toxicity assessment of nanomaterials: methods and challenges. *Analytical and Bioanalytical Chemistry* 398:589–605.
57. Tiede K, Boxall AB, Tear SP, Lewis J, David H, Hasselvo M (2008) Detection and characterization of engineered nanoparticles in food and the environment. *Food Additives and Contaminants* 25:795–821.
58. Jose-Yacaman M, Marin-Almazo M, Ascencio J (2001) High resolution TEM studies on palladium nanoparticles. *Journal of Molecular Catalysis A* 173:61–74.
59. Chuklanov A, Ziganshina S, Bukharaev A (2006) Computer program for the grain analysis of AFM images of nanoparticles placed on a rough surface. *Surface Interface Analysis* 38:679–681.
60. Baatz M, Arini N, Schape A, Binnig G, Linssen B (2006) Object-oriented image analysis for high content screening: detailed quantification of cells and sub cellular structures with the Cellenger software. *Cytometry A* 69:652–658.
61. Dhawan A, Sharma V, Parmar D (2009) Nanomaterials: a challenge for toxicologists. *Nanotoxicology* 3:1–9.
62. Navarro E, Baun A, Behra R, Hartmann NB, Filser J, Miao AJ, Quigg A, Santschi PH, Sigg L (2008) Environmental behavior and ecotoxicity of engineered nanoparticles to algae, plants, and fungi. *Ecotoxicology (London, England)* 17:372–386.
63. Buffle J, Wilkinson K, Stoll S, Filella M, Zhang J (1998) A generalized description of aquatic colloidal interactions: the three-colloidal component approach. *Environmental Science and Technology* 32:2887–2899.

64. Kretzschmar R, Sticher H (1997) Transport of humic-coated iron oxide colloids in a sandy soil: influence of Ca^{2+} and trace metals. *Environmental Science and Technology* 31:3497–3504.
65. Kahru A, Dubourguier HC, Blinova I, Ivask A, Kasemets K (2008) Biotests and biosensors for ecotoxicology of metal oxide nanoparticles: a minireview. *Sensors* 8:5153–5170.
66. Kahru A, Dubourguier HC (2010) From ecotoxicology to nanoecotoxicology. *Toxicology* 269:105–119.
67. Baun A, Sorensen SN, Rasmussen RF, Hartmann NB, Koch CB (2008) Toxicity and bioaccumulation of xenobiotic organic compounds in the presence of aqueous suspensions of aggregates of nano-C(60). *Aquatic Toxicology (Amsterdam, Netherlands)* 86:379–387.
68. Yang L, Watts DJ (2005) Particle surface characteristics may play an important role in phytotoxicity of alumina nanoparticles. *Toxicology Letters* 158:122–132.
69. Knauer K, Sobek A, Bucheli TD (2007) Reduced toxicity of diuron to the freshwater green alga *Pseudokirchneriella subcapitata* in the presence of black carbon. *Aquatic Toxicology (Amsterdam, Netherlands)* 83:143–148.
70. Baun A, Hansen SF (2008) Environmental challenges for nanomedicine. *Nanomedicine* 3:605–608.
71. Sharma V, Singh SK, Anderson D, Tobin DJ, Dhawan A (2011) Zinc oxide nanoparticle induced genotoxicity in primary human epidermal keratinocytes. *Journal of Nanoscience and Nanotechnology* 11:3782–3788.
72. Kumar A, Pandey AK, Singh SS, Shanker R, Dhawan A (2011) A flow cytometric method to assess nanoparticle uptake in bacteria. *Cytometry A* doi:10.1002/cyto.a.21085.
73. Suzuki H, Toyooka T, Ibuki Y (2007) Simple and easy method to evaluate uptake potential of nanoparticles in mammalian cells using a flow cytometric light scatter analysis. *Environmental Science and Technology* 41:3018–3024.
74. Neal AL (2008) What can be inferred from bacterium-nanoparticle interactions about the potential consequences of environmental exposure to nanoparticles? *Ecotoxicology (London, England)* 17:362–371.
75. OECD (1997) OECD Guideline for Testing of Chemicals, Bacterial Reverse Mutation Test (No. 471).
76. Oda Y, Nakamura S, Oki I, Kato T, Shinagawa H (1985) Evaluation of the new system (umu-test) for the detection of environmental mutagens and carcinogens. *Mutation Research* 147:219–229.
77. Justus T, Thomas SM (1998) Construction of a umuC'-luxAB plasmid for the detection of mutagenic DNA repair via luminescence. *Mutation Research* 398:131–141.
78. MerschSundermann V, Klopman G, Rosenkranz H (1996) Chemical structure and genotoxicity: studies of the SOS chromotest. *Mutation Research Review in Genetic Toxicology* 340:81–91.
79. Ptitsyn LR, Horneck G, Komova O, Kozubek S, Krasavin EA, Bonev M, Rettberg P (1997) A biosensor for environmental genotoxin screening based on an SOS lux assay in recombinant *Escherichia coli* cells. *Applied and Environmental Microbiology* 63:4377–4384.
80. Vollmer AC, Belkin S, Smulski DR, Van Dyk TK, LaRossa RA (1997) Detection of DNA damage by use of *Escherichia coli* carrying *recA'*::lux, *uvrA'*::lux, or *alkA'*::lux reporter plasmids. *Applied and Environmental Microbiology* 63:2566–2571.
81. Norman A, Hansen L, Sorensen S (2005) Construction of a ColD *cda* promoter-based SOS-green fluorescent protein whole-cell biosensor with higher sensitivity toward genotoxic compounds than constructs based on *recA*, *umuDC*, or *sul4* promoters. *Applied and Environmental Microbiology* 71:2338–2346.
82. Dhawan A, Bajpayee M, Parmar D (2009) Comet assay: a reliable tool for the assessment of DNA damage in different models. *Cell Biology and Toxicology* 25:5–32.
83. Robbens J, Dardenne F, Devriese L, De Coen W, Blust R (2010) *Escherichia coli* as a bioreporter in ecotoxicology. *Applied Microbiology and Biotechnology* 88:1007–1025.

84. Manukhov IV, Kotova V, Mal'dov DK, Il'ichev AV, Bel'kov AP, Zavid'gel'skii GB (2008) [Induction of oxidative stress and SOS response in *Escherichia coli* by plant extracts: the role of hydroperoxides and the synergistic effect of simultaneous treatment with cisplatinum]. *Mikrobiologiya* 77:590–597.
85. Loui C, Chang AC, Lu S (2009) Role of the ArcAB two-component system in the resistance of *Escherichia coli* to reactive oxygen stress. *BMC Microbiology* 9:183.
86. Lee JH, Youn CH, Kim BC, Gu MB (2007) An oxidative stress-specific bacterial cell array chip for toxicity analysis. *Biosensors and Bioelectronics* 22:2223–2229.

Chapter 18

Nano-Silver Toxicity: Emerging Concerns and Consequences in Human Health

Indarchand Gupta, Nelson Duran, and Mahendra Rai

18.1 Introduction

Nanotechnology is one of the key technologies of the twenty-first century and hence there has been vast progress and increased funding in overall technological research on nanomaterials. Nanotechnology deals with structures of the size 100 nm and less, and involves developing materials or devices within that size (Roco 1999).

Nanotechnology is being used to create many new materials and devices with a wide range of applications: transparent sunscreens and cosmetics, odor and wrinkle-repellent clothing, long-lasting paints, electronic and sports equipment, fuel catalysts, building equipment, a small number of medicines, and even food products are some examples of nanotechnology that have reached the public (Rai et al. 2009). According to a recent report, there are over 800 consumer products already available containing nanomaterials, costing US\$147 billion in 2007, projected is a rise to \$3.1 trillion by 2015 (Lux report 2008). Out of these materials, it is expected that the demand for nanotechnology in medical products will grow by more than 17% annually to reach an estimated US\$53 billion market in 2011, with the largest share in pharmaceutical applications expected to reach , US\$110 billion in 2016 (Gangloff 2007). Therefore, the nanotechnology market annually requires a large amount of raw nanomaterials, ranging from nano-sized metals and metal oxide nanoparticles to carbon nanotubes and composites (Thayer 2007; Park 2007) to manufacture diverse range of nano-based products.

I. Gupta • M. Rai (✉)

Department of Biotechnology, SGB Amravati University, Amravati, Maharashtra, India
e-mail: mkrai123@rediffmail.com; pmkrai@hotmail.com

N. Duran

Chemistry Institute, Biological Chemistry Laboratory, University of Campinas, Campinas, SP, Brazil

Center of Natural and Human Sciences (CCNH), Universidade Federal do ABC (UFABC), Santo André, SP, Brazil

Out of vast range of nano-based products available today, metal nanoparticles are of utmost interest since they are most often used in manufacturing and medicine. Within several metal nanoparticles, silver nanoparticles have a wide array of applications including food packaging, odor-resistant textiles, antimicrobial agents, household appliances and medical devices, etc. (Woodrow Wilson International Center for Scholars 2007).

Such manufacturing and consumer utilization produces multiple sources for the release of these materials into the environment (Borm et al. 2006b), food supplies and other routes of non-voluntary entry into the human body (Theodore and Kunz 2005). Hence, human exposure to these nanomaterials through many different routes is being reported and is set to increase dramatically in the coming years. This growth in exposure to nanomaterials invites debate on the future implications of nanotechnology.

Nanotoxicology is emerging as an important sub-discipline of nanotechnology. It refers to the study of the interactions of nanostructures with biological systems putting emphasis on elucidating the relationship between the physical and chemical properties of nanostructures with induction of toxic biological responses. The toxicity of nanomaterials is often linked to their smaller size because smaller particles have a greater reactive surface area than larger particles, are more chemically reactive and produce large numbers of reactive oxygen species that include free radicals (Nel et al. 2006). Additionally, as highlighted by Barandiaran (2007), there are issues of site-specific accumulation and translocation between organs and tissues. The small-sized nanomaterials are easily taken up by the human body as compared to larger particles, crossing biological membranes and accessing cells, tissues and organs (Holsapple et al. 2005).

18.2 Nanotoxicity: Risk to Researchers and Workers

Persons producing or working with or consuming nanomaterials are potentially at the highest risk. Researchers and workers in the nanotechnology industries are considered at primary risk of exposure through inhalation, dermal contact, or ingestion (Thomas et al. 2006).

As a part of a government-wide coordination effort, the Occupational Safety and Health Administration (OSHA), Department of Labor, USA, is working with other agencies to deal with issues related to the impact of nanomaterials on human health and the environment. OSHA confirms that the number of workers involved in the research, manufacturing, production, and disposal of nano-products is growing. Similarly, the U.S. Environment Protection Agency (EPA) has proposed the conditional registration of an antimicrobial pesticide product, HeiQ AGS-20, containing nano-silver as a new active ingredient for a period of 4 years. This product has been proposed for use as a preservative for textiles. As a condition of registration, EPA is requiring additional product chemistry, toxicology, exposure, and environmental data. The agency will evaluate the data during this period in order to confirm that it

will not cause any harmful effect to humans and the environment and thus will be safe for use (Pesticide News Story 2010).

Unfortunately, the occupational health risks coupled with nanoparticles are not yet understood. Indeed, little information exists on exposure routes, potential exposure levels and how these factors relate to toxicity. Therefore, toxicological research requires top priority to anticipate the health requirement of workers associated with the synthesis or handling of nanomaterials.

A large number of nano-based products are available to the consumer. For each of these uses, there is concern over the lack of data about use and consequences to the consumer. Additionally, consumer use will contaminate the environment. Benn and Westerhoff (2008) reported that ordinary laundering of socks impregnated with Ag nanoparticles causes their release into the water as downstream contaminants. Therefore, there is an urgent need to understand the toxicity of silver nanoparticles to consumers.

Dermal exposure to nanoscale materials occurs because the nanoparticle formulation enhances penetration of active ingredients of cosmetics into the skin thereby improving their effectiveness (Thomas et al. 2006) (Fig. 18.1). Nanomaterials are embedded into the matrix of sporting equipment to permit long-term release. Moreover, nanotechnology is used to generate textile products with valuable properties including wrinkle-free and stain-resistant clothing (Wakelyn 1994; Thomas et al. 2006).

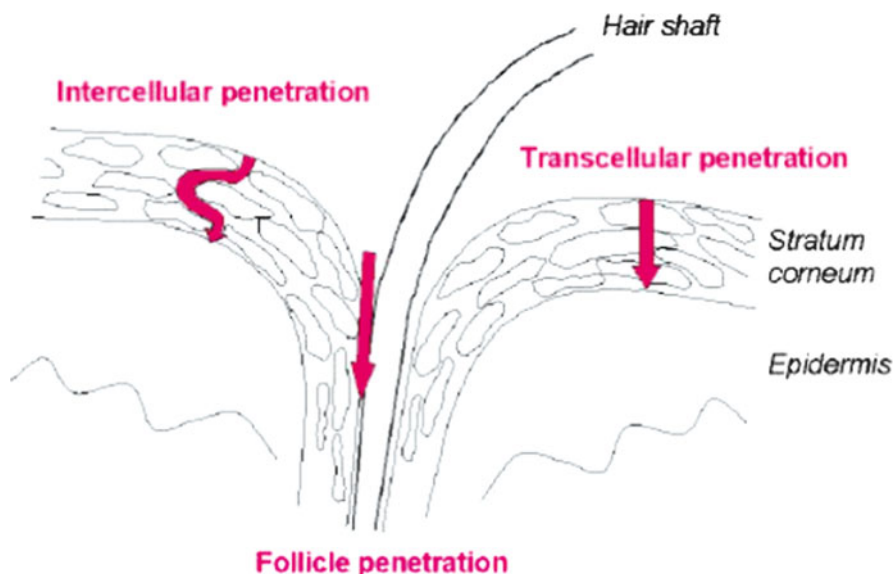


Fig. 18.1 Penetration pathways of topically applied substances through the skin. The nanoparticles can enter the skin by intercellular penetration through the stratum corneum by transcellular penetration or follicular penetration (Taken with permission from Borm et al. 2006b)

18.3 Routes of Exposure

18.3.1 Through Inhalation

Many studies have revealed that there is a direct association between morbidity and mortality in the general population and daily concentrations of suspended particulate matter (PM), especially of the ultrafine fraction defined as being smaller than 100 nm (i.e. with nanoparticle dimensions) (Dockery and Pope III 1994; Peters et al. 1997). Geiser and Kreyling (2010) reported an association between the presence of nanoparticles in inhaled air at the workplace and acute morbidity and even mortality in elderly persons.

High concentrations of ultrafine particles (20–80 nm) in the ambient air are related to several adverse health effects in humans. Some of these health consequences may occur via inhalation of ultrafine particles (UFPs) followed by their translocation to other organs (Fig. 18.2). Wichmann and Peters (2000) have shown considerably stronger pulmonary inflammatory effects when tested at equal mass dose with their fine (40–300 nm) counterparts. These effects are (1) local

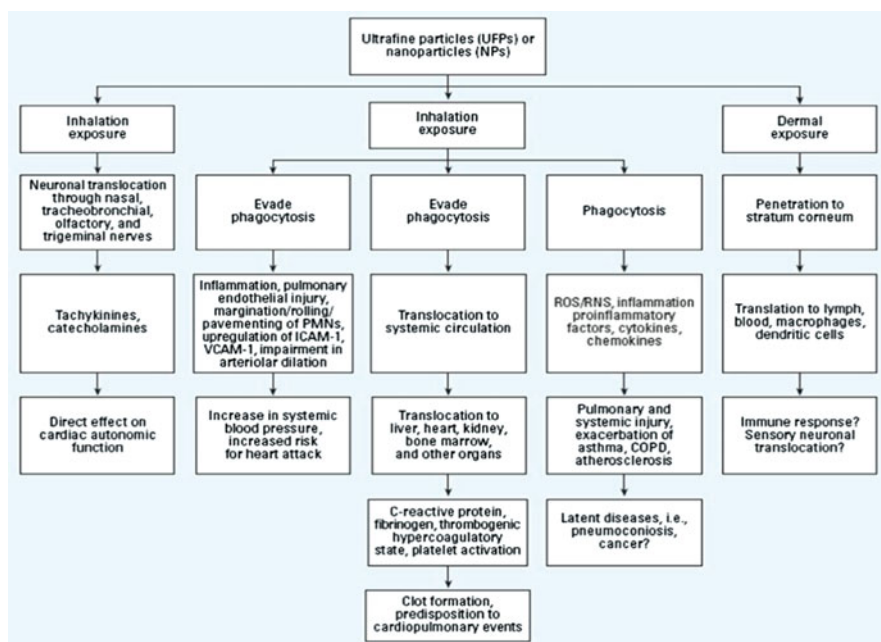


Fig. 18.2 Hypothetical scheme of potential interactions that may occur via inhalation of UFPs and translocation to other organs. *ICAM-1* intracellular adhesion molecule-1; *PMNs* polymorphonuclear leukocytes; *RNS* reactive nitrogen species; *VCAM-1* vascular adhesion molecule-1. The scheme also shows suspected interactions (indicated by a *question mark*) leading to sequences of events that may cause cardiovascular and pulmonary morbidity and mortality (Taken with permission from Gwinn and Vallyathan 2006)

effects on the lung and (2) systemic effects that impact the cardiovascular system (Donaldson et al. 2001). There are some reports signifying that exposure to ultrafine particulate air pollution (<100 nm) is associated with increased prevalence of cardiovascular diseases (Wichmann and Peters 2000; Ibaldo-Mulli et al. 2002; Peters and Pope 2002; Lanki et al. 2006). The nanoparticles enter the circulation and extrapulmonary tissues (Nemmar et al. 2001, 2002; Oberdorster et al. 2002) with possibly up to 15% of the inhaled dose reaching the capillaries (Geiser et al. 2005).

Human exposure to manufactured particulate matter in the nano-size range also presents a risk to consumers as well as to occupational workers. These studies raise questions about the possible adverse health implications for large-scale, uncontrolled commercial production and distribution of nanoparticles (Colvin 2003; Borm and Kreyling 2004; Nel et al. 2006; Borm et al. 2006a; Unfried et al. 2007).

18.3.2 Through Gastrointestinal Tract

Nanomaterials can be ingested directly through food and water or if used in cosmetics or as drugs or drug delivery devices. Nanomaterial-containing products are available in the market and most of them are used orally. Nanoparticles cleared from the respiratory tract via a mucociliary escalator can subsequently be ingested into the gastrointestinal tract (Chen et al. 2006).

Very few researchers have studied the uptake and disposition of nanomaterials by the gastrointestinal tract. These nanoparticles are taken up into the blood circulation after ingestion (Jani et al. 1994; Yamago et al. 1995). Possibly, both particle surface chemistry and particle size affects the gastrointestinal tract uptake of nanoparticles. Thus, it poses an easier route of entry of nanoparticles into the blood and thereby to other body systems.

18.3.3 Through Skin

It is a well-known fact that the human skin is imperfect; it is not an impenetrable barrier. Many drugs applied onto the skin gets permeated through the skin. A potentially important uptake route of nanoparticles is through dermal exposure. So there arises a question: do similar responses occur with nanoparticles of titanium dioxide and zinc oxide applied on the surface of the skin in the form of sunscreens (Tyner et al. 2009; Barnard 2010)? It is observed that micronized titanium dioxide preparations used in sunscreens are aggregated on the surface of the stratum corneum (Pflucker et al. 2001). Similar results were obtained in a penetration study of micronized zinc oxide of mean particle size of 40 nm: it does not penetrate through the stratum corneum (Borm et al. 2006b).

Ruptured skin can be an easy portal of entry even for larger (0.5–7 µm) particles. For instance, soil particles get accumulated in the inguinal lymph nodes of people

who often run or walk barefoot, thereby causing elephantiac lymphedema (Corachan et al. 1988; Blundell et al. 1989). Tinkle et al. (2003) hypothesized that unbroken skin when flexed – as in wrist movements – would make the epidermis permeable for nano-sized particles suggesting that acne, eczema, shaving wounds or severe sunburn may enable skin uptake of nanomaterials more readily.

Quantum dots were found to actually penetrate through this layer finally localizing within the epidermal and dermal layers (Ryman-Rasmussen et al. 2006). Similarly, in another example, the fullerene-based peptides were also observed to penetrate the skin (Rouse et al. 2007). With AgNPs, macroscopic observations showed no gross irritation in porcine skin, whereas microscopic and ultra-structural observations showed areas of focal inflammation on the surface and in the upper stratum corneum layers. AgNPs silver nanoparticles activated the mast cells causing the symptom of agyria that develops with Ag ion use (Kakurai et al. 2003). However, there are many facets of NP interaction that require further experimentation to resolve mechanisms of toxicity.

18.4 Development of Methodology to Better Dissect Cytotoxicity

In vitro toxicological evaluation methods are important tools for toxicological study. According to the inter-agency National Toxicology Program, it is recommended that a new entity should be classified as per its plausible risks. Thus, each entity should be tested by a set of tests designed to characterize a given risk and to analyze the mechanisms for related outcomes. From such studies, it should be possible to strengthen the scientific base for risk evaluation, and to provide material to aid the understanding of all stakeholders. It is, therefore, important to develop methods to analyze the effects of shape, size and surface on the activity of the NPs both *in vitro* and *in vivo* (Clancy et al. 2010). An assessment regime considering traditional pharmacology and toxicology approaches will play an important role in shaping public health policy.

18.5 Rationale Behind *In Vitro* Study

Cell-based assays are presently considered essential to toxicity testing (Nel et al. 2006; Lewinski et al. 2008). These assays of nanomaterials commonly interface the selected nanoparticle with an appropriate cell phenotype (Jones and Grainger 2009).

Primary cell lines are more representative of tissue and hence are ideal for *in vitro* toxicity studies. However, secondary cell lines are easy to maintain and are preferred in most toxicological studies for better reproducibility of data.

The *in vitro* studies are fast, cheap and allow greater control over the experiments. They mimic realistic conditions, thereby reducing the number of laboratory animals required for the testing (Marquis et al. 2009). They are also helpful in predicting the starting doses for *in vivo* acute toxicity testing. Moreover, these assays are compatible with available tools for mechanistic evaluation of toxicity.

A variety of assays are reported based on viability, proliferation and activation of cells. To assess cell viability (cytotoxicity), several different assays are being utilized. Activity staining with MTT (3-(4,5-Dimethylthiazol-2-yl)-2,5-diphenyltetrazolium bromide), and assessment of membrane integrity by the neutral red assay or monitoring the release of lactate dehydrogenase (LDH) are commonly used (Fotakis and Timbrell 2006). The use of these assays has been discussed in the next section specifically for silver nanoparticles (AgNPs).

18.6 Silver Nanoparticles and Cytotoxicity

Silver, a naturally occurring precious metal, is the 47th element in the periodic table with an atomic weight of 107.8. Silver has two natural isotopes, 106.90 Ag and 108.90 Ag. It has been used in a large range of applications including fashioning into ornaments and utensils, traded jewelry, and as the basis for many monetary systems. Today's uses include preparing electrical contacts and conductors, in mirrors and in catalysis of chemical reactions.

Ancient civilizations were aware of silver's bactericidal properties (Hill and Pillsbury 1939) and such uses continue today (Margaret et al. 2006; Sarkar et al. 2007). Silver ions are effective against many pathogens such as bacteria (Morones et al. 2005; Zhang and Sun 2007), viruses, fungi, and yeast with no toxicity to humans. However, the downside is the neutralization of ions in biological fluids and argyria and delayed wound healing upon long-term use. Due to its broad spectrum activity, effectiveness and lower costs, the search for newer and superior silver-based antimicrobial agents is necessary. Among the various particles available, AgNPs have been the focus of increasing interest and are being considered as a precursor and as an excellent candidate for therapeutic purposes.

18.6.1 Cellular Uptake

The NPs appear to gain intracellular locations to achieve their reprogramming of eukaryotic cell metabolism. Asharani et al. (2009a, b), demonstrated uptake of AgNPs to occur by clathrin-mediated endocytosis and macropinocytosis (Fig. 18.3). They have suggested that cancer cells may be more susceptible than normal cells. They compared responses of the normal human lung fibroblast line (IMR-90), chosen because it is a common route of exposure to NPs, with the human glioblastoma cell

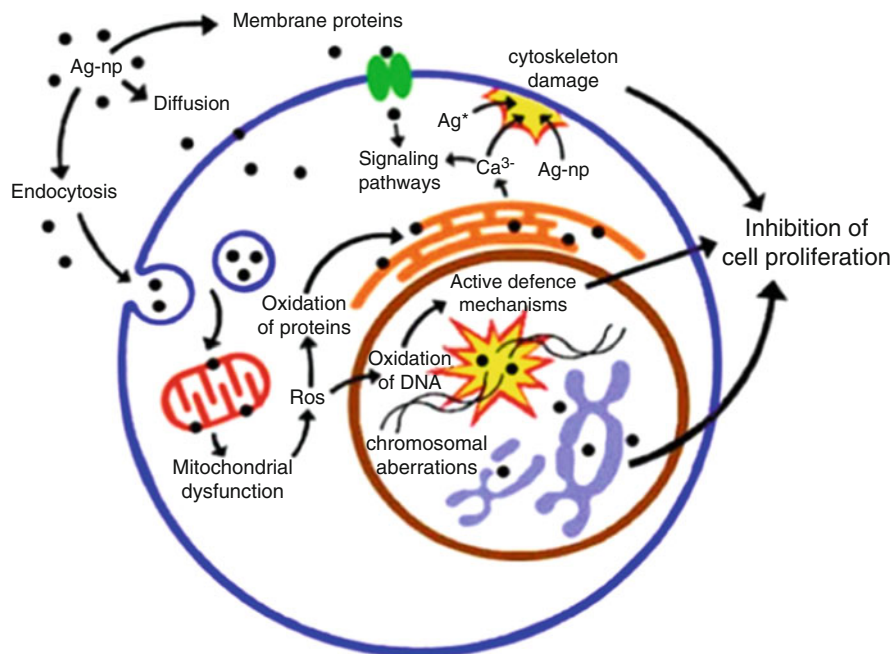


Fig. 18.3 The schematic representation of mechanism of AgNPs toxicity based on experimental data. Silver nanoparticles can enter into the cell through endocytosis, diffusion or membrane proteins. The higher concentration of Ag^+ ions inhibits Ca^{2+} release from the cytoplasm. Repeated calcium influx and efflux in mitochondria could result in mitochondrial membrane damage, resulting in ROS production and inhibition of ATP synthesis. The generated ROS damages DNA, affecting its replication, chromosomal morphology and segregation, thereby leading to inhibition of cell division (Taken with permission from Asharani et al. 2009b)

line (U251), reasoning that after entry into the body, AgNPs are known to localize in the brain. The work of Asharani et al. (2009a, b) thus opened up new avenues about the anti-cancerous effect of silver nanoparticles. But further detailed study is needed to confirm the hypothesis that silver nanoparticles have specific activity against the cancerous cells as compared to normal cells. If this is so, then the mechanism lying behind such a differential activity of nanoparticles should be explored. These studies can be useful in future to prepare or formulate the anti-cancerous drug by using silver nanoparticles.

18.6.2 High Doses of AgNPs Induce Cell Death

In 2005, Hussain and his colleagues (2005) evaluated acute toxic effects of silver nanoparticles *in vitro* with the rat liver-derived cell line BRL 3A. They demonstrated that AgNPs (15 and 30 nm sizes) caused a concentration-dependent

increase in cytotoxicity with significant action from doses of 5–50 $\mu\text{g/mL}$. Braydich-Stolle et al. (2005) assessed the suitability of a mouse spermatogonial stem cell line, C18-4, as a model to assess nanotoxicity in male germ line *in vitro*. Their evaluations suggested the drastic reduction in mitochondrial function and cell viability. In agreement with these studies are findings by Carlson et al. (2008), examining the size-dependent interactions of hydrocarbon-coated silver nanoparticles (15, 30 and 55 nm size) with macrophages. Both AgNPs with diameters 15 and 30 nm appeared to be toxic in the MTT at low concentrations (5 and ~ 10 $\mu\text{g/mL}$) whereas the 55-nm NPs were less active.

Other examples of AgNPs cytotoxicity have been published including: Soto et al. (2006) with a murine lung macrophage cell line and the alveolar macrophage (THB-1) cell line; Greulich et al. (2009) and human mesenchymal stem cells at the concentration from 3.5 to 50 $\mu\text{g/mL}$; and Miura and Shinohara (2009) with HeLa cells found toxic only at higher levels, i.e. 80 $\mu\text{g Ag/mL}$. These findings suggest both size- and concentration-dependent toxic effects of silver nanoparticles. From this discussion, it is imperative that smaller-sized nanoparticles show the greater toxic effect, and similar results can be obtained at higher concentrations.

18.6.3 Apoptosis: A Crucial Mechanism Behind Cell Death

Apoptosis is a physiological/pathophysiological form of cell death. During this process, certain biochemical and morphological changes occur, including cell volume decrease, caspase activation, chromatin condensation, DNA laddering, and cell fragmentation (Shimizu et al. 2004).

Several mechanisms have been reported to date including the detail of the mechanism involved in the induction of apoptosis. It can be initiated by various exogenous and endogenous stimuli such as ultraviolet radiation, oxidative stress, and genotoxic chemicals (Rastogi et al. 2009). Thus, apoptosis can be induced by various pathways.

Apoptosis can occur via activation of the tumor suppressor protein p53, which is activated in response to DNA damage, UV radiation and a range of chemotherapeutic drugs. It is then followed by induction of apoptosis-regulating pathways involving the mitochondria (Vogelstein et al. 2000; Kakkar and Singh 2007) (Fig. 18.4). It is a key tumor suppressor protein prone to DNA damage-induced apoptosis (Clarke et al. 1993). It is functionally conserved in multicellular animals including human cells (Schumacher et al. 2001). There are genes which get up-regulated and down-regulated in the process of apoptosis and their number is still increasing (Singh and Khar 2005).

The apoptosis can also be induced by reactive oxygen species (ROS), which are known to function via the mitochondria (Bosca et al. 2005; Fong et al. 2007). ROS generation precedes mitochondrial permeability transition, cytochrome c release, and caspase activation (Garcia-Ruiz et al. 2000), thereby leading to apoptosis (Fig. 18.5).

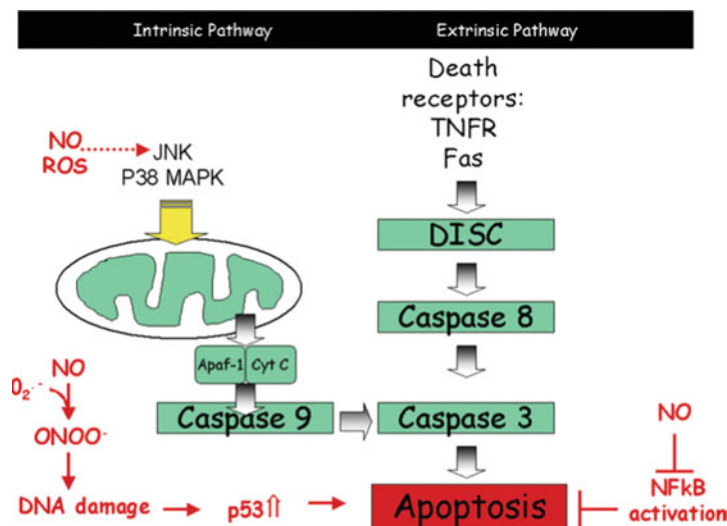


Fig. 18.4 A schematic representation depicting the impact of NO and ROS on the intrinsic and extrinsic pathways that regulate apoptosis. The intrinsic pathway is activated by cellular stress and signals through survival kinases to the mitochondria which then involve caspase 9 through cytochrome c release. The extrinsic pathway is driven by signaling from death receptors such as the tumor necrosis factor- α (*TNF- α*) receptor, Fas through death-inducing signaling complex (*DISC*) (Taken with permission from Roberts et al. 2009)

The caspase pathway is another mechanism for the initiation of apoptosis. It is an aspartic acid-directed cysteine protease mechanism which initiates and carries out apoptosis. Malfunctioning of this pathway may lead to tumor development, and neurodegenerative as well as several types of autoimmune disorder (Danial and Korsmeyer 2004; Ghavami et al. 2009; Green et al. 2009).

18.6.3.1 AgNPs Cause Apoptosis

Several findings have demonstrated a connection between cell death induced by AgNPs and changed expression of apoptosis-related genes and activation of functions associated with apoptosis (Lee et al. 2011; Cha et al. 2008). Ahamed and co-workers (Ahamed et al. 2008) demonstrated that the apoptosis-connected transcription factor p53 was up-regulated after treatment with both uncoated 25-nm AgNPs and AgNPs coated with a polysaccharide in mouse embryonic stem (mES) cells and mouse embryonic fibroblasts (MEF). The uncoated particles agglomerated, while the coated particles dispersed (Murdock et al. 2007), which was supported by their findings (Ahamed et al. 2008). Agglomeration of uncoated AgNPs correlated with exclusion from the nucleus and mitochondria while the coated AgNPs were distributed throughout the cell. There was also increased expression from the gene encoding Rad51, a protein involved in DNA double-strand breakage repair and

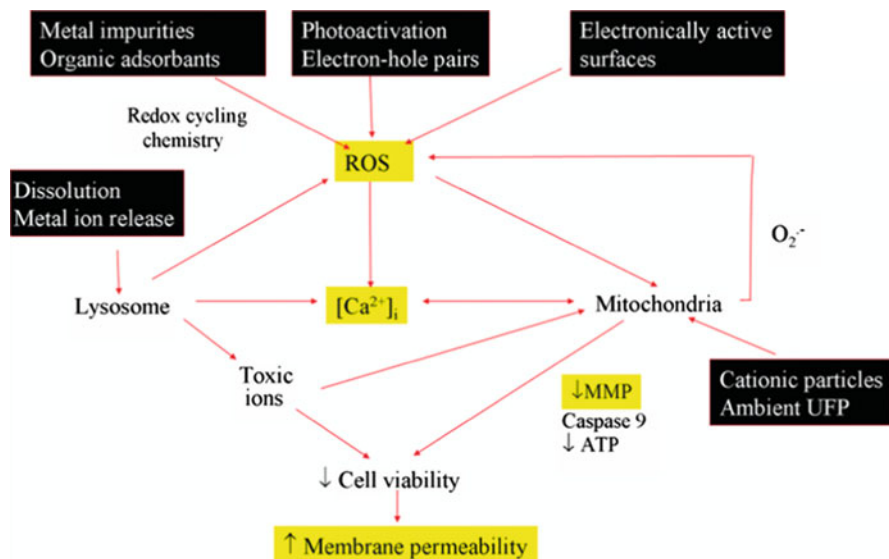


Fig. 18.5 Schematic representation to illustrate the interrelatedness of cellular responses to nanoparticle-induced ROS production. Nanomaterials induce ROS production as a direct consequence of specific material properties or as a consequence of triggering cellular injury responses leading to oxidant radical generation. ROS production could trigger a range of oxidative stress effects. The induction of cellular toxicity at the highest level of oxidative stress involves a number of interrelated cellular responses that include intracellular Ca^{2+} release and mitochondrial perturbation leading to cell death with accompanying changes in cell membrane integrity and nuclear PI uptake. Here, it is demonstrated that nanoparticles engage this toxic oxidative stress pathway through an event sequence that includes particle dissolution, shedding of nanoparticles, $[\text{Ca}^{2+}]$ flux, superoxide generation, and mitochondrial perturbation. The schematic outlines the particle characteristics that could culminate in cytotoxicity (Taken with permission from George et al. 2010)

accumulation. It is well known that double-strand breakage in DNA induces the phosphorylation of histone H2AX at serine 139, which is a specialized histone involved in double strand break repair (Chicheportiche et al. 2007; Ismail and Hendzel 2008). The phosphorylation of this histone was observed to a greater extent with the above-mentioned polysaccharide surface-functionalized (coated) AgNPs.

Additionally, severe DNA damage could also induce apoptosis in cell, where Annexin V protein, a factor involved in apoptosis, is involved (Wang and Kirsch 2006). Thus, apoptotic response can be measured by finding the Annexin V protein expression level by western blot analysis. Ahamed et al. (2008) found the higher expression of Annexin V in coated AgNP-treated MEF cells as compared to the uncoated.

AgNPs are shown to induce caspase-3 activity, one of the key molecules in apoptosis because its activation is often considered as the point of no return for the cell (Cohen 1997). Increase in the caspase-3 activity upon AgNPs-treatment in cancer cell lines has also been reported (Arora et al. 2008). The caspase-3 assay of Bovine retinal endothelial cells (BRECs) showed an increase in caspase-3 level during treatment with silver nanoparticles (Kalishwaralal et al. 2009).

Hsin et al. (2008) studied apoptosis in Ag NPs-challenged NIH3T3 fibroblast cells. Key indicators of apoptosis included release of cytochrome c into the cytosol and translocation of Bax to mitochondria, showing a mitochondrial dependence. Previously, Almofti et al. (2003) found that Ag^+ toxicity in rat liver mitochondria was caused by an increase in the mitochondrial membrane permeability and following release of cytochrome c. Whether the mitochondrial-driven apoptosis observed with the NPs is dependent on ion release awaits proof.

Part of the cellular responses to AgNPs involves the accumulation of reactive oxygen species (ROS). Studies with caudate, frontal cortex and hippocampus of mice brain (Rahman et al. 2009) showed that AgNPs induce oxidative stress and reactive oxygen species. Reactive oxygen species (ROS) increased in a concentration-dependent manner in rat liver cells treated with 10, 25 and 50 $\mu\text{g}/\text{mL}$ of Ag (15- and 100-nm particles) and GSH was depleted (Hussain et al. 2005). Similarly, Carlson et al. (2008) found ROS accumulation after treatments with 15 nm AgNPs at 25 and 50 $\mu\text{g}/\text{mL}$. Kim et al. (2008) showed that AgNPs (25 nm) induced toxicological changes in several organs, including the heart and in cells *in vitro*.

From this discussion, it can be concluded that silver nanoparticles upon entry at high concentration into mammalian cells induces apoptosis, finally leading to its death. The up-regulation of certain genes, generation of ROS, and induction of the caspase pathway are some routes which initiate apoptosis in the cell after their exposure to nano-silver. However, still more study is needed to ensure the exact mechanism of action of silver nanoparticles which cause damage to eukaryotic cells, especially mammalian cells.

18.6.4 Mechanism of Action: Ions Versus NPs

There is confusion in the literature regarding the mechanism of action of AgNPs over the release of ions from the NPs. For instance, Navarro et al. (2008) claimed that AgNPs toxicity could be explained by the release of Ag^+ from the particles which damage cells. Factors that govern the release are not clarified but may relate to particle shape, size, etc. Ingress of AgNPs into cells would result in the intracellular release of Ag ions that could trigger responses different from direct treatments of cells with ions that have a barrier to internal transport through the cell membranes (Bury and Wood 1999). Santoro et al. (2007), after studying the effect of nanosilver as an antimicrobial agent against bacterial colonization surrounding the eye lens, suggested that the toxic effects could be induced from the production of silver ions from nanoparticles released into the culture media. Indeeds treatments with AgNPs and Ag^+ ions caused differential expression from oxidative stress-related genes: expression of the catalase gene was higher with ion treatment than in cells treated with AgNPs (Kim et al. 2009); whether such finding signifies unique mechanisms for the NPs is unresolved. Release of ions from the AgNPs, perhaps at cellular sites that are not available to the ion or at concentrations below ion dosage, seems logical to explain these differences.

The mechanism of action of Ag ions, however, is not fully understood in spite of its historical usage for human medical needs. Wood et al. (1996) reported that Ag⁺ correlated toxicity in fish with disturbance of ionic regulation. *In vitro* studies with primary culture of rainbow trout hepatocytes showed AgNPs at 2.5–4.9 mg/L were highly cytotoxic (Hussain et al. 2005).

Almofti et al. (2003) related the release of cytochrome c in rat liver mitochondria to interaction of the ion with –SH groups of the mitochondrial membrane proteins causing changes in mitochondrial membrane permeability. Palmeira (2008) confirmed toxicity of AgNPs to mitochondrial function in rat liver cells. Gopinath and colleagues (2008) using hamster kidney and colon cancers cells showed that in a 6-h exposure AgNPs inhibited the growth of both types of cells, they claimed through apoptosis. These reports illustrate the potential effects of AgNPs and Ag ions towards different human and animal cells.

18.6.5 Reprogramming of Endothelial Proliferation

The endothelium is the thin layer of cells that lines the interior surface of all blood vessels. It is the target for many medical therapies as it is involved in pathophysiological conditions such as angiogenesis, atherosclerosis, tumor growth, myocardial infarction, limb and cardiac ischemia, restenosis, etc. Therefore, Kalishwaralal et al. (2009) studied the effect of biologically-synthesized AgNPs on bovine retinal endothelial cells (BREC), an *in vitro* model for studies on the retina. Vascular endothelial growth factor (VEGF) is the factor which is found to induce cell proliferation and migration in primary cultures of bovine retinal endothelial cells. The bio-AgNPs significantly blocked the VEGF-induced BREC cell proliferation and their migration (Peters et al. 2004; Yamawaki and Iwai 2006; Kalishwaralal et al. 2009).

Other studies have also examined cell proliferation. Rosas-Hernández et al. (2009) determined anti-proliferative and proliferative effects of 45-nm silver nanoparticles on coronary endothelial cells (CECs). At low concentrations (1.0–10 µg/mL), the AgNPs inhibited cell proliferation, due possibly to apoptosis or other mechanisms of necrosis and cellular arrest. At high concentrations (50–100 µg/mL), a significant proliferative effect was induced. They speculate that proliferation is linked with: (1) endothelial NO production (Ziche and Morbidelli 2000), itself an external inducer of apoptosis (REF) only at the higher AgNPs concentration, and (2) an increase in LDH release only at the lower concentration. LDH release is an indicator of antiproliferative effects (Boop and Lettieri 2008).

Shin et al. (2007) found that the proliferation of peripheral blood mononuclear cells (PBMCs) was impaired by 15-mg/L doses of AgNPs stabilized by polymer encapsulation. There were profound effects on the production of cytokines by these cells: production of INF-γ and TNF-α was inhibited at 10 mg/L whereas formation

of IL-5 was less affected. It means that silver nanoparticles might more effectively inhibit inflammations associated with infections.

18.6.6 Toxic Effects of AgNPs on Different Systems

18.6.6.1 Neurological Effects

Rahman et al. (2009) evaluated the effects of AgNPs on gene expression in different regions of the mouse brain. AgNPs of 25 nm size caused genes associated with oxidative stress and antioxidant defenses genes to be differentially expressed in the caudate, frontal cortex, and hippocampus of mice. Up-regulated genes included: *Fmo2*, *Txnip*, glutathione peroxidase (*Gpx3*), glutathione reductase (*Gsr*), NADPH oxidase (*Nox1*), superoxide dismutase 2, mitochondrial (*Sod2*), Thioredoxin reductase 3 (*Txnrd3*), and Parkinson' disease (*Park7*) and Peroxiredoxin6 (*Prdx6*) genes. *Fmo* gene is concerned with the oxidative metabolism of various xenobiotics but also with the oxidation of reduced glutathione (GSH) to glutathione disulfide (Cereda et al. 2006), *Txnip* plays a role in beta cell glucose toxicity, and induces the intrinsic mitochondrial pathway of apoptosis (Chen and Schluesener 2008). However, *Gpx2* gene, encoding another isozyme of glutathione peroxidase was found down-regulated fivefold in the frontal cortex of mouse brain after the treatment with 1,000 mg/kg Ag-25 nanoparticles. Deficiency of this enzyme increases extracellular oxidative stress thereby promoting platelet activation and leading to a cerebral venous thrombophilic state (Voetsch et al. 2008).

Several studies have revealed that silver nanoparticles, following entry into the systemic blood supply, can induce blood–brain barrier (BBB) dysfunction, astrocyte swelling and neuronal degeneration (Sharma et al. 2009a, b). Exposure to silver nanoparticles has been reported to modulate many genes linked with motor neuron disorder and immune cell function, demonstrating potential neurotoxicity and immunotoxicity in mice. It mainly increases the aquaporin 1 (Aqp1) expression and decreases *Kns2* gene in the brains of AgNP-treated mice. AQP1 is a transmembrane protein which plays an important role in maintaining the homeostasis though water selective channels, while KNS2 is required for the transport of the amyloid precursor protein in neurons (Lee et al. 2010). These changes in gene expression suggest that the chronic exposure silver nanoparticles can result in neurodegenerative disease.

18.6.6.2 Immunological Effects

As stated above, the BBB permeability of nanoparticles has been found to be related to the immunotoxicity. Trickler et al. (2010) examined the interactions of nanosilver (25, 40, and 80 nm) with cerebral microvasculature and found an association of proinflammatory mediators like TNF, IL-1B, and PGE₂ which can

increase BBB permeability. Previously, Carlson et al. (2008) reported the production of morphologically abnormal cells with adherence characteristics after the uptake of AgNPs at high doses after 24 h in alveolar macrophages. These cells also responded significantly showing an inflammatory effect by releasing TNF, MIP-2 and IL-1B. Additionally, cellular viability significantly diminished with increasing doses from 10 to 75 $\mu\text{g}/\text{cm}^3$ of Ag-NPs (15 and 30 nm) following 24 h of exposure. These reports together provide evidence that systemic exposure to AgNPs induces inflammatory effects.

18.6.6.3 Respiratory Effects

Prolonged inhalation of silver nanoparticles seems to affect the normal functioning of lung. This has been supported by the histopathological examination of silver nanoparticle-exposed lung. It causes chronic alveolar inflammation, thickening of alveolar cell walls and small granulomatous lesions (Sung et al. 2008). At the cellular level, it has been confirmed that silver nanoparticles induced stress in associated genes including metallothionein (MT1H, MT1X, and MT2A) and heat shock protein (HSPA4L, HSPH). Likewise, they also induced expression levels of cell cycle checkpoint-related genes like *BIRC5*, *BUB1B*, *CCNA2*, *CDC25B*, *CDC20*, and *CKS*, which may cause the dysregulated proliferation of cells (Kawata et al. 2009). Ji et al. (2007) reported concentration-dependent increases in the silver content of liver following the inhalation of silver nanoparticles for 5 days/week for 4 weeks. This accumulation is possibly due to mucociliary transport and subsequent swallowing of the nanoparticles leading to absorption in the gastrointestinal tract and detectable accumulation in the liver. Ingestion of colloidal silver has also been linked with liver and kidney damage in rats, which are considered to be highly metabolic organs of the body (Kim et al. 2010). Remarkably, silver concentrations were found to be accumulated two to three times higher in female rats as compared to the male rats (Sung et al. 2009). After inhalation, silver nanoparticles were also found to be distributed in kidneys after 28-day (Kim et al. 2007) and 90-day oral and 90-day inhalation studies (Sung et al. 2009).

18.6.6.4 Reproductive Effects

Toxicants that damage normal reproductive functions are an important health issue. Different nanoparticles are one of these. Like BBB, nanoparticles also cross the blood–testes barrier and get accumulated in the male reproductive system, thus having potential adverse effects on the sperm cells. AgNPs can interfere with the cell signaling pathway within sperm cells, thus inhibiting their growth. This toxicity of silver nanoparticles to mammalian germline stem cells specifies the potential of these particles to interfere in general with the male reproductive system (Braydich-Stolle et al. 2005). Further work by Braydich-Stolle et al. (2010) showed that silver nanoparticles reduce the spermatogonial stem cell viability and proliferation in

a size- and concentration-dependent manner with smaller nanoparticles (10–25 nm diameter) inducing a greater decrease in cell viability than larger ones (80 nm diameter).

18.6.6.5 Developmental Defects

The potential toxicity of silver nanoparticles can be assessed by utilizing a well-recognised model in developmental biology and genetics such as the zebrafish (*Danio rerio*). These embryos are transparent. Additionally, they possess a high degree of homology to the human genome, offering an economically feasible, medium-throughput screening platform for noninvasive real-time assessments of toxicity. Therefore, taking advantage of these features of zebrafish, Asharani et al. (2008) studied the toxicity of silver nanoparticles on them. In their study, they found that silver nanoparticles caused concentration-dependent toxicity by hampering the normal development resulting in abnormal body axes, twisted notochord, slow blood flow, pericardial edema and cardiac arrhythmia, with increased apoptosis in zebrafish embryos. In another study, Chae et al. (2009) suggested that the AgNPs led to cellular and DNA damage in Japanese medaka (*Oryzias latipes*). Additionally, carcinogenic and oxidative stresses on genes related to metal detoxification/metabolism regulation and radical scavenging action were also reported to be induced. In contrast, the ionic silver led to an induction of inflammatory response and metallic detoxification processes in the liver of the exposed fish, but resulted in a lower overall stress response when compared with the AgNPs. Eventually, such assessments using the aquatic model organisms like zebrafish will lead to the identification of nanomaterial characteristics that come up with negligible or no toxicity and help to get more balanced designs of materials on the nanoscale.

18.6.6.6 Genotoxic Effects

Many reports have confirmed the genotoxic effects of silver nanoparticles. Recently, Wise Sr. et al. (2010) observed that AgNPs were cytotoxic as well as genotoxic to fish cells in a concentration-dependent manner. They investigated the cytotoxicity and genotoxicity using 30-nm silver nanospheres by exposing them to the *Oryzias latipes* cell line. The silver nanoparticles induced cell death at 0.05–5 $\mu\text{g}/\text{cm}^2$ and chromosomal aberration and aneuploidy at 0.05–0.3 $\mu\text{g}/\text{cm}^2$. On the other hand, Lu et al. (2010a) reported that the citrate-coated colloidal silver nanoparticles at 100 $\mu\text{g}/\text{mL}$ level did not show a genotoxic effect, while the citrate-coated powder form of the AgNPs were found to be toxic.

Hence, nanogenotoxicity needs to be studied in detail to improve our current understanding.

18.6.7 Toxicity at the Microbial Level

AgNPs are toxic to microbial cells at lower levels than those used to demonstrate metabolic effects with human and animal cells. This sensitivity accounts for the proliferation in the use of AgNPs, and ions in products where control of microbial growth is desired such as in the food and medical industries. For instance, growth of cells of the yeast *Saccharomyces cerevisiae*, and the human pathogens *Escherichia coli* and *Staphylococcus. Aureus*, were reported to be at significantly lower concentrations, 0.7, 0.35, and 3.5 µg/L respectively (Kim et al. 2007). Likewise, the metallothionein-deficient (*mtl-2*) mutant strain of *Caenorhabditis elegans* demonstrated greater sensitivity to AgNP than a wild-type strain (Meyer et al. 2010). Gajjar et al. (2009) reported that the AgNPs were equivalent to Ag ions for their lethal dose against a soil pseudomonad. Early events in toxicity appear to be at the level of inhibition of the electron transfer chain and membrane function (Gajjar et al. 2009). What accounts for the differences in sensitivity between animal and microbial cells remains to be resolved. Indeed, the microbial cells possess more complicated and layered cell wall structures than mammalian cells, yet they are more sensitive. So, physical barriers to cytoplasmic influx do not alone explain the findings. Resistance mechanisms are documented for prokaryotic cells and involve efflux pumps to lower cytoplasmic levels of Ag ions and chaperone binding proteins (Rensing et al. 1999; Bagai et al. 2008)

Chromosomal detection of AgNPs (25 µg/mL) in exposed fibroblast cells by fluorescence in situ hybridization (FISH) revealed a 10% increase of chromosomal aberration as compared to treatment with high doses (50 and 100 µg/mL). Cancer cell treatments also showed the same extent of response (Asharani et al. 2009b). There are some studies using AgNPs as antimicrobial agents in bone cement (Alt et al. 2004), while Braydich-Stolle et al. (2005) have shown that silver nanoparticles could be toxic for the bone-lining cells and other tissues.

18.7 Conclusions and Future Directions

The concerns about human exposure to the nanomaterials require us to find solutions to use the NPs with less risk. An understanding of potential negative impacts has to be part of NP safety. It is essential to look at both sides of the story in order to discover the harmful effects of NPs. Currently, we cannot provide a quantifiable exposure assessment. The current methodology lacks the desired sensitivity, reliability and correlation with *in vivo* activity. Therefore, there is a need to develop new methods which can provide accurate exposure risks of NPs both *in vitro* and *in vivo*.

Having a remarkable surface area with small particle size, NPs do have an impact on membrane surfaces, and translocation into animal bodies by ingestion, inhalation or skin contact and translocation to the brain has been demonstrated.

Understanding the effects of skin contact is especially pertinent as AgNPs are often applied topically as antimicrobials as pastes to skin. Many *in vitro* studies that have shown toxic properties of cell challenge by AgNPs through apoptosis, DNA damage, oxidative stress and inflammatory responses have been documented.

Most studies focus on *in vitro* cell culture and how this relates to whole body exposure is an existing challenge. Though silver nanoparticles have been found to be good at destroying cancerous cells, *in vivo* target specificity is needed. For example, if a pregnant women ingests the nanoparticles then many questions regarding the various adverse effects on the fetus require to be answered. Therefore, we need better methods to understand the mechanisms of intracellular uptake, to quantify intracellular NPs in tissues and organs and to differentiate the NPs from Ag ions.

Health and environmental risks are products of both hazards and exposures. Moreover, hazard data from toxicity studies can be confounded with the concept of health risk. Therefore, occupational safety and health programs should include risk management based on recognition of the nanomaterial hazards. Exposure potentials of these nanomaterials should be evaluated and novel applications of control measures should be developed to reduce the risk so that it is better “to be safe rather than saying sorry”.

Acknowledgements This work is supported by Council of Scientific and Industrial Research, New Delhi and Indo-Brazil Joint Research Project funded by Department of Science and Technology, New Delhi, India. The authors thank Professor Anne Anderson, Biology Department, Utah State University, USA for critical suggestions.

References

- Ahamed M, Karns M, Goodson M, Rowe J, Hussain SM, Schlager JJ, Hong Y (2008) DNA damage response to different surface chemistry of silver nanoparticles in mammalian cells. *Toxicol Appl Pharmacol* 233: 404–410.
- Almofti MR, Ichikawa T, Yamashita K, Terada H, Shinohara Y (2003) Silver ion induces a cyclosporine a-insensitive permeability transition in rat liver mitochondria and release of apoptogenic cytochrome. *C J Biochem* 134(1): 43–49.
- Alt V, Bechert T, Steinrucke P, Wagener M, Seidel P, Dingeldein E, Domann E, Schnettler R (2004) An *in vitro* assessment of the antibacterial properties and cytotoxicity of nanoparticulate silver bone cement. *Biomateria* 25: 4383–4391.
- Arora S, Jain J, Rajwade JM, Paknikar KM (2008) Cellular responses induced by silver nanoparticles: *in vitro* studies. *Toxicol Lett* 179: 93–100.
- Asharani PV, Wu YL, Gong Z, Valiyaveettil S (2008) Toxicity of silver nanoparticles in zebrafish models. *Nanotechnology* 19 255102 doi 10.1088/0957-4484/19/25/255102.
- Asharani PV, Mun GLK, Hande MP, Valiyaveettil S (2009a) Cytotoxicity and genotoxicity of silver nanoparticles in human cells. *ACS Nano* 3: 279–290.
- Asharani PV, Hande M P, Valiyaveettil S (2009b) Anti-proliferative activity of silver nanoparticles. *BMC Cell Bio* 10(65): [Online] Available at <http://www.biomedcentral.com/1471-2121/10/65>. Accessed on 24 July 2010.

- Bagai I, Rensing C, Blackburn NJ, McEvoy MM (2008) Direct metal transfer between periplasmic proteins identifies a bacterial copper chaperone. *Biochemistry* 47(44): 11408–11414.
- Barandiaran J (2007) Regulating Berkeley's nanotech future. *Policy Matters* 5(1): 31–38.
- Barnard AS (2010) One-to-one comparison of sunscreen efficacy, aesthetics and potential nanotoxicity. *Nat Nanotechnol* 5: 271–274.
- Blundell G, Henderson WJ, Price EW (1989) Soil particles in the tissues of the foot in endemic elephantiasis of the lower legs. *Ann Trop Med Parasitol* 83: 381–385.
- Boop SK, Lettieri T (2008) Comparison of four different colorimetric and fluorometric cytotoxicity assays in a zebrafish liver cell line. *BMC Pharmacol* 8: 8–19.
- Born PJA, Kreyling W (2004) Toxicological hazards of inhaled nanoparticles- potential implication for drug delivery. *J Nanosci Nanotechnol* 4(6): 1–11.
- Born PJA, Klaessig FC, Landry TD, Moudgil B, Pauluhn J, Thomas K, Trottier R, Wood S (2006a) Research strategies for safety evaluation of nanomaterials, part V: role of dissolution in biological fate and effects of nanoscale particles. *Toxicol Sci* 90: 23–32.
- Born PJA, Robbins D, Haubold S, Kuhlbusch T, Fissan H, Donaldson K, Schins R, Stone V, Kreyling W, Lademann J, Krutmann J, Warheit J, Oberdorster E (2006b) The potential risks of nanomaterials: a review carried out for ECETOC. Part Fibre Toxicol 3: 11. [Online] Available at <http://www.particleandfibretoxicology.com/content/3/1/11>. Accessed on 29 July 2010.
- Bosca L, Zeini M, Traves PG, Hortelano S (2005) Nitric oxide and cell viability in inflammatory cells: a role for NO in macrophage function and fate. *Toxicology* 208: 249–258.
- Benn, TM, Westerhoff P (2008) Nanoparticle silver released into water from commercially available socks fabrics. *Environ Sci Technol* 42(18): 7025–7026.
- Braydich-Stolle L, Hussain S, Schlager JJ, Hofmann MC (2005) *In vitro* cytotoxicity of nanoparticles in mammalian germline stem cells. *Toxicol Sci* 88(2): 412–419.
- Braydich-Stolle LK, Lucas B, Schrand A, Murdock RC, Lee T, Schlager JJ, Hussain SM, Hofmann MC (2010) Silver nanoparticles disrupt GDNF/Fyn kinase signaling in spermatogonial stem cells. *Toxicol Sci* 116(2): 577–589.
- Bury NR, Wood CM (1999) Mechanism of branchial apical silver uptake by rainbow trout is via the proton-coupled Na⁺ channel. *Am J Physiol* 277: 1385–1391.
- Carlson C, Hussain SM, Schrand AM, Braydich-Stolle LK, Hess KL, Jones RL, Schlager JJ (2008) Unique cellular interaction of silver nanoparticles: size-dependent generation of reactive oxygen species. *J Phys Chem B* 112: 13608–13619.
- Cha K, Hong HW, Choi YG, Lee MJ, Park JH, Chae HK, Ryu G, Myung H (2008) Comparison of acute responses of mice livers to short-term exposure to nano-sized or micro-sized silver particles. *Biotechnol Lett* 30:1893–1899
- Chae YJ, Pham CH, Lee J, Bae E, Yi J, Gu MB (2009) Evaluation of the toxic impact of silver nanoparticles on Japanese medaka (*Oryzias latipes*). *Aqu Toxicol* 94: 320–327.
- Cereda C, Gabanti E, Corato M, de Silvestri A, Alimonti D, Cova E, Malaspina A, Ceroni M (2006) Increased incidence of FMO1 gene single nucleotide polymorphisms in sporadic amyotrophic lateral sclerosis. *Amyotroph Lateral Scler* 7: 227–234.
- Chen X, Schluesener HJ (2008) Nanosilver: a nanoproduct in medical application. *Toxicol Lett* 176: 1–12.
- Chen Z, Meng H, Xing G, Chen C, Zhao Y, Jia G, Wang T, Yuan H, Ye C, Zhao F, Chai Z, Zhu C, Fang X, Ma B, Wan L (2006) Acute toxicological effects of copper nanoparticles *in vivo*. *Toxicol Lett* 163(2): 109–120.
- Chicheportiche A, Bernardino-Sgherri J, de-Massy B, Dutrillaux B (2007) Characterization of Spo11-dependent and independent phospho-H2AX foci during meiotic prophase I in the male mouse. *J Cell Sci* 120: 1733–1742.
- Clancy AA, Gregoriou Y, Yaehne K, Cramb DT (2010) Measuring properties of nanoparticles in embryonic blood vessels: towards a physicochemical basis for nanotoxicity. *Chem Phys Lett* 488(4–6): 99–111.
- Clarke AR, Purdie CA, Harrison DJ, Morris RG, Bird CC, Hooper ML, Wyllie AH (1993) Thymocyte apoptosis induced by p53-dependent and independent pathways. *Nature* 362: 849–852.
- Cohen GM (1997) Caspases: the executioners of apoptosis. *Biochem J* 1: 326–330.

- Colvin VL (2003) The potential environmental impact of engineered nanomaterials. *Nat Biotechnol* 21: 1166–1170.
- Corachan M, Tura JM, Campo E, Soley M, Traveria A (1988) Prodoconiosis in equatorial Guinea. Report of two cases from different geographical environments. *Trop Geogr Med* 40: 359–364.
- Danial NN, Korsmeyer SJ (2004) Cell death: critical control points. *Cell* 116: 205–219.
- Dockery DW, Pope C A III (1994) Acute respiratory effects of particulate air pollution. *Annu Rev Public Health* 15: 107–132.
- Donaldson K, Stone V, Seaton A, MacNee W (2001) Ambient particle inhalation and the cardiovascular system: potential mechanisms. *Environ Health Perspect* 109(Suppl 4): 523–527.
- Fong CC, Zhang Y, Zhang Q, Tzang CH, Fong WF, Wu RS, Yang M (2007) Dexamethasone protects RAW264.7 macrophages from growth arrest and apoptosis induced by H₂O₂ through alteration of gene expression patterns and inhibition of nuclear factor-kappa B (NF-kappaB) activity. *Toxicology* 236: 16–28.
- Fotakis G, Timbrell JA (2006) *In vitro* cytotoxicity assays: comparison of LDH, neutral red, MTT and protein assay in hepatoma cell lines following exposure to cadmium chloride. *Toxicol Lett* 160: 171–177.
- Gajjar P, Pettee B, Britt DW, Huang W, Johnson WP, Anderson J (2009) Antimicrobial activities of commercial nanoparticles against an environmental soil microbe, *Pseudomonas putida* KT2440. *J Bio Eng* 3:9 doi:[10.1186/1754-1611-3-9](https://doi.org/10.1186/1754-1611-3-9)
- Gangloff C (2007) US demand for nanotechnology medical products to approach \$53 billion in 2011. [Online] Available at http://www.nanotech-now.com/news.cgi?story_id=21109. Accessed on 29 July 2010.
- Garcia-Ruiz C, Colell A, Paris R, Fernández-Checa JC (2000) Direct interaction of GD3 ganglioside with mitochondria generates reactive oxygen species followed by mitochondrial permeability transition, cytochrome c release, and caspase activation. *FASEB J* 14: 847–858.
- Geiser M, Rothen-Rutishauser B, Kapp N, Schürch S, Kreyling W, Schulz H, Semmler M, Hof VI, Heyder J, Gehr P (2005) Ultrafine particles cross cellular membranes by nonphagocytic mechanisms in lungs and in cultured cells. *Environ Health Perspect* 113(11): 1555–1560.
- Geiser M, Kreyling WG (2010) Deposition and biokinetics of inhaled nanoparticles. *Part Fibre Toxicol* 7: 2. [Online] Available at <http://creativecommons.org/licenses/by/2.0>. Accessed on 29 July 2010.
- George S, Pokhrel S, Xia, T, Gilbert B, Ji Z, Schowalter M, Rosenauer A, Damoiseaux R, Bradley KA, Madler L, Nel AE (2010) Use of a rapid cytotoxicity screening approach to engineer a safer zinc oxide nanoparticle through iron doping. *ACS Nano* 4(1): 15–29.
- Ghavami S, Hashemi M, Ande SR, Yeganeh B, Xiao W, Eshraghi M, Bus CJ, Kadkhoda K, Wiehac E, Halayko AJ, Los M (2009) Apoptosis and cancer: mutations within caspase genes. *J Med Genet* doi:[10.1136/jmg.2009.066944](https://doi.org/10.1136/jmg.2009.066944).
- Gopinath P, Gogoi SK, Chattopadhyay A, Ghosh SS (2008) Implications of silver nanoparticle induced cell apoptosis for *in vitro* gene therapy. *Nanotechnology* 19: 1–10.
- Green DR, Ferguson T, Zitvogel L, Kroemer G (2009) Immunogenic and tolerogenic cell death. *Nat Rev Immunol* 9: 353–363.
- Greulich C, Kittler S, Eppler M, Muhr G, Koller M (2009) Studies on the biocompatibility and the interaction of silver nanoparticles with human mesenchymal stem cells (hMSCs). *Langenbecks Arch Surg* 394 (3): 495–502.
- Gwinn MR, Vallyathan V (2006) Nanoparticles: health effects—pros and cons. *Environ Health Perspect* 114(12): 1818–1825.
- Hill WR, Pillsbury DM (1939) *Argyria: The Pharmacology of Silver*. Baltimore, MD, Williams & Wilkins, pp. 128–132.
- Holsapple M, Farland W, Landry T, Monteiro-Riviere N, Carter J, Walker N, Thomas K (2005) Research strategies for safety evaluation of nanomaterials, Part II: Toxicological and safety evaluation of nanomaterials, current challenges and data needs. *Toxicol Sci* 88(1): 12–17.

- Hsin Y H, Chen CF, Huang S, Shih TS, Lai PS, Chueh PJ (2008) The apoptotic effect of nanosilver is mediated by a ROS- and JNK-dependent mechanism involving the mitochondrial pathway in NIH3T3 cells. *Toxicol Lett* 179: 130–139.
- Hussain SM, Hess KL, Gearhart JM, Geiss KT, Schlager JJ (2005) *In vitro* toxicology of nanoparticles in BRL 3A rat liver cells. *Toxicol In Vitro* 19: 975–983.
- Ibald-Mulli A, Wichmann HE, Kreyling W, Peters A (2002) Epidemiological evidence on health effects of ultrafine particles. *J Aerosol Med* 15: 189–201.
- Ismail IH, Hendzel MJ (2008) The gamma-H2A.X: is it just a surrogate marker of double-strand breaks or much more?. *Environ Mol Mutagen* 49: 73–82.
- Jani PU, McCarthy DE, Florence AT (1994) Titanium dioxide (rutile) particles uptake from the rat GI tract and translocation to systemic organs after oral administration. *J Pharm* 105: 157–168.
- Ji JH, Jung JH, Kim SS, Yoon JU, Park JD, Choi BS, Chung YH, Kwon IH, Jeong J, Han BS, Shin JH, Sung JH, Song KS, Yu IJ (2007) Twenty-eight-day inhalation toxicity study of silver nanoparticles in Sprague-Dawley rats. *Inhal Toxicol* 19: 857–871.
- Jones CF, Grainger W (2009) *In vitro* assessments of nanomaterial toxicity. *Adv Drug Deliv Rev* 61: 438–456.
- Kakkar P, Singh BK (2007) Mitochondria: a hub of redox activities and cellular distress control. *Mol Cell Biochem* 305: 235–253.
- Kawata K, Osawa M, Okabe S (2009) *In vitro* toxicity of silver nanoparticles at noncytotoxic doses to HepG2 human hepatoma cells. *Environ Sci Technol* 43(15): 6046–6051.
- Kim JS, Kuk E, Yu KN, Kim JH, Park SJ, Lee HJ, Kim SH, Park YK, Park Y H, Hwang CY, Kim YK, Lee YS, Jeong DH, Cho MH (2007) Antimicrobial effects of silver nanoparticles. *Nanomed: NBM* 3: 95–101.
- Kim YS, Kim JS, Cho HS, Rha DS, Kim JM (2008) Twenty-eight-day oral toxicity, genotoxicity and gender-related tissue distribution of silver nanoparticles in Sprague–Dawley rats. *Inhal Toxicol* 20: 575–583.
- Kim S, Choi JE, Choi J, Chung K, Park K, Yi J, Ryu D (2009) Oxidative stress-dependent toxicity of silver nanoparticles in human hepatoma cells. *Toxicol In Vitro* 23: 1076–1084.
- Kim YS, Song MY, Park JD, Song KS, Ryu HR, Chung YH, Chang HK, Lee JH, Oh KH, Kelman BJ, Hwang IK, Yu IJ (2010) Subchronic oral toxicity of silver nanoparticles. *Part and Fibre Toxicol*, 7:20.[Online] Available at <http://www.particleandfibretoxicology.com/content/7/1/20>. Accessed on 13 August 2010.
- Kalishwaralal K, Banumathi E, Ram Kumar Pandian S, Deepak V, Muniyandi J, Eom SH, Gurunathan S (2009) Silver nanoparticles inhibit VEGF induced cell proliferation and migration in bovine retinal endothelial cells. *Colloids Surf B Biointerfaces* 73(1): 51–57.
- Lanki T, de Hartog JJ, Heinrich J, Hoek G, Janssen NA, Peters A, Stölzel M, Timonen KL, Vallius M, Vanninen E, Pekkanen J (2006) Can we identify sources of fine particles responsible for exercise-induced ischemia on days with elevated air pollution? The ULTRA Study. *Environ Health Perspect* 114: 655–660.
- Lee H-Y, Choi Y-J, Jung E-J, Yin H-Q, Kwon J-T, Kim J-E, Im H-T, Cho M-H, Kim J-H, Kim H-Y, Lee B-H (2010) Genomics-based screening of differentially expressed genes in the brains of mice exposed to silver nanoparticles via inhalation. *J Nanopart Res* 12: 1567–1578.
- Lee YS, Kim DW, Lee YH, Oh JH, Yoon S, Choi MS, Lee SK, Kim JW, Lee K, Song CW (2011) Silver nanoparticles induce apoptosis and G2/M arrest via PKC ζ -dependent signaling in A549 lung cells. *Arch Toxicol* doi: 10.1007/s00204-011-0714-1.
- Lewinski N, Colvin V, Drezek R (2008) Cytotoxicity of nanoparticles. *Small* 4(1): 26–49.
- Lu W, Senapati D, Wang S, Tovmachenko O, Singh AK, Yu H, Ray PC (2010) Effect of surface coating on the toxicity of silver nanomaterials on human skin keratinocytes. *Chem Phys Lett* 487: 92–96.
- Marquis BJ, Love SA, Braun KL, Haynes CL (2009) Analytical methods to assess nanoparticle toxicity. *Analyst* 134: 425–439.

- Meyer JN, Lord CA, Yang XY, Turner EA, Badireddy AR, Marinakos SM, Chilkoti A, Wiesner MR, Auffan M (2010) Intracellular uptake and associated toxicity of silver nanoparticles in *Caenorhabditis elegans*. *Aquat Toxicol* 100(2): 140–150.
- Miura N, Shinohara Y (2009) Cytotoxic effect and apoptosis induction by silver nanoparticles in HeLa cells. *Biochem Biophys Res Commun* 390(3): 733–737.
- Lux report (2008) Nanomaterials state of the market Q3 2008: stealth success, broad impact. [Online] Available at: <http://portal.luxresearchinc.com/research/document/3735>. Accessed on 24 July 2010.
- Kakurai M, Demitsu T, Umemoto N, Ohtsuki M, Nakagawa H (2003) Activation of mast cells by silver particles in a patient with localized argyria due to implantation of acupuncture needles. *Br J Dermatol* 148(4): 822.
- Margaret Ip, Lui SL, Poon VKM, Lung I, Burd A (2006) Antimicrobial activities of silver dressings: an *in vivo* comparison. *J Med Microbiol* 55: 59–63.
- Morones JR, Elechiguerra JL, Camacho A, Holt K, Kouri JB, Ramirez JT, Yacaman MJ (2005) The bactericidal effect of silver nanoparticles. *Nanotechnology* 16: 2346–2353.
- Murdock RC, Braydich-Stolle L, Schrand AM, Schlager JJ, Hussain SM (2007) Characterization of nanomaterial dispersion in solution prior to *in vitro* exposure using dynamic light scattering technique. *Toxicol Sci* 101: 239–253.
- Navarro E, Piccapietra F, Wagner B, Marconi F, Kaegi R, Odzak N, Sigg L, Behra R (2008) Toxicity of silver nanoparticles to *Clamydomonas reinhardtii*. *Environ Sci Technol* 42: 8959–8964.
- Nel A, Xia T, Maedler L, Li N (2006) Toxic potential of materials at the nanolevel. *Science* 311 (5761): 622–627.
- Nemmar A, Vanbilloen H, Hoylaerts MF, Hoet PHM, Verbruggen A, Nemery B (2001) Passage of intratracheally instilled ultrafine particles from the lung into the systemic circulation in hamster. *Am J Respir Crit Care Med* 164: 1665–1668.
- Nemmar A, Hoet, PHM, Vanquickenborne, B, Dinsdale D, Thomeer M., Hoylaerts MF, Vanbilloen H, Mortelmans L, Nemery B (2002) Passage of inhaled particles into the blood circulation in humans. *Circulation* 105: 411–414.
- Oberdorster G, Sharp Z, Atudorei V, Elder A, Gelein R, Lunts A, Kreyling W, Cox C (2002) Extrapulmonary translocation of ultrafine carbon particles following whole-body inhalation exposure of rats. *J Toxicol Environ Health* 65(20): 1531–1543.
- Palmeira CM (2008) *In vitro* assessment of silver nanoparticles toxicity in hepatic mitochondrial function. EOARD Grand FA8655-07-3047. Final Report. IMAR-Mitochondrial Research Group. Coimbra, Portugal. [Online] Available at <http://handle.dtic.mil/100.2/ADA491040>. Accessed on 29 July 2010.
- Park B (2007) Current and Future Applications of Nanotechnology, in Nanotechnology. In: Harrison RM, Hester RE, eds. *Consequences for Human Health and the Environment*. The Royal Society of Chemistry, Cambridge, UK.
- Peters A, Pope CA III (2002) Cardiopulmonary mortality and air pollution. *Lancet* 360(9341): 1184–1185.
- Peters A, Wichmann HE, Tuch T, Heinrich J, Heyder J (1997) Respiratory effects are associated with the number of ultrafine particles. *Am J Resp Crit Care Med* 155: 1376–1383.
- Peters K, Unger RE, Kirkpatrick CJ, Gatti AM, Monari E (2004) Effects of nano-scaled particles on endothelial cell function *in vitro*: studies on viability, proliferation and inflammation. *J Mater Sci Mater Med* 15: 321–325.
- Pflucker F, Wendel V, Hohenberg H, Gärtner E, Will T, Pfeiffer S, Wepf R, Gers-Barlag H (2001) The human stratum corneum layer: an effective barrier against dermal uptake of different forms of topically applied micronised titanium dioxide. *Skin Pharmacol Appl Skin Physiol* 14 (Suppl 1): 92–97.
- Rahman MF, Wang J, Patterson TA, Saini UT, Robinson BL, Newport GD, Murdock RC, Schlager JJ, Hussain SM, Ali SF (2009) Expression of genes related to oxidative stress in the mouse brain after exposure to silver-25 nanoparticles. *Toxicol Lett* 187: 15–21.
- Rai M, Yadav A, Gade A (2009) Silver nanoparticles as a new generation of antimicrobials. *Biotechnol Adv* 27(1): 76–83.

- Rastogi RP, Richam, Sinha RP (2009) Apoptosis: molecular mechanisms and pathogenicity. *EXCLI J* 8: 155–181.
- Rensing C, Ghosh M, Rosen BP (1999) Families of soft-metal-ion-transporting ATPases. *J Bacteriol* 181(19): 5891–5897.
- Roberts RA, Laskin DL, Smith CV, Robertson FM, Allen EMG, Doorn JA, Slikkerk W (2009) Nitrate and oxidative stress in toxicology and disease. *Toxicol Sci* 112(1): 4–16.
- Roco MC (1999) Nanoparticles and nanotechnology research. *J Nanopart Res* 1: 1–6.
- Rosas-Hernández H, Jiménez-Badillo S, Martínez-Cuevas PP, Gracia-Espino E, Terrones H, Terrones M, Hussain SM, Ali SF, González C (2009) Effects of 45-nm silver nanoparticles on coronary endothelial cells and isolated rat aortic rings. *Toxicol Lett* 191(2–3): 305–313.
- Rouse JG, Yang J, Ryman-Rasmussen JP, Barron AR, Monteiro-Riviere NA (2007) Effects of mechanical flexion on the penetration of fullerene amino acid-derivatized peptide nanoparticles through skin. *Nano Lett* 7: 155–160.
- Ryman-Rasmussen JP, Riviere JE, Monteiro-Riviere NA (2006) Penetration of intact skin by quantum dots with diverse physicochemical properties. *Toxicol Sci* 91: 159–165.
- Santoro CM, Duchsherer NL, Grainger DW (2007) Antimicrobial efficacy and ocular cell toxicity from silver nanoparticles. *Nanobiotechnology* 3(2): 55–65.
- Sarkar S, Sharma C, Yog R, Periakaruppan A, Jejelowo O, Thomas R, Barrera EV, Rice-Ficht AC, Wilson BL, Ramesh GT (2007) Analysis of stress responsive genes induced by single-walled carbon nanotubes in BJ foreskin cells. *J Nanosci Nanotechnol* 7: 584–592.
- Schumacher B, Hofmann K, Boulton S, Gratner A (2001) The *C. elegans* homolog of the p53 tumor suppressor is required for DNA damage-induced apoptosis. *Curr Biol* 11: 1722–1727.
- Sharma HS, Ali SF, Hussain SM, Schlager JJ, Sharma A (2009a) Influence of engineered nanoparticles from metals on the bloodbrain barrier permeability, cerebral blood flow, brain edema and neurotoxicity. An experimental study in the rat and mice using biochemical and morphological approaches. *J Nanosci Nanotechnol* 9: 5055–5072.
- Sharma HS, Ali SF, Tian ZR, Hussain SM, Schlager JJ, Sjoquist PO, Sharma A, Muresanu DF (2009b) Chronic treatment with nanoparticles exacerbate hyperthermia induced blood-brain barrier breakdown, cognitive dysfunction and brain pathology in the rat. Neuroprotective effects of nanowired-antioxidant compound H-290/51. *J Nanosci Nanotechnol* 9: 5073–5090.
- Shimizu T, Numata T, Okada Y (2004) A role of reactive oxygen species in apoptotic activation of volume-sensitive Cl⁻ channel. *Proc Natl Acad Sci* 101(17): 6770–6773.
- Shin S, Ye M, Kim H, Kang H (2007) The effects of nano-silver on the proliferation and cytokine expression by peripheral blood mononuclear cells. *Int Immunopharmacol* 7: 1813–1818.
- Singh S, Khar A (2005) Differential gene expression during apoptosis induced by a serum factor: Role of mitochondrial F0-F1 ATP synthase complex. *Apoptosis* 10: 1469–1482.
- Soto K, Carrasco A, Powell TG, Murr LE, Garza KM (2006) Biological effects of nanoparticulate materials. *Mat Sci Eng art C* 26: 1421–1427.
- Suksanpaisan L, Susantat T, Smith DR (2009) Characterization of dengue virus entry into HepG2 cells. *J Biomed Sci* 16: 17. [Online] Available at <http://www.jbiomedsci.com/content/16/1/17>. Accessed on 28 July 2010.
- Sung JH, Ji JH, Yoon JU, Kim DS, Song MY, Jeong J, Han BS, Han JH, Chung YH, Kim J, Kim TS, Chang HK, Lee EJ, Lee JH, Yu IJ (2008) Lung function changes in Sprague-Dawley rats after prolonged inhalation exposure to silver nanoparticles. *Inhal Toxicol* 20(6): 567–574.
- Sung JH, Ji JH, Park JD, Yoon JU, Kim DS, Jeon KS, Song MY, Jeong J, Han BS, Han JH, Chung YH, Chang HK, Lee JH, Cho MH, Kelman BJ, Yu J (2009) Subchronic inhalation toxicity of silver nanoparticles. *Toxicol Sci* 108(2): 452–461.
- Thayer AM (2007) Carbon nanotubes by the metric ton. *Chem Eng News* 85(46): 29–35.
- Theodore L, Kunz RG (2005) Nanotechnology/ Environmental Overview. In: Theodore L, ed. *Nanotechnology: Environmental Implications and Solutions*. Hoboken, NJ, John Wiley & Sons Inc., pp. 1–60.
- Thomas T, Thomas K, Sadrieh N, Savage N, Adair P, Bronaugh R (2006) Research strategies for safety evaluation of nanomaterials, Part VII: evaluating consumer exposure to nanoscale materials. *Toxicol Sci* 91(1): 14–19.

- Tinkle SS, Antonini JM, Rich BA, Roberts JR, Salmen R, DePree K, Adkins EJ (2003) Skin as a route of exposure and sensitization in chronic beryllium disease. *Environ Health Perspect* 111 (9): 1202–1208.
- Trickler WJ, Lantz SM, Murdock RC, Schrand AM, Robinson BL, Newport GD, Schlager JJ, Oldenburg SJ, Paule MG, Slikker W Jr, Hussain SM, Ali SF (2010) Silver nanoparticle induced blood-brain barrier inflammation and increased permeability in primary rat brain microvessel endothelial cells. *Toxicol Sci* 118(1): 160–70.
- Tyner KM, Wokovich AM, Doub WH, Buhse LF, Sung Li-Piin, Watson SS, Sadrieh N (2009) Comparing methods for detecting and characterizing metal oxide nanoparticles in unmodified commercial sunscreens. *Nanomedicine* 4: 145–159.
- Unfried K, Albrecht C, Klotz LO, von Mikecz A, Grether-Beck S, Schins RPF (2007) Cellular responses to nanoparticles: target structures and mechanisms. *Nanotoxicology* 1(1): 52–71.
- Voetsch B, Jin RC, Bieri C, Deus-Silva L, Camargo EC, Annichino-Bizacchi JM, Handy DE, Loscalzo J (2008) Role of promoter polymorphisms in the plasma glutathione peroxidase (Gpx3) gene as a risk factor for cerebral venous thrombosis. *Stroke* 39: 303–307.
- Vogelstein B, Lane D, Levine AJ (2000) Surfing the p53 network. *Nature* 408: 307–310.
- Wise JP Sr, Goodale BC, Wise SS, Craig GA, Pongan AF, Walter RB, Thompson WD, Ng AK, Aboueissa AM, Mitani H, Spalding MJ, Mason MD (2010) Silver nanospheres are cytotoxic and genotoxic to fish cells. *Aquat Toxicol* 97: 34–41.
- Woodrow Wilson International Center for Scholars (2007) Nanotechnology Consumer Products Inventory. [Online] Available via DIALOG http://www.nanotechproject.org/inventories/consumer/analysis_draft/. Accessed 31 October 2008
- Wakelyn PJ (1994) Cotton yarn manufacturing. In: Ivester AL, Neefus JD, eds. *ILO Encyclopedia of Occupational Health and Safety*, 4th ed. International Labour Office, Geneva, Switzerland, pp. 89.9–89.11.
- Wang, W, Kirsch, T (2006) Annexin V/ β 5 Integrin Interactions Regulate Apoptosis of Growth Plate Chondrocytes. *J Biol Chem* 281: 30848–30856.
- Wichmann H-E, Peters A (2000) Epidemiological evidence of the effects of ultrafine particle exposure. *Phil Trans Royal Soc Lond* 358: 2751–2769.
- Wood CM, Hogstrand C, Galvez F, Munger RS (1996) The physiology of waterborne silver toxicity in freshwater rainbow trout (*Oncorhynchus mykiss*) I. The effects of ionic Ag⁺. *Aquat Toxicol* 35: 93–109.
- Yamago S, Tokuyama H, Nakamura E, Kikuchi K, Kananishi S, Sueki K, Nakahara H, Enomoto S, Ambe F (1995) *In vivo* biological behavior of a water-miscible fullerene: ¹⁴C labeling, absorption, distribution, excretion and acute toxicity. *Chem Biol* 2: 385–389.
- Yamawaki H, Iwai N (2006) Mechanisms underlying nano-sized air-pollution mediated progression of atherosclerosis: carbon black causes cytotoxic injury/inflammation and inhibits cell growth in vascular endothelial cells. *Circ J* 70: 129–140.
- Zhang Y, Sun J (2007) A study on the bio-safety for nano-silver as anti-bacterial materials. *Chin J Med Instrum* 31: 35–38.
- Ziche M, Morbidelli L (2000) Nitric oxide in angiogenesis. *J Neurooncol* 50: 139–148.

Index

A

Absorbents/filter agents 16
Absorption, distribution, metabolism and excretion (ADME) 416
Acalypha indica, silver nanoparticles 344
Acrylamide/titania 128
Activated carbon 16
Adenosine triphosphate (ATP) 4, 74
Ag/graphene oxide 61
Ag-CSN (silver-loaded chitosan nanoparticles) 381
Ag-HPAMAM-NH₂ 54
AgNPs. *see* Silver nanoparticles
Algae, copper 111
Alkyl hydroxy peroxidase 516
Allyl acetylacetone 128
Amino acids 298
– silver 339
Ammonium hexafluorotitanate 13
Amorphous calcium phosphate (ACP) 411
Anatase 56
Antiadhesives 409
Antibacterial potential 360
Antifouling 32, 136, 194, 271
Anti-biofilm 32, 34
Apoptosis 533
– AgNPs 534
Argyria 74
Atmospheric pressure CVD (APCVD) 433
Atomic force microscopy (AFM) 185

B

Bacteria, silver nanoparticles 341
Benzophenone tetracarboxylic dianhydride (BTDA) 125

Bioavailability 511
Biocompatibility, oral 416
Biofilms, formation 29, 123, 139, 196, 258, 325
– oral infections 396
Biogenic synthesis 337
Bio-reporters 514
Botallackite 93

C

Cadmium nanoparticles 338, 352
Calcium silicate–Ag 377
Candidosis 396, 399
Capsicum annuum extract, silver nanoparticles 342
Carbon fiber, silver treatment 18
Carbon nanofibers (CNFs) 56
Carbon nanotubes (CNTs) 90, 244, 381, 430, 452, 471
– paper coating 441
Carboxybetaine 33
Cardiovascular implants 69
Cascade photoreactor 472
Casein phosphopeptide (CPP) 411
Catalase 124
Catheters, silver deposition 324
Cationic antibacterial peptides 30
Cell death, AgNPs 532
Cell membrane, direct damage, silver 7
Cellular respiration 4, 7
Cellular uptake 531
Chemical vapor deposition (CVD) 13, 433
Chitlac 63
Chitosan 55, 380, 409
– films, nanoclays 383
– *N*-halamine-based 293

Cloisite 382
 Coatings, inorganic silver composites 13, 19
 Coenzyme A (CoA) 124
 Colloidal-silver-impregnated ceramic filter 488
 Contact angle (CA) 200
 Copper, antimicrobial activity 97, 225
 Copper-bound chitosan-attached cellulose 90
 Copper-fluoropolymer (Cu-CFx) 413
 Copper-loaded carboxymethyl-chitosan (CMCS-Cu) 91
 Copper nanoparticles (CuNPs) 87, 225, 339, 353, 403
 – antibacterial 85, 229, 403
 – antifungal 237
 – chitosan 90
 – MWCNTs 90
 – synthesis 87, 353
 – toxicity 339
 Copper nanorods (CuNRs) 87
 Copper oxide (CuO) 97, 404
 – health risk 419
 Copper(II) acetylacetonate 87
 Curcacycline, silver nanoparticles 344
 Cytotoxicity 364, 419, 514, 530

D

DAPI (diamidino-2-phenylindole) 194
 Dehydroascorbate reductase (DHAR) 346
 Dental caries 396, 398
 Deposition 316
 Dermal exposure 527
 Dichlorofluorescein diacetate 516
 Dip-coating 317, 428
 Disinfecting medical devices 69
 Disinfection by-products (BDPs) 465
 Dithiothreitol 5
 DNA, binding 203
 – damage 74
 – silver ions 5, 64
 – silver nanoparticles ring 51
 Dopamine-containing polymers 22
 Dynamic light scattering (DLS) 202

E

Ecotoxicity 166, 497, 518
 Electrophoretic mobility shift assay (EMSA) 203
 Electroporation 480
 Electrospinning 431
 Electrosynthesis 291

Endothelial proliferation, reprogramming 537
 Energy dispersive spectroscopy (EDS) 188, 190
 Epifluorescence microscopy 193
 Etching 317
 Ethylene glycol dimethyl ether (EGDME) 431
 Ethylene-vinyl alcohol/titania 138
 Experimental composite adhesives (ECAs) 412
 Exposure 528

F

Fabrics, biocidal silver 25
 Fibers, coating modification 15
 Field emission SEM (FeSEM) 188
 Films, inorganic silver composites 13, 19
 Flame-assisted CVD (FACVD) 433
 Food packaging 70, 375, 456
 – silver 70
 Fouling 13, 29, 291
 FT-IR 200
 Fullerenes 471
 Fungi, copper 108
 – silver nanoparticles 340

G

Gastrointestinal tract uptake 528
 Genomics 517
 Genotoxicity 514
 Geraniol, silver nanoparticles 343
 Glass, antimicrobial modification 12
 Glutathione 517
 Gold nanoparticles 338, 348, 404
 Graphene oxide (GO) 429, 444
 Gum arabic 55
 Gum disease 396, 398
N-Halamines 291
 – polystyrenes 292

H

Health 37, 69, 86, 172, 364, 387, 481, 490, 498, 525
 Hyaluronic acid-catechol (HA-C) 22
 Hydrogels 24, 244, 400
 Hydrogen peroxide 516
 Hydroperoxidase I (katG) 516
 Hydroxyapatite (HA) 19, 56, 408, 410
 – copper-doped 93
 2-Hydroxyethyl methacrylate (HEMA) 24

I

Implantable devices 69
Industrial applications 367
Inhalation 528
Ions vs NPs 536
IR spectroscopy 199
Iron nanoparticles 339, 354

K

Kirby-Bauer disk diffusion test 10

L

Laser scanning confocal microscopy (LSCM) 192
Layer-by-Layer (LbL) self-assembly 19
Layered double hydroxides (LDHs) 385
Leather, silver deposition 328
Lipid peroxidation (LPO) 516
Lipoteichoic acids (LTA) 169

M

Magnetron sputtering (MS) 317, 431
Material fouling 29
Medicago sativa, silver nanoparticles 344
Medical alloy implants 13
Membrane lipids 65
Mercaptoethanol 5
Metal hydroxides 380
Metal ions, dissolved 275
Metal oxides 151, 378, 404
Methacrylic acid (MA)/titania 128
Methyl methacrylate (MMA)/titania 126
Methylene bisacrylamide 128
Mg(OH)₂ 380
Microbe-based reporters 514
Microbial control, silver 71
Minimum biocidal concentration (MBC), copper 98, 403
– silver 9
Minimum inhibitory concentration (MIC), copper 98, 403
– silver 9, 67, 199
– zinc 167
Molecular imprinting polymer-coated titania 127
Montmorillonites 382
Multidrug resistance 29
Multilayered films 245
Multi-walled nanotubes (MWNT) 381, 430, 442, 484
Mutation 6

N

Nanoclays 382
Nanoparticles, immobilization 86, 89, 242, 470
Nanostructured calcium silicate (NCS) 377
Nanotoxicity 526
Nicotinamide adenine dinucleotide (NADH) 5, 50
Nisin loading/retention 386
Nitric oxide 516
NMR 196

O

Oligo ethylene glycol (OEG) 32
Oral infections, biofilms 395
– nanometals 400
Organically modified montmorillonites (OMMT) 382
Oxidative stress 516
Oxydianiline 125

P

Packaging, antimicrobial, silver 70
Palladium nanoparticles 339, 354
PAMPS [poly(2-acrylamido-2-methyl-1-propanesulfonic acid)] 23
Paper, antibacterial 427
– point-of-use water treatment 480
PEO-PPO-PEO 129
Peptides, silver 339
Peri-implantitis 398
Periodontal disease 396, 398
Phanerochaete chrysosporium 50
PHMA [poly(2-hydroxy-4-*N*-methacrylamidobenzoic acid)]-doped polypyrrole film 23
Phosphate efflux 5
Phosphobetaine 33
Phosphonium polymers 32
Photoacoustic spectroscopy (PAS) 195
Photocatalysis 120
Photodynamic therapy (PDT), oral infections 414
Photokilling 120, 139
Photoreactors, flow-through 471
Photoreduction 319
Phyllanthin, silver nanoparticles 343
Physical vapor deposition (PVD) 13
Pigments 15
Plasma treatment 317
Platinum nanoparticles 339, 355

- Polyaniline/titania 130
 Polycarboxybetaine (PCB) 33
 Polydimethylsiloxane (PDMS) 54
 Polyetheretherketone (PEEK),
 Ag/hydroxyapatite (HA) 19
 Polyethersulfone (PES), silver-filled
 asymmetric 71
 – titania 136
 Polyethylene/titania 137
 Polyethylene glycol (PEG) 32
 Polyethylene terephthalate (PET) 20, 69
 Polyethyleneimine (PEI) 20, 22
 – catechol (PEI-C) 22
 Polyimide/titania 125
 Polymer matrix 411
 Polymeric films, nanometals 413
 Polymethylmethacrylate (PMMA)/bentonite/
 Cu 89
 – titania 126, 129, 134
 Polypropylene/titania 129, 137
 Polyrhodanine 55
 Polystyrene/titania 136
 Polysulfobetaine (PSB) 33
 Polytetrafluoroethylene (PTFE) 20
 Polyvinylacetate (PVAc) 125
 Polyvinylpyrrolidone (PVP) 48, 56, 71
 Poly(acrylic acid) (PAA) 128
 Poly(allylamine chloride) (PAH) 128
 Poly(allylamine hydrochloride) (PAH) 20
 Poly(amide–imide)/titania 125
 Poly(butyl acrylate-*co*-methylmethacrylate-*co*-
 (3-methacryloxypropyl)
 trimethoxysilane) 135
 Poly(diallyldimethylammonium chloride)
 (PDADMAC) 25
 Poly(dihydroperfluorooctyl acrylate)
 (PFOA) 54
 Poly(3-hydroxybutyrate-*co*-3-
 hydroxyvalerate) (PHBV) 62
 Poly(imide siloxane)/titania 126
 Poly(lactic-*co*-glycolic acid) (PLGA) 415
 Poly(L-lactide) 55
 Poly(methyl methacrylate) (PMMA) 62
 Poly(methyl methacrylate-*co*-butyl
 methacrylate-*co*-methacrylic acid) 135
 Poly[2-methoxy-5-(2-ethyl-hexyloxy)
 phenylenevinylene] 137
 Poly(styrene-*alt*-maleic anhydride) (PSMA)/
 titania 134
 Poly(tBAM-*co*-EGDMA)/anatase 142
 Poly(trimethylhexamethyleneterephthalamide)
 125
 Poly(vinyl chloride) (PVC)/titania 136
 Powder X-ray diffraction (XRD) 202
 Pr³⁺-activated upconversion materials 486
 Proteomics 517
- Q**
- Quaternary ammonium poly (ethylene imine)
 (QA-PEI) 408, 416
 Quaternary ammonium polymers 31, 408
 Quercetin, silver nanoparticles 345, 347
- R**
- Rayleigh scattering 202
 Reactive oxygen species (ROS) 7, 17, 74,
 165, 259, 362, 420, 516
 – apoptosis 533
 Respiration 4, 7
- S**
- Scanning electron microscopy (SEM) 187
 Scanning probe microscopy (SPM) 185
 Scanning transmission X-ray microscopy
 (STXM) 191
 Selenium nanoparticles 339, 357
 Silica, oral anti-adhesive 409
 Silicon, oral anti-adhesive 409
 Silver 3, 48, 181, 266, 313, 338, 466
 – bacterial resistance 27
 – colloidal 6
 – ecological impact 74
 – inorganic composites 12
 – interaction with bacterial cells 364
 – wound dressing materials 67
 Silver coatings, deposition 317
 Silver colloids, polyethyleneimine (PEI)-
 stabilized 245
 Silver ion 3, 58, 315, 402
 Silver metal clusters, deposition 319
 Silver nanomaterials, direct damage to cell
 membrane 7
 – reduction of silver ions 17
 Silver nanoparticles (AgNPs)
 – antibacterial 213, 450
 – antifungal 215, 237
 – antimicrobial 226, 266, 313, 360,
 402, 450
 – antiviral 217
 – bioactivity 58, 212
 – complications 219, 525
 – cytotoxicity 531
 – developmental defects 540

- food packaging 376
 - genotoxic effects 540
 - HIV-1 217
 - immunological effects 538
 - neurological effects 538
 - paper coating 440
 - polyethylene oxide (PEO) 431
 - reproductive effects 539
 - respiratory effects 539
 - synergism with ampicillin 363
 - synthesis 48, 339
 - toxicity 525
 - Silver nanopowder 6
 - Silver nanowires (AgNWs) 478
 - Silver sulfadiazine 3, 58, 74
 - Silver–amino acid interaction 4
 - Silver-based antimicrobial nanocomposites 47
 - Silver-binding peptides 339
 - Silver–biopolymer nanocomposites 54
 - Silver–cellulose 54
 - Silver–chitosan 55
 - Silver-coated silicone catheters 69
 - Silver–copper nanopowder 6
 - Silver–DNA interaction 4
 - Silver–hydroxyapatite/titania 56
 - Silver–inorganic nanocomposites 56, 60
 - Silver-loaded acetate hollow fibers 62
 - Silver–lysozyme nanoparticle 51
 - Silver–poly(amidoamine) 53
 - Silver–polyaniline 52
 - Silver–polymer nanocomposites 52, 61
 - Silver–polyrhodanine 55
 - Silver–thiol interactions 7
 - Silver(I) complexes 57, 58
 - saccharinate 58
 - Single-wall nanotube (SWNT) 381, 430, 442
 - Skin 527, 529
 - Sodium zincate 161
 - Spent mushroom substrate (SMS) 50
 - Spin-coating 427
 - Sputtering 95, 156, 317, 413, 431
 - Sulfobetaine 33
 - Supercritical carbon dioxide 53
 - Superoxide dismutase 124
 - Superoxide radical 516
 - Surface coating, ZnO 170
 - Surface free energy 200
 - Synergism, silver nanoparticles/ampicillin 363
- T**
- Tannic acid, silver nanoparticles 343
 - Tellurium nanoparticles 339, 359
 - Tetraethylorthosilicate (TEOS) 12, 56
 - Tetrapropylorthotitanate (TPOT) 125
 - Textiles, biocidal silver 25
 - coating modification 15
 - fibers, silver deposition 320
 - Thiol groups, biocides interaction 4
 - Tissue scaffolds 68
 - Titanium alkoxide 13
 - Titanium dioxide 15, 56, 120, 256, 406, 435, 444, 468
 - disinfection capability 120
 - food packaging 378
 - nanotube/CdS electrodes 475
 - paper 435
 - polymeric nanocomposites 124
 - Titanium nanoparticles 339, 360
 - Tooth surfaces 396
 - Tourmaline nanocrystals 385
 - Toxicity 517
 - microbial 541
 - nanomaterial-based films 454
 - oral cavity 416
 - Toxicology 47, 72, 364, 386
 - Tributyl tin (TBT) 291
 - 3-(Trimethoxysilyl)propyl methacrylate (MSMA)/titania 126
- U**
- Uptake 511
 - UV-C 486
 - UV-Vis 196
- V**
- Vacuum filtration 429
 - Viral particles, silver 70
- W**
- Waste water treatment, silver nanoparticles 71, 74
 - Water-borne diseases 465
 - Water disinfection 465
 - silver 71
 - Water sterilization, high speed 478
 - Water treatment 465
 - Wound dressing 68
- Z**
- Zeolites 16, 93, 111, 216, 402
 - Zinc oxide 151, 258, 405, 450

- antimicrobial activity 161, 258
- crystal structure 152
- food packaging 379
- mechanism 165
- minimal inhibitory concentration (MIC) 167
- paper coating 440
- ROS 165, 174, 259
- sepiolite 171
- toxicity 171
- Zone of inhibition (ZOI) 10, 22, 98, 108

About the Editors

Nicola Cioffi

Nicola Cioffi graduated in Chemistry – *summa cum laude* – at the University of Bari in 1997, studying the ascorbic acid oxidation cascade. In 2001, he obtained a PhD in Chemistry of Innovative Materials at the University of Bari, working on the development, characterization, and analytical application of novel nanostructured materials such as metal nanoparticles, organic/inorganic nano-composites and conductive polymer thin films.

In 2001, he received the “Best Young Researcher” Award from the Analytical Chemistry Division of the Italian Chemical Society.

From November 2001 to December 2004, he held several post-doctoral fellowships, still working on the synthesis, characterization, and device application of nanomaterials. In 2004, he was awarded a fellowship from the Italian Section of the Human Proteome Organization on the use of mass spectrometry techniques for proteomics research. Since 2005, he has been Assistant Professor at the Chemistry Department of the University of Bari.

He serves as referee for 27 international journals and is a member of five Editorial Boards. He co-edited special issues of *Sensor Letters* and *Molecules* journals. His scientific output includes several invited seminars, 9 book chapters, 81 papers and 2 editorials in peer-reviewed journals and textbooks, 3 European patents, 10 extended abstracts and 150 conference communications.

Nicola Cioffi’s research interests are in the field of nanomaterials for the life sciences, including: sensors (gas- & vapor-sensors, biosensors), bio-analysis, nanomaterials for mass spectrometry and proteomics research, antibacterial/bioactive nanomaterials, catalysts for green chemistry, and surface analysis of novel materials.

Mahendra Rai

Professor Mahendra Rai is Head of the Department of Biotechnology at SGB Amravati University in Maharashtra, India. He has published 200 research papers, more than 100 popular articles in Indian and foreign journals and edited 25 books. He is a member of several scientific societies and has been a national Scholar for five years. He has received several prestigious awards, including the Father T.A. Mathias award (1989) from the All India Association for Christian Higher Education, and the Medini award (1999) from the Department of Environment and Forest, Government of India. He has also received a SERC visiting fellowship by the Department of Science and Technology (1996), an INSA visiting fellowship by the Indian National Science Academy (1998) and TWAS-UNESCO Associateship (2002), Italy. He has approximately three decades of teaching and research experience.

The main focus of Professor Rai's research is biological synthesis of nanoparticles, understanding the mechanism involved, and their bioactivity.